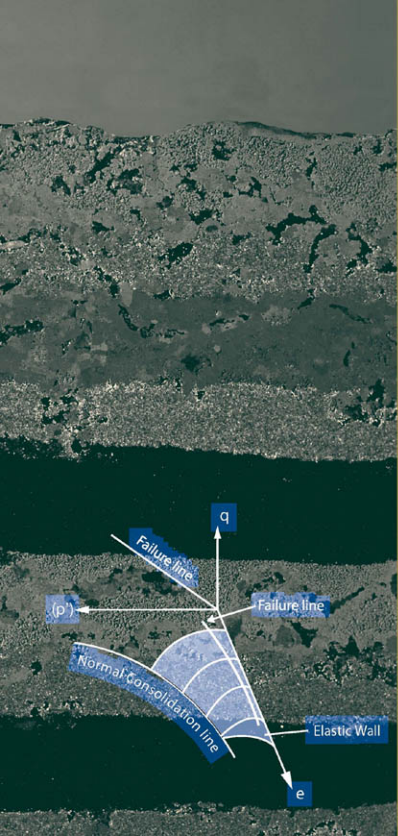


SOIL
Mechanics
AND
Foundations

3rd Edition



This page intentionally left blank

THIRD EDITION

SOIL MECHANICS AND FOUNDATIONS

MUNI BUDHU

*Professor, Department of Civil Engineering & Engineering Mechanics
University of Arizona*



JOHN WILEY & SONS, INC.

VICE PRESIDENT AND EXECUTIVE PUBLISHER
ACQUISITIONS EDITOR
EDITORIAL ASSISTANT
PRODUCTION SERVICES MANAGER
SENIOR PRODUCTION EDITOR
EXECUTIVE MARKETING MANAGER
EXECUTIVE MEDIA EDITOR
CREATIVE DIRECTOR
DESIGNER
PHOTO EDITOR
SENIOR ILLUSTRATION EDITOR
PRODUCTION SERVICES
COVER IMAGE

Don Fowley
Jennifer Welter
Alexandra Spicehandler
Dorothy Sinclair
Janet Foxman
Christopher Ruel
Tom Kulesa
Harry Nolan
Wendy Lai
Sheena Goldstein
Anna Melhorn
Brendan Short/Aptara
© Hans Pfletschinger/Peter Arnold Images/Photolibrary

This book was set in 10/12 Times Ten LT Std by Aptara®, Inc. and printed and bound by Hamilton Printing Company. The cover was printed by Hamilton Printing Company.

This book is printed on acid-free paper. (∞)

Founded in 1807, John Wiley & Sons, Inc. has been a valued source of knowledge and understanding for more than 200 years, helping people around the world meet their needs and fulfill their aspirations. Our company is built on a foundation of principles that include responsibility to the communities we serve and where we live and work. In 2008, we launched a Corporate Citizenship Initiative, a global effort to address the environmental, social, economic, and ethical challenges we face in our business. Among the issues we are addressing are carbon impact, paper specifications and procurement, ethical conduct within our business and among our vendors, and community and charitable support. For more information, please visit our website: www.wiley.com/go/citizenship.

Copyright © 2011, 2007, 2000 John Wiley & Sons, Inc. All rights reserved. No part of this publication may be reproduced, stored in a retrieval system or transmitted in any form or by any means, electronic, mechanical, photocopying, recording, scanning or otherwise, except as permitted under Sections 107 or 108 of the 1976 United States Copyright Act, without either the prior written permission of the Publisher, or authorization through payment of the appropriate per-copy fee to the Copyright Clearance Center, Inc., 222 Rosewood Drive, Danvers, MA 01923, website www.copyright.com. Requests to the Publisher for permission should be addressed to the Permissions Department, John Wiley & Sons, Inc., 111 River Street, Hoboken, NJ 07030-5774, (201) 748-6011, fax (201) 748-6008, website www.wiley.com/go/permissions.

Evaluation copies are provided to qualified academics and professionals for review purposes only, for use in their courses during the next academic year. These copies are licensed and may not be sold or transferred to a third party. Upon completion of the review period, please return the evaluation copy to Wiley. Return instructions and a free of charge return shipping label are available at www.wiley.com/go/returnlabel. Outside of the United States, please contact your local representative.

Library of Congress Cataloging-in-Publication Data

Budhu, M.

Soil mechanics and foundations / Muni Budhu.—3rd ed.
p. cm.

Includes bibliographical references.

ISBN 978-0-470-55684-9 (hardback)

1. Soil mechanics. 2. Foundations. I. Title.

TA710.B765 2010

624.1'5136—dc22

2010023265

Printed in the United States of America

10 9 8 7 6 5 4 3 2 1

PREFACE

This textbook is written for an undergraduate course in soil mechanics and foundations. It has three primary objectives. The first is to present basic concepts and fundamental principles of soil mechanics and foundations in a simple pedagogy using the students' background in mechanics, physics, and mathematics. The second is to integrate modern learning principles, teaching techniques, and learning aids to assist students in understanding the various topics in soil mechanics and foundations. The third is to provide a solid background knowledge to hopefully launch students in their lifelong learning of geotechnical engineering issues.

Some of the key features of this textbook are:

- Topics are presented thoroughly and systematically to elucidate the basic concepts and fundamental principles without diluting technical rigor.
- A large number of example problems are solved to demonstrate or to provide further insights into the basic concepts and applications of fundamental principles.
- The solution of each example is preceded by a strategy, which is intended to teach students to think about possible solutions to a problem before they begin to solve it. Each solution provides a step-by-step procedure to guide the student in problem solving.
- A “What you should be able to do” list at the beginning of each chapter alerts readers to what they should have learned after studying each chapter, to help students take responsibility for learning the material.
- Web-based applications including interactive animations, interactive problem solving, interactive step-by-step examples, virtual soils laboratory, e-quizzes, and much more are integrated with this textbook.

With the proliferation and accessibility of computers, programmable calculators, and software, students will likely use these tools in their practice. Consequently, computer program utilities and generalized equations that the students can program into their calculators are provided rather than charts.

The content of the book has been significantly enhanced in the third edition:

- **Reorganization of chapters**—Several chapters in the second edition are now divided into multiple chapters for ease of use.
- **Enhancement of content**—The content of each chapter has been enhanced by adding updated materials and more explanations. In particular, significant improvements have been made not only to help interpret soil behavior but also to apply the basic concepts to practical problems.
- **Examples and problems**—More examples, with more practical “real-world” situations, and more problems have been added. The examples have been given descriptive titles to make specific examples easier to locate.

ACKNOWLEDGMENTS

I am grateful to the many reviewers who offered many valuable suggestions for improving this textbook. The following persons were particularly helpful in reviewing the third edition: Juan Lopez, geotechnical engineer, Golder Associates, Houston, TX; Walid Toufig, graduate student, University of Arizona, Tucson, AZ; and Ibrahim Adiyaman, graduate student, University of Arizona, Tucson, AZ.

Ms. Jenny Welter, Mr. Bill Webber, and the staff of John Wiley & Sons were particularly helpful in getting this book completed. Additional resources are available online at www.wiley.com/college/budhu.

Also available from the Publisher: *Foundations and Earth Retaining Structures*, by Muni Budhu

ISBN: 978-0471-47012-0

Website: www.wiley.com/college/budhu

A companion lab manual is available from the Publisher: *Soil Mechanics Laboratory Manual*, by Michael Kalinski

The soil mechanics course is often accompanied by a laboratory course, to introduce students to common geotechnical test methods, test standards, and terminology. Michael Kalinski of the University of Kentucky has written a lab manual introducing students to the most common soil mechanics tests, and has included laboratory exercises and data sheets for each test. Brief video demonstrations are also available online for each of the experiments described in this manual.

Soil Mechanics Laboratory Manual, by Michael Kalinski

Website: www.wiley.com/college/kalinski

NOTES for Students and Instructors

PURPOSES OF THIS BOOK

This book is intended to present the principles of soil mechanics and its application to foundation analyses. It will provide you with an understanding of the properties and behavior of soils, albeit not a perfect understanding. The design of safe and economical geotechnical structures or systems requires considerable experience and judgment, which cannot be obtained by reading this or any other textbook. It is hoped that the fundamental principles and guidance provided in this textbook will be a base for lifelong learning in the science and art of geotechnical engineering.

The goals of this textbook in a course on soil mechanics and foundation are as follows:

1. To understand the physical and mechanical properties of soils.
2. To determine parameters from soil testing to characterize soil properties, soil strength, and soil deformations.
3. To apply the principles of soil mechanics to analyze and design simple geotechnical systems.

LEARNING OUTCOMES

When you complete studying this textbook you should be able to:

- Describe soils and determine their physical characteristics such as grain size, water content, and void ratio.
- Classify soils.
- Determine compaction of soils.
- Understand the importance of soil investigations and be able to plan a soil investigation.
- Understand the concept of effective stress.
- Determine total and effective stresses and porewater pressures.
- Determine soil permeability.
- Determine how surface stresses are distributed within a soil mass.
- Specify, conduct, and interpret soil tests to characterize soils.
- Understand the stress-strain behavior of soils.
- Understand popular failure criteria for soils and their limitations.
- Determine soil strength and deformation parameters from soil tests, for example, Young's modulus, friction angle, and undrained shear strength.
- Discriminate between "drained" and "undrained" conditions.
- Understand the effects of seepage on the stability of structures.
- Estimate the bearing capacity and settlement of structures founded on soils.
- Analyze and design simple foundations.
- Determine the stability of earth structures, for example, retaining walls and slopes.

ASSESSMENT

You will be assessed on how well you absorb and use the fundamentals of soil mechanics. Three areas of assessment are incorporated in the Exercise sections of this textbook. The first area, called “Theory,” is intended for you to demonstrate your knowledge of the theory and extend it to uncover new relationships. The questions under “Theory” will help you later in your career to address unconventional issues using fundamental principles. The second area, called “Problem Solving,” requires you to apply the fundamental principles and concepts to a wide variety of problems. These problems will test your understanding and use of the fundamental principles and concepts. The third area, called “Practical,” is intended to create practical scenarios in which you can use not only the subject matter in the specific chapter but also prior materials that you have encountered. These problems try to mimic some aspects of real situations and give you a feel for how the materials you have studied so far can be applied in practice. Communication is at least as important as the technical details. In many of these “Practical” problems you are placed in a situation in which you must convince stakeholders of your technical competence. A quiz at the end of each chapter is at www.wiley.com/college/budhu to test your general knowledge of the subject matter.

SUGGESTIONS FOR PROBLEM SOLVING

Engineering is, foremost, about problem solving. For most engineering problems, there is no unique method or procedure for finding solutions. Often, there is no unique solution to an engineering problem. A suggested problem-solving procedure is outlined below.

1. Read the problem carefully; note or write down what is given and what you are required to find.
2. Draw clear diagrams or sketches wherever possible.
3. Devise a strategy to find the solution. Determine what principles, concepts, and equations are needed to solve the problem.
4. When performing calculations, make sure that you are using the correct units.
5. Check whether your results are reasonable.

The units of measurement used in this textbook follow the SI system. Engineering calculations are approximations and do not result in exact numbers. All calculations in this book are rounded, at the most, to two decimal places except in some exceptional cases, for example, void ratio.

WEBSITE

Additional materials are available at www.wiley.com/college/budhu. The National Science Digital Library site “Grow” (www.grow.arizona.edu) contains a collection of learning and other materials on geotechnical engineering.

NOTES for Instructors

I would like to present some guidance to assist you in using this book in undergraduate geotechnical engineering courses based on my own experiences in teaching this material.

DESCRIPTION OF CHAPTERS

The philosophy behind each chapter is to seek coherence and to group topics that are directly related to each other. This is a rather difficult task in geotechnical engineering because topics are intertwined. Attempts have been made to group topics based on whether they relate directly to the physical characteristics of soils or mechanical behavior or are applications of concepts to analysis of geotechnical systems. The sequencing of the chapters is such that the preknowledge required in a chapter is covered in previous chapters.

Chapter 1 sets the introductory stage of informing the students of the importance of geotechnical engineering. Most of the topics related to the physical characteristics of soils are grouped in Chapters 2 through 5. Chapter 2 deals with basic geology, soil composition, and particle sizes. Chapter 3 is about soils investigations and includes in situ and laboratory tests. The reasons for these tests will become clear after Chapters 4 through 10 are completed. In Chapter 4, phase relationships, index properties, and soil classification and compaction are presented. Chapter 5 describes soil compaction and why it is important. One-dimensional flow of water and wellpoints are discussed in Chapter 6.

Chapter 7 deals with stresses, strains, and elastic deformation of soils. Most of the material in this chapter builds on course materials that students would have encountered in their courses in statics and strength of materials. Often, elasticity is used in preliminary calculations in analyses and design of geotechnical systems. The use of elasticity to find stresses and settlement of soils is presented and discussed. Stress increases due to applied surface loads common to geotechnical problems are described. Students are introduced to stress and strain states and stress and strain invariants. The importance of effective stresses and seepage in soil mechanics is emphasized.

Chapter 8 presents stress paths. Here basic formulation and illustrations of stress paths are discussed. Drained and undrained conditions are presented within the context of elasticity. In Chapter 9, the basic concepts of consolidation are presented with methods to calculate consolidation settlement. The theory of one-dimensional consolidation is developed to show students the theoretical framework from which soil consolidation settlement is interpreted and the parameters required to determine time rate of settlement. The oedometer test is described, and procedures to determine the various parameters for settlement calculations are presented.

Chapter 10 deals with the shear strength of soils and the tests (laboratory and field) required for its determination. Failure criteria are discussed using the student's background in strength of materials (Mohr's circle) and in statics (dry friction). Soils are treated as a dilatant-frictional material rather than the conventional cohesive-frictional material. Typical stress-strain responses of sand and clay are presented and discussed. The implications of drained and undrained conditions on the shear strength of soils are discussed. Laboratory and field tests to determine the shear strength of soils are described. Some of the failure criteria for soils are presented and their limitations are discussed.

Chapter 11 deviates from traditional undergraduate textbook topics that present soil consolidation and strength as separate issues. In this chapter, deformation and strength are integrated within the framework of critical state soil mechanics using a simplified version of the modified Cam-clay model. The emphasis is on understanding the mechanical behavior of soils rather than presenting the mathematical

formulation of critical state soil mechanics and the modified Cam-clay model. The amount of mathematics is kept to the minimum needed for understanding and clarification of important concepts. Projection geometry is used to illustrate the different responses of soils when the loading changes under drained and undrained loading. Although this chapter deals with a simplification and an idealization of real soils, the real benefit is a simple framework, which allows the students to think about possible soil responses if conditions change from those originally conceived, as is usual in engineering practice. It also allows them to better interpret soil test results and estimate possible soil responses from different loading conditions.

Chapter 12 deals with bearing capacity and settlement of footings. Here bearing capacity and settlement are treated as a single topic. In the design of foundations, the geotechnical engineer must be satisfied that the bearing capacity is sufficient and the settlement at working load is tolerable. Indeed, for most shallow footings, it is settlement that governs the design, not bearing capacity. Limit equilibrium analysis is introduced to illustrate the method that has been used to find the popular bearing capacity equations and to make use of the student's background in statics (equilibrium) to introduce a simple but powerful analytical tool. A set of bearing capacity equations for general soil failure that has found general use in geotechnical practice is presented. These equations are simplified by breaking them down into two categories—one relating to drained condition, the other to undrained condition. Elastic, one-dimensional consolidation and Skempton and Bjerrum's (1957) method of determining settlement are presented. The elastic method of finding settlement is based on work done by Gazetas et al. (1985), who described problems associated with the Janbu, Bjerrum, and Kjaernali (1956) method that is conventionally quoted in textbooks. The application of knowledge gained in Chapter 11 to shallow footing design is presented.

Pile foundations are described and discussed in Chapter 13. Methods for finding bearing capacity and settlement of single and group piles are presented.

Chapter 14 is about two-dimensional steady-state flow through soils. Solutions to two-dimensional flow using flownets and the finite difference technique are discussed. Emphases are placed on seepage, porewater pressure, and instability. This chapter normally comes early in most current textbooks. The reason for placing this chapter here is because two-dimensional flow influences the stability of earth structures (retaining walls and slopes), discussion of which follows in Chapters 15 and 16. A student would then be able to make the practical connection of two-dimensional flow and stability of geotechnical systems readily.

Lateral earth pressures and their use in the analysis of earth-retaining systems and simple braced excavations are presented in Chapter 15. Gravity and flexible retaining walls, in addition to reinforced soil walls, are discussed. Guidance is provided as to what strength parameters to use in drained and undrained conditions.

Chapter 16 is about slope stability. Here stability conditions are described based on drained or undrained conditions.

Appendix A allows easy access to frequently used typical soil parameters and correlations. Appendix B shows charts to determine the increases in vertical stress and elastic settlement of uniformly loaded circular foundation. Appendix C contains charts for the determination of the increases in vertical stress for uniformly loaded circular and rectangular footings resting on finite soil layers. Appendix D contains charts for the determination of lateral earth pressure coefficients presented by Kerisel and Absi (1990).

CHAPTER LAYOUT

The **Introduction** of each chapter attempts to capture the student's attention, to present the learning objectives, and to inform the student of what prior knowledge is needed to master the material. At the end of the introduction, the importance of the learning material in the chapter is described. The intention is to give the student a feel for the kind of problem that he or she should be able to solve on completion of the chapter.

Definitions of Key Terms are presented to alert and introduce the students to new terms in the topics to be covered. A section on **Questions to Guide Your Reading** is intended to advise the students on key information that they should grasp and absorb. These questions form the core for the end-of-chapter quiz.

Each topic is presented thoroughly, with the intention of engaging the students and making them feel involved in the process of learning. At various stages, **Essential Points** are summarized for reinforcement. **Examples** are solved at the end of each major topic to illustrate problem-solving techniques, and to reinforce and apply the basic concepts. A **What's Next** section serves as a link between articles and informs students about this connection. This prepares them for the next topic and serves as a break point for your lectures. A **Summary** at the end of each chapter reminds students, in a general way, of key information. The **Exercises** or problems are divided into three sections. The first section contains problems that are theoretically based, the second section contains problems suitable for problem solving, and the third section contains problems biased toward application. This gives you flexibility in setting up problems based on the objectives of the course.

ADDITIONAL MATERIALS

Additional materials are and will be available at <http://www.wiley.com/college/budhu>. These materials include:

1. Interactive animation of certain concepts.
2. Interactive problem solving.
3. Spreadsheets.
4. PowerPoint slides.
5. Software applications.
6. A quiz for each chapter.

CONTENTS

PREFACE **iii**

NOTES FOR STUDENTS AND INSTRUCTORS **v**

NOTES FOR INSTRUCTORS **vii**

CHAPTER 1 INTRODUCTION TO SOIL MECHANICS AND FOUNDATIONS **1**

- 1.0 Introduction **1**
- 1.1 Marvels of Civil Engineering—The Hidden Truth **2**
- 1.2 Geotechnical Lessons from Failures **3**

CHAPTER 2 GEOLOGICAL CHARACTERISTICS AND PARTICLE SIZES OF SOILS **5**

- 2.0 Introduction **5**
- 2.1 Definitions of Key Terms **5**
- 2.2 Questions to Guide Your Reading **6**
- 2.3 Basic Geology **6**
 - 2.3.1 Earth's Profile **6**
 - 2.3.2 Plate Tectonics **6**
 - 2.3.3 Composition of the Earth's Crust **7**
 - 2.3.4 Discontinuities **8**
 - 2.3.5 Geologic Cycle and Geological Time **8**
- 2.4 Composition of Soils **10**
 - 2.4.1 Soil Formation **10**
 - 2.4.2 Soil Types **10**
 - 2.4.3 Clay Minerals **11**
 - 2.4.4 Surface Forces and Adsorbed Water **12**
 - 2.4.5 Soil Fabric **13**
- 2.5 Determination of Particle Size of Soils—ASTM D 422 **15**
 - 2.5.1 Particle Size of Coarse-Grained Soils **15**
 - 2.5.2 Particle Size of Fine-Grained Soils **16**
 - 2.5.3 Characterization of Soils Based on Particle Size **17**
- 2.6 Comparison of Coarse-Grained and Fine-Grained Soils for Engineering Use **24**
- 2.7 Summary **24**
 - Self-Assessment **25**
 - Exercises **25**

CHAPTER 3 SOILS INVESTIGATION **26**

- 3.0 Introduction **26**
- 3.1 Definitions of Key Terms **27**
- 3.2 Questions to Guide Your Reading **27**

- 3.3 Purposes of a Soils Investigation **27**
- 3.4 Phases of a Soils Investigation **27**
- 3.5 Soils Exploration Program **29**
 - 3.5.1 Soils Exploration Methods **29**
 - 3.5.2 Soil Identification in the Field **32**
 - 3.5.3 Number and Depths of Boreholes **34**
 - 3.5.4 Soil Sampling **35**
 - 3.5.5 Groundwater Conditions **36**
 - 3.5.6 Soils Laboratory Tests **37**
 - 3.5.7 Types of In Situ or Field Tests **37**
 - 3.5.8 Types of Laboratory Tests **43**
- 3.6 Soils Report **46**
- 3.7 Summary **47**
 - Self-Assessment **47**
 - Exercises **47**

CHAPTER 4 PHYSICAL SOIL STATES AND SOIL CLASSIFICATION **48**

- 4.0 Introduction **48**
- 4.1 Definitions of Key Terms **49**
- 4.2 Questions to Guide Your Reading **49**
- 4.3 Phase Relationships **50**
- 4.4 Physical States and Index Properties of Fine-Grained Soils **61**
- 4.5 Determination of the Liquid, Plastic, and Shrinkage Limits **64**
 - 4.5.1 Casagrande Cup Method—ASTM D 4318 **64**
 - 4.5.2 Plastic Limit Test—ASTM D 4318 **65**
 - 4.5.3 Fall Cone Method to Determine Liquid and Plastic Limits **65**
 - 4.5.4 Shrinkage Limit—ASTM D 427 and D 4943 **66**
- 4.6 Soil Classification Schemes **70**
 - 4.6.1 Unified Soil Classification System **71**
 - 4.6.2 American Society for Testing and Materials (ASTM) Classification System **71**
 - 4.6.3 AASHTO Soil Classification System **74**
 - 4.6.4 Plasticity Chart **76**
- 4.7 Engineering Use Chart **76**
- 4.8 Summary **80**
 - Self-Assessment **81**
 - Practical Examples **81**
 - Exercises **83**

CHAPTER 5 SOIL COMPACTION 87

5.0	Introduction	87
5.1	Definitions of Key Terms	88
5.2	Questions to Guide Your Reading	88
5.3	Basic Concept	88
5.4	Proctor Compaction Test—ASTM D 1140 and ASTM D 1557	89
5.5	Interpretation of Proctor Test Results	91
5.6	Benefits of Soil Compaction	95
5.7	Field Compaction	96
5.8	Compaction Quality Control	97
5.8.1	Sand Cone—ASTM D 1556	97
5.8.2	Balloon Test—ASTM D 2167	100
5.8.3	Nuclear Density Meter—ASTM D 2922, ASTM D 5195	100
5.8.4	Comparison Among the Popular Compaction Quality Control Tests	101
5.9	Summary	102
	Self-Assessment	102
	Practical Example	102
	Exercises	103

CHAPTER 6 ONE-DIMENSIONAL FLOW OF WATER THROUGH SOILS 105

6.0	Introduction	105
6.1	Definitions of Key Terms	105
6.2	Questions to Guide Your Reading	105
6.3	Head and Pressure Variation in a Fluid at Rest	106
6.4	Darcy's Law	109
6.5	Empirical Relationships for k	111
6.6	Flow Parallel to Soil Layers	116
6.7	Flow Normal to Soil Layers	117
6.8	Equivalent Hydraulic Conductivity	117
6.9	Determination of the Hydraulic Conductivity	118
6.9.1	Constant-Head Test	118
6.9.2	Falling-Head Test	119
6.9.3	Pumping Test to Determine the Hydraulic Conductivity	122
6.10	Groundwater Lowering by Wellpoints	124
6.11	Summary	126
	Self-Assessment	126
	Practical Example	126
	Exercises	127

CHAPTER 7 STRESSES, STRAINS, AND ELASTIC DEFORMATIONS OF SOILS 131

7.0	Introduction	131
7.1	Definitions of Key Terms	133
7.2	Questions to Guide Your Reading	133
7.3	Stresses and Strains	133
7.3.1	Normal Stresses and Strains	133
7.3.2	Volumetric strain	134
7.3.3	Shear Stresses and Shear Strains	134

7.4	Idealized Stress–Strain Response and Yielding	135
7.4.1	Material Responses to Normal Loading and Unloading	135
7.4.2	Material Response to Shear Forces	137
7.4.3	Yield Surface	138
7.5	Hooke's Law	139
7.5.1	General State of Stress	139
7.5.2	Principal Stresses	140
7.5.3	Displacements from Strains and Forces from Stresses	140
7.6	Plane Strain and Axial Symmetric Conditions	141
7.6.1	Plane Strain Condition	141
7.6.2	Axisymmetric Condition	142
7.7	Anisotropic, Elastic States	145
7.8	Stress and Strain States	146
7.8.1	Mohr's Circle for Stress States	147
7.8.2	Mohr's Circle for Strain States	148
7.9	Total and Effective Stresses	150
7.9.1	The Principle of Effective Stress	151
7.9.2	Effective Stresses Due to Geostatic Stress Fields	152
7.9.3	Effects of Capillarity	153
7.9.4	Effects of Seepage	154
7.10	Lateral Earth Pressure at Rest	161
7.11	Stresses in Soil from Surface Loads	163
7.11.1	Point Load	163
7.11.2	Line Load	165
7.11.3	Line Load Near a Buried Earth-Retaining Structure	166
7.11.4	Strip Load	166
7.11.5	Uniformly Loaded Circular Area	168
7.11.6	Uniformly Loaded Rectangular Area	170
7.11.7	Approximate Method for Rectangular Loads	172
7.11.8	Vertical Stress Below Arbitrarily Shaped Area	175
7.11.9	Embankment Loads	177
7.11.10	Infinite Loads	178
7.12	Summary	178
	Self-Assessment	178
	Practical Examples	178
	Exercises	181

CHAPTER 8 STRESS PATH 186

8.0	Introduction	186
8.1	Definitions of Key Terms	187
8.2	Questions to Guide Your Reading	187
8.3	Stress and Strain Invariants	187
8.3.1	Mean Stress	187
8.3.2	Deviatoric or Shear Stress	187

8.3.3 Volumetric Strain 188 8.3.4 Deviatoric or Distortional or Shear Strain 188 8.3.5 Axisymmetric Condition, $\sigma'_2 = \sigma'_3$ or $\sigma_2 = \sigma_3; \varepsilon_2 = \varepsilon_3$ 188 8.3.6 Plane Strain, $\varepsilon_2 = 0$ 188 8.3.7 Hooke's Law Using Stress and Strain Invariants 189 8.4 Stress Paths 191 8.4.1 Basic Concept 191 8.4.2 Plotting Stress Paths Using Stress Invariants 192 8.4.3 Plotting Stress Paths Using Two-Dimensional Stress Parameters 196 8.4.4 Procedure for Plotting Stress Paths 197 8.5 Summary 203 Self-Assessment 203 Practical Example 203 Exercises 205	9.4.4 Procedure to Calculate Primary Consolidation Settlement 218 9.4.5 Thick Soil Layers 219 9.5 One-Dimensional Consolidation Theory 225 9.5.1 Derivation of Governing Equation 225 9.5.2 Solution of Governing Consolidation Equation Using Fourier Series 227 9.5.3 Finite Difference Solution of the Governing Consolidation Equation 229 9.6 Secondary Compression Settlement 234 9.7 One-Dimensional Consolidation Laboratory Test 235 9.7.1 Oedometer Test 235 9.7.2 Determination of the Coefficient of Consolidation 236 9.7.2.1 Root Time Method (Square Root Time Method) 236 9.7.2.2 Log Time Method 237 9.7.3 Determination of Void Ratio at the End of a Loading Step 238 9.7.4 Determination of the Past Maximum Vertical Effective Stress 239 9.7.5 Determination of Compression and Recompression Indices 240 9.7.6 Determination of the Modulus of Volume Change 240 9.7.7 Determination of the Secondary Compression Index 241 9.8 Relationship Between Laboratory and Field Consolidation 243 9.9 Typical Values of Consolidation Settlement Parameters and Empirical Relationships 245 9.10 Preconsolidation of Soils Using Wick Drains 246 9.11 Summary 249 Self-Assessment 250 Practical Examples 250 Exercises 257
CHAPTER 9 ONE-DIMENSIONAL CONSOLIDATION SETTLEMENT OF FINE-GRAINED SOILS 207	
CHAPTER 10 SHEAR STRENGTH OF SOILS 261	
 9.0 Introduction 207 9.1 Definitions of Key Terms 208 9.2 Questions to Guide Your Reading 209 9.3 Basic Concepts 209 9.3.1 Instantaneous Load 210 9.3.2 Consolidation Under a Constant Load—Primary Consolidation 211 9.3.3 Secondary Compression 211 9.3.4 Drainage Path 212 9.3.5 Rate of Consolidation 212 9.3.6 Effective Stress Changes 212 9.3.7 Void Ratio and Settlement Changes Under a Constant Load 213 9.3.8 Effects of Vertical Stresses on Primary Consolidation 213 9.3.9 Primary Consolidation Parameters 216 9.3.10 Effects of Loading History 215 9.3.11 Overconsolidation Ratio 216 9.3.12 Possible and Impossible Consolidation Soil States 216 9.4 Calculation of Primary Consolidation Settlement 216 9.4.1 Effects of Unloading/Reloading of a Soil Sample Taken from the Field 216 9.4.2 Primary Consolidation Settlement of Normally Consolidated Fine-Grained Soils 217 9.4.3 Primary Consolidation Settlement of Overconsolidated Fine-Grained Soils 218	 10.0 Introduction 261 10.1 Definitions of Key Terms 262 10.2 Questions to Guide Your Reading 262 10.3 Typical Response of Soils to Shearing Forces 262 10.3.1 Effects of Increasing the Normal Effective Stress 265 10.3.2 Effects of Overconsolidation Ratio 266 10.3.3 Effects of Drainage of Excess Porewater Pressure 267 10.3.4 Effects of Cohesion 267

10.3.5 Effects of Soil Tension 268	11.3.3 Soil Yielding 328
10.3.6 Effects of Cementation 269	11.3.4 Prediction of the Behavior of Normally Consolidated and Lightly Overconsolidated Soils Under Drained Condition 329
10.4 Four Models for Interpreting the Shear Strength of Soils 269	11.3.5 Prediction of the Behavior of Normally Consolidated and Lightly Overconsolidated Soils Under Undrained Condition 332
10.4.1 Coulomb's Failure Criterion 270	11.3.6 Prediction of the Behavior of Heavily Overconsolidated Soils Under Drained and Undrained Condition 335
10.4.2 Taylor's Failure Criterion 274	11.3.7 Prediction of the Behavior of Coarse-Grained Soils Using CSM 337
10.4.3 Mohr-Coulomb Failure Criterion 275	11.3.8 Critical State Boundary 337
10.4.4 Tresca Failure Criterion 277	11.3.9 Volume Changes and Excess Porewater Pressures 338
10.5 Practical Implications of Failure Criteria 278	11.3.10 Effects of Effective and Total Stress Paths 338
10.6 Interpretation of the Shear Strength of Soils 280	11.4 Elements of the Critical State Model 339
10.7 Laboratory Tests to Determine Shear Strength Parameters 286	11.4.1 Yield Surface 339
10.7.1 A Simple Test to Determine Friction Angle of Clean, Coarse-Grained Soils 286	11.4.2 Critical State Parameters 340
10.7.2 Shear Box or Direct Shear Test 286	11.4.2.1 Failure Line in (p', q) Space 340
10.7.3 Conventional Triaxial Apparatus 291	11.4.2.2 Failure Line in (p', e) Space 342
10.7.4 Unconfined Compression (UC) Test 293	11.5 Failure Stresses from the Critical State Model 345
10.7.5 Consolidated Drained (CD) Compression Test 295	11.5.1 Drained Triaxial Test 345
10.7.6 Consolidated Undrained (CU) Compression Test 300	11.5.2 Undrained Triaxial Test 347
10.7.7 Unconsolidated Undrained (UU) Test 304	11.6 Modifications of CSM and Their Practical Implications 361
10.8 Porewater Pressure Under Axisymmetric Undrained Loading 305	11.7 Relationships from CSM that Are of Practical Significance 365
10.9 Other Laboratory Devices to Measure Shear Strength 307	11.7.1 Relationship Between Normalized Yield (peak) Shear Stress and Critical State Shear Stress Under Triaxial Drained Condition 365
10.9.1 Simple Shear Apparatuses 307	11.7.2 Relationship Among the Tension Cutoff, Mean Effective Stress, and Preconsolidation Stress 367
10.9.2 True Triaxial Apparatus 311	11.7.3 Relationship Among Undrained Shear Strength, Critical State Friction Angle, and Preconsolidation Ratio 369
10.9.3 Hollow-Cylinder Apparatus 312	11.7.4 Relationship Between the Normalized Undrained Shear Strength at the Critical State for Normally Consolidated and Overconsolidated Fine-Grained Soils 370
10.10 Field Tests 313	11.7.5 Relationship Between the Normalized Undrained Shear Strength of One-Dimensionally Consolidated or K_o -Consolidated and Isotropically Consolidated Fine-Grained Soils 371
10.10.1 Vane Shear Test (VST) 313	
10.10.2 The Standard Penetration Test (SPT) 313	
10.10.3 Cone Penetrometer Test (CPT) 314	
10.11 Specifying Laboratory Strength Tests 314	
10.12 Empirical Relationships for Shear Strength Parameters 314	
10.13 Summary 316	
Self-Assessment 316	
Practical Examples 316	
Exercises 320	
CHAPTER 11 A CRITICAL STATE MODEL TO INTERPRET SOIL BEHAVIOR 324	
11.0 Introduction 324	
11.1 Definitions of Key Terms 325	
11.2 Questions to Guide Your Reading 325	
11.3 Basic Concepts 326	
11.3.1 Parameter Mapping 326	
11.3.2 Failure Surface 328	

11.7.6	Relationship Between the Normalized Undrained Shear Strength at Initial Yield and at Critical State for Overconsolidated Fine-Grained Soils Under Triaxial Test Condition	374	12.8	Bearing Capacity of Layered Soils	445
11.7.7	Undrained Shear Strength Under Direct Simple Shear (plane strain) Condition	376	12.9	Building Codes Bearing Capacity Values	447
11.7.8	Relationship Between Direct Simple Shear Tests and Triaxial Tests	377	12.10	Settlement	448
11.7.9	Relationship for the Application of Drained and Undrained Conditions in the Analysis of Geosystems	378	12.11	Settlement Calculations	450
11.7.10	Relationship Among Excess Porewater Pressure, Preconsolidation Ratio, and Critical State Friction Angle	381	12.11.1	Immediate Settlement	450
11.7.11	Undrained Shear Strength of Clays at the Liquid and Plastic Limits	382	12.11.2	Primary Consolidation Settlement	454
11.7.12	Vertical Effective Stresses at the Liquid and Plastic Limits	382	12.12	Determination of Bearing Capacity and Settlement of Coarse-Grained Soils from Field Tests	457
11.7.13	Compressibility Indices (λ and C_c) and Plasticity Index	382	12.12.1	Standard Penetration Test (SPT)	457
11.7.14	Undrained Shear Strength, Liquidity Index, and Sensitivity	383	12.12.2	Cone Penetration Test (CPT)	460
11.7.15	Summary of Relationships Among Some Soil Parameters from CSM	383	12.12.3	Plate Load Test (PLT)	463
11.8	Soil Stiffness	389	12.13	Shallow Foundation Analysis Using CSM	464
11.9	Strains from the Critical State Model	393	11.13.1	Heavily Overconsolidated Fine-Grained Soil	465
11.9.1	Volumetric Strains	393	12.13.2	Dense, Coarse-Grained Soils	471
11.9.2	Shear Strains	395	12.14	Horizontal Elastic Displacement and Rotation	485
11.10	Calculated Stress–Strain Response	399	12.15	Summary	486
11.10.1	Drained Compression Tests	400		Self-Assessment	487
11.10.2	Undrained Compression Tests	400		Practical Examples	487
11.11	Application of CSM to Cemented Soils	407		Exercises	506
11.12	Summary	408			
	Self-Assessment	409			
	Practical Examples	409			
	Exercises	418			
CHAPTER 12 BEARING CAPACITY OF SOILS AND SETTLEMENT OF SHALLOW FOUNDATIONS 422					
12.0	Introduction	422			
12.1	Definitions of Key Terms	423			
12.2	Questions to Guide Your Reading	424			
12.3	Allowable Stress and Load and Resistance Factor Design	425			
12.4	Basic Concepts	426			
12.4.1	Soil Response to a Loaded Footing	426			
12.4.2	Conventional Failure Surface Under a Footing	428			
12.5	Collapse Load Using the Limit Equilibrium Method	429			
12.6	Bearing Capacity Equations	431			
12.7	Mat Foundations	443			
CHAPTER 13 PILE FOUNDATIONS 509					
13.0	Introduction	509			
13.1	Definitions of Key Terms	509			
13.2	Questions to Guide Your Reading	510			
13.3	Types of Piles and Installations	511			
13.3.1	Concrete Piles	512			
13.3.2	Steel Piles	512			
13.3.3	Timber Piles	512			
13.3.4	Plastic Piles	512			
13.3.5	Composites	512			
13.3.6	Pile Installation	514			
13.4	Basic Concept	515			
13.5	Load Capacity of Single Piles	521			
13.6	Pile Load Test (ASTM D 1143)	522			
13.7	Methods Using Statics for Driven Piles	531			
13.7.1	α -Method	531			
13.7.1.1	Skin Friction	531			
13.7.1.2	End Bearing	531			
13.7.2	β -Method	532			
13.7.2.1	Skin Friction	532			
13.7.2.2	End Bearing	534			
13.8	Pile Load Capacity of Driven Piles Based on SPT and CPT Results	539			
13.8.1	SPT	540			
13.8.2	CPT	540			
13.9	Load Capacity of Drilled Shafts	544			
13.10	Pile Groups	546			
13.11	Elastic Settlement of Piles	552			
13.12	Consolidation Settlement Under a Pile Group	554			

13.13	Procedure to Estimate Settlement of Single and Group Piles 555	15.7	Application of Lateral Earth Pressures to Retaining Walls 627	
13.14	Settlement of Drilled Shafts 559	15.8	Types of Retaining Walls and Modes of Failure 630	
13.15	Piles Subjected to Negative Skin Friction 560	15.9	Stability of Rigid Retaining Walls 633	
13.16	Pile-Driving Formulas and Wave Equation 562	15.9.1	Translation 633	
13.17	Laterally Loaded Piles 563	15.9.2	Rotation 634	
13.18	Micropiles 567	15.9.3	Bearing Capacity 634	
13.19	Summary 568 Self-Assessment 568 Practical Examples 568 Exercises 575	15.9.4	Deep-Seated Failure 634	
CHAPTER 14 TWO-DIMENSIONAL FLOW OF WATER THROUGH SOILS 579				
14.0	Introduction 579	15.9.5	Seepage 635	
14.1	Definitions of Key Terms 579	15.9.6	Procedures to Analyze Rigid Retaining Walls 635	
14.2	Questions to Guide Your Reading 580	15.10	Stability of Flexible Retaining Walls 643	
14.3	Two-Dimensional Flow of Water Through Porous Media 580	15.10.1	Analysis of Sheet Pile Walls in Uniform Soils 643	
14.4	Flownet Sketching 583	15.10.2	Analysis of Sheet Pile Walls in Mixed Soils 645	
14.4.1	Criteria for Sketching Flownets 583	15.10.3	Consideration of Tension Cracks in Fine-Grained Soils 645	
14.4.2	Flownet for Isotropic Soils 583	15.10.4	Methods of Analyses 646	
14.4.3	Flownet for Anisotropic Soil 585	15.10.5	Analysis of Cantilever Sheet Pile Walls 648	
14.5	Interpretation of Flownet 586	15.10.6	Analysis of Anchored Sheet Pile Walls 648	
14.5.1	Flow Rate 586	15.11	Braced Excavation 659	
14.5.2	Hydraulic Gradient 586	15.12	Mechanical Stabilized Earth Walls 666	
14.5.3	Static Liquefaction, Heaving, Boiling, and Piping 586	15.12.1	Basic Concepts 667	
14.5.4	Critical Hydraulic Gradient 587	15.12.2	Stability of Mechanical Stabilized Earth Walls 667	
14.5.5	Porewater Pressure Distribution 587	15.13	Other Types of Retaining Walls 675	
14.5.6	Uplift Forces 587	15.13.1	Modular Gravity Walls 675	
14.6	Finite Difference Solution for Two-Dimensional Flow 592	15.13.2	In Situ Reinforced Walls 676	
14.7	Flow Through Earth Dams 598	15.13.3	Chemically Stabilized Earth Walls (CSE) 676	
14.8	Soil Filtration 602	15.14	Summary 676 Self-Assessment 676 Practical Examples 676 Exercises 682	
14.9	Summary 603 Self-Assessment 603 Practical Examples 603 Exercises 606	CHAPTER 15 STABILITY OF EARTH-RETAINING STRUCTURES 610		
15.0	Introduction 610	CHAPTER 16 SLOPE STABILITY 687		
15.1	Definitions of Key Terms 611	16.0	Introduction 687	
15.2	Questions to Guide Your Reading 611	16.1	Definitions of Key Terms 687	
15.3	Basic Concepts of Lateral Earth Pressures 612	16.2	Questions to Guide Your Reading 688	
15.4	Coulomb's Earth Pressure Theory 620	16.3	Some Types of Slope Failure 688	
15.5	Rankine's Lateral Earth Pressure for a Sloping Backfill and a Sloping Wall Face 623	16.4	Some Causes of Slope Failure 689	
15.6	Lateral Earth Pressures for a Total Stress Analysis 625	16.4.1	Erosion 689	

16.5	Infinite Slopes	692
16.6	Two-Dimensional Slope Stability Analyses	697
16.7	Rotational Slope Failures	697
16.8	Method of Slices	699
16.8.1	Bishop's Method	699
16.8.2	Janbu's Method	702
16.8.3	Cemented Soils	703
16.9	Application of the Method of Slices	704
16.10	Procedure for the Method of Slices	705
16.11	Stability of Slopes with Simple Geometry	713
16.11.1	Taylor's Method	713
16.11.2	Bishop–Morgenstern Method	714
16.12	Factor of Safety (FS)	715
16.13	Summary	716
	Self-Assessment	716
	Practical Example	716
	Exercises	719

APPENDIX A A COLLECTION OF FREQUENTLY USED SOIL PARAMETERS AND CORRELATIONS **723**

APPENDIX B DISTRIBUTION OF VERTICAL STRESS AND ELASTIC DISPLACEMENT UNDER A UNIFORM CIRCULAR LOAD **730**

APPENDIX C DISTRIBUTION OF SURFACE STRESSES WITHIN FINITE SOIL LAYERS **731**

APPENDIX D LATERAL EARTH PRESSURE COEFFICIENTS (KERISEL AND ABSI, 1990) **734**

REFERENCES **738**

INDEX **742**

INTRODUCTION TO SOIL MECHANICS AND FOUNDATIONS

1.0 INTRODUCTION

Soils are natural resources. They are necessary for our existence. They provide food, shelter, construction materials, and gems. They protect the environment and provide support for our buildings. In this textbook, we will deal with soils as construction materials and as support for structures on and within them.

Soils are the oldest and most complex engineering materials. Our ancestors used soils as a construction material for flood protection and shelters. Western civilization credits the Romans for recognizing the importance of soils in the stability of structures. Roman engineers, especially Vitruvius, who served during the reign of Emperor Augustus in the first century B.C., paid great attention to soil types (sand, gravel, etc.) and to the design and construction of solid foundations. There was no theoretical basis for design; experience from trial and error was relied upon.

Coulomb (1773) is credited as the first person to use mechanics to solve soil problems. He was a member of the French Royal Engineers, who were interested in protecting old fortresses that fell easily from cannon fire. To protect the fortresses from artillery attack, sloping masses of soil were placed in front of them (Figure 1.1). The enemy had to tunnel below the soil mass and the fortress to attack. Of course, the enemy then became an easy target. The mass of soil applies a lateral force to the fortress that could cause it to topple over or could cause it to slide away from the soil mass. Coulomb attempted to determine the lateral force so that he could evaluate the stability of the fortress. He postulated that a wedge of soil ABC (Figure 1.1) would fail along a slip plane BC, and this wedge would push the wall out or topple it over as it moved down the slip plane.

Movement of the wedge along the slip plane would occur only if the soil resistance along the wedge were overcome. Coulomb assumed that the soil resistance was provided by friction between the particles, and the problem became one of a wedge sliding on a rough (frictional) plane, which you may have analyzed in your physics or mechanics course. Coulomb tacitly defined a failure criterion for soils. Today, Coulomb's failure criterion and method of analysis still prevail.

From the early twentieth century, the rapid growth of cities, industry, and commerce required myriad building systems—for example, skyscrapers, large public buildings, dams for electric power generation, reservoirs for water supply and irrigation, tunnels, roads and railroads, port and harbor facilities, bridges, airports and runways, mining activities, hospitals, sanitation systems, drainage systems, and towers for communication systems. These building systems require stable and economic foundations, and new questions about soils were asked. For example, what is the state of stress in a soil mass, how can one design safe and economic foundations, how much would a building settle, and what is the stability of structures founded on or within soil? We continue to ask these questions and to try to find answers as

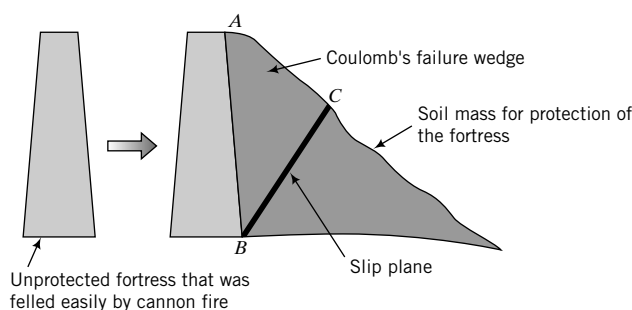


FIGURE 1.1
Unprotected and protected fortress.

new issues have confronted us. Some of these new issues include removing toxic compounds from soil and water, designing foundations and earth structures to mitigate damage from earthquakes and other natural hazards, and designing systems to protect the environment and be sustainable.

To answer these questions we needed the help of some rational method, and, consequently, soil mechanics was born. Karl Terzaghi (1883–1963) is the undisputed father of soil mechanics. The publication of his book *Erdbaumechanik* in 1925 laid the foundation for soil mechanics and brought recognition to the importance of soils in engineering activities. Soil mechanics, also called geotechnique or geotechnics or geomechanics, is the application of engineering mechanics to the solution of problems dealing with soils as a foundation and as a construction material. Engineering mechanics is used to understand and interpret the properties, behavior, and performance of soils.

Soil mechanics is a subset of geotechnical engineering, which involves the application of soil mechanics, geology, and hydraulics to the analysis and design of geotechnical systems such as dams, embankments, tunnels, canals and waterways, foundations for bridges, roads, buildings, and solid waste disposal systems. Every application of soil mechanics involves uncertainty because of the variability of soils—their stratification, composition, and engineering properties. Thus, engineering mechanics can provide only partial solutions to soil problems. Experience and approximate calculations are essential for the successful application of soil mechanics to practical problems. Many of the calculations in this textbook are approximations.

Stability and economy are two tenets of engineering design. In geotechnical engineering, the uncertainties of the performance of soils, the uncertainties of the applied loads, and the vagaries of natural forces nudge us to compromise between sophisticated and simple analyses or to use approximate methods. Stability should never be compromised for economy. An unstable structure compromised to save a few dollars can result in death and destruction.

1.1 MARVELS OF CIVIL ENGINEERING—THE HIDDEN TRUTH

The work that geotechnical engineers do is often invisible once construction is completed. For example, four marvelous structures—the Willis Tower (formerly called the Sears Tower, Figure 1.2), the Empire State Building (Figure 1.3), the Taj Mahal (Figure 1.4), and the Hoover Dam (Figure 1.5)—grace us with their engineering and architectural beauty. However, if the foundations, which are invisible, on which these structures stand were not satisfactorily designed, then these structures would not exist. A satisfactory foundation design requires the proper application of soil mechanics principles, accumulated experience, and good judgment.



FIGURE 1.2

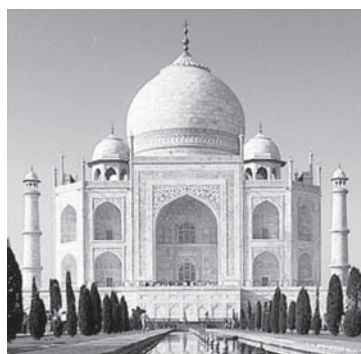
Willis Tower (formerly the Sears Tower). (© Bill Bachmann/Photo Researchers.)

FIGURE 1.3

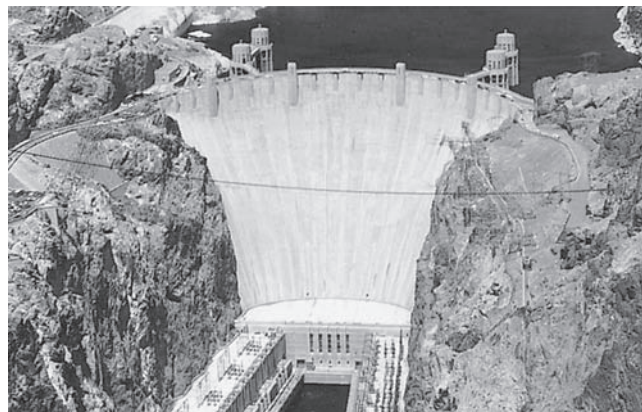
Empire State Building. (© Rafael Macia/Photo Researchers.)

**FIGURE 1.4**

Taj Mahal. (© Will & Deni McIntyre/Photo Researchers.)

**FIGURE 1.5**

Hoover Dam. (Courtesy Bureau of Reclamation, U.S. Department of the Interior. Photo by E. E. Hertzog.)



The stability and life of any structure—a building, an airport, a road, dams, levees, natural slopes, power plants—depend on the stability, strength, and deformation of soils. If the soil fails, structures founded on or within it will fail or be impaired, regardless of how well these structures are designed. Thus, successful civil engineering projects are heavily dependent on geotechnical engineering.

1.2 GEOTECHNICAL LESSONS FROM FAILURES

All structures that are founded on earth rely on our ability to design safe and economic foundations. Because of the natural vagaries of soils, failures do occur. Some failures have been catastrophic and have caused severe damage to lives and property; others have been insidious. Failures occur because of inadequate site and soil

investigations; unforeseen soil and water conditions; natural hazards; poor engineering analysis, design, construction, and quality control; damaging postconstruction activities; and usage outside the design conditions. When failures are investigated thoroughly, we obtain lessons and information that will guide us to prevent similar types of failure in the future. Some types of failure caused by natural hazards (earthquakes, hurricanes, etc.) are difficult to prevent, and our efforts must be directed toward solutions that mitigate damages to lives and properties.

One of the earliest failures that was investigated and contributed to our knowledge of soil behavior is the failure of the Transcona Grain Elevator in 1913 (Figure 1.6). Within 24 hours after loading the grain elevator at a rate of about 1 m of grain height per day, the bin house began to tilt and settle. Fortunately, the structural damage was minimal and the bin house was later restored. No borings were done to identify the soils and to obtain information on their strength. Rather, an open pit about 4 m deep was made for the foundations and a plate was loaded to determine the bearing strength of the soil.

The information gathered from the Transcona Grain Elevator failure and the subsequent detailed soil investigation was used (Peck and Bryant, 1953; Skempton, 1951) to verify the theoretical soil bearing strength. Peck and Bryant found that the applied pressure from loads imposed by the bin house and the grains was nearly equal to the calculated maximum pressure that the soil could withstand, thereby lending support to the theory for calculating the bearing strength of soft clay soils. We also learn from this failure the importance of soil investigations, soils tests, and the effects of rate of loading.

The Transcona Grain Elevator was designed at a time when soil mechanics was not yet born. One eyewitness (White, 1953) wrote: "Soil Mechanics as a special science had hardly begun at that time. If as much had been known then as is now about the shear strength and behavior of soils, adequate borings would have been taken and tests made and these troubles would have been avoided. We owe more to the development of this science than is generally recognized."

We have come a long way in understanding soil behavior since the founding of soil mechanics by Terzaghi in 1925. We continue to learn more daily through research on and experience from failures, and your contribution to understanding soil behavior is needed. Join me on a journey of learning the fundamentals of soil mechanics and its applications to practical problems so that we can avoid failures or, at least, reduce the probability of their occurrence.



FIGURE 1.6 Failure of the Transcona Grain Elevator. (Photo courtesy of Parrish and Heimbecker Limited.)

GEOLOGICAL CHARACTERISTICS AND PARTICLE SIZES OF SOILS

2.0 INTRODUCTION

The purpose of this chapter is to introduce you to basic geology and particle sizes of soils.

When you complete this chapter, you should be able to:

- Appreciate the importance of geology in geotechnical engineering.
- Understand the formation of soils.
- Determine particle size distribution of a soil mass.
- Interpret grading curves.

Importance

Geology is important for successful geotechnical engineering practice. One of the primary tasks of a geotechnical engineer is to understand the character of the soil at a site. Soils, derived from the weathering of rocks, are very complex materials and vary widely. There is no certainty that a soil in one location will have the same properties as the soil just a few centimeters away. Unrealized geological formations and groundwater conditions have been responsible for failures of many geotechnical systems and increased construction costs. As a typical practical scenario, let us consider the design and construction of a bridge as part of a highway project. You are required to design the bridge foundation and abutment. To initiate a design of the foundation and the abutment, you have to know the geology of the site including the soil types, their spatial variations, groundwater conditions, and potential for damage from natural hazards such as earthquakes. You, perhaps working with geologists, will have to plan and conduct a site investigation and interpret the data. In the next chapter, you will learn about site investigation. In this chapter, you will learn basic geology of importance to geotechnical engineers, descriptions of soils, and particle size distributions.

2.1 DEFINITIONS OF KEY TERMS

Dip is the downward separation of a bedding plane.

Faults are ground fractures.

Minerals are chemical elements that constitute rocks.

Rocks are the aggregation of minerals into a hard mass.

Soils are materials that are derived from the weathering of rocks.

Strike is the horizontal surface separation of a layer or bedding plane.

Effective particle size (D_{10}) is the average particle diameter of the soil at 10 percentile; that is, 10% of the particles are smaller than this size (diameter).

Average particle diameter (D_{50}) is the average particle diameter of the soil.

2.2 QUESTIONS TO GUIDE YOUR READING

1. Why is geology important in geotechnical engineering?
2. What is engineering soil?
3. What is the composition of soils?
4. What are the main minerals in soils?
5. How is soil described?
6. What are the differences between coarse-grained and fine-grained soils?
7. What is a grading curve?
8. How do you determine the particle size distribution in soils?
9. How do you interpret a grading curve?

2.3 BASIC GEOLOGY

2.3.1 Earth's Profile

Our planet Earth has an average radius of 6373 km and a mean mass density of 5.527 g/cm^3 compared with a mean mass density of soil particles of 2.7 g/cm^3 and water of 1 g/cm^3 . Studies from elastic waves generated by earthquakes have shown that the earth has a core of heavy metals, mostly iron, of mass density 8 g/cm^3 surrounded by a mantle. The mantle consists of two parts, upper mantle and lower mantle. The upper mantle is solid rock while the lower mantle is molten rock. Above the upper mantle is the crust, which may be as much as 50 km thick in the continental areas (Figure 2.1) and as little as 7 km thick in oceanic areas.

2.3.2 Plate Tectonics

The crust and part of the upper mantle, about 100 km thick, make up the lithosphere. Below the lithosphere is the asthenosphere, which is about 150 km thick. The lithosphere is fragmented into about 20 large plates—large blocks of rocks—that slide against and move toward, away from, and under each other above hot molten materials in the asthenosphere. The theory governing the movements of the plates is called plate tectonics. Plate tectonics is based on *uniformitarianism*, which states that the earth's forces and processes are continuous rather than catastrophic and the present is similar to the past.

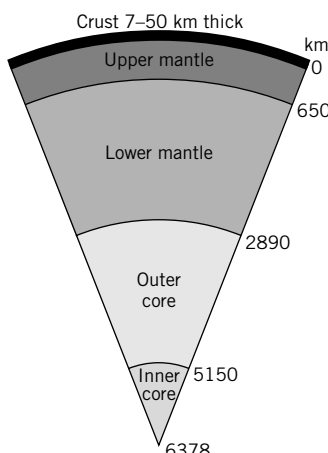


FIGURE 2.1
A sector of the earth.

The plates move slowly relative to each other but occasionally jerk, sending the energy contained in the straining rock in all directions. The energy is transmitted as shock waves. When these waves reach the surface, the ground shaking that occurs is referred to as an earthquake. The adjustment of the plates after an earthquake causes another set of shock waves that are referred to as aftershocks. The point at which the earthquake originates is called the focus and the point directly above it on the earth's surface is called the epicenter.

As the shock waves move to the earth's surface from the focus, they separate into body waves and surface waves. These waves travel at different velocities. Body waves comprise compression, or primary, P waves, and distortional, or shear, S waves. P waves are the first to arrive at the surface, followed by the S waves. Surface waves comprise Love (LQ) waves and Raleigh (LR) waves. These surface waves have large amplitudes and long periods.

The amount of seismic energy released is defined by the magnitude (M) of the earthquake. On the Richter scale, M is a logarithmic scale that ranges from 0 to 9. An earthquake of M = 2 is barely felt, while an earthquake of M = 7 could cause extensive damage.

At the edges of the plates, three phenomena are of particular importance:

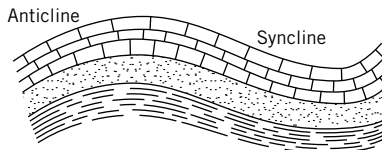
1. A fault zone that occurs when the plates slide past each other.
2. A subduction zone that occurs when the plates move toward each other, causing one plate to move beneath the other.
3. A spreading zone that occurs when the plates move away from each other.

2.3.3 Composition of the Earth's Crust

The materials that comprise the earth's crust are sediments and rock. Sediments are solid fragments of inorganic or organic material resulting from the weathering of rocks and are transported and deposited by wind, water, or ice. Rocks are classified into three groups—igneous, sedimentary, and metamorphic—based on the earth's process that forms them.

Igneous rocks are formed from magma (molten rock materials) emitted from volcanoes that has cooled and solidified. Sedimentary rocks are formed from sediments and animal and plant materials that are deposited in water or on land on the earth's surface and then subjected to pressures and heat. The heat and pressures that are involved in forming sedimentary rocks are low in comparison to those for igneous rocks. Metamorphic rocks are formed deep within the earth's crust from the transformation of igneous, sedimentary, and even existing metamorphic rocks into denser rocks. Their appearance and texture are variable. For engineering purposes, foliation (layering caused by parallel alignment of minerals), weak minerals, and cleavage planes are particularly important because they are planes of weakness. No melting takes place, so the original chemical composition of the original rock remains unchanged. The rock texture generally becomes coarser-grained.

Sedimentary rocks are of particular importance to geotechnical engineers because they cover about 75% of the earth's surface area with an average thickness of 0.8 km. The sediments that comprise sedimentary rocks may be bonded (cemented) together by minerals, chemicals, and electrical attraction or may be loose. Clastic sedimentary rocks are small pieces of rocks cemented together by minerals such as carbonates (calcite, CaCO_3) or sulfates (gypsum, $\text{CaSO}_4 [+2\text{H}_2\text{O}]$). Examples of clastic sedimentary rocks are sandstones formed from sand cemented by minerals and found on beaches and sand dunes; shales formed from clay and mud and found in lakes and swamps; and conglomerates formed from sand and gravels at the bottom of streams. Chemical sedimentary rocks are minerals such as halite (rock salt), calcite, and gypsum that have been formed from elements dissolved in water (e.g., the material found in Death Valley, California). Organic sedimentary rocks are formed from organic materials such as plants, bones, and shells. Coal is an organic sedimentary rock formed deep in the earth from the compaction of plants.

**FIGURE 2.2** Simple folding.

2.3.4 Discontinuities

Rock masses are seldom homogeneous and continuous. Rather, they consist of discontinuities that control the strength and displacements of the rock masses and the stability of any structure founded on them. Discontinuities in sedimentary rocks are called bedding planes. These bedding planes are planes that separate different bodies of sedimentary deposits. In metamorphic rocks they are called foliation planes. In igneous rocks they are called joints. However, the term *joint* is used generically to describe most discontinuities in rock masses. The terms *strike* and *dip* are used to describe the geometry of a bedding plane. Strike is the horizontal surface separation of a layer or bedding plane. Dip is the downward separation of a bedding plane.

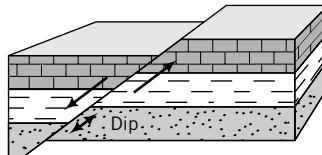
Rock masses may be distorted by folding. There are a variety of folds (Figure 2.2) are anticlines—rock mass folded upward (convex)—and synclines—rock mass folded downward (concave). Folding results in unequal distribution of stresses within the rock mass and can cause major problems in civil engineering construction through uneven release of stresses.

The movements of the plates cause ground fractures called faults. The three predominant faults are normal, thrust, and strike/slip. Tension causes normal fault (Figure 2.3a). An example of a normal fault is the Teton Mountains in Wyoming. Compression causes thrust or reverse fault (Figure 2.3b). Shear causes strike/slip fault (Figure 2.3c). An example of a strike/slip fault is the San Andreas Fault in California. Faults are rarely simple. They normally consist of different types of faulting.

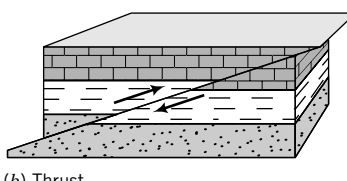
2.3.5 Geologic Cycle and Geological Time

The formation of rocks and sediments is a continuous process known as the geologic cycle. Sediments are transformed by heat and pressure into rocks and then the rocks are eroded into sediments. The cycle has neither a starting point nor an ending point. There are three main geological principles, given by Nicolaus Steno (1638–1687), that govern the geologic cycle:

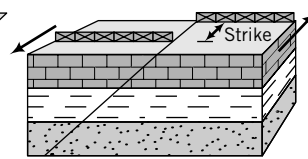
1. *Principle of original horizontality*, which states that sediments are deposited in layers parallel to the earth's surface.
2. *Principle of original continuity*, which states that depositions are sheetlike and are only terminated in contact with existing solid surfaces. Deformities occur from subsequent forces in the earth.



(a) Normal



(b) Thrust



(c) Strike-slip

FIGURE 2.3

Three types of faults: (a) normal, (b) thrust, and (c) strike/slip.



FIGURE 2.4 Layered sediments as seen in the Grand Canyon. The youngest layer is the topmost layer. The deformation of the layers depends on, among other factors, the material properties, confinement pressures, strain rate, and temperatures.

(Age Fotostock America, Inc.)

3. *Principle of superposition*, which states that the age of a deposition is directly related to the order of deposition. Older layers are generally below younger layers.

Evidence of these principles is clearly seen in the Grand Canyon (Figure 2.4).

Geological time is the dating of past events. The ages of the earth's materials are measured by radioactive methods. Potassium-argon dating (potassium is found in igneous rocks and is transformed into argon by radioactivity) and rubidium-strontium dating (rubidium is found in metamorphic rocks and is transformed into strontium by radioactivity) are the popular and the most useful radioactive dating methods. The time periods (million years) in Figure 2.5 have been assigned based on past bioactivity, but mainly on carbon 14 (C_{14}) dating. Geological dating provides estimates of the frequency of occurrence of volcanic eruptions, earthquakes, landslides, floods, erosion, and temperature variations.

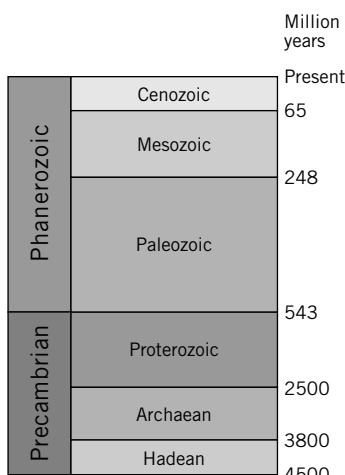


FIGURE 2.5
Geological time.

THE ESSENTIAL POINTS ARE:

1. Knowledge of geology is important for the successful practice of geotechnical engineering.
2. The earth's surface (lithosphere) is fractured into about 20 mobile plates. Interaction of these plates causes volcanic activity and earthquakes.
3. The three groups of rocks are igneous, sedimentary, and metamorphic. Igneous rocks are formed from magma (molten rock materials) emitted from volcanoes that has cooled and solidified. Sedimentary rocks are formed from sediments and animal and plant materials that are deposited in water or on land on the earth's surface and then subjected to pressures and heat. Metamorphic rocks are formed deep within the earth's crust from the transformation of igneous and sedimentary rocks into denser rocks. They are foliated and have weak minerals and cleavage planes.
4. Sedimentary rocks are of particular importance to geotechnical engineers because they cover about 75% of the earth's surface area.
5. Rock masses are inhomogeneous and discontinuous.

What's next . . . Now that you have a basic knowledge of geology, we will begin our study of engineering soils.

2.4 COMPOSITION OF SOILS

2.4.1 Soil Formation

Soils are formed from the physical and chemical weathering of rocks. Physical weathering involves reduction of size without any change in the original composition of the parent rock. The main agents responsible for this process are exfoliation, unloading, erosion, freezing, and thawing. Chemical weathering causes both reductions in size and chemical alteration of the original parent rock. The main agents responsible for chemical weathering are hydration, carbonation, and oxidation. Often, chemical and physical weathering take place in concert.

Soils that remain at the site of weathering are called residual soils. These soils retain many of the elements that comprise the parent rock. Alluvial soils, also called fluvial soils, are soils that were transported by rivers and streams. The composition of these soils depends on the environment under which they were transported and is often different from the parent rock. The profile of alluvial soils usually consists of layers of different soils. Much of our construction activity has been and is occurring in and on alluvial soils. Glacial soils are soils that were transported and deposited by glaciers. Marine soils are soils deposited in a marine environment.

2.4.2 Soil Types

Common descriptive terms such as gravels, sands, silts, and clays are used to identify specific textures in soils. We will refer to these soil textures as soil types; that is, sand is one soil type, clay is another. Texture refers to the appearance or feel of a soil. Sands and gravels are grouped together as coarse-grained soils. Clays and silts are fine-grained soils. Coarse-grained soils feel gritty and hard. Fine-grained soils feel smooth. The coarseness of soils is determined from knowing the distribution of particle sizes, which is the primary means of classifying coarse-grained soils. To characterize fine-grained soils, we need further information on the types of minerals present and their contents. The response of fine-grained soils to loads, known as the mechanical behavior, depends on the type of predominant minerals present.

Currently, many soil descriptions and soil types are in usage. A few of these are listed below.

- *Alluvial soils* are fine sediments that have been eroded from rock and transported by water, and have settled on river and stream beds.

- *Calcareous soil* contains calcium carbonate and effervesces when treated with hydrochloric acid.
- *Caliche* consists of gravel, sand, and clay cemented together by calcium carbonate.
- *Colluvial soils* (colluvium) are soils found at the base of mountains that have been eroded by the combination of water and gravity.
- *Eolian soils* are sand-sized particles deposited by wind.
- *Expansive soils* are clays that undergo large volume changes from cycles of wetting and drying.
- *Glacial soils* are mixed soils consisting of rock debris, sand, silt, clays, and boulders.
- *Glacial till* is a soil that consists mainly of coarse particles.
- *Glacial clays* are soils that were deposited in ancient lakes and subsequently frozen. The thawing of these lakes revealed soil profiles of neatly stratified silt and clay, sometimes called varved clay. The silt layer is light in color and was deposited during summer periods, while the thinner, dark clay layer was deposited during winter periods.
- *Gypsum* is calcium sulfate formed under heat and pressure from sediments in ocean brine.
- *Lacustrine soils* are mostly silts and clays deposited in glacial lake waters.
- *Lateritic soils* are residual soils that are cemented with iron oxides and are found in tropical regions.
- *Loam* is a mixture of sand, silt, and clay that may contain organic material.
- *Loess* is a wind-blown, uniform, fine-grained soil.
- *Marine soils* are sand, silts, and clays deposited in salt or brackish water.
- *Marl* (marlstone) is a mud (see definition of mud below) cemented by calcium carbonate or lime.
- *Mud* is clay and silt mixed with water into a viscous fluid.

2.4.3 Clay Minerals

Minerals are crystalline materials and make up the solids constituent of a soil. The mineral particles of fine-grained soils are platy. Minerals are classified according to chemical composition and structure. Most minerals of interest to geotechnical engineers are composed of oxygen and silicon—two of the most abundant elements on earth. Silicates are a group of minerals with a structural unit called the silica tetrahedron. A central silica cation (positively charged ion) is surrounded by four oxygen anions (negatively charged ions), one at each corner of the tetrahedron (Figure 2.6a). The charge on a single tetrahedron is -4 , and to achieve a neutral charge cations must be added or single tetrahedrons must be linked to each other sharing oxygen ions. Silicate minerals are formed by the addition of cations and interactions of tetrahedrons. Silica tetrahedrons combine to form sheets, called silicate sheets or laminae, which are thin layers of silica tetrahedrons in which three oxygen ions are shared between adjacent tetrahedrons (Figure 2.6b). Silicate sheets may contain other structural units such as alumina sheets. Alumina sheets are formed by combination of alumina minerals, which consists of an aluminum ion surrounded by six oxygen or hydroxyl atoms in an octahedron (Figure 2.6c, d).

The main groups of crystalline materials that make up clays are the minerals kaolinite, illite, and montmorillonite. Kaolinite has a structure that consists of one silica sheet and one alumina sheet bonded together into a layer about 0.72 nm thick and stacked repeatedly (Figure 2.7a). The layers are held together by hydrogen bonds. Tightly stacked layers result from numerous hydrogen bonds. Kaolinite is common in clays in humid tropical regions. Illite consists of repeated layers of one alumina sheet sandwiched by two silicate sheets (Figure 2.7b). The layers, each of thickness 0.96 nm , are held together by potassium ions.

Montmorillonite has a structure similar to illite, but the layers are held together by weak van der Waals forces. Montmorillonite belongs to the smectite clay family. It is an aluminum smectite with a

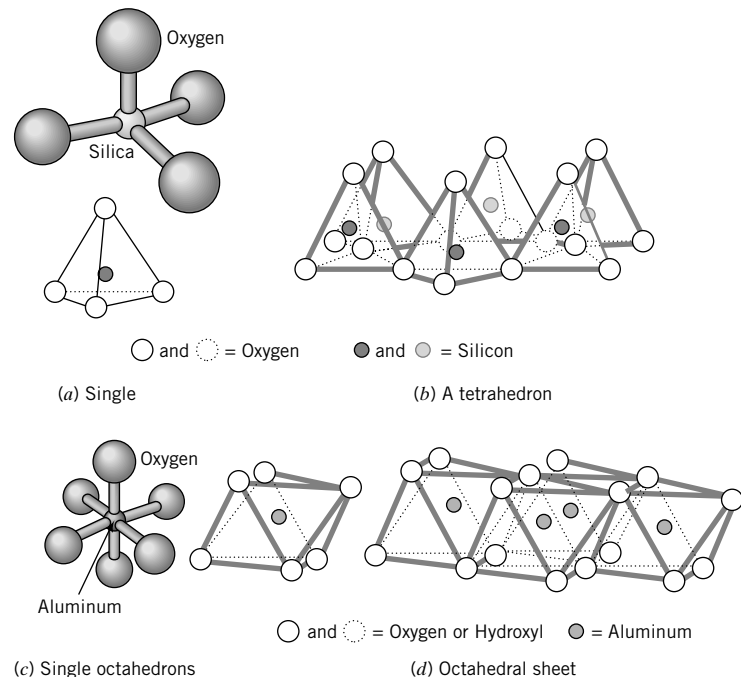


FIGURE 2.6
 (a) Silica tetrahedrons, (b) silica sheets, (c) single aluminum octahedrons, and (d) aluminum sheets.

small amount of Al^{+3} replaced by Mg^{2+} . This causes a charge inequity that is balanced by exchangeable cations Na^+ or Ca^{2+} and oriented water (Figure 2.7c). Additional water can easily enter the bond and separate the layers in montmorillonite, causing swelling. If the predominant exchangeable cation is Ca^{2+} (calcium smectite), there are two water layers, while if it is Na^+ (sodium smectite), there is usually only one water layer. Sodium smectite can absorb enough water to cause the particles to separate. Calcium smectites do not usually absorb enough water to cause particle separation because of their divalent cations. Montmorillonite is often called a swelling or expansive clay.

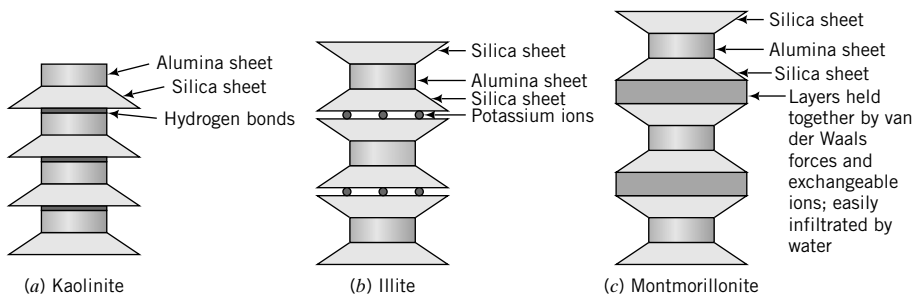


FIGURE 2.7 Structure of kaolinite, illite, and montmorillonite.

2.4.4 Surface Forces and Adsorbed Water

If we subdivide a body, the ratio of its surface area to its volume increases. For example, a cube with sides of 1 cm has a surface area of 6 cm^2 . If we subdivide this cube into smaller cubes with sides of 1 mm, the original volume is unchanged but the surface area increases to 60 cm^2 . The surface area per unit mass (specific surface) of sands is typically 0.01 m^2 per gram, while for clays it is as high as 1000 m^2 per gram (montmorillonite). The specific surface of kaolinite ranges from 10 to 20 m^2 per gram, while that of illite

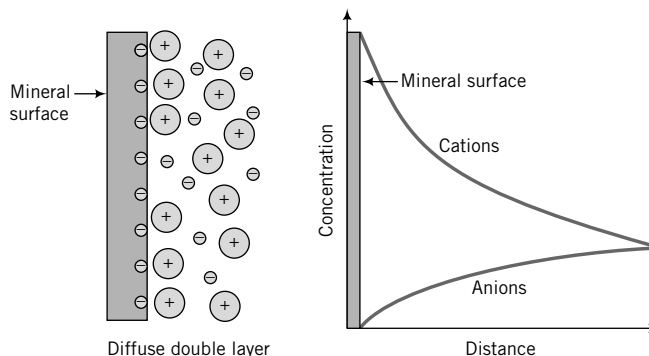


FIGURE 2.8 Diffuse double layer.

ranges from 65 to 100 m² per gram. The surface area of 45 grams of illite is equivalent to the area of a football field. Because of the large surface areas of fine-grained soils, surface forces significantly influence their behavior compared to coarse-grained soils. The clay–water interaction coupled with the large surface areas results in clays having larger water-holding capacity in a large number of smaller pore spaces compared with coarse-grained soils.

The surface charges on fine-grained soils are negative (anions). These negative surface charges attract cations and the positively charged side of water molecules from surrounding water. Consequently, a thin film or layer of water, called adsorbed water, is bonded to the mineral surfaces. The thin film or layer of water is known as the diffuse double layer (Figure 2.8). The largest concentration of cations occurs at the mineral surface and decreases exponentially with distance away from the surface (Figure 2.8).

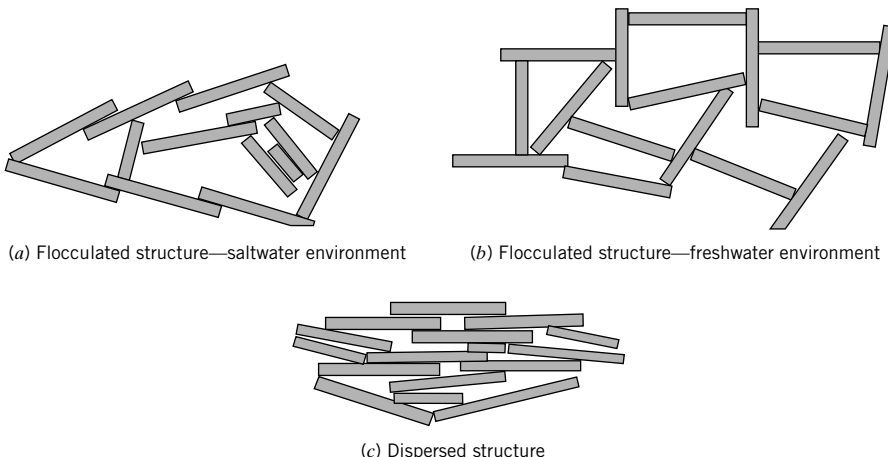
Surface forces on clay particles are of two types. One type, called attracting forces, is due to London–van der Waals forces. These forces are far-reaching and decrease in inverse proportion to l^2 (l is the distance between two particles). The other type, called repelling forces, is due to the diffuse double layer. Around each particle is an ionic cloud. When two particles are far apart, the electric charge on each is neutralized by equal and opposite charge of the ionic cloud around it. When the particles move closer together such that the clouds mutually penetrate each other, the negative charges on the particles cause repulsion.

Drying of most soils, with the exception of gypsum, using an oven for which the standard temperature is $105 \pm 5^\circ\text{C}$, cannot remove the adsorbed water. The adsorbed water influences the way a soil behaves. For example, plasticity in soils, which we will deal with in Chapter 4, is attributed to the adsorbed water. Toxic chemicals that seep into the ground contaminate soil and groundwater. Knowledge of the surface chemistry of fine-grained soils is important in understanding the migration, sequestration, rerelease, and ultimate removal of toxic compounds from soils.

Our main concern in this book is with the physical and mechanical properties of soils. Accordingly, we will not deal with the surface chemistry of fine-grained soils. You may refer to Mitchell (1993) for further information on the surface chemistry of fine-grained soils that are of importance to geotechnical and geoenvironmental engineers.

2.4.5 Soil Fabric

Soil particles are assumed to be rigid. During deposition, the mineral particles are arranged into structural frameworks that we call soil fabric (Figure 2.9). Each particle is in random contact with neighboring particles. The environment under which deposition occurs influences the structural framework that is formed. In particular, the electrochemical environment has the greatest influence on the kind of soil fabric that is formed during deposition of fine-grained soils.

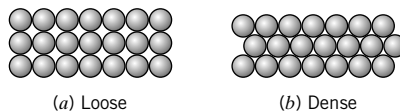
**FIGURE 2.9** Soil fabric.

Two common types of soil fabric—flocculated and dispersed—are formed during soil deposition of fine-grained soils, as shown schematically in Figure 2.9. A flocculated structure, formed in a saltwater environment, results when many particles tend to orient parallel to one another. A flocculated structure, formed in a freshwater environment, results when many particles tend to orient perpendicular to one another. A dispersed structure occurs when a majority of the particles orient parallel to one another.

Any loading (tectonic or otherwise) during or after deposition permanently alters the soil fabric or structural arrangement in a way that is unique to that particular loading condition. Consequently, the history of loading and changes in the environment is imprinted in the soil fabric. The soil fabric is the brain; it retains the memory of the birth of the soil and subsequent changes that occur.

The spaces between the mineral particles are called voids, which may be filled with liquids (essentially water), gases (essentially air), and cementitious materials (e.g., calcium carbonate). Voids occupy a large proportion of the soil volume. Interconnected voids form the passageway through which water flows in and out of soils. If we change the volume of voids, we will cause the soil to either compress (settle) or expand (dilate). Loads applied by a building, for example, will cause the mineral particles to be forced closer together, reducing the volume of voids and changing the orientation of the structural framework. Consequently, the building settles. The amount of settlement depends on how much we compress the volume of voids. The rate at which the settlement occurs depends on the interconnectivity of the voids. Free water, not the adsorbed water, and/or air trapped in the voids must be forced out for settlement to occur. The decrease in volume, which results in settlement of buildings and other structures, is usually very slow (almost ceaseless) in fine-grained soils because these soils have large surface areas compared with coarse-grained soils. The larger surface areas provide greater resistance to the flow of water through the voids.

If the rigid (mostly quartz) particles of coarse-grained soils can be approximated by spheres, then the loosest packing (maximum voids space) would occur when the spheres are stacked one on top of another (Figure 2.10a). The densest packing would occur when the spheres are packed in a staggered pattern, as shown in Figure 2.10b. Real coarse-grained soils consist of an assortment of particle sizes and shapes, and consequently the packing is random. From your physics course, mass is volume multiplied by density. The density of soil particles is approximately 2.7 grams/cm³. For spherical soil particles of diameter D (cm), the mass is $2.7 \times \frac{\pi D^3}{6}$. So the number of particles per gram of soil is $\frac{0.7}{D^3}$. Thus, 1 gram of a fine sand of diameter 0.015 cm would consist of about 207,400 particles.

**FIGURE 2.10**

Loose and dense packing of spheres.

THE ESSENTIAL POINTS ARE:

- 1. Soils are derived from the weathering of rocks and are commonly described by textural terms such as gravels, sands, silts, and clays.**
- 2. Physical weathering causes reduction in size of the parent rock without change in its composition.**
- 3. Chemical weathering causes reduction in size and chemical composition that differs from the parent rock.**
- 4. Clays are composed of three main types of mineral—kaolinite, illite, and montmorillonite.**
- 5. The clay minerals consist of silica and alumina sheets that are combined to form layers. The bonds between layers play a very important role in the mechanical behavior of clays. The bond between the layers in montmorillonite is very weak compared with kaolinite and illite. Water can easily enter between the layers in montmorillonite, causing swelling.**
- 6. A thin layer of water, called adsorbed water, is bonded to the mineral surfaces of soils. This layer significantly influences the physical and mechanical characteristics of fine-grained soils.**

What's next . . . In most soils, there is a distribution of particle sizes that influences the response of soils to loads and to the flow of water. We will describe methods used in the laboratory to find particle sizes of soils.

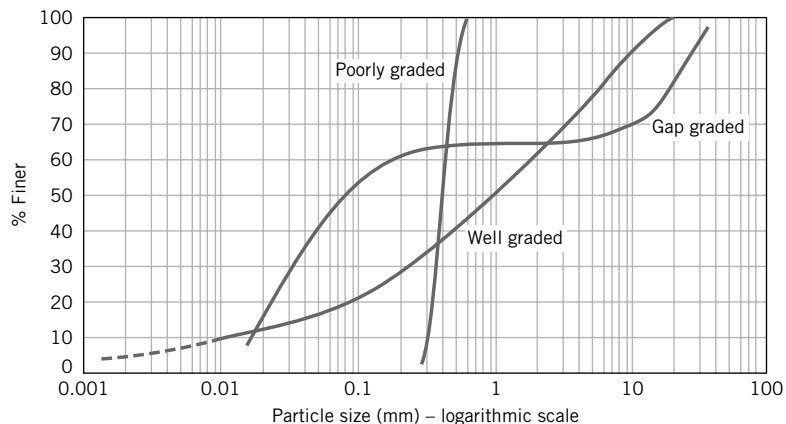
2.5 DETERMINATION OF PARTICLE SIZE OF SOILS—ASTM D 422

2.5.1 Particle Size of Coarse-Grained Soils

The distribution of particle sizes or average grain diameter of coarse-grained soils—gravels and sands—is obtained by screening a known weight of the soil through a stack of sieves of progressively finer mesh size. A typical stack of sieves is shown in Figure 2.11.

**FIGURE 2.11**

Stack of sieves.

**FIGURE 2.12** Particle size distribution curves.

Each sieve is identified by either a number that corresponds to the number of square holes per linear inch of mesh or the size of the opening. Large sieve (mesh) openings (25.4 mm to 6.35 mm) are designated by the sieve opening size, while smaller sieve sizes are designated by numbers. The particle diameter in the screening process, often called sieve analysis, is the maximum dimension of a particle that will pass through the square hole of a particular mesh. A known weight of dry soil is placed on the largest sieve (the top sieve) and the nest of sieves is then placed on a vibrator, called a sieve shaker, and shaken. The nest of sieves is dismantled, one sieve at a time. The soil retained on each sieve is weighed, and the percentage of soil retained on each sieve is calculated. The results are plotted on a graph of percent of particles finer than a given sieve size (not the percent retained) as the ordinate versus the logarithm of the particle sizes, as shown in Figure 2.12. The resulting plot is called a particle size distribution curve or, simply, the gradation curve. Engineers have found it convenient to use a logarithmic scale for particle size because the ratio of particle sizes from the largest to the smallest in a soil can be greater than 10^4 .

Let W_i be the weight of soil retained on the i th sieve from the top of the nest of sieves and W be the total soil weight. The percent weight retained is

$$\% \text{ retained on } i\text{th sieve} = \frac{W_i}{W} \times 100 \quad (2.1)$$

The percent finer is

$$\% \text{ finer than } i\text{th sieve} = 100 - \sum_{i=1}^i (\% \text{ retained on } i\text{th sieve}) \quad (2.2)$$

You can use mass instead of weight. The unit of mass is grams or kilograms.

2.5.2 Particle Size of Fine-Grained Soils

The screening process cannot be used for fine-grained soils—silts and clays—because of their extremely small size. The common laboratory method used to determine the size distribution of fine-grained soils is a hydrometer test (Figure 2.13). The hydrometer test involves mixing a small amount of soil into a suspension and observing how the suspension settles in time. Larger particles will settle quickly, followed by smaller particles. When the hydrometer is lowered into the suspension, it will sink into the suspension until the buoyancy force is sufficient to balance the weight of the hydrometer.

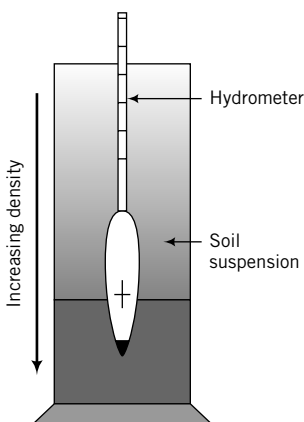


FIGURE 2.13
Hydrometer in soil–water suspension.

The length of the hydrometer projecting above the suspension is a function of the density, so it is possible to calibrate the hydrometer to read the density of the suspension at different times. The calibration of the hydrometer is affected by temperature and the specific gravity of the suspended solids. You must then apply a correction factor to your hydrometer reading based on the test temperatures.

Typically, a hydrometer test is conducted by taking a small quantity of a dry, fine-grained soil (approximately 50 grams) and thoroughly mixing it with distilled water to form a paste. The paste is placed in a 1-liter glass cylinder, and distilled water is added to bring the level to the 1-liter mark. The glass cylinder is then repeatedly shaken and inverted before being placed in a constant-temperature bath. A hydrometer is placed in the glass cylinder and a clock is simultaneously started. At different times, the hydrometer is read. The diameter D (cm) of the particle at time t_D (seconds) is calculated from Stokes's law as

$$D = \sqrt{\frac{18\mu z}{(G_s - 1)\rho_w g t_D}} \quad (2.3)$$

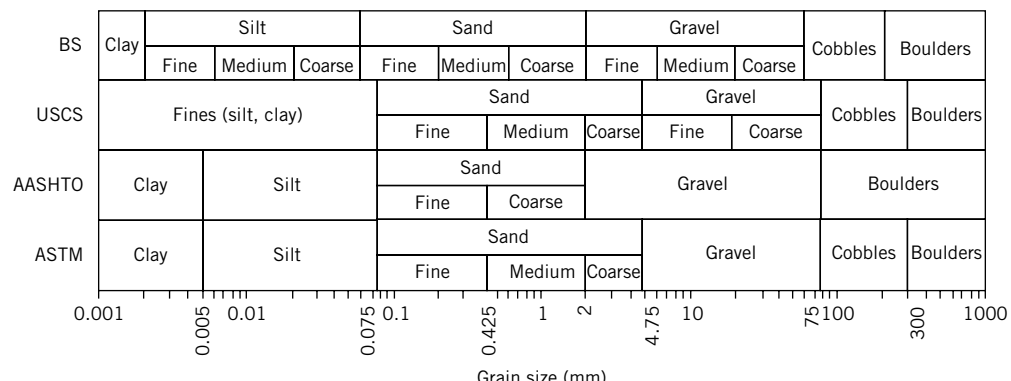
where μ is the viscosity of water [0.01 gram/(cm.s) at 20°C], z is the depth (cm), ρ_w is the density of water (1 gram/cm³), g is the acceleration due to gravity (981 cm/s²), and G_s is the specific gravity of the soil particles. For most soils, $G_s \approx 2.7$.

In the application of Stokes's law, the particles are assumed to be free-falling spheres with no collision. But the mineral particles of clays are platelike, and collision of particles during sedimentation is unavoidable. Also, Stokes's law is valid only for laminar flow with Reynolds number ($Re = \frac{vD\gamma_w}{\mu g}$, where v is velocity, D is the diameter of the particle, γ_w is the unit weight of water, μ is the dynamic viscosity of water at 20°C, and g is the acceleration due to gravity) smaller than 1. Laminar flow prevails for particle sizes in the range $0.001 \text{ mm} < D_s < 0.1 \text{ mm}$. By using the material passing the No. 200 sieve (average particle size $<0.075 \text{ mm}$), laminar flow is automatically satisfied for particles less than 0.001 mm. Particles smaller than 0.001 mm are colloids. Electrostatic forces influence the motion of colloids, and Stokes's law is not valid. Brownian motion describes the random movement of colloids.

The results of the hydrometer test suffice for most geotechnical engineering needs. For more accurate size distribution measurements in fine-grained soils, other, more sophisticated methods are available (e.g., light-scattering methods). The dashed line in Figure 2.12 shows a typical particle size distribution for fine-grained soils.

2.5.3 Characterization of Soils Based on Particle Size

The grading curve is used for textural classification of soils. Various classification systems have evolved over the years to describe soils based on their particle size distribution. Each system was developed for

**FIGURE 2.14** Comparison of four systems for describing soils based on particle size.

a specific engineering purpose. In Figure 2.14, four systems are compared. These are the Unified Soil Classification System (USCS), the American Society for Testing and Materials (ASTM) (a modification of the USCS system), the American Association of State Highway and Transportation Officials (AASHTO), and the British Standards (BS). We will discuss soil classification in more detail in Chapter 4.

In this book we will use the ASTM system. Soils will be separated into two categories. One category is coarse-grained soils that are delineated if more than 50% of the soil is greater than 0.075 mm (No. 200 sieve). The other category is fine-grained soils that are delineated if more than 50% of the soil is finer than 0.075 mm. Coarse-grained soils are subdivided into gravels and sands, while fine-grained soils are divided into silts and clays. Each soil type—gravel, sand, silt, and clay—is identified by grain size, as shown in Table 2.1. Clays have particle sizes less than 0.002 mm. Real soils consist of a mixture of particle sizes.

The selection of a soil for a particular use may depend on the assortment of particles it contains. Two coefficients have been defined to provide guidance on distinguishing soils based on the distribution of the particles. One of these is a numerical measure of uniformity, called the *uniformity coefficient*, Cu, defined as

$$Cu = \frac{D_{60}}{D_{10}} \quad (2.4)$$

where D_{60} is the diameter of the soil particles for which 60% of the particles are finer, and D_{10} is the diameter of the soil particles for which 10% of the particles are finer. Both of these diameters are obtained from the grading curve.

TABLE 2.1 Soil Types, Descriptions, and Average Grain Sizes According to ASTM D 2487

Soil type	Description	Average grain size
Gravel	Rounded and/or angular bulky hard rock, coarsely divided	Coarse: 75 mm to 19 mm Fine: 19 mm to 4.75 mm
Sand	Rounded and/or angular hard rock, finely divided	Coarse: 4.75 mm to 2.0 mm (No. 10) Medium: 2.0 mm to 0.425 mm (No. 40) Fine: 0.425 mm to 0.075 mm (No. 200)
Silt	Particle size between clay and sand. Exhibit little or no strength when dried.	0.075 mm to 0.002 mm
Clay	Particles are smooth and mostly clay minerals. Exhibit significant strength when dried; water reduces strength.	<0.002 mm

The other coefficient is the *coefficient of curvature*, C_c (other terms used are the coefficient of gradation and the coefficient of concavity), defined as

$$C_c = \frac{(D_{30})^2}{D_{10} D_{60}} \quad (2.5)$$

where D_{30} is the diameter of the soil particles for which 30% of the particles are finer. The average particle diameter is D_{50} .

A soil that has a uniformity coefficient of <4 contains particles of uniform size (approximately one size). The minimum value of C_u is 1 and corresponds to an assemblage of particles of the same size. The gradation curve for a poorly graded soil is almost vertical (Figure 2.12). Humps in the gradation curve indicate two or more poorly graded soils. Higher values of uniformity coefficient (>4) indicate a wider assortment of particle sizes. A soil that has a uniformity coefficient of >4 is described as a well-graded soil and is indicated by a flat curve (Figure 2.12). The coefficient of curvature is between 1 and 3 for well-graded soils. The absence of certain grain sizes, termed gap-graded, is diagnosed by a coefficient of curvature outside the range 1 to 3 and a sudden change of slope in the particle size distribution curve, as shown in Figure 2.12.

Poorly graded soils are sorted by water (e.g., beach sands) or by wind. Gap-graded soils are also sorted by water, but certain sizes were not transported. Well-graded soils are produced by bulk transport processes (e.g., glacial till). The uniformity coefficient and the coefficient of concavity are strictly applicable to coarse-grained soils.

The diameter D_{10} is called the effective size of the soil and was described by Allen Hazen (1892) in connection with his work on soil filters. The effective size is the diameter of an artificial sphere that will produce approximately the same effect as an irregularly shaped particle. The effective size is particularly important in regulating the flow of water through soils, and can dictate the mechanical behavior of soils since the coarser fractions may not be in effective contact with each other; that is, they float in a matrix of finer particles. The higher the D_{10} value, the coarser the soil and the better the drainage characteristics.

Particle size analyses have many uses in engineering. They are used to select aggregates for concrete, soils for the construction of dams and highways, soils as filters, and material for grouting and chemical injection. In Chapter 4, you will learn about how the particle size distribution is used with other physical properties of soils in a classification system designed to help you select soils for particular applications.

THE ESSENTIAL POINTS ARE:

- 1. A sieve analysis is used to determine the grain size distribution of coarse-grained soils.**
- 2. For fine-grained soils, a hydrometer analysis is used to find the particle size distribution.**
- 3. Particle size distribution is represented on a semilogarithmic plot of % finer (ordinate, arithmetic scale) versus particle size (abscissa, logarithmic scale).**
- 4. The particle size distribution plot is used to delineate the different soil textures (percentages of gravel, sand, silt, and clay) in a soil.**
- 5. The effective size, D_{10} , is the diameter of the particles of which 10% of the soil is finer. D_{10} is an important value in regulating flow through soils and can significantly influence the mechanical behavior of soils.**
- 6. D_{50} is the average grain size diameter of the soil.**
- 7. Two coefficients—the uniformity coefficient and the coefficient of curvature—are used to characterize the particle size distribution. Poorly graded soils have uniformity coefficients <4 and steep gradation curves. Well-graded soils have uniformity coefficients >4 , coefficients of curvature between 1 and 3, and flat gradation curves. Gap-graded soils have coefficients of curvature <1 or >3 , and one or more humps on the gradation curves.**

EXAMPLE 2.1 Calculating Particle Size Distribution and Interpretation of Soil Type from a Sieve Analysis Test

A sieve analysis test was conducted on 650 grams of soil. The results are as follows.

Sieve no.	9.53 mm (3/8")	4	10	20	40	100	200	Pan
Opening (mm)	9.53	4.75	2	0.85	0.425	0.15	0.075	
Mass retained (grams)	0	53	76	73	142	85	120.5	99.8

Determine (a) the amount of coarse-grained and fine-grained soils, and (b) the amount of each soil type based on the ASTM system.

Strategy Calculate the % finer and plot the gradation curve. Extract the amount of coarse-grained soil (particle sizes ≥ 0.075 mm) and the amount of fine-grained soil (particle sizes < 0.075 mm). Use Table 2.1 to guide you to get the amount of each soil type.

Solution 2.1

Step 1: Set up a table or a spreadsheet to do the calculations.

A	B	C	D	E	F
Sieve no.	Opening (mm)	Mass retained (grams) M_r	% Retained (100 $\times M_r/M_t$)	Σ (% Retained) (Σ column D)	% Finer (100 – column E)
9.53 mm (3/8")	9.53	0	0.0	0.0	100.0
4	4.75	53	8.2	8.2	91.8
10	2	76	11.7	19.9	80.1
20	0.85	73	11.2	31.1	68.9
40	0.425	142	21.9	52.9	47.1
100	0.15	85.4	13.1	66.1	33.9
200	0.075	120.5	18.5	84.6	15.4
Pan		99.8	15.4		
	SUM	649.7	100.0		
	$M_t =$	649.7			

Note: In the sieve analysis test, some mass is lost because particles are stuck in the sieves. Use the sum of the mass after the test.

Step 2: Plot grading curve. See Figure E2.1.

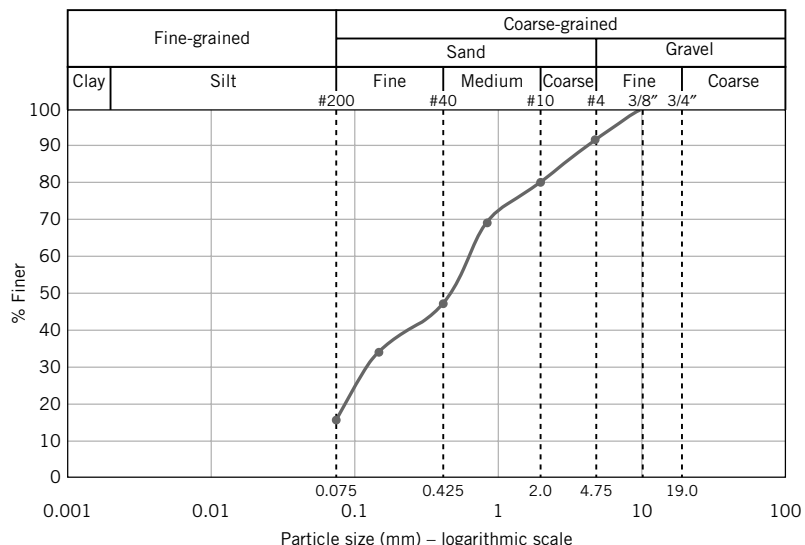


FIGURE E2.1 Grading curve.

Step 3: Extract soil type.

- (a) The amount of fine-grained soil is the % finer than the No. 200 sieve (opening = 0.075 mm). The amount of coarse-grained soil is the % coarser than the No. 200 sieve, i.e., cumulative % retained on the No. 200 sieve.
% fine-grained soil = 15.4%
% coarse-grained soil = $100 - 15.4 = 84.6\%$

(b)

Fine gravel (%) = 8.2
Total gravel (%) = 8.2
Coarse sand (%) = 11.7
Medium sand (%) = 33.0
Fine sand (%) = 31.7
Total sand (%) = 76.4
Silt + clay (%) = 15.4

EXAMPLE 2.2 Interpreting Sieve Analysis Data

A sample of a dry, coarse-grained material of mass 500 grams was shaken through a nest of sieves, and the following results were obtained:

Sieve no.	Opening (mm)	Mass retained (grams)
4	4.75	0
10	2.00	14.8
20	0.85	98
40	0.425	90.1
100	0.15	181.9
200	0.075	108.8
Pan		6.1

- (a) Plot the particle size distribution (gradation) curve.
(b) Determine (1) the effective size, (2) the average particle size, (3) the uniformity coefficient, and (4) the coefficient of curvature.
(c) Determine the textural composition of the soil (i.e., the amount of gravel, sand, etc.).

Strategy The best way to solve this type of problem is to make a table to carry out the calculations and then plot a gradation curve. Total mass (M) of dry sample used is 500 grams, but on summing the masses of the retained soil in column 2 we obtain 499.7 grams. The reduction in mass is due to losses mainly from a small quantity of soil that gets stuck in the meshes of the sieves. You should use the “after sieving” total mass of 499.7 grams in the calculations.

Solution 2.2**Step 1:** Tabulate data to obtain % finer.

See table below.

Sieve no.	Mass retained (grams), M_r	% Retained $(M_r/M) \times 100$	$\Sigma (\%)$ Retained	% Finer
4	0	0	0	$100 - 0 = 100$
10	14.8	3.0	3.0	$100 - 3.0 = 97.0$
20	98.0	19.6	22.6	$100 - 22.6 = 77.4$
40	90.1	18.0	40.6	$100 - 40.6 = 59.4$
100	181.9	36.4	77.0	$100 - 77 = 23.0$
200	108.8	21.8	98.8	$100 - 98.8 = 1.2$
Pan	6.1	1.2		
Total mass $M = 499.7$		100.0		

add check

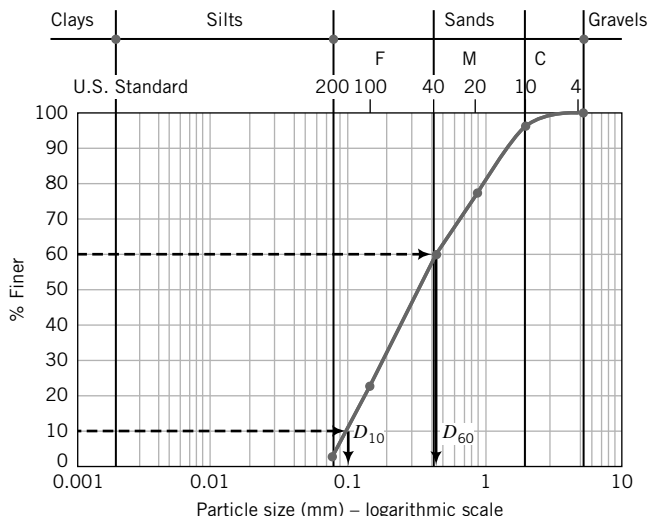


FIGURE E2.2
Particle size distribution curve.

Step 2: Plot the gradation curve.

See Figure E2.2 for a plot of the gradation curve.

Step 3: Extract the effective size.

$$\text{Effective size} = D_{10} = 0.1 \text{ mm}$$

Step 4: Extract percentages of gravel, sand, silt, and clay.

$$\begin{aligned}\text{Gravel} &= 0\% \\ \text{Sand} &= 98.8\% \\ \text{Silt and clay} &= 1.2\%\end{aligned}$$

Step 5: Calculate Cu and Cc.

$$Cu = \frac{D_{60}}{D_{10}} = \frac{0.45}{0.1} = 4.5$$

$$Cc = \frac{(D_{30})^2}{D_{10}D_{60}} = \frac{0.18^2}{0.1 \times 0.45} = 0.72$$

EXAMPLE 2.3 Calculation of Particle Diameter from Hydrometer Test Data

At a certain stage in a hydrometer test, the vertical distance moved by soil particles of a certain size over a period of 1 minute is 0.8 cm. The temperature measured is 20°C. If the specific gravity of the soil particles is 2.7, calculate the diameter of the particles using Stokes's law. Are these silt or clay particles?

Strategy For this problem use Equation 2.3, making sure that the units are consistent.

Solution 2.3

Step 1: Calculate the particle diameter using Stokes's law.

$$\mu = 0.01 \text{ gram}/(\text{cm.s}) \text{ at } 20^\circ\text{C}, \rho_w = 1 \text{ gram}/\text{cm}^3 \text{ at } 20^\circ\text{C}, g = 981 \text{ cm/s}^2, t_D = 1 \times 60 = 60 \text{ seconds}$$

$$D = \sqrt{\frac{18\mu z}{(G_s - 1)p_w g t_D}} = \sqrt{\frac{18 \times 0.01 \times 0.8}{(2.7 - 1) \times 1 \times 981 \times 60}} = 0.0012 \text{ cm} = 0.012 \text{ mm}$$

Step 2: Identify the soil type.

Silt particles have sizes between 0.075 mm and 0.002 mm.

Therefore, the soil particles belong to the silt fraction of the soil.

EXAMPLE 2.4 Interpreting Hydrometer Analysis

The soil passing the No. 200 sieve in Example 2.1 was used to conduct a hydrometer test. The results are shown in the table below. What are the amounts of clays and silts in the soil?

Time (min)	Hydrometer reading (gram/liter)	Temperature (°C)	Corrected distance of fall (cm)	Grain size (mm)	% Finer by weight
1	40.0	22.5	8.90	0.0396	82.2
2	34.0	22.5	9.21	0.0285	68.8
3	32.0	22.0	9.96	0.0243	64.2
4	30.0	22.0	10.29	0.0214	59.7
8	27.0	22.0	10.96	0.0156	53.1
15	25.0	21.5	11.17	0.0116	48.4
30	23.0	21.5	11.45	0.0083	43.9
60	21.0	21.5	11.96	0.0060	39.5
240	17.0	20.0	12.45	0.0031	30.0
900	14.0	19.0	13.10	0.0017	22.9

Strategy Plot % finer versus grain size (log scale) and extract % of grain size finer than 0.002.

Solution 2.4

Step 1: Plot % finer versus grain size (log scale).

See Figure E2.4.

Step 2: Extract % finer than 0.002 mm.

$$\% \text{ finer than } 0.002 \text{ mm} = 24.5\%$$

$$\% \text{ clay in the soil in Example 2.1 is } (24.5/100) \times 15.4 = 3.8\%$$

$$\% \text{ silt} = 15.4 - 3.9 = 11.6\%$$

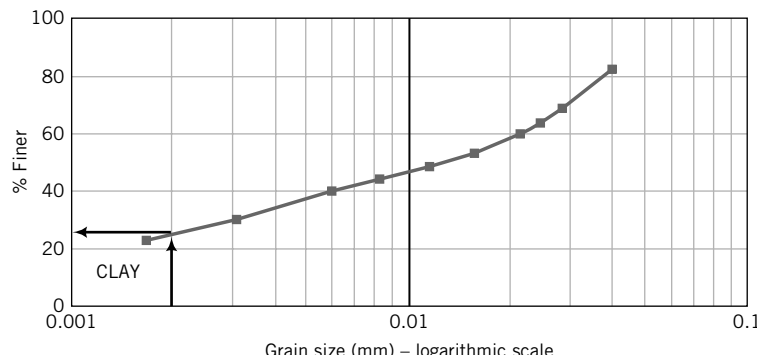


FIGURE E2.4 Grading curve.

What's next . . . Coarse-grained and fine-grained soils have different characteristics for engineering purposes. In the next section, a broad comparison between coarse-grained and fine-grained soils is presented.

2.6 COMPARISON OF COARSE-GRAINED AND FINE-GRAINED SOILS FOR ENGINEERING USE

Coarse-grained soils have good load-bearing capacities and good drainage qualities, and their strength and volume change characteristics are not significantly affected by change in moisture conditions under static loading. They are practically incompressible when dense, but significant volume changes can occur when they are loose. Vibrations accentuate volume changes in loose, coarse-grained soils by rearranging the soil fabric into a dense configuration.

Fine-grained soils have poor load-bearing capacities compared with coarse-grained soils. Fine-grained soils are practically impermeable, change volume and strength with variations in moisture conditions, and are susceptible to frost. The engineering properties of coarse-grained soils are controlled mainly by the grain size of the particles and their structural arrangement. The engineering properties of fine-grained soils are controlled by mineralogical factors rather than grain size. Thin layers of fine-grained soils, even within thick deposits of coarse-grained soils, have been responsible for many geotechnical failures, and therefore you need to pay special attention to fine-grained soils.

In this book, we will deal with soil as a construction and a foundation material. We will not consider soils containing organic material or the parent material of soils, rock. We will label our soils as engineering soils to distinguish our consideration of soils from that of geologists, agronomists, and soil scientists, who have additional interests in soils not related to construction activities.

THE ESSENTIAL POINTS ARE:

1. Fine-grained soils have much larger surface areas than coarse-grained soils and are responsible for the major physical and mechanical differences between coarse-grained and fine-grained soils.
2. The engineering properties of fine-grained soils depend mainly on mineralogical factors.
3. Coarse-grained soils have good load-bearing capacities and good drainage qualities, and their strength and volume-change characteristics are not significantly affected by changes in moisture conditions.
4. Fine-grained soils have poor load-bearing capacities and poor drainage qualities, and their strength and volume-change characteristics are significantly affected by changes in moisture conditions.

2.7 SUMMARY

Geological understanding of soils is important for successful geotechnical engineering practice. Of the three main groups of rocks—igneous, sedimentary, and metamorphic—sedimentary rocks are of particular importance to geotechnical engineers because they comprise nearly 75% of the earth's surface. Soils are derived from the weathering of rocks by physical and chemical processes. The main groups of soils for engineering purposes from these processes are coarse-grained soils—sand and gravels—and fine-grained soils—silts and clays. Particle size is sufficient to identify coarse-grained soils. Fine-grained soils require mineralogical characterization in addition to particle size for identification. Coarse-grained and fine-grained soils have different engineering properties. The behavior of fine-grained soils is strongly influenced by moisture content changes. The behavior of coarse-grained soils under static loading is not influenced by moisture content changes.

Self-Assessment

Access Chapter 2 at <http://www.wiley.com/college/budhu> to take the end-of-chapter quiz to test your understanding of this chapter.



EXERCISES

- 2.1** (a) What are the three layers that make up the earth's internal structure?
 (b) What is the composition of each of the layers?
- 2.2** (a) Describe the differences among the three key groups of rocks.
 (b) Explain why sedimentary rocks are of particular importance to geotechnical engineers.
 (c) Are rock masses homogeneous and continuous? Explain.
- 2.3** (a) How are soils formed?
 (b) What are the agents responsible for weathering of rocks?
- 2.4** (a) What is a mineral?
 (b) Describe the differences among the three main clay minerals.
 (c) Why are silicates the most common minerals?
- 2.5** Why does montmorillonite undergo large volume change in contact with water?
- 2.6** In your area, choose a project under construction or a recently constructed project such as a road or a building. Describe the geology of the site.
- 2.7** Collect soils and rocks in your neighborhood and write a description of each. The description should include color, hardness, stratifications, jointing (if any), etc.
- 2.8** (a) What is soil fabric?
 (b) What is the name for the spaces between mineral particles?
 (c) Why are the spaces between mineral particles important to geoengineers?
 (d) Explain the differences between a flocculated and a dispersed structure.
- 2.9** (a) What are the six categories of soil types identified in the ASTM classification system?
 (b) For which soil type are surface forces important? Why?
 (c) What is adsorbed water?
 (d) Can you remove the adsorbed water by oven-drying at 105°C? Explain.
- 2.10** A particle size analysis on a soil sample yields the following data:
- | Sieve no. | 3/8" | 4 | 10 | 20 | 60 | 200 | Pan |
|-----------------------|------|------|-----|------|------|-------|-----|
| Sieve size (mm) | 9.53 | 4.75 | 2.0 | 0.84 | 0.25 | 0.074 | — |
| Mass retained (grams) | 0 | 310 | 580 | 380 | 260 | 680 | 210 |
- (a) Plot the particle size distribution curve.
 (b) Determine the amount of coarse-grained and fine-grained soils in the sample.
- 2.11** The following results were obtained from sieve analyses of two soils:
- | Sieve no. | Opening (mm) | Soil A | Soil B |
|-----------|--------------|--------|--------|
| 4 | 4.75 | 0 | 0 |
| 10 | 2.00 | 20.2 | 48.2 |
| 20 | 0.85 | 25.7 | 19.6 |
| 40 | 0.425 | 40.4 | 60.3 |
| 100 | 0.15 | 18.1 | 37.2 |
| 200 | 0.075 | 27.2 | 22.1 |
| Pan | | 68.2 | 5.6 |
- Hydrometer tests of these soils give the following results: Soil A, % finer than 0.002 mm = 48%; Soil B, % finer than 0.002 mm = 2%.
- (a) Plot the gradation curve for each soil on the same graph.
 (b) How much coarse-grained and fine-grained soils are in each soil?
 (c) What are the percentages of clay and silt in each soil?
 (d) Determine D_{10} for each soil.
 (e) Determine the uniformity coefficient and the coefficient of concavity for each soil.
 (f) Describe the gradation curve (e.g., well graded) for each soil.

3.0 INTRODUCTION

The purpose of this chapter is to give you a brief introduction to a site or soils investigation.

When you complete this chapter, you should be able to:

- Plan a soils investigation.
- Describe soils in the field.
- Appreciate the limitations of a soils investigation.

Importance

Geological forces and processes often result in inhomogeneous and discontinuous formations that significantly influence the stability and costs of civil engineering works. The amount of investigation needed to characterize a site economically, the type and methods of construction, and natural geological hazards such as earthquakes, volcanic activity, and groundwater conditions are important geological factors that must be considered in the practice of geotechnical engineering. Many failures of structures, causing loss of lives and property, have resulted from unrealized geological conditions. Consider the geology at a potential construction site in a county, as shown in Figure 3.1. To map these geological features requires applications of geophysical methods and a series of closely spaced boreholes. The precise size of each geological feature is difficult to ascertain. In building a skyscraper, for example, you must have knowledge of the geological features under and within the vicinity of the building to design a safe and economical foundation.

Most of the theories we will be using in later chapters to predict and understand the response of a soil are based on the assumption of a homogeneous soil mass. But soils are rarely homogeneous, as illustrated in Figure 3.1. Thus, we will be treating soils as ideal or hypothetical materials and use statistical average properties. However, in many cases, statistical average values could mislead because a weak or discontinuous soil layer at a particular location may control the stability of a geotechnical system (e.g., a foundation).

A soils investigation is an essential part of the design and construction of a proposed structural system (buildings, dams, roads and highways, etc.). Soils are identified, observed, and recovered during a soils investigation of a proposed site. Usually soils investigations are conducted only on a fraction of a proposed site because it would be prohibitively expensive to conduct an extensive investigation of a whole site. We then have to make estimates and judgments based on information from a limited set of observations, and from field and laboratory test data that will have profound effects on the performance and costs of structures constructed at a site.

A practical situation is as follows. A subdivision consisting of 3000 homes, a shopping center, water and sewer plants, utilities, and an office complex is planned for a 200-hectare (approximately 300-acre) site in your neighborhood. As part of the permitting, preliminary design, and construction processes, a soils report is required. You are assigned to plan and execute the soils investigation and write the report.

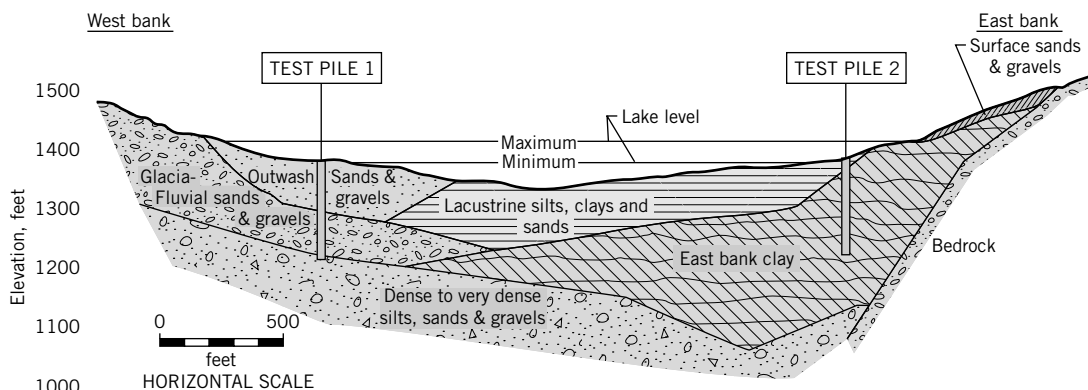


FIGURE 3.1 Soil profile at a construction site. (Source: McCammon and Golder, 1970.)

3.1 DEFINITIONS OF KEY TERMS

SPT is the standard penetration test.

N is the number of blows for the last 305-mm penetration of an STP sampler.

Soil sensitivity (S_t) is the ratio of the intact strength to the disturbed strength.

3.2 QUESTIONS TO GUIDE YOUR READING

1. What are the purposes of a soils investigation?
2. How do you plan and execute a soils investigation?
3. How do you interpret the information from a soils investigation?
4. How do you report the results?
5. What should be included in a soils report?

3.3 PURPOSES OF A SOILS INVESTIGATION

A soils investigation program is necessary to provide information for design and construction, environmental assessment, and project due diligence (*due diligence* is the process of evaluating a prospective project to facilitate business decisions by the owner). The purposes of a soils investigation are:

1. To evaluate the general suitability of the site for the proposed project.
2. To enable an adequate and economical design to be made.
3. To disclose and make provision for difficulties that may arise during construction due to ground and other local conditions.

3.4 PHASES OF A SOILS INVESTIGATION

The scope of a soils investigation depends on the type, size, and importance of the structure; the client; the engineer's familiarity with the soils at the site; and local building codes. Structures that are sensitive to settlement such as machine foundations and high-use buildings usually require a more thorough soils investigation than a foundation for a house. A client may wish to take a greater risk than normal to save money and set limits on the type and extent of the site investigation. You should be cautious about any attempt to reduce the extent of a soils investigation below a level that is desirable for assuming

acceptable risks for similar projects on or within similar ground conditions. If the geotechnical engineer is familiar with a site, he/she may undertake a very simple soils investigation to confirm his/her experience. Some local building codes have provisions that set out the extent of a site investigation. It is mandatory that a visit be made to the proposed site.

A soils investigation has three components. The first component is done prior to design. The second component is done during the design process. The third component is done during construction. The second and third components are needed for contingencies. The first component is generally more extensive and is conducted in phases. These phases are as follows:

Phase I. This phase is sometimes called “desk study.” It involves collection of available information such as a site plan; type, size, and importance of the structure; loading conditions; previous geotechnical reports; maps, including topographic maps, aerial photographs, still photographs, satellite imagery, and geologic maps; and newspaper clippings. An assortment of maps giving geology, contours and elevations, climate, land use, aerial photos, regional seismicity, and hydrology are available on the Internet (e.g., <http://www.usgs.gov>). Geographical information system (GIS)—an integration of software, hardware, and digital data to capture, manage, analyze and display spatial information—can be used to view, share, understand, question, interpret, and visualize data in ways that reveal relationships, patterns, and trends. GIS data consist of discrete objects such as roads and continuous fields such as elevation. These are stored either as raster or vector objects. Google Earth (<http://earth.google.com>) can be used to view satellite imagery, maps, terrain, and 3D structures. You can also create project maps using Google Earth.



Phase II. Preliminary reconnaissance or a site visit to provide a general picture of the topography and geology of the site. It is necessary that you take with you on the site visit all the information gathered in Phase I to compare with the current conditions of the site. Your site visit notes should include the following:

- Photographs of the site and its neighborhood.
- Access to the site for workers and equipment.
- Sketches of all fences, utility posts, driveways, walkways, drainage systems, and so on.
- Utility services that are available, such as water and electricity.
- Sketches of topography including all existing structures, cuts, fills, ground depression, ponds, and so on.
- The state of any existing building at the site or nearby. Your notes should include exterior and interior cracks, any noticeable tilt, type of construction (e.g., brick or framed stucco building), evidence of frost damage, molds, and any exceptional features.
- Geological features from any exposed area such as a road cut.
- Occasionally, a few boreholes may be dug to explore the site.

Phase III. Detailed soils exploration. The objectives of a detailed soils exploration are:

- To determine the geological structure, which should include the thickness, sequence, and extent of the soil strata.
- To determine the groundwater conditions.
- To obtain disturbed and undisturbed samples for laboratory tests.
- To conduct in situ tests.

See Section 3.5 for more details.

Phase IV. Laboratory testing. The objectives of laboratory tests are:

- To classify the soils.
- To determine soil strength, failure stresses and strains, stress-strain response, permeability, compactibility, and settlement parameters. Not all of these may be required for a project.

Phase V. Write a report. The report must contain a clear description of the soils at the site, methods of exploration, soil stratigraphy, in situ and laboratory test methods and results, and the location of the groundwater. You should include information on and/or explanations of any unusual soil, water-bearing stratum, and any soil and groundwater conditions such as frost susceptibility or waterlogged areas that may be troublesome during construction.

THE ESSENTIAL POINTS ARE:

- 1. A soils investigation is necessary to determine the suitability of a site for its intended purpose.**
- 2. A soils investigation is conducted in phases. Each phase affects the extent of the next phase.**
- 3. A clear, concise report describing the conditions of the ground, soil stratigraphy, soil parameters, and any potential construction problems must be prepared for the client.**

What's next . . . In the next section, we will study how a soils exploration program (Phase III) is normally conducted.

3.5 SOILS EXPLORATION PROGRAM

A soils exploration program usually involves test pits and/or soil borings (boreholes). During the site visit (Phase II), you should work out most of the soils exploration program. A detailed soils exploration consists of:

1. Determining the need for and extent of geophysical exploration.
2. Preliminary location of each borehole and/or test pit.
3. Numbering of the boreholes or test pits.
4. Planned depth of each borehole or test pit.
5. Methods and procedures for advancing the boreholes.
6. Sampling instructions for at least the first borehole. The sampling instructions must include the number of samples and possible locations. Changes in the sampling instructions often occur after the first borehole.
7. Determining the need for and types of in situ tests.
8. Requirements for groundwater observations.

3.5.1 Soils Exploration Methods

The soils at a site can be explored using one or more of the following methods.

- Geophysical methods—nondestructive techniques used to provide spatial information on soils, rocks, and hydrological and environmental conditions. Popular methods are:
 1. Ground-penetrating radar (GPR)

GPR, also called *georadar*, is a high-resolution, high-frequency (10 MHz to 1000 MHz) electromagnetic wave technique for imaging soils and ground structures. An antenna is used to transmit and recover radar pulses generated by a pulse generator. The returned pulse is then processed to produce images of the soil profile. The key geotechnical uses are soil profile imaging and location of buried objects. GPR produces continuous-resolution images of the soil profile with very little soil disturbance. GPR is not suitable for highly conductive (>15 milliohms/m) wet clays and silts. GPR resolution decreases with depth.
 2. Seismic surveys

Seismic investigations utilize the fact that surface waves travel with different velocities through different materials. The subsurface interfaces are determined by recording the magnitude and

travel time of the seismic waves, essentially compression waves (P waves), at a point some distance from the source of the wave. The velocity of propagation is the most important parameter in the application of seismic methods. The densities and elastic properties of the geological materials control the velocity of propagation. When a seismic wave encounters a boundary between two elastic media, the wave energy is transmitted by *reflection*, *refraction*, and *diffraction*. Seismic reflection and refraction are used in geotechnical site characterization.

In seismic reflection tests, the travel times of waves reflected from subsurface interfaces are measured by geophones. Geophones are motion-sensitive transducers that convert ground motion to electric signals. The travel times are correlated to depth, size, and shape of the interfaces. The angle of reflection of the waves is a function of the material density contrast. Seismic reflection is used when high resolution of soil profile is required, especially at large depths (>50 m).

Seismic refraction surveys are very similar to seismic reflection surveys except that refraction waves are measured and the source geophone is placed at a greater distance. The latter enables the recording of seismic waves that are primarily horizontal rather than vertical. In most refraction surveys, only the initial P waves are recorded. The seismic refraction method is used to determine the depth and thickness of the soil profile and the existence of buried structures.

For shallow depths of investigation, the ground surface is pounded by a sledgehammer to generate the seismic waves; for large depths, a small explosive charge is used. Seismic methods are sensitive to noise and vibration. Various filtering techniques are used to reduce background noise and vibration. Multichannel analysis of surface waves (MASW) is used to map spatial changes in low-velocity materials. A soil profile interpreted from MASW is shown in Figure 3.2.

To get information on the stiffnesses of soil layers, crosshole seismic tests are used. The seismic source is located in one borehole and the geophone is located in an adjacent borehole. The P and S (shear) wave velocities are calculated from the arrival times and the geophone distances. These are then used to calculate the soil stiffnesses.

Downhole seismic tests are used to detect layering and the strength of the layers. The seismic source is located on the surface and geophones are located in a borehole.

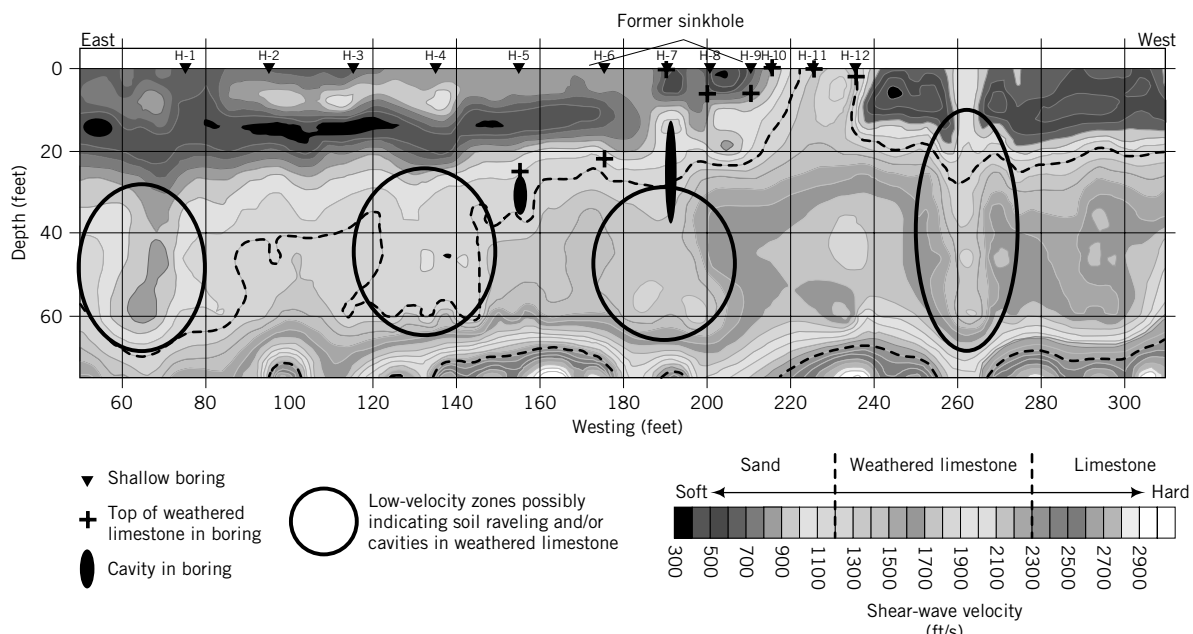


FIGURE 3.2 Soil profile from a multichannel analysis of surface waves from seismic tests.
(Source: Courtesy of Lynn Yuhr, Technos, Inc.)

3. Electrical resistivity

Electrical resistivity measurements can be used for identification and quantification of depth of groundwater, detection of clays, and measurement of groundwater conductivity. Soil resistivity, measured in ohm-centimeters (ohm-cm), varies with moisture content and temperature changes. In general, an increase in soil moisture results in a reduction in soil resistivity. The pore fluid provides the only electrical path in sands, while both the pore fluid and the surface charged particles provide electrical paths in clays. Resistivities of wet fine-grained soils are generally much lower than those of wet coarse-grained soils. The difference in resistivity between a soil in a dry and in a saturated condition may be several orders of magnitude.

The method of measuring subsurface resistivity involves placing four electrodes in the ground in a line at equal spacing, applying a measured AC current to the outer two electrodes, and measuring the AC voltage between the inner two electrodes. A measured resistance is calculated by dividing the measured voltage by the measured current. This resistance is then multiplied by a geometric factor that includes the spacing between each electrode to determine the apparent resistivity.

Electrode spacings of 0.75, 1.5, 3.0, 6.0, and 12.0 m are typically used for shallow depths (<10 m) of investigations. Greater electrode spacings of 1.5, 3.0, 6.0, 15.0, 30.0, 100.0, and 150.0 m are typically used for deeper investigations. The depth of investigation is typically less than the maximum electrode spacing. Water is introduced to the electrode holes as the electrodes are driven into the ground to improve electrical contact. A subsurface resistivity profile is typically performed by making successive measurements at several electrode spacings at one location. A soil profile from resistivity measurements is shown in Figure 3.3.

4. Other geophysical methods of geotechnical engineering interests

- (a) Gamma density, or gamma-gamma, measures electron density and can be used to estimate the total soil density or porosity.
- (b) Neutron porosity measures hydrogen density. It is used for porosity estimation below the groundwater level.
- (c) Sonic-VDL measures the seismic velocity. It is useful to measure soil stiffnesses and to detect bedrock elevation.
- (d) Microgravity is used to detect changes in subsurface densities and is particularly good at detecting cavities. A gravimeter is used at discrete points on the earth's surface to detect small changes in gravity. These changes are called gravity anomalies and are related to density changes.

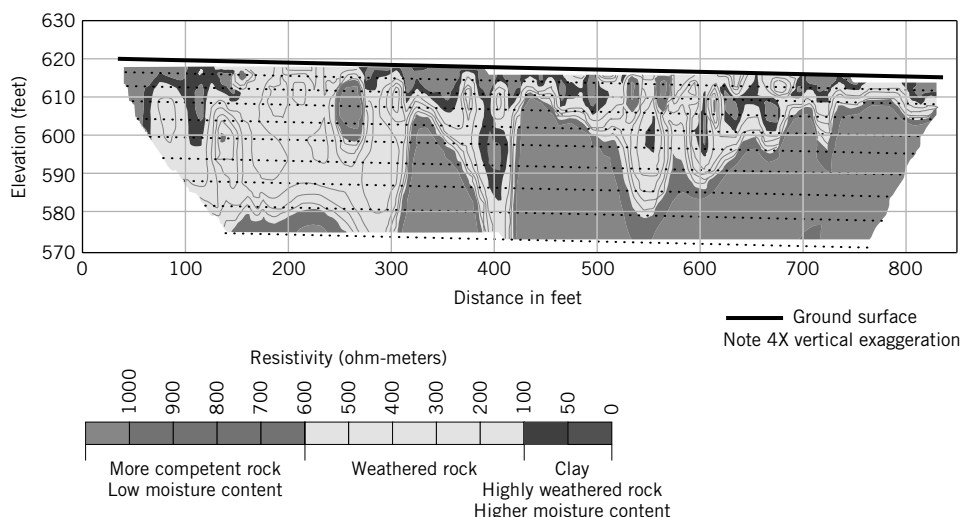


FIGURE 3.3 Soil profile from electrical resistivity tests. (Courtesy of Lynn Yuhr, Technos, Inc.)

- Trial pits or test pits. A pit is dug by hand using shovels or with a machine such as a backhoe. This method can provide excellent shallow-depth soil stratigraphy.
- Hand or power augers. These are tools used to quickly create a hole about 100 mm to 250 mm in diameter in the ground. You can inspect the soil and take undisturbed samples for lab tests.
- Wash boring. Water is pumped through a hollow rod that may or may not be equipped with a drill bit to remove soil from a borehole. The washings can be used to estimate the soil types.
- Rotary rigs. These are mechanical devices used to drill boreholes, extract soil samples, and facilitate in situ tests.

The advantages and disadvantages of each of these methods are shown in Table 3.1.

3.5.2 Soil Identification in the Field

In the field, the predominant soil types based on texture are identified by inspection. Gravels and sands are gritty and the individual particles are visible. Silts easily crumble, and water migrates to the surface on application of pressure. Clays fail this water migration test since water flows very slowly through clays. Clays feel smooth, greasy, and sticky to the touch when wet but are very hard and strong when dry.

Common descriptive terms and methods of identification are as follows.

Color: Color is not directly related to engineering properties of soils, but is related to soil mineralogy and texture.

Gray and bluish: unoxidized soils

White and cream: calcareous soils

Red and yellow: oxidized soils

Black and dark brown: soils containing organic matter

Moisture: Appearance due to water is described as wet, dry, or moist.

Structure:

Homogeneous: Color and texture feel the same throughout.

Nonhomogeneous: Color and texture vary.

Shape: Angular, subangular, subrounded, rounded, flaky.

Weathering: Fresh, decomposed, weathered.

Carbonate: Effervesces with acid. Add a small amount of hydrochloric acid and check if soil effervesces. If it does, it contains carbonate.

Smell: Organic soils give off a strong odor that intensifies with heat. Nonorganic soils have a subtle odor with the addition of water.

Feel: Use feel to distinguish between sand, silts, and clays.

Sand has a gritty feel.

Silt has a rough feel similar to fine sandpaper.

Clay feels smooth and greasy. It sticks to fingers and is powdery when dry.

Consistency: Very stiff: Finger pressure barely dents soil, but it cracks under significant pressure.

Stiff: Finger pressure dents soil.

Firm: Soil can be molded using strong finger pressure.

Soft: Easily molded by finger.

Very soft: Soil flows between fingers when fist is closed.

Dilatancy: Place a small amount of the soil in your palm and shake horizontally. Then strike it with the other hand. If the surface is slurry and water appears, the soil probably has a large amount of silt.

TABLE 3.1 Advantages and Disadvantages of Soil Exploration Methods

Method	Advantages	Disadvantages
Geophysical methods Ground penetration radar Seismic surveys Electrical resistivity Microgravity	<ul style="list-style-type: none"> • Nondestructive • Quick • Provide stratigraphy, groundwater, and relative wetness • Relatively inexpensive • Provide subsurface geologic information with which to plan detailed soils investigations 	<ul style="list-style-type: none"> • No soil samples • Limited design parameters • Site may not have enough real estate to conduct tests adequately • Much of the information is qualitative
Test pits A pit is dug either by hand or by a backhoe.	<ul style="list-style-type: none"> • Cost-effective • Provide detailed information on stratigraphy • Large quantities of disturbed soils are available for testing • Large blocks of undisturbed samples can be carved out from the pits • Field tests can be conducted at the bottom of the pit 	<ul style="list-style-type: none"> • Depth limited to about 6 m • Deep pits uneconomical • Excavation below groundwater and into rock difficult and costly • Too many pits may scar site and require backfill soils
Hand augers The auger is rotated by turning and pushing down on the handlebar.	<ul style="list-style-type: none"> • Cost-effective • Not dependent on terrain • Portable • Low headroom required • Used in uncased holes • Groundwater location can easily be identified and measured 	<ul style="list-style-type: none"> • Depth limited to about 6 m • Labor-intensive • Undisturbed samples can be taken only for soft clay deposits • Cannot be used in rock, stiff clays, dry sand, or caliche soils
Power augers Truck mounted and equipped with continuous-flight augers that bore a hole 100 to 250 mm in diameter. Augers can have a solid or hollow stem.	<ul style="list-style-type: none"> • Quick • Used in uncased holes • Undisturbed samples can be obtained quite easily • Drilling mud not used • Groundwater location can easily be identified 	<ul style="list-style-type: none"> • Depth limited to about 15 m; at greater depth drilling becomes difficult and expensive • Site must be accessible to motorized vehicle
Wash boring Water is pumped to bottom of borehole and soil washings are returned to surface. A drill bit is rotated and dropped to produce a chopping action.	<ul style="list-style-type: none"> • Can be used in difficult terrain • Low equipment costs • Used in uncased holes 	<ul style="list-style-type: none"> • Depth limited to about 30 m • Slow drilling through stiff clays and gravels • Difficulty in obtaining accurate location of groundwater level • Undisturbed soil samples cannot be obtained
Rotary drills A drill bit is pushed by the weight of the drilling equipment and rotated by a motor.	<ul style="list-style-type: none"> • Quick • Can drill through any type of soil or rock • Can drill to depths of 7500 m • Undisturbed samples can easily be recovered 	<ul style="list-style-type: none"> • Expensive equipment • Terrain must be accessible to motorized vehicle • Difficulty in obtaining location of groundwater level • Additional time required for setup and cleanup

Packing: Coarse-grained soils are described as:

- Very loose: collapses with slight disturbance; open structure
- Loose: collapses upon disturbance; open structure
- Medium dense: indents when pushed firmly
- Dense: barely deforms when pushed by feet or by stomping
- Very dense: impossible to depress with stomping

3.5.3 Number and Depths of Boreholes

It is practically impossible and economically infeasible to completely explore the whole project site. You have to make judgments on the number, location, and depths of borings to provide sufficient information for design and construction. The number and depths of borings should cover the zone of soil that would be affected by the structural loads. There is no fixed rule to follow. In most cases, the number and depths of borings are governed by experience based on the geological character of the ground, the importance of the structure, the structural loads, and the availability of equipment. Building codes and regulatory bodies provide guidelines on the minimum number and depths of borings.

The number of boreholes should be adequate to detect variations of the soils at the site. If the locations of the loads on the footprint of the structure are known (this is often not the case), you should consider drilling at least one borehole at the location of the heaviest load. As a guide, a minimum of three boreholes should be drilled for a building area of about 250 m^2 (2500 ft^2) and about five for a building area of about 1000 m^2 ($10,000 \text{ ft}^2$). Some guidelines on the minimum number of boreholes for buildings and for due diligence in subdivisions are given in Table 3.2. Some general guidance on the depth of boreholes is provided in the following:

- In compressible soils such as clays, the borings should penetrate to at least between 1 and 3 times the width of the proposed foundation below the depth of embedment or until the stress increment due to the heaviest foundation load is less than 10%, whichever is greater.
- In very stiff clays and dense, coarse-grained soils, borings should penetrate 5 m to 6 m to prove that the thickness of the stratum is adequate.
- Borings should penetrate at least 3 m into rock.
- Borings must penetrate below any fills or very soft deposits below the proposed structure.
- The minimum depth of boreholes should be 6 m unless bedrock or very dense material is encountered.

General guidelines for the minimum number or frequency of boreholes and their minimum depths for common geotechnical structures are shown in Table 3.3.

TABLE 3.2 Guidelines for the Minimum Number of Boreholes for Buildings and Subdivisions Based on Area

Buildings		Subdivisions	
Area (m^2)	No. of boreholes (minimum)	Area (m^2)	No. of boreholes (minimum)
<100	2	<4000	2
250	3	8000	3
500	4	20,000	4
1000	5	40,000	5
2000	6	80,000	7
5000	7	400,000	15
6000	8		
8000	9		
10,000	10		

TABLE 3.3 Guidelines for the Minimum Number or Frequency and Depths of Boreholes for Common Geostructures

Geostructure	Minimum number of boreholes	Minimum depth
Shallow foundation for buildings	1, but generally boreholes are placed at node points along grids of sizes varying from $15\text{ m} \times 15\text{ m}$ to $40\text{ m} \times 40\text{ m}$	5 m or $1B$ to $3B$, where B is the foundation width
Deep (pile) foundation for buildings	Same as shallow foundations	25 m to 30 m; if bedrock is encountered, drill 3 m into it
Bridge	Abutments: 2 Piers: 2	25 m to 30 m; if bedrock is encountered, drill 3 m into it
Retaining walls	Length $< 30\text{ m}$: 1 Length $> 30\text{ m}$: 1 every 30 m, or 1 to 2 times the height of the wall	1 to 2 times the wall height Walls located on bedrock: 3 m into bedrock
Cut slopes	Along length of slope: 1 every 60 m; if the soil does not vary significantly, 1 every 120 m On slope: 3	6 m below the bottom of the cut slope
Embankments including roadway (highway, motorway)	1 every 60 m; if the soil does not vary significantly, 1 every 120 m	The greater of $2 \times$ height or 6 m

3.5.4 Soil Sampling

The objective of soil sampling is to obtain soils of satisfactory size with minimum disturbance for observations and laboratory tests. Soil samples are usually obtained by attaching an open-ended, thin-walled tube—called a Shelby tube or, simply, a sampling tube—to drill rods and forcing it down into the soil.

The tube is carefully withdrawn, hopefully with the soil inside it. Soil disturbances occur from several sources during sampling, such as friction between the soil and the sampling tube, the wall thickness of the sampling tube, the sharpness of the cutting edge, and the care and handling of the sample tube during transportation. To minimize friction, the sampling tube should be pushed instead of driven into the ground.

Sampling tubes that are in common use have been designed to minimize sampling disturbances. One measure of the effects of sampler wall thickness is the recovery ratio defined as L/z , where L is the length of the sample and z is the distance that the sampler was pushed. Higher wall thickness leads to a greater recovery ratio and greater sampling disturbance.

One common type of soil sampler is the “Shelby tube,” which is a thin-walled, seamless steel tube of diameter 50 or 75 mm and length of 600–900 mm (Figure 3.4a). Another popular sampler is the “standard” sampler, also known as the split spoon sampler (split barrel sampler), which has an inside diameter of 35 mm and an outside diameter of 51 mm (Figure 3.4b). The sampler has a split barrel that is held together using a screw-on driving shoe at the bottom end and a cap at the upper end. In some

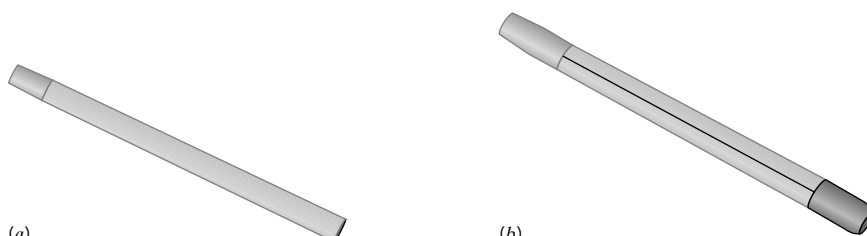


FIGURE 3.4 (a) A thin-walled tube and (b) A split barrel sampler.

countries a steel liner is used inside the sampler, but in the United States it is standard practice not to use this liner. Consequently, the soil sample has a greater diameter. The results of SPT (see Section 3.5.7b) are different for lined and unlined samplers. The thicker wall of the standard sampler permits higher driving stresses than the Shelby tube, but does so at the expense of higher levels of soil disturbances. Split spoon samples are disturbed. They are used for visual examination and for classification tests.

3.5.5 Groundwater Conditions

If you dig a hole into a soil mass that has all the voids filled with water (fully saturated), you will observe water in the hole up to a certain level. This water level is called groundwater level or groundwater table.

The top of the groundwater level is under atmospheric pressure and is sometimes called the free surface. We will denote groundwater level by the symbol ∇ . Many construction failures, court battles, and construction cost overruns are due to the nonidentification or nondisclosure of groundwater conditions at a site. The water table invariably fluctuates depending on environmental conditions (e.g., rainfall patterns, winter rains, monsoons, drought), human activities (e.g., pumping groundwater from wells and drawdown during construction), and geological conditions.

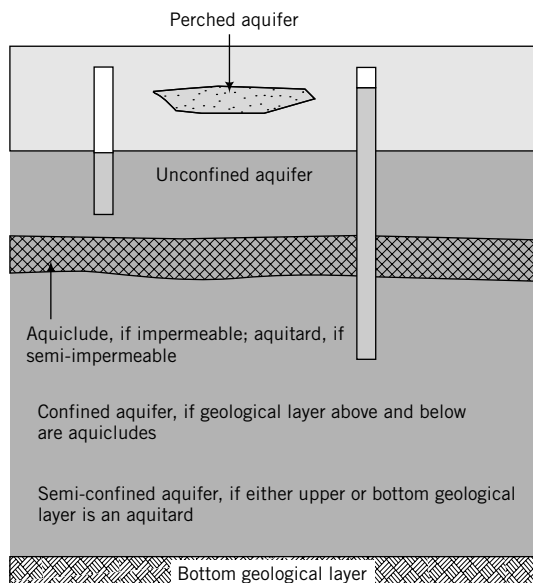


FIGURE 3.5
Unconfined, confined,
and perched aquifers;
aquitard; and aquiclude.

The water-bearing soils below the groundwater level are called an aquifer. Aquifers can be unconfined or confined or semiconfined (Figure 3.5). In an unconfined aquifer the groundwater level is free to fluctuate up and down, depending on the availability of water. During winter and spring, the groundwater level usually rises. In drier months, the groundwater level drops.

Aquifers are sometimes separated by geological formations that may restrict groundwater flow. If the formations are impermeable, such as fine-grained soils (e.g., clay) and/or nonporous rock, they are called aquiclude. If the formations are semi-impermeable, they are called aquitard.

A confined aquifer is a water-bearing stratum that is confined by aquiclude (impermeable geological formations) above and below it. The water held in an unconfined aquifer is under pressure because of the confinement. If one of the impermeable formations, usually the top, is penetrated, water can rise above the ground surface. In some unconfined aquifers, water has risen more than 50 m above the aquifer surface during well drilling. Confined aquifers (also called artesian aquifers) are not directly affected by seasonal climatic changes. There is really no true confined aquifer, as some infiltration does occur from the overlying soil or rock. The geological formations are rarely continuous, especially in alluvial aquifers. Often, the aquifer consists of fingerings or zones or lenses of impermeable and semi-impermeable

materials. Sometimes a zone or zones of water is/are collected within the unsaturated geological formation. These are known as perched aquifers, and the groundwater levels within them are called perched water tables. If these perched aquifers are not identified and reported in the soils report, they may cause instability, construction problems, and litigation.

You should identify not only the groundwater level and any special conditions (e.g., artesian condition) but also the possible range of groundwater level fluctuations.

3.5.6 Soils Laboratory Tests

Samples are normally taken from the field for laboratory tests to characterize the physical and mechanical (strength and deformation) properties. These parameters are used to design foundations and to determine the use of soils as a construction material. Disturbed samples such as from a standard sampler are usually used for visual inspection and for tests to determine the physical properties such as plasticity and grain size and shape. Undisturbed samples such as from a thin-walled sampler are used for both physical and mechanical properties. Test results, especially those that relate to the mechanical properties, are strongly affected by sampling, handling, transportation, and sample preparation disturbances. Care must therefore be exercised to protect the intact condition of the soil samples. Wax is often used to coat the soil samples to prevent moisture losses.

3.5.7 Types of In Situ or Field Tests

Over the years, several in situ testing devices have emerged to characterize the soil and to measure strength and deformation properties. The most popular devices are:

1. Vane shear test (VST)
2. Standard penetration test (SPT)
3. Cone penetrometer test (CPT)
4. Pressuremeter test (PMT)
5. Flat plate dilatometer (DMT)

(a) Vane Shear Test (VST)—ASTM D 2573 The shear vane device consists of four thin metal blades welded orthogonally (90°) to a rod (Figure 3.6). The vane is pushed, usually from the bottom of a borehole, to the desired depth. A torque is applied at a rate of 6° per minute by a torque head device located above the soil surface and attached to the shear vane rod.

After the maximum torque is obtained, the shear vane is rotated an additional 8 to 10 revolutions to measure the residual torque, T_{res} . The ratio of the maximum torque to the residual torque is the soil sensitivity, S_t , where

$$S_t = \frac{T_{max}}{T_r} \quad (3.1)$$

Sensitivity is a measure of the reduction of undrained shear strength (see Chapter 10) due to soil disturbance. The results of a vane shear test are displayed as undrained or vane shear strength versus depth.

The VST is simple, inexpensive, and quick to perform, and the equipment is widely available. The insertion of the vane causes soil remolding. Higher blade thickness results in greater remolding and lower soil strengths. The blade thickness should not exceed 5% of the vane diameter. Errors in the measurements of the torque include excessive friction, variable rotation, and calibration. The VST cannot be used for coarse-grained soils and very stiff clays.

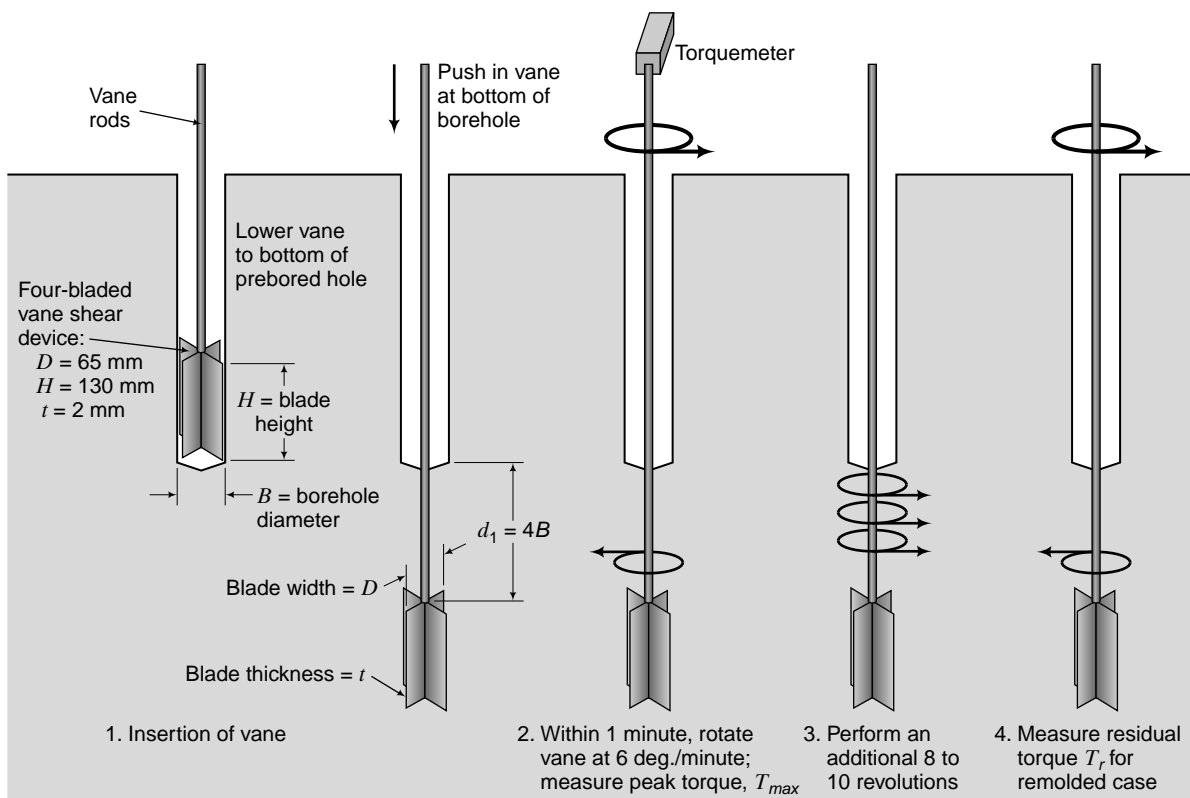


FIGURE 3.6 Vane shear tester. (Source: Professor Paul Mayne, Georgia Tech.)

(b) The Standard Penetration Test (SPT)—ASTM D 1586 The standard penetration test (SPT) was developed circa 1927 and it is perhaps the most popular field test. The SPT is performed by driving a standard split spoon sampler into the ground by blows from a drop hammer of mass 63.5 kg falling 760 mm (Figure 3.7). The sampler is driven 152 mm (6 in.) into the soil at the bottom of a borehole, and the number of blows (N) required to drive it an additional 304 mm is counted. The number of blows (N) is called the standard penetration number.

The word “standard” is a misnomer for the standard penetration test. Several methods are used in different parts of the world to release the hammer. Also, different types of anvils, rods, and rod lengths are prevalent. Various corrections are applied to the N values to account for energy losses, overburden pressure, rod length, and so on. It is customary to correct the N values to a rod energy ratio of 60%. The rod energy ratio is the ratio of the energy delivered to the split spoon sampler to the free-falling energy of the hammer. The corrected N values are denoted as N_{60} and given as

$$N_{60} = N \left(\frac{ER_r}{60} \right) = NC_E \quad (3.2)$$

where ER_r is the energy ratio and C_E is the 60% rod energy ratio correction factor. Correction factors for rod lengths, sampler type, borehole diameter, and equipment (60% rod energy ratio correction) are given in Table 3.4.

We can write a composite correction factor, C_{RSBE} , for the correction factors given in Table 3.4 as

$$C_{RSBE} = C_R C_S C_B C_E \quad (3.3)$$

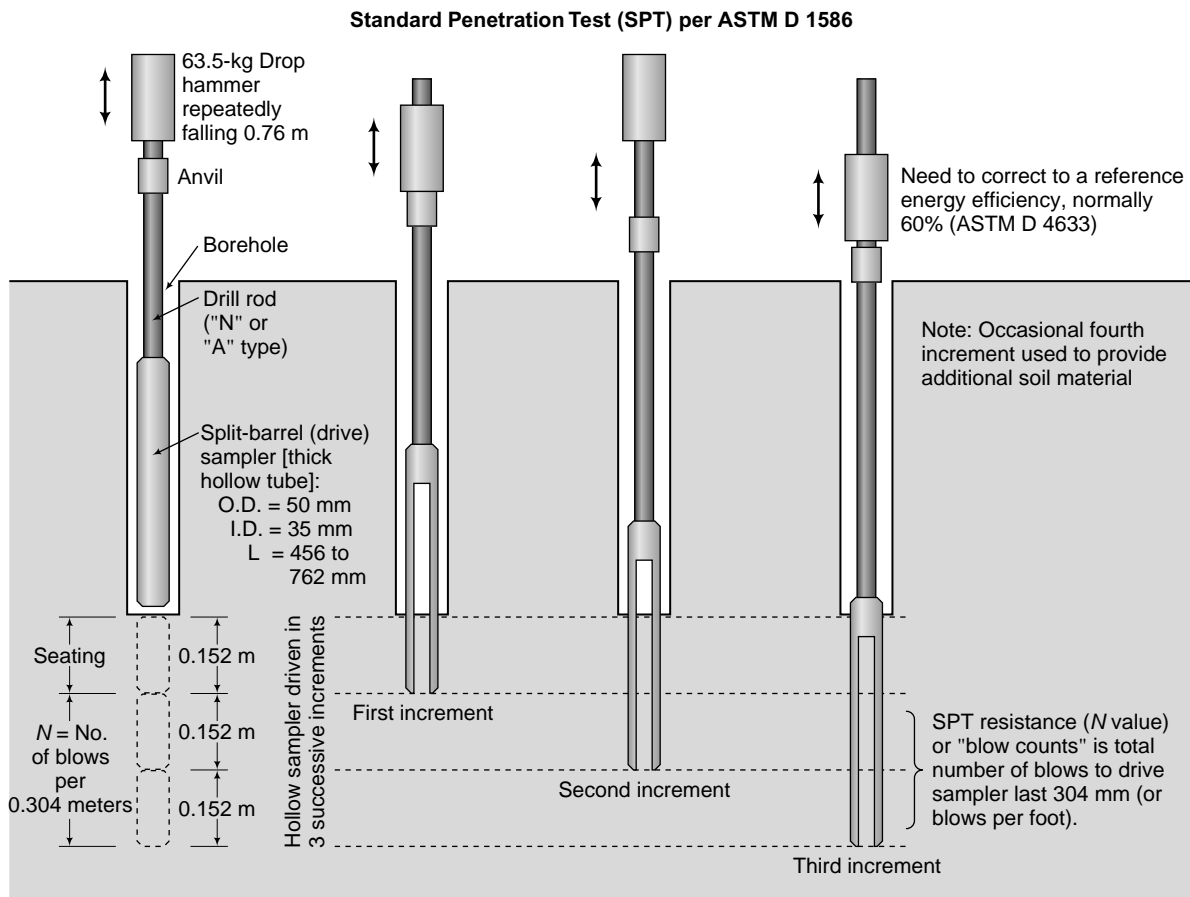


FIGURE 3.7 Driving sequence in an SPT test. (Source: Professor Paul Mayne, Georgia Tech.)

where C_R , C_S , C_B , and C_E are correction factors for rod length, sampler type, bore hole diameter, and rod energy correction, respectively.

The corrected N value is

$$N_{cor} = C_{RSBE}N \quad (3.4)$$

Equation (3.4) gives only a partially corrected N value. Additional correction factors will be discussed in Chapter 12. Compactness of coarse-grained soils based on N values is given in Table 3.5.

The SPT is very useful for determining changes in stratigraphy and locating bedrock. Also, you can inspect the soil in the split spoon sampler to describe the soil profile and extract disturbed samples for laboratory tests.

The SPT is simple and quick to perform. The equipment is widely available and can penetrate dense materials. SPT results have been correlated with engineering properties of soils, bearing capacity, and settlement of foundations. Most of these correlations are, however, weak. There are multiple sources of errors including test performance and the use of nonstandard equipment. Test performance errors include a faulty method of lifting and dropping the hammer, improper cleaning of the bottom of the borehole before the test commences, and not maintaining the groundwater level, if one is encountered. These errors give N values that are not representative of the soil. SPT tests are unreliable for coarse gravel, boulders, soft clays, silts, and mixed soils containing boulders, cobbles, clays, and silts.

TABLE 3.4 Correction Factors for Rod Length, Sampler Type, and Borehole Size

Correction factor	Item	Correction factor
C_R	Rod length (below anvil)	$C_R = 0.05L + 0.61; 4 \text{ m} < L \leq 6 \text{ m}$ $C_R = -0.0004L^2 + 0.017L + 0.83; 6 \text{ m} < L < 20 \text{ m}$ $C_R = 1; L \geq 20 \text{ m}$ $L = \text{rod length}$
C_S	Standard sampler U.S. sampler without liners	$C_S = 1.0$ $C_S = 1.2$
C_B	Borehole diameter: 65 mm to 115 mm (2.5 in. to 4.5 in.) 152 mm (6 in.) 200 mm (8 in.)	$C_B = 1.0$ $C_B = 1.05$ $C_B = 1.15$
C_E	Equipment: Safety hammer (rope, without Japanese "throw" release) Donut hammer (rope, without Japanese "throw" release) Donut hammer (rope, with Japanese "throw" release) Automatic-trip hammer (donut or safety type)	$C_E = 0.7-1.2$ $C_E = 0.5-1.0$ $C_E = 1.1-1.4$ $C_E = 0.8-1.4$

SOURCE: Youd et al. (2001) and Seed et al. (2003).

TABLE 3.5 Compactness of Coarse-Grained Soils Based on N Values

N	Compactness
0–4	Very loose
4–10	Loose
10–30	Medium
30–50	Dense
>50	Very dense

EXAMPLE 3.1 Correcting SPT Values

The blow counts for an SPT test at a depth of 6 m in a coarse-grained soil at every 0.152 m are 8, 12, and 15. A donut automatic trip hammer and a standard sampler were used in a borehole 152 mm in diameter.

- (a) Determine the N value.
- (b) Correct the N value for rod length, sampler type, borehole size, and energy ratio to 60%.
- (c) Make a preliminary description of the compactness of the soil.

Strategy The N value is the sum of the blow counts for the last 0.304 m of penetration. Just add the last two blow counts.

Solution 3.1

Step 1: Add the last two blow counts.

$$N = 12 + 15 = 27$$

Step 2: Apply correction factors.

From Table 3.4, $C_R = 0.05L + 0.61$; $4 \text{ m} < L \leq 6 \text{ m}$. Therefore, $C_R = 0.91$ for rod length of 6 m, $C_S = 1.0$ for standard sampler, and $C_B = 1.05$ for a borehole of diameter 152 mm. For a donut automatic trip hammer, $C_E = 0.8$ to 1.4; use $C_E = 1$.

$$N_{cor} = C_{RSBE}N = 0.91 \times 1.0 \times 1.05 \times 1 \times 27 = 26$$

Step 3: Use Table 3.5 to describe the compactness.

For $N = 27$, the soil is medium dense.

(c) The Cone Penetrometer Test (CPT)—ASTM D 5778 The cone penetrometer is a cone with a base area of 10 cm^2 and cone angle of 60° (Figure 3.8a) that is attached to a rod. An outer sleeve encloses the rod. The thrusts required to drive the cone and the sleeve into the ground at a rate of 2 cm/s are measured independently so that the end resistance or cone resistance and side friction or sleeve resistance may be estimated separately. Although originally developed for the design of piles, the cone penetrometer has also been used to estimate the bearing capacity and settlement of foundations.

The piezocone (uCPT or CPTu) is a cone penetrometer that has porous elements inserted into the cone or sleeve to allow for porewater pressure measurements (Figure 3.8b). The measured porewater pressure depends on the location of the porous elements. A load cell is often used to measure the force of penetration. The piezocone is a very useful tool for soil profiling. Researchers have claimed that the

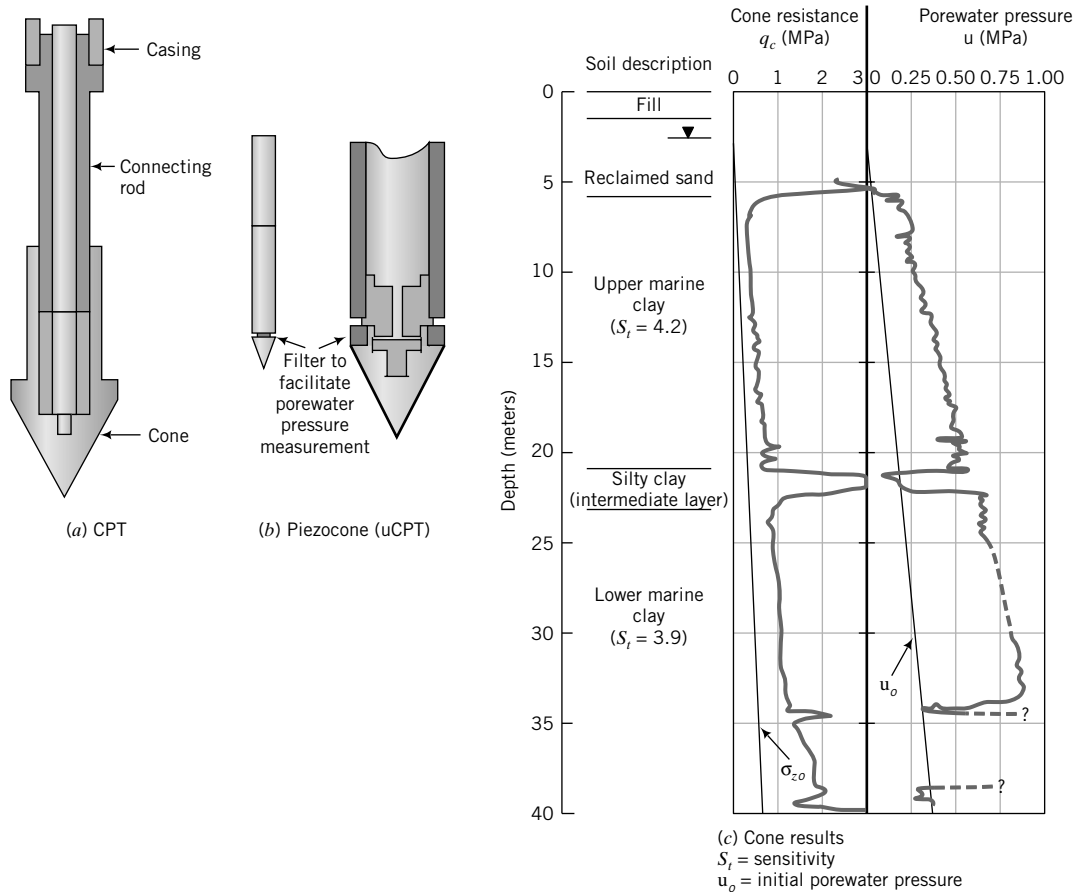


FIGURE 3.8 (a) CPT and (b) piezocone. (c) Piezocone results. (From Chang, 1988.)

piezocone provides useful data to estimate the shear strength, bearing capacity, and consolidation characteristics of soils. Typical results from a piezocone are shown in Figure 3.8c.

Other CPT variants include the seismic cone (SCPT) and the vision cone (VisCPT or VisCPTu). In the SCPT, geophones are installed inside the cone. Hammers on the surface are used to produce surface disturbances, and the resulting seismic waves are recorded by the geophones (usually three). The recorded data are then analyzed to give damping characteristics and soil strength parameters.

The VisCPT and VisCPTu have miniature cameras installed in the CPT probe that provide continuous images of the soil adjacent to the cone. Through image processing, the soil texture can be inferred. The VisCPTu can also be used to detect liquefiable soils.

Regardless of which CPT probe is used, the results are average values of the soil resistance over a length of about 10 cone diameters—about 5 diameters above the tip plus about 5 diameters below the tip. In layered soils, the soil resistances measured by the cone may not represent individual layers, especially thin layers (<5 cone diameters).

The cone resistance is influenced by several soil variables such as stress level, soil density, stratigraphy, soil mineralogy, soil type, and soil fabric. Results of CPT have been correlated with laboratory tests to build empirical relationships for strength and deformation parameters. Investigators have also related CPT results to other field tests, particularly SPT.

CPT is quick to perform, with fewer performance errors compared with SPT. It can provide continuous records of soil conditions. CPT cannot be used in dense, coarse-grained soils (e.g., coarse gravel, boulders) and mixed soils containing boulders, cobbles, clays, and silts. The cone tip is prone to damage from contact with dense objects. The more sophisticated uCPT, SCPT, and VisCPT usually require specialists to perform and to interpret the results.

(d) Pressuremeters—ASTM D 4719-87 (1994) The Menard pressuremeter (Figure 3.9a) is a probe that is placed at the desired depth in an unlined borehole, and pressure is applied to a measuring cell of the probe. The stresses near the probe are shown in Figure 3.9b. The pressure applied is analogous to the expansion of a cylindrical cavity. The pressure is raised in stages at constant time intervals, and volume changes are recorded at each stage. A pressure–volume change curve is then drawn from which the elastic modulus, shear modulus, and undrained shear strength may be estimated.

One of the disadvantages of the Menard pressuremeter is that it has to be inserted into a predrilled hole, and consequently the soil is disturbed. The Cambridge Camkometer (Figure 3.10) is a self-boring pressuremeter, which minimizes soil disturbances. Pressure is applied to radially expand a rubber membrane, which is built into the side wall of the Camkometer, and a feeler gauge measures the radial

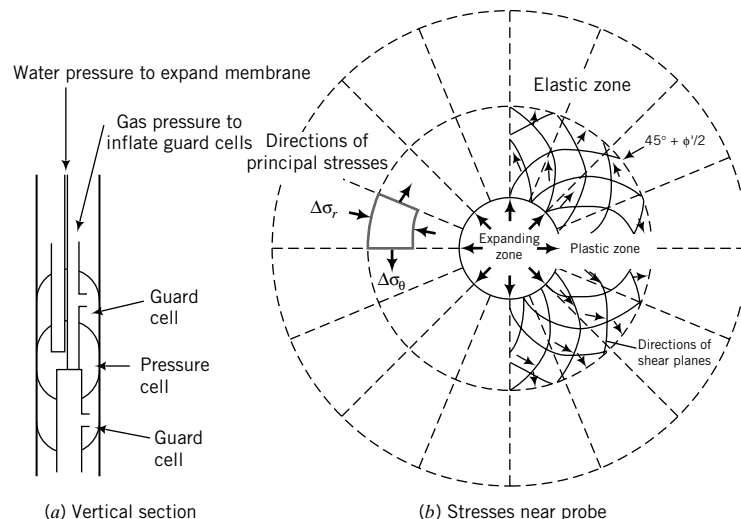


FIGURE 3.9
(a) Menard pressuremeter
and (b) stresses near the
probe.

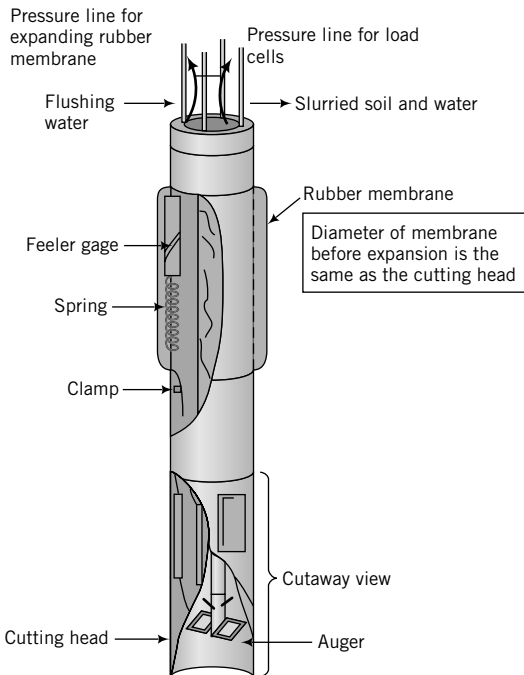


FIGURE 3.10
Schematic of Cambridge Camkometer. (Redrawn from Wroth and Hughes, 1973.)

displacement. Thus, the stress-strain response of the soil can be obtained. Interpretation of the pressuremeter test is beyond the scope of this book.

Pressuremeter tests provide measurement of horizontal stress and estimates of shear modulus and shear strength. Soil disturbance is small when self-boring pressuremeters are used. Pressuremeters are more costly than CPT and the flat plate dilatometer (Section 3.5.7e) and are not widely available. The drainage condition is unknown, and this leads to uncertainty in the interpretation of the test data to estimate the shear modulus and shear strength.

(e) Flat Plate Dilatometer (DMT) The flat plate dilatometer consists of a tapered blade 95 mm wide, 15 mm thick, and 240 mm long (Figure 3.11). On the flat face, the dilatometer is a flexible steel membrane 60 mm in diameter that, when inflated, pushes the soil laterally. The blade is attached to drill rods and is pushed into the soil at a rate of 2 cm/s by a drill rig. Tests are normally conducted every 200 mm. The pneumatic pressures (a) to bring the membrane flush with the soil surface, (b) to push the soil laterally for a distance of 1.1 mm, and (c) at which the membrane returns to its original position are recorded.

Results from dilatometers have been related to undrained shear strength, lateral earth pressures, overconsolidation ratio, and elastic modulus. DMT is simple and quick to conduct. It provides reasonable estimates of horizontal stress and is less costly than the pressuremeter test. Dilatometers cause significant remolding of the soil before the test commences, and the results obtained should be used with caution. The dilatometer test is best suited for clays and sands.

3.5.8 Types of Laboratory Tests

Laboratory tests are needed to classify soils and to determine strength, settlement, and stiffness parameters for design and construction. They allow for better control of the test conditions applied to the soil

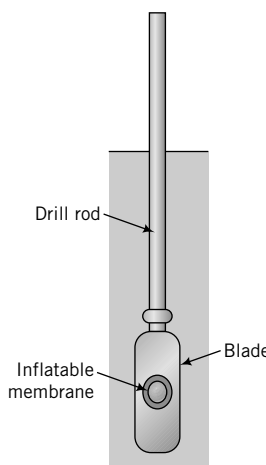


FIGURE 3.11
Flat plate dilatometer.

TABLE 3.6 Summary of Laboratory Tests to Determine Physical Properties

Physical properties	ASTM	Test objective	Parameters determined	Purpose
Specific gravity	D 854	To determine the specific gravity of soils	G_s	To calculate soil density
Grain size determination	D 422 D 1140	To determine the grain size distribution	D_{10} , D_{50} $Cu = \frac{D_{10}}{D_{60}}$ $CC = \frac{D_{30^2}}{D_{10}D_{60}}$	Soil classification
Water content	D 2216	To determine the water content of a soil	w	Qualitative information on strength and deformation
Index test	D 4318	To determine the water content at which soil changes phases	PL, LL, PI, SL, LI	Soil classification; qualitative information on strength and settlement
Compaction	D 698 D 1557	To determine the maximum dry density and optimum water content	$(\gamma_d)_{max}$, w_{opt}	Specification of compaction in the field
Permeability	D 2434	To determine the hydraulic conductivity	k	Estimate of flow of water and seepage forces; stability analysis
Maximum and minimum dry density	D 4253 D 4254	To determine the maximum and minimum dry density of coarse-grained soil	e_{max} e_{min}	Soil classification

than in situ tests. Laboratory test samples are invariably disturbed, and the degree of disturbance can significantly affect the test results. Sufficient care must be taken to reduce testing disturbances. Laboratory tests can be divided into two classes: Class I tests are tests to determine the physical properties; Class II tests are used to determine the mechanical properties. Tables 3.6 and 3.7 summarize these tests. You will learn about them and the meaning and importance of the soil parameters that they measure in later chapters of this textbook.

THE ESSENTIAL POINTS ARE:

1. A number of tools are available for soil exploration. You need to use judgment as to the type that is appropriate for a given project.
2. Significant care and attention to details are necessary to make the results of a soils investigation meaningful.

TABLE 3.7 Summary of Laboratory Mechanical Tests

Test	ASTM	Stress condition	Drainage condition	Soil type	Parameters	Advantages	Disadvantages
Direct shear (DS)	D 3080	Plane strain—stress or strain control	Drained	Coarse-grained	ϕ'_{cs} , ϕ'_{pr} , α_p	<ul style="list-style-type: none"> • Simple • Quick • Commonly available 	<ul style="list-style-type: none"> • Soil fails on predetermined failure plane • Nonuniform stress distribution • Strains cannot be determined
Triaxial (T)	D 4767 D 2850 D 2166 (for UC tests)	Axisymmetric stress or strain control	Drained or undrained	All	ϕ'_{cs} , ϕ'_{pr} , s_{ur} , E , and M	<ul style="list-style-type: none"> • Versatile—two stresses (axial and radial stresses) can be controlled independently • Commonly available 	<ul style="list-style-type: none"> • Principal axes rotate only by 90° instantaneously • Nonuniform stress distribution—reduce by lubricating platen
One-dimensional consolidation	D 2435 D 4186 D 5333 D 454	Axisymmetric	Drained	Fine-grained	C_o , C_r , C_a , C_v , σ'_{zc} , m_v or λ , κ , p'_c	<ul style="list-style-type: none"> • Simple • Readily available 	• One-dimensional
Direct simple shear (DSS)		Plane strain	Drained (constant load) or undrained (constant volume)	All	ϕ'_{cs} , ϕ'_{pr} , s_{ur} , G	<ul style="list-style-type: none"> • Principal axes rotate during test • Closely approximates many field conditions 	<ul style="list-style-type: none"> • Nonuniform stress and strain distributions • Not readily available

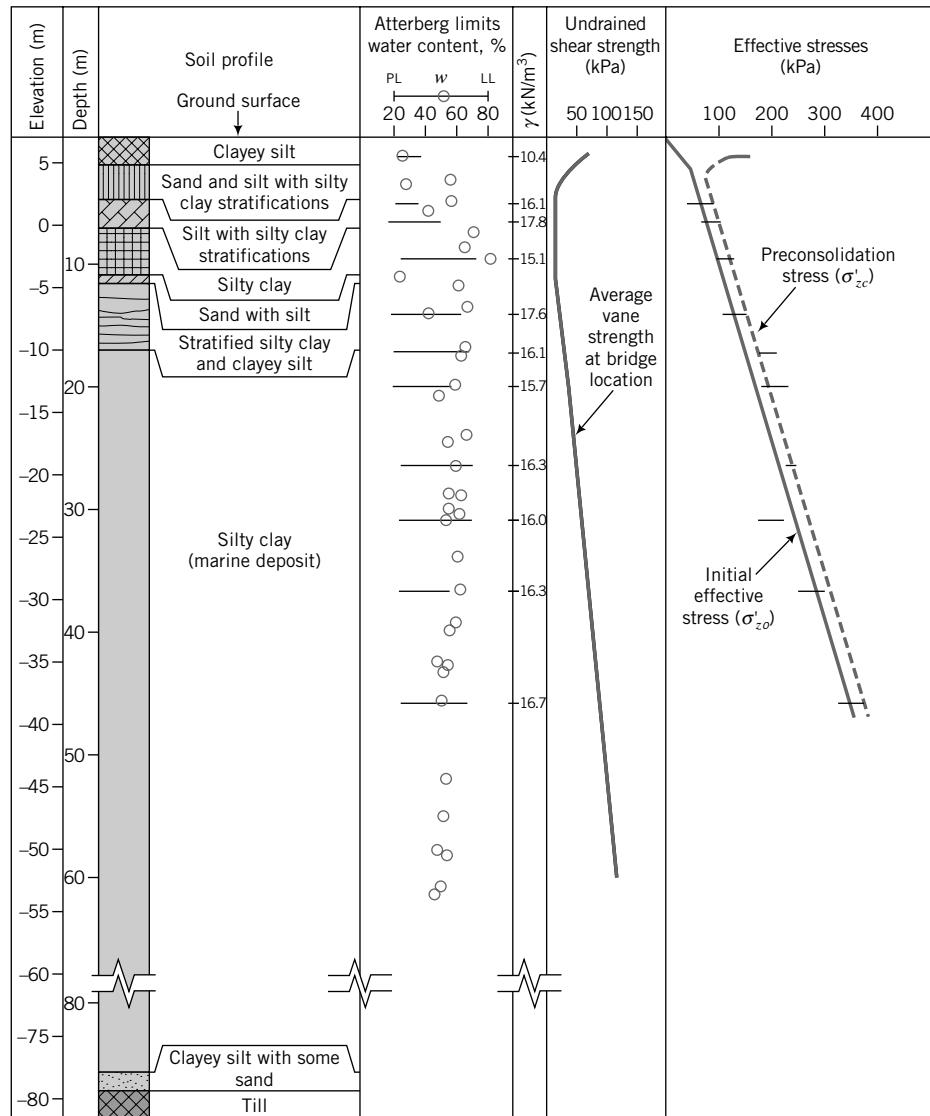


FIGURE 3.12 A borehole log. (Redrawn from Blanchet et al., 1980.)

3.6 SOILS REPORT

A clear, concise, and accurate report of the site investigation must be prepared. The report should contain at a minimum the following:

1. A document (often a letter) authorizing the investigation.
2. A summary of the work done and recommendations (about one page).
3. Scope of work.
4. Description of the site.
5. Details of the types of investigation conducted, soil and groundwater information including lab and field test results, assumptions and limitations of the investigation, and possible construction difficulties. Soil boring logs (a typical one is shown in Figure 3.12) are normally used to summarize the soil

data. A log of each boring should be performed by the geotechnical field personnel. Typically, the boring log should contain the following:

- (a) Name of project and location, including street name.
 - (b) Location of boring—station and offset.
 - (c) Date boring was performed.
 - (d) Surface elevation.
 - (e) Depth and thickness of each stratum, with fill pattern to quickly identify different soil types. A legend of the fill pattern must be included in the soils report.
 - (f) Depths at which samples or in situ tests were conducted, with sample or test numbers.
 - (g) Soil classification of each stratum.
 - (h) Depth to water (if encountered).
6. Analysis and interpretation of the data collected.
 7. Recommendations for design and construction, with discussions of any special provisions.

3.7 SUMMARY

At a project site, the soils must be identified and characterized through a soils investigation. Such an investigation is done in phases and may include geophysical investigations, boreholes, and field and laboratory tests. At the completion of a soils investigation, the client normally requires a carefully written report.

Self-Assessment

Access Chapter 3 at <http://www.wiley.com/college/budhu> to take the end-of-chapter quiz to test your understanding of this chapter.

EXERCISES

- 3.1** In your area, choose a project under construction or a recently constructed project such as a road or a building. Obtain the soils (geotechnical) report and review it.
- 3.2** Obtain borehole logs from a building site in your area. Describe the geology, the methods used in the soils exploration, and the type of field tests used, if any.
- 3.3** On Google Earth (earth.google.com), locate where you live. Conduct a Phase 1 (desk study) investigation, assuming that a five-story office building (50 m wide \times 75 m long \times 18 m high) is planned for that location.
- 3.4** A property developer wants to build a subdivision consisting of 500 residences, a shopping mall, and five office buildings near your college. Assume that the total area is 50 hectares. The developer hires you to conduct a soils investigation as part of the due diligence process. Describe how you would conduct this investigation.

PHYSICAL SOIL STATES AND SOIL CLASSIFICATION

4.0 INTRODUCTION

In engineering, we disassemble complex systems into parts and then study each part and its relationship to the whole. We will do the same for soils. Soils will be dismantled into three constituents, and we will examine how the proportions of each constituent characterize soils. We will also describe tests to determine the physical states of soils. The results of these tests and determination of particle size distribution (Chapter 2) allow us to classify soils.

When you complete this chapter, you should be able to:

- Determine the proportions of the main constituents in a soil.
- Understand how water changes the states of soils, particularly fine-grained soils.
- Determine index properties of soils.
- Classify soils.

Importance

Soils are naturally complex, multiphase materials. They are generally a matrix of an assortment of particles (solids), fluids, and gases. Each influences the behavior of the soil mass as a whole. Unless we understand the composition of a soil mass, we will be unable to estimate how it will behave under loads and how we can use it as a construction material. Geoengineers have devised classification systems based on the results of simple, quick soil tests. These systems help us make decisions about the suitability of particular types of soils for typical geoengineering systems.

Here are two sample practical situations. A highway is proposed to link the city of Noscut to the village of Windsor Forest. The highway route will pass through a terrain that is relatively flat and is expected to be flooded by a 100-year storm event. To support the highway, an embankment will be constructed from soils trucked to the site from two possible pits. You, the geotechnical engineer, are to advise a stakeholders' committee consisting of engineers, farmers, community representatives, and lawyers on the estimated cost of the embankment. In arriving at a cost, you must consider the suitability of the soil in each of the two pits for the embankment, the amount of soil, and the number of truckloads required. A highway under construction is shown in Figure 4.1.

The Palm Islands in Dubai, United Arab Emirates, were constructed in the Arabian Sea using several million cubic meters of sand and rock dredged from the Persian Gulf. The islands, referred to as the "Eighth Wonder of the World," are examples of challenging geotechnical engineering design and construction that require the use of the topics covered in this chapter. These islands are in the shape of palm trees. Rock breakwaters—structures constructed for coastal protection—form the edges of the palm leaves and are filled in by sand sprayed from dredging ships. Learn more about these islands and similar projects by searching the Internet using the key words "Palm Islands Dubai."



FIGURE 4.1 A highway under construction.

4.1 DEFINITIONS OF KEY TERMS

Water content (w) is the ratio of the weight of water to the weight of solids.

Void ratio (e) is the ratio of the volume of void space to the volume of solids.

Porosity (n) is the ratio of the volume of void to the total volume of soil.

Degree of saturation (S) is the ratio of the volume of water to the volume of void.

Bulk unit weight (γ) is the weight density, that is, the weight of a soil per unit volume.

Saturated unit weight (γ_{sat}) is the weight of a saturated soil per unit volume.

Dry unit weight (γ_d) is the weight of a dry soil per unit volume.

Effective unit weight (γ') is the weight of soil solids in a submerged soil per unit volume.

Relative density (D_r) is an index that quantifies the degree of packing between the loosest and densest state of coarse-grained soils.

Swell factor (SF) is the ratio of the volume of excavated material to the volume of in situ material (sometimes called borrow pit material or bank material).

Liquid limit (LL) is the water content at which a soil changes from a plastic state to a liquid state.

Plastic limit (PL) is the water content at which a soil changes from a semisolid to a plastic state.

Shrinkage limit (SL) is the water content at which a soil changes from a solid to a semisolid state without further change in volume.

4.2 QUESTIONS TO GUIDE YOUR READING

1. What are the constituents of soils?
2. What are the relationships among the constituents?
3. What are the effects of water on soils?
4. What are the Atterberg limits?

5. What are index tests and how are they conducted?
6. What are the purposes of classifying soils?
7. How do I classify a soil?
8. Is there a unique soil classification system?

4.3 PHASE RELATIONSHIPS

Soil is composed of solids, liquids, and gases (Figure 4.2a). The solid phase may be minerals, organic matter, or both. As mentioned before, we will not deal with organic matter in this textbook. The spaces between the solids (soil particles) are called voids. Water is often the predominant liquid and air is the predominant gas. We will use the terms water and air instead of liquid and gas. The soil water is called porewater and plays a very important role in the behavior of soils under load. If all the voids are filled by water, the soil is saturated. Otherwise, the soil is unsaturated. If all the voids are filled with air, the soil is said to be dry.

We can idealize the three phases of soil, as shown in Figure 4.2b. The physical properties of soils are influenced by the relative proportions of each of these phases. The total volume of the soil is the sum of the volume of solids (V_s), volume of water (V_w), and volume of air (V_a); that is,

$$V = V_s + V_w + V_a = V_s + V_v \quad (4.1)$$

where

$$V_v = V_w + V_a$$

is the volume of voids. The weight of the soil is the sum of the weight of solids (W_s) and the weight of water (W_w). The weight of air is negligible. Thus,

$$W = W_s + W_w \quad (4.2)$$

The following definitions have been established to describe the proportion of each constituent in soil. Each equation can be presented with different variables. The most popular and convenient forms are given. You should try to memorize these relationships. When you work on these relationships, think about a bread dough in which you have to reconstruct the amount of the constituent ingredients—for example, the amount of flour or water. If you add too much water to a bread dough, it becomes softer and more malleable. The same phenomenon occurs in fine-grained soils.

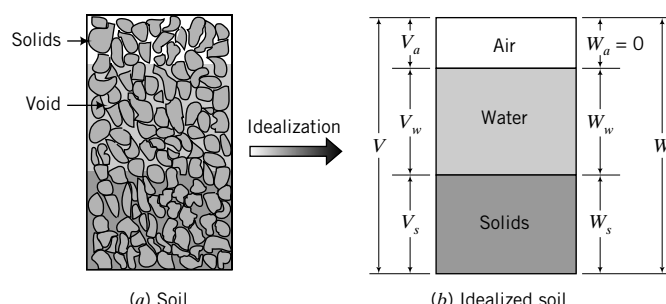


FIGURE 4.2
Soil phases.

1. Water content (w) is the ratio, often expressed as a percentage, of the weight of water to the weight of solids:

$$w = \frac{W_w}{W_s} \times 100\% \quad (4.3)$$

The water content of a soil is found by weighing a sample of the soil and then placing it in an oven at $110 \pm 5^\circ\text{C}$ until the weight of the sample remains constant, that is, all the absorbed water is driven out. For most soils, a constant weight is achieved in about 24 hours. The soil is removed from the oven, cooled, and then weighed. The detailed procedure to determine the water content of soils is described in ASTM D 2216. It is a common mistake to use the total weight in the denominator. Remember, it is the weight (or mass) of the solids.

2. Void ratio (e) is the ratio of the volume of void space to the volume of solids. Void ratio is usually expressed as a decimal quantity.

$$e = \frac{V_v}{V_s} \quad (4.4)$$

3. Specific volume (V') is the volume of soil per unit volume of solids:

$$V' = \frac{V}{V_s} = 1 + e \quad (4.5)$$

This equation is useful in relating volumes, as shown in Example 4.6 and in the calculation of volumetric strains (Chapter 7).

4. Porosity (n) is the ratio of the volume of voids to the total volume. Porosity is usually expressed as a percentage.

$$n = \frac{V_v}{V} \quad (4.6)$$

Porosity and void ratio are related by the expression

$$n = \frac{e}{1 + e} \quad (4.7)$$

Let us prove Equation (4.7). We will start with the basic definition [Eq. (4.6)] and then algebraically manipulate it to get Equation (4.7). The total volume is decomposed into the volume of solids and the volume of voids, and then both the numerator and denominator are divided by the volume of solids; that is,

$$n = \frac{V_v}{V} = \frac{V_v}{V_s + V_v} = \frac{V_v/V_s}{V_s/V_s + V_v/V_s} = \frac{e}{1 + e}$$

The porosity of soils can vary widely. If the particles of coarse-grained soils were spheres, the maximum and minimum porosities would be 48% and 26%, respectively. This is equivalent to maximum and minimum void ratios of 0.91 and 0.35, respectively. The void ratios of real coarse-grained soils vary between 1 and 0.3. Clay soils can have void ratios greater than 1.

5. Specific gravity (G_s) is the ratio of the weight of the soil solids to the weight of water of equal volume:

$$G_s = \frac{W_s}{V_s \gamma_w} \quad (4.8)$$

where $\gamma_w = 9.81 \text{ kN/m}^3$ is the unit weight of water. We will use $\gamma_w = 9.8 \text{ kN/m}^3$ in this book. The specific gravity of soils ranges from approximately 2.6 to 2.8. For most problems, G_s can be assumed, with little error, to be equal to 2.7.

The procedure to determine the specific gravity of soils is described in ASTM D 854. Two types of container are used to determine the specific gravity. One is a pycnometer, which is used for coarse-grained soils. The other is a 50-mL density bottle, which is used for fine-grained soils. The container is weighed and a small quantity of dry soil is placed in it. The mass of the container and the dry soil is determined. De-aired water is added to the soil in the container. The container is then agitated to remove air bubbles. When all air bubbles have been removed, the container is filled with de-aired water. The mass of container, soil, and water is determined. The contents of the container are discarded and the container is thoroughly cleaned. De-aired water is added to fill the container, and the mass of the container and water is determined.

Let M_1 be the mass of the container; M_2 be the mass of the container and dry soil; M_3 be the mass of the container, soil, and water; and M_4 be the mass of the container and water. The mass of dry soil is $M_s = M_2 - M_1$, the mass of water displaced by the soil particles is $M_5 = M_4 - M_3 + M_s$, and $G_s = M_s/M_5$.

6. Degree of saturation (S) is the ratio, often expressed as a percentage, of the volume of water to the volume of voids:

$$S = \frac{V_w}{V_v} = \frac{wG_s}{e} \quad \text{or} \quad Se = wG_s \quad (4.9)$$

If $S = 1$ or 100%, the soil is saturated. If $S = 0$, the soil is bone-dry. It is practically impossible to obtain a soil with $S = 0$.

7. Unit weight is the weight of a soil per unit volume. We will use the term **bulk unit weight**, γ , to denote unit weight:

$$\gamma = \frac{W}{V} = \left(\frac{G_s + Se}{1 + e} \right) \gamma_w \quad (4.10)$$

Special Cases

(a) Saturated unit weight ($S = 1$):

$$\gamma_{sat} = \left(\frac{G_s + e}{1 + e} \right) \gamma_w \quad (4.11)$$

(b) Dry unit weight ($S = 0$):

$$\gamma_d = \frac{W_s}{V} = \left(\frac{G_s}{1 + e} \right) \gamma_w = \frac{\gamma}{1 + w} \quad (4.12)$$

(c) Effective or buoyant unit weight is the weight of a saturated soil, surrounded by water, per unit volume of soil:

$$\gamma' = \gamma_{sat} - \gamma_w = \left(\frac{G_s - 1}{1 + e} \right) \gamma_w \quad (4.13)$$

TABLE 4.1 Typical Values of Unit Weight for Soils

Soil type	γ_{sat} (kN/m ³)	γ_d (kN/m ³)
Gravel	20–22	15–17
Sand	18–20	13–16
Silt	18–20	14–18
Clay	16–22	14–21

Typical values of unit weight of soils are given in Table 4.1.

8. Relative density (D_r) is an index that quantifies the degree of packing between the loosest and densest possible state of coarse-grained soils as determined by experiments:

$$D_r = \frac{e_{max} - e}{e_{max} - e_{min}} \quad (4.14)$$

where e_{max} is the maximum void ratio (loosest condition), e_{min} is the minimum void ratio (densest condition), and e is the current void ratio.

The relative density can also be written as

$$D_r = \frac{\gamma_d - (\gamma_d)_{min}}{(\gamma_d)_{max} - (\gamma_d)_{min}} \left\{ \frac{(\gamma_d)_{max}}{\gamma_d} \right\} \quad (4.15)$$

ASTM D 4253 and ASTM D 4254 outline procedures for the determination of maximum and minimum void ratios for coarse-grained soils. The maximum void ratio is obtained by pouring dry sand, for example, into a mold of volume (V) 2830 cm³ using a funnel. The sand that fills the mold is weighed. If the weight of the sand is W , then by combining Equations (4.10) and (4.12) we get $e_{max} = G_s \gamma_w (V/W) - 1$. The minimum void ratio is determined by vibrating the sand with a weight imposing a vertical stress of 13.8 kPa on top of the sand. Vibration occurs for 8 minutes at a frequency of 3600 Hz and amplitude of 0.064 mm. From the weight of the sand (W_1) and the volume (V_1) occupied by it after vibration, we can calculate the minimum void ratio using $e_{min} = G_s \gamma_w (V_1/W_1) - 1$.

The relative density correlates very well with the strength of coarse-grained soils—denser soils being stronger than looser soils. A description of sand based on relative density and porosity is given in Table 4.2.

TABLE 4.2 Description of Coarse-Grained Soils Based on Relative Density and Porosity

D_r (%)	Porosity, n (%)	Description
0–20	100–80	Very loose
20–40	80–60	Loose
40–70	60–30	Medium dense or firm
70–85	30–15	Dense
85–100	<15	Very dense

9. Swell factor (SF) or free swell factor is the ratio of the volume of excavated material to the volume of in situ material (sometimes called borrow pit material or bank material):

$$SF = \frac{\text{Volume of excavated material}}{\text{Volume of in situ material}} \times 100 (\%) \quad (4.16)$$

Free swell ranges for some clay minerals are shown in Table 4.3.

TABLE 4.3 Ranges of Free Swell for Some Clay Minerals

Clay minerals	Free swell (%)
Calcium montmorillonite (Ca-smectite)	45–145
Sodium montmorillonite (Na-smectite)	1400–1600
Illite	15–120
Kaolinite	5–60

What's next . . . Eight examples will be used to illustrate how to solve a variety of problems involving the constituents of soils. In the first example, we will derive some of the equations describing relationships among the soil constituents.

EXAMPLE 4.1 *Deriving Soil Constituent Relationships*

Prove the following relationships:

$$(a) S = \frac{wG_s}{e}$$

$$(b) \gamma_d = \frac{\gamma}{1 + w}$$

$$(c) \gamma = \left(\frac{G_s + Se}{1 + e} \right) \gamma_w = \frac{G_s \gamma_w (1 + w)}{1 + e}$$

Strategy The proofs of these equations are algebraic manipulations. Start with the basic definition and then manipulate the basic equation algebraically to get the desired form.

Solution 4.1

(a) For this relationship, we proceed as follows:

Step 1: Write down the basic equation.

$$S = \frac{V_w}{V_v}$$

Step 2: Manipulate the basic equation to get the desired equation.

You want to get e in the denominator, and you have V_v . You know that $V_v = eV_s$ and V_w is the weight of water divided by the unit weight of water. From the definition of water content, the weight of water is wW_s . Here is the algebra:

$$V_v = eV_s; \quad V_w = \frac{W_w}{\gamma_w} = \frac{wW_s}{\gamma_w}$$

$$S = \frac{wW_s}{e\gamma_w V_s} = \frac{G_s w}{e}$$

(b) For this relationship, we proceed as follows:

Step 1: Write down the basic equation.

$$\gamma_d = \frac{W_s}{V}$$

Step 2: Manipulate the basic equation to get the new form of the equation.

$$\gamma_d = \frac{W_s}{V} = \frac{W - W_w}{V} = \frac{W}{V} - \frac{wW_s}{V} = \gamma - w\gamma_d$$

$$\therefore \gamma_d + w\gamma_d = \gamma$$

$$\gamma_d = \frac{\gamma}{1 + w}$$

(c) For this relationship, we proceed as follows:

Step 1: Start with the basic equation.

$$\gamma = \frac{W}{V}$$

Step 2: Manipulate the basic equation to get the new form of the equation.

$$\gamma = \frac{W}{V} = \frac{W_s + W_w}{V_s + V_v} = \frac{W_s + wW_s}{V_s + V_v}$$

Substituting $w = Se/G_s$ and $V_v = eV_s$, we obtain

$$\begin{aligned}\gamma &= \frac{W_s(1 + Se/G_s)}{V_s(1 + e)} \\ &= \frac{G_s\gamma_w(1 + Se/G_s)}{1 + e} = \frac{G_s\gamma_w(1 + w)}{1 + e}\end{aligned}$$

or

$$\gamma = \left(\frac{G_s + Se}{1 + e} \right) \gamma_w$$

EXAMPLE 4.2 Specific Gravity of a Coarse-Grained Soil

An ASTM D 854 test was conducted on a sand. The data are as shown below. Calculate the specific gravity.

Mass of pycnometer	= 38.2 grams
Mass of pycnometer and dry soil	= 64.3 grams
Mass of pycnometer, dry soil, and water	= 154.8 grams
Mass of pycnometer and water	= 138.5 grams

Strategy Prepare a table of the data and carry out the calculations as given in Section 4.3 (5. Specific gravity).

Solution 4.2

M_1 = mass of pycnometer	= 38.2 grams
M_2 = mass of pycnometer and dry soil	= 64.3 grams
M_3 = mass of pycnometer, dry soil, and water	= 154.8 grams
M_4 = mass of pycnometer and water	= 138.5 grams
M_s = mass of dry soil = $M_2 - M_1$	= 26.1 grams
M_5 = mass of water displaced by soil particles = $M_4 - M_3 + M_s$	= 9.8 grams
Specific gravity, $G_s = M_s/M_5$	2.66

EXAMPLE 4.3 Calculation of Void Ratio and Porosity

A container of volume $2.83 \times 10^{-3} \text{ m}^3$ weighs 9.8 N. Dry sand was poured to fill the container. The container and the sand weigh 52.3 N. Calculate (a) the void ratio and (b) the porosity. Describe the condition of the soil (loose or dense). Assume $G_s = 2.7$.

Strategy Since you know the volume and the dry unit weight, you can calculate the dry density and then find e using Equation (4.12). The porosity can be found using the void ratio–porosity relationship.

Solution 4.3

Step 1: Calculate the weight of dry sand.

$$\begin{aligned}\text{Weight of sand and container} &= 52.3 \text{ N} \\ \text{Weight of container} &= 9.8 \text{ N} \\ \text{Weight of dry sand, } W_s &= 52.3 - 9.8 = 42.5 \text{ N} = 0.0425 \text{ kN}\end{aligned}$$

Step 2: Calculate dry unit weight.

$$\gamma_d = \frac{W_s}{V} = \frac{0.0425}{2.83 \times 10^{-3}} = 15 \text{ kN/m}^3$$

Step 3: Calculate the void ratio.

$$\text{Equation (4.12):} \quad \gamma_d = \frac{W_s}{V} = \frac{G_s}{1+e} \gamma_w$$

Solving for e , we get

$$e = G_s \frac{\gamma_w}{\gamma_d} - 1 = 2.7 \frac{9.8}{15} - 1 = 0.764$$

Step 4: Calculate the porosity.

$$\text{Equation (4.7):} \quad n = \frac{e}{1+e} = \frac{0.764}{1+0.764} = 0.43 = 43\%$$

Step 5: Describe the soil.

Table 4.2: For $n = 43\%$, the sand is medium dense or firm.

EXAMPLE 4.4 Calculating Soil Constituents

A sample of saturated clay was placed in a container and weighed. The weight was 6 N. The clay in its container was placed in an oven for 24 hours at 105°C. The weight reduced to a constant value of 5 N. The weight of the container is 1 N. If $G_s = 2.7$, determine the (a) water content, (b) void ratio, (c) bulk unit weight, (d) dry unit weight, and (e) effective unit weight.

Strategy Write down what is given and then use the appropriate equations to find the unknowns. You are given the weight of the natural soil, sometimes called the wet weight, and the dry weight of the soil. The difference between these will give the weight of water, and you can find the water content by using Equation (4.3). You are also given a saturated soil, which means that $S = 1$.

Solution 4.4

Step 1: Write down what is given.

$$\text{Weight of sample + container} = 6 \text{ N}$$

$$\text{Weight of dry sample + container} = 5 \text{ N}$$

Step 2: Determine the weight of water and the weight of dry soil.

$$\text{Weight of water: } W_w = 6 - 5 = 1 \text{ N}$$

$$\text{Weight of dry soil: } W_d = 5 - 1 = 4 \text{ N}$$

Step 3: Determine the water content.

$$w = \frac{W_w}{W_s} \times 100 = \frac{1}{4} \times 100 = 25\%$$

Note: The denominator is the weight of solids, not the total weight.

Step 4: Determine the void ratio.

$$e = \frac{wG_s}{S} = \frac{0.25 \times 2.7}{1} = 0.675$$

Step 5: Determine the bulk unit weight.

$$\gamma = \frac{W}{V} = \frac{G_s \gamma_w (1 + w)}{1 + e} \quad (\text{see Example 4.1})$$

$$\gamma = \frac{2.7 \times 9.8(1 + 0.25)}{1 + 0.675} = 19.7 \text{ kN/m}^3$$

In this case the soil is saturated, so the bulk unit weight is equal to the saturated unit weight.

Step 6: Determine the dry unit weight.

$$\gamma_d = \frac{W_s}{V} = \left(\frac{G_s}{1 + e} \right) \gamma_w = \frac{2.7}{1 + 0.675} \times 9.8 = 15.8 \text{ kN/m}^3$$

or

$$\gamma_d = \left(\frac{\gamma}{1 + w} \right) = \frac{19.7}{1 + 0.25} = 15.8 \text{ kN/m}^3$$

Step 7: Determine the effective unit weight.

$$\gamma' = \left(\frac{G_s - 1}{1 + e} \right) \gamma_w = \left(\frac{2.7 - 1}{1 + 0.675} \right) \times 9.8 = 9.9 \text{ kN/m}^3$$

or

$$\gamma' = \gamma_{sat} - \gamma_w = 19.7 - 9.8 = 9.9 \text{ kN/m}^3$$

EXAMPLE 4.5 Calculation of Water Content of an Unsaturated Soil

The void space in a soil sample consists of 80% air and 20% water. The dry unit weight is $\gamma_d = 15.7 \text{ kN/m}^3$ and $G_s = 2.7$. Determine the water content.

Strategy You can calculate the void ratio from Equation (4.12) and the degree of saturation because you know the amount of air and water in the voids. Then use Equation (4.9) to find the water content.

Solution 4.5

Step 1: Calculate the void ratio from the dry unit weight.

$$\gamma_d = \frac{G_s \gamma_w}{1 + e}$$

$$e = \frac{G_s \gamma_w}{\gamma_d} - 1 = \frac{2.7 \times 9.8}{15.7} - 1 = 0.685$$

Step 2: Calculate the water content.

$$Se = w G_s$$

$$w = Se/G_s$$

We need to find the degree of saturation, as this is the only unknown value apart from w .

The degree of saturation is the ratio of the volume of water to the volume of voids. Since the volume of water is 20% of the void volume, the degree of saturation is 20%, i.e., $S = 0.2$.

$$w = \frac{Se}{G_s} = \frac{0.2 \times 0.685}{2.7} = 0.051 = 5.1\%$$

Alternatively:

You could substitute $e = w G_s/S$ in the equation for dry unit weight in Step 1 and find w directly instead of finding e first.

EXAMPLE 4.6 Determination of Aggregate Requirement for a Roadway

Aggregates from a material storage site are required for the embankment of a roadway. The porosity of the aggregates at the storage site is 80%, and the desired porosity of the compacted aggregates in the embankment is 20%. For a section of the embankment 7.6 m wide \times 0.61 m compacted thickness \times 305 m long, calculate the volume of aggregates required.

Strategy The simplest way is to find a relationship between the n and the volume of the aggregate.

Solution 4.6

Step 1: Calculate the volume of the embankment.

$$V_{emb} = 7.6 \times 0.61 \times 305 = 1414 \text{ m}^3$$

Step 2: Calculate the volume of aggregate required.

Let V_{ss} = volume required from the storage site, and V_{emb} = volume of embankment.

$$\frac{V_{ss}}{V_{emb}} = \frac{1 + e_{ss}}{1 + e_{emb}} = \frac{1 - \frac{e_{emb}}{1 + e_{emb}}}{1 - \frac{e_{ss}}{1 + e_{ss}}} = \frac{1 - n_{emb}}{1 - n_{ss}} = \frac{1 - 0.2}{1 - 0.8} = 4$$

$$V_{emb} = 4 \times 1414 = 5656 \text{ m}^3$$

EXAMPLE 4.7 Application of Soil Constituent Relationships to a Practical Problem

An embankment for a highway is to be constructed from a soil compacted to a dry unit weight of 18 kN/m^3 . The clay has to be trucked to the site from a borrow pit. The bulk unit weight of the soil in the borrow pit is 17 kN/m^3 and its natural water content is 5%. Calculate the volume of clay from the borrow pit required for 1 cubic meter of embankment. The swell factor is 1.2 (20% free swell). Assume $G_s = 2.7$.

Strategy This problem can be solved in many ways. We will use two of these ways. One way is direct; the other a bit longer. In the first way, we are going to use the ratio of the dry unit weight of the compacted soil to that of the borrow pit soil to determine the volume. In the second way, we will use the specific volume. In this case, we need to find the void ratio for the borrow pit clay and the desired void ratio for the embankment. We can then relate the specific volumes of the embankment and the borrow pit clay.

Solution 4.7

Step 1: Find the dry unit weight of the borrow pit soil.

$$\gamma_d = \frac{\gamma}{1 + w} = \frac{17}{1 + 0.05} = 16.2 \text{ kN/m}^3$$

Step 2: Find the volume of borrow pit soil required.

Without consideration of swell factor:

$$\text{Volume of borrow pit soil required per } \text{m}^3 = \frac{(\gamma_d)_{compacted \text{ soil}}}{(\gamma_d)_{borrow \text{ pit} \text{ soil}}} = \frac{18}{16.2} = 1.11 \text{ m}^3$$

With consideration of swell factor:

$$\text{Volume required} = \text{SF} \times \text{volume of borrow pit soil required} = 1.2 \times 1.11 = 1.33 \text{ m}^3$$

Alternatively:

Step 1: Define parameters for the borrow pit and embankment. Let

V'_1, e_1 = specific volume and void ratio, respectively, of borrow pit clay
 V'_2, e_2 = specific volume and void ratio, respectively, of compacted clay

Step 2: Determine e_1 and e_2 .

$$\gamma_d = \frac{\gamma}{1 + w} = \frac{17}{1 + 0.05} = 16.2 \text{ kN/m}^3$$

But

$$\gamma_d = \frac{G_s}{1 + e_1} \gamma_w$$

and therefore

$$e_1 = G_s \frac{\gamma_w}{\gamma_d} - 1 = 2.7 \left(\frac{9.8}{16.2} \right) - 1 = 0.633$$

Similarly,

$$e_2 = G_s \frac{\gamma_w}{\gamma_d} - 1 = 2.7 \left(\frac{9.8}{18} \right) - 1 = 0.47$$

Step 3: Determine the volume of borrow pit material.

$$\frac{V'_1}{V'_2} = \frac{1 + e_1}{1 + e_2}$$

Therefore,

$$V'_1 = V'_2 \frac{1 + e_1}{1 + e_2} = 1 \left(\frac{1 + 0.633}{1 + 0.47} \right) = 1.11 \text{ m}^3$$

Considering the swell, we get

$$\text{Volume required} = \text{SF} \times \text{volume of borrow pit soil required} = 1.2 \times 1.11 = 1.33 \text{ m}^3$$

EXAMPLE 4.8 Application of Soil Constituent Relationships to a Practical Problem

If the borrow soil in Example 4.7 were to be compacted to attain a dry unit weight of 18 kN/m³ at a water content of 7%, determine the amount of water required per cubic meter of embankment, assuming no loss of water during transportation.

Strategy Since water content is related to the weight of solids and not the total weight, we need to use the data given to find the weight of solids.

Solution 4.8

Step 1: Determine the weight of solids per unit volume of borrow pit soil.

$$W_s = \frac{\gamma}{1 + w} = \frac{17}{1 + 0.05} = 16.2 \text{ kN/m}^3$$

Step 2: Determine the amount of water required.

$$\text{Additional water} = 7 - 5 = 2\%$$

$$\text{Weight of water} = W_w = wW_s = 0.02 \times 16.2 = 0.32 \text{ kN}$$

$$V_w = \frac{W_w}{\gamma_w} = \frac{0.32}{9.8} = 0.033 \text{ m}^3 = 33 \text{ liters}$$

What's next . . . Water significantly influences the strength and deformation of fine-grained soils. In the next section, we discuss how water changes the state of fine-grained soils.

4.4 PHYSICAL STATES AND INDEX PROPERTIES OF FINE-GRAINED SOILS

The physical and mechanical behavior of fine-grained soils is linked to four distinct states: solid, semisolid, plastic, and liquid, in order of increasing water content. Let us consider a soil initially in a liquid state that is allowed to dry uniformly. If we plot a diagram of volume versus water content as shown in Figure 4.3, we can locate the original liquid state as point *A*. As the soil dries, its water content reduces and, consequently, so does its volume (see Figure 4.2b).

At point *B*, the soil becomes so stiff that it can no longer flow as a liquid. The boundary water content at point *B* is called the liquid limit; it is denoted by LL. As the soil continues to dry, there is a range of water content at which the soil can be molded into any desired shape without rupture. The soil at this state is said to exhibit plastic behavior—the ability to deform continuously without rupture. But if drying is continued beyond the range of water content for plastic behavior, the soil becomes a semisolid. The soil cannot be molded now without visible cracks appearing. The water content at which the soil changes from a plastic to a semisolid is known as the plastic limit, denoted by PL. The range of water contents over which the soil deforms plastically is known as the plasticity index, PI:

$$\text{PI} = \text{LL} - \text{PL} \quad (4.17)$$

As the soil continues to dry, it comes to a final state called the solid state. At this state, no further volume change occurs since nearly all the water in the soil has been removed. The water content at which the soil changes from a semisolid to a solid is called the shrinkage limit, denoted by SL. The shrinkage limit is useful for the determination of the swelling and shrinking capacity of soils. The liquid and plastic limits are called the Atterberg limits after their originator, Swedish soil scientist A. Atterberg (1911).

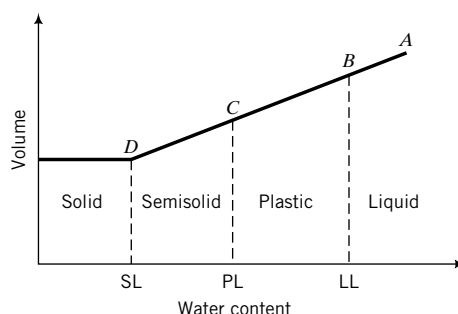


FIGURE 4.3
Changes in soil states
as a function of soil volume
and water content.

TABLE 4.4 Description of the Strength of Fine-Grained Soils Based on Liquidity Index

Values of LI	Description of soil strength
LI < 0	Semisolid state—high strength, brittle, (sudden) fracture is expected
0 < LI < 1	Plastic state—intermediate strength, soil deforms like a plastic material
LI > 1	Liquid state—low strength, soil deforms like a viscous fluid

We have changed the state of fine-grained soils by changing the water content. Since engineers are interested in the strength and deformation of materials, we can associate specific strength characteristics with each of the soil states. At one extreme, the liquid state, the soil has the lowest strength and the largest deformation. At the other extreme, the solid state, the soil has the largest strength and the lowest deformation. A measure of soil strength using the Atterberg limits is known as the liquidity index (LI) and is expressed as

$$LI = \frac{w - PL}{PI} \quad (4.18)$$

The liquidity index is the ratio of the difference in water content between the natural or in situ water content of a soil and its plastic limit to its plasticity index. Table 4.4 shows a description of soil strength based on values of LI.

Typical values for the Atterberg limits for soils are shown in Table 4.5. The Atterberg limits depend on the type of predominant mineral in the soil. If montmorillonite is the predominant mineral, the liquid limit can exceed 100%. Why? Recall that the bond between the layers in montmorillonite is weak and large amounts of water can easily infiltrate the spaces between the layers. In the case of kaolinite, the layers are held relatively tightly and water cannot easily infiltrate between the layers in comparison with montmorillonite. Therefore, you can expect the Atterberg limits for kaolinite to be, in general, much lower than those for either montmorillonite or illite.

Skempton (1953) showed that for soils with a particular mineralogy, the plasticity index is linearly related to the amount of the clay fraction. He coined a term called activity (A) to describe the importance of the clay fractions on the plasticity index. The equation for A is

$$A = \frac{PI}{\text{Clay fraction (\%)}} \quad (4.19)$$

TABLE 4.5 Typical Atterberg Limits for Soils

Soil type	LL (%)	PL (%)	PI (%)
Sand		Nonplastic	
Silt	30–40	20–25	10–15
Clay	40–150	25–50	15–100
Minerals			
Kaolinite	50–60	30–40	10–25
Illite	95–120	50–60	50–70
Montmorillonite	290–710	50–100	200–660

TABLE 4.6 Activity of Clay-Rich Soils

Description	Activity, A
Inactive	<0.75
Normal	0.75–1.25
Active	1.25–2
Very (highly) active (e.g., bentonite)	>6
Minerals	
Kaolinite	0.3–0.5
Illite	0.5–1.3
Na-montmorillonite	4–7
Ca-montmorillonite	0.5–2.0

You should recall that the clay fraction is the amount of particles less than 2 μm . Activity is one of the factors used in identifying expansive or swelling soils. Typical values of activity are given in Table 4.6.

EXAMPLE 4.9 Calculation of Plasticity Index, Liquidity Index, and Activity

A fine-grained soil has a liquid limit of 300% and a plastic limit of 55%. The natural water content of the soil in the field is 80% and the clay content is 60%.

- (a) Determine the plasticity index, the liquidity index, and the activity.
- (b) What is the soil state in the field?
- (c) What is the predominant mineral in this soil?
- (d) If this soil were under a concrete slab used as a foundation for a building and water were to seep into it from watering of a lawn, what would you expect to happen to the foundation?

Strategy Use Equations (4.16–4.19) and Tables 4.4, 4.5, and 4.6 to answer the questions asked.

Solution 4.9

Step 1: Calculate the plasticity index, liquidity index, and activity.

(a) $\text{PI} = \text{LL} - \text{PL} = 300 - 55 = 245\%$

$$\text{LI} = \frac{w - \text{PL}}{\text{PI}} = \frac{80 - 55}{245} = 0.1$$

$$A = \frac{\text{PI}}{\text{Clay fraction (\%)}} = \frac{245}{60} = 4.1$$

Step 2: Determine the state of the soil in the field.

- (b) Based on Table 4.4, the soil with $\text{LI} = 0.1$ is at the low end of the plastic state.

Step 3: Determine the predominant mineral.

- (c) From Tables 4.5 and 4.6, the predominant mineral is montmorillonite (most likely Na-montmorillonite).

Step 4: Determine the consequences of water seeping into the soil.

(d) Seepage from lawn watering will cause the soil to expand (montmorillonite is an expansive soil). Because the water content in the montmorillonite will not increase uniformly under the foundation, the expansion will not be uniform. More expansion will occur at the edge of the slab because the water content will be greater there. Consequently, the concrete foundation will curl upward at the edge and most likely crack. Construction on expansive soils requires special attention to water management issues such as drainage and landscape. Generally, plants and lawns should be at least 3 m away from the edge of the foundation and the land should be sculpted to drain water away from the foundation.

What's next . . . In the next section we discuss tests, called index tests, to determine the Atterberg limits and shrinkage limits of fine-grained soils.

4.5 DETERMINATION OF THE LIQUID, PLASTIC, AND SHRINKAGE LIMITS

4.5.1 Casagrande Cup Method—ASTM D 4318

The liquid limit is determined from an apparatus (Figure 4.4) that consists of a semispherical brass cup that is repeatedly dropped onto a hard rubber base from a height of 10 mm by a cam-operated mechanism. Arthur Casagrande (1932) developed this apparatus, and the procedure for the test is called the Casagrande cup method.

A dry powder of the soil is mixed with distilled water into a paste and placed in the cup to a thickness of about 12.5 mm. The soil surface is smoothed and a groove is cut into the soil using a standard grooving tool. The crank operating the cam is turned at a rate of 2 revolutions per second, and the number of blows required to close the groove over a length of 12.5 mm is counted and recorded. A specimen of soil within the closed portion is extracted for determination of the water content. The liquid limit is defined as the water content at which the groove cut into the soil will close over a distance of 12.5 mm following 25 blows. This is difficult to achieve in a single test. Four or more tests at different water contents are usually required for terminal blows (number of blows to close the groove over a distance of 12.5 mm) ranging from 10 to 40. The results are presented in a plot of water content (ordinate, arithmetic scale) versus terminal blows (abscissa, logarithmic scale) as shown in Figure 4.5.

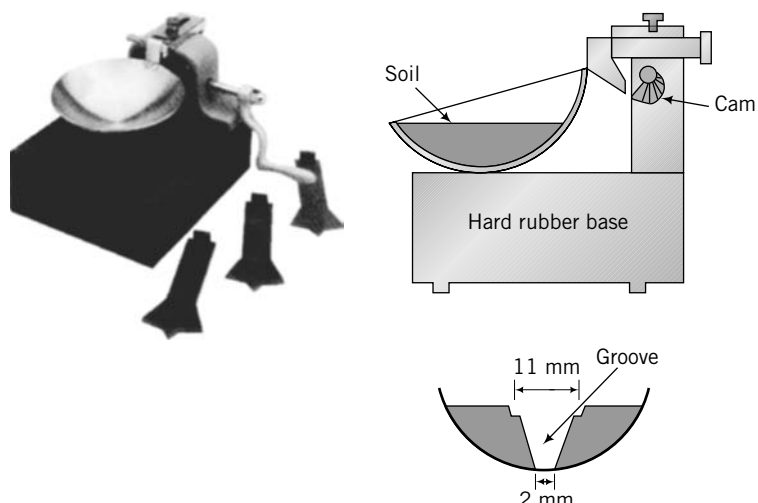
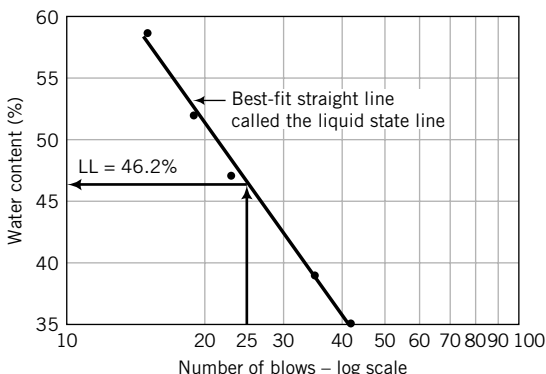


FIGURE 4.4 Cup apparatus for the determination of liquid limit.
(Photo courtesy of Geotest.)

**FIGURE 4.5**

Typical liquid limit results from the Casagrande cup method.

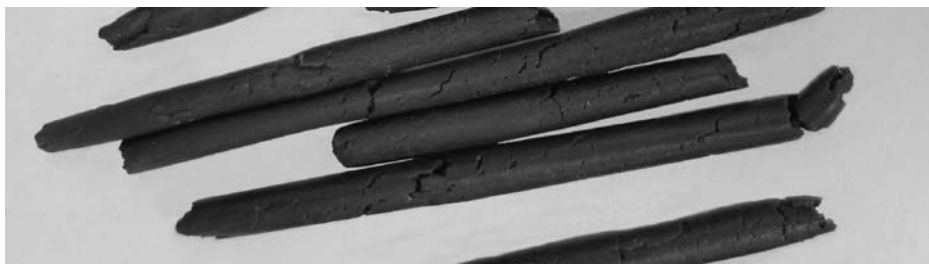
The best-fit straight line to the data points, usually called the flow line, is drawn. We will call this line the liquid state line to distinguish it from flow lines used in describing the flow of water through soils. The liquid limit is read from the graph as the water content on the liquid state line corresponding to 25 blows.

The cup method of determining the liquid limit has many shortcomings. Two of these are:

1. The tendency of soils of low plasticity to slide and to liquefy with shock in the cup rather than to flow plastically.
2. Sensitivity to operator technique and to small differences in apparatus.

4.5.2 Plastic Limit Test—ASTM D 4318

The plastic limit is determined by rolling a small clay sample into threads and finding the water content at which threads approximately 3 mm in diameter will just start to crumble (Figure 4.6). Two or more determinations are made, and the average water content is reported as the plastic limit.

**FIGURE 4.6** Soil at plastic limit.

4.5.3 Fall Cone Method to Determine Liquid and Plastic Limits

A fall cone test, popular in Europe and Asia, appears to offer a more accurate (less prone to operator's errors) method of determining both the liquid and plastic limits. In the fall cone test (Figure 4.7), a cone with an apex angle of 30° and total mass of 80 grams is suspended above, but just in contact with, the soil sample. The cone is permitted to fall freely for a period of 5 seconds. The water content corresponding to a cone penetration of 20 mm defines the liquid limit.

The sample preparation is similar to the cup method except that the sample container in the fall cone test has a different shape and size (Figure 4.7). Four or more tests at different water contents are also required because of the difficulty of achieving the liquid limit from a single test. The results are plotted as water content (ordinate, logarithmic scale) versus penetration (abscissa, logarithmic scale), and

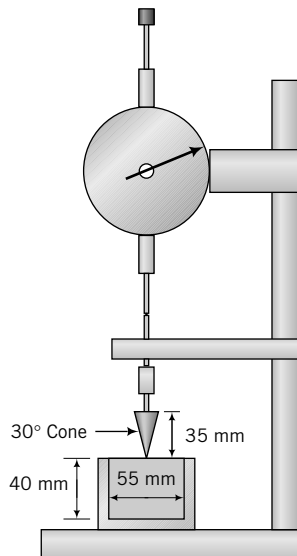


FIGURE 4.7
Fall cone apparatus.

the best-fit straight line (liquid state line) linking the data points is drawn (Figure 4.8). The liquid limit is read from the plot as the water content on the liquid state line corresponding to a penetration of 20 mm.

The plastic limit is found by projecting the best fit-straight line backward to intersect the water content axis at a depth of penetration of 1 mm. The water content at this depth of penetration (1 mm) is C. The plastic limit is given as (Feng, 2000):

$$PL = C(2)^m \quad (4.20)$$

where m is the slope (taken as positive) of the best-fit straight line. If you use a spreadsheet program, you can obtain C and m from a power trend line function that gives the best-fit equation.

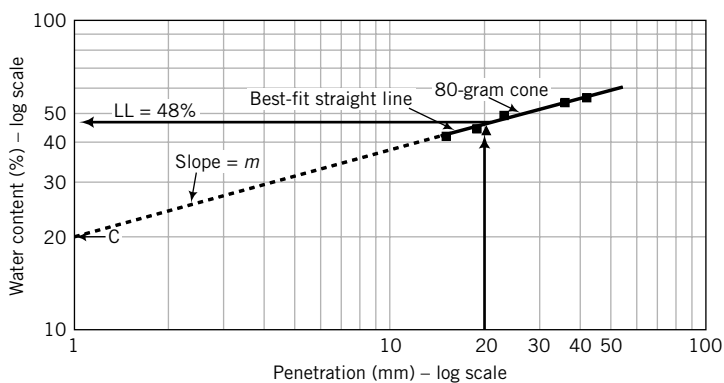


FIGURE 4.8 Typical fall cone test results.

4.5.4 Shrinkage Limit—ASTM D 427 and D 4943

The shrinkage limit is determined as follows. A mass of wet soil, M_1 , is placed in a porcelain dish 44.5 mm in diameter and 12.5 mm high and then oven-dried. The volume of oven-dried soil is determined

by using mercury (ASTM D 427) to occupy the vacant spaces caused by shrinkage. The mass of the mercury is determined, and the volume decrease caused by shrinkage can be calculated from the known density of mercury. The shrinkage limit is calculated from

$$SL = \left(\frac{M_1 - M_2}{M_2} - \frac{V_1 - V_2}{M_2} \frac{\gamma_w}{g} \right) \times 100 = \left(w - \frac{V_1 - V_2}{M_2} \frac{\gamma_w}{g} \right) \times 100 \quad (4.21)$$

where M_1 is the mass of the wet soil, M_2 is the mass of the oven-dried soil, w is water content (not in percentage), V_1 is the volume of wet soil, V_2 ($= \frac{\text{mass of mercury}}{\text{density of mercury}}$) is the volume of the oven-dried soil, and g is the acceleration due to gravity (9.8 m/s^2).

The linear shrinkage ratio, LS, is

$$LS = 1 - \sqrt[3]{\frac{V_2}{V_1}} \quad (4.22)$$

The shrinkage ratio is

$$SR = \frac{M_2 g}{V_2 \gamma_w} \quad (4.23)$$

The range of water content from the plastic limit to the shrinkage limit is called the shrinkage index (SI),

$$SI = PL - SL \quad (4.24)$$

The shrinkage limit can be estimated from the liquid limit and plasticity index by the following empirical expression:

$$SL = 46.4 \left(\frac{LL + 45.5}{PI + 46.4} \right) - 43.5 \quad (4.25)$$

where LL and PI are in percent.

THE ESSENTIAL POINTS ARE:

- 1. Fine-grained soils can exist in one of four states: solid, semisolid, plastic, or liquid.**
- 2. Water is the agent that is responsible for changing the states of soils.**
- 3. A soil gets weaker if its water content increases.**
- 4. Three limits are defined based on the water content that causes a change of state. These are the liquid limit—the water content that caused the soil to change from a liquid to a plastic state; the plastic limit—the water content that caused the soil to change from a plastic to a semisolid; and the shrinkage limit—the water content that caused the soil to change from a semisolid to a solid state. All these limiting water contents are found from laboratory tests.**
- 5. The plasticity index defines the range of water content for which the soil behaves like a plastic material.**
- 6. The liquidity index gives a qualitative measure of strength.**
- 7. The soil strength is lowest at the liquid state and highest at the solid state.**

EXAMPLE 4.10 Interpreting Casagrande's Cup Data

A liquid limit test, conducted on a soil sample in the cup device, gave the following results:

Number of blows	10	19	23	27	40
Water content (%)	60.0	45.2	39.8	36.5	25.2

Two determinations for the plastic limit gave water contents of 20.3% and 20.8%. Determine (a) the liquid limit and plastic limit, (b) the plasticity index, (c) the liquidity index if the natural water content is 27.4%, and (d) the void ratio at the liquid limit if $G_s = 2.7$. If the soil were to be loaded to failure, would you expect a brittle failure?

Strategy To get the liquid limit, you must make a semilogarithmic plot of water content versus number of blows. Use the data to make your plot, then extract the liquid limit (water content on the liquid state line corresponding to 25 blows). Two determinations of the plastic limit were made, and the differences in the results were small. So, use the average value of water content as the plastic limit.

Solution 4.10

Step 1: Plot the data.

See Figure E4.10.

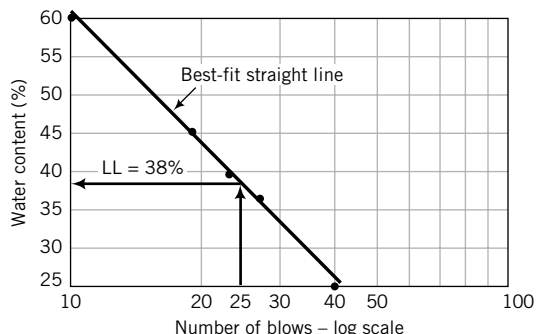


FIGURE E4.10

Plot of the liquid state line for the liquid limit by the Casagrande cup method.

Step 2: Extract the liquid limit.

The water content on the liquid state line corresponding to a terminal blow of 25 gives the liquid limit.

$$LL = 38\%$$

Step 3: Calculate the plastic limit.

The plastic limit is

$$PL = \frac{20.3 + 20.8}{2} = 20.6\%$$

Step 4: Calculate PI.

$$PI = LL - PL = 38 - 20.6 = 17.4\%$$

Step 5: Calculate LI.

$$LI = \frac{(w - PL)}{PI} = \frac{27.4 - 20.6}{17.4} = 0.39$$

Step 6: Calculate the void ratio.

Assume the soil is saturated at the liquid limit. For a saturated soil, $e = wG_s$. Thus,

$$e_{LL} = LLG_s = 0.38 \times 2.7 = 1.03$$

Brittle failure is not expected, as the soil is in a plastic state ($0 < LI < 1$).

EXAMPLE 4.11 Interpreting Fall Cone Data

The results of a fall cone test are shown in the table below.

Cone mass	80-gram cone				
Penetration (mm)	5.5	7.8	14.8	22	32
Water content (%)	39.0	44.8	52.5	60.3	67

Determine (a) the liquid limit, (b) the plastic limit, (c) the plasticity index, and (d) the liquidity index if the natural water content is 46%.

Strategy Adopt the same strategy as in Example 4.10. Make a plot of water content versus penetration, both at logarithmic scale. Use the data to make your plot, then extract the liquid limit (water content on the liquid state line corresponding to 20 mm). Find the water content difference between the two liquid state lines at any fixed penetration. Use this value to determine the plastic limit from Equation (4.20).

Solution 4.11

Step 1: Plot the data.

See Figure E4.11.

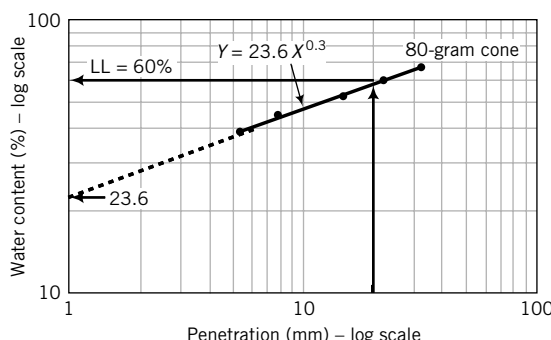


FIGURE E4.11
Plot of fall cone results.

Step 2: Extract the liquid limit.

$$LL = 60\%$$

Step 3: Determine the plastic limit.

The best-fit straight line for the 80-gram cone is $Y = 23.6X^{0.3}$ where Y is water content and X is penetration. Therefore, $C = 23.6$ and $m = 0.3$. From Equation (4.20):

$$\begin{aligned} PL &= C(2)^m = 23.6(2)^{0.3} \\ &= 29\% \end{aligned}$$

Step 4: Determine PI.

$$\text{PI} = \text{LL} - \text{PL} = 60 - 29 = 31\%$$

Step 5: Determine LI.

$$\text{LI} = \frac{w - \text{PL}}{\text{PI}} = \frac{46 - 29}{31} = 0.55$$

EXAMPLE 4.12 Determination of the Shrinkage Limit

The following results were recorded in a shrinkage limit test using mercury. Determine the shrinkage limit.

Mass of container	17.5 grams
Mass of wet soil and container	78.1 grams
Mass of dish	130.0 grams
Mass of dish and displaced mercury	462.0 grams
Mass of dry soil and container	64.4 grams

Strategy Use a table to conduct the calculation based on Equation (4.21).

Solution 4.12

Step 1: Set up a table or, better yet, use a spreadsheet to carry out the calculations.

M_c = mass of container	17.5 grams
M_{wc} = mass of wet soil and container	78.1 grams
M_d = mass of dish	130.0 grams
M_{dm} = mass of dish and displaced mercury	462.0 grams
ρ_m = density of mercury	13.6 grams/cm ³
M_{dc} = mass of dry soil and container	64.4 grams
V_1 = volume of wet soil	32.4 cm ³
V_2 = volume of oven-dried soil	24.4 cm ³
M_1 = mass of wet soil	60.6 grams
M_2 = mass of dry soil	46.9 grams
Shrinkage limit = $((M_1 - M_2)/M_2) - ((V_1 - V_2)/M_2) \gamma_w/g$ 100	12.1%

What's next . . . We now know how to obtain some basic soil data—particle size and indices—from quick, simple tests. The question that arises is: What do we do with these data? Engineers would like to use them to get a first impression on the use and possible performance of a soil for a particular purpose such as a construction material for an embankment. This is currently achieved by classification systems. Next, we will study a few of these systems.

4.6 SOIL CLASSIFICATION SCHEMES

A classification scheme provides a method of identifying soils in a particular group that would likely exhibit similar characteristics. In Chapter 2, Section 5, you were introduced to how some of these schemes classify soils based on particle size only. Soil classification is used to specify a certain soil type that is best suited for a given application. Also, it can be used to establish a soil profile along a desired cross section of a soil mass. There are several classification schemes available. Each was devised for a specific use. For example, the American Association of State Highway and Transportation Officials (AASHTO) developed one scheme that classifies soils according to their usefulness in roads and highways, while the

Unified Soil Classification System (USCS) was originally developed for use in airfield construction but was later modified for general use.

4.6.1 Unified Soil Classification System

The USCS is neither too elaborate nor too simplistic. The USCS uses symbols for the particle size groups. These symbols and their representations are G—gravel, S—sand, M—silt, and C—clay. These are combined with other symbols expressing gradation characteristics—W for well graded and P for poorly graded—and plasticity characteristics—H for high and L for low, and a symbol, O, indicating the presence of organic material. A typical classification of CL means a clay soil with low plasticity, while SP means a poorly graded sand. The flowcharts shown in Figures 4.9a and 4.9b provide systematic means of classifying a soil according to the USCS.

4.6.2 American Society for Testing and Materials (ASTM) Classification System

The American Society for Testing and Materials classification system (ASTM-CS) is nearly identical to the USCS. ASTM-CS uses the same symbols as USCS but provides a better scheme for mixed soils, i.e., soils consisting of mixtures of, for example, sand, gravel, and clay. Soils are classified by group symbols and group names. For example, we can have a soil with a group symbol, SW-SM, and group name, which describes the soil, as “well-graded sand with silt” if the gravel content is less than 15%. Flowcharts to classify soils based on the ASTM-CS are shown in Figures 4.10a, 4.10b, and 4.10c.

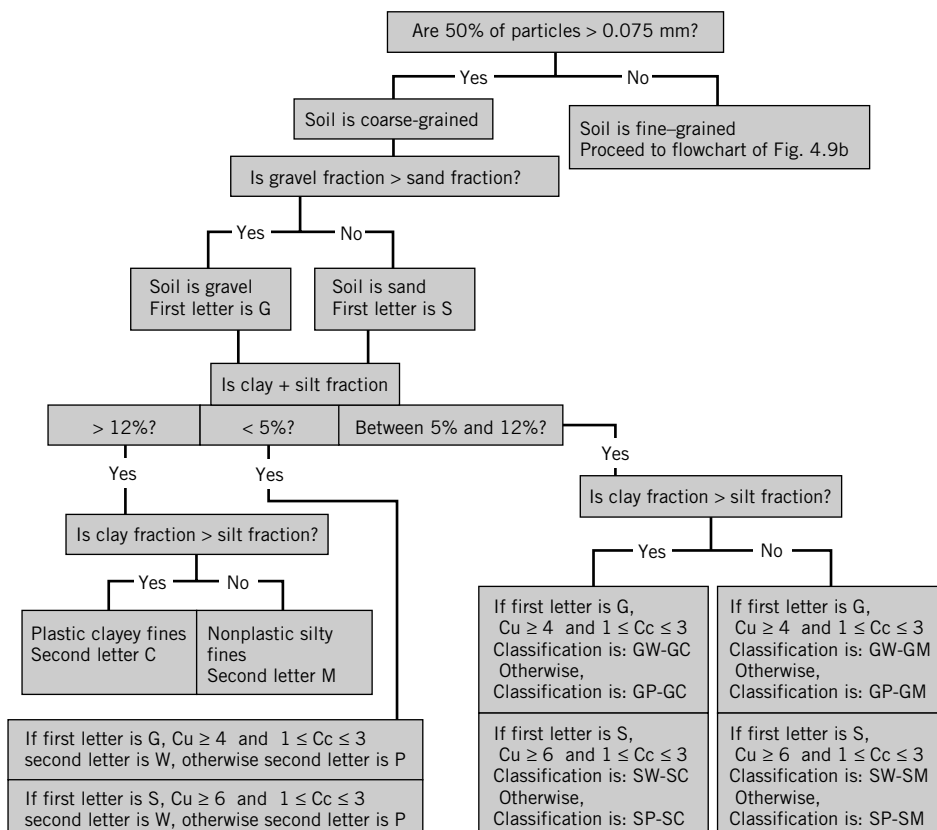


FIGURE 4.9a Unified Soil Classification System flowchart for coarse-grained soils.

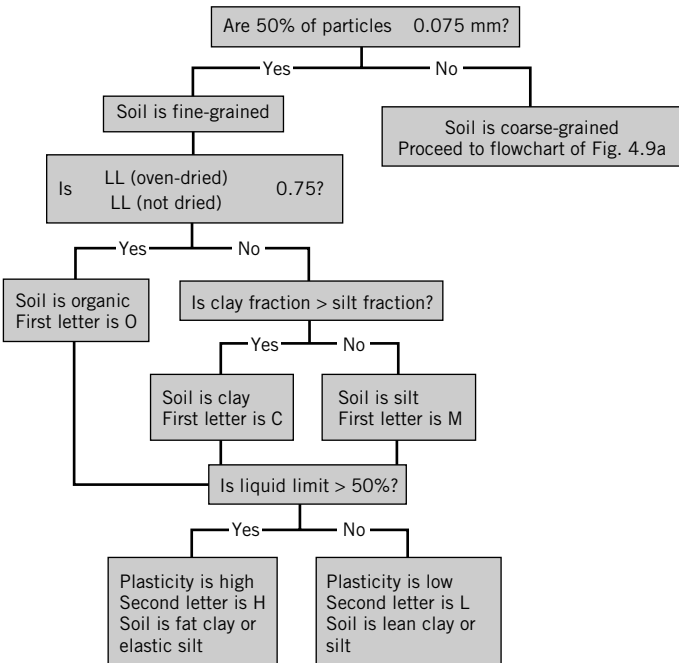


FIGURE 4.9b Unified Soil Classification System flowchart for fine-grained soils.

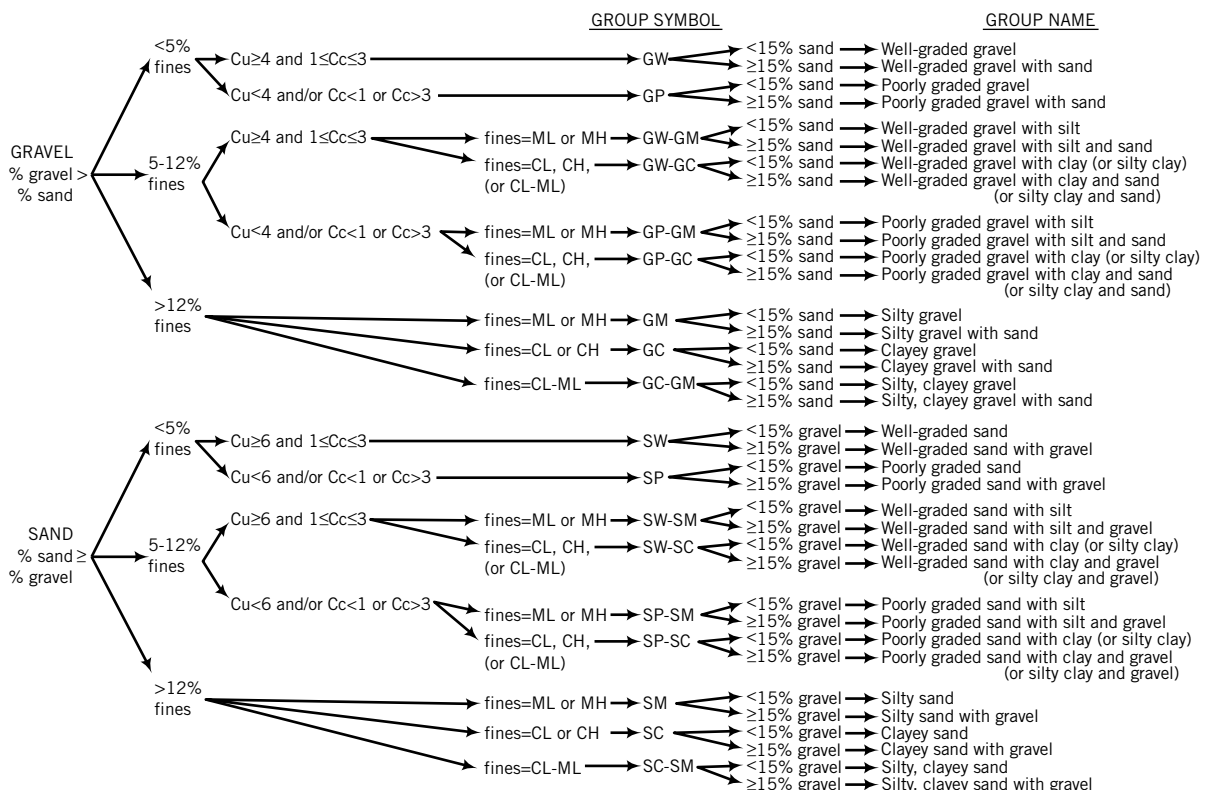


FIGURE 4.10a Flowchart for classifying coarse-grained soils more than 50% retained on No. 200 sieve.
(Source: Reprinted with permission from ASTM D 2487-10 Standard Practice for Classification of Soils for Engineering Purposes, copyright ASTM International, 100 Barr Harbor Drive, West Conshohocken, PA 19428.)

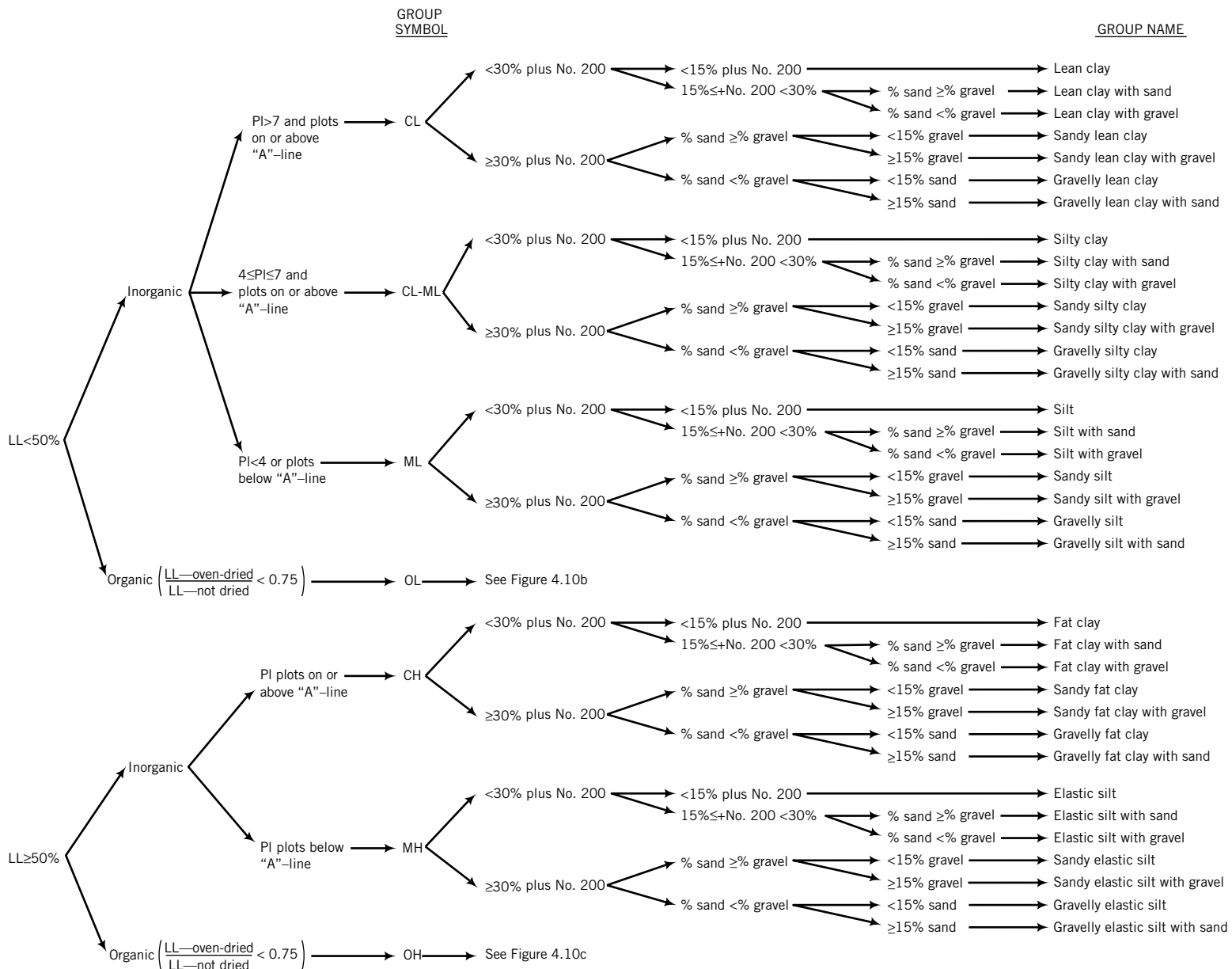


FIGURE 4.10b Flowchart for classifying inorganic fine-grained soils (50% or more fines). (Source: Reprinted with permission from ASTM D 2487-10 Standard Practice for Classification of Soils for Engineering Purposes, copyright ASTM International, 100 Barr Harbor Drive, West Conshohocken, PA 19428.)

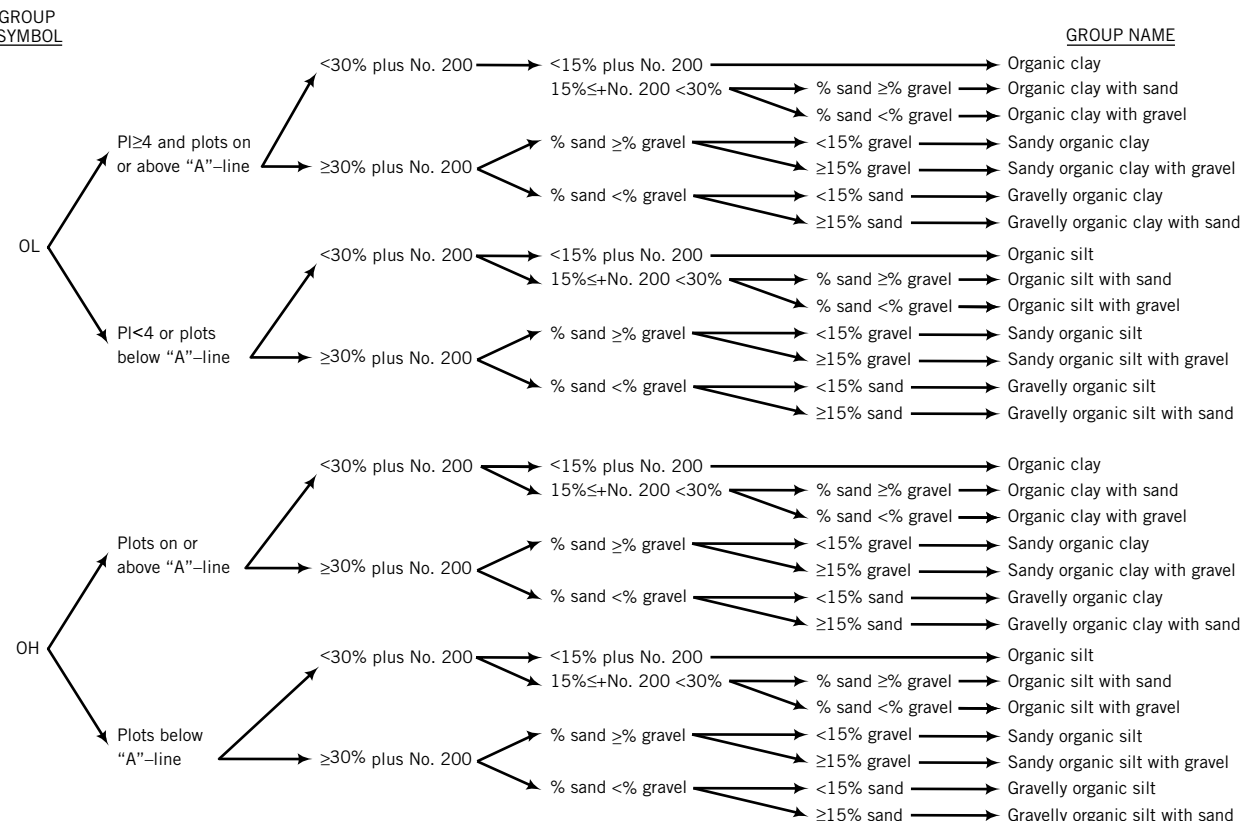


FIGURE 4.10c Flowchart for classifying organic fine-grained soils (50% or more fines). (Source: Reprinted with permission from ASTM D 2487-10 Standard Practice for Classification of Soils for Engineering Purposes, copyright ASTM International, 100 Barr Harbor Drive, West Conshohocken, PA 19428.)

4.6.3 AASHTO Soil Classification System

The AASHTO soil classification system is used to determine the suitability of soils for earthworks, embankments, and road bed materials (subgrade—natural material below a constructed pavement; subbase—a layer of soil above the subgrade; and base—a layer of soil above the subbase that offers high stability to distribute wheel loads). According to AASHTO, granular soils are soils in which 35% or less are finer than the No. 200 sieve (0.075 mm). Silt-clay soils are soils in which more than 35% are finer than the No. 200 sieve. (Table 4.7)

TABLE 4.7 Soil Types, Average Grain Size, and Description According to AASHTO

Gravel	75 mm to 2 mm (No. 10 sieve)
Sand	2 mm (No. 10 sieve) to 0.075 mm (No. 200 sieve)
Silt & Clay	<0.075 mm (No. 200 sieve) Silty: PI < 10% Clayey: PI > 11%

The AASHTO system classifies soils into seven major groups, A-1 through A-7. The first three groups, A-1 through A-3, are granular (coarse-grained) soils, while the last four groups, A-4 through A-7, are silt-clay (fine-grained) soils (Table 4.8).

Silt and clay soils are located within the plasticity chart, as shown in Figure 4.12.

A group index (GI) value is appended in parentheses to the main group to provide a measure of quality of a soil as highway subgrade material. The group index is given as

$$\text{Group Index: GI} = (F - 35)[0.2 + 0.005(\text{LL} - 40)] + 0.01(F - 15)(\text{PI} - 10) \quad (4.26)$$

where F is percent passing No. 200 sieve and the other terms have been defined before. The GI index is reported to the nearest whole number (2.4 reported as 2; 2.5 reported as 3), and if $\text{GI} < 0$, it is set to 0.

GI for groups A-1-a, A-1-b, A-2-4, A-2-5, and A-3 is zero. For groups A-2-6 and A-2-7, the partial group index equation

$$\text{GI} = 0.01(F - 15)(\text{PI} - 10) \quad (4.27)$$

is used. The higher the group index, the lower the quality of the soil as a subgrade material. The GI should not exceed 20 for any of groups A-4 through A-7.

TABLE 4.8A AASHTO Classification of Soils and Soil-Aggregate Mixtures

General Classification	Granular Materials (35% or less passing No. 200)			Silt-Clay Materials (More than 35% passing No. 200)			
	A-1	A-3 ^A	A-2	A-4	A-5	A-6	A-7
Sieve analysis, % passing							
No. 10 (2.00 mm)
No. 40 (425 m)	50 max	51 min
No. 200 (75 m)	25 max	10 max	35 max	35 min	36 min	35 min	35 max
Characteristics of fraction							
passing No. 40 (425 m)							B
Liquid limit	B	40 max	41 min	40 max	B
Plasticity index	6 max	N.P.	B	40 max	10 max	11 min	
General rating as subgrade	Excellent to Good			Fair to Poor			

^AThe placing of A-3 before A-2 is necessary in the “left to right elimination process” and does not indicate superiority of A-3 over A-2.

^BSee Table 4.8B for values.

Reprinted with permission of American Association of State Highway and Transportation Officials.

TABLE 4.8B AASHTO Classification of Soils and Soil-Aggregate Mixtures

General Classification	Granular Materials (35% or less passing No. 200)			Silt-Clay Materials (More than 35% passing No. 200)			
	A-1	A-3	A-2	A-4	A-5	A-6	A-7
Group Classification	A-1-a	A-1-b	A-3	A-2-4	A-2-5	A-2-6	A-2-7
Sieve analysis, % passing							
No. 10 (2.00 mm)	50 max
No. 40 (425 m)	30 max	50 max	51 min
No. 200 (75 m)	15 max	25 max	10 max	35 max	35 max	35 max	35 min
Characteristics of fraction							
passing No. 40 (425 m)							
Liquid limit	40 max	41 max	40 max	41 min	40 max
Plasticity index	6 max	N.P.	10 max	10 max	11 min	11 min	10 max
Usual types of significant	Stone Fragments,	Fine	Silty or Clayey	Gravel and Sand			
constituent materials	Gravel and Sand				Silty Soils	Clayey Soils	
General rating as subgrade	Excellent to Good			Fair to Poor			

Reprinted with permission of American Association of State Highway and Transportation Officials.

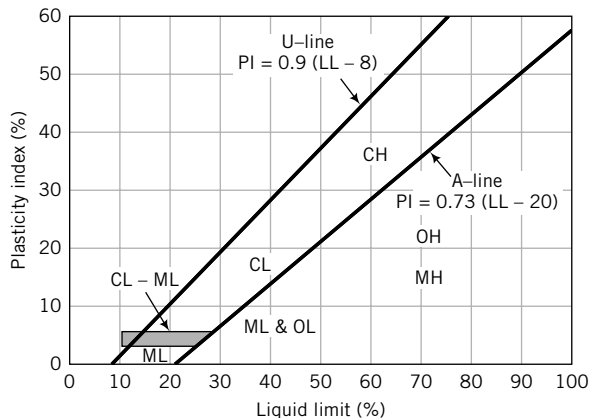


FIGURE 4.11
Plasticity chart.

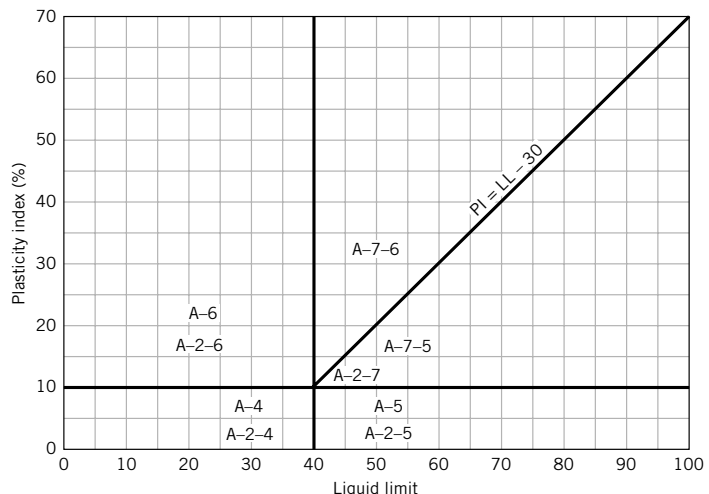


FIGURE 4.12
AASHTO classification of silt and clay within the plasticity chart.

4.6.4 Plasticity Chart

Experimental results from soils tested from different parts of the world were plotted on a graph of plasticity index (ordinate) versus liquid limit (abscissa). It was found that clays, silts, and organic soils lie in distinct regions of the graph. A line defined by the equation

$$PI = 0.73(LL - 20)\% \quad (4.28)$$

called the “A-line,” delineates the boundaries between clays (above the line) and silts and organic soils (below the line), as shown in Figure 4.11. A second line, the U-line, expressed as $PI = 0.9(LL - 8)\%$, defines the upper limit of the correlation between plasticity index and liquid limit. If the results of your soil tests fall above the U-line, you should be suspicious of your results and repeat your tests.

AASHTO’s classification of fine-grained soils is represented on the plasticity chart as shown in Figure 4.12.

4.7 ENGINEERING USE CHART

You may ask: “How do I use a soil classification to select a soil for a particular type of construction, for example, a dam?” Geotechnical engineers have prepared charts based on experience to assist you in selecting a soil for a particular construction purpose. One such chart is shown in Table 4.9 on pages 78–79.

The numerical values 1 to 9 are ratings, with 1 being the best. The chart should only be used to provide guidance and to make a preliminary assessment of the suitability of a soil for a particular use. You should not rely on such descriptions as “excellent” shear strength or “negligible” compressibility to make final design and construction decisions. We will deal later (Chapters 9 and 10) with more reliable methods to determine strength and compressibility properties.

EXAMPLE 4.13 Soil Classification According to USCS and ASTM-CS

Particle size analyses were carried out on two soils—Soil A and Soil B—and the particle size distribution curves are shown in Figure E4.13. The Atterberg limits for the two soils are:

Soil	LL	PL
A	26 (oven-dried; assume same for not dried)	18
B	Nonplastic	

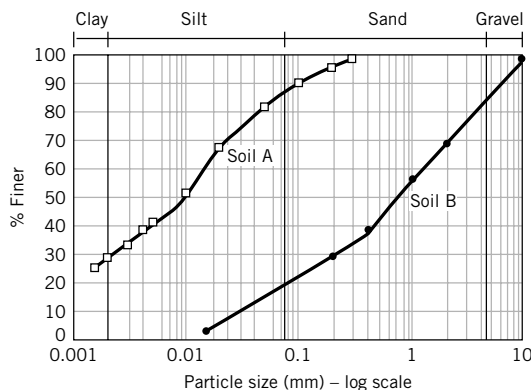


FIGURE E4.13
Particle size distributions.

- (a) Classify these soils according to USCS and ASTM-CS.
- (b) Is either of the soils organic?
- (c) In a preliminary assessment, which of the two soils is a better material for the core of a rolled earth dam?

Strategy If you examine the flowcharts of Figures 4.9a and 4.9b, you will notice that you need to identify the various soil types based on texture: for example, the percentage of gravel or sand. Use the particle size distribution curve to extract the different percentages of each soil type, and then follow the flowchart. To determine whether your soil is organic or inorganic, plot your Atterberg limits on the plasticity chart and check whether the limits fall within an inorganic or organic soil region.

Solution 4.13

Step 1: Determine the percentages of each soil type from the particle size distribution curve.

Constituent	Soil A	Soil B
Percent of particles greater than 0.075 mm	12	80
Gravel fraction (%)	0	16
Sand fraction (%)	12	64
Silt fraction (%)	59	20
Clay fraction (%)	29	0

TABLE 4.9 Engineering Use Chart (after Wagner, 1957)

Typical names of soil groups	Group symbols	Important properties			
		Permeability when compacted	Shearing strength when compacted and saturated	Compressibility when compacted and saturated	Workability as a construction material
Well-graded gravels, gravel–sand mixtures, little or no fines	GW	Pervious	Excellent	Negligible	Excellent
Poorly graded gravels, gravel–sand mixtures, little or no fines	GP	Very pervious	Good	Negligible	Good
Silty gravels, poorly graded gravel–sand–silt mixtures	GM	Semipervious to impervious	Good	Negligible	Good
Clayey gravels, poorly graded gravel–sand–clay mixtures	GC	Impervious	Good to fair	Very low	Good
Well-graded sands, gravelly sands, little or no fines	SW	Pervious	Excellent	Negligible	Excellent
Poorly graded sands, gravelly sands, little or no fines	SP	Pervious	Good	Very low	Fair
Silty sands, poorly graded sand–silt mixtures	SM	Semipervious to impervious	Good	Low	Fair
Clayey sands, poorly graded sand–clay mixtures	SC	Impervious	Good to fair	Low	Good
Inorganic silts and very fine sands, rock flour, silty or clayey fine sands with slight plasticity	ML	Semipervious to impervious	Fair	Medium	Fair
Inorganic clays of low to medium plasticity, gravelly clays, sandy clays, silty clays, lean clays	CL	Impervious	Fair	Medium	Good to fair
Organic silts and organic silt–clays of low plasticity	OL	Semipervious to impervious	Poor	Medium	Fair
Inorganic silts, micaceous or diatomaceous fine sandy or silty soils, elastic silts	MH	Semipervious to impervious	Fair to poor	High	Poor
Inorganic clays of high plasticity, fat clays	CH	Impervious	Poor	High	Poor
Organic clays of medium to high plasticity	OH	Impervious	Poor	High	Poor
Peat and other highly organic soils	Pt	—	—	—	—

Step 2: Use the flowcharts.

Soil A: % < No. 200 (% fines) = 59 + 29 = 88%, % sand > % gravel, gravel < 15%; LL (oven-dried) to LL (not dried) ratio = 1

USCS: Because 50% of the particles are less than 0.075 mm, use flowchart 4.9b.

Soil is ML (silt of low plasticity, or a lean silt).

ASTM-CS: The soil has more than 50% fines; use Figure 4.10b.

Group symbol = ML, group name = sandy silt

Relative desirability for various uses										
Rolled earth dams			Canal sections			Foundations		Roadways		
Homogeneous embankment	Core	Shell	Erosion resistance	Compacted earth lining	Seepage important	Seepage not important	Frost heave not possible	Frost heave possible	Fills Surfacing	
—	—	1	1	—	—	1	1	1	1	3
—	—	2	2	—	—	3	3	3	3	—
2	4	—	4	4	1	4	4	9	5	5
1	1	—	3	1	2	6	5	5	5	1
—	—	3 if gravelly	6	—	—	2	2	2	2	4
—	—	4 if gravelly	7 if gravelly	—	—	5	6	4	—	—
4	5	—	8 if gravelly	5 erosion critical	3	7	8	10	6	6
3	2	—	5	2	4	8	7	6	2	—
6	6	—	—	6 erosion critical	6	9	10	11	—	—
5	3	—	9	3	5	10	9	7	7	—
8	8	—	—	7 erosion critical	7	11	11	12	—	—
9	9	—	—	—	8	12	12	13	—	—
7	7	—	10	8 volume change critical	9	13	13	8	—	—
10	10	—	—	—	10	14	14	14	—	—
—	—	—	—	—	—	—	—	—	—	—

Soil B: % < No. 200 = 20% (silt), % sand > % gravel, gravel = 16%

USCS: Because 50% of the particles are greater than 0.075 mm, use flowchart 4.9a.

Soil is SM (silty sand).

ASTM-CS: Soil has less than 50% fines; use Figure 4.10a.

Group symbol = SM, group name = silty sand with gravel

Step 3: Plot the Atterberg limits on the plasticity chart.

Soil A: PI = 26 – 18 = 8%

The point (26, 8) falls above the A-line; the soil is inorganic.

Soil B: Nonplastic and inorganic

Step 4: Use Table 4.9 to make a preliminary assessment.

Soil B, with a rating of 5, is better than Soil B, with a rating of 6, for the dam core.

EXAMPLE 4.14 AASHTO Soil Classification

Classify Soils A and B in Example 4.13 according to the AASHTO system. Which soil is better for a subgrade?

Strategy Determine if 35% or more of the particles are passing the No. 200 sieves. If so, the soil is one of A-4 through A-7. If not, it is one of A-1 through A-3. Extract the amount passing No. 10 and No. 40 and then use Table 4.8. You should also calculate GI.

Solution 4.14

Step 1: Determine % passing No. 200 sieve.

Soil A: 88% passing No. 200, i.e., > 35% passing No. 200; Soil B: 20% passing No. 200, i.e., < 35% passing No. 200.

Soil A is silty clay; Soil B is granular.

Step 2: Make a table of values according to Table 4.8.

Sieve no.	Soil A	Soil B
No. 10 % finer	100	70
No. 40 % finer	100	40
No. 200 % finer	88	20
LL (%)	26	18
PI (%)	8	NP

$$\text{Soil A: GI} = (F - 35)[0.2 + 0.005(LL - 40)] + 0.01(F - 15)(PI - 10) = (88 - 35)[0.2 + 0.005(26 - 40)] + 0.01(88 - 15)(8 - 10) = 5.4 = 5$$

Soil B is nonplastic. Therefore, GI = 0.

Step 3: Use Table 4.8 with the values in Step 2 to classify the soils.

Soil A is A-4 (5). Note: The value in parentheses is GI.

Soil B is A-1-b (stone fragments, gravel, and sand).

Step 4: Decide which soil is better for a subgrade material.

According to Table 4.8, Soil B (A-1-b) is an excellent material for a subgrade. Soil A is fair to poor. Soil B is then the preferable material.

4.8 SUMMARY

We have dealt with a large body of basic information on the physical properties of soils. Soils are conveniently idealized as three-phase materials: solids, water, and air. The physical properties of a soil depend on the relative proportion of these constituents in a given mass. Soils are classified into groups by their particle sizes and Atterberg limits. Soils within the same group are likely to have similar mechanical behavior and construction use. Some of the main physical parameters for soils are the particle sizes, void ratio, liquid limit, plastic limit, shrinkage limit, and plasticity and liquidity indices. Water can significantly change the characteristics of soils.

Self-assessment

Access Chapter 4 at <http://www.wiley.com/college/budhu> to take the end-of-chapter quiz to test your understanding of this chapter.

Practical Examples

EXAMPLE 4.15 Calculating Soil Quantities for a Highway Embankment

An embankment for a highway 30 m wide and 1.5 m in compacted thickness is to be constructed from a sandy soil trucked from a borrow pit. The water content of the sandy soil in the borrow pit is 15% and its void ratio is 0.69. The swell index is 1.2. The specification requires the embankment to be compacted to a dry unit weight of 18 kN/m³. Determine, for a 1-km length of embankment, the following:

- (a) The weight of sandy soil from the borrow pit required to construct the embankment.
- (b) The number of truckloads of sandy soil required for the construction. The full capacity of each truck is 22.2 m³, and local government regulations require a maximum loaded capacity of 90%.
- (c) The weight of water per truckload of sandy soil.
- (d) The degree of saturation of the sandy soil in situ.

Strategy The strategy is similar to that adopted in Example 4.7.

Solution 4.15

Step 1: Calculate γ_d for the borrow pit material.

$$\gamma_d = \frac{G_s \gamma_w}{1 + e} = \frac{2.7 \times 9.8}{1 + 0.69} = 15.7 \text{ kN/m}^3$$

Step 2: Determine the volume of borrow pit soil required.

Volume of finished embankment: $V = 30 \times 1.5 \times 1 = 45 \text{ m}^3$

Volume of borrow pit soil required: $\frac{(\gamma_d)_{\text{required}}}{(\gamma_d)_{\text{borrow pit}}} \times V = \frac{18}{15.7} \times 45 \times 10^3 = 51.6 \times 10^3 \text{ m}^3$

Volume of borrow pit material required considering swell = $1.2 \times 51.6 \times 10^3 = 61.9 \times 10^3 \text{ m}^3$

Step 3: Determine the number of trucks required.

$$\text{Number of trucks} = \frac{51.6 \times 10^3}{10} = 5160$$

Step 4: Determine the weight of water required.

Weight of dry soil in one truckload: $W_d = 10 \times 15.7 = 157 \text{ kN}$

Weight of water: $wW_d = 0.15 \times 157 = 23.6 \text{ kN}$

Step 5: Determine the degree of saturation.

$$S = \frac{wG_s}{e} = \frac{0.15 \times 2.7}{0.69} = 0.59 = 59\%$$

EXAMPLE 4.16 Calculating Soil Quantities and Cost for a Dam

An earth dam requires 1 million cubic meters of soil compacted to a void ratio of 0.8. In the vicinity of the proposed dam, three borrow pits were identified as having suitable materials. The cost of purchasing the soil and the cost of excavation are the same for each borrow pit. The only cost difference is transportation cost. The table below provides the void ratio and the transportation cost for each borrow pit. Which borrow pit would be the most economical?

Borrow pit	Void ratio	Swell factor	Transportation cost (\$/m ³)
1	1.8	1.1	\$0.60
2	0.9	1.2	\$1.00
3	1.5	1.1	\$0.75

Strategy The specific volume is very useful in this problem to find the desired volume of borrow pit material.

Solution 4.16

Step 1: Define parameters and set up relevant equations. Let V_o, e_o be the specific volume and void ratio of the compacted soil in the dam, and V_i, e_i be the specific volume and void ratio of the soil from the borrow pits, where $i = 1, 2, 3$. Now,

$$\frac{V_i}{V_o} = \frac{1 + e_i}{1 + e_o}$$

and

$$V_i = V_o \left(\frac{1 + e_i}{1 + e_o} \right) = \frac{1 \times 10^6}{1 + 0.8} (1 + e_i)$$

Step 2: Determine the volume of soil from each borrow pit. Substituting the void ratio from the table into the last equation and multiplying by the swell factor, we obtain

$$V_1 = 1,555,555 \times 1.1 = 1,711,111 \text{ m}^3$$

$$V_2 = 1,055,555 \times 1.2 = 1,266,666 \text{ m}^3$$

$$V_3 = 1,388,888 \times 1.1 = 1,527,777 \text{ m}^3$$

Step 3: Determine transportation costs.

$$V_1 = 1,711,111 \times 0.6 = \$1,026,667$$

$$V_2 = 1,266,666 \times 1.0 = \$1,266,666$$

$$V_3 = 1,527,777 \times 1.1 = \$1,680,555$$

Borrow pit 1 is therefore the most economical.

EXAMPLE 4.17 Estimating Soil Profile Based on Soil Classification

Three boreholes (BH) along a proposed road intersection are shown in Figure E4.17a and b. The soils in each borehole were classified using ASTM-CS. Sketch a soil profile along the center line.

Strategy Assume that the boreholes are all along the center line. You should align the boreholes relative to a single elevation and then sketch the soil profile using ASTM-CS.

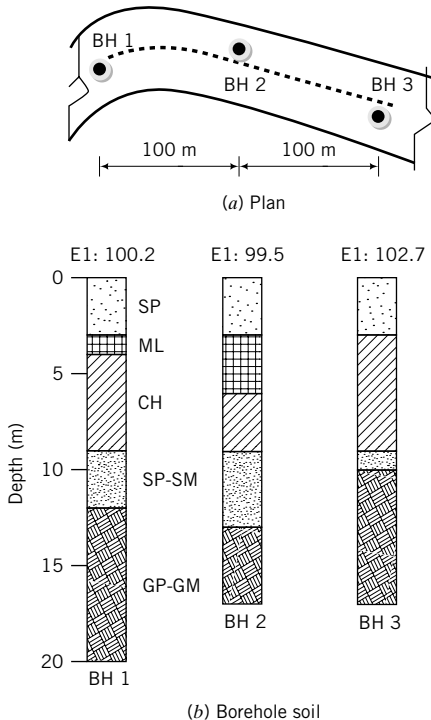
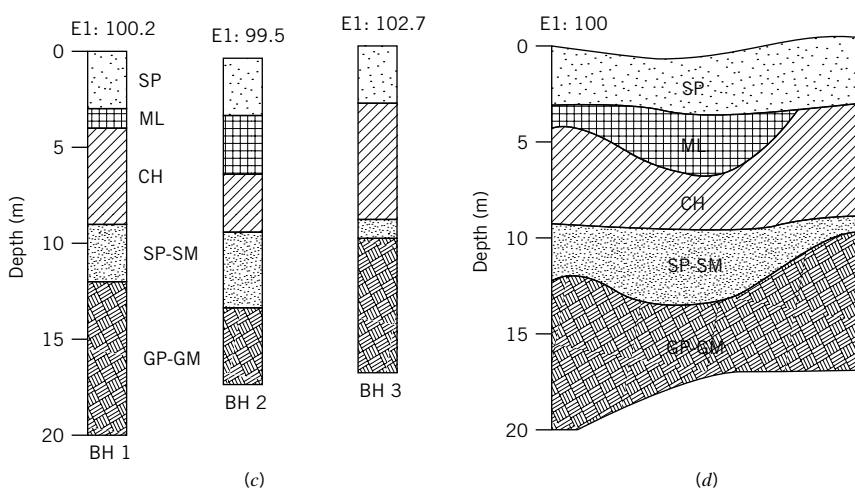
Solution 4.17

Step 1: Align the boreholes relative to a single elevation.

See Figure E4.17c.

Step 2: Sketch soil profile.

Draw smooth curves around each corresponding soil type in the boreholes, as shown in Figure E4.17d. These curves are estimates. The low plasticity silt (ML) is only present in boreholes 1 and 2. You have to make an estimate as to where this layer of silt ends before BH 3.

**FIGURE E4.17a, b****FIGURE E4.17c, d**

EXERCISES

Theory

4.1 Prove the following relations:

$$(a) \quad \gamma_d = \frac{G_s \gamma_w}{1 + e}$$

$$(b) \quad S = \frac{w G_s (1 - n)}{n}$$

$$(c) \quad \gamma = \gamma_d + S n \gamma_w$$

$$(d) \quad \gamma' = \gamma_d + \gamma_w (n - 1)$$

In the above equations, n is the porosity as a ratio, not as a percentage.

4.2 Show that

$$D_r = \frac{\gamma_d - (\gamma_d)_{min}}{(\gamma_d)_{max} - (\gamma_d)_{min}} \left\{ \frac{(\gamma_d)_{max}}{\gamma_d} \right\}$$

4.3 Tests on a soil gave the following results: $G_s = 2.7$ and $e = 1.96$. Make a plot of degree of saturation versus water content for this soil.

4.4 Assuming soil particles to be spheres, derive equations for the maximum and minimum porosities, and maximum and minimum void ratios.

Problem Solving

Interactive Problem Solving

Access <http://www.wiley.com/college/budhu>, Chapter 4, and click on Problem Solver to interactively solve problems similar to some in this chapter.

Assume $G_s = 2.7$, where necessary, for solving the following problems.

4.5 A cylinder has 500 cm^3 of water. After a mass of 100 grams of sand is poured into the cylinder and all air bubbles are removed by a vacuum pump, the water level rises to 537.5 cm^3 . Determine the specific gravity of the sand.

4.6 An ASTM D 854 test was done on a sand. The data are as shown below. Calculate the specific gravity.

Mass of pycnometer = 40.1 grams

Mass of pycnometer and dry soil = 65.8 grams

Mass of pycnometer, dry soil, and water = 154.5 grams

Mass of pycnometer and water = 138.5 grams

4.7 The wet mass of a sample of saturated soil is 520 grams. The dry mass, after oven-drying, is 400 grams. Determine the (a) water content, (b) void ratio, (c) saturated unit weight, and (d) effective unit weight.

4.8 A soil sample has a bulk unit weight of 19.8 kN/m^3 at a water content of 10%. Determine the void ratio, percentage air in the voids (air voids), and the degree of saturation of this sample.

4.9 A wet sand sample has a volume of $4.64 \times 10^{-4} \text{ m}^3$ and weighs 8 N. After oven-drying, the weight reduces to 7.5 N. Calculate the water content, void ratio, and degree of saturation.

4.10 A saturated silty clay encountered in a deep excavation is found to have a water content of 23.5%. Determine its porosity and bulk unit weight.

4.11 A soil sample of diameter 37.5 mm and length 75 mm has a wet weight of 1.32 N and dry weight of 1.1 N. Determine (a) the degree of saturation, (b) the porosity, (c) the bulk unit weight, and (d) the dry unit weight.

4.12 The mass of a wet sample of soil and its container is 0.33 kg. The dry mass of the soil and its container is 0.29 kg. The mass of the container is 0.06 kg and its volume is $0.15 \times 10^{-3} \text{ m}^3$. Determine the following.

- (a) The bulk, dry, and saturated unit weights of the soil.
- (b) The void ratio and the degree of saturation.
- (c) How much air void is in the soil?
- (d) The weight of water required to saturate 1 m^3 of this soil.

4.13 A sand has a natural water content of 5% and bulk unit weight of 18.0 kN/m^3 . The void ratios corresponding to the densest and loosest state of this soil are 0.51 and 0.87. Find the relative density and degree of saturation.

4.14 The void ratio of a soil is 1.2. Determine the bulk and effective unit weights for the following degrees of saturation: (a) 75%, (b) 95%, and (c) 100%. What is the percentage error in the bulk unit weight if the soil is 95% saturated but assumed to be 100% saturated?

4.15 The following results were obtained from a liquid limit test on a clay using the Casagrande cup device.

Number of blows	6	12	20	28	32
Water content (%)	52.5	47.1	43.2	38.6	37.0

- (a) Determine the liquid limit of this clay.
- (b) If the natural water content is 38% and the plastic limit is 23%, calculate the liquidity index.
- (c) Do you expect a brittle type of failure for this soil? Justify your answer.

4.16 The following data were recorded from a liquid limit test on a clay using the Casagrande cup device.

Test number	Container (grams)	Container and wet soil (grams)	Container and dry soil (grams)	Blow count
	W_c	W_w	W_d	N
1	45.3	57.1	54.4	28
2	43.0	59.8	56.0	31
3	45.2	61.7	57.9	22
4	45.6	58.4	55.3	18

Determine the liquid limit.

4.17 A fall cone test was carried out on a soil to determine its liquid and plastic limits using a cone of mass 80 grams. The following results were obtained:

80-gram cone				
Penetration (mm)	8	15	19	28
Water content (%)	43.1	52.0	56.1	62.9

Determine (a) the liquid and plastic limits and (b) the plasticity index. If the soil contains 45% clay, calculate the activity.

- 4.18** The following results were recorded in a shrinkage limit test using mercury

Mass of container	17.0 grams
Mass of wet soil and container	72.3 grams
Mass of dish	132.40 grams
Mass of dish and displaced mercury	486.1 grams
Mass of dry soil and container	58.2 grams
Volume of wet soil	32.4 cm ³

Determine the shrinkage limit, the linear shrinkage, and the shrinkage ratio. The density of mercury is 13.6 grams/cm³.

- 4.19** The results of a particle size analysis of a soil are given in the following table. No Atterberg limit tests were conducted.

Sieve no.	9.53 mm (3/8")	4	10	20	40	100	200
% finer	100	89.8	70.2	62.5	49.8	28.6	4.1

- (a) Would you have conducted Atterberg limit tests on this soil? Justify your answer.
 - (b) Classify the soil according to USCS, ASTM-CS, and AASHTO.
 - (c) Is this soil a good foundation material? Justify your answer.
- 4.20** The results of a particle size analysis of a soil are given in the following table. Atterberg limit tests gave LL = 62% and PL = 38%. The clay content is 37%.

Sieve no.	9.53 mm (3/8")	4	10	20	40	100	200
% finer	100	90.8	84.4	77.5	71.8	65.6	62.8

- (a) Classify the soil according to ASTM-CS and AASHTO.
- (b) Rate this soil as a subgrade for a highway.

Practical

- 4.21** The water contents of soil samples taken at different depths are given in the table below.

Depth (m)	1	2	3	4	5	6
w (%)	21.3	23.6	6.1	32.7	41.5	42.0

The groundwater level is at the surface. Assume $G_s = 2.7$.

- (a) Plot on the same graph (a) depth versus water content and (b) depth versus saturated unit weight.
- (b) Are there any questionable water content values? If so, at what depth?
- (c) If the water contents are all correct, what type or types of soils (e.g., clay, sand) are probably at the site?

- 4.22** A fine-grained soil has a liquid limit of 200% and a plastic limit of 45%. The natural water content of the soil in the field is 60% and the clay content is 63%.

- (a) Calculate the plasticity index, the liquidity index, and the activity.
- (b) What is the soil state (e.g., liquid) in the field?
- (c) What is the predominant mineral in this soil?
- (d) This soil is under a rectangular concrete slab, 15 m × 50 m, used as a foundation for a building. A water pipe, 100 mm in diameter, is located in a trench 450 mm below the center of the slab. The trench running along the length of the slab, 300 mm wide and 450 mm deep, was backfilled with the same soil. If this pipe were to leak, what effect would it have on the foundation? Draw a neat sketch of the existing trench and pipe, and show in another sketch how you would mitigate any water-related issue from the pipe and the soil. Explain why your mitigation method is better than the existing construction.

- 4.23** An elliptical artificial island is required for a reclamation project. The major axis of the ellipse is 10 km and the minor axis is 7.5 km (Figure P4.23). A rock breakwater, 100 m thick, forms the edges of the island. The area within the breakwater is to be filled with sand. The sand in its loosest state has a porosity of 90% and the desired porosity, when compacted, is 20%. Assuming the average thickness of the completed island is 100 m, determine the quantity of sand required.

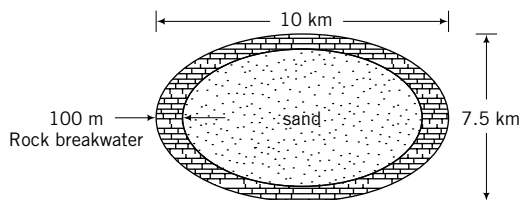
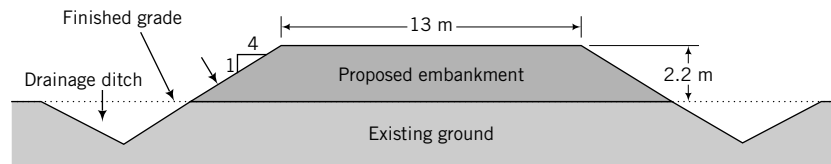
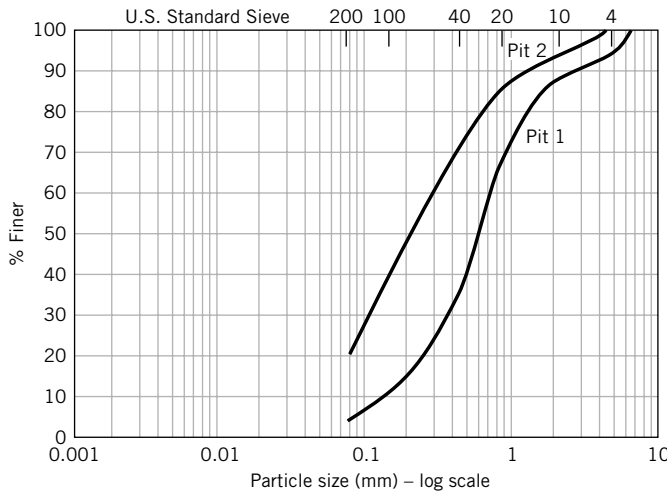


FIGURE P4.23

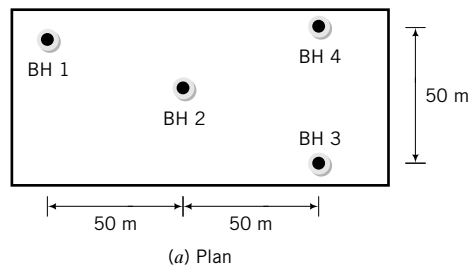
- 4.24** The highway embankment from Noscut to Windsor Forest, described in the sample practical situation, is 10 km long. The average cross section of the embankment is shown in Figure P4.24a. The gradation curves for the soils at the two borrow pits are shown in Figure P4.24b. Pit 1 is located 5 km from the start of the embankment, while pit 2 is 3 km away. Estimated costs for various earthmoving

**FIGURE P4.24a****FIGURE P4.24b**

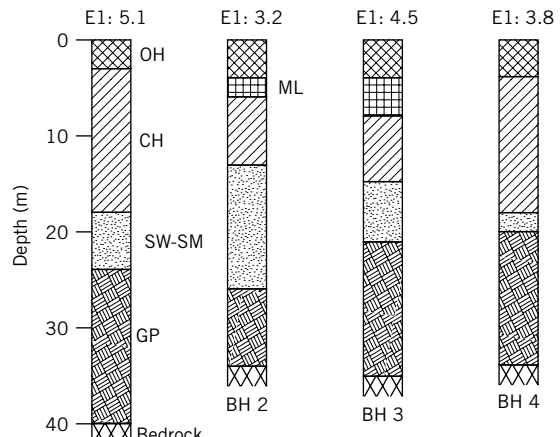
operations are shown in the table below. You are given 10 minutes by the stakeholders' committee to present your recommendations. Prepare your presentation. The available visual aid equipment is an LCD projector.

Operation	Cost	
	Pit 1	Pit 2
Purchase and load borrow pit material at site, haul 2 km round-trip, and spread with 200 HP dozer	\$10/m ³	\$12/m ³
Extra mileage charge for each km	\$0.50/m ³	\$0.55/m ³
Compaction	\$1.02/m ³	\$1.26/m ³
Miscellaneous	\$1.10/m ³	\$0.85/m ³

- 4.25** The soil profiles for four boreholes (BH) at a site proposed for an office building are shown in Figure P4.25. The soils in each borehole were classified using ASTM-CS. Sketch the soil profiles along a diagonal line linking boreholes 1, 2, and 3 and along a line linking boreholes 3 and 4.



(a) Plan

**FIGURE P4.25**

5.0 INTRODUCTION

Soil compaction is the densification—reduction in void ratio—of a soil through the expulsion of air. This is normally achieved by using mechanical compactors, rollers, and rammers with the addition of water. We will discuss the fundamentals of soil compaction, compaction tests, field compaction, and quality control in the field.

When you complete this chapter, you should be able to:

- Understand the importance of soil compaction.
- Determine maximum dry unit weight and optimum water content.
- Specify soil compaction criteria for field applications.
- Identify suitable equipment for field compaction.
- Specify soil compaction quality control tests.

Importance

Soil compaction is perhaps the least expensive method of improving soils. It is a common practice in all types of building systems on and within soils. As a sample practical situation, we consider a levee. A levee—a long earthen embankment, sometimes called a dike or dyke, used to retain and/or regulate water levels in rivers—is to be constructed from soil trucked from a borrow pit. You are required to (a) determine the suitability of the soil for the levee, (b) specify compaction criteria, and (c) specify quality control methods.

On Monday morning, August 29, 2005, Hurricane Katrina slammed into New Orleans, Louisiana, USA, as a Category 3 storm. Over 1800 persons lost their lives, and massive property damage occurred. Much of the damage was due to floods from the catastrophic failure of the levee system (Figure 5.1). Hurricane Katrina is claimed to be the largest natural disaster in the history of the United States, with



FIGURE 5.1 Failure of a section of a levee from Hurricane Katrina.
(© ROBYN BECK/AFP/Getty Images/NewsCom.)

estimated damages exceeding \$100 billion. Several investigations were conducted on the design and construction of the levee systems. The reports of many of these investigations are available on the World Wide Web (e.g., <http://www.asce.org/static/hurricane/whitehouse.cfm>). One of the lessons from failures such as from Hurricane Katrina is that in designing any geotechnical structure you ought to consider a systems approach. You must consider how your part of the problem fits into the whole project and the implications if anything goes wrong with your part—that is, you should take a holistic approach.

5.1 DEFINITIONS OF KEY TERMS

Compaction is the densification of soils by the expulsion of air.

Maximum dry unit weight (γ_d) is the maximum unit weight that a soil can attain using a specified means of compaction.

Optimum water content (w_{opt}) is the water content required to allow a soil to attain its maximum dry unit weight following a specified means of compaction.

5.2 QUESTIONS TO GUIDE YOUR READING

1. What is soil compaction?
2. What is the importance of soil compaction?
3. What factors affect soil compaction?
4. How is soil compaction achieved in the laboratory?
5. What are the requirements for soil compaction in the field?
6. What types of equipment are used for soil compaction?
7. How is soil compaction monitored in the field?

5.3 BASIC CONCEPT

Let's reexamine Equation (4.12) for dry unit weight, that is,

$$\gamma_d = \left(\frac{G_s}{1 + e} \right) \gamma_w = \frac{\gamma}{1 + w} = \left(\frac{G_s}{1 + wG_s/S} \right) \gamma_w \quad (5.1)$$

The extreme-right-hand term was obtained by replacing e by $e = wG_s/S$. How can we increase the dry unit weight? Examination of Equation (5.1) reveals that we have to reduce the void ratio; that is, w/S must be reduced since G_s is constant. The theoretical maximum dry unit weight is obtained when $S = 1$ ($S = 100\%$); that is,

$$e_{min} = wG_s \quad (5.2)$$

A plot of the theoretical dry unit weight versus water content for different degrees of compaction is shown in Figure 5.2. The theoretical dry unit weight decreases as the water content increases because the soil solids are heavier than water for the same volume occupied. Recall that the specific gravity of the soil solids is on average 2.7. That is, the mass of the soil solids is 2.7 times the mass of water for the same volume occupied. The theoretical dry unit weight decreases as the degree of saturation decreases. The mass of air is negligible, so as air replaces water in the void space, the volume of soil remains constant but its mass decreases. Thus, the dry unit weight decreases. The curve corresponding to $S = 100\%$ is the saturation line, sometimes called the zero air voids curve. The achievement of zero air voids by compaction is rare.

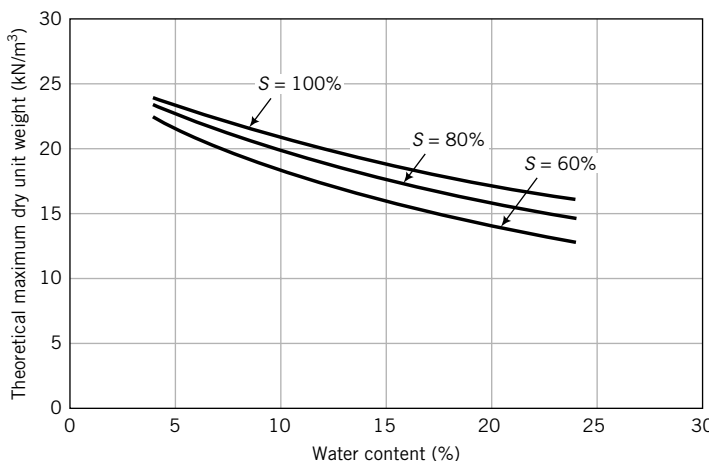


FIGURE 5.2 Theoretical maximum dry unit weight–water content relationship for different degrees of saturation.

The curves shown in Figure 5.2 were obtained as follows:

1. Assume a fixed value of S , say, $S = 1$ (100% saturation), in Equation (5.1).
2. Substitute arbitrarily chosen values of w .
3. With the fixed value of S and either an estimated value of G_s ($= 2.7$) or a known value, find γ_d for each value of w using Equation (5.1).
4. Plot the results of γ_d versus w .
5. Repeat for a different value of S , if desired.

What's next . . . In the next section, a laboratory test that is commonly used to determine the maximum dry unit weight and optimum water content is briefly described.

5.4 PROCTOR COMPACTION TEST—ASTM D 1140 AND ASTM D 1557

A laboratory test called the standard Proctor test was developed to deliver a standard amount of mechanical energy (compactive effort) to determine the maximum dry unit weight of a soil. In the standard Proctor test, a dry soil specimen is mixed with water and compacted in a cylindrical mold of volume $9.44 \times 10^{-4} \text{ m}^3$ (standard Proctor mold) by repeated blows from the mass of a hammer, 2.5 kg, falling freely from a height of 305 mm (Figure 5.3). The soil is compacted in three layers, each of which is subjected to 25 blows.

The energy imparted by the hammer is

$$E_{\text{comp}} = m_h g \frac{h_d}{V} N_b N_l \quad (5.3)$$

where m_h is the mass of the hammer, g is the acceleration due to gravity, h_d is the height of fall of the hammer, V is the volume of compacted soil, N_b is the number of blows, and N_l is the number of layers. Thus, the compaction energy of the standard Proctor test is

$$E_{\text{comp}} = 2.5 \times 9.8 \frac{0.305}{9.44 \times 10^{-4}} \times 25 \times 3 \times 10^{-3} = 594 \text{ kJ/m}^3$$

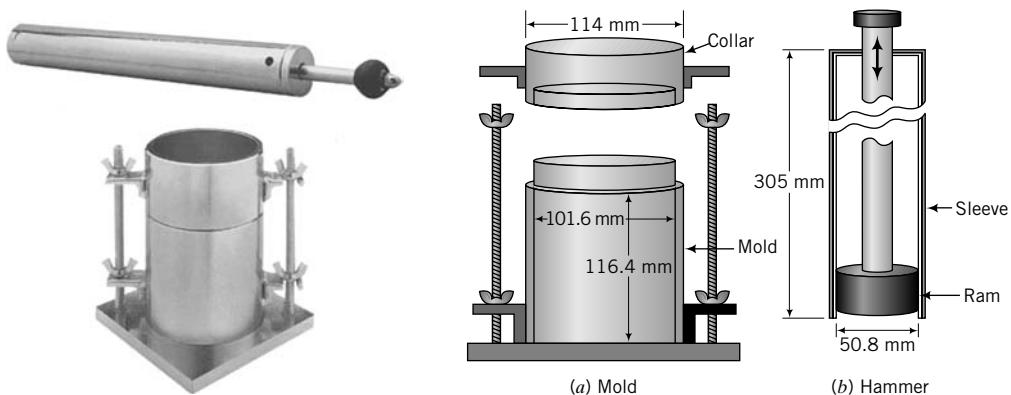


FIGURE 5.3 Compaction apparatus. (Photo courtesy of Geotest.)

For most projects, the standard Proctor test is satisfactory. For projects involving heavy loads, such as runways to support heavy aircraft loads, a modified Proctor test was developed. In this test, the hammer has a mass 4.54 kg and falls freely from a height of 457 mm. The soil is compacted in five layers with 25 blows per layer in the standard Proctor mold. The compaction energy of the modified Proctor test compaction test is 2695 kJ/m^3 , about 4.5 times the energy of the standard Proctor test.

Four or more tests are conducted on the soil using different water contents. The last test is identified when additional water causes the bulk unit weight of the soil to decrease. The results are plotted as dry unit weight (ordinate) versus water content (abscissa). Typical dry unit weight–water content plots are shown in Figure 5.4.

Clays usually yield bell-shaped curves. Sands often show an initial decrease in dry unit weight, attributed to capillary tension that restrains the free movement of soil particles, followed by a hump. Some soils—those with liquid limit less than 30% and fine, poorly graded sands—may produce one or more humps before the maximum dry unit weight is achieved.

The water content at which the maximum dry unit weight, $(\gamma_d)_{max}$, is achieved is called the optimum water content (w_{opt}). At water contents below optimum (dry of optimum), air is expelled and water facilitates the rearrangement of soil grains into a denser configuration—the number of soil grains per unit volume of soil increases. At water contents just above optimum (wet of optimum), the compactive effort cannot expel more air and additional water displaces soil grains, thus decreasing the number of

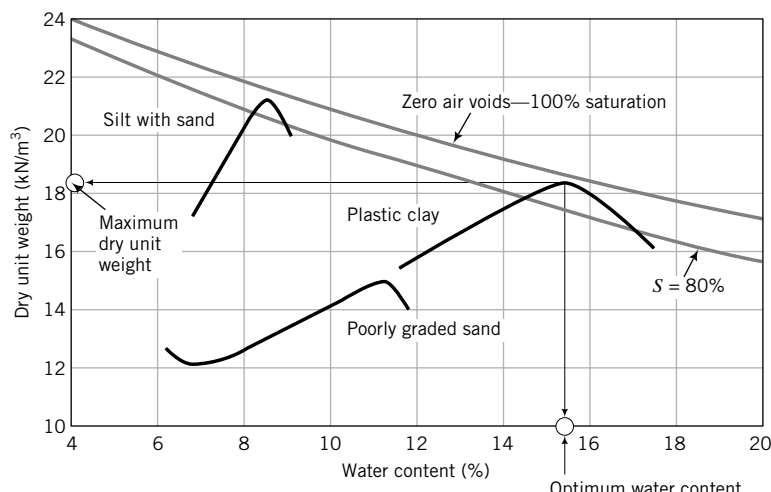
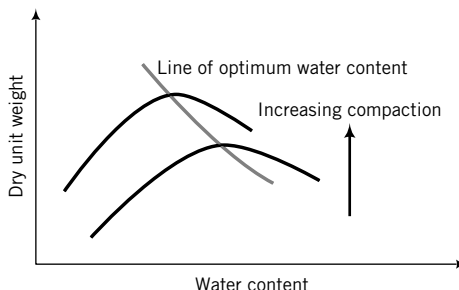


FIGURE 5.4 Dry unit weight–water content curves.

**FIGURE 5.5**

Effect of increasing compaction efforts on the dry unit weight–water content relationship.

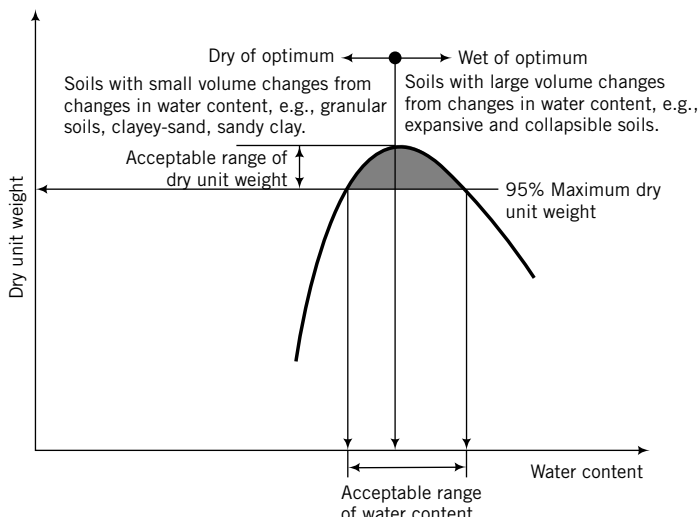
soil grains per unit volume of soil. Consequently, the dry unit weight decreases. The modified Proctor test, using higher levels of compaction energy, achieves a higher maximum dry unit weight at a lower optimum water content than the standard test (Figure 5.5). The degree of saturation is also lower at higher levels of compaction than in the standard compaction test.

The soil is invariably unsaturated at the maximum dry unit weight, that is, $S < 1$. We can determine the degree of saturation at the maximum dry unit weight using Equation (5.1). We know $\gamma_d = (\gamma_d)_{max}$ and $w = w_{opt}$ from our Proctor test results. If G_s is known, we can solve Equation (5.1) for S . If G_s is unknown, you can substitute a value of 2.7 with little resulting error in most cases.

What's next . . . In the next section, you will learn how to interpret the Proctor test for practical applications.

5.5 INTERPRETATION OF PROCTOR TEST RESULTS

Knowledge of the optimum water content and the maximum dry unit weight of soils is very important for construction specifications of soil improvement by compaction. Specifications for earth structures (embankments, footings, etc.) usually call for a minimum of 95% of Proctor maximum dry unit weight. This level of compaction can be attained at two water contents—one before the attainment of the maximum dry unit weight, or dry of optimum, the other after attainment of the maximum dry unit weight, or wet of optimum (Figure 5.6). Normal practice is to compact the soil dry of optimum. Compact the soil wet of optimum for swelling (expansive) soils, soil liners for solid waste landfills, and projects where soil volume changes from changes in moisture conditions are intolerable.

**FIGURE 5.6** Illustration of compaction specification of soils in the field.

When a heavily compacted soil mass (near to maximum dry unit weight) is sheared, it tends to expand (dilate) and gets looser. Usually this expansion is not uniform; some parts of the soil mass are looser than other parts. The flow rate of water in the soil will increase as water can easily (compared to the intact one) flow through the looser parts, possibly leading to catastrophic failure. Heavily compacted soils tend to show sudden decrease in strength when sheared. In engineering, if failure is to occur we prefer that it occurs gradually rather than suddenly so that mitigation measures can be implemented. In some earth structures (for example, earth dams) you should try to achieve a level of compaction that would cause the soil to behave ductile (ability to deform without rupture). This may require compaction wet of optimum at levels less than 95% of the maximum dry unit weight (approximately 80% to 90% of maximum dry unit weight).

EXAMPLE 5.1 Calculating Dry Unit Weight from Proctor Test Data

The wet mass of one of the standard Proctor test samples is 1806 grams at a water content of 8%. The volume of the standard Proctor test sample is $9.44 \times 10^{-4} \text{ m}^3$. Determine the bulk and dry unit weights.

Strategy From the wet mass and its volume, you can calculate the bulk unit weight. Divide the bulk unit weight by 1 plus the water content to find the dry unit weight.

Solution 5.1

Step 1: Find the bulk unit weight.

$$\gamma = \frac{W}{V} = \frac{(1806/1000) \times 9.8}{9.44 \times 10^{-4}} = 18,749 \text{ N/m}^3 = 18.7 \text{ kN/m}^3$$

(1806 grams is divided by 1000 to give kilograms. 1 kg = 9.8 N)

Step 2: Find the dry unit weight.

$$\gamma_d = \frac{\gamma}{1 + w} = \frac{18.7}{1 + 0.08} = 17.3 \text{ kN/m}^3$$

EXAMPLE 5.2 Interpreting Compaction Data (1)

The results of a standard compaction test are shown in the table below.

Water content (%)	6.2	8.1	9.8	11.5	12.3	13.2
Bulk unit weight (kN/m^3)	16.9	18.7	19.5	20.5	20.4	20.1

- (a) Determine the maximum dry unit weight and optimum water content.
- (b) What is the dry unit weight and water content at 95% standard compaction, dry of optimum?
- (c) Determine the degree of saturation at the maximum dry density.
- (d) Plot the zero air voids line.

Strategy Compute γ_d and then plot the results of γ_d versus w (%). Extract the required information.

Solution 5.2

Step 1: Use a table or a spreadsheet program to tabulate γ_d .

Use Equation (4.12) to find the dry unit weight and Equation (5.2) and (5.1) to calculate the dry unit weight for $S = 1$.

Water content	Bulk unit weight (kN/m ³)	Dry unit weight (kN/m ³) $\gamma_d = \frac{\gamma}{1 + w}$	Zero air voids	
			Water content (%)	Dry unit weight (kN/m ³) $\gamma_d = \left(\frac{G_s}{1 + wG_s/S} \right) \gamma_w;$ $S = 1$
6.2	16.9	15.9	6	22.8
8.1	18.7	17.3	8	21.8
9.8	19.5	17.8	10	20.8
11.5	20.5	18.4	12	20.0
12.3	20.4	18.2	14	19.2
13.2	20.1	17.8		

Step 2: Plot graphs as shown in Figure E5.2

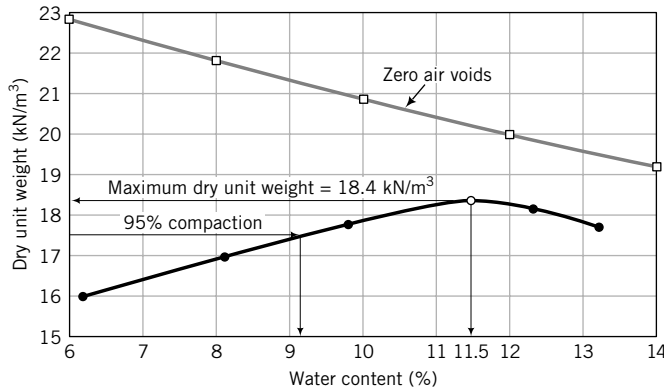


FIGURE E5.2 Compaction test results.

Step 3: Extract the desired values.

$$(\gamma_d)_{\max} = 18.4 \text{ kN/m}^3, \quad w_{opt} = 11.5\%$$

At 95% compaction, $\gamma_d = 18.4 \times 0.95 = 17.5 \text{ kN/m}^3$ and $w = 9.2\%$ (from graph).

Step 4: Calculate the degree of saturation at maximum dry unit weight.

Algebraically manipulate Equation (5.1) to find S as

$$S = \frac{wG_s(\gamma_d)_{\max}/\gamma_w}{G_s - (\gamma_d)_{\max}/\gamma_w} = \frac{0.115 \times 2.7 \times (18.4/9.8)}{2.7 - 18.4/9.8} = 0.71 = 71\%$$

EXAMPLE 5.3 *Interpreting Compaction Data (2)*

The detailed results of a standard compaction test are shown in the table below. Determine the maximum dry unit weight and optimum water content.

Diameter of mold = 101.4 mm

Height of mold = 116.7 mm

Mass of mold, $M = 4196.50$ grams

Unit weight data		Water content data		
Mass of wet soil and mold (grams) M_{wm}	Mass of can and wet soil (grams) M_w	Mass of can and dry soil (grams) M_d	Mass of can (grams) M_c	
5906.00	114.92	111.48	46.50	
6056.00	163.12	155.08	46.43	
6124.00	190.43	178.64	46.20	
6156.00	193.13	178.24	46.50	
6103.00	188.77	171.58	46.10	

Strategy This example is similar to Example 5.2 except that you have to calculate the water content as you would do in an actual test.

Solution 5.3

Step 1: Set up a spreadsheet or a table to do the calculations.

$$\text{Volume of mold} = \frac{\pi}{4} \times 0.1014^2 \times 0.1167 = 942.4 \times 10^{-6} \text{ m}^3$$

Water content calculations				Dry unit weight calculations		
Mass of can and wet soil (grams) M_w	Mass of can and dry soil (grams) M_d	Mass of can (grams) M_c	Water content (%)	Mass of wet soil and mold (grams) M_{wm}	Mass of wet soil (grams) M_w	Dry unit weight (γ_d kN/m 3)
114.92	111.48	46.50	5.30	5906.00	1709.5	16.9
163.12	155.08	46.43	7.40	6056.00	1859.5	18.0
190.43	178.64	46.20	8.90	6124.00	1927.5	18.4
193.13	178.24	46.50	11.30	6156.00	1959.5	18.3
188.77	171.58	46.10	13.70	6103.00	1906.5	17.5

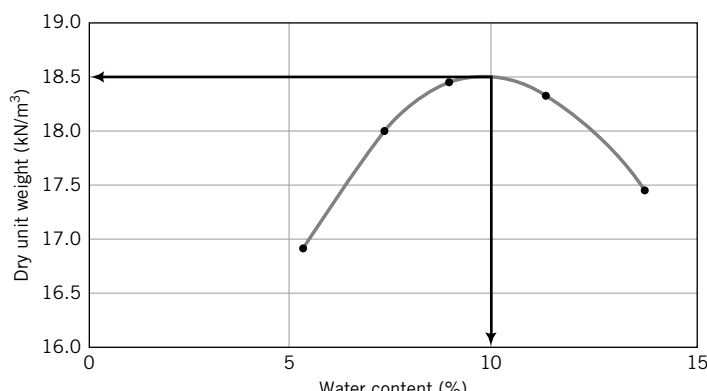
$$\text{Dry unit weight} = \frac{\text{mass of wet soil} \times \text{acceleration due to gravity}}{\text{Volume of mold} (1 + \text{water content})}$$

Step 2: Plot dry unit weight versus water content curve.

See Figure E5.3.

Step 3: Extract the results.

Maximum dry unit weight = 18.5 kN/m 3 ; optimum water content = 10%

**FIGURE E5.3**

What's next . . . Why is soil compaction important? This question is addressed in the next section.

5.6 BENEFITS OF SOIL COMPACTION

Compaction is the most popular technique for improving soils. The soil fabric is forced into a dense configuration by the expulsion of air using mechanical effort with or without the assistance of water. The benefits of compaction are:

1. Increased soil strength.
2. Increased load-bearing capacity.
3. Reduction in settlement (lower compressibility).
4. Reduction in the flow of water (water seepage).
5. Reduction in soil swelling (expansion) and collapse (soil contraction).
6. Increased soil stability.
7. Reduction in frost damage.

Improper compaction can lead to:

1. Structural distress from excessive total and differential settlements.
2. Cracking of pavements, floors, and basements.
3. Structural damage to buried structures, water and sewer pipes, and utility conduits.
4. Soil erosion.

THE ESSENTIAL POINTS ARE:

1. Compaction is the densification of a soil by the expulsion of air and the rearrangement of soil particles.
2. The Proctor test is used to determine the maximum dry unit weight and the optimum water content and serves as the reference for field specifications of compaction.
3. Higher compactive effort increases the maximum dry unit weight and reduces the optimum water content.
4. Compaction increases strength, lowers compressibility, and reduces the rate of flow water through soils.

What's next . . . In the next section, general guidelines to help you specify field compaction equipment are presented.

5.7 FIELD COMPACTION

A variety of mechanical equipment is used to compact soils in the field. Compaction is accomplished by static and vibratory vertical forces. Static vertical forces are applied by deadweights that impart pressure and/or kneading action to the soil mass. Sheepsfoot rollers (Figure 5.7a), grid rollers, rubber-tired rollers, drum rollers (Figure 5.7b), loaders, and scrapers are examples of equipment that apply static vertical forces. Vibratory vertical forces are applied by engine-driven systems with rotating eccentric weights or spring/piston mechanisms that impart a rapid sequence of blows to the soil surface. The soil is compacted by pressure and rearranging of the soil structure by either impact or vibration. Common types of vibrating equipment are vibrating plate compactors, vibrating rollers, and vibrating sheepsfoot rollers. Vibrating sheepsfoot and impact rammers are impact compactors.



FIGURE 5.7

Two types of machinery for field compaction: (a) a sheepsfoot roller and (b) a drum-type roller. (Photos courtesy of Vibromax America, Inc.)

TABLE 5.1 Comparison of Field Compactors for Various Soil Types

Material	Lift thickness (mm)	Compaction type				
		Static		Dynamic		
		Pressure with kneading	Kneading with pressure	Vibration	Impact	Compactability
Gravel	300+	Not applicable	Very good	Good	Poor	Very easy
Sand	250±	Not applicable	Good	Excellent	Poor	Easy
Silt	150±	Good	Excellent	Poor	Good	Difficult
Clay	150±	Very good	Good	No	Excellent	Very difficult

The soil mass is compacted in layers called lifts. The lift thickness rarely exceeds 300 mm. Coarse-grained soils are compacted in lifts between 250 mm and 300 mm while fine-grained soils are compacted in lifts ranging between 100 mm and 150 mm. The stresses imparted by compactors, especially static compactors, decrease with lift depth. Consequently, the top part of the lift is subjected to greater stresses than the bottom and attains a higher degree of compaction. Lower lift thickness is then preferable for uniform compaction. A comparison of various types of field compactors and the type of soils they are suitable for is shown in Table 5.1. Generally, it is preferable to specify the amount of compaction desired based on the relevant Proctor test and let the contractor select the appropriate equipment. You will have to ensure that the contractor has the necessary experience.

What's next . . . When you specify the amount of compaction desired for a project, you need to ensure that the specifications are met. In next section, three popular apparatuses for compaction quality control tests are discussed.

5.8 COMPACTION QUALITY CONTROL

A geotechnical engineer needs to check that field compaction meets specifications. A measure of the degree of compaction (DC) is the ratio of the measured dry unit weight achieved to the desired dry unit weight.

$$DC = \frac{\text{Measured dry unit weight}}{\text{Desired dry unit weight}} \quad (5.4)$$

Various types of equipment are available to check the amount of compaction achieved in the field. Three popular pieces of equipment are (1) the sand cone, (2) the balloon, and (3) nuclear density meters.

5.8.1 Sand Cone—ASTM D 1556

A sand cone apparatus is shown in Figure 5.8. It consists of a glass or plastic jar with a funnel attached to the neck of the jar.

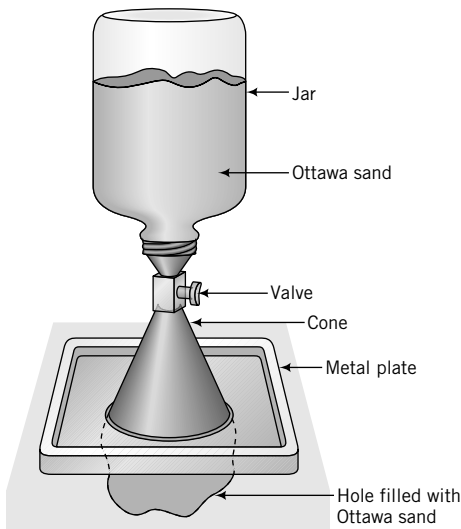


FIGURE 5.8
A sand cone apparatus.

The procedure for a sand cone test is as follows:

1. Fill the jar with a standard sand—a sand with known density—and determine the weight of the sand cone apparatus with the jar filled with sand (W_1). The American Society for Testing and Materials (ASTM) recommends Ottawa sand as the standard.
2. Determine the weight of sand to fill the cone (W_2).
3. Excavate a small hole in the soil and determine the weight of the excavated soil (W_3).
4. Determine the water content of the excavated soil (w).
5. Fill the hole with the standard sand by inverting the sand cone apparatus over the hole and opening the valve.
6. Determine the weight of the sand cone apparatus with the remaining sand in the jar (W_4).
7. Calculate the unit weight of the soil as follows:

$$\text{Weight of sand to fill hole} = W_s = W_1 - (W_2 + W_4)$$

$$\text{Volume of hole} = V = \frac{W_s}{(\gamma_d)_{\text{Ottawa sand}}}$$

$$\text{Weight of dry soil} = W_d = \frac{W_3}{1 + w}$$

$$\text{Dry unit weight} = \gamma_d = \frac{W_d}{V}$$

EXAMPLE 5.4 Interpreting Sand Cone Test Results

A sand cone test was conducted during the compaction of a roadway embankment. The data are as follows.

Calibration to find dry unit weight of the standard sand

Mass of Proctor mold	4178 grams
Mass of Proctor mold and sand	5609 grams
Volume of mold	0.00095 m ³

Calibration of sand cone

Mass of sand cone apparatus and jar filled with sand	5466 grams
Mass of sand cone apparatus with remaining sand in jar	3755 grams

Sand cone test results

Mass of sand cone apparatus and jar filled with sand	7387 grams
Mass of excavated soil	1827 grams
Mass of sand cone apparatus with remaining sand in jar	3919 grams
Water content of excavated soil	4.8%

(a) Determine the dry unit weight.

(b) The standard Proctor maximum dry unit weight of the roadway embankment soil is 16 kN/m^3 at an optimum water content of 4.2%, dry of optimum. The specification requires a minimum dry unit weight of 95% of Proctor maximum dry unit weight. Is the specification met? If not, how can it be achieved?

Strategy Set up a spreadsheet to carry out the calculations following the method described for the sand cone test. Compare the measured field dry unit weight with the specification requirement to check satisfaction.

Solution 5.4

Step 1: Set up a spreadsheet or a table and carry out calculations following the method described for the sand cone test.

Calibration to find dry unit weight of standard sand

Mass of Proctor mold, M_1	4178 grams
Mass of Proctor mold + sand, M_2	5609 grams
Volume of mold, V_1	0.00095 m^3
Dry unit weight of sand in cone, $\gamma_{dc} = (M_2 - M_1) \times g / V_1$	14.8 kN/m^3

Calibration of sand cone

Mass of sand cone apparatus + jar filled with sand, M_3	5466 grams
Mass of sand cone apparatus with remaining sand in jar, M_4	3755 grams
Mass of sand to fill cone, M_2	1711 grams

Sand cone test results

Mass of sand cone apparatus + jar filled with sand, M_1	7387 grams
Mass of excavated soil, M_3	1827 grams
Mass of sand cone apparatus with remaining sand in jar, M_4	3919 grams
Mass of sand to fill hole, $M_s = M_1 - (M_2 + M_4)$	1757 grams
Volume of hole, $V = M_s \times 9.8 \times 10^{-6} / \gamma_{dc}$	0.0011664 m^3
Water content of excavated soil, w	4.8%
Mass of dry soil, $M_d = M_3 / (1 + w)$	1743 grams
Dry unit weight = $M_d \times 9.8 \times 10^{-6} / V$	14.6 kN/m^3

Step 2: Compare specification with sand cone results.

$$\text{Minimum dry unit weight required} = 0.95 \times 16 = 15.2 \text{ kN/m}^3$$

The sand cone test result gives a dry unit weight of 14.6 kN/m^3 . The degree of compaction is $DC = 14.6/15.2 = 96\%$. Therefore, the specification is not met.

Step 3: Decide on how best to meet the specification.

The water content in the field is 4.8%, while the Proctor test gave an optimum water content of 4.2%. Thus, too much water was added to the embankment soil (the soil was compacted wet of optimum). The contractor should aerate the compacted soil. The dry unit weight and water content should be rechecked and the embankment recompacted as needed.

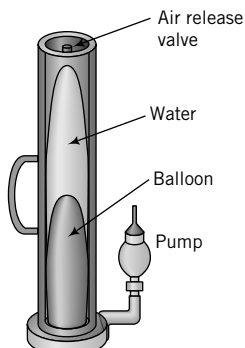


FIGURE 5.9
Balloon test device.

5.8.2 Balloon Test—ASTM D 2167

The balloon test apparatus (Figure 5.9) consists of a graduated cylinder with a centrally placed balloon. The cylinder is filled with water. The procedure for the balloon test is as follows:

1. Fill the cylinder with water and record its volume, V_1 .
2. Excavate a small hole in the soil and determine the weight of the excavated soil (W).
3. Determine the water content of the excavated soil (w).
4. Use the pump to invert the balloon to fill the hole.
5. Record the volume of water remaining in the cylinder, V_2 .
6. Calculate the unit weight of the soil as follows:

$$\gamma = \frac{W}{V_1 - V_2}; \quad \gamma_d = \frac{\gamma}{1 + w}$$

The balloon test is not often used.

5.8.3 Nuclear Density Meter—ASTM D 2922, ASTM D 5195

The nuclear density apparatus (Figure 5.10) is a versatile device to rapidly obtain the unit weight and water content of the soil nondestructively. Soil particles cause radiation to scatter to a detector tube, and



FIGURE 5.10
Nuclear density meter. (Photo courtesy
of Seaman Nuclear Corp.)

the amount of scatter is counted. The scatter count rate is inversely proportional to the unit weight of the soil. If water is present in the soil, the hydrogen in water scatters the neutrons, and the amount of scatter is proportional to the water content. The radiation source is either radium or radioactive isotopes of cesium and americium. The nuclear density apparatus is first calibrated using the manufacturer's reference blocks. This calibration serves as a reference to determine the unit weight and water content of a soil at a particular site.

There are two types of measurements:

1. Backscatter, in which the number of backscattered gamma rays detected by the counter is related to the soil's unit weight. The depth of measurement is 50 mm to 75 mm.
2. Direct transmission, in which the number of rays detected by the counter is related to the soil's unit weight. The depth of measurement is 50 mm to 200 mm.

5.8.4 Comparison Among the Three Popular Compaction Quality Control Tests

A comparison among the three compaction quality control tests is shown in Table 5.2.

TABLE 5.2 Comparison Among the Three Popular Compaction Quality Control Tests

Material	Sand cone	Balloon	Nuclear density meter
Advantages	<ul style="list-style-type: none"> • Low cost • Accurate • Large sample 	<ul style="list-style-type: none"> • Low to moderate cost • Fewer computational steps compared to sand cone • Large sample 	<ul style="list-style-type: none"> • Quick • Direct measurement of unit weight and water content
Disadvantages	<ul style="list-style-type: none"> • Slow; many steps required • Standard sand in hole has to be retrieved • Unit weight has to be computed • Difficult to control density of sand in hole • Possible void space under plate • Hole can reduce in size through soil movement • Hole can cave in (granular materials) 	<ul style="list-style-type: none"> • Slow • Extra care needed to prevent damage to balloon, especially in gravelly materials • Unit weight has to be computed • Difficult to obtain accurate hole size • Possible void space under plate • Hole can reduce in size through soil movement • Hole can cave in (granular materials) 	<ul style="list-style-type: none"> • High cost • Radiation certification required for operation • Water content error can be significant • Surface preparation needed • Radiation backscatter can be hazardous

THE ESSENTIAL POINTS ARE:

1. A variety of field equipment is used to obtain the desired compaction.
2. The sand cone apparatus, the balloon apparatus, and the nuclear density meter are three types of equipment used for compaction quality control in the field.
3. It is generally best to allow the contractor to select and use the appropriate equipment to achieve the desired compaction.

5.9 SUMMARY

Compaction—the densification of a soil by expulsion of air and forcing the soil particles closer together—is a popular method for improving soils. The laboratory test to investigate the maximum dry unit weight and the optimum water content is the Proctor test. This standard test is used in most applications. For heavy loads, the modified Proctor test is used. Various types of equipment are available to achieve specified compaction. You need to select the appropriate equipment based on the soil type and the availability of the desired equipment.

Self-Assessment



Access Chapter 5 at <http://www.wiley.com/college/budhu> to take the end-of-chapter quiz to test your understanding of this chapter.

Practical Example

EXAMPLE 5.5 Interpreting Standard Proctor Test Results and Specifying Field Compaction Equipment

The standard Proctor test for a gravelly sand (24% gravel, 76% sand) to be used as a base course (a soil layer above the existing soil) of a highway embankment is shown in Figure E5.5a.

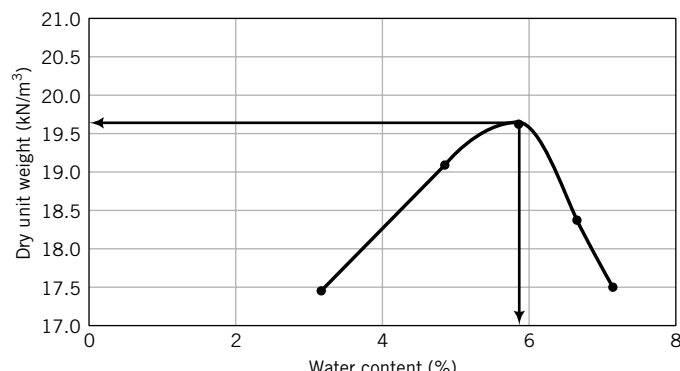


FIGURE E5.5a

- (a) Specify the compaction criteria for the field.
- (b) Recommend field compaction equipment that would achieve the desired compaction.
- (c) Specify an appropriate quality control test.

Strategy Because the soil is a gravelly sand, it is best to specify compaction dry of optimum.

Solution 5.5

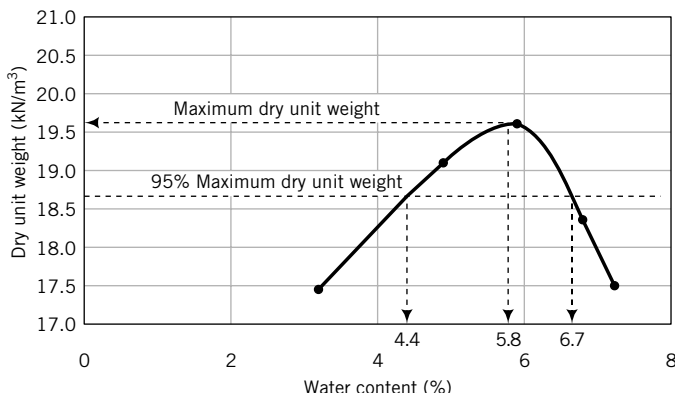
Step 1: Determine maximum dry unit weight and optimum water content.

The maximum dry unit weight and optimum water content are $19.6 \text{ kN}/\text{m}^3$ and 5.8%, respectively.

Step 2: Specify dry unit weight and water content.

Specify 95% standard Proctor test to be compacted dry of optimum (Figure E5.5b).

$$\gamma_d = 18.6 \text{ kN}/\text{m}^3; w = 4.4\%$$

**FIGURE E5.5b****Step 3:** Determine field method of compaction.

The soil contains a larger proportion of sand than gravel. From Table 5.1, a vibrating roller is excellent for sand and good for gravel. Specify a vibrating roller.

Step 4: Specify quality control equipment.

Either the sand cone or the nuclear density meter is suitable.

EXERCISES

Assume $G_s = 2.7$, where necessary, for solving the following problems.

Theory

- 5.1** Discuss the effects of not dropping the hammer in a standard Proctor test from a height of 305 mm. Plot a graph of energy versus hammer height from 250 mm to 400 mm in steps of 50 mm to discuss the effects. Assume the mold, hammer mass, number of layers (3), and number of blows (25) are all constants.

- 5.2 (a)** Plot the theoretical dry unit weight versus water content using the following data.

Water content (%)	4	5	8	10	12
Degree of saturation, S (%)	20	30	60	70	75

- (b)** Determine the maximum dry unit weight and optimum water content.

Problem Solving

- 5.3** A soil at a mining site is classified according to USCS as GW-GM.

- (a)** Would this soil be suitable for the base course of a road?

- (b)** What type of field compaction equipment would you recommend?

- (c)** How would you check that the desired compaction is achieved in the field?

- (d)** Would you specify compaction dry or wet of optimum? Why?

- 5.4** The water content in one of five standard Proctor test samples is 15.2%. The corresponding degree of saturation is 85%. Calculate the dry unit weight if $G_s = 2.67$.

- 5.5** The data from a standard Proctor test are shown in the table below.

- (a)** Determine the maximum dry unit weight and the optimum water content.

- (b)** Plot the zero air voids line.

- (c)** Determine the degree of saturation at the maximum dry unit weight.

Diameter of mold	101.4 mm
Height of mold	116.7 mm
Mass of mold	4196.50 grams
Specific gravity, G_s	2.69

Unit weight determination		Water content determination		
Mass of wet soil and mold (grams)	Mass of can and wet soil (grams)	Mass of can and dry soil (grams)	Mass of can (grams)	
5906	108.12	105.10	42.10	
6013	98.57	94.90	40.90	
6135	121.90	114.70	42.70	
6156	118.39	110.50	42.50	
6103	138.02	126.80	41.80	

Practical

5.6 A fine-grained soil has 60% clay with LL = 220%, PL = 45%, and a natural water content of 6%. A standard Proctor test was carried out in the laboratory and the following data were recorded.

Diameter of mold	101.40 mm
Height of mold	116.70 mm
Mass of mold	4196.50 grams
Specific gravity, G_s	2.69

Unit weight determination		Water content determination		
Mass of wet soil and mold (grams)	Mass of can and wet soil (grams)	Mass of can and dry soil (grams)	Mass of can (grams)	
6257	105.05	103.10	42.10	
6356	100.69	97.90	40.90	
6400	114.71	110.70	42.70	
6421	134.26	128.50	42.50	
6400	109.34	104.80	41.80	

- (a) Determine the maximum dry unit weight and optimum water content.
- (b) If the desired compaction in the field is 95% of the standard Proctor test results, what values of dry unit weight and water content would you specify? Explain why you select these values.
- (c) What field equipment would you specify to compact the soil in the field, and why?
- (d) How would you check that the specified dry unit weight and water content are achieved in the field?

5.7 Standard Proctor compaction test results on a sandy clay (35% sand, 55% clay, and 10% silt), taken from a borrow pit, are given in the following table.

Water content (%)	4.2	5.1	7.8	9.2	12
Dry unit weight (kN/m^3)	16.9	18.1	19.6	19.5	18.5

The sandy clay in the borrow pit has a porosity of 65% and a water content of 5.2%. A highway embankment is to be constructed using this soil.

- (a) Specify the compaction (dry unit weight and water content) to be achieved in the field. Justify your specification.
- (b) How many cubic meters of borrow pit soil are needed for 1 cubic meter of highway fill?
- (c) How much water per unit volume is required to meet the specification?
- (d) How many truckloads of soil will be required for a $100,000\text{-m}^3$ highway embankment? Each truck has a load capacity of 22.5 m^3 and regulations require a maximum load capacity of 90%.
- (e) Determine the cost for $100,000\text{ m}^3$ of compacted soil based on the following:

Purchase and load borrow pit material at site, haul 2 km round-trip, and spread with 200 HP dozer = $\$15/\text{m}^3$; extra mileage charge for each km = $\$0.5/\text{m}^3$; round-trip distance = 10 km; compaction = $\$1.02/\text{m}^3$.

- 5.8 A sand cone test was conducted for quality control during the compaction of sandy clay. The data are as follows.

Calibration to find dry unit weight of the standard sand	
Mass of Proctor mold	4178 grams
Mass of Proctor mold and sand	5609 grams
Volume of mold	0.00095 m^3
Calibration of sand cone	
Mass of sand cone apparatus and jar filled with sand	5466 grams
Mass of sand cone apparatus with remaining sand in jar	3755 grams
Sand cone test results	
Mass of sand cone apparatus and jar filled with sand	7387 grams
Mass of excavated soil	2206 grams
Mass of sand cone apparatus with remaining sand in jar	3919 grams
Water content of excavated soil	9.2%

- (a) Determine the dry unit weight.
- (b) The standard Proctor maximum dry unit weight of the sandy clay is 178 kN/m^3 at an optimum water content of 10%. The specification requires 95% Proctor dry unit weight at acceptable water contents ranging from 9% to 10.8%. Is the specification met? Justify your answer.

CHAPTER 6

ONE-DIMENSIONAL FLOW OF WATER THROUGH SOILS

6.0 INTRODUCTION

In this chapter, we will discuss one-dimensional flow of water through soils. Two-dimensional flow of water is presented in Chapter 14.

When you complete this chapter, you should be able to:

- Determine the rate of flow of water through soils.
- Determine the hydraulic conductivity of soils.
- Appreciate the importance of flow of water through soils.

Importance

We have discussed particle sizes and index properties, and used these to classify soils. You know that water changes the soil states in fine-grained soils; the greater the water content in a soil, the weaker it is. Soils are porous materials, much like sponges. Water can flow between the interconnected voids. Particle sizes and the structural arrangement of the particles influence the rate of flow.

The flow of water has caused instability and failure of many geotechnical structures (e.g., roads, bridges, dams, and excavations). The key physical property that governs the flow of water in soils is hydraulic conductivity (also called permeability). A sample practical application is as follows. An excavation is required to construct the basement of a building. During construction, the base of the excavation needs to be free of water. The engineer decides to use a retaining wall around the excavation to keep it dry. Water from outside the excavation will flow under the wall. This can lead to instability as well as flooding of the excavation. To determine the length of the wall to keep the excavation dry, the soil's hydraulic conductivity must be known.

6.1 DEFINITIONS OF KEY TERMS

Groundwater is water under gravity that fills the soil pores.

Head (H) is the mechanical energy per unit weight.

Hydraulic conductivity, sometimes called the coefficient of permeability, (k) is a proportionality constant used to determine the flow velocity of water through soils.

Porewater pressure (u) is the pressure of water within the soil pores.

6.2 QUESTIONS TO GUIDE YOUR READING

1. What causes the flow of water through soils?
2. What law describes the flow of water through soils?
3. What is hydraulic conductivity and how is it determined?
4. What are the typical values of hydraulic conductivities for coarse-grained and fine-grained soils?

6.3 HEAD AND PRESSURE VARIATION IN A FLUID AT REST

We will be discussing gravitational flow of water under a steady-state condition. You may ask: “What is a steady-state condition?” Gravitational flow can only occur if there is a gradient. Flow takes place downhill. The steady-state condition occurs if neither the flow nor the porewater pressure changes with time. Recall from Chapter 4 that porewater pressure is the water pressure within the voids.

Darcy's law governs the flow of water through soils. But before we delve into Darcy's law, we will discuss an important principle in fluid mechanics—Bernoulli's principle—that is essential in understanding flow through soils.

If you cap one end of a tube, fill the tube with water, and then rest it on your table (Figure 6.1), the height of water with reference to your table is called the pressure head (h_p). Head refers to the mechanical energy per unit weight. If you raise the tube above the table, the mechanical energy or total head increases.

You now have two components of total head—the pressure head (h_p) and the elevation head (h_z). If water were to flow through the tube with a velocity v under a steady-state condition, then we would have an additional head due to the velocity, given as $v^2/2g$. The total head, H , according to Bernoulli's principle, is

$$H = h_z + h_p + \frac{v^2}{2g} \quad (6.1)$$

The flow is assumed to be steady, inviscid (no change in viscosity), incompressible (no change in volume), and irrotational (fluid particles do not spin).

The elevation or potential head is referenced to an arbitrary datum, and the total head will change depending on the choice of the datum position. Therefore, it is essential that you identify your datum position in solutions to flow problems. Pressures are defined relative to atmospheric pressure (atmospheric pressure is 101.3 kPa at a temperature of 15°C). This is called gage pressure. The gage pressure at the groundwater level (free surface) is zero. The velocity of flow through soils is generally small (<1 cm/s) and we usually neglect the velocity head. The total head in soils is then

$$H = h_z + h_p = h_z + \frac{u}{\gamma_w} \quad (6.2)$$

where $u = h_p \gamma_w$ is the porewater pressure.

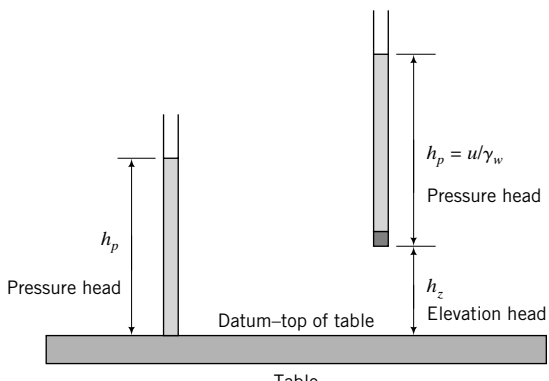
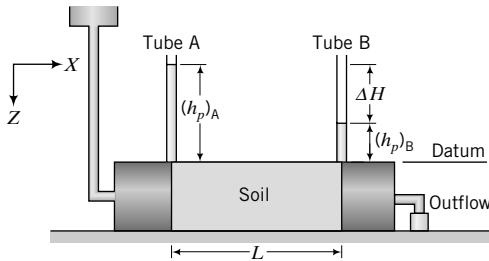


FIGURE 6.1

Illustration of elevation and pressure heads.

**FIGURE 6.2**

Head loss due to flow of water through soil.

Consider a cylinder containing a soil mass with water flowing through it at a constant rate, as depicted in Figure 6.2. If we connect two tubes, A and B, called piezometers, at a distance L apart, the water will rise to different heights in each of the tubes. The height of water in tube B near the exit is lower than that in tube A. Why? As the water flows through the soil, energy is dissipated through friction with the soil particles, resulting in a loss of head. The head loss between A and B, assuming decrease in head, is positive and our datum arbitrarily selected at the top of the cylinder is $\Delta H = (h_p)_A - (h_p)_B$. In general, the head loss is the total head at A minus the total head at B.

The ordinary differential equation to describe one-dimensional pressure variation of a fluid at rest (acceleration equal to zero) is

$$\frac{dp}{dz} = \gamma_w \quad (6.3)$$

The fluid pressure difference between two vertical points, z_1 and z_2 , below the free surface (Figure 6.3) is

$$\int_{p_1}^{p_2} dp = \gamma_w \int_{z_1}^{z_2} z$$

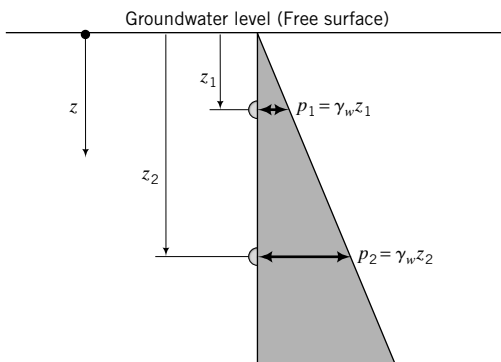
Performing the integration gives

$$p_2 - p_1 = \gamma_w(z_2 - z_1) \quad (6.4)$$

At the free surface ($z_1 = 0$), the (gage) pressure is zero ($p_1 = 0$) and $z_2 = z_w$, so the fluid pressure variation (called the hydrostatic pressure distribution) is

$$p = u = \gamma_w z_w \quad (6.5)$$

where z_w is the depth from the groundwater level.

**FIGURE 6.3**

Hydrostatic or porewater pressure variation below the groundwater level.

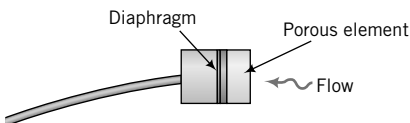


FIGURE 6.4
Schematic of a porewater pressure transducer.

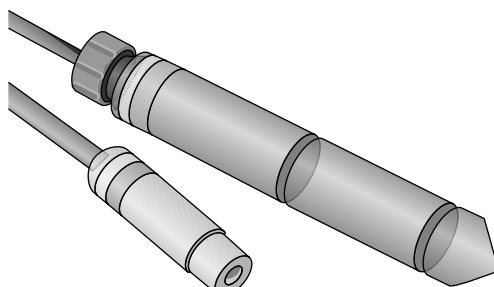


FIGURE 6.5
Piezometers.

Porewater pressures are measured by porewater pressure transducers (Figure 6.4) or by piezometers (Figure 6.5). In a porewater pressure transducer, water passes through a porous material and pushes against a metal diaphragm to which a strain gauge is attached. The strain gauge is usually wired into a Wheatstone bridge. The porewater pressure transducer is calibrated by applying known pressures and measuring the electrical voltage output from the Wheatstone bridge. Piezometers are porous tubes that allow the passage of water. In a simple piezometer, you can measure the height of water in the tube from a fixed elevation and then calculate the porewater pressure by multiplying the height of water by the unit weight of water. A borehole cased to a certain depth acts like a piezometer. Modern piezometers are equipped with porewater pressure transducers for electronic reading and data acquisition.

EXAMPLE 6.1 Determination of Hydraulic Heads

Determine (a) the variations of the elevation, pressure, and total heads through the soil when the pressure gage in the experimental setup shown in Figure E6.1a has a pressure of 19.6 kPa, and (b) the elevation, pressure, and total heads in the middle of the soil.

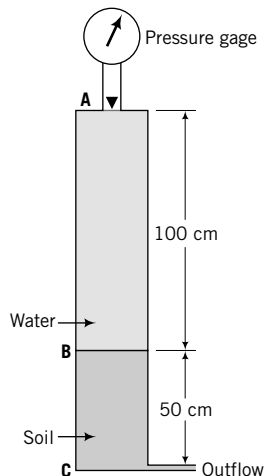


FIGURE E6.1a

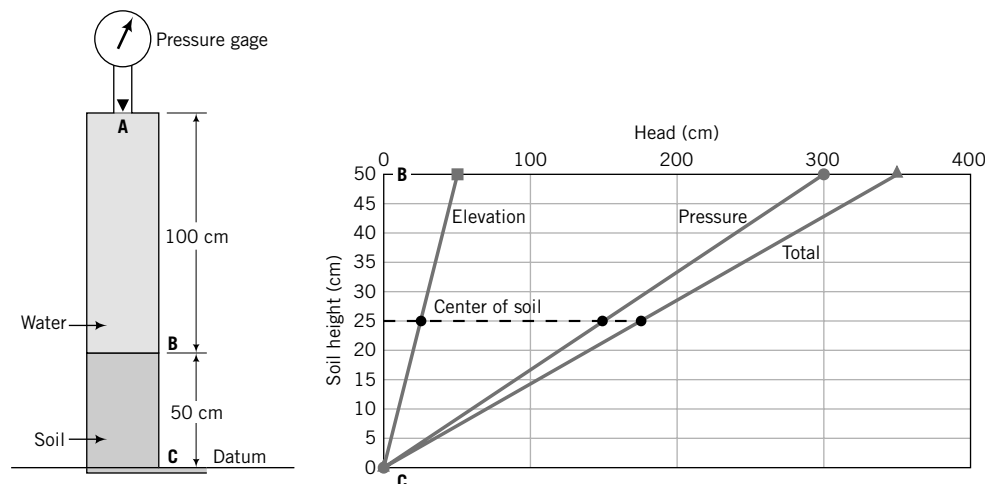


FIGURE E6.1b

Strategy The first thing you need to do is to define your datum. Outflows or exits are good choices; the pressure head there is zero. The pressure from the pressure gage should be converted to a pressure head by dividing by the unit weight of water (9.8 kN/m^3). To determine the pressure head at a point, assume that you connect a small tube at that point and then figure out how high the water will rise in the tube.

Solution 6.1

Step 1: Define the datum position. Choose C as datum (Figure E6.1b).

Step 2: Determine the heads.

Top of soil—B

Pressure gage = 19.6 kPa; equivalent pressure head = pressure/unit weight of water = $19.6/9.8 = 2 \text{ m} = 200 \text{ cm}$

Elevation head = 50 cm; pressure head of water above B + pressure gage head = $100 + 200 = 300 \text{ cm}$; total head = elevation head + pressure head = $50 + 300 = 350 \text{ cm}$

Bottom of soil—C

Elevation head = 0 cm; pressure head = 0 cm; total head = $0 + 0 = 0 \text{ cm}$

Step 3: Determine the heads at the center of the soil.

The heads are linearly distributed through the soil. Therefore, the heads are proportional to the soil height.

At the center of the soil, elevation head = 25 cm, pressure head = $300/2 = 150 \text{ cm}$, and the total head = $25 + 150 = 175 \text{ cm}$.

6.4 DARCY'S LAW

Darcy (1856) proposed that average flow velocity through soils is proportional to the gradient of the total head. The flow in any direction, j , is

$$v_j = k_j \frac{dH}{dx_j} \quad (6.6)$$

where v is the average flow velocity, k is a coefficient of proportionality called the hydraulic conductivity (sometimes called the coefficient of permeability), and dH is the change in total head over a distance dx .

The unit of measurement for k is length/time, that is, cm/s. With reference to Figure 6.2, Darcy's law becomes

$$v_x = k_x \frac{\Delta H}{L} = k_x i \quad (6.7)$$

where $i = \Delta H/L$ is the hydraulic gradient. Darcy's law is valid for all soils if the flow is laminar.

The average velocity, v , calculated from Equation (6.7) is for the cross-sectional area normal to the direction of flow. Flow through soils, however, occurs only through the interconnected voids. The velocity through the void spaces is called seepage velocity (v_s) and is obtained by dividing the average velocity by the porosity of the soil:

$$v_s = \frac{k_j}{n} i \quad (6.8)$$

The volume rate of flow, q_j , or, simply, flow rate is the product of the average velocity and the cross-sectional area:

$$q_j = v_j A = A k_j i \quad (6.9)$$

The unit of measurement for q_j is m³/s or cm³/s. The conservation of flow (law of continuity) stipulates that the volume rate of inflow (q_j)_{in} into a soil element must equal the volume rate of outflow, (q_j)_{out}, or, simply, inflow must equal outflow: (q_j)_{in} = (q_j)_{out}.

The hydraulic conductivity depends on

1. *Soil type*: Coarse-grained soils have higher hydraulic conductivities than fine-grained soils. The water in the double layer in fine-grained soils significantly reduces the seepage pore space.
2. *Particle size*: Hydraulic conductivity depends on D_{50}^2 (or D_{10}^2) for coarse-grained soils.
3. *Pore fluid properties, particularly viscosity*: $k_1 : k_2 \approx \mu_2 : \mu_1$, where μ is dynamic viscosity (dynamic viscosity of water is 1.12×10^{-3} N.s/m² at 15.6°C) and the subscripts 1 and 2 denote two types of pore fluids in a given soil.
4. *Void ratio*: $k_1 : k_2 \approx e_1^2 : e_2^2$, where subscripts 1 and 2 denote two types of soil fabric for coarse-grained soils. This ratio is useful in comparing the hydraulic conductivities of similar soils with different void ratios. However, two soils with the same void ratio can have different hydraulic conductivities.
5. *Pore size*: The greater the interconnected pore space, the higher the hydraulic conductivity. Large pores do not indicate high porosity. The flow of water through soils is related to the square of the pore size, and not the total pore volume.
6. *Homogeneity, layering, and fissuring*: Water tends to seep quickly through loose layers, through fissures, and along the interface of layered soils. Catastrophic failures can occur from such seepage.
7. *Entrapped gases*: Entrapped gases tend to reduce the hydraulic conductivity. It is often very difficult to get gas-free soils. Even soils that are under groundwater level and are assumed to be saturated may still have some entrapped gases.
8. *Validity of Darcy's law*: Darcy's law is valid only for laminar flow (Reynolds number less than 2100). Fancher et al. (1933) gave the following criterion for the applicability of Darcy's law for hydraulic conductivity determination:

$$\frac{v D_s \gamma_w}{\mu g} \leq 1 \quad (6.10)$$

where v is velocity, D_s is the diameter of a sphere of equivalent volume to the average soil particles, μ is dynamic viscosity of water (1.12×10^{-3} N.s/m² at 15.6°C), and g is the acceleration due to gravity.

Typical ranges of k_z for various soil types are shown in Table 6.1.

TABLE 6.1 Hydraulic Conductivity for Common Soil Types

Soil type	k_z (cm/s)	Description	Drainage
Clean gravel (GW, GP)	>1.0	High	Very good
Clean sands, clean sand and gravel mixtures (SW, SP)	1.0 to 10^{-3}	Medium	Good
Fine sands, silts, mixtures comprising sands, silts, and clays (SM-SC)	10^{-3} to 10^{-5}	Low	Poor
Weathered and fissured clays			
Silt, silty clay (MH, ML)	10^{-5} to 10^{-7}	Very low	Poor
Homogeneous clays (CL, CH)	< 10^{-7}	Practically impervious	Very poor

Homogeneous clays are practically impervious. Two popular uses of “impervious” clays are in dam construction to curtail the flow of water through the dam and as barriers in landfills to prevent migration of effluent to the surrounding area. Clean sands and gravels are pervious and can be used as drainage materials or soil filters. The values shown in Table 6.1 are useful only to prepare estimates and in preliminary design.

6.5 EMPIRICAL RELATIONSHIPS FOR k

For a homogeneous soil, the hydraulic conductivity depends predominantly on the interconnected pore spaces. You should recall that the pore space (void ratio) is dependent on the soil fabric or structural arrangement of the soil grains. Taylor (1948) proposed a relationship linking k with void ratio as

$$k_z = D_{50}^2 \frac{\gamma_w}{\mu} \frac{C_1 e^3}{1 + e} \quad (6.11)$$

where C_1 is a constant related to shape that can be obtained from laboratory experiments. A number of empirical relationships have been proposed linking k_z to void ratio and grain size for coarse-grained soils. Hazen (1930) proposed one of the early relationships as

$$k_z = CD_{10}^2 \text{ (unit: cm/s)} \quad (6.12)$$

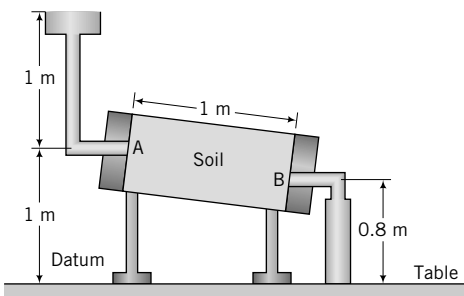
where C is a constant varying between 0.4 and 1.4 if the unit of measurement of D_{10} is mm. Typically, $C = 1.0$. Hazen's tests were done on sands with D_{10} ranging from 0.1 mm to 3 mm and $Cu < 5$. Other relationships were proposed for coarse-grained and fine-grained soils by Samarasinghe et al. (1982), Kenny et al. (1984), and others. One has to be extremely cautious in using empirical relationships for k_z because it is very sensitive to changes in void ratio, interconnected pore space, and the homogeneity of your soil mass.

THE ESSENTIAL POINTS ARE:

1. The flow of water through soils is governed by Darcy's law, which states that the average flow velocity is proportional to the hydraulic gradient.
2. The proportionality coefficient in Darcy's law is called the hydraulic conductivity, k .
3. The value of k_z is influenced by the void ratio, pore size, interconnected pore space, particle size distribution, homogeneity of the soil mass, properties of the pore fluid, and the amount of undissolved gas in the pore fluid.
4. Homogeneous clays are practically impervious, while sands and gravels are pervious.

EXAMPLE 6.2 Calculating Flow Parameters

A soil sample 10 cm in diameter is placed in a tube 1 m long. A constant supply of water is allowed to flow into one end of the soil at A, and the outflow at B is collected by a beaker (Figure E6.2). The average amount of water collected is 1 cm³ for every 10 seconds. The tube is inclined as shown in Figure E6.2. Determine the (a) hydraulic gradient, (b) flow rate, (c) average velocity, (d) seepage velocity if $e = 0.6$, and (e) hydraulic conductivity.

**FIGURE E6.2**

Strategy In flow problems, you must define a datum position. So your first task is to define the datum position and then find the difference in total head between A and B. Use the head difference to calculate the hydraulic gradient and use Equations (6.7) to (6.9) to solve the problem.

Solution 6.2

Step 1: Define the datum position. Select the top of the table as the datum.

Step 2: Find the total heads at A (inflow) and B (outflow).

$$H_A = (h_p)_A + (h_z)_A = 1 + 1 = 2 \text{ m}$$

$$H_B = (h_p)_B + (h_z)_B = 0 + 0.8 = 0.8 \text{ m}$$

Step 3: Find the hydraulic gradient.

$$\Delta H = H_A - H_B = 2 - 0.8 = 1.2 \text{ m}$$

$$L = 1 \text{ m}; \quad i = \frac{\Delta H}{L} = \frac{1.2}{1} = 1.2$$

If you were to select the outflow, point B, as the datum, then $H_A = 1 \text{ m} + 0.2 \text{ m} = 1.2 \text{ m}$ and $H_B = 0$. The head loss is $\Delta H = 1.2 \text{ m}$, which is the same value we obtained using the table's top as the datum. It is often simpler, for calculation purposes, to select the exit flow position as the datum.

Step 4: Determine the flow rate.

Volume of water collected, $Q = 1 \text{ cm}^3, t = 10 \text{ seconds}$

$$q_z = \frac{Q}{t} = \frac{1}{10} = 0.1 \text{ cm}^3/\text{s}$$

Step 5: Determine the average velocity.

$$q_z = Av$$

$$A = \frac{\pi \times (\text{diam})^2}{4} = \frac{\pi \times 10^2}{4} = 78.5 \text{ cm}^2$$

$$v = \frac{q_z}{A} = \frac{0.1}{78.5} = 0.0013 \text{ cm/s}$$

Step 6: Determine seepage velocity.

$$v_s = \frac{v}{n}$$

$$n = \frac{e}{1 + e} = \frac{0.6}{1 + 0.6} = 0.38$$

$$v_s = \frac{0.0013}{0.38} = 0.0034 \text{ cm/s}$$

Step 7: Determine the hydraulic conductivity. From Darcy's law, $v = k_z i$.

$$\therefore k_z = \frac{v}{i} = \frac{0.0013}{1.2} = 10.8 \times 10^{-4} \text{ cm/s}$$

EXAMPLE 6.3 Calculating Hydraulic Heads and Application to a Practical Scenario

A drainage pipe (Figure E6.3a) became completely blocked during a storm by a plug of sand 1.5 m long, followed by another plug of a mixture of clays, silts, and sands 0.5 m long. When the storm was over, the water level above ground was 1 m. The hydraulic conductivity of the sand is 2 times that of the mixture of clays, silts, and sands.

- (a) Plot the variation of pressure, elevation, and total head over the length of the pipe.
- (b) Calculate the porewater pressure at (1) the center of the sand plug and (2) the center of the mixture of clays, silts, and sands.
- (c) Find the average hydraulic gradients in the sand and in the mixture of clays, silts, and sands.

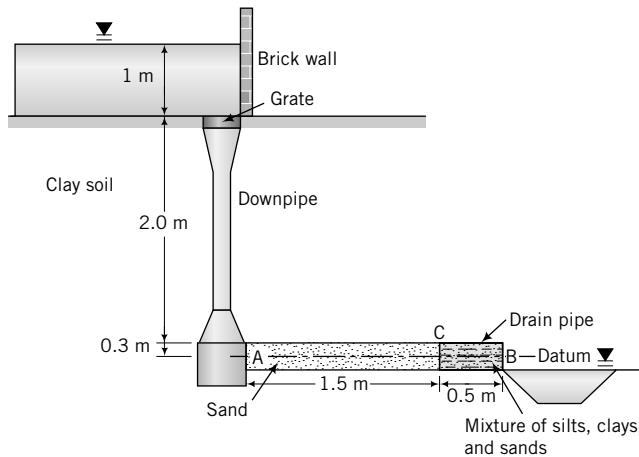


FIGURE E6.3a Illustration of blocked drainage pipe.

Strategy You need to select a datum. From the information given, you can calculate the total head at A and B. The difference in head is the head loss over both plugs, but you do not know how much head is lost in the sand and in the mixture of clays, silts, and sands. The continuity equation provides the key to finding the head loss over each plug.

Solution 6.3

Step 1: Select a datum.

Select the exit at B along the centerline of the drainage pipe as the datum.

Step 2: Determine heads at A and B.

$$(h_z)_A = 0 \text{ m}, \quad (h_p)_A = 0.3 + 2 + 1 = 3.3 \text{ m}, \quad H_A = 0 + 3.3 = 3.3 \text{ m}$$

$$(h_z)_B = 0 \text{ m}, \quad (h_p)_B = 0 \text{ m}, \quad H_B = 0 \text{ m}$$

Step 3: Determine the head loss in each plug.

Head loss between A and B is $|H_B - H_A| = 3.3 \text{ m}$ (decrease in head taken as positive). Let ΔH_1 , L_1 , k_1 , and q_1 be the head loss, length, hydraulic conductivity, and flow in the sand; let ΔH_2 , L_2 , k_2 , and q_2 be the head loss, length, hydraulic conductivity, and flow in the mixture of clays, silts, and sands. Now,

$$q_1 = A k_1 \frac{\Delta H_1}{L_1} = A \times 2k_2 \frac{\Delta H_1}{L_1}$$

$$q_2 = A k_2 \frac{\Delta H_2}{L_2} = A \times k_2 \frac{\Delta H_2}{L_2}$$

From the continuity equation, $q_1 = q_2$.

$$\therefore A \times 2k_2 \frac{\Delta H_1}{L_1} = A k_2 \frac{\Delta H_2}{L_2}$$

Solving, we get

$$\frac{\Delta H_1}{\Delta H_2} = \frac{L_1}{2L_2} = \frac{1.5}{2 \times 0.5} = 1.5$$

$$\Delta H_1 = 1.5 \Delta H_2 \tag{1}$$

However, we know that

$$\Delta H_1 + \Delta H_2 = \Delta H = 3.3 \text{ m} \tag{2}$$

Solving for ΔH_1 and ΔH_2 from Equations (1) and (2), we obtain

$$\Delta H_1 = 1.98 \text{ m} \quad \text{and} \quad \Delta H_2 = 3.3 - 1.98 = 1.32 \text{ m}$$

Step 4: Calculate heads at the junction of the two plugs.

$$\text{Total head at C} = H_C = H_A - \Delta H_1 = 3.3 - 1.98 = 1.32 \text{ m}$$

$$(h_z)_C = 0$$

$$(h_p)_C = H_C - (h_z)_C = 1.32 \text{ m}$$

Step 5: Plot distribution of heads.

See Figure E6.3b.

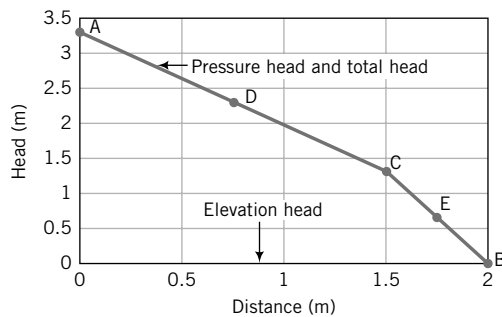


FIGURE E6.3b Variation of elevation, pressure, and total heads along pipe.

Step 6: Calculate porewater pressures.

Let D be the center of the sand.

$$(h_p)_D = \frac{(h_p)_A + (h_p)_C}{2} = \frac{3.3 + 1.32}{2} = 2.31 \text{ m}$$

$$u_D = 2.31 \times \gamma_w = 2.31 \times 9.8 = 22.6 \text{ kPa}$$

Let E be the center of the mixture of clays, silts, and sands.

$$(h_p)_E = \frac{(h_p)_C + (h_p)_B}{2} = \frac{1.32 + 0}{2} = 0.66 \text{ m}$$

$$u_E = 0.66 \times 9.8 = 6.5 \text{ kPa}$$

Step 7: Find the average hydraulic gradients.

$$i_1 = \frac{\Delta H_1}{L_1} = \frac{1.98}{1.5} = 1.32$$

$$i_2 = \frac{\Delta H_2}{L_2} = \frac{1.32}{0.5} = 2.64$$

EXAMPLE 6.4 Calculating Hydrostatic Pressures

The groundwater level in a soil mass is 2 m below the existing surface. Plot the variation of hydrostatic pressure with depth up to a depth of 10 m.

Strategy Since the hydrostatic pressure is linearly related to depth, the distribution will be a straight line starting from the groundwater level, not the surface.

Solution 6.4

Step 1: Plot hydrostatic pressure distribution.

$$p = u = \gamma_w z_w = 9.8 z_w$$

At a depth of 10 m, $z_w = 10 - 2 = 8$ m and $p = u = 9.8 \times 8 = 78.4$ kPa
 The slope of the hydrostatic pressure distribution = 9.8 kN/m³.
 See Figure E6.4.

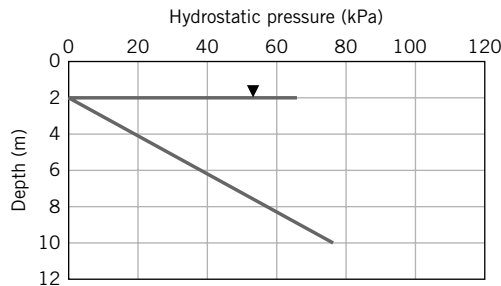


FIGURE E6.4

What's next . . . We have considered flow only through homogeneous soils. In reality, soils are stratified or layered with different soil types. In calculating flow through layered soils, an average or equivalent hydraulic conductivity representing the whole soil mass is determined from the permeability of each layer. Next, we will consider flow of water through layered soil masses: One flow occurs parallel to the layers, the other flow occurs normal to the layers.

6.6 FLOW PARALLEL TO SOIL LAYERS

When the flow is parallel to the soil layers (Figure 6.6), the hydraulic gradient is the same at all points. The flow through the soil mass as a whole is equal to the sum of the flow through each of the layers. There is an analogy here with the flow of electricity through resistors in parallel. If we consider a unit width (in the y direction) of flow and use Equation (6.9), we obtain

$$q_x = Av = (1 \times H_o)k_{x(eq)}i = (1 \times z_1)k_{x1}i + (1 \times z_2)k_{x2}i + \cdots + (1 \times z_n)k_{xn}i \quad (6.13)$$

where H_o is the total thickness of the soil mass, $k_{x(eq)}$ is the equivalent permeability in the horizontal (x) direction, z_1 to z_n are the thicknesses of the first to the n th layers, and k_{x1} to k_{xn} are the horizontal hydraulic conductivities of the first to the n th layer. Solving Equation (6.13) for $k_{x(eq)}$, we get

$$k_{x(eq)} = \frac{1}{H_o}(z_1k_{x1} + z_2k_{x2} + \cdots + z_nk_{xn}) \quad (6.14)$$

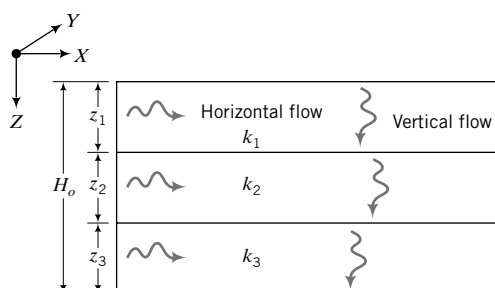


FIGURE 6.6 Flow through stratified layers.

6.7 FLOW NORMAL TO SOIL LAYERS

For flow normal to the soil layers, the head loss in the soil mass is the sum of the head losses in each layer:

$$\Delta H = \Delta h_1 + \Delta h_2 + \cdots + \Delta h_n \quad (6.15)$$

where ΔH is the total head loss, and Δh_1 to Δh_n are the head losses in each of the n layers. The velocity in each layer is the same. The analogy to electricity is flow of current through resistors in series. From Darcy's law, we obtain

$$k_{z(eq)} \frac{\Delta H}{H_o} = k_{z1} \frac{\Delta h_1}{z_1} = k_{z2} \frac{\Delta h_2}{z_2} = \cdots = k_{zn} \frac{\Delta h_n}{z_n} \quad (6.16)$$

where $k_{z(eq)}$ is the equivalent hydraulic conductivity in the vertical (z) direction and k_{z1} to k_{zn} are the vertical hydraulic conductivities of the first to the n th layer. Solving Equations (6.15) and (6.16) leads to

$$k_{z(eq)} = \frac{H_o}{\frac{z_1}{k_{z1}} + \frac{z_2}{k_{z2}} + \cdots + \frac{z_n}{k_{zn}}} \quad (6.17)$$

Values of $k_{z(eq)}$ are generally less than $k_{x(eq)}$ —sometimes as much as 10 times less.

6.8 EQUIVALENT HYDRAULIC CONDUCTIVITY

The equivalent hydraulic conductivity for flow parallel and normal to soil layers is

$$k_{eq} = \sqrt{k_{x(eq)} k_{z(eq)}} \quad (6.18)$$

EXAMPLE 6.5 Vertical and Horizontal Flows in Layered Soils

A canal is cut into a soil with a stratigraphy shown in Figure E6.5. Assuming flow takes place laterally and vertically through the sides of the canal and vertically below the canal, determine the equivalent hydraulic conductivity in the horizontal and vertical directions. The vertical and horizontal hydraulic conductivities for each layer are assumed to be the same. Calculate the ratio of the equivalent horizontal hydraulic conductivity to the equivalent vertical hydraulic conductivity for flow through the sides of the canal.

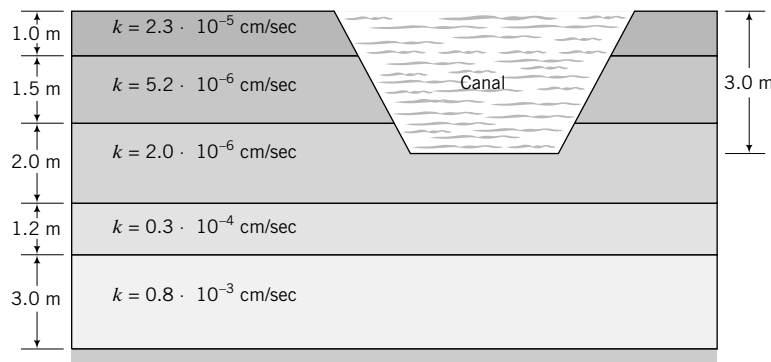


FIGURE E6.5

Strategy Use Equation (6.14) to find the equivalent horizontal hydraulic conductivity over the depth of the canal (3.0 m) and then use Equation (6.17) to find the equivalent vertical hydraulic conductivity below the canal. To make the calculations easier, convert all exponential quantities to a single exponent.

Solution 6.5

Step 1: Find $k_{x(eq)}$ and $k_{z(eq)}$ for flow through the sides of the canal.

$$H_o = 3 \text{ m}$$

$$\begin{aligned} k_{x(eq)} &= \frac{1}{H_o}(z_1k_{x1} + z_2k_{x2} + \dots + z_nk_{xn}) \\ &= \frac{1}{3}(1 \times 0.23 \times 10^{-6} + 1.5 \times 5.2 \times 10^{-6} + 0.5 \times 2 \times 10^{-6}) \\ &= 3 \times 10^{-6} \text{ cm/s} \end{aligned}$$

$$\begin{aligned} k_{z(eq)} &= \frac{H_o}{\frac{z_1}{k_{z1}} + \frac{z_2}{k_{z2}} + \dots + \frac{z_n}{k_{zn}}} \\ &= \frac{3}{\frac{1}{10^{-6}} \left(\frac{1}{0.23} + \frac{1.5}{5.2} + \frac{0.5}{2} \right)} = 0.61 \times 10^{-6} \text{ cm/s} \end{aligned}$$

Step 2: Find the $k_{x(eq)}/k_{z(eq)}$ ratio.

$$\frac{k_{x(eq)}}{k_{z(eq)}} = \frac{3 \times 10^{-6}}{0.61 \times 10^{-6}} = 4.9$$

Step 3: Find $k_{z(eq)}$ below the bottom of the canal.

$$H_o = 1.5 + 1.2 + 3.0 = 5.7 \text{ m}$$

$$\begin{aligned} k_{z(eq)} &= \frac{H_o}{\frac{z_1}{k_{z1}} + \frac{z_2}{k_{z2}} + \dots + \frac{z_n}{k_{zn}}} = \frac{5.7}{\frac{1.5}{2 \times 10^{-6}} + \frac{1.2}{30 \times 10^{-6}} + \frac{3}{800 \times 10^{-6}}} \\ &= 7.2 \times 10^{-6} \text{ cm/s} \end{aligned}$$

What's next . . . In order to calculate flow, we need to know the hydraulic conductivity k_z . We will discuss how this is determined in the laboratory and in the field.

6.9 DETERMINATION OF THE HYDRAULIC CONDUCTIVITY



Virtual Laboratory

Access www.wiley.com/college/budhu, Chapter 6; click on Virtual Lab, and select constant-head test to conduct an interactive virtual constant-head permeability test. After you complete the virtual constant-head test, select the falling-head test and conduct a virtual falling-head permeability test.

6.9.1 Constant-Head Test

The constant-head test is used to determine the hydraulic conductivity of coarse-grained soils. A typical constant-head apparatus is shown in Figure 6.7. Water is allowed to flow through a cylindrical sample

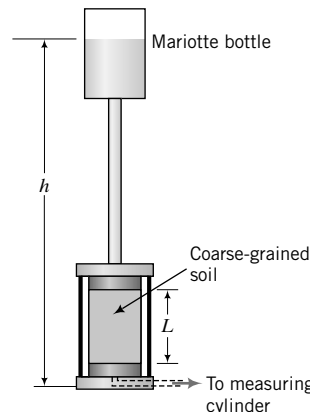


FIGURE 6.7
A constant-head test setup.

of soil under a constant head (h). The outflow (Q) is collected in a graduated cylinder at a convenient duration (t).

With reference to Figure 6.7,

$$\Delta H = h \quad \text{and} \quad i = \frac{\Delta H}{L} = \frac{h}{L}$$

The flow rate through the soil is $q_z = Q/t$, where Q is the total quantity of water collected in the measuring cylinder over time t .

From Equation (6.9),

$$k_z = \frac{q_z}{Ai} = \frac{QL}{tAh} \quad (6.19)$$

where k_z is the hydraulic conductivity in the vertical direction and A is the cross-sectional area.

The viscosity of the fluid, which is a function of temperature, influences the value of k_z . The experimental value ($k_{T^\circ C}$) is corrected to a baseline temperature of $20^\circ C$ using

$$k_{20^\circ C} = k_{T^\circ C} \frac{\mu_{T^\circ C}}{\mu_{20^\circ C}} = k_{T^\circ C} R_T \quad (6.20)$$

where μ is the dynamic viscosity of water, T is the temperature in $^\circ C$ at which the measurement was made, and $R_T = \mu_{T^\circ C}/\mu_{20^\circ C}$ is the temperature correction factor that can be calculated from

$$R_T = 2.42 - 0.475 \ln(T) \quad (6.21)$$

6.9.2 Falling-Head Test

The falling-head test is used for fine-grained soils because the flow of water through these soils is too slow to get reasonable measurements from the constant-head test. A compacted soil sample or a sample extracted from the field is placed in a metal or acrylic cylinder (Figure 6.8). Porous stones are positioned at the top and bottom faces of the sample to prevent its disintegration and to allow water to percolate through it. Water flows through the sample from a standpipe attached to the top of the cylinder. The head of water (h) changes with time as flow occurs through the soil. At different times, the head of water

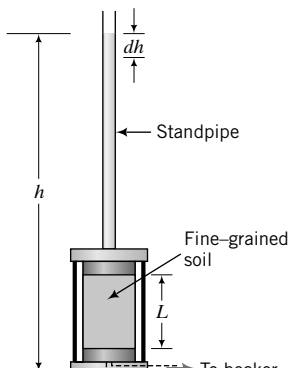


FIGURE 6.8
A falling-head test setup.

is recorded. Let dh be the drop in head over a time period dt . The velocity or rate of head loss in the tube is

$$v = -\frac{dh}{dt}$$

and the inflow of water to the soil is

$$(q_z)_{in} = av = -a \frac{dh}{dt}$$

where a is the cross-sectional area of the tube. We now appeal to Darcy's law to get the outflow:

$$(q_z)_{out} = Aki = Ak \frac{h}{L}$$

where A is the cross-sectional area, L is the length of the soil sample, and h is the head of water at any time t . The continuity condition requires that $(q_z)_{in} = (q_z)_{out}$. Therefore,

$$-a \frac{dh}{dt} = Ak \frac{h}{L}$$

By separating the variables (h and t) and integrating between the appropriate limits, the last equation becomes

$$\frac{Ak}{aL} \int_{t_1}^{t_2} dt = - \int_{h_1}^{h_2} \frac{dh}{h}$$

and the solution for k in the vertical direction is

$$k = k_z = \frac{aL}{A(t_2 - t_1)} \ln\left(\frac{h_1}{h_2}\right)$$

(6.22)

The hydraulic conductivity is corrected using Equation (6.20).

THE ESSENTIAL POINTS ARE:

1. The constant-head test is used to determine the hydraulic conductivity of coarse-grained soils.
2. The falling-head test is used to determine the hydraulic conductivity of fine-grained soils.

EXAMPLE 6.6 Interpretation of Constant-Head Test Data

A sample of sand, 5 cm in diameter and 15 cm long, was prepared at a porosity of 60% in a constant-head apparatus. The total head was kept constant at 30 cm and the amount of water collected in 5 seconds was 40 cm³. The test temperature was 20°C. Calculate the hydraulic conductivity and the seepage velocity.

Strategy From the data given, you can readily apply Darcy's law to find k_z .

Solution 6.6

Step 1: Calculate the sample cross-sectional area, hydraulic gradient, and flow.

$$D = 5 \text{ cm}$$

$$A = \frac{\pi \times D^2}{4} = \frac{\pi \times 5^2}{4} = 19.6 \text{ cm}^2$$

$$\Delta H = 30 \text{ cm}$$

$$i = \frac{\Delta H}{L} = \frac{30}{15} = 2$$

$$Q = 40 \text{ cm}^3$$

$$q_z = \frac{Q}{t} = \frac{40}{5} = 8 \text{ cm}^3/\text{s}$$

Step 2: Calculate k_z .

$$k_z = \frac{q_z}{Ai} = \frac{8}{19.6 \times 2} = 0.2 \text{ cm/s}$$

Step 3: Calculate the seepage velocity.

$$v_s = \frac{k_z i}{n} = \frac{0.2 \times 2}{0.6} = 0.67 \text{ cm/s}$$

EXAMPLE 6.7 Interpretation of Falling-Head Test Data

The data from a falling-head test on a silty clay are:

Cross-sectional area of soil = 80 cm²

Length of soil = 10 cm

Initial head = 90 cm

Final head = 84 cm

Duration of test = 15 minutes

Diameter of tube = 6 mm

Temperature = 22°C

Determine k .

Strategy Since this is a falling-head test, you should use Equation (6.22). Make sure you are using consistent units.

Solution 6.7

Step 1: Calculate the parameters required in Equation (6.22).

$$a = \frac{\pi \times (6/10)^2}{4} = 0.28 \text{ cm}^2$$

$$A = 80 \text{ cm}^2 \text{ (given)}$$

$$t_2 - t_1 = 15 \times 60 = 900 \text{ seconds}$$

Step 2: Calculate k_z .

$$k_z = \frac{aL}{A(t_2 - t_1)} \ln\left(\frac{h_1}{h_2}\right) = \frac{0.28 \times 10}{80 \times 900} \ln\left(\frac{90}{84}\right) = 2.7 \times 10^{-6} \text{ cm/s}$$

From Equation (6.21), $R_T = 2.42 - 0.475 \ln(T) = 2.42 - 0.475 \ln(22) = 0.95$

$$k_{20^\circ\text{C}} = k_z R_T = 2.7 \times 10^{-6} \times 0.95 = 2.6 \times 10^{-6} \text{ cm/s}$$

What's next . . . In the constant-head test and the falling-head test, we determined the hydraulic conductivity of only a small volume of soil at a specific location in a soil mass. In some cases, we have to use remolded or disturbed soil samples. In addition, if field samples are used, they are invariably disturbed by sampling processes (see Chapter 3). The hydraulic conductivity is sensitive to alteration in the fabric of the soil and, consequently, there are doubts about the accuracy of representing the in situ soil conditions using laboratory permeability tests. There are several field methods to determine the hydraulic conductivity. Next, we will discuss one popular method.

6.9.3 Pumping Test to Determine the Hydraulic Conductivity

One common method of determining the hydraulic conductivity in the field is by pumping water at a constant flow rate from a well and measuring the decrease in groundwater level at observation wells (Figure 6.9). The equation, called the simple well formula, is derived using the following assumptions.

1. The water-bearing layer (called an aquifer) is unconfined and nonleaky.
2. The pumping well penetrates through the water-bearing stratum and is perforated only at the section that is below the groundwater level.

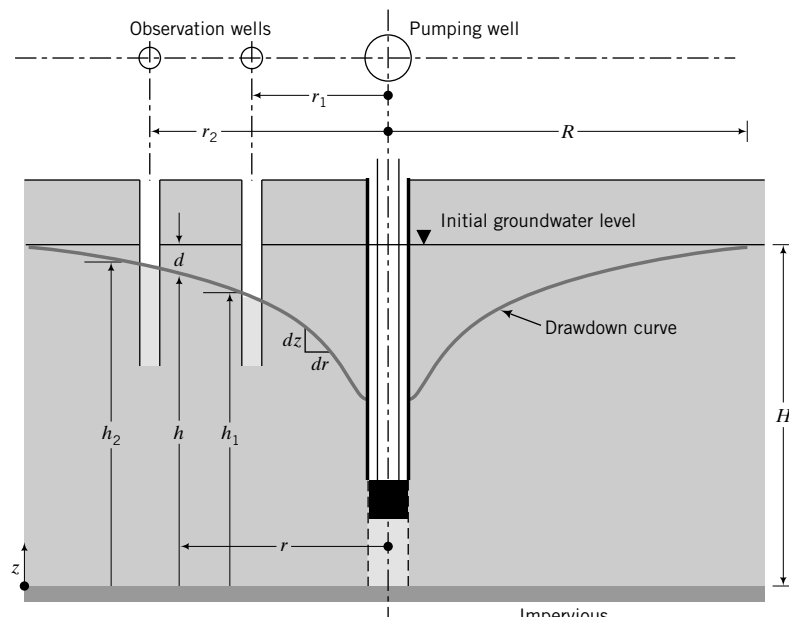


FIGURE 6.9 Layout of a pump test to determine k_z

3. The soil mass is homogeneous, isotropic, and of infinite size.
4. Darcy's law is valid.
5. Flow is radial toward the well.
6. The hydraulic gradient at any point in the water-bearing stratum is constant and is equal to the slope of groundwater surface (Dupuit's assumption).

Let dz be the drop in total head over a distance dr . Then, according to Dupuit's assumption, the hydraulic gradient is

$$i = \frac{dz}{dr}$$

The area of flow at a radial distance r from the center of the pumping well is

$$A = 2\pi r z$$

where z is the thickness of an elemental volume of the pervious soil layer.

From Darcy's law, the flow is

$$q_z = 2\pi r z k \frac{dz}{dr}$$

We need to rearrange the above equation and integrate it between the limits r_1 and r_2 and h_1 and h_2 :

$$q_z \int_{r_1}^{r_2} \frac{dr}{r} = 2k\pi \int_{h_1}^{h_2} z dz \quad (6.23)$$

Completing the integration leads to

$$k = \frac{q_z \ln(r_2/r_1)}{\pi(h_2^2 - h_1^2)}$$

(6.24)

With measurements of r_1 , r_2 , h_1 , h_2 , and q_v (flow rate of the pump), k can be calculated from Equation (6.24). This test is only practical for coarse-grained soils.

Pumping tests lower the groundwater, which then causes stress changes in the soil. Since the groundwater is not lowered uniformly, as shown by the drawdown curve in Figure 6.9, the stress changes in the soil will not be even. Consequently, pumping tests near existing structures can cause these structures to settle unevenly. You should consider the possibility of differential settlement on existing structures when you plan a pumping test.

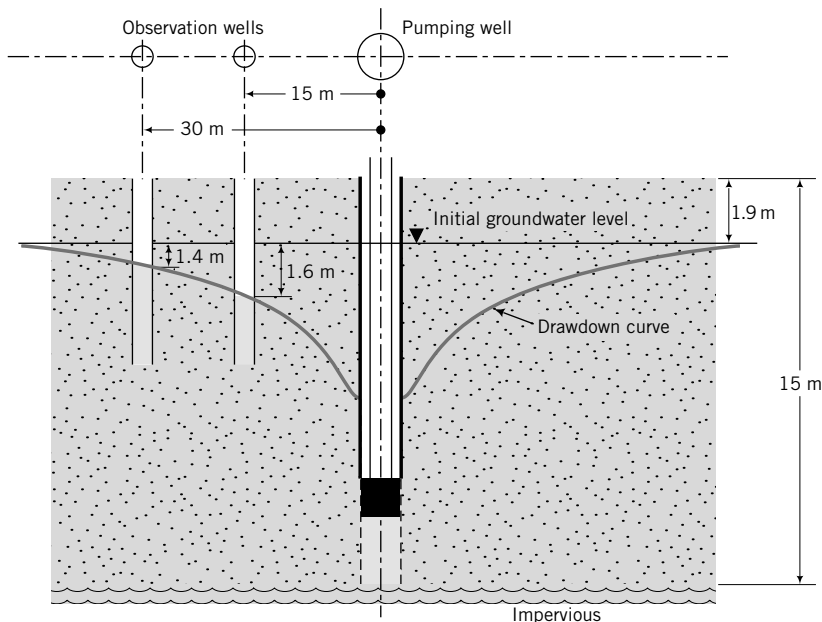
EXAMPLE 6.8 Interpretation of Pumping Test Data

A pumping test was carried out in a soil bed of thickness 15 m and the following measurements were recorded. Rate of pumping was $10.6 \times 10^{-3} \text{ m}^3/\text{s}$; drawdowns in observation wells located at 15 m and 30 m from the center of the pumping well were 1.6 m and 1.4 m, respectively, from the initial groundwater level. The initial groundwater level was located at 1.9 m below ground level. Determine k .

Strategy You are given all the measurements to directly apply Equation (6.24) to find k . You should draw a sketch of the pump test to identify the values to be used in Equation (6.24).

Solution 6.8

Step 1: Draw a sketch of the pump test with the appropriate dimensions—see Figure E6.8.

**FIGURE E6.8**

Step 2: Substitute given values in Equation (6.24) to find k .

$$r_2 = 30 \text{ m}, \quad r_1 = 15 \text{ m}, \quad h_2 = 15 - (1.9 + 1.4) = 11.7 \text{ m}$$

$$h_1 = 15 - (1.9 + 1.6) = 11.5 \text{ m}$$

$$k = \frac{q_z \ln(r_2/r_1)}{\pi(h_2^2 - h_1^2)} = \frac{10.6 \times 10^{-3} \ln(30/15)}{\pi(11.7^2 - 11.5^2)10^4} = 5.0 \times 10^{-2} \text{ cm/s}$$

6.10 GROUNDWATER LOWERING BY WELLPOINTS

Sometimes it is necessary to temporarily lower the groundwater level for construction of foundations. The process of lowering the groundwater is called dewatering and is accomplished by inserting wellpoints around the excavation for the foundations. A wellpoint system consists of an interconnected network of wells (pipes) installed around the perimeter of an excavation (Figure 6.10). The wells are installed in rows and the spacing depends on the soil type and the hydraulic conductivity. The spacing in clean sands with water depth of about 5 m is about 1 m to 1.5 m.

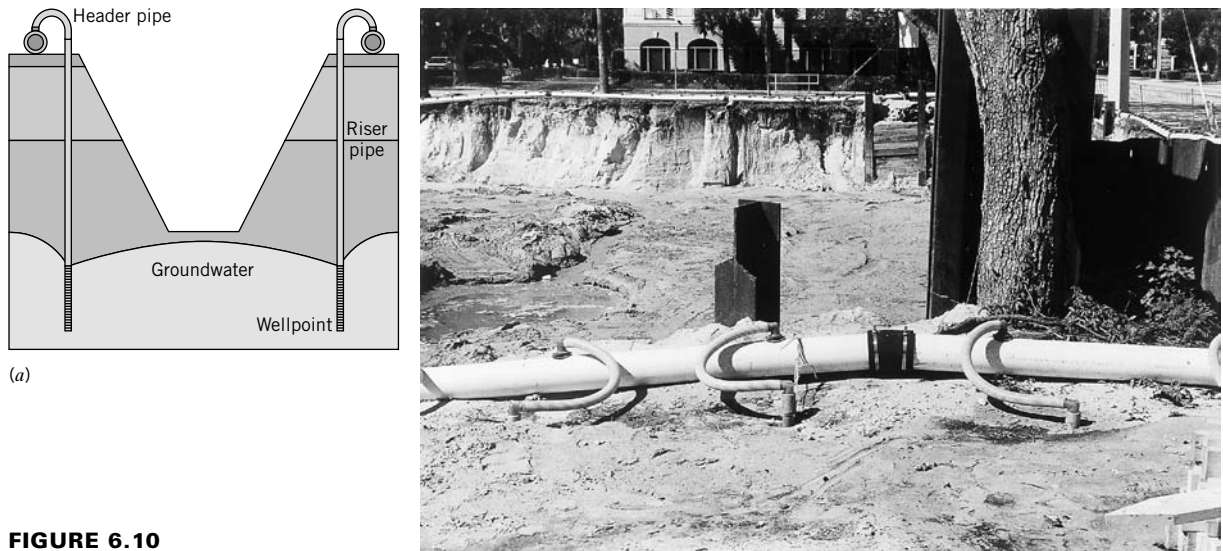
Reconsidering Figure 6.9, the drawdown, d , is

$$d = H - h \quad (6.25)$$

The radius of influence, R , of the depression cone is the radius at which the drawdown is zero. The flow rate or discharge between the limits r and R and h and H can be found from Equation (6.23) as

$$q_w = \frac{k\pi(H^2 - h^2)}{\ln\left(\frac{R}{r}\right)} \quad (6.26)$$

Solving for h , we get

**FIGURE 6.10**

Wellpoint system for an excavation. (b)

$$h = \pm \sqrt{H^2 - \frac{q_w \ln\left(\frac{R}{r}\right)}{k\pi}} \quad (6.27)$$

Therefore, at any point with coordinates (r, z) , the drawdown is

$$d = H \pm \sqrt{H^2 - \frac{q_w \ln\left(\frac{R}{r}\right)}{k\pi}} \quad (6.28)$$

The positive sign is used when water is pumped into the well and the negative sign is used when water is pumped from the well. The maximum drawdown, d_{max} , occurs at the well face, i.e., $r = r_o$, and from Equation (6.28),

$$d_{max} = H \pm \sqrt{H^2 - \frac{q_w \ln\left(\frac{R}{r_o}\right)}{k\pi}} \quad (6.29)$$

The radius of influence of the depression cone is found from experience and can be estimated (Slichter, 1899) from

$$R = 3000d_{max}\sqrt{k}; d \text{ is in m and } k \text{ is in m/s.} \quad (6.30)$$

Equation (6.30) does not have a theoretical basis and is not dimensionally correct. However, it has been satisfactorily applied in practice. An equation (Kozeny, 1933) that is dimensionally correct is

$$R = \sqrt{12 \frac{t}{n} \sqrt{\frac{q_w k}{\pi}}} \quad (6.31)$$

where t (sec) is duration for a discharge, q_w (m^3/s), n is porosity, and k is the average hydraulic conductivity (m/s). The predictions of R from Equations (6.30) and (6.31) are normally significantly different.

However, the discharge is not very sensitive to the accuracy of R because the changes in $\ln\left(\frac{R}{r}\right)$ are small for large changes in $\left(\frac{R}{r}\right)$. The accuracy of R has significant impact for drawdown near existing buildings. For closely spaced wellpoints, a two-dimensional flow analysis (Chapter 14) is required.

EXAMPLE 6.9 Interpretation of Wellpoint Data

A wellpoint of 0.1 m radius in a permeable soil layer 7 m thick has a constant discharge of 0.05 m³/s in a 24-hour operation. The soil parameters are $k = 0.004$ m/s and $e = 0.5$. Determine the radius of influence and the maximum drawdown.

Strategy Use Kozeny's (1933) equation for R and then use Equation (6.29) to calculate d_{max} .

Solution 6.9

Step 1: Calculate R .

$$n = \frac{e}{1 + e} = \frac{0.5}{1 + 0.5} = 0.33$$

$$R = \sqrt{12 \frac{t}{n} \sqrt{\frac{q_w k}{\pi}}} = R = \sqrt{12 \frac{24 \times 3600}{0.33} \sqrt{\frac{0.05 \times 0.004}{\pi}}} = 158.3 \text{ m}$$

Compare R using Slichter's equation.

$$R = 3000d_{max}\sqrt{k} = 3000 \times 2.56\sqrt{0.004} = 485.7 \text{ m}$$

The value of d_{max} was inserted from Step 2.

Step 2: Calculate d_{max} .

$$d_{max} = H - \sqrt{H^2 - \frac{q_w \ln\left(\frac{R}{r_o}\right)}{k\pi}} = 7 - \sqrt{7^2 - \frac{0.05 \ln\left(\frac{158.3}{0.1}\right)}{0.004\pi}} = 2.56 \text{ m}$$

6.11 SUMMARY

Flow of water through soils is governed by Darcy's law, which states that the velocity is proportional to the hydraulic gradient. The proportionality constant is the hydraulic conductivity. The hydraulic conductivity depends on soil type, particle size, pore fluid properties, void ratio, pore size, homogeneity, layering and fissuring, and entrapped gases. In coarse-grained soils the hydraulic conductivity is determined using a constant-head test, while for fine-grained soils a falling-head test is used. In the field, a pumping test is used to determine the hydraulic conductivity. Wellpoints are used at a construction site to lower the groundwater level.

Self-Assessment



Access Chapter 6 at <http://www.wiley.com/college/budhu> to take the end-of-chapter quiz to test your understanding of this chapter.

Practical Example

EXAMPLE 6.10 Application of Flow Data to a Canal

A ditch is required for a utility line near an ephemeral canal, which at the time of excavation was filled with water, as shown in Figure E6.10. The average vertical and horizontal hydraulic conductivities are 1×10^{-5} cm/s and 2×10^{-4} cm/s, respectively. Assuming a 1-m length of ditch, determine the flow rate of water into it.

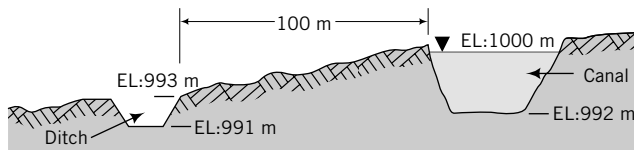


FIGURE E6.10

Strategy You need to determine an equivalent hydraulic conductivity and then calculate the flow rate using Darcy's law. However, to calculate the flow rate, you need to determine the hydraulic gradient. To do so, find the difference in total head between the canal and the ditch, and then divide by the length of the flow.

Solution 6.10

Step 1: Calculate an equivalent hydraulic conductivity.

$$k_{eq} = \sqrt{k_z k_x} = \sqrt{10^{-5} \times 2 \times 10^{-4}} = 4.5 \times 10^{-5} \text{ cm/s}$$

Step 2: Determine the hydraulic gradient.

Take datum as the bottom of the ditch.

Elevation head at base of ditch = 0, pressure head at base of ditch = 0; total head at ditch = 0

Elevation head at base of canal = 1 m, pressure head at base of canal = 8 m; total head at canal = 9 m

Head difference, $\Delta h = 9 \text{ m}$

$$\text{Slope} \approx \tan^{-1}\left(\frac{100 - 993}{100}\right) = 4^\circ$$

$$\text{Average length of flow path, } L = \frac{100}{\cos(4^\circ)} = 100.2 \text{ m}$$

$$i = \frac{\Delta h}{L} = \frac{9}{100.2} = 0.09$$

Step 3: Calculate the flow rate.

Assume flow parallel to the slope and consider a vertical section of the ditch.

$$A = (993 - 991) \times 1 = 2 \text{ m}^2$$

$$q_i = AK_{eq}i = 2 \times (4.5 \times 10^{-5}/100) \times 0.09 = 0.81 \times 10^{-7} \text{ m}^3/\text{s}$$

EXERCISES

Theory

- 6.1 A pump test is carried out to determine the hydraulic conductivity of a confined aquifer, as shown in Figure P6.1 on page 128. Show that the equation for k is

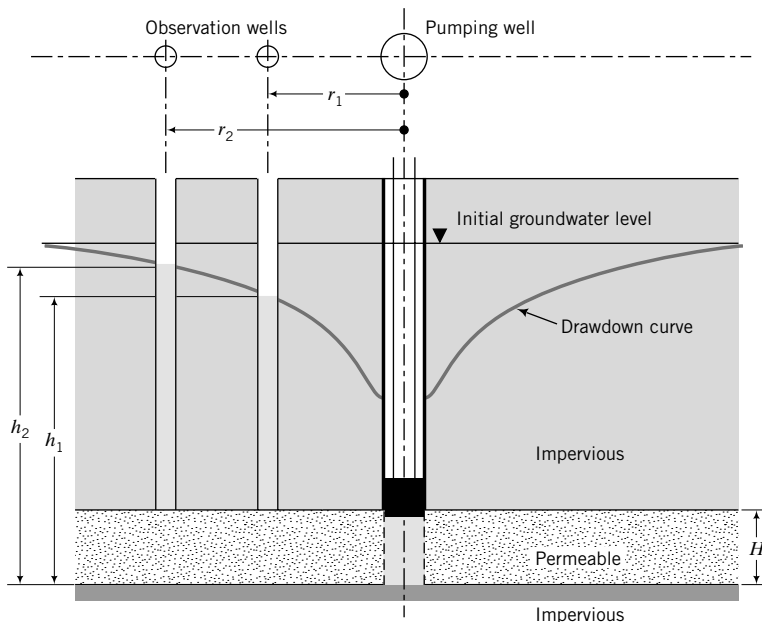
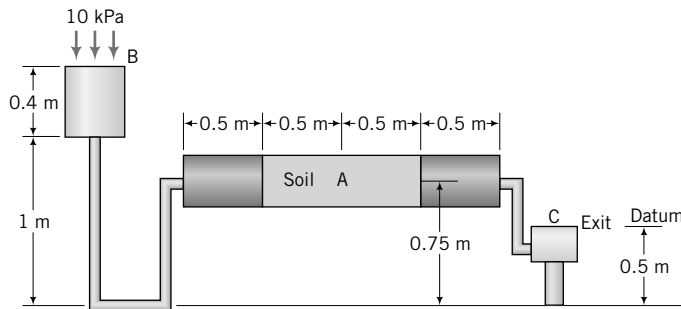
$$k = \frac{q \ln(r_1/r_2)}{2\pi H(h_1 - h_2)}$$

Problem Solving

- 6.2 Determine the pressure head, elevation head, and total head at A, B, and C for the arrangement shown in

Figure P6.2 on page 128. Take the water level at exit as datum. (*Hint:* You need to convert the pressure 10 kPa to head.)

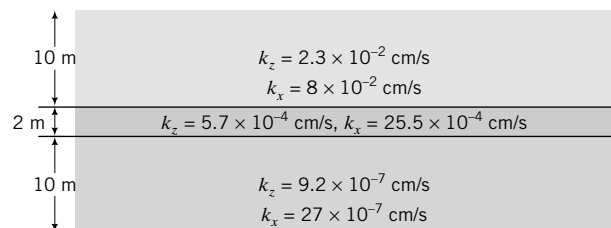
- 6.3 The groundwater level in a soil layer 10 m thick is located at 3 m below the surface. (a) Plot the distribution of hydrostatic pressure with depth. (b) If the groundwater were to rise to the surface, plot on the same graph as (a), using a different line type, the distribution of hydrostatic pressure with depth. (c) Repeat (b), but the groundwater is now 2 m above the ground surface (flood condition). Interpret and discuss these plots with respect to the effects of fluctuating groundwater levels.

**FIGURE P6.1****FIGURE P6.2**

- 6.4** In a constant-head permeability test, a sample of soil 12 cm long and 6 cm in diameter discharged $1.5 \times 10^{-3} \text{ m}^3$ of water in 10 minutes. The head difference in two piezometers A and B located at 1 cm and 11 cm, respectively, from the bottom of the sample is 2 cm. Determine the hydraulic conductivity of the soil. What is the soil type tested?
- 6.5** A constant-head test was conducted on a sample of soil 15 cm long and 60 cm^2 in cross-sectional area. The quantity of water collected was 50 cm^3 in 20 seconds under a head difference of 24 cm. Calculate the hydraulic conductivity. If the porosity of the sand is 55%, calculate the average velocity and the seepage velocity. Estimate the hydraulic conductivity of a similar soil with a porosity of 35% from the results of this test.
- 6.6** A falling-head permeability test was carried out on a clay soil of diameter 10 cm and length 15 cm. In 1 hour the head

in the standpipe of diameter 5 mm dropped from 68 cm to 50.2 cm. Calculate the hydraulic conductivity of this clay.

- 6.7** Calculate the equivalent hydraulic conductivity for the soil profile shown in Figure P6.7.

**FIGURE P6.7**

- 6.8** A pumping test was carried out to determine the average hydraulic conductivity of a sand deposit 20 m

thick overlying impermeable clay. The discharge from the pumping well was $10 \times 10^{-3} \text{ m}^3/\text{s}$. Drawdowns in the observation wells located 15 m and 30 m from the centerline of the pumping well were 2.1 m and 1.6 m, respectively. Groundwater table was reached at 3.2 m below the ground surface. Determine the hydraulic conductivity of the sand. Estimate the effective grain size using Hazen's equation.

Practical

- 6.9** An excavation is proposed for a square area near the bend of a river, as shown in Figure P6.9. It is expected that the flow of water into the excavation will come through the silt layer. Pumping tests reveal an average horizontal hydraulic conductivity of $2 \times 10^{-5} \text{ cm/s}$ in the

silt layer. The excavation has to be kept dry. Determine the flow (q_i) into the excavation.

- 6.10** Groundwater is pumped for domestic use from an unconfined aquifer (water-bearing sand layer). The thickness of the clay layer above the sand layer is 20 m and its initial porosity is 40%. After 10 years of pumping, the porosity is reduced to 30%. Determine the subsidence of the clay surface.

- 6.11** A canal is dug parallel to a river, as shown in Figure P6.11. A sandy-silt seam of average thickness 0.5 m cuts across the otherwise impermeable clay. The average vertical and horizontal hydraulic conductivities are $1.5 \times 10^{-5} \text{ cm/s}$ and $15 \times 10^{-5} \text{ cm/s}$, respectively. Assuming a 1-m length of canal, determine the flow rate of water from the canal to the river.

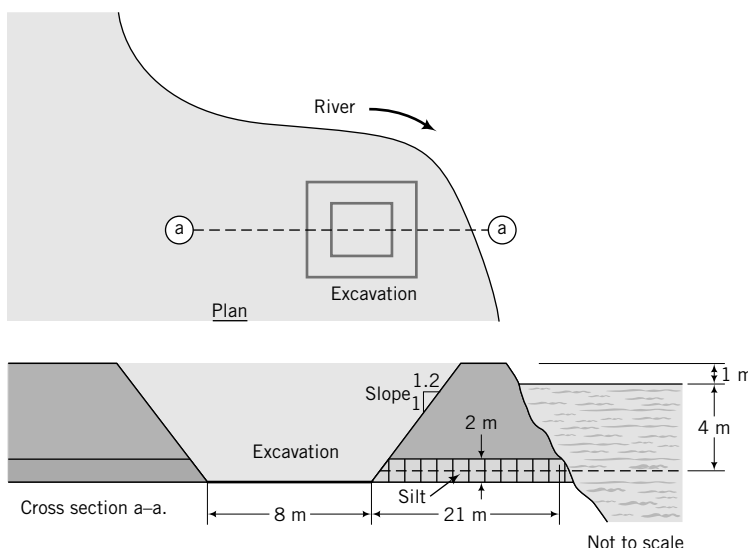


FIGURE P6.9

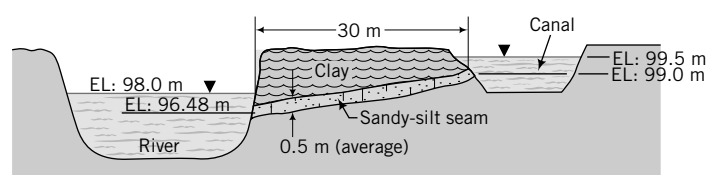


FIGURE P6.11

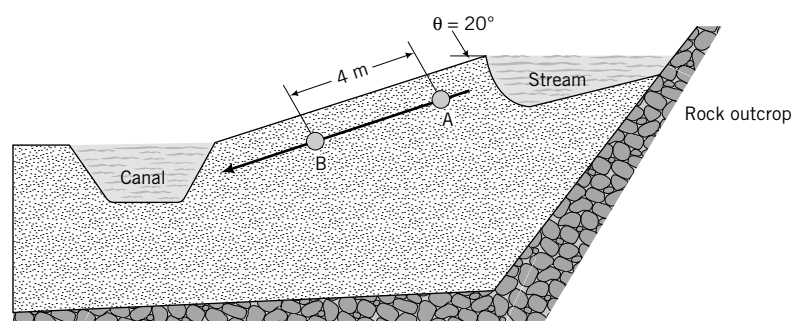


FIGURE P6.12

- 6.12** An excavation is made for a canal that is fed by a stream, as shown in Figure P6.12. The measured flow into the canal is $0.25 \times 10^{-4} \text{ m}^3/\text{s}$ per unit area. Two porewater pressure transducers, A and B, placed along a line parallel to the slope and approximately at the canal mid-height gave readings of 3 kPa and 2.5 kPa. Assuming flow parallel to the slope, estimate the hydraulic conductivity.
- 6.13** A well of 0.1 m radius is part of a wellpoint network to keep an excavation dry (Figure P6.13). The groundwater

at the far edge of the excavation must be 0.5 m below the base.

- (a) Calculate the radius of influence.
- (b) Calculate the maximum drawdown.
- (c) Plot the drawdown curve.
- (d) For the radius of influence in (a), (i) calculate the discharge if the well radius increases to 0.2 m, and (ii) compare it to the discharge for the 0.1-m-radius well.

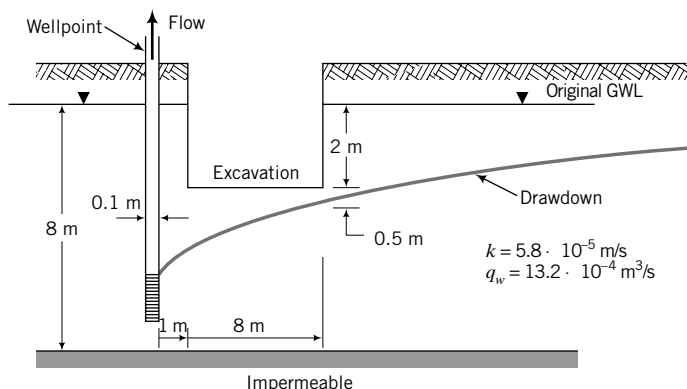


FIGURE P6.13

STRESSES, STRAINS, AND ELASTIC DEFORMATIONS OF SOILS

7.0 INTRODUCTION

In this chapter, we will review some fundamental principles of mechanics and strength of materials and apply these principles to soils treated as elastic porous materials. This chapter contains a catalog of a large number of equations for soil stresses and strains. You may become weary of these equations, but they are necessary for analyses of the mechanical behavior of soils. You do not have to memorize these equations except the fundamental ones.

When you complete this chapter, you should be able to:

- Calculate stresses and strains in soils (assuming elastic behavior) from external loads.
- Calculate elastic settlement.
- Calculate stress states.
- Calculate effective stresses.

You will use the following principles learned from statics and strength of materials:

- Stresses and strains
- Mohr's circle
- Elasticity—Hooke's law

Importance

You would have studied in mechanics the stresses imposed on homogeneous, elastic, rigid bodies by external forces. Soils are not homogeneous, elastic, rigid bodies, so the determination of stresses and strains in soils is a particularly difficult task. You may ask: "If soils are not elastic materials, then why do I have to study elastic methods of analysis?" Here are some reasons why a knowledge of elastic analysis is advantageous.

An elastic analysis of an isotropic material involves only two constants—Young's modulus and Poisson's ratio—and thus if we assume that soils are isotropic elastic materials, then we have a powerful, but simple, analytical tool to predict a soil's response under loading. We will have to determine only the two elastic constants from our laboratory or field tests.

A geotechnical engineer must ensure that a geotechnical structure must not collapse under any anticipated loading condition and that settlement under working load (a fraction of the collapse load) must be within tolerable limits. We would prefer the settlement under working loads to be elastic so that no permanent settlement would occur. To calculate the elastic settlement, we have to use an elastic analysis. For example, in designing foundations on coarse-grained soils, we normally assume that the settlement is elastic, and we then use elastic analysis to calculate the settlement.

An important task of a geotechnical engineer is to determine the stresses and strains that are imposed on a soil mass by external loads. It is customary to assume that the strains in the soils are small, and this assumption allows us to apply our knowledge of mechanics of elastic bodies to soils. Small strains mean infinitesimal strains. For a realistic description of soils, elastic analysis is not satisfactory. We need soil models that can duplicate the complexity of soil behavior. However, even for complex soil models, an elastic analysis is a first step.

Various types of surface loads or stresses are applied to soils. For example, an oil tank will impose a uniform, circular, vertical stress on the surface of the soil while an unsymmetrical building may impose a nonuniform vertical stress. We would like to know how the surface stresses are distributed within the soil mass and the resulting deformations. The induced stresses can lead to soil failure, or the deformations may be intolerable. Here is a sample practical situation. Two storage tanks are to be founded on a deep layer of stiff, saturated clay. Your client and the mechanical engineer who is designing the pipe works need an estimate of the settlement of the tanks when they are completely filled. Because of land restrictions, your client desires that the tanks be as close as possible to each other. If two separate foundations are placed too close to each other, the stresses in the soil induced by each foundation will overlap and cause intolerable tilting of the structures and their foundations. An example of tilting of structures caused by stress overlap is shown in Figure 7.1.

The settlement of soils is caused by the stress transmitted to the soil particles. This stress is called effective stress. It is important that you know how to calculate effective stress in soils.

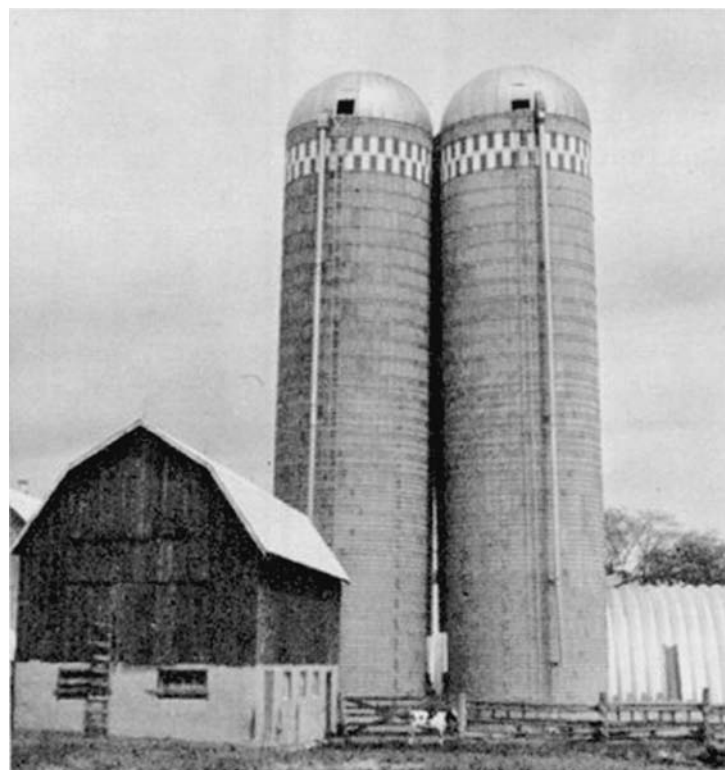


FIGURE 7.1 The “kissing” silos. (Bozozuk, 1976, permission from National Research Council of Canada.) These silos tilt toward each other at the top because stresses in the soil overlap at and near the internal edges of their foundations. The foundations are too close to each other.

7.1 DEFINITIONS OF KEY TERMS

Stress, or intensity of loading, is the load per unit area. The fundamental definition of stress is the ratio of the force ΔP acting on a plane ΔS to the area of the plane ΔS when ΔS tends to zero; Δ denotes a small quantity.

Effective stress (σ') is the stress carried by the soil particles.

Total stress (σ) is the stress carried by the soil particles and the liquids and gases in the voids.

Strain, or intensity of deformation, is the ratio of the change in a dimension to the original dimension or the ratio of change in length to the original length.

Stress (strain) state at a point is a set of stress (strain) vectors corresponding to all planes passing through that point. Mohr's circle is used to graphically represent stress (strain) state for two-dimensional bodies.

Porewater pressure, u , is the pressure of the water held in the soil pores.

Isotropic means the material properties are the same in all directions, and also the loadings are the same in all directions.

Anisotropic means the material properties are different in different directions, and also the loadings are different in different directions.

Elastic materials are materials that return to their original configuration on unloading and obey Hooke's law.

Plastic materials do not return to their original configuration on unloading.

7.2 QUESTIONS TO GUIDE YOUR READING

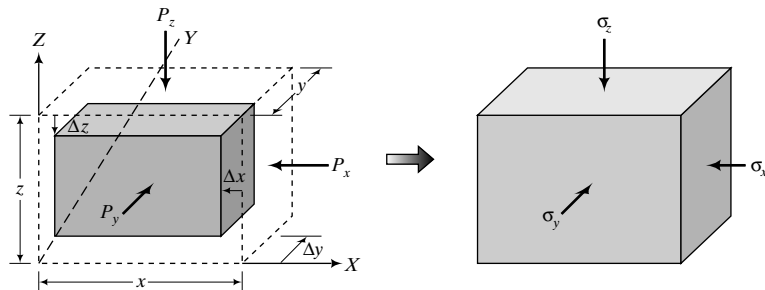
1. What are normal and shear stresses?
2. What is stress state and how is it determined?
3. Is soil an elastic material?
4. What are the limitations in analyzing soils based on the assumption that they (soils) are elastic materials?
5. What are shear strains, vertical strains, volumetric strains, and deviatoric strains?
6. How do I use elastic analysis to estimate the elastic settlement of soils, and what are the limitations?
7. What are the differences between plane strain and axisymmetric conditions?
8. How do I determine the stresses and strains/displacements imposed on a soil mass by external loads?
9. What is effective stress?
10. Is deformation a function of effective or total stress?

7.3 STRESSES AND STRAINS

7.3.1 Normal Stresses and Strains

Consider a cube of dimensions $x = y = z$ that is subjected to forces P_x, P_y, P_z , normal to three adjacent sides, as shown in Figure 7.2. The normal stresses are

$$\sigma_z = \frac{P_z}{xy}, \quad \sigma_x = \frac{P_x}{yz}, \quad \sigma_y = \frac{P_y}{xz} \quad (7.1)$$

**FIGURE 7.2** Stresses and displacements due to applied loads.

Let us assume that under these forces the cube compressed by Δx , Δy , and Δz in the X , Y , and Z directions. The strains in these directions, assuming they are small (infinitesimal), are

$$\epsilon_z = \frac{\Delta z}{z}, \quad \epsilon_x = \frac{\Delta x}{x}, \quad \epsilon_y = \frac{\Delta y}{y} \quad (7.2)$$

7.3.2 Volumetric Strain

The volumetric strain is

$$\epsilon_p = \epsilon_x + \epsilon_y + \epsilon_z \quad (7.3)$$

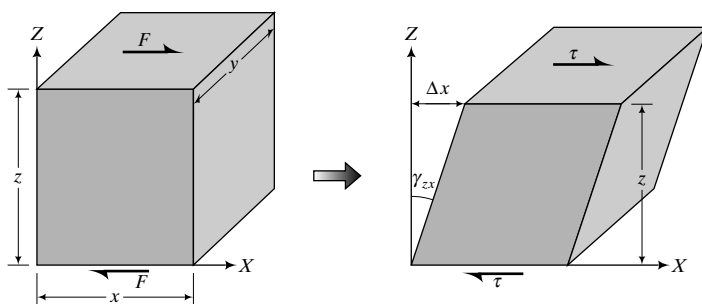
7.3.3 Shear Stresses and Shear Strains

Let us consider, for simplicity, the XZ plane and apply a force F that causes the square to distort into a parallelogram, as shown in Figure 7.3. The force F is a shearing force, and the shear stress is

$$\tau = \frac{F}{xy} \quad (7.4)$$

Simple shear strain is a measure of the angular distortion of a body by shearing forces. If the horizontal displacement is Δx , the shear strain or simple shear strain, γ_{zx} , is

$$\gamma_{zx} = \tan^{-1} \frac{\Delta x}{z}$$

**FIGURE 7.3** Shear stresses and shear strains.

For small strains, $\tan \gamma_{zx} = \gamma_{zx}$, and therefore

$$\gamma_{zx} = \frac{\Delta x}{z} \quad (7.5)$$

If the shear stress on a plane is zero, the normal stress on that plane is called a principal stress. We will discuss principal stresses later. In geotechnical engineering, compressive stresses in soils are assumed to be positive. Soils cannot sustain any appreciable tensile stresses, and we normally assume that the tensile strength of soils is negligible. Strains can be compressive or tensile.

THE ESSENTIAL POINTS ARE:

1. A normal stress is the load per unit area on a plane normal to the direction of the load.
2. A shear stress is the load per unit area on a plane parallel to the direction of the shear force.
3. Normal stresses compress or elongate a material; shear stresses distort a material.
4. A normal strain is the change in length divided by the original length in the direction of the original length.
5. Principal stresses are normal stresses on planes of zero shear stress.
6. Soils can only sustain compressive stresses.

What's next . . . What happens when we apply stresses to a deformable material? From the last section, you may answer that the material deforms, and you are absolutely correct. Different materials respond differently to applied loads. Next, we will examine some typical responses of deformable materials to applied loads to serve as a base for characterizing the loading responses of soils.

7.4 IDEALIZED STRESS-STRAIN RESPONSE AND YIELDING

7.4.1 Material Responses to Normal Loading and Unloading

If we apply an incremental vertical load, ΔP , to a deformable cylinder (Figure 7.4) of cross-sectional area A , the cylinder will compress by, say, Δz and the radius will increase by Δr . The loading condition we apply here is called uniaxial loading. The change in vertical stress is

$$\Delta\sigma_z = \frac{\Delta P}{A} \quad (7.6)$$

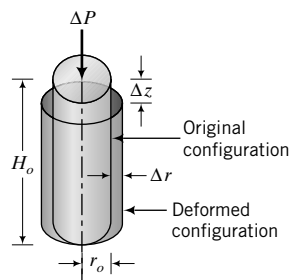


FIGURE 7.4
Forces and displacements
on a cylinder.

TABLE 7.1 Typical Values of Poisson's Ratio

Soil type	Description	ν^a
Clay	Soft	0.35–0.40
	Medium	0.30–0.35
	Stiff	0.20–0.30
Sand	Loose	0.15–0.25
	Medium	0.25–0.30
	Dense	0.25–0.35

^aThese values are effective values, ν' .

The vertical and radial strains are, respectively,

$$\Delta\epsilon_z = \frac{\Delta z}{H_o} \quad (7.7)$$

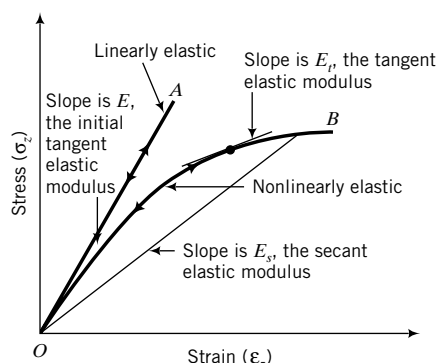
$$\Delta\epsilon_r = \frac{\Delta r}{r_o} \quad (7.8)$$

where H_o is the original length and r_o is the original radius. In Equations (7.7) and (7.8), a negative sign should be inserted for expansion and a positive sign for compression. Thus, for radial expansion, Equation (7.8) should have a negative sign. It is not included here for generality. The ratio of the radial (or lateral) strain to the vertical strain is called Poisson's ratio, ν , defined as

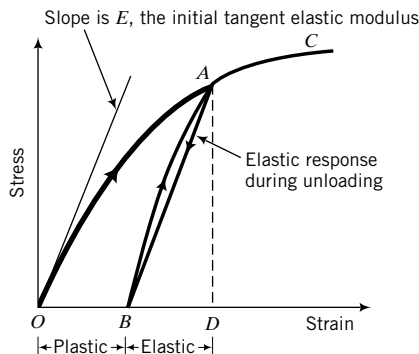
$$\nu = \frac{-\Delta\epsilon_r}{\Delta\epsilon_z} \quad (7.9)$$

Typical values of Poisson's ratio for soil are listed in Table 7.1.

We can plot a graph of $\sigma_z = \Sigma\Delta\sigma_z$ versus $\epsilon_z = \Sigma\Delta\epsilon_z$. If, for equal increments of ΔP , we get the same value of Δz , then we will get a straight line in the graph of σ_z versus ϵ_z , as shown by OA in Figure 7.5. If at some stress point, say, at A (Figure 7.5), we unload the cylinder and it returns to its original configuration, the material comprising the cylinder is called a *linearly elastic* material. Suppose for equal increments of ΔP we get different values of Δz , but on unloading the cylinder it returns to its original configuration. Then a plot of the stress-strain relationship will be a curve, as illustrated by OB in Figure 7.5. In this case, the material comprising the cylinder is called a *nonlinearly elastic* material. If we apply a load P_1 that causes a displacement Δz_1 on an elastic material and a second load P_2 that causes a displacement Δz_2 ,

**FIGURE 7.5**

Linear and nonlinear stress-strain curves of an elastic material.

**FIGURE 7.6**

Idealized stress-strain curves of an elastoplastic material.

then the total displacement is $\Delta z = \Delta z_1 + \Delta z_2$. Elastic materials obey the principle of superposition. The order in which the load is applied is not important; we could apply P_2 first and then P_1 , but the final displacement would be the same.

Some materials—soil is one of them—do not return to their original configurations after unloading. They exhibit a stress-strain relationship similar to that depicted in Figure 7.6, where OA is the loading response, AB the unloading response, and BC the reloading response. The strains that occur during loading, OA , consist of two parts—an elastic or recoverable part, BD , and a plastic or unrecoverable part, OB . Such material behavior is called *elastoplastic*. Part of the loading response is elastic, the other plastic.

As engineers, we are particularly interested in the plastic strains since these are the result of permanent deformations of the material. But to calculate the permanent deformation, we must know the elastic deformation. Here, elastic analyses become useful. The stress at which permanent deformation initiates is called the yield stress.

The *elastic modulus* or *initial tangent elastic modulus* (E) is the slope of the stress-strain line for linear isotropic material (Figure 7.5). For a nonlinear elastic material, either the tangent modulus (E_t) or the secant modulus (E_s) or both is determined from the stress-strain relationship (Figure 7.5). The *tangent elastic modulus* is the slope of the tangent to the stress-strain point under consideration. The *secant elastic modulus* is the slope of the line joining the origin $(0, 0)$ to some desired stress-strain point. For example, some engineers prefer to determine the secant modulus by using a point on the stress-strain curve corresponding to the maximum stress, while others prefer to use a point on the stress-strain curve corresponding to a certain level of strain, for example, 1% or one-half the maximum stress (the corresponding secant elastic modulus is normally denoted by E_{50}). The tangent elastic modulus and the secant elastic modulus are not constants. These moduli tend to decrease as shear strains increase. It is customary to determine the *initial tangent elastic modulus* for an elastoplastic material by unloading it and calculating the initial slope of the unloading line as the initial tangent elastic modulus (Figure 7.6).

Strictly speaking, these moduli determined as indicated are not true elastic moduli. The true elastic moduli are determined by small, incremental loading and unloading of the soil. If the stress-strain path followed during the loading is the same as the path followed during unloading, then the slope gives the true elastic modulus.

7.4.2 Material Response to Shear Forces

Shear forces distort materials. A typical response of an elastoplastic material to simple shear is shown in Figure 7.7. The initial shear modulus (G_i) is the slope of the initial straight portion of the τ_{zx} versus γ_{zx} curve. The secant shear modulus (G) is the slope of a line from the desired shear stress–shear strain point to the origin of the τ_{zx} versus γ_{zx} plot (Figure 7.7).

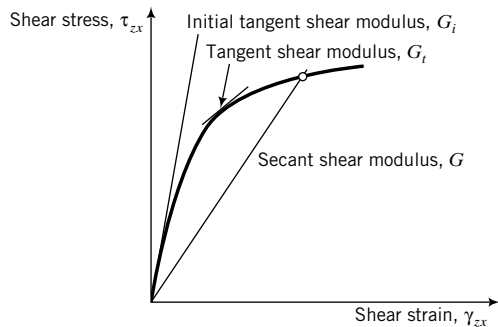


FIGURE 7.7
Shear stress–shear strain response
of elastoplastic material.

7.4.3 Yield Surface

Let us consider a more complex situation than the uniaxial loading of a cylinder (Figure 7.8a). In this case, we are going to apply increments of vertical and radial stresses. Since we are not applying any shear stresses, the axial stresses and radial stresses are principal stresses: $\sigma_z = \sigma_1 = \Sigma \Delta \sigma_z$ and $\sigma_r = \sigma_3 = \Sigma \Delta \sigma_r$, respectively. Let us, for example, set σ_3 to zero and increase σ_1 . The material will yield at some value of σ_1 , which we will call $(\sigma_1)_y$, and plots as point A in Figure 7.8b. If, alternatively, we set $\sigma_1 = 0$ and increase σ_3 , the material will yield at $(\sigma_3)_y$ and is represented by point B in Figure 7.8b. We can then subject the cylinder to various combinations of σ_1 and σ_3 and plot the resulting yield points. Linking the yield points results in a curve, AB, which is called the *yield curve* or *yield surface*, as shown in Figure 7.8b. A material subjected to a combination of stresses that lies below this curve will respond elastically (recoverable deformation). If loading is continued beyond the yield stress, the material will respond elastoplastically (irrecoverable or permanent deformations occur). If the material is isotropic, the yield surface will be symmetrical about the σ_1 and σ_3 axes.

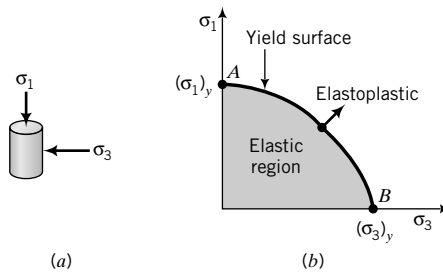


FIGURE 7.8
Elastic, yield, and elastoplastic
stress states.

THE ESSENTIAL POINTS ARE:

1. An elastic material recovers its original configuration on unloading; an elastoplastic material undergoes both elastic (recoverable) and plastic (permanent) deformation during loading.
2. Soils are elastoplastic materials.
3. At small strains soils behave like an elastic material, and thereafter like an elastoplastic material.
4. The locus of the stresses at which a soil yields is called a yield surface. Stresses below the yield stress cause the soil to respond elastically; stresses beyond the yield stress cause the soil to respond elastoplastically.

What's next . . . In the next two sections, we will write the general expression for Hooke's law, which is the fundamental law for linear elastic materials, and then consider two loading cases appropriate to soils.

7.5 HOOKE'S LAW

Access www.wiley.com/college/budhu, and click Chapter 7 and then elastic.xls for a spreadsheet to calculate stresses and strains using Hooke's law.

7.5.1 General State of Stress

Stresses and strains for a linear, isotropic, elastic soil are related through Hooke's law. For a general state of stress (Figure 7.9), Hooke's law is

$$\begin{Bmatrix} \epsilon_x \\ \epsilon_y \\ \epsilon_z \\ \gamma_{xy} \\ \gamma_{yz} \\ \gamma_{zx} \end{Bmatrix} = \frac{1}{E} \begin{bmatrix} 1 & -\nu & -\nu & 0 & 0 & 0 \\ -\nu & 1 & -\nu & 0 & 0 & 0 \\ -\nu & -\nu & 1 & 0 & 0 & 0 \\ 0 & 0 & 0 & 2(1+\nu) & 0 & 0 \\ 0 & 0 & 0 & 0 & 2(1+\nu) & 0 \\ 0 & 0 & 0 & 0 & 0 & 2(1+\nu) \end{bmatrix} \begin{Bmatrix} \sigma_x \\ \sigma_y \\ \sigma_z \\ \tau_{xy} \\ \tau_{yz} \\ \tau_{zx} \end{Bmatrix} \quad (7.10)$$

where E is the elastic (or Young's) modulus and ν is Poisson's ratio. Equation (7.10) is called the elastic equation or elastic stress-strain constitutive equation. From Equation (7.10), we have, for example,

$$\gamma_{zx} = \frac{2(1+\nu)}{E} \tau_{zx} = \frac{\tau_{zx}}{G} \quad (7.11)$$

where

$$G = \frac{E}{2(1+\nu)} \quad (7.12)$$

is the shear modulus. We will call E , G , and ν the elastic parameters. Only two of these parameters—either E or G and ν —are required to solve problems dealing with isotropic, elastic materials. We can calculate G from Equation (7.12), if E and ν are known. Poisson's ratio for soils is not easy to determine, and a direct way to obtain G is to subject the material to shearing forces, as described in Section 7.4.2. For nonlinear elastic materials, the tangent modulus or the secant modulus is used in Equation (7.10) and the calculations are done incrementally for small increments of stress.

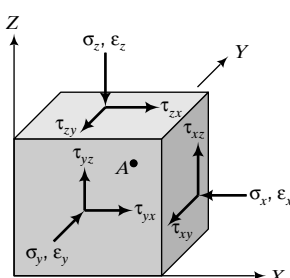


FIGURE 7.9
General state of stress.

TABLE 7.2 Typical Values of E and G

Soil type	Description	E^a(MPa)	G^a(MPa)
Clay	Soft	1–15	0.5–5
	Medium	15–30	5–15
	Stiff	30–100	15–40
Sand	Loose	10–20	5–10
	Medium	20–40	10–15
	Dense	40–80	15–35

^aThese are average secant elastic moduli for drained condition (see Chapter 10).

The elastic and shear moduli for soils depend on the stress history, the direction of loading, and the magnitude of the applied strains. In Chapter 10 we will study a few tests that are used to determine E and G , and in Chapter 11 we will explore the details of the use of E and G in the mechanical analyses of soils. Typical values of E and G are shown in Table 7.2.

7.5.2 Principal Stresses

If the stresses applied to a soil are principal stresses, then Hooke's law reduces to

$$\begin{Bmatrix} \varepsilon_1 \\ \varepsilon_2 \\ \varepsilon_3 \end{Bmatrix} = \frac{1}{E} \begin{bmatrix} 1 & -\nu & -\nu \\ -\nu & 1 & -\nu \\ -\nu & -\nu & 1 \end{bmatrix} \begin{Bmatrix} \sigma_1 \\ \sigma_2 \\ \sigma_3 \end{Bmatrix} \quad (7.13)$$

The matrix on the right-hand side of Equation (7.13) is called the compliance matrix. The inverse of Equation (7.13) is

$$\begin{Bmatrix} \sigma_1 \\ \sigma_2 \\ \sigma_3 \end{Bmatrix} = \frac{E}{(1+\nu)(1-2\nu)} \begin{bmatrix} 1-\nu & \nu & \nu \\ \nu & 1-\nu & \nu \\ \nu & \nu & 1-\nu \end{bmatrix} \begin{Bmatrix} \varepsilon_1 \\ \varepsilon_2 \\ \varepsilon_3 \end{Bmatrix} \quad (7.14)$$

The matrix on the right-hand side of Equation (7.14) is called the stiffness matrix. If you know the stresses and the material parameters E and ν , you can use Equation (7.13) to calculate the strains; or if you know the strains, E , and ν , you can use Equation (7.14) to calculate the stresses.

7.5.3 Displacements from Strains and Forces from Stresses

The displacements and forces are obtained by integration. For example, the vertical displacement, Δz , is

$$\Delta z = \int \varepsilon_z dz \quad (7.15)$$

and the axial force is

$$P_z = \int \Delta \sigma_z dA \quad (7.16)$$

where dz is the height or thickness of the element and dA is the elemental area.

THE ESSENTIAL POINTS ARE:

- 1. Hooke's law applies to a linearly elastic material.**
- 2. As a first approximation, you can use Hooke's law to calculate stresses, strains, and elastic settlement of soils.**
- 3. For nonlinear materials, Hooke's law is used with an approximate elastic modulus (tangent modulus or secant modulus) and the calculations are done for incremental increases in stresses or strains.**

What's next . . . The stresses and strains in three dimensions become complicated when applied to real problems. For practical purposes, many geotechnical problems can be solved using two-dimensional stress and strain parameters. In the next section, we will discuss two conditions that simplify the stress and strain states of soils.

7.6 PLANE STRAIN AND AXIAL SYMMETRIC CONDITIONS

7.6.1 Plane Strain Condition

There are two conditions of stresses and strains that are common in geotechnical engineering. One is the *plane strain* condition in which the strain in one direction is zero. As an example of a plane strain condition, let us consider an element of soil, A, behind a retaining wall (Figure 7.10). Because the displacement that is likely to occur in the Y direction (Δ_y) is small compared with the length in this direction, the strain tends to zero; that is, $\epsilon_y = \Delta_y/y \approx 0$. We can then assume that soil element A is under a plane strain condition. Since we are considering principal stresses, we will map the X, Y, and Z directions as 3, 2, and 1 directions. In the case of the retaining wall, the Y direction (2 direction) is the zero strain direction, and therefore $\epsilon_2 = 0$ in Equation (7.13).

Hooke's law for a plane strain condition is

$$\epsilon_1 = \frac{1 + \nu}{E} [(1 - \nu)\sigma_1 - \nu\sigma_3] \quad (7.17)$$

$$\epsilon_3 = \frac{1 + \nu}{E} [(1 - \nu)\sigma_3 - \nu\sigma_1] \quad (7.18)$$

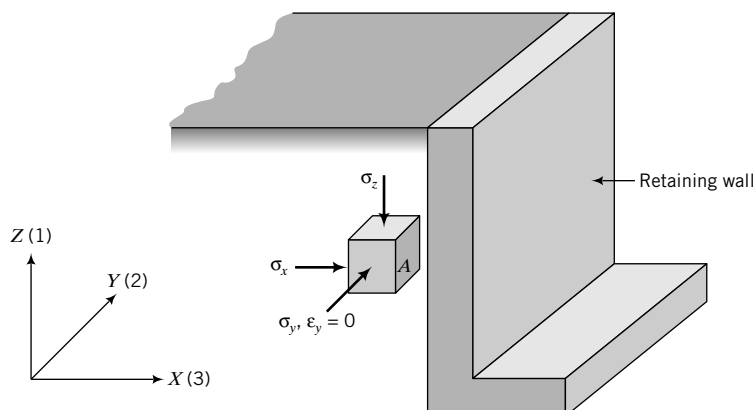


FIGURE 7.10 Plane strain condition in a soil element behind a retaining wall.

and

$$\sigma_2 = \nu(\sigma_1 + \sigma_3) \quad (7.19)$$

In matrix form, Equations (7.17) and (7.18) become

$$\begin{Bmatrix} \varepsilon_1 \\ \varepsilon_3 \end{Bmatrix} = \frac{1+\nu}{E} \begin{bmatrix} 1-\nu & -\nu \\ -\nu & 1-\nu \end{bmatrix} \begin{Bmatrix} \sigma_1 \\ \sigma_3 \end{Bmatrix} \quad (7.20)$$

The inverse of Equation (7.20) gives

$$\begin{Bmatrix} \sigma_1 \\ \sigma_3 \end{Bmatrix} = \frac{E}{(1+\nu)(1-2\nu)} \begin{bmatrix} 1-\nu & \nu \\ \nu & 1-\nu \end{bmatrix} \begin{Bmatrix} \varepsilon_1 \\ \varepsilon_3 \end{Bmatrix} \quad (7.21)$$

7.6.2 Axisymmetric Condition

The other condition that occurs in practical problems is *axial symmetry*, or the *axisymmetric* condition, where two stresses are equal. Let us consider a water tank or an oil tank founded on a soil mass, as illustrated in Figure 7.11.

The radial stresses (σ_r) and circumferential stresses (σ_θ) on a cylindrical element of soil directly under the center of the tank are equal because of axial symmetry. The oil tank will apply a uniform vertical (axial) stress at the soil surface and the soil element will be subjected to an increase in axial stress, $\Delta\sigma_z = \Delta\sigma_1$, and an increase in radial stress, $\Delta\sigma_r = \Delta\sigma_\theta = \Delta\sigma_3$. Will a soil element under the edge of the tank be under an axisymmetric condition? The answer is no, since the stresses at the edge of the tank are all different; there is no symmetry.

Hooke's law for the axisymmetric condition is

$$\varepsilon_1 = \frac{1}{E} [\sigma_1 - 2\nu\sigma_3] \quad (7.22)$$

$$\varepsilon_3 = \frac{1}{E} [(1-\nu)\sigma_3 - \nu\sigma_1] \quad (7.23)$$

or, in matrix form,

$$\begin{Bmatrix} \varepsilon_1 \\ \varepsilon_3 \end{Bmatrix} = \frac{1}{E} \begin{bmatrix} 1 & -2\nu \\ -\nu & 1-\nu \end{bmatrix} \begin{Bmatrix} \sigma_1 \\ \sigma_3 \end{Bmatrix} \quad (7.24)$$

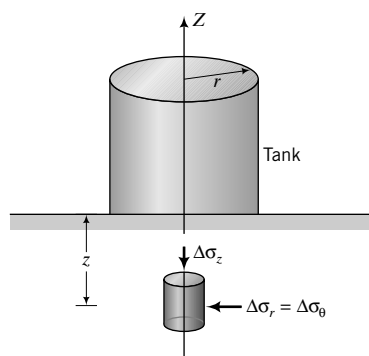


FIGURE 7.11
Axisymmetric condition on a soil element under the center of a tank.

The inverse of Equation (7.24) gives

$$\begin{Bmatrix} \sigma_1 \\ \sigma_3 \end{Bmatrix} = \frac{E}{(1 + \nu)(1 - 2\nu)} \begin{bmatrix} 1 - \nu & 2\nu \\ \nu & 1 \end{bmatrix} \begin{Bmatrix} \epsilon_1 \\ \epsilon_3 \end{Bmatrix} \quad (7.25)$$

Plane strain and axisymmetric stress conditions are ideal conditions. In reality, the stress conditions imposed on soils are much more complicated.

THE ESSENTIAL POINTS ARE:

1. A plane strain condition is one in which the strain in one or more directions is zero or small enough to be neglected.
2. An axisymmetric condition is one in which two stresses are equal.

EXAMPLE 7.1 Application of Hooke's Law for Plane Strain Condition

A retaining wall moves outward, causing a lateral strain of 0.1% and a vertical strain of 0.05% on a soil element located 3 m below ground level. Assuming the soil is a linear, isotropic, elastic material with $E = 5000$ kPa and $\nu = 0.3$, calculate the increase in stresses imposed. If the retaining wall is 6 m high and the stresses you calculate are the average stresses, determine the lateral force increase per unit length of wall.

Strategy You will have to make a decision whether to use the plane strain or axisymmetric condition and then use the appropriate equation. You are asked to find the increase in stresses, so it is best to write the elastic equations in terms of increment. The retaining wall moves outward, so the lateral strain is tensile (−) while the vertical strain is compressive (+). The increase in lateral force is found by integration of the average lateral stress increase.

Solution 7.1

Step 1: Determine the appropriate stress condition and write the appropriate equation.

The soil element is likely to be under the plane strain condition ($\epsilon_2 = 0$); use Equation (7.21).

$$\begin{Bmatrix} \Delta\sigma_1 \\ \Delta\sigma_3 \end{Bmatrix} = \frac{5000}{(1 + 0.3)(1 - 2 \times 0.3)} \begin{bmatrix} 1 - 0.3 & 0.3 \\ 0.3 & 1 - 0.3 \end{bmatrix} \begin{Bmatrix} 0.0005 \\ -0.001 \end{Bmatrix}$$

Step 2: Solve the equation.

$$\Delta\sigma_1 = 9615.4 \{ (0.7 \times 0.0005) + [0.3 \times (-0.001)] \} = 0.5 \text{ kPa}$$

$$\Delta\sigma_3 = 9615.4 \{ (0.3 \times 0.0005) + [0.7 \times (-0.001)] \} = -5.3 \text{ kPa}$$

The negative sign means reduction.

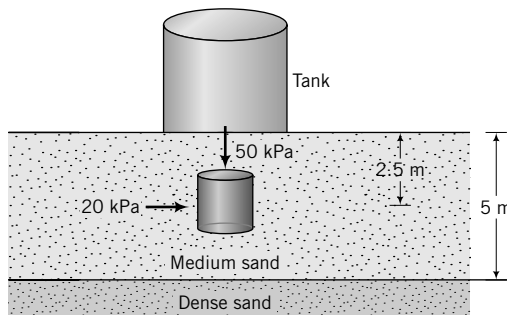
Step 3: Calculate the lateral force per unit length.

$$\Delta\sigma_3 = \Delta\sigma_x$$

$$\Delta P_x = \int_0^6 \Delta\sigma_x dA = - \int_0^6 5.3(dx \times 1) = -[5.3x]_0^6 = -31.8 \text{ kN/m}$$

EXAMPLE 7.2 Application of Hooke's Law for Axisymmetric Condition

An oil tank is founded on a layer of medium sand 5 m thick underlain by a deep deposit of dense sand. The geotechnical engineer assumed, based on experience, that the settlement of the tank would occur from settlement in the medium sand. The vertical and lateral stresses at the middle of the medium sand directly under the center

**FIGURE E7.2**

of the tank are 50 kPa and 20 kPa, respectively. The values of E and ν are 20 MPa and 0.3, respectively. Assuming a linear, isotropic, elastic material behavior, calculate the strains imposed in the medium sand and the vertical settlement.

Strategy You have to decide on the stress conditions on the soil element directly under the center of the tank. Once you make your decision, use the appropriate equations to find the strains and then integrate the vertical strains to calculate the settlement. Draw a diagram illustrating the problem.

Solution 7.2

Step 1: Draw a diagram of the problem—see Figure E7.2.

Step 2: Decide on a stress condition.

The element is directly under the center of the tank, so the axisymmetric condition prevails.

Step 3: Choose the appropriate equations and solve.

Use Equation (7.24).

$$\begin{Bmatrix} \Delta\epsilon_1 \\ \Delta\epsilon_3 \end{Bmatrix} = \frac{1}{20 \times 10^3} \begin{bmatrix} 1 & -0.6 \\ -0.3 & 0.7 \end{bmatrix} \begin{Bmatrix} 50 \\ 20 \end{Bmatrix}$$

Using algebra, we get

$$\Delta\epsilon_1 = \frac{1}{20 \times 10^3} [1 \times 50 - 0.6 \times 20] = 1.9 \times 10^{-3}$$

$$\Delta\epsilon_3 = \frac{1}{20 \times 10^3} [-0.3 \times 50 + 0.7 \times 20] = -5 \times 10^{-5}$$

Step 4: Calculate vertical displacement.

$$\Delta\epsilon_1 = \Delta\epsilon_z$$

$$\Delta z = \int_0^5 \Delta\epsilon_z dz = [1.9 \times 10^{-3} z]_0^5 = 9.5 \times 10^{-3} \text{ m} = 9.5 \text{ mm}$$

What's next . . . We have used the elastic equations to calculate stresses, strains, and displacements in soils assuming that soils are linear, isotropic, elastic materials. Soils, in general, are not linear, isotropic, elastic materials. We will briefly discuss anisotropic, elastic materials in the next section.

7.7 ANISOTROPIC, ELASTIC STATES

Anisotropic materials have different elastic parameters in different directions. Anisotropy in soils results from essentially two causes.

1. The manner in which the soil is deposited. This is called structural anisotropy and it is the result of the kind of soil fabric that is formed during deposition. You should recall (Chapter 2) that the soil fabric produced is related to the history of the environment in which the soil is formed. A special form of structural anisotropy occurs when the horizontal plane is a plane of isotropy. We call this form of structural anisotropy transverse anisotropy.
2. The difference in stresses in the different directions. This is known as stress-induced anisotropy.

Transverse anisotropy, also called cross anisotropy, is the most prevalent type of anisotropy in soils. If we were to load the soil in the vertical direction (Z direction) and repeat the same loading in the horizontal direction, say, the X direction, the soil would respond differently; its stress-strain characteristics and strength would be different in these directions. However, if we were to load the soil in the Y direction, the soil's response would be similar to the response obtained in the X direction. The implication is that a soil mass will, in general, respond differently depending on the direction of the load. For transverse anisotropy, the elastic parameters are the same in the lateral directions (X and Y directions) but are different from the vertical direction.

To fully describe anisotropic soil behavior we need 21 elastic constants (Love, 1927), but for transverse anisotropy we need only five elastic constants; these are E_z , E_x , ν_{xx} , ν_{zx} , and ν_{zz} . The first letter in the double subscripts denotes the direction of loading and the second letter denotes the direction of measurement. For example, ν_{zx} means Poisson's ratio determined from the ratio of the strain in the lateral direction (X direction) to the strain in the vertical direction (Z direction) with the load applied in the vertical direction (Z direction).

In the laboratory, the direction of loading of soil samples taken from the field is invariably vertical. Consequently, we cannot determine the five desired elastic parameters from conventional laboratory tests. Graham and Housby (1983) suggested a method to overcome the lack of knowledge of the five desired elastic parameters in solving problems on transverse anisotropy. However, their method is beyond the scope of this book.

For axisymmetric conditions, the transverse anisotropic, elastic equations are

$$\begin{Bmatrix} \Delta\epsilon_z \\ \Delta\epsilon_r \end{Bmatrix} = \begin{bmatrix} \frac{1}{E_z} & \frac{-2\nu_{rz}}{E_r} \\ \frac{-\nu_{rz}}{E_z} & \frac{(1-\nu_{rr})}{E_r} \end{bmatrix} \begin{Bmatrix} \Delta\sigma_z \\ \Delta\sigma_r \end{Bmatrix} \quad (7.26)$$

where the subscript z denotes vertical and r denotes radial. By superposition, $\nu_{rz}/\nu_{rz} = E_r/E_z$.

THE ESSENTIAL POINTS ARE:

1. Two forms of anisotropy are present in soils. One is structural anisotropy, which is related to the history of loading and environmental conditions during deposition, and the other is stress-induced anisotropy, which results from differences in stresses in different directions.
2. The prevalent form of structural anisotropy in soils is transverse anisotropy; the soil properties and the soil response in the lateral directions are the same but are different from those in the vertical direction.
3. You need to find the elastic parameters in different directions of a soil mass to determine elastic stresses, strains, and displacements.

EXAMPLE 7.3 Application of Hooke's Law for Transverse Anisotropic Soils

Redo Example 7.2, but now the soil under the oil tank is an anisotropic, elastic material with $E_z = 20 \text{ MPa}$, $E_r = 25 \text{ MPa}$, $\nu_{rz} = 0.15$, and $\nu_{rr} = 0.3$.

Strategy The solution of this problem is a straightforward application of Equation (7.26).

Solution 7.3

Step 1: Determine ν_{zr} (by superposition).

$$\frac{\nu_{rz}}{\nu_{zr}} = \frac{E_r}{E_z}$$

$$\nu_{zr} = \frac{20}{25} \times 0.15 = 0.12$$

Step 2: Find the strains.

Use Equation (7.26).

$$\begin{Bmatrix} \Delta\epsilon_z \\ \Delta\epsilon_r \end{Bmatrix} = 10^{-3} \begin{bmatrix} \frac{1}{20} & \frac{-2 \times 0.15}{25} \\ \frac{-0.12}{20} & \frac{(1 - 0.3)}{25} \end{bmatrix} \begin{Bmatrix} 50 \\ 20 \end{Bmatrix}$$

The solution is $\epsilon_z = 2.26 \times 10^{-3} = 0.23\%$ and $\epsilon_r = 0.26 \times 10^{-3} = 0.03\%$.

Step 3: Determine vertical displacement.

$$\Delta z = \int_0^5 \epsilon_z dz = [2.26 \times 10^{-3} z]_0^5 = 11.3 \times 10^{-3} \text{ m} = 11.3 \text{ mm}$$

The vertical displacement in the anisotropic case is about 19% more than in the isotropic case (Example 7.2). Also, the radial strain is tensile for the isotropic case but compressive in the anisotropic case for this problem.

What's next . . . We now know how to calculate stresses and strains in soils if we assume soils are elastic, homogeneous materials. One of the important tasks for engineering works is to determine strength or failure of materials. We can draw an analogy of the strength of materials with the strength of a chain. The chain is only as strong as its weakest link. For soils, failure may be initiated at a point within a soil mass and then propagate through it; this is known as progressive failure. The stress state at a point in a soil mass due to applied boundary forces may be equal to the strength of the soil, thereby initiating failure. Therefore, as engineers, we need to know the stress state at a point due to applied loads. We can use Equation (7.10) to find stress states, but geoengineers have been using a two-dimensional stress system based on Mohr's circle. We will discuss stress and strain states next using your knowledge of Mohr's circle in strength of materials.

7.8 STRESS AND STRAIN STATES

Access www.wiley.com/college/budhu, and click Chapter 7 and then Mohrcircle.zip to download an application to plot, interpret, and explore a variety of stress states interactively.



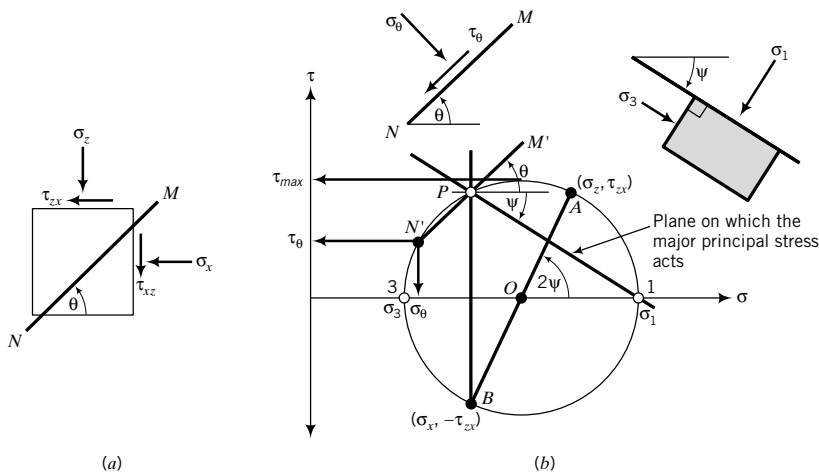


FIGURE 7.12 Stresses on a two-dimensional element and Mohr's circle.

7.8.1 Mohr's Circle for Stress States

Suppose a cuboidal sample of soil is subjected to the stresses shown in Figure 7.9. We would like to know what the stresses are at a point, say, A , within the sample due to the applied stresses. One approach to find the stresses at A , called the stress state at A , is to use Mohr's circle. The stress state at a point is the set of stress vectors corresponding to all planes passing through that point. For simplicity, we will consider a two-dimensional element with stresses, as shown in Figure 7.12a. Let us draw Mohr's circle. First, we have to choose a sign convention. We have already decided that compressive stresses are positive for soils. We will assume counterclockwise shear is positive and $\sigma_z > \sigma_x$. The two coordinates of the circle are (σ_z, τ_{zx}) and $(\sigma_x, -\tau_{zx})$. Recall from your strength of materials course that, for equilibrium, $\tau_{xz} = -\tau_{zx}$; these are called complementary shear stresses and are orthogonal to each other. Plot these two coordinates on a graph of shear stress (ordinate) and normal stress (abscissa), as shown by A and B in Figure 7.12b. Draw a circle with AB as the diameter. The circle crosses the normal stress axis at 1 and 3. The stresses at these points are the major principal stress, σ_1 , and the minor principal stress, σ_3 .

The principal stresses are related to the stress components $\sigma_z, \sigma_x, \tau_{zx}$ by

$$\sigma_1 = \frac{\sigma_z + \sigma_x}{2} + \sqrt{\left(\frac{\sigma_z - \sigma_x}{2}\right)^2 + \tau_{zx}^2} \quad (7.27)$$

$$\sigma_3 = \frac{\sigma_z + \sigma_x}{2} - \sqrt{\left(\frac{\sigma_z - \sigma_x}{2}\right)^2 + \tau_{zx}^2} \quad (7.28)$$

The angle between the major principal stress plane and the horizontal plane (ψ) is

$$\tan \psi = \frac{\tau_{zx}}{\sigma_1 - \sigma_x} \quad (7.29)$$

The stresses on a plane oriented at an angle θ from the major principal stress plane are

$$\sigma_\theta = \frac{\sigma_1 + \sigma_3}{2} + \frac{\sigma_1 - \sigma_3}{2} \cos 2\theta \quad (7.30)$$

$$\tau_\theta = \frac{\sigma_1 - \sigma_3}{2} \sin 2\theta \quad (7.31)$$

The stresses on a plane oriented at an angle θ from the horizontal plane are

$$\sigma_\theta = \frac{\sigma_z + \sigma_x}{2} + \frac{\sigma_z - \sigma_x}{2} \cos 2\theta + \tau_{zx} \sin 2\theta \quad (7.32)$$

$$\tau_\theta = \tau_{zx} \cos 2\theta - \frac{\sigma_z - \sigma_x}{2} \sin 2\theta \quad (7.33)$$

In the above equations, θ is positive for counterclockwise orientation.

The maximum (principal) shear stress is at the top of the circle with magnitude

$$\tau_{max} = \frac{\sigma_1 - \sigma_3}{2} \quad (7.34)$$

For the stresses shown in Figure 7.9 we would get three circles, but we have simplified the problem by plotting one circle for stresses on all planes perpendicular to one principal direction.

The stress σ_z acts on the horizontal plane and the stress σ_x acts on the vertical plane for our case. If we draw these planes in Mohr's circle, they intersect at a point, P . Point P is called the pole of the stress circle. It is a special point because any line passing through the pole will intersect Mohr's circle at a point that represents the stresses on a plane parallel to the line. Let us see how this works. Suppose we want to find the stresses on a plane inclined at an angle θ from the horizontal plane, as depicted by MN in Figure 7.12a. Once we locate the pole, P , we can draw a line parallel to MN through P as shown by $M'N'$ in Figure 7.12b. The line $M'N'$ intersects the circle at N' and the coordinates of N' , $(\sigma_\theta, \tau_\theta)$, represent the normal and shear stresses on MN .

7.8.2 Mohr's Circle for Strain States

So far, we have studied stress states. The strain state is found in a similar manner to the stress state. With reference to Figure 7.13, the principal strains are

$$\text{Major principal strain: } \epsilon_1 = \frac{\epsilon_z + \epsilon_x}{2} + \sqrt{\left(\frac{\epsilon_z - \epsilon_x}{2}\right)^2 + \left(\frac{\gamma_{zx}}{2}\right)^2} \quad (7.35)$$

$$\text{Major principal strain: } \epsilon_3 = \frac{\epsilon_z + \epsilon_x}{2} - \sqrt{\left(\frac{\epsilon_z - \epsilon_x}{2}\right)^2 + \left(\frac{\gamma_{zx}}{2}\right)^2} \quad (7.36)$$

where γ_{zx} is called the engineering shear strain or simple shear strain.

The maximum simple shear strain is

$$\gamma_{max} = \epsilon_1 - \epsilon_3 \quad (7.37)$$

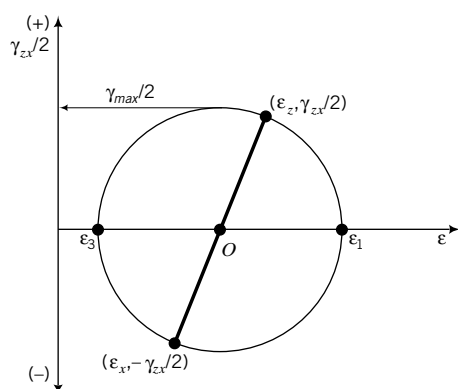


FIGURE 7.13
Mohr's circle of strain.

In soils, strains can be compressive or tensile. There is no absolute reference strain. For stresses, we can select atmospheric pressure as the reference, but not so for strains. Usually, we deal with changes or increments of strains resulting from stress changes.

THE ESSENTIAL POINTS ARE:

1. Mohr's circle is used to find the stress state or strain state from a two-dimensional set of stresses or strains on a soil.
2. The pole on a Mohr's circle identifies a point through which any plane passing through it will intersect the Mohr's circle at a point that represents the stresses on that plane.

EXAMPLE 7.4 Mohr's Circle for Stress State

A sample of soil ($0.1 \text{ m} \times 0.1 \text{ m}$) is subjected to the forces shown in Figure E7.4a. Determine (a) σ_1 , σ_3 , and Ψ ; (b) the maximum shear stress; and (c) the stresses on a plane oriented at 30° counterclockwise from the major principal stress plane.

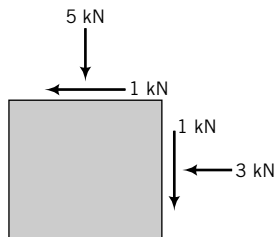


FIGURE E7.4a

Strategy There are two approaches to solve this problem. You can use either Mohr's circle or the appropriate equations. Both approaches will be used here.

Solution 7.4

Step 1: Find the area.

$$\text{Area: } A = 0.1 \times 0.1 = 10^{-2} \text{ m}^2$$

Step 2: Calculate the stresses.

$$\sigma_z = \frac{\text{Force}}{\text{Area}} = \frac{5}{10^{-2}} = 500 \text{ kPa}$$

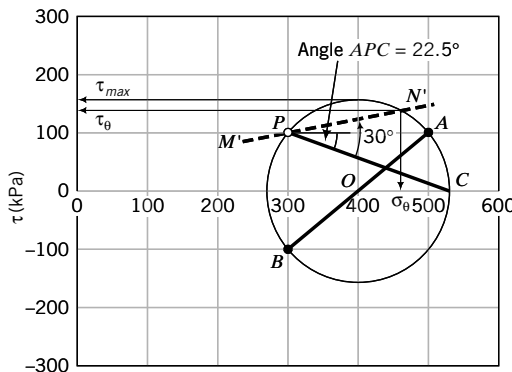
$$\sigma_x = \frac{3}{10^{-2}} = 300 \text{ kPa}$$

$$\tau_{zx} = \frac{1}{10^{-2}} = 100 \text{ kPa}; \quad \tau_{xz} = -\tau_{zx} = -100 \text{ kPa}$$

Step 3: Draw Mohr's circle and extract σ_1 , σ_3 , and τ_{max} .

Mohr's circle is shown in Figure E7.4b.

$$\sigma_1 = 540 \text{ kPa}, \quad \sigma_3 = 260 \text{ kPa}, \quad \tau_{max} = 140 \text{ kPa}$$

**FIGURE E7.4b**

Step 4: Draw the pole on Mohr's circle. The pole of Mohr's circle is shown by point P in Figure E7.4b.

Step 5: Determine ψ .

Draw a line from P to σ_1 and measure the angle between the horizontal plane and this line.

$$\psi = 22.5^\circ$$

Alternatively, the angle $AOC = 2\psi = 45^\circ$.

$$\therefore \psi = 22.5^\circ$$

Step 6: Determine the stresses on a plane inclined at 30° from the major principal stress plane.

Draw a line M^1N^1 through P with an inclination of 30° from the major principal stress plane, angle CPN' . The coordinate at point N' is (470, 120).

Alternatively:

Step 1: Use Equations (7.27) to (7.29) and (7.34) to find σ_1 , σ_3 , ψ , and τ_{max} .

$$\sigma_1 = \frac{500 + 300}{2} + \sqrt{\left(\frac{500 - 300}{2}\right)^2 + 100^2} = 541.4 \text{ kPa}$$

$$\sigma_3 = \frac{500 + 300}{2} - \sqrt{\left(\frac{500 - 300}{2}\right)^2 + 100^2} = 258.6 \text{ kPa}$$

$$\tan \psi = \frac{\tau_{yx}}{\sigma_1 - \sigma_3} = \frac{100}{541.4 - 300} = 0.414$$

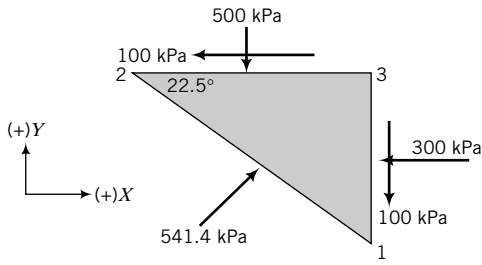
$$\therefore \psi = 22.5^\circ$$

$$\tau_{max} = \frac{\sigma_1 - \sigma_3}{2} = \frac{541.4 - 258.6}{2} = 141.4 \text{ kPa}$$

Check Equilibrium

$$\text{Length of } 2 - 3 = 0.1 \text{ m}$$

$$\text{Length of } 3 - 1 = 0.1 \times (\tan 22.5^\circ) = 0.0414 \text{ m}$$

**FIGURE E7.4c**

$$\text{Length of } 1 - 2 = 0.1 / (\cos 22.5^\circ) = 0.1082 \text{ m}$$

$$\sum F_x = 0: -300 \times 0.0414 - 100 \times 0.1 + 541.4 \times 0.1082 \times \cos(22.5^\circ) = 0$$

$$\sum F_y = 0: -100 \times 0.0414 - 500 \times 0.1 + 541.4 \times 0.1082 \times \sin(22.5^\circ) = 0$$

Step 2: Use Equations (7.30) and (7.31) to find σ_θ and τ_θ .

$$\sigma_\theta = \frac{541.4 + 258.6}{2} + \frac{541.4 - 258.6}{2} \cos(2 \times 30) = 470.7 \text{ kPa}$$

$$\tau_\theta = \frac{541.4 - 258.6}{2} \sin(2 \times 30) = 122.5 \text{ kPa}$$

What's next . . . The stresses we have calculated are for soils as solid elastic materials. We have not accounted for the pressure within the soil pore spaces. In the next section, we will discuss the principle of effective stresses that accounts for the pressures within the soil pores. This principle is the most important principle in soil mechanics.

7.9 TOTAL AND EFFECTIVE STRESSES

7.9.1 The Principle of Effective Stress

The deformations of soils are similar to the deformations of structural framework such as a truss. The truss deforms from changes in loads carried by each member. If the truss is loaded in air or submerged in water, the deformations under a given load will remain unchanged. Deformations of the truss are independent of hydrostatic pressure. The same is true for soils.

Let us consider an element of a *saturated soil* subjected to a normal stress, σ , applied on the horizontal boundary, as shown in Figure 7.14. The stress σ is called the *total stress*, and for equilibrium (Newton's third law) the stresses in the soil must be equal and opposite to σ . The resistance or reaction to σ is provided by a combination of the stresses from the solids, called *effective stress* (σ'), and from water in the pores, called *porewater pressure* (u). We will denote effective stresses by a prime ('') following the symbol for normal stress, usually σ . The equilibrium equation is

$$\sigma = \sigma' + u \quad (7.38)$$

so that

$$\sigma' = \sigma - u \quad (7.39)$$

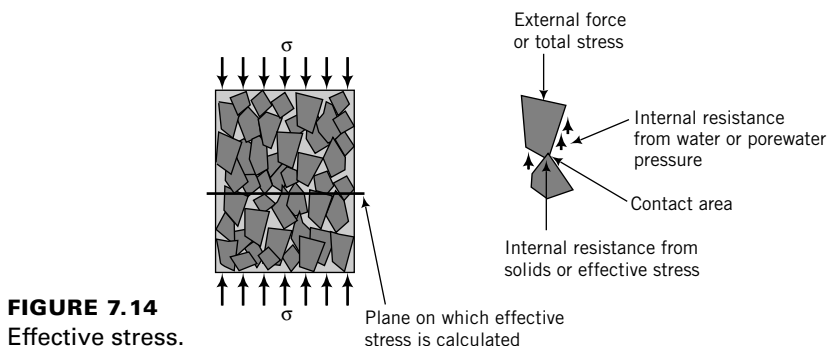


FIGURE 7.14
Effective stress.

Equation (7.39) is called the *principle of effective stress* and was first recognized by Terzaghi (1883–1963) in the mid-1920s during his research into soil consolidation (Chapter 9). **The principle of effective stress is the most important principle in soil mechanics. Deformations of soils are a function of effective stresses, not total stresses. The principle of effective stresses applies only to normal stresses and not to shear stresses.** The porewater cannot sustain shear stresses, and therefore the soil solids must resist the shear forces. Thus $\tau = \tau'$, where τ is the total shear stress and τ' is the effective shear stress. The effective stress is not the contact stress between the soil solids. Rather, it is the average stress on a plane through the soil mass.

Soils cannot sustain tension. Consequently, the effective stress cannot be less than zero. Porewater pressures can be positive or negative. The latter are sometimes called suction or suction pressure.

For unsaturated soils, the effective stress (Bishop et al., 1960) is

$$\sigma' = \sigma - u_a + \chi(u_a - u) \quad (7.40)$$

where u_a is the pore air pressure, u is the porewater pressure, and χ is a factor depending on the degree of saturation. For dry soil, $\chi = 0$; for saturated soil, $\chi = 1$. Values of χ for a silt are shown in Figure 7.15.

7.9.2 Effective Stresses Due to Geostatic Stress Fields

The effective stress in a soil mass not subjected to external loads is found from the unit weight of the soil and the depth of groundwater. Consider a soil element at a depth z below the ground surface, with the groundwater level (GWL) at ground surface (Figure 7.16a). The total vertical stress is

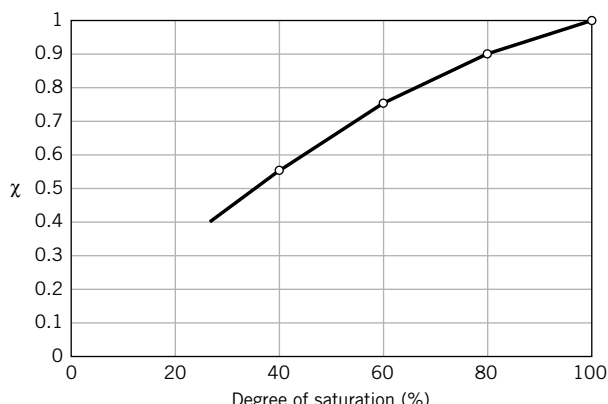


FIGURE 7.15
Values of χ for a silt at different degrees of saturation.

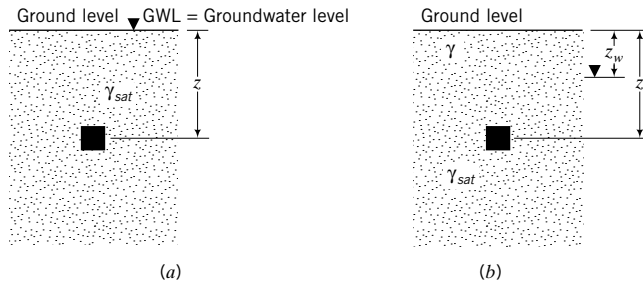


FIGURE 7.16 Soil element at a depth z with groundwater level (a) at ground level and (b) below ground level.

$$\sigma = \gamma_{sat}z \quad (7.41)$$

The porewater pressure is

$$u = \gamma_w z \quad (7.42)$$

and the effective stress is

$$\sigma' = \sigma - u = \gamma_{sat}z - \gamma_w z = (\gamma_{sat} - \gamma_w)z = \gamma'z \quad (7.43)$$

If the GWL is at a depth z_w below ground level (Fig. 7.16b), then

$$\sigma = \gamma z_w + \gamma_{sat}(z - z_w) \quad \text{and} \quad u = \gamma_w(z - z_w)$$

The effective stress is

$$\begin{aligned} \sigma' &= \sigma - u = \gamma z_w + \gamma_{sat}(z - z_w) - \gamma_w(z - z_w) \\ &= \gamma z_w + (\gamma_{sat} - \gamma_w)(z - z_w) = \gamma z_w + \gamma'(z - z_w) \end{aligned}$$

7.9.3 Effects of Capillarity

In silts and fine sands, the soil above the groundwater can be saturated by capillary action. You would have encountered capillary action in your physics course when you studied menisci. We can get an understanding of capillarity in soils by idealizing the continuous void spaces as capillary tubes. Consider a single idealized tube, as shown in Figure 7.17. The height at which water will rise in the tube can be found from statics. Summing forces vertically (upward forces are negative), we get

$$\Sigma F_z = \text{weight of water} - \text{the tension forces from capillary action}$$

that is,

$$\frac{\pi d^2}{4} z_c \gamma_w - \pi d T \cos \theta = 0 \quad (7.44)$$

Solving for z_c , we get

$$z_c = \frac{4T \cos \theta}{d \gamma_w} \quad (7.45)$$

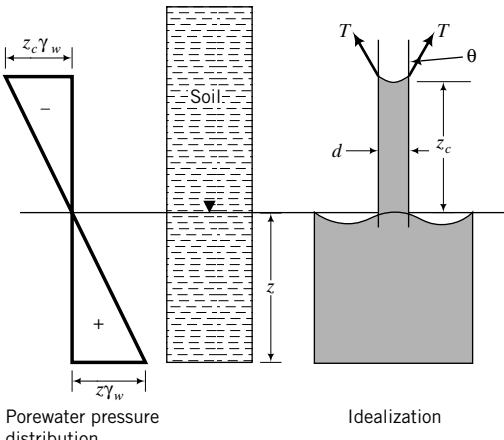


FIGURE 7.17
Capillary simulation
in soils.

where T is the surface tension (force per unit length), θ is the contact angle, z_c is the height of capillary rise, and d is the diameter of the tube representing the diameter of the void space. The surface tension of water is 0.073 N/m and the contact angle of water with a clean glass surface is 0. Since T , θ , and γ_w are constants,

$$z_c \propto \frac{1}{d} \quad (7.46)$$

For soils, d is assumed to be equivalent to $0.1 D_{10}$ where D_{10} is the effective size. The interpretation of Equation (7.46) is that the smaller the soil pores, the higher the capillary zone. The capillary zone in fine sands will be larger than for medium or coarse sands.

The porewater pressure due to capillarity is negative (suction), as shown in Figure 7.17, and is a function of the size of the soil pores and the water content. At the groundwater level, the porewater pressure is zero and decreases (becomes negative) as you move up the capillary zone. The effective stress increases because the porewater pressure is negative. For example, for the capillary zone, z_c , the porewater pressure at the top is $-z_c \gamma_w$ and the effective stress is $\sigma' = \sigma - (-z_c \gamma_w) = \sigma + z_c \gamma_w$.

The approach we have taken to interpret capillary action in soils is simple, but it is sufficient for most geotechnical applications. For a comprehensive treatment of capillary action, you can refer to Adamson (1982).

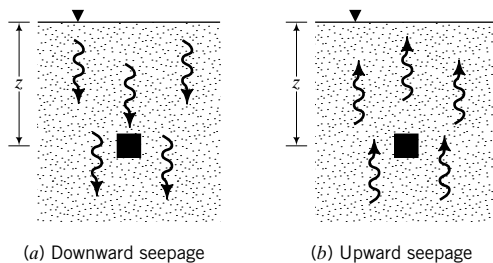
7.9.4 Effects of Seepage

In Chapter 6, we discussed one-dimensional flow of water through soils. As water flows through soil it exerts a frictional drag on the soil particles, resulting in head losses. The frictional drag is called seepage force in soil mechanics. It is often convenient to define seepage as the seepage force per unit volume (it has units similar to unit weight), which we will denote by j_s . If the head loss over a flow distance, L , is Δh , the seepage force is

$$j_s = \frac{\Delta h \gamma_w}{L} = i \gamma_w \quad (7.47)$$

If seepage occurs downward (Figure 7.18a), then the seepage stresses are in the same direction as the gravitational effective stresses. From static equilibrium, the resultant vertical effective stress is

$$\sigma'_z = \gamma' z + i z \gamma_w = \gamma' z + j_s z \quad (7.48)$$

**FIGURE 7.18**

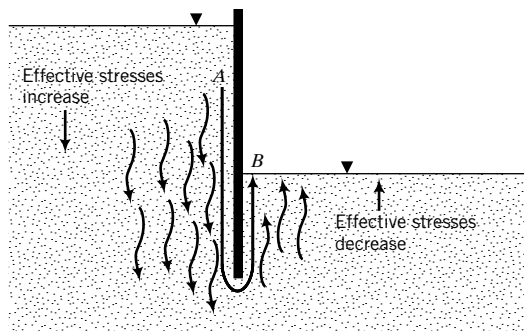
Seepage in soils. (a) Downward seepage

(b) Upward seepage

If seepage occurs upward (Figure 7.18b), then the seepage stresses are in the opposite direction to the gravitational effective stresses. From static equilibrium, the resultant vertical effective stress is

$$\sigma'_z = \gamma' z - iz\gamma_w = \gamma' z - j_s z \quad (7.49)$$

Seepage forces play a very important role in destabilizing geotechnical structures. For example, a cantilever retaining wall, shown in Figure 7.19, depends on the depth of embedment for its stability. The retained soil (left side of wall) applies an outward lateral pressure to the wall, which is resisted by an inward lateral resistance from the soil on the right side of the wall. If a steady quantity of water is available on the left side of the wall, for example, from a broken water pipe, then water will flow from the left side to the right side of the wall. The path followed by a particle of water is depicted by *AB* in Figure 7.19, and as water flows from *A* to *B*, head loss occurs. The seepage stresses on the left side of the wall are in the direction of the gravitational stresses. The effective stress increases and, consequently, an additional outward lateral force is applied on the left side of the wall. On the right side of the wall, the seepage stresses are upward and the effective stress decreases. The lateral resistance provided by the embedment is reduced. Seepage stresses in this problem play a double role (increase the lateral disturbing force and reduce the lateral resistance) in reducing the stability of a geotechnical structure. In Chapters 14 through 15, you will study the effects of seepage on the stability of several types of geotechnical structures.

**FIGURE 7.19**

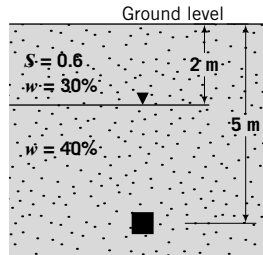
Effects of seepage on the effective stresses near a retaining wall.

THE ESSENTIAL POINTS ARE:

1. The effective stress represents the average stress carried by the soil solids and is the difference between the total stress and the porewater pressure.
2. The effective stress principle applies only to normal stresses and not to shear stresses.
3. Deformations of soils are due to effective, not total, stress.
4. Soils, especially silts and fine sands, can be affected by capillary action.
5. Capillary action results in negative porewater pressures and increases the effective stresses.
6. Downward seepage increases the resultant effective stress; upward seepage decreases the resultant effective stress.

EXAMPLE 7.5 Calculating Vertical Effective Stress

Calculate the effective stress for a soil element at depth 5 m in a uniform deposit of soil, as shown in Figure E7.5. Assume that the pore air pressure is zero.

**FIGURE E7.5**

Strategy You need to get unit weights from the given data, and you should note that the soil above the groundwater level is not saturated.

Solution 7.5

Step 1: Calculate unit weights.

Above groundwater level

$$\gamma = \left(\frac{G_s + Se}{1 + e} \right) \gamma_w = \frac{G_s(1 + w)}{1 + e} \gamma_w$$

$$Se = wG_s, \quad \therefore e = \frac{0.3 \times 2.7}{0.6} = 1.35$$

$$\gamma = \frac{2.7(1 + 0.3)}{1 + 1.35} \times 9.8 = 14.6 \text{ kN/m}^3$$

Below groundwater level

Soil is saturated, $S = 1$.

$$e = wG_s = 0.4 \times 2.7 = 1.08$$

$$\gamma_{sat} = \left(\frac{G_s + e}{1 + e} \right) \gamma_w = \left(\frac{2.7 + 1.08}{1 + 1.08} \right) 9.8 = 17.8 \text{ kN/m}^3$$

Step 2: Calculate the effective stress.

$$\text{Total stress: } \sigma_z = 2\gamma + 3\gamma_{sat} = 2 \times 14.6 + 3 \times 17.8 = 82.6 \text{ kPa}$$

$$\text{Porewater pressure: } u = 3\gamma_w = 3 \times 9.8 = 29.4 \text{ kPa}$$

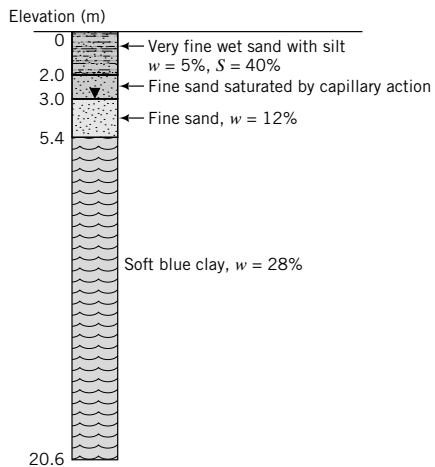
$$\text{Effective stress: } \sigma'_z = \sigma_z - u = 82.6 - 29.4 = 53.2 \text{ kPa}$$

Alternatively:

$$\sigma'_z = 2\gamma + 3(\gamma_{sat} - \gamma_w) = 2\gamma + 3\gamma' = 2 \times 14.6 + 3(17.8 - 9.8) = 53.2 \text{ kPa}$$

EXAMPLE 7.6 Calculating and Plotting Vertical Effective Stress Distribution

A borehole at a site reveals the soil profile shown in Figure E7.6a. Plot the distribution of vertical total and effective stresses with depth. Assume pore air pressure is zero.

**FIGURE E7.6a**

Strategy From the data given, you will have to find the unit weight of each soil layer to calculate the stresses. You are given that the 1.0 m of fine sand above the groundwater level is saturated by capillary action. Therefore, the porewater pressure in this 1.0 m zone is negative.

Solution 7.6

Step 1: Calculate the unit weights.

0–2 m

$$S = 40\% = 0.4; \quad w = 0.05$$

$$e = \frac{wG_s}{S} = \frac{0.05 \times 2.7}{0.4} = 0.34$$

$$\gamma = \frac{G_s(1 + w)}{1 + e} \gamma_w = \frac{2.7(1 + 0.05)}{1 + 0.34} 9.8 = 20.7 \text{ kN/m}^3$$

2–5.4 m

$$S = 1; \quad w = 0.12$$

$$e = wG_s = 0.12 \times 2.7 = 0.32$$

$$\gamma_{sat} = \left(\frac{G_s + e}{1 + e} \right) \gamma_w = \left(\frac{2.7 + 0.32}{1 + 0.32} \right) 9.8 = 22.4 \text{ kN/m}^3$$

5.4–20.6 m

$$S = 1; \quad w = 0.28$$

$$e = wG_s = 0.28 \times 2.7 = 0.76$$

$$\gamma_{sat} = \left(\frac{2.7 + 0.76}{1 + 0.76} \right) 9.8 = 19.3 \text{ kN/m}^3$$

Step 2: Calculate the stresses using a table or a spreadsheet program.

Depth (m)	Thickness (m)	σ_z (kPa)	u (kPa)	$\sigma'_z = \sigma - u$ (kPa)
0	0	0	0	0
2	2	$20.7 \times 2 = 41.4$	$-1 \times 9.8 = -9.8$	51.2
3	1	$41.4 + 22.4 \times 1 = 63.8$	0	63.8
5.4	2.4	$63.8 + 22.4 \times 2.4 = 117.6$	$2.4 \times 9.8 = 23.5$	94.1
20.6	15.2	$117.6 + 19.3 \times 15.2 = 411$	$23.5 + 15.2 \times 9.8 = 172.5$ or $17.6 \times 9.8 = 172.5$	238.5

Step 3: Plot the stresses versus depth—see Figure E7.6b.

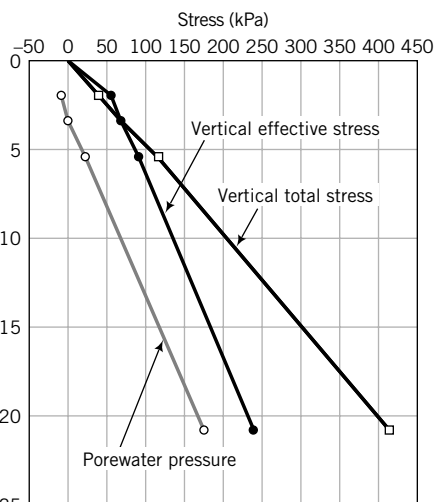


FIGURE E7.6b

EXAMPLE 7.7 Effects of Seepage on Effective Stress

Water is seeping downward through a soil layer, as shown in Figure E7.7. Two piezometers (A and B) located 2 m apart (vertically) showed a head loss of 0.2 m. Calculate the resultant vertical effective stress for a soil element at a depth of 6 m.

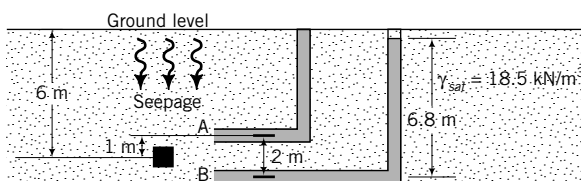


FIGURE E7.7

Strategy You have to calculate the seepage stress. But to obtain this you must know the hydraulic gradient, which you can find from the data given.

Solution 7.7

Step 1: Find the hydraulic gradient.

$$\Delta H = 0.2 \text{ m}; \quad L = 2 \text{ m}; \quad i = \frac{\Delta H}{L} = \frac{0.2}{2} = 0.1$$

Step 2: Determine the effective stress.

Assume the hydraulic gradient is the average for the soil mass; then

$$\sigma'_z = (\gamma_{sat} - \gamma_w)z + i\gamma_w z = (18.5 - 9.8)6 + 0.1 \times 9.8 \times 6 = 58.1 \text{ kPa}$$

EXAMPLE 7.8 Effects of Groundwater Condition on Effective Stress

- (a) Plot the total and effective stresses and porewater pressure with depth for the soil profile shown in Figure E7.8a for steady-state seepage condition. A porewater pressure transducer installed at the top of the sand layer gives a pressure of 58.8 kPa. Assume $G_s = 2.7$ and neglect pore air pressure.
- (b) If a borehole were to penetrate the sand layer, how far would the water rise above the groundwater level?

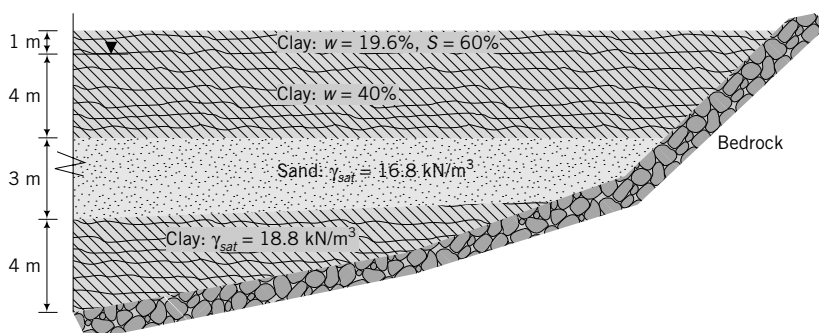


FIGURE E7.8a

Strategy You have to calculate the unit weight of the top layer of clay. From the soil profile, the groundwater appears to be under artesian condition, so the effective stress would change sharply at the interface of the top clay layer and the sand. It is best to separate the soil above the groundwater from the soil below the groundwater. So, divide the soil profile into artificial layers.

Solution 7.8

Step 1: Divide the soil profile into artificial layers.

See Figure E7.8b.

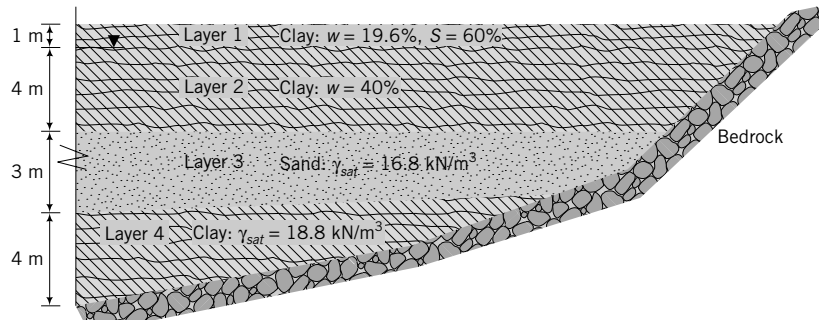


FIGURE E7.8b

Step 2: Find the unit weight of the top clay layers.

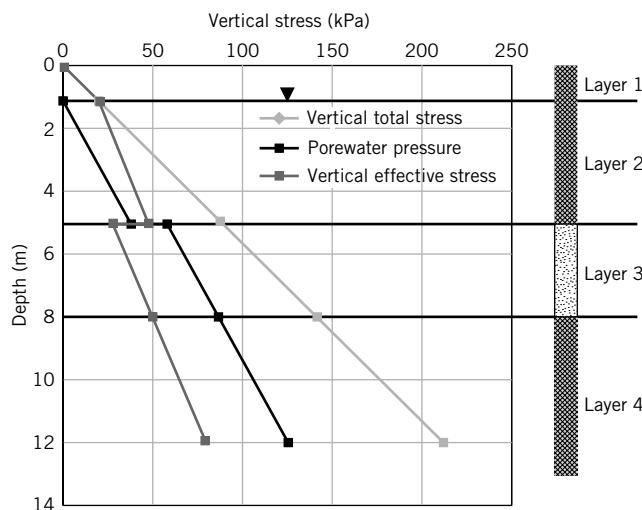
$$\text{Above groundwater level: } \gamma = \frac{G_s + Se}{1 + e} \gamma_w = \frac{G_s(1 + w)}{1 + \frac{wG_s}{S}} \gamma_w = \frac{2.7(1 + 0.196)}{1 + \frac{0.196 \times 2.7}{0.6}} \times 9.8 = 16.8 \text{ kN/m}^3$$

$$\text{Below groundwater level: } \gamma_{sat} = \frac{G_s + e}{1 + e} \gamma_w = \frac{G_s(1 + w)}{1 + wG_s} \gamma_w = \frac{2.7(1 + 0.12)}{1 + 0.12 \times 2.7} \times 9.8 = 17.8 \text{ kN/m}^3$$

Step 3: Determine the effective stress.

See spreadsheet. Note: The porewater pressure at the top of the sand is 58.8 kPa.

Layer	Depth (m)	Thickness (m)	γ (kN/m ³)	σ_z (kPa)	u (kPa)	σ'_z (kPa)
1 - top	0			0	0	0
1 - bottom	1	1	16.8	16.8	0.0	16.8
2 - top	1	4	17.8	16.8	0.0	16.8
2 - bottom	5			88.0	39.2	48.8
3 - top	5	3	16.8	88.0	58.8	29.2
3 - bottom	8			138.4	88.2	50.2
4 - top	8	4	18.8	138.4	88.2	50.2
4 - bottom	12			213.6	127.4	86.2

Step 4: Plot vertical stress and porewater pressure distributions with depth.**FIGURE E7.8c***Note:*

- (1) The vertical effective stress changes abruptly at the top of the sand layer due to the artesian condition.
- (2) For each layer or change in condition (groundwater or unit weight), the vertical stress at the bottom of the preceding layer acts a surcharge, transmitting a uniform vertical stress of equal magnitude to all subsequent layers. As an example, the vertical total stress at the bottom of layer 2 is 88 kPa. This stress is transferred to both layers 3 and 4. Thus, the vertical total stress at the bottom of layer 3 from its own weight is $3 \times 16.8 = 50.4$ kPa, and adding the vertical total stress from the layers above gives $88 + 50.4 = 138.4$ kPa.

Step 5: Calculate the height of water.

$$h = \frac{58.8}{9.8} = 6 \text{ m}$$

Height above existing groundwater level = $6 - 4 = 2$ m, or 1 m above ground level.

What's next . . . We have only considered vertical stresses. But an element of soil in the ground is also subjected to lateral stresses. Next, we will introduce an equation that relates the vertical and lateral effective stresses.

7.10 LATERAL EARTH PRESSURE AT REST

The ratio of the horizontal principal effective stress to the vertical principal effective stress is called the lateral earth pressure coefficient at rest (K_o), that is,

$$K_o = \frac{\sigma'_3}{\sigma'_1} \quad (7.50)$$

The at-rest condition implies that no deformation occurs. We will revisit the at-rest coefficient in later chapters. You must remember that K_o applies only to effective principal, not total principal, stresses. To find the lateral total stress, you must add the porewater pressure. Remember that the porewater pressure is hydrostatic and, at any given depth, the porewater pressures in all directions are equal.

For a soil that was never subjected to effective stresses higher than its current effective stress (normally consolidated soil), $K_o = K_o^{nc}$ is reasonably predicted by an equation suggested by Jaky (1944) as

$$K_o^{nc} \approx 1 - \sin \phi'_{cs} \quad (7.51)$$

where ϕ'_{cs} is a fundamental frictional soil constant that will be discussed in Chapter 10.

The value of K_o^{nc} is constant. During unloading or reloading, the soil stresses must adjust to be in equilibrium with the applied stress. This means that stress changes take place not only vertically but also horizontally. For a given surface stress, the changes in horizontal total stresses and vertical total stresses are different, but the porewater pressure changes in every direction are the same. Therefore, the current effective stresses are different in different directions. A soil in which the current effective stress is lower than the past maximum stress is called an overconsolidated soil (to be discussed further in Chapter 9). The K_o values for overconsolidated soils are not constants. We will denote K_o for overconsolidated soils as K_o^{oc} . Various equations have been suggested linking K_o^{oc} to K_o^{nc} . One equation that is popular and found to match test data reasonably well is an equation proposed by Meyerhof (1976) as

$$K_o^{oc} = K_o^{nc}(\text{OCR})^{1/2} = (1 - \sin \phi'_{cs})(\text{OCR})^{1/2} \quad (7.52)$$

where OCR is the overconsolidation ratio (see Chapter 9 for more information), defined as the ratio of the past vertical effective stress to the current vertical effective stress.

EXAMPLE 7.9 Calculating Horizontal Effective and Total Stresses

Calculate the horizontal effective stress and the horizontal total stress for the soil element at 5 m in Example 7.5 if $K_o = 0.5$.

Strategy The stresses on the horizontal and vertical planes on the soil element are principal stresses (no shear stress occurs on these planes). You need to apply K_o to the effective principal stress and then add the porewater pressure to get the lateral total principal stress.

Solution 7.9

Step 1: Calculate the horizontal effective stress.

$$K_o = \frac{\sigma'_3}{\sigma'_1} = \frac{\sigma'_x}{\sigma'_z}; \quad \sigma'_x = K_o \sigma'_z = 0.5 \times 53.2 = 26.6 \text{ kPa}$$

Step 2: Calculate the horizontal total stress.

$$\sigma_x = \sigma'_x + u = 26.6 + 29.4 = 56 \text{ kPa}$$

EXAMPLE 7.10 Calculating Horizontal Total and Effective Stresses from Dissipation of Excess Porewater Pressure

Determine the horizontal effective and total stresses on a normally consolidated soil sample for:

- (a) time: $t = t_1, \Delta u = 20 \text{ kPa}$
- (b) time: $t \rightarrow \infty, \Delta u = 0$

The vertical total stress is 100 kPa and the frictional constant $\phi'_{cs} = 30^\circ$.

Strategy The horizontal earth pressure coefficient must be applied to the vertical effective stress, not the vertical total stress. You need to calculate the vertical effective stress, then the horizontal effective stress. Add the excess porewater pressure to the horizontal effective stress to find the horizontal total stress.

Solution 7.10

Step 1: Calculate the vertical effective stresses.

$$\sigma'_z = \sigma_z - \Delta u$$

- (a) $\sigma'_z = 100 - 20 = 80 \text{ kPa}$
- (b) $\sigma'_z = 100 - 0 = 100 \text{ kPa}$

Step 2: Calculate the horizontal effective stress.

$$K_o^{nc} = 1 - \sin \phi'_{cs} = 1 - \sin 30^\circ = 0.5$$

$$\sigma'_x = K_o^{nc} \sigma'_z$$

- (a) $\sigma'_x = 0.5 \times 80 = 40 \text{ kPa}$
- (b) $\sigma'_x = 0.5 \times 100 = 50 \text{ kPa}$

Step 3: Calculate the total horizontal stresses.

$$\sigma_x = \sigma'_x + \Delta u$$

- (a) $\sigma_x = 40 + 20 = 60 \text{ kPa}$
- (b) $\sigma_x = 50 + 0 = 50 \text{ kPa}$

What's next . . . The stresses we have considered so far are called geostatic stresses, and when we considered elastic deformation of soils, the additional stresses imposed on the soil were given. But in practice, we have to find these additional stresses from applied loads located either on the ground surface or within the soil mass. We will use elastic analysis to find these additional stresses. Next, we will consider increases in stresses from a number of common surface loads. You will encounter myriad equations. You are not expected to remember these equations, but you are expected to know how to use them.

7.11 STRESSES IN SOIL FROM SURFACE LOADS



Computer Program Utility

Access www.wiley.com/college/budhu, and click on Chapter 7 and then STRESS.zip to download and run a computer application to obtain the stress increases and displacements due to surface loads. You can use this program to explore stress changes due to different types of loads, and prepare and print Newmark charts for vertical stresses beneath arbitrarily shaped loads (described in Section 7.11.8). This computer program will also be helpful in solving problems in later chapters.

The distribution of stresses within a soil from applied surface loads or stresses is determined by assuming that the soil is a semi-infinite, homogeneous, linear, isotropic, elastic material. A semi-infinite mass is bounded on one side and extends infinitely in all other directions; this is also called an “elastic half-space.” For soils, the horizontal surface is the bounding side. Because of the assumption of a linear elastic soil mass, we can use the principle of superposition. That is, the stress increase at a given point in a soil mass in a certain direction from different loads can be added together.

Surface loads are divided into two general classes, finite and infinite. However, these are qualitative classes and are subject to interpretation. Examples of finite loads are point loads, circular loads, and rectangular loads. Examples of infinite loads are fills and surcharges. The relative rigidity of the foundation (a system that transfers the load to the soil) to the soil mass influences the stress distribution within the soil. The elastic solutions presented are for flexible loads and do not account for the relative rigidity of the soil foundation system. If the foundation is rigid, the stress increases are generally lower (15% to 30% less for clays and 20% to 30% less for sands) than those calculated from the elastic solutions presented in this section. Traditionally, the stress increases from the elastic solutions are not adjusted because soil behavior is nonlinear and it is better to err on the conservative side. The increases in soil stresses from surface loads are total stresses. These increases in stresses are resisted initially by both the porewater and the soil particles.

Equations and charts for several types of flexible surface loads based on the above assumptions are presented. Most soils exist in layers with finite thicknesses. The solution based on a semi-infinite soil mass will not be accurate for these layered soils. In Appendix C, you will find selected graphs and tables for vertical stress increases in one-layer and two-layer soils. A comprehensive set of equations for a variety of loading situations is available in Poulos and Davis (1974).

7.11.1 Point Load

Boussinesq (1885) presented a solution for the distribution of stresses for a point load applied on the soil surface. An example of a point load is the vertical load transferred to the soil from an electric power line pole.

The increases in stresses on a soil element located at point A (Figure 7.20a) due to a point load, Q , are

$$\Delta\sigma_z = \frac{3Q}{2\pi z^2 \left[1 + \left(\frac{r}{z} \right)^2 \right]^{5/2}} \quad (7.53)$$

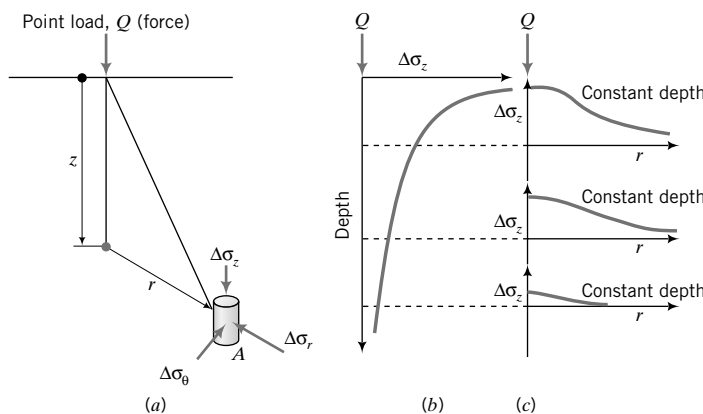


FIGURE 7.20 Point load and vertical stress distribution with depth and radial distance.

$$\Delta\sigma_r = \frac{Q}{2\pi} \left(\frac{3r^2z}{(r^2+z^2)^{5/2}} - \frac{1-2\nu}{r^2+z^2+z(r^2+z^2)^{1/2}} \right) \quad (7.54)$$

$$\Delta\sigma_\theta = \frac{Q}{2\pi} (1-2\nu) \left(\frac{z}{(r^2+z^2)^{3/2}} - \frac{1}{r^2+z^2+z(r^2+z^2)^{1/2}} \right) \quad (7.55)$$

$$\Delta\tau_{rz} = \frac{3Q}{2\pi} \left[\frac{rz^2}{(r^2+z^2)^{5/2}} \right] \quad (7.56)$$

where ν is Poisson's ratio. Most often, the increase in vertical stress is needed in practice. Equation (7.53) can be written as

$$\Delta\sigma_z = \frac{Q}{z^2} I \quad (7.57)$$

where I is an influence factor, and

$$I = \frac{3}{2\pi} \frac{1}{\left[1 + \left(\frac{r}{z} \right)^2 \right]^{5/2}} \quad (7.58)$$

The distributions of the increase in vertical stress from Equations (7.57) and (7.58) reveal that the increase in vertical stress decreases with depth (Figure 7.20b) and radial distance (Figure 7.20c).

The vertical displacement is

$$\Delta z = \frac{Q(1+\nu)}{2\pi Ez \left[1 + \left(\frac{r}{z} \right)^2 \right]^{1/2}} \left[2(1-\nu) + \frac{1}{1 + \left(\frac{r}{z} \right)^2} \right] \quad (7.59)$$

and the radial displacement is

$$\Delta r = \frac{Q(1+\nu)}{2\pi Ez \left[1 + \left(\frac{r}{z} \right)^2 \right]^{1/2}} \left[\frac{\left(\frac{r}{z} \right)}{\left\{ 1 + \left(\frac{r}{z} \right)^2 \right\}} - \frac{(1-2\nu)\left(\frac{r}{z} \right)}{\left\{ 1 + \left(\frac{r}{z} \right)^2 \right\}^{1/2} + 1} \right] \quad (7.60)$$

where E is Young's modulus.

EXAMPLE 7.11 Vertical Stress Increase Due to a Point Load

A pole carries a vertical load of 200 kN. Determine the vertical total stress increase at a depth 5 m (a) directly below the pole and (b) at a radial distance of 2 m.

Strategy The first step is to determine the type of surface load. The load carried by the pole can be approximated to a point load. You can then use the equation for the vertical stress increase for a point load.

Solution 7.11

Step 1: Determine the load type.

Assume the load from the pole can be approximated by a point load.

Step 2: Use the equation for a point load. Use Equation (7.57):

$$z = 5 \text{ m}, \quad Q = 200 \text{ kN}; \quad \text{Under load, } r = 0, \quad \therefore \frac{r}{z} = 0$$

$$\text{From Equation (7.58): } \frac{r}{z} = 0, \quad I = \frac{3}{2\pi} = 0.48$$

$$\Delta\sigma_z = \frac{Q}{z^2} I = \frac{200}{5^2} \times 0.48 = 3.8 \text{ kPa}$$

Step 3: Determine the vertical stress at the radial distance.

$$r = 2 \text{ m}, \quad \frac{r}{z} = \frac{2}{5} = 0.4, \quad I = \frac{3}{2\pi} \frac{1}{[1 + (0.4)^2]^{5/2}} = 0.33$$

$$\Delta\sigma_z = \frac{200}{5^2} \times 0.33 = 2.6 \text{ kPa}$$

7.11.2 Line Load

With reference to Figure 7.21a, the increases in stresses due to a line load, Q (force/length), are

$$\Delta\sigma_z = \frac{2Qz^3}{\pi(x^2 + z^2)^2} \quad (7.61)$$

$$\Delta\sigma_x = \frac{2Qx^2z}{\pi(x^2 + z^2)^2} \quad (7.62)$$

$$\Delta\tau_{zx} = \frac{2Qxz^2}{\pi(x^2 + z^2)^2} \quad (7.63)$$

A practical example of a line load is the load from a long brick wall.

7.11.3 Line Load Near a Buried Earth-Retaining Structure

The increase in lateral stress on a buried earth-retaining structure (Figure 7.21b) due to a line load of intensity Q (force/length) is

$$\Delta\sigma_x = \frac{4Qa^2b}{\pi H_o(a^2 + b^2)^2} \quad (7.64)$$

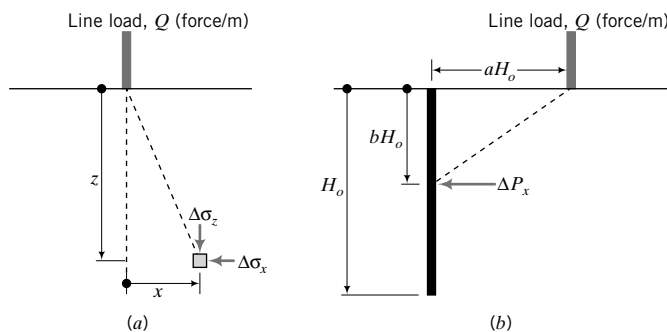


FIGURE 7.21 (a) Line load and (b) line load near a retaining wall.

The increase in lateral force is

$$\Delta P_x = \frac{2Q}{\pi(a^2 + 1)} \quad (7.65)$$

7.11.4 Strip Load

A strip load is the load transmitted by a structure of finite width and infinite length on a soil surface. Two types of strip loads are common in geotechnical engineering. One is a load that imposes a uniform stress on the soil, for example, the middle section of a long embankment (Figure 7.22a). The other is a load that induces a triangular stress distribution over an area of width B (Figure 7.22b). An example of a strip load with a triangular stress distribution is the stress under the side of an embankment.

The increases in stresses due to a surface stress q_s (force/area) are as follows:

(a) Area transmitting a uniform stress (Figure 7.22a)

$$\Delta\sigma_z = \frac{q_s}{\pi} [\alpha + \sin \alpha \cos(\alpha + 2\beta)] \quad (7.66)$$

$$\Delta\sigma_x = \frac{q_s}{\pi} [\alpha - \sin \alpha \cos(\alpha + 2\beta)] \quad (7.67)$$

$$\Delta\tau_{zx} = \frac{q_s}{\pi} [\sin \alpha \sin(\alpha + 2\beta)] \quad (7.68)$$

where q_s is the applied surface stress.

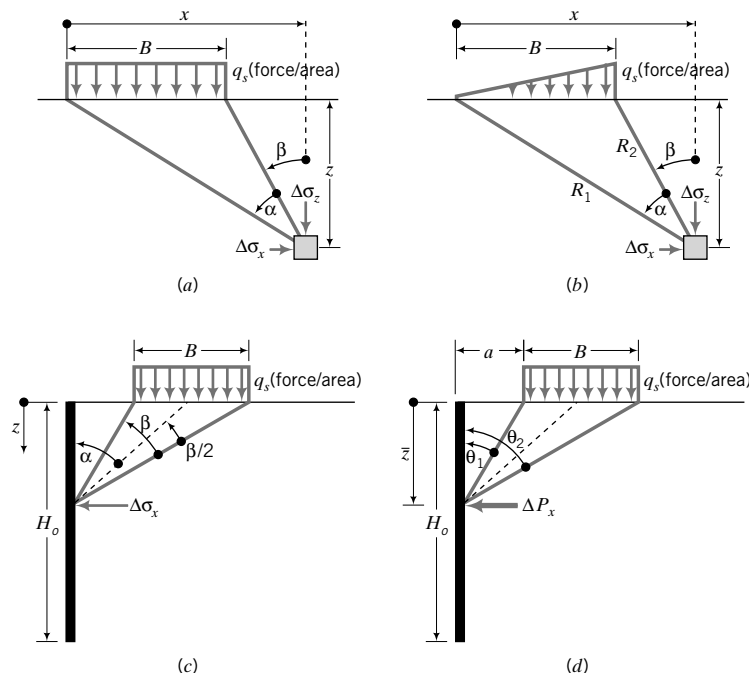


FIGURE 7.22 Strip load imposing (a) a uniform surface stress and (b) a linear varying surface stress. (c) Strip load imposing a uniform surface stress near a retaining wall and (d) lateral force on a retaining wall from a strip load imposing a uniform surface stress.

The vertical displacement due to a strip loading is useful only as relative displacement between two points not located at infinity. The relative vertical displacement between the center of the strip load $(0, 0)$ and a point at the surface $(x, 0)$ is

$$\Delta z(x, 0) - \Delta z(0, 0) = \frac{2q_s(1 - v^2)}{\pi E} \left\{ \left(x - \frac{B}{2} \right) \ln \left| x - \frac{B}{2} \right| - \left(x + \frac{B}{2} \right) \ln \left| x + \frac{B}{2} \right| + B \ln \left(\frac{B}{2} \right) \right\} \quad (7.69)$$

(b) Area transmitting a triangular stress (Figure 7.22b)

$$\Delta \sigma_z = \frac{q_s}{\pi} \left(\frac{x}{B} \alpha - \frac{1}{2} \sin 2\beta \right) \quad (7.70)$$

$$\Delta \sigma_x = \frac{q_s}{\pi} \left(\frac{x}{B} \alpha - \frac{z}{B} \ln \frac{R_1^2}{R_2^2} + \frac{1}{2} \sin 2\beta \right) \quad (7.71)$$

$$\Delta \tau_{zx} = \frac{q_s}{2\pi} \left(1 + \cos 2\beta - 2 \frac{z}{B} \alpha \right) \quad (7.72)$$

The relative vertical displacement between the center of the strip load $(0, 0)$ and a point at the surface $(x, 0)$ is

$$\Delta z(x, 0) - \Delta z(0, 0) = \frac{q_s(1 - v^2)}{\pi E \left(\frac{B}{2} \right)} \left\{ \frac{B^2}{2} \ln B - \frac{x^2}{2} \ln x + \left(\frac{x^2}{2} - \frac{B^2}{2} \right) \ln |B - x| + \frac{B}{2} x \right\} \quad (7.73)$$

(c) Area transmitting a uniform stress near a retaining wall (Figure 7.22c, d)

$$\Delta \sigma_x = \frac{2q_s}{\pi} (\beta - \sin \beta \cos 2\alpha) \quad (7.74)$$

The lateral force and its location were derived by Jarquio (1981) and are

$$\Delta P_x = \frac{q_s}{90} [H_o(\theta_2 - \theta_1)] \quad (7.75)$$

$$\bar{z} = \frac{H_o^2(\theta_2 - \theta_1) - (R_1 - R_2) + 57.3BH_o}{2H_o(\theta_2 - \theta_1)} \quad (7.76)$$

where

$$\theta_1 = \tan^{-1} \left(\frac{a}{H_o} \right), \quad \theta_2 = \tan^{-1} \left(\frac{a + B}{H_o} \right)$$

$$R_1 = (a + B)^2(90 - \theta_2), \quad \text{and} \quad R_2 = a^2(90 - \theta_1)$$

7.11.5 Uniformly Loaded Circular Area

An example of a circular area that transmits stresses to a soil mass is a circular foundation of an oil or water tank. The increases of vertical and radial stresses under the center of a circular area of radius r_o are

$$\Delta \sigma_z = q_s \left[1 - \left(\frac{1}{1 + (r_o/z)^2} \right)^{3/2} \right] = q_s I_c \quad (7.77)$$

where

$$I_c = \left[1 - \left(\frac{1}{1 + (r_o/z)^2} \right)^{3/2} \right]$$

is an influence factor and

$$\Delta\sigma_r = \Delta\sigma_\theta = \frac{q_s}{2} \left[(1 + 2\nu) - \frac{4(1 + \nu)}{[1 + (r_o/z)^2]^{1/2}} + \frac{1}{[1 + (r_o/z)^2]^{3/2}} \right] \quad (7.78)$$

The vertical elastic settlement at the surface due to a circular flexible loaded area is

$$\text{Below center of loaded area: } \Delta z = \frac{q_s D (1 - \nu^2)}{E} \quad (7.79)$$

$$\text{Below edge: } \Delta z = \frac{2}{\pi} \frac{q_s D (1 - \nu^2)}{E} \quad (7.80)$$

where $D = 2r_o$ is the diameter of the loaded area. The vertical stress increases and vertical elastic settlements at all points in the soil mass from a circular loaded area are shown in Appendix B.

EXAMPLE 7.12 Vertical Stress Increase Due to a Ring Load

A silo is supported on a ring foundation, as shown in Figure E7.12a. The total vertical load is 4 MN. (a) Plot the vertical stress increase with depth up to 8 m under the center of the ring (point O , Figure E7.12a). (b) Determine the maximum vertical stress increase and its location.

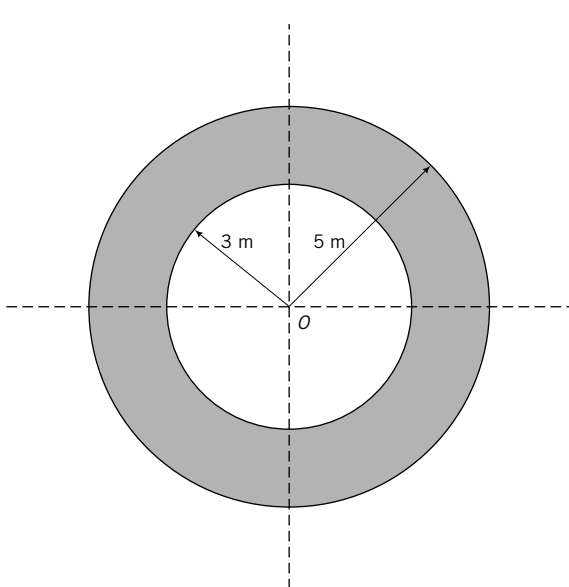


FIGURE E7.12a

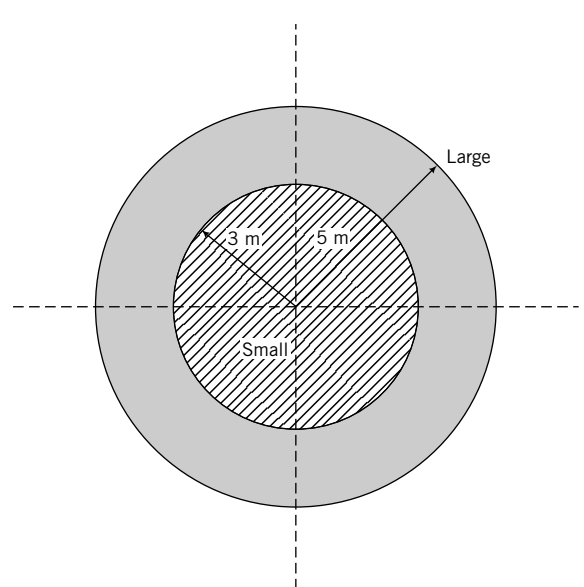


FIGURE E7.12b

Strategy To use the equation for a uniform circular area to simulate the ring foundation, you need to create two artificial circular foundations, one with a radius of 5 m and the other with a radius of 3 m. Both foundations must be fully loaded with the applied uniform, vertical stress. By subtracting the vertical stress increase of the smaller foundation from the larger foundation, you would obtain the vertical stress increase from the ring foundation. You are applying here the principle of superposition.

Solution 7.12

Step 1: Identify the loading type.

It is a uniformly loaded ring foundation.

Step 2: Calculate the imposed surface stress.

$$r_2 = 5 \text{ m}, \quad r_1 = 3 \text{ m}$$

$$\text{Area} = \pi(r_2^2 - r_1^2) = \pi(5^2 - 3^2) = 16\pi \text{ m}^2$$

$$q_s = \frac{Q}{A} = \frac{4000}{16\pi} = 79.6 \text{ kPa}$$

Step 3: Create two solid circular foundations of radii 5 m and 3 m.

See Figure E7.12b. Let “large” denotes the foundation of radius 5 m and “small” denotes the foundation of radius 3 m.

Step 4: Create a spreadsheet to do the calculations.

Ring load

Load	4000 kN
Outer radius	5 m
Inner radius	3 m
Area	50.3 m ²
q_s	79.6 kPa

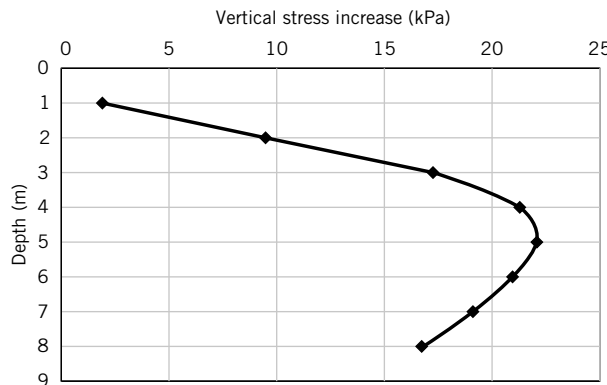
z	Large		Small		I_{diff}	$\Delta\sigma_z (\text{kPa})$
	r/z	$(I_c)_{large}$	r _o /z	$(I_c)_{small}$		
1	7.00	0.992	3.00	0.968	0.024	1.9
2	2.50	0.949	1.50	0.829	0.119	9.5
3	1.67	0.864	1.00	0.646	0.217	17.3
4	1.25	0.756	0.75	0.488	0.268	21.3
5	1.00	0.646	0.60	0.369	0.277	22.0
6	0.83	0.547	0.50	0.284	0.262	20.9
7	0.71	0.461	0.43	0.223	0.238	18.9
8	0.63	0.390	0.38	0.179	0.211	16.8

The coefficients I_c were obtained from the application program, STRESS.zip. You can download this application from www.wiley.com/college/budhu.

Step 5: Plot the vertical stress increase variation with depth.

See Figure E7.12c.



**FIGURE E7.12c**

Step 6: Determine the maximum vertical stress increase and depth of occurrence.

From Figure E7.12c, the maximum vertical stress increase is 22 kPa and the depth of occurrence is 5 m from the surface.

7.11.6 Uniformly Loaded Rectangular Area

Many structural foundations are rectangular or approximately rectangular in shape. The increases in stresses below the corner of a rectangular area of width B and length L are

$$\Delta\sigma_z = \frac{q_s}{2\pi} \left[\tan^{-1} \frac{LB}{zR_3} + \frac{LBz}{R_3} \left(\frac{1}{R_1^2} + \frac{1}{R_2^2} \right) \right] \quad (7.81)$$

$$\Delta\sigma_x = \frac{q_s}{2\pi} \left[\tan^{-1} \frac{LB}{zR_3} - \frac{LBz}{R_1^2 R_3} \right] \quad (7.82)$$

$$\Delta\sigma_y = \frac{q_s}{2\pi} \left[\tan^{-1} \frac{LB}{zR_3} - \frac{LBz}{R_2^2 R_3} \right] \quad (7.83)$$

$$\Delta\tau_{zx} = \frac{q_s}{2\pi} \left[\frac{B}{R_2} - \frac{z^2 B}{R_1^2 R_3} \right] \quad (7.84)$$

where $R_1 = (L^2 + z^2)^{1/2}$, $R_2 = (B^2 + z^2)^{1/2}$, and $R_3 = (L^2 + B^2 + z^2)^{1/2}$.

These equations can be written as

$$\Delta\sigma_z = q_s I_z \quad (7.85)$$

$$\Delta\sigma_x = q_s I_x \quad (7.86)$$

$$\Delta\sigma_y = q_s I_y \quad (7.87)$$

$$\Delta\tau_{zx} = q_s I_\tau \quad (7.88)$$

where I denotes the influence factor. The influence factor for the vertical stress is

$$I_z = \frac{1}{4\pi} \left[\frac{2mn\sqrt{m^2 + n^2 + 1}}{m^2 + n^2 + m^2n^2 + 1} \left(\frac{m^2 + n^2 + 2}{m^2 + n^2 + 1} \right) + \tan^{-1} \left(\frac{2mn\sqrt{m^2 + n^2 + 1}}{m^2 + n^2 - m^2n^2 + 1} \right) \right] \quad (7.89)$$

where $m = B/z$ and $n = L/z$. You can program your calculator or use a spreadsheet program to find I_z . You must be careful in the last term (\tan^{-1}) in programming. If $m^2 + n^2 + 1 < m^2n^2$, then you have to add π to the bracketed quantity in the last term. The distribution of vertical stress below a uniformly loaded square foundation is shown in Figure 7.23. The increase in vertical stress is about 10% below a depth of

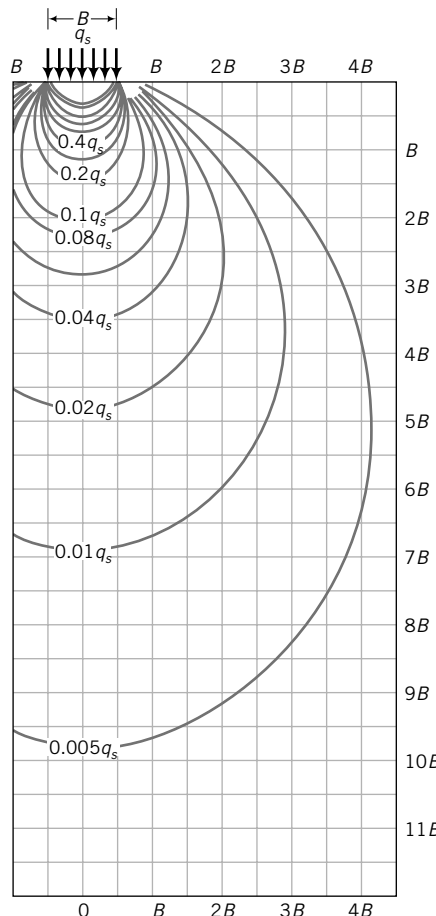


FIGURE 7.23 Vertical stress contour below a square foundation.

$2B$; B is the diameter of the foundation. The vertical stress decreases from the center of the foundation outward, reaching a value of about 10% at a horizontal distance of $B/2$ from the edge at a depth of B . A chart for I_z for the corner of rectangular loaded area is shown in Figure 7.24 on page 172. You would have to calculate $m = B/z$ and $n = L/z$ and read I_z from the chart; m and n are interchangeable. In general, the vertical stress increase is less than 10% of the surface stress when $z > 2B$.

The vertical elastic settlement at the ground surface under a rectangular flexible surface load is

$$\Delta z = \frac{q_s B (1 - \nu^2)}{E} I_s \quad (7.90)$$

where I_s is a settlement influence factor that is a function of the L/B ratio (L is length and B is width). Setting $\xi_s = L/B$, the equations for I_s are

At center of a rectangle (Giroud, 1968):

$$I_s = \frac{2}{\pi} \left[\ln(\xi_s + \sqrt{1 + \xi_s^2}) + \xi_s \ln \frac{1 + \sqrt{1 + \xi_s^2}}{\xi_s} \right] \quad (7.91)$$

At corner of a rectangle (Giroud, 1968):

$$I_s = \frac{1}{\pi} \left[\ln(\xi_s + \sqrt{1 + \xi_s^2}) + \xi_s \ln \frac{1 + \sqrt{1 + \xi_s^2}}{\xi_s} \right] \quad (7.92)$$

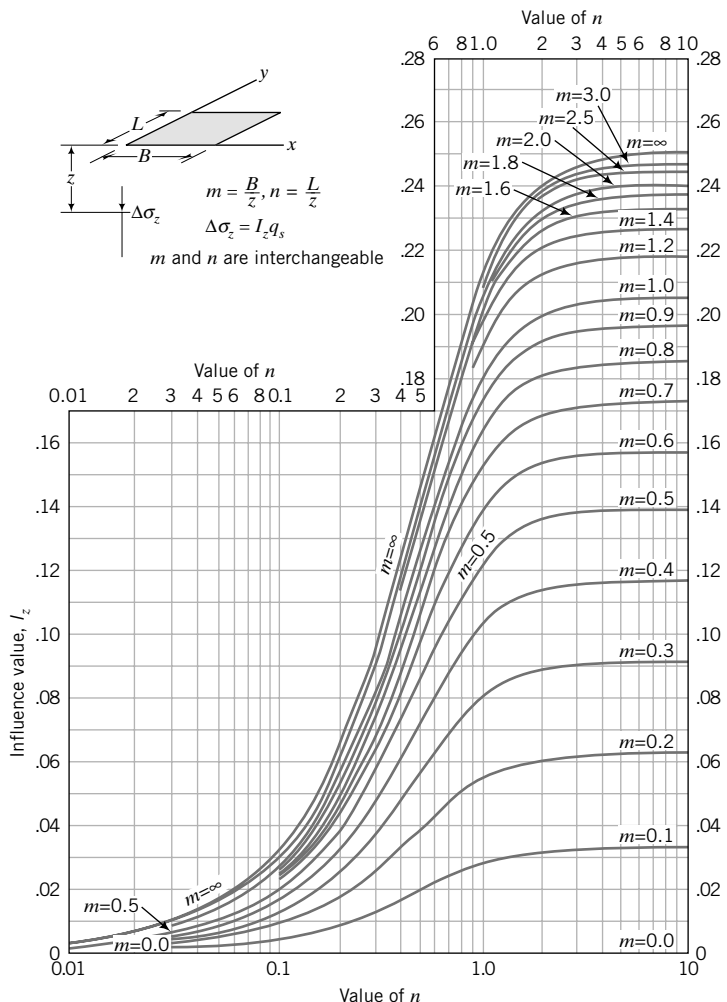


FIGURE 7.24 Influence factor for calculating the vertical stress increase under the corner of a rectangle. (Source: NAV-FAC-DM 7.1.)

The above equations can be simplified to the following for $\xi_s \geq 1$:

$$\text{At center of a rectangle: } I_s \approx 0.62 \ln(\xi_s) + 1.12 \quad (7.93)$$

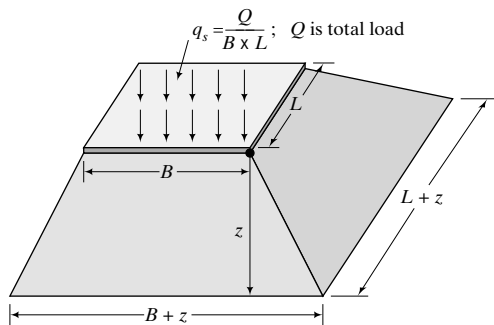
$$\text{At corner of a rectangle: } I_s \approx 0.31 \ln(\xi_s) + 0.56 \quad (7.94)$$

7.11.7 Approximate Method for Rectangular Loads

In preliminary analyses of vertical stress increases under the center of rectangular loads, geotechnical engineers often use an approximate method (sometimes called the 2:1 method). The surface load on an area $B \times L$ is dispersed at a depth z over an area $(B + z) \times (L + z)$, as illustrated in Figure 7.25. The vertical stress increase under the center of the load is

$$\Delta\sigma_z = \frac{Q}{(B + z)(L + z)} = \frac{q_s BL}{(B + z)(L + z)} \quad (7.95)$$

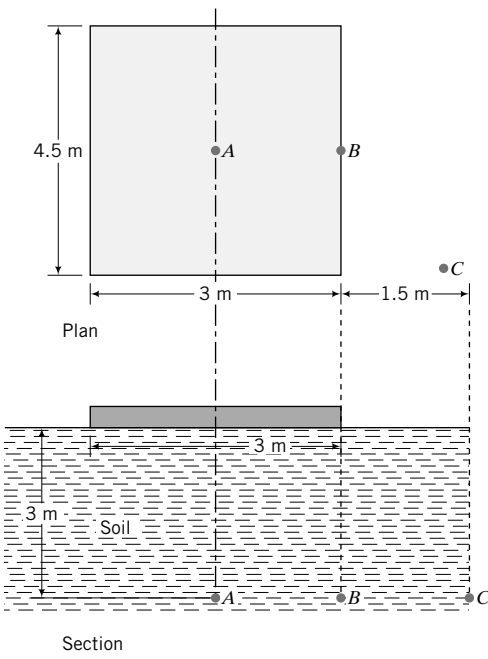
The approximate method is reasonably accurate (compared with Boussinesq's elastic solution) when $z > B$.

**FIGURE 7.25**

Dispersion of load for approximate increase in vertical stress under a rectangular loaded area

EXAMPLE 7.13 Vertical Stress Increase Due to a Rectangular Load

A rectangular concrete slab, $3 \text{ m} \times 4.5 \text{ m}$, rests on the surface of a soil mass. The load on the slab is 2025 kN. Determine the vertical stress increase at a depth of 3 m (a) under the center of the slab, point A (Figure E7.13a); (b) under point B (Figure E7.13a); and (c) at a distance of 1.5 m from a corner, point C (Figure E7.13a).

**FIGURE E7.13a**

(a)

Strategy The slab is rectangular and the equations for a uniformly loaded rectangular area are for the corner of the area. You should divide the area so that the point of interest is a corner of a rectangle(s). You may have to extend the loaded area if the point of interest is outside it (loaded area). The extension is fictitious, so you have to subtract the fictitious increase in vertical stress for the extended area.

Solution 7.13

Step 1: Identify the loading type.

It is a uniformly loaded rectangle.

Step 2: Divide the rectangle so that the center is a corner.

In this problem, all four rectangles, after the subdivision, are equal (Figure E7.13b; point C is excluded for simplicity), so you only need to find the vertical stress increase for one rectangle of size $B = 1.5\text{ m}$, $L = 2.25\text{ m}$ and multiply the results by 4.

$$m = \frac{B}{z} = \frac{1.5}{3} = 0.5; \quad n = \frac{L}{z} = \frac{2.25}{3} = 0.75$$

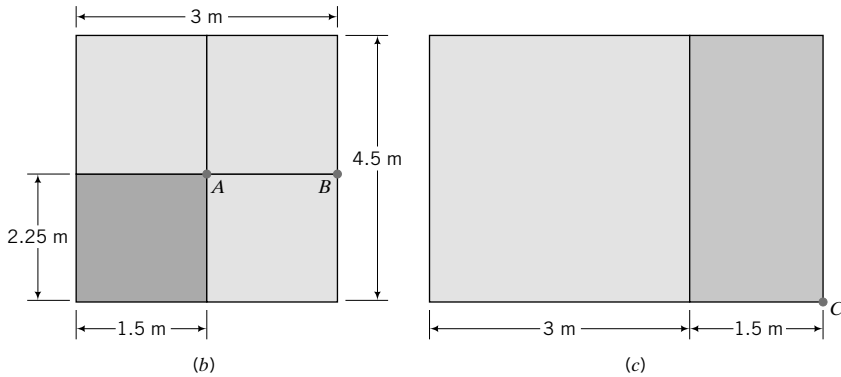


FIGURE E7.13b, c

From the chart in Figure 7.24, $I_z = 0.107$.

Step 3: Find the vertical stress increase at the center of the slab (point A, Figure E7.13b).

$$q_s = \frac{Q}{A} = \frac{2025}{3 \times 4.5} = 150 \text{ kPa}$$

$$\Delta\sigma_z = 4q_s I_z = 4 \times 150 \times 0.105 = 63 \text{ kPa}$$

Note: The approximate method [Equation (7.95)] gives

$$\Delta\sigma_z = \frac{Q}{(B+z)(L+z)} = \frac{2025}{(3+3)(4.5+3)} = 45 \text{ kPa}$$

which is about 30% less than the elastic solution.

Step 4: Find the vertical stress increase for point B.

Point B is at the corner of two rectangles, each of width 3 m and length 2.25 m. You need to find the vertical stress increase for one rectangle and multiply the result by 2.

$$m = \frac{3}{3} = 1; \quad n = \frac{2.25}{3} = 0.75$$

From the chart in Figure 7.24, $I_z = 0.158$.

$$\Delta\sigma_z = 2q_s I_z = 2 \times 150 \times 0.158 = 47.4 \text{ kPa}$$

You should note that the vertical stress increase at B is lower than at A, as expected.

Step 5: Find the stress increase for point C.

Stress point C is outside the rectangular slab. You have to extend the rectangle to C (Figure E7.13c) and find the stress increase for the large rectangle of width $B = 4.5\text{ m}$, length $L = 4.5\text{ m}$ and then subtract the stress increase for the smaller rectangle of width $B = 1.5\text{ m}$ and length $L = 4.5\text{ m}$.

Large rectangle

$$m = \frac{4.5}{3} = 1.5, \quad n = \frac{4.5}{3} = 1.5; \quad \text{from chart in Figure 7.24, } I_z = 0.22$$

Small rectangle

$$m = \frac{1.5}{3} = 0.5, \quad n = \frac{4.5}{3} = 1.5; \quad \text{from chart in Figure 7.24, } I_z = 0.13$$

$$\Delta\sigma_z = q_s \Delta I_z = 150 \times (0.22 - 0.13) = 13.5 \text{ kPa}$$

7.11.8 Vertical Stress Below Arbitrarily Shaped Areas

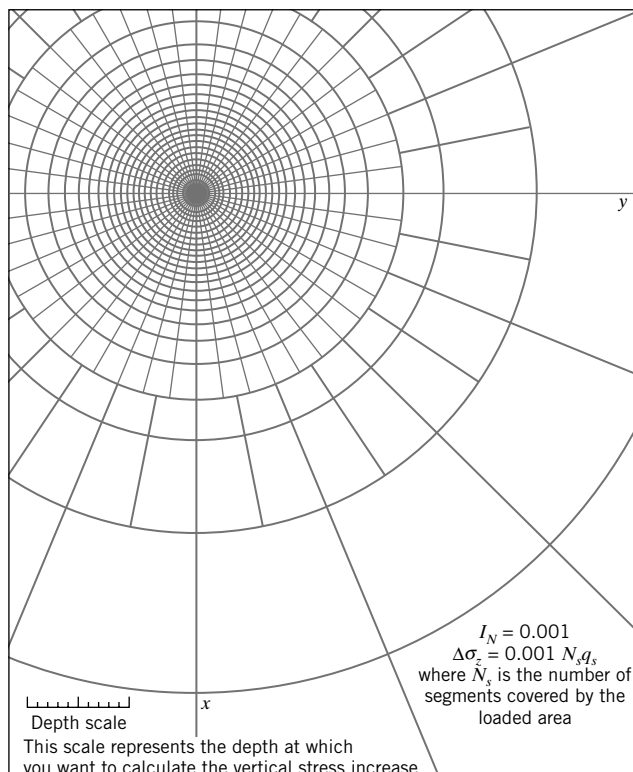
Newmark (1942) developed a chart to determine the increase in vertical stress due to a uniformly loaded area of any shape. The chart consists of concentric circles divided by radial lines (Figure 7.26). The area of each segment represents an equal proportion of the applied surface stress at a depth z below the surface. If there are 10 concentric circles and 20 radial lines, the stress on each circle is $q_s/10$ and on each segment is $q_s/(10 \times 20)$. The radius-to-depth ratio of the first (inner) circle is found by setting $\Delta\sigma_z = 0.1q_s$ in Equation (7.77), that is,

$$0.1q_s = q_s \left[1 - \left\{ \frac{1}{1 + (r_o/z)^2} \right\}^{3/2} \right]$$

from which $r_o/z = 0.27$. For the other circles, substitute the appropriate value for $\Delta\sigma_z$; for example, for the second circle $\Delta\sigma_z = 0.2q_s$, and find r_o/z . The chart is normalized to the depth; that is, all dimensions are scaled by a factor initially determined for the depth. Every chart should show a scale and an influence factor I_N . The influence factor for Figure 7.26 is 0.001.

The procedure for using Newmark's chart is as follows:

- Set the scale, shown on the chart, equal to the depth at which the increase in vertical stress is required. We will call this the depth scale.



2. Identify the point below the loaded area where the stress is required. Let us say this point is A .
3. Plot the loaded area, scaling its plan dimension using the depth scale with point A at the center of the chart.
4. Count the number of segments (N_s) covered by the scaled loaded area. If certain segments are not fully covered, you can estimate what fraction is covered.
5. Calculate the increase in vertical stress as $\Delta\sigma_z = q_s I_N N_s$.

EXAMPLE 7.14 Vertical Stress Increase Due to an Irregular Loaded Area

The plan of a foundation of uniform thickness for a building is shown in Figure E7.14a. Determine the vertical stress increase at a depth of 4 m below the centroid. The foundation applies a vertical stress of 200 kPa on the soil surface.

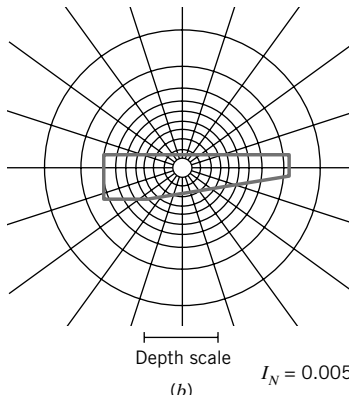
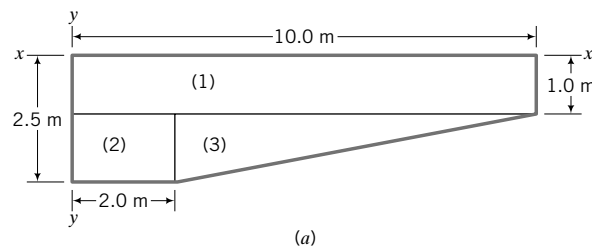


FIGURE E7.14a, b

Strategy You need to locate the centroid of the foundation, which you can find using the given dimensions. The shape of the foundation does not fit neatly into one of the standard shapes (e.g., rectangles or circles) discussed. The convenient method to use for this (odd) shape foundation is Newmark's chart.

Solution 7.14

Step 1: Find the centroid.

Divide the loaded area into a number of regular shapes. In this example, we have three. Take the sum of moments of the areas about $y-y$ (Figure E7.14a) and divide by the sum of the areas to get \bar{x} . Take moments about $x-x$ (Figure E7.14a) to get \bar{y} .

$$\bar{x} = \frac{(1.0 \times 10.0 \times 5.0) + (1.5 \times 2.0 \times 1.0) + \left[\frac{1}{2} \times 8.0 \times 1.5 \times \left(2 + \frac{1}{3} \times 8.0 \right) \right]}{(1.0 \times 10.0) + (1.5 \times 2.0) + \frac{1}{2} \times 8.0 \times 1.5} = \frac{81}{19} = 4.26 \text{ m}$$

$$\bar{y} = \frac{(1 \times 10 \times 0.5) + (1.5 \times 2 \times 1.75) + \left[\frac{1}{2} \times 8.0 \times 1.5 \times \left(1.0 + \frac{1.5}{3} \right) \right]}{(1.0 \times 10.0) + (1.5 \times 2.0) + \frac{1}{2} \times 8.0 \times 1.5} = \frac{19.25}{19} \approx 1 \text{ m}$$

Step 2: Scale and plot the foundation on a Newmark's chart.

The scale on the chart is set equal to the depth. The centroid is located at the center of the chart and the foundation is scaled using the depth scale (Figure E7.14b).

Step 3: Count the number of segments covered by the foundation.

$$N_s = 61$$

Step 4: Calculate the vertical stress increase.

$$\Delta\sigma_z = q_s I_N N_s = 200 \times 0.005 \times 61 = 61 \text{ kPa}$$

7.11.9 Embankment Loads

Loads from an embankment can be considered as a combination of a rectangle and two triangular strip loads. The vertical stress increase due to an embankment load is shown in Figure 7.27. The applied vertical, surface stress is the height of the embankment multiplied by the unit weight of the embankment (fill) material.

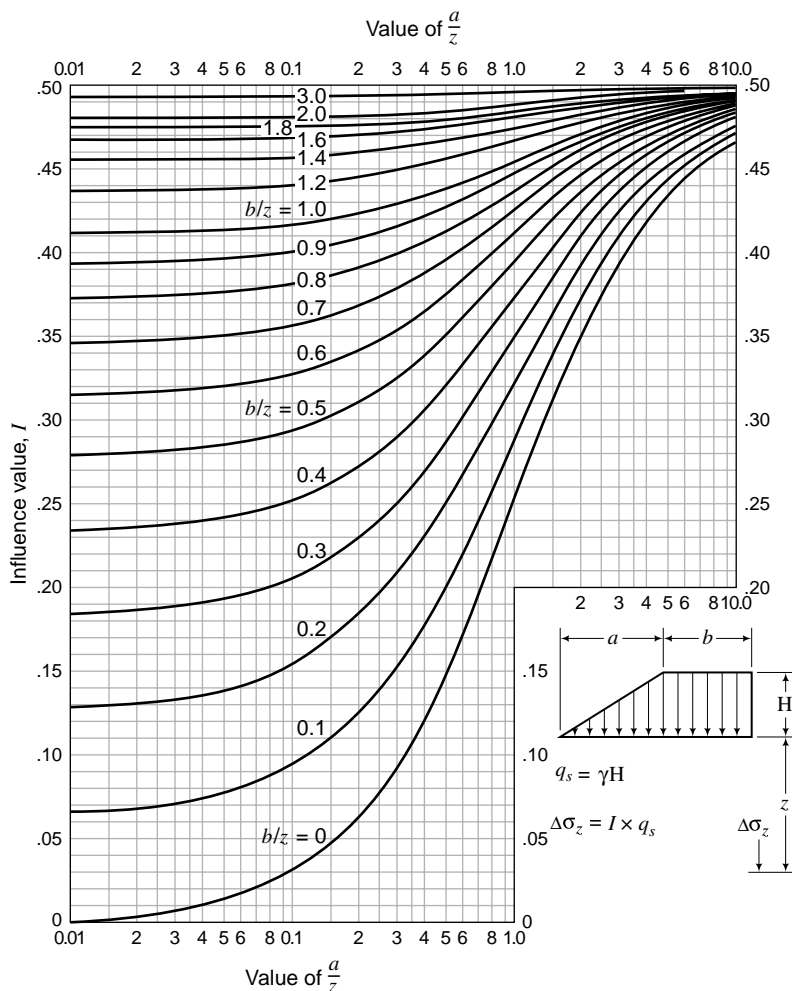


FIGURE 7.27
Vertical stress increase
due to an embankment.

7.11.10 Infinite Loads

Uniform loads of large lateral extent such as fills and surcharges are assumed to be transferred to the soil as a uniformly distributed vertical stress throughout the depth. For example, if a fill of unit weight 15 kN/m³ and height 2 m is placed on the surface of a soil, then the vertical stress at any depth below the surface is $2 \times 15 = 30$ kPa.

THE ESSENTIAL POINTS ARE:

1. The increases in stresses below a surface load are found by assuming the soil is an elastic, semi-infinite mass.
2. Various equations are available for the increases in stresses from surface loading.
3. The stress increase at any depth depends on the shape and distribution of the surface load.
4. A stress applied at the surface of a soil mass by a loaded area decreases with depth and lateral distance away from the center of the loaded area.
5. The vertical stress increases are generally less than 10% of the surface stress when the depth-to-width ratio is greater than 2.

7.12 SUMMARY

Elastic theory provides a simple, first approximation to calculate the deformation of soils at small strains. You are cautioned that the elastic theory cannot adequately describe the behavior of most soils, and more involved theories are required. The most important principle in soil mechanics is the principle of effective stress. Soil deformation is due to effective, not total, stresses. Applied surface stresses are distributed such that their magnitudes decrease with depth and distance away from their points of application.

Self-Assessment



Access Chapter 7 at <http://www.wiley.com/college/budhu> to take the end-of-chapter quiz to test your understanding of this chapter.

Practical Examples

EXAMPLE 7.15 Vertical Stress Increase Due to an Electric Power Transmission Pole

A Douglas fir electric power transmission pole is 12 m above ground level and embedded 2 m into the ground. The butt diameter is 450 mm and the tip diameter (the top of the pole) is 320 mm. The weight of the pole, cross arms, and wires is 33 kN. Assuming the pole transmits the load as a point load, plot the vertical stress increase with depth up to a depth where the stress increase is less than 5 kPa along the center of the pole.

Strategy This is a straightforward application of Boussinesq's equation.

Solution 7.15

Step 1: Calculate vertical stress increase.

At center of pole, $r = 0, r/z = 0$.

$$\text{Equation (7.58): } I = \frac{3}{2\pi} = 0.477$$

The vertical stress increase with depth is shown in the table below.

z (m)	r/z	I	$\Delta\sigma_z$ Equation (7.57) (kPa)
0.1	0.00	0.477	1577.6
0.2	0.00	0.477	393.9
0.5	0.00	0.477	63.0
1	0.00	0.477	17.8
2	0.00	0.477	3.9

Step 2: Plot the vertical stress distribution with depth.

See Figure E7.15.

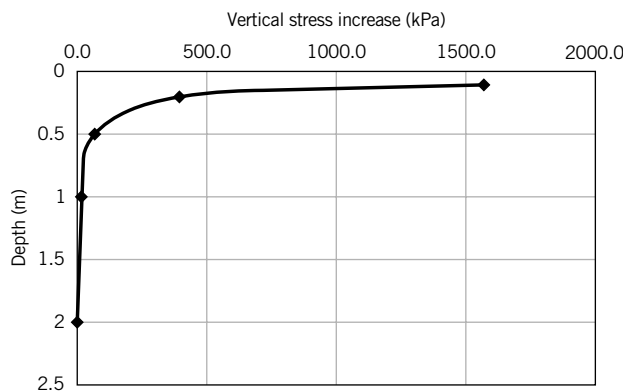


FIGURE E7.15

EXAMPLE 7.16 Height of Embankment to Obtain a Desired Vertical Stress Increase

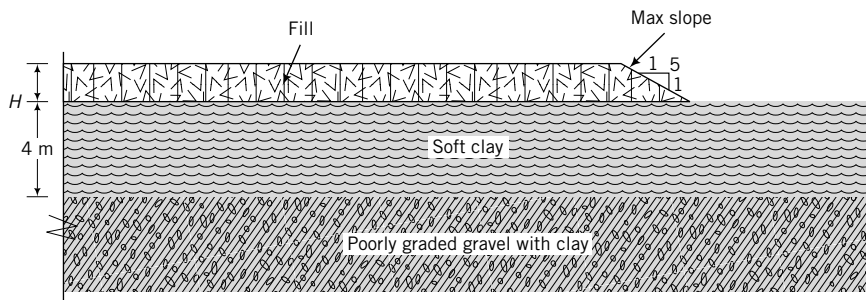
A route for a proposed highway passes through a 2-km stretch of soft clay (ASTM-CS: CH) approximately 4 m thick underlain by poorly graded gravel with clay (ASTM-CS: GP-GC). The geotechnical engineer estimated the settlement (Chapter 9) of the soft clay due to the pavement and traffic loads and found that it is intolerable. One solution is to preload the soft clay by constructing a temporary embankment in stages. Each loading stage will remain on the soft clay for about 6 months to allow the porewater to drain and to cause the clay to settle. The loading must be of such a magnitude that the soft clay would not fail. The estimated maximum vertical stress increase at the center of the soil clay layer along a vertical line through the center of the embankment for the first stage of the loading is 20 kPa. Calculate the height of embankment required if the pavement width is 8 m and the embankment slope cannot exceed 1 (V): 1.5 (H). The unit weight of the fill is 16 kN/m³.

Strategy The solution of this type of problem may require iteration. The constraints on the problem are the maximum vertical stress increase and the slope of the embankment. Since you are given the maximum vertical stress increase, you need to find a (Figure 7.27) and use the maximum slope of the embankment to find H .

Solution 7.16

Step 1: Make a sketch of the problem.

See Figure E7.16.

**FIGURE E7.16**

Step 2: Calculate $\frac{b}{z}$ ratio.

$$\frac{b}{z} = \frac{4}{2} = 2; \frac{a}{z}$$
 ratio has to be determined.

Step 3: Determine I required.

From Figure 7.27, $I = 0.48$ for $\frac{b}{z} = 2$ and $\frac{a}{z} = 0.001$ to 2 .

Step 4: Determine a/z ratio required.

Since Figure 7.27 only gives the vertical stress increase for one half the embankment load, you have to divide the desired vertical stress increase by 2.

$$\therefore \frac{\Delta\sigma_z}{2} = q_s I = \gamma H I = 16 H I$$

$$I = \frac{20}{2 \times 16 H} = \frac{1}{1.6 H}$$

Since the minimum value of a is $1.5H$, then

$$I = \frac{1}{1.6 H} = \frac{1}{1.6 \frac{a}{1.5}} = \frac{0.94}{a}$$

$$a = \frac{0.94}{I} = \frac{0.94}{0.48} = 1.96 \text{ m}; \frac{a}{z} = \frac{1.96}{2} = 0.88, \text{ which lies within the range } 0.001 \text{ to } 2.$$

Therefore, $I = 0.48$.

If $\frac{a}{z}$ were not within the range 0.001 to 2, then you would have to do iterations by choosing a value of I for $\frac{b}{z} = 2$ and then check that $\frac{a}{z}$ corresponds to that value of I .

Step 5: Determine H required.

$$H = \frac{a}{1.5} = \frac{1.96}{1.5} = 1.3 \text{ m}$$

EXAMPLE 7.17 Vertical Stress Increase Due to a Foundation

A building foundation of width 10 m and length 40 m transmits a load of 80 MN to a deep deposit of stiff saturated clay (Figure E7.17a). The elastic modulus of the clay varies with depth (Figure E7.17b) and $v = 0.32$. Estimate the elastic settlement of the clay under the center of the foundation.

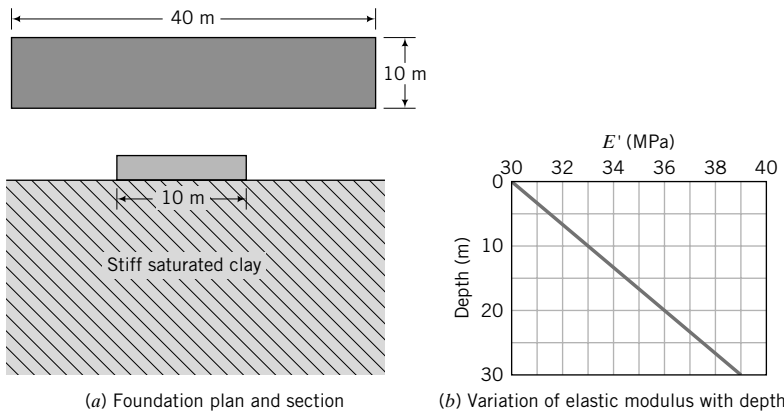


FIGURE E7.17

Strategy The major decision in this problem is what depth to use to determine an appropriate elastic modulus. One option is to use an average elastic modulus over a depth of $2B$ or $3B$. Beyond a depth of about $2B$, the vertical stress increase is less than 10%. Let us use a depth of $3B$.

Solution 7.17

Step 1: Find the applied vertical surface stress.

$$q_s = \frac{Q}{A} = \frac{80 \times 10^3}{10 \times 40} = 200 \text{ kPa}$$

Step 2: Determine the elastic modulus.

Assume an effective depth of $3B = 3 \times 10 = 30 \text{ m}$.
The average value of E is 34.5 MPa.

Step 3: Calculate the vertical settlement.

$$\text{Use Equation(7.90): } \Delta z = \frac{q_s B (1 - \nu^2)}{E} I_s$$

$$\frac{L}{B} = \frac{40}{10} = 4, \quad I_s = 0.62 \ln \left(\frac{L}{B} \right) + 1.12 = 0.62 \ln (4) + 1.12 = 1.98$$

$$\Delta z = \frac{200 \times 5 \times (1 - 0.32^2)}{34.5 \times 10^6} 1.98 = 51.5 \times 10^{-6} \text{ m} = 51.5 \times 10^{-3} \text{ mm}$$

EXERCISES

Theory

- 7.1** An elastic soil is confined laterally and is axially compressed under drained conditions. In soil mechanics, the loading imposed on the soil is called K_o compression or consolidation. Show that under the K_o condition,

$$\frac{\sigma'_x}{\sigma'_z} = \frac{\nu'}{1 - \nu'}$$

where ν' is Poisson's ratio for drained condition.

- 7.2** Show that if an elastic, cylindrical soil is confined in the lateral directions, the constrained elastic modulus is

$$E_c = \frac{E'(1 - \nu')}{(1 + \nu')(1 - 2\nu')}$$

where E' = Young's modulus and ν' is Poisson's ratio for drained condition.

- 7.3** The increase in porewater pressure in a saturated soil is given by $\Delta u = \Delta\sigma_3 + A(\Delta\sigma_1 - \Delta\sigma_3)$. Show that if the

soil is a linear, isotropic, elastic material, $A = \frac{1}{3}$ for the axisymmetric condition.

Problem Solving

Stresses and strains

- 7.4** A cylindrical soil, 75 mm in diameter and 150 mm long, is axially compressed. The length decreases to 147 mm and the radius increases by 0.3 mm. Calculate:
- The axial and radial strains
 - The volumetric strains
 - Poisson's ratio
- 7.5** A cylindrical soil, 75 mm in diameter and 150 mm long, is radially compressed. The length increases to 153 mm and the radius decreases to 37.2 mm. Calculate:
- The axial and radial strains
 - The volumetric strains
- 7.6** A soil, 100 mm \times 150 mm \times 20 mm high, is subjected to simple shear deformation (see Figure 7.3). The normal force in the Z direction is 1 kN and the shear force is 0.5 kN. The displacements at the top of the soil in the X and Z directions are $\Delta x = 1$ mm and $\Delta z = 1$ mm. Calculate:
- The shear and normal stresses
 - The axial and shear strains

Elastic deformation

- 7.7** A long embankment is located on a soil profile consisting of 4 m of medium clay followed by 8 m of medium-to-dense sand on top of bedrock. A vertical settlement of 5 mm at the center of the embankment was measured during construction. Assuming all the settlement is elastic and occurs in the medium clay, determine the average stresses imposed on the medium clay under the center of the embankment using the elastic equations. The elastic parameters are $E = 15$ MPa and $\nu = 0.3$. (Hint: Assume the lateral strain is zero.)
- 7.8** An element of soil (sand) behind a retaining wall is subjected to an increase in vertical stress of 5 kPa and a decrease in lateral stress of 25 kPa. Determine the change in vertical and lateral strains, assuming the soil is a linearly elastic material with $E = 20$ MPa and $\nu = 0.3$.

Stress state using Mohr's circle

- 7.9** A cylindrical specimen of soil is compressed by an axial principal stress of 500 kPa and a radial principal stress of 200 kPa. Plot Mohr's circle of stress and determine (a) the maximum shear stress and (b) the normal and shear stresses on a plane inclined at 30° counterclockwise from the horizontal.
- 7.10** A soil specimen (100 mm \times 100 mm \times 100 mm) is subjected to the forces shown in Figure P7.10. Determine

mine (a) the magnitude of the principal stresses, (b) the orientation of the principal stress plane to the horizontal, (c) the maximum shear stress, and (d) the normal and shear stresses on a plane inclined at 20° clockwise to the horizontal.

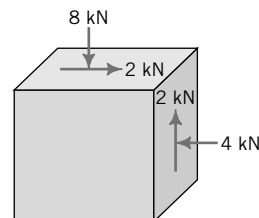


FIGURE P7.10

- 7.11** The initial principal stresses at a certain depth in a clay soil are 100 kPa on the horizontal plane and 50 kPa on the vertical plane. Construction of a surface foundation induces additional stresses consisting of a vertical stress of 45 kPa, a lateral stress of 20 kPa, and a counterclockwise (with respect to the horizontal plane) shear stress of 40 kPa. Plot Mohr's circle (1) for the initial state of the soil and (2) after construction of the foundation. Determine (a) the change in magnitude of the principal stresses, (b) the change in maximum shear stress, and (c) the change in orientation of the principal stress plane resulting from the construction of the foundation.

Effective stress

- 7.12** Plot the distribution of total stress, effective stress, and pore-water pressure with depth for the soil profile shown in Figure P7.12. Neglect capillary action and pore air pressure.

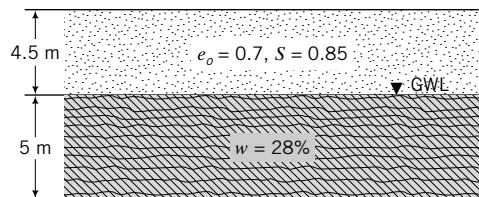
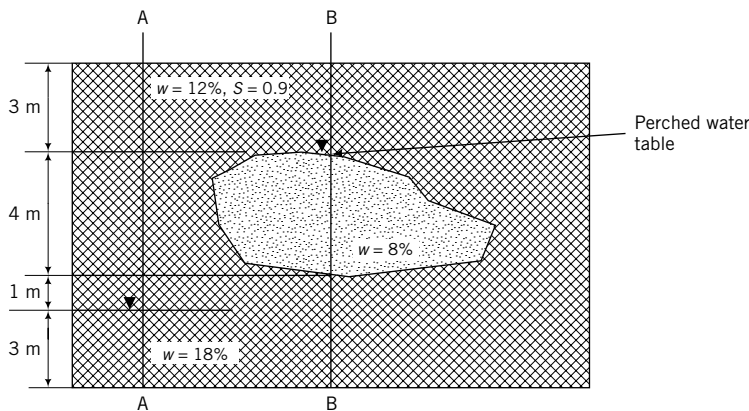


FIGURE P7.12

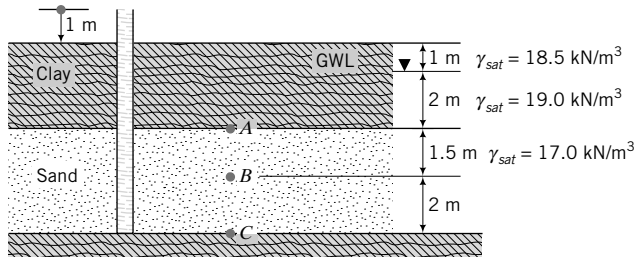
- 7.13** If the groundwater in problem 7.12 were (a) to rise to the surface, (b) to rise 2 m above the surface, and (c) to rapidly decrease from 2 m above the surface to 1 m below its present level, determine and plot the distributions of vertical effective and total stresses and porewater pressure with depth.
- 7.14** At what depth would the vertical effective stress in a deep deposit of clay be 100 kPa, if $e = 1.1$? The groundwater level is at 1 m below ground surface and $S = 95\%$ above the groundwater level. Neglect pore air pressure.
- 7.15** A culvert is to be constructed in a bed of sand ($e = 0.5$) for drainage purposes. The roof of the culvert will be

**FIGURE P7.18**

located 3 m below ground surface. Currently, the ground-water level is at ground surface. But, after installation of the culvert, the groundwater level is expected to drop to 2 m below ground surface. Calculate the change in vertical effective stress on the roof of the culvert after installation. You can assume the sand above the ground-water level is saturated.

- 7.16** A soil profile consists of 10-m-thick fine sand of effective size 0.15 mm above a very thick layer of clay. Groundwater level is at 3 m below the ground surface. (a) Determine the height of capillary rise, assuming that the equivalent capillary tube diameter is 10% of the effective size and the sand surface is similar to smooth glass. (b) Plot the distribution of vertical effective stress and porewater pressure with depth if the void ratio of the sand is 0.6 and the degree of saturation is 90%. Neglect pore air pressure.

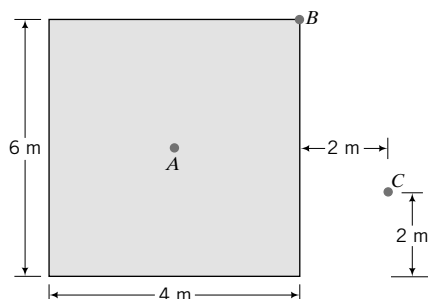
- 7.17** A soil profile consists of a clay layer underlain by a sand layer, as shown in Figure P7.17. If a tube is inserted into the bottom sand layer and the water level rises to 1 m above the ground surface, determine the vertical effective stresses and porewater pressures at *A*, *B*, and *C*. If K_o is 0.5, determine the lateral effective and lateral total stresses at *A*, *B*, and *C*. What is the value of the porewater pressure at *A* to cause the vertical effective stress there to be zero?

**FIGURE P7.17**

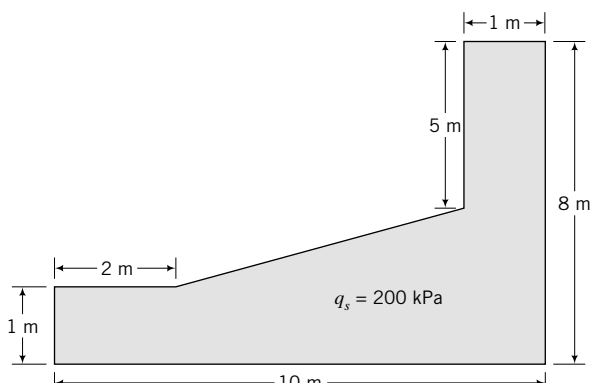
- 7.18** A soil section, as shown in Figure P7.18, has a perched groundwater level. Plot the vertical total and effective stresses and porewater pressures with depth along sections A-A and B-B. Neglect pore air pressure.

Stresses in soil from surface loads

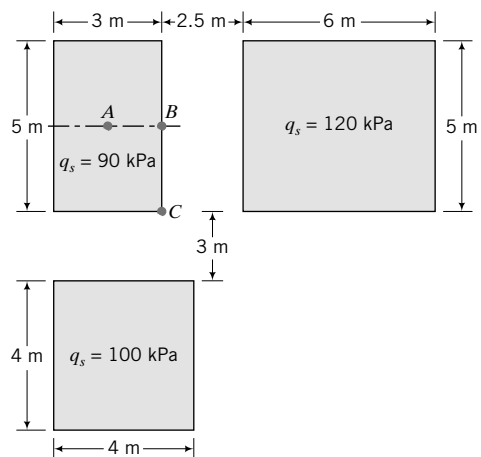
- 7.19** A pole is held vertically on a soil surface by three equally spaced wires tied to the top of the pole. Each wire has a tension of 1 kN and is inclined at 45° to the vertical. Calculate:
- The increase in vertical stress at a depth 1 m below the surface
 - The amount of elastic settlement below the axis of the pole if $E = 40 \text{ MPa}$ and $\nu = 0.45$
- 7.20** A rectangular foundation $4 \text{ m} \times 6 \text{ m}$ (Figure P7.20) transmits a stress of 100 kPa on the surface of a soil deposit. Plot the distribution of increases of vertical stresses with depth under points *A*, *B*, and *C* up to a depth of 20 m. At what depth is the increase in vertical stress below *A* less than 10% of the surface stress?

**FIGURE P7.20**

- 7.21** Determine the increase in vertical stress at a depth of 5 m below the centroid of the foundation shown in Figure P7.21.

**FIGURE P7.21**

- 7.22** Three foundations are located next to each other (Figure P7.22). Determine the stress increases at *A*, *B*, and *C* at a depth of 2 m below the ground surface.

**FIGURE P7.22**

Practical

- 7.23** You are the geotechnical engineer for a proposed office building in a densely clustered city. The office building will be constructed adjacent to an existing office complex. The soil at the site is a deposit of very dense sand with $E = E' = 45 \text{ MPa}$ and $\nu = \nu' = 0.3$. The sand rests on a deep deposit of dense gravel. The existing high-rise complex is founded on a concrete slab, $100 \text{ m} \times 120 \text{ m}$, located at 2 m below ground surface, and transmits a load of 2400 MN to the soil. Your office foundation is $50 \text{ m} \times 80 \text{ m}$ and transmits a load of 1000 MN . You also intend to locate your foundation at 2 m below ground level. The front of your building is aligned with the existing office complex, and the side distance is 0.5 m. The lesser dimension of each building is the frontal dimension. The owners of the existing building are concerned about possible settlement of their building due to your building. You are invited to a meeting with your client,

the owners of the existing building, and their technical staff. You are expected to determine what effects your office building would have on the existing building. You only have one hour to make the preliminary calculations. You are expected to present the estimated increase in stresses and settlement of the existing office complex will due to the construction of your office building. Prepare your analysis and presentation.

- 7.24** A house (plan dimension: $10 \text{ m} \times 15 \text{ m}$) is located on a deep deposit of sand mixed with some clays and silts. The groundwater at the time the house was completed was 0.5 m below the surface. A utility trench, 4 m deep, was later dug on one side along the length of the house. Any water that accumulated in the trench was pumped out so that the trench remained dry. Because of a labor dispute, work on laying the utility in the trench ceased, but the open trench was continuously pumped. Sometime during the dispute, the owners noticed cracking of the walls in the house. Assuming $S = 0.9$ for the soil above the groundwater level and a void ratio of 0.7, write a short, preliminary technical report (not more than a page) to the owner explaining why the cracks developed. The walls of the trench did not move laterally. The hydraulic conductivities of the soil in the vertical and horizontal directions are $0.5 \times 10^{-4} \text{ cm/sec}$ and $2.3 \times 10^{-4} \text{ cm/sec}$, respectively. The calculations should be in an appendix to the report. Neglect pore air pressure.

- 7.25** A farmer requires two steel silos to store wheat. Each silo is 8 m in external diameter and 10 m high. The foundation for each silo is a circular concrete slab thickened at the edge. The total load of each silo filled with wheat is 9552 kN . The soil consists of a 30 m thick deposit of medium clay above a deep deposit of very stiff clay. The farmer desires that the silos be a distance of 2 m apart and hires you to recommend whether this distance is satisfactory. The area is subjected to a gust wind speed of 100 kilometers per hour.

- Plot the distribution of vertical stress increase at the edges and at the center of one of the silos up to a depth of 16 m. Assume the soft clay layer is semi-infinite and the concrete slab is flexible. Use a spreadsheet to tabulate and plot your results.
- Calculate the elastic settlement at the surface of one of the silos at the edges and at the center, assuming $E = 30 \text{ MPa}$ and $\nu = 0.7$.
- Calculate the elastic tilt of the foundation of one of the silos and sketch the deformed shape of the foundation slab.
- Would the tops of the silos touch each other based on the elastic tilt? Show calculations in support of your answer.
- What minimum separation distance would you recommend? Make clear sketches to explain your recommendation to the owner.

- (f) Explain how the wind would alter the stress distribution below the silos. (*Hint:* Use the charts in Appendix B.)
- 7.26** A water tank, 15 m in diameter and 10 m high, is proposed for a site where there is an existing pipeline (Figure P7.26). Plot the distribution of vertical and lateral stress increases imposed by the water tank on the pipeline along one-half the circumference nearest to the tank. The empty tank's weight (dead load) is 350 kN. Assume the water tank is filled to its capacity.

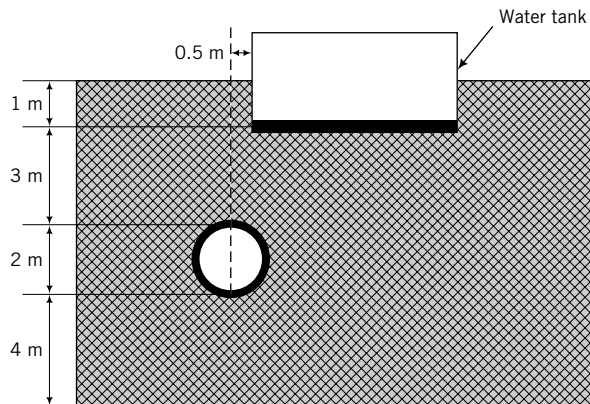


FIGURE P7.26

- 7.27** A developer proposes to construct an apartment building near an existing retaining wall (Figure P7.27). The building of width 12 m and length 300 m (parallel to the retaining wall) will impose a surface stress of 150 kPa. In the preliminary design, the long edge of the building is located 1 m from the wall. Assume the building load can be treated as a strip load.

- (a) Plot the distribution of the lateral force increase with depth up to a depth of 4 m.
- (b) What is the maximum value of the lateral force increase, and where does it occur?
- (c) If the embedment depth of the retaining wall is 4 m, calculate the maximum additional moment about the base of the wall (point O in Figure P7.27) from constructing the building.
- (d) What advice would you give to the developer regarding how far the apartment should be located from the existing retaining wall?

- 7.28** A 10-m-thick, water-bearing sand layer (permeable), called an aquifer, is sandwiched between a 6-m clay layer (impermeable) at the top and bedrock (impermeable) at the bottom. The groundwater level is at the ground surface. An open pipe is placed at the top of the sand layer. Water in the pipe rises to a height of 5 m above the groundwater level. The water contents of the clay and sand are 52% and 8%, respectively.
- (a) Does an artesian condition exist? Why?
- (b) Plot the distribution of vertical total and effective stresses, and porewater pressure with depth up to a depth of 10 m.
- (c) If K_o of the clay is 0.5 and K_o of the sand is 0.45, plot the distribution of lateral total and effective stresses.
- (d) An invert (surface of the bottom arc) level of 4 m from the ground surface is proposed for a water pipe 2 m in diameter. Draw the soil profile and locate the water pipe. Explain any issue (justify with calculations) with locating the water pipe at the proposed invert level.

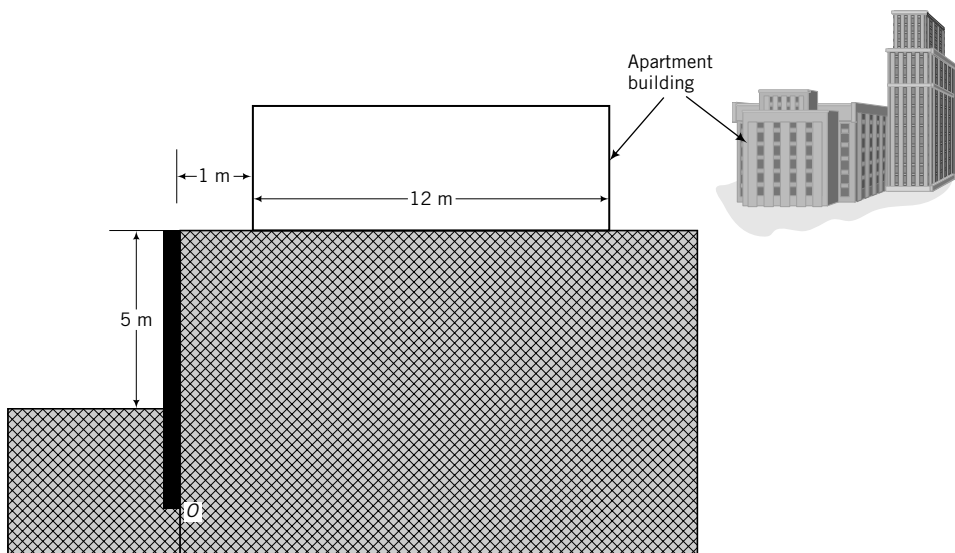


FIGURE P7.27

STRESS PATH

8.0 INTRODUCTION

In this chapter, you will learn about stress paths and their importance in understanding soil behavior under loads. When you complete this chapter, you should be able to:

- Calculate stresses and strains invariants.
- Plot stress paths for common soil loadings.
- Understand the difference between total and effective stress paths.

Importance

The stresses and strains discussed in Chapter 7 are all dependent on the axis system chosen. We have arbitrarily chosen the Cartesian coordinate and the cylindrical coordinate systems. We could, however, define a set of stresses and strains that are independent of the axis system. Such a system, which we will discuss in this chapter, will allow us to use generalized stress and strain parameters to analyze and interpret soil behavior. In particular, we will be able to represent a three-dimensional system of stresses and strains by a two-dimensional system.

We have examined how applied surface stresses are distributed in soils as if soils were linear, isotropic, elastic materials. Different structures will impose different stresses and cause the soil to respond differently. For example, an element of soil under the center of an oil tank will experience a continuous increase or decrease in vertical stress while the tank is being filled or emptied. However, the soil near a retaining earth structure will suffer a reduction in lateral stress if the wall moves out. These different loading conditions would cause the soil to respond differently. Therefore, we need to trace the history of stress increases/decreases in soils to evaluate possible soil responses, and to conduct tests that replicate the loading history of the in situ soil. Figure 8.1 shows an excavation near a high-rise building. The



FIGURE 8.1 An excavation near a high-rise building. The applied loading history of soil elements at the same depth at the edge of the excavation and at, say, the center of the building will be different.

applied loading history of soil elements at the same depth at the edge of the excavation and at, say, the center of the building is different, and the soil will respond differently.

8.1 DEFINITIONS OF KEY TERMS

Mean stress, p , is the average stress on a body or the average of the orthogonal stresses in three dimensions.

Deviatoric stress, q , is the shear or distortional stress or stress difference on a body.

Stress path is a graphical representation of the locus of stresses on a body.

Isotropic means the same material properties in all directions and also the same loading in all directions.

8.2 QUESTIONS TO GUIDE YOUR READING

1. What are mean and deviatoric stresses?
2. What is a stress path?
3. What is the significance of stress paths in practical problems?

8.3 STRESS AND STRAIN INVARIANTS

Stress and strain invariants are measures that are independent of the axis system. We will define stress invariants that provide measures of (1) mean stress and (2) deviatoric or distortional or shear stress, and strain invariants that provide measures of (1) volumetric strains and (2) deviatoric or distortional or shear strains.

8.3.1 Mean Stress

$$p = \frac{\sigma_1 + \sigma_2 + \sigma_3}{3} = \frac{\sigma_x + \sigma_y + \sigma_z}{3} \quad (8.1)$$

On a graph with orthogonal principal stress axes $\sigma_1, \sigma_2, \sigma_3$, the mean stress is the space diagonal (Figure 8.2). Mean stress causes volume changes.

8.3.2 Deviatoric or Shear Stress

$$q = \frac{1}{\sqrt{2}}[(\sigma_1 - \sigma_2)^2 + (\sigma_2 - \sigma_3)^2 + (\sigma_3 - \sigma_1)^2]^{1/2} \quad (8.2)$$

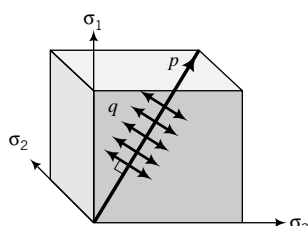


FIGURE 8.2 Mean and deviatoric stresses.

A line normal to the mean stress, as illustrated in Figure 8.2, represents the deviatoric stress. Deviatoric stress causes distortions or shearing of a soil mass. Equation (8.2) can be written in terms of normal and shear stresses as

$$q = \frac{1}{\sqrt{2}} \{ [(\sigma_{xx} - \sigma_{yy})^2 + (\sigma_{yy} - \sigma_{zz})^2 + (\sigma_{zz} - \sigma_{xx})^2] + 6\tau_{xy}^2 + 6\tau_{yz}^2 + 6\tau_{zx}^2 \}^{1/2} \quad (8.3)$$

8.3.3 Volumetric Strain

$$\varepsilon_p = \varepsilon_1 + \varepsilon_2 + \varepsilon_3 = \varepsilon_x + \varepsilon_y + \varepsilon_z \quad (8.4)$$

8.3.4 Deviatoric or Distortional or Shear Strain

$$\varepsilon_q = \frac{\sqrt{2}}{3} [(\varepsilon_1 - \varepsilon_2)^2 + (\varepsilon_2 - \varepsilon_3)^2 + (\varepsilon_3 - \varepsilon_1)^2]^{1/2} \quad (8.5)$$

8.3.5 Axisymmetric Condition, $\sigma'_2 = \sigma'_3$ or $\sigma_2 = \sigma_3$; $\varepsilon_2 = \varepsilon_3$

$$p' = \frac{\sigma'_1 + 2\sigma'_3}{3} \quad \text{and} \quad p = \frac{\sigma_1 + 2\sigma_3}{3} \quad (8.6)$$

$$p' = p - u \quad (8.7)$$

$$q = \sigma_1 - \sigma_3; \quad q' = \sigma'_1 - \sigma'_3 = (\sigma_1 - \Delta u) - (\sigma_3 - \Delta u) = \sigma_1 - \sigma_3 \quad (8.8)$$

Therefore, $q = q'$; shear is unaffected by porewater pressures.

$$\varepsilon_p = \varepsilon_1 + 2\varepsilon_3 \quad (8.9)$$

$$\varepsilon_q = \frac{2}{3}(\varepsilon_1 - \varepsilon_3) \quad (8.10)$$

8.3.6 Plane Strain, $\varepsilon_2 = 0$

$$p' = \frac{\sigma'_1 + \sigma'_2 + \sigma'_3}{3} \quad \text{and} \quad p = \frac{\sigma_1 + \sigma_2 + \sigma_3}{3} \quad (8.11)$$

$$p' = p - u \quad (8.12)$$

$$q' = q = \frac{1}{\sqrt{2}} [(\sigma'_1 - \sigma'_2)^2 + (\sigma'_2 - \sigma'_3)^2 + (\sigma'_3 - \sigma'_1)^2]^{1/2} \quad (8.13)$$

or

$$q = q' = \frac{1}{\sqrt{2}} [(\sigma_1 - \sigma_3)^2 + (\sigma_2 - \sigma_3)^2 + (\sigma_3 - \sigma_1)^2]^{1/2} \quad (8.14)$$

$$\varepsilon_p = \varepsilon_1 + \varepsilon_3 \quad (8.15)$$

$$\varepsilon_q = \frac{2}{3}(\varepsilon_1^2 + \varepsilon_3^2 - \varepsilon_1 \varepsilon_3)^{1/2} \quad (8.16)$$

8.3.7 Hooke's Law Using Stress and Strain Invariants

The stress and strain invariants for an elastic material are related as follows:

$$\varepsilon_p^e = \frac{1}{K'} p' \quad (8.17)$$

where

$$K' = \frac{p'}{\varepsilon_p^e} = \frac{E'}{3(1 - 2\nu')} \quad (8.18)$$

is the effective bulk modulus and the superscript *e* denotes elastic.

$$\varepsilon_q^e = \frac{1}{3G} q \quad (8.19)$$

where

$$G = G' = \frac{E'}{2(1 + \nu')} \quad (8.20)$$

is called the shear modulus. Hooke's law in terms of the stress and strain invariants is

$$\begin{Bmatrix} p' \\ q \end{Bmatrix} = \begin{bmatrix} K' & 0 \\ 0 & 3G \end{bmatrix} \begin{Bmatrix} \varepsilon_p^e \\ \varepsilon_q^e \end{Bmatrix} \quad (8.21)$$

Equation (8.21) reveals that for a linear, isotropic, elastic material, shear stresses do not cause volume changes and mean effective stresses do not cause shear deformation.

We can generate a generalized Poisson's ratio by eliminating E' from Equations (8.18) and (8.20), as follows:

$$\text{Equation (8.18): } E' = 3K'(1 - 2\nu')$$

$$\text{Equation (8.20): } E' = 2G(1 + \nu')$$

$$\therefore \frac{3K'(1 - 2\nu')}{2G(1 + \nu')} = 1$$

and

$$\nu' = \frac{3K' - 2G}{2G + 6K'} \quad (8.22)$$

THE ESSENTIAL POINTS ARE:

1. Stress and strain invariants are independent of the chosen axis system.
2. Stress and strain invariants are convenient measures to determine the effects of a general state of stresses and strains on soils.
3. Mean stress represents the average stress on a soil, while deviatoric stress represents the average shear or distortional stress.

EXAMPLE 8.1 Calculating Stress and Strain Invariants for Axisymmetric Loading

A cylindrical sample of soil 50 mm in diameter and 100 mm long is subjected to an axial effective principal stress of 400 kPa and a radial effective principal stress of 100 kPa. The axial and radial displacements are 0.5 mm and -0.04 mm, respectively. Assuming the soil is an isotropic, elastic material, calculate (a) the mean and deviatoric stresses, (b) the volumetric and shear (distortional) strains, and (c) the shear, bulk, and elastic moduli.

Strategy This is a straightforward problem. You only need to apply the equations given in the previous section. The negative sign for the radial displacement indicates an expansion.

Solution 8.1

Step 1: Calculate the mean and deviatoric stresses.

$$\sigma'_1 = \sigma'_z = 400 \text{ kPa}, \quad \sigma'_3 = \sigma'_r = 100 \text{ kPa}$$

(a)

$$p' = \frac{\sigma'_z + 2\sigma'_r}{3} = \frac{400 + 2 \times 100}{3} = 200 \text{ kPa}$$

$$q = q' = \sigma'_z - \sigma'_r = 400 - 100 = 300 \text{ kPa}$$

Step 2: Calculate the volumetric and shear strains.

$$\Delta z = 0.5 \text{ mm}, \quad \Delta r = -0.04 \text{ mm}, \quad r = 50/2 = 25 \text{ mm}, \quad L = 100 \text{ mm}$$

(b)

$$\varepsilon_z = \varepsilon_1 = \frac{\Delta z}{L} = \frac{0.5}{100} = 0.005$$

$$\varepsilon_r = \varepsilon_3 = \frac{\Delta r}{r} = \frac{-0.04}{25} = -0.0016$$

$$\varepsilon_p^e = \varepsilon_z + 2\varepsilon_r = 0.005 - 2 \times 0.0016 = 0.0018 = 0.18\%$$

$$\varepsilon_q^e = \frac{2}{3}(\varepsilon_z - \varepsilon_r) = \frac{2}{3}(0.005 + 0.0016) = 0.0044 = 0.44\%$$

Step 3: Calculate the moduli.

(c)

$$K' = \frac{p'}{\varepsilon_p^e} = \frac{200}{0.0018} = 111,111 \text{ kPa}$$

$$G = \frac{q}{3\varepsilon_q^e} = \frac{300}{3 \times 0.0044} = 22,727 \text{ kPa}$$

but

$$G = \frac{E'}{2(1 + \nu')} \quad \text{and} \quad \nu' = \frac{3K' - 2G}{2G + 6K'} = \frac{3 \times 111,111 - 2 \times 22,727}{2 \times 22,727 + 6 \times 111,111} = 0.4$$

$$\therefore E' = 2G(1 + \nu') = 2 \times 22,727(1 + 0.4) = 63,636 \text{ kPa}$$

What's next . . . In the next section, a method of keeping track of the loading history of a soil is described.

8.4 STRESS PATHS

8.4.1 Basic Concept

Consider two marbles representing two particles of a coarse-grained soil. Let us fix one marble in a hemispherical hole and stack the other on top of it (Figure 8.3a). We are constructing a one-dimensional system in which relative displacement of the two marbles will occur at the contact. Let us incrementally apply a vertical, concentric force, F_z , on the top marble. We will call this loading A. The forces at the contact are equal to the applied loads, and the marbles are forced together vertically. No relative displacement between the marbles occurs. For the system to become unstable or to fail, the applied forces must crush the marbles. We can make a plot of our loading by arbitrarily choosing an axis system. Let us choose a Cartesian system, with the X axis representing the horizontal forces and the Z axis representing the vertical forces. We can represent loading A by a line OA , as shown in Figure 8.3c. The line OA is called a load path or a force path.

Let us now apply the same force at an angle θ to the X axis in the ZX plane (Figure 8.3b) and call this loading B. There are now two components of force. One component is $F_x = F \cos \theta$ and the other is $F_z = F \sin \theta$. If the frictional resistance at the contacts of the two marbles is less than the horizontal force, the top marble will slide relative to the bottom. You should recall from your mechanics or physics course that the frictional resistance is μF_z (Coulomb's law), where μ is the coefficient of friction at the contact between the two marbles. Our one-dimensional system now has two modes of instability or failure—one due to relative sliding and the other due to crushing of the marbles. The force path for loading B is represented by OB in Figure 8.3c. The essential point or principle is that the response, stability, and failure of the system depend on the force path.

Soils, of course, are not marbles, but the underlying principle is the same. The soil fabric can be thought of as a space frame, with the soil particles representing the members of the frame and the particle

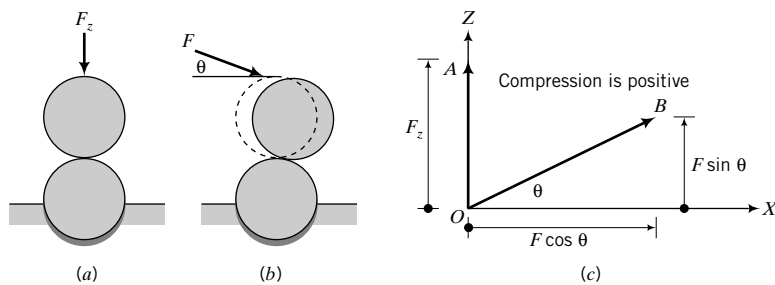


FIGURE 8.3 Effects of force paths on a one-dimensional system of marbles.

contacts representing the joints. The response, stability, and failure of the soil fabric or the space frame depend on the stress path.

Stress paths are presented in a plot showing the relationship between stress parameters and provide a convenient way to allow a geotechnical engineer to study the changes in stresses in a soil caused by loading conditions. We can, for example, plot a two-dimensional graph of σ_1 versus σ_3 or σ_2 , which will give us a relationship between these stress parameters. However, the stress invariants, being independent of the axis system, are more convenient to use.

8.4.2 Plotting Stress Paths Using Stress Invariants

We will explore stress paths for a range of loading conditions. We will use a cylindrical soil sample for illustrative purposes and subject it to several loading conditions. Let us apply equal increments of axial and radial stresses ($\Delta\sigma_z = \Delta\sigma_r = \Delta\sigma$) to an initially stress-free sample, as illustrated in the inset figure labeled “1” in Figure 8.4. Since we are not applying any shearing stresses on the horizontal and vertical boundaries, the axial and radial stresses are principal stresses; that is, $\Delta\sigma_z = \Delta\sigma_1$ and $\Delta\sigma_r = \Delta\sigma_3$.

The loading condition we are applying is called isotropic compression; that is, the stresses in all directions are equal ($\Delta\sigma_1 = \Delta\sigma_2 = \Delta\sigma_3$). We will call this loading condition loading 1. It is often convenient to work with increments of stresses in determining stress paths. Consequently, we are going to use the incremental form of the stress invariants. The stress invariants for isotropic compression are

$$\Delta p_1 = \frac{\Delta\sigma_1 + 2\Delta\sigma_3}{3} = \frac{\Delta\sigma_1 + 2\Delta\sigma_1}{3} = \Delta\sigma_1$$

$$\Delta q_1 = \Delta\sigma_1 - \Delta\sigma_3 = \Delta\sigma_1 - \Delta\sigma_1 = 0$$

The subscript 1 on p and q denotes loading 1.

Let us now prepare a graph with axes p (abscissa) and q (ordinate), as depicted in Figure 8.4. We will call this graph the p - q plot. The initial stresses on the soil sample are zero; that is, $p_o = 0$ and $q_o = 0$. The stresses at the end of loading 1 are

$$p_1 = p_o + \Delta p_1 = 0 + \Delta\sigma_1 = \Delta\sigma_1$$

$$q_1 = q_o + \Delta q_1 = 0 + 0 = 0$$

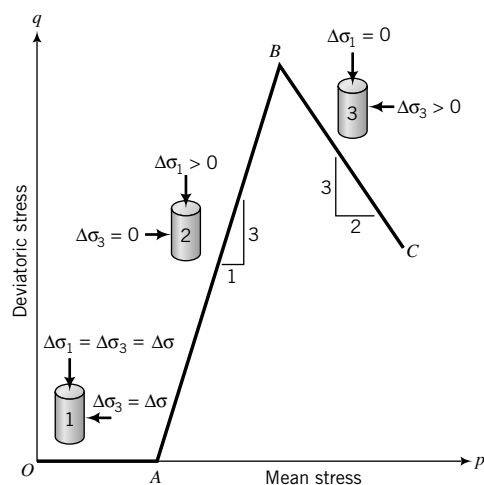


FIGURE 8.4
Stress paths.

and are shown as coordinate A in Figure 8.4. The line OA is called the stress path for isotropic compression. The slope of OA is

$$\frac{\Delta q_1}{\Delta p_1} = 0$$

Let us now apply loading 2 by keeping σ_3 constant, that is, $\Delta\sigma_3 = 0$, but continue to increase σ_1 , that is, $\Delta\sigma_1 > 0$ (insert figure labeled “2” in Figure 8.4). Increases in the stress invariants for loading 2 are

$$\Delta p_2 = \frac{\Delta\sigma_1 + 2 \times 0}{3} = \frac{\Delta\sigma_1}{3}$$

$$\Delta q_2 = \Delta\sigma_1 - 0 = \Delta\sigma_1$$

and the stress invariants at the end of loading 2 are

$$p_2 = p_1 + \Delta p_2 = \Delta\sigma_1 + \frac{\Delta\sigma_1}{3} = \frac{4}{3}\Delta\sigma_1$$

$$q_2 = q_1 + \Delta q_2 = 0 + \Delta\sigma_1 = \Delta\sigma_1$$

Point B in Figure 8.4 represents (q_2, p_2) , and the line AB is the stress path for loading 2. The slope of AB is

$$\frac{\Delta q_2}{\Delta p_2} = \frac{\Delta\sigma_1}{(\Delta\sigma_1/3)} = 3$$

Let us make another change to the loading conditions. We will now keep σ_1 constant ($\Delta\sigma_1 = 0$) and then increase σ_3 ($\Delta\sigma_3 > 0$), as illustrated by the inset figure labeled “3” in Figure 8.4. The increases in stress invariants are

$$\Delta p_3 = \frac{0 + 2\Delta\sigma_3}{3} = \frac{2\Delta\sigma_3}{3}$$

$$\Delta q_3 = 0 - \Delta\sigma_3 = -\Delta\sigma_3$$

The stress invariants at the end of loading 3 are

$$p_3 = p_2 + \Delta p_3 = \frac{4}{3}\Delta\sigma_1 + \frac{2}{3}\Delta\sigma_3$$

$$q_3 = q_2 + \Delta q_3 = \Delta\sigma_1 - \Delta\sigma_3$$

The stress path for loading 3 is shown as BC in Figure 8.4. The slope of BC is

$$\frac{\Delta q_3}{\Delta p_3} = \frac{-\Delta\sigma_3}{\frac{2}{3}\Delta\sigma_3} = -\frac{3}{2}$$

You should note that q decreases but p increases for stress path BC .

So far, we have not discussed whether the soil was allowed to drain or not. You will recall that the soil solids and the porewater (Section 7.9) must carry the applied increase in stresses in a saturated

soil. If the soil porewater is allowed to drain from the soil sample, the increase in stress carried by the porewater, called excess porewater pressure (Δu), will continuously decrease to zero and the soil solids will have to support all of the increase in applied stresses. We will assume that during loading 1, the excess porewater was allowed to drain; this is called the drained condition in geotechnical engineering. The type of loading imposed by loading 1 is called isotropic consolidation. In Chapter 9, we will discuss isotropic consolidation further. Since the excess porewater pressure (Δu_1) dissipates as water drains from the soil, the mean effective stress at the end of each increment of loading 1 is equal to the mean total stress; that is,

$$\Delta p'_1 = \Delta p_1 - \Delta u_1 = \Delta p_1 - 0 = \Delta p$$

The effective stress path (ESP) and the total stress path (TSP) are the same and represented by OA in Figure 8.5. You should note that we have used dual labels, p' , p , for the horizontal axis in Figure 8.5. This dual labeling allows us to use one plot to represent both the effective and total stress paths.

We will assume that for loadings 2 and 3 the excess porewater pressures were prevented from draining out of the soil. In geotechnical engineering, the term *undrained* is used to denote a loading situation in which the excess porewater cannot drain from the soil. The implication is that the volume of our soil sample remains constant. In Chapter 10, we will discuss drained and undrained loading conditions in more detail. For loading 2, the total stress path is AB . In this book, we will represent total stress paths by dashed lines.

If our soil were an isotropic, elastic material, then according to Equation (8.17), written in incremental form,

$$\Delta \varepsilon_p^e = \frac{\Delta p'}{K'} = 0 \quad (8.23)$$

The solution of Equation (8.23) leads to either $\Delta p' = 0$ or $K' = \infty$. There is no reason why K' should be ∞ . The act of preventing the drainage of the excess porewater cannot change the (effective) bulk modulus of the soil solids. Remember the truss analogy we used for effective stresses. The same analogy is applicable here. The only tenable solution is $\Delta p' = 0$. We can also write Equation (8.23) in terms of total stresses; that is,

$$\Delta \varepsilon_p^e = \frac{\Delta p}{K} = 0 \quad (8.24)$$

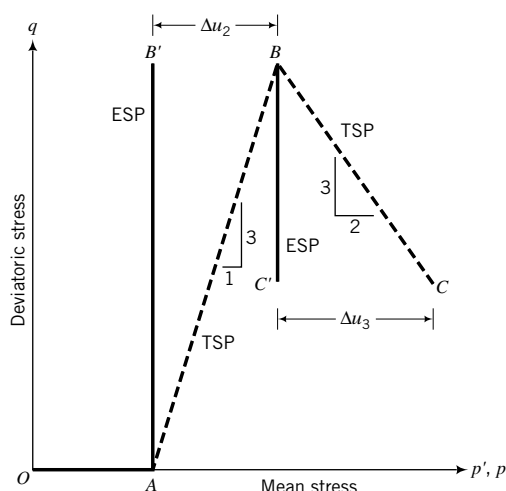


FIGURE 8.5
Total and effective stress paths.

where $K = E_u/3(1 - 2\nu_u)$ and the subscript u denotes undrained condition. In this case, Δp cannot be zero since this is the change in mean total stress from the applied loading. Therefore, the only tenable solution is $K = K_u = \infty$, which leads to $\nu_u = 0.5$. The implications of Equations (8.23) and (8.24) for a linear, isotropic, elastic soil under undrained conditions are:

1. The change in mean effective stress is zero and, consequently, the effective stress path is vertical.
2. The undrained bulk modulus is ∞ and $\nu_u = 0.5$.

The deviatoric stress is unaffected by porewater pressure changes. We can write Equation (8.20) in terms of total stress parameters as

$$G = G_u = \frac{E_u}{2(1 + \nu_u)}$$

Since $G = G_u = G'$, then

$$\frac{E_u}{2(1 + \nu_u)} = \frac{E'}{2(1 + \nu')}$$

and, by substituting $\nu_u = 0.5$, we obtain

$$E_u = \frac{1.5E'}{(1 + \nu')} \quad (8.25)$$

For many soils, $\nu' \approx \frac{1}{3}$ and, as a result, $E_u \approx 1.1E'$; that is, the undrained elastic modulus is about 10% greater than the effective elastic modulus.

The effective stress path for loading 2, assuming our soil sample behaves like an isotropic, elastic material, is represented by AB' (Figure 8.5); the coordinates of B' are

$$\begin{aligned} p'_2 &= p'_1 + \Delta p'_2 = p'_1 + 0 = \Delta\sigma_1 \\ q_2 &= q_1 + \Delta q_2 = 0 + \Delta\sigma_1 = \Delta\sigma_1 \end{aligned}$$

The difference in mean stress between the TSP and the ESP at a fixed value of q is the change in excess porewater pressure. That is, the magnitude of a horizontal line between the TSP and ESP is the change in excess porewater pressure. The maximum change in excess porewater pressure at the end of loading 2 is

$$\Delta u_2 = p_2 - p'_2 = \frac{4}{3}\Delta\sigma_1 - \Delta\sigma_1 = \frac{1}{3}\Delta\sigma_1$$

For loading 3, the ESP for an elastic soil is BC' and the maximum change in excess porewater pressure is denoted by CC' (Figure 8.5).

Soils only behave as elastic materials over a small range of strains, and therefore the condition $\Delta p' = 0$ under undrained loading has only limited application. Once the soil yields, the ESP tends to bend. In Chapter 11, we will discuss how soil yielding affects the ESP.

You can use the above procedure to determine the stress paths for any loading condition. For example, let us confine our soil sample laterally, that is, we are keeping the diameter constant, $\Delta\varepsilon_r = 0$, and incrementally increasing σ_1 under drained conditions (Figure 8.6). The loading condition we are imposing on our sample is called one-dimensional compression.

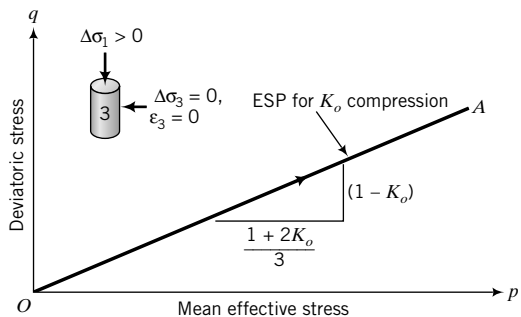


FIGURE 8.6 One-dimensional compression stress path.

The increase in lateral effective stress for an increment of vertical stress $\Delta\sigma_1$ under the drained condition is given by Equation (7.50) as $\Delta\sigma_3 = \Delta\sigma'_3 = K_o\Delta\sigma'$. The stress invariants are

$$\Delta p' = \frac{\Delta\sigma'_1 + 2\Delta\sigma'_3}{3} = \frac{\Delta\sigma'_1 + 2K_o\Delta\sigma'}{3} = \Delta\sigma'_1\left(\frac{1 + 2K_o}{3}\right)$$

$$\Delta q = \Delta q' = \Delta\sigma'_1 - \Delta\sigma'_3 = \Delta\sigma'_1 - K_o\Delta\sigma'_1 = \Delta\sigma'_1(1 - K_o)$$

The slope of the TSP is equal to the slope of the ESP; that is,

$$\frac{\Delta q}{\Delta p'} = \frac{\Delta q}{\Delta p} = \frac{3(1 - K_o)}{1 + 2K_o}$$

The one-dimensional compression stress path is shown in Figure 8.6.

8.4.3 Plotting Stress Paths Using Two-Dimensional Stress Parameters

For two-dimensional stresses, we can use an alternative stress path presentation based on Mohr's circle. We can define

$$t = \frac{\sigma_1 - \sigma_3}{2} = \frac{\sigma'_1 - \sigma'_3}{2} \quad (8.26)$$

$$s = \frac{\sigma_1 + \sigma_3}{2}; \quad s' = \frac{\sigma'_1 + \sigma'_3}{2} \quad (8.27)$$

where t and s are the radius and center of Mohr's circle, respectively, and represent the maximum shear stress and mean stress, respectively. This representation of stress neglects the effects of the intermediate principal stresses and is appropriate for plane stress condition. However, some geotechnical engineers use s' or s and t for convenience, especially for plane strain condition, because we often do not know the value of the intermediate stress mobilized from conventional laboratory and field test equipment. Recall that in a plane strain test the intermediate principal stress is not zero. So, by using s' or s and t space, we are setting the intermediate principal stress to zero or a constant value. The s' or s and t space is best used for plane stress condition (one principal stress equals zero). But plane stress condition rarely, if at all, represents conditions in the field.

You should be aware that the predicted changes in excess porewater pressure, which depend on mean stress p , would be different for stress path representations in (p, q) space and (s, t) space. For example, let us consider the triaxial compression test (axial stress increases and radial stress remains constant) for a linear, isotropic, elastic soil for which the TSP is represented by AB and the ESP is represented by AB' (Figure 8.7a, b). The predicted change in excess porewater pressure for (p, q) space (Figure 8.7a) is

$$\Delta u = \Delta p = \frac{\Delta\sigma_1 + 0 + 0}{3} = \frac{\Delta\sigma_1}{3}; \quad \Delta\sigma_2 = \Delta\sigma_3 = 0$$

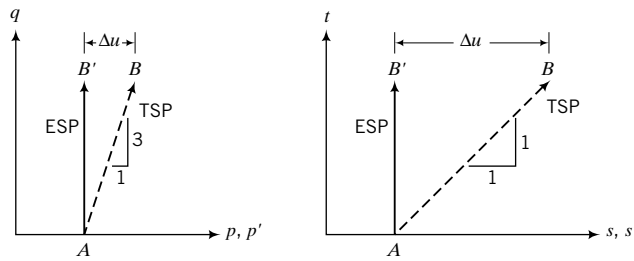


FIGURE 8.7 Total and effective stress path in (p, q) and (s, t) spaces.

For the (s, t) space (Figure 8.7b),

$$\Delta u = \Delta s = \frac{\Delta \sigma_1 + 0}{2} = \frac{\Delta \sigma_1}{2}$$

Thus, interpreting the excess porewater pressure from the stress path in (s, t) space would lead to a 50% greater excess porewater pressure than from the stress path in (p, q) space, because the intermediate stress is not accounted for in the (s, t) space. The slope of the TSP is also different for the two-stress-path space.

For the (p, q) space, the TSP for triaxial compression (TC) is $\frac{\Delta q}{\Delta p} = 3$, while in (s, t) space it is $\frac{\Delta t}{\Delta s} = 1$. In the literature, p or p' and q are sometimes used to denote the stress state characterized by s or s' and t .

THE ESSENTIAL POINTS ARE:

1. A stress path is a graphical representation of stresses in stress space. For convenience, stress paths are plotted as deviatoric stress (q) on the ordinate versus mean effective stress (p') and/or mean total stress (p) on the abscissa.
2. The effective stress path for a linear, elastic soil under the undrained condition is vertical; that is, $\Delta p' = 0$ or $\Delta s' = 0$.
3. The mean stress difference between the total stress path and the effective stress path is the excess porewater pressure.
4. The response, stability, and failure of soils depend on stress paths.

8.4.4 Procedure for Plotting Stress Paths

A summary of the procedure for plotting stress paths is as follows:

1. Determine the loading conditions drained or undrained, or both.
2. Calculate the initial loading values of p'_o , p_o , and q_o .
3. Set up a graph of p' (and p , if you are going to also plot the total stress path) as the abscissa and q as the ordinate. Plot the initial values of (p'_o, q_o) and (p_o, q_o) .
4. Determine the increase in stresses $\Delta \sigma_1$, $\Delta \sigma_2$, and $\Delta \sigma_3$. These stresses can be negative.
5. Calculate the increase in stress invariants $\Delta p'$, Δp , and Δq . These stress invariants can be negative.
6. Calculate the current stress invariants as $p' = p'_o + \Delta p'$, $p = p_o + \Delta p$, and $q = q_o + \Delta q$. The current value of p' cannot be negative, but q can be negative.
7. Plot the current stress invariants (p', q) and (p, q) .
8. Connect the points identifying effective stresses, and do the same for total stresses.

9. Repeat items 4 to 8 for the next loading condition.
10. The excess porewater pressure at a desired level of deviatoric stress is the mean stress difference between the total stress path and the effective stress path. Remember that for a drained loading condition, $\text{ESP} = \text{TSP}$, and for an undrained condition, the ESP for a linear, elastic soil is vertical.

The procedure for plotting stress paths in (s, t) space is similar, except that the appropriate equations are Equations (8.26) and (8.27).

EXAMPLE 8.2 Stress Paths Due to Axisymmetric Loading (Triaxial Test)

Two cylindrical specimens of a soil, A and B, were loaded as follows. Both specimens were isotropically loaded by a stress of 200 kPa under drained conditions. Subsequently, the radial stress applied on specimen A was held constant and the axial stress was incrementally increased to 440 kPa under undrained conditions. The axial stress on specimen B was held constant and the radial stress incrementally reduced to 50 kPa under drained conditions. Plot the total and effective stress paths for each specimen, assuming the soil is a linear, isotropic, elastic material. Calculate the maximum excess porewater pressure in specimen A.

Strategy The loading conditions on both specimens are axisymmetric. The easiest approach is to write the mean stress and deviatoric stress equations in terms of increments and make the necessary substitutions.

Solution 8.4

Step 1: Determine loading condition.

Loading is axisymmetric, and both drained and undrained conditions are specified.

Step 2: Calculate initial stress invariants for isotropic loading path.

For axisymmetric, isotropic loading under drained conditions, $\Delta u = 0$,

$$\Delta p' = \frac{\Delta\sigma'_a + 2\Delta\sigma'_r}{3} = \frac{\Delta\sigma'_1 + 2\Delta\sigma'_1}{3} = \Delta\sigma'_1 = 200 \text{ kPa}$$

$p_o = p'_o = 200$ kPa, since the soil specimens were loaded from a stress-free state under drained conditions.

$$q_o = q'_o = 0$$

Step 3: Set up a graph and plot initial stress points.

Create a graph with axes p' and p as the abscissa and q as the ordinate and plot the isotropic stress path with coordinates $(0, 0)$ and $(200, 0)$, as shown by OA in Figure E8.2.

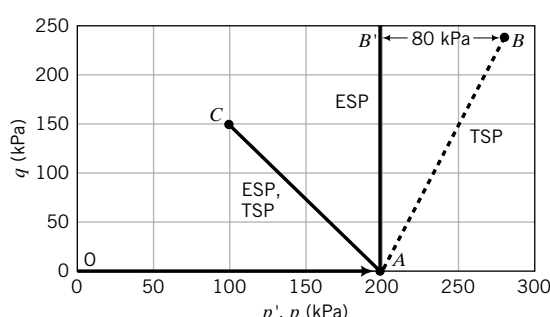


FIGURE E8.2

Step 4: Determine the increases in stresses.

Specimen A

We have (1) an undrained condition, Δu is not zero, and (2) no change in the radial stress, but the axial stress is increased to 440 kPa. Therefore,

$$\Delta\sigma_3 = 0, \quad \Delta\sigma_1 = 440 - 200 = 240 \text{ kPa}$$

Specimen B

Drained loading ($\Delta u = 0$); therefore, TSP = ESP.

Axial stress held constant, $\Delta\sigma_1 = \Delta\sigma'_1 = 0$; radial stress decreases to 50 kPa; that is,

$$\Delta\sigma_3 = \Delta\sigma'_3 = 50 - 200 = -150 \text{ kPa}$$

Step 5: Calculate the increases in stress invariants.

Specimen A

$$\Delta p = \frac{\Delta\sigma_1 + 2\Delta\sigma_3}{3} = \frac{240 + 2 \times 0}{3} = 80 \text{ kPa}$$

$$\Delta q = \Delta\sigma_1 - \Delta\sigma_3 = 240 - 0 = 240 \text{ kPa}$$

$$\text{Slope of total stress path} = \frac{\Delta q}{\Delta p} = \frac{240}{80} = 3$$

Specimen B

$$\Delta p = \Delta p' = \frac{\Delta\sigma'_1 + 2\Delta\sigma'_3}{3} = \frac{0 + 2 \times (-150)}{3} = -100 \text{ kPa}$$

$$\Delta q = \Delta\sigma_1 - \Delta\sigma_3 = 0 - (-150) = 150 \text{ kPa}$$

$$\text{Slope of ESP (or TSP)} = \frac{\Delta q}{\Delta p'} = \frac{150}{-100} = -1.5$$

Step 6: Calculate the current stress invariants.

Specimen A

$$p = p_o + \Delta p = 200 + 80 = 280 \text{ kPa}, \quad q = q' = q_o + \Delta q = 0 + 240 = 240 \text{ kPa}$$

$$p' = p_o + \Delta p' = 200 + 0 = 200 \text{ kPa} \text{ (elastic soil)}$$

Specimen B

$$p = p' = p_o + \Delta p = 200 - 100 = 100 \text{ kPa}$$

$$q = q_o + \Delta q' = 0 + 150 = 150 \text{ kPa}$$

Step 7: Plot the current stress invariants.

Specimen A

Plot point B as (280, 240); plot point B' as (200, 240).

Specimen B

Plot point C as (100, 150).

Step 8: Connect the stress points.

Specimen A

AB in Figure E8.2 shows the total stress path and AB' shows the effective stress path.

Specimen B

AC in Figure E8.2 shows the ESP and TSP.

Step 9: Determine the excess porewater pressure.

Specimen A

BB' shows the maximum excess porewater pressure. The mean stress difference is $280 - 200 = 80$ kPa.

EXAMPLE 8.3 Stress Paths in (p, q) and (s, t) Spaces for Soil Elements Next to an Excavation

A long excavation is required in a stiff saturated soil for the construction of a building. Consider two soil elements. One, element A, is directly at the bottom of the excavation along the center line and the other, element B, is at the open face (Figure E8.3a).

- (a) Plot the stress paths in (p, q) and (s, t) spaces for elements A and B.
- (b) If the soil is an isotropic, linear elastic material, predict the excess porewater pressures.

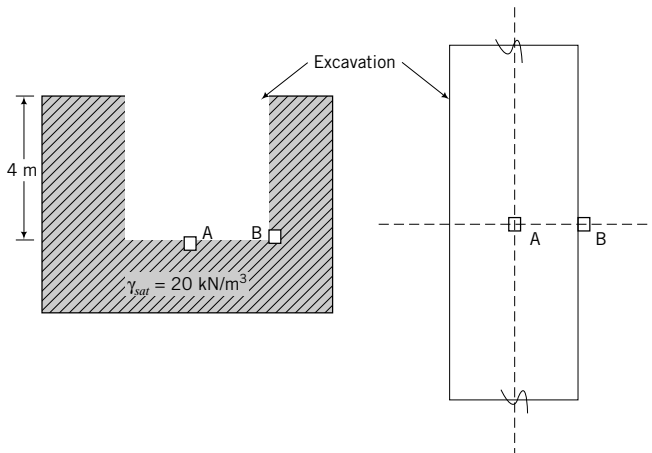


FIGURE E8.3a

Strategy Determine the loading condition and then write the mean stress and deviatoric stress equations in terms of increments.

Solution 8.3

Step 1: Determine loading condition.

Element A is under axisymmetric condition and will be subjected to reduction in vertical and lateral stresses. The increases in lateral stresses are much lower than the increases in vertical stresses. Element B is under plane strain condition and will be subjected to reduction in lateral stresses with no change in vertical stresses.

Step 2: Calculate initial stresses.

Elements A and B have the same initial stresses.

$$\sigma_z = \sigma'_z = 4 \times 20 = 80 \text{ kPa}$$

$$\sigma_x = \sigma'_x = \sigma_y = \sigma'_y = 0.6 \times 80 = 48 \text{ kPa}$$

Note: All stresses are principal stresses.

$$p_o = p'_o = \frac{\sigma_x + \sigma_y + \sigma_z}{3} = \frac{80 + 48 + 48}{3} = 58.7 \text{ kPa}$$

$$q_o = \sigma_z - \sigma_x = (80 - 48) = 32 \text{ kPa}$$

$$s_o = s'_o = \frac{\sigma_z + \sigma_x}{2} = \frac{80 + 48}{2} = 64 \text{ kPa}$$

$$t_o = \frac{\sigma_z - \sigma_x}{2} = \frac{80 - 48}{2} = 16 \text{ kPa}$$

Step 3: Determine the changes in stresses.

Element A: The vertical total stress decreases and, as a first approximation, the changes in lateral stress are small and can be neglected.

$$\Delta p = \frac{\Delta\sigma_x + \Delta\sigma_y + \Delta\sigma_z}{3} = \frac{0 + 0 + (-\Delta\sigma_z)}{3} = \frac{-\Delta\sigma_z}{3} = \frac{-80}{3} \text{ kPa}$$

$$\Delta q = (-\Delta\sigma_z) - \Delta\sigma_x = -\Delta\sigma_z - 0 = -\Delta\sigma_z = -80 \text{ kPa}$$

$$\text{slope} = \frac{\Delta q}{\Delta p} = \frac{-\Delta\sigma_z}{\frac{-80}{3}} = 3$$

$$\Delta s = \frac{(-\Delta\sigma_z) + \Delta\sigma_x}{2} = \frac{-\Delta\sigma_z + 0}{2} = \frac{-\Delta\sigma_z}{2} = -40 \text{ kPa}$$

$$\Delta t = \frac{\Delta\sigma_z - \Delta\sigma_x}{2} = \frac{-\Delta\sigma_z - 0}{2} = \frac{-\Delta\sigma_z}{2} = -40 \text{ kPa}$$

$$\text{slope} = \frac{\Delta t}{\Delta s} = \frac{\frac{-\Delta\sigma_z}{2}}{\frac{-80}{3}} = 1$$

Element B: The vertical total stress remains constant, but the lateral stress in the X direction decreases. The change in lateral stress in the Y direction is small and can be neglected.

$$\Delta p = \frac{\Delta\sigma_x + \Delta\sigma_y + \Delta\sigma_z}{3} = \frac{(-\Delta\sigma_x) + 0 + 0}{3} = \frac{-\Delta\sigma_x}{3} = \frac{-48}{3} = -16 \text{ kPa}$$

$$\Delta q = \Delta\sigma_z - (-\Delta\sigma_x) = 0 + \Delta\sigma_x = \Delta\sigma_x = 48 \text{ kPa}$$

$$\text{slope} = \frac{\Delta q}{\Delta p} = \frac{\Delta \sigma_x}{\frac{-\Delta \sigma_x}{3}} = -3$$

$$\Delta s = \frac{\Delta \sigma_z + (-\Delta \sigma_x)}{2} = \frac{0 - \Delta \sigma_x}{2} = \frac{-\Delta \sigma_x}{2} = -24 \text{ kPa}$$

$$\Delta t = \frac{\Delta \sigma_z - \Delta \sigma_x}{2} = \frac{0 - (-\Delta \sigma_x)}{2} = \frac{\Delta \sigma_x}{2} = 24 \text{ kPa}$$

$$\text{slope} = \frac{\Delta \sigma_x}{\Delta s} = \frac{\frac{\Delta \sigma_x}{2}}{\frac{-\Delta \sigma_x}{2}} = -1$$

Step 4: Plot stress paths.

See Figure E8.3b.

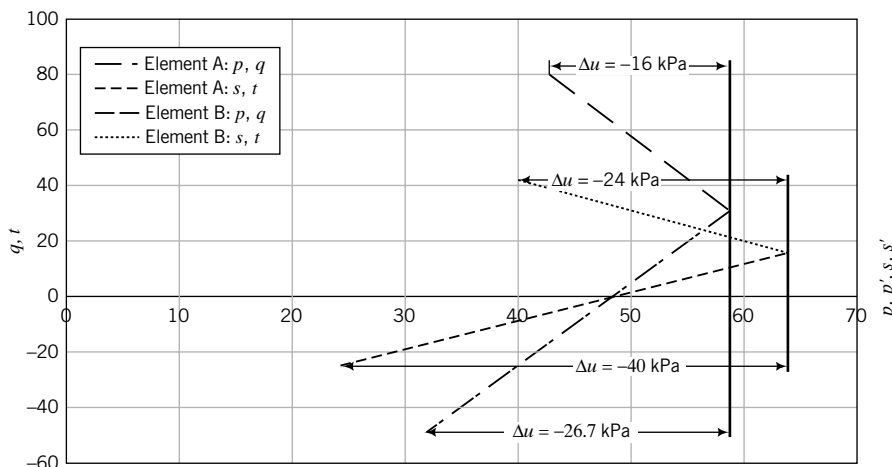


FIGURE E8.3b

Step 5: Summarize results.

Element	Space	Slope	u (kPa)
A	p, q	3	-26.7
A	s, t	1	-40
B	p, q	-3	-16
B	s, t	-1	-24

Both elements A and B are unloaded. Element A is unloaded by removing the initial vertical stress, while element B is unloaded by removing the lateral stress. The changes in deviatoric stress for element A are negative, indicating extension, i.e., the lateral stress changes are greater than the vertical stress changes. This is similar to laterally squeezing a pop can. The changes in deviatoric stress for element B are positive values, indicating compression, i.e., the vertical stress changes are greater than the lateral stress changes. This is similar to compressing a pop can vertically and causing lateral bulging (radial extension). The negative porewater pressures (suction) are due to these extensions.

8.5 SUMMARY

Stress paths provide a useful means through which the history of loading of a soil can be followed. The mean effective stress changes for a linear, isotropic, elastic soil are zero under undrained loading, and the effective stress path is a vector parallel to the deviatoric stress axis, with the q ordinate equal to the corresponding state on the total stress path. The difference in mean stress between the total stress path and the effective stress path gives the excess porewater pressure at a desired value of deviatoric stress.

Self-Assessment

Access Chapter 8 at <http://www.wiley.com/college/budhu> to take the end-of-chapter quiz to test your understanding of this chapter.

Practical Example

EXAMPLE 8.4 Stress Paths Under a Foundation for a Multistory Building

A square foundation (a slab of concrete), $4 \text{ m} \times 4 \text{ m}$, is required to support one of the column loads from a three-story building. The foundation base is located at ground surface and weighs 160 kN . Each story applies a load of 720 kN . The soil is a stiff, saturated, overconsolidated clay with a saturated unit weight of 20 kN/m^3 and $K_o^{oc} = 1$. Groundwater is at 10 m below the surface. The building was to be constructed rapidly, but after the second story was nearly completed, work stopped for a period of 1 year. A transducer at a depth 5 m below the center of the foundation measured the porewater pressure. When work resumed after the 1-year hiatus, the excess porewater pressure developed during construction dissipated by 50%. Assume the stiff clay behaves like an isotropic, linear elastic material. For the soil element at 5 m :

- (a) Plot the total and effective stress paths in (p, q) space before construction stopped.
- (b) Predict the excess porewater pressures just before construction stopped.
- (c) Plot the total and effective stress paths in (p, q) space after construction resumed.
- (d) Predict the excess porewater pressures after construction resumed.

Strategy Determine the initial stresses and the calculate the stress increase from the surface applied stresses. Write the mean stress and deviatoric stress equations in terms of increments.

Solution 8.4

Step 1: Calculate initial stresses.

The soil element under the center of the foundation is under asymmetric condition. Groundwater is below the soil element at 5 m , so it has no effect. The initial total and effective stresses are the same because the porewater pressure is zero.

$$\sigma_z = \sigma'_z = 5 \times 20 = 100 \text{ kPa}$$

$$\sigma_x = \sigma'_x = \sigma_y = \sigma'_y = K_o^{oc} \sigma'_z = 1 \times 100 = 100 \text{ kPa}$$

Note: All stresses are principal stresses.

$$p_o = p'_o = \frac{\sigma_x + \sigma_y + \sigma_z}{3} = \frac{100 + 100 + 100}{3} = 100 \text{ kPa}$$

$$q_o = \sigma_z - \sigma_x = (100 - 100) = 0 \text{ kPa}$$

Step 2: Determine the changes in stresses up to the end of construction of the second story.

The total load at the completion of the second story is $160 + 720 + 720 = 1600 \text{ kN}$.

$$q_s = \frac{1600}{4 \times 4} = 100 \text{ kPa}$$

Use the computer program STRESS. $L = B = 4/2 = 2 \text{ m}$, $z = 5 \text{ m}$.

$$\Delta\sigma_z = 4 \times 6 = 24 \text{ kPa}; \quad \Delta\sigma_x = \Delta\sigma_y = 4 \times 0.29 = 1.2 \text{ kPa}$$

Notice that the changes in lateral stresses are only about 5% of the change in vertical stress. We can, as a first approximation, set the changes in lateral stresses at zero because they are small. The multiplier 4 is used because the initial calculations are only valid for the interior corner of one-fourth of the square foundation.

$$\Delta p = \frac{\Delta\sigma_x + \Delta\sigma_y + \Delta\sigma_z}{3} = \frac{0 + 0 + 24}{3} = 8 \text{ kPa}$$

$$\Delta q = \Delta\sigma_z - \Delta\sigma_x = 24 - 0 = 24 \text{ kPa}$$

$$\text{slope} = \frac{\Delta q}{\Delta p} = \frac{24}{8} = 3$$

$$\text{Current stresses: } p_1 = p_o + \Delta p = 100 + 8 = 108 \text{ kPa}$$

$$q_1 = q_o + \Delta q = 0 + 24 = 24 \text{ kPa}$$

$$p'_1 = p'_o + \Delta p' = 100 + 0 = 100 \text{ kPa}$$

Since the soil is linearly elastic, the change in mean effective stress is zero. Also, the deviatoric (shear) stress is unaffected by changes in porewater pressures.

Step 3: Plot stress paths.

See Figure E8.4.

TSP is represented by OA . ESP is represented by OA' .

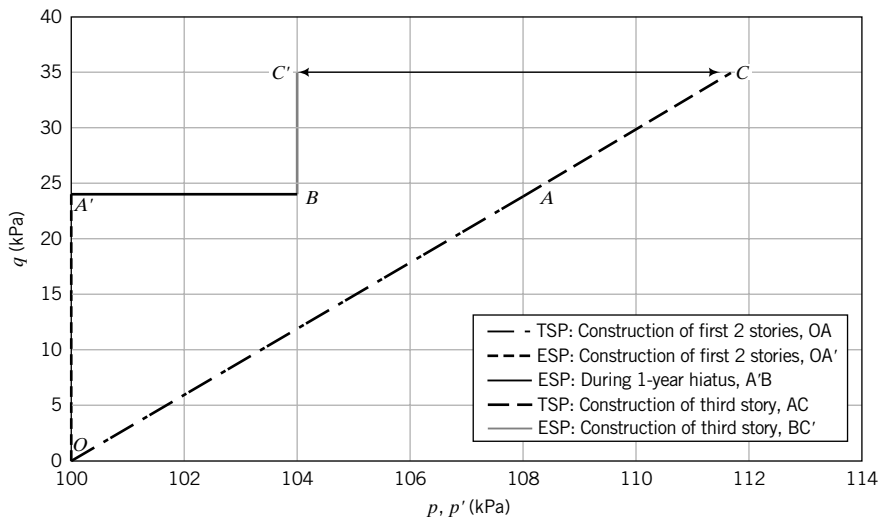


FIGURE E8.4

Step 4: Calculate the excess porewater pressure.

The excess porewater pressure is the mean stress difference between the total and effective stress paths. The magnitude of the excess porewater pressure is represented by AA' .

$$\Delta u = \Delta p = 8 \text{ kPa}$$

Step 5: Determine the excess porewater pressure just before construction resumes.

Amount of excess porewater pressure dissipated = $0.5 \times 8 = 4 \text{ kPa}$

Amount of excess porewater pressure present = $8 - 4 = 4 \text{ kPa}$

Because the excess porewater decreases, the mean effective stress will increase by a similar amount.

$$\text{Current stresses: } p'_2 = p_1' + \Delta u = 100 + 4 = 104 \text{ kPa}$$

$$q_1 = q_o + \Delta q = 0 + 24 = 24 \text{ kPa}$$

Note: There is no change in q .

The stress path as the excess porewater pressure dissipates is represented by A'B in Figure E8.4.

Step 6: Determine the changes in stresses due to the construction of the third story.

The additional load is 720 kN.

$$q_s = \frac{720}{4 \times 4} = 45 \text{ kPa}$$

Because in the calculation of increase in soil stresses from surface stresses we are assuming an isotropic, elastic soil (Chapter 7), then we can simply use proportion to calculate the increase in stresses due to the additional surface stress.

$$\Delta\sigma_z = 24 \times \frac{45}{100} = 10.8 \text{ kPa}$$

$$\Delta p = \frac{\Delta\sigma_x + \Delta\sigma_y + \Delta\sigma_z}{3} = \frac{0 + 0 + 10.8}{3} = 3.6 \text{ kPa}$$

$$\Delta q = \Delta\sigma_z - \Delta\sigma_x = 10.8 - 0 = 10.8 \text{ kPa}$$

$$\text{slope} = \frac{\Delta q}{\Delta p} = \frac{10.8}{3.6} = 3$$

$$\text{Current stresses: } p_3 = p_1 + \Delta p = 108 + 3.6 = 111.6 \text{ kPa}$$

$$q_3 = q_1 + \Delta q = 24 + 10.8 = 34.8 \text{ kPa}$$

$$p'_3 = p'_2 + \Delta p' = 104 + 0 = 104 \text{ kPa}$$

Step 7: Plot stress paths.

See Figure E8.4.

TSP is represented by AC. ESP is represented by BC'.

Step 8: Calculate the excess porewater pressure.

The excess porewater pressure is the mean stress difference between the total and effective stress paths. The magnitude of the excess porewater pressure is represented by CC'.

$$\Delta u = \Delta p = 111.6 - 104 = 7.6 \text{ kPa}$$

EXERCISES

Theory

- 8.1** If the axial stress on a cylindrical sample of soil is decreased and the radial stress is increased by twice the decrease in axial stress, show that the stress path has a slope $q/p = -3$. Plot the stress path.

- 8.2** The initial mean effective stress on a soil is p'_o and the deviatoric stress is $q = 0$. If the soil is a linear, isotropic, elastic material, plot the total and effective stress paths for the following axisymmetric undrained loading condition: (a) $\Delta\sigma_3 = \frac{1}{2}\Delta\sigma_1$, and (b) $\Delta\sigma_3 = -\frac{1}{2}\Delta\sigma_1$.

Problem Solving

- 8.3** A cylindrical sample of soil is isotropically compressed under drained condition with a vertical stress of 100 kPa and a radial stress of 100 kPa. Subsequently, the axial stress was held constant and the radial stress was increased to 300 kPa under an undrained condition.
- Create a graph with the x -axis as p, p' and the y -axis as q . Calculate and plot the initial mean effective stress and deviatoric stress.
 - Calculate the increase in mean total stress and deviatoric stress.
 - Plot the current total and effective stress paths (assume the soil is a linear, isotropic, elastic material).
 - Determine the slopes of the total and effective stress paths and the maximum excess porewater pressure.
- 8.4** A cylindrical sample of soil is isotropically compressed under drained condition with a vertical stress of 100 kPa and a radial stress of 100 kPa. Subsequently, the axial stress was held constant and the radial stress was increased to 300 kPa under an undrained condition.
- Create a graph with the x -axis as s, s' and the y -axis as t . Calculate and plot the initial mean effective stress and deviatoric stress.
 - Calculate the increase in mean total stress and deviatoric stress.
 - Plot the total and effective stress paths (assume the soil is a linear, isotropic, elastic material).
 - Determine the slopes of the total and effective stress paths and the maximum excess porewater pressure.
- 8.5** The initial effective stresses on a saturated soil element at a certain depth in a soil mass are $\sigma'_1 = 80$ kPa, $\sigma'_2 = 40$ kPa, and $\sigma'_3 = 40$ kPa. The groundwater level is below the depth of the soil element. A sudden outward movement of a retaining wall that was retaining the soil resulted in the following changes in stresses: $\Delta\sigma_1 = 0$ kPa, $\Delta\sigma_2$ (parallel to wall) = -10 kPa, and $\Delta\sigma_3$ (normal to wall) = -40 kPa.
- Plot the initial stress state and the total stress path in (p, q) space.
 - Plot the effective stress path assuming that the soil is a linearly elastic material.
 - Determine the maximum excess porewater pressure.
- 8.6** The initial effective stresses on a saturated soil element at a certain depth in a soil mass are $\sigma'_1 = 40$ kPa, $\sigma'_2 = 20$ kPa,

and $\sigma'_3 = 20$ kPa. The groundwater level is below the soil element. The changes in stresses on the soil element are shown in Figure P8.6.

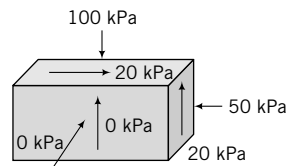


FIGURE P8.6

- Calculate the change in principal total stresses.
- Plot the total stress path in (p, q) space.
- Plot the effective stress path assuming that the soil is a linearly elastic material, and determine the maximum excess porewater pressure.

Practical

- 8.7** An oil tank (10 m in diameter) is to be constructed on a 10-m-thick layer of soft, normally consolidated clay classified as CH. Its saturated unit weight is 18.8 kN/m^3 and the lateral earth pressure coefficient at rest is $K_o = 0.5$. Groundwater is at the surface. The clay is underlain by a sand classified as SP. The estimated settlement of the tank is intolerable. The geotechnical engineer proposes to preload the soft clay by constructing the tank and then filling it with water in stages. The dead load of the tank and its foundation will impose a uniform vertical stress of 25 kPa at the ground surface. The water level in the tank for the first stage of loading is 2 m. For a soil element at a depth of 5 m under the center of the tank:
- Calculate the initial mean total and effective stresses and the initial deviatoric stresses. Create a graph with the x -axis as p, p' and the y -axis as q . Plot the initial stress state.
 - Calculate the total vertical stress applied at the ground surface when the tank is filled with 2 m of water.
 - Calculate the increase in vertical and lateral stresses on the soil element due to the total applied surface stress when the tank is filled with 2 m of water.
 - Calculate the increase in mean total stress and deviatoric stress due to the total applied surface stress when the tank is filled with 2 m of water.
 - Plot the total stress path when the tank is filled with 2 m of water. Clearly label this stress path.
 - If the soft clay were to behave as an isotropic, elastic material, plot the effective stress path and calculate the increase in porewater pressure.

ONE-DIMENSIONAL CONSOLIDATION SETTLEMENT OF FINE-GRAINED SOILS

9.0 INTRODUCTION

In this chapter, we will consider one-dimensional consolidation settlement of fine-grained soils. We will restrict settlement consideration to the vertical direction. We will (1) develop the basic concepts of consolidation, (2) apply them to estimate consolidation settlement from applied loads, (3) formulate the theory of one-dimensional consolidation and use it to predict the time rate of settlement, and (4) show how to determine settlement parameters.

After you have studied this chapter, you should:

- Have a basic understanding of soil consolidation under vertical loads.
- Be able to calculate one-dimensional consolidation settlement and time rate of settlement.

You will make use of the following concepts learned from the previous chapters and your courses in mechanics and mathematics.

- Stresses in soils—effective stresses and vertical stress increases from surface loads (Chapter 7)
- Strains in soils—vertical and volumetric strains (Chapters 7 and 8)
- Elasticity (Chapter 7)
- Flow of water through soils (Chapter 6, Darcy's law)
- Solutions of partial differential equations

Importance

Under loads, all soils will settle, causing settlement of structures founded on or within them. If the settlement is not kept to a tolerable limit, the desired use of the structure may be impaired and the design life of the structure may be reduced. Structures may settle uniformly or nonuniformly. The latter condition is called differential settlement and is often the crucial design consideration.

The Leaning Tower of Pisa is the classic example of differential settlement (Figure 9.1). Construction of the tower started in 1173, and by the end of 1178 when two-thirds of the tower was completed, it had tilted. Since then the tower has been settling differentially. The foundation of the tower is located about 3 m into a bed of silty sand that is underlain by 30 m of soft clay resting on a deposit of sand. A sand layer approximately 5 m thick intersects the clay. The structure of the tower is intact, but its function is impaired by differential settlement.

The total settlement usually consists of three parts—immediate or elastic compression, primary consolidation, and secondary compression. We have considered elastic settlement in Chapter 7, and we will consider some modifications to the elastic analysis for practical applications in Chapter 12. In this chapter, we will deal with primary consolidation and secondary compression.

**FIGURE 9.1**

The Leaning Tower of Pisa.
(© Photo Disc Inc./Getty Images.)

9.1 DEFINITIONS OF KEY TERMS

Consolidation is the time-dependent settlement of soils resulting from the expulsion of water from the soil pores.

Primary consolidation is the change in volume of a fine-grained soil caused by the expulsion of water from the voids and the transfer of stress from the excess porewater pressure to the soil particles.

Secondary compression is the change in volume of a fine-grained soil caused by the adjustment of the soil fabric (internal structure) after primary consolidation has been completed.

Excess porewater pressure, Δu , is the porewater pressure in excess of the current equilibrium porewater pressure. For example, if the porewater pressure in a soil is u_o and a load is applied to the soil so that the existing porewater pressure increases to u_1 , then the excess porewater pressure is $\Delta u = u_1 - u_o$.

Drainage path, H_{dr} , is the longest vertical path that a water particle will take to reach the drainage surface.

Past maximum vertical effective stress, σ'_{zc} , is the maximum vertical effective stress that a soil was subjected to in the past.

Normally consolidated soil is one that has never experienced vertical effective stresses greater than its current vertical effective stress ($\sigma'_{zo} = \sigma'_{zc}$).

Overconsolidated soil is one that has experienced vertical effective stresses greater than its existing vertical effective stress ($\sigma'_{zo} < \sigma'_{zc}$).

Overconsolidation ratio, **OCR**, is the ratio by which the current vertical effective stress in the soil was exceeded in the past ($OCR = \sigma'_{zc}/\sigma'_{zo}$).

Compression index, **C_c**, is the slope of the normal consolidation line in a plot of the logarithm of vertical effective stress versus void ratio.

Unloading/reloading index or recompression index, C_r , is the average slope of the unloading/reloading curves in a plot of the logarithm of vertical effective stress versus void ratio.

Modulus of volume compressibility, m_s , is the slope of the curve between two stress points in a plot of vertical effective stress versus vertical strain.

9.2 QUESTIONS TO GUIDE YOUR READING

1. What is the process of soil consolidation?
2. What is the difference between consolidation and compaction?
3. What is the governing equation for one-dimensional consolidation?
4. What are the assumptions made in one-dimensional consolidation theory?
5. How is the excess porewater pressure distributed within the soil when a load is applied and after various elapsed times?
6. What factors determine the consolidation settlement of soils?
7. What are the average degree of consolidation, time factor, modulus of volume compressibility, and compression and recompression indices?
8. What is the difference between primary consolidation and secondary compression?
9. What is the drainage path for single drainage and double drainage?
10. Why do we need to carry out consolidation tests, how are they conducted, and what parameters are deduced from the test results?
11. How are time rate of settlement and consolidation settlement calculated?
12. Are there significant differences between the calculated settlements and field settlements?

9.3 BASIC CONCEPTS

In our development of the various ideas on consolidation settlement, we will assume:

- A homogeneous, saturated soil
- The soil particles and the water to be incompressible
- Vertical flow of water
- The validity of Darcy's law
- Small strains

We will conduct a simple experiment to establish the basic concepts of the one-dimensional consolidation settlement of fine-grained soils. Let us take a thin, soft, saturated sample of clay and place it between porous stones in a rigid, cylindrical container with a frictionless inside wall (Figure 9.2a). The porous stones are used to facilitate drainage of the porewater from the top and bottom faces of the soil. The top half of the soil will drain through the top porous stone and the bottom half of the soil will drain through the bottom porous stone. A platen on the top porous stone transmits applied loads to the soil. Expelled water is transported by plastic tubes to a burette. A valve is used to control the flow of the expelled water into the burette. Three porewater pressure transducers are mounted in the side wall of the cylinder to measure the excess porewater pressure near the porous stone at the top (A), at a distance of one-quarter the height (B), and at mid-height of the soil (C). Excess porewater pressure is the additional porewater pressure induced in a soil mass by loads. A displacement gage with its stem on the platen keeps track of the vertical settlement of the soil.

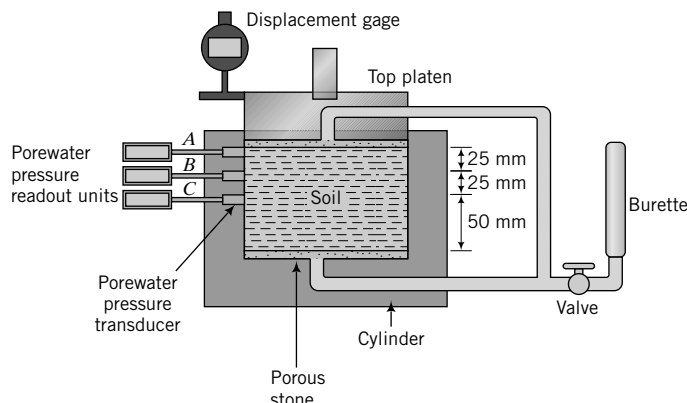


FIGURE 9.2a Experimental setup for illustrating basic concepts of consolidation.

We will assume that the porewater and the soil particles are incompressible, and the initial porewater pressure is zero. The volume of excess porewater that drains from the soil is then a measure of the volume change of the soil resulting from the applied loads. Since the side wall of the container is rigid, no radial displacement can occur. The lateral and circumferential strains are then equal to zero ($\epsilon_r = \epsilon_\theta = 0$), and the volumetric strain ($\epsilon_p = \epsilon_z + \epsilon_\theta + \epsilon_r$) is equal to the vertical strain, $\epsilon_z = \Delta z/H_o$, where Δz is the change in height or thickness and H_o is the initial height or thickness of the soil.

9.3.1 Instantaneous Load

Let us now apply a load P to the soil through the load platen and keep the valve closed. Since no excess porewater can drain from the soil, the change in volume of the soil is zero ($\Delta V = 0$) and no load or stress is transferred to the soil particles ($\Delta\sigma'_z = 0$). The porewater carries the total load. The initial excess porewater pressure in the soil (Δu_o) is then equal to the change in applied vertical stress, $\Delta\sigma_z = P/A$, where A is the cross-sectional area of the soil, or more appropriately, the change in mean total stress, $\Delta p = (\Delta\sigma_z + 2\Delta\sigma_r)/3$, where $\Delta\sigma_r$ is the change in radial stress. For our thin soil layer, we will assume that the initial excess porewater pressure will be distributed uniformly with depth so that at every point in the soil layer, the initial excess porewater pressure is equal to the applied vertical stress. For example, if $\Delta\sigma_z = 100$ kPa, then $\Delta u_o = 100$ kPa, as shown in Figure 9.2b.

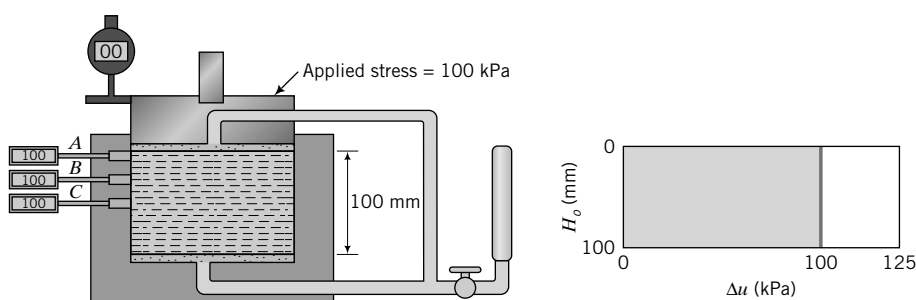


FIGURE 9.2b Instantaneous or initial excess porewater pressure when a vertical load is applied.

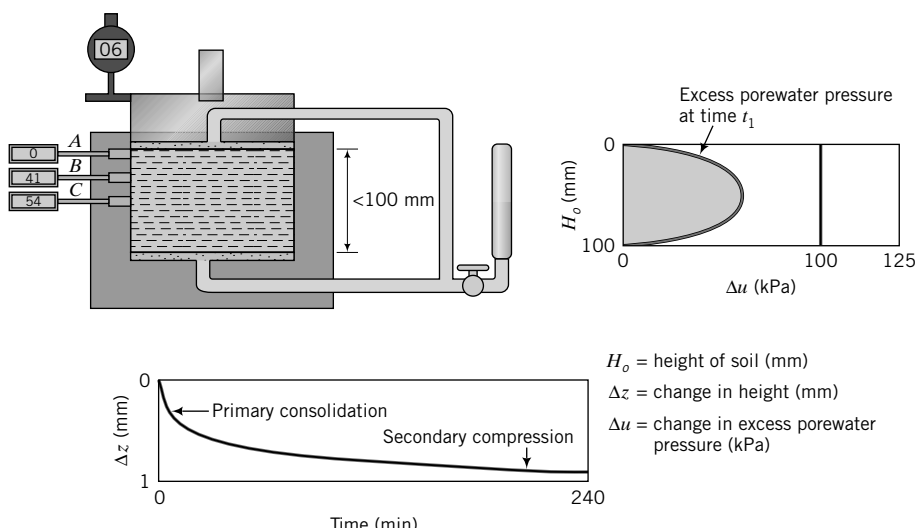


FIGURE 9.2c Excess porewater pressure distribution and settlement during consolidation.

9.3.2 Consolidation Under a Constant Load—Primary Consolidation

Let us now open the valve and allow the initial excess porewater to drain. The total volume of soil at time t_1 decreases by the amount of excess porewater that drains from it, as indicated by the change in volume of water in the burette (Figure 9.2c). At the top and bottom of the soil sample, the excess porewater pressure is zero because these are the drainage boundaries. The decrease of initial excess porewater pressure at the middle of the soil (position C) is the slowest because a water particle must travel from the middle of the soil to either the top or bottom boundary to exit the system.

You may have noticed that the settlement of the soil (Δz) with time t (Figure 9.2c) is not linear. Most of the settlement occurs shortly after the valve is opened. The rate of settlement, $\Delta z/t$, is also much faster soon after the valve is opened compared with later times. Before the valve is opened, an initial hydraulic head, $\Delta u_o/\gamma_w$, is created by the applied vertical stress. When the valve is opened, the initial excess porewater is forced out of the soil by this initial hydraulic head. With time, the initial hydraulic head decreases and, consequently, smaller amounts of excess porewater are forced out. An analogy can be drawn with a pipe containing pressurized water that is ruptured. A large volume of water gushes out as soon as the pipe is ruptured, but soon after, the flow becomes substantially reduced. We will call the initial settlement response soon after the valve is opened the early time response, or primary consolidation. Primary consolidation is the change in volume of the soil caused by the expulsion of water from the voids and the transfer of load from the excess porewater pressure to the soil particles.

9.3.3 Secondary Compression

Theoretically, primary consolidation ends when $\Delta u_o = 0$. The later time settlement response is called secondary compression, or creep. Secondary compression is the change in volume of a fine-grained soil caused by the adjustment of the soil fabric (internal structure) after primary consolidation has been completed. The term “consolidation” is reserved for the process in which settlement of a soil occurs from changes in effective stresses resulting from decreases in excess porewater pressure. The rate of settlement from secondary compression is very slow compared with that from primary consolidation.

We have separated primary consolidation and secondary compression. In reality, the distinction is not clear because secondary compression occurs as part of the primary consolidation phase, especially in soft clays. The mechanics of consolidation is still not fully understood, and to make estimates of settlement it is convenient to separate primary consolidation and secondary compression.

9.3.4 Drainage Path

The distance of the longest vertical path taken by a particle to exit the soil is called the length of the drainage path. Because we allowed the soil to drain on the top and bottom faces (double drainage), the length of the drainage path, H_{dr} , is

$$H_{dr} = \frac{H_{av}}{2} = \frac{H_o + H_f}{4} \quad (9.1)$$

where H_{av} is the average height and H_o and H_f are the initial and final heights, respectively, under the current loading. If drainage is permitted from only one face of the soil, then $H_{dr} = H_{av}$. Shorter drainage paths will cause the soil to complete its settlement in a shorter time than a longer drainage path. You will see later that, for single drainage, our soil sample will take four times longer to reach a particular settlement than for double drainage.

9.3.5 Rate of Consolidation

The rate of consolidation for a homogeneous soil depends on the soil's hydraulic conductivity (permeability), the thickness, and the length of the drainage path. A soil with a hydraulic conductivity lower than that of our current soil will take longer to drain the initial excess porewater, and settlement will proceed at a slower rate.

9.3.6 Effective Stress Changes

Since the applied vertical stress (total stress) remains constant, then according to the principle of effective stress ($\Delta\sigma'_z = \Delta\sigma_z - \Delta u$), any reduction of the initial excess porewater pressure must be balanced by a corresponding increase in vertical effective stress. Increases in vertical effective stresses lead to soil settlement caused by changes to the soil fabric. As time increases, the initial excess porewater continues to dissipate and the soil continues to settle (Figure 9.2c).

After some time, usually within 24 hours for many small soil samples tested in the laboratory, the initial excess porewater pressure in the middle of the soil reduces to approximately zero, and the rate of decrease of the volume of the soil becomes very small. Since the initial excess porewater pressure becomes zero, then, from the principle of effective stress, all of the applied vertical stress is transferred to the soil; that is, the vertical effective stress is equal to the vertical total stress ($\Delta\sigma'_z = \Delta\sigma_z$).

THE ESSENTIAL POINTS ARE:

- When a load is applied to a saturated soil, all of the applied stress is supported initially by the porewater (initial excess porewater pressure); that is, at $t = 0$, $\Delta u_o = \sigma_z$ or $\Delta u_o = \Delta p$. The change in effective stress is zero ($\Delta\sigma'_z = 0$).**
- If drainage of porewater is permitted, the initial excess porewater pressure decreases and soil settlement (Δz) increases with time; that is, $\Delta u(t) < \Delta u_o$ and $\Delta z > 0$. Since the change in total stress is zero ($\Delta\sigma_z = 0$), then the change in effective stress is equal to the change in excess porewater pressure [$\Delta u_o - \Delta u(t)$].**
- When $t \rightarrow \infty$, the change in volume and the change in excess porewater pressure of the soil approach zero; that is, $\Delta V \rightarrow 0$ and $\Delta u_o \rightarrow 0$. The change in vertical effective stress is $\Delta\sigma'_z = \Delta\sigma_z$.**
- Soil settlement is not linearly related to time except very early in the consolidation process.**
- The change in volume of the soil is equal to the volume of initial excess porewater expelled.**
- The rate of settlement depends on the hydraulic conductivity (permeability) of the soil.**

9.3.7 Void Ratio and Settlement Changes Under a Constant Load

The initial volume (specific volume) of a soil is $V = 1 + e_o$ (Chapter 3), where e_o is the initial void ratio. The change in volume of the soil (ΔV) is equal to the change in void ratio (Δe). We can calculate the volumetric strain from the change in void ratio as

$$\epsilon_p = \frac{\Delta V}{V} = \frac{\Delta e}{1 + e_o} \quad (9.2)$$

Since for one-dimensional consolidation the radial strains and the circumferential strains are zero ($\epsilon_r = \epsilon_\theta = 0$), then $\epsilon_z = \epsilon_p$. We can write a relationship between settlement and the change in void ratio as

$$\epsilon_z = \frac{\Delta z}{H_o} = \frac{\Delta e}{1 + e_o} \quad (9.3)$$

where H_o is the initial height of the soil. We can rewrite Equation (9.3) as

$$\Delta z = H_o \frac{\Delta e}{1 + e_o} \quad (9.4)$$

We are going to use ρ_{pc} to denote primary consolidation settlement rather than Δz , so

$$\rho_{pc} = H_o \frac{\Delta e}{1 + e_o} \quad (9.5)$$

The void ratio at any time under load P is

$$e = e_o - \Delta e = e_o - \frac{\Delta z}{H_o} (1 + e_o) = e_o \left(1 - \frac{\Delta z}{H_o}\right) - \frac{\Delta z}{H_o} \quad (9.6)$$

For a saturated soil, $e_o = wG_s$, where w is the water content. Therefore, we can write Equation (9.6) as

$$e = wG_s \left(1 - \frac{\Delta z}{H_o}\right) - \frac{\Delta z}{H_o} \quad (9.7)$$

9.3.8 Effects of Vertical Stresses on Primary Consolidation

We can apply additional loads to the soil and for each load increment we can calculate the final void ratio from Equation (9.6) and plot the results, as shown by segment AB in Figure 9.3 on page 216. Three types of graph are shown in Figure 9.3 to illustrate three different arbitrary ways of plotting the data from our test. Figure 9.3a is an arithmetic plot of the void ratio versus vertical effective stress. Figure 9.3b is a similar plot except the vertical effective stress is plotted on a logarithmic scale. Figure 9.3c is an arithmetic plot of the vertical strain (ϵ_z) versus vertical effective stress. The segment AB in Figures 9.3a and 9.3c is not linear because the settlement that occurs for each increment of loading brings the soil to a denser state from its initial state, and the soil's permeability decreases. Therefore, doubling the load from a previous increment, for example, would not cause a twofold increase in settlement. The segment AB (Figure 9.3a–c) is called the virgin consolidation line, or normal consolidation line (NCL). In a plot of σ'_z (log scale) versus e , the NCL is approximately a straight line.

At some value of vertical effective stress, say, σ'_{zc} , let us unload the soil incrementally. Each increment of unloading is carried out only after the soil reaches equilibrium under the previous loading step.

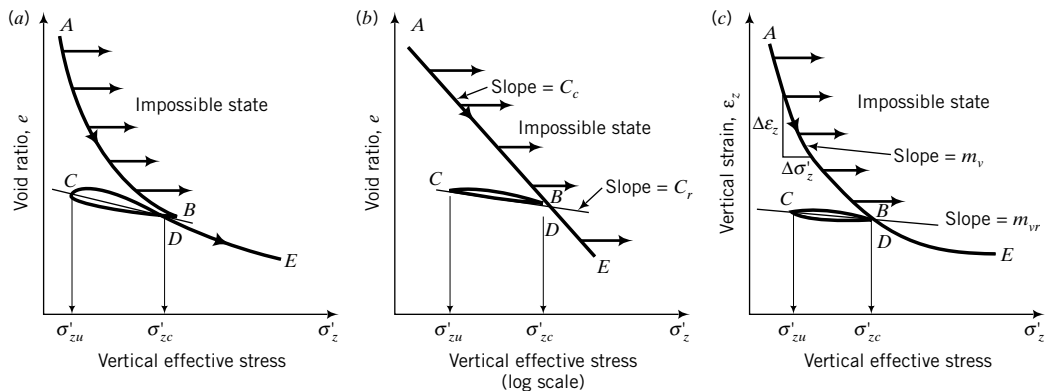


FIGURE 9.3 Three plots of settlement data from soil consolidation.

When an increment of load is removed, the soil will start to swell by absorbing water from the burette. The void ratio increases, but the increase is much less than the decrease in void ratio for the same magnitude of loading that was previously applied.

Let us reload the soil after unloading it to, say, σ'_{zc} . The reloading path CD is convex compared with the concave unloading path BC . One reason for this is the evolving soil structure (soil particles arrangement) during loading and unloading. At each loading/unloading stage, the soil particles are reorganized into a different structural framework to resist the load. The average slopes of the unloading path and the reloading path are not equal, but the difference is assumed to be small. We will represent the unloading-reloading path by an average slope BC and refer to it as the recompression line or the unloading-reloading line (URL).

A comparison of the soil's response with typical material responses to loads as shown in Figures 7.5 and 7.6 reveals that soils can be considered to be an elastoplastic material (see Figure 7.6). The path BC represents the elastic response, while the path AB represents the elastoplastic response of the soil. Loads that cause the soil to follow path BC will produce elastic settlement (recoverable settlement of small magnitude). Loads that cause the soil to follow path AB will produce settlements that have both elastic and plastic (permanent) components.

Once the past maximum vertical effective stress, σ'_{zc} , is exceeded, the slope of the path followed by the soil, DE , is approximately the same as that of the initial loading path, AB . Unloading and reloading the soil at any subsequent vertical effective stress would result in a soil's response similar to paths $BCDE$.

9.3.9 Primary Consolidation Parameters

The primary consolidation settlement of the soil (settlement that occurs along path AB in Figure 9.3) can be expressed through the slopes of the curves in Figure 9.3. We are going to define two slopes for primary consolidation. One is called the coefficient of compression or compression index, C_c , and is obtained from the plot of e versus $\log \sigma'_z$ (Figure 9.3b) as

$$C_c = -\frac{e_2 - e_1}{\log \frac{(\sigma'_z)_2}{(\sigma'_z)_1}} \quad (\text{no units}) \quad (9.8)$$

where the subscripts 1 and 2 denote two arbitrarily selected points on the NCL.

The other is called the modulus of volume compressibility, m_v , and is obtained from the plot of ϵ_z versus σ'_z (Figure 9.3c) as

$$m_v = -\frac{(\epsilon_z)_2 - (\epsilon_z)_1}{(\sigma'_z)_2 - (\sigma'_z)_1} \quad \left(\frac{\text{m}^2}{\text{kN}} \right) \quad (9.9)$$

where the subscripts 1 and 2 denote two arbitrarily selected points on the NCL.

Similarly, we can define the slope BC in Figure 9.3b as the recompression index, C_r , which we can express as

$$C_r = -\frac{e_2 - e_1}{\log \frac{(\sigma'_z)_2}{(\sigma'_z)_1}} \quad (9.10)$$

where the subscripts 1 and 2 denote two arbitrarily selected points on the URL.

The slope BC in Figure 9.3c is called the modulus of volume recompressibility, m_{vr} , and is expressed as

$$m_{vr} = -\frac{(\varepsilon_z)_2 - (\varepsilon_z)_1}{(\sigma'_z)_2 - (\sigma'_z)_1} \left(\frac{\text{m}^2}{\text{kN}} \right) \quad (9.11)$$

where the subscripts 1 and 2 denote two arbitrarily selected points on the URL.

From Hooke's law, we know that Young's modulus of elasticity is

$$E'_c = \frac{\Delta\sigma'_z}{\Delta\varepsilon_z} = \frac{E'(1 - \nu')}{(1 + \nu')(1 - 2\nu')} \quad (9.12)$$

where the subscript c denotes constrained because we are constraining the soil to settle only in one direction (one-dimensional consolidation), E' is Young's modulus based on effective stresses, and ν' is Poisson's ratio. We can rewrite Equation (9.12) as

$$E'_c = \frac{1}{m_{vr}} \quad (9.13)$$

The slopes C_c , C_r , m_v , and m_{vr} are positive values to satisfy our sign convention of compression or recompression as positive.

9.3.10 Effects of Loading History

In our experiment, we found that during reloading the soil follows the normal consolidation line when the past maximum vertical effective stress is exceeded. The history of loading of a soil is locked in its fabric, and the soil maintains a memory of the past maximum effective stress. To understand how the soil will respond to loads, we have to unlock its memory. If a soil were to be consolidated to stresses below its past maximum vertical effective stress, then settlement would be small because the soil fabric was permanently changed by a higher stress in the past. However, if the soil were to be consolidated beyond its past maximum effective stress, settlement would be large for stresses beyond its past maximum effective stress because the soil fabric would now undergo further change from a current loading that is higher than its past maximum effective stress.

The practical significance of this soil behavior is that if the loading imposed on the soil by a structure is such that the vertical effective stress in the soil does not exceed its past maximum vertical effective stress, the settlement of the structure would be small, otherwise significant permanent settlement would occur. The past maximum vertical effective stress defines the limit of elastic behavior. For stresses that are lower than the past maximum vertical effective stress, the soil will follow the URL and we can reasonably assume that the soil will behave like an elastic material. For stresses greater than the past maximum vertical effective stress, the soil would behave like an elastoplastic material.

9.3.11 Overconsolidation Ratio

We will create a demarcation for soils based on their consolidation history. We will label a soil whose current vertical effective stress or overburden effective stress, σ'_{zo} , is less than its past maximum vertical effective stress, σ'_{zc} , as an overconsolidated soil. An overconsolidated soil will follow a vertical effective stress versus void ratio path similar to *CDE* (Figure 9.3) during loading. The degree of overconsolidation, called overconsolidation ratio, OCR, is defined as

$$\text{OCR} = \frac{\sigma'_{zc}}{\sigma'_{zo}} \quad (9.14)$$

If $\text{OCR} = 1$, the soil is normally consolidated soil. Normally consolidated soils follow paths similar to *ABE* (Figure 9.3). The overconsolidation ratio of soils has been observed to decrease with depth, eventually reaching a value of 1 (normally consolidated state).

9.3.12 Possible and Impossible Consolidation Soil States

The normal consolidation line delineates possible from impossible soil states. Unloading a soil or reloading it cannot bring it to soil states right of the normal consolidation line, which we will call impossible soil states (Figure 9.3). Possible soil states only occur on or to the left of the normal consolidation line.

THE ESSENTIAL POINTS ARE:

1. Path *AB* (Figure 9.3), called the **normal consolidation line (NCL)**, describes the response of a normally consolidated soil—a soil that has never experienced a vertical effective stress greater than its current vertical effective stress. The NCL is approximately a straight line in a plot of $\log \sigma'_z$ versus e and is defined by a slope, C_c , called the **compression index**.
2. A normally consolidated soil would behave like an elastoplastic material. That is, part of the settlement under the load is recoverable, while the other part is permanent.
3. An overconsolidated soil has experienced vertical effective stresses greater than its current vertical effective stress.
4. An overconsolidated soil will follow paths such as *CDE* (Figure 9.3). For stresses below the past maximum vertical effective stress, an overconsolidated soil would behave approximately like an elastic material, and settlement would be small. However, for stresses greater than the past maximum vertical effective stress, an overconsolidated soil will behave like an elastoplastic material, similar to a normally consolidated soil.

What's next . . . Next, we will consider how to use the basic concepts to calculate one-dimensional settlement.

9.4 CALCULATION OF PRIMARY CONSOLIDATION SETTLEMENT

9.4.1 Effects of Unloading/Reloading of a Soil Sample Taken from the Field

Let us consider a soil sample that we wish to take from the field at a depth z (Figure 9.4a). We will assume that the groundwater level is at the surface. The current vertical effective stress or overburden effective stress is

$$\sigma'_{zo} = (\gamma_{sat} - \gamma_w)z = \gamma'z$$

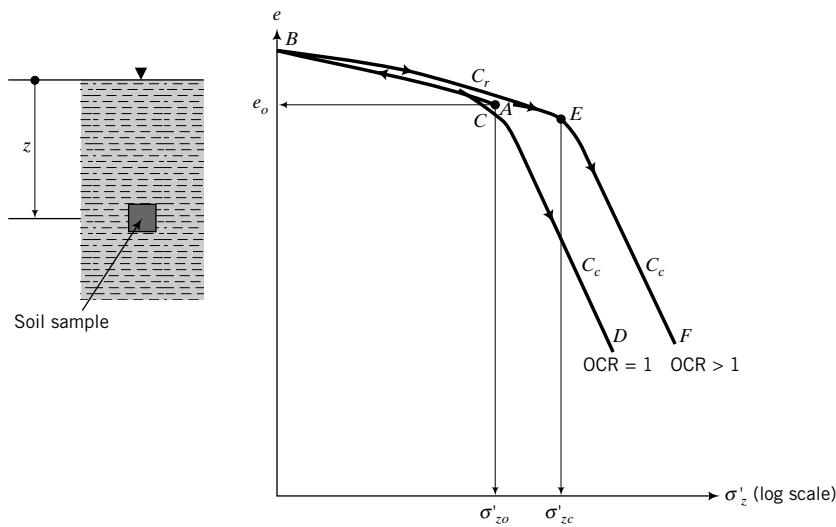


FIGURE 9.4 (a) Soil sample at a depth z below ground surface.
(b) Expected one-dimensional settlement response.

and the current void ratio can be found from γ_{sat} using Equation 4.13. On a plot of σ'_z (log scale) versus e , the current vertical effective stress can be represented as A , as depicted in Figure 9.4b.

To obtain a sample, we would have to make a borehole and remove the soil above it. The act of removing the soil and extracting the sample reduces the total stress to zero; that is, we have fully unloaded the soil. From the principle of effective stress [Equation (7.38)], $\sigma'_z = -\Delta u$. Since σ' cannot be negative—that is, soil cannot sustain tension—the porewater pressure must be negative. As the porewater pressure dissipates with time, volume changes (swelling) occur. Using the basic concepts of consolidation described in Section 9.3, the sample will follow an unloading path AB (Figure 9.4b). The point B does not correspond to zero effective stress because we cannot represent zero on a logarithmic scale. However, the effective stress level at the start of the logarithmic scale is assumed to be small (≈ 0). If we were to reload our soil sample, the reloading path followed would depend on the OCR. If $\text{OCR} = 1$ (normally consolidated soil), the path followed during reloading would be BCD (Figure 9.4b). The average slope of ABC is C_r . Once σ'_{zo} is exceeded, the soil will follow the normal consolidation line, CD , of slope C_c . If the soil were overconsolidated, $\text{OCR} > 1$, the reloading path followed would be BDF because we have to reload the soil beyond σ'_{zc} before it behaves like a normally consolidated soil. The average slope of ABE is C_r , and the slope of EF is C_c . The point E marks the past maximum vertical effective stress. Later in this chapter, we will determine the position of E from laboratory tests (Section 9.7).

9.4.2 Primary Consolidation Settlement of Normally Consolidated Fine-Grained Soils

Let us consider a site consisting of a normally consolidated soil on which we wish to construct a building. We will assume that the increase in vertical stress due to the building at depth z , where we took our soil sample, is $\Delta\sigma_z$. (Recall that you can find $\Delta\sigma_z$ using the methods described in Section 7.11.) The final vertical stress is

$$\sigma'_{fin} = \sigma'_{zo} + \Delta\sigma_z \quad (9.15)$$

The increase in vertical stress will cause the soil to settle following the NCL, and the primary consolidation settlement is

$$\rho_{pc} = H_o \frac{\Delta e}{1 + e_o} = \frac{H_o}{1 + e_o} C_c \log \frac{\sigma'_{fin}}{\sigma'_{zo}}; \quad \text{OCR} = 1 \quad (9.16)$$

where $\Delta e = C_c \log (\sigma'_{fin}/\sigma'_{zo})$.

9.4.3 Primary Consolidation Settlement of Overconsolidated Fine-Grained Soils

If the soil is overconsolidated, we have to consider two cases depending on the magnitude of $\Delta\sigma_z$. We will approximate the curve in the σ'_z (log scale) versus e space as two straight lines, as shown in Figure 9.5. In Case 1, the increase in $\Delta\sigma_z$ is such that $\sigma'_{fin} = \sigma'_{zo} + \Delta\sigma_z$ is less than σ'_{zc} (Figure 9.5a). In this case, consolidation occurs along the URL and

$$\rho_{pc} = \frac{H_o}{1 + e_o} C_r \log \frac{\sigma'_{fin}}{\sigma'_{zo}}; \quad \sigma'_{fin} < \sigma'_{zc} \quad (9.17)$$

In Case 2, the increase in $\Delta\sigma_z$ is such that $\sigma'_{fin} = \sigma'_{zo} + \Delta\sigma_z$ is greater than σ'_{zc} (Figure 9.5b). In this case, we have to consider two components of settlement—one along the URL and the other along the NCL. The equation to use in Case 2 is

$$\rho_{pc} = \frac{H_o}{1 + e_o} \left(C_r \log \frac{\sigma'_{zc}}{\sigma'_{zo}} + C_c \log \frac{\sigma'_{fin}}{\sigma'_{zc}} \right); \quad \sigma'_{fin} > \sigma'_{zc} \quad (9.18)$$

or

$$\rho_{pc} = \frac{H_o}{1 + e_o} \left[C_r \log (\text{OCR}) + C_c \log \frac{\sigma'_{fin}}{\sigma'_{zc}} \right]; \quad \sigma'_{fin} > \sigma'_{zc} \quad (9.19)$$

9.4.4 Procedure to Calculate Primary Consolidation Settlement

The procedure to calculate primary consolidation settlement is as follows:

1. Calculate the current vertical effective stress (σ'_{zo}) and the current void ratio (e_o) at the center of the soil layer for which settlement is required.

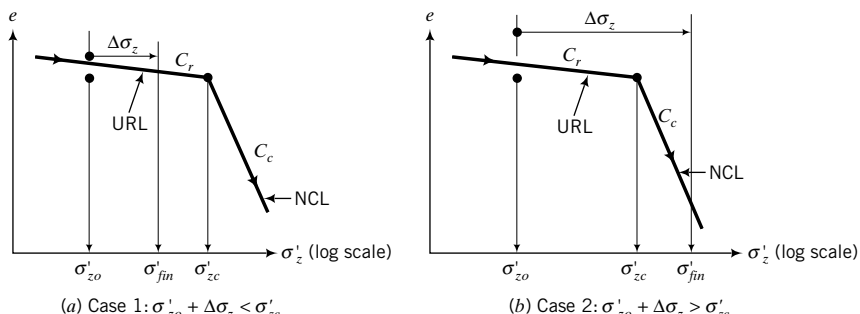


FIGURE 9.5 Two cases to consider for calculating settlement of overconsolidated fine-grained soils.

2. Calculate the applied vertical stress increase ($\Delta\sigma_z$) at the center of the soil layer using the appropriate method in Section 7.11.
3. Calculate the final vertical effective stress $\sigma'_{fin} = \sigma'_{zo} + \Delta\sigma_z$.
4. Calculate the primary consolidation settlement.

(a) If the soil is normally consolidated ($OCR = 1$), the primary consolidation settlement is

$$\rho_{pc} = \frac{H_o}{1 + e_o} C_c \log \frac{\sigma'_{fin}}{\sigma'_{zo}}$$

(b) If the soil is overconsolidated and $\sigma'_{fin} < \sigma'_{zc}$, the primary consolidation settlement is

$$\rho_{pc} = \frac{H_o}{1 + e_o} C_r \log \frac{\sigma'_{fin}}{\sigma'_{zc}}$$

(c) If the soil is overconsolidated and $\sigma'_{fin} > \sigma'_{zc}$, the primary consolidation settlement is

$$\rho_{pc} = \frac{H_o}{1 + e_o} \left[C_r \log (OCR) + C_c \log \frac{\sigma'_{fin}}{\sigma'_{zc}} \right]$$

where H_o is the thickness of the soil layer.

You can also calculate the primary consolidation settlement using m_v . However, unlike C_c , which is constant, m_v varies with stress levels. You should compute an average value of m_v over the stress range σ'_{zo} to σ'_{fin} . To reduce the effects of nonlinearity, the vertical effective stress difference should not exceed 100 kPa in calculating m_v or m_{vr} . The primary consolidation settlement, using m_v , is

$$\rho_{pc} = H_o m_v \Delta\sigma_z \quad (9.20)$$

The advantage of using Equation (9.20) is that m_v is readily determined from displacement data in consolidation tests; you do not have to calculate void ratio changes from the test data as required to determine C_c .

9.4.5 Thick Soil Layers

For better accuracy, when dealing with thick layers ($H_o > 2$ m), you should divide the soil layer into sublayers (about two to five sublayers) and find the settlement for each sublayer. Add up the settlement of each sublayer to find the total primary consolidation settlement. You must remember that the value of H_o in the primary consolidation equations is the thickness of the sublayer. An alternative method is to use a harmonic mean value of the vertical stress increase for the sublayers in the equations for primary consolidation settlement. The harmonic mean stress increase is

$$\Delta\sigma_z = \frac{n(\Delta\sigma_z)_1 + (n - 1)(\Delta\sigma_z)_2 + (n - 2)(\Delta\sigma_z)_3 + \dots + (\Delta\sigma_z)_n}{n + (n - 1) + (n - 2) + \dots + 1} \quad (9.21)$$

where n is the number of sublayers and the subscripts 1, 2, etc., mean the first (top) layer, the second layer, and so on. The advantage of using the harmonic mean is that the settlement is skewed in favor of the upper part of the soil layer. You should recall from Chapter 7 that the increase in vertical stress decreases with depth. Therefore, the primary consolidation settlement of the upper portion of the soil layer can be expected to be more than the lower portion because the upper portion of the soil layer is subjected to higher vertical stress increases.

EXAMPLE 9.1 *Consolidation Settlement of a Normally Consolidated Clay*

The soil profile at a site for a proposed office building consists of a layer of fine sand 10.4 m thick above a layer of soft, normally consolidated clay 2 m thick. Below the soft clay is a deposit of coarse sand. The groundwater table was observed at 3 m below ground level. The void ratio of the sand is 0.76 and the water content of the clay is 43%. The building will impose a vertical stress increase of 140 kPa at the middle of the clay layer. Estimate the primary consolidation settlement of the clay. Assume the soil above the water table to be saturated, $C_c = 0.3$, and $G_s = 2.7$.

Strategy You should write down what is given or known and draw a diagram of the soil profile (see Figure E9.1). In this problem, you are given the stratigraphy, groundwater level, vertical stress increase, and the following soil parameters and soil condition:

$$e_o \text{ (for sand)} = 0.76; \quad w \text{ (for clay)} = 43\%$$

$$H_o = 2 \text{ m}, \quad \Delta\sigma_z = 140 \text{ kPa}, \quad C_c = 0.3, \quad G_s = 2.7$$

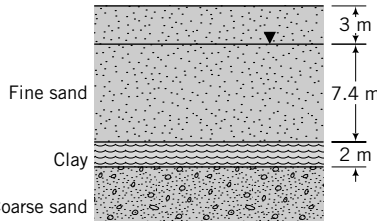


FIGURE E9.1

Since you are given a normally consolidated clay, the primary consolidation settlement response of the soil will follow path *ABE* (Figure 9.3). The appropriate equation to use is Equation (9.16).

Solution 9.1

Step 1: Calculate σ'_{zo} and e_o at the center of the clay layer.

$$\text{Sand: } \gamma_{sat} = \left(\frac{G_s + e}{1 + e} \right) \gamma_w = \left(\frac{2.7 + 0.76}{1 + 0.76} \right) 9.8 = 19.3 \text{ kN/m}^3$$

$$\gamma' = \left(\frac{G_s - 1}{1 + e} \right) \gamma_w = \left(\frac{2.7 - 1}{1 + 0.76} \right) 9.8 = 9.5 \text{ kN/m}^3$$

$$\text{or } \gamma' = \gamma_{sat} - \gamma_w = 19.3 - 9.8 = 9.5 \text{ kN/m}^3$$

$$\text{Clay: } e_o = wG_s = 2.7 \times 0.43 = 1.16$$

$$\gamma' = \left(\frac{G_s - 1}{1 + e} \right) \gamma_w = \left(\frac{2.7 - 1}{1 + 1.16} \right) 9.8 = 7.7 \text{ kN/m}^3$$

The vertical effective stress at the mid-depth of the clay layer is

$$\sigma'_{zo} = (19.3 \times 3) + (9.5 \times 7.4) + (7.7 \times 1) = 135.9 \text{ kPa}$$

Step 2: Calculate the increase of stress at the mid-depth of the clay layer. You do not need to calculate $\Delta\sigma_z$ for this problem. It is given as $\Delta\sigma_z = 140 \text{ kPa}$.

Step 3: Calculate σ'_{fin} .

$$\sigma'_{fin} = \sigma'_{zo} + \Delta\sigma_z = 135.9 + 140 = 275.9 \text{ kPa}$$

Step 4: Calculate the primary consolidation settlement.

$$\rho_{pc} = \frac{H_o}{1 + e_o} C_c \log \frac{\sigma'_{fin}}{\sigma'_{zo}} = \frac{2}{1 + 1.16} \times 0.3 \log \frac{275.9}{135.9} = 0.085 \text{ m} = 85 \text{ mm}$$

EXAMPLE 9.2 Consolidation Settlement of an Overconsolidated Clay

Assume the same soil stratigraphy as in Example 9.1. But now the clay is overconsolidated with an $OCR = 2.5$, $w = 38\%$, and $C_r = 0.05$. All other soil values given in Example 9.1 remain unchanged. Determine the primary consolidation settlement of the clay.

Strategy Since the soil is overconsolidated, you will have to check whether σ'_{zc} is less than or greater than the sum of the current vertical effective stress and the applied vertical stress increase at the center of the clay. This check will determine the appropriate equation to use. In this problem, the unit weight of the sand is unchanged but the clay has changed.

Solution 9.2

Step 1: Calculate σ'_{zo} and e_o at mid-depth of the clay layer.

You should note that this settlement is small compared with the settlement obtained in Example 9.1.

$$\text{Clay: } e_o = wG_s = 0.38 \times 2.7 = 1.03$$

$$\gamma' = \left(\frac{G_s - 1}{1 + e} \right) \gamma_w = \left(\frac{2.7 - 1}{1 + 1.03} \right) 9.8 = 8.2 \text{ kN/m}^3$$

$$\sigma'_{zo} = (19.3 \times 3) + (9.5 \times 7.4) + (8.2 \times 1) = 136.4 \text{ kPa}$$

(Note that the increase in vertical effective stress from the unit weight change in this overconsolidated clay is very small.)

Step 2: Calculate the past maximum vertical effective stress.

$$\sigma'_{zc} = \sigma'_{zo} \times OCR = 136.4 \times 2.5 = 341 \text{ kPa}$$

Step 3: Calculate σ'_{fin} .

$$\sigma'_{fin} = \sigma'_{zo} + \Delta\sigma_z = 136.4 + 140 = 276.4 \text{ kPa}$$

Step 4: Check if σ'_{fin} is less than or greater than σ'_{zc} .

$$(\sigma'_{fin} = 276.4 \text{ kPa}) < (\sigma'_{zc} = 341 \text{ kPa})$$

Therefore, use Equation (9.17).

Step 5: Calculate the total primary consolidation settlement.

$$\rho_{pc} = \frac{H_o}{1 + e_o} C_r \log \frac{\sigma'_{fin}}{\sigma'_{zo}} = \frac{2}{1 + 1.03} \times 0.05 \log \frac{276.4}{136.4} = 0.015 \text{ m} = 15 \text{ mm}$$

EXAMPLE 9.3 Consolidation Settlement of a Lightly Overconsolidated Clay

Assume the same soil stratigraphy and soil parameters as in Example 9.2 except that the clay has an overconsolidation ratio of 1.5. Determine the primary consolidation settlement of the clay.

Strategy Since the soil is overconsolidated, you will have to check whether σ'_{zc} is less than or greater than the sum of the current vertical effective stress and the applied vertical stress at the center of the clay. This check will determine the appropriate equation to use.

Solution 9.3

Step 1: Calculate σ'_{zo} and e_o .

From Example 9.2, $\sigma'_{zo} = 136.4$ kPa.

Step 2: Calculate the past maximum vertical effective stress.

$$\sigma'_{zc} = \sigma'_{zo} \times \text{OCR} = 136.4 \times 1.5 = 204.6 \text{ kPa}$$

Step 3: Calculate σ'_{fin} .

$$\sigma'_{fin} = \sigma'_{zo} + \Delta\sigma_z = 136.4 + 140 = 276.4 \text{ kPa}$$

Step 4: Check if σ'_{fin} is less than or greater than σ'_{zc} .

$$(\sigma'_{fin} = 276.4 \text{ kPa}) > (\sigma'_{zc} = 204.6 \text{ kPa})$$

Therefore, use either Equation (9.18) or (9.19).

Step 5: Calculate the total primary consolidation settlement.

$$\rho_{pc} = \frac{H_o}{1 + e_o} \left(C_r \log \frac{\sigma'_{zc}}{\sigma'_{zo}} + C_c \log \frac{\sigma'_{fin}}{\sigma'_{zc}} \right) = \frac{2}{1 + 1.03} \times \left(0.05 \log \frac{204.6}{136.4} + 0.3 \log \frac{276.4}{204.6} \right) = 0.047 \text{ m} = 47 \text{ mm}$$

or

$$\rho_{pc} = \frac{H_o}{1 + e_o} \left[C_r \log (\text{OCR}) + C_c \log \frac{\sigma'_{fin}}{\sigma'_{zc}} \right] = \frac{2}{1 + 1.03} \times \left(0.05 \log 1.5 + 0.3 \log \frac{276.4}{204.6} \right) = 0.047 \text{ m} = 47 \text{ mm}$$

EXAMPLE 9.4 Consolidation Settlement Using m_v

A vertical section through a building foundation at a site is shown in Figure E9.4. The average modulus of volume compressibility of the clay is $m_v = 5 \times 10^{-5} \text{ m}^2/\text{kN}$. Determine the primary consolidation settlement.

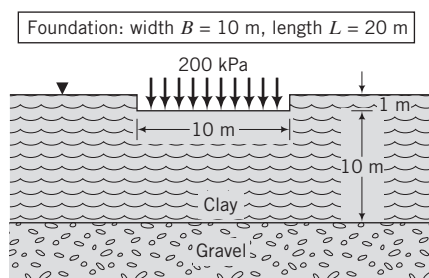


FIGURE E9.4

Strategy To find the primary consolidation settlement, you need to know the vertical stress increase in the clay layer from the building load. Since the clay layer is finite, we will have to use the vertical stress influence values in Appendix C. If we assume a rough base, we can use the influence values specified by Milovic and Tournier (1971) or, if we assume a smooth base, we can use the values specified by Sovinc (1961). The clay layer is 10 m thick, so it is best to subdivide the clay layer into sublayers ≤ 2 m thick.

Solution 9.4

Step 1: Find the vertical stress increase at the center of the clay layer below the foundation. Divide the clay layer into five sublayers, each of thickness 2 m—that is, $H_o = 2$ m. Find the vertical stress increase at the middle of each sublayer under the center of the rectangular foundation. Assume a rough base and use Table C1 (Appendix C).

$$B = 10 \text{ m}, \quad L = 20 \text{ m}, \quad \frac{L}{B} = 2, \quad q_s = 200 \text{ kPa}$$

Layer	z (m)	$\frac{z}{B}$	I_{zp}	$\Delta\sigma_z = I_{zp}q_s$ (kPa)
1	1	0.1	0.992	198.4
2	3	0.3	0.951	190.2
3	5	0.5	0.876	175.2
4	7	0.7	0.781	156.2
5	9	0.9	0.686	137.2

Step 2: Calculate the primary consolidation settlement.

Use Equation (9.20).

$$\rho_{pc} = \sum_{i=1}^n (H_o m_v \Delta\sigma_z)_i = 2 \times 5 \times 10^{-5} \times (198.4 + 190.2 + 175.2 + 156.2 + 137.2) = 0.086 \text{ m} = 86 \text{ mm}$$

Alternatively:

Use the harmonic mean value of $\Delta\sigma_z$ with $n = 5$; that is, Equation (9.21).

$$\Delta\sigma_z = \frac{5(198.4) + 4(190.2) + 3(175.2) + 2(156.2) + 1(137.2)}{5 + 4 + 3 + 2 + 1} = 181.9 \text{ kPa}$$

$$\rho_{pc} = 10 \times 5 \times 10^{-5} \times 181.9 = 0.091 \text{ m} = 91 \text{ mm}$$

The greater settlement in this method results from the bias toward the top layer.

EXAMPLE 9.5 Estimating OCR Variation with Depth

A laboratory test on a saturated clay taken at a depth of 10 m below the ground surface gave the following results: $C_c = 0.3$, $C_r = 0.08$, $OCR = 5$, $w = 23\%$, and $G_s = 2.7$. The groundwater level is at the surface. Determine and plot the variation of water content and overconsolidation ratio with depth up to 50 m.

Strategy The overconsolidation state lies on the unloading/reloading line (Figure 9.3), so you need to find an equation for this line using the data given. Identify what given data are relevant to finding the equation for the unloading/reloading line. Here you are given the slope, C_r , so you need to use the other data to find the complete question. You can find the coordinate of one point on the unloading/reloading line from the water content and the depth, as shown in Step 1.

Solution 9.5

Step 1: Determine e_o and σ'_{zo} .

The soil is saturated, so $S = 1$.

$$\gamma' = \left(\frac{G_s - 1}{1 + e} \right) \gamma_w = \left(\frac{2.7 - 1}{1 + 0.621} \right) 9.8 = 10.3 \text{ kN/m}^3$$

$$e_o = G_s w = 2.7 \times 0.23 = 0.621$$

$$\sigma'_{zo} = \gamma' z = 10.3 \times 10 = 103 \text{ kPa}$$

Step 2: Determine the past maximum vertical effective stress.

$$\sigma'_{zc} = \sigma'_{zo} \times \text{OCR} = 103 \times 5 = 515 \text{ kPa}$$

Step 3: Find the equation for the URL (slope BC in Figure E9.5a).

$$e_B = e_o - C_r \log \frac{\sigma'_{zc}}{\sigma'_{zo}}$$

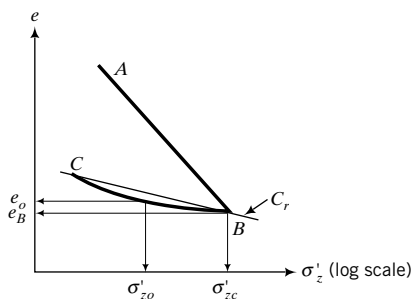


FIGURE E9.5a

Therefore,

$$e_B = 0.621 - 0.08 \log (5) = 0.565$$

Hence, the equation for the unloading/reloading line is

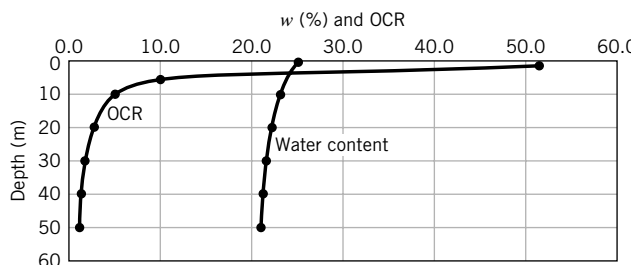
$$e = 0.565 + 0.08 \log (\text{OCR}) \quad (1)$$

Substituting $e = wG_s$ ($G_s = 2.7$) and $\text{OCR} = 515/\gamma'z$ ($\gamma' = 10.3 \text{ kN/m}^3$, z is depth) in Equation (1) gives

$$w = 0.209 + 0.03 \log \left(\frac{50}{z} \right)$$

You can now substitute values of z from 1 to 50 and find w and then substitute $e = wG_s$ in Equation (1) to find the OCR. The table below shows the calculated values and the results, which are plotted in Figure E9.5b.

Depth	w(%)	OCR
1	26.0	51.4
5	23.9	10
10	23.0	5
20	22.1	2.5
30	21.6	1.7
40	21.2	1.2
50	20.9	1.0

**FIGURE E9.5b**

You should note that the soil becomes normally consolidated as the depth increases. This is a characteristic of real soils.

What's next . . . So far, we have only considered how to determine the final primary consolidation settlement. This settlement might take months or years to occur, depending essentially on the hydraulic conductivity (permeability) of the soil, the soil thickness, drainage conditions, and the magnitude of the applied stress. Geotechnical engineers have to know the magnitude of the final primary consolidation settlement and also the rate of settlement so that the settlement at any given time can be evaluated.

The next section deals with a theory to determine the settlement at any time. Several assumptions are made in developing this theory. However, you will see that many of the observations we made in Section 9.3 are well described by this theory.

9.5 ONE-DIMENSIONAL CONSOLIDATION THEORY

9.5.1 Derivation of Governing Equation

We now return to our experiment described in Section 9.3 to derive the theory for time rate of settlement using an element of the soil sample of thickness dz and cross-sectional area $dA = dx dy$ (Figure 9.6). We will assume the following:

1. The soil is saturated, isotropic, and homogeneous.
2. Darcy's law is valid.
3. Flow only occurs vertically.
4. The strains are small.

We will use the following observations made in Section 9.3:

1. The change in volume of the soil (ΔV) is equal to the change in volume of porewater expelled (ΔV_w), which is equal to the change in the volume of the voids (ΔV_v). Since the area of the soil

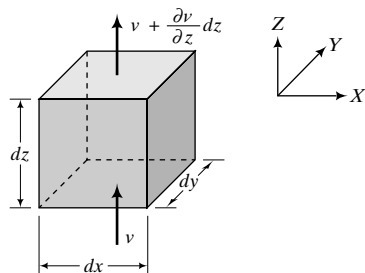


FIGURE 9.6
One-dimensional flow through a two-dimensional soil element.

is constant (the soil is laterally constrained), the change in volume is directly proportional to the change in height.

2. At any depth, the change in vertical effective stress is equal to the change in excess porewater pressure at that depth. That is, $\partial\sigma'_z = \partial u$.

For our soil element in Figure 9.6, the inflow of water is $v dA$ and the outflow over the elemental thickness dz is $[v + (\partial v / \partial z)dz] dA$. Recall from Chapter 6 that the flow rate is the product of the velocity and the cross-sectional area normal to its (velocity) direction. The change in flow is then $(\partial v / \partial z)dz dA$. The rate of change in volume of water expelled, which is equal to the rate of change of volume of the soil, must equal the change in flow. That is,

$$\frac{\partial V}{\partial t} = \frac{\partial v}{\partial z} dz dA \quad (9.22)$$

Recall [Equation (9.2)] that the volumetric strain $\epsilon_p = \partial V/V = \partial e/(1 + e_o)$, and therefore

$$\partial V = \frac{\partial e}{1 + e_o} dz dA = m_v \partial\sigma'_z dz dA = m_v \partial u dz dA \quad (9.23)$$

Substituting Equation (9.23) into Equation (9.22) and simplifying, we obtain

$$\frac{\partial v}{\partial z} = \frac{\partial u}{\partial t} m_v \quad (9.24)$$

The one-dimensional flow of water from Darcy's law is

$$v = k_z i = k_z \frac{\partial h}{\partial z} \quad (9.25)$$

where k_z is the hydraulic conductivity in the vertical direction.

Partial differentiation of Equation (9.25) with respect to z gives

$$\frac{\partial v}{\partial z} = k_z \frac{\partial^2 h}{\partial z^2} \quad (9.26)$$

The porewater pressure at any time from our experiment in Section 9.3 is

$$u = h \gamma_w \quad (9.27)$$

where h is the height of water in the burette.

Partial differentiation of Equation (9.27) with respect to z gives

$$\frac{\partial^2 h}{\partial z^2} = \frac{1}{\gamma_w} \frac{\partial^2 u}{\partial z^2} \quad (9.28)$$

By substitution of Equation (9.28) into Equation (9.26), we get

$$\frac{\partial v}{\partial z} = \frac{k_z}{\gamma_w} \frac{\partial^2 u}{\partial z^2} \quad (9.29)$$

Equating Equation (9.24) and Equation (9.29), we obtain

$$\frac{\partial u}{\partial t} = \frac{k_z}{m_v \gamma_w} \frac{\partial^2 u}{\partial z^2} \quad (9.30)$$

We can replace $\frac{k_z}{m_v \gamma_w}$ by a coefficient C_v called the coefficient of consolidation.

The units for C_v are length²/time, for example, cm²/min. Rewriting Equation (9.30) by substituting C_v , we get the general equation for one-dimensional consolidation as

$$\frac{\partial u}{\partial t} = C_v \frac{\partial^2 u}{\partial z^2} \quad (9.31)$$

This equation describes the spatial variation of excess porewater pressure (Δu) with time (t) and depth (z). It is a common equation in many branches of engineering. For example, the heat diffusion equation commonly used in mechanical engineering is similar to Equation (9.31) except that temperature, T , replaces u and heat factor, K , replaces C_v . Equation (9.31) is called the Terzaghi one-dimensional consolidation equation because Terzaghi (1925) developed it.

In the derivation of Equation (9.31), we tacitly assumed that k_z and m_v are constants. This is usually not the case because as the soil consolidates, the void spaces are reduced and k_z decreases. Also, m_v is not linearly related to σ'_z (Figure 9.3c). The consequence of k_z and m_v not being constants is that C_v is not a constant. In practice, C_v is assumed to be a constant, and this assumption is reasonable only if the stress changes are small enough such that k_z and m_v do not change significantly.

THE ESSENTIAL POINTS ARE:

1. The one-dimensional consolidation equation allows us to predict the changes in excess porewater pressure at various depths within the soil with time.
2. We need to know the excess porewater pressure at a desired time because we have to determine the vertical effective stress to calculate the primary consolidation settlement.

What's next . . . In the next section, the solution to the one-dimensional consolidation equation is found for the case where the soil can drain from the top and bottom boundaries using two methods. One method is based on the Fourier series and the other method is based on the finite difference numerical scheme. The latter is simpler in programming and in spreadsheet applications for any boundary condition.

9.5.2 Solution of Governing Consolidation Equation Using Fourier Series

The solution of any differential equation requires a knowledge of the boundary conditions. By specification of the initial distribution of excess porewater pressures at the boundaries, we can obtain solutions for the spatial variation of excess porewater pressure with time and depth. Various distributions of porewater pressures within a soil layer are possible. Two of these are shown in Figure 9.7. One of these is a uniform distribution of initial excess porewater pressure with depth (Figure 9.7a). This may occur in a thin layer of fine-grained soils. The other (Figure 9.7b) is a triangular distribution. This may occur in a thick layer of fine-grained soils.

The boundary conditions for a uniform distribution of initial excess porewater pressure in which double drainage occurs are

When $t = 0$, $\Delta u = \Delta u_o = \Delta\sigma_z$.

At the top boundary, $z = 0$, $\Delta u = 0$.

At the bottom boundary, $z = 2H_{dr}$, $\Delta u = 0$, where H_{dr} is the length of the drainage path.

A solution for the governing consolidation equation, Equation (9.31), which satisfies these boundary conditions, is obtained using the Fourier series,

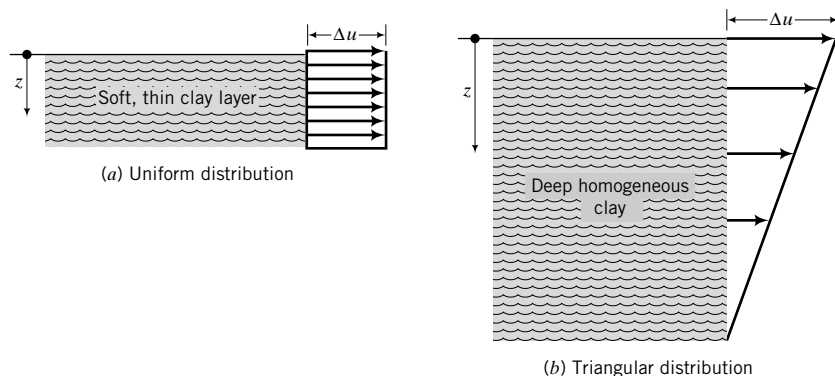


FIGURE 9.7 Two types of excess porewater pressure distribution with depth: (a) uniform distribution with depth in a thin layer and (b) triangular distribution with depth in a thick layer.

$$\Delta u(z, t) = \sum_{m=0}^{\infty} \frac{2\Delta u_o}{M} \sin\left(\frac{Mz}{H_{dr}}\right) \exp(-M^2 T_v) \quad (9.32)$$

where $M = (\pi/2)(2m + 1)$ and m is a positive integer with values from 0 to ∞ and

$$T_v = \frac{C_v t}{H_{dr}^2} \quad (9.33)$$

where T_v is known as the time factor; it is a dimensionless term.

A plot of Equation (9.32) gives the variation of excess porewater pressure with depth at different times. Let us examine Equation (9.32) for an arbitrarily selected isochrone at any time t or time factor T_v , as shown in Figure 9.8. At time $t = 0$ ($T_v = 0$), the initial excess porewater pressure, Δu_o , is equal to the applied vertical stress throughout the soil layer. As soon as drainage occurs, the initial excess porewater pressure will immediately fall to zero at the permeable boundaries. The maximum excess porewater pressure occurs at the center of the soil layer because the drainage path there is the longest, as obtained earlier in our experiment in Section 9.3.

At time $t > 0$, the total applied vertical stress increment $\Delta\sigma_z$ at a depth z is equal to the sum of the vertical effective stress increment $\Delta\sigma'_z$ and the excess porewater pressure Δu_z . After considerable time ($t \rightarrow \infty$), the excess porewater pressure decreases to zero and the vertical effective stress increment becomes equal to the vertical total stress increment.

We now define a parameter, U_z , called the degree of consolidation or consolidation ratio, which gives us the amount of consolidation completed at a particular time and depth. This parameter can be expressed mathematically as

$$U_z = 1 - \frac{\Delta u_z}{\Delta u_o} = 1 - \sum_{m=0}^{\infty} \frac{2}{M} \sin\left(\frac{Mz}{H_{dr}}\right) \exp(-M^2 T_v) \quad (9.34)$$

The consolidation ratio is equal to zero everywhere at the beginning of the consolidation $\Delta u_z = \Delta u_o$ but increases to unity as the initial excess porewater pressure dissipates.

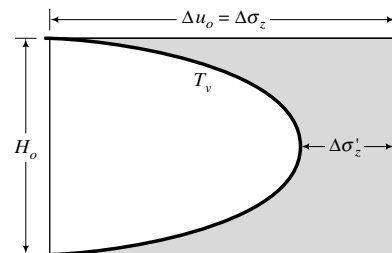


FIGURE 9.8
An isochrone illustrating the theoretical excess porewater pressure distribution with depth.

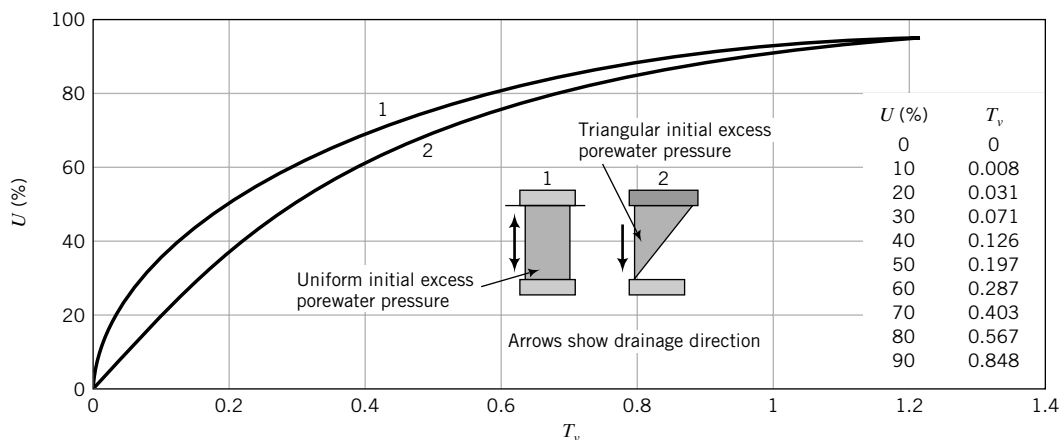


FIGURE 9.9 Relationship between time factor and average degree of consolidation for a uniform distribution and a triangular distribution of initial excess porewater pressure.

A geotechnical engineer is often concerned with the average degree of consolidation, U , of a whole layer at a particular time rather than the consolidation at a particular depth. The shaded area in Figure 9.8 represents the amount of consolidation of a soil layer at any given time. The average degree of consolidation can be expressed mathematically from the solution of the one-dimensional consolidation equation as

$$U = 1 - \sum_{m=0}^{\infty} \frac{2}{M^2} \exp(-M^2 T_v) \quad (9.35)$$

Figure 9.9 shows the variation of the average degree of consolidation with time factor T_v for a uniform and a triangular distribution of excess porewater pressure.

A convenient set of equations for double drainage, found by the curve fitting Figure 9.9, is

$$T_v = \frac{\pi}{4} \left(\frac{U}{100} \right)^2 \quad \text{for } U < 60\% \quad (9.36)$$

and

$$T_v = 1.781 - 0.933 \log(100 - U) \quad \text{for } U \geq 60\% \quad (9.37)$$

The time factor corresponding to every 10% of average degree of consolidation for double drainage conditions is shown in the inset table in Figure 9.9. The time factors corresponding to 50% and 90% consolidation are often used in interpreting consolidation test results. You should remember that $T_v = 0.848$ for 90% consolidation, and $T_v = 0.197$ for 50% consolidation.

9.5.3 Finite Difference Solution of the Governing Consolidation Equation



Computer Program Utility

Access www.wiley.com/college/budhu and click on Chapter 9 for a spreadsheet solution of the finite difference equation of the one-dimensional consolidation equation. You can modify the copy of this spreadsheet to solve other problems. Read this section before accessing the spreadsheet.

Numerical methods (finite difference, finite element, and boundary element) provide approximate solutions to differential and integral equations for boundary conditions in which closed-form solutions

(analytical solutions) are not possible. We will use the finite difference method here to find a solution to the consolidation equation because it involves only the expansion of the differential equation using Taylor's theorem and can easily be adopted for spreadsheet applications.

Using Taylor's theorem,

$$\frac{\partial u}{\partial t} = \frac{1}{\Delta t}(u_{i,j+1} - u_{i,j}) \quad (9.38)$$

and

$$\frac{\partial^2 u}{\partial z^2} = \frac{1}{(\Delta z)^2}(u_{i-1,j} - 2u_{i,j} + u_{i+1,j}) \quad (9.39)$$

where (i, j) denotes a nodal position at the intersection of row i and column j . Columns represent time divisions and rows represent soil depth divisions. The assumption implicit in Equation (9.38) is that the excess porewater pressure between two adjacent nodes changes linearly with time. This assumption is reasonable if the distance between the two nodes is small. Substituting Equations (9.38) and (9.39) in the governing consolidation equation (9.31) and rearranging, we get

$$u_{i,j+1} = u_{i,j} + \frac{C_v \Delta t}{(\Delta z)^2}(u_{i-1,j} - 2u_{i,j} + u_{i+1,j}) \quad (9.40)$$

Equation (9.40) is valid for nodes that are not boundary nodes. There are special conditions that apply to boundary nodes. For example, at an impermeable boundary, no flow across it can occur and, consequently, $\partial u / \partial z = 0$, for which the finite difference equation is

$$\frac{\partial u}{\partial z} = 0 = \frac{1}{2\Delta z}(u_{i-1,j} - u_{i+1,j}) = 0 \quad (9.41)$$

and the governing consolidation equation becomes

$$u_{i,j+1} = u_{i,j} + \frac{C_v \Delta t}{(\Delta z)^2}(2u_{i-1,j} - 2u_{i,j}) \quad (9.42)$$

To determine how the porewater pressure is distributed within a soil at a given time, we have to establish the initial excess porewater pressure at the boundaries. Once we do this, we have to estimate the variation of the initial excess porewater pressure within the soil. We may, for example, assume a linear distribution of initial excess porewater pressure with depth if the soil layer is thin or has a triangular distribution for a thick soil layer. If you cannot estimate the initial excess porewater pressure, you can guess reasonable values for the interior of the soil or use linear interpolation. Then you successively apply Equation (9.40) to each interior nodal point and replace the old value by the newly calculated value until the old value and the new value differ by a small tolerance. At impermeable boundaries, you have to apply Equation (9.42).

The procedure to apply the finite difference form of the governing consolidation equation to determine the variation of excess porewater pressure with time and depth is as follows:

1. Divide the soil layer into a depth-time grid (Figure 9.10). Rows represent subdivisions of the depth, columns represent subdivisions of time. Let's say we divide the depth into m rows and the time into n columns; then $\Delta z = H_o/m$ and $\Delta t = t/n$, where H_o is the thickness of the soil layer and t is the total time. A nodal point represents the i th depth position and the j th elapsed time. To avoid convergence problems, researchers have found that $\alpha = C_v \Delta t / (\Delta z)^2$ must be less than $\frac{1}{2}$. This places a limit on the number of subdivisions in the grid. Often, the depth is subdivided arbitrarily and the time step Δt is selected so that $\alpha < \frac{1}{2}$. In many practical situations, $\alpha = 0.25$ usually ensures convergence.

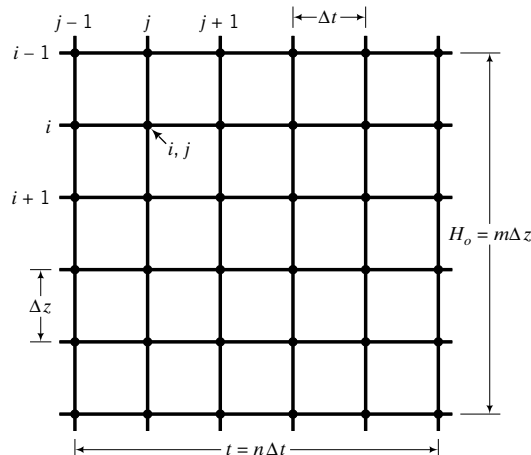


FIGURE 9.10 Division of a soil layer into a depth (row)-time (column) grid.

2. Identify the boundary conditions. For example, if the top boundary is a drainage boundary, then the excess porewater pressure there is zero. If, however, the top boundary is an impermeable boundary, then no flow can occur across it and Equation (9.42) applies.
3. Estimate the distribution of initial excess porewater pressure and determine the nodal initial excess porewater pressures.
4. Calculate the excess porewater pressure at interior nodes using Equation (9.40) and at impermeable boundary nodes using Equation (9.42). If the boundary is permeable, then the excess porewater pressure is zero at all nodes on this boundary.

THE ESSENTIAL POINTS ARE:

1. An ideal soil (isotropic, homogeneous, saturated) is assumed in developing the governing one-dimensional consolidation equation.
2. Strains are assumed to be small.
3. Excess porewater pressure dissipation depends on time, soil thickness, drainage conditions, and the hydraulic conductivity (permeability) of the soil.
4. The decrease in initial excess porewater pressure causes an equivalent increase in vertical effective stress and settlement increases.
5. The average degree of consolidation is conventionally used to find the time rate of settlement.

EXAMPLE 9.6 Change in Vertical Effective Stress at a Given Degree of Consolidation

A soft clay layer 1.5 m thick is sandwiched between layers of sand. The initial vertical total stress at the center of the clay layer is 200 kPa and the porewater pressure is 100 kPa. The increase in vertical stress at the center of the clay layer from a building foundation is 100 kPa. What are the vertical effective stress and excess porewater pressure at the center of the clay layer when 60% consolidation occurs?

Strategy You are given the increment in applied stress and the degree of consolidation. You know that the initial change in excess porewater pressure is equal to the change in applied vertical stress. From the data given, decide on the appropriate equation, which in this case is Equation (9.34).

Solution 9.6

Step 1: Calculate the initial excess porewater pressure.

$$\Delta u_o = \Delta \sigma_z = 100 \text{ kPa}$$

Step 2: Calculate the current excess porewater pressure at 60% consolidation.

$$\Delta u_z = \Delta u_o(1 - U_z) = 100(1 - 0.6) = 40 \text{ kPa}$$

Step 3: Calculate the vertical total stress and total excess porewater pressure.

$$\text{Vertical total stress: } \Delta \sigma_z = 200 + 100 = 300 \text{ kPa}$$

$$\text{Total porewater pressure: } 100 + 40 = 140 \text{ kPa}$$

Step 4: Calculate the current vertical effective stress.

$$\sigma'_z = \sigma_z - \Delta u_z = 300 - 140 = 160 \text{ kPa}$$

Alternatively:

Step 1: Calculate the initial vertical effective stress.

$$\text{Initial vertical effective stress} = 200 - 100 = 100 \text{ kPa}$$

Step 2: Same as Step 2 above.

Step 3: Calculate the increase in vertical effective stress at 60% consolidation.

$$\Delta \sigma'_z = 100 - 40 = 60 \text{ kPa}$$

Step 4: Calculate the current vertical effective stress.

$$\sigma'_z = 100 + 60 = 160 \text{ kPa}$$

EXAMPLE 9.7 Application of Finite Difference Method to Calculate Porewater Pressure Distribution

A layer of soft clay, 5 m thick, is drained at the top surface only. The initial excess porewater pressure from an applied load at time $t = 0$ is distributed according to $\Delta u_o = 80 - 2z^2$, where z is the depth measured from the top boundary. Determine the distribution of excess porewater pressure with depth after 6 months using the finite difference method. The coefficient of consolidation, C_v , is $8 \times 10^{-4} \text{ cm}^2/\text{s}$.

Strategy Divide the clay layer into, say, five equal layers of 1 m thickness and find the value of the initial excess porewater pressure at each node at time $t = 0$ using $\Delta u_o = 80 - 2z^2$. Then find a time step Δt that will lead to $\alpha < \frac{1}{2}$. The top boundary is a drainage boundary. Therefore, the excess porewater pressure is zero for all times at all nodes along this boundary. Use a spreadsheet or write a short program to do the iterations to solve the governing consolidation equation. You must note that the bottom boundary is not a drainage boundary, and the relevant equation to use for the nodes at this boundary is Equation (9.42).

Solution 9.7

Step 1: Divide the soil layer into a grid.

Divide the depth into five layers, that is, $m = 5$.

$$\Delta z = \frac{H_o}{m} = \frac{5}{5} = 1 \text{ m}$$

$$C_v = 8 \times 10^{-4} \text{ cm}^2/\text{s} = 8 \times 10^{-8} \text{ m}^2/\text{s} = 2.52 \text{ m}^2/\text{yr}$$

Assume five time steps, that is, $n = 5$ and $\Delta t = \frac{t}{n} = \frac{0.5}{5} = 0.1$ yr.

$$\alpha = \frac{C_v \Delta t}{\Delta z^2} = \frac{2.52 \times 0.1}{1^2} = 0.252 < 0.5$$

Step 2: Identify boundary conditions.

The bottom boundary is impermeable; therefore, Equation (9.42) applies to the nodes along this boundary. The top boundary is pervious; therefore, the excess porewater pressure is zero at all times greater than zero.

Step 3: Determine the distribution of initial excess porewater pressure.

You are given the distribution of initial excess porewater pressure as $\Delta u_o = 80 - 2z^2$. At time $t = 0$ (column 1), insert the nodal values of initial excess porewater pressure. For example, at row 2, column 1 (node 2), $\Delta u_o = 80 - 2 \times 1^2 = 78$ kPa. The initial excess porewater pressures are listed in column 1; see the table below.

Step 4: Calculate the excess porewater pressure at each node of the grid. The governing equation, except at the impermeable boundary, is

$$u_{i,j+1} = u_{i,j} + 0.252(u_{i-1,j} - 2u_{i,j} + u_{i+1,j})$$

Let us calculate the excess porewater pressure after 0.1 yr at the node located at row 2, column 2.

$$u_{2,1+1} = 78 + 0.252(0 - 2 \times 78 + 72) = 57 \text{ kPa}$$

At the bottom impermeable boundary (row 6, column 2), we have to apply Equation (9.42), which is

$$u_{i,j+1} = u_{i,j} + 0.252(2u_{i-1,j} - 2u_{i,j})$$

Therefore,

$$u_{6,1+1} = 30 + 0.252(2 \times 48 - 2 \times 30) = 39 \text{ kPa}$$

The complete results after 6 months using a spreadsheet are shown in the table below. The results are plotted in Figure E9.7.

Column	1	2	3	4	5	6
	Time (yr)					
Depth (m)	0.00	0.10	0.20	0.30	0.4	0.5
0.0	0.0	0.0	0.0	0.0	0.0	0.0
1.0	78.0	57	46.3	39.4	34.5	30.7
2.0	72.0	71	65.0	59.1	54.0	49.7
3.0	62.0	61	60.0	58.4	56.5	54.5
4.0	48.0	47	48.5	50.0	51.0	51.6
5.0	30.0	39	43.0	45.8	47.9	49.5

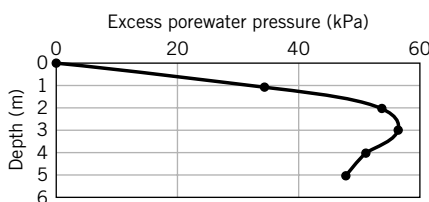


FIGURE E9.7

What's next . . . We have described only primary consolidation settlement. The other part of the total consolidation settlement is secondary compression, which will be discussed next.

9.6 SECONDARY COMPRESSION SETTLEMENT

You will recall from our experiment in Section 9.3 that consolidation settlement consists of two parts. The first part is primary consolidation, which occurs at early times. The second part is secondary compression, or creep, which takes place under a constant vertical effective stress. The physical reasons for secondary compression in soils are not fully understood. One plausible explanation is the expulsion of water from micropores; another is viscous deformation of the soil structure.

We can make a plot of void ratio versus the logarithm of time from our experimental data in Section 9.3, as shown in Figure 9.11. Primary consolidation is assumed to end at the intersection of the projection of the two straight parts of the curve.

The secondary compression index is

$$C_\alpha = -\frac{(e_t - e_p)}{\log(t/t_p)} = \frac{|\Delta e|}{\log(t/t_p)}; \quad t > t_p \quad (9.43)$$

where (t_p, e_p) is the coordinate at the intersection of the tangents to the primary consolidation and secondary compression parts of the logarithm of time versus void ratio curve, and (t, e_t) is the coordinate of any point on the secondary compression curve, as shown in Figure 9.11. The secondary consolidation settlement is

$$\rho_{sc} = \frac{H_o}{(1 + e_p)} C_\alpha \log\left(\frac{t}{t_p}\right) \quad (9.44)$$

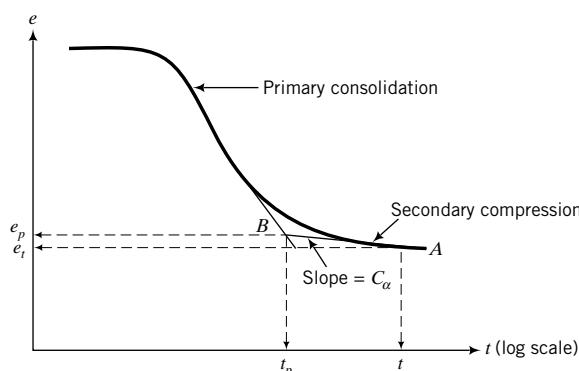


FIGURE 9.11
Secondary compression.

What's next . . . You will recall that there are several unknown parameters in the theoretical solution of the one-dimensional consolidation equation. We need to know these parameters to calculate consolidation settlement and rate of settlement for fine-grained soils. The one-dimensional consolidation test is used to find these parameters. This test is usually one of the tests that you will perform in the laboratory component of your course. In the next section, the test procedures will be briefly discussed, followed by a discussion of the methods used to determine the various soil consolidation parameters.

9.7 ONE-DIMENSIONAL CONSOLIDATION LABORATORY TEST



Virtual Laboratory

Access www.wiley.com/college/budhu and click on Chapter 9 for a virtual consolidation test.

9.7.1 Oedometer Test

The one-dimensional consolidation test, called the oedometer test, is used to find C_c , C_r , C_α , C_v , m_v , and σ'_{zc} . The hydraulic conductivity, k_z , can also be calculated from the test data. The experimental arrangement we used in Section 9.3 is similar to an oedometer test setup. The details of the test apparatus and the testing procedures are described in ASTM D 2435. A disk of soil is enclosed in a stiff metal ring and placed between two porous stones in a cylindrical container filled with water, as shown in Figure 9.12. A metal load platen mounted on top of the upper porous stone transmits the applied vertical stress (vertical total stress) to the soil sample. Both the metal platen and the upper porous stone can move vertically inside the ring as the soil settles under the applied vertical stress. The ring containing the soil sample can be fixed to the container by a collar (fixed ring cell, Figure 9.12b) or is unrestrained (floating ring cell, Figure 9.12c).

Incremental loads, including unloading sequences, are applied to the platen, and the settlement of the soil at various fixed times under each load increment is measured by a displacement gage. Each load increment is allowed to remain on the soil until the change in settlement is negligible and the excess porewater pressure developed under the current load increment has dissipated. For many soils, this usually occurs within 24 hours, but longer monitoring times may be required for exceptional soil types, for example, montmorillonite. Each load increment is doubled. The ratio of the load increment to the previous load is called the load increment ratio (LIR); conventionally, LIR = 1. To determine C_r , the soil sample is unloaded using a load decrement ratio—load decrement divided by current load—of 2.

At the end of the oedometer test, the apparatus is dismantled and the water content of the sample is determined. It is best to unload the soil sample to a small pressure before dismantling the apparatus, because if you remove the final consolidation load completely, a negative excess porewater pressure

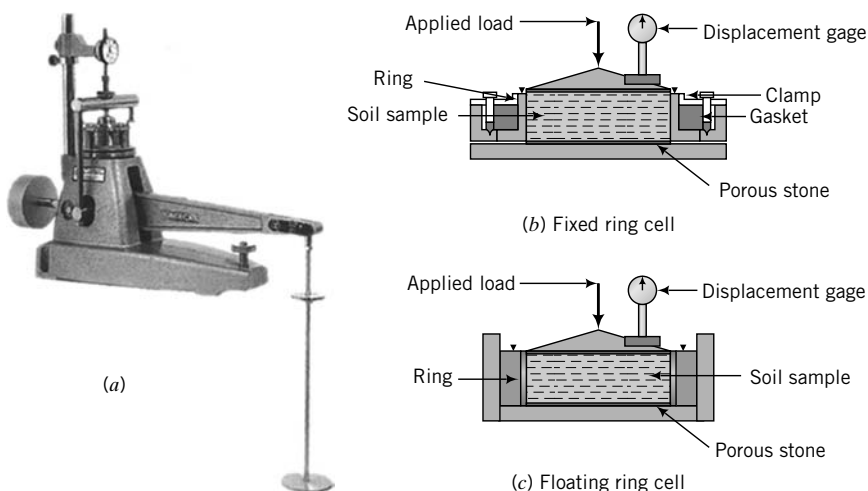


FIGURE 9.12 (a) A typical consolidation apparatus (photo courtesy of Geotest), (b) a fixed ring cell, and (c) a floating ring cell.

that equals the final consolidation pressure will develop. This negative excess porewater pressure can cause water to flow into the soil and increase the soil's water content. Consequently, the final void ratio calculated from the final water content will be erroneous.

The data obtained from the one-dimensional consolidation test are as follows:

1. Initial height of the soil, H_o , which is fixed by the height of the ring.
2. Current height of the soil at various time intervals under each load (time-settlement data).
3. Water content at the beginning and at the end of the test, and the dry weight of the soil at the end of the test.

You now have to use these data to determine C_c , C_r , C_α , C_v , m_v , and σ'_{zc} . We will start with finding C_v .

9.7.2 Determination of the Coefficient of Consolidation

There are two popular methods that can be used to calculate C_v . Taylor (1942) proposed one method, called the root time method. Casagrande and Fadum (1940) proposed the other method, called the log time method. The root time method utilizes the early time response, which theoretically should appear as a straight line in a plot of square root of time versus displacement gage reading.

9.7.2.1 Root Time Method (Square Root Time Method) Let us arbitrarily choose a point, C , on the displacement versus square root of time factor gage reading, as shown in Figure 9.13. We will assume that this point corresponds to 90% consolidation ($U = 90\%$) for which $T_v = 0.848$ (Figure 9.9). If point C were to lie on a straight line, the theoretical relationship between U and T_v would be $U = 0.98\sqrt{T_v}$; that is, if you substitute $T_v = 0.848$, you get $U = 90\%$.

At early times, the theoretical relationship between U and T_v is given by Equation (9.36); that is,

$$U = \sqrt{\frac{4}{\pi} T_v} = 1.13\sqrt{T_v}; \quad U < 0.6$$

The laboratory early time response is represented by the straight line OA in Figure 9.13. You should note that O is below the initial displacement gage reading because there is an initial compression of the

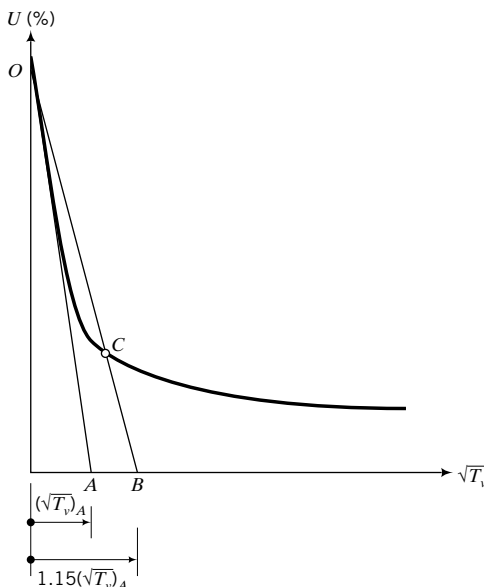


FIGURE 9.13 Correction of laboratory early time response to determine C_v .

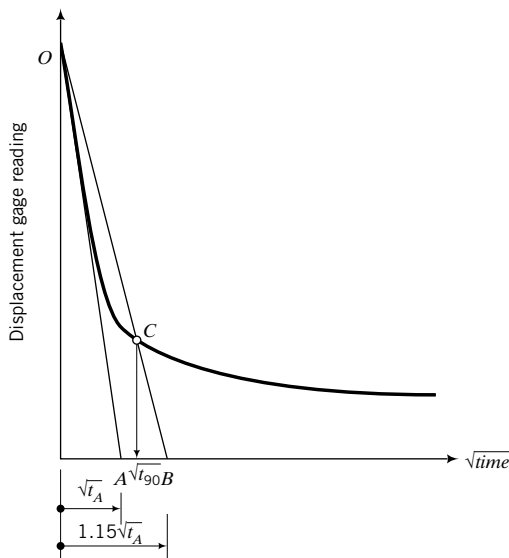


FIGURE 9.14
Root time method to determine C_v .

soil before consolidation begins. This compression can be due to the breaking of particle bonds in lightly cemented soils. The ratio of the gradient of OA and the gradient of the theoretical early time response, line OCB , is

$$\frac{1.13\sqrt{T_v}}{0.98\sqrt{T_v}} = 1.15$$

We can use this ratio to establish the time when 90% consolidation is achieved in the one-dimensional consolidation test.

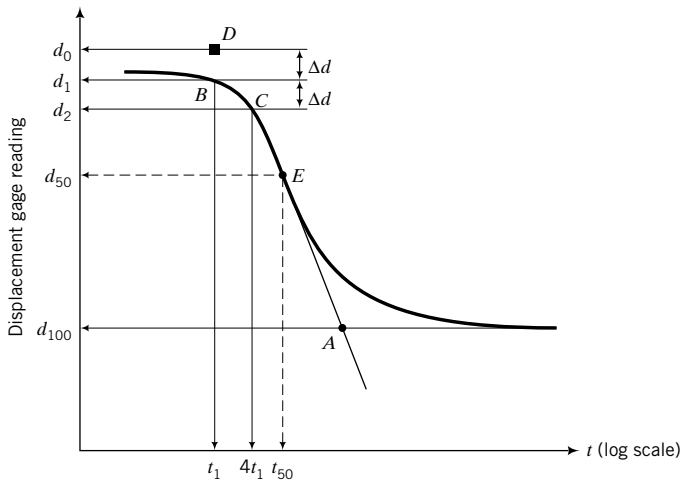
The procedure, with reference to Figure 9.14, is as follows:

1. Plot the displacement gage readings versus square root of times.
2. Draw the best straight line through the initial part of the curve intersecting the ordinate (displacement reading) at O and the abscissa ($\sqrt{\text{time}}$) at A .
3. Note the time at point A ; let us say it is $\sqrt{t_A}$.
4. Locate a point B , $1.15\sqrt{t_A}$, on the abscissa.
5. Join OB .
6. The intersection of the line OB with the curve, point C , gives the displacement gage reading and the time for 90% consolidation (t_{90}). You should note that the value read off the abscissa is $\sqrt{t_{90}}$. Now when $U = 90\%$, $T_v = 0.848$ (Figure 9.9) and from Equation (9.31) we obtain

$$C_v = \frac{0.848H_{dr}^2}{t_{90}} \quad (9.45)$$

where H_{dr} is the length of the drainage path.

9.7.2.2 Log Time Method In the log time method, the displacement gage readings are plotted against the times (log scale). The logarithm of times is arbitrary and is only used for convenience. A typical curve obtained is shown in Figure 9.15. The theoretical early time settlement response in a plot of

**FIGURE 9.15** Root time method to determine C_v .

logarithm of times versus displacement gage readings is a parabola (Section 9.3). The experimental early time curve is not normally a parabola, and a correction is often required.

The procedure, with reference to Figure 9.15, is as follows:

1. Project the straight portions of the primary consolidation and secondary compression to intersect at A . The ordinate of A , d_{100} , is the displacement gage reading for 100% primary consolidation.
2. Correct the initial portion of the curve to make it a parabola. Select a time t_1 , point B , near the head of the initial portion of the curve ($U < 60\%$) and then another time t_2 , point C , such that $t_2 = 4t_1$.
3. Calculate the difference in displacement reading, $\Delta d = d_2 - d_1$, between t_2 and t_1 . Plot a point D at a vertical distance Δd from B . The ordinate of point D is the corrected initial displacement gage reading, d_o , at the beginning of primary consolidation.
4. Calculate the ordinate for 50% consolidation as $d_{50} = (d_{100} + d_o)/2$. Draw a horizontal line through this point to intersect the curve at E . The abscissa of point E is the time for 50% consolidation, t_{50} .
5. You will recall (Figure 9.9) that the time factor for 50% consolidation is 0.197, and from Equation (9.31) we obtain

$$C_v = \frac{0.197 H_{dr}^2}{t_{50}} \quad (9.46)$$

The log time method makes use of the early (primary consolidation) and later time responses (secondary compression), while the root time method only utilizes the early time response, which is expected to be a straight line. In theory, the root time method should give good results except when nonlinearities arising from secondary compression cause substantial deviations from the expected straight line. These deviations are most pronounced in fine-grained soils with organic materials.

9.7.3 Determination of Void Ratio at the End of a Loading Step

To determine σ'_{zc} , C_c , C_r , and C_α , we need to know the void ratio for each loading step. Recall that at the end of the consolidation test, we determined the water content (w) of the soil sample. Using these data, initial height (H_o), and the specific gravity (G_s) of the soil sample, you can calculate the void ratio for each loading step as follows:

1. Calculate the final void ratio, $e_{fin} = wG_s$, where w is the water content determined at the end of the test.

2. Calculate the total consolidation settlement of the soil sample during the test, $(\Delta z)_{fin} = d_{fin} - d_i$, where d_{fin} is the final displacement gage reading and d_i is the displacement gage reading at the start of the test.
3. Back-calculate the initial void ratio, using Equation (9.7), as

$$e_o = \frac{e_{fin} + \frac{(\Delta z)_{fin}}{H_o}}{1 - \frac{(\Delta z)_{fin}}{H_o}}$$

4. Calculate e for each loading step using Equation (9.6) or Equation (9.7).

9.7.4 Determination of the Past Maximum Vertical Effective Stress

Now that we have calculated e for each loading step, we can plot a graph of the void ratio versus the vertical effective stress (log scale), as shown in Figure 9.16. We will call Figure 9.16 the e versus σ'_z (log scale) curve. You will now determine the past maximum vertical effective stress using a method proposed by Casagrande (1936).

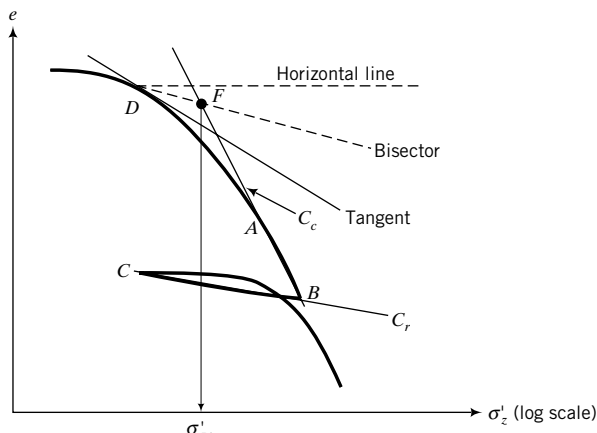
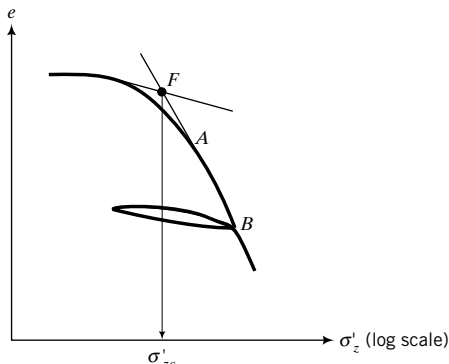


FIGURE 9.16 Determination of the past maximum vertical effective stress using Casagrande's method.

The procedure, with reference to Figure 9.16, is as follows:

1. Identify the point of maximum curvature, point D , on the initial part of the curve.
2. Draw a horizontal line through D .
3. Draw a tangent to the curve at D .
4. Bisect the angle formed by the tangent and the horizontal line at D .
5. Extend backward the straight portion of the curve (the normal consolidation line), BA , to intersect the bisector line at F .
6. The abscissa of F is the past maximum vertical effective stress, σ'_{zc} .

A simpler method that is also used in practice is to project the straight portion of the initial recompression curve to intersect the backward projection of the normal consolidation line at F , as shown in Figure 9.17. The abscissa of F is σ'_{zc} .

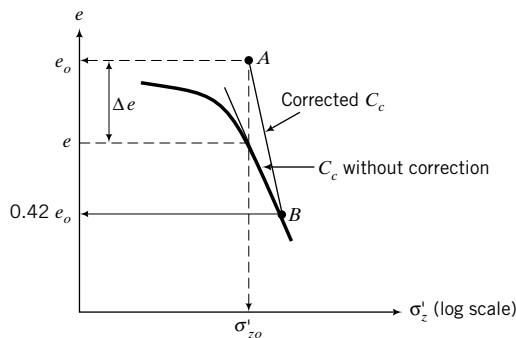
**FIGURE 9.17**

A simplified method of determining the past maximum vertical effective stress.

Both of these methods are based on individual judgment. The actual value of σ'_{zc} for real soils is more difficult to ascertain than described above. Degradation of the soil from its intact condition caused by sampling, transportation, handling, and sample preparation usually does not produce the ideal curve shown in Figure 9.16.

9.7.5 Determination of Compression and Recompression Indices

The slope of the normal consolidation line, BA , gives the compression index, C_c . To determine the recompression index, C_r , draw a line (BC) approximately midway between the unloading and reloading curves (Figure 9.16). The slope of this line is the recompression index (C_r).

**FIGURE 9.18**

Schmertmann's method to correct C_c for soil disturbances.

Field observations indicate that, in many instances, the predictions of the total settlement and the rate of settlement using oedometer test results do not match recorded settlement from actual structures. Disturbances from sampling and sample preparation tend to decrease C_c and C_v . Schmertmann (1953) suggested a correction to the laboratory curve to obtain a more representative in situ value of C_c . His method is as follows. Locate a point A at coordinate (σ'_{zo}, e_o) and a point B at ordinate $0.42e_o$ on the laboratory e versus σ'_z (log scale) curve, as shown in Figure 9.18. The slope of the line AB is the corrected value for C_c .

9.7.6 Determination of the Modulus of Volume Change

The modulus of volume compressibility, m_v , is found from plotting a curve similar to Figure 9.3c and determining the slope, as shown in this figure. You do not need to calculate void ratio to determine m_v . You need the final change in height at the end of each loading (Δz), and then you calculate the vertical strain, $\varepsilon_z = \Delta z/H_o$, where H_o is the initial height. The modulus of volume compressibility is not constant

but depends on the range of vertical effective stress that is used in the calculation. A representative value for m_v can be obtained by finding the slope between the current vertical effective stress and the final vertical effective stress ($\sigma'_{zo} + \Delta\sigma_z$) at the center of the soil layer in the field or 100 kPa, whichever is less.

9.7.7 Determination of the Secondary Compression Index

The secondary compression index, C_α , can be found by making a plot similar to Figure 9.11. You should note that Figure 9.11 is for a single load. The value of C_α usually varies with the magnitude of the applied loads and other factors such as the LIR.

What's next . . . Three examples and their solutions are presented next to show you how to find various consolidation soil parameters, as discussed above. The first two examples are intended to illustrate the determination of the compression indices and how to use them to make predictions. The third example illustrates how to find C_v using the root time method.

EXAMPLE 9.8 Calculating C_c from Test Data

At a vertical stress of 200 kPa, the void ratio of a saturated soil sample tested in an oedometer is 1.52 and lies on the normal consolidation line. An increment of vertical stress of 150 kPa compresses the sample to a void ratio of 1.43.

- Determine the compression index, C_c , of the soil.
- The sample was unloaded to a vertical stress of 200 kPa, and the void ratio increased to 1.45. Determine the slope of the recompression index, C_r .
- What is the overconsolidation ratio of the soil at stage (b)?
- If the soil were reloaded to a vertical stress of 500 kPa, what void ratio would be attained?

Strategy Draw a sketch of the soil response on a plot of vertical effective stress (log scale) versus void ratio. Use this sketch to answer the various questions.

Solution 9.8

Step 1: Determine C_c .

C_c is the slope AB shown in Figure E9.8.

$$C_c = \frac{-(1.43 - 1.52)}{\log(350/200)} = 0.37$$

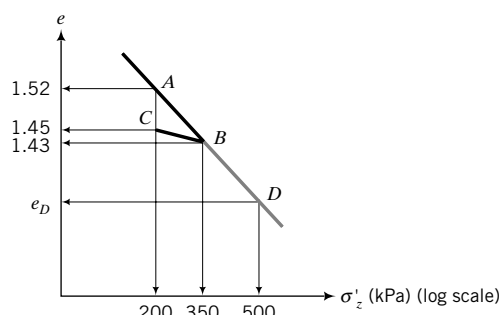


FIGURE E9.8

Step 2: Determine C_r .

C_r is the slope of BC in Figure E9.8.

$$C_r = \frac{-(1.43 - 1.45)}{\log(350/200)} = 0.08$$

Step 3: Determine the overconsolidation ratio.

Past maximum vertical effective stress: $\sigma'_{zc} = 350$ kPa

Current vertical effective stress: $\sigma'_z = 200$ kPa

$$\text{OCR} = \frac{\sigma'_{zc}}{\sigma'_z} = \frac{350}{200} = 1.75$$

Step 4: Calculate the void ratio at 500 kPa.

The void ratio at 500 kPa is the void ratio at D on the normal consolidation line (Figure E9.8).

$$e_D = e_B - C_c \log\left(\frac{500}{350}\right) = 1.43 - 0.37 \log 1.43 = 1.37$$

EXAMPLE 9.9 Determination of Elastic Parameters, m_{vr} and E'_c

During a one-dimensional consolidation test, the height of a normally consolidated soil sample at a vertical effective stress of 200 kPa was 18 mm. The vertical effective stress was reduced to 50 kPa, causing the soil to swell by 0.5 mm. Determine m_{vr} and E'_c .

Strategy From the data, you can find the vertical strain. You know the increase in vertical effective stress, so the appropriate equations to use to calculate m_{vr} and E'_c are Equations (9.11) and (9.12).

Solution 9.9**Step 1:** Calculate the vertical strain.

$$\Delta\varepsilon_{zr} = \frac{\Delta z}{H_o} = \frac{0.5}{18} = 0.028$$

Step 2: Calculate the modulus of volume recompressibility.

$$m_{vr} = \frac{\Delta\varepsilon_{zr}}{\Delta\sigma'_z} = \frac{0.028}{150} = 1.9 \times 10^{-4} \text{ m}^2/\text{kN}$$

Step 3: Calculate the constrained elastic modulus.

$$E'_c = \frac{1}{m_{vr}} = \frac{1}{1.9 \times 10^{-4}} = 5263 \text{ kPa}$$

EXAMPLE 9.10 Determination of C_v Using Root Time Method

The following readings were taken for an increment of vertical stress of 20 kPa in an oedometer test on a saturated clay sample 75 mm in diameter and 20 mm thick. Drainage was permitted from the top and bottom boundaries.

Time (min)	0.25	1	2.25	4	9	16	25	36	24 hours
ΔH (mm)	0.12	0.23	0.33	0.43	0.59	0.68	0.74	0.76	0.89

Determine the coefficient of consolidation using the root time method.

Strategy Plot the data in a graph of displacement reading versus \sqrt{t} and follow the procedures in Section 9.7.2.1.

Solution 9.10

Step 1: Make a plot of settlement (decrease in thickness) versus \sqrt{t} , as shown in Figure E9.10.

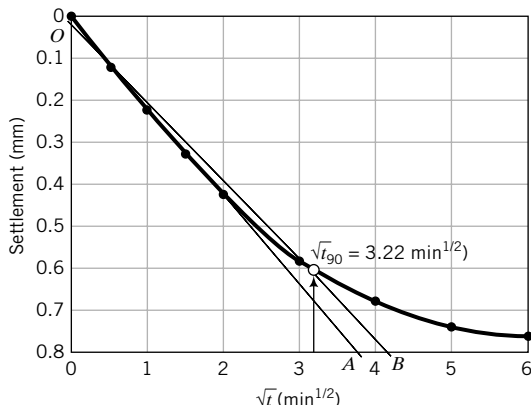


FIGURE E9.10

Step 2: Follow the procedures outlined in Section 9.7.2.1 to find t_{90} .

From Figure E9.10,

$$\sqrt{t_{90}} = 3.22 \text{ min}^{1/2}; \quad t_{90} = 10.4 \text{ min}$$

Step 3: Calculate C_v from Equation (9.45).

$$C_v = \frac{0.848 H_{dr}^2}{t_{90}}$$

where H_{dr} is the length of the drainage path. The current height is $20 - 0.89 = 19.1 \text{ mm}$. From Equation (9.1),

$$H_{dr} = \frac{H_o + H_f}{4} = \frac{20 + 19.1}{4} = 9.8 \text{ mm}$$

$$\therefore C_v = \frac{0.848 \times 9.8^2}{10.4} = 7.8 \text{ mm}^2/\text{min}$$

What's next . . . We have described the consolidation test of a small sample of soil and the soil consolidation parameters that can be obtained. What is the relationship between this small test sample and the soil in the field? Can you readily calculate the settlement of the soil in the field based on the results of your consolidation test? The next section provides the relationship between the small test sample and the soil in the field.

9.8 RELATIONSHIP BETWEEN LABORATORY AND FIELD CONSOLIDATION

The time factor (T_v) provides a useful expression to estimate the settlement in the field from the results of a laboratory consolidation test. If two layers of the same clay have the same degree of consolidation, then their time factors and coefficients of consolidation are the same. Hence,

$$T_v = \frac{(C_v t)_{lab}}{(H_{dr}^2)_{lab}} = \frac{(C_v t)_{field}}{(H_{dr}^2)_{field}} \quad (9.47)$$

and, by simplification,

$$\frac{t_{field}}{t_{lab}} = \frac{(H_{dr}^2)_{field}}{(H_{dr}^2)_{lab}} \quad (9.48)$$

What's next . . . The following example shows you how to find the expected field settlement from consolidation test results for a particular degree of consolidation.

EXAMPLE 9.11 Time-Settlement Calculations

A sample, 75 mm in diameter and 20 mm high, taken from a clay layer 10 m thick, was tested in an oedometer with drainage at the upper and lower boundaries. It took the laboratory sample 15 minutes to reach 50% consolidation.

- (a) If the clay layer in the field has the same drainage condition as the laboratory sample, calculate how long it will take the 10-m clay layer to achieve 50% and 90% consolidation.
- (b) How much more time would it take the 10-m clay layer to achieve 50% consolidation if drainage existed on only one boundary?

Strategy You are given all the data to directly use Equation (9.48). For part (a) there is double drainage in the field and the lab, so the drainage path is one-half the soil thickness. For part (b) there is single drainage in the field, so the drainage path is equal to the soil thickness.

Solution 9.11

- (a) We proceed as follows:

Step 1: Calculate the drainage path.

$$(H_{dr})_{lab} = \frac{20}{2} = 10 \text{ mm} = 0.01 \text{ m}; \quad (H_{dr})_{field} = \frac{10}{2} = 5 \text{ m}$$

Step 2: Calculate the field time using Equation (9.48).

$$t_{field} = \frac{t_{lab}(H_{dr}^2)_{field}}{(H_{dr}^2)_{lab}} = \frac{15 \times 5^2}{0.01^2} = 375 \times 10^4 \text{ min} = 7.13 \text{ years}$$

- (b) We proceed as follows:

Step 1: Calculate the drainage path.

$$(H_{dr})_{lab} = \frac{20}{2} = 10 \text{ mm} = 0.01 \text{ m}; \quad (H_{dr})_{field} = 10 \text{ m}$$

Step 2: Calculate field time using Equation (9.48).

$$t_{field} = \frac{t_{lab}(H_{dr}^2)_{field}}{(H_{dr}^2)_{lab}} = \frac{15 \times 10^2}{0.01} = 15 \times 10^6 \text{ min} = 28.54 \text{ years}$$

You should take note that if drainage exists on only one boundary rather than both boundaries of the clay layer, the time taken for a given percent consolidation in the field is four times longer.

What's next . . . Several empirical equations are available linking consolidation parameters to simple, less time-consuming soil tests such as the Atterberg limits and water content tests. In the next section, some of these relationships are presented.

9.9 TYPICAL VALUES OF CONSOLIDATION SETTLEMENT PARAMETERS AND EMPIRICAL RELATIONSHIPS

Some relationships between simple soil tests and consolidation settlement parameters are given below. You should be cautious in using these relationships because they may not be applicable to your soil type.

Typical range of values

$$C_c = 0.1 \text{ to } 0.8$$

$$C_r = 0.015 \text{ to } 0.35; \text{ also, } C_r \approx C_c/5 \text{ to } C_c/10$$

$$C_\alpha/C_c = 0.03 \text{ to } 0.08$$

Empirical relationships

$$C_c = 0.009 (\text{LL} - 10)$$

$$C_c = 0.40(e_o - 0.25)$$

$$C_c = 0.01(w - 5)$$

$$C_c = 0.37(e_o + 0.003 \text{ LL} - 0.34)$$

$$C_c = 0.00234 \text{ LL } G_s$$

$$C_r = 0.15(e_o + 0.007)$$

$$C_r = 0.003(w + 7)$$

$$C_r = 0.126(e_o + 0.003 \text{ LL} - 0.06)$$

$$C_r = 0.000463 \text{ LL } G_s$$

$$C_c = 1.35 \text{ PI (remolded clays)}$$

Reference

Terzaghi and Peck, 1967

Azzouz et al., 1976

Azzouz et al., 1976

Azzouz et al., 1976

Nagaraj and Murthy, 1986

Azzouz et al., 1976

Azzouz et al., 1976

Azzouz et al., 1976

Nagaraj and Murthy, 1985

Schofield and Wroth, 1968

w is the natural water content (%), LL is the liquid limit (%), e_o is the initial void ratio, and PI is the plasticity index.

Typical values of C_v are shown in Table 9.1.

TABLE 9.1 Typical Values of C_v

Soil	C_v	
	($\text{cm}^2/\text{s} \times 10^{-4}$)	(m^2/yr)
Boston blue clay (CL)	40±20	12±6
Organic silt (OH)	2–10	0.6–3
Glacial lake clays (CL)	6.5–8.7	2.0–2.7
Chicago silty clay (CL)	8.5	2.7
Swedish medium sensitive clays (CL-CH)		
1. laboratory	0.4–0.7	0.1–0.2
2. field	0.7–3.0	0.2–1.0
San Francisco Bay mud (CL)	2–4	0.6–1.2
Mexico City clay (MH)	0.9–1.5	0.3–0.5

SOURCE: Carter and Bentley, 1991

What's next . . . Sometimes we may have to build structures on a site for which the calculated settlement of the soil is intolerable. One popular method to reduce the consolidation settlement to tolerable limits is to preload the soil and use wick drains to speed up the drainage of the excess porewater pressure. Next, we will discuss wick drains.

9.10 PRECONSOLIDATION OF SOILS USING WICK DRAINS



Computer Program Utility

Access www.wiley.com/college/budhu and click Chapter 9 for a spreadsheet on wick drains (wick.xls).

The purpose of wick drains is to accelerate the consolidation settlement of soft, saturated clays by reducing the drainage path. A wick drain is a prefabricated drainage strip that consists of a plastic core surrounded by a nonwoven polypropylene geotextile jacket (Figure 9.19). The geotextile (a filter fabric) allows passage of water into the core that is then pumped out. A wick drain is installed by enclosing the drain in a tubular steel mandrel and supporting it at the base by an anchor plate. The mandrel is then driven into the soil by a vibratory rig or pushed by a hydraulic rig. At the desired depth, the mandrel is removed, the drain and anchor plate remain in place, and the drain is cut off with a tail about 300 mm long. The effect of drains on the soil consolidation is illustrated in Figure 9.20. A wick drain in which one end is on an impervious boundary is called a half-closed drain (Figure 9.21). Sometimes the drain may penetrate into a pervious layer below an impervious layer, allowing the porewater to be expelled from the top and bottom of the drain. Such a drain provides two-way drainage and would accelerate the consolidation of the soil. Recall that for one-dimensional consolidation, two-way drainage reduces the time for a given degree of consolidation by four times compared with single drainage.

The governing equation for axisymmetric radial drainage is

$$\frac{\partial u}{\partial t} = C_h \left(\frac{\partial^2 u}{\partial r^2} + \frac{1}{r} \frac{\partial u}{\partial r} \right) \quad (9.49)$$

where r is the radial distance from the center of the drain and C_h is the coefficient of consolidation in the horizontal or radial direction. The boundary conditions to solve Equation (9.49) are:

$$\text{At } r = r_d: \quad u = 0 \quad \text{when } t > 0$$

$$\text{At } r = R: \quad \frac{\partial u}{\partial r} = 0$$

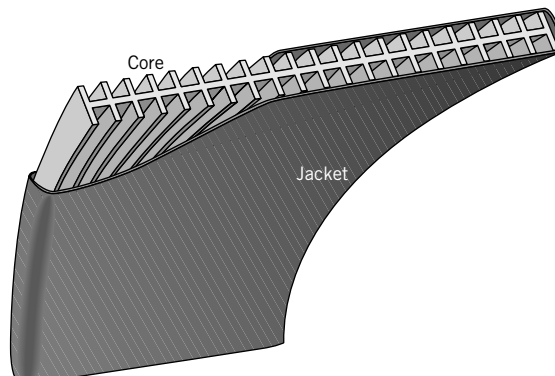


FIGURE 9.19
Wick drain.

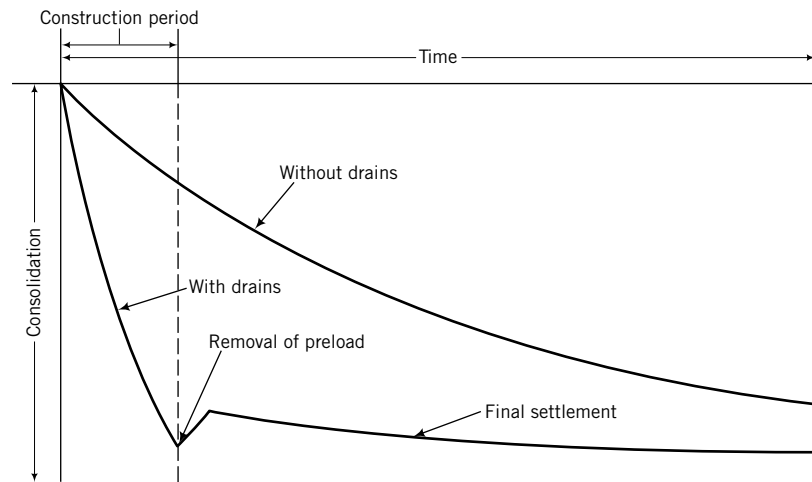


FIGURE 9.20 Effects of wick drains on time to achieve a given degree of consolidation.

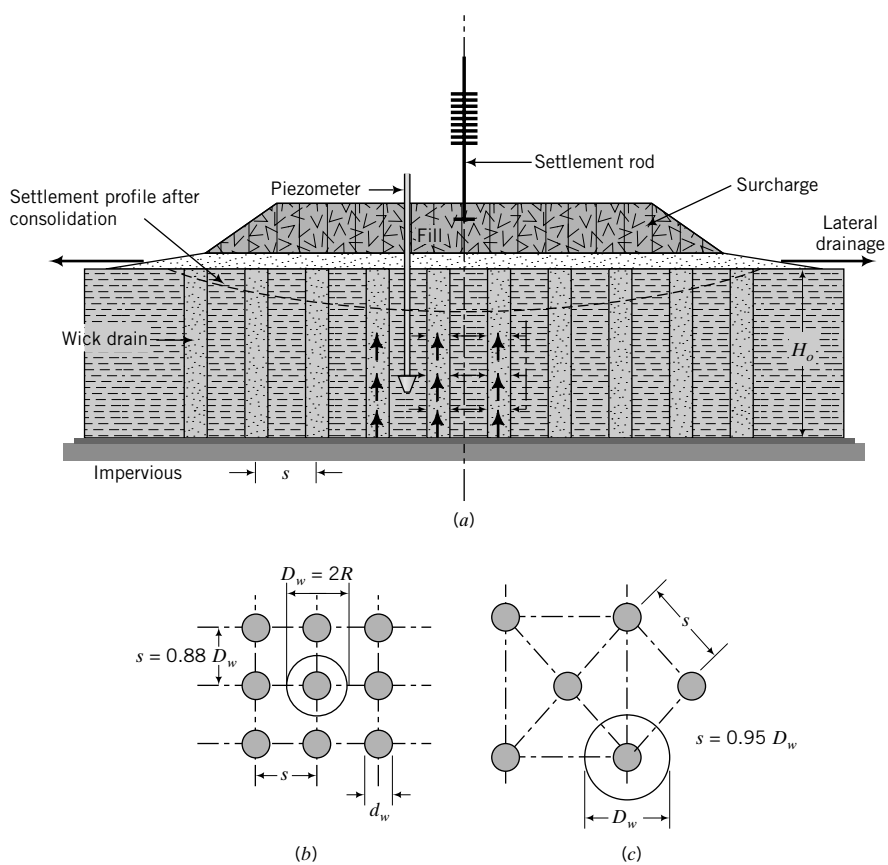


FIGURE 9.21 (a) Vertical section of a half-closed wick drain. (b) Plan of a square grid wick drain. (c) Plan of a triangular grid wick drain.

and the initial condition is $t = 0, u = u_o$, where r_d is the radius of the drains, t is time, and R is the radius of the cylindrical influence zone (Figure 9.21). Richart (1959) reported solutions for Equation (9.49) for two cases—free strain and equal strain. Free strain occurs when the surface load is uniformly distributed (flexible foundation, Figure 9.21) and the resulting surface settlement is uneven. Equal strain occurs when the surface settlement is forced to be uniform (rigid foundation) and the resulting surface load is not uniformly distributed. Richart showed that the differences in the two cases are small and the solution for equal strain is often used in practice.

The time factor for consolidation in the vertical direction is given by Equation (9.33), while the time factor for consolidation in the radial direction (T_r) is

$$T_r = \frac{C_h t}{4R^2} \quad (9.50)$$

The hydraulic conductivity of the soil in the horizontal or radial direction is sometimes much greater (2 to 10 times for many soils) than in the vertical direction (Chapter 6) and, consequently, C_h is greater than C_v , usually $C_h/C_v \approx 1.2$ to 2. During drilling of the borehole and installation of the drain, a thin layer of soil at the interface of the drain is often remolded. This thin layer of remolded soil is called a smear zone. The values of C_v and C_h are often much lower in the smear zone than in the natural soil. It is customary to use reduced values of C_v and C_h to account for the smear zone.

The average degree of consolidation for vertical and radial dissipation of porewater pressure (U_{vr}) is

$$U_{vr} = 1 - (1 - U)(1 - U_r) \quad (9.51)$$

where U is the average degree of consolidation for vertical drainage [Equation (9.35)] and U_r is the average degree of consolidation for radial drainage.

The flow into wick drains is predominantly radial. Assuming no soil disturbances during installation, the time for soil consolidation for a finite vertical discharge capacity is

$$t = \frac{D_w^2}{8C_h} \left[\frac{1}{1 - \left(\frac{d_w}{D_w} \right)^2} \ln \frac{D_w}{d_w} - 0.75 + 0.25 \left(\frac{d_w}{D_w} \right)^2 + z\pi(2L - z) \frac{k}{q_w} \right] \ln \frac{1}{1 - U} \quad (9.52)$$

where t is time(s) required to achieve the desired consolidation, D_w is diameter (m) of the zone of influence, C_h is the coefficient of consolidation for horizontal flow (m^2/s), d_w (m) = $2(h + b)/\pi$ is the equivalent drain diameter, b (m) is the width and h (m) is the thickness of the drain, z (m) is the distance to flow point, L (m) is the effective drain length (total drain length when drainage occurs at one end only, half length when drainage occurs at both ends), k (m/s) is the hydraulic conductivity of the soil (usually, either the radial or equivalent k value is used), q_w (m^3/s) is discharge capacity of the wick drain at a gradient of 1, and U is average degree of consolidation. For a square arrangement of drains, the spacing, s , is about $0.88D_w$, while for a triangular arrangement, $s = 0.95D_w$.

The spacing of the wick drains is the primary design parameter for a desired amount of settlement in a desired time period. The other design parameter is the surcharge height. In general, by varying the spacing and surcharge height, the designer can obtain the most economical combination of wick spacing, consolidation time, and surcharge height for a project.

EXAMPLE 9.12 Spacing of Wick Drains

A foundation for a structure is to be constructed on a soft deposit of clay, 20 m thick. Below the soft clay is a stiff, overconsolidated clay. The calculated settlement cannot be tolerated, and it was decided that the soft soil should be preconsolidated by an embankment equivalent to the building load to achieve 90% consolidation in 12 months. Wick

drains are required to speed up the time for soil consolidation. The wick drains are 100 mm wide and 3 mm thick, with a discharge of $0.1 \times 10^{-6} \text{ m}^3/\text{s}$. The properties of the soils are $k = 0.01 \times 10^{-8} \text{ m/s}$ and $C_h = 1 \times 10^{-8} \text{ m}^2/\text{s}$. The distance to the flow point is 10 m and the system is half-closed. Determine the spacing of the wick drains arranged in a square grid.



Strategy You have to assume a spacing such that the calculated time using Equation (9.52) matches the desired time of 12 months. It is best to set up a spreadsheet to do this calculation and use the Goal Seek function. Such a spreadsheet is available at www.wiley.com/college/budhu.

Solution 9.12

The spreadsheet solution follows.

A	B	C	D	E
1				
2 Spacing	s	0.97	m	
3 Drain configuration		s	s = square, t = triangular	
4 Drain width	h	100	mm	
5 Thickness	b	3	mm	
6 Degree of consolidation	U	90	%	
7 Coef. of horiz. consolidation	C_h	1	$\times 10^{-8} \text{ m}^2/\text{s}$	
8 Desired time	t	365	days	
9 Soil thickness	L	20	m	
10 Distance to flow point	z	10	m	
11 Discharge capacity	q_w	0.1	$\times 10^{-6} \text{ m}^3/\text{s}$	
12 Soil permeability	k_s	0.01	$\times 10^{-8} \text{ m/s}$	
13 Diameter of influence	D_w	1.107	m	
14 Equivalent diameter	d_w	65.57	mm	
15 k/q_w ratio		0.1	$\times 10^{-2}$	
16 Calculated time		365	days	
17				

Cell C16 is Equation (9.52). Using the Goal Seek function in Excel with the following input:

Set cell	C16
To value	365
By changing cell	C2

The spreadsheet calculations give a spacing of 0.97 m. Use 1 m spacing.

9.11 SUMMARY

Consolidation settlement of a soil is a time-dependent process that depends on the hydraulic conductivity and thickness of the soil, and the drainage conditions. When an increment of vertical stress is applied to a soil, the instantaneous (initial) excess porewater pressure is equal to the vertical stress increment. With time, the initial excess porewater pressure decreases, the vertical effective stress increases by the amount of decrease of the initial excess porewater pressure, and settlement increases. The consolidation settlement is made up of two parts—the early time response called primary consolidation and a later time response called secondary compression.

Soils retain a memory of the past maximum effective stress, which may be erased by loading to a higher stress level. If the current vertical effective stress on a soil was never exceeded in the past (a normally consolidated soil), it would behave elastoplastically when stressed. If the current vertical effective stress on a soil was exceeded in the past (an overconsolidated soil), it would behave elastically (approximately) for stresses less than its past maximum effective stress.

Self-Assessment



Access Chapter 9 at <http://www.wiley.com/college/budhu> to take the end-of-chapter quiz to test your understanding of this chapter.

Practical Examples

EXAMPLE 9.13 Lateral Stress During Soil Consolidation in the Lab

A soil was consolidated in an oedometer to a vertical stress of 100 kPa and then unloaded incrementally to 50 kPa. The excess porewater pressure is zero. If the frictional soil constant ϕ'_{cs} is 25° , determine the lateral stress.

Strategy The soil in this case becomes overconsolidated—the past maximum vertical effective stress is 100 kPa and the current effective stress is 50 kPa. You need to find K_o^{nc} and then K_o^{oc} using the OCR of your soil. (See Section 7.10.)

Solution 9.13

Step 1: Calculate K_o^{nc} .

$$\text{Equation (7.51): } K_o^{nc} = 1 - \sin \phi'_{cs} = 1 - \sin 25 = 0.58$$

Step 2: Calculate OCR.

$$\text{OCR} = \frac{\sigma'_{zc}}{\sigma'_{zo}} = \frac{100}{50} = 2$$

Step 3: Calculate K_o^{oc} .

$$\text{Equation (7.52): } K_o^{oc} = K_o^{nc}(\text{OCR})^{1/2} = 0.58(2)^{1/2} = 0.82$$

Step 4: Calculate the lateral effective stress.

$$\sigma'_x = K_o^{oc} \sigma'_{zo} = 0.82 \times 50 = 41 \text{ kPa}$$

Step 5: Calculate the lateral total stress.

$$\sigma_x = \sigma'_x + \Delta u = 41 + 0 = 41 \text{ kPa}$$

EXAMPLE 9.14 Consolidation Settlement Due to a Foundation

A foundation for an oil tank is proposed for a site with a soil profile, as shown in Figure E9.14a. A specimen of the fine-grained soil, 75 mm in diameter and 20 mm thick, was tested in an oedometer in a laboratory. The initial water content was 62% and $G_s = 2.7$. The vertical stresses were applied incrementally—each increment remaining on the specimen until the porewater pressure change was negligible. The cumulative settlement values at the end of each loading step are as follows:

Vertical stress (kPa)	15	30	60	120	240	480
Settlement (mm)	0.10	0.11	0.21	1.13	2.17	3.15

The time–settlement data when the vertical stress was 200 kPa are:

Time (min)	0	0.25	1	4	9	16	36	64	100
Settlement (mm)	0	0.22	0.42	0.6	0.71	0.79	0.86	0.91	0.93

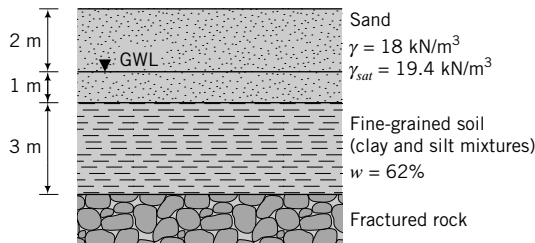


FIGURE E9.14a

The tank, when full, will impose vertical stresses of 90 kPa and 75 kPa at the top and bottom of the fine-grained soil layer, respectively. You may assume that the vertical stress is linearly distributed in this layer.

- Determine the primary consolidation settlement of the fine-grained soil layer when the tank is full.
- Calculate and plot the settlement–time curve.

Strategy To calculate the primary consolidation settlement, you need to know C_c and C_r or m_v , and σ'_{zo} , $\Delta\sigma$, and σ'_{zc} . Use the data given to find the values of these parameters. You may use the methods in Section 7.11 to calculate $\Delta\sigma_z$, although it is best for this problem to use the stress increase in Appendix C, as the fine-grained soil layer is of finite thickness. To find time for a given degree of consolidation, you need to find C_v from the data.

Solution 9.14

Step 1: Find C_v using the root time method.

Use the data from the 240 kPa load step to plot a settlement versus $\sqrt{\text{time}}$ curve, as depicted in Figure E9.14b. Follow the procedures set out in Section 9.7 to find C_v . From the curve, $t_{90} = 1.2 \text{ min}$.

Height of sample at beginning of loading = $20 - 1.2 = 18.8 \text{ mm}$

Height of sample at end of loading = $20 - 2.17 = 17.83 \text{ mm}$

$$H_{dr} = \frac{H_o + H_f}{4} = \frac{18.8 + 17.83}{4} = 9.16 \text{ mm}$$

$$C_v = \frac{T_v H_{dr}^2}{t_{90}} = \frac{0.848 \times (9.16)^2}{1.2} = 59.3 \text{ mm}^2/\text{min}$$

$$= 59.3 \times 10^{-6} \text{ m}^2/\text{min}$$

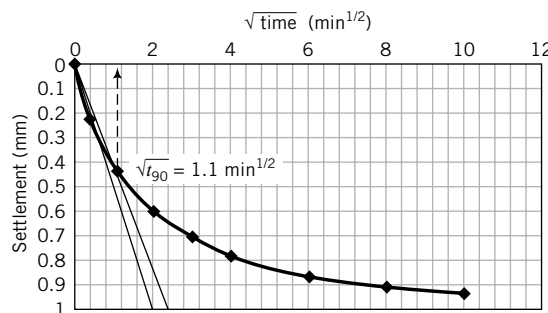


FIGURE E9.14b

Step 2: Determine the void ratio at the end of each load step.

$$\text{Initial void ratio: } e_o = wG_s = 0.62 \times 2.7 = 1.67$$

$$\begin{aligned} \text{Equation (9.6): } e &= e_o - \frac{\Delta z}{H_o}(1 + e_o) = 1.67 - \frac{\Delta z}{20}(1 + 1.67) \\ &= 1.67 - 13.35 \times 10^{-2} \Delta z \end{aligned}$$

The void ratio for each load step is shown in the table below.

σ'_z (kPa)	15	30	60	120	240	480
Void ratio	1.66	1.65	1.64	1.52	1.38	1.25

A plot of $e - \log \sigma'_z$ versus e is shown in Figure E9.14c.

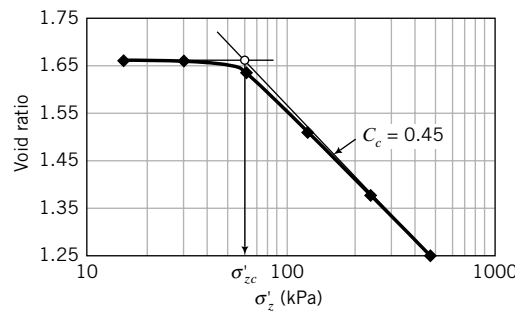


FIGURE E9.14c

Step 3: Determine σ'_{zc} and C_c .

Follow the procedures in Section 9.7 to find σ'_{zc} .

$$\sigma'_{zc} = 60 \text{ kPa}$$

$$C_c = \frac{1.52 - 1.25}{\log \left(\frac{480}{120} \right)} = 0.45$$

Step 4: Calculate σ'_{zo} .

$$\text{Clay: } \gamma_{sat} = \frac{G_s + e_o}{1 + e_o} \gamma_w = \left(\frac{2.7 + 1.67}{1 + 1.67} \right) 9.8 = 16 \text{ kN/m}^3$$

$$\sigma'_{zo} = (18 \times 2) + (19.4 - 9.8)1 + (16 - 9.8)1.5 = 54.9 \text{ kPa}$$

Step 5: Calculate settlement.

$$\text{OCR} = \frac{\sigma'_{zc}}{\sigma'_{zo}} = \frac{60}{54.9} = 1.1$$

For practical purposes, the OCR is very close to 1; that is, $\sigma'_z \approx \sigma'_{zc}$. Therefore, the soil is normally consolidated. Also, inspection of the e versus $\log \sigma'_z$ curve shows that C_c is approximately zero, which lends further support to the assumption that the soil is normally consolidated.

$$\rho_{pc} = \frac{H_o}{1 + 1.67} 0.45 \left(\frac{\sigma'_{zo} + \Delta \sigma_z}{\sigma'_{zo}} \right) = 0.17 H_o \log \left(\frac{\sigma'_{zo} + \Delta \sigma_z}{\sigma'_{zo}} \right)$$

Divide the clay layer into three sublayers 1.0 m thick and compute the settlement for each sublayer. The primary consolidation settlement is the sum of the settlement of each sublayer. The vertical stress increase in the fine-grained soil layer is

$$90 - \left(\frac{90 - 75}{3} \right) z = 90 - 5z$$

where z is the depth below the top of the layer. Calculate the vertical stress increase at the center of each sublayer and then the settlement from the above equation. The table below summarizes the computation.

Layer	z (m)	σ'_{zo} at center of sublayer (kPa)	$\Delta\sigma_z$ (kPa)	$\sigma'_{zo} + \Delta\sigma_z$ (kPa)	ρ_{pc} (mm)
1	0.5	48.7	87.5	136.2	75.9
2	1.5	54.9	82.5	137.4	67.7
3	2.5	61.1	77.5	138.6	60.5
		Total		204.1	

Alternatively, by considering the 3-m fine-grained soil layer as a whole and taking the average vertical stress increment, we obtain

$$\rho_{pc} = \frac{3000}{1 + 1.67} 0.45 \log \left(\frac{137.4}{54.9} \right) = 201.4 \text{ mm}$$

In general, the former approach is more accurate for thick layers.

Step 6: Calculate settlement-time values.

$$C_v = 59.3 \times 10^{-6} \times 60 \times 24 = 85,392 \times 10^{-6} \text{ m}^2/\text{day}$$

$$t = \frac{T_v H_{dr}^2}{C_v} = \frac{T_v \times (\frac{3}{2})^2}{85,392 \times 10^{-6}} = 26.3 T_v \text{ days}$$

The calculation of settlement at discrete times is shown in the table below and the data are plotted in Figure E9.14d.

U (%)	T_v	Settlement (mm)	
		$\rho_{pc} \times \frac{U}{100}$	$t = 26.3 T_v$ (days)
10	0.008	20.4	0.2
20	0.031	20.8	0.8
30	0.071	61.3	1.9
40	0.126	81.6	3.3
50	0.197	102.1	5.2
60	0.287	122.5	7.6
70	0.403	142.9	10.6
80	0.567	163.3	14.9
90	0.848	183.7	22.3

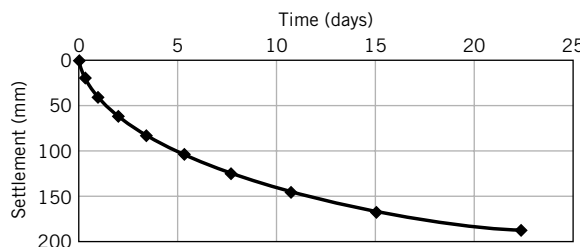


FIGURE E9.14d

EXAMPLE 9.15 Estimating Consolidation Settlement Due to Unexpected Field Condition

A geotechnical engineer made a preliminary settlement analysis for a foundation of an office building that is to be constructed at a location where the soil strata contain a compressible clay layer. She calculated 50 mm of primary consolidation settlement. The building will impose an average vertical stress of 150 kPa in the clay layer. As often happens in design practice, design changes are required. In this case, the actual thickness of the clay is 30% more than the original soil profile indicated and, during construction, the groundwater table has to be lowered by 2 m. Estimate the new primary consolidation settlement.

Strategy From Section 9.3, the primary consolidation settlement is proportional to the thickness of the soil layer and also to the increase in vertical stress [see Equation (9.20)]. Use proportionality to find the new primary consolidation settlement.

Solution 9.15

Step 1: Estimate the new primary consolidation settlement due to the increase in thickness.

$$\frac{(\rho_{pc})_n}{(\rho_{pc})_o} = \frac{H_n}{H_o}$$

where subscripts o and n denote original and new, respectively.

$$(\rho_{pc})_n = 50 \times \frac{1.3H_o}{H_o} = 65 \text{ mm}$$

Step 2: Estimate primary consolidation settlement from vertical stress increase due to lowering of the groundwater level.

Increase in vertical effective stress due to lowering of water table = $2 \times 9.8 = 19.6 \text{ kPa}$.

Primary consolidation settlement is also proportional to the vertical effective stress:

$$\frac{(\rho_{pc})_n}{(\rho_{pc})_o} = \frac{(\sigma'_z)_n}{(\sigma'_z)_o}$$

$$\therefore (\rho_{pc})_n = 65 \times \frac{(150 + 19.6)}{150} = 73.5 \text{ mm}$$

EXAMPLE 9.16 Consolidation Differential Settlement in Nonuniform Soil

The foundations supporting two columns of a building are shown in Figure E9.16. An extensive soil investigation was not carried out, and it was assumed in the design of the foundations that the clay layer had a uniform thickness of 1.2 m. Two years after construction the building settled, with a differential settlement of 10 mm. Walls of the building began to crack. The doors have not jammed, but by measuring the out-of-vertical distance of the doors,

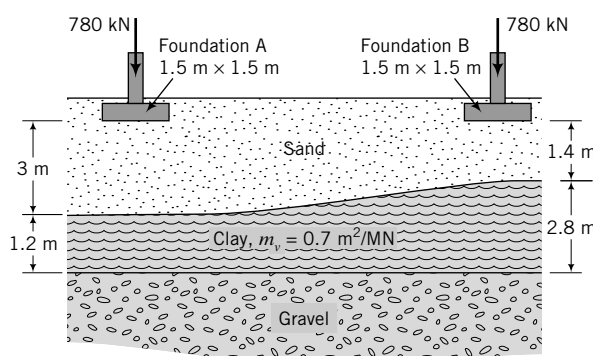


FIGURE E9.16

it is estimated that they would become jammed if the differential settlement exceeded 24 mm. A subsequent soil investigation showed that the thickness of the clay layer was not uniform but varies, as shown in Figure E9.16. The owners would like to get an estimate of the expected total differential settlement and how long it will take before the doors become jammed.

Strategy Determine the settlement under each foundation, and then calculate the differential settlement. Since you know the differential settlement that occurs over a two-year period after construction, you can find the degree of consolidation and then use this information to calculate the expected time for the doors to become jammed.

Solution 9.16

Step 1: Calculate the vertical stress increase at the center of the clay layer under each foundation. Let's use the approximate method, Equation (7.95).

$$\Delta\sigma_z = \frac{P}{(B+z)(L+z)}$$

$$(\Delta\sigma_z)_A = \frac{780}{(1.5+3.6)(1.5+3.6)} = 30 \text{ kPa}$$

$$(\Delta\sigma_z)_B = \frac{780}{(1.5+2.8)(1.5+2.8)} = 42.2 \text{ kPa}$$

Note: For a more accurate value of $\Delta\sigma_z$ you should use the vertical stress increase due to surface loads on multilayered soils (Poulos and Davis, 1974).

Step 2: Calculate the primary consolidation settlement.

Use $\rho_{pc} = H_o m_v \Delta\sigma$ to calculate the primary consolidation settlement.

$$(\rho_{pc})_A = 1.2 \times 0.7 \times 10^{-3} \times 30 = 25.2 \times 10^{-3} \text{ m} = 25.2 \text{ mm}$$

$$(\rho_{pc})_B = 2.8 \times 0.7 \times 10^{-3} \times 42.2 = 82.7 \times 10^{-3} \text{ m} = 82.7 \text{ mm}$$

Step 3: Calculate the differential settlement.

$$\text{Differential settlement: } \delta = 82.7 - 25.2 = 57.5 \text{ mm}$$

Step 4: Calculate the time for 24-mm differential settlement to occur.

$$\text{Current differential settlement: } \delta_c = 10 \text{ mm}$$

$$\text{Degree of consolidation: } U = \frac{\delta_c}{\delta} = \frac{10}{57.5} = 0.17$$

$$T_v = \frac{4}{\pi} U^2 = \frac{4}{\pi} \times 0.17^2 = 0.037$$

$$C_v = \frac{T_v H_{dr}^2}{t} = \frac{0.037 \times (2.8/2)^2}{2} = 0.036 \text{ m}^2/\text{yr}$$

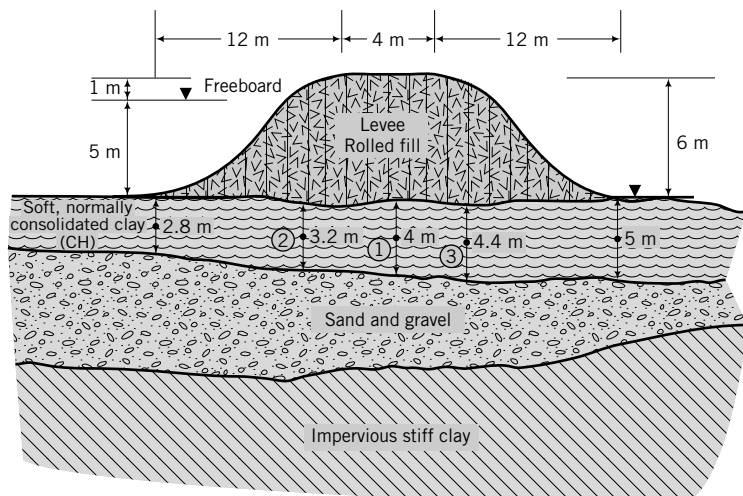
$$\text{For 24-mm differential settlement: } U = \frac{24}{57.5} = 0.42, \quad T_v = \frac{4}{\pi} \times 0.42^2 = 0.225$$

$$t = \frac{T_v H_{dr}^2}{C_v} = \frac{0.225 \times (2.8/2)^2}{0.036} = 12.25 \text{ years}$$

Therefore, in the next 10.25 years, the total differential settlement would be 24 mm.

EXAMPLE 9.17 Settlement of a Levee

A recently constructed levee (a long embankment) is shown in Figure E9.17a. It was constructed from compacted earthen fill (rolled fill). Statistical analysis from climatic data and other data such as historical wave heights shows that a freeboard of 1 m is required. If soil settlement is not considered, (a) determine how much the freeboard would be compromised, and (2) estimate the settlement profile under the levee. Only a limited set of data was available for the soft, normally consolidated clay. These data are $w = 55.6\%$, $LL = 68\%$, and $PL = 30\%$.

**FIGURE E9.17a**

Strategy The soil data are extremely limited. You can use empirical equations in Section 9.9 to estimate the compression index. To find the vertical stress distribution, use a combination of a surface strip load with uniform stress distribution and with a triangular stress distribution. You can use Figure 7.27, but this is only useful for the center of the levee. As a geotechnical engineer, you should obtain more data from at least consolidation and shear tests.

Step 1: Estimate soil parameters and calculate surface stress.

$$\text{From Section 9.9: } C_c = 0.009 (LL - 10) = 0.009 (68 - 10) = 0.52$$

$$q_s = \gamma H_o = 18 \times 6 = 108 \text{ kPa}$$

$$e_o = w G_s = 0.556 \times 2.7 = 1.5$$

$$\gamma' = \frac{G_s - 1}{1 + e_o} \gamma_w = \frac{2.7 - 1}{1 + 1.5} \times 9.8 = 6.7 \text{ kN/m}^3$$

Step 2: Estimate increase in stress at the center of the soft clay.

Using the program STRESS, we get the following vertical stress increase at the center of the clay. Select three points at the center of the soft clay, as shown in Figure E9.17a. The increases in vertical stresses calculated for these three points are shown in Figure E9.17b.

q_s (kPa)	108	108	108	108	108
B (m)	12	4	4	4	12
x (m)	12	0	2	4	12
z (m)	1.6	1.6	2	2.2	2.2
$\Delta\sigma_z$ (kPa)	49.4	52.7	88.4	51	47.8
	$+ 17.2$				
	2		1		3

FIGURE E9.17b Point (see Figure E9.17a)

The additional vertical stress increase of 17.2 kPa at the center of the levee is due to the two triangular loads. The input to the stress program for this stress increase is $q_s = 108 \text{ kPa}$, $B = 12 \text{ m}$, $x = 14 \text{ m}$ ($12 \text{ m} + 4/2 \text{ m}$), and $z = 2 \text{ m}$. You have to double the result because you have two triangles.

Step 3: Estimate the settlement.

Since the soil is normally consolidated, $\text{OCR} = 1$. Use Equation (9.16) to calculate the settlement, i.e.,

$$\rho_{pc} = \frac{H_o}{1 + e_o} C_c \log \frac{\sigma'_{fin}}{\sigma'_{zo}}$$

A spreadsheet is used to do the calculations, as shown below.

Point	$H \text{ (m)}$	$\Delta\sigma_z \text{ (kPa)}$	$\sigma'_{zo} \text{ (kPa)}$	$\sigma'_{fin} \text{ (kPa)}$	$\rho_{pc} \text{ (m)}$
1	4	105.6	13.4	119.0	0.79
2	3.2	102.1	10.7	112.8	0.68
3	4.4	98.8	14.7	113.5	0.81

The settlement at the edges of the levee base would be approximately zero. Note that although the vertical stress increases at points 2 and 3 are about the same, the settlement at point 3 is greater because the thickness of the soft clay is greater there.

The average reduction in freeboard is $(0.79 + 0.68 + 0.81)/3 = 0.76 \text{ m}$.

Step 4: Sketch the settlement profile.

The estimated settlement profile is shown in Figure E9.17c. This diagram is not to scale.

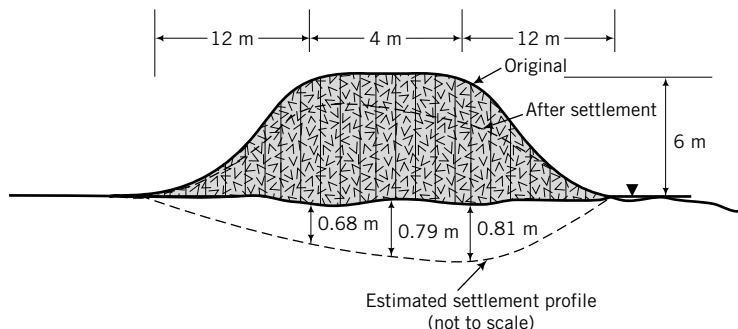


FIGURE E9.17c

EXERCISES

For all problems, assume $G_s = 2.7$ unless otherwise stated.

Theory

- 9.1** A clay soil of thickness H is allowed to drain on the top boundary through a thin sand layer. A vertical stress of σ is applied to the clay. The excess porewater pressure distribution is linear in the soil layer, with a value of u_t at the top boundary and u_b ($u_b > u_t$) at the bottom boundary. The excess porewater pressure at the top boundary is not zero because the sand layer was partially blocked. Derive an equation for the excess porewater pressure distribution with soil thickness and time.

- 9.2** A soil layer of thickness H_o has only single drainage through the top boundary. The excess porewater pressure distribution when a vertical stress, σ , is applied varies parabolically, with a value of zero at the top boundary and u_b at the bottom boundary. Show that

$$C_v = \frac{H_o^2}{2u_b} \frac{d\sigma'}{dt} \quad \text{and} \quad k_z = \frac{\gamma_w H_o}{2u_b} \frac{dH_o}{dt}$$

- 9.3** Show that, for a linear elastic soil,

$$m_{vr} = \frac{(1 + v')(1 - 2v')}{E'(1 - v')}$$

- 9.4** Show that, if an overconsolidated soil behaves like a linear elastic material,

$$K_o^{oc} = (\text{OCR})K_o^{nc} - \frac{\nu'}{1 - \nu'}(\text{OCR} - 1)$$

- 9.5** The excess porewater pressure distribution in a 10-m-thick clay varies linearly from 100 kPa at the top to 10 kPa at the bottom of the layer when a vertical stress is applied. Assuming drainage only at the top of the clay layer, determine the excess porewater pressure in 1 year's time using the finite difference method if $C_v = 1.5 \text{ m}^2/\text{yr}$.
- 9.6** At a depth of 4 m in a clay deposit, the overconsolidation ratio is 3.0. Plot the variation of overconsolidation ratio and water content with depth for this deposit up to a depth of 15 m. The recompression index is $C_r = 0.05$, and the water content at 4 m is 32%. The groundwater level is at the ground surface.

- 9.7** The overconsolidation ratio of a saturated clay at a depth of 5 m is 6.0, and its water content is 38%. It is believed that the clay has become overconsolidated as a result of erosion. Calculate the thickness of the soil layer that was eroded. Assume that the groundwater level is at the ground surface for both the past and present conditions.

Problem Solving

- 9.8** An oedometer test on a saturated clay soil gave the following results: $C_c = 0.2$, $C_r = 0.04$, $\text{OCR} = 4.5$. The existing vertical effective stress in the field is 130 kPa. A building foundation will increase the vertical stress at the center of the clay by 50 kPa. The thickness of the clay layer is 2 m and its water content is 28%.

- (a) Calculate the primary consolidation settlement.
 (b) What would be the difference in settlement if OCR were 1.5 instead of 4.5?

- 9.9** A building is expected to increase the vertical stress at the center of a 2-m-thick clay layer by 100 kPa. If $m_v = 4 \times 10^{-4} \text{ m}^2/\text{kN}$, calculate the primary consolidation settlement.

- 9.10** Two adjacent bridge piers rest on clay layers of different thickness but with the same properties. Pier 1 imposes a stress increment of 100 kPa to a 3-m-thick layer, while Pier 2 imposes a stress increment of 150 kPa to a 5-m-thick layer. What is the differential settlement between the two piers if $m_v = 3 \times 10^{-4} \text{ m}^2/\text{kN}$?

- 9.11** The table below shows data recorded during an oedometer test on a soil sample for an increment of vertical stress of 200 kPa. At the start of the loading, the sample height was 19.17 mm.

Time (min)	0	0.25	1	4	9	16	36	64	100
Settlement (mm)	0	0.30	0.35	0.49	0.61	0.73	0.90	0.95	0.97

After 24 hours, the settlement was negligible and the void ratio was 1.20, corresponding to a sample height of 18.2 mm. Determine C_v using the root time and the log time methods.

- 9.12** A sample of saturated clay of height 20 mm and water content 30% was tested in an oedometer. Loading and unloading of the sample were carried out. The thickness H_f of the sample at the end of each stress increment/decrement is shown in the table below.

σ'_z (kPa)	100	200	400	200	100
H_f (mm)	20	19.31	18.62	18.68	18.75

- (a) Plot the results as void ratio versus σ'_z (log scale).
 (b) Determine C_c and C_r .
 (c) Determine m_v between $\sigma'_z = 200$ kPa and $\sigma'_z = 300$ kPa.

- 9.13** A sample of saturated clay, taken from a depth of 5 m, was tested in a conventional oedometer. The table below gives the vertical effective stress and the corresponding thickness recorded during the test.

σ'_z (kPa)	100	200	400	800	1600	800	400	100
h (mm)	19.2	19.0	17.0	14.8	12.6	13.1	14.3	15.9

The water content at the end of the test was 40% and the initial height was 20 mm.

- (a) Plot a graph of void ratio versus σ'_z (log scale).
 (b) Determine C_c and C_r .
 (c) Determine m_v between $\sigma'_z = 400$ kPa and $\sigma'_z = 500$ kPa.
 (d) Determine the relationship between e (void ratio) and h (thickness).
 (e) Determine σ'_{zc} using Casagrande's method.

- 9.14** The following data were recorded in an oedometer test on a clay sample 100 mm in diameter and 30 mm high.

Load (N)	0	50	100	200	400	800	0
Displacement gage reading (mm)	0	0.48	0.67	0.98	1.24	1.62	1.4

At the end of the test, the wet mass of the sample was 507.3 grams and, after oven-drying, its dry mass was 412.5 grams. The specific gravity was 2.65.

- (a) Calculate the void ratio at the end of the test.
 (b) Calculate the void ratio at the end of each loading step.
 (c) Calculate the initial thickness of the soil sample from the initial void ratio and compare this with the initial thickness.
 (d) Determine m_v between $\sigma'_z = 50$ kPa and $\sigma'_z = 150$ kPa.

9.15 A laboratory consolidation test on a 20-mm-thick sample of soil shows that 90% consolidation occurs in 30 minutes. Plot a settlement (degree of consolidation)-time curve for a 10-m layer of this clay in the field for (a) single drainage and (b) double drainage.

9.16 A clay layer below a building foundation settles 15 mm in 200 days after the building was completed. According to the oedometer results, this settlement corresponds to an average degree of consolidation of 25%. Plot the settlement-time curve for a 10-year period, assuming double drainage.

9.17 An oil tank is to be sited on a soft alluvial deposit of clay. Below the soft clay is a thick layer of stiff clay. It was decided that a circular embankment, 10 m in diameter, with wick drains inserted into the soft clay would be constructed to preconsolidate it. The height of the embankment is 6 m, and the unit weight of the soil comprising the embankment is 18 kN/m³. The following data are available: thickness of soft clay = 7 m, $k = 1 \times 10^{-10}$ m/s, and $C_h = 0.6 \text{ m}^2/\text{yr}$. The desired degree of consolidation is 90% in 12 months. Determine the spacing of a square grid of the wick drains. Assume wick drain of size 100 mm × 3 mm and $q_w = 0.1 \times 10^{-6}$ m³/s. The flow point distance is 4 m. Assume a half-closed system.

Practical

9.18 Figure P9.18 shows the soil profile at a site for a proposed office building. It is expected that the vertical stress at the top of the clay will increase by 150 kPa and at the bottom by 90 kPa. Assuming a linear stress distribution within the clay, calculate the consolidation settlement. (Hint: You should divide the clay into five equal layers, compute the settlement for each layer, and then find the total settlement.) Groundwater level is at the top of the clay layer. An oedometer test on a sample of the clay

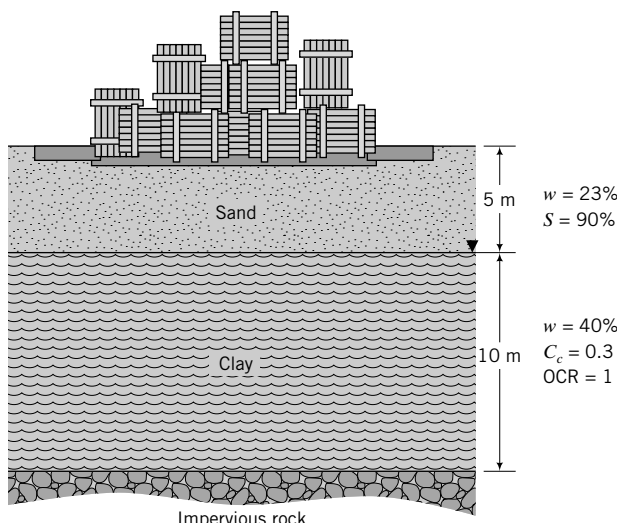


FIGURE P9.18

revealed that 90% consolidation on a 20-mm-thick sample occurred in 40 minutes. The sample was drained on the upper and lower boundaries. How long will it take for 50% consolidation to occur in the field?

9.19 A borehole at a site for a proposed building reveals the following soil profile:

0–5 m	Dense sand, $\gamma = 18 \text{ kN/m}^3$, $\gamma_{sat} = 19 \text{ kN/m}^3$
At 4 m	Groundwater level
5–10 m	Soft, normally consolidated clay, $\gamma_{sat} = 17.5 \text{ kN/m}^3$
Below 10 m	Impervious rock

A building is to be constructed on this site with its foundation at 2 m below ground level. The building load is 30 MN and the foundation is rectangular with a width of 10 m and length of 15 m. A sample of the clay was tested in an oedometer, and the following results were obtained:

Vertical stress (kPa)	50	100	200	400	800
Void ratio	0.945	0.895	0.815	0.750	0.705

Calculate the primary consolidation settlement. Assuming that the primary consolidation took 5 years to achieve in the field, calculate the secondary compression for a period of 10 years beyond primary consolidation. The secondary compression index is $C_s/6$. [Hint: Determine e_p for your σ'_{fin} from a plot of e versus σ'_z (log scale).]

9.20 Water is pumped from an aquifer, as shown in Figure P9.20, for domestic use. The original groundwater level was at the top of the soft clay and dropped by 10 m. The ground surface subsided.

(a) Assuming that the subsidence is due to the settlement of the soft clay, estimate the settlement of the ground surface.

(b) A decision was made to recharge the aquifer by pumping water from a canal. If the groundwater level were to return to its original level, would the ground surface return to its original elevation? If so, why? If not, why not? Show calculations to support your answer. How much recovery (expansion of soil) is possible using the one-dimensional consolidation theory?

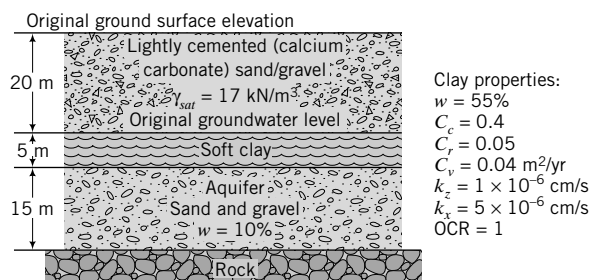


FIGURE P9.20

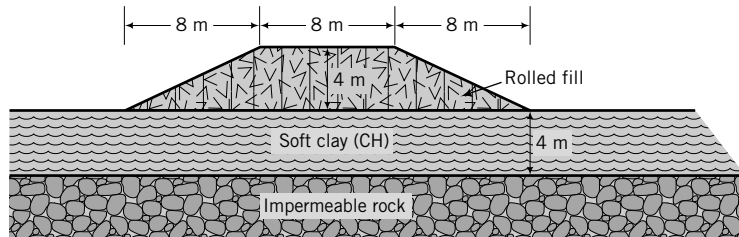


FIGURE P9.21

9.21 A route for a proposed 8-m-wide highway crosses a region with a 4-m-thick saturated, soft, normally consolidated clay (CH) above impermeable rock. Groundwater level is 1 m below the surface. The geotechnical data available during the preliminary design stage consist of Atterberg limits ($LL = 68\%$ and $PL = 32\%$) and the natural water content ($w = 56\%$). Based on experience, the geotechnical engineer estimated the coefficient of consolidation at 8 m^2 per year. To limit settlement, a 4-m-high embankment will be constructed as a surcharge from fill of unit weight 16 kN/m^3 . (Figure P9.21).

- (a) Estimate the compression and recompression indices. (Hint: See Section 9.9.)
- (b) Estimate the total primary consolidation settlement under the center of the embankment.
- (c) Plot a time-settlement curve under the center of the embankment.
- (d) How many years will it take for 50% consolidation to occur?
- (e) Explain how you would speed up the consolidation.
- (f) Estimate the rebound (heave) when the surcharge is removed.

(g) Sketch a settlement profile along the base of the embankment. Would the settlement be uniform along the base? Explain your answer.

9.22 A covered steel (unit weight = 80 kN/m^3) tank, 15 m in diameter \times 10 m high and with 20-mm wall thickness, is filled with liquid (unit weight = 9 kN/m^3) up to a height of 9.9 m. The tank sits on a concrete (unit weight = 25 kN/m^3) foundation, 15 m in diameter \times 0.6 m thick. The foundation rests on the surface of a 5-m-thick soft, normally consolidated clay above a thick layer of gravel. The geotechnical data of the clay are: $C_c = 0.6$, $C_r = 0.08$, $C_v = 10 \text{ m}^2/\text{year}$, and $w = 48\%$. Groundwater level is 0.5 m below the surface. Assume the foundation is flexible.

- (a) Calculate the primary consolidation settlement at the center of the tank.
- (b) Calculate the differential consolidation settlement between the center and the edge of the tank.
- (c) Calculate the time for 50% consolidation to occur.
- (d) The tank was loaded to half its capacity and kept there for 2 years. Calculate the settlement. The tank was then drained; calculate the rebound.

CHAPTER 10

SHEAR STRENGTH OF SOILS

10.0 INTRODUCTION

In this chapter we will define, describe, and determine the shear strength of soils. When you complete this chapter, you should be able to:

- Determine the shear strength of soils.
- Understand the differences between drained and undrained shear strength.
- Determine the type of shear test that best simulates field conditions.
- Interpret laboratory and field test results to obtain shear strength parameters.

You will use the following principles learned from previous chapters and other courses.

- Stresses, strains, Mohr's circle of stresses and strains, and stress paths (Chapter 7)
- Friction (statics and/or physics)

Importance

The safety of any geotechnical structure is dependent on the strength of the soil. If the soil fails, a structure founded on it can collapse, endangering lives and causing economic damage. The strength of soils is therefore of paramount importance to geotechnical engineers. The word *strength* is used loosely to mean shear strength, which is the internal frictional resistance of a soil to shearing forces. Shear strength is required to make estimates of the load-bearing capacity of soils and the stability of geotechnical structures, and in analyzing the stress-strain characteristics of soils.

Figure 10.1 shows homes in precarious positions because the shear strength of the soil within the slope was exceeded. Would you like one of these homes to be yours? The content of this chapter will



FIGURE 10.1 Shear failure of soil under several homes. (©Vince Streano/Corbis.)

help you to understand the shear behavior of soils so that you can prevent catastrophes like that shown in Figure 10.1.

10.1 DEFINITIONS OF KEY TERMS

Shear strength of a soil (τ_f) is the maximum internal resistance to applied shearing forces.

Effective friction angle (ϕ') is a measure of the shear strength of soils due to friction.

Cementation (c_{cm}) is a measure of the shear strength of a soil from forces that cement the particles.

Soil tension (c_t) is a measure of the apparent shear strength of a soil from soil suction (negative pore-water pressures or capillary stresses).

Cohesion (c_o) is a measure of the intermolecular forces.

Undrained shear strength (s_u) is the shear strength of a soil when sheared at constant volume.

Apparent cohesion (C) is the apparent shear strength at zero normal effective stress.

Critical state is a stress state reached in a soil when continuous shearing occurs at constant shear stress to normal effective stress ratio and constant volume.

Dilation is a measure of the change in volume of a soil when the soil is distorted by shearing.

10.2 QUESTIONS TO GUIDE YOUR READING

1. What is meant by the shear strength of soils?
2. What factors affect the shear strength?
3. How is shear strength determined?
4. What are the assumptions in the Coulomb, Tresca, Taylor, and Mohr–Coulomb failure criteria?
5. Do soils fail on a plane?
6. What are the differences among peak, critical, and residual effective friction angles?
7. What are peak shear strength, critical shear strength, and residual shear strength?
8. Are there differences between the shear strengths of dense and loose sands, or between normally consolidated and overconsolidated clays?
9. What are the differences between drained and undrained shear strengths?
10. Under what conditions should the drained shear strength or the undrained shear strength parameters be used?
11. What laboratory and field tests are used to determine shear strength?
12. What are the differences among the results of various laboratory and field tests?
13. How do I know what laboratory test to specify for a project?

10.3 TYPICAL RESPONSE OF SOILS TO SHEARING FORCES

The shear strength of a soil is its resistance to shearing stresses. We are going to describe the behavior of two groups of soils when they are subjected to shearing forces. One group, called uncemented soils, has very weak interparticle bonds. The other group, called cemented soils, has strong interparticle bonds through ion exchange or substitution. The particles of cemented soils are chemically bonded or cemented together. An example of a cemented soil is caliche, which is a mixture of clay, sand, and gravel cemented by calcium carbonate.

Let us incrementally deform two samples of soil by applying simple shear deformation (Figure 10.2) to each of them. One sample, which we call Type I, represents mostly loose sands and normally

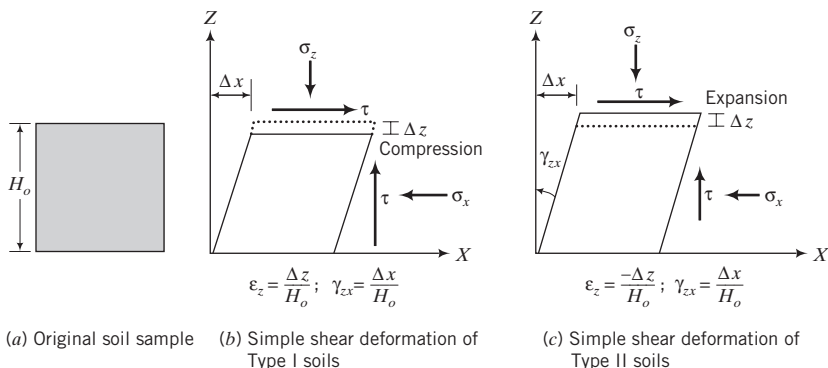


FIGURE 10.2 Simple shear deformation of Type I and Type II soils.

consolidated and lightly overconsolidated clays ($OCR \leq 2$). The other, which we call Type II, represents mostly dense sands and overconsolidated clays ($OCR > 2$). In classical mechanics, simple shear deformation refers to shearing under constant volume. In soil mechanics, we relax this restriction (constant volume) because we wish to know the volume change characteristics of soils under simple shear (Figure 10.2). The implication is that the mathematical interpretation of simple shear tests becomes complicated because we now have to account for the influence of volumetric strains on soil behavior. Since in simple shear $\epsilon_x = \epsilon_y = 0$, the volumetric strain is equal to the vertical strain, $\epsilon_z = \Delta z / H_o$, where Δz is the vertical displacement (positive for compression) and H_o is the initial sample height. The shear strain is the small angular distortion expressed as $\gamma_{zx} = \Delta x / H_o$, where Δx is the horizontal displacement.

We are going to summarize the important features of the responses of these two groups of soils—Type I and Type II—when subjected to a constant vertical (normal) effective stress and increasing shear strain. We will consider the shear stress versus the shear strain, the strain versus the shear strain, and the void ratio versus the shear strain responses, as illustrated in Figure 10.3. The vertical strain and volumetric strain are synonymous in discussing the response of soils in this section.

Type I soils—loose sands, normally consolidated and lightly overconsolidated clays ($OCR \leq 2$)—are observed to:

- Show gradual increase in shear stresses as the shear strain increases (strain-hardens) until an approximately constant shear stress, which we will call the critical state shear stress, τ_{cs} , is attained (Figure 10.3a).
- Compress, that is, they become denser (Figure 10.2b and Figure 10.3b, c) until a constant void ratio, which we will call the critical ratio, e_{cs} , is reached (Figure 10.3c).

Type II soils—dense sands and heavily overconsolidated clays ($OCR > 2$)—are observed to:

- Show a rapid increase in shear stress reaching a peak value, τ_p , at low shear strains (compared to Type I soils) and then show a decrease in shear stress with increasing shear strain (strain-softens), ultimately attaining a critical state shear stress (Figure 10.3a). The strain-softening response generally results from localized failure zones called shear bands (Figure 10.4). These shear bands are soil pockets that have loosened and reached the critical state shear stress. Between the shear bands are denser soils that gradually loosen as shearing continues. The initial thickness of shear bands was observed from laboratory tests to be about 10 to 15 grain diameters. The soil mass within a shear band undergoes intense shearing, while the soil masses above and below it behave as rigid bodies. The development of shear bands depends on the boundary conditions imposed on the soil, the homogeneity of the soil, the grain size, uniformity of loads, and initial density.

When a shear band develops in some types of overconsolidated clays, the particles become oriented parallel to the direction of the shear band, causing the final shear stress of these clays to decrease below the critical state shear stress. We will call this type of soil Type II-A, and the final shear stress attained the residual shear stress, τ_r . Type I soils at very low normal effective stress can also exhibit a peak shear stress during shearing.

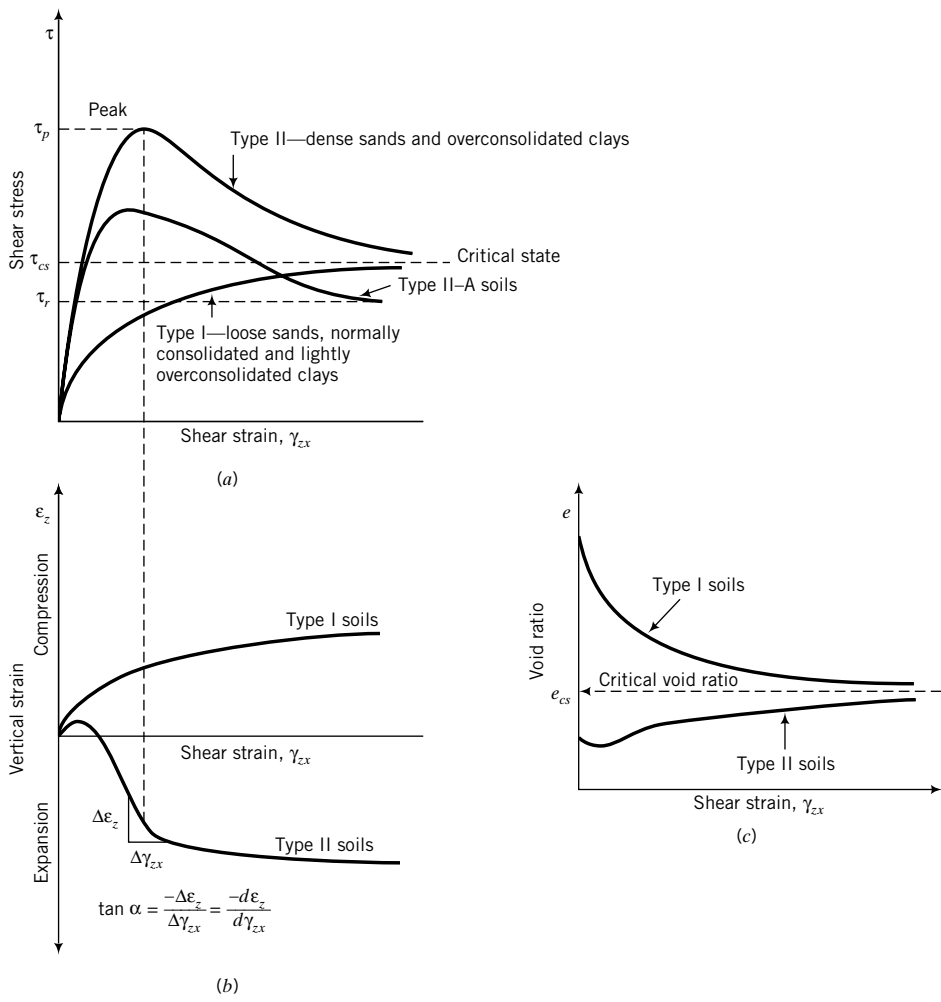


FIGURE 10.3 Response of soils to shearing.

- Compress initially (attributed to particle adjustment) and then expand, that is, they become looser (Figure 10.2c and Figure 10.3b, c) until a critical void ratio (the same void ratio as in Type I soils) is attained.

The critical state shear stress is reached for all soils when no further volume change occurs under continued shearing. We will use the term *critical state* to define the stress state reached by a soil when



FIGURE 10.4 Radiographs of shear bands in a dense fine sand (the white circles are lead shot used to trace internal displacements; white lines are shear bands). (After Budhu, 1979.)

no further change in shear stress and volume occurs under continuous shearing at a constant normal effective stress.

10.3.1 Effects of Increasing the Normal Effective Stress

So far, we have only used a single normal effective stress in our presentation of the responses of Type I and Type II soils. What is the effect of increasing the normal effective stress? For Type I soils, the amount of compression and the magnitude of the critical state shear stress will increase (Figure 10.5a, b). For Type II soils, the peak shear stress tends to disappear, the critical shear stress increases, and the change in volume expansion decreases (Figure 10.5a, b).

If we were to plot the peak shear stress and the critical state shear stress for each constant normal effective stress for Type I and II soils, we would get:

1. An approximate straight line (OA, Figure 10.5c) that links all the critical state shear stress values of Type I and Type II soils. We will call the angle between OA and the σ'_n axis the critical state friction angle, ϕ'_{cs} . The line OA will be called the failure envelope because any shear stress that lies on it is a critical state shear stress.
2. A curve (OBCA, Figure 10.5c) that links all peak shear stress values for Type II soils. We will call OBC (the curved part of OBCA) the peak shear stress envelope because any shear stress that lies on it is a peak shear stress.

At large normal effective stresses, the peak shear stress for Type II soils is suppressed, and only a critical state shear stress is observed and appears as a point (point 9) located on OA (Figure 10.5c). For Type II-A soils, the residual shear stresses would lie on a line OD below OA. We will call the angle between OD and the σ'_n axis the residual friction angle, ϕ'_r . As the normal effective stress increases, the

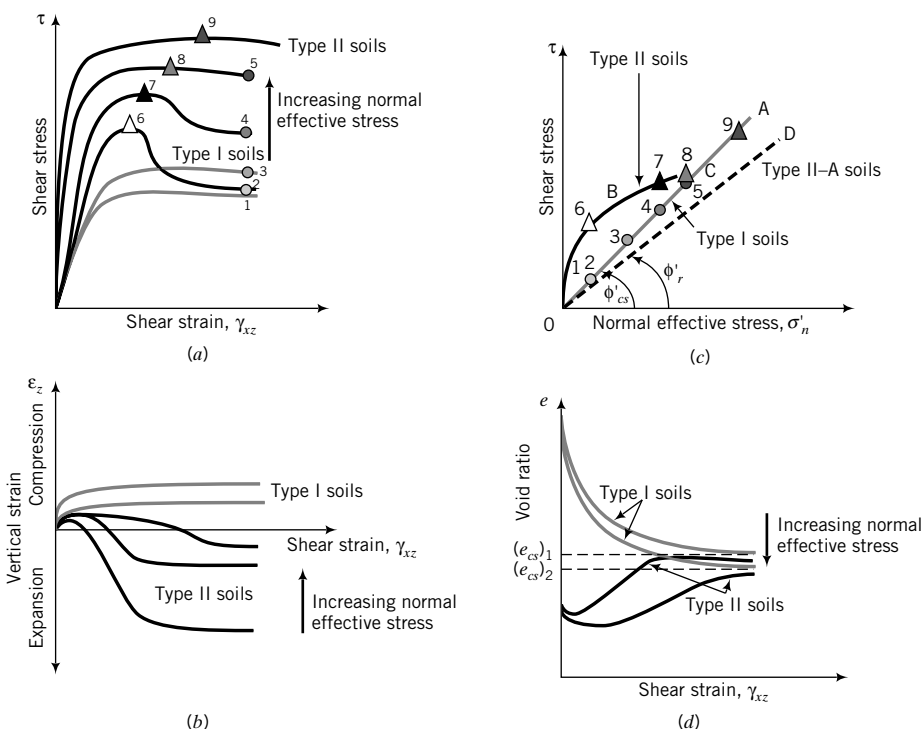


FIGURE 10.5 Effects of increasing normal effective stresses on the response of soils.

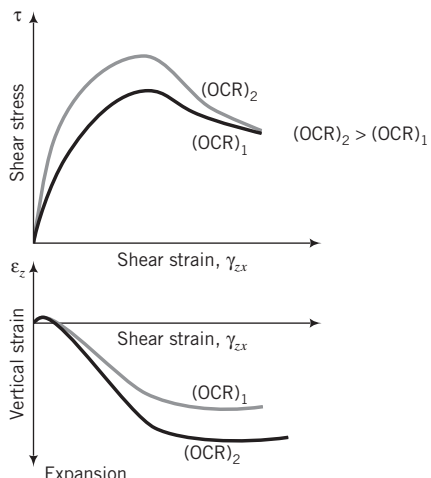


FIGURE 10.6
Effects of OCR on peak strength
and volume expansion.

critical void ratio decreases (Figure 10.5d). Thus, the critical void ratio is dependent on the magnitude of the normal effective stress.

10.3.2 Effects of Overconsolidation Ratio

The initial state of the soil dictates the response of the soil to shearing forces. For example, two overconsolidated homogeneous soils with different overconsolidation ratios but the same mineralogical composition would exhibit different peak shear stresses and volume expansion, as shown in Figure 10.6. The higher overconsolidated soil gives a higher peak shear strength and greater volume expansion.

THE ESSENTIAL POINTS ARE:

1. Type I soils—loose sands and normally consolidated and lightly overconsolidated clays—strain-harden to a critical state shear stress and compress toward a critical void ratio.
2. Type II soils—dense sands and overconsolidated clays—reach a peak shear stress, strain-soften to a critical state shear stress, and expand toward a critical void ratio after an initial compression at low shear strains.
3. The peak shear stress of Type II soils is suppressed and the volume expansion decreases when the normal effective stress is large.
4. Just before peak shear stress is attained in Type II soils, shear bands develop. Shear bands are loose pockets or bands of soil masses that have reached the critical state shear stress. Denser soil masses adjacent to shear bands gradually become looser as shearing continues.
5. All soils reach a critical state, irrespective of their initial state, at which continuous shearing occurs without changes in shear stress and volume for a given normal effective stress.
6. The critical state shear stress and the critical void ratio depend on the normal effective stress. Higher normal effective stresses result in higher critical state shear stresses and lower critical void ratios. The critical void ratio is not a fundamental soil property.
7. At large strains, the particles of some overconsolidated clays become oriented parallel to the direction of shear bands, and the final shear stress attained is lower than the critical state shear stress.
8. Higher overconsolidation ratios of homogeneous soils result in higher peak shear stresses and greater volume expansion.

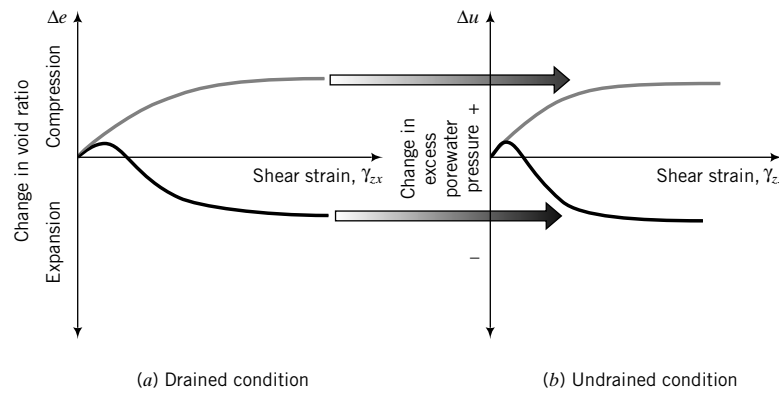


FIGURE 10.7 Effects of drained and undrained conditions on volume changes.

10.3.3 Effects of Drainage of Excess Porewater Pressure

You were introduced to drained and undrained conditions when we discussed stress paths in Chapter 8. Drained condition occurs when the excess porewater pressure developed during loading of a soil dissipates, i.e., $\Delta u = 0$. Undrained condition occurs when the excess porewater pressure cannot drain, at least quickly, from the soil; that is, $\Delta u \neq 0$. The existence of either condition—drained or undrained—depends on the soil type, the geological formation (fissures, sand layers in clays, etc.), and the rate of loading. In reality, neither condition is true. They are limiting conditions that set up the bounds within which the true condition lies.

The rate of loading under the undrained condition is often much faster than the rate of dissipation of the excess porewater pressure, and the volume-change tendency of the soil is suppressed. The result of this suppression is a change in excess porewater pressure during shearing. A soil with a tendency to compress during drained loading will exhibit an increase in excess porewater pressure (positive excess porewater pressure, Figure 10.7) under undrained condition, resulting in a decrease in effective stress. A soil that expands during drained loading will exhibit a decrease in excess porewater pressure (negative excess porewater pressure, Figure 10.7) under undrained condition, resulting in an increase in effective stress. These changes in excess porewater pressure occur because the void ratio does not change during undrained loading; that is, the volume of the soil remains constant.

During the life of a geotechnical structure, called the long-term condition, the excess porewater pressure developed by a loading dissipates, and drained condition applies. Clays usually take many years to dissipate the excess porewater pressures. During construction and shortly after, called the short-term condition, soils with low permeability (fine-grained soils) do not have sufficient time for the excess porewater pressure to dissipate, and undrained condition applies. The hydraulic conductivity of coarse-grained soils is sufficiently large that under static loading conditions the excess porewater pressure dissipates quickly. Consequently, undrained condition does not apply to clean, coarse-grained soils under static loading, but only to fine-grained soils and to mixtures of coarse- and fine-grained soils. Dynamic loading, such as during an earthquake, is imposed so quickly that even coarse-grained soils do not have sufficient time to dissipate the excess porewater pressure, and undrained condition applies.

A summary of the essential differences between drained and undrained conditions is shown in Table 10.1.

10.3.4 Effects of Cohesion

The term *cohesion*, C , as used conventionally in geotechnical engineering, is an apparent shear strength that captures the effects of intermolecular forces (c_o), soil tension (c_t), and cementation (c_{cm}) on the

TABLE 10.1 Differences Between Drained and Undrained Loading

Condition	Drained	Undrained
Excess porewater pressure	-0	Not zero; could be positive or negative
Volume change	Compression Expansion	Positive excess porewater pressure Negative excess porewater pressure
Consolidation	Yes, fine-grained soils	No
Compression	Yes	Yes, but lateral expansion must occur so that the volume change is zero
Analysis	Effective stress	Total stress
Design strength parameters	ϕ'_{cs} (or ϕ'_p or ϕ'_f)	s_u

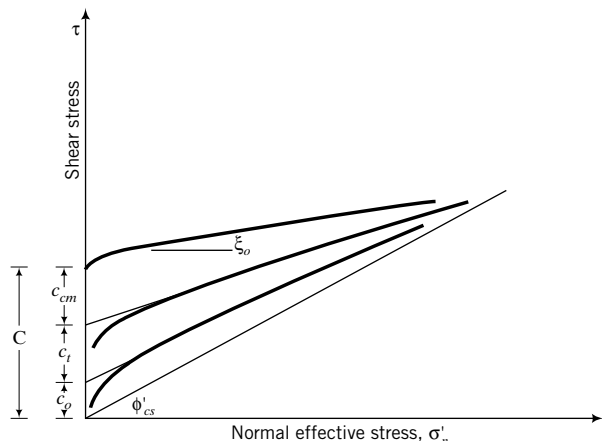
shear strength of soils. In this textbook, we will separate these effects. Cohesion, c_o , represents the action of intermolecular forces on the shear strength of soils. These forces do not contribute significant shearing resistance for practical consideration and will be neglected. In a plot of peak shear stress versus normal effective stress using shear test data, an intercept shear stress, c_o , would be observed (Figure 10.8) when a best-fit straight line is used as the trend line.

10.3.5 Effects of Soil Tension

Soil tension is the result of surface tension of water on soil particles in unsaturated soils. A suction pressure (negative porewater pressure from capillary stresses) is created that pulls the soil particles together. Recall that the effective stress is equal to total stress minus porewater pressure. Thus, if the porewater pressure is negative, the normal effective stress increases. For soil as a frictional material, this normal effective stress increase leads to a gain in shearing resistance. The intergranular friction angle or critical state friction angle does not change.

Soil tension can be very large, sometimes exceeding 1000 kPa (equivalent to the pressure from about 100 m of water). If the soil becomes saturated, the soil tension reduces to zero. Thus, any gain in shear strength from soil tension is only temporary. It can be described as an apparent shear strength, c_t . In practice, you should not rely on this gain in shear strength, especially for long-term loading.

There are some situations, such as shallow excavations in fine-grained soils that will be opened for a very short time, in which you can use the additional shear strength (apparent shear strength) to your advantage. Without soil tension, the soil would collapse and these excavations might need to be braced by using steel, concrete, or wood panels. With soil tension, you may not need these bracings because the apparent shear strength allows the soil to support itself over a limited depth (see Chapter 15), resulting in cost savings. However, local experience is required to successfully use soil tension to your advantage.

**FIGURE 10.8**

Peak shear stress envelope for soils resulting from cohesion, soil tension, and cementation.

Unsaturated soils generally behave like Type II soils because negative excess porewater pressure increases the normal effective stress and, consequently, the shearing resistance. In a plot of peak shear stress versus normal effective stress using shear test data, an intercept shear stress, c_t , would be observed (Figure 10.8).

10.3.6 Effects of Cementation

Nearly all natural soils have some degree of cementation, wherein the soil particles are chemically bonded. Salts such as calcium carbonate (CaCO_3) are the main natural compounds for cementing soil particles. The degree of cementation can vary widely, from very weak bond strength (soil crumbles under finger pressure) to the bond strength of weak rocks.

Cemented soils possess shear strength even when the normal effective stress is zero. They behave much like Type II soils except that they have an initial shear strength, c_{cm} , under zero normal effective stress. In this textbook, we will call this initial shear strength the cementation strength. In a plot of peak shear stress versus normal effective stress using shear test data, an intercept shear stress, c_{cm} , would be observed (Figure 10.8). The slope angle, ξ_o , of the best-fit straight line from shear test data is the apparent friction angle (Figure 10.8).

The shear strength from cementation is mobilized at small shear strain levels ($<0.001\%$). In most geotechnical structures, the soil mass is subjected to much larger shear strains. You need to be cautious in utilizing c_{cm} in design because at large shear strains, any shear strength due to cementation in the soil will be destroyed. Also, the cementation of natural soils is generally nonuniform. Thus, over the footprint of your structure the shear strength from cementation will vary.

THE ESSENTIAL POINTS ARE:

- 1. Volume changes that occur under drained condition are suppressed under undrained condition.**
The result of this suppression is that a soil with a compression tendency under drained condition will respond with positive excess porewater pressures during undrained condition, and a soil with an expansion tendency during drained condition will respond with negative excess porewater pressures during undrained condition.
- 2. Cohesion, defined as the shearing resistance from intermolecular forces, is generally small for consideration in geotechnical application.**
- 3. Soil tension resulting from surface tension of water on soil particles in unsaturated soils creates an apparent shear resistance that disappears when the soil is saturated. You need to be cautious in utilizing this additional shearing resistance in certain geotechnical applications such as shallow excavations.**
- 4. Cementation—the chemical bonding of soil particles—is present to some degree in all natural soils. It imparts shear strength to the soil at zero normal effective stress. The shear strain at which this shear strength is mobilized is very small. You should be cautious in using this shear strength in designing geotechnical systems because in most of these systems the shear strain mobilized is larger than that required to mobilize the shear strength due to cementation.**

What's next . . . You should now have a general idea of the responses of soils to shearing forces. How do we interpret these responses using mechanical models? In the next section, four models are considered.

10.4 FOUR MODELS FOR INTERPRETING THE SHEAR STRENGTH OF SOILS

In this section, we will examine four soil models to help us interpret the shear strength of soils. A soil model is an idealized representation of the soil to allow us to understand its response to loading and other external events. By definition, then, a soil model should not be expected to capture all the intricacies

of soil behavior. Each soil model may have a different set of assumptions and may only represent one or more aspects of soil behavior.

10.4.1 Coulomb's Failure Criterion

Soils, in particular granular soils, are endowed by nature with slip planes. Each contact of one soil particle with another is a potential micro slip plane. Loadings can cause a number of these micro slip planes to align in the direction of least resistance. Thus, we can speculate that a possible mode of soil failure is slip on a plane of least resistance. Recall from your courses in statics or physics that impending slip between two rigid bodies was the basis for Coulomb's frictional law. For example, if a wooden block is pushed horizontally across a table (Figure 10.9a), the horizontal force (H) required to initiate movement, according to Coulomb's frictional law, is

$$H = \mu W \quad (10.1)$$

where μ is the coefficient of static sliding friction between the block and the table and W is the weight of the block. The angle between the resultant force and the normal force is called the friction angle, $\phi' = \tan^{-1} \mu$.

Coulomb's law requires the existence or the development of a critical sliding plane, also called slip plane. In the case of the wooden block on the table, the slip plane is the horizontal plane at the interface between the wooden block and the table. Unlike the wooden block, we do not know where the sliding plane is located in soils.

In terms of stresses, Coulomb's law is expressed as

$$\tau_f = (\sigma'_n)_f \tan \phi' \quad (10.2)$$

where $\tau_f (= T/A$, where T is the shear force at impending slip and A is the area of the plane parallel to T) is the shear stress when slip is initiated, and $(\sigma'_n)_f$ is the normal effective stress on the plane on which slip is initiated. The subscript f denotes failure, which, according to Coulomb's law, occurs when rigid body movement of one body relative to another is initiated. Failure does not necessarily mean collapse, but is the impeding movement of one rigid body relative to another.

If you plot Coulomb's equation (10.2) on a graph of shear stress, τ_f , versus normal effective stress, $(\sigma'_n)_f$, you get a straight line similar to OA (Figure 10.5) if $\phi' = \phi'_{cs}$. Thus, Coulomb's law may be used to model soil behavior at critical state. But what about modeling the peak behavior that is characteristic of Type II soils?

You should recall from Chapter 4 that soils can have different unit weights depending on the arrangement of the particles. Let us simulate two extreme arrangements of soil particles for

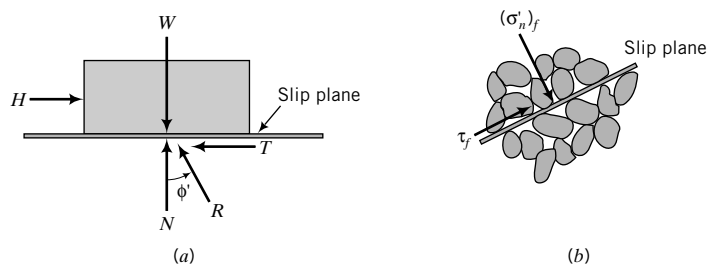


FIGURE 10.9 (a) Slip of a wooden block. (b) A slip plane in a soil mass.

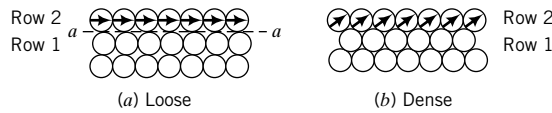


FIGURE 10.10 Packing of disks representing loose and dense sand.

coarse-grained soils—one loose, the other dense. We will assume that the soil particles are spheres. In two dimensions, arrays of spheres become arrays of disks. The loose array is obtained by stacking the spheres one on top of another, while the dense packing is obtained by staggering the rows, as illustrated in Figure 10.10.

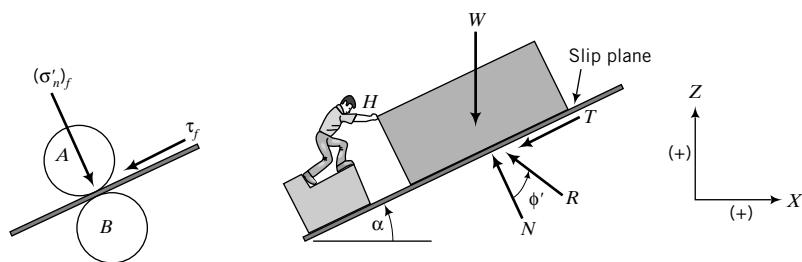
For simplicity, let us consider the first two rows. If we push (shear) row 2 relative to row 1 in the loose assembly, sliding would be initiated on the horizontal plane, $a-a$, consistent with Coulomb's frictional law [Equation (10.2)]. Once motion is initiated, the particles in the loose assembly would tend to move into the void spaces. The direction of movement would have a downward component, that is, compression.

In the dense packing, relative sliding of row 2 with respect to row 1 is restrained by the interlocking of the disks. Sliding, for the dense assembly, would be initiated on an inclined plane rather than on a horizontal plane. For the dense assembly, the particles must ride up over each other or be pushed aside, or both. The direction of movement of the particles would have an upward component, that is, expansion.

We are going to use our knowledge of statics to investigate impending sliding of particles up or down a plane to assist us in interpreting the shearing behavior of soils using Coulomb's frictional law. The shearing of the loose array can be idealized by analogy with the sliding of our wooden block on the horizontal plane. At failure,

$$\frac{\tau_f}{(\sigma'_n)_f} = \frac{H}{W} = \tan\phi' \quad (10.3)$$

Consider two particles A and B in the dense assembly and draw the free-body diagram of the stresses at the sliding contact between A and B , as depicted in Figure 10.11. We now appeal to our wooden block for an analogy to describe the shearing behavior of the dense array. For the dense array, the wooden block is placed on a plane oriented at an angle α to the horizontal (Figure 10.11b). Our goal is to find the horizontal force to initiate movement of the block up the incline. You may have solved this problem in statics. Anyway, we are going to solve it again. At impending motion, $T = \mu N$, where N is the normal force. Using the force equilibrium equations in the X and Z directions, we get



(a) Stresses on failure plane (b) Simulated shearing of a dense array of particles

FIGURE 10.11 Simulation of failure in dense sand.

$$\Sigma F_x = 0: H - N \sin \alpha - \mu N \cos \alpha = 0 \quad (10.4)$$

$$\Sigma F_z = 0: N \cos \alpha - \mu N \sin \alpha - W = 0 \quad (10.5)$$

Solving for H and W , we obtain

$$H = N(\sin \alpha + \mu \cos \alpha) \quad (10.6)$$

$$W = N(\cos \alpha - \mu \sin \alpha) \quad (10.7)$$

Dividing Equation (10.6) by Equation (10.7) and simplifying, we obtain

$$\frac{H}{W} = \frac{\mu + \tan \alpha}{1 - \mu \tan \alpha} = \frac{\tan \phi' + \tan \alpha}{1 - \tan \phi' \tan \alpha}$$

By analogy with the loose assembly, we can replace H by τ_f and W by $(\sigma'_n)_f$, resulting in

$$\tau_f = (\sigma'_n)_f \frac{\tan \phi' + \tan \alpha}{1 - \tan \phi' \tan \alpha} = (\sigma'_n)_f \tan(\phi' + \alpha) \quad (10.8)$$

Let us investigate the implications of Equation (10.8). If $\alpha = 0$, Equation (10.8) reduces to Coulomb's frictional Equation (10.2). If α increases, the shear strength, τ_f , gets larger. For instance, assume $\phi' = 30^\circ$ and $(\sigma'_n)_f$ is constant; then, for $\alpha = 0$ we get $\tau_f = 0.58(\sigma'_n)_f$, but if $\alpha = 10^\circ$ we get $\tau_f = 0.84(\sigma'_n)_f$, that is, an increase of 45% in shear strength for a 10% increase in α .

If the normal effective stress increases on our dense disk assembly, the amount of "riding up" of the disks will decrease. In fact, we can impose a sufficiently high normal effective stress to suppress the "riding up" tendencies of the dense disks assembly. Therefore, the ability of the dense disks assembly to expand depends on the magnitude of the normal effective stress. The lower the normal effective stress, the greater the value of α . The net effect of α due to normal effective stress increases is that the failure envelope becomes curved, as illustrated by *OBC* in Figure 10.12, which is similar to the expected peak shear stress response of Type II soils (Figure 10.5c).

The geometry of soil grains and their structural arrangements are much more complex than our loose and dense assembly of disks. However, the model using disks is applicable to soils if we wish to interpret their (soils') shear strength using Coulomb's frictional law. In real soils, the particles are randomly distributed and often irregular. Shearing of a given volume of soil would cause impending slip of some particles to occur up the plane while others occur down the plane. The general form of Equation (10.8) is then

$$\tau_f = (\sigma'_n)_f \tan(\phi' \pm \alpha) \quad (10.9)$$

where the positive sign refers to soils in which the net movement of the particles is initiated up the plane and the negative sign refers to net particle movement down the plane.

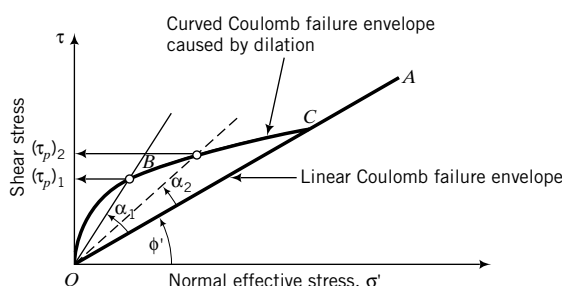


FIGURE 10.12
Effects of dilation on Coulomb's failure envelope.

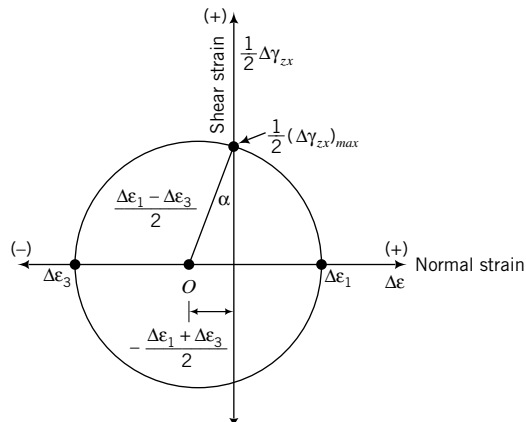


FIGURE 10.13
Mohr's circle of strain and angle of dilation.

We will call the angle, α , the dilation angle. It is a measure of the change in volumetric strain with respect to the change in shear strain. Soils that have positive values of α expand during shearing, while soils with negative values of α contract during shearing. In Mohr's circle of strain (Figure 10.13), the dilation angle is

$$\alpha = \sin^{-1}\left(-\frac{\Delta\epsilon_1 + \Delta\epsilon_3}{\Delta\epsilon_1 - \Delta\epsilon_3}\right) = \sin^{-1}\left(-\frac{\Delta\epsilon_1 + \Delta\epsilon_3}{(\Delta\gamma_{zx})_{max}}\right) \quad (10.10)$$

where Δ denotes change. The negative sign is used because we want α to be positive when the soil is expanding. You should recall that compression is taken as positive in soil mechanics.

If a soil mass is constrained in the lateral directions, the dilation angle is represented (Figure 10.3b) as

$$\alpha = \tan^{-1}\left(\frac{-\Delta z}{\Delta x}\right) \quad (10.11)$$

Dilation is not a peculiarity of soils, but occurs in many other materials, for example, rice and wheat. The ancient traders of grains were well aware of the phenomenon of volume expansion of grains. However, it was Osborne Reynolds (1885) who described the phenomenon of dilatancy and brought it to the attention of the scientific community. Dilation can be seen in action at a beach. If you place your foot on beach sand just following a receding wave, you will notice that the initially wet, saturated sand around your foot momentarily appears to be dry (whitish color). This occurs because the sand mass around your foot dilates, sucking water up into the voids. This water is released, showing up as surface water, when you lift up your foot.

For cemented soils, Coulomb's frictional law can be written as

$$\tau_f = c_{cm} + (\sigma'_n)_f \tan(\xi_o) \quad (10.12)$$

where c_{cm} is the cementation strength (Figure 10.8) and ξ_o is the apparent friction angle. Neither c_{cm} nor ξ_o is a fundamental soil parameter. Also, adding the cementation strength to the apparent frictional strength $[(\sigma'_n)_f \tan \xi_o]$ is not strictly correct since they are not mobilized at the same shear strains.

Coulomb's model applies strictly to soil failures that occur along a slip plane, such as a joint or the interface of two soils or the interface between a structure and a soil. Stratified soil deposits such as overconsolidated varved clays (regular layered soils that depict seasonal variations in deposition) and fissured clays are likely candidates for failure following Coulomb's model, especially if the direction of shearing is parallel to the direction of the bedding plane.

THE ESSENTIAL POINTS ARE:

1. Shear failure of soils may be modeled using Coulomb's frictional law, $\tau_f = (\sigma'_n)_f \tan(\phi' \pm \alpha)$, where τ_f is the shear stress when slip is initiated, $(\sigma'_n)_f$ is the normal effective stress on the slip plane, ϕ' is the friction angle, and α is the dilation angle.
2. The effect of dilation is to increase the shear strength of the soil and cause the Coulomb's failure envelope to be curved.
3. Large normal effective stresses tend to suppress dilation.
4. At the critical state, the dilation angle is zero.
5. For cemented soils, Coulomb's frictional law is $\tau_f = c_{cm} + (\sigma'_n)_f \tan(\xi_o)$ where c_{cm} is called the cementation strength and ξ_o is the apparent friction angle.

10.4.2 Taylor's Failure Criterion

Taylor (1948) used an energy method to derive a simple soil model. He assumed that the shear strength of soil is due to sliding friction from shearing and the interlocking of soil particles. Consider a rectangular soil element that is sheared by a shear stress τ under a constant vertical effective stress σ'_z (Figure 10.2c). Let us assume that the increment of shear strain is $d\gamma$ and the increment of vertical strain is $d\varepsilon_z$.

The external energy (force \times distance moved in the direction of the force or stress \times compatible strain) is $\tau d\gamma$. The internal energy is the work done by friction, $\mu_f \sigma'_z d\gamma$, where μ_f is the static, sliding friction coefficient and the work done by the movement of the soil against the vertical effective stress, $\pm \sigma'_z d\varepsilon_z$. The negative sign indicates the vertical strain is in the opposite direction (expansion) to the direction of the vertical effective stress. The energy $\pm \sigma'_z d\varepsilon_z$ is the interlocking energy due to the arrangement of the soil particles or soil fabric.

For equilibrium,

$$\tau d\gamma = \mu_f \sigma'_z d\gamma \pm \sigma'_z d\varepsilon_z$$

Dividing by $\sigma'_z d\gamma$, we get

$$\frac{\tau}{\sigma'_z} = \mu_f \pm \frac{d\varepsilon_z}{d\gamma} \quad (10.13)$$

At critical state, $\mu_f = \tan \phi'_{cs}$ and $\alpha = \frac{d\varepsilon_z}{d\gamma} = 0$. Therefore,

$$\left(\frac{\tau}{\sigma'_z} \right)_{cs} = \tan \phi'_{cs} \quad (10.14)$$

At peak shear strength,

$$-\frac{d\varepsilon_z}{d\gamma} = \tan \alpha_p$$

Therefore,

$$\left(\frac{\tau}{\sigma'_z} \right)_p = \tan \phi'_{cs} + \tan \alpha_p \quad (10.15)$$

where the subscripts, cs and p , denote critical state and peak, respectively.

Unlike Coulomb failure criterion, Taylor failure criterion does not require the assumption of any physical mechanism of failure, such as a plane of sliding. It can be applied at every stage of loading

for soils that are homogeneous and deform under plane strain conditions similar to simple shear. This failure criterion would not apply to soils that fail along a joint or an interface between two soils. Taylor failure criterion gives a higher peak dilation angle than Coulomb failure criterion.

Equation (10.13) applies to two-dimensional stress systems. An extension of Taylor failure criterion to account for three-dimensional stress is presented in Chapter 11. Neither Taylor nor Coulomb failure criterion explicitly considers the rotation of the soil particles during shearing.

THE ESSENTIAL POINTS ARE:

1. The shear strength of soils is due to friction and to interlocking of soil particles.
2. The critical state shear strength is: $\tau_{cs} = (\sigma'_n)_f \tan \phi'_{cs}$
3. The peak shear strength is: $\tau_p = (\sigma'_n)_f (\tan \phi'_{cs} + \tan \alpha_p)$.

10.4.3 Mohr-Coulomb Failure Criterion

Coulomb's frictional law for finding the shear strength of soils requires that we know the friction angle and the normal effective stress on the slip plane. Both of these are not readily known because soils are usually subjected to a variety of stresses. You should recall from Chapter 7 that Mohr's circle can be used to determine the stress state within a soil mass. By combining Mohr's circle for finding stress states with Coulomb's frictional law, we can develop a generalized failure criterion.

Let us draw a Coulomb frictional failure line, as illustrated by AB in Figure 10.14, and subject a cylindrical sample of soil to principal effective stresses so that Mohr's circle touches the Coulomb failure line. Of course, several circles can share AB as the common tangent, but we will show only one for simplicity. The point of tangency is at B [$\tau_f, (\sigma'_n)_f$] and the center of the circle is at O . We are going to discuss mostly the top half of the circle; the bottom half is a reflection of the top half. The major and minor principal effective stresses at failure are $(\sigma'_1)_f$ and $(\sigma'_3)_f$. Our objective is to find a relationship between the principal effective stresses and ϕ' at failure. We will discuss the appropriate ϕ' later in this section.

From the geometry of Mohr's circle,

$$\sin \phi' = \frac{OB}{OA} = \frac{\frac{(\phi'_1)_f - (\sigma'_3)_f}{2}}{\frac{(\sigma'_1)_f + (\sigma'_3)_f}{2}}$$

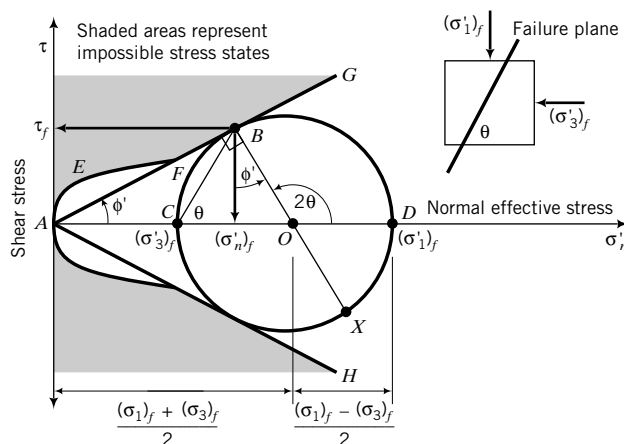


FIGURE 10.14 The Mohr-Coulomb failure envelope.

which reduces to

$$\sin \phi' = \frac{(\sigma'_1)_f - (\sigma'_3)_f}{(\sigma'_1)' + (\sigma'_3)'_f} \quad (10.16)$$

Rearranging Equation (10.16) gives

$$\frac{(\sigma'_1)_f}{(\sigma'_3)_f} = \frac{1 + \sin \phi'}{1 - \sin \phi'} = \tan^2\left(45 + \frac{\phi'}{2}\right) = K_p \quad (10.17)$$

or

$$\frac{(\sigma'_3)_f}{(\sigma'_1)_f} = \frac{1 - \sin \phi'}{1 + \sin \phi'} = \tan^2\left(45 - \frac{\phi'}{2}\right) = K_a \quad (10.18)$$

where K_p and K_a are called the passive and active earth pressure coefficients. In Chapter 15, we will discuss K_p and K_a and use them in connection with the analysis of earth-retaining walls. The angle $BCO = \theta$ represents the inclination of the failure plane (BC) or slip plane to the plane on which the major principal effective stress acts in Mohr's circle. Let us find a relationship between θ and ϕ' . From the geometry of Mohr's circle (Figure 10.14),

$$\begin{aligned} \angle BOC &= 90 - \phi' \quad \text{and} \quad \angle BOD = 2\theta = 90^\circ + \phi' \\ \therefore \theta &= 45 + \frac{\phi'}{2} = \frac{\pi}{4} + \frac{\phi'}{2} \end{aligned} \quad (10.19)$$

The failure stresses (the stresses on the plane BC) are

$$(\sigma'_n)_f = \frac{\sigma'_1 + \sigma'_3}{2} - \frac{\sigma'_1 - \sigma'_3}{2} \sin \phi' \quad (10.20)$$

$$\tau_f = \frac{\sigma'_1 - \sigma'_3}{2} \cos \phi' \quad (10.21)$$

The Mohr–Coulomb (MC) failure criterion is a limiting stress criterion, which requires that stresses in the soil mass cannot lie within the shaded region shown in Figure 10.14. That is, the soil cannot have stress states greater than the failure stress state. The shaded areas are called regions of impossible stress states. For dilating soils, the bounding curve for possible stress states is the failure envelope, $AEBF$. For nondilating soils, the bounding curve is the linear line AFB . The MC failure criterion derived here is independent of the intermediate principal effective stress σ'_2 , and does not consider the strains at which failure occurs.

Because MC is a limiting stress criterion, the failure lines AG and AH (Figure 10.14) are fixed lines in $[\tau, \sigma'_n]$ space. The line AG is the failure line for compression, while the line AH is the failure line for extension (soil elongates; the lateral effective stress is greater than the vertical effective stress). The shear strength in compression and in extension from interpreting soil strength using the MC failure criterion is identical. In reality, this is not so.

When the stresses on a plane within the soil mass reach the failure line (plane), they must remain there under further loading. For example, point B (Figure 10.14) is on the MC failure line, AG , but point X is not on the failure line, AH . When additional loading is applied, point B must remain on the failure line, AG . The Mohr circle must then gradually rotate clockwise until point X lies on the failure line, AH . In this way, stresses on more planes reach failure. We could have the reverse, whereby point X is on the failure line, AH , and point B is not on the failure line, AG . For certain geotechnical projects, such as in

open excavations in soft soils, this may be the case. In practice, our main concern is when failure is first achieved, point *B* in Figure 10.14, rather than with the postfailure behavior.

Traditionally, failure criteria are defined in terms of stresses. Strains are considered at working stresses (stresses below the failure stresses) using stress-strain relationships (also called constitutive relationships) such as Hooke's law. Strains are important because although the stress or load imposed on a soil may not cause it to fail, the resulting strains or displacements may be intolerable. We will describe in Chapter 11 a simple model that considers the effects of the intermediate principal effective stress and strains on soil behavior.

If we normalize (make the quantity a number, i.e., no units) Equation (10.16) by dividing the numerator and denominator by $(\sigma'_3)_f$, we get

$$\sin \phi' = \frac{\frac{(\sigma'_1)_f}{(\sigma'_3)_f} - 1}{\frac{(\sigma'_1)_f}{(\sigma'_3)_f} + 1} \quad (10.22)$$

The implication of this equation is that the MC failure criterion defines failure when the maximum principal effective stress ratio, called maximum effective stress obliquity, $\frac{(\sigma'_1)_f}{(\sigma'_3)_f}$, is achieved and not when the maximum shear stress, $[(\sigma'_1 - \sigma'_3)/2]_{max}$, is achieved. The failure shear stress is then less than the maximum shear stress.

THE ESSENTIAL POINTS ARE:

- 1. Coupling Mohr's circle with Coulomb's frictional law allows us to define shear failure based on the stress state of the soil.**
- 2. Failure occurs, according to the Mohr-Coulomb failure criterion, when the soil reaches the maximum principal effective stress obliquity, that is, $(\frac{\sigma'_1}{\sigma'_3})_{max}$.**
- 3. The failure plane or slip plane is inclined at an angle $\theta = \pi/4 + \phi'/2$ to the plane on which the major principal effective stress acts.**
- 4. The maximum shear stress, $\tau_{max} = [(\sigma'_1 - \sigma'_3)/2]_{max}$, is not the failure shear stress.**

10.4.4 Tresca Failure Criterion

The shear strength of a fine-grained soil under undrained condition is called the undrained shear strength, s_u . We use the Tresca failure criterion—shear stress at failure is one-half the principal stress difference—to interpret the undrained shear strength. The undrained shear strength, s_u , is the radius of the Mohr total stress circle; that is,

$$s_u = \frac{(\sigma_1)_f - (\sigma_3)_f}{2} = \frac{(\sigma'_1)_f - (\sigma'_3)_f}{2} \quad (10.23)$$

as shown in Figure 10.15a. The shear strength under undrained loading depends only on the initial void ratio or the initial water content. An increase in initial normal effective stress, sometimes called confining pressure, causes a decrease in initial void ratio and a larger change in excess porewater pressure when a soil is sheared under undrained condition. The result is that the Mohr's circle of total stress expands and the undrained shear strength increases (Figure 10.15b). Thus, s_u is not a fundamental soil property. The value of s_u depends on the magnitude of the initial confining pressure or the initial void ratio. Analyses of soil strength and soil stability problems using s_u are called total stress analyses (TSA).

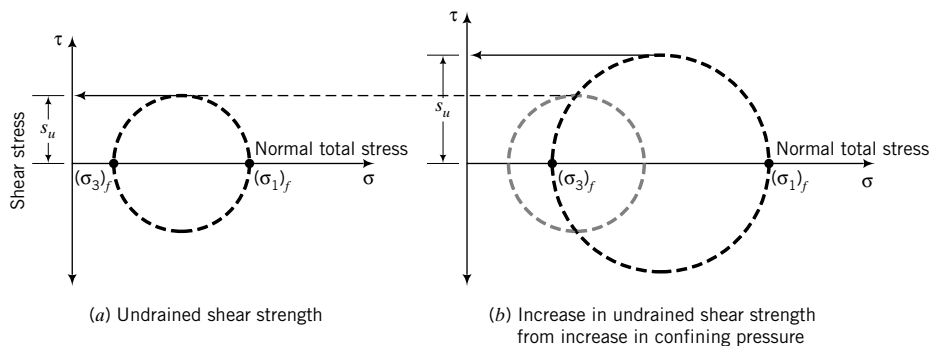


FIGURE 10.15 Mohr's circles for undrained conditions.

THE ESSENTIAL POINTS ARE:

1. For a total stress analysis, which applies to fine-grained soils, the shear strength parameter is the undrained shear strength, s_u .
2. Tresca failure criterion is used to interpret the undrained shear strength.
3. The undrained shear strength depends on the initial void ratio. It is not a fundamental soil shear strength parameter.

What's next . . . In the next section, we will discuss the implications of the failure criteria presented for soils. You need to be aware of some important ramifications of these criteria when you use them to interpret soil strength for practical applications.

10.5 PRACTICAL IMPLICATIONS OF THE FAILURE CRITERIA

When we interpret soil failure using Coulomb, Mohr–Coulomb, Tresca, or Taylor failure criteria, we are using a particular mechanical model. For example, Coulomb's failure criterion is based on a sliding block model. For this and the Mohr–Coulomb failure criterion, we assume that:

1. There is a slip plane upon which one part of the soil mass slides relative to the other. Each part of the soil above and below the slip plane is a rigid mass. However, soils generally do not fail on a slip plane. Rather, in dense soils, there are pockets or bands of soil that have reached critical state while other pockets are still dense. As the soil approaches peak shear stress and beyond, more dense pockets become loose as the soil strain-softens. At the critical state, the whole soil mass becomes loose and behaves like a viscous fluid. Loose soils do not normally show slip planes or shear bands, and strain-harden to the critical state.
2. No deformation of the soil mass occurs prior to failure. In reality, significant soil deformation (shear strains $\sim 2\%$) is required to mobilize the peak shear stress and much more (shear strains $> 10\%$) for the critical state shear stress.
3. Failure occurs according to Coulomb by impending, frictional sliding along a slip plane, and according to Mohr–Coulomb when the maximum stress obliquity on a plane is mobilized.

The Coulomb and Mohr–Coulomb failure criteria are based on limiting stress. Stresses within the soil must either be on the slip plane or be below it. Taylor failure criterion considers not only the forces acting on the soil mass, but also the deformation that occurs from these forces. That is, failure is a combination of the forces and the resulting deformation. Tresca's criterion, originally proposed as a yield criterion in solid mechanics, has been adopted in soil mechanics as a failure (limiting stress) criterion. It is not the same as the Mohr–Coulomb failure criterion.

TABLE 10.2 Differences Among the Four Failure Criteria

Name	Failure criteria	Soil treated as	Best used for	Test data interpretation*
Coulomb	Failure occurs by impending, frictional sliding on a slip plane.	Rigid, frictional material	Layered or fissured overconsolidated soils or a soil where a prefailure plane exists	Direct shear
Mohr–Coulomb	Failure occurs by impending, frictional sliding on the plane of maximum principal effective stress obliquity.	Rigid, frictional material	Long-term (drained condition) strength of overconsolidated fine-grained and dense coarse-grained soils	Triaxial
Tresca	Failure occurs when one-half the maximum principal stress difference is achieved.	Homogeneous solid	Short-term (undrained condition) strength of fine-grained soils	Triaxial
Taylor	Failure occurs from sliding (frictional strength) and interlocking of soil particles.	Deformable, frictional solid	Short-term and long-term strength of homogeneous soils	Direct simple shear

*See Sections 10.7 and 10.11 for descriptions of these tests.

With the exception of Taylor's criterion, none of the failure criteria provide information on the shear strains required to initiate failure. Strains (shear and volumetric) are important in the evaluation of shear strength and deformation of soils for design of safe foundations, slopes, and other geotechnical systems. Also, these criteria do not consider the initial state (e.g., the initial stresses, overconsolidation ratio, and initial void ratio) of the soil. In reality, failure is influenced by the initial state of the soil. In Chapter 11, we will develop a simple model in which we will consider the initial state and strains at which soil failure occurs. A summary of the key differences among the four soil failure criteria is given in Table 10.2.

We are going to define three regions of soil states, as illustrated in Figure 10.16, and consider practical implications of soils in these regions.

Region I. Impossible soil states. A soil cannot have soil states above the boundary AEFB.

Region II. Impending instability (risky design). Soil states within the region AEFA (Figure 10.16a) or 1-2-3 (Figure 10.16b) are characteristic of dilating soils that show peak shear strength and are

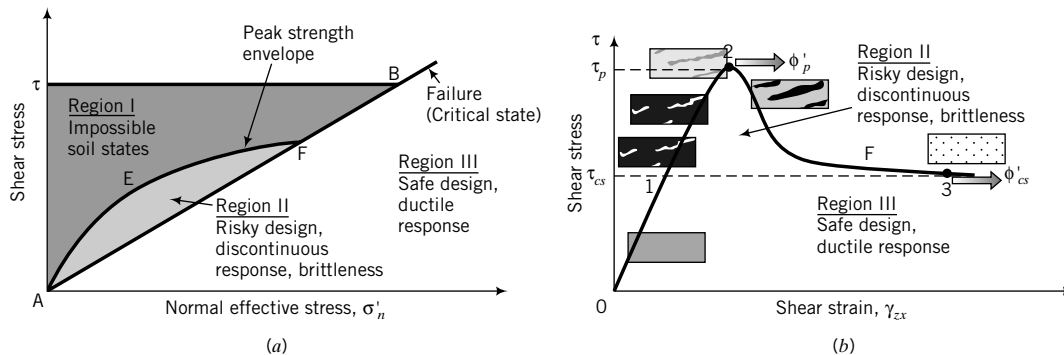


FIGURE 10.16 Interpretation of soil states.

associated with the formation of shear bands. The shear bands consist of soils that have reached the critical state and are embedded within soil zones with high interlocking stresses due to particle rearrangement. These shear bands grow as the peak shear strength is mobilized and as the soil strain-softens subsequent to the critical state.

Soil stress states within AEFA (Figure 10.16a) or 1-2-3 (Figure 10.16b) are analogous to brittle material-type behavior. Brittle material (e.g., cast iron) will fail suddenly. Because of the shear bands that are formed within Region II, the soil permeability increases, and if water is available it will migrate to and flow through them. This could lead to catastrophic failures in soil structures such as slopes, since the flow of water through the shear bands could trigger flow slides. Design that allows the soil to mobilize stress states that lie within Region II can be classified as a risky design. Soil stress states that lie on the curve AEF can lead to sudden failure (collapse). We will call this curve the peak strength envelope (a curve linking the loci of peak shear strengths).

Region III. Stable soil states (safe design). One of your aims as a geotechnical engineer is to design geotechnical systems on the basis that if the failure state were to occur, the soil would not collapse suddenly but would continuously deform under constant load. This is called ductility. Soil states that are below the failure line or failure envelope AB (Figure 10.16a) or 0-1-3 (Figure 10.16b) would lead to safe design. Soil states on AB are failure (critical) states

When designing geotechnical systems, geotechnical engineers must consider both drained and undrained conditions to determine which of these conditions is critical. The decision on what shear strength parameters to use depends on whether you are considering the short-term (undrained) or the long-term (drained) condition. In the case of analyses for drained condition, called effective stress analyses (ESA), the shear strength parameters are ϕ'_p and ϕ'_{cs} . The value of ϕ'_{cs} is constant for a soil regardless of its initial condition and the magnitude of the normal effective stress. But the value of ϕ'_p depends on the normal effective stress. In the case of fine-grained soils, the shear strength parameter for short-term loading is s_u . To successfully use s_u in design, the initial condition, especially the initial vertical effective stress and the overconsolidation ratio, must be known.

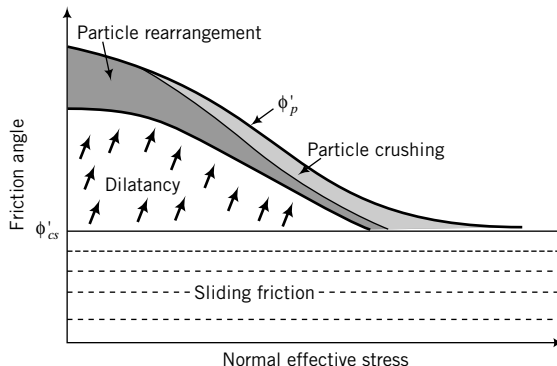
THE ESSENTIAL POINTS ARE:

1. Soil states above the peak shear strength boundary are impossible.
2. Soil states within the peak shear strength boundary and the failure line (critical state) are associated with brittle, discontinuous soil responses and risky design.
3. Soil states below the failure line lead to ductile responses and are safe.
4. You should not rely on ϕ'_p in geotechnical design, because the amount of dilation one measures in laboratory or field tests may not be mobilized by the soil under construction loads. You should use ϕ'_{cs} unless experience dictates otherwise. A higher factor of safety is warranted if ϕ'_p rather than ϕ'_{cs} is used in design.

What's next . . . In the next section, we will define and describe various parameters to interpret the shear strength of soils. You should read this section carefully because it is an important juncture in our understanding of the shear strength of soils for soil stability analyses and design considerations.

10.6 INTERPRETATION OF THE SHEAR STRENGTH OF SOILS

In this book, we will interpret the shear strength of soils based on their capacity to dilate. Dense sands and overconsolidated clays ($OCR > 2$) tend to show peak shear stresses and expand (positive dilation angle), while loose sands and normally consolidated and lightly overconsolidated clays do not show peak shear stresses except at very low normal effective stresses and tend to compress (negative dilation

**FIGURE 10.17**

Contribution of sliding friction, dilatancy, crushing, and rearrangement of particles on the peak shear strength of soils.

angle). In our interpretation of shear strength, we will describe soils as dilating soils when they exhibit peak shear stresses at $\alpha > 0$, and nondilating soils when they exhibit no peak shear stress and attain a maximum shear stress at $\alpha = 0$. However, a nondilating soil does not mean that it does not change volume (expand or contract) during shearing. The terms *dilating* and *nondilating* refer only to particular stress states (peak and critical) during soil deformation.

The peak shear strength of a soil is provided by a combination of the shearing resistance due to sliding (Coulomb's frictional sliding), dilatancy effects, crushing, and rearrangement of particles (Figure 10.17). At low normal effective stresses, rearrangement of soil particles and dilatancy are more readily facilitated than at high normal effective stresses. At high normal effective stresses, particle crushing significantly influences the shearing resistance. However, it is difficult to determine the amount of the shear strength contributed by crushing and the arrangement of particles from soil test results. In this textbook, we will take a simple approach. We will assume that the shear strength of an uncemented soil is a combination of shearing resistance due to frictional sliding of particles and dilatancy. That is, we are combining the shearing resistances due to crushing, rearrangement of particles, and dilatancy into one.

We will refer to key soil shear strength parameters using the following notation. The peak shear strength, τ_p , is the peak shear stress attained by a dilating soil (Figure 10.3). The dilation angle at peak shear stress will be denoted as α_p . The shear stress attained by all soils at large shear strains ($\gamma_{zx} > 10\%$), when the dilation angle is zero, is the critical state shear strength denoted by τ_{cs} . The void ratio corresponding to the critical state shear strength is the critical void ratio denoted by e_{cs} . The effective friction angle corresponding to the critical state shear strength and critical void ratio is ϕ'_{cs} .

The peak effective friction angle for a dilating soil according to Coulomb's model is

$$\phi'_p = \phi'_{cs} + \alpha_p \quad (10.24)$$

Test results (Bolton, 1986) show that for plane strain tests,

$$\phi'_p = \phi'_{cs} + 0.8\alpha_p \quad (10.25)$$

We will continue to use Equation (10.24), but in practice you can make the adjustment [Equation (10.25)] suggested by Bolton (1986).

Typical values of ϕ'_{cs} , ϕ'_p , and ϕ' for soils are shown in Table 10.3. The peak dilatancy angle, α_p , generally has values ranging from 0° to 15° .

We will drop the term *effective* in describing friction angle and accept it by default, such that effective critical state friction angle becomes critical state friction angle, ϕ'_{cs} , and effective peak friction angle becomes peak friction angle, ϕ'_p . Table 10.4 provides a summary of the equations for each soil model at peak and at critical state.

For soils that exhibit residual shear strength, replace ϕ'_{cs} by ϕ'_r in the critical state column of Table 10.4. The residual shear strength is very important in the analysis and design of slopes in heavily overconsolidated clays and previously failed slopes.

TABLE 10.3 Ranges of Friction Angles for Soils (degrees)

Soil type	ϕ'_{cs}	ϕ'_p	ϕ'_r
Gravel	30–35	35–50	
Mixtures of gravel and sand with fine-grained soils	28–33	30–40	
Sand	27–37*	32–50	
Silt or silty sand	24–32	27–35	
Clays	15–30	20–30	5–15

*Higher values (32°–37°) in the range are for sands with significant amount of feldspar (Bolton, 1986). Lower values (27°–32°) in the range are for quartz sands.

TABLE 10.4 Summary of Equations for the Four Failure Criteria

Name	Peak	Critical state
Coulomb	$\tau_p = (\sigma'_n)_f \tan(\phi'_{cs} + \alpha_p) = (\sigma'_n)_f \tan \phi'_p$	$\tau_{cs} = \tau_f = (\sigma'_n)_f \tan \phi'_{cs}$
Mohr–Coulomb	$\sin \phi'_p = \frac{(\sigma'_1)_p - (\sigma'_3)_p}{(\sigma'_1)_p + (\sigma'_3)_p}$ $\frac{(\sigma'_3)_p}{(\sigma'_1)_p} = \frac{1 - \sin \phi'_p}{1 + \sin \phi'_p} = \tan^2\left(45^\circ - \frac{\phi'_p}{2}\right)$ <p>Inclination of the failure plane to the plane on which the major principal effective stress acts.</p>	$\sin \phi'_{cs} = \frac{(\sigma'_1)_{cs} - (\sigma'_3)_{cs}}{(\sigma'_1)_{cs} + (\sigma'_3)_{cs}}$ $\frac{(\sigma'_3)_{cs}}{(\sigma'_1)_{cs}} = \frac{1 - \sin \phi'_{cs}}{1 + \sin \phi'_{cs}} = \tan^2\left(45^\circ - \frac{\phi'_{cs}}{2}\right)$ <p>Inclination of the failure plane to the plane on which the major principal effective stress acts.</p>
Tresca	$\theta_p = \frac{\pi}{4} + \frac{\phi'_p}{2}$ <p>Stresses on failure plane</p> $(\sigma'_n)_p = \left(\frac{\sigma'_1 + \sigma'_3}{2} - \frac{\sigma'_1 - \sigma'_3}{2} \sin \phi'_p \right)_p$ $\tau_p = \left(\frac{\sigma'_1 - \sigma'_3}{2} \right)_p \cos \phi'_p$ $(s_u)_p = \frac{(\sigma_1)_p - (\sigma_3)_p}{2}$	$\theta_{cs} = \frac{\pi}{4} + \frac{\phi'_{cs}}{2}$ <p>Stresses on failure plane</p> $(\sigma'_n)_{cs} = \left(\frac{\sigma'_1 + \sigma'_3}{2} - \frac{\sigma'_1 - \sigma'_3}{2} \sin \phi'_{cs} \right)_{cs}$ $\tau_{cs} = \left(\frac{\sigma'_1 - \sigma'_3}{2} \right)_{cs} \cos \phi'_{cs}$ $(s_u)_{cs} = \frac{(\sigma_1)_{cs} - (\sigma_3)_{cs}}{2}$
Taylor	$\tau_p = (\sigma'_n)_f (\tan \phi'_{cs} + \tan \alpha_p)$	$\tau_{cs} = \tau_f = (\sigma'_n)_f \tan \phi'_{cs}$

If the shear stress (τ) induced in a soil is less than the peak or critical shear strength, then the soil has reserved shear strength, and we can characterize this reserved shear strength by a factor of safety (FS).

$$\text{For peak condition in dilating soils: } \text{FS} = \frac{\tau_p}{\tau} \quad (10.26)$$

$$\text{For critical state condition in all soils: } \text{FS} = \frac{\tau_{cs}}{\tau} \quad (10.27)$$

THE ESSENTIAL POINTS ARE:

1. The friction angle at the critical state, ϕ'_{cs} , is a fundamental soil parameter.
2. The friction angle at peak shear stress for dilating soils, ϕ'_p , is not a fundamental soil parameter but depends on the capacity of the soil to dilate.

EXAMPLE 10.1 Application of Coulomb and Taylor Failure Criteria

A dry sand was tested in a shear device. The shear force–shear displacement for a normal force of 100 N is shown in Figure E10.1a.

- Is the soil a dense or loose sand?
- Identify and determine the peak shear force and critical state shear force.
- Calculate the peak and critical state friction angles and the peak dilation angle using Coulomb's model.
- Determine the peak dilation angle using Taylor's model.
- If the sand were loose, determine the critical state shear stress for a normal effective stress of 200 kPa using Coulomb's model.

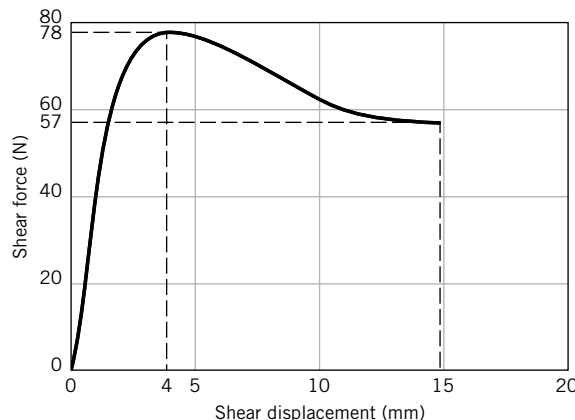


FIGURE E10.1a

Strategy Identify the peak and critical state shear force. The friction angle is the arctangent of the ratio of the shear force to the normal force. The constant shear force at large displacement gives the critical state shear force. From this force, you can calculate the critical state friction angle. Similarly, you can calculate ϕ'_p from the peak shear force.

Solution 10.1

Step 1: Determine whether soil is dense or loose. Since the curve shows a peak, the soil is likely to be dense.

Step 2: Identify peak and critical state shear forces.

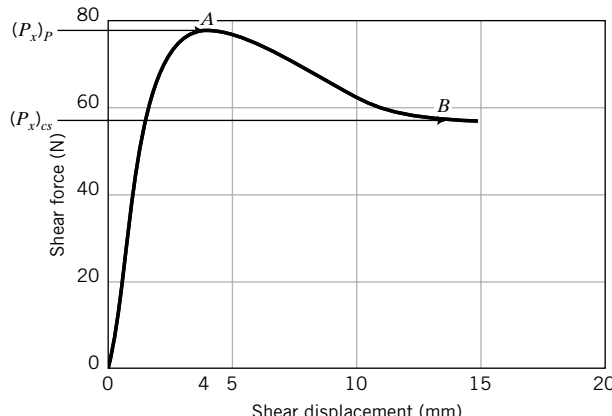


FIGURE E10.1b

With reference to Figure E10.1b, point A is the peak shear force and point B is the critical state shear force.

Step 3: Read values of peak and critical state shear forces from the graph in Figure E10.1b.

$$(P_x)_p = 78 \text{ N}$$

$$(P_x)_{cs} = 57 \text{ N}$$

$$P_z = 100 \text{ N}$$

Step 4: Determine friction angles.

$$\phi'_p = \tan^{-1}\left(\frac{(P_x)_p}{P_z}\right) = \tan^{-1}\left(\frac{78}{100}\right) = 38^\circ$$

$$\phi'_{cs} = \tan^{-1}\left(\frac{(P_x)_{cs}}{P_z}\right) = \tan^{-1}\left(\frac{57}{100}\right) = 29.7^\circ$$

Step 5: Determine peak dilation angle using Coulomb's model.

$$\alpha_p = \phi'_p - \phi'_{cs} = 38 - 29.7 = 8.3^\circ$$

Step 6: Calculate the peak dilation angle using Taylor's method.

$$\tan \alpha_p = \frac{(P_x)_p}{P_z} - \tan \phi'_{cs}$$

$$\alpha_p = \tan^{-1}\left(\frac{78}{100} - 0.57\right) = 11.9^\circ$$

Step 7: Calculate critical state shear stress.

$$\tau_{cs} = \tau_f = \sigma'_n \tan \phi'_{cs} = 200 \tan(29.7^\circ) = 200 \times 0.257 = 114 \text{ kPa}$$

EXAMPLE 10.2 Application of Mohr-Coulomb Failure Criterion

A cylindrical soil sample was subjected to axial principal effective stresses (σ'_1) and radial principal effective stresses (σ'_3). The soil could not support additional stresses when $\sigma'_1 = 300$ kPa and $\sigma'_3 = 100$ kPa. (1) Determine the friction angle and the inclination of the slip plane to the horizontal. (2) Determine the stresses on the failure plane. (3) Determine the maximum shear stress. (4) Is the maximum shear stress equal to the failure shear stress? Assume no significant dilatational effects.

Strategy Since there are no significant dilation effects, $\phi' = \phi'_{cs}$.

Solution 10.2

Step 1: Find ϕ'_{cs} .

$$\begin{aligned} \sin \phi'_{cs} &= \frac{(\sigma'_1)_{cs} - (\sigma'_3)_{cs}}{(\sigma'_1)_{cs} + (\sigma'_3)_{cs}} = \frac{300 - 100}{300 + 100} = \frac{2}{4} = \frac{1}{2} \\ \therefore \phi'_{cs} &= 30^\circ \end{aligned}$$

Step 2: Find θ .

$$\theta_{cs} = 45^\circ + \frac{\phi'_{cs}}{2} = 45^\circ + \frac{30^\circ}{2} = 60^\circ$$

Step 3: Calculate the stresses on the failure plane.

$$(\sigma'_n)_{cs} = \left(\frac{\sigma'_1 + \sigma'_3}{2} - \frac{\sigma'_1 - \sigma'_3}{2} \sin \phi'_{cs} \right)_{cs} = \left(\frac{300 + 100}{2} - \frac{300 - 100}{2} \sin 30^\circ \right)_{cs} = 150 \text{ kPa}$$

$$\tau_{cs} = \left(\frac{\sigma'_1 - \sigma'_3}{2} \right)_{cs} \cos \phi'_{cs} = \left(\frac{300 - 100}{2} \right) \cos 30^\circ = 86.6 \text{ kPa}$$

Step 4: Calculate the maximum shear stress.

$$\tau_{max} = \left(\frac{\sigma'_1 - \sigma'_3}{2} \right) = \left(\frac{300 - 100}{2} \right) = 100 \text{ kPa}$$

Step 5: Check if the maximum shear stress is equal to the failure shear stress.

$$\tau_{max} = 100 \text{ kPa} > \tau_{cs} = 86.6 \text{ kPa}$$

The maximum shear stress is greater than the failure shear stress.

EXAMPLE 10.3 Failure Stress Due to a Foundation Using Mohr–Coulomb Criterion

Figure E10.3 shows the soil profile at a site for a proposed building. The soil is a homogeneous, poorly graded sand. Determine the increase in vertical effective stress at which a soil element at a depth of 3 m, under the center of the building, will fail if the increase in lateral effective stress is 20% of the increase in vertical effective stress. The coefficient of lateral earth pressure at rest, K_o , is 0.5. Assume all stresses are principal stresses.

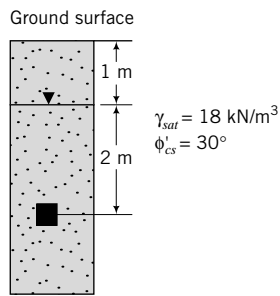


FIGURE E10.3

Strategy You are given a homogeneous deposit of sand and its properties. Use the data given to find the initial stresses, and then use the Mohr–Coulomb equation to solve the problem. Since the soil element is under the center of the building, axisymmetric conditions prevail. Also, you are given that $\Delta\sigma'_3 = 0.2\Delta\sigma'_1$. Therefore, all you need to do is find $\Delta\sigma'_1$.

Solution 10.3

Step 1: Find the initial effective stresses at a depth of 3 m.

Assume the top 1 m of soil to be saturated.

$$\sigma'_{zo} = (\sigma'_1)_o = (18 \times 3) - 9.8 \times 2 = 34.4 \text{ kPa}$$

The subscript o denotes original or initial.

The lateral earth pressure is

$$(\sigma'_x)_o = (\sigma'_3)_o = K_o(\sigma'_z)_o = 0.5 \times 34.4 = 17.2 \text{ kPa}$$

Step 2: Find $\Delta\sigma'_1$.

$$\text{At failure: } \frac{(\sigma'_1)_{cs}}{(\sigma'_3)_{cs}} = \frac{1 + \sin\phi'_{cs}}{1 - \sin\phi'_{cs}} = \frac{1 + \sin 30^\circ}{1 - \sin 30^\circ} = 3$$

But

$$(\sigma'_1)_f = (\sigma'_1)_{cs} = (\sigma'_1)_o + \Delta\sigma'_1 \quad \text{and} \quad (\sigma'_3)_f = (\sigma'_3)_c = (\sigma'_3)_o + 0.2\Delta\sigma'_1$$

where $\Delta\sigma'_1$ is the additional vertical effective stress to bring the soil to failure.

$$\therefore \frac{(\sigma'_1)_o + \Delta\sigma'_1}{(\Delta\sigma'_3)_o + 0.2\Delta\sigma'_1} = \frac{34.4 + \Delta\sigma'_1}{17.2 + 0.2\Delta\sigma'_1} = 3$$

The solution is $\Delta\sigma'_1 = 43$ kPa.

What's next . . . We have identified the shear strength parameters (ϕ'_{cs} , ϕ'_p , ϕ'_r and s_u) that are important for analyses and design of geotechnical systems. A variety of laboratory tests and field tests are used to determine these parameters. We will describe many of these tests and the interpretation of the results. You may have to perform some of these tests in the laboratory section of your course.

10.7 LABORATORY TESTS TO DETERMINE SHEAR STRENGTH PARAMETERS



Virtual Laboratory

Access www.wiley.com/college/budhu and click on Chapter 10 to conduct a virtual direct shear test and a virtual triaxial test.

10.7.1 A Simple Test to Determine Friction Angle of Clean Coarse-Grained Soils

The critical state friction angle, ϕ'_{cs} , for a clean coarse-grained soil can be found by pouring the soil into a loose heap on a horizontal surface and measuring the slope angle of the heap relative to the horizontal. This angle is sometimes called the angle of repose, but it closely approximates ϕ'_{cs} .

10.7.2 Shear Box or Direct Shear Test

A popular apparatus to determine the shear strength parameters is the shear box. This test is useful when a soil mass is likely to fail along a thin zone under plane strain conditions. The shear box (Figure 10.18) consists of a horizontally split, open metal box. Soil is placed in the box, and one-half of the box is moved relative to the other half. Failure is thereby constrained along a thin zone of soil on the horizontal plane (AB). Serrated or grooved metal plates are placed at the top and bottom faces of the soil to generate the shearing force.

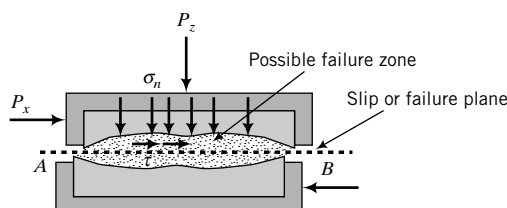


FIGURE 10.18
Shear box.

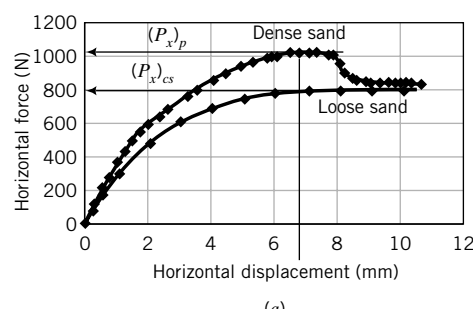
Vertical forces are applied through a metal platen resting on the top serrated plate. Horizontal forces are applied through a motor for displacement control or by weights through a pulley system for load control. Most shear box tests are conducted using displacement control because we can get both the peak shear force and the critical shear force. In load control tests, you cannot get data beyond the maximum or peak shear force.

The horizontal displacement, Δx , the vertical displacement, Δz , the vertical loads, P_z , and the horizontal loads, P_x , are measured. Usually, three or more tests are carried out on a soil sample using three different constant vertical forces. Failure is determined when the soil cannot resist any further increment of horizontal force. The stresses and strains in the shear box test are difficult to calculate from the forces and displacements measured. The stresses in the thin (dimension unknown) constrained failure zone (Figure 10.18) are not uniformly distributed, and strains cannot be determined.

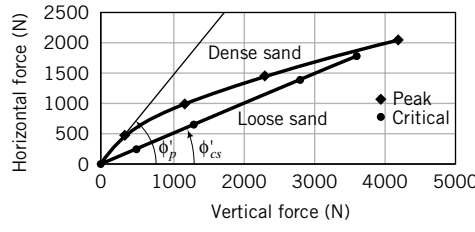
The shear box apparatus cannot prevent drainage, but one can get an estimate of the undrained shear strength of clays by running the shear box test at a fast rate of loading so that the test is completed quickly. Generally, three or more tests are performed on a soil. The soil sample in each test is sheared under a constant vertical force, which is different in each test. The data recorded for each test are the horizontal displacements, the horizontal forces, the vertical displacements, and the constant vertical force under which the test is conducted. From the recorded data, you can find the following strength parameters: τ_p , τ_{cs} , ϕ'_p , ϕ'_{cs} , α (and s_u , if fine-grained soils are tested quickly). Coulomb failure criterion is used to determine the shear strength. Taylor failure criterion may also be used, but Coulomb failure is better suited for the direct shear test. The strength parameters are generally determined from plotting the data, as illustrated in Figure 10.19 for sand.

Only the results of one test at a constant value of P_z are shown in Figure 10.19a, b. The results of $(P_x)_p$ and $(P_x)_{cs}$ plotted against P_z for all tests are shown in Figure 10.19c. If the soil is dilatant, it would exhibit a peak shear force (Figure 10.19a, dense sand) and expand (Figure 10.19b, dense sand), and the failure envelope would be curved (Figure 10.19c, dense sand). The peak shear stress is the peak shear force divided by the cross-sectional area (A) of the test sample; that is,

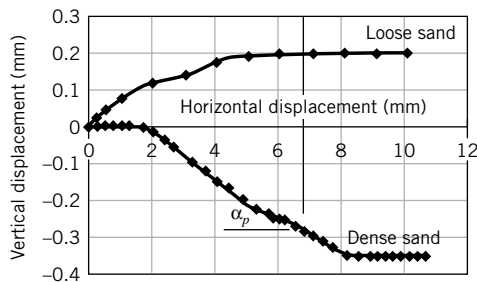
$$\tau_p = \frac{(P_x)_p}{A} \quad (10.28)$$



(a)



(c)



(b)

FIGURE 10.19 Results from a shear box test on a dense and a loose sand.

The critical shear stress is

$$\tau_{cs} = \frac{(P_x)_{cs}}{A} \quad (10.29)$$

In a plot of vertical forces versus horizontal forces (Figure 10.19c), the points representing the critical horizontal forces should ideally lie along a straight line through the origin. Experimental results usually show small deviations from this straight line, and a “best-fit” straight line is conventionally drawn. The angle subtended by this straight line and the horizontal axis is ϕ'_{cs} . Alternatively,

$$\phi'_{cs} = \tan^{-1} \frac{(P_x)_{cs}}{P_z} \quad (10.30)$$

For dilatant soils, the angle between a line from the origin to each peak horizontal force that does not lie on the “best-fit” straight line in Figure 10.19c and the abscissa (normal effective stress axis) represents a value of ϕ'_p at the corresponding vertical force. Recall from Section 10.5 that ϕ'_p is not constant, but varies with the magnitude of the normal effective stress (P_z/A). Usually, the normal effective stress at which ϕ'_p is determined should correspond to the maximum anticipated normal effective stress in the field. The value of ϕ'_p is largest at the lowest value of the applied normal effective stress, as illustrated in Figure 10.19c. You would determine ϕ'_p by drawing a line from the origin to the point representing the peak horizontal force at the desired normal force, and measuring the angle subtended by this line and the horizontal axis. Alternatively,

$$\phi'_p = \tan^{-1} \frac{(P_x)_p}{P_z} \quad (10.31)$$

You can also determine the peak dilation angle directly for each test from a plot of horizontal displacement versus vertical displacement, as illustrated in Figure 10.19b. The peak dilation angle is

$$\alpha_p = \tan^{-1} \left(\frac{-\Delta z}{\Delta x} \right) \quad (10.32)$$

We can find α_p from

$$\alpha_p = \phi'_p - \phi'_{cs} \quad (10.33)$$

EXAMPLE 10.4 Interpretation of Shear Box Test Using Coulomb Failure Criterion

The shear box test results of two samples of the same soil but with different initial unit weights are shown in the table below. Sample A did not show peak value, but sample B did.

Soil	Test number	Vertical force (N)	Horizontal force (N)
A	Test 1	250	150
	Test 2	500	269
	Test 3	750	433
B	Test 1	100	98
	Test 2	200	175
	Test 3	300	210
	Test 4	400	248

Determine the following:

- (a) ϕ'_{cs}
- (b) ϕ'_p at vertical forces of 200 N and 400 N for sample B
- (c) The dilation angle at vertical forces of 200 N and 400 N for sample B

Strategy To obtain the desired values, it is best to plot a graph of vertical force versus horizontal force.

Solution 10.4

Step 1: Plot a graph of the vertical forces versus failure horizontal forces for each sample. See Figure E10.4.

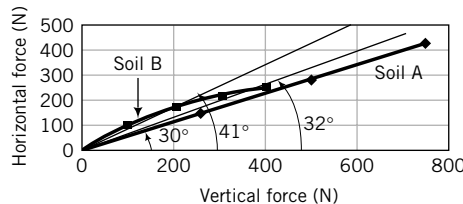


FIGURE E10.4

Step 2: Extract ϕ'_{cs} .

All the plotted points for sample A fall on a straight line through the origin. Sample A is a nondilatant soil, possibly a loose sand or a normally consolidated clay. The effective friction angle is $\phi'_{cs} = 30^\circ$.

Step 3: Determine ϕ'_p .

The horizontal forces corresponding to vertical forces at 200 N and 400 N for sample B do not lie on the straight line corresponding to ϕ'_{cs} . Therefore, each of these forces has a ϕ'_p associated with it.

$$(\phi'_p)_{200\text{ N}} = \tan^{-1}\left(\frac{175}{200}\right) = 41.2^\circ$$

$$(\phi'_p)_{400\text{ N}} = \tan^{-1}\left(\frac{248}{400}\right) = 31.8^\circ$$

Step 4: Determine α_p .

$$\alpha_p = \phi'_p - \phi'_{cs}$$

$$(\alpha_p)_{200\text{ N}} = 41.2 - 30 = 11.2^\circ$$

$$(\alpha_p)_{400\text{ N}} = 31.8 - 30 = 1.8^\circ$$

Note that as the normal force increases, α_p decreases.

EXAMPLE 10.5 Predicting the Shear Stress at Failure Using Coulomb Failure Criterion

The critical state friction angle of a soil is 28° . Determine the critical state shear stress if the normal effective stress is 200 kPa.

Strategy This is a straightforward application of the Coulomb failure criterion.

Solution 10.5

Step 1: Determine the failure shear stress.

$$\tau_f = \tau_{cs} = (\sigma'_n)_f \tan \phi'_{cs}$$

$$\tau_{cs} = 200 \tan 28^\circ = 106.3 \text{ kPa}$$

EXAMPLE 10.6 *Interpreting Shear Box Test Data Using Coulomb Failure Criterion*

The data recorded during a shear box test on a sand sample, $10 \text{ cm} \times 10 \text{ cm} \times 3 \text{ cm}$, at a constant vertical force of 1200 N are shown in the table below. A negative sign denotes vertical expansion.

- Plot graphs of (1) horizontal forces versus horizontal displacements, and (2) vertical displacements versus horizontal displacements.
- Would you characterize the behavior of this sand as that of a dense or a loose sand? Explain your answer.
- Determine (1) the maximum or peak shear stress, (2) the critical state shear stress, (3) the peak dilation angle, (4) ϕ'_p , and (5) ϕ'_{cs} .

Horizontal displacement (mm)	Horizontal force (N)	Vertical displacement (mm)	Horizontal displacement (mm)	Horizontal force (N)	Vertical displacement (mm)
0.00	0.00	0.00	6.10	988.29	-0.40
0.25	82.40	0.00	6.22	988.29	-0.41
0.51	157.67	0.00	6.48	993.68	-0.45
0.76	249.94	0.00	6.60	998.86	-0.46
1.02	354.31	0.00	6.86	991.52	-0.49
1.27	425.72	0.01	7.11	999.76	-0.51
1.52	488.90	0.00	7.37	1005.26	-0.53
1.78	538.33	0.00	7.75	1002.51	-0.57
2.03	571.29	-0.01	7.87	994.27	-0.57
2.41	631.62	-0.03	8.13	944.83	-0.58
2.67	663.54	-0.05	8.26	878.91	-0.58
3.30	759.29	-0.09	8.51	807.50	-0.58
3.68	807.17	-0.12	8.64	791.02	-0.59
4.06	844.47	-0.16	8.89	774.54	-0.59
4.45	884.41	-0.21	9.14	766.30	-0.60
4.97	928.35	-0.28	9.40	760.81	-0.59
5.25	939.34	-0.31	9.65	760.81	-0.59
5.58	950.32	-0.34	9.91	758.06	-0.60
5.72	977.72	-0.37	10.16	758.06	-0.59
5.84	982.91	-0.37	10.41	758.06	-0.59
5.97	988.29	-0.40	10.67	755.32	-0.59

Strategy After you plot the graphs, you can get an idea as to whether you have a loose or a dense sand. A dense sand may show a peak horizontal force in the plot of horizontal force versus horizontal displacement, and would expand.

Solution 10.6

Step 1: Plot graphs.

See Figure E10.6.

Step 2: Determine whether the sand is dense or loose.

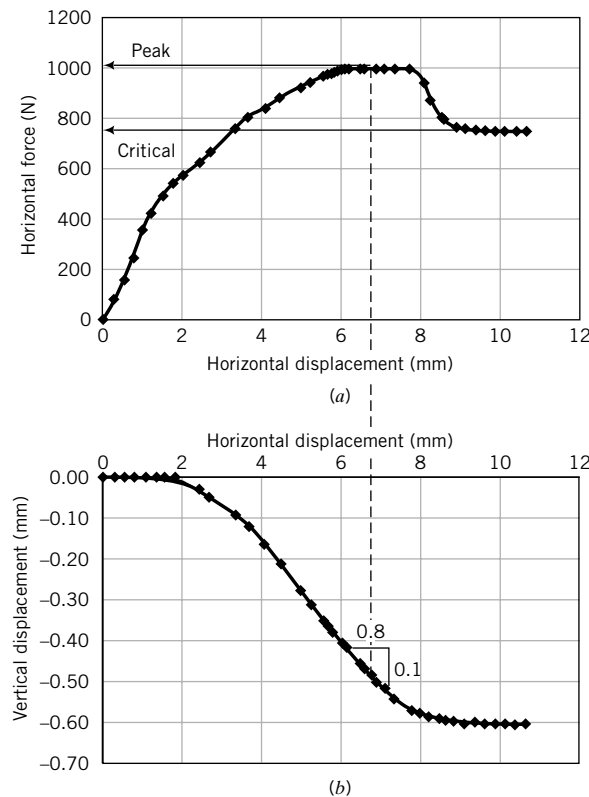
The sand appears to be dense—it showed a peak horizontal force and has dilated.

Step 3: Extract the required values.

Cross-sectional area of sample: $A = 10 \times 10 = 100 \text{ cm}^2 = 10^{-2} \text{ m}^2$

$$\tau_p = \frac{(P_x)_p}{A} = \frac{1005 \text{ N}}{10^{-2}} \times 10^{-3} = 100.5 \text{ kPa}$$

$$\tau_{cs} = \frac{(P_x)_{cs}}{A} = \frac{758 \text{ N}}{10^{-2}} \times 10^{-3} = 75.8 \text{ kPa}$$

**FIGURE E10.6**

$$\alpha_p = \tan^{-1}\left(\frac{-\Delta z}{\Delta x}\right) = \tan^{-1}\left(\frac{0.1}{0.8}\right) = 7.1^\circ$$

$$\text{Normal effective stress: } \sigma'_n = \left(\frac{1200 \text{ N}}{10^{-2}}\right) \times 10^{-3} = 120 \text{ kPa}$$

$$\phi'_p = \tan^{-1}\left(\frac{\tau_p}{\sigma'_n}\right) = \tan^{-1}\left(\frac{100.5}{120}\right) = 39.9^\circ$$

$$\phi'_{cs} = \tan^{-1}\left(\frac{\tau_{cs}}{\sigma'_n}\right) = \tan^{-1}\left(\frac{75.8}{120}\right) = 32.3^\circ$$

Also,

$$\alpha_p = \phi'_p - \phi'_{cs} = 39.9 - 32.3 = 7.6^\circ$$

10.7.3 Conventional Triaxial Apparatus

A widely used apparatus to determine the shear strength parameters and the stress-strain behavior of soils is the triaxial apparatus. The name is a misnomer since two, not three, stresses can be controlled. In the triaxial test, a cylindrical sample of soil, usually with a length-to-diameter ratio of 2, is subjected to either controlled increases in axial stresses or axial displacements and radial stresses. The sample is laterally confined by a membrane, and radial stresses are applied by pressuring water in a chamber (Figure 10.20). The axial stresses are applied by loading a plunger. If the axial stress is greater

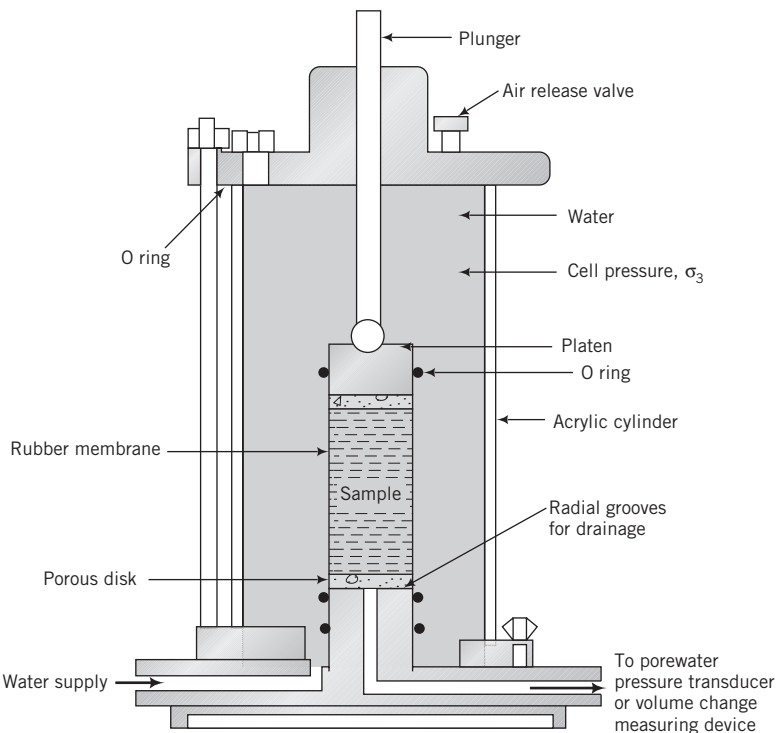


FIGURE 10.20 Schematic of a triaxial cell.

than the radial stress, the soil is compressed vertically and the test is called triaxial compression. If the radial stress is greater than the axial stress, the soil is compressed laterally and the test is called triaxial extension.

The applied stresses are principal stresses and the loading condition is axisymmetric. For compression tests, we will denote the radial stresses σ_r as σ_3 and the axial stresses σ_z as σ_1 . For extension tests, we will denote the radial stresses σ_r as σ_1 and the axial stresses σ_z as σ_3 .

The average stresses and strains on a soil sample in the triaxial apparatus for compression tests are as follows:

$$\text{Axial total stress: } \sigma_1 = \frac{P_z}{A} + \sigma_3 \quad (10.34)$$

$$\text{Deviatoric stress: } \sigma_1 - \sigma_3 = \frac{P_z}{A} \quad (10.35)$$

$$\text{Axial strain: } \epsilon_1 = \frac{\Delta z}{H_o} \quad (10.36)$$

$$\text{Radial strain: } \epsilon_3 = \frac{\Delta r}{r_o} \quad (10.37)$$

$$\text{Volumetric strain: } \epsilon_p = \frac{\Delta V}{V_o} = \epsilon_1 + 2\epsilon_3 \quad (10.38)$$

$$\text{Deviatoric strain: } \epsilon_q = \frac{2}{3}(\epsilon_1 - \epsilon_3) \quad (10.39)$$

where P_z is the load on the plunger, A is the cross-sectional area of the soil sample, r_o is the initial radius of the soil sample, Δr is the change in radius, V_o is the initial volume, ΔV is the change in volume, H_o is the initial height, and Δz is the change in height. We will call the plunger load the deviatoric load, and

the corresponding stress the deviatoric stress, $q = (\sigma_1 - \sigma_3)$. The shear stress is $\tau = \frac{q}{2}$.

The area of the sample changes during loading, and at any given instance the area is

$$A = \frac{V}{H} = \frac{V_o - \Delta V}{H_o - \Delta z} = \frac{V_o \left(1 - \frac{\Delta V}{V_o}\right)}{H_o \left(1 - \frac{\Delta z}{H_o}\right)} = \frac{A_o (1 - \varepsilon_p)}{1 - \varepsilon_1} \quad (10.40)$$

where $A_o (= \pi r_o^2)$ is the initial cross-sectional area and H is the current height of the sample. The dilation angle for a triaxial test is given by Equation (10.10).

The triaxial apparatus is versatile because we can (1) independently control the applied axial and radial stresses, (2) conduct tests under drained and undrained conditions, and (3) control the applied displacements or stresses.

A variety of stress paths can be applied to soil samples in the triaxial apparatus. However, only a few stress paths are used in practice to mimic typical geotechnical problems. We will discuss the tests most often used, why they are used, and typical results obtained.

10.7.4 Unconfined Compression (UC) Test

The purpose of this test is to determine the undrained shear strength of saturated clays quickly. In the UC test, no radial stress is applied to the sample ($\sigma_3 = 0$). The axial (plunger) load, P_z , is increased rapidly until the soil sample fails, that is, it cannot support any additional load. The loading is applied quickly so that the porewater it cannot drain from the soil; the sample is sheared at constant volume.

The stresses applied on the soil sample and the total stress path followed are shown in Figure 10.21a,b. The effective stress path is unknown, since porewater pressure changes are not normally measured. Mohr's circle using total stresses is depicted in Figure 10.21c. If the excess porewater pressures

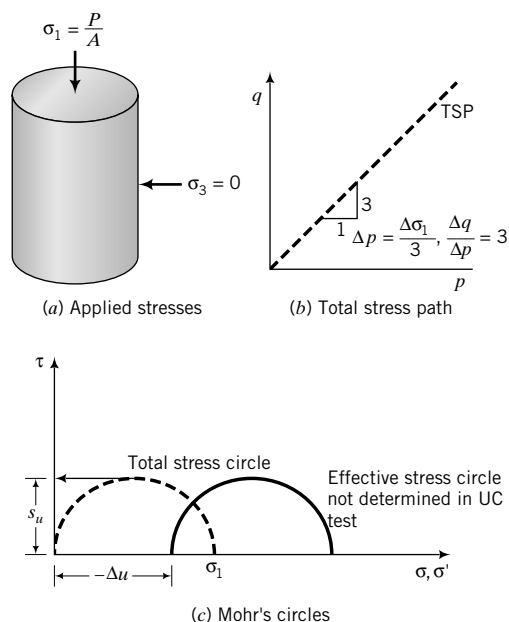


FIGURE 10.21 Stresses, stress paths, and Mohr's circles for UC test.

were to be measured, they would be negative. The theoretical reason for negative excess porewater pressures is as follows. Since $\sigma_3 = 0$, then from the principle of effective stresses, $\sigma'_3 = \sigma_3 - \Delta u = 0 - \Delta u = -\Delta u$. The effective radial stress, σ'_3 , cannot be negative because uncemented soils cannot sustain tension. Therefore, the excess porewater pressure must be negative so that σ'_3 is positive. Mohr's circle of effective stresses would be to the right of the total stress circle, as shown in Figure 10.21c.

The Tresca failure criterion is used to interpret the results of the UC test. The undrained shear strength is

$$s_u = \frac{P_z}{2A} = \frac{1}{2}\sigma_1 \quad (10.41)$$

where, from Equation (10.40), $A = A_o = (1 - \varepsilon_1)$ (no volume change, i.e., $\varepsilon_p = 0$). If the peak load is used, you will get $(s_u)_p$. If the load at critical state is used, you will get $(s_u)_{cs}$. The undrained elastic modulus, E_u , is determined from a plot of ε_1 versus σ_1 .

The results from UC tests are used to:

- Estimate the short-term bearing capacity of fine-grained soils for foundations.
- Estimate the short-term stability of slopes.
- Compare the shear strengths of soils from a site to establish soil strength variability quickly and cost-effectively (the UC test is cheaper to perform than other triaxial tests).
- Determine the stress-strain characteristics under fast (undrained) loading conditions.

EXAMPLE 10.7 Undrained Shear Strength from a UC Test Using Tresca Failure Criterion

An unconfined compression test was carried out on a saturated clay sample. The maximum (peak) load the clay sustained was 127 N and the vertical displacement was 0.8 mm. The size of the sample was 38 mm diameter \times 76 mm long. Determine the undrained shear strength. Draw Mohr's circle of stress for the test and locate s_u .

Strategy Since the test is a UC test, $\sigma_3 = 0$ and $(\sigma_1)_f$ is the failure axial stress. You can find s_u by calculating one-half the failure axial stress.

Solution 10.7

Step 1: Determine the sample area at failure.

Diameter $D_o = 38$ mm; length $H_o = 76$ mm.

$$A_o = \frac{\pi \times D_o^2}{4} = \frac{\pi \times 0.038^2}{4} = 11.3 \times 10^{-4} \text{ m}^2, \quad \varepsilon_1 = \frac{\Delta z}{H_o} = \frac{0.8}{76} = 0.01$$

$$A = \frac{A_o}{1 - \varepsilon_1} = \frac{11.3 \times 10^{-4}}{1 - 0.01} = 11.4 \times 10^{-4} \text{ m}^2$$

Step 2: Determine the major principal stress at failure.

$$(\sigma_1)_p = \frac{P_z}{A} = \frac{127 \times 10^{-4}}{11.4 \times 10^{-4}} = 111.4 \text{ kPa}$$

Step 3: Calculate s_u .

$$(s_u)_p = \frac{(\sigma_1)_p - (\sigma_3)_p}{2} = \frac{111.4 - 0}{2} = 55.7 \text{ kPa}$$

Step 4: Draw Mohr's circle.

See Figure E10.7. The values extracted from the graphs are

$$(\sigma_3)_p = 0, \quad (\sigma_1)_p = 111 \text{ kPa}, \quad (s_u)_p = 56 \text{ kPa}$$

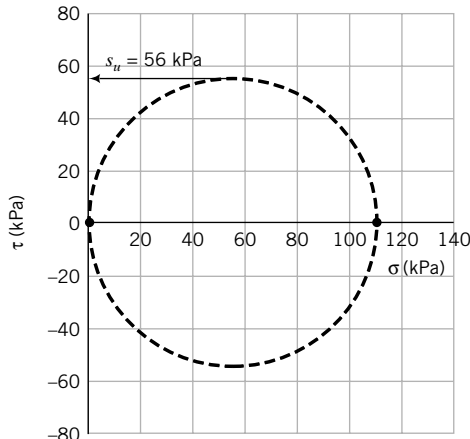


FIGURE E10.7

10.7.5 Consolidated Drained (CD) Compression Test

The purpose of a CD test is to determine the drained shear strength parameters, ϕ'_{cs} and ϕ'_p , to analyze long-term loading of a soil mass. The effective elastic moduli for drained condition E' and E'_s are also obtained from this test. A consolidated drained compression test is performed in two stages. The first stage is consolidating the soil to a desired effective stress level by pressurizing the water in the cell and allowing the soil sample to drain until the excess porewater pressure dissipates. In the second stage, the pressure in the cell (cell pressure or confining pressure) is kept constant, and additional axial loads or displacements are added very slowly until the soil sample fails. The displacement rate (or strain rate) used must be slow enough to allow the excess porewater pressure to dissipate. Because the hydraulic conductivity of fine-grained soils is much lower than that of coarse-grained soils, the displacement rate for testing fine-grained soils is much lower than for coarse-grained soils. Drainage of the excess porewater is permitted and the amount of water expelled is measured. It is customary to perform a minimum of three tests at different cell pressures. The stresses on the soil sample for the two stages of a CD test are as follows:

Stage 1: Isotropic consolidation phase

$$\Delta\sigma_1 = \Delta\sigma_3 = \Delta\sigma'_1 = \Delta\sigma'_3; \quad \Delta\sigma_1 > 0, \quad \Delta u = 0$$

When the load is applied, the initial excess porewater pressure for a saturated soil is equal to the cell pressure, that is, $\Delta u = \Delta\sigma_3$. At the end of the consolidation phase, the excess porewater pressure dissipates; that is, $\Delta u = 0$.

$$\Delta p' = \Delta p = \frac{\Delta\sigma_1 + 2\Delta\sigma_1}{3} = \Delta\sigma_1; \quad \Delta q = \Delta\sigma_1 - \Delta\sigma_3 = 0, \quad \text{and } \frac{\Delta q}{\Delta p'} = \frac{\Delta q}{\Delta p} = 0$$

Stage 2: Shearing phase

$$\Delta\sigma_1 = \Delta\sigma'_1 > 0; \quad \Delta\sigma_3 = \Delta\sigma'_3 = 0; \quad \Delta u = 0$$

Therefore,

$$\Delta p' = \Delta p = \frac{\Delta\sigma'_1}{3}; \quad \Delta q = \Delta\sigma'_1; \quad \frac{\Delta q}{\Delta p'} = \frac{\Delta q}{\Delta p} = 3$$

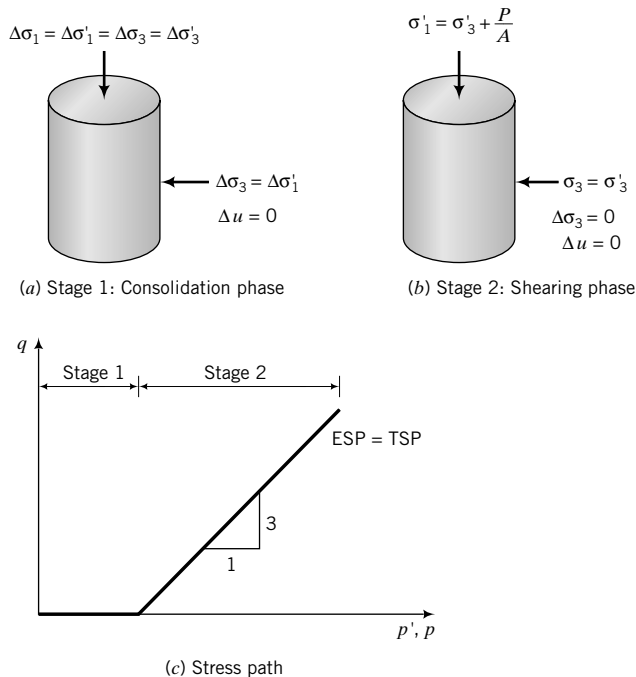


FIGURE 10.22
Stresses and stress paths during a CD test.

The stresses and stress path applied are illustrated in Figure 10.22. The change in volume of the soil is measured by continuously recording the volume of water expelled. The volumetric strain is

$$\varepsilon_p = \frac{\Delta V}{V_o} = \varepsilon_1 + 2\varepsilon_3 \quad (10.42)$$

where ΔV is the change in volume and V_o is the original volume of the soil. Also, the axial displacements are recorded and the axial strain is calculated as $\varepsilon_1 = \Delta z/H_o$. The radial strains are calculated by rearranging Equation (10.42) to yield

$$\varepsilon_3 = \frac{1}{2}(\varepsilon_p - \varepsilon_1) \quad (10.43)$$

The maximum shear strain is

$$(\gamma_{zx})_{max} = (\varepsilon_1 - \varepsilon_3)_{max} \quad (10.44)$$

which, by substitution of Equation (10.43), gives

$$(\gamma_{zx})_{max} = \frac{1}{2}(3\varepsilon_1 - \varepsilon_p) \quad (10.45)$$

Since the CD test is a drained test, a single test can take several days if the hydraulic conductivity of the soil is low (e.g., fine-grained soils). Typical results of consolidated drained tests on a sand are shown in Figure 10.23. The Mohr–Coulomb failure criterion is used to interpret the results of a CD test.

The elastic moduli for drained conditions, E' and E'_s , are obtained from the CD test from the plot of deviatoric stress, $(\sigma'_1 - \sigma'_3)$, as ordinate and ε_1 as abscissa, as shown in Figure 10.23a. The results of CD tests are used to determine the long-term stability of slopes, foundations, retaining walls, excavations, and other earthworks.

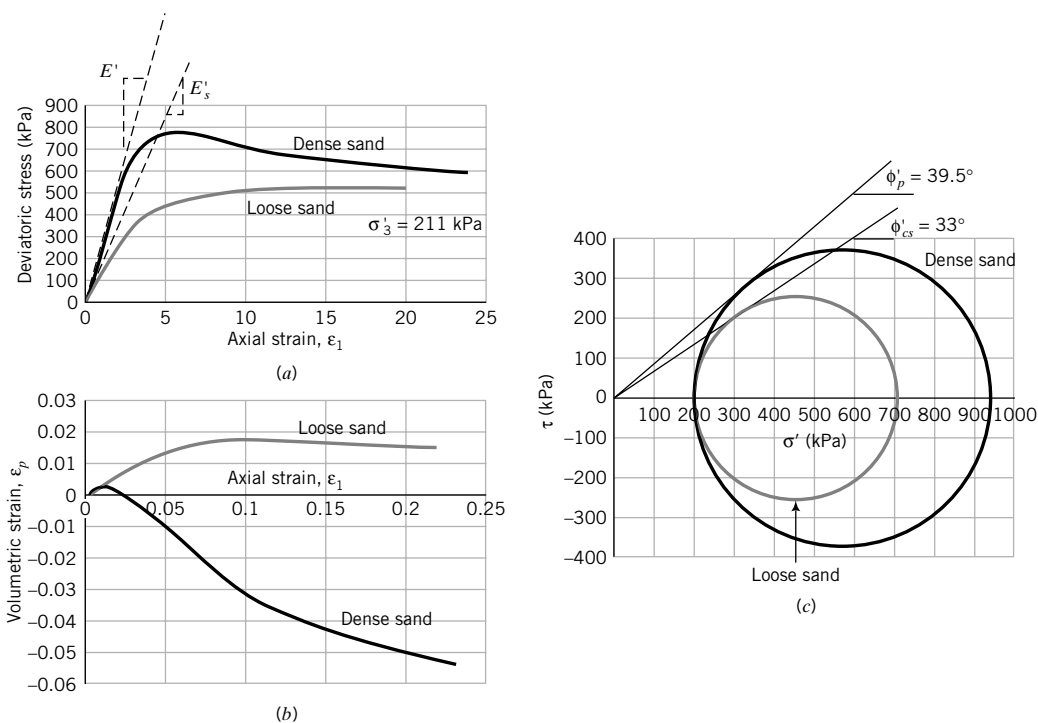


FIGURE 10.23 Results from CD tests on dense and loose sand. (From *The Measurement of Soil Properties in the Triaxial Test*, by Bishop and Henkel, Edward Arnold, 1962.)

EXAMPLE 10.8 Interpreting CD Triaxial Test Data Using Mohr–Coulomb Failure Criterion

The results of three CD tests on 38-mm-diameter and 76-mm-long samples of a soil at failure are as follows:

Test number	σ'_3 (kPa)	Deviatoric stress (kPa)
1	100	247.8 (peak)
2	180	362.0 (peak)
3	300	564 (no peak observed)

The detailed results for Test 1 are as follows. The negative sign indicates expansion.

Δz (mm)	ΔV (cm^3)	Axial load = P_z (N)
0	0.00	0.0
0.152	0.02	61.1
0.228	0.03	94.3
0.38	-0.09	124.0
0.76	-0.50	201.5
1.52	-1.29	257.5
2.28	-1.98	292.9
2.66	-2.24	298.9
3.04	-2.41	298.0
3.8	-2.55	279.2
4.56	-2.59	268.4
5.32	-2.67	252.5
6.08	-2.62	238.0
6.84	-2.64	229.5
7.6	-2.66	223.2
8.36	-2.63	224.3

- (a) Determine the friction angle for each test.
- (b) Determine τ_p , τ_{cs} , E' , and E'_s at peak shear stress for Test 1.
- (c) Determine ϕ'_{cs} .
- (d) Determine α_p for Test 1.

Strategy From a plot of deviatoric stress versus axial strain for Test 1, you will get τ_p , τ_{cs} , E' , and E'_s . The friction angles can be calculated or found from Mohr's circle.

Solution 10.8

Step 1: Determine the friction angles. Use a table to do the calculations.

Test no.	σ'_3 (kPa)	$\sigma'_1 - \sigma'_3$ (kPa)	σ'_1 (kPa)	$\sigma'_1 + \sigma'_3$ (kPa)	$\phi' = \sin^{-1}\left(\frac{\sigma'_1 - \sigma'_3}{\sigma'_1 + \sigma'_3}\right)$
Test 1	100	247.8	347.8	447.8	33.6° (peak)
Test 2	180	362	542	722	30.1° (peak)
Test 3	300	564	864	1164	29°

Alternatively, plot Mohr's circles and determine the friction angles, as shown for Test 1 and Test 2 in Figure E10.8a.

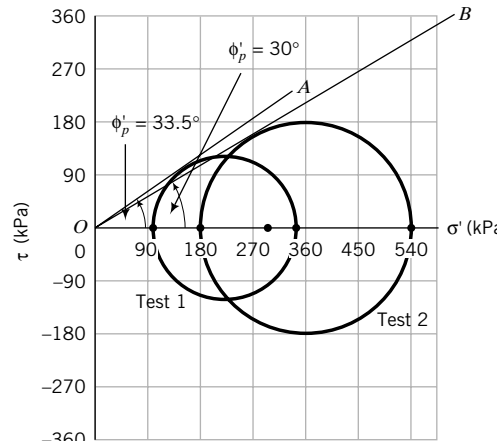


FIGURE E10.8a

Step 2: Determine τ_p and τ_{cs} from a plot of deviatoric stress versus axial strain response for Test 1.

$$\text{The initial area is } A_o = \frac{\pi D_o^2}{4} = \frac{\pi \times 38^2}{4} = 1134 \text{ mm}^2$$

$$V_o = A_o H_o = 1134 \times 76 = 86,184 \text{ mm}^2$$

$$A = \frac{A_o(1 - \varepsilon_p)}{1 - \varepsilon_1}$$

The deviatoric stress, q , is the axial load (P_z) divided by the cross-sectional area of the sample.

$A_o = 1134 \text{ mm}^2$					
$\Delta z (\text{mm})$	$\varepsilon_1 = \frac{\Delta z}{H_o}$	$\Delta V (\text{cm}^3)$	$\varepsilon_p = \frac{\Delta V}{V_o}$	$A (\text{mm}^2)$	$q = P_z/A (\text{kPa})$
0.00	0.00	0.00	0.00	1134	0
0.15	0.20	0.02	0.02	1136	53.8
0.23	0.30	0.03	0.03	1137	82.9
0.38	0.50	-0.09	-0.10	1141	108.7
0.76	1.00	-0.50	-0.58	1152	174.9
1.52	2.00	-1.29	-1.50	1175	219.2
2.28	3.00	-1.98	-2.30	1196	244.9
2.66	3.50	-2.24	-2.60	1206	247.8
3.04	4.00	-2.41	-2.80	1215	245.3
3.80	5.00	-2.55	-2.97	1229	227.1
4.56	6.00	-2.59	-3.01	1243	215.9
5.32	7.00	-2.67	-3.10	1257	200.8
6.08	8.00	-2.62	-3.05	1270	187.3
6.84	9.00	-2.64	-3.07	1285	178.7
7.60	10.00	-2.66	-3.09	1299	171.8
8.36	11.00	-2.63	-3.06	1313	170.7

Extract τ_p and τ_{cs} .

$$\tau_p = \frac{(\sigma'_1 - \sigma'_3)_p}{2} = \frac{247.8}{2} = 124 \text{ kPa}, \quad \tau_{cs} = \frac{(\sigma'_1 - \sigma'_3)_{cs}}{2} = \frac{170.7}{2} = 85.4 \text{ kPa}$$

See the above table for calculations and Figure E10.8b for a plot of the results.

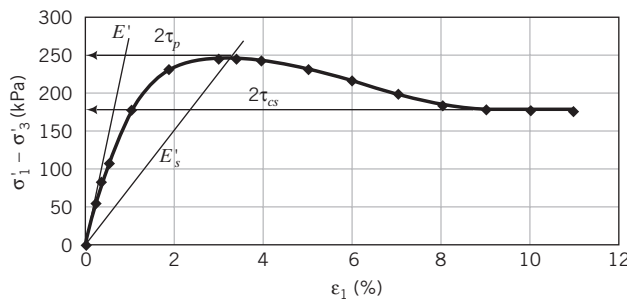


FIGURE E10.8b

Step 3: Determine E' and E'_s .

The initial slope of Figure E10.8b gives E' and the slope of the line from the origin to $q_p = 2\tau_p$ gives E'_s .

$$E' = \frac{54}{0.002} = 27,000 \text{ kPa}$$

$$E'_s = \frac{247.8}{0.035} = 7081 \text{ kPa}$$

Step 4: Determine ϕ'_{cs}

The deviatoric stress and the volumetric change appear to be constant from about $\varepsilon_1 \approx 10\%$. We can use the result at $\varepsilon_1 = 11\%$ to determine ϕ'_{cs} .

$$(\sigma'_3)_{cs} = 100 \text{ kPa}, (\sigma'_1)_{cs} = 170.7 + 100 = 270.7 \text{ kPa}$$

$$\phi'_{cs} = \sin^{-1} \left(\frac{\sigma'_1 - \sigma'_3}{\sigma'_1 + \sigma'_3}_{cs} \right) = \sin^{-1} \left(\frac{170.7}{270.7 + 100} \right) = 27.4^\circ$$

Step 5: Determine α_p

$$\alpha_p = \phi'_p - \phi'_{cs} = 33.6 - 27.4 = 6.2^\circ$$

10.7.6 Consolidated Undrained (CU) Compression Test

The purpose of a CU test is to determine the undrained and drained shear strength parameters (s_u, ϕ'_{cs}, ϕ'_p). The CU test is conducted in a similar manner to the CD test except that after isotropic consolidation, the axial load is increased under undrained condition and the excess porewater pressure is measured. The applied stresses are as follows:

Stage 1: Isotropic consolidation phase

$$\Delta\sigma_1 = \Delta\sigma_3 = \Delta\sigma'_1 = \Delta\sigma'_3; \quad \Delta\sigma_1 > 0, \quad \Delta u = 0$$

Therefore,

$$\Delta p' = \Delta p = \Delta\sigma_1; \quad \Delta q = 0, \quad \frac{\Delta q}{\Delta p'} = \frac{\Delta q}{\Delta p} = 0$$

Stage 2: Shearing phase

$$\Delta\sigma_1 > 0, \quad \Delta\sigma_3 = 0; \quad \Delta\sigma'_1 = \Delta\sigma_1 - \Delta u, \quad \Delta\sigma'_3 = -\Delta u$$

$$\Delta p = \frac{\Delta\sigma_1}{3}; \quad \Delta q = \Delta\sigma_1, \quad \frac{\Delta q}{\Delta p} = 3$$

$$\Delta p' = \Delta p - \Delta u = \frac{\Delta\sigma_1}{3} - \Delta u$$

$$\Delta q = \Delta\sigma_1, \quad \frac{\Delta q}{\Delta p'} = \frac{\Delta\sigma_1}{\frac{\Delta\sigma_1}{3} - \Delta u} = \frac{3}{1 - \frac{3\Delta u}{\Delta\sigma_1}}$$

While the total stress path is determinate, the effective stress path can be determined only if we measure the changes in excess porewater pressures. The stresses on the soil samples and the stress paths in a CU test are illustrated in Figure 10.24. The effective stress path is nonlinear because when the soil yields, the excess porewater pressures increase nonlinearly, causing the ESP to bend.

In a CU test, the volume of the soil is constant during the shear phase. Therefore,

$$\epsilon_p = \epsilon_1 + 2\epsilon_3 = 0 \quad (10.46)$$

which leads to

$$\epsilon_3 = -\frac{\epsilon_1}{2} \quad (10.47)$$

The axial displacement is measured and $\epsilon_1 = \Delta z/H_o$ is calculated. The maximum shear strain is

$$(\gamma_{zx})_{max} = \epsilon_1 - \epsilon_3 = \epsilon_1 - \left(-\frac{\epsilon_1}{2}\right) = 1.5\epsilon_1 \quad (10.48)$$

The elastic moduli E_u and $(E_u)_s$ are determined from a plot of $(\sigma_1 - \sigma_3)$ as ordinate and ϵ_1 as abscissa.

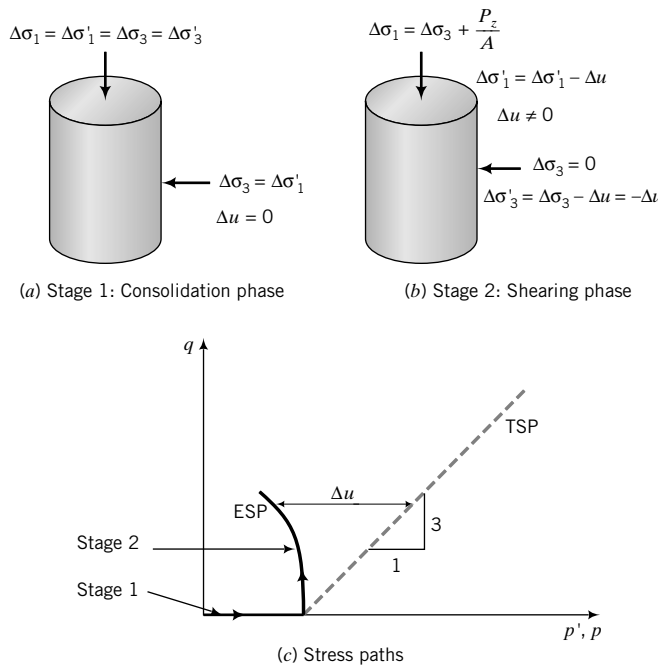


FIGURE 10.24 Stresses and stress paths for triaxial CU test.

Typical results from a CU test are shown in Figure 10.25 on page 304. Two sets of Mohr's circles at failure can be drawn, as depicted in Figure 10.25 on page 304. One represents total stress condition, and the other effective stress condition. For each test, Mohr's circle representing the total stresses has the same size as Mohr's circle representing the effective stresses, but they are separated horizontally by the excess porewater pressure. Mohr's circle of effective stresses is shifted to the right if the excess porewater pressure at failure is negative and to the left if the excess porewater pressure is positive. The Mohr–Coulomb failure criterion is used to interpret the shear strength using the effective stress circles. The shear strength parameters are ϕ'_{cs} and ϕ'_p .

The Tresca failure criterion is used to interpret the undrained shear strength using the total stress circles. Each Mohr's circle of total stress is associated with a particular value of s_u because each test has a different initial water content resulting from the different confining pressure, or applied consolidating stresses. The value of s_u is obtained by drawing a horizontal line from the top of the desired Mohr's circle of total stress to intersect the vertical shear axis. The intercept is s_u . The value of s_u at a cell pressure of about 830 kPa is 234 kPa, as shown in Figure 10.25. Alternatively, you can calculate s_u from

$$s_u = \frac{(\sigma_1 - \sigma_3)_f}{2} = \frac{(P_z)_{max}}{2A} \quad (10.49)$$

If the peak load is used, you will get $(s_u)_p$. If the load at critical state is used, you will get $(s_u)_{cs}$. You would normally determine s_u at the maximum anticipated stress level in the field. The value of s_u reported must be accompanied by the value of the initial ratio and the value of the overconsolidation ratio used in the test.

The CU test is the most popular triaxial test because you can obtain not only s_u but also ϕ'_{cs} and ϕ'_p , and most tests can be completed within a few minutes after consolidation, compared with more than a day for a CD test. Fine-grained soils with low k values must be sheared slowly to allow the excess porewater pressure to equilibrate throughout the test sample. The results from CU

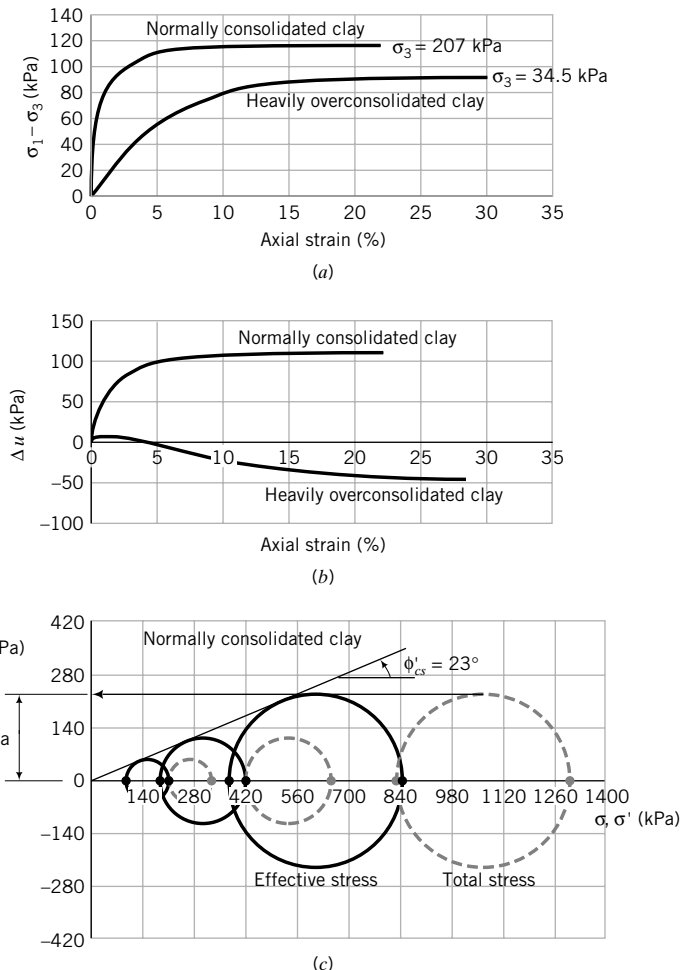


FIGURE 10.25 Triaxial CU tests on clays. (From *The Measurement of Soil Properties in the Triaxial Test*, by Bishop and Henkel, Edward Arnold, 1962.)

tests are used to analyze the stability of slopes, foundations, retaining walls, excavations, and other earthworks.

EXAMPLE 10.9 Interpreting CU Triaxial Test Data

A CU test was conducted on a saturated clay soil by isotropically consolidating the soil using a cell pressure of 150 kPa and then incrementally applying loads on the plunger while keeping the cell pressure constant. At large axial strains ($\approx 15\%$), the axial stress exerted by the plunger was approximately constant at 160 kPa and the porewater pressure recorded was constant at 54 kPa. Determine (a) s_u and (b) ϕ'_{cs} . Illustrate your answer by plotting Mohr's circle for total and effective stresses.

Strategy You can calculate the effective strength parameters by using the Mohr–Coulomb failure criterion or you can determine them from plotting Mohr's circle. Remember that the (axial) stress imposed by the plunger is not the major principal stress σ_1 , but $(\sigma_1 - \sigma_3) = (\sigma'_1 - \sigma'_3)$. Since the axial stress and the porewater

pressure remain approximately constant at large strains, we can assume that critical state condition has been achieved. The Tresca failure criterion must be used to determine s_u .

Solution 10.9

Step 1: Calculate the stresses at failure.

$$\frac{P_z}{A} = (\sigma_1)_f - (\sigma_3)_f = 160 \text{ kPa}$$

$$(\sigma_1)_{cs} = \frac{P_z}{A} + \sigma_3 = 160 + 150 = 310 \text{ kPa}$$

$$(\sigma'_1)_{cs} = (\sigma_1)_{cs} - \Delta u_{cs} = 310 - 54 = 256 \text{ kPa}$$

$$(\sigma_3)_{cs} = 150 \text{ kPa}, \quad (\sigma'_3)_{cs} = (\sigma_3)_{cs} - \Delta u_{cs} = 150 - 54 = 96 \text{ kPa}$$

Step 2: Determine the undrained shear strength.

$$s_u = (s_u)_{cs} = \frac{(\sigma_1)_{cs} - (\sigma_3)_{cs}}{2} = \frac{160}{2} = 80 \text{ kPa}$$

Step 3: Determine ϕ'_{cs} .

$$\sin \phi'_{cs} = \frac{(\sigma_1)_{cs} - (\sigma_3)_{cs}}{(\sigma_1)_{cs} + (\sigma_3)_{cs}} = \frac{160}{256 + 96} = 0.45$$

$$\phi'_{cs} = 26.7^\circ$$

Step 4: Draw Mohr's circle.

See Figure E10.9.

$$\phi'_{cs} = 27^\circ$$

$$(s_u)_{cs} = 80 \text{ kPa}$$

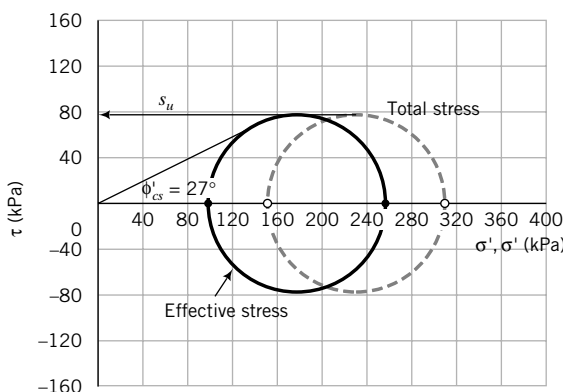


FIGURE E10.9

10.7.7 Unconsolidated Undrained (UU) Test

The purpose of a UU test is to determine the undrained shear strength of a saturated soil. The UU test consists of applying a cell pressure to the soil sample without drainage of porewater followed by increments of axial stress. The cell pressure is kept constant and the test is completed very quickly because in neither of the two stages—consolidation and shearing—is the excess porewater pressure allowed to drain. The stresses applied are:

Stage 1: Isotropic compression (not consolidation) phase

$$\begin{aligned}\Delta\sigma_1 &= \Delta\sigma_3, \quad \Delta u \neq 0 \\ \Delta p &= \Delta\sigma_1, \quad \Delta q = 0, \quad \frac{\Delta q}{\Delta p} = 0\end{aligned}$$

Stage 2: Shearing phase

$$\begin{aligned}\Delta\sigma_1 &> 0, \quad \Delta\sigma_3 = 0 \\ \Delta p &= \frac{\Delta\sigma_1}{3}, \quad \Delta q = \Delta\sigma_1, \quad \frac{\Delta q}{\Delta p} = 3\end{aligned}$$

Two or more samples of the same soil and the same initial void ratio are normally tested at different cell pressures. Each Mohr's circle is the same size, but the circles are translated horizontally by the difference in the magnitude of the cell pressures. Mohr's circles, stresses, and stress paths for a UU test are shown in Figure 10.26. Only the total stress path is known, since the porewater pressures are not measured to enable the calculation of the effective stresses.

The undrained shear strength, s_u , and the undrained elastic moduli, E_u and $(E_u)_s$, are obtained from a UU test. Tresca failure criterion is used to interpret the UU test. The UU tests, like the UC tests, are

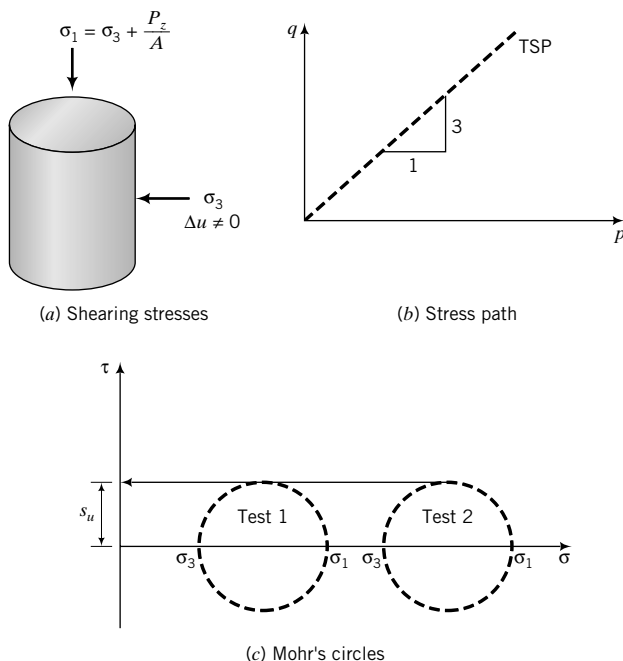


FIGURE 10.26
Stresses, stress path, and
Mohr's circles for UU tests.

quick and inexpensive compared with CD and CU tests. The advantage that the UU test has over the UC test is that the soil sample is stressed in the lateral direction to simulate the field condition. Both the UU and UC tests are useful in preliminary analyses for the design of slopes, foundations, retaining walls, excavations, and other earthworks.

EXAMPLE 10.10 Undrained Shear Strength from a UU Triaxial Test

A UU test was conducted on saturated clay. The cell pressure was 200 kPa and the peak deviatoric stress was 220 kPa. Determine the undrained shear strength.

Strategy You can calculate the radius of the total stress circle to give $(s_u)_p$, but a plot of Mohr's circle is instructive.

Solution 10.10

Step 1: Draw Mohr's circle.

See Figure E10.10.

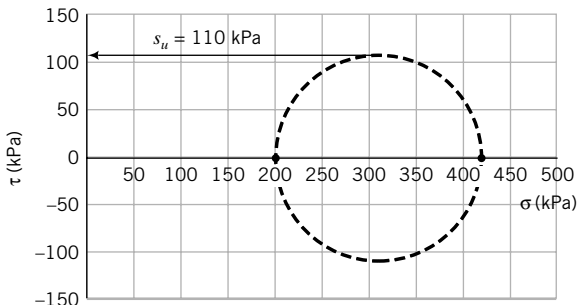


FIGURE E10.10

Step 2: Determine the undrained shear strength.

Draw a horizontal line to the top of Mohr's circle. The intersection of the horizontal line with the ordinate is the undrained shear strength.

$$(s_u)_p = 110 \text{ kPa}$$

$$\text{By calculation: } (s_u)_p = \frac{(\sigma_1)_p - (\sigma_3)_p}{2} = \frac{220}{2} = 110 \text{ kPa}$$

What's next . . . In the UU test and sometimes in the CU test, the excess porewater pressures are not measured. However, we need to know the magnitude of the excess porewater pressures to calculate effective stresses. Next, we will present a method to predict the excess porewater pressure from axisymmetric tests.

10.8 POREWATER PRESSURE UNDER AXISYMMETRIC UNDRAINED LOADING

The porewater pressure changes in soils are due to the changes in mean total and deviatoric stresses. Skempton (1954) proposed the following equation to determine the porewater pressure under axisymmetric conditions:

$$\Delta u = B[\Delta\sigma_3 + A(\Delta\sigma_1 - \Delta\sigma_3)] \quad (10.50)$$

TABLE 10.5 A_f Values

Type of clay	A_f
Highly sensitive	0.75 to 1.0
Normally consolidated	0.5 to 1
Compacted sandy clay	0.25 to 0.75
Lightly overconsolidated clays	0 to 0.5
Compacted clay-gravel	-0.25 to 0.25
Heavily overconsolidated clays	-0.5 to 0

SOURCE: From *The Measurement of Soil Properties in the Triaxial Test*, by Bishop and Henkel, Edward Arnold, 1962.

where $\Delta\sigma_3$ is the increase in lateral principal stress, $\Delta\sigma_1 - \Delta\sigma_3$ is the deviatoric stress increase, B is a coefficient indicating the level of saturation, and A is an excess porewater pressure coefficient. The A coefficient is due to the deviatoric stress. The coefficient B is 1 for saturated soils and 0 for dry soils. However, B is not directly correlated with saturation except at high values of saturation ($S > 90\%$). At failure,

$$A = A_f = \left(\frac{\Delta u_q}{\Delta\sigma_1 - \Delta\sigma_3} \right)_f \quad (10.51)$$

where Δu_q is the change in excess porewater pressure resulting from changes in deviatoric (shear) stresses. Experimental results of A_f presented by Skempton (1954) are shown in Table 10.5. The coefficient A was found to be dependent on the overconsolidation ratio (OCR). A typical variation of A_f with OCR is shown in Figure 10.27.

Equation (10.50) is very useful in determining whether a soil is saturated in an axisymmetric test. Let us manipulate Equation (10.50) by dividing both sides by $\Delta\sigma_3$, resulting in

$$\frac{\Delta u}{\Delta\sigma_3} = B \left[1 + A \left(\frac{\Delta\sigma_1}{\Delta\sigma_3} - 1 \right) \right] \quad (10.52)$$

During isotropic consolidation, $\Delta\sigma_3 = \Delta\sigma_1$ and Equation (10.52) becomes

$$\frac{\Delta u}{\Delta\sigma_3} = B \quad (10.53)$$

If a soil is saturated, then $B = 1$ and $\Delta u = \Delta\sigma_3$. That is, if we increase the consolidation stress or confining pressure by $\Delta\sigma_3$, the instantaneous excess porewater pressure change must be equal to the increase of confining pressure. Equation (10.53) then provides a basis to evaluate the level of saturation of a soil sample in an axisymmetric test. The coefficients A and B are referred to as Skempton's porewater pressure coefficients.

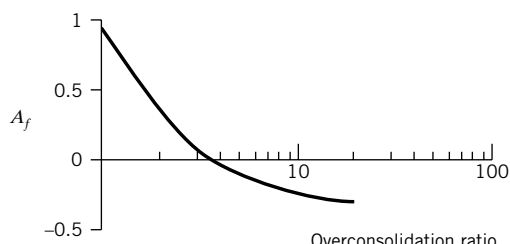


FIGURE 10.27
Variation of OCR with A_f .

THE ESSENTIAL POINTS ARE:

- Under an axisymmetric loading condition, the porewater pressure can be predicted using Skempton's porewater pressure coefficients, A and B .
- For a saturated soil, $B = 1$.

What's next . . . In the next section, we will briefly describe a few other laboratory apparatuses to determine the shear strength of soils. These apparatuses are more complex and were developed to more closely represent the field stresses on the laboratory soil sample than the triaxial and direct shear apparatuses.

10.9 OTHER LABORATORY DEVICES TO MEASURE SHEAR STRENGTH

There are several other types of apparatuses that are used to determine the shear strength of soils in the laboratory. These apparatuses are, in general, more sophisticated than the shear box and the triaxial apparatus.

10.9.1 Simple Shear Apparatuses

The purpose of a simple shear test is to determine shear strength parameters and the stress-strain behavior of soils under loading conditions that closely simulate plane strain and allow for the principal axes of stresses and strains to rotate. Principal stress rotations also occur in the direct shear test, but are indeterminate. The stress states in soils for many geotechnical structures are akin to simple shear.

There are two types of commercially available simple shear devices. One deforms an initial cuboidal sample under plane strain conditions into a parallelepiped (Figure 10.28a). The sample is contained in a box made by stacking square hollow plates between two platens. The top platen can be maintained at a fixed height for constant-volume tests or allowed to move vertically to permit volume change to occur (constant load test). By displacing the bottom of the box relative to the top, the soil is transformed from a cube to a parallelepiped.

A load cell mounted on the top platen measures the excess porewater pressures. The lateral stresses are deduced from one of the hollow plates outfitted with strain gages. The stresses and strains deduced from measurements in the cuboidal simple shear apparatus are shown in Figure 10.28b. If the excess porewater pressures are measured in undrained (constant-volume) tests, then the effective stresses can be determined.

The other apparatus tests a cylindrical sample whose vertical side is enclosed by a wire-reinforced rubber membrane (Figure 10.28c). Rigid, rough metal plates are placed at the top and bottom of the sample. Displacing the top of the sample relative to the bottom deforms the sample. The vertical and horizontal loads (usually on the top boundary) as well as displacements on the boundaries are measured, and thus the average normal and shear stresses and boundary strains can be deduced. In the cylindrical apparatus, the stresses measured are σ_z and τ_{zx} , and the test is referred to as direct simple shear.

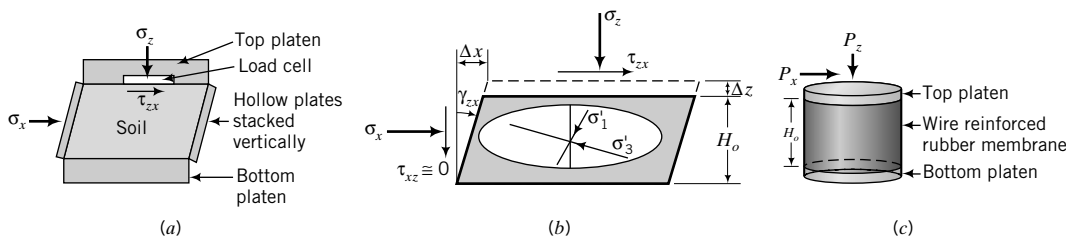


FIGURE 10.28 Cuboidal simple shear apparatus: (a) simple shear box, (b) stresses imposed on samples, and (c) direct simple shear.

Simple shear apparatuses do not subject the sample as a whole to uniform stresses and strains. However, the stresses and strains in the central region of the sample are uniform. In simple shear, the strains are $\varepsilon_x = \varepsilon_y = 0$, $\varepsilon_z = \Delta z/H_o$, and $\gamma_{zx} = \Delta x/H_o$. A plot of shear stress τ_{zx} versus γ_{zx} is used to determine G .

The shear displacement Δx must be applied in small increments to comply with the above definition. The principal strains from Equations (7.35) and (7.36) are

$$\varepsilon_1 = \frac{1}{2} (\varepsilon_z + \sqrt{\varepsilon_z^2 + \gamma_{zx}^2}) \quad (10.54)$$

$$\varepsilon_3 = \frac{1}{2} (\varepsilon_z - \sqrt{\varepsilon_z^2 + \gamma_{zx}^2}) \quad (10.55)$$

and

$$(\gamma_{zx})_{max} = \varepsilon_1 - \varepsilon_3 = \sqrt{\varepsilon_z^2 + \gamma_{zx}^2} \quad (10.56)$$

The dilation angle is determined from Equation (10.10). Taylor failure criterion is suitable for interpreting the results of simple shear tests. You can also use Mohr–Coulomb failure criterion with the effective stresses to determine ϕ'_{cs} and ϕ'_p , and Tresca failure criterion with the total stresses to determine s_u .

EXAMPLE 10.11 Interpreting Simple Shear Test Data

A cuboidal soil sample, with 50-mm sides, was tested in a simple shear device. The soil volume was maintained constant by adjusting the vertical load. At failure, the vertical load (P_z) was 500 N, the horizontal load (P_x) was 375 N, and the shear load (T) was 150 N. The excess porewater pressure developed was 60 kPa.

- (a) Plot Mohr's circles for total and effective stresses.
- (b) Determine the friction angle and the undrained shear strength, assuming the soil is nondilating.
- (c) Determine the failure stresses.
- (d) Find the magnitudes of the principal effective stresses and the inclination of the major principal axis of stress to the horizontal.
- (e) Determine the shear and normal stresses on a plane oriented at 20° clockwise from the horizontal.

Strategy Draw a diagram of the forces on the soil sample, calculate the stresses, and plot Mohr's circle. You can find all the required values from Mohr's circle or you can calculate them. You must use effective stresses to calculate the friction angle. We will assume critical state condition, as the soil is nondilating.

Solution 10.11

Step 1: Determine the total and effective stresses.

$$\sigma_z = \frac{P_z}{A} = \frac{500 \times 10^{-3}}{(0.05)^2} = 200 \text{ kPa}$$

$$\sigma_x = \frac{P_x}{A} = \frac{375 \times 10^{-3}}{(0.05)^2} = 150 \text{ kPa}$$

$$\tau_{zx} = \frac{T}{A} = \frac{150 \times 10^{-3}}{(0.05)^2} = 60 \text{ kPa}$$

$$\sigma'_z = \sigma_z - \Delta u = 200 - 60 = 140 \text{ kPa}$$

$$\sigma'_x = \sigma_x - \Delta u = 150 - 60 = 90 \text{ kPa}$$

Step 2: Draw Mohr's circle of total and effective stresses.

See Figure E10.11.

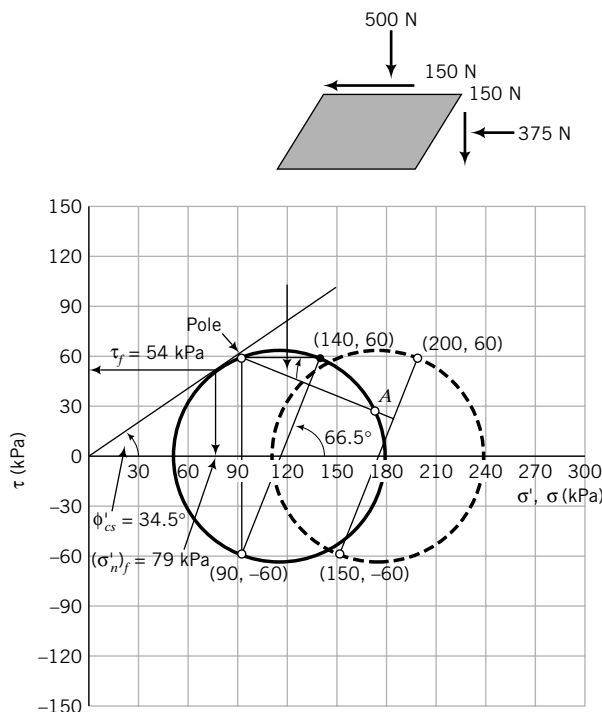


FIGURE E10.11

Step 3: Determine ϕ'_{cs} and s_u .

Draw a tangent to Mohr's circle of effective stress from the origin of the axes.

$$\text{From Mohr's circle: } \phi'_{cs} = 34.5^\circ$$

The undrained shear strength is found by drawing a horizontal line from the top of Mohr's circle of total stresses to intersect the ordinate.

$$(s_u)_{cs} = 65 \text{ kPa}$$

Step 4: Determine the failure stresses.

At the point of tangency of the failure envelope and Mohr's circle of effective stress, we get

$$\tau_{cs} = 54 \text{ kPa}, \quad (\sigma'_n)_{cs} = 79 \text{ kPa}$$

Step 5: Determine σ'_1 , σ'_3 , and ψ .

From Mohr's circle of effective stress, we get

$$(\sigma'_1)_{cs} = 180 \text{ kPa} \quad \text{and} \quad (\sigma'_3)_{cs} = 50 \text{ kPa}; \quad 2\psi = 66.5^\circ \quad \text{and} \quad \psi = 33.3^\circ$$

Step 6: Determine the stresses on a plane oriented at 20° .

Identify the pole, as shown in Figure E10.11. Draw a line inclined at 20° to the horizontal from the pole, as shown in Figure E10.11. Remember that we are using counterclockwise shear as positive. Point A gives the stresses on a plane oriented at 20° from the horizontal.

$$\tau_{20} = 30 \text{ kPa}; \quad \sigma'_{20} = 173 \text{ kPa}$$

Alternatively, by calculation,

$$\text{Equation (7.27): } (\sigma'_1)_{cs} = \frac{140 + 90}{2} + \sqrt{\left(\frac{140 - 90}{2}\right)^2 + 60^2} = 180 \text{ kPa}$$

$$\text{Equation (7.28): } (\sigma'_3)_{cs} = \frac{140 + 90}{2} - \sqrt{\left(\frac{140 - 90}{2}\right)^2 + 60^2} = 50 \text{ kPa}$$

$$(s_u)_{cs} = \frac{(\sigma'_1 - \sigma'_3)_{cs}}{2} = \frac{180 - 50}{2} = 65 \text{ kPa}$$

$$\phi'_{cs} = \sin^{-1}\left(\frac{\sigma'_1 - \sigma'_3}{\sigma'_1 + \sigma'_3}\right) = \sin^{-1}\left(\frac{180 - 50}{180 + 50}\right) = 34.4^\circ$$

$$\text{Equation (7.29): } \tan\psi = \frac{\tau_{zx}}{\sigma'_1 - \sigma'_x} = \frac{60}{180 - 90} = 0.67; \quad \psi = 33.7^\circ$$

$$\begin{aligned} \text{Equation (7.32): } (\sigma'_n)_{20} &= \frac{140 + 90}{2} + \frac{140 - 90}{2} \cos 40^\circ + 60 \sin 40^\circ \\ &= 172.7 \text{ kPa} \end{aligned}$$

$$\text{Equation (7.33): } \tau_{20} = 60 \cos 40^\circ - \frac{140 - 90}{2} \sin 40^\circ = 29.9 \text{ kPa}$$

EXAMPLE 10.12 Interpreting Strains from a Simple Shear Test

A cuboidal soil sample, with 50-mm sides, was tested under drained conditions in a simple shear apparatus, and the maximum shear stress occurred when the shear displacement was 1 mm and the vertical movement was -0.05 mm .

- (a) Plot Mohr's circle of strain.
- (b) Determine the principal strains.
- (c) Determine the maximum shear strain.
- (d) Determine the dilation angle, α .

Strategy Calculate the vertical and shear strains and then plot Mohr's circle of strain. You can determine all the required values from Mohr's circle or you can calculate them.

Solution 10.12

Step 1: Determine the strains.

$$\varepsilon_z = \frac{\Delta z}{H_o} = -\frac{0.05}{50} = -0.001$$

(negative sign because the sample expands; compression is positive)

$$\varepsilon_x = \varepsilon_y = 0$$

$$\gamma_{zx} = \frac{\Delta x}{H_o} = \frac{1}{50} = 0.02$$

Step 2: Plot Mohr's circle of strain and determine ε_1 , ε_3 , $(\gamma_{zx})_{max}$, and α .

See Mohr's circle of strain, Figure E10.12.

$$\varepsilon_1 = 9.5 \times 10^{-3}, \quad \varepsilon_3 = -10.5 \times 10^{-3}$$

$$\alpha = 3^\circ$$

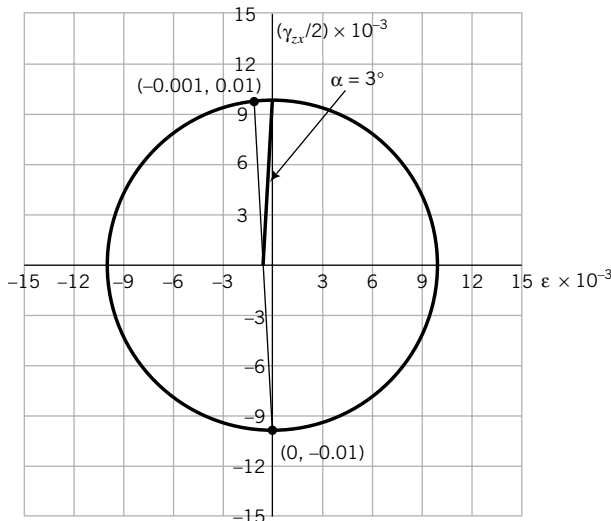


FIGURE E10.12

By calculation,

$$\text{Equation (7.35): } \varepsilon_1 = \frac{1}{2}(-0.001 + \sqrt{(-0.001)^2 + (0.02)^2}) = 9.5 \times 10^{-3}$$

$$\text{Equation (7.36): } \varepsilon_3 = \frac{1}{2}(-0.001 - \sqrt{(-0.001)^2 + (0.02)^2}) = -10.5 \times 10^{-3}$$

10.9.2 True Triaxial Apparatus

The purpose of a true triaxial test is to determine soil behavior and properties by loading the soil in three dimensions. In a true triaxial test, a cuboidal sample is subjected to independent displacements or stresses on three Cartesian axes. Displacements are applied through a system of rigid metal plates moving perpendicularly and tangentially to each face, as shown by the arrows in Figure 10.29a. Pressure

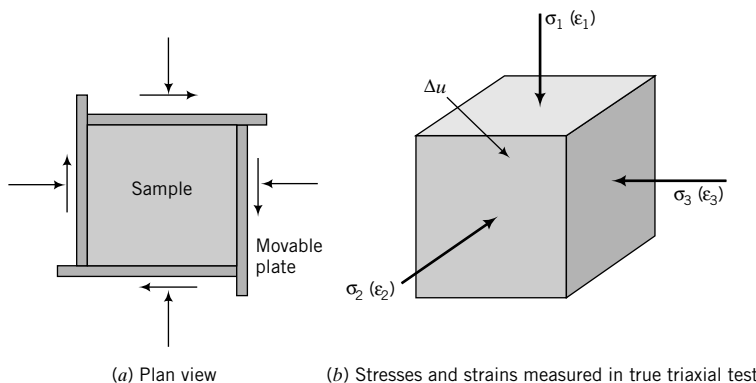


FIGURE 10.29 Schematic of true triaxial cell and stresses imposed on a sample of soil.

transducers are fixed to the inside of the faces to measure the three principal stresses. Like the conventional triaxial apparatus, the directions of principal stresses are prescribed and can only be changed instantaneously through an angle of 90° . The stresses and strains that can be measured in a true triaxial test are shown in Figure 10.29b.

10.9.3 Hollow-Cylinder Apparatus

The purpose of a hollow-cylinder test is to determine soil properties from a variety of plane strain stress paths. In the hollow-cylinder apparatus (Figure 10.30a), a hollow, thin-walled cylindrical sample is enclosed in a pressure chamber and can be subjected to vertical loads or displacements, radial stresses on the inner and outer cylindrical surfaces, and a torque, as shown in Figure 10.30b.

The vertical stress acting on a typical element of soil in this device is

$$\sigma_z = \frac{P_z}{A}$$

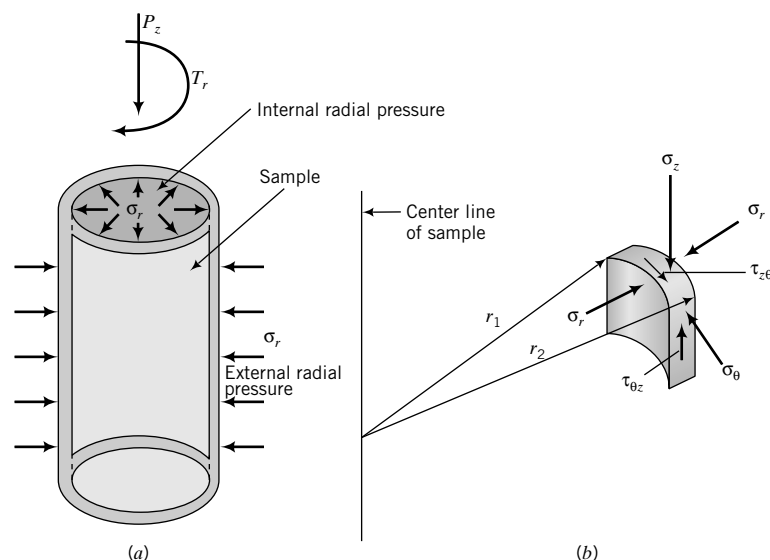
If the internal and external radial pressures are equal, then

$$\sigma_r = \sigma_\theta$$

The shearing stress applied is

$$\tau_{z\theta} = \frac{3T_r}{2\pi(r_2^3 - r_1^3)} \quad (10.57)$$

where T_r is the applied torque and r_1 and r_2 are the inner and outer radii. We can obtain ϕ' , ϕ'_{cs} , s_u , and G from the hollow-cylinder test.



Note: The internal radial pressure can be different from the external radial pressure.

FIGURE 10.30 (a) Hollow-cylinder cell and (b) stresses on an element of soil.

What's next . . . Sampling disturbances and sample preparation for laboratory tests may significantly impair the shear strength parameters. Consequently, a variety of field tests (Chapter 3) have been developed to obtain more reliable soil shear strength parameters by testing soils in situ. Field test results are often related to laboratory test results using empirical factors. In the next section, the shear strength parameters from popular in situ tests are presented.

10.10 FIELD TESTS

10.10.1 Vane Shear Test (VST)

The undrained shear strength from a vane shear test (Chapter 3, Section 3.5.7a) is calculated from

$$s_u = \frac{2T}{\pi d^3(h/d + \frac{1}{3})} \quad (10.58)$$

where T is the maximum torque, h is the height, and d is the diameter of the vane.

10.10.2 The Standard Penetration Test (SPT)

Results from SPT (Chapter 3) have been correlated to several soil parameters. Most of these correlations are weak. Typical correlation among N values, relative density, and ϕ' are given in Tables 10.6 and 10.7. You should be cautious in using the correlation in Table 10.6. SPTs are not recommended for fine-grained soils, so the correlation shown in Table 10.7 should be used only to provide an assessment of the relative shear strength of fine-grained soils.

TABLE 10.6 Correlation of N , N_{60} , γ , D_r , and ϕ' for Coarse-Grained Soils

N	N_{60}	Compactness	γ (kN/m ³)	D_r (%)	ϕ' (degrees)
0–4	0–3	Very loose	11–13	0–20	26–28
4–10	3–9	Loose	14–16	20–40	29–34
10–30	9–25	Medium	17–19	40–70	35–40*
30–50	25–45	Dense	20–21	70–85	38–45*
>50	>45	Very dense	>21	>85	>45*

*These values correspond to ϕ'_p .

TABLE 10.7 Correlation of N_{60} and s_u for Saturated Fine-Grained Soils

N_{60}	Description	s_u (kPa)
0–2	Very soft	<10
3–5	Soft	10–25
6–9	Medium	25–50
10–15	Stiff	50–100
15–30	Very stiff	100–200
>30	Extremely stiff	>200

10.10.3 Cone Penetrometer Test (CPT)

The cone resistance q_c is normally correlated with the undrained shear strength. Several adjustments are made to q_c . One correlation equation is

$$s_u = \frac{q_c - \sigma_z}{N_k} \quad (10.59)$$

where N_k is a cone factor that depends on the geometry of the cone and the rate of penetration. Average values of N_k as a function of plasticity index can be estimated from

$$N_k = 19 - \frac{\text{PI} - 10}{5}; \quad \text{PI} > 10 \quad (10.60)$$

Results of cone penetrometer tests have been correlated with the peak friction angle. A number of correlations exist. Based on published data for sand (Robertson and Campanella, 1983), you can estimate ϕ'_p using

$$\phi'_p = 35^\circ + 11.5 \log\left(\frac{q_c}{30\sigma'_{zo}}\right); \quad 25^\circ < \phi'_p < 50^\circ \quad (10.61)$$

THE ESSENTIAL POINTS ARE:

1. Various field tests are used to determine soil strength parameters.
2. You should be cautious in using these correlations of field test results, especially SPT, with soil strength parameters in design.

What's next . . . In the next section, the types of strength tests to specify for typical practical situations are presented.

10.11 SPECIFYING LABORATORY STRENGTH TESTS

It is desirable to test soil samples under the same loading and boundary conditions that would likely occur in the field. Often, this is difficult to accomplish because the loading and boundary conditions in the field are uncertain. Even if they were known to a high degree of certainty, it would be difficult and perhaps costly to devise the required laboratory apparatus. We then have to specify lab tests from conventional devices that best simulate the field conditions. A few practical cases are shown in Figure 10.31 with the recommended types of tests.

What's next . . . Several empirical relationships have been proposed to obtain soil strength parameters from laboratory tests, for example, the Atterberg limits, or from statistical analyses of field and laboratory test results. Some of these relationships are presented in the next section.

10.12 EMPIRICAL RELATIONSHIPS FOR SHEAR STRENGTH PARAMETERS

Some suggested empirical relationships for the shear strength of soils are shown in Table 10.8. These relationships should only be used as a guide and in preliminary design calculations.

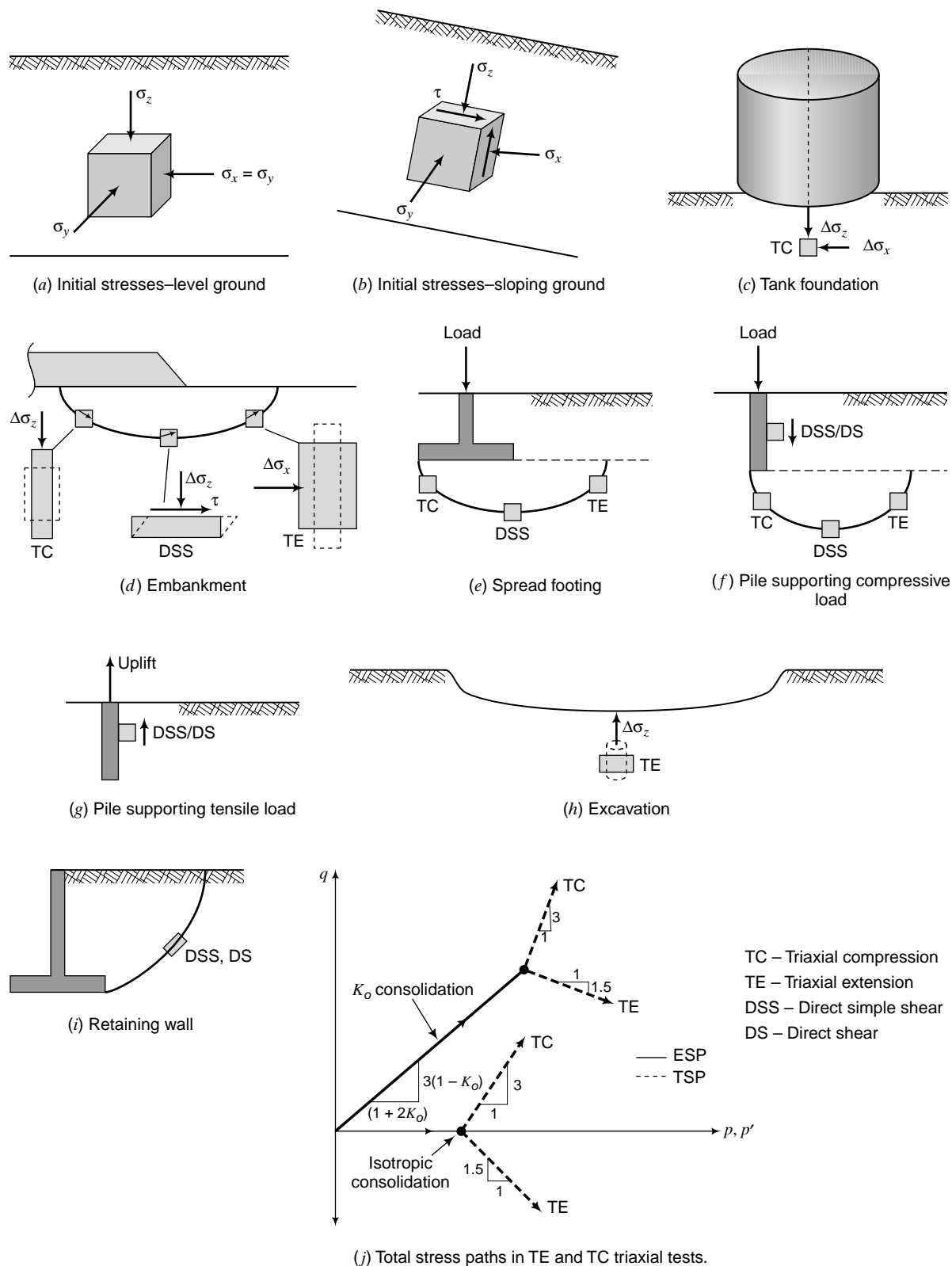


FIGURE 10.31 Some practical cases and the laboratory strength tests to specify.

TABLE 10.8 Empirical Soil Strength Relationships

Soil type	Equation	Reference
Normally consolidated clays	$\left(\frac{s_u}{\sigma'_z}\right)_{nc} = 0.11 + 0.0037 \text{ PI}$	Skempton (1957)
	$\left(\frac{s_u}{\sigma'_{zo}}\right) = 0.22$	
Overconsolidated clays	$\frac{(s_u/\sigma'_z)_{oc}}{(s_u/\sigma'_z)_{nc}} = (\text{OCR})^{0.8}$ See Note 1.	Ladd et al. (1977)
	$\frac{s_u}{\sigma'_z} = (0.23 \pm 0.04)\text{OCR}^{0.8}$ See Note 1.	
Clean quartz sand	$\phi'_p = \phi'_{cs} + 3D_r(10 - \ln p'_f) - 3$, where p'_f is the mean effective stress at failure (in kPa) and D_r is relative density. This equation should only be used if $12 > (\phi'_p - \phi'_{cs}) > 0$.	Bolton (1986)

Note 1: These are applicable to direct simple shear tests. The estimated undrained shear strength from triaxial compression tests would be about 1.4 times greater.

10.13 SUMMARY

The strength of soils is interpreted using four failure criteria. Each criterion is suitable for a certain class of problem. For example, Coulomb failure criterion is best used in situations where planar slip planes may develop. All soils, regardless of their initial state of stress, will reach a critical state characterized by continuous shearing at constant shear-to-normal-effective-stress ratio and constant volume. The initial void ratio of a soil and the normal effective stresses determine whether the soil will dilate or not. Dilating soils often exhibit (1) a peak shear stress and then strain-soften to a constant shear stress, and (2) initial contraction followed by expansion toward a critical void ratio. Nondilating soils (1) show a gradual increase of shear stress, ultimately reaching a constant shear stress, and (2) contract toward a critical void ratio. The shear strength parameters are the friction angles (ϕ'_p and ϕ'_{cs}) for drained conditions and s_u for undrained conditions. Only ϕ'_{cs} is a fundamental soil strength parameter.

A number of laboratory and field tests are available to determine the shear strength parameters. All these tests have shortcomings. You should use careful judgment in deciding what test should be used for a particular project. Also, you must select the appropriate failure criterion to interpret the test results.

Self-Assessment

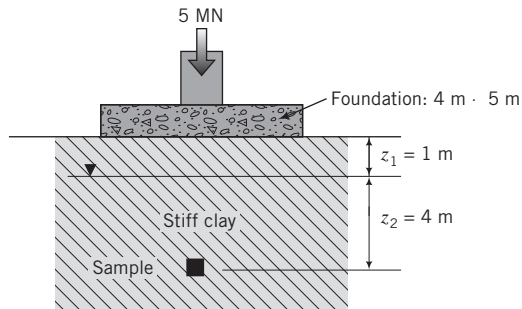


Access Chapter 10 at <http://www.wiley.com/college/budhu> to take the end-of-chapter quiz to test your understanding of this chapter.

Practical Examples

EXAMPLE 10.13 Failure Calculations for a Foundation

A rectangular foundation $4 \text{ m} \times 5 \text{ m}$ transmits a total load of 5 MN to a deep, uniform deposit of stiff, overconsolidated clay with an OCR = 4 and $\gamma_{sat} = 18 \text{ kN/m}^3$ (Figure E10.13). Groundwater level is at 1 m below the ground surface. A CU test was conducted on a soil sample taken at a depth 5 m below the center of the foundation. The results obtained are $(s_u)_p = 40 \text{ kPa}$, $\phi'_p = 28^\circ$, and $\phi'_{cs} = 24^\circ$. Determine if the soil will reach the failure state for short-term and long-term loading conditions. If the soil does not reach the failure state, what are the factors of safety for short-term and long-term loading conditions? Assume the soil above the groundwater level is saturated.

**FIGURE E10.13**

Strategy The key is to find the stresses imposed on the soil at a depth of 5 m and check whether the imposed shear stress exceeds the critical shear strength. For short-term condition, the critical shear strength is s_u , while for long-term conditions the critical shear strength is $(\sigma'_n)_f \tan \phi'_{cs}$.

Solution 10.13

Step 1: Determine the initial stresses.

$$\sigma'_z = \sigma'_1 = \gamma_{sat} z_1 + (\gamma_{sat} - \gamma_w) z_2 = (18 \times 1) + (18 - 9.8)4 = 50.8 \text{ kPa}$$

$$K_o^{oc} = K_o^{nc}(\text{OCR})^{0.5} = (1 - \sin \phi'_{cs})(\text{OCR})^{0.5} = (1 - \sin 24^\circ)(4)^{0.5} = 1.2$$

$$\sigma'_3 = K_o^{oc} \sigma'_z = 1.2 \times 50.8 = 61 \text{ kPa}$$

$$\sigma_1 = \sigma'_z + z_2 \gamma_w = 50.8 + 4 \times 9.8 = 90 \text{ kPa}$$

$$\sigma_3 = \sigma'_3 + z_2 \gamma_w = 61 + 4 \times 9.8 = 100.2 \text{ kPa}$$

Step 2: Determine the vertical stress increases at $z = 5 \text{ m}$ under the center of the rectangular foundation.

Use Equation (7.85) or the computer program, STRESS, at www.wiley.com/college/budhu.



$$\Delta\sigma_z = 71.1 \text{ kPa}, \quad \Delta\sigma_x = 5.1 \text{ kPa}$$

Neglect the effect of the shear stress, $\Delta\tau_{zx}$.

Step 3: Determine imposed shear stress for short-term loading.

$$\text{Current vertical total stress: } (\sigma_1)_T = \sigma_1 + \Delta\sigma_z = 90 + 71.1 = 161.1 \text{ kPa}$$

$$\text{Current horizontal total stress: } (\sigma_1)_T = \sigma_3 + \Delta\sigma_x = 100.2 + 5.1 = 105.3 \text{ kPa}$$

$$\text{Current shear stress: } \tau_u = \frac{(\sigma_1)_T - (\sigma_3)_T}{2} = \frac{161.1 - 105.3}{2} = 28 \text{ kPa} < 40 \text{ kPa}$$

The soil will not reach the peak stress state.

$$\text{Factor of safety: } \text{FS} = \frac{(s_u)_p}{\tau_u} = \frac{40}{28} = 1.4$$

Step 4: Determine failure shear stress for long-term loading.

For long-term loading, we will assume that all the excess porewater pressure dissipated.

$$\text{Final effective stresses: } (\sigma'_1)_F = \sigma'_1 + \Delta\sigma_z = 50.8 + 71.1 = 121.9 \text{ kPa}$$

$$(\sigma'_3)_F = \sigma'_3 + \Delta\sigma_x = 61 + 5.1 = 66.1 \text{ kPa}$$

$$\text{Angle of friction mobilized: } \phi' = \sin^{-1}\left(\frac{\sigma'_1 - \sigma'_3}{\sigma'_1 + \sigma'_3}\right) = \sin^{-1}\left(\frac{121.9 - 66.1}{121.9 + 66.1}\right) = 17^\circ$$

The critical state angle of friction is 24° , which is greater than ϕ' . Therefore, failure would not occur.

$$\text{Factor of safety based on critical state: } \text{FS} = \frac{\tan 24^\circ}{\tan 17^\circ} = 1.5$$

$$\text{Factor of safety based on peak state: } \text{FS} = \frac{\tan 28^\circ}{\tan 17^\circ} = 1.7$$

EXAMPLE 10.14 Specifying Lab Tests for a Dam

An earth dam is proposed for a site consisting of a homogeneous stiff clay, as shown in Figure E10.14a. You, the geotechnical engineer, are required to specify soil strength tests to determine the stability of the dam. One of the critical situations is the possible failure of the dam by a rotational slip plane in the stiff clay. What laboratory strength tests would you specify and why?

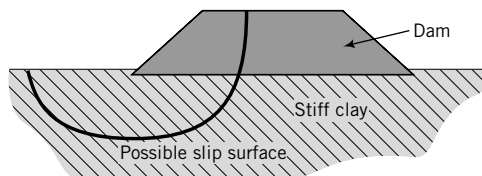


FIGURE E10.14a

Strategy The key is to determine the stress states for short-term and long-term conditions along the failure surface.

Solution 10.14

Step 1: Determine stresses along the failure surface.

Let us select three points—*A*, *B*, and *C*—on the possible failure surface. The rotational slip surface will introduce compression on element *A*, shear on element *B*, and extension on element *C* (Figure E10.14b). The stresses on element *A* are analogous to a triaxial compression test. Element *B* will deform in a manner compatible with simple shear, while element *C* will suffer from an upward thrust that can be simulated by a triaxial extension test.

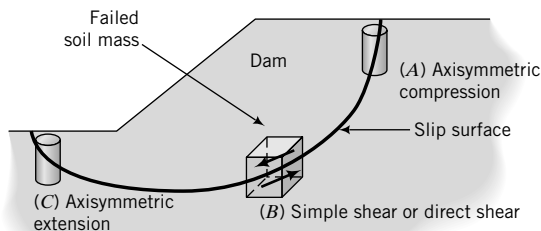


FIGURE E10.14b

Step 2: Make recommendations.

The following strength tests are recommended.

(a) Triaxial CU compression tests with porewater pressure measurements. Parameters required are ϕ'_p , ϕ'_{cs} , and s_u .

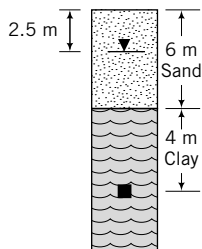
(b) Direct simple shear constant-volume tests.

Parameters required are ϕ'_p , ϕ'_{cs} , and s_u . If a direct simple shear apparatus is unavailable, then direct shear (shear box) tests should be substituted.

Undrained tests should be carried out at the maximum anticipated stress on the soil. You can determine the stress increases from the dam using the methods described in Chapter 7.

EXAMPLE 10.15 Estimation of s_u

You have contracted a laboratory to conduct soil tests for a site, which consists of a layer of sand, 6 m thick, with $\gamma_{sat} = 18 \text{ kN/m}^3$. Below the sand is a deep, soft, bluish clay with $\gamma_{sat} = 20 \text{ kN/m}^3$ (Figure E10.15). The site is in a remote area. Groundwater level was located at 2.5 m below the surface. You specified a consolidation test and a triaxial consolidated undrained test for samples of the soil taken at 10 m below ground surface. The consolidation test shows that the clay is lightly overconsolidated, with an OCR = 1.3. The undrained shear strength at a cell pressure approximately equal to the initial vertical stress is 72 kPa. Do you think the undrained shear strength value is reasonable, assuming the OCR of the soil is accurate? Show calculations to support your thinking.

**FIGURE E10.15**

Strategy Because the site is in a remote area, it is likely that you may not find existing soil results from neighboring constructions. In such a case you can use empirical relationships as guides, but you are warned that soils are notorious for having variable strengths.

Solution 10.15

Step 1: Determine the initial effective stresses.

Assume that the sand above the groundwater level is saturated.

$$\sigma'_{zo} = (18 \times 2.5) + (18 - 9.8) \times 3.5 + (20 - 9.8) \times 4 = 114.5 \text{ kPa}$$

$$\sigma'_{zc} = \sigma'_{zo} \times \text{OCR} = 114.5 \times 1.3 = 148.9 \text{ kPa}$$

Step 2: Determine s_u/σ'_{zo} .

$$\frac{s_u}{\sigma'_{zo}} = \frac{72}{114.5} = 0.63$$

Step 3: Use empirical equations from Table 10.8

$$\text{Jamiolkowski et al. (1985): } \frac{s_u}{\sigma'_{zo}} = (0.23 \pm 0.04)\text{OCR}^{0.8}$$

$$\begin{aligned} \text{Range of } \frac{s_u}{(\sigma'_{zo})}: & \quad 0.19(\text{OCR})^{0.8} \text{ to } 0.27(\text{OCR})^{0.8} \\ & = 0.19(1.3)^{0.8} \text{ to } 0.27(1.3)^{0.8} \\ & = 0.23 \text{ to } 0.33 < 0.63 \end{aligned}$$

The Jamiolkowski et al. (1985) expression is applicable to DSS. Triaxial compression tests usually give s_u values higher than DSS. Using a factor of 1.4 (see Note 1, Table 10.18), we get

$$\left(\frac{s_u}{\sigma'_{zo}} \right) = 0.32 \text{ to } 0.46 < 0.63$$

The differences between the reported results and the empirical relationships are substantial. The undrained shear strength is therefore suspicious. One possible reason for such high shear strength is that the water content at which the soil was tested is lower than the natural water content. This could happen if the soil sample extracted from the field was not properly sealed to prevent moisture loss. You should request a repeat of the test.

EXERCISES

Theory

- 10.1** A CD triaxial test was conducted on a loose sand. The axial stress was held constant and the radial stress was increased until failure occurred. At critical state, the radial stress was greater than the axial stress. Show, using Mohr's circle and geometry, that the slip plane is inclined at $\pi/4 - \phi'_{cs}/2$ to the horizontal plane.
- 10.2** The initial stresses on a soil are $\sigma'_1 = \sigma'_z$ and $\sigma'_3 = K_o \sigma'_z$, where K_o is the lateral earth pressure coefficient at rest (see Chapter 7). The soil was then brought to failure (critical state) by reducing σ'_3 while keeping σ'_1 constant. At failure, $\sigma'_3 = K \sigma'_1$, where K is a lateral earth pressure coefficient. Show that

$$\frac{\tau_{cs}}{\tau_{zx}} = \frac{1 - K}{1 - K_o} \cos \phi'_{cs}$$

where τ_{zx} is the maximum shear stress under the initial stresses and τ_{cs} is the failure (critical) shear stress.

- 10.3** Sand is placed on a stiff clay slope, as shown in Figure P10.3. (a) Show that sand will be unstable (i.e., fail by sliding) if $\theta > \phi'$. (b) Does the thickness of the sand layer influence impending failure? (c) If $\phi' = 25^\circ$ and $\theta = 23^\circ$, determine the factor of safety.

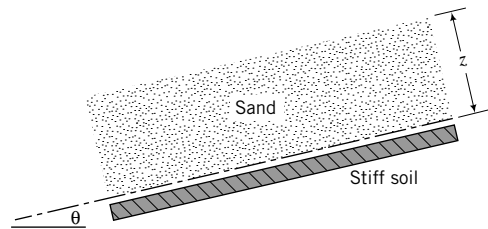


FIGURE P10.3

Problem Solving

- 10.4** A structure will impose a normal effective stress of 100 kPa and a shear stress of 30 kPa on a plane inclined at 58° to the horizontal. The critical state friction angle of the soil is 25° . Will the soil fail? If not, what is the factor of safety?
- 10.5** Figure P10.5 shows the stress-strain behavior of a soil. Determine the peak and critical shear stresses. Esti-

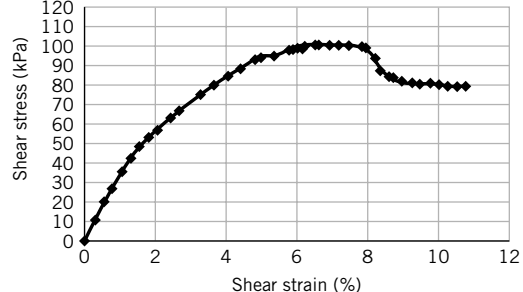


FIGURE P10.5

mate the peak and critical state friction angle and the peak dilation angle using (i) Coulomb's model, and (ii) Taylor's model. The normal effective stress is 160 kPa.

- 10.6** The following results were obtained from three direct shear (shear box) tests on a sample of sandy clay. The cross section of the shear box is $6 \text{ cm} \times 6 \text{ cm}$.

Normal force (N)	1250	1000	500	250
Shearing force (N)	506	405	325	255

- (a) Which failure criterion is appropriate to interpret this data set?
 (b) Determine the critical state friction angle.
 (c) If the soil is dilatant, determine ϕ'_p at a normal force of 250 N.

- 10.7** The results of a direct shear test on a dense sand are shown in the table below. Determine ϕ'_p , ϕ'_{cs} , and α_p . The vertical force is 200 N. The sample area is $100 \text{ mm} \times 100 \text{ mm}$ and the sample height is 20 mm. In the table, Δx , Δz , and P_x are the horizontal and vertical displacements and horizontal (shear) force, respectively.

Δx (mm)	Δz (mm)	P_x (N)
0	0	0
0.25	0	17.7
0.38	0.02	19.3
0.76	0.04	40.3
1.52	0.03	83.3
2.67	-0.04	127.2
3.18	-0.09	137.4
4.06	-0.15	155.9
5.08	-0.22	169.6
6.1	-0.26	176.8
6.6	-0.28	177.7
7.11	-0.28	172.9
8.13	-0.28	161.2
9.14	-0.28	159.8
10.16	-0.28	158.8

- 10.8** Repeat Problem 10.7, but use Taylor's model instead of Coulomb's model and assume that the data are from a direct simple shear test.

- 10.9** A cylindrical sample of soil 50 mm in diameter \times 100 mm long was subjected to axial and radial effective stresses. When the vertical displacement was 2 mm, the soil failed. The stresses at critical state are $(\sigma'_1)_{cs} = 280 \text{ kPa}$ and $(\sigma'_3)_{cs} = 100 \text{ kPa}$. The change in soil volume at failure was 800 mm^3 . (i) Which failure criterion is appropriate to interpret the test data? (ii) Determine (a) the axial strain at failure, (b) the volumetric strain at failure, (c) the critical state friction angle, and (d) the inclination of the slip plane to the horizontal plane.

- 10.10** An unconfined compression test was conducted on a compacted soil sample 50 mm in diameter \times 100 mm long. The sample is 86% saturated but you can assume it is fully saturated. The peak axial force recorded was 230 N, and the sample shortened by 2 mm. (a) Which failure criterion is appropriate to interpret the test data? (b) Determine the undrained shear strength. (c) Explain how your results may be affected by the saturation level of the sample.

- 10.11** A CD test was conducted on a sample of dense sand 38 mm in diameter \times 76 mm long. The cell pressure was 200 kPa. The results are shown in the table below.

- (a) Determine the ϕ'_p , ϕ'_{cs} , α_p , τ_p , E' , and E'_s .
- (b) If $\nu' = 0.3$, calculate G .

Axial displacement (mm)	Axial load (N)	Change in volume ($1 \times 10^3 \text{ mm}^3$)
0	0	0
0.3	128.1	0.1
0.6	225.9	0.1
1.0	338.9	0.1
1.3	451.8	-0.25
1.6	508.3	-0.7
1.9	564.8	-1.9
3.2	604.3	-2.7
5.2	593.0	-3.2
6.4	576.0	-3.4
7.1	564.8	-3.5
9.7	525.2	-3.6
12.9	497.0	-3.7
15.5	480.0	-3.7

- 10.12** CU tests were carried out on two samples of a clay. Each sample was isotropically consolidated before the axial stress was increased. The following results were obtained. Sample I results are at the peak deviatoric stress while sample II results are at critical state.

Sample no.	σ_3 (kPa)	$\sigma_1 - \sigma_3$ (kPa)	Δu (kPa)
I	420	320	205
II	690	365	350

- (a) Draw Mohr's circles (total and effective stresses) for each test on the same graph.
- (b) Why are the total stress circles not the same size?
- (c) Determine the friction angle for each test.
- (d) Determine the undrained shear strength at a cell pressure, $(\sigma_3)_f$, of 690 kPa.
- (e) Determine the stresses on the failure plane for each sample.

- 10.13** CU tests were conducted on samples of a compacted clay. Each sample was saturated before shearing. The results,

when no further change in excess porewater pressure or deviatoric stress occurred, are shown in the table below. Determine (a) ϕ'_{cs} and (b) s_u at a cell pressure of 420 kPa.

σ_3 (kPa)	$(\sigma_1 - \sigma_3)$ (kPa)	Δu (kPa)
140	636	-71
280	1008	-51.2
420	1323	-19.4

- 10.14** The failure stresses and excess porewater pressures for three samples of a loose sand in CU tests are given below.

Sample no.	$(\sigma_3)_f$ (kPa)	$(\sigma_1 - \sigma_3)_f$ (kPa)	Δu_f (kPa)
1	210	123	112
2	360	252	162
3	685	448	323

- (a) Plot Mohr's circle of effective stress from these data.
- (b) Determine the friction angle for each test.
- (c) If the sand were to be subjected to a vertical effective stress of 300 kPa, what magnitude of horizontal effective stress would cause failure?
- (d) Determine the inclination of (1) the failure plane and (2) the plane of maximum shear stress to the horizontal plane for Test 2.
- (e) Determine the failure stresses for Test 1.
- (f) Is the failure shear stress the maximum shear stress? Give reasons.

- 10.15** A CU triaxial test was carried out on a silty clay that was isotropically consolidated using a cell pressure of 125 kPa. The following data were obtained:

Axial load (kPa)	Axial strain, ϵ_1 (%)	Δu (kPa)
0	0	0
5.5	0.05	4.0
11.0	0.12	8.6
24.5	0.29	19.1
28.5	0.38	29.3
35.0	0.56	34.8
50.5	1.08	41.0
85.0	2.43	49.7
105.0	4.02	55.8
120.8	9.15	59.0

- (a) Plot the deviatoric stress against axial strain and excess porewater pressure against axial strain.
- (b) Determine the undrained shear strength and the friction angle.
- (c) Determine E' and E'_s .
- (d) Determine Skempton's A_f .

- 10.16** Three CU tests with porewater pressure measurements were made on a clay soil. The results at failure are shown on page 324.

σ_3 (kPa)	$\sigma_1 - \sigma_3$ (kPa)	Δu (kPa)
150	87.5	80
275	207.5	115
500	345.0	230

- 10.17** The following data at failure were obtained from two CU tests on a soil:
- | Test | σ_3 (kPa) | $\sigma_1 - \sigma_3$ (kPa) | Δu (kPa) |
|------|------------------|-----------------------------|------------------|
| 1 | 100 | 240 | -60 |
| 2 | 150 | 270 | -90 |

- (a) Determine the friction angle for each test.
 (b) Determine the change in dilation angle between the two tests, if a CD test were carried out.
 (c) Determine the undrained shear strength for each test.

- 10.18** A CU test on a stiff, overconsolidated clay at a constant cell pressure of 150 kPa gave a peak deviatoric stress of 448 kPa. The corresponding excess porewater pressure was -60 kPa. Determine the friction angle. Is this the critical state friction angle? Explain your answer.

- 10.19** The results of UU and CU tests on samples of a soil are shown below. Determine (a) the friction angle and (b) s_u at a cell pressure of 210 kPa in the CU tests. Predict the excess porewater pressure at failure for each of the UU test samples.

Type of test	σ_3 (kPa)	$(\sigma_1 - \sigma_3)$ (kPa)	Δu (kPa)
UU	57	105	To be determined
	210	246	To be determined
CU	57	74.2	11.9
	133	137.9	49.0
	210	203	86.1

- 10.20** The failure stresses in a simple shear constant-volume test are shown in the table below.

Total normal stress on the horizontal plane	300 kPa
Total normal stress on the vertical plane	200 kPa
Total shear stress on the horizontal and vertical planes	100 kPa
Porewater pressure	50 kPa

- (a) Draw Mohr's circles of total and effective stresses and determine the magnitude of the principal effective stresses and direction of the major principal effective stresses.
 (b) Determine the friction angle assuming the soil is nondilatational.
 (c) Determine the undrained shear strength. Assume the shear stress on the horizontal plane is counterclockwise.

Practical

- 10.21** You are in charge of designing a retaining wall. What laboratory tests would you specify for the backfill soil? Give reasons.

- 10.22** The following results were obtained from CU tests on a clay soil that is the foundation material for an embankment:

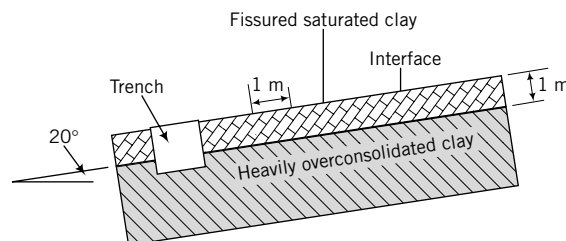
σ_3 (kPa)	$\sigma_1 - \sigma_3$ (kPa)	Δu (kPa)
300	331	111
400	420	160
600	487	322

Recommend the shear strength parameters to be used for short-term and long-term analyses. The maximum confining pressure (cell pressure) at the depth of interest is 300 kPa.

- 10.23** An embankment is being constructed to preload a foundation for an oil tank using a soil of unit weight $\gamma_{sat} = 18 \text{ kN/m}^3$. The soil below the embankment has a friction angle $\phi'_{cs} = 25^\circ$. The Skempton's pore pressure parameters found from triaxial tests are $A_f = 0.2$ and $B = 0.9$. It is proposed to raise the embankment from 3 m to 6 m. Assume (i) the increases in stresses are principal stresses, (ii) the dissipation of excess pore pressure during this stage of construction is negligible, and (iii) the increase in the lateral total pressure at any point is 0.2 times the increase in vertical total pressure. Determine the following:

- (a) Increase in the vertical total stress ($\Delta\sigma_z$) at the base of the embankment.
 (b) Increase in the lateral total stress ($\Delta\sigma_z$) at 0.5 m below the base of the embankment. Assume the vertical stress at the base is fully transferred to the soil at 0.5 m depth.
 (c) Increase in porewater pressure (Δu) at 0.5 m below the base of the embankment.
 (d) Vertical effective stress increase ($\Delta\sigma'_1$) at 0.5 m below the base of the embankment when it achieves a height of 6 m.

- 10.24** A trench is proposed for utilities along a very long slope that consists of two soils. The top soil is a fissured

**FIGURE P10.24**

saturated clay ($\gamma_{sat} = 20 \text{ kN/m}^3$, $\phi'_{cs} = 25^\circ$, $(s_u)_{cs} = 20 \text{ kPa}$) and the soil below it is a thick, heavily overconsolidated, stiff saturated clay with $(s_u)_p = 80 \text{ kPa}$ (Figure P10.24). The groundwater level is 8 m below the ground surface. One of the potential failure mechanisms consists of the top clay sliding as a rigid block at the interface. Consider a 1-m length of slope. Calculate the factor of safety (failure shear stress/shear stress imposed) of the slope for (a) short-term and (b) long-term conditions. Assume that the friction angle at the interface of the two soils is 25° .

- 10.25** Direct shear (shear box) tests were conducted on a moist, fine sand with $D_{50} = 0.2 \text{ mm}$. The fines content (particles less than 0.075 mm) is less than 1%. The results of the tests are:

Vertical load (N)	270	540	1080
Horizontal load (N)	184	334	662

- (a) Plot the vertical load versus the horizontal load.
- (b) Do the data align with a straight line through the origin? If not, explain why it is not so, assuming that the data are correct.
- (c) Recommend the friction angle to be used for the foundation design of a 10-story-high building. Explain your recommendation.

- 10.26** The results of a direct simple shear, constant volume test on an overconsolidated clay with $OCR = 4$ at critical state are $\tau_{cs} = 63 \text{ kPa}$, $\Delta u = 12 \text{ kPa}$, and $\sigma_z = 100 \text{ kPa}$. (a) Determine the undrained shear strength. (b) Is the test result reasonable? Explain your answer.

A CRITICAL STATE MODEL TO INTERPRET SOIL BEHAVIOR

11.0 INTRODUCTION

In this chapter, a simple soil model that combines consolidation and shear strength to interpret and predict soil responses to static loading is presented. When you complete this chapter, you should be able to:

- Estimate failure stresses for soil.
- Estimate strains at failure.
- Understand the relationship among soil parameters.
- Estimate whether drained or undrained condition would be critical for practical problems.
- Estimate whether a soil will show a peak shear stress or not.
- Predict stress-strain characteristics of soils from a few parameters obtained from simple soil tests.
- Evaluate possible soil stress states and failure if the loading on a geotechnical system were to change.

You will make use of all the materials you studied in Chapters 2 to 10, but particularly:

- Index properties
- Effective stresses, stress invariants, and stress paths
- Primary consolidation
- Shear strength

Importance

So far, we have painted individual pictures of soil behavior. We have looked at the physical characteristics of soils, one-dimensional flow of water through soils, stresses in soils from surface loads, effective stresses, stress paths, one-dimensional consolidation, and shear strength. You know that if you consolidate a soil to a higher stress state than its current one, the shear strength of the soil will increase. But the amount of increase depends on the soil type, the loading conditions (drained or undrained condition), and the stress paths. Therefore, the individual pictures should all be linked together. But how?

In this chapter, we are going to take the individual pictures and build a mosaic that will provide a basis for us to interpret and anticipate soil behavior. Our mosaic is mainly intended to unite consolidation and shear strength. Real soils, of course, require a complex mosaic, not only because soils are natural, complex materials, but also because the loads and loading paths cannot be anticipated accurately.

Our mosaic will provide a simple framework to describe, interpret, and anticipate soil responses to various loadings. The framework is essentially a theoretical model based on critical state soil mechanics—critical state model (Schofield and Wroth, 1968). Laboratory and field data, especially results from soft, normally consolidated clays, lend support to the underlying concepts embodied in the development of the critical state model. The emphasis in this chapter will be on using the critical state model to provide a generalized understanding of soil behavior rather than on the mathematical formulation.

The critical state model (CSM) we are going to study is a simplification and an idealization of soil behavior. However, the CSM captures the behavior of soils that are of greatest importance to geotechnical engineers. The central idea in the CSM is that all soils will fail on a unique failure surface in (p', q, e) space (see book cover). Thus, the CSM incorporates volume changes in its failure criterion, unlike the Mohr–Coulomb failure criterion, which defines failure only as the attainment of the maximum stress obliquity. According to the CSM, the failure stress state is insufficient to guarantee failure; the soil structure must also be loose enough.

The CSM is a tool to make estimates of soil responses when you cannot conduct sufficient soil tests to completely characterize a soil at a site or when you have to predict the soil's response from changes in loading during and after construction. Although there is a debate about the application of the CSM to real soils, the ideas behind the CSM are simple. It is a very powerful tool to get insights into soil behavior, especially in the case of the “what-if” situation. There is also a plethora of soil models in the literature that have critical state as their core. By studying the CSM, albeit a simplified version in this chapter, you will be able to better understand these other soil models.

A practical scenario is as follows. An oil tank is to be constructed on a soft alluvial clay. It was decided that the clay would be preloaded with a circular embankment imposing a stress at least equal to the total applied stress of the tank when filled. Wick drains (Chapter 9) are to be used to accelerate the consolidation process. The foundation for the tank is a circular slab of concrete, and the purpose of the preloading is to reduce the total settlement of the foundation. You are required to advise the owners on how the tank should be filled during preloading to prevent premature failure and to achieve the desired settlement. After preloading, the owners decided to increase the height of the tank. You are requested to determine whether the soil has enough shear strength to support an additional increase in tank height, and if so, the amount of settlement that can be expected. The owners are reluctant to finance any further preloading and soil testing.

11.1 DEFINITIONS OF KEY TERMS

Preconsolidation ratio (R_o) is the ratio by which the current mean effective stress in the soil was exceeded in the past ($R_o = p'_c/p'_o$, where p'_c is the preconsolidation mean effective stress, or, simply, preconsolidation stress, and p'_o is the current mean effective stress).

Compression index (λ) is the slope of the normal consolidation line in a plot of void ratio versus the natural logarithm of mean effective stress.

Unloading/reloading index, or recompression index (κ), is the average slope of the unloading/reloading curves in a plot of void ratio versus the natural logarithm of mean effective stress.

Critical state line (CSL) is a line that represents the failure state of soils. In (p', q) space, the critical state line has a slope M , which is related to the friction angle of the soil at the critical state. In $(e, \ln p')$ space, the critical state line has a slope λ , which is parallel to the normal consolidation line. In three-dimensional (p', q, e) space (see book cover), the critical state line becomes a critical state surface.

11.2 QUESTIONS TO GUIDE YOUR READING

1. What is soil yielding?
2. What is the difference between yielding and failure in soils?
3. What parameters affect the yielding and failure of soils?
4. Does the failure stress depend on the consolidation pressure?
5. What are the critical state parameters, and how can you determine them from soil tests?
6. Are strains important in soil failure?

7. What are the differences in the stress-strain responses of soils due to different stress paths?
8. What are the differences in behavior of soils under drained and undrained conditions?
9. Are the results from triaxial compression tests and direct simple shear the same? If not, how do I estimate the shear strength of a soil under direct simple shear from the results of triaxial compression, or vice versa?
10. How do I estimate the shear strength of a soil in the field from the results of lab tests?
11. How do loading (stress) paths affect the response of soils?

11.3 BASIC CONCEPTS



Interactive Concept Learning

Access www.wiley.com/college/budhu, click on Chapter 11, and download an interactive lesson (criticalstate.zip) (1) to learn the basic concepts of the critical state model, (2) to calculate yield and failure stresses and strains, (3) to calculate yield stresses and strains, and (4) to predict stress-strain responses for both drained and undrained conditions.

11.3.1 Parameter Mapping

In our development of the basic concepts on critical state, we are going to map certain plots we have studied in Chapters 8, 9, and 10 using stress and strain invariants and concentrate on a saturated soil under axisymmetric loading. However, the concepts and method hold for any loading condition. Rather than plotting σ'_n versus τ , we will plot the data as p' versus q (Figure 11.1a). This means that you must know the principal stresses acting on the element. For axisymmetric (triaxial) condition, you only need to know two principal stresses.

The Coulomb failure line in (σ'_n, τ) space of slope $\phi'_{cs} = \tan^{-1}[\tau_{cs}/(\sigma'_n)]$ is now mapped in (p', q) space as a line of slope $M = q_f/p_f$, where the subscript f denotes failure. Instead of a plot of σ'_z versus e , we will plot the data as p' versus e (Figure 11.1b), and instead of σ'_n (log scale) versus e , we will plot p' (ln scale) versus e (Figure 11.1c). The p' (ln scale) versus e plot will be referred to as the $(\ln p', e)$ plot.

We will denote the slope of the normal consolidation line (NCL) in the plot of p' (ln scale) versus e as λ and the unloading/reloading (URL) line as κ . The NCL is a generic normal consolidation line. In the initial development of the CSM in this textbook, the NCL is the same as the isotropic consolidation line (ICL). Later, we will differentiate ICL from the one-dimensional consolidation line (K_o CL). All these consolidation lines have the same slope. There are now relationships between ϕ'_{cs} and M , C_c and λ , and C_r and κ . The relationships for the slopes of the normal consolidation line, λ , and the unloading/reloading line, κ , are

$$\lambda = \frac{C_c}{\ln(10)} = \frac{C_c}{2.3} = 0.434 C_c \quad (11.1)$$

$$\kappa = \frac{C_r}{\ln(10)} = \frac{C_r}{2.3} = 0.434 C_r \quad (11.2)$$

Both λ and κ are positive for compression. For many soils, κ/λ has values within the range $\frac{1}{10}$ to $\frac{1}{5}$. We will formulate the relationship between ϕ'_{cs} and M later. The overconsolidation ratio using stress invariants, called preconsolidation ratio, is

$$R_o = \frac{p'_c}{p'_o} \quad (11.3)$$

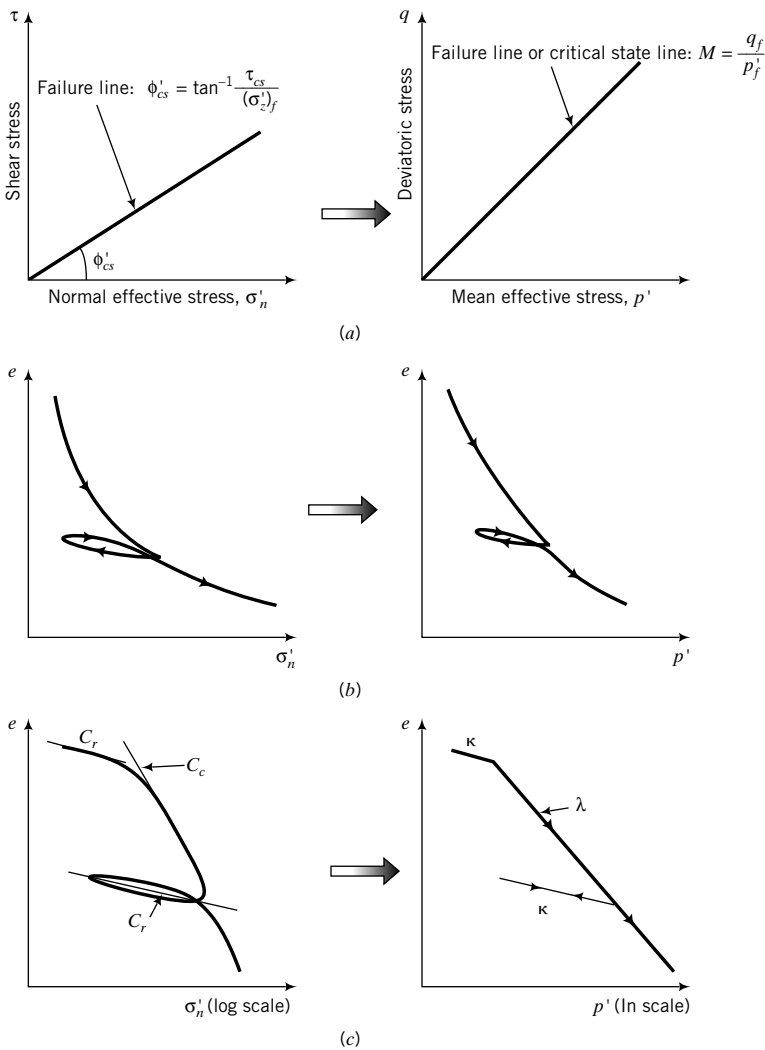


FIGURE 11.1 Mapping of strength and consolidation parameters.

where p'_o is the initial mean effective stress or overburden mean pressure and p'_c is the preconsolidation mean effective stress or, simply, preconsolidation stress. The preconsolidation ratio, R_o , defined by Equation (11.3) is not equal to OCR [Equation (9.13)] except for soils that have been isotropically consolidated.

EXAMPLE 11.1 Calculation of λ and κ from One-Dimensional Consolidation Test Results

The results of one-dimensional consolidation tests on a clay are $C_c = 0.69$ and $C_r = 0.16$. Calculate λ and κ .

Strategy This solution is a straightforward application of Equations (11.1) and (11.2).

Solution 11.1

Step 1: Calculate λ and κ .

$$\lambda = \frac{C_c}{2.3} = \frac{0.69}{2.3} = 0.3$$

$$\kappa = \frac{C_r}{2.3} = \frac{0.16}{2.3} = 0.07$$

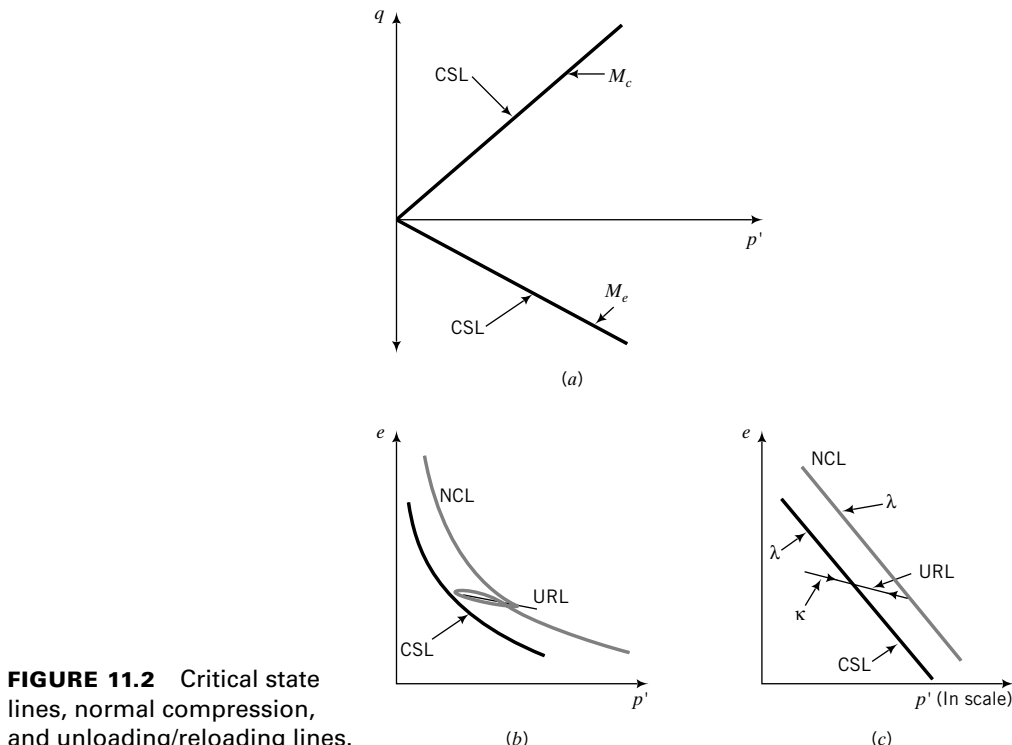


FIGURE 11.2 Critical state lines, normal compression, and unloading/reloading lines.

11.3.2 Failure Surface

The fundamental concept in CSM is that a unique failure surface exists in (p', q, e) space (see book cover), which defines failure of a soil irrespective of the history of loading or the stress paths followed. Failure and critical state are synonymous. We will refer to the failure line as the critical state line (CSL) in this chapter. You should recall that critical state is a constant stress state characterized by continuous shear deformation at constant volume. In stress space (p', q) the CSL is a straight line of slope $M = M_c$, for compression, and $M = M_e$, for extension (Figure 11.2a). Extension does not mean tension but refers to the case where the lateral stress is greater than the vertical stress. There is a corresponding CSL in (p', e) space (Figure 11.2b) or $(\ln p', e)$ space (Figure 11.2c) that is parallel to the normal consolidation line.

We can represent the CSL in a single three-dimensional plot with axes p', q, e (see book cover), but we will use the projections of the failure surface in the (q, p') space and the (p', e) space for simplicity. The failure surface shown on the book cover does not define limiting stresses as Coulomb or Mohr–Coulomb failure surfaces. It is a failure surface based on a particular set of stress and strain invariants [$p, q, \epsilon_p, \epsilon_q$; see Equations (8.1) to (8.5)] that leads to energy balance (input energy = output or dissipated energy) for soil as a continuum. Coulomb and Mohr–Coulomb failure surfaces are failure surfaces or planes in which the soil masses above and below them are rigid bodies. These failure planes are planes of discontinuity.

11.3.3 Soil Yielding

You should recall from Chapter 7 (Figure 7.8) that there is a yield surface in stress space that separates stress states that produce elastic responses from stress states that produce plastic responses. We are going to use the yield surface in (p', q) space (Figure 11.3) rather than (σ'_1, σ'_3) space so that our interpretation of soil responses is independent of the axis system.

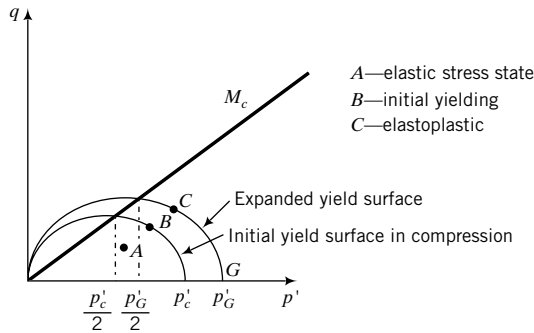


FIGURE 11.3 Expansion of the yield surface.

The yield surface is assumed to be an ellipse, and its initial size or major axis is determined by the preconsolidation stress, p'_c . Experimental evidence (Wong and Mitchell, 1975) indicates that an elliptical yield surface is a reasonable approximation for soils. The higher the preconsolidation stress, the larger the initial ellipse. We will consider the yield surface for compression, but the ideas are the same for extension except that the minor axis of the elliptical yield surface in extension is smaller than in compression.

All combinations of q and p' that are within the yield surface, for example, point A in Figure 11.3, will cause the soil to respond elastically. If a combination of q and p' lies on the initial yield surface (point B , Figure 11.3), the soil yields in a similar fashion to the yielding of a steel bar. Any tendency of a stress combination to move outside the current yield surface is accompanied by an expansion of the current yield surface, such that during plastic loading the stress point (p', q) lies on the expanded yield surface and not outside, as depicted by C . Effective stress paths such as BC (Figure 11.3) cause the soil to behave elastoplastically.

If the soil is unloaded from any stress state below failure, the soil will respond like an elastic material. As the initial yield surface expands, the elastic region gets larger. Expansion of the initial yield surface simulates strain-hardening materials such as loose sands and normally and lightly overconsolidated clays. The initial yield surface can also contract, simulating strain-softening materials such as dense sands and heavily overconsolidated clays. You can think of the yield surface as a balloon. Blowing up the balloon (applying pressure; loading) is analogous to the expansion of the yield surface. Releasing the air (gas) from the balloon (reducing pressure; unloading) is analogous to the contraction of the yield surface.

The critical state line intersects every yield surface at its crest. Thus, the intersection of the initial yield surface and the critical state line is at a mean effective stress $\frac{p'_c}{2}$, and for the expanded yield surface it is at $\frac{p'_G}{2}$.

11.3.4 Prediction of the Behavior of Normally Consolidated and Lightly Overconsolidated Soils Under Drained Condition

Let us consider a hypothetical situation to illustrate the ideas presented so far. We are going to try to predict how a sample of soil of initial void ratio e_o will respond when tested under drained condition in a triaxial apparatus, that is, a standard CD test. You should recall that the soil sample in a CD test is isotropically consolidated and then axial loads or displacements are applied, keeping the cell pressure constant. We are going to consolidate our soil sample up to a maximum mean effective stress p'_c , and then unload it to a mean effective stress p'_o such that $R_o = p'_c/p'_o < 2$. The limits imposed on R_o are only for presenting the basic ideas on CSM. More details on delineating lightly overconsolidated from heavily overconsolidated soils will be presented in Section 11.7.

On a plot of p' versus e (Figure 11.4b), the isotropic consolidation path is represented by AC . You should recall from Figure 11.1 that the line AC maps as the normal consolidation line (NCL) of slope λ . Because we are applying isotropic loading, the line AC is called the isotropic consolidation line (ICL).

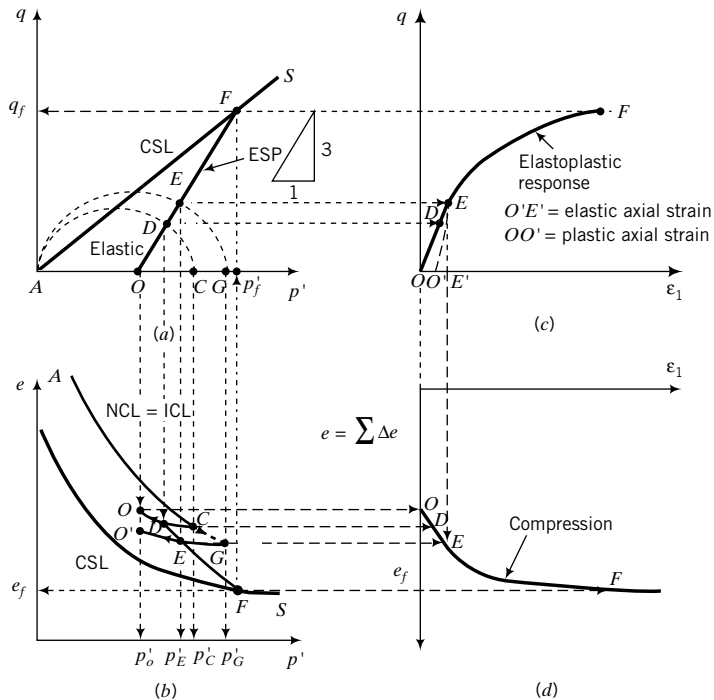


FIGURE 11.4 Illustrative predicted results from a triaxial CD test on a lightly overconsolidated soil ($1 < R_o \leq 2$) using CSM.

As we consolidate the soil gradually from A to C and unload it gradually to O , the stress paths followed in the (p', q) space are $A \rightarrow C$ and $C \rightarrow O$, respectively (Figure 11.4a). We can also sketch a curve (CO , Figure 11.4b) to represent the unloading of the soil in (p', e) space. The line CO is then the unloading/reloading line of slope, κ , in $(\ln p', e)$ space.

The preconsolidation mean effective stress, p'_c , determines the size of the initial yield surface. Since the maximum mean effective stress applied is the mean effective stress at C , then AC is the major principal axis of the ellipse representing the initial yield surface. A semiellipse is sketched in Figure 11.4a to illustrate the initial yield surface for compression. We can draw a line, AS , of slope, M_c , from the origin to represent the critical-state line (CSL) in (p', q) space, as shown in Figure 11.4a. In (p', e) space, the critical state line is parallel to the normal consolidation line (NCL), as shown in Figure 11.4b. Of course, we do not know, as yet, the slope $M = M_c$, or the equations to draw the initial yield surface and the CSL in (p', e) space. We have simply selected arbitrary values. Later, we are going to develop equations to define the slope M , the shape of the yield surface, and the critical state line in (p', e) space or $(\ln p', e)$ space. The CSL intersects the initial yield surface and all subsequent yield surfaces at $\frac{p'_c}{2}$, where p'_c is the (generic) current preconsolidation mean effective stress. For example, when the yield surface expands with a major axis, say AG , the CSL will intersect it at $\frac{p'_G}{2}$.

Let us now shear the soil sample at its current mean effective stress, p'_c , by increasing the axial stress, keeping the cell pressure, σ_3 , constant, and allowing the sample to drain. Because the soil is allowed to drain, the total stress is equal to the effective stress. That is, $(\Delta\sigma_1 = \Delta\sigma'_1 > 0)$ and $(\Delta\sigma_3 = \Delta\sigma'_3 > 0)$. You should recall from Chapter 10 that the effective stress path for a standard triaxial CD test has a slope $q/p' = 3$

(Proof: $\frac{\Delta q}{\Delta p'} = \frac{\Delta\sigma'_1 - \Delta\sigma'_3}{\Delta\sigma'_1 + 2\Delta\sigma'_3} = \frac{\Delta\sigma'_1 - 0}{\Delta\sigma'_1 + 2 \times 0} = 3$). The effective stress path (ESP) is shown by OF in

Figure 11.4a. The ESP is equal to the total stress path (TSP) because this is a drained test. The effective stress path intersects the initial yield surface at D . All stress states from O to D lie within the initial yield surface and, therefore, from O to D on the ESP the soil behaves elastically.

Assuming linear elastic response of the soil, we can draw a line OD in (ϵ_1, q) space (Figure 11.4c) to represent the elastic stress-strain response. At this stage we do not know the slope of OD , but later you will learn how to get this slope. Since the line CO in (p', e) space represents the unloading/reloading line (URL), the elastic response must lie along this line. The change in void ratio is $\Delta e = e_D - e_o$ (Figure 11.4b) and we can plot the axial strain (ϵ_1) versus e response, as shown by OD in Figure 11.4d.

Further loading from D along the stress path OF causes the soil to yield. The initial yield surface expands (Figure 11.4a) and the stress-strain is no longer elastic but elastoplastic (Chapter 7). At some arbitrarily chosen small increment of loading beyond initial yield, point E along the ESP, the size (major axis) of the yield surface is p'_G (G in Figure 11.4a). There must be a corresponding point G on the NCL in (p', e) space, as shown in Figure 11.4b. The increment of loading shown in Figure 11.4 is exaggerated. Normally, the stress increment should be very small because the soil behavior is no longer elastic. The stress is now not directly related to strain but is related to the plastic strain increment.

The total change in void ratio as you load the sample from D to E is DE (Figure 11.4b). Since E lies on the expanded yield surface with a past mean effective stress, p'_G , then E must be on the unloading line, GO' , as illustrated in Figure 11.4b. If you unload the soil sample from E back to O (Figure 11.4a), the soil will follow an unloading path, EO' , parallel to OC , as shown in Figure 11.4b. In the stress-strain plot, the unloading path will be EO' (Figure 11.4c). The length OO' on the axial strain axis is the plastic (permanent) axial strain, while the length OE' is the elastic axial strain.

We can continue to add increments of loading along the ESP until the CSL is intersected. At this stage, the soil fails and cannot provide additional shearing resistance to further loading. The deviatoric stress, q , and the void ratio, e , remain constant. The failure stresses are p'_f and q_f (Figure 11.4a) and the failure void ratio is e_f (Figure 11.4b). In general, it is the ratio $\frac{q_f}{p'_f}$ ($= M$) and e_f that are constants. For each increment of loading, we can determine Δe and plot ϵ_1 versus $\Sigma \Delta e$ [or $\epsilon_p = (\Sigma \Delta e)/(1 + e_o)$], as shown in Figure 11.4d. We can then sketch the stress-strain curve and the path followed in (p', e) space.

Let us summarize the key elements so far about our model.

1. During isotropic consolidation, the stress state must lie on the mean effective stress axis in (p', q) space and also on the NCL in (p', e) space.
2. All stress states on an ESP within and on the yield surface must lie on the unloading/reloading line through the current preconsolidation mean effective stress. For example, any point on the semiellipse, AEG , in Figure 11.4a has a corresponding point on the unloading/reloading line, $O'G$. Similarly, any point on the ESP from, say, E will also lie on the unloading/reloading line $O'G$. In reality, we are projecting the mean effective stress component of the stress state onto the unloading/reloading line.
3. All stress states on the unloading/reloading line result in elastic response.
4. Consolidation (e.g., stress paths along the p' axis) cannot lead to soil failure. Soils fail by the application of shearing stresses following ESP with slopes greater than the slope of the CSL for compression.
5. Any stress state on an ESP directed outward from the current yield surface causes further yielding. The yield surface expands.
6. Unloading from any expanded yield surface produces elastic response.
7. Once yielding is initiated, the stress-strain curve becomes nonlinear, with an elastic strain component and a plastic strain component.
8. The critical state line intersects each yield surface at its crest. The corresponding mean effective stress is one-half the mean effective stress of the major axis of the ellipse representing the yield surface.
9. Failure occurs when the ESP intersects the CSL and the change in volume is zero.

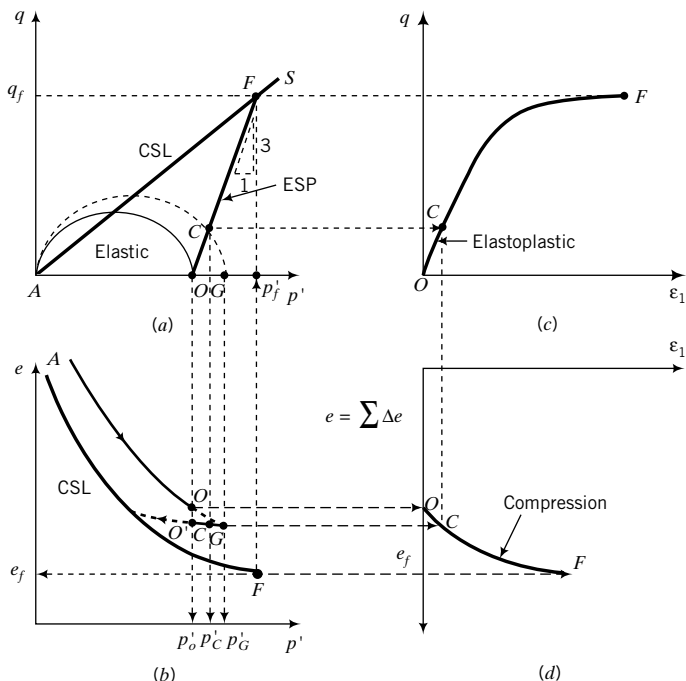


FIGURE 11.5 Illustrative predicted results from a CD triaxial test on a normally consolidated soil ($R_o = 1$) using CSM.

10. The soil must yield before it fails.
11. Each point on one of the plots in Figure 11.4 has a corresponding point on another plot. Thus, each point on any plot can be obtained by projection, as illustrated in Figure 11.4. Of course, the scale of the axis on one plot must match the scale of the corresponding axis on the other plot. For example, point F on the failure line, AS , in (p', q) space must have a corresponding point F on the failure line in (p', e) space.

In the case of a normally consolidated soil, the past mean effective stress is equal to the current mean effective stress (O in Figure 11.5a, b). The point O is on the initial yield surface. So, upon loading, the soil will yield immediately. There is no initial elastic region. An increment of effective stress corresponding to C in Figure 11.5 will cause the initial yield surface to expand. The preconsolidation mean effective stress is now p'_G and must lie at the juncture of the normal consolidation line and the unloading/reloading line. Since C is on the expanded yield surface, it must have a corresponding point on the unloading/reloading line through G . If you unload the soil from C , you will now get an elastic response ($C \rightarrow O'$, Figure 11.5b). The soil sample has become overconsolidated. Continued incremental loading along the ESP will induce further incremental yielding until failure is attained.

11.3.5 Prediction of the Behavior of Normally Consolidated and Lightly Overconsolidated Soils Under Undrained Condition

Instead of a standard triaxial CD test, we could have conducted a standard triaxial CU test after consolidating the sample. The slope of the TSP is 3. We do not know the ESP as yet. Let us examine what would occur to a lightly overconsolidated soil under undrained condition according to our CSM. We will use the abscissa as a dual axis for both p' and p (Figure 11.6). We know (Chapter 10) that for undrained condition the soil volume remains constant, that is, $\Delta e = 0$. Constant volume does not mean that there is no induced volumetric strain in the soil sample as it is sheared. Rather, it means that the elastic volumetric strain is balanced by an equal and opposite amount of plastic

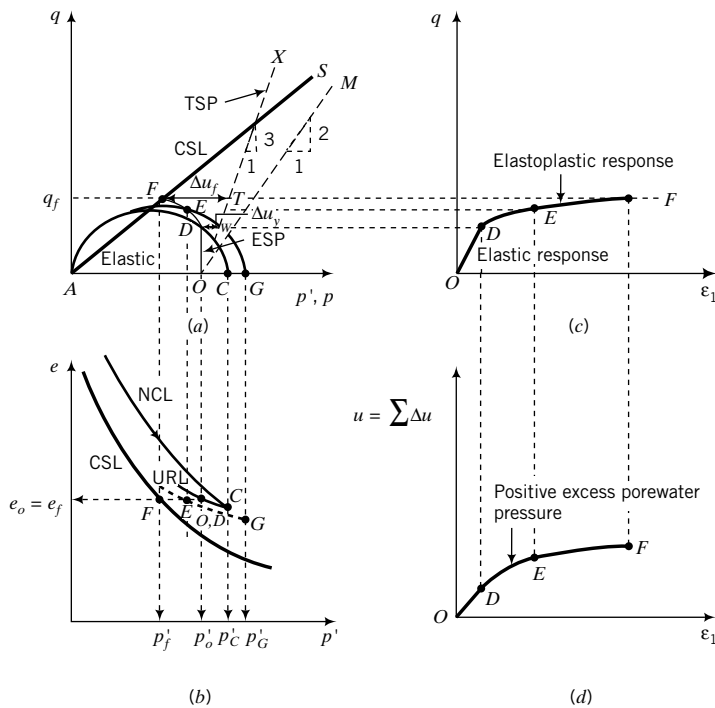


FIGURE 11.6 Illustrative predicted results from a triaxial CU test on a lightly overconsolidated soil using the CSM ($1 < R_o \leq 2$).

volumetric strains. We also know from Chapters 8 and 10 that the ESP for a linear elastic soil is vertical, that is, the change in mean effective stress, $\Delta p'$, is zero.

Because the change in volume is zero, the mean effective stress at failure can be represented by drawing a horizontal line from the initial void ratio to intersect the critical state line in (p', e) space, as illustrated by OF in Figure 11.6b. Projecting a vertical line from the mean effective stress at failure in (p', e) space to intersect the critical state line in (p', q) space gives the deviatoric stress at failure (Figure 11.6a). The initial yield stresses (p'_y, q_y), point D in Figure 11.6a, are obtained from the intersection of the ESP and the initial yield surface. Points O and D are coincident in the (p', e) plot, as illustrated in Figure 11.6b, because $\Delta p' = 0$. The ESP (OD in Figure 11.6a) produces elastic response.

Continued loading beyond initial yield will cause the initial yield surface to expand. For example, any point E between D and F on the constant void ratio line will be on an expanded yield surface (AEG) in (p', q) space. Also, point E must be on a URL line through G (Figure 11.6b). The ESP from D curves left toward F on the critical state line as excess porewater pressure increases significantly after initial yield.

The TSP has a slope of 3, as illustrated by OX in Figure 11.6a. The difference in mean stress between the total stress path and the effective path gives the change in excess porewater pressure. The excess porewater pressures at initial yield and at failure are represented by the horizontal lines DW and FT , respectively.

The undrained shear response of a soil is independent of the TSP. The shearing response would be the same if we imposed a TSP OM (Figure 11.6a), of slope, say, 2 (V):1 (H) rather than 3 (V):1 (H), where V and H are vertical and horizontal values. The TSP is only important in finding the total excess porewater pressure under undrained loading.

The intersection of the TSP with the critical state line is not the failure point, because failure and deformation of a soil mass depend on effective stress, not total stress. By projection, we can

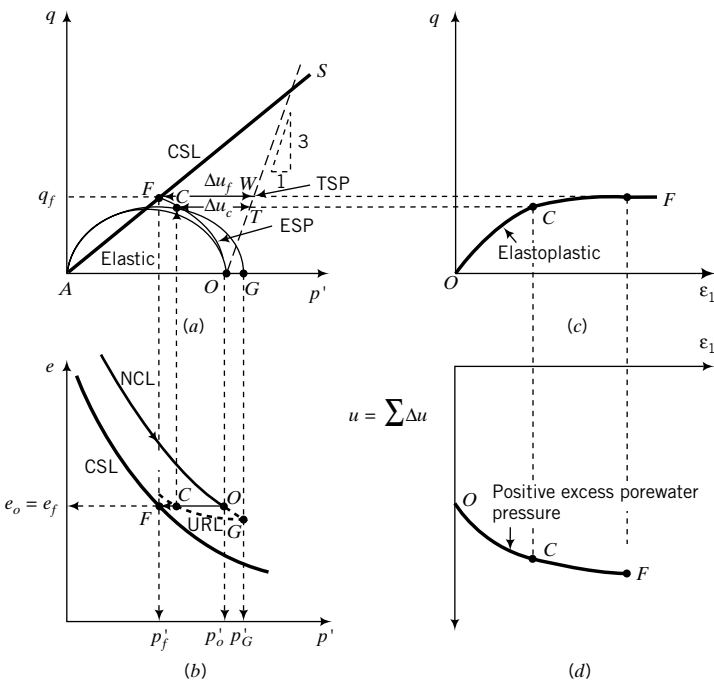


FIGURE 11.7 Illustrative predicted results from a triaxial CU test on a normally consolidated soil using the CSM ($R_o = 1$).

sketch the stress–strain response and the excess porewater pressure versus axial strain, as illustrated in Figure 11.6c, d.

For normally consolidated soils, yielding begins as soon as the soil is loaded (Figure 11.7). The ESP curves toward F on the failure line. A point C on the constant volume line, OF , in Figure 11.7b will be on an expanded yield surface and also on the corresponding URL (Figure 11.7a, b). The excess porewater pressures at C and F are represented by the horizontal lines CT and FW , respectively.

Let us summarize the key elements for undrained loading of lightly overconsolidated and normally consolidated soils from our model.

1. Under undrained loading, also called constant-volume loading, the total volume remains constant. This is represented in (p', e) space by a horizontal line from the initial mean effective stress to the failure line.
2. The portion of the ESP in (p', q) space that lies within the initial yield surface is represented by a vertical line from the initial mean effective stress to the initial yield surface. The soil behaves elastically, and the change in mean effective stress is zero.
3. Normally consolidated soils do not show an initial elastic response. They yield as soon as the loading is applied.
4. Loading beyond initial yield causes the soil to behave as a strain-hardening elastoplastic material. The initial yield surface expands.
5. The difference in mean total and mean effective stress at any stage of loading gives the excess porewater pressure at that stage of loading.
6. The response of soils under undrained condition is independent of the total stress path. The total stress path is only important in finding the total excess porewater pressure.

11.3.6 Prediction of the Behavior of Heavily Overconsolidated Soils Under Drained and Undrained Condition

So far we have considered normally and lightly overconsolidated soils ($R_o \leq 2$). What is the situation regarding heavily overconsolidated soils, that is, $R_o > 2$? Whether a soil behaves in a normally consolidated or a lightly overconsolidated or a heavily overconsolidated manner depends not only on R_o but also on the effective stress path. We can model a heavily overconsolidated soil by unloading it from its preconsolidation stress so that $p'_c/p'_o > 2$, as shown by point O in Figure 11.8a, b. Heavily overconsolidated soils have initial stress states that lie to the left of the critical state line in (p', e) space. The ESP for a standard triaxial CD test has a slope of 3 and intersects the initial yield surface at D . Therefore, from O to D the soil behaves elastically, as shown by OD in Figure 11.8b, c. The intersection of the ESP with the critical state line is at F (Figure 11.8a), so that the yield surface must contract as the soil is loaded to failure beyond initial yield. The initial yield shear stress is analogous to the peak shear stress for dilating soils. From D , the soil volume expands (Figure 11.8b, d), and the soil strain softens (Figure 11.8c) to failure at F . Remember that soil yielding must occur before failure. So, the soil must follow the path $O \rightarrow D \rightarrow F$ and not $O \rightarrow F \rightarrow D$.

The simulated volumetric response is shown in Figure 11.8d. From O to D (the elastic phase), the soil contracts. After initial yielding, the soil expands (dilates) up to failure and remains at constant volume (constant void ratio) thereafter.

The CSM simulates the mechanical behavior of heavily overconsolidated soils as elastic materials up to the peak shear stress and thereafter elastoplastically as the imposed loading causes

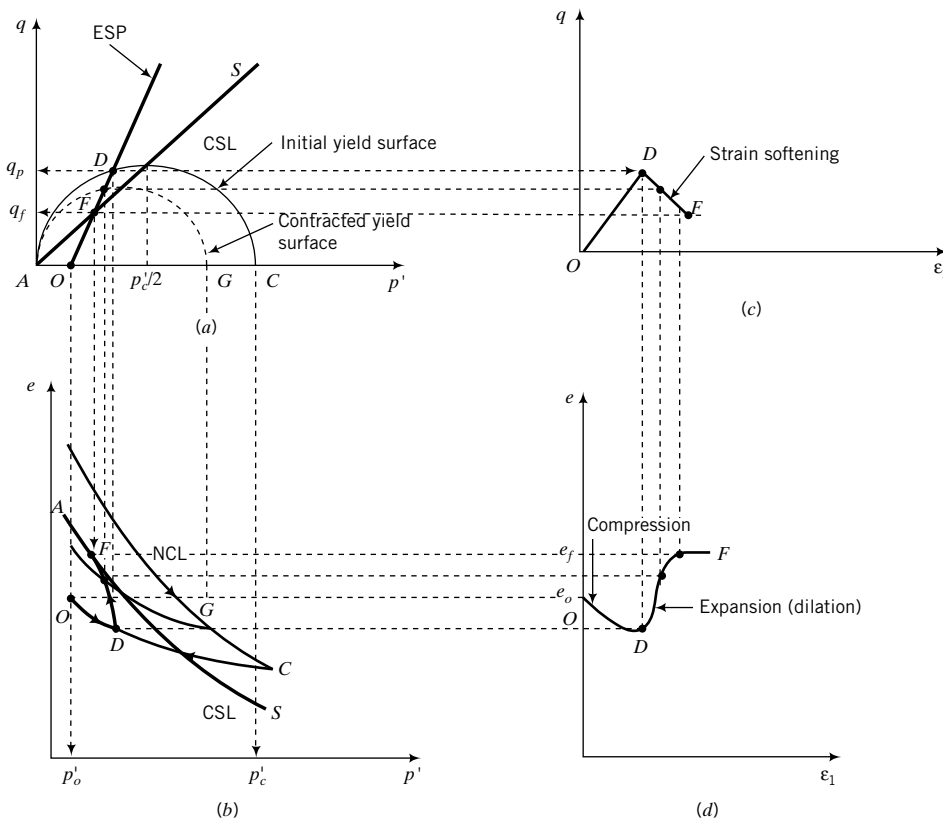


FIGURE 11.8 Illustrative predicted results from a triaxial CD test on a heavily overconsolidated soil ($R_o > 2$) using the CSM.

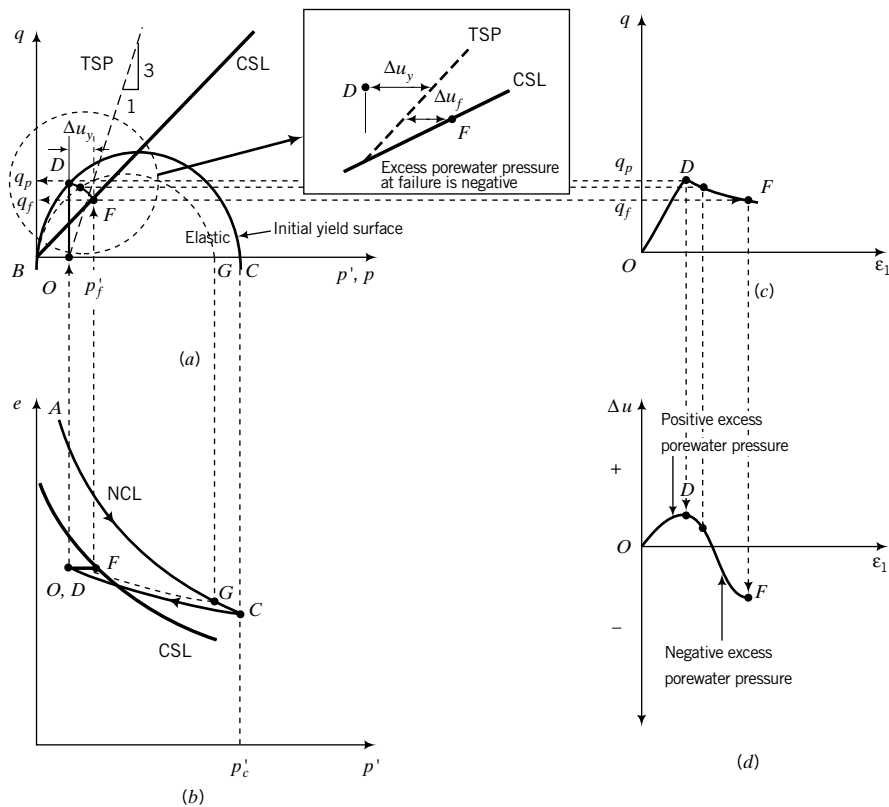


FIGURE 11.9 Illustrative predicted results from a triaxial CU test on a heavily overconsolidated soil ($R_o > 2$) using the CSM.

the soil to strain-soften toward the critical state line. In reality, heavily overconsolidated soils may behave elastoplastically before the peak shear stress is achieved, but this behavior is not captured by the simple CSM described here.

In the case of a standard triaxial CU test on heavily overconsolidated soils, the path to failure in (p', e) space is OF , as shown in Figure 11.9b, because no change in volume occurs. In the (p', q) space (Figure 11.9a), the soil will yield at D and then fail at F . So the path to failure is $O \rightarrow D \rightarrow F$. All stress states from O to D are within the initial yield surface, so the soil behaves like an elastic material. The ESP is then represented by a vertical line. Any stress state between D and F must have a corresponding point at the intersection of a URL line and the constant volume line, OF (Figure 11.9b). The yield surface from D to F contracts.

The tendency for the soil to contract from O to D induces positive excess porewater pressures, while the tendency to expand (D to F) induces negative excess porewater pressures (Figure 11.9d). The excess porewater pressures at initial yield, Δu_y , and at failure, Δu_f , are shown in the inset of Figure 11.9a. The excess porewater pressure at failure is negative ($p'_f > p_f$).

Let us summarize the key elements for undrained loading of heavily overconsolidated soils from our model.

- Under undrained loading, the total volume remains constant. This is represented in (p', e) space by a horizontal line from the initial mean effective stress to the failure line.
- The portion of the ESP in (p', q) space that lies within the initial yield surface is represented by a vertical line from the initial mean effective stress to the initial yield surface. The soil behaves elastically, and the change in mean effective stress is zero.

3. After initial yield, the soil may strain-soften (the initial yield surface contracts) or may strain-harden (the initial yield surface expands) to the critical state.
4. During elastic deformation under drained condition, the soil volume decreases (contracts), and after initial yield the soil volume increases (expands) to the critical state and does not change volume thereafter.
5. During elastic deformation under undrained condition, the soil develops positive excess porewater pressures, and after initial yield the soil develops negative excess porewater pressures up to the critical state. Thereafter, the excess porewater pressure remains constant.
6. The response of the soil under undrained condition is independent of the total stress path.

11.3.7 Prediction of the Behavior of Coarse-Grained Soils Using CSM

CSM is applicable to all soils. However, there are some issues about coarse-grained soils that require special considerations. Laboratory test data show that the NCL and CSL lines for coarse-grained soils are not well defined as straight lines in $(\ln p', e)$ space (Figure 11.10) compared to those for fine-grained soils. The particulate nature of coarse-grained soils with respect to shape, size, roughness, structural arrangement (packing), particle hardness, and stiffness often leads to localized discontinuities. Tests using X rays on coarse-grained soils show shear banding (Figure 10.4) and nonuniform distribution of strains, even at low strains ($<1\%$). Averaged stresses and strains normally deduced from measurements in soil test equipment cannot be relied upon to validate CSM. CSM is based on treating soils as continua, with smooth changes in stresses and strains. CSM cannot be used when shear bands occur. Other models (e.g., Coulomb or Mohr–Coulomb) may be more appropriate than CSM. However, the soil within the shear band is generally at critical state, and it is likely to behave as a viscous fluid.

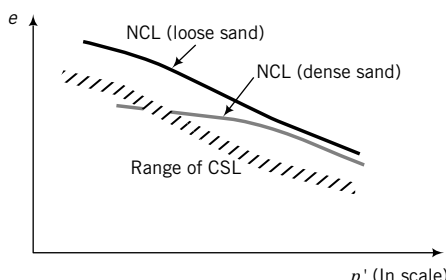


FIGURE 11.10 Illustrative volumetric responses of coarse-grained soils.

Overconsolidation ratio and preconsolidation ratio are useful strictly for fine-grained soils. There is no standard technique to determine the preconsolidation stress for coarse-grained soils. There have been attempts to define a new state parameter for coarse-grained soils within the CSM framework, with some success. These attempts are beyond the scope of this textbook. Despite the nonlinearity of the NCL and the CSL in $(\ln p', e)$ space for coarse-grained soils, and the difficulties in determining R_o or OCR, the framework by which CSM describes and integrates strength and deformation is still outstanding for all soils.

11.3.8 Critical State Boundary

The CSL serves as a boundary separating normally consolidated and lightly overconsolidated soils from heavily overconsolidated soils (Figure 11.11). Stress states that lie to the right of the CSL will result in compression and strain-hardening of the soil; stress states that lie to the left of the CSL will result in expansion and strain-softening of the soil. More detailed analysis of how a soil will likely behave is given in Section 11.7.

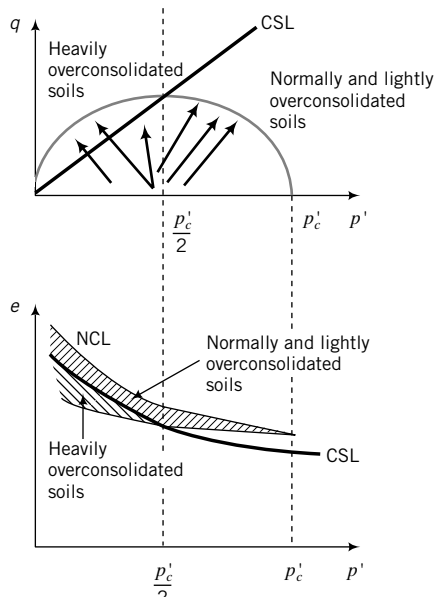


FIGURE 11.11 State boundary for normally and lightly overconsolidated soils and heavily overconsolidated soils.

11.3.9 Volume Changes and Excess Porewater Pressures

If you compare the responses of soils in drained and undrained tests as predicted by the CSM, you will notice that compression in drained tests translates as positive excess porewater pressures in undrained tests, and expansion in drained tests translates as negative excess porewater pressures in undrained tests. The CSM also predicts that normally consolidated and lightly overconsolidated soils strain-harden to failure, while heavily overconsolidated soils strain-soften to failure. The predicted responses from the CSM then qualitatively match observed soil responses (Chapter 10).

11.3.10 Effects of Effective and Total Stress Paths

The response of a soil depends on the ESP. Effective stress paths with slopes less than the slope of the CSL (OA , Figure 11.12) will not produce shear failure in the soil because the ESP will never intersect the critical state line. You can load a normally consolidated or a lightly overconsolidated soil with an ESP that causes it to respond like an overconsolidated soil, as shown by OBF in Figure 11.12. Effective stress paths similar to OBF are possible in soil excavation. Remember that a soil must yield (B) before it fails (F). So the stress path to failure is $O \rightarrow B \rightarrow F$. The TSP has no effect on the soil response under undrained condition.

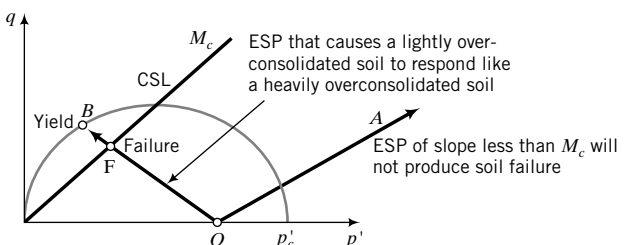


FIGURE 11.12 Effects of effective stress paths on soil response.

THE ESSENTIAL POINTS ARE:

- 1. There is a unique critical state line in (p', q) space and a corresponding critical state line in (p', e) space for a soil.**
- 2. There is an initial yield surface whose size depends on the preconsolidation mean effective stress.**
- 3. The soil will behave elastically for stresses that are within the yield surface and elastoplastically for stresses directed outside the yield surface.**
- 4. The yield surface expands for normally and lightly overconsolidated soils and contracts for heavily overconsolidated soils when the applied effective stresses exceed the initial yield stress.**
- 5. The initial stress state of normally consolidated soils, $R_o = 1$, lies on the initial surface.**
- 6. Every stress state must lie on an expanded or contracted yield surface and on a corresponding URL.**
- 7. Failure occurs when the ESP intersects the CSL and the change in volume is zero.**
- 8. A soil must yield before it fails.**
- 9. The excess porewater pressure is the difference in mean stress between the TSP and the ESP at a desired value of deviatoric stress.**
- 10. The critical state model qualitatively captures the essential features of soil responses under drained and undrained loading.**

What's next . . . You were given an illustration using projection geometry of the essential ingredients of the critical state model. There were many unknowns. For example, you did not know the slope of the critical state line and the equation of the yield surface. In the next section we will develop equations to find these unknowns. Remember that our intention is to build a simple mosaic coupling the essential features of consolidation and shear strength.

11.4 ELEMENTS OF THE CRITICAL STATE MODEL

11.4.1 Yield Surface

The equation for the yield surface is an ellipse given by

$$(p')^2 - p'p'_c + \frac{q^2}{M^2} = 0 \quad (11.4a)$$

We can rewrite Equation (11.4a) as

$$q^2 = M^2 p'(p'_c - p') \quad (11.4b)$$

or

$$q = \pm M \sqrt{p'(p'_c - p')} \quad (11.4c)$$

or

$$q = \pm M p' \sqrt{\left(\frac{p'_c}{p'} - 1 \right)} \quad (11.4d)$$

or

$$p'_c = p' + \frac{q^2}{M^2 p'} \quad (11.4e)$$

The theoretical basis for the yield surface is presented by Schofield and Wroth (1968) and Roscoe and Burland (1968). You can draw the initial yield surface from the initial stresses on the soil if you know the values of M and p'_c .

EXAMPLE 11.2 Plotting the Initial Yield Surface

A clay soil was consolidated to a mean effective stress of 250 kPa. If $M = M_c = 0.94$, plot the yield surface.

Strategy For values of p' from 0 to p'_c , find the corresponding values of q using Equation (11.4d). Then plot the results.

Solution 11.2

Step 1: Solve for q using values of p' from 0 to p'_c .

You can set up a spreadsheet to solve for q using various values of p' from 0 to $p'_c = 250$ kPa, or you can use your calculator. For example, putting $p' = 100$ kPa in Equation (11.4d) gives

$$q = \pm 0.94 \times 100 \left[\frac{250}{100} - 1 \right]^{\frac{1}{2}} = \pm 115.1 \text{ kPa}$$

Step 2: Plot initial yield surface.

See Figure E11.2 (only the top half of the ellipse is shown).

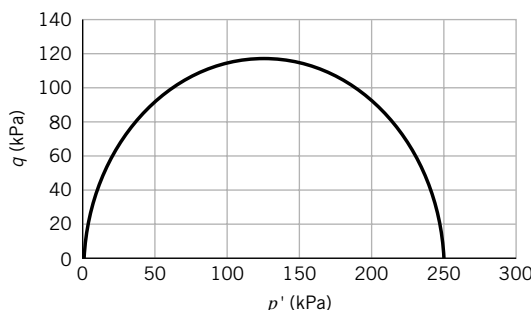


FIGURE E11.2

11.4.2 Critical State Parameters

11.4.2.1 Failure Line in (p', q) Space The failure line in (p', q) space is

$$q_f = Mp'_f \quad (11.5)$$

where q_f is the deviatoric stress at failure, M is a frictional constant, and p'_f is the mean effective stress at failure. By default, the subscript f denotes failure and is synonymous with critical state. For compression, $M = M_c$, and for extension, $M = M_e$. The critical state line intersects the yield surface at $p'_c/2$.

We can build a convenient relationship between M and ϕ'_{cs} for axisymmetric compression and extension and plane strain conditions as follows.

Axisymmetric Compression

$$M_c = \frac{q_f}{p'_f} = \frac{(\sigma'_1 - \sigma'_3)_f}{\left(\frac{\sigma'_1 + 2\sigma'_3}{3}\right)_f} = \frac{3\left(\frac{\sigma'_1}{\sigma'_3} - 1\right)_f}{\left(\frac{\sigma'_1}{\sigma'_3} + 2\right)_f}$$

We know from Chapter 10 that

$$\left(\frac{\sigma'_1}{\sigma'_3}\right)_f = \frac{1 + \sin\phi'_{cs}}{1 - \sin\phi'_{cs}}$$

Therefore,

$$M_c = \frac{6 \sin\phi'_{cs}}{3 - \sin\phi'_{cs}} \quad (11.6)$$

or

$$\sin\phi'_{cs} = \frac{3M_c}{6 + M_c} \quad (11.7)$$

Axisymmetric Extension In an axisymmetric (triaxial) extension, the radial stress is the major principal stress. Since in axial symmetry the radial stress is equal to the circumferential stress, we get

$$p'_f = \left(\frac{2\sigma'_1 + \sigma'_3}{3}\right)_f$$

$$q_f = (\sigma'_1 - \sigma'_3)_f$$

and

$$M_e = \frac{q_f}{p'_f} = \frac{\left(2\frac{\sigma'_1}{\sigma'_3} + 1\right)_f}{\left(\frac{\sigma'_1}{\sigma'_3} - 1\right)_f} = \frac{6 \sin\phi'_{cs}}{3 + \sin\phi'_{cs}} \quad (11.8)$$

or

$$\sin\phi'_{cs} = \frac{3M_e}{6 - M_e} \quad (11.9)$$

An important point to note is that while the friction angle, ϕ'_{cs} , is the same for compression and extension, the slope of the critical state line in (p', q) space is not the same (Figure 11.13). Therefore, the failure deviatoric stresses in compression and extension are different. Since $M_e < M_c$, the failure deviatoric stress of a soil in extension is lower than that for the same soil in compression.

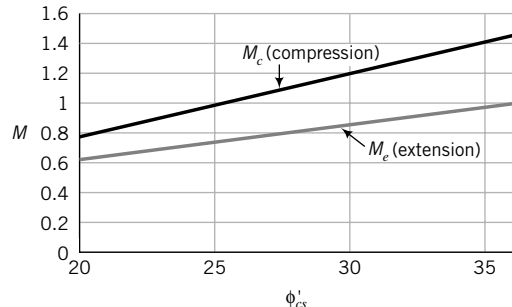


FIGURE 11.13 Variation of the frictional constant M with critical state friction angle.

Plane Strain In plane strain, one of the strains is zero. In Chapter 7, we selected $\varepsilon_2 = 0$; thus, $\sigma'_2 \neq 0$. In general, we do not know the value of σ'_2 unless we have special research equipment to measure it. If $\sigma'_2 = C(\sigma'_1 + \sigma'_3)$, where $C = 0.5$, then

$$M = M_{ps} = \sqrt{3} \sin \phi'_{cs} \quad (11.10)$$

Taking $C = 0.5$ presumes zero elastic compressibility. The subscript ps denotes plane strain. The constant, C , using a specially designed simple shear device (Budhu, 1984) on a sand, was shown to be approximately $\frac{1}{2} \tan \phi'_{cs}$. As an exercise, you can derive Equation (11.10) by following the derivation of M_c , but with p' and q defined, as given by Equations (8.1) and (8.2).

11.4.2.2 Failure Line in (p', e) Space Let us now find the equation for the critical state line in (p', e) space. We will use the $(\ln p', e)$ plot, as shown in Figure 11.14c. The CSL is parallel to the normal consolidation line and is represented by

$$e_f = e_\Gamma - \lambda \ln p'_f \quad (11.11)$$

where e_Γ is the void ratio on the critical state line when $p' = 1$ (Γ is the Greek uppercase letter gamma). This value of void ratio serves as an anchor for the CSL in (p', e) space and $(\ln p', e)$ space. The value of e_Γ depends on the units chosen for the p' scale. In this book, we will use kPa for the units of p' .

We will now determine e_Γ from the initial state of the soil. Let us isotropically consolidate a soil to a mean effective stress p'_c , and then isotropically unload it to a mean effective stress p'_o (Figure 11.14a, b). Let X be the intersection of the unloading/reloading line with the critical state line. The mean effective stress at X is $p'_c/2$, and from the unloading/reloading line,

$$e_X = e_o + \kappa \ln \frac{p'_o}{p'_c/2} \quad (11.12)$$

where e_o is the initial void ratio. From the critical state line,

$$e_X = e_\Gamma - \lambda \ln \frac{p'_c}{2} \quad (11.13)$$

Therefore, combining Equations (11.12) and (11.13), we get

$$e_\Gamma = e_o + (\lambda - \kappa) \ln \frac{p'_c}{2} + \kappa \ln p'_o \quad (11.14)$$

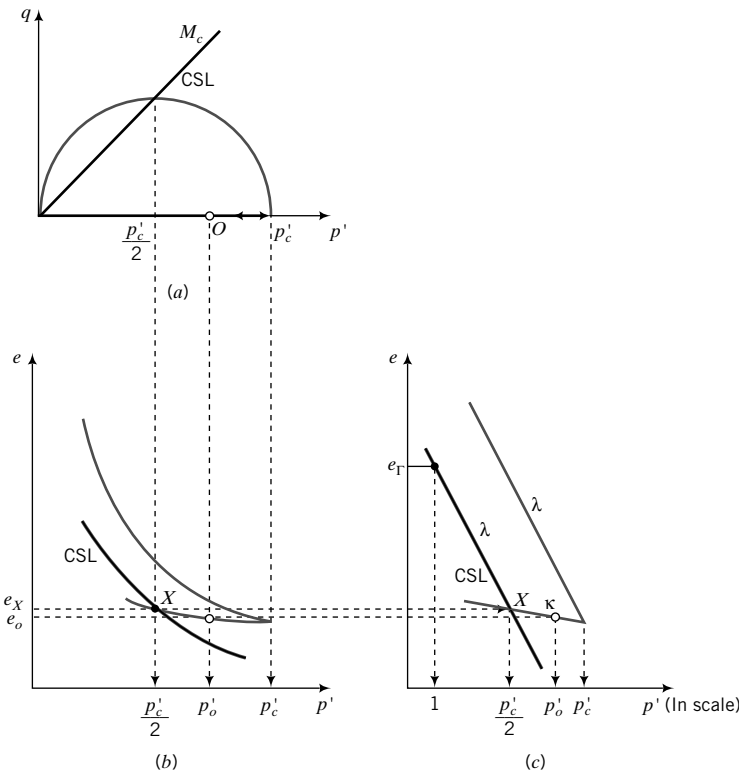


FIGURE 11.14 Void ratio, e_T , to anchor critical state line.

THE ESSENTIAL CRITICAL STATE PARAMETERS ARE:

- λ—Compression index, which is obtained from an isotropic or a one-dimensional consolidation test.
- κ—Unloading/reloading index or recompression index, which is obtained from an isotropic or a one-dimensional consolidation test.
- M—Critical state frictional constant.

To use the critical state model, you must also know the initial stresses, for example, p' , e_o , and p'_c , and the initial void ratio, e_o .

EXAMPLE 11.3 Calculation of M and Failure Stresses in Extension

A standard triaxial CD test at a constant cell pressure, $\sigma_3 = \sigma'_3 = 120$ kPa, was conducted on a sample of normally consolidated clay. At failure, $q = \sigma'_1 - \sigma'_3 = 140$ kPa.

- Calculate M_c .
- Calculate p'_f .
- Determine the deviatoric stresses at failure if an extension test were to be carried out so that failure occurs at the same mean effective stress.

Strategy You are given the final stresses, so you have to use these to compute ϕ'_{cs} and then use Equation (11.6) to calculate M_c and Equation (11.8) to calculate M_e . You can then calculate q_f for the extension test by proportionality.

Solution 11.3

Step 1: Find the major principal stress at failure.

$$(\sigma'_1)_f = (\sigma'_1 - \sigma'_3) + \sigma'_3 = 140 + 120 = 260 \text{ kPa}$$

Step 2: Find p'_f .

$$p'_f = \left(\frac{\sigma'_1 + 2\sigma'_3}{3} \right)_f = \frac{260 + 2 \times 120}{3} = 166.7 \text{ kPa}$$

Step 3: Find ϕ'_{cs} .

$$\begin{aligned} \sin \phi'_{cs} &= \frac{\sigma'_1 - \sigma'_3}{\sigma'_1 + \sigma'_3} = \frac{140}{260 + 120} = 0.37 \\ \phi'_{cs} &= 21.6^\circ \end{aligned}$$

Step 4: Find M_c and M_e .

$$M_c = \frac{6 \sin \phi'_{cs}}{3 - \sin \phi'_{cs}} = \frac{6 \times 0.37}{3 - 0.37} = 0.84$$

$$M_e = \frac{6 \sin \phi'_{cs}}{3 + \sin \phi'_{cs}} = \frac{6 \times 0.37}{3 + 0.37} = 0.66$$

Step 5: Find q_f for extension.

$$q_f = \frac{0.66}{0.84} \times 140 = 110 \text{ kPa}; \quad p'_f = \frac{q_f}{M_e} = \frac{110}{0.66} = 166.7 \text{ kPa}$$

EXAMPLE 11.4 Determination of λ , κ , and e_T

A saturated soil sample is isotropically consolidated in a triaxial apparatus, and a selected set of data is shown in the table. Determine λ , κ , and e_T .

Condition	Cell pressure (kPa)	Final void ratio
Loading	200	1.72
	1000	1.20
Unloading	500	1.25

Strategy Make a sketch of the results in $(\ln p', e)$ space to provide a visual aid for solving this problem.

Solution 11.4

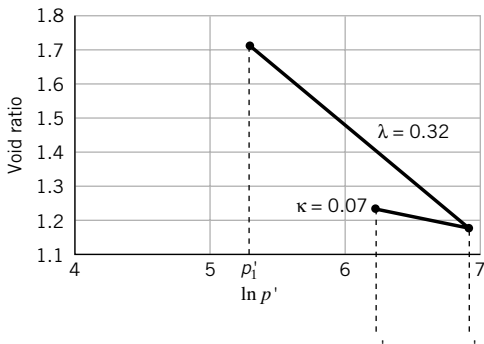
Step 1: Make a plot of $\ln p'$ versus e .

See Figure E11.4.

Step 2: Calculate λ .

From Figure E11.4,

$$\lambda = -\frac{\Delta e}{\ln(p'_e) - \ln(p'_i)} = -\frac{1.20 - 1.72}{6.91 - 5.3} = 0.32$$

**FIGURE E11.4**

Note: Figure E.11.4 is not a semilog (base e) plot. The abscissa is $\ln p'$. If the data were plotted on a semilog (base e) plot, then

$$\lambda = -\frac{\Delta e}{\ln(p'_c/p'_1)} = -\frac{1.20 - 1.72}{\ln\left(\frac{1000}{200}\right)} = 0.32$$

Step 3: Calculate κ .

From Figure E11.4,

$$\kappa = -\frac{\Delta e}{\ln(p'_c) - \ln(p'_o)} = -\frac{1.20 - 1.25}{6.91 - 6.21} = 0.07$$

Step 4: Calculate e_Γ .

$$\begin{aligned} e_\Gamma &= e_o + (\lambda - \kappa) \ln \frac{p'_c}{2} + \kappa \ln p'_o \\ &= 1.25 + (0.32 - 0.07) \ln \frac{1000}{2} + 0.07 \ln 500 = 3.24 \end{aligned}$$

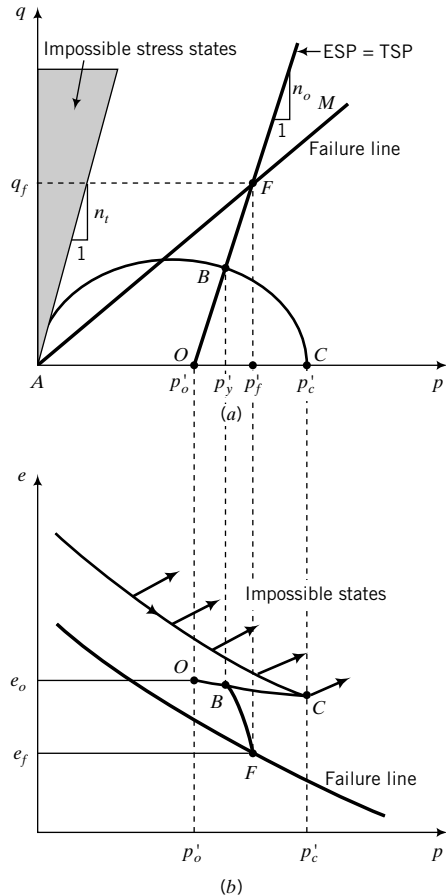
What's next . . . We now know the key parameters to use in the CSM. Next, we will use the CSM to predict the shear strength of soils.

11.5 FAILURE STRESSES FROM THE CRITICAL STATE MODEL

11.5.1 Drained Triaxial Test

Let us consider a standard triaxial CD test in which we isotropically consolidate a soil to a mean effective stress p'_c and unload it isotropically to a mean effective stress of p'_o (Figure 11.15a) such that $R_o \leq 2$. The slope of the ESP = TSP is 3, as shown by OF in Figure 11.15a. The ESP will intersect the critical state line at F . We need to find the stresses at F . The equation for the ESP is

$$q_f = 3(p'_f - p'_o) \quad (11.15)$$

**FIGURE 11.15**

Failure in a drained test on a lightly overconsolidated soil.

The equation for the critical state line, using a generic M , which for compression is M_c and for extension is M_e , is

$$q_f = Mp'_f \quad (11.16)$$

The intersection of these two lines is found by combining Equations (11.15) and (11.16), which gives

$$p'_f = \frac{3p'_o}{3 - M} \quad (11.17)$$

and

$$q_f = Mp'_f = \frac{3Mp'_o}{3 - M} \quad (11.18)$$

In general, if the slope of the ESP = n_o , then Equations (11.17) and (11.18) become

$$p'_f = \frac{n_o p'_o}{n_o - M} \quad (11.19)$$

and

$$q_f = Mp'_f = \frac{n_o Mp'_o}{n_o - M} \quad (11.20)$$

Let us examine Equations (11.19) and (11.20). If $M = M_c = n_o$, then $p'_f \rightarrow \infty$ and $q_f \rightarrow \infty$. Therefore, M_c cannot have a value of n_o because soils cannot have infinite strength. If $M_c > n_o$, then p'_f is negative and q_f is negative. Of course, p'_f cannot be negative because soil cannot sustain tension. Therefore, we cannot have a value of M_c greater than n_o . Therefore, the region bounded by a slope $q/p' = n_o$ originating from the origin and the deviatoric stress axis represents impossible soil states (Figure 11.15a). We will call this line the tension line. For standard triaxial tests, $n_o = n_t = 3$, where n_t is the slope of the tension line. For extension triaxial tests, the slope of the tension line is $n_t = -\frac{3}{2}$. In the case of plane strain tests, if tension is parallel to the minor principal effective stress (σ'_3) and $\sigma'_2 = 0.5(\sigma'_1 + \sigma'_3)$, then the slope of the tension line $n_t = \sqrt{3}$. (You should prove this as an exercise.)

Also, you should recall from Chapter 9 that soil states to the right of the normal consolidation line are impossible (Figure 11.15b). We have now delineated regions in stress space (p', q) and in void ratio versus mean effective stress space—that is, (p', e) space—that are possible for soils. Soil states cannot exist outside these regions.

For overconsolidated soil, the initial yield stress is attained when the ESP intersects the initial yield surface, point B in Figure 11.15a. The coordinate for the yield stresses is found by setting $q = q_y = n_o(p'_y - p'_o)$ and $p' = p'_y$. Thus,

$$n_o(p'_y - p'_o) = \pm M p'_y \sqrt{\left(\frac{p'_c}{p'_y} - 1\right)} \quad (11.21)$$

Solving for p'_y gives

$$p'_y = p'_p = \frac{(M^2 p'_c + 2n_o^2 p'_o) + \sqrt{(M^2 p'_c + 2n_o^2 p'_o)^2 - 4n_o^2(M^2 + n_o^2)(p'_o)^2}}{2(M^2 + n_o^2)} \quad (11.22)$$

Dividing the numerator on the right-hand side of Equation (11.22) by p'_o gives

$$\begin{aligned} p'_y &= \frac{p'_o \left[\left(M^2 \frac{p'_c}{p'_o} + 2n_o^2 \right) + \sqrt{\left(M^2 \frac{p'_c}{p'_o} + 2n_o^2 \right)^2 - 4n_o^2(M^2 + n_o^2)} \right]}{2(M^2 + n_o^2)} \\ &= \frac{p'_o [(M^2 R_o + 2n_o^2) + \sqrt{(M^2 R_o + 2n_o^2)^2 - 4n_o^2(M^2 + n_o^2)}]}{2(M^2 + n_o^2)} \end{aligned} \quad (11.23)$$

The yield shear stress is

$$\tau_y = \frac{q_y}{2} = \frac{n_o(p'_y - p'_o)}{2} \quad (11.24)$$

For the standard triaxial test, $n_o = 3$.

11.5.2 Undrained Triaxial Test

In an undrained test, the total volume change is zero. That is, $\Delta V = 0$ or $\Delta e_p = 0$ or $\Delta e = 0$ (Figure 11.16) and, consequently,

$$e_f = e_o = e_\Gamma - \lambda \ln p'_f \quad (11.25)$$

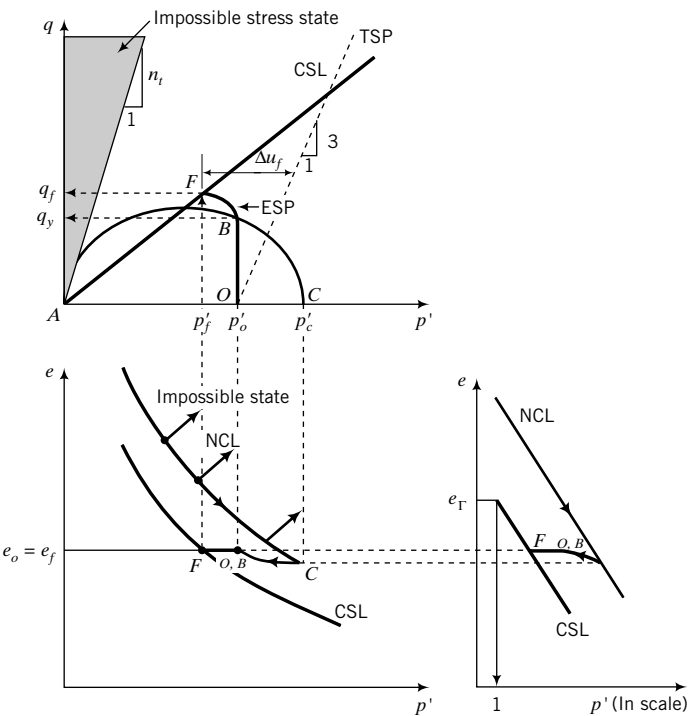


FIGURE 11.16 Failure in an undrained test on a lightly overconsolidated soil.

By rearranging Equation (11.25), we get

$$p'_f = \exp\left(\frac{e_f - e_o}{\lambda}\right) \quad (11.26)$$

Since $q_f = Mp'_f$, then

$$q_f = M \exp\left(\frac{e_f - e_o}{\lambda}\right) \quad (11.27)$$

Recall from Section 11.3.5 that the shear behavior of soils under undrained condition is independent of the total stress path. Equation (11.27) confirms this, as it has no parameter that is related to the total stress path. The undrained shear strength, denoted by s_u , is defined as one-half the deviatoric stress at failure. That is,

$$(s_u)_f = \frac{q_f}{2} = \frac{M}{2} \exp\left(\frac{e_f - e_o}{\lambda}\right) \quad (11.28)$$

It is valid for normally consolidated, lightly overconsolidated, and heavily overconsolidated soils. For a given soil, M , λ , and e_f are constants and the only variable in Equation (11.28) is the initial void ratio. Therefore, the undrained shear strength of a particular saturated fine-grained soil depends only on the initial void ratio or initial water content. You should recall that we discussed this in Chapter 10 but did not show any mathematical proof. Also, s_u is not a fundamental soil property because it depends on the initial state of the soil.

We can use Equation (11.28) to compare the undrained shear strengths of two samples of the same soil tested at different void ratio, or to predict the undrained shear strength of one sample if we know the undrained shear strength of the other. Consider two samples, A and B, of the same soil. The ratio of their undrained shear strength is

$$\frac{(s_u)_A}{(s_u)_B} = \frac{\left[\exp\left(\frac{e_\Gamma - e_o}{\lambda}\right) \right]_A}{\left[\exp\left(\frac{e_\Gamma - e_o}{\lambda}\right) \right]_B} = \exp\left(\frac{(e_o)_B - (e_o)_A}{\lambda}\right)$$

For a saturated soil, $e_o = wG_s$ and we can then rewrite the above equation as

$$\frac{(s_u)_A}{(s_u)_B} = \exp\left[\frac{G_s(w_B - w_A)}{\lambda}\right] \quad (11.29)$$

Let us examine the difference in undrained shear strength for a 1% difference in water content between samples A and B. We will assume that the water content of sample B is greater than that of sample A, that is, $(w_B - w_A)$ is positive, $\lambda = 0.15$ (a typical value for a silty clay), and $G_s = 2.7$. Putting these values into Equation (11.29), we get

$$\frac{(s_u)_A}{(s_u)_B} = 1.20$$

That is, a 1% increase in water content causes a reduction in undrained shear strength of 20% for this soil. The implication for soil testing is that you should preserve the water content of soil samples, especially samples taken from the field, because the undrained shear strength can be significantly altered by even small changes in water content.

The ESP is vertical ($\Delta p' = 0$) within the initial yield surface, and after the soil yields, the ESP bends toward the critical state line, as the excess porewater pressure increases considerably after yield. The excess porewater pressure at failure is found from the difference between the mean total stress and the corresponding mean effective stress at failure. It consists of two components. One component, called the shear component, Δu_f^s (Figure 11.17, FA), is related to the shearing behavior. The other component, called the total stress component, Δu_f^t (Figure 11.17, AB), is connected not to the shearing behavior but to the total stress path. If two samples of the same soil at the same initial stress state are subjected to two different TSP, say, OT and OR in Figure 11.17, the shear component of the excess porewater pressure would be the same, but the total stress path component would be different (compare AB and AD in Figure 11.17). The total excess porewater pressure at failure (critical state) is

$$\Delta u_f = \Delta u_f^s + \Delta u_f^t = (p'_o - p'_f) + \frac{q_f}{n_o} \quad (11.30)$$

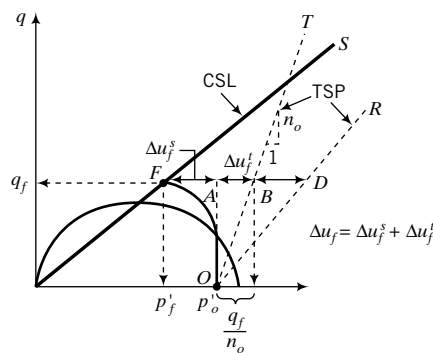


FIGURE 11.17

Excess porewater pressures during undrained loading.

Substituting $q_f = Mp'_f$ in Equation (11.30), we get

$$\Delta u_f = p'_o - p'_f + \frac{Mp'_f}{n_o} = p'_o + p'_f \left(\frac{M}{n_o} - 1 \right) \quad (11.31)$$

By substituting Equation (11.26) into Equation (11.31), we obtain

$$\Delta u_f = p'_o + \left(\frac{M}{n_o} - 1 \right) \exp \left(\frac{e_\Gamma - e_o}{\lambda} \right) \quad (11.32)$$

For a standard triaxial CU test, $n_o = 3$, and

$$\Delta u_f = p'_o + \left(\frac{M}{3} - 1 \right) \exp \left(\frac{e_\Gamma - e_o}{\lambda} \right) \quad (11.33)$$

The right-hand side of Equation (11.28) can be transformed into mean effective stress terms by substituting Equation (11.14) and carrying out algebraic manipulations. However, we will use a more elegant mathematical method (Wroth, 1984). We start by defining an equivalent stress originally proposed by Hvorslev (1937). The equivalent effective stress is the mean effective stress on the NCL that has the same void ratio as the current mean effective stress. With reference to Figure 11.18, the equivalent effective stress for point O on the URL is p'_a .

Let us consider two samples of the same soil. One of them, sample I, is normally consolidated to C in Figure 11.18, i.e., $R_o = 1$. The other, sample II, is normally consolidated to C and then unloaded to O . That is, sample II is heavily overconsolidated, with R_o greater than 2. The intersection of the CSL with the URL is at X and the mean effective stress is $\frac{p'_c}{2}$. Both samples are to be loaded to failure under undrained condition. Sample I will fail at D on the CSL, while sample II will fail at F on the CSL. The equivalent effective stress for sample I is p'_c , while for sample II it is p'_a . Note that sample I is on both the NCL and the URL. The change in void ratio from A to C on the NCL is

$$e_a - e_c = \lambda \ln \frac{p'_c}{p'_a} \quad (11.34)$$

The change in void ratio from O to C on the URL is

$$e_o - e_c = \kappa \ln \frac{p'_c}{p'_o} = \kappa \ln R_o \quad (11.35)$$

Now $e_a = e_o$, and thus

$$\lambda \ln \frac{p'_c}{p'_a} = \kappa \ln R_o \quad (11.36)$$

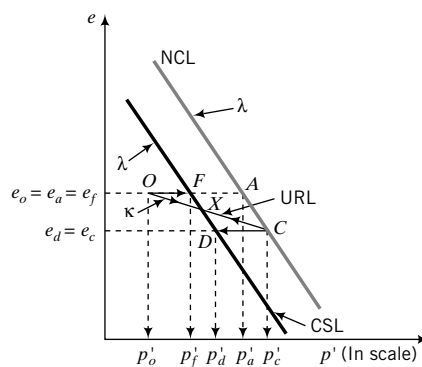


FIGURE 11.18

Normal consolidation, unloading/reloading, and critical state lines in (p', e) space.

Points F and X are on the CSL. By similar triangles (FOX and AOC), we get

$$\lambda \ln \frac{p'_x}{p'_f} = \kappa \ln \frac{p'_x}{p'_o} \quad (11.37)$$

By subtracting both sides of Equation (11.37) from $\lambda \ln \frac{p'_x}{p'_o}$, we get

$$\lambda \ln \frac{p'_x}{p'_o} - \lambda \ln \frac{p'_x}{p'_f} = \lambda \ln \frac{p'_x}{p'_o} - \kappa \ln \frac{p'_x}{p'_o} \quad (11.38)$$

which simplifies to

$$\lambda \ln \frac{p'_f}{p'_o} = (\lambda - \kappa) \ln \frac{p'_x}{p'_o} \quad (11.39)$$

Substituting $p'_x = \frac{p'_c}{2}$ and $R_o = \frac{p'_c}{p'_o}$ into Equation (11.39) gives

$$\lambda \ln \frac{p'_f}{p'_o} = (\lambda - \kappa) \ln \frac{\frac{p'_c}{2}}{p'_o} = (\lambda - \kappa) \ln \left(\frac{R_o}{2} \right) \quad (11.40)$$

Simplifying Equation (11.40) gives

$$\frac{p'_f}{p'_o} = \left(\frac{R_o}{2} \right)^\Lambda \quad (11.41)$$

where $\Lambda = \frac{\lambda - \kappa}{\lambda} = 1 - \frac{\kappa}{\lambda} = \frac{C_c - C_r}{C_c} = 1 - \frac{C_r}{C_c}$ is the plastic volumetric strain ratio (Schofield and Wroth, 1968); Λ is Greek uppercase letter lambda. An approximate value for Λ is 0.8. The undrained shear strength at the critical state is then

$$(s_u)_f = \frac{q_f}{2} = \frac{Mp'_f}{2} = \frac{Mp'_o}{2} \left(\frac{R_o}{2} \right)^\Lambda \quad (11.42)$$

Equation (11.28) and Equation (11.42) will predict the same value of undrained shear strength at the critical state. These equations are just representations of the undrained shear strength with different parameters. Equation (11.28) is advantageous if the water content is known.

Heavily overconsolidated fine-grained or dense-to-medium-dense coarse-grained soils may exhibit a peak shear stress and then strain-soften to the critical state (Figure 11.9). However, the attainment of a peak stress depends on the initial stress state and the ESP. Recall that according to CSM, soils would behave elastically up to the initial yield stress (peak deviatoric stress), q_y . By substituting $p' = p'_o$ and $q = q_y$ in the equation for the yield surface [Equation (11.4d)], we obtain

$$q_y = Mp'_o \sqrt{\frac{p'_c}{p'_o} - 1} = Mp'_o \sqrt{R_o - 1}; \quad R_o > 1 \quad (11.43)$$

The undrained shear strength for fine-grained soils at initial yield is

$$(s_u)_y = \frac{M}{2} p'_o \sqrt{R_o - 1}; \quad R_o > 1 \quad (11.44)$$

We will discuss the implications of Equation (11.44) for the design of geosystems in Section 11.7.

THE ESSENTIAL POINTS ARE:

1. The intersection of the ESP and the critical state line gives the failure stresses.
2. The undrained shear strength depends only on the initial void ratio.
3. Small changes in water content can significantly alter the undrained shear strength.
4. The undrained shear strength is independent of the total stress path.

EXAMPLE 11.5 Predicting Yield Stresses for Drained Condition

A clay sample was isotropically consolidated under a cell pressure of 250 kPa in a triaxial test and then unloaded isotropically to a mean effective stress of 100 kPa. A standard CD test is to be conducted on the clay sample by keeping the cell pressure constant and increasing the axial stress. Predict the yield stresses, p'_y and q_y , if $M = 0.94$.

Strategy This is a standard triaxial CD test. The ESP has a slope $n_o = 3$. The yield stresses can be found from the intersection of the ESP and the initial yield surface. The initial yield surface is known, since $p'_c = 250$ kPa and $M = 0.94$.

Solution 11.5

Step 1: Make a sketch or draw a scaled plot of the initial yield surface.

$$(p')^2 - 250p'_c + \frac{q_y^2}{(0.94)^2} = 0$$

The yield surface is the same as in Example 11.2. See Figure E11.5.

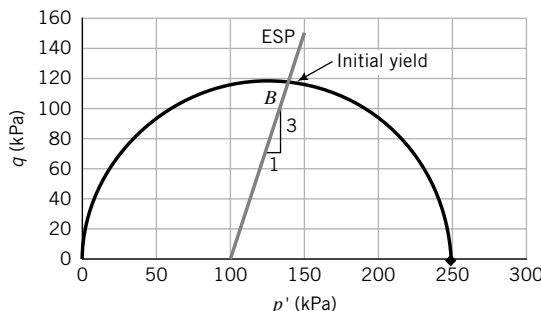


FIGURE E11.5

Step 2: Find the equation for the ESP.

The equation for the ESP is

$$p' = p'_o + \frac{q}{3}$$

See Figure E11.5.

Step 3: Find the intersection of the ESP with the initial yield surface.

Let $B = (p'_y, q_y)$ be the yield stresses at the intersection of the initial yield surface with the ESP (Figure E11.5). At B , the equation for the yield surface is

$$(p')^2 - 250p'_c + \frac{q_y^2}{(0.94)^2} = 0 \quad (1)$$

At B , the equation for the ESP is

$$p'_y = p'_o + \frac{q_y}{3} \quad (2)$$

Inserting Equation (2) into Equation (1), we can solve for q_y as follows:

$$\begin{aligned} \left(p'_o + \frac{q_y}{3} \right)^2 - 250 \left(p'_o + \frac{q_y}{3} \right) + \frac{q_y^2}{(0.94)^2} &= 0 \\ = \left(100 + \frac{q_y}{3} \right)^2 - 250 \left(100 + \frac{q_y}{3} \right) + \frac{q_y^2}{(0.94)^2} &= 0 \end{aligned}$$

The solution gives $q_y = 117$ kPa and -103.5 kPa. Since the test is compression, the correct solution is $q_y = 117$ kPa (see Figure E11.5).

Solving for p'_y from Equation (2) gives

$$p'_y = p'_o + \frac{q_y}{3} = 100 + \frac{117}{3} = 139 \text{ kPa}$$

You can also use Equation (11.23). Try this for yourself.

EXAMPLE 11.6 Predicting Yield Stresses for Undrained Condition

Repeat Example 11.5, except that the clay was sheared under undrained condition. In addition, calculate the excess porewater pressure at initial yield.

Strategy In this case, the TSP has a slope $n_o = 3$. Since the soil will behave elastically within the initial yield surface, the ESP is vertical (see Chapter 8). The yield stresses can be found from the intersection of the ESP and the initial yield surface.

Solution 11.6

Step 1: Identify given parameters.

$$p'_o = 100 \text{ kPa}, \quad p'_c = 250 \text{ kPa}, \quad R_o = \frac{p'_c}{p'_o} = \frac{250}{100} = 2.5$$

$$M = 0.94$$

Step 2: Calculate yield stresses.

$$q_y = Mp'_o\sqrt{R_o - 1} = 0.94 \times 100\sqrt{2.5 - 1} = 115 \text{ kPa}$$

$$p'_y = p'_o = 100 \text{ kPa}$$

See Figure E11.6.

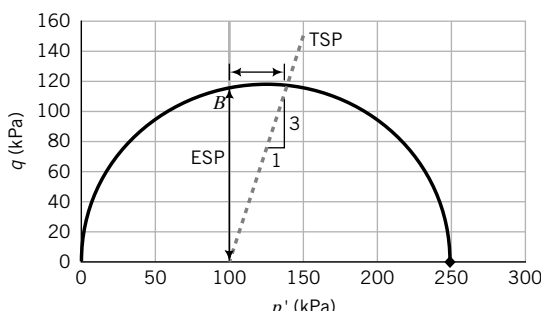


FIGURE E11.6

Step 3: Calculate the total mean stress at yield.

$$p_y = p_o + \frac{q_y}{3} = 100 + \frac{115}{3} = 138.3 \text{ kPa}$$

Step 4: Calculate the excess porewater pressure at yield.

$$\Delta u_y = p_y - p'_o = 138.3 - 100 = 38.3 \text{ kPa}$$

EXAMPLE 11.7 Estimating the Initial Size of the Yield Surface and Initial Yield Stresses for a K_o - (normally) Consolidated Soil in the Field

- (a) Estimate the size of the yield surface for a soil element at a depth of 5 m in a very soft, K_o -consolidated clay, as shown in Figure E11.7a. Groundwater level is at ground surface.
- (b) Estimate the mean and deviatoric stresses at initial yield.

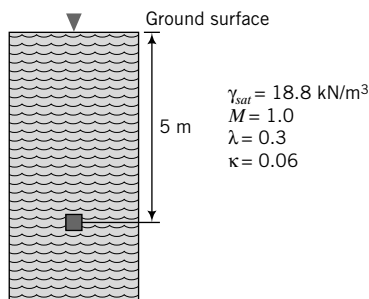


FIGURE E11.7a

Strategy You need to calculate the initial stresses and then use Equation (11.4).

Solution 11.7

Step 1: Calculate the initial stresses.

$$\sigma_{zo} = 5 \times 18.8 = 94 \text{ kPa}; \quad u_o = 5 \times 9.8 = 49 \text{ kPa}; \quad \sigma'_{zo} = 94 - 49 = 45 \text{ kPa}$$

or

$$\begin{aligned} \sigma'_{zo} &= 5 \times (18.8 - 9.8) = 45 \text{ kPa} \\ \sin \phi_{cs} &= \frac{3M_c}{6 + M_c} = \frac{3 \times 1}{6 + 1} = \frac{3}{7} = 0.43 \\ K_o &= 1 - \sin \phi'_{cs} = 1 - 0.43 = 0.57 \\ \sigma'_{xo} &= K_o \times \sigma'_{zo} = 0.57 \times 45 = 25.7 \text{ kPa} \\ p'_o &= \frac{\sigma'_{zo} + 2\sigma'_{xo}}{3} = \frac{45 + 2 \times 25.7}{3} = 32.1 \text{ kPa} \\ q_o &= \sigma'_{zo} - \sigma'_{xo} = 45 - 25.7 = 19.3 \text{ kPa} \end{aligned}$$

Step 2: Solve for p'_c using the yield surface equation.

The equation for the initial yield surface is given by Equation (11.4e) as

$$\begin{aligned} p'_c &= \frac{q_o^2}{M^2 p'_o} + p'_o \\ \therefore p'_c &= \frac{19.3^2}{1^2 \times 32.1} + 32.1 = 43.7 \text{ kPa} \end{aligned}$$

Step 3: Estimate stresses at initial yield.

$$p'_y = p'_o = 32.1 \text{ kPa}; \quad q_y = q_o = 19.3 \text{ kPa}$$

See Figure E11.7b for a plot of the initial yield surface and initial yield point, O .

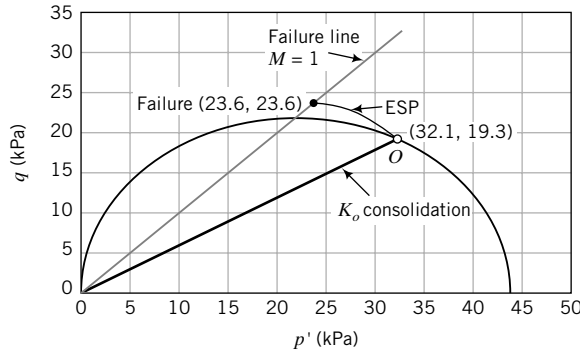


FIGURE E11.7b

EXAMPLE 11.8 Predicting Failure Stresses for a K_o - (normally) Consolidated Soil in the Field

- (a) For the soil element in Example 11.7, what additional stresses, $\Delta p'$ and Δq , will cause it to fail under undrained condition?
- (b) Predict the undrained shear strength.

Strategy You need to calculate the failure stresses for undrained loading. From the given data, calculate e_o and e_Γ , then find the failure stresses. The additional stresses are the differences between the initial and failure stresses.

Solution 11.8

Step 1: Find e_o and e_Γ .

$$\gamma_{sat} = \left(\frac{G_s + e_o}{1 + e_o} \right) \gamma_w$$

$$e_o = \left(\frac{G_s - \frac{\gamma_{sat}}{\gamma_w}}{\frac{\gamma_{sat}}{\gamma_w} - 1} \right) = \left(\frac{2.7 - \frac{18.8}{9.8}}{\frac{18.8}{9.8} - 1} \right) = 0.84$$

$$e_\Gamma = e_o + (\lambda - \kappa) \ln \frac{p'_c}{2} + \kappa \ln p'_o$$

$$= 0.84 + (0.3 - 0.06) \ln \frac{43.7}{2} + 0.06 \ln (32.1) = 1.788$$

Step 2: Find failure stresses.

$$p'_f = \exp \left(\frac{e_\Gamma - e_o}{\lambda} \right) = \exp \left(\frac{1.788 - 0.84}{0.3} \right) = 23.6 \text{ kPa}$$

Since $q_f = Mp'_f$, then $q_f = 1 \times 23.6 = 23.6 \text{ kPa}$.

You will get the same result using Equation (11.41).

Step 3: Find increase in stresses to cause failure.

$$\Delta p'_f = p'_f - p'_o = 23.6 - 32.1 = -8.5 \text{ kPa}$$

$$\Delta q_f = q_f - q_o = 23.6 - 19.3 = 4.3 \text{ kPa}$$

Note that there is no initial elastic state for a normally consolidated soil.

See Figure E11.7b.

Step 4: Calculate the undrained shear strength.

$$(s_u)_f = \frac{q_f}{2} = \frac{23.6}{2} = 11.8 \text{ kPa}$$

EXAMPLE 11.9 Predicting Yield and Failure Stresses and Excess Porewater Pressures

Two specimens, A and B, of a clay were each isotropically consolidated under a cell pressure of 300 kPa and then unloaded isotropically to a mean effective stress of 200 kPa. A CD test is to be conducted on specimen A and a CU test is to be conducted on specimen B.

- (a) Estimate, for each specimen, (a) the yield stresses, p'_y , q_y , $(\sigma'_1)_y$, and $(\sigma'_3)_y$; and (b) the failure stresses p'_f , q_f , $(\sigma'_1)_f$, and $(\sigma'_3)_f$.
- (b) Estimate for sample B the excess porewater pressure at yield and at failure.

The soil parameters are $\lambda = 0.3$, $\kappa = 0.05$, $e_o = 1.10$, and $\phi'_{cs} = 30^\circ$. The cell pressure was kept constant at 200 kPa.

Strategy Both specimens have the same consolidation history but are tested under different drainage conditions. The yield stresses can be found from the intersection of the ESP and the initial yield surface. The initial yield surface is known since $p'_c = 300$ kPa, and M can be found from ϕ'_{cs} . The failure stresses can be obtained from the intersection of the ESP and the critical state line. It is always a good habit to sketch the q versus p' and the e versus p' graphs to help you solve problems using the critical state model. You can also find the yield and failure stresses using graphical methods, as described in the alternative solution.

Solution 11.9

Step 1: Calculate M_c .

$$M_c = \frac{6 \sin 30^\circ}{3 - \sin 30^\circ} = 1.2$$

Step 2: Calculate e_Γ .

With $p'_o = 200$ kPa and $p'_c = 300$ kPa,

$$\begin{aligned} e_\Gamma &= e_o + (\lambda - \kappa) \ln \frac{p'_c}{2} + \kappa \ln p'_o \\ &= 1.10 + (0.3 - 0.05) \ln \frac{300}{2} + 0.05 \ln 200 = 2.62 \end{aligned}$$

Step 3: Make a sketch or draw scaled plots of q versus p' and e versus p' .

See Figure E11.9a, b.

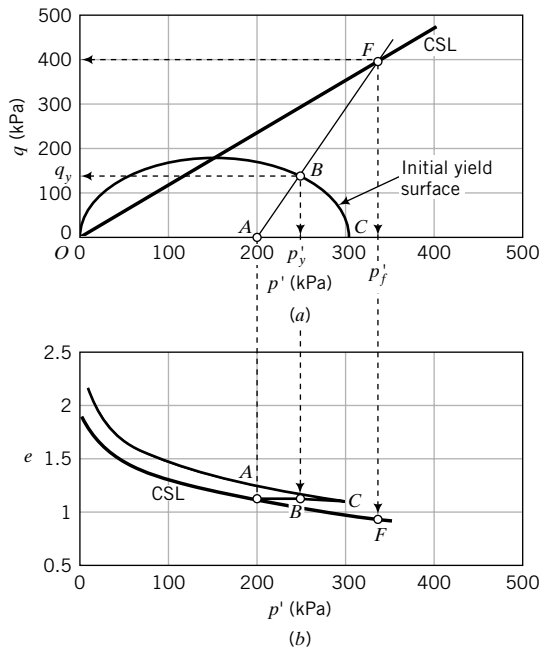
Step 4: Find the yield stresses.

Drained Test Let p'_y and q_y be the yield stress (point B in Figure E11.9a). From the equation for the yield surface [Equation (11.4d)],

$$q_y = \pm M p'_y \sqrt{\left(\frac{p'_c}{p'_y} - 1 \right)} = \pm 1.2 p'_y \sqrt{\left(\frac{300}{p'_y} - 1 \right)} \quad (1)$$

From the ESP,

$$q_y = 3(p'_y - p'_o) = 3p'_y - 600 \quad (2)$$

**FIGURE E11.9a, b**

Solving Equations (1) and (2) for p'_y and q_y gives two solutions: $p'_y = 140.1$ kPa, $q_y = -179.6$ kPa; and $p'_y = 246.1$ kPa, $q_y = 138.2$ kPa. Of course, $q_y = -179.6$ kPa is not possible because we are conducting a compression test. The yield stresses are then $p'_y = 246.1$ kPa, $q_y = 138.2$ kPa.

Now,

$$q_y = (\sigma'_1)_y - (\sigma'_3)_y = 138.2 \text{ kPa}; \quad (\sigma'_3)_f = 200 \text{ kPa}$$

Solving for $(\sigma'_1)_f$ gives

$$(\sigma'_1)_f = 138.2 + 200 = 338.2 \text{ kPa}$$

Undrained Test The ESP for the undrained test is vertical for the region of stress paths below the yield stress, that is, $\Delta p' = 0$. From the yield surface [Equation (11.4d)] for $p' = p'_y = p'_o$, we get

$$q = q_y = \pm M p'_o \sqrt{\left(\frac{p'_c}{p'_o} - 1 \right)} = \pm 1.2 \times 200 \sqrt{\left(\frac{300}{200} - 1 \right)} = 169.7 \text{ kPa}$$

From the TSP, we can find p_y (B' , Figure E11.9c):

$$p_y = p'_o + \frac{q_y}{3} = 200 + \frac{169.7}{3} = 256.6 \text{ kPa}$$

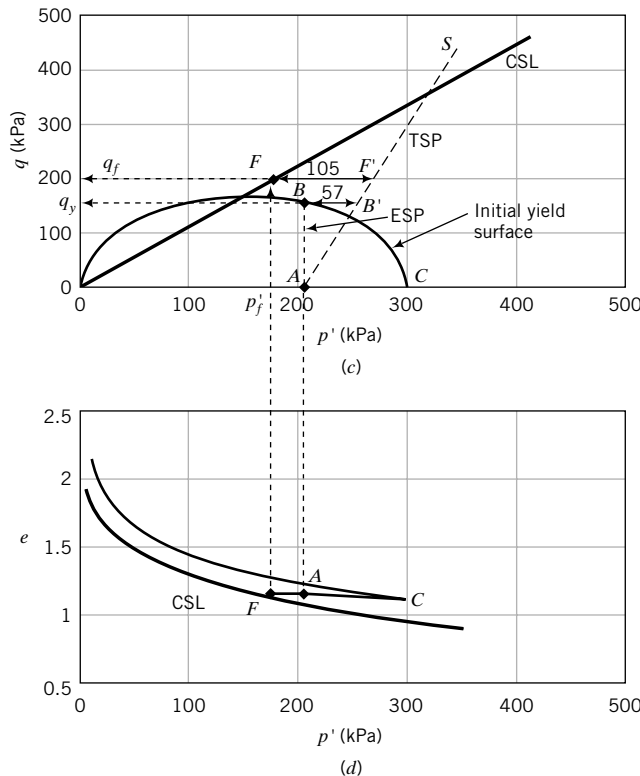
The excess porewater pressure at yield is

$$\Delta u_y = p_y - p'_y = p_y - p'_o = 256.6 - 200 = 56.6 \text{ kPa}$$

Now,

$$p'_y = p'_o = \frac{(\sigma'_1)_y + 2(\sigma'_3)_y}{3} = 200 \text{ kPa}$$

$$q_y = (\sigma'_1)_y - (\sigma'_3)_y = 169.7 \text{ kPa}$$

**FIGURE E11.9c, d**

Solving for $(\sigma'_1)_y$ and $(\sigma'_3)_y$ gives

$$(\sigma'_1)_y = 313.3 \text{ kPa}; \quad (\sigma'_3)_y = 143.4 \text{ kPa}$$

Check

$$(\sigma_3)_y = (\sigma'_3)_y + \Delta u_y = 143.4 + 56.6 = 200 \text{ kPa}$$

Step 5: Find the failure stresses.

Drained Test

$$\text{Equation (11.17): } p'_f = \frac{3 \times 200}{3 - 1.2} = 333.3 \text{ kPa}$$

$$\text{Equation (11.18): } q_f = 1.2 \times 333.3 = 400 \text{ kPa}$$

Now,

$$q_F = (\sigma'_1)_f - (\sigma'_3)_f = 400 \text{ kPa} \quad \text{and} \quad (\sigma'_3)_f = 200 \text{ kPa}$$

Solving for $(\sigma'_1)_f$, we get

$$(\sigma'_1)_f = 400 + 200 = 600 \text{ kPa}$$

Undrained Test

$$\Lambda = \frac{\lambda - \kappa}{\lambda} = \frac{0.3 - 0.05}{0.3} = 0.833; \quad R_o = 300/200 = 1.5$$

$$\text{Equation (11.41): } p'_f = p'_o \left(\frac{R_o}{2} \right)^{\Lambda} = 200 \left(\frac{1.5}{2} \right)^{0.833} = 157 \text{ kPa}$$

$$\text{Equation (11.5): } q_f = 1.2 \times 157 = 188.4 \text{ kPa}$$

Alternatively:

$$\text{Equation (11.26): } p'_f = \exp \left(\frac{2.62 - 1.10}{0.3} \right) = 158.6 \text{ kPa}$$

$$\text{Equation (11.5): } q_f = 1.2 \times 158.6 = 190.3 \text{ kPa}$$

The difference between the results of Equation (11.41) and Eq. (11.26) is due to rounding errors.

Now,

$$p'_f = \frac{(\sigma'_1)_f + 2(\sigma'_3)_f}{3} = 158.6 \text{ kPa}$$

$$q_f = (\sigma'_1)_f - (\sigma'_3)_f = 190.4 \text{ kPa}$$

Solving for $(\sigma'_1)_f$ and $(\sigma'_3)_f$, we find

$$(\sigma'_1)_f = 285.5 \text{ kPa} \quad \text{and} \quad (\sigma'_3)_f = 95.1 \text{ kPa}$$

We can find the excess porewater pressure at failure from either Equation (11.34),

$$\Delta u_f = 200 + \left(\frac{1.2}{3} - 1 \right) \exp \left(\frac{2.62 - 1.10}{0.3} \right) = 104.9 \text{ kPa}$$

or

$$\Delta u_f = \sigma_3 - (\sigma'_3)_f = 200 - 95.1 = 104.9 \text{ kPa}$$

Graphical Method We need to find the equations for the normal consolidation line and the critical state lines.

Normal Consolidation Line Void ratio at preconsolidation stress:

$$e_c = e_o - \kappa \ln \frac{p'_c}{p'_o} = 1.10 - 0.05 \ln \frac{300}{200} = 1.08$$

Void ratio at $p' = 1 \text{ kPa}$ on NCL:

$$e_n = e_c + \lambda \ln p'_c = 1.08 + 0.3 \ln 300 = 2.79$$

The equation for the normal consolidation line is then

$$e = 2.79 - 0.3 \ln p'$$

The equation for the unloading/reloading line is

$$e = 1.08 + 0.05 \ln \frac{p'_c}{p'}$$

The equation for the critical state line in $(\ln p', e)$ space is

$$e = 2.62 - 0.3 \ln p'$$

Now you can plot the normal consolidation line, the unloading/reloading line, and the critical state line, as shown in Figure E11.9b.

Plot Initial Yield Surface The yield surface [Equation (11.4d)] is

$$q = \pm 1.2p' \sqrt{\frac{300}{p'} - 1}$$

For $p' = 0$ to 300, plot the initial yield surface, as shown in Figure E11.9a.

Plot Critical State Line The critical state line is

$$q = 1.2p'$$

and is plotted as OF in Figure E11.9a.

Drained Test The ESP for the drained test is

$$p' = 200 + \frac{q}{3}$$

and is plotted as AF in Figure E11.9a. The ESP intersects the initial yield surface at B and the yield stresses are $p'_y = 240$ kPa and $q_y = 138$ kPa. The ESP intersects the critical state line at F , and the failure stresses are $p'_f = 333$ kPa and $q_f = 400$ kPa.

Undrained Test For the undrained test, the initial void ratio and the final void ratio are equal. Draw a horizontal line from A to intersect the critical state line in (p', e) space at F (Figure E11.9d). Project a vertical line from F to intersect the critical state line in (p', q) space at F (Figure E11.9c). The failure stresses are $p'_f = 159$ kPa and $q_f = 190$ kPa. Draw the TSP, as shown by AS in Figure E11.16c. The ESP within the elastic region is vertical, as shown by AB . The yield stresses are $p'_y = 200$ kPa and $q_y = 170$ kPa. The excess porewater pressures are:

At yield—horizontal line BB' : $\Delta u_y = 57$ kPa

At failure—horizontal line FF' : $\Delta u_f = 105$ kPa

EXAMPLE 11.10 Predicting s_u in Compression and Extension Tests on a Heavily Overconsolidated Clay

Determine the undrained shear strength at initial yield in (a) a CU compression test and (b) a CU extension test for a clay soil with $R_o = 5$, $p'_o = 70$ kPa, and $\phi'_{cs} = 25^\circ$.

Strategy Since you are given ϕ'_{cs} , you should use Equations 11.6 and 11.8 to find M_c and M_e . Use Equation (11.44) to solve the problem.

Solution 11.10

Step 1: Calculate M_c and M_e .

$$M_c = \frac{6 \sin \phi'_{cs}}{3 - \sin \phi'_{cs}} = \frac{6 \sin 25^\circ}{3 - \sin 25^\circ} = 0.98$$

$$M_e = \frac{6 \sin \phi'_{cs}}{3 + \sin \phi'_{cs}} = 0.74$$

Step 2: Calculate s_u .

Use Equation (11.44).

$$\text{Compression: } (s_u)_y = \frac{0.98}{2} \times 70\sqrt{5 - 1} = 68.6 \text{ kPa}$$

$$\text{Extension: } (s_u)_y = \frac{0.74}{2} \times 70\sqrt{5 - 1} = 51.8 \text{ kPa}$$

Or, by proportion,

$$\text{Extension: } (s_u)_y = \frac{0.74}{0.98} \times 68.6 = 51.8 \text{ kPa}$$

EXAMPLE 11.11 Effects of Change of Water Content on s_u

The in situ water content of a soil sample is 48%. The water content decreases to 44% due to transportation of the sample to the laboratory and during sample preparation. What difference in undrained shear strength could be expected if $\lambda = 0.13$ and $G_s = 2.7$?

Strategy The solution to this problem is a straightforward application of Equation (11.29).

Solution 11.11

Step 1: Determine the difference in s_u values.

Use Equation (11.29).

$$\frac{(s_u)_{lab}}{(s_u)_{field}} = \exp \frac{[G_s(w_{field} - w_{lab})]}{\lambda} = \exp \left[\frac{2.7(0.48 - 0.44)}{0.13} \right] = 2.3$$

The laboratory undrained shear strength would probably show an increase over the in situ undrained shear strength by a factor greater than 2.

What's next . . . In the next section, we consider some practical implications of the CSM.

11.6 MODIFICATIONS OF CSM AND THEIR PRACTICAL IMPLICATIONS

The CSM is the foundation of many popular soil models used in numerical analyses. CSM have been shown to be particularly good in simulations of normally and lightly overconsolidated fine-grained soils, but not as good for heavily overconsolidated clays and coarse-grained soils. Various modifications in the literature have been made to CSM so as to model more complex loading conditions than those described so far in this chapter and to better describe heavily overconsolidated clays and coarse-grained soils. We are going to make some simple modifications to CSM to improve its versatility in modeling a wide range of soil types and to establish some additional conceptual understanding of soil behavior.

We considered a particular shape of the yield surface in developing the concept of critical state model. Other shapes of yield surfaces have been developed and used in predicting soil responses. For example, Schofield and Wroth (1968) developed a bullet-shaped yield surface using energy methods. For heavily overconsolidated soils, the peak (initial yield) shear strength occurs on the initial yield surface, which in our case is an ellipse. Experimental data from shear box tests on heavily overconsolidated clays presented by Hvorslev (1937) reveal that the locus of peak shear strength is approximately a straight line. In considering heavily overconsolidated fine-grained soils, we will replace that portion of the initial elliptical yield surface on the left side of the critical state line by the straight line found by Hvorslev. This line defines limiting stress states and is not a yield surface.

In Figure 11.19a, b, AT , At , and ac are lines that separate possible from impossible states; ac is the normal consolidation line; AT and At delineate limiting tensile stress states labeled TL; AF and gf are the critical state or failure lines; TF is Hvorslev's surface, labeled HV surface. Line ct is an unloading/reloading line.

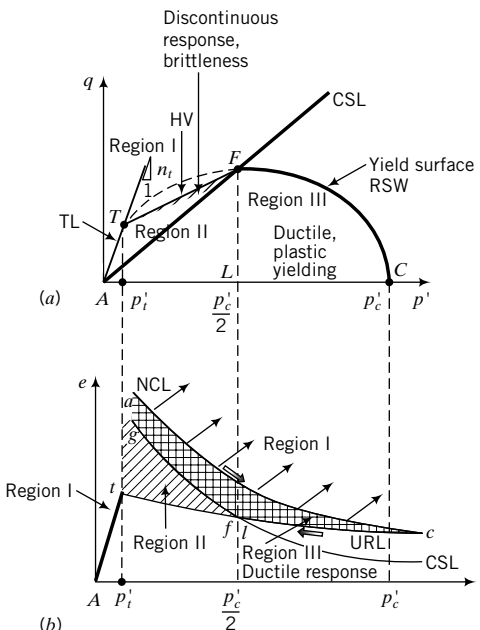


FIGURE 11.19
Regional description and expected responses of soil.

The HV surface defines stress states at incipient instability and is fixed in stress space. It lies between $p' = \frac{p'_c}{2}$ and p'_t , where p'_t is mean effective stress at the intersection of the TL and the HV surfaces. The surface FC is a yield surface and not a limiting stress surface. It is labeled RSW (after Roscoe, Schofield, and Wroth, 1958). Unlike the HV surface, the RSW surface is not fixed in stress space. It can expand or contract. It is bounded by the critical state line and the mean effective stress axis [isotropic stress path in (p', q) space]. Soil stress states on AT will cause the soil to fail in tension. Recall that uncemented soils cannot sustain tension.

We are going to describe three regions of soil behavior, as in Section 10.7.

Region I. Soil stress states within Region I are impossible. During unloading the soil cannot follow paths right of the normal consolidation line, ac (Figure 11.19b). Also, uncemented soils cannot have stress states left of the tension line, AT or At .

Region II. Soil stress states within Region II, area $ATFA$ (Figure 11.19a), would cause the soil to behave elastically, but on approaching the HV surface it may exhibit discontinuous response and fail with one or more bifurcations. In laboratory shear tests, it has been observed that just prior to achieving the peak shear strength and during strain softening, preferential zones of dilation (shear bands, Figure 10.4) develop. Due to progressive softening, the size of these preferential zones of dilation increases during postpeak shear deformation.

The permeability or hydraulic conductivity of the soil (especially within the shear bands or preferential zones of dilation) increases and, if water is present, this increased permeability can lead to sudden failure due to seepage (for example, flow slides on a slope). The presence of preferential zones of dilation as the soil mass strain-softens renders CSM inadmissible because CSM treats soils as continua. Calculations using CSM in the strain-softening regime of soil behavior cannot be expected to be accurate.

Loads that bring the soil to stress states near or on the HV surface present a high safety risk.

Region III. Soil stress states within Region III ($AFCA$, Figure 11.19a) will cause the soil to behave in a ductile manner. It is desirable to design geotechnical systems such that the soil will behave in

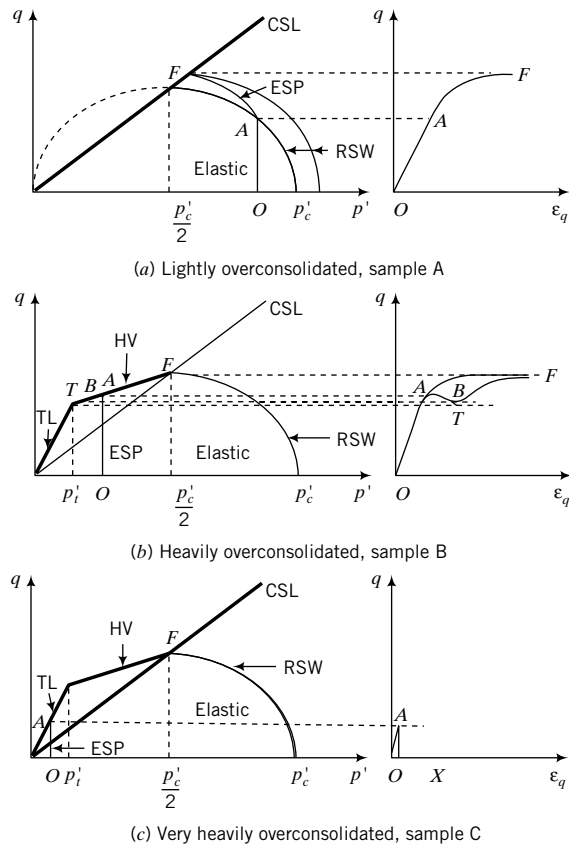


FIGURE 11.20 Theoretical responses of lightly overconsolidated, heavily overconsolidated, and very heavily overconsolidated soils from modifications of CSM.

a ductile manner under anticipated loadings. Soil states on the CSL are failure states. Your design loads should not bring the soil state to failure under any anticipated loading condition.

Let us examine the behavior of three samples of the same soil in undrained triaxial tests. The first, sample A, is lightly overconsolidated, $2 > R_o > 1$. The second, sample B, is heavily overconsolidated, $R_t > R_o > 2$, where $R_t = \frac{p'_c}{p'_t}$. The third, sample C, is very heavily overconsolidated, $R_o > R_t$. The theoretical response of the lightly overconsolidated soil is shown in Figure 11.20a. From O to A the soil behaves elastically [recall that the ESP for an elastic soil under undrained condition is vertical in (p', q) space]. At A , the soil yields, and as further loading is applied the initial yield surface (RSW) expands, excess porewater pressures increase, and the soil fails at F . The deviatoric stress-deviatoric strain relationship is shown as OAF in the right-hand side plot of Figure 11.20a. The soil stress-strain response is that of a ductile material. The tension line and the HV surface are deliberately not shown in Figure 11.20a for clarity. They play no role in the stress-strain response of soils as ductile materials.

The theoretical response of the heavily overconsolidated soil is shown in Figure 11.20b. From O to A the soil behaves elastically. At A , the soil reaches the HV surface, and CSM no longer applies. Since the HV surface is a limiting stress surface, the stress state of any soil element must be either on this surface or below it. In reality, as A is approached the soil may start to develop discontinuities. When the HV is reached, significant redistribution of stresses within the soil occurs in ways that are difficult to predict.

Failure (or failure mode) on the HV surface is generally driven by one or more narrow shear bands. When this happens, the lateral strains are approximately zero. Deformation of the soil is then essentially one-dimensional (vertical). The soil mass within the shear bands are at critical state. This type

of failure mode is called localization. In fact, as stated before, the shear bands may initiate just before the HV surface is reached and can cause a fluttering type of response. We will disregard this fluttering effect and regard the onset of instability as when the effective stress path reaches the HV surface. Recall that the soil is no longer a continuum when the HV surface is reached.

Various responses of the soil can occur after the HV surface is reached, depending on how the stresses are redistributed (sometimes called load shedding). We can consider three stress redistribution cases (Figure 11.20b). For case 1, the stresses may be redistributed to induce the stress state to move up the HV surface toward the critical state line, path *A* to *F*. The stress-strain response would be similar to a strain-hardening type of response, as illustrated by *OAF* in the right-hand side plot of Figure 11.20b. From *A* to *F*, the soil is a discontinuous material, with more of the soil mass approaching critical state. At *F*, a sufficient amount of soil mass, but not necessarily the whole soil mass, has attained critical state. The soil may continue to show a strain-hardening type of response beyond *F* as load shedding continues. Eventually, the soil mass as a whole would reach critical state at very large strains.

For case 2, the applied stresses may cause the stress state to move down toward the tension line, path *AB*, and then move upward toward the critical state line. The deviatoric stress-deviatoric strain relationship for this case is shown by *OABF*. The soil would exhibit a strain-softening type of response, *AB*, and then a strain-hardening type of response, *BF*. For case 3, the stress state may move down the HV surface toward the tension line and fail by tension at *T*. The deviatoric stress-deviatoric strain relationship for this case is shown by *OAT*. The deviatoric strain is indeterminate after *T* is reached using classical continuum mechanics. Another possible case is that the soil stress state can initially move toward *F* and then later move toward *T*. This case is not shown in Figure 11.20b for clarity. Sketch the response for this case as an exercise.

The theoretical response of the very heavily overconsolidated soil is shown in Figure 11.20c. From *O* to *A* the soil behaves elastically. At *A*, the soil reaches the tension line and fails in tension. The soil mass becomes discontinuous and the post-tension behavior is difficult to predict. One possible post-tension case is that the deviatoric stress becomes zero after the effective stress path reaches the tension line. The deviatoric stress-deviatoric strain relationship for this case is shown by *OAX*. The deviatoric strain is indeterminate after *A* is reached.

THE ESSENTIAL POINTS ARE:

- 1. Soil stress states for normally and lightly overconsolidated soils between the CSL and the p' axis are expected to induce an initial elastic response followed by a strain-hardening response by the expansion of the RSW surface until failure occurs on the CSL. These soils exhibit ductile response.**
- 2. Soil stress states for heavily overconsolidated soils are expected to induce an initial elastic response up to the HV surface.**
- 3. The response of the soil after the HV surface is reached depends on how the stresses are redistributed with the soil mass. Four possible responses are (1) a strain-hardening type of response and then failure on the CSL, (2) a strain-softening type of response followed by a strain-hardening type of response and then failure on the CSL, (3) a strain-softening response and failure by tension, and (4) a strain-hardening response followed by a strain-softening type of response and failure by tension.**
- 4. It is desirable to design geotechnical systems such that the soil will behave in a ductile manner under anticipated loadings.**

What's next . . . We have discussed the basis for CSM; derived equations to calculate the failure and yield stresses, failure and yield void ratio, and failure and yield excess porewater pressures; and made some modifications. CSM allows us to build a number of relationships, for example, relationships between drained and undrained conditions, yielding and critical state, and peak and critical state stresses. In the next section, we build some key relationships using CSM to further our understanding of soil behavior and to relate these to practice.

11.7 RELATIONSHIPS FROM CSM THAT ARE OF PRACTICAL SIGNIFICANCE

In this section, we will explore some relationships of practical interest by manipulating the various equations we have derived using CSM. One way of building relationships is to use dimensionless quantities. We learned from CSM that the initial state of the soil strongly influences its behavior. So, we will normalize (make dimensionless) stress parameters such as p'_y , q_p ($= q_y$), and τ_f by dividing them by the initial mean effective stress, p'_o . We will also use ϕ'_{cs} , wherever possible, as the base for relationships because it is a fundamental soil property. Only compression will be considered, but the relationships will be cast in terms of a generic M value. You can replace M by M_e in the derived relationships for soil extension consideration. CSM parameters will be used to build the relationships and then be converted to soil parameters familiar to practicing engineers where necessary. Some of the benefits of these relationships are:

1. They impart further insights into the mechanical behavior of soils.
2. They allow us to use a few well-established soil parameters obtained from simple soil tests such as one-dimensional consolidation and triaxial tests to predict soil strength for various field conditions.
3. They provide us with guidance as to what condition (drained or undrained) would likely be critical in analyzing the safety of geosystems.
4. They allow us to convert the shear strength from axisymmetric tests (triaxial) to plane strain tests (direct simple shear).
5. They guide us to the kind of analysis (elastic or elastoplastic) that may be appropriate for geosystems design.
6. They help us to estimate under what conditions a soil would likely exhibit a peak shear stress.
7. They define limits to provide guidance on when a soil will behave in a ductile manner or show discontinuous response.

11.7.1 Relationship Between Normalized Yield (peak) Shear Stress and Critical State Shear Stress Under Triaxial Drained Condition

Normalizing (making dimensionless) Equation (11.23) by dividing both sides of it by p'_o , we get

$$\frac{p'_y}{p'_o} = \frac{(M^2 R_o + 2n_o^2) + \sqrt{(M^2 R_o + 2n_o^2)^2 - 4n_o^2(M^2 + n_o^2)}}{2(M^2 + n_o^2)} \quad (11.45)$$

Similarly, Equation (11.24) becomes

$$\frac{\tau_y}{p'_o} = \frac{n_o \left(\frac{p'_y}{p'_o} - 1 \right)}{2} \quad (11.46)$$

For the standard triaxial CD test, $n_o = 3$ and Equation (11.45) can be written as

$$\frac{p'_y}{p'_o} = \frac{(M^2 R_o + 18) + \sqrt{(M^2 R_o + 18)^2 - 36(M^2 + 9)}}{2(M^2 + 9)} \quad (11.47)$$

Similarly, Equation (11.46) and Equation (11.20) become

$$\frac{\tau_y}{p'_o} = \frac{3\left(\frac{p'_y}{p'_o} - 1\right)}{2} \quad (11.48)$$

and

$$\frac{\tau_f}{p'_o} = \frac{3M}{2(3 - M)} \quad (11.49)$$

We define a ratio, α_{pcs} , to relate the normalized initial yield shear stress to the normalized shear stress at the critical state for triaxial drained test. Thus,

$$\alpha_{pcs} = \frac{\frac{\tau_y}{p'_o}}{\frac{\tau_f}{p'_o}} = \frac{\frac{3\left(\frac{p'_y}{p'_o} - 1\right)}{2}}{\frac{3M}{2(3 - M)}} = \frac{\left(\frac{p'_y}{p'_o} - 1\right)(3 - M)}{M} \quad (11.50)$$

For triaxial compression, M is given by Equation (11.6), and by substitution in Equation (11.50) we get

$$\alpha_{pcs} = \frac{\frac{\tau_y}{p'_o}}{\frac{\tau_f}{p'_o}} = \frac{1.5\left(\frac{p'_y}{p'_o} - 1\right)(1 - \sin \phi'_{cs})}{\sin \phi'_{cs}} \quad (11.51)$$

A plot of Equation (11.51) showing the relationship among α_{pcs} , R_o , and ϕ'_{cs} is shown in Figure 11.21.

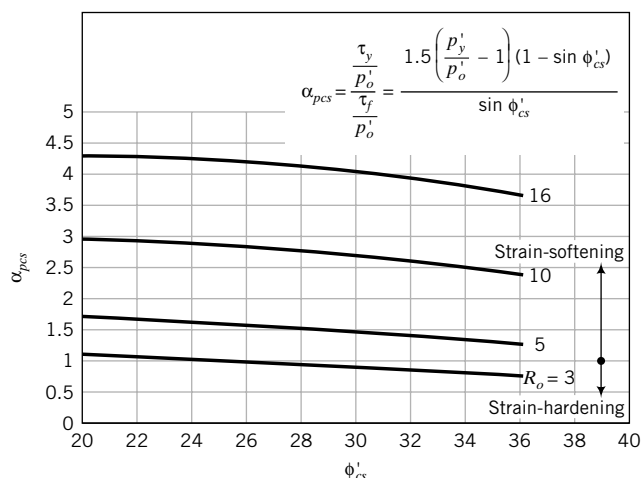


FIGURE 11.21 Variation of initial yield (peak) shear stress to critical state shear strength with critical state friction angle for different values of R_o under drained triaxial compression.

Soils that have $\alpha_{pcs} < 1$ would not show a peak shear strength and would behave in a ductile manner. They would strain-harden to failure (critical state). For example, if a soil has an $R_o = 3$ and $\phi'_{cs} = 30^\circ$, then $\alpha_{pcs} = 0.9$ (Figure 11.21). Therefore, the initial yield shear stress is 0.9 times the critical state shear stress. Such a soil would not show a peak shear stress. Recall that according to CSM the soil will behave elastically for shear stresses below the initial shear stress. Therefore, if your geosystem is located on a soil with $R_o = 3$ and $\phi'_{cs} = 30^\circ$, and is loaded axisymmetrically as in a standard triaxial test, the soil will behave elastically for imposed shear stresses less than 0.9 times the critical state shear stress. An elastic analysis would then be valid according to CSM. Otherwise, an elastoplastic analysis would have to be carried out.

Soils with $\alpha_{pcs} > 1$ would show a peak shear strength and then strain-soften to the critical state. If the HV surface is employed, these soils will show localization. Soils with $R_o > 4.4$ show peak shear stress for all values of critical state friction angles (Figure 11.21). If a soil has an $R_o = 10$ and $\phi'_{cs} = 30^\circ$, then $\alpha_{pcs} = 2.7$. The normalized peak (initial yield) shear stress is 2.7 times the normalized critical state shear strength. An elastic analysis would then be valid for imposed shear stresses less than the peak shear stress.

The value of α_{pcs} tends to decrease with increasing critical friction angle (Figure 11.21). R_o does not cover the full range because of the tension limit (see Section 11.7.2).

Normally consolidated soils are not shown in Figure 11.21 because they do not show an initial elastic response. They yield as soon as the load is applied. Therefore, an elastoplastic analysis has to be carried out for the analysis of geosystems founded on normally consolidated soils.

We have only considered an effective stress path similar to the standard triaxial drained test. For other effective stress paths, we can use the general expressions, Equations (11.45) and (11.46).

11.7.2 Relationships Among the Tension Cutoff, Mean Effective Stress, and Preconsolidation Stress

Certain effective stress paths can cause uncemented soils, essentially fine-grained uncemented soils, to fail on the tension line (Figure 11.19), i.e., the soil ruptures and tension cracks develop. The mean effective stress at the intersection of the initial yield surface and the tension line is found from Equation (11.4e) by substituting $p' = p'_t$ and $q = q_t = n_t p'_t$, where the subscript t denotes tension and n_t is the slope of the tension line. Thus,

$$p'_c = p'_t + \frac{q_t^2}{M^2 p'_t} = p'_t + \frac{(n_t p'_t)^2}{M^2 p'_t} = p'_t \left(1 + \frac{n_t^2}{M^2} \right) \quad (11.52)$$

Solving for p'_t , we get

$$p'_t = \frac{p'_c}{\left(1 + \frac{n_t^2}{M^2} \right)} \quad (11.53)$$

For triaxial compression, $n_t = 3$,

$$\frac{p'_c}{p'_t} = t_c = \frac{1}{\left(1 + \frac{3^2}{M^2} \right)} = \frac{1}{1 + \frac{9}{\left(\frac{6 \sin \phi'_{cs}}{3 - \sin \phi'_{cs}} \right)^2}} \quad (11.54)$$

The inverse of Equation (11.54) gives the preconsolidation ratio for tension cutoff. Thus,

$$\frac{p'_c}{p'_t} = R_t = \left(1 + \frac{n_t^2}{M^2} \right) \quad (11.55)$$

That is, for triaxial compression,

$$R_t = 1 + \frac{9}{\left(\frac{6 \sin \phi'_{cs}}{3 - \sin \phi'_{cs}}\right)^2} = 1 + \frac{1}{\left(\frac{2 \sin \phi'_{cs}}{3 - \sin \phi'_{cs}}\right)^2} \quad (11.56)$$

For plane strain, $n_t = \sqrt{3}$ and $M = \sqrt{3} \sin \phi'_{cs}$. Therefore,

$$t_c = \frac{1}{1 + \frac{(\sqrt{3})^2}{(\sqrt{3} \sin \phi'_{cs})^2}} = \frac{\sin^2 \phi'_{cs}}{1 + \sin^2 \phi'_{cs}} \quad (11.57)$$

and

$$R_t = \frac{1 + \sin^2 \phi'_{cs}}{\sin^2 \phi'_{cs}} \quad (11.58)$$

A plot of Equation (11.58) for different values of critical state friction angle is shown in Figure 11.22. The practical implication of Equation (11.58) is that fine-grained soils under undrained loading would rupture on the tension line at certain limiting values of R_t . For example, if $\phi'_{cs} = 20^\circ$, then for $R_o = R_t > 16$ ($OCR \approx 57$; see Section 11.7.5 or Figure 11.29) the soil would fail in tension, while if $\phi'_{cs} = 36^\circ$, the limiting $R_o = R_t$ is 5 ($OCR \approx 5.5$; see Section 11.7.5 or Figure 11.29). You need then to be extra-careful as a geotechnical engineer when dealing with heavily overconsolidated fine-grained soils.

When the soil ruptures, it is no longer a continuum. The rupture normalized undrained shear strength is

$$\left(\frac{s_u}{p'_o}\right)_t = \frac{n_t}{2} \quad (11.59)$$

For triaxial compression,

$$\left(\frac{s_u}{p'_o}\right)_t = 1.5 \quad (11.60)$$

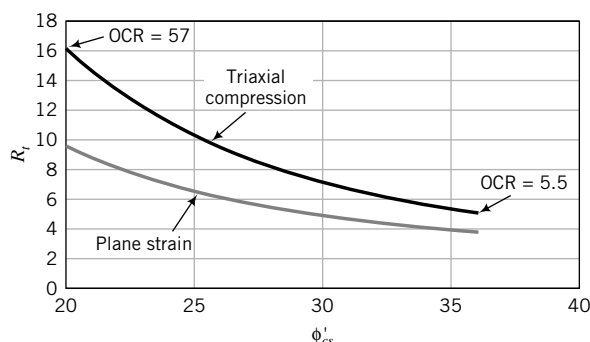


FIGURE 11.22 Tension cutoff preconsolidation ratio.

For plane strain,

$$\left(\frac{s_u}{p'_o} \right)_t = \frac{\sqrt{3}}{2} = 0.866 \quad (11.61)$$

11.7.3 Relationships Among Undrained Shear Strength, Critical State Friction Angle, and Preconsolidation Ratio

Dividing both sides of Equation (11.42) by p'_o , we get

$$\frac{(s_u)_f}{p'_o} = \frac{M}{2} \left(\frac{R_o}{2} \right)^\Lambda \quad (11.62)$$

The ratio at the left-hand side of Equation (11.62) is called the normalized undrained shear strength at critical state. It is dimensionless. For triaxial compression on an isotropically consolidated soil, $p'_o = \sigma'_{zo}$, and Equation (11.62) becomes

$$\left[\frac{(s_u)_f}{\sigma'_{zo}} \right]_{ic} = \frac{3 \sin \phi'_{cs}}{3 - \sin \phi'_{cs}} \left(\frac{R_o}{2} \right)^\Lambda \quad (11.63)$$

The subscript ic denotes isotropic consolidation. The practical implication of Equation (11.63) is that it provides a relationship among the undrained shear strength, the critical state friction angle, and the preconsolidation ratio. The critical state friction is a fundamental soil property; the undrained shear strength is not. A plot of Equation (11.63) is shown in Figure 11.23 for $\Lambda = 0.8$. This plot shows that the undrained shear strength increases with R_o for a given fine-grained soil. For example, if the normalized undrained shear strength for an isotropically consolidated fine-grained soil is 1 and $R_o = 5$, then the corresponding critical state friction angle is 24° .

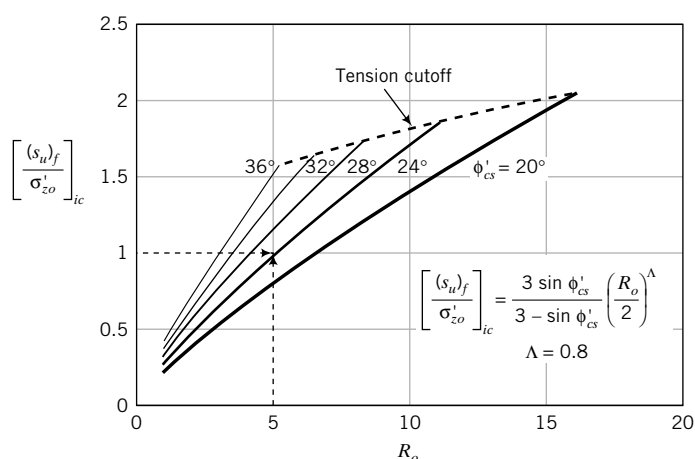


FIGURE 11.23 Variation of theoretical normalized undrained shear strength at critical state with critical state friction angle and R_o for isotropically consolidated fine-grained soils under triaxial compression.

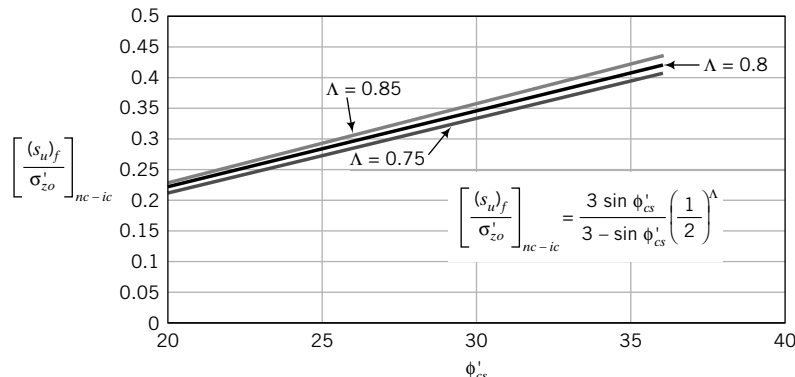


FIGURE 11.24 Variation of theoretical normalized undrained shear strength ratio at critical state for a normally consolidated soil with critical state friction angle and Λ .

For normally consolidated soils, $R_o = 1$, and Equation (11.63) becomes

$$\left[\frac{(s_u)_f}{\sigma'_{zo}} \right]_{nc-ic} = \frac{M}{2} \left(\frac{1}{2} \right)^\Lambda = \frac{3 \sin \phi'_{cs}}{3 - \sin \phi'_{cs}} \left(\frac{1}{2} \right)^\Lambda \quad (11.64)$$

A plot of Equation (11.64) is shown in Figure 11.24 for practical ranges of Λ . Some soils may have Λ lower than 0.75, but rarely greater than 0.85. The maximum difference in the predicted undrained shear strength ratio at critical state for Λ between 0.75 and 0.85 is only about 10%. The subscript $nc-ic$ refers to a normally consolidated soil from isotropic loading.

Soil test results (Mesri, 1975) show that $\frac{s_u}{\sigma'_{zo}} = 0.22$. CSM shows that $\frac{s_u}{\sigma'_{zo}}$ depends on R_o and ϕ'_{cs} . The value of $\frac{s_u}{\sigma'_{zo}}$ from Equation (11.64) for $\phi'_{cs} = 20^\circ$ for $R_o = 1$ is 0.22, or you can use Figure 11.24 to get the same result.

11.7.4 Relationship Between the Normalized Undrained Shear Strength at the Critical State for Normally Consolidated and Overconsolidated Fine-Grained Soils

Let us now define a ratio, α_R , between the normalized undrained shear strength ratio at critical state for an overconsolidated fine-grained soil and the undrained shear strength ratio at critical state for the same soil but normally consolidated. From Equations (11.63) and (11.64), α_R is

$$\alpha_R = \frac{\left[\frac{(s_u)_f}{\sigma'_{zo}} \right]_{oc-ic}}{\left[\frac{(s_u)_f}{\sigma'_{zo}} \right]_{nc-ic}} = \frac{\frac{M}{2} \left(\frac{R_o}{2} \right)^\Lambda}{\frac{M}{2} \left(\frac{1}{2} \right)^\Lambda} = (R_o)^\Lambda \quad (11.65)$$

where the subscript $oc-ic$ refers to an overconsolidated soil from isotropic loading. A plot of Equation (11.65) for Λ ranging from 0.75 to 0.85 is shown in Figure 11.25. The practical implication of Equation (11.65) is that the normalized undrained shear strength at the critical state is proportional to the pre-consolidation ratio. Therefore, if, say, the undrained shear strength of a fine-grained soil at the critical state is known for a normally consolidated soil, then we can predict the undrained shear strength at any preconsolidation ratio for that same soil. For example, if the normalized undrained shear strength of a normally consolidated fine-grained soil is 0.25, then the normalized undrained shear strength of the same soil with a preconsolidation ratio of 10 from Equation (11.65) or Figure 11.25 is 6.3 times greater,

that is, $\left[\frac{(s_u)_f}{\sigma'_{zo}} \right]_{oc} = 6.3 \times 0.25 = 1.58$ for $\Lambda = 0.8$.

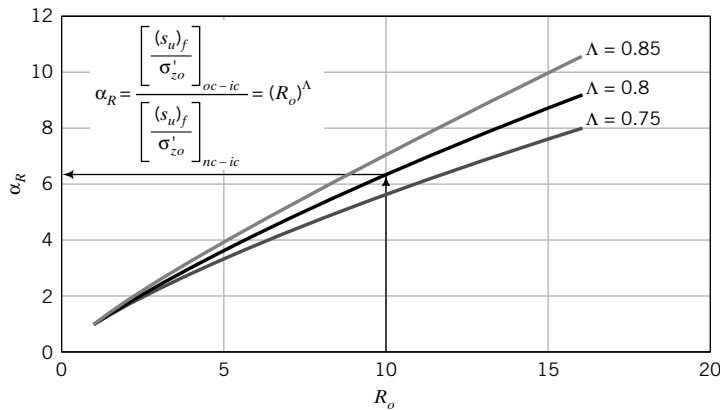


FIGURE 11.25 Variation of theoretical normalized undrained shear strength ratio at critical state for an overconsolidated soil to that of a normally consolidated soil for different values of Λ .

11.7.5 Relationship Between the Normalized Undrained Shear Strength of One-Dimensionally Consolidated or K_o -Consolidated and Isotropically Consolidated Fine-Grained Soils

Soils in the field are one-dimensionally consolidated or K_o -consolidated. The K_o consolidation line (K_o CL) is parallel to the ICL (Figure 11.26). Under K_o consolidation, $p'_o = \frac{(1+2K_o^{oc})}{3}\sigma'_{zo}$; K_o^{oc} is the lateral earth pressure coefficient at rest for overconsolidated soils. For normally consolidated soils, use K_o^{nc} . Therefore, the K_o consolidation line is shifted left by $\left(\sigma'_{zo} - \frac{(1+2K_o^{oc})}{3}\sigma'_{zo}\right) = \frac{2(1-K_o^{oc})}{3}\sigma'_{zo}$. In effect, the

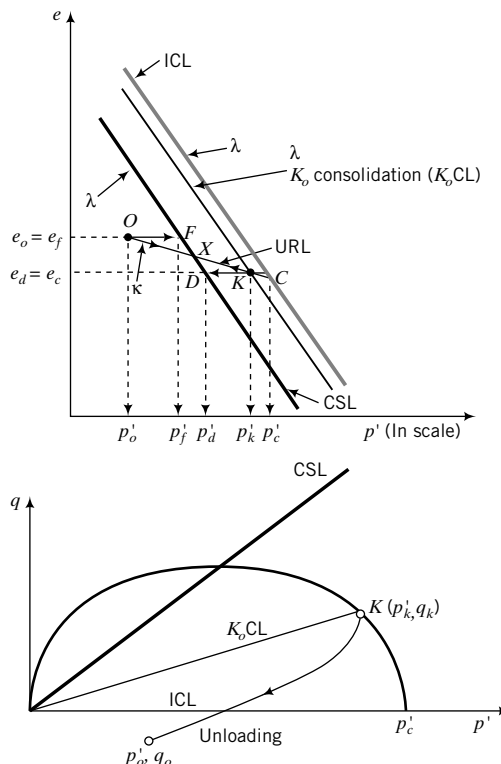


FIGURE 11.26
Loading and unloading
a K_o -consolidated fine-
grained soil.

simple CSM is treating a K_o consolidated soil as if it were an overconsolidated soil with respect to isotropic consolidation. For example, the stress point K located on the K_o consolidation line must also be on a URL from the isotropic consolidation line. That is, point K must be on the line OC . From Equation (11.62), we obtain, by substitution for p'_o ,

$$\left[\frac{(s_u)_f}{\sigma'_{zo}} \right]_{K_o CL} = \frac{(1 + 2K_o^{oc})}{3} \frac{M}{2} \left(\frac{R_o}{2} \right)^\Lambda \quad (11.66)$$

Substituting $K_o^{oc} \approx (1 - \sin \phi'_{cs}) \text{OCR}^{\frac{1}{2}}$ and $M = \frac{6 \sin \phi'_{cs}}{3 - \sin \phi'_{cs}}$ into Equation (11.66), we get

$$\left[\frac{(s_u)_f}{\sigma'_{zo}} \right]_{K_o CL} \approx \frac{3 \sin \phi'_{cs}}{3 - \sin \phi'_{cs}} \frac{\left[1 + 2(1 - \sin \phi'_{cs}) \text{OCR}^{\frac{1}{2}} \right]}{3} \left(\frac{R_o}{2} \right)^\Lambda \quad (11.67)$$

Now R_o has to be calculated based on the preconsolidation stress, p'_c (see Figure 11.27). From Equation (11.4e),

$$p'_c = p'_k + \frac{q_k^2}{M^2 p'_k} \quad (11.68)$$

Dividing both sides of the above equation by p'_o , we obtain

$$\frac{p'_c}{p'_o} = R_o = \frac{p'_k}{p'_o} + \frac{q_k^2}{M^2 p'_k p'_o} \quad (11.69)$$

We now insert the following into Equations (11.68) and (11.69).

$$\begin{aligned} p'_o &= \frac{(1 + 2K_o^{oc})}{3} \sigma'_{zo} \approx \frac{\left[1 + 2(1 - \sin \phi'_{cs}) \text{OCR}^{\frac{1}{2}} \right]}{3} \sigma'_{zo} \\ p'_k &= \frac{(1 + 2K_o^{nc})}{3} \sigma'_{zc} \approx \frac{\left[1 + 2(1 - \sin \phi'_{cs}) \right]}{3} \sigma'_{zc} \approx \frac{(3 - 2 \sin \phi'_{cs})}{3} \sigma'_{zc} \\ q_k &= (1 - K_o^{nc}) \sigma'_{zc} \approx [1 - (1 - \sin \phi'_{cs})] \sigma'_{zc} \approx (\sin \phi'_{cs}) \sigma'_{zc} \end{aligned}$$

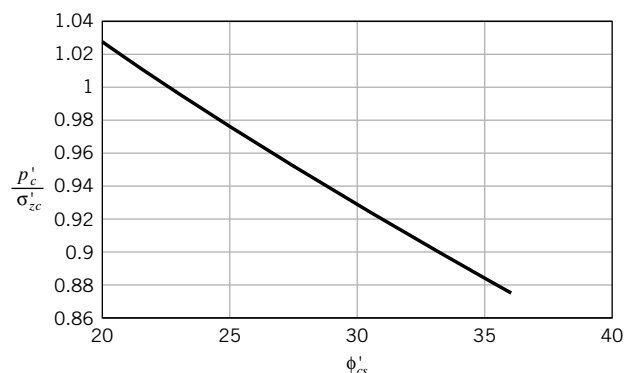


FIGURE 11.27 Relationship among critical state friction angle and preconsolidation stress and maximum past vertical effective stress.

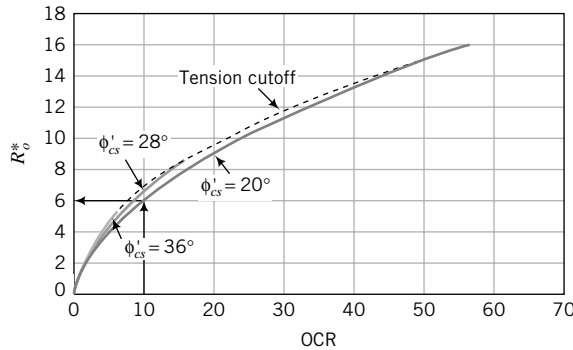


FIGURE 11.28 Variation of R_o^* with OCR for one-dimensionally consolidated fine-grained soils.

In doing so, we get for axisymmetric loading, after simplification,

$$\frac{p'_c}{\sigma'_{zc}} \approx \frac{1}{3} \left[(3 - 2 \sin \phi'_{cs}) - \frac{(3 - \sin \phi'_{cs})^2}{4(2 \sin \phi'_{cs} - 3)} \right] \quad (11.70)$$

A plot of Equation (11.70) is shown in Figure 11.27, which provides an easy means of determining the preconsolidation stress from the past maximum vertical effective stress.

The preconsolidation ratio is

$$R_o = \frac{p'_c}{p'_o} = R_o^* \approx \frac{\left[(3 - 2 \sin \phi'_{cs}) - \frac{(\sin \phi'_{cs} - 3)^2}{4(2 \sin \phi'_{cs} - 3)} \right]}{1 + 2(1 - \sin \phi'_{cs}) \text{OCR}^{\frac{1}{2}}} \quad (11.71)$$

The superscript * is used to differentiate R_o , defined using stress invariants from isotropic loading, from the K_o -consolidated loading. A plot of Equation (11.71) is shown in Figure 11.28. You cannot replace R_o directly by $\text{OCR} = \frac{\sigma'_{zc}}{\sigma'_{zo}}$ that is obtained from the one-dimensional consolidation test in the relationships we have developed based on CSM. Rather, you need to convert OCR to R_o using Equation (11.71) or extract the appropriate R_o from Figure 11.28. For example, if $\text{OCR} = 10$ and $\phi'_{cs} = 20^\circ$, then $R_o^* = R_o = 6$.

The ratio of the normalized undrained shear strength under K_o consolidation and the normalized undrained shear strength under isotropic consolidation at critical state, α_{K_o-ic} , is

$$\alpha_{K_o-ic} = \frac{\left[\frac{(s_u)_f}{\sigma'_{zo}} \right]_{K_o \text{CL}}}{\left[\frac{(s_u)_f}{\sigma'_{zo}} \right]_{ic}} = \frac{\frac{(1 + 2K_o^{oc}) M}{3} \left(\frac{R_o^*}{2} \right)^\Lambda}{\frac{M}{2} \left(\frac{R_o}{2} \right)^\Lambda} \approx \frac{1}{3} \left(1 + 2(1 - \sin \phi'_{cs}) \text{OCR}^{\frac{1}{2}} \right) \left(\frac{R_o^*}{R_o} \right)^\Lambda \quad (11.72)$$

where R_o^* is found from Equation (11.71). For isotropically consolidated fine-grained soils, $R_o = \text{OCR} = 1$. Equation (11.72) reduces to

$$(\alpha_{K_o-ic})_{nc} \approx \frac{1}{3} (3 - 2 \sin \phi'_{cs}) \left(1 - \frac{(\sin \phi'_{cs} - 3)^2}{4(2 \sin \phi'_{cs} - 3)(3 - 2 \sin \phi'_{cs})} \right)^\Lambda \quad (11.73)$$

The values of $(\alpha_{K_o-ic})_{nc}$ for $\Lambda = 0.8$ and different values of ϕ'_{cs} are plotted in Figure 11.29. A K_o -consolidated fine-grained soil with $\text{OCR} = 1$ and $\phi'_{cs} = 30^\circ$ would have a normalized undrained shear strength that is about 0.87 times the normalized undrained shear strength of the same soil isotropically consolidated. The practical implication is that the undrained shear strengths from standard triaxial isotropically

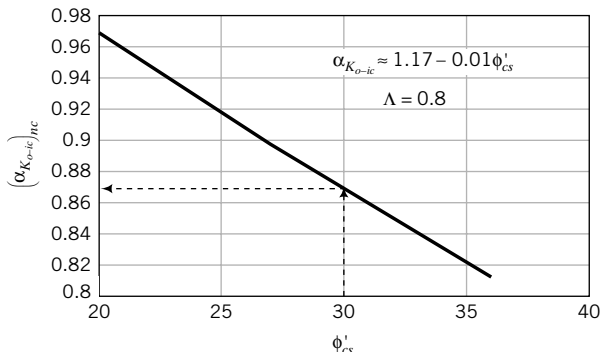


FIGURE 11.29 Variation of theoretical normalized undrained shear strength at critical state for K_o -consolidated soils to that of isotropically consolidated soils.

consolidated tests have to be converted for field application. Equations (11.72) and (11.73) or Figure 11.29 provide the theoretical factor for such a conversion.

11.7.6 Relationship Between the Normalized Undrained Shear Strength at Initial Yield and at Critical State for Overconsolidated Fine-Grained Soils Under Triaxial Test Condition

We can develop a relationship between the normalized undrained shear strength at initial yield and at the critical state for overconsolidated fine-grained soils. We know from Chapter 10 and Section 11.4 that under a certain initial stress state and effective stress path, a soil can exhibit a peak shear stress and then strain-soften to the critical state. CSM allows us to establish what initial soil states will cause a fine-grained soil to show a peak undrained shear strength. Let us denote the ratio of the normalized undrained shear strength at initial yield to the normalized shear strength at the critical state as α_{ycs} . From Equations (11.42) and (11.43), we obtain

$$\alpha_{ycs} = \frac{\frac{(s_u)_y}{p'_o}}{\frac{(s_u)_f}{p'_o}} = \frac{\frac{M}{2}\sqrt{R_o - 1}}{\frac{M}{2}\left(\frac{R_o}{2}\right)^{\Lambda}} = \frac{\sqrt{R_o - 1}}{\left(\frac{R_o}{2}\right)^{\Lambda}} \quad (11.74)$$

A plot of Equation (11.74) is shown in Figure 11.30 for Λ in the range 0.75 to 0.85. When $\alpha_{ycs} > 1$, the normalized yield undrained shear strength is greater than the normalized critical state undrained shear strength. This occurs over a limited range of R_o . For $\Lambda = 0.8$, the range is $2 < R_o < 4$. Since for each soil type there is a limiting value of R_o at which rupture would occur, then there is a cutoff value $R_o = R_t$ for each value of critical state friction angle (see Figure 11.22). Figure 11.30 is applicable to $\phi'_{cs} = 20^\circ$.

The practical significance of α_{ycs} is to estimate the undrained shear strength at initial yield from knowing the undrained shear strength at the critical state and vice versa. Knowing the initial yield stress allows you to use an elastic analysis to analyze your geosystem.

Recall from Figure 11.19 that Hvorslev found that peak shear stresses when normalized to the equivalent effective stress for overconsolidated fine-grained soils lie along the line TF . The slope of this line (TF in Figure 11.31) is

$$m = \frac{\frac{Mp'_c}{2} - n_t t_c p'_c}{\frac{p'_c}{2} - t_c p'_c} = \frac{0.5M - n_t t_c}{0.5 - t_c} = \frac{M - 2n_t t_c}{1 - 2t_c} \quad (11.75)$$

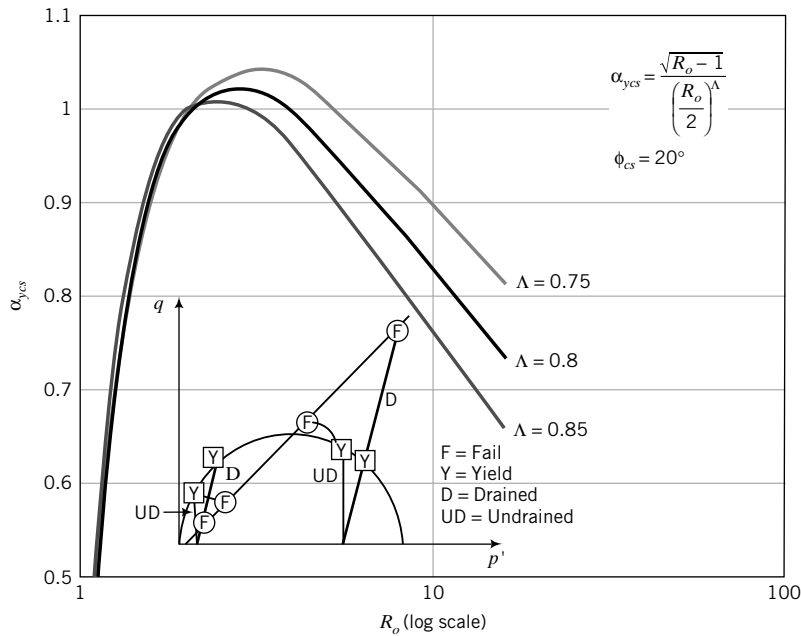


FIGURE 11.30 Variation of theoretical normalized yield to critical state undrained shear strength for isotropically consolidated fine-grained soils under undrained condition.

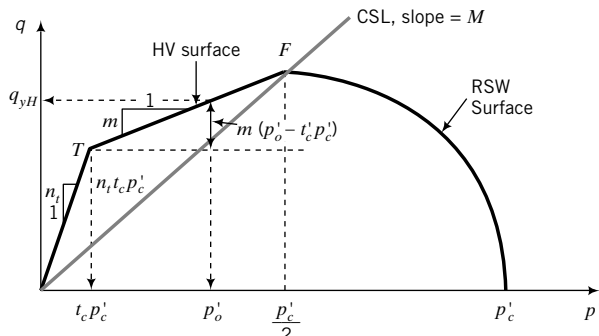


FIGURE 11.31 Hvorslev's limiting stress surface within CSM.

where \$n_t\$ is the slope of the tension line and \$t_c\$ is the intersection of the HV surface with the tension line given by Equation (11.55). Recall that in the triaxial compression test, \$n_t = 3\$. The initial deviatoric stress on the HV surface, \$q_{yH}\$, is then

$$q_{yH} = m(p'_o - t_c p'_c) + n_t t_c p'_c = p'_o[m(1 - t_c R_o) + n_t t_c R_o] \quad (11.76)$$

where \$\frac{p'_c}{2} \geq p'_o \geq t_c p'_c\$ and the subscript \$yH\$ denotes the limiting stress state on reaching the HV surface.

The normalized undrained shear strength of the soil on reaching the HV surface is

$$\frac{(s_u)_{yH}}{p'_o} = 0.5 \left[\frac{M - 2t_c n_t}{1 - 2t_c} (1 - t_c R_o) + t_c n_t R_o \right] \quad (11.77)$$

A plot of Equation (11.77) is shown in Figure 11.32. For \$R_o < 2\$, stable yielding would occur. For each value of critical state friction angle, there is a critical \$R_o = R_i\$ at which the soil would rupture (tension

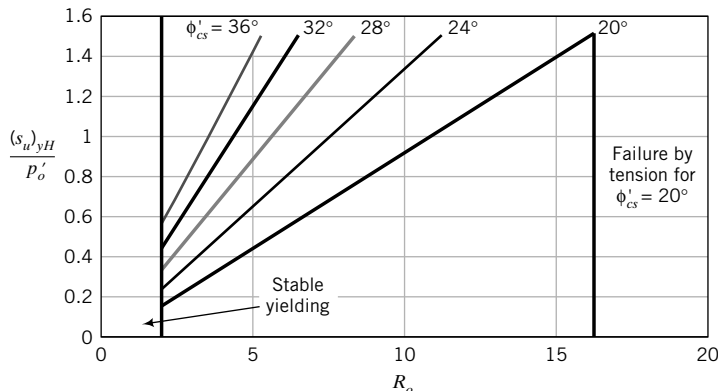


FIGURE 11.32 Variation of theoretical normalized undrained shear strength on the Hvorslev's surface for isotropically consolidated fine-grained soils.

limit), as discussed previously. The end point of the curve for each critical state friction angle in Figure 11.32 indicates the tension limit. The practical significance of Equation (11.77) is that it is an expression to calculate the limiting stresses (incipient instability) for heavily overconsolidated fine-grained soils.

11.7.7 Undrained Shear Strength Under Direct Simple Shear (plane strain) Condition

For plane strain condition, $M_{ps} \approx \sqrt{3} \sin \phi'_{cs}$ (Equation 11.10). If $\sigma'_2 = C(\sigma'_1 + \sigma'_3)$ where $C = 0.5$, then

$$p'_o = \frac{\sigma'_1 + \sigma'_2 + \sigma'_3}{3} = \frac{\sigma'_1 + 0.5(\sigma'_1 + \sigma'_3) + \sigma'_3}{3} = \frac{1}{2}(\sigma'_1 + \sigma'_3)$$

So, for a K_o -consolidated fine-grained soil in a direct simple shear test (initial shear stress is zero; $\sigma'_3 = \sigma'_{zo} = K_o^{oc} \sigma'_1 = K_o^{oc} \sigma'_{zo}$),

$$\left[\frac{(s_u)_f}{\sigma'_{zo}} \right]_{DSS} = \frac{1}{2}(1 + K_o^{oc}) \frac{\sqrt{3} \sin \phi'_{cs}}{2} \left(\frac{R_o^*}{2} \right)^\Lambda = \frac{\sqrt{3}}{4} \left[1 + (1 - \sin \phi'_{cs}) \text{OCR}^{\frac{1}{2}} \right] \sin \phi'_{cs} \left(\frac{R_o^*}{2} \right)^\Lambda \quad (11.78)$$

Equation (11.78) with $\Lambda = 0.8$ and $\text{OCR} = 1$ is plotted in Figure 11.33, where the results of direct simple shear tests on different normally consolidated fine-grained soils are also plotted. The agreement between the predicted (theoretical) results from Equation (11.78) and the experimental data is quite good. The experimental data are based on a simple interpretation of normalized undrained shear strength whereby the shear stress on the horizontal plane is divided by the vertical effective stress. Equation (11.78) is based on considering the complete stress state of the soil. Let us see what would happen if we were to limit our consideration to the stresses on the horizontal plane in the direct simple shear test. In this case, $p'_o = \sigma'_{zo}$ and $R_o^* = \text{OCR}$, and Equation (11.78) becomes

$$\left[\frac{(s_u)_f}{\sigma'_{zo}} \right]_{DSS} = \frac{\sqrt{3} \sin \phi'_{cs}}{2} \left(\frac{\text{OCR}}{2} \right)^\Lambda \quad (11.79)$$

For a normally consolidated fine-grained soil, $\text{OCR} = 1$ and $\Lambda = 0.8$. Equation (11.79) then reduces to

$$\left[\frac{(s_u)_f}{\sigma'_{zo}} \right]_{DSS} \approx 0.5 \sin \phi'_{cs} \quad (11.80)$$

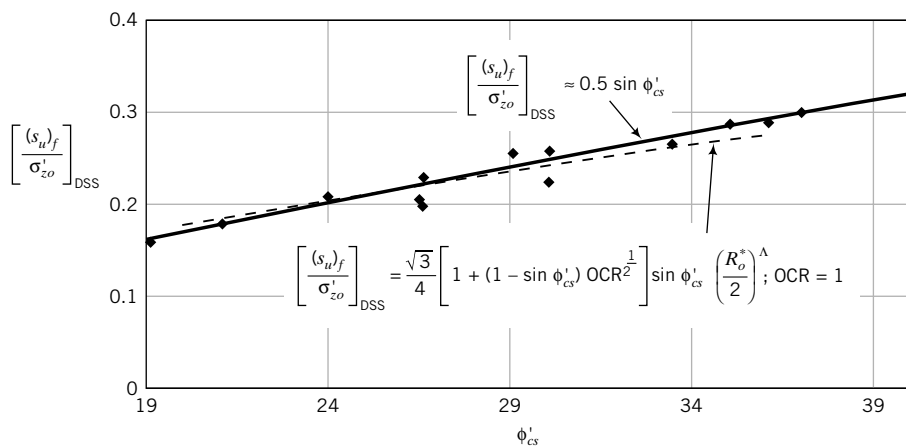


FIGURE 11.33 Variation of theoretical normalized undrained shear strength at critical state for normally consolidated fine-grained soils under direct simple shear and comparison with experimental data shown by the symbols. (Data extracted from Mayne et al., 2009.)

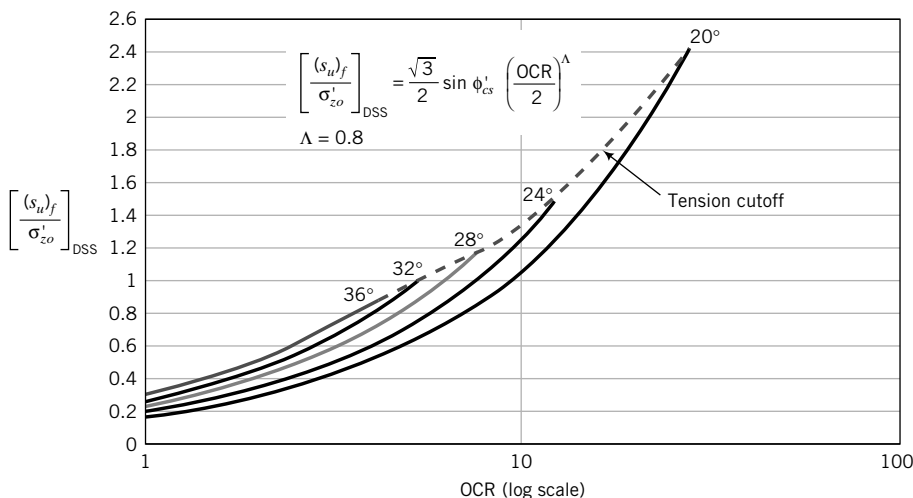


FIGURE 11.34 Variation of theoretical normalized undrained shear strength at critical state with OCR and critical state friction angle for direct simple shear tests.

The agreement between the predicted normalized undrained shear strength from Equation (11.80) and the test data is excellent (Figure 11.33). The exponent $\Lambda = 0.8$ has been shown (Wroth, 1984) to be an excellent fit to direct simple shear test data. The theoretical DSS results for different OCR are shown in Figure 11.34.

11.7.8 Relationship Between Direct Simple Shear Tests and Triaxial Tests

In practice, direct simple shear apparatus are not as readily available compared with triaxial apparatus. However, the stress states imposed by the majority of geosystems are similar to direct simple shear (plane strain). Therefore, if we could find a relationship between triaxial test results (axisymmetric condition) and direct simple shear results, it would allow us to use results from triaxial tests to analyze

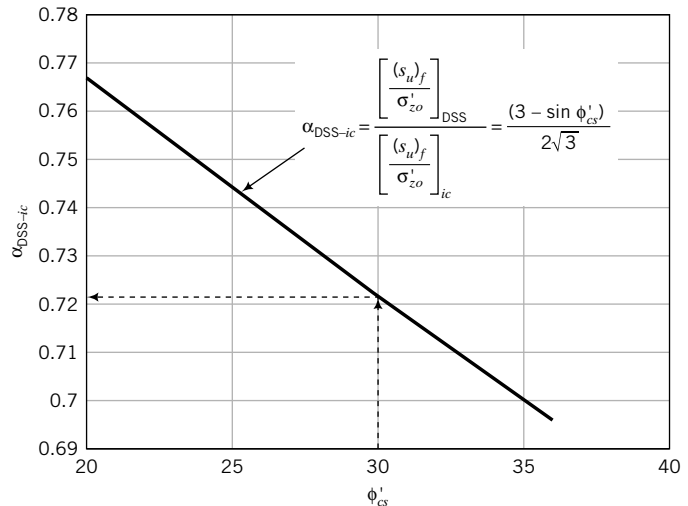


FIGURE 11.35 Variation of the theoretical ratio of normalized undrained shear strength at critical state for direct simple shear tests to that of triaxial isotropically consolidated tests.

geosystems for which the imposed stress state is best simulated by direct simple shear. Recall that in the triaxial test we can only rotate the principal axis of stress by 90° instantaneously, whereby in the direct simple shear test the principal axes of stress rotate gradually. In the field, many structural loads impose gradual rotation of the principal axis of stress.

The ratio of the normalized undrained shear strength of a fine-grained soil under direct simple shear and the normalized undrained shear strength of the same soil isotropically consolidated and then sheared under triaxial undrained condition, α_{DSS-ic} , is

$$\alpha_{DSS-ic} = \frac{\left[\frac{(s_u)_f}{\sigma'_{zo}} \right]_{DSS}}{\left[\frac{(s_u)_f}{\sigma'_{zo}} \right]_{ic}} = \frac{\frac{\sqrt{3} \sin \phi'_{cs} (R_o^*)^\Lambda}{2} \left(\frac{R_o^*}{2} \right)^\Lambda}{\frac{3 \sin \phi'_{cs} (R_o)^{\Lambda}}{3 - \sin \phi'_{cs}} \left(\frac{R_o}{2} \right)^\Lambda} = \frac{(3 - \sin \phi'_{cs})}{2\sqrt{3}} \left(\frac{R_o^*}{R_o} \right)^\Lambda = \frac{(3 - \sin \phi'_{cs})}{2\sqrt{3}} \quad (11.81)$$

since, in this case, $\frac{R_o^*}{R_o} = 1$.

A plot of Equation (11.81) is shown in Figure 11.35. The normalized undrained shear strength in a direct simple shear test is always less than that in the triaxial test on isotropically consolidated samples of the same soil. Suppose the critical state friction angle of a fine-grained soil is 30°; then the normalized undrained shear strength from a triaxial isotropically consolidated sample must be multiplied by about 0.72 to estimate the undrained shear strength of the same soil sample subjected to direct simple shear test. Recall that ϕ'_{cs} is a fundamental soil property and, as such, it is independent of the type of test.

The practical implication is that triaxial test results from isotropically consolidated samples must be corrected to apply to the analysis of geosystems in which the stress states are best simulated by direct simple shear. Examples of these geosystems are retaining walls and slopes. In the case of slopes, the design safety margin is generally small ($1 < FS \leq 1.5$; FS is factor of safety). If you do not account for the reduction in undrained shear strength from triaxial test results, the risk of failure increases.

11.7.9 Relationship for the Application of Drained and Undrained Conditions in the Analysis of Geosystems

In the analysis of geosystems on or within fine-grained soils, we often consider two limit conditions—short-term and long-term conditions. Short-term condition (undrained condition) is assumed to simulate

the stress state during and soon after construction. Long-term condition (drained condition) is assumed to simulate the stress state during the life of the structure or when the excess porewater pressure has dissipated. We can now build a relationship between a soil at an initial stress state subjected to undrained loading and the same soil at the same initial stress state subjected to drained loading. We define a ratio, α_{SL} , to describe the ratio of the shear strength of a soil under undrained short-term condition (S in the subscript) to the shear strength under long-term condition (L in the subscript). From Equations (11.20) and (11.49), we get

$$\alpha_{SL} = \frac{\frac{(s_u)_f}{p'_o}}{\frac{\tau_f}{p'_o}} = \frac{\frac{M}{2} \left(\frac{R_o}{2}\right)^\Lambda}{\frac{M}{2} \frac{n_o}{n_o - M}} = \frac{(n_o - M)}{n_o} \left(\frac{R_o}{2}\right)^\Lambda \quad (11.82)$$

For the standard triaxial test condition, $n_o = 3$ and Equation (11.82) becomes

$$\alpha_{SL} = \frac{(3 - M)}{3} \left(\frac{R_o}{2}\right)^\Lambda \quad (11.83)$$

Substituting Equation (11.6) into Equation (11.83) and simplifying, we get

$$\alpha_{SL} = \frac{3(1 - \sin \phi'_{cs})}{(3 - \sin \phi'_{cs})} \left(\frac{R_o}{2}\right)^\Lambda \quad (11.84)$$

Two plots of Equation (11.84) are shown in Figure 11.36 for $\Lambda = 0.8$ and different values of R_o . The same data are plotted on both graphs for ease of use. When α_{SL} is less than 1, the normalized shear strength under undrained condition at critical state is lower than that under drained condition. Therefore, undrained loading would be critical. On average, this occurs for soils with R_o less than about 3. The actual value of R_o for which undrained condition is critical depends on the critical state friction value. Higher critical state friction angles result in higher R_o at which undrained condition is critical. Drained condition is critical when $\alpha_{SL} > 1$ because the normalized undrained shear strength at critical state is greater than the normalized drained shear strength at critical state.

This relationship is of practical importance because it provides guidance on which one of these conditions would be critical. A soil with different R_o would have different critical (design) conditions. For example, if $\phi'_{cs} = 30^\circ$, $R_o = 1$, and $\Lambda = 0.8$, then from Figure 11.36a, $\alpha_{SL} = 0.35$. Therefore, undrained loading would be critical. But if $R_o = 5$ for the same soil, $\alpha_{ySL} = 1.25$ and drained loading would be critical. Equation (11.84) applies only to critical state condition.

If we were to consider peak (initial yield) stress state, then

$$\alpha_{ySL} = \frac{\frac{(s_u)_y}{p'_o}}{\frac{\tau_y}{p'_o}} = \frac{\frac{M}{2} \sqrt{R_o - 1}}{\frac{3(p'_y - 1)}{2(p'_o - 1)}} = \frac{M \sqrt{R_o - 1}}{3 \left(\frac{p'_y}{p'_o} - 1\right)} = \frac{2 \sin \phi'_{cs}}{(3 - \sin \phi'_{cs})} \frac{\sqrt{R_o - 1}}{\left(\frac{p'_y}{p'_o} - 1\right)} \quad (11.85)$$

Equation (11.85) is plotted in Figure 11.37. If we were to compare Fig.11.36b with Figure 11.37, we would notice that drained and undrained conditions are approximately reversed. For $R_o < 2$, drained loading is critical, but for $R_o > 2$, undrained loading is critical. Consider a tank foundation on an overconsolidated clay with OCR = 10 and $\phi'_{cs} = 28^\circ$. Which of undrained or drained loading would be critical for soil yielding? From Figure 11.28, $R_o = 6.5$ for OCR = 10. From Figure 11.37, $\alpha_{ySL} = 0.78$, and therefore yielding under undrained condition would be critical. However, if we were to consider failure (critical state), $\alpha_{SL} = 1.3$ (Figure 11.36) and drained loading would be critical.

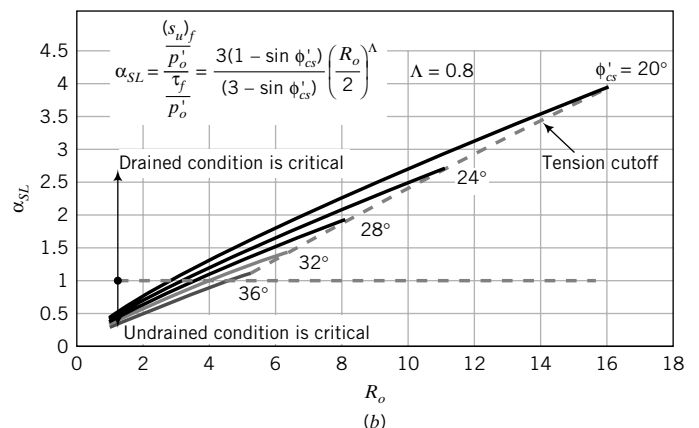
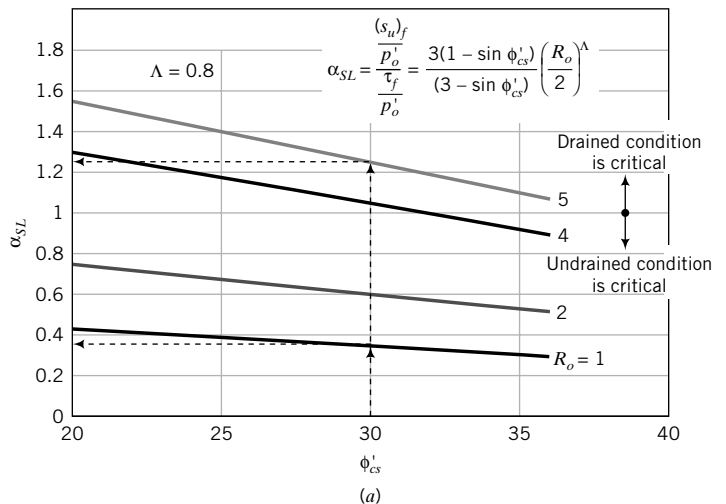


FIGURE 11.36 Theoretical ratio of normalized undrained shear strength at critical state to the normalized shear strength at critical state under drained condition for different R_o . The same data are plotted in the two graphs for ease of use.

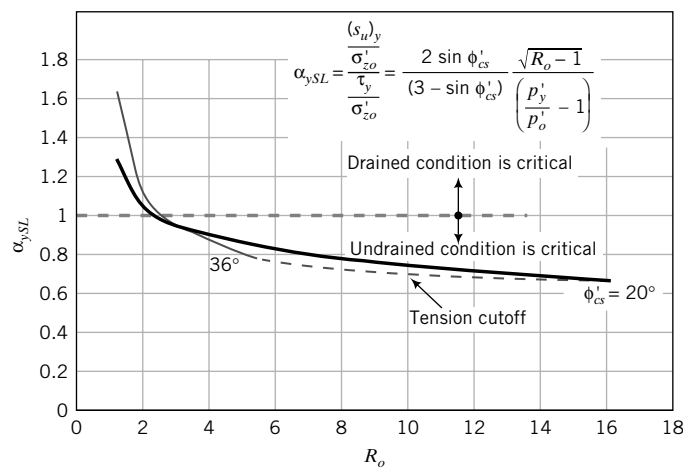


FIGURE 11.37 Theoretical ratio of normalized undrained shear strength at initial yield to the normalized initial yield shear stress under drained condition for different R_o .

11.7.10 Relationship Among Excess Porewater Pressure, Preconsolidation Ratio, and Critical State Friction Angle

Recall (Chapter 10) that Skempton (1954) proposed the A and B porewater pressure coefficients for the triaxial test; A is related to the shear component and B is related to the degree of saturation. We can use CSM to establish the theoretical A coefficient and its relationship to R_o and ϕ'_{cs} . Let us consider the excess porewater pressure at failure (critical state) for a saturated soil. From Equation (10.51),

$$A_f = \frac{\Delta u_f}{(\Delta \sigma_1)_f - (\Delta \sigma_3)_f} \quad (11.86)$$

For the standard triaxial undrained test, $(\Delta \sigma_3)_f = 0$ since the cell pressure is held constant and the axial (deviator) stress is increased to bring the soil to failure. Thus, $q_f = (\Delta \sigma_1)_f$ and

$$A_f = \frac{\Delta u_f}{q_f} \quad (11.87)$$

Substitution of Equation (11.30) into Equation (11.87) gives

$$A_f = \frac{\left(p'_o - \frac{q_f}{M} \right) + \frac{q_f}{3}}{q_f} = \frac{1}{M} \left(\frac{p'_o}{p'_f} - 1 \right) + \frac{1}{3} = \frac{1}{M} \left[\left(\frac{R_o}{2} \right)^{-\Lambda} - 1 \right] + \frac{1}{3} \quad (11.88)$$

or

$$A_f = \frac{3 - \sin \phi'_{cs}}{6 \sin \phi'_{cs}} \left[\left(\frac{R_o}{2} \right)^{-\Lambda} - 1 \right] + \frac{1}{3} \quad (11.89)$$

The shear component of the excess porewater pressures is the first part of the right-hand side of Equation (11.89), while the last part, $\frac{1}{3}$, is the total stress path component. A plot of Equation (11.89) is shown in Figure 11.38. The A_f is dependent not only on R_o but also on ϕ'_{cs} . Recall that Skempton's A_f is dependent only on the R_o .

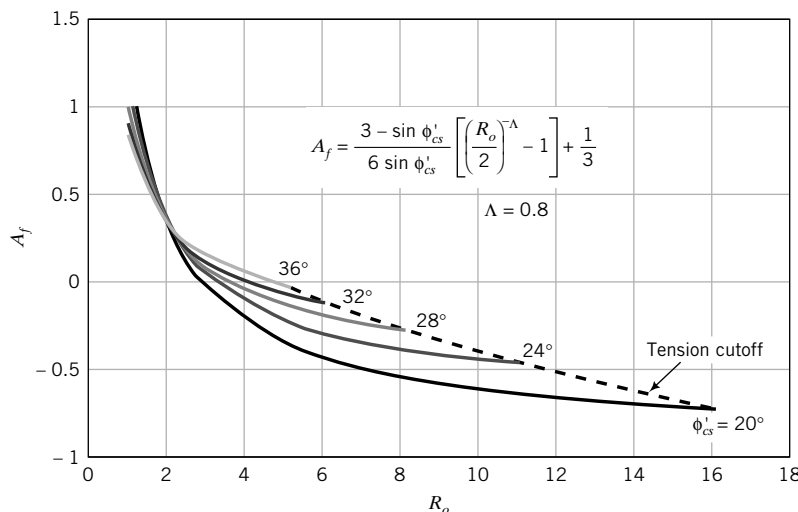


FIGURE 11.38 Variation of A_f with R_o and critical state friction angle.

11.7.11 Undrained Shear Strength of Clays at the Liquid and Plastic Limits

Wood (1990), using test results reported by Youssef et al. (1965) and Dumbleton and West (1970), showed that

$$\frac{(s_u)_{PL}}{(s_u)_{LL}} = R \quad (11.90)$$

where R depends on activity (Chapter 3) and varies between 30 and 100, and the subscripts PL and LL denote plastic limit and liquid limit, respectively. Wood and Wroth (1978) recommend a value of $R = 100$ as reasonable for most soils (R up to 170 has been reported in the literature). The recommended value of $(s_u)_{LL}$, culled from the published data, is 2 kPa (the test data showed variations between 0.9 and 8 kPa) and that for $(s_u)_{PL}$ is 200 kPa. Since most soils are within the plastic range, these recommended values place lower (2 kPa) and upper (200 kPa) limits on the undrained shear strength of disturbed or remolded clays.

11.7.12 Vertical Effective Stresses at the Liquid and Plastic Limits

Wood (1990) used results from Skempton (1970) and recommended that

$$(\sigma'_z)_{LL} = 8 \text{ kPa} \quad (11.91)$$

The test results showed that $(\sigma'_z)_{LL}$ varies from 6 to 58 kPa. Laboratory and field data also showed that the undrained shear strength is proportional to the vertical effective stress. Therefore,

$$(\sigma'_z)_{PL} = R(\sigma'_z)_{LL} \approx 800 \text{ kPa} \quad (11.92)$$

11.7.13 Compressibility Indices (λ and C_c) and Plasticity Index

The compressibility index C_c or λ is usually obtained from a consolidation test. In the absence of consolidation test results, we can estimate C_c or λ from the plasticity index. With reference to Figure 11.39,

$$-(e_{PL} - e_{LL}) = \lambda \ln \frac{(\sigma'_z)_{PL}}{(\sigma'_z)_{LL}} = \lambda \ln R$$

Now, $e_{LL} = w_{LL} G_s$, $e_{PL} = w_{PL} G_s$, and $G_s = 2.7$. Therefore, for $R = 100$,

$$LL - PL = \frac{\lambda}{2.7} \ln R \approx 1.7\lambda$$

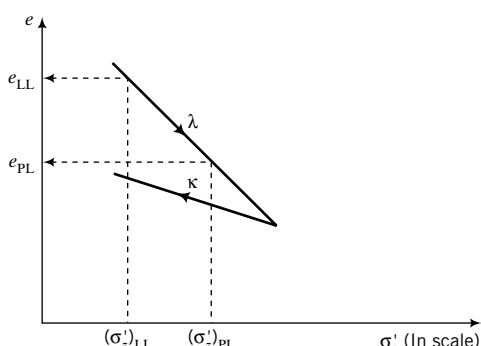


FIGURE 11.39 Illustrative graph of e versus σ'_z (In scale).

and

$$\lambda \approx 0.59 \text{ PI} \quad (11.93)$$

or

$$C_c = 2.3 \lambda \approx 1.35 \text{ PI} \quad (11.94)$$

Equation (11.93) indicates that the compression index increases with the plasticity index.

11.7.14 Undrained Shear Strength, Liquidity Index, and Sensitivity

Let us build a relationship between liquidity index and undrained shear strength. The undrained shear strength of a soil at a water content w , with reference to its undrained shear strength at the plastic limit, is obtained from Equation (11.29) as

$$\frac{(s_u)_w}{(s_u)_{PL}} = \exp\left(G_s \frac{(PL - w)}{\lambda}\right)$$

Putting $G_s = 2.7$ and $\lambda = 0.59 \text{ PI}$ in the above equation, and recalling that

$$LI = \frac{w - PL}{PI}$$

we get

$$(s_u)_w = (s_u)_{PL} \exp(-4.6 LI) \approx 200 \exp(-4.6 LI) \quad (11.95)$$

Clays laid down in saltwater environments and having flocculated structure (Chapter 2) often have in situ (natural) water contents higher than their liquid limit but do not behave like a viscous liquid in their natural state. The flocculated structure becomes unstable when fresh water leaches out the salt. The undistributed or intact undrained shear strengths of these clays are significantly greater than their disturbed or remolded undrained shear strengths. The term sensitivity, S_t , is used to define the ratio of the intact undrained shear strength to the remolded undrained shear strength:

$$S_t = \frac{(s_u)_i}{(s_u)_r} \quad (11.96)$$

where i denotes intact and r denotes remolded. By substituting Equation (11.95) into Equation (11.96), we obtain

$$(s_u)_r \approx 200 \exp(-4.6 LI) \quad (11.97)$$

For values of $S_t > 8$, the clay is called a quick clay. Quick clay, when disturbed, can flow like a viscous liquid ($LI > 1$). Bjerrum (1954) reported test data on quick clays in Scandinavia, which yield an empirical relationship between S_t and LI as

$$LI = 1.2 \log_{10} S_t \quad (11.98)$$

11.7.15 Summary of Relationships Among Some Soil Parameters from CSM

Table A.14 (Appendix A) provides a summary of the relationships among some soil parameters from CSM. The approximate expressions for practical use were obtained by a curve fitting the CSM expressions. The approximate expressions should be used to get a quick estimate during preliminary design. They are accurate to about 10% or less.

EXAMPLE 11.12 Predicting the Shear Strength of a Fine-Grained Soil Using CSM

A standard undrained triaxial test was performed on a fine-grained soil in a normally consolidated state. The cell pressure was 100 kPa, and the axial stress at failure (critical state) was 70 kPa. Assuming $\Lambda = 0.8$,

- Determine the normalized undrained shear strength.
- Estimate ϕ'_{cs} .
- Estimate the undrained shear strength at critical state of the same soil if it were overconsolidated with $R_o = 5$. Assume the preconsolidation stress is the same.
- Estimate the undrained shear strength at critical state of the same soil if it were to be subjected to direct simple shear.
- The same soil exists in the field as a 10-m-thick layer with a saturated unit weight of 19.8 kN/m³. Groundwater is at the surface. Estimate the undrained shear strength at a depth of 5 m if OCR = 4.
- Estimate the excess porewater pressure in the test.

Strategy Use the relationships given in Section 11.7 to answer the questions.

Solution 11.12

Step 1: Calculate the normalized undrained shear strength.

$$(s_u)_f = \frac{q_f}{2} = \frac{70}{2} = 35 \text{ kPa}$$

$$\frac{(s_u)_f}{p'_o} = \frac{35}{100} = 0.35$$

Note that the initial mean effective stress is 100 kPa. But, at failure, this value changes because of the development of excess porewater pressures.

Step 2: Estimate the critical state friction angle.

From Figure 11.24 or Equation (11.63) with $\frac{s_u}{p'_o} = 0.35$ and $\Lambda = 0.8$, $\phi'_{cs} = 30^\circ$.

Step 3: Calculate M_c .

$$M_c = \frac{6 \sin 30^\circ}{3 - \sin 30^\circ} = 1.2$$

Step 4: Calculate the undrained shear strength for $R_o = 5$.

$$\left[\frac{(s_u)_f}{p'_o} \right]_{R_o=5} = \frac{(s_u)_f}{p'_o} (R_o)^\Lambda = 0.35 \times (5)^{0.8} = 1.27$$

Since $R_o = 5$, then $p'_o = \frac{p'_c}{R_o} = \frac{100}{5} = 20 \text{ kPa}$.

$$[(s_u)_f]_{R_o=5} = 1.27 \times 20 = 25.4 \text{ kPa}$$

Step 5: Estimate the undrained shear strength for DSS.

$$\left[\frac{(s_u)_f}{\sigma'_{zo}} \right]_{DSS} \approx 0.5 \sin \phi'_{cs} \approx 0.5 \sin 30^\circ = 0.25$$

$$[(s_u)_f]_{DSS} = 0.25 \times 100 = 25 \text{ kPa}$$

Step 6: Estimate the shear strength of the soil in the field.

$$\text{OCR} = 4$$

$$R_o^* = \frac{\left[(3 - 2 \sin \phi'_{cs}) - \frac{(\sin \phi'_{cs} - 3)^2}{4(2 \sin \phi'_{cs} - 3)} \right]}{1 + 2(1 - \sin \phi'_{cs}) \text{OCR}^{\frac{1}{2}}} \text{OCR} = \frac{\left[(3 - 2 \sin 30^\circ) - \frac{(\sin 30^\circ - 3)^2}{4(2 \sin 30^\circ - 3)} \right]}{1 + 2(1 - \phi'_{cs} \sin 30^\circ) 4^{\frac{1}{2}}} 4 = 3.7$$

From Equation (11.72) with $R_o = 1$,

$$\begin{aligned} \left[\frac{(s_u)_f}{\sigma'_{zo}} \right]_{K_0 \text{CL}} &\approx \left[\frac{(s_u)_f}{\sigma'_{zo}} \right]_{ic} \frac{[1 + 2(1 - \sin \phi'_{cs}) \text{OCR}^{\frac{1}{2}}](R_o^*)^{\Lambda}}{3} \\ &\approx 0.35 \times \frac{[1 + 2(1 - \sin 30^\circ) 4^{\frac{1}{2}}](3.7)^{0.8}}{3} = 1 \end{aligned}$$

The vertical effective stress in the field is $5 \times (19.8 - 9.8) = 50$ kPa. Therefore,

$$[(s_u)_f]_{K_0 \text{CL}} = 50 \times 1 \approx 50 \text{ kPa}$$

Step 7: Estimate the excess porewater pressure.

$$\begin{aligned} p'_f &= \frac{q_f}{M} = \frac{70}{1.2} = 58.3 \text{ kPa} \\ p_f &= p'_o + \frac{q_f}{3} = 100 + \frac{70}{3} = 123.3 \text{ kPa} \\ \Delta u_f &= p_f - p'_f = 123.3 - 58.3 = 65 \text{ kPa} \end{aligned}$$

EXAMPLE 11.13 Predicting the Peak and Critical State Shear Strength of a Sand from Knowing the Angle of Repose

A dry sand sample is slowly poured on a table and the angle of repose is measured as 30° . A triaxial drained compression test is to be carried out on a specimen of this soil by applying incremental cell pressures starting from 12.5 kPa and doubling each increment thereafter. Each increment will remain on the specimen for about 15 minutes. After a maximum cell pressure of 400 kPa, the specimen will be incrementally unloaded to a cell pressure of 40 kPa. The specimen will then be sheared by increasing the axial stress and keeping the cell pressure constant.

- (a) Predict the shear stress at critical state using CSM.
- (b) Will the sand show a peak shear stress? If so, calculate the peak shear stress.
- (c) Calculate the normalized undrained shear strength.
- (d) Over what range of shear stress would the sand behave like a linearly elastic material?
- (e) Calculate the shear stress at the critical state if the soil were to be subjected to direct simple shear condition following an ESP with a slope of 2.5.

Strategy The angle of repose is approximately equal to the critical state friction angle. We will use this value to find M , and then we can unleash the power of CSM for predicting the shear strength of soils from very few soil parameters.

Solution 11.13

Step 1: Estimate the critical state friction angle.

The critical state friction angle is approximately equal to the angle of repose.

$$\phi'_{cs} = 30^\circ$$

Step 2: Calculate M_c .

$$M_c = \frac{6 \sin 30^\circ}{3 - \sin 30^\circ} = 1.2$$

Step 3: Calculate the shear stress at critical state.

$$p'_o = 40 \text{ kPa}, \quad p'_c = 400 \text{ kPa}, \quad R_o = \frac{p'_c}{p'_o} = \frac{400}{40} = 10$$

Since the test is a standard triaxial drained test, the slope of the ESP is 3.

$$\frac{\tau_f}{p'_o} = \frac{3M}{2(3 - M)} = \frac{3 \times 1.2}{2(3 - 1.2)} = 1$$

$$\tau_f = 1 \times p'_o = 40 \text{ kPa}$$

Step 4: Determine if the sand will exhibit a peak shear stress.

From Figure 11.22, with $\phi'_{cs} = 30^\circ$ and $R_o = 10$, $\alpha_{pcs} = 2.7$. Therefore, the sand is likely to show a peak shear stress.

Step 5: Calculate the (peak) shear stress at initial yield.

$$\frac{\tau_y}{p'_o} = \alpha_{pcs} \times \frac{\tau_f}{p'_o} = 2.7 \times 1 = 2.7$$

$$\tau_y = 2.7 \times p'_o = 2.7 \times 40 = 108 \text{ kPa}$$

By calculation:

$$\begin{aligned} \frac{p'_y}{p'_o} &= \frac{(M^2 R_o + 18) + \sqrt{(M^2 R_o + 18)^2 - 36(M^2 + 9)}}{2(M^2 + 9)} \\ &= \frac{(1.2^2 \times 10 + 18) + \sqrt{(1.2^2 \times 10 + 18)^2 - 36(1.2^2 + 9)}}{2(1.2^2 + 9)} = 2.8 \\ \frac{\tau_y}{p'_o} &= \frac{3\left(\frac{p'_y}{p'_o} - 1\right)}{2} = \frac{3(2.8 - 1)}{2} = 2.7 \\ \tau_y &= 2.7 \times p'_o = 2.7 \times 40 = 108 \text{ kPa} \end{aligned}$$

Step 6: Determine the range in which the sand will behave like an elastic material.

The range of shear stress for which the soil will behave like an elastic material is 0 to 108 kPa.

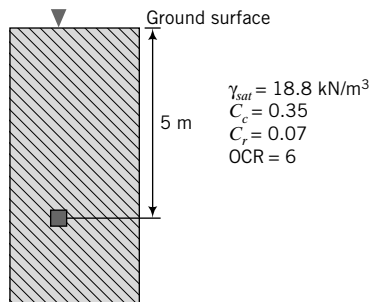
Step 7: Calculate critical state shear stress for DSS.

$$n_o = 2.5, \quad M = \sqrt{3} \sin \phi'_{cs} = \sqrt{3} \sin 30^\circ = 0.866$$

$$\tau_{cs} = \frac{1}{2} \frac{n_o M p'_o}{(n_o - M)} = \frac{1}{2} \frac{2.5 \times 0.866 \times 40}{(2.5 - 0.866)} = 26.5 \text{ kPa}$$

EXAMPLE 11.14 Estimating the Undrained Shear Strength for Direct Simple Shear for Field Application Based on the Result from a Triaxial Undrained Compression Test

A soil sample, 50 mm in diameter and 450 mm long, was extracted in a sampling tube from the ground such that its center is at 5 m below the surface (Figure E11.14a). Groundwater is at the surface. The sample was coated in wax to prevent water content changes. One specimen, 50 mm in diameter \times 25 mm thick, from the sampling tube was used

**FIGURE E11.14a**

for a one-dimensional consolidation test. Another specimen, 50 mm in diameter \times 100 mm long, near the center of the sampling tube was used to conduct a standard triaxial undrained compression test. The soil technician, who conducted the two tests according to ASTM standards, reported the following results from the consolidation test: $\gamma_{sat} = 18.8 \text{ kN/m}^3$, $C_c = 0.35$, $C_r = 0.07$, and $\text{OCR} = 6$. For the triaxial undrained compression test, the technician consolidated the specimen by increasing the cell pressure up to 300 kPa. Each increment of cell pressure was kept constant for 24 hours, and the specimen was permitted to drain the excess porewater pressure. When the cell pressure of 300 kPa was achieved and more than 95% of the excess porewater pressure was drained from the specimen, the drainage valves were closed and the specimen sheared by increasing the axial stress. The cell pressure of 300 kPa was held constant during shearing. The soil technician reported a maximum axial load at failure of 330 N at a vertical compression of 1 mm. She also reported that the soil in the sampling tube seems homogeneous.

- (a) Calculate the undrained shear strength.
- (b) Calculate the normalized undrained shear strength.
- (c) Is this the undrained shear strength at critical state? If not, estimate the normalized undrained shear strength at critical state using CSM.
- (d) Estimate the critical state friction angle.
- (e) Is the undrained triaxial test on the lab specimen representative of the undrained strength of the soil in the field? If not, estimate its value.
- (f) If a geosystem were to impose a stress state analogous to direct simple shear, estimate the undrained shear strength you would use in the analysis.

Strategy The solution to this problem makes use of several of the relationships in Section 11.7. You are given the maximum axial load and it is uncertain whether this is the peak or critical state load. You can make an assumption as to which one and then check your assumption. The soil in the field is K_o -consolidated, while in the lab the soil sample is isotropically consolidated. So you need to correct the test results.

Solution 11.14

Step 1: Calculate the undrained shear strength.

$$P_{max} = 330 \text{ N}, \Delta L = 1 \text{ mm}; \quad L = 100 \text{ mm}; \quad \varepsilon_z = \frac{\Delta L}{L} = \frac{1}{100} = 0.01$$

$$D = 50 \text{ mm, initial area, } A_o = \frac{\pi D^2}{4} = \frac{\pi (0.05)^2}{4} = 1.96 \times 10^{-3} \text{ m}^2$$

$$A = \frac{A_o}{(1 - \varepsilon_z)} = \frac{1.96 \times 10^{-3}}{(1 - 0.01)} = 1.98 \times 10^{-3} \text{ m}^2$$

$$q = \frac{P_{max}}{A} = \frac{330 \times 10^{-3}}{1.98 \times 10^{-3}} = 166.7 \text{ kPa}$$

$$s_u = \frac{q}{2} = \frac{166.7}{2} = 83.4 \text{ kPa}$$

Step 2: Calculate the normalized undrained shear strength.

$$(p'_o)_{lab} = 300 \text{ kPa}$$

$$\frac{s_u}{(p'_o)_{lab}} = \frac{83.4}{300} = 0.278$$

Step 3: Check if the normalized undrained shear strength is at critical state or at initial yield.

We do not know whether the cell pressure of 300 kPa applied by the soil technician is below or above the preconsolidation stress. Let's assume that it is above the preconsolidation stress and then check if the assumption is valid. In this case, R_o in the test is equal to 1, and from Figure 11.24 with

$\frac{s_u}{(p'_o)_{lab}} = \frac{s_u}{(\sigma'_{zo})_{lab}} = 0.278$ and $\Lambda = \frac{C_c - C_r}{C_c} = \frac{0.35 - 0.07}{0.35} = 0.8$, we get $\phi'_{cs} = 24.5^\circ$. You can also use Equation (11.64) to find ϕ'_{cs} .

The initial stresses for the soil in the field are:

$$\sigma_{zo} = 5 \times 18.8 = 94 \text{ kPa}; \quad u_o = 5 \times 9.8 = 49 \text{ kPa}; \quad \sigma'_{zo} = 94 - 49 = 45 \text{ kPa}$$

or

$$\sigma'_{zo} = 5 \times (18.8 - 9.8) = 45 \text{ kPa}$$

$$M_c = \frac{6 \sin \phi'_{cs}}{3 - \sin \phi'_{cs}} = \frac{6 \sin 24.5^\circ}{3 - \sin 24.5^\circ} = 0.96$$

$$K_o^{nc} = 1 - \sin \phi'_{cs} = 1 - 0.41 = 0.59$$

$$K_o^{oc} = K_o^{nc} \text{ OCR}^{\frac{1}{2}} = 0.59 \times 6^{\frac{1}{2}} = 1.45$$

$$\sigma'_{xo} = K_o^{oc} \times \sigma'_{zo} = 1.45 \times 45 = 65.3 \text{ kPa}$$

$$p'_o = \frac{\sigma'_{zo} + 2\sigma'_{xo}}{3} = \frac{45 + 2 \times 65.3}{3} = 58.5 \text{ kPa}$$

$$q_o = \sigma'_{zo} - \sigma'_{xo} = 45 - 65.3 = -20.3 \text{ kPa}$$

$$\sigma'_{zc} = 6 \times 45 = 270 \text{ kPa}$$

$$p'_k = \sigma'_{zo} \left(\frac{1 + 2k_o^{nc}}{3} \right) = 270 \left(\frac{1 + 2 \times 0.59}{3} \right) = 196.2 \text{ kPa}$$

$$q_k = \sigma'_{zc} (1 - K_o^{nc}) = 270 (1 - 0.59) = 110.7 \text{ kPa}$$

$$p'_c = p'_o + \frac{q_o^2}{M^2 p'_o} = 196.2 + \frac{110.7^2}{0.96^2 \times 196.2} = 264 \text{ kPa}$$

See the initial stresses illustrated in Figure E11.14b.

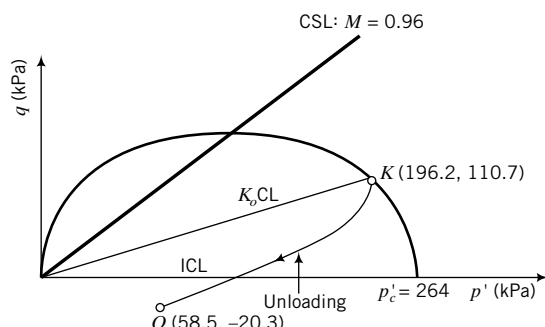


FIGURE E11.14b

The cell pressure of 300 kPa applied in the lab test is higher than the preconsolidation stress ($= 264$ kPa). Therefore, the specimen in the lab is reconsolidated along the ICL. The normalized undrained shear strength from the test is the critical state value.

Step 4: Estimate the critical state friction angle.

$$\phi'_{cs} = 24.5^\circ \text{ (see Step 3)}$$

Step 5: Check if the undrained triaxial test from the soil specimen is representative of the undrained strength of the soil in the field.

The R_o used in the lab test is 1 and the soil specimen was isotropically consolidated, while the OCR of the soil in the field is 6 and was K_o -consolidated.

$$\begin{aligned} R_o^* &= \frac{\left[(3 - 2 \sin \phi'_{cs}) - \frac{(\sin \phi'_{cs} - 3)^2}{4(2 \sin \phi'_{cs} - 3)} \right]}{1 + 2(1 - \sin \phi'_{cs}) \text{OCR}^{\frac{1}{2}}} \text{OCR} \\ &= \frac{\left[(3 - 2 \sin 24.5^\circ) - \frac{(\sin 24.5^\circ - 3)^2}{4(2 \sin 24.5^\circ - 3)} \right]}{1 + 2(1 - \sin 24.5^\circ) 4^{\frac{1}{2}}} \times 6 = 4.6 \end{aligned}$$

From Equation (11.72) with $R_o = 1$,

$$\begin{aligned} \left[\frac{(s_u)_f}{\sigma'_{zo}} \right]_{field} &\approx \left[\frac{(s_u)_f}{p'_o} \right]_{ic} \frac{\left(1 + 2(1 - \sin \phi'_{cs}) \text{OCR}^{\frac{1}{2}} \right) (R_o^*)^{\lambda}}{3} \\ &\approx 0.278 \times \frac{\left(1 + 2(1 - \sin 24.5^\circ) 6^{\frac{1}{2}} \right) (4.6)^{0.8}}{3} = 1.21 \end{aligned}$$

The vertical effective stress in the field is 45 kPa. Therefore,

$$[(s_u)_f]_{field} = 45 \times 1.21 \approx 54.7 \text{ kPa}$$

Step 6: Estimate the undrained shear strength for direct shear simple shear.

$$\begin{aligned} \left[\frac{(s_u)_{cs}}{\sigma'_{zo}} \right]_{DSS} &= \frac{\sqrt{3} \sin \phi'_{cs}}{2} \left(\frac{\text{OCR}}{2} \right)^{\lambda} \approx 0.5 \sin \phi'_{cs} \text{OCR}^{0.8} = 0.5 \sin 24.5^\circ \times 6^{0.8} = 0.87 \\ [(s_u)_{cs}]_{DSS} &\approx 0.87 \sigma'_{zo} = 0.87 \times 45 = 39 \text{ kPa} \end{aligned}$$

What's next . . . We have estimated failure stresses. We also need to know the deformations or strains. But before we can get the strains from the stresses we need to know the elastic, shear, and bulk moduli. In the next section, we will use the CSM to determine these moduli.

11.8 SOIL STIFFNESS

The effective elastic modulus, E' , or the shear modulus, G , and the effective bulk modulus, K' , characterize soil stiffness. In practice, E' or G and K' are commonly obtained from triaxial or simple shear tests. We can obtain an estimate of E' or G and K' using the critical state model and results from axisymmetric, isotropic consolidation tests. The void ratio during unloading/reloading is described by

$$e = e_k - \kappa \ln p' \quad (11.99)$$

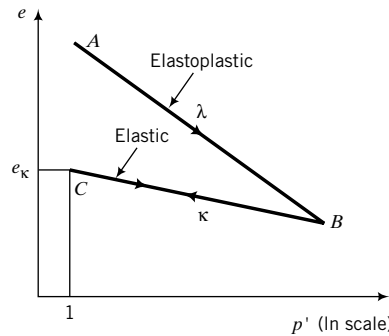


FIGURE 11.40 Loading and unloading/reloading (elastic) response of soils in $(\ln p', e)$ space.

where e_k is the void ratio on the unloading/reloading line at $p' = 1$ unit of stress (Figure 11.40). The unloading/reloading path BC (Figure 11.40) is reversible, which is a characteristic of elastic materials. Differentiating Equation (11.99) gives

$$de = -\kappa \frac{dp'}{p'} \quad (11.100)$$

The elastic volumetric strain increment is

$$d\varepsilon_p^e = -\frac{de}{1 + e_o} = \frac{\kappa}{1 + e_o} \frac{dp'}{p'} \quad (11.101)$$

But, from Equation (8.17),

$$d\varepsilon_p^e = \frac{dp'}{K'}$$

Therefore,

$$\frac{dp'}{K'} = \frac{\kappa}{1 + e_o} \frac{dp'}{p'}$$

Solving for K' , we obtain

$$K' = \frac{p'(1 + e_o)}{\kappa} \quad (11.102)$$

From Equation (8.18),

$$E' = 3K'(1 - 2\nu')$$

Therefore,

$$E' = \frac{3p'(1 + e_o)(1 - 2\nu')}{\kappa} \quad (11.103)$$

Also, from Equation (8.20),

$$G = \frac{E'}{2(1 + \nu')}$$

Therefore,

$$G = \frac{3p'(1 + e_o)(1 - 2\nu')}{2\kappa(1 + \nu')} = \frac{1.5p'(1 + e_o)(1 - 2\nu')}{\kappa(1 + \nu')} \quad (11.104)$$

Equations (11.106) and (11.104) indicate that the elastic constants, E' and G , are proportional to the mean effective stress. This implies nonlinear elastic behavior, and therefore calculations must be

carried out incrementally. For overconsolidated soils, Equations (11.103) and (11.104) provide useful estimates of E' and G from conducting an isotropic consolidation test, which is a relatively simple soil test. However, it was argued (Zytnski et al., 1978) that relating E' , G , and K' to the in situ stress state leads to unrealistically low values for fine-grained soils. Randolph et al. (1979) recommended that G should be related to the historically maximum value of K' , such that

$$K'_{max} = \frac{1 + e_c}{\kappa} p'_c \quad (11.105)$$

where p'_c is the preconsolidation mean effective stress and e_c is the void ratio corresponding to p'_c .

$$e_c = e_o - \kappa \ln \frac{p'_c}{p'_o} = e_o - \kappa \ln R_o \quad (11.106)$$

Therefore, from Equation (8.18),

$$E' = \frac{3 p'_c (1 + e_c) (1 - 2\nu')}{\kappa} \quad (11.107)$$

From Equation (8.20),

$$G = \frac{1.5 p'_c (1 + e_c) (1 - 2\nu')}{\kappa (1 + \nu')} \quad (11.108)$$

In this textbook, we will continue to use Equations (11.103) and (11.104) to maintain the simple framework of CSM. For practical geotechnical problems, you should consider using Equations (11.105), (11.107), and (11.108) for fine-grained soils.

Soil stiffness is influenced by the amount of shear strains applied. Increases in shear strains tend to lead to decreases in G and E' , while increases in volumetric strains lead to decreases in K' . The net effect is that the soil stiffness decreases with increasing strains.

It is customary to identify three regions of soil stiffness based on the level of applied shear strains. At small shear strains (γ or ϵ_q usually $< 0.001\%$), the soil stiffness is approximately constant (Figure 11.41) and the soil behaves like a linearly elastic material. At intermediate shear strains between 0.001% and 1%, the soil stiffness decreases significantly and the soil behavior is elastoplastic (nonlinear). At large strains ($\gamma > 1\%$), the soil stiffness decreases slowly to an approximately constant value as the soil approaches critical state. At the critical state, the soil behaves like a viscous fluid.

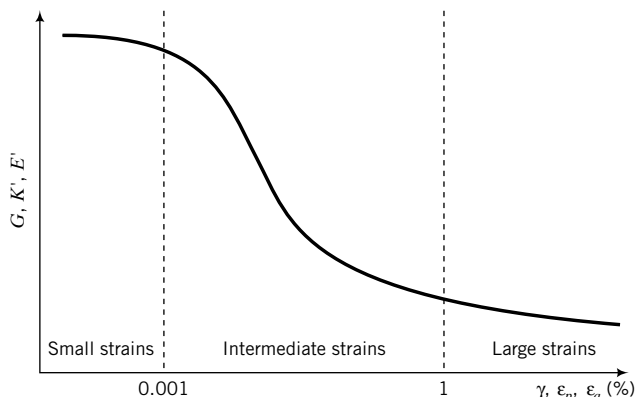


FIGURE 11.41 Schematic variation of shear, bulk, and Young's elastic moduli with strain levels.

In practical problems, the shear strains are in the intermediate range, typically $\gamma < 0.1\%$. However, the shear strain distribution within the soil is not uniform. The shear strains decrease with distance away from a structure, and local shear strains near the edge of a foundation slab, for example, can be much greater than 0.1%. The implication of a nonuniform shear strain distribution is that the soil stiffness varies within the loaded region of the soil. Consequently, large settlements and failures are usually initiated in the loaded soil region where the soil stiffness is the lowest.

In conventional laboratory tests, it is not practical to determine the soil stiffness at shear strains less than 0.001% because of inaccuracies in the measurement of the soil displacements due to displacements of the apparatuses themselves and to resolution and inaccuracies of measuring instruments. The soil stiffness at small strains is best determined in the field using wave propagation techniques. In one such technique, vibrations are created at the soil surface or at a prescribed depth in the soil, and the shear wave velocity (V_{sh}) is measured. The shear modulus at small strains is calculated from

$$G = \frac{\gamma(V_{sh})^2}{g} \quad (11.109)$$

where γ is the bulk unit weight of the soil and g is the acceleration due to gravity. In the laboratory, the shear modulus at small strains can be determined using a resonance column test (Drnevich, 1967). The resonance column test utilizes a hollow-cylinder apparatus (Chapter 10) to induce resonance of the soil sample. Resonance column tests show that G depends not only on the level of shear strain but also on void ratio, overconsolidation ratio, and mean effective stress. Various empirical relationships have been proposed linking G to e , overconsolidation ratio, and p' . Two such relationships are presented below.

Jamiolkowski et al. (1985) for Clays

$$G = \frac{198}{e^{1.3}} (R_o)^a \sqrt{p'} \text{ MPa} \quad (11.110)$$

where G is the initial shear modulus, p' is the mean effective stress (MPa), and a is a coefficient that depends on the plasticity index, as follows:

PI (%)	<i>a</i>
0	0
20	0.18
40	0.30
60	0.41
80	0.48
≥ 100	0.50

Seed and Idriss (1970) for Sands

$$G = k_1 \sqrt{p'} \text{ MPa} \quad (11.111)$$

<i>e</i>	<i>k</i> ₁	<i>D</i> _r (%)	<i>k</i> ₁
0.4	484	30	235
0.5	415	40	277
0.6	353	45	298
0.7	304	60	360
0.8	270	75	408
0.9	235	90	484

EXAMPLE 11.15 Calculation of Soil Stiffness

The in situ water content of a saturated soil sample taken at a depth of 5 m is 37%. The groundwater level is at 6 m below the surface. The results from a one-dimensional consolidation test on the sample are $\lambda = 0.3$, $\kappa = 0.05$, and $OCR = 1$. If $K_o = 0.5$ and $\nu' = 0.3$, calculate the effective elastic and bulk moduli and the shear modulus.

Strategy The solution to this problem is a straightforward application of stiffness equations.

Solution 11.15

Step 1: Determine the initial void ratio.

$$e = wG_s = 0.37 \times 2.7 = 1.0$$

Step 2: Determine the initial mean effective stress.

$$\gamma_{sat} = \left(\frac{G_s + e_o}{1 + e_o} \right) \gamma_w = \left(\frac{2.7 + 1}{1 + 1} \right) 9.8 = 18.1 \text{ kN/m}^3$$

$$\sigma'_{zo} = \gamma_{sat}z = 18.1 \times 5 = 90.5 \text{ kPa}$$

$$p'_o = \frac{(1 + 2K_o)}{3} \sigma'_{zo} = \frac{1 + 2 \times 0.5}{3} \times 90.5 = 60.3 \text{ kPa}$$

Step 3: Determine stiffnesses.

$$E' = \frac{3p'(1 + e_o)(1 - 2\nu')}{\kappa} = \frac{3 \times 90.5(1 + 1)(1 - 2 \times 0.3)}{0.05} = 4344 \text{ kPa}$$

$$K' = \frac{p'(1 + e_o)}{\kappa} = \frac{90.5 \times (1 + 1)}{0.05} = 3620 \text{ kPa}$$

$$G = \frac{E'}{2(1 + \nu')} = \frac{4344}{2 \times (1 + 0.3)} = 1671 \text{ kPa}$$

What's next . . . Now that we know how to calculate the shear and bulk moduli, we can move on to determine strains, which we will consider next.

11.9 STRAINS FROM THE CRITICAL STATE MODEL

11.9.1 Volumetric Strains

The total change in volumetric strains consists of two parts: the recoverable part (elastic) and the unrecoverable part (plastic). We can write an expression for the total change in volumetric strain as

$$\Delta\varepsilon_p = \Delta\varepsilon_p^e + \Delta\varepsilon_p^p \quad (11.112)$$

where the superscripts e and p denote elastic and plastic, respectively. Let us consider a soil sample that is isotropically consolidated to a mean effective stress p'_c and unloaded to a mean effective stress p'_o , as represented by ACO in Figure 11.42a and b. In a CD test, the soil will yield at D . Let us now consider a small increment of stress, DE , which causes the yield surface to expand, as shown in Figure 11.42a.

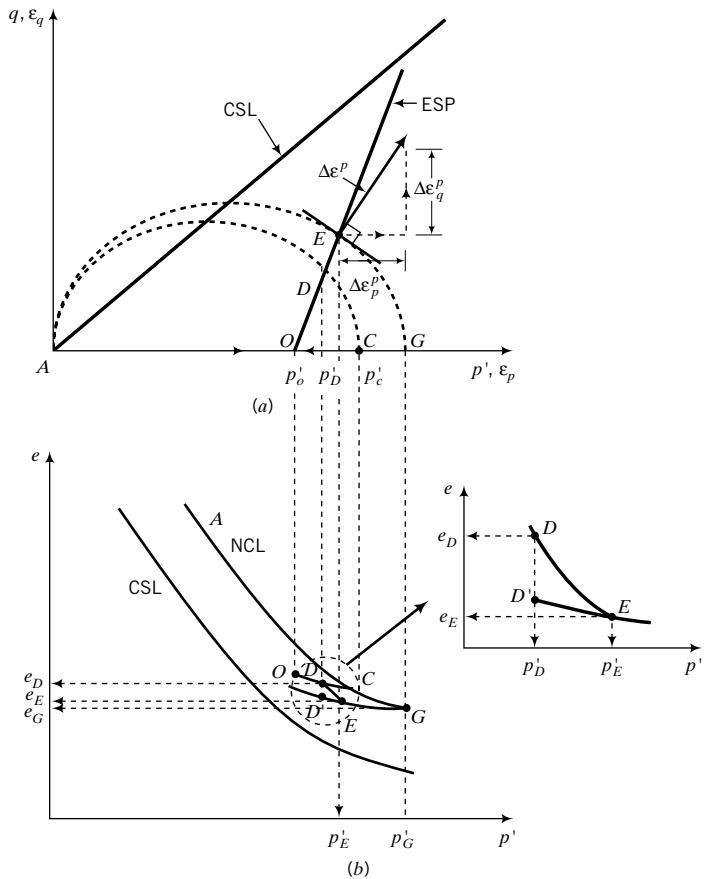


FIGURE 11.42 Determination of plastic strains.

The change in void ratio for this stress increment is $\Delta e = e_D - e_C$ (Figure 11.42).

$$e_D = e_C + \kappa \ln \frac{p'_C}{p'_D}$$

$$e_E = e_G + \kappa \ln \frac{p'_G}{p'_E}$$

but

$$e_G = e_C + \lambda \ln \frac{p'_G}{p'_C}$$

Therefore,

$$e_D - e_C = \Delta e = (\lambda - \kappa) \ln \left(\frac{p'_G}{p'_C} \right) + \kappa \ln \left(\frac{p'_E}{p'_D} \right)$$

The corresponding total change in volumetric strain is

$$\Delta \epsilon_p = \frac{\Delta e}{1 + e_o} = \frac{1}{1 + e_o} \left\{ (\lambda - \kappa) \ln \frac{p'_G}{p'_C} + \kappa \ln \frac{p'_E}{p'_D} \right\} \quad (11.113)$$

The volumetric elastic strain component is represented by ED' . That is, if you were to unload the soil from E back to its previous stress state at D , the rebound would occur along an unloading/reloading line associated with the maximum mean effective stress for the yield surface on which unloading starts. The elastic change in volumetric strain from E to D' is

$$\Delta\epsilon_p^e = \frac{\Delta e}{1 + e_o} = \frac{e_{D'} - e_E}{1 + e_o} = \frac{\kappa}{1 + e_o} \ln \frac{p'_E}{p'_D} \quad (11.114)$$

We get a positive value of $\Delta\epsilon_p^e$ because rather than computing the rebound (expansion) from E to D' , we compute the compression from D' to E .

The volumetric elastic strains can also be computed from Equation (8.17) as

$$\Delta\epsilon_p^e = \frac{\Delta p'}{K'} \quad (11.115)$$

The change in volumetric plastic strain is

$$\Delta\epsilon_p^p = \Delta\epsilon_p - \Delta\epsilon_p^e = \left(\frac{\lambda - \kappa}{1 + e_o} \right) \ln \frac{p'_G}{p'_C} \quad (11.116)$$

Under undrained conditions, the total volumetric change is zero. Consequently, from Equation (11.112),

$$\Delta\epsilon_p^e = -\Delta\epsilon_p^p \quad (11.117)$$

11.9.2 Shear Strains

Let the yield surface be represented by

$$F = (p')^2 - p'p'_c + \frac{q^2}{M^2} = 0 \quad (11.118)$$

To find the shear or deviatoric strains, we will assume that the resultant plastic strain increment, $\Delta\epsilon^p$, for an increment of stress is normal to the yield surface (Figure 11.42a). Normally, the plastic strain increment should be normal to a plastic potential function, but we are assuming here that the plastic potential function, and the yield surface (yield function, F) are the same. A plastic potential function is a scalar quantity that defines a vector in terms of its location in space. Classical plasticity demands that the surfaces defined by the yield and plastic potential coincide. If they do not, then basic work restrictions are violated. However, advanced soil mechanics theories often use different surfaces for yield and potential functions to obtain more realistic stress-strain relationships. The resultant plastic strain increment has two components—a deviatoric or shear component, $\Delta\epsilon_q^p$, and a volumetric component, $\Delta\epsilon_p^p$, as shown in Figure 11.42a. We already found $\Delta\epsilon_p^p$ in the previous section.

Since we know the equation for the yield surface [Equation (11.118)], we can find the normal to it by differentiation of the yield function with respect to p' and q . The tangent or slope of the yield surface is

$$dF = 2p'dp' - p'_cdp' + 2q \frac{dq}{M^2} = 0 \quad (11.119)$$

Rearranging Equation (11.119), we obtain the slope as

$$\frac{dq}{dp'} = \left(\frac{p'_c/2 - p'}{q/M^2} \right) \quad (11.120)$$

The normal to the yield surface is

$$-\frac{1}{dq/dp'} = -\frac{dp'}{dq}$$

From Figure 11.42a, the normal, in terms of plastic strains, is $d\epsilon_q^p/d\epsilon_p^p$. Therefore,

$$\frac{d\epsilon_q^p}{d\epsilon_p^p} = -\frac{dp'}{dq} = -\frac{q/M^2}{p_c'/2 - p'} \quad (11.121)$$

which leads to

$$d\epsilon_q^p = d\epsilon_p^p \frac{q}{M^2(p' - p_c'/2)} \quad (11.122)$$

The elastic shear strains can be obtained from Equation (8.19) as

$$\Delta\epsilon_q^e = \frac{1}{3G} \Delta q \quad (11.123)$$

These equations for strain increments are valid only for small changes in stress. For example, you cannot use these equations to calculate the failure strains by simply substituting the failure stresses for p' and q . You have to calculate the strains for small increments of stresses up to failure and then sum each component of strain separately. We need to do this because the critical state model considers soils as elastoplastic materials and not linearly elastic materials.

EXAMPLE 11.16 Calculation of Strains

A sample of clay was isotropically consolidated to a mean effective stress of 225 kPa and was then unloaded to a mean effective stress of 150 kPa, at which stress $\epsilon_o = 1.4$. A standard triaxial CD test is to be conducted. Calculate (a) the elastic strains at initial yield, and (b) the total volumetric and deviatoric strains for an increase of deviatoric stress of 12 kPa after initial yield. For this clay, $\lambda = 0.16$, $\kappa = 0.05$, $\phi_{cs}' = 25.5^\circ$, and $v' = 0.3$.

Strategy It is best to sketch diagrams similar to Figure 11.4 to help you visualize the solution to this problem. Remember that the strains within the yield surface are elastic.

Solution 11.16

Step 1: Calculate initial stresses, R_o and M_c .

$$p'_c = 225 \text{ kPa}, \quad p'_o = 150 \text{ kPa}$$

$$R_o = \frac{225}{150} = 1.5$$

$$M_c = \frac{6 \sin \phi_{cs}'}{3 - \sin \phi_{cs}'} = \frac{6 \sin 25.5^\circ}{3 - \sin 25.5^\circ} = 1$$

Step 2: Determine the initial yield stresses.

The yield stresses are the stresses at the intersection of the initial yield surface and the effective stress path.

$$\text{Equation for the yield surface: } (p')^2 - p'p'_c + \frac{q^2}{M_c^2} = 0$$

$$\text{Equation of the ESP: } p' = p'_o + \frac{q}{3}$$

$$\text{At the initial yield point } D \text{ (Figure 11.4): } p'_y = p'_o + \frac{q_y}{3} = 150 + \frac{q_y}{3}$$

Substituting $p' = p'_y$, $q = q_y$, and the values for M_c and p'_c into the equation for the initial yield surface [Equation (11.4a)] gives

$$\left(150 + \frac{q_y}{3}\right)^2 - \left(150 + \frac{q_y}{3}\right)225 + \frac{q_y^2}{1^2} = 0$$

Simplification results in

$$q_y^2 + 22.5q_y - 10,125 = 0$$

The solution for q_y is $q_y = 90$ kPa or $q_y = -112.5$ kPa. The correct answer is $q_y = 90$ kPa since we are applying compression to the soil sample. Therefore,

$$p'_y = 150 + \frac{q'_y}{3} = 150 + \frac{90}{3} = 180 \text{ kPa}$$

Step 3: Calculate the elastic strains at initial yield.

Elastic volumetric strains

$$\text{Elastic volumetric strains: } \Delta\epsilon_p^e = \frac{\kappa}{1 + e_o} \ln \frac{p'_y}{p'_o} = \frac{0.05}{1 + 1.4} \ln \frac{180}{150} = 38 \times 10^{-4}$$

Alternatively, you can use Equation (11.115). Take the average value of p' from p'_o to p'_y to calculate K' .

$$p'_{av} = \frac{p'_o + p'_y}{2} = \frac{150 + 180}{2} = 165 \text{ kPa}$$

$$K' = \frac{p'(1 + e_o)}{\kappa} = \frac{165(1 + 1.4)}{0.05} = 7920 \text{ kPa}$$

$$\Delta\epsilon_p^e = \frac{\Delta p'}{K'} = \frac{180 - 150}{7920} = 38 \times 10^{-4}$$

Elastic shear strains

$$G = \frac{1.5p'(1 + e_o)(1 - 2\nu')}{\kappa(1 + \nu')} = \frac{1.5 \times 165(1 + 1.4)(1 - 2 \times 0.3)}{0.05(1 + 0.3)} = 3655 \text{ kPa}$$

$$\Delta\epsilon_q^e = \frac{\Delta q}{3G} = \frac{90}{3 \times 3655} = 82 \times 10^{-4}$$

Alternatively:

Void ratio corresponding to p'_c is:

$$e_c = e_o - \kappa \ln \frac{p'_c}{p'_o} = 1.4 - 0.05 \ln \frac{225}{150} = 1.38$$

$$\text{Equation (11.115): } K'_{max} = \frac{1 + e_c}{\kappa} p'_c = \frac{1 + 1.38}{0.05} \times 225 = 10,710 \text{ kPa}$$

$$\text{Equation (11.108): } G = \frac{1.5p'_c(1 + e_c)(1 - 2\nu')}{\kappa(1 + \nu')} = \frac{1.5 \times 225 \times (1 + 1.38)(1 - 2 \times 0.3)}{0.05(1 + 0.3)} = 4943 \text{ kPa}$$

The elastic shear strains computed using G from Equation (11.108) would be $\left(\frac{4943 - 3655}{3655}\right) \times 100 = 35\%$

less than using G from Equation (11.104). For heavily overconsolidated clays, Equation (11.108) would give more realistic values of G than Equation (11.104). For this problem, we will continue to use Equation (11.104).

Step 4: Determine expanded yield surface.

After initial yield: $\Delta q = 12 \text{ kPa}$

$$\therefore \Delta p' = \frac{\Delta q}{3} = \frac{12}{3} = 4 \text{ kPa}$$

The stresses at E (Figure 11.4) are $p'_E = p'_y + \Delta p = 180 + 4 = 184 \text{ kPa}$, and

$$q_E = q_y + \Delta q = 90 + 12 = 102 \text{ kPa}$$

The preconsolidation mean effective stress (major axis) of the expanded yield surface is obtained by substituting $p'_E = 184 \text{ kPa}$ and $q_E = 102 \text{ kPa}$ in the equation for the yield surface [Equation (11.4e)]:

$$p'_c = p'_o + \frac{q^2}{M^2 p'_o} = 184 + \frac{102^2}{1^2 \times 184} = 240.5 \text{ kPa}$$

Step 5: Calculate strain increments after yield.

$$\begin{aligned} \Delta \varepsilon_p &= \frac{1}{1 + e_o} \left\{ (\lambda - \kappa) \ln \frac{p'_G}{p'_C} + \kappa \ln \frac{p'_E}{p'_D} \right\} = \frac{1}{1 + 1.4} \left\{ (0.16 - 0.05) \ln \frac{240.5}{225} + 0.05 \ln \frac{184}{180} \right\} = 35 \times 10^{-4} \\ \Delta \varepsilon_p^p &= \frac{\lambda - \kappa}{1 + e_o} \ln \frac{p'_G}{p'_C} = \frac{0.16 - 0.05}{1 + 1.4} \ln \frac{240.5}{225} = 31 \times 10^{-4} \\ \Delta \varepsilon_q^p &= \Delta \varepsilon_p^p \frac{q_E}{M_c^2 [p'_E - (p'_c)_E/2]} = 31 \times 10^{-4} \frac{102}{1^2 (184 - 240.5/2)} \\ &= 50 \times 10^{-4} \end{aligned}$$

Assuming that G remains constant, we can calculate the elastic shear strain from

$$\text{Equation (11.123): } \Delta \varepsilon_q^e = \frac{\Delta q}{3G} = \frac{12}{3 \times 3655} = 11 \times 10^{-4}$$

Step 6: Calculate total strains.

$$\text{Total volumetric strains: } \varepsilon_p = \Delta \varepsilon_p^e + \Delta \varepsilon_p = (38 + 35)10^{-4} = 73 \times 10^{-4}$$

$$\text{Total shear strains: } \varepsilon_q = \Delta \varepsilon_q^e + \Delta \varepsilon_q^p = [(82 + 11) + 50]10^{-4} = 173 \times 10^{-4}$$

EXAMPLE 11.17 Expansion of Yield Surface

Show that the yield surface in an undrained test increases such that

$$p'_c = (p'_c)_{prev} \left(\frac{p'_{prev}}{p'} \right)^{\kappa/(\lambda - \kappa)}$$

where p'_c is the current value of the major axis of the yield surface, $(p'_c)_{prev}$ is the previous value of the major axis of the yield surface, p'_{prev} is the previous value of mean effective stress, and p' is the current value of mean effective stress.

Strategy Sketch an e versus $\ln p'$ diagram and then use it to prove the equation given.

Solution 11.17

Step 1: Sketch an e versus $\ln p'$ diagram.

See Figure E11.17.

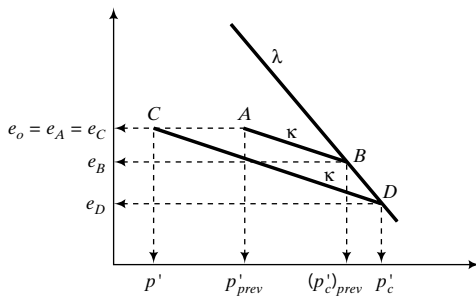


FIGURE E11.17

Step 2: Prove the equation.

Line AB

$$e_B - e_A = \kappa \ln \left(\frac{(p'_c)_{prev}}{p'_{prev}} \right) \quad (1)$$

Line CD

$$e_D - e_C = \kappa \ln \frac{p'_c}{p'} \quad (2)$$

Subtracting Equation (2) from Equation (1), noting that $e_A = e_C$, we obtain

$$e_D - e_B = \kappa \ln \left\{ \frac{(p'_c)_{prev}}{p'_{prev}} \right\} - \kappa \ln \frac{p'_c}{p'} \quad (3)$$

But, from the normal consolidation line BD, we get

$$e_D - e_B = \lambda \ln \left\{ \frac{p'_c}{(p'_c)_{prev}} \right\} \quad (4)$$

Substituting Equation (4) into Equation (3) and simplifying gives

$$\begin{aligned} \lambda \ln \left[\frac{p'_c}{(p'_c)_{prev}} \right] &= \kappa \ln \left[\frac{(p'_c)_{prev}}{(p')_{prev}} \right] - \kappa \ln \left(\frac{p'_c}{p'} \right) \\ p'_c &= (p'_c)_{prev} \left(\frac{p'_{prev}}{p'} \right)^{\kappa / (\lambda - \kappa)} \end{aligned}$$

What's next . . . We have calculated the yield stresses, the failure stresses, and strains for a given stress increment. In the next section, a procedure is outlined to calculate the stress-strain, volume change, and excess porewater pressure responses of a soil using the critical state model.

11.10 CALCULATED STRESS-STRAIN RESPONSE



Computer Program Utility

Access www.wiley.com/college/budhu and click Chapter 11 and the criticalstate.xls to calculate and plot the stress-strain responses of drained and undrained compression tests. You can predict the stress-strain response, volume changes, and excess porewater pressure from the initial stress state to the failure stress state using the methods described in the previous sections. The required soil parameters are p'_o , e_o , p'_c , or OCR, λ , κ , ϕ'_{cs} , and v' . The procedures for a given stress path are as follows.

11.10.1 Drained Compression Tests

- Determine the mean effective stress and the deviatoric stress at initial yield, that is, p'_y and q_y , by finding the coordinates of the intersection of the initial yield surface with the effective stress path. For a CD test,

$$p'_y = \frac{(M^2 p'_c + 2n_o^2 p'_o) + \sqrt{(M^2 p'_c + 2n_o^2 p'_o)^2 - 4n_o^2(M^2 + n_o^2)(p'_o)^2}}{2(M^2 + n_o^2)} \quad (11.124)$$

$$q_y = n_o(p'_y - p'_o) \quad (11.125)$$

where n_o is the slope of the ESP and $M = M_c$. For the standard triaxial drained test, $n_o = 3$.

- Calculate the mean effective stress and deviatoric stress at failure using Equations (11.19) and (11.20).
- Calculate G using Equation (11.104) or Equation (11.108). Use an average value of $p' [p' = (p'_o + p'_f)/2]$ to calculate G if Equation (11.108) is used.
- Calculate the initial elastic volumetric strain using Equation (11.115) and initial elastic deviatoric strain using Equation (11.123).
- Divide the ESP between the initial yield stresses and the failure stresses into a number of equal stress increments. Small increment sizes (<5% of the stress difference between q_f and q_y) tend to give a more accurate solution than larger increment sizes.

For each mean effective stress increment up to failure:

- Calculate the preconsolidation stress, p'_c , for each increment; that is, you are calculating the major axis of the ellipse using Equation (11.4e).
- Calculate the total volumetric strain increment using Equation (11.113).
- Calculate the plastic volumetric strain using Equation (11.116).
- Calculate the plastic deviatoric strain increment using Equation (11.122).
- Calculate the elastic deviatoric strain increment using Equation (11.123).
- Add the plastic and elastic deviatoric strain increments to give the total deviatoric strain increment.
- Sum the total volumetric strain increments (ϵ_p).
- Sum the total deviatoric shear strain increments (ϵ_q).
- Calculate

$$\epsilon_1 = \frac{3\epsilon_q + \epsilon_p}{3} = \epsilon_q + \frac{\epsilon_p}{3} \quad (11.126)$$

- If desired, you can calculate the principal effective stresses for axisymmetric compression from

$$\sigma'_1 = \frac{2q}{3} + p' \quad \text{and} \quad \sigma'_3 = p' - \frac{q}{3} \quad (11.127)$$

The last value of mean effective stress should be about $0.99p'_f$ to prevent instability in the solution.

11.10.2 Undrained Compression Tests

- Determine the mean effective stress and the deviatoric stress at initial yield, that is, p'_y and q_y . Remember that the effective stress path within the initial yield surface is vertical. Therefore, $p_y (= p'_o)$ and q_y are found by determining the intersection of a vertical line originating at p'_o with the initial yield surface. The equation to determine q_y for an isotropically consolidated soil is

$$q_y = Mp'_o \sqrt{\frac{p'_c}{p'_o} - 1} \quad (11.128)$$

If the soil is heavily overconsolidated, then $q_y = q_p$.

2. Calculate the mean effective and deviatoric stress at failure from Equations (11.41) and (11.16).
3. Calculate G using Equation (11.104) or Equation (11.108).
4. Calculate the initial elastic deviatoric strain from Equation (11.123).
5. Divide the horizontal distance between the initial mean effective stress, p'_o , and the failure mean effective stress, p'_f , in the (p', e) plot into a number of equal mean effective stress increments. You need to use small stress increment size, usually less than $0.05(p'_o - p'_f)$.

For each increment of mean effective stress, calculate the following:

6. Determine the preconsolidation stress after each increment of mean effective stress from

$$p'_c = (p'_c)_{prev} \left(\frac{p'_{prev}}{p'} \right)^{\kappa/(\lambda-\kappa)}$$

where the subscript *prev* denotes the previous increment, p'_c is the current preconsolidation stress or the current size of the major axis of the yield surface, and p' is the current mean effective stress.

7. Calculate q at the end of each increment from

$$q = Mp' \sqrt{\frac{p'_c}{p'} - 1}$$

8. Calculate the volumetric elastic strain increment from Equation (11.115).
9. Calculate the volumetric plastic strain increment. Since the total volumetric strain is zero, the volumetric plastic strain increment is equal to the negative of the volumetric elastic strain increment; that is, $\Delta\varepsilon_p^p = -\Delta\varepsilon_p^e$.
10. Calculate the deviatoric plastic strain increment from Equation (11.122).
11. Calculate the deviatoric elastic strain increment from Equation (11.123).
12. Add the deviatoric elastic and plastic strain increments to get the total deviatoric strain increment.
13. Sum the total deviatoric strain increments. For undrained conditions, $\varepsilon_1 = \varepsilon_q$.
14. Calculate the current mean total stress from the TSP. Remember, you know the current value of q from Step 7. For a standard triaxial CU test, $p = p'_o + q/n_o$ where $n_o = 3$.
15. Calculate the change in excess porewater pressure by subtracting the current mean effective stress from the current mean total stress.

EXAMPLE 11.18 Predicting Stress-Strain Responses for Drained and Undrained Conditions



Computer Program Utility

Access www.wiley.com/college/budhu and click Chapter 11 and the criticalstate.xls to calculate and plot the stress-strain responses of drained and undrained compression tests. You can predict the stress-strain response, volume changes, and excess porewater pressure from the initial stress state to the failure stress state using the methods described in the previous sections. The required soil parameters are p'_o , e_o , p'_c , or OCR , λ , κ , ϕ'_{cs} , and ν' . The procedures for a given stress path are as follows.

Estimate and plot the stress-strain curve, volume changes (drained conditions), and excess porewater pressures (undrained conditions) for two samples of the same soil. The first sample, sample A, is to be subjected to conditions similar to a standard triaxial CD test, and the second sample, sample B, is to be subjected to conditions similar to a

standard triaxial CU test. The soil parameters are $\lambda = 0.25$, $\kappa = 0.05$, $\phi'_{cs} = 24^\circ$, $v' = 0.3$, $e_o = 1.15$, $p'_o = 200$ kPa, and $p'_c = 250$ kPa.

Strategy Follow the procedures listed in Section 11.9. A spreadsheet can be prepared to do the calculations. However, you should manually check some of the spreadsheet results to be sure that you entered the correct formulation. A spreadsheet will be used here, but we will calculate the results for one increment for each sample.

Solution 11.18

$$\text{Calculate } M_c: \quad M_c = \frac{6 \sin \phi'_{cs}}{3 - \sin \phi'_{cs}} = \frac{6 \sin 24^\circ}{3 - \sin 24^\circ} = 0.94$$

$$\begin{aligned} \text{Calculate } e_r: \quad e_r &= e_o + (\lambda - \kappa) \ln \frac{p'_c}{2} + \kappa \ln p'_o \\ &= 1.15 + (0.25 - 0.05) \ln \frac{250}{2} + 0.05 \ln 200 = 2.38 \end{aligned}$$

For the standard triaxial test, $n_o = 3$.

Each step corresponds to the procedures listed in Section 11.9.

Sample A, Drained Test

Step 1:

$$\begin{aligned} p'_y &= \frac{(M^2 p'_c + 2n_o^2 p'_o) + \sqrt{(M^2 p'_c + 2n_o^2 p'_o)^2 - 4n_o^2(M^2 + n_o^2)(p'_o)^2}}{2(M^2 + n_o^2)} \\ &= \frac{(0.94^2 \times 250 + 2 \times 9 \times 200) + \sqrt{(0.94^2 \times 250 + 2 \times 9 \times 200)^2 - 4 \times 9 \times (0.94^2 + 9)(200)^2}}{2(0.94^2 + 9)} \\ &= 224 \text{ kPa} \\ q_y &= 3(p'_y - p'_o) = 3(224 - 200) = 72 \text{ kPa} \end{aligned}$$

Step 2:

$$p'_f = \frac{3p'_o}{3 - M};$$

$$p'_f = \frac{3 \times 200}{3 - 0.94} = 291.3 \text{ kPa}, \quad q_f = Mp'_f = 0.94 \times 291.3 = 273.8 \text{ kPa}$$

Step 3:

$$p'_{av} = \frac{200 + 224}{2} = 212 \text{ kPa}$$

$$G = \frac{1.5p'(1 + e_o)(1 - 2v')}{\kappa(1 + v')} = \frac{1.5 \times 212(1 + 1.15) \times (1 - 2 \times 0.3)}{0.05(1 + 0.3)} = 4207 \text{ kPa}$$

Step 4:

$$(\Delta \epsilon_q^e)_{initial} = \frac{\Delta q}{3G} = \frac{71.9}{3 \times 4207} = 5.7 \times 10^{-3}$$

$$(\Delta \epsilon_p^e)_{initial} = \frac{\kappa}{1 + e_o} \ln \frac{p'_y}{p'_o} = \frac{0.05}{1 + 1.15} \ln \frac{224}{200} = 2.6 \times 10^{-3}$$

Step 5:

Let $\Delta p' = 4$ kPa; then $\Delta q = n_o \times \Delta p' = 3 \times 4 = 12$ kPa.

First stress increment after the initial yield follows.

Step 6:

$$p' = 224 + 4 = 228 \text{ kPa}, \quad q = 71.9 + 12 = 83.9 \text{ kPa}$$

$$p'_c = p' + \frac{q^2}{M^2 p'} = 228 + \frac{83.9^2}{0.94^2 \times 228} = 262.9 \text{ kPa}$$

Step 7: $\Delta\epsilon_p = \frac{1}{1+e_o} \left\{ (\lambda - \kappa) \ln \frac{p'_G}{p'_c} + \kappa \ln \frac{p'_E}{p'_D} \right\} = \frac{1}{1+1.15} \left\{ (0.25 - 0.05) \ln \frac{262.9}{250} + 0.05 \ln \frac{228}{224} \right\} = 5.1 \times 10^{-3}$

Step 8: $\Delta\epsilon_p^p = \frac{\lambda - \kappa}{1+e_o} \ln \frac{p_G}{p'_c} = \frac{(0.25 - 0.05)}{1+1.15} \ln \frac{262.9}{250} = 4.6 \times 10^{-3}$

Step 9: $\Delta\epsilon_q^p = \Delta\epsilon_p^p \frac{q}{M^2(p' - p'_c/2)} = 4.6 \times 10^{-3} \frac{83.9}{0.94^2(228 - 262.9/2)} = 4.5 \times 10^{-3}$

Step 10: Assuming G is constant,

$$\Delta\epsilon_q^e = \frac{\Delta q}{3G} = \frac{12}{3 \times 4207} = 1.0 \times 10^{-3}$$

Step 11: $\Delta\epsilon_q = \Delta\epsilon_q^e + \Delta\epsilon_q^p = (1.0 + 4.5) \times 10^{-3} = 5.5 \times 10^{-3}$

Step 12: $\epsilon_p = (\Delta\epsilon_p^e)_{initial} + \Delta\epsilon_p = (2.6 + 5.1) \times 10^{-3} = 7.7 \times 10^{-3}$

Step 13: $\epsilon_q = (\Delta\epsilon_q^e)_{initial} + \Delta\epsilon_q = (5.7 + 5.5) \times 10^{-3} = 11.2 \times 10^{-3}$

Step 14: $\epsilon_1 = \epsilon_q + \frac{\epsilon_p}{3} = \left(11.2 + \frac{7.7}{3} \right) \times 10^{-3} = 13.8 \times 10^{-3}$

The spreadsheet program and the stress-strain plots are shown in the table below and in Figure E11.18a, b. There are some slight differences between the calculated values shown above and the spreadsheet because of number rounding.

Drained Case

Given data		Calculated values			
λ	0.25	M	0.94	$\Delta p'$	4 kPa*
κ	0.05	R_o	1.25	Δq	12 kPa
ϕ'_{cs}	24	e_f	2.38	G	4207.0 kPa
e_o	1.15	p'_f	291.4 kPa	$\Delta\epsilon_p^e$	0.0026
p'_o	200 kPa	q_f	274.2 kPa	$\Delta\epsilon_q^e$	0.0057
p'_c	250 kPa	p'_v	224.0 kPa		
v'	0.3	q_v	71.9 kPa		

*Selected increment.

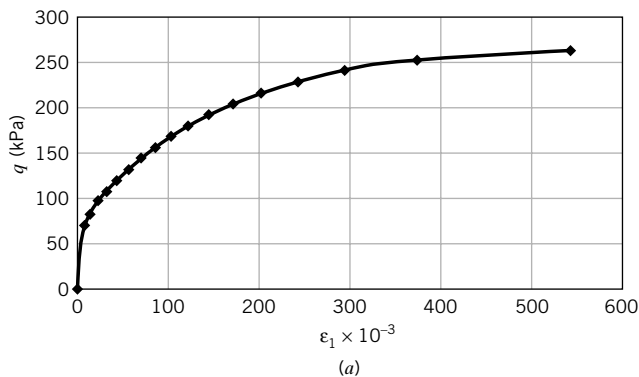
Tabulation

p' (kPa)	$\Sigma\Delta q$ (kPa)	q (kPa)	p'_c (kPa)	$\Delta\epsilon_p \times 10^{-3}$	$\epsilon_p = \sum \Delta\epsilon_p \times 10^{-3}$	$\epsilon_p^p \times 10^{-3}$	$\epsilon_q^p \times 10^{-3}$	$\epsilon_q^e \times 10^{-3}$	$\Delta\epsilon_q \times 10^{-3}$	$\Delta\epsilon_q = \sum \epsilon_q \times 10^{-3}$	$\epsilon_1 \times 10^{-3}$
0	0	0	0	0.0	0.0	0.0	0.0	0.0	0.0	0.0	0.0
224.0	0.0	71.9	250.0	2.6	2.6	0.0	0.0	5.7	5.7	5.7	6.6
228.0	12.0	83.9	262.8	5.1	7.7	4.6	4.6	1.0	5.5	11.2	13.8
232.0	24.0	95.9	276.7	6.4	14.1	4.8	5.5	1.0	6.5	177	22.4
236.0	36.0	107.9	291.6	6.5	20.6	4.9	6.6	1.0	7.6	25.3	32.1
240.0	48.0	119.9	307.6	6.6	27.2	4.9	7.8	1.0	8.7	34.0	43.0
244.0	60.0	131.9	324.4	6.6	33.8	5.0	9.1	1.0	10.0	44.0	55.2

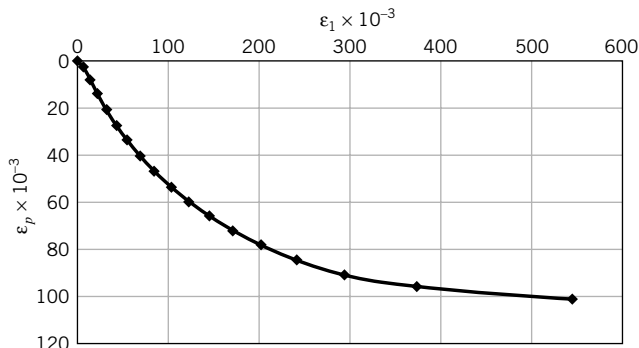
(continued)

Tabulation (continued)

p' (kPa)	$\Sigma \Delta q$ (kPa)	q (kPa)	p'_c (kPa)	$\Delta \varepsilon_{p'}$ $\times 10^{-3}$	$\varepsilon_p = \Sigma \Delta \varepsilon_p$ $\times 10^{-3}$	ε_p^p $\times 10^{-3}$	ε_q^p $\times 10^{-3}$	ε_q^e $\times 10^{-3}$	$\Delta \varepsilon_q$ $\times 10^{-3}$	$\Delta \varepsilon_q = \Delta \varepsilon_q$ $\times 10^{-3}$	ε_1 $\times 10^{-3}$
248.0	72.0	143.9	342.2	6.6	40.3	5.0	10.5	1.0	11.4	55.4	68.9
252.0	84.0	155.9	360.8	6.5	46.9	4.9	12.1	1.0	13.1	68.5	84.1
256.0	96.0	167.9	380.3	6.5	53.3	4.9	14.1	1.0	15.0	83.5	101.3
260.0	108.0	179.9	400.5	6.4	59.7	4.8	16.4	1.0	17.3	100.8	120.8
264.0	120.0	191.9	421.4	6.3	66.0	4.7	19.3	1.0	20.3	121.1	143.1
268.0	132.0	203.9	443.1	6.2	72.2	4.7	23.1	1.0	24.1	145.2	169.2
272.0	144.0	215.9	465.4	6.1	78.3	4.6	28.4	1.0	29.4	174.6	200.6
276.0	156.0	227.9	488.4	5.9	84.2	4.5	36.3	1.0	37.3	211.9	239.9
280.0	168.0	239.9	512.0	5.8	90.0	4.4	49.7	1.0	50.6	262.5	292.5
284.0	180.0	251.9	536.2	5.7	95.7	4.3	77.1	1.0	78.1	340.5	372.4
288.0	192.0	263.9	561.0	5.6	101.3	4.2	167.7	1.0	168.7	509.2	543.0



(a)



(b)

FIGURE E11.18a, b**Sample B, Undrained Test**

Step 1:
$$q_y = Mp'_o \sqrt{\frac{p'_c}{p'_o} - 1} = 0.94 \times 200 \sqrt{\frac{250}{200} - 1} = 94 \text{ kPa}$$

Step 2:
$$p'_f = \exp\left(\frac{e_f - e_o}{\lambda}\right) = \exp\left(\frac{2.38 - 1.15}{0.25}\right) = 137 \text{ kPa}$$

$$q_f = Mp'_f = 0.94 \times 137 = 128.8 \text{ kPa}$$

Step 3: $G = \frac{1.5p'(1 + e_o)(1 - 2\nu')}{\kappa(1 + \nu')} = \frac{1.5 \times 200(1 + 1.15) \times (1 - 2 \times 0.3)}{0.05(1 + 0.3)} = 3969.2 \text{ kPa}$

Step 4: $(\Delta\varepsilon_q^e)_{initial} = \frac{\Delta q}{3G} = \frac{94}{3 \times 3969.2} = 7.9 \times 10^{-3}$

Step 5: Let $\Delta p' = 3 \text{ kPa}$.
First stress increment after the initial yield follows.

Step 6: $p' = p'_o - \Delta p' = 200 - 3 = 197 \text{ kPa}$

$$p'_c = (p'_c)_{prev} \left(\frac{p'_{prev}}{p'} \right)^{\kappa/(\lambda-\kappa)} = 250 \left(\frac{200}{197} \right)^{0.05/(0.25-0.05)} = 250.9 \text{ kPa}$$

Step 7: $q = Mp' \sqrt{\frac{p'_c}{p'} - 1} = 0.94 \times 197 \sqrt{\frac{250.9}{197} - 1} = 97 \text{ kPa}$

Step 8: $\Delta\varepsilon_p^e = \frac{\kappa}{1 + e_o} \ln \frac{p'_{prev}}{p'} = \frac{0.05}{1 + 1.15} \ln \frac{200}{197} = 0.35 \times 10^{-3}$

Step 9: $\Delta\varepsilon_p^p = -\Delta\varepsilon_p^e = -0.35 \times 10^{-3}$

Step 10: Compression is positive.

$$\Delta\varepsilon_q^p = \Delta\varepsilon_p^p \frac{q}{M^2(p' - p'_c/2)} = 0.35 \times 10^{-3} \frac{97}{0.94^2(197 - 250.9/2)} = 0.54 \times 10^{-3}$$

Step 11: $\Delta\varepsilon_q^e = \frac{\Delta q}{3G} = \frac{97 - 94.1}{3 \times 3969.2} = 0.24 \times 10^{-3}$

Step 12: $\Delta\varepsilon_q = \varepsilon_q^e + \Delta\varepsilon_q^p = (0.24 + 0.54) \times 10^{-3} = 0.78 \times 10^{-3}$

Step 13: $\varepsilon_q = \varepsilon_1 = (\Delta\varepsilon_q^e)_{initial} + \Delta\varepsilon_q = (7.9 + 0.78) \times 10^{-3} = 8.7 \times 10^{-3}$

Step 14: $p = p'_o + \frac{q}{3} = 200 + \frac{97}{3} = 232.3 \text{ kPa}$

Step 15: $\Delta u = p - p' = 232.3 - 197 = 35.3 \text{ kPa}$

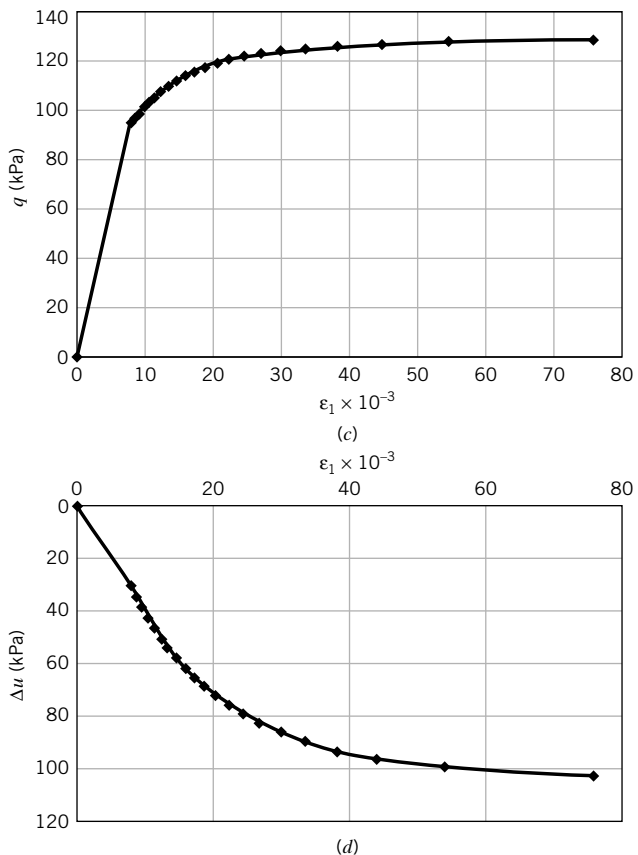
The spreadsheet program and the stress-strain plots are shown in the table below and Figure E11.18c, d.

Undrained Triaxial Test

Given data	Calculated values		
λ	0.25	M	0.94
κ	0.05	R_o	1.25
ϕ'_{cs}	24	e_Γ	2.38
e_o	1.15	p'_f	137.3 kPa
p'_o	200 kPa	q_f	129.2 kPa
p'_c	250 kPa	p'_y	200.0 kPa
ν'	0.3	q_y	94.1 kPa
		Δu_f	105.8 kPa

Tabulation

p' (kPa)	p'_c (kPa)	q (kPa)	$\Delta\varepsilon_p^e \times 10^{-3}$	$\Delta\varepsilon_p^p \times 10^{-3}$	$\Delta\varepsilon_q^p \times 10^{-3}$	$\Delta\varepsilon_p^e \times 10^{-3}$	$\Delta\varepsilon_q \times 10^{-3}$	$\varepsilon_q = \sum \Delta\varepsilon_q \times 10^{-3}$	$\varepsilon_1 \times 10^{-3}$	p (kPa)	Δu (kPa)
0	0	0		0.0	0.0	0.0	0.0	0.0	0.0	0	0
200.0	250.0	94.1	0.0	0.0	0.0	7.9	7.9	7.9	7.9	231.4	31.4
197.0	250.9	97.0	-0.4	0.4	0.5	0.2	0.8	8.7	8.7	232.3	35.3
194.0	251.9	99.7	-0.4	0.4	0.6	0.2	0.8	9.5	9.5	233.2	39.2
191.0	252.9	102.3	-0.4	0.4	0.6	0.2	0.9	10.4	10.4	234.1	43.1
188.0	253.9	104.7	-0.4	0.4	0.7	0.2	0.9	11.3	11.3	234.9	46.9
185.0	254.9	107.0	-0.4	0.4	0.8	0.2	1.0	12.3	12.3	235.7	50.7
182.0	256.0	109.2	-0.4	0.4	0.9	0.2	1.0	13.3	13.3	236.4	54.4
179.0	257.0	111.2	-0.4	0.4	1.0	0.2	1.1	14.4	14.4	237.1	58.1
176.0	258.1	113.1	-0.4	0.4	1.1	0.2	1.2	15.7	15.7	237.7	61.7
173.0	259.2	114.9	-0.4	0.4	1.2	0.2	1.3	17.0	17.0	238.3	65.3
170.0	260.4	116.6	-0.4	0.4	1.3	0.1	1.5	18.5	18.5	238.9	68.9
167.0	261.5	118.2	-0.4	0.4	1.5	0.1	1.7	20.2	20.2	239.4	72.4
164.0	262.7	119.7	-0.4	0.4	1.7	0.1	1.9	22.0	22.0	239.9	75.9
161.0	263.9	121.1	-0.4	0.4	2.0	0.1	2.1	24.2	24.2	240.4	79.4
158.0	265.2	122.5	-0.4	0.4	2.4	0.1	2.5	26.7	26.7	240.8	82.8
155.0	266.4	123.7	-0.4	0.4	2.9	0.1	3.0	29.6	29.6	241.2	86.2
152.0	267.8	124.8	-0.5	0.5	3.5	0.1	3.6	33.3	33.3	241.6	89.6
149.0	269.1	125.9	-0.5	0.5	4.6	0.1	4.6	37.9	37.9	242.0	93.0
146.0	270.5	126.9	-0.5	0.5	6.3	0.1	6.4	44.3	44.3	242.3	96.3
143.0	271.9	127.8	-0.5	0.5	9.9	0.1	9.9	54.2	54.2	242.6	99.6
140.0	273.3	128.6	-0.5	0.5	21.4	0.1	21.5	75.7	75.7	242.9	102.9
138.0	274.3	129.1	-0.3	0.3	57.4	0.0	57.5	133.2	133.2	243.0	105.0

**FIGURE E11.18c, d**

11.11 APPLICATION OF CSM TO CEMENTED SOILS

We can adopt the basic tenets of CSM to provide a framework for understanding the stress-strain and failure responses of cemented soils. In most cases, natural soils are cemented with various degrees of cementation. One cementing agent is calcium carbonate that is commonly found in groundwater. Under favorable conditions, calcium carbonate crystallizes; fills up some void spaces, reducing the void ratio of the uncemented soil; and bonds soil particles.

Let us consider an isotropically and normally consolidated, uncemented soil with a current mean effective stress, p'_o (Figure 11.43). Recall that for normally consolidated soils, $p'_c = p'_o$. The initial yield surface for the normally consolidated, uncemented soil is ABO . Now, assume that the soil becomes cemented, with the cementing agent filling a portion of the void and the soil remaining saturated. Let C_m be the ratio of the volume of the cementing agent to the total initial soil volume. Then the change in porosity is C_m and the change (decrease) in void ratio is $C_m(1 + e_o)$, where e_o is the initial void ratio of the uncemented soil. This decrease in void ratio occurs without any change in mean effective stress, so point O on the NCL for the uncemented soil (Figure 11.43b) moves vertically downward to point O' . The cementation has the following effects.

1. It causes a change in the state of the soil, converting it from a normally consolidated state to an overconsolidated state. Point O' must then be on an unloading/reloading line for the cemented soil.
2. The slopes of the NCL, λ_{cm} , and the URL, κ_{cm} , of the cemented soil are lower than those of the uncemented soil.
3. The cemented soil is now associated with a new, expanded RSW surface, FC . The preconsolidation stress for the cemented soil, p'_{cm} , is found as follows. From the compression line for the uncemented soil,

$$e_{cm} = e_o - \lambda \ln \frac{p'_{cm}}{p'_o} \quad (11.129)$$

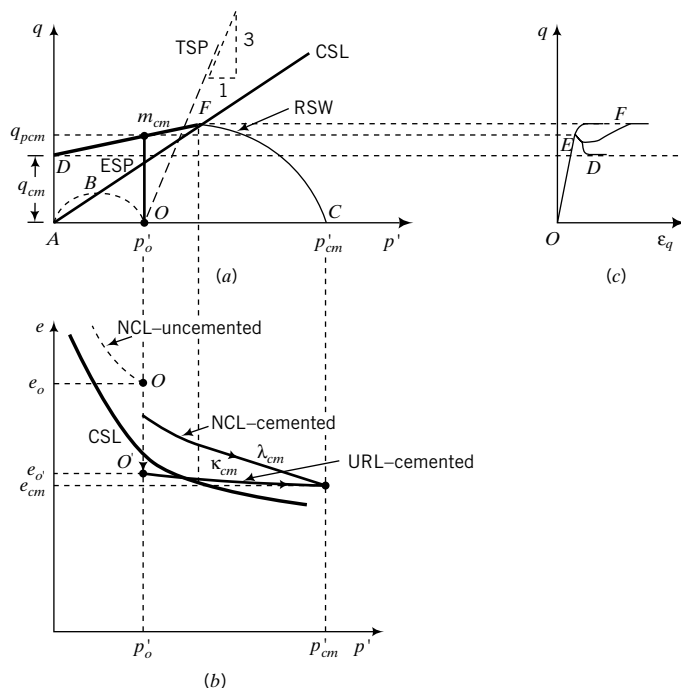


FIGURE 11.43 Application of CSM to cemented soils.

while from the unloading/reloading line for the cemented soil,

$$e_{cm} = e_{o'} - \kappa_{cm} \ln \frac{p'_{cm}}{p'_o} \quad (11.130)$$

Subtracting Equation (11.129) from Equation (11.130), we get

$$e_o - e_{o'} = (\lambda - \kappa_{cm}) \ln \frac{p'_{cm}}{p'_o}$$

But $\Delta e_{cm} = e_o - e_{o'} = C_m(1 + e_o)$. Therefore, solving for p'_{cm} , we obtain

$$p'_{cm} = p'_o \exp \left[\frac{C_m(1 + e_o)}{(\lambda - \kappa_{cm})} \right] \quad (11.131)$$

The CSL of the cemented and uncemented soil is the same provided the volume of soil particles is greater than the volume of the particles of the cementing agent. The degree of overconsolidation depends on the type and amount of the cementing agent. The theoretical expected stress-strain responses of cemented soils would be similar to those of the heavily and very heavily overconsolidated uncemented soils shown in Figure 11.20b, c. The difference between the limiting stress surface, DF , for cemented soils and Hvorslev's surface for the uncemented soils is that there is no tension cutoff. The bonding of the particles by the cementing agent confers a tensile resistance, q_{cm} , to the soil.

Failure of cemented soils generally occurs in a diffused failure mode. One or more bifurcations would initiate instability when the ESP approaches or reaches the surface, DF . The stress-strain response of cemented soils cannot be simulated using classical continuum mechanics when bifurcation occurs. Three possible stress-strain responses are shown in Figure 11.43.

The shear strength of cemented soil, τ_{cm} , on the limiting stress surface is

$$\tau_{pcm} = \frac{1}{2}(q_{cm} + m_{cm}p'_o) \quad (11.132)$$

where m_{cm} is the slope of the limiting stress surface. Neither m_{cm} nor q_{cm} is a fundamental soil parameter. They both depend on the type, amount, and distribution of the cementing agent within the soil mass. The value of m_{cm} is found from shear tests by plotting the peak deviatoric stress versus the mean effective stress.

11.12 SUMMARY

In this chapter, a simple critical state model (CSM) was used to provide insights into soil behavior. The model replicates the essential features of soil behavior. The key feature of the critical state model is that every soil fails on a unique surface in (p', q, e) space. According to the CSM, the failure stress state is insufficient to guarantee failure; the soil must also be loose enough (reaches the critical void ratio). Every sample of the same soil will fail on a stress state that lies on the critical state line regardless of any differences in the initial stress state, stress history, and stress path among samples.

The model makes use of an elliptical yield surface that expands to simulate hardening or contracts to simulate softening during loading. Expansion and contraction of the yield surface are related to the normal consolidation line of the soil. Imposed stress states that lie within the initial yield surface will cause the soil to behave elastically. Imposed stress states that lie outside the initial yield surface will cause the soil to yield and to behave elastoplastically. Each imposed stress state that causes the soil to yield must lie on a yield surface and on an unloading/reloading line corresponding to the preconsolidation mean effective stress associated with the current yield surface.

The CSM is intended not to replicate all the details of the behavior of real soils but to serve as a simple framework from which we can interpret and understand important features of soil behavior. Several relationships of practical importance were derived based on CSM. These relationships must be used with caution because of the simplifying assumptions made in their derivation.

Self-Assessment

Access Chapter 11 at <http://www.wiley.com/college/budhu> to take the end-of-chapter quiz to test your understanding of this chapter.

Practical Examples

EXAMPLE 11.19 Evaluating Soil Test Results Using Critical State Concepts

You requested a laboratory to carry out soil tests on samples of soils extracted at different depths from a borehole. The laboratory results are shown in Table E11.19a. The tests at depth 5.2 m were repeated and the differences in results were about 10%. The average results are reported for this depth. Are any of the results suspect? If so, which are?

TABLE E11.19a

Depth (m)	w (%)	PL (%)	LL (%)	s_u (kPa)	λ
2.1	22	12	32	102	0.14
3	24	15	31	10	0.12
4.2	29	15	29	10	0.09
5.2	24	17	35	35	0.1
6.4	17	13	22	47	0.07
8.1	23	12	27	85	0.1

Strategy It appears that the results at depth 5.2 m are accurate. Use the equations in Section 11.7 to predict λ and s_u and then compare the predicted with the laboratory test results.

Solution 11.19

Step 1: Prepare a table and calculate λ and s_u .

Use Equation (11.93) to predict λ and Equation (11.95) to predict s_u . See Table E11.19b.

TABLE E11.19b

Depth (m)	Laboratory results				Calculated results				
	w (%)	PL (%)	LL (%)	s_u (kPa)	λ	PI	LI	λ	s_u (kPa)
2.1	22	12	32	102	0.14	20	0.50	0.12	20.1
3	24	15	31	10	0.12	16	0.56	0.096	15.0
4.2	29	15	29	10	0.09	14	1.00	0.084	2.0
5.2	24	17	35	35	0.1	18	0.39	0.108	33.4
6.4	17	13	22	47	0.07	9	0.44	0.054	25.9
8.1	23	12	27	85	0.1	15	0.73	0.09	6.9
Average	23.2	14.0	29.3						
STD ^a	3.5	1.8	4.1						

^aSTD is standard deviation.

Step 2: Compare laboratory test results with predicted results.

The s_u value at 2.1 m is suspect because all the other values seem reasonable. The predicted value of s_u at depth 4.2 m is low in comparison with the laboratory test results. However, the water content at this depth is the highest reported, but the plasticity index is about average. If the water content were about

24% (the average of the water content just above and below 4.2 m), the predicted s_u would be 10.4 kPa, compared with 10 kPa from laboratory tests. The water content at 4.2 m is therefore suspect.

The s_u value at 6.4 m, water content, and liquid limit appear suspicious. Even if the water content were taken as the average for the borehole, the s_u values predicted (≈ 1 kPa) would be much lower than the laboratory results. You should repeat the tests for the sample taken at 6.4 m. The s_u value at 8.1 m is suspect because all the other values seem reasonable at these depths.

EXAMPLE 11.20 Foundation Design on an Overconsolidated Clay

A foundation (a slab of concrete) resting on the surface of a saturated overconsolidated clay is to be designed to support a column load including the weight of the foundation of 400 kN. Groundwater level is at 4 m below the surface. A one-dimensional consolidation test on a sample of the clay at its natural water content of $w = 20\%$ and taken at a depth of 1 m gave the following results: $C_c = 0.46$, $C_r = 0.115$, and $OCR = 8$. Atterberg limit tests gave $LL = 59\%$ and $PL = 29\%$. No other tests were conducted. For a preliminary design, assume a square foundation of size $2 \text{ m} \times 2 \text{ m}$.

- Determine if the increase in stresses from the foundation will cause the clay at a depth of $\frac{B}{2} = 1 \text{ m}$ to reach the limiting stress condition (HV surface).
- If the clay does not reach the limiting stresses, calculate the factor of safety.
- Assuming that the stress state at the depth of 1 m represents the average stress state over a thickness of 2 m of the clay, calculate the settlement (compression) of the foundation when it is fully loaded (short-term settlement). Is this settlement elastic or elastoplastic?
- How much long-term settlement would occur from the dissipation of the excess porewater pressure?
- Estimate the total settlement.

Strategy We have only a limited amount of information from two simple soil tests. We can use the correlations of simple soil tests results using CSM given in Table 11.1 to estimate any needed parameters.

Solution 11.20

Step 1: Calculate initial values.

Make a sketch of the problem. See Figure E11.20a.

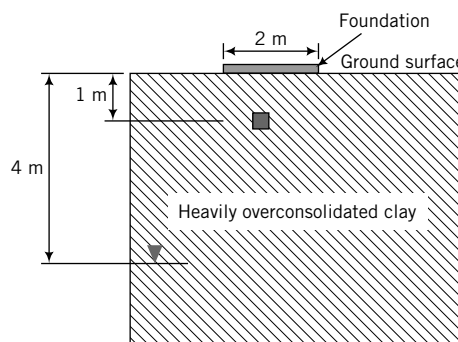


FIGURE E11.20a

$$e_o = wG_s = 0.2 \times 2.7 = 0.54$$

$$\gamma_{sat} = \left(\frac{G_s + e_o}{1 + e_o} \right) \gamma_w = \left(\frac{2.7 + 0.54}{1 + 0.54} \right) 9.8 = 20.6 \text{ kN/m}^3$$

$$\sigma'_{zo} = \gamma_{sat}z = 20.6 \times 1 = 20.6 \text{ kPa}$$

$$\sigma'_{zc} = OCR \times \sigma'_{zo} = 8 \times 20.6 = 164.8 \text{ kPa}$$

$$\phi'_{cs} = \sin^{-1} \left[0.35 - 0.1 \ln \left(\frac{PI}{100} \right) \right] = \sin^{-1} \left[0.35 - 0.1 \ln \left(\frac{30}{100} \right) \right] = 28^\circ$$

$$M_c = \frac{6 \sin \phi'_{cs}}{3 - \sin \phi'_{cs}} = \frac{6 \sin 28^\circ}{3 - \sin 28^\circ} = 1.11$$

$$K_o^{nc} = 1 - \sin \phi'_{cs} = 1 - \sin 28^\circ = 0.53$$

$$K_o^{oc} = K_o^{nc} \text{OCR}^{\frac{1}{2}} = 0.53 \times 8^{\frac{1}{2}} = 1.5$$

$$\kappa = \frac{C_r}{2.3} = \frac{0.115}{2.3} = 0.05$$

The initial and past consolidation stresses in the field are:

$$\text{Current: } p'_o = p_o = \frac{1 + 2K_o^{oc}}{3} \sigma'_{zo} = \frac{1 + 2 \times 1.5}{3} \times 20.6 = 27.5 \text{ kPa}$$

$$\text{Past: } p'_k = \frac{1 + 2K_o^{nc}}{3} \sigma'_{zc} = \frac{1 + 2 \times 0.53}{3} \times 164.8 = 113.2 \text{ kPa}$$

$$\text{Current: } q_o = \sigma'_{zo}(1 - K_o^{oc}) = 20.6 \times (1 - 1.5) = -10.3 \text{ kPa}$$

$$\text{Past: } q_k = \sigma'_{zc}(1 - K_o^{nc}) = 164.8 \times (1 - 0.53) = 77.5 \text{ kPa}$$

Note: As a result of the overconsolidation, the current lateral effective stress is greater than the vertical effective stress (see Figure E11.20b). The consolidation (effective) stress path is $A \rightarrow K$ and the unloading (effective) stress path is $K \rightarrow O$ in Figure E11.20b.

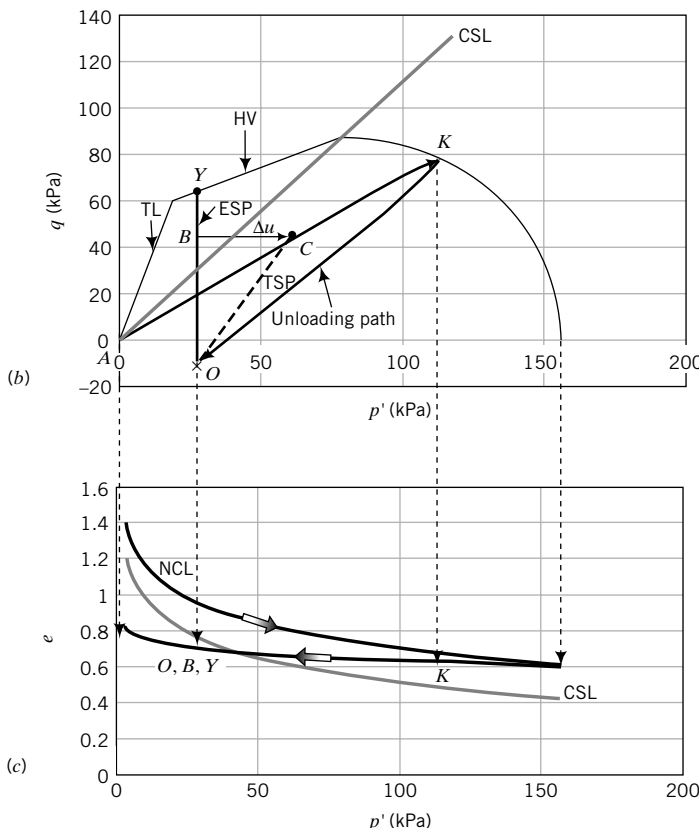


FIGURE E11.20b, c

Find p'_c using Equation (11.4e). That is,

$$p'_c = p'_k + \frac{q_k^2}{M^2 p'_k} = 113.2 + \frac{77.5^2}{1.11^2 \times 113.2} = 156.3 \text{ kPa}$$

$$R_o = \frac{p'_c}{p'_o} = \frac{156.3}{27.5} = 5.7$$

Step 2: Calculate increase in stresses from the surface load.

$$q_s = \frac{400}{2 \times 2} = 100 \text{ kPa}$$

From the program STRESS, the increase in vertical and lateral stresses under the center of the foundation for input $B = L = 2/2 = 1 \text{ m}$, $q_s = 100 \text{ kPa}$, and $z = 1 \text{ m}$ is

$$\Delta\sigma_z = 70 \text{ kPa}; \quad \Delta\sigma_x = 15 \text{ kPa}; \quad \Delta\sigma_y = 15 \text{ kPa}$$

Assume these are principal stresses.

$$\Delta p = \frac{70 + 2 \times 15}{3} = \frac{100}{3} = 33.3 \text{ kPa}$$

$$\Delta q = 70 - 15 = 55 \text{ kPa}$$

$$\frac{\Delta q}{\Delta p} = \frac{55}{\frac{100}{3}} = 1.65$$

Step 3: Calculate stresses after the foundation is loaded.

$$p = p_o + \Delta p = 27.5 + 33.3 = 60.8 \text{ kPa}$$

$$q = q_o + \Delta q = -10.3 + 55 = 44.7 \text{ kPa}$$

The total stress path is $O \rightarrow C$ in Figure E11.20b.

Step 4: Calculate stresses on the HV surface.

Axisymmetric condition is assumed at the center of the foundation, $n_t = 3$.

$$t_c = \frac{1}{\left(1 + \frac{n_t^2}{M^2}\right)} = \frac{1}{\left(1 + \frac{3^2}{1.11^2}\right)} = 0.12$$

$$R_t = \frac{1}{t_c} = \frac{1}{0.12} = 8.3 > R_o; \quad \text{therefore, soil will not fail in tension}$$

$$m = \frac{M - 2t_c n_t}{1 - 2t_c} = \frac{1.11 - 2 \times 0.12 \times 3}{1 - 2 \times 0.12} = 0.51$$

The deviatoric stress on the HV surface, q_{yH} , is

$$q_{yH} = p'_o [m(1 - t_c R_o) + t_c n_t R_o]$$

$$= 27.5[0.51(1 - 0.12 \times 5.7) + 0.12 \times 3 \times 5.7] = 61 \text{ kPa}$$

Step 5: Determine if the applied stress will bring the soil to the HV surface.

Since $q = 44.7 \text{ kPa} < q_{yH} = 61 \text{ kPa}$, the soil stress state will be below the HV surface.

Step 6: Determine the factor of safety.

$$\text{FS} = \frac{q_{yH}}{q} = \frac{61}{44.7} = 1.36$$

Step 7: Calculate short-term settlement.

Since the stresses from the foundation loads are below the HV surface, the soil will behave elastically, and we can use the elastic stiffness parameters in Section 11.8 to calculate the settlement. For heavily overconsolidated soils, use

$$E' = \frac{3p'_c(1 + e_c)(1 - 2\nu')}{\kappa}$$

where

$$e_c = e_o - \kappa \ln(R_o) = 0.54 - 0.05 \times \ln(5.7) = 0.453$$

Assume $\nu' = 0.35$; then

$$E' = \frac{3 \times 156.3(1 + 0.453)(1 - 2 \times 0.35)}{0.05} = 4088 \text{ kPa}$$

$$G = \frac{E'}{2(1 + \nu')} = \frac{4088}{2(1 + 0.35)} = 1514 \text{ kPa}$$

The average change in vertical strain for short-term condition is

$$\Delta\epsilon_z = \Delta\epsilon_q = \frac{\Delta q}{3G} = \frac{55}{3 \times 1514} = 0.0121$$

The settlement is

$$\Delta\epsilon_z H = \Delta\epsilon_z B = 0.0121 \times 2000 \approx 24 \text{ mm}$$

Step 8: Calculate the long-term settlement.

For long-term condition, the excess porewater pressure dissipates. The change in effective stress is equal to the change in excess porewater pressure, i.e., $\Delta p' = \Delta u = \frac{100}{3} \text{ kPa}$.

$$\Delta e = \kappa \ln\left(\frac{p'_o + \Delta p}{p'_o}\right) = 0.05 \times \ln\left(\frac{27.5 + \frac{100}{3}}{27.5}\right) = 0.04$$

The average vertical strain is

$$\Delta\epsilon_z = \frac{\Delta e}{1 + e_o} = \frac{0.04}{1 + 0.54} = 0.026$$

The long-term settlement is

$$\Delta\epsilon_z H = \Delta\epsilon_z B = 0.026 \times 2000 = 52 \text{ mm}$$

Step 9: Calculate the total settlement.

The total settlement = $24 + 52 = 76$ mm.

EXAMPLE 11.21 Predicting Soil Response Under a Tank Foundation

An oil tank foundation is to be located on a very soft clay, 6 m thick, underlain by a deep deposit of stiff clay. Soil tests at a depth of 3 m gave the following results: $\lambda = 0.24$, $\kappa = 0.05$, $\phi'_{cs} = 30^\circ$, $OCR = 1.2$, and $w = 55\%$. The unit weight of the oil is 8.5 kN/m^3 . The tank has a diameter of 8 m and is 5 m high. The dead load of the tank and its foundation is 350 kN. Because of the expected large settlement, it was decided to preconsolidate the soil by quickly filling the tank with water and then allowing consolidation to take place. To reduce the time to achieve the desired level of consolidation, sand drains were installed at the site.

- (a) Determine if a soil element at 3 m below the tank will yield if the tank is filled to capacity.
- (b) Would the soil element at 3 m below the tank fail if the tank is filled to capacity?
- (c) What levels of water will cause the soil element to yield and to fail?
- (d) Would the soil element yield under the dead load only?
- (e) Assuming the stress state of the soil element at 3 m depth represents the average, determine the short-term, long-term, and total settlements under the dead load.
- (f) The dead load was applied and kept there until the excess porewater pressure dissipated. What height of water will now bring the soil element to failure?

Strategy The soil is one-dimensionally consolidated before the tank is placed on it. The loads from the tank will force the soil to consolidate along a path that depends on the applied stress increments. A soil element under the center of the tank will be subjected to axisymmetric loading conditions. If the tank is loaded quickly, then undrained conditions apply and the task is to predict the failure stresses and then use them to calculate the surface stresses that would cause failure. After consolidation, the undrained shear strength will increase and you will have to find the new failure stresses.

Solution 11.21

Step 1: Calculate initial values.

$$e_o = wG_s = 0.55 \times 2.7 = 1.49$$

$$K_o^{nc} = 1 - \sin \phi'_{cs} = 1 - \sin 30^\circ = 0.5$$

$$K_o^{oc} = K_o^{nc}(OCR)^{1/2} = 0.5 \times (1.2)^{1/2} = 0.55$$

$$\gamma' = \frac{G_s - 1}{1 + e_o} \gamma_w = \frac{2.7 - 1}{1 + 1.49} \times 9.8 = 6.69 \text{ kN/m}^3$$

$$\sigma'_{zo} = \gamma' z = 6.69 \times 3 = 20.1 \text{ kPa}$$

$$\sigma'_{xo} = K_o^{oc} \sigma'_{zo} = 0.55 \times 20.1 = 11.1 \text{ kPa}$$

$$\sigma'_{zc} = OCR \times \sigma'_{zo} = 1.2 \times 20.1 = 24.1 \text{ kPa}$$

$$M_c = \frac{6 \sin \phi'_{cs}}{3 - \sin \phi'_{cs}} = \frac{6 \sin 30^\circ}{3 - \sin 30^\circ} = 1.2$$

$$\Lambda = 1 - \frac{\kappa}{\lambda} = 1 - \frac{0.05}{0.24} = 0.79$$

The stresses on the initial yield surface are:

$$p'_k = \frac{1 + 2K_o^{nc}}{3} \sigma'_{zc} = \frac{1 + 2 \times 0.5}{3} \times 24.1 = 16.1 \text{ kPa}$$

$$q_k = (1 - K_o^{nc})\sigma'_{zc} = (1 - 0.5) \times 24.1 = 12.1 \text{ kPa}$$

$$p'_o = \frac{1 + 2K_o^{oc}}{3}\sigma'_{zc} = \frac{1 + 2 \times 0.55}{3} \times 20.1 = 14.1 \text{ kPa}$$

$$q_o = (1 - K_o^{oc})\sigma'_{zo} = (1 - 0.55) \times 20.1 = 9 \text{ kPa}$$

You need to calculate the preconsolidation stress on the isotropic consolidation line (point *I*, Figure E11.21). You should note that (p'_k, q_k) lies on the initial yield surface (point *K*, Figure E11.21).

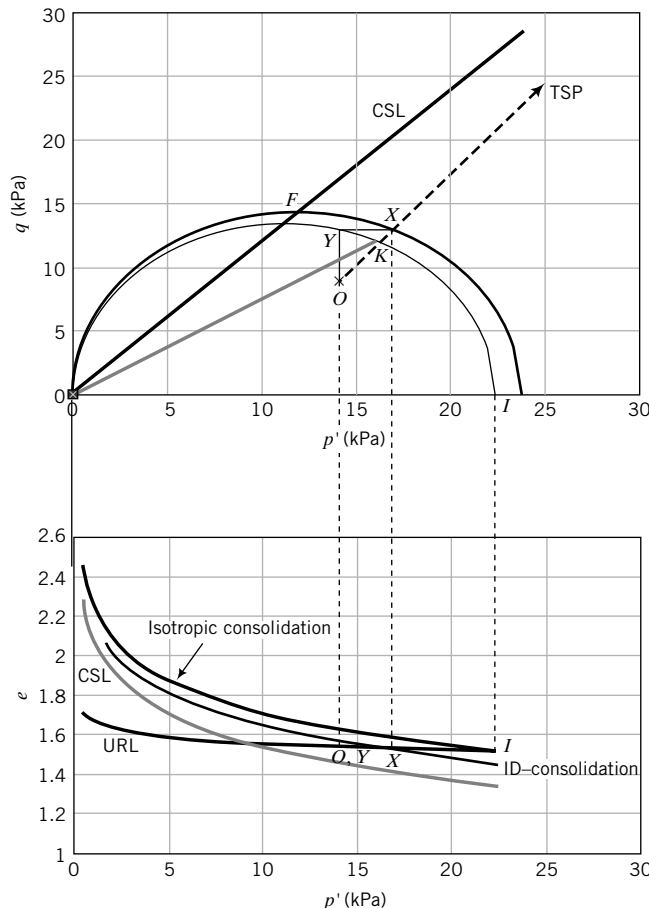


FIGURE E11.21

Find p'_c using Equation (11.4e), i.e.,

$$p'_c = p'_k + \frac{(p'_k)^2}{M^2 p'_k} = 16.1 + \frac{12.1^2}{1.2^2 \times 16.1} = 22.4 \text{ kPa}$$

$$R_o = \frac{p'_c}{p'_o} = \frac{22.4}{14.1} = 1.59$$

Find the void ratio on the CSL for $p' = 1$ kPa.

$$e_\Gamma = e_o + (\lambda - \kappa) \ln \frac{p'_c}{2} + \kappa \ln p'_o = 1.49 + (0.24 - 0.05) \ln \frac{22.4}{2} + 0.05 \ln 14.1 = 2.08$$

Step 2: Calculate the stress increase from the tank and also the consolidation stress path.

$$\text{Area of tank: } A = \frac{\pi D^2}{4} = \frac{\pi \times 8^2}{4} = 50.27 \text{ m}^2$$

$$\text{Vertical surface stress from water: } \gamma_w h = 9.8 \times 5 = 49 \text{ kPa}$$

$$\text{Vertical surface stress from dead load: } \frac{350}{50.27} = 7 \text{ kPa}$$

$$\text{Total vertical surface stress: } q_s = 49 + 7 = 56 \text{ kPa}$$

Vertical stress increase:

$$\Delta\sigma_z = q_s \left[1 - \left(\frac{1}{1 - (r/z)^2} \right)^{3/2} \right] = q_s \left[1 - \left(\frac{1}{1 + (4/3)^2} \right)^{3/2} \right] = 0.78q_s$$

Radial stress increase:

$$\begin{aligned} \Delta\sigma_r &= \frac{q_s}{2} \left((1 + 2v) - \frac{2(1 + v)}{[1 + (r/z)^2]^{1/2}} + \frac{1}{[1 + (r/z)^2]^{3/2}} \right) \\ &= \frac{q_s}{2} \left((1 + 2 + 0.5) - \frac{2(1 + 0.5)}{\left[1 + \left(\frac{4}{3} \right)^2 \right]^{1/2}} + \frac{1}{\left[1 + \left(\frac{4}{3} \right)^2 \right]^{3/2}} \right) = 0.21q_s \end{aligned}$$

$$\frac{\Delta\sigma_r}{\Delta\sigma_z} = \frac{0.21}{0.78} = 0.27$$

$$\Delta\sigma_z = 0.78 \times 56 = 43.7 \text{ kPa}, \quad \Delta\sigma_r = 0.21 \times 56 = 11.8 \text{ kPa}$$

$$\Delta p_{app} = \frac{0.78q_s + 2 \times 0.21q_s}{3} = 0.4q_s = 0.4 \times 56 = 22.4 \text{ kPa}$$

$$\Delta q_{app} = 0.78q_s - 0.21q_s = 0.57q_s = 0.57 \times 56 = 31.9 \text{ kPa}$$

$$\text{Slope of TSP = ESP during consolidation: } \frac{\Delta q_{app}}{\Delta p_{app}} = \frac{0.57q_s}{0.4q_s} = 1.42$$

Step 3: Calculate the initial yield stresses and excess porewater pressure at yield.

The yield stresses (point C, Figure E11.21) are found from Equation (11.4d). That is,

$$q_y = Mp'_o \sqrt{\frac{p'_c}{p_o} - 1} = Mp'_o \sqrt{R_o - 1} = 1.2 \times 14.1 \sqrt{1.59 - 1} = 13 \text{ kPa}$$

$$p'_y = p'_o = 14.1 \text{ kPa}, \quad \Delta q_y = q_y - q_o = 13 - 9 = 4 \text{ kPa}$$

The excess porewater pressure at yield is

$$\Delta u_y = \Delta p_y = \frac{\Delta q_y}{1.42} = \frac{4}{1.42} = 2.8 \text{ kPa}$$

Step 4: Check if soil yields when the tank is filled to capacity.

Since Δq_{app} ($= 31.9 \text{ kPa}$) $>$ Δq_y ($= 4 \text{ kPa}$), the soil will yield.

Step 5: Check if the soil element will fail when the tank is filled to capacity.

$$q_f = Mp'_o \left(\frac{R_o}{2} \right)^{\Lambda} = 1.2 \times 14.1 \times \left(\frac{1.59}{2} \right)^{0.79} = 14.1 \text{ kPa}$$

$$\Delta q_f = q_f - q_o = 14.1 - 9 = 5.1 \text{ kPa} < \Delta q_{app} = 31.9 \text{ kPa}$$

The soil element will fail. (See point F in Figure E11.21; F is on the failure line.)

Step 6: Determine heights of water to cause yielding and failure. When the soil element yields or fails, the elastic distribution of surface stresses is invalid. However, to get an estimate, we will assume that it is valid.

At initial yield: $\Delta q_y = 4 \text{ kPa}$

The change in surface stress (initial surface stress is zero) is

$$\Delta q_s = \frac{\Delta q_y}{0.57} = \frac{4}{0.57} = 7 \text{ kPa}$$

$$\Delta h_w = \frac{\Delta q_s}{\gamma_w} = \frac{7}{9.8} = 0.72 \text{ m}$$

At initial failure: $\Delta q_f = 14.1 - 9 = 5.1 \text{ kPa}$

$$\Delta q_s = \frac{\Delta q_f}{0.57} = \frac{5.1}{0.57} = 8.9 \text{ kPa}$$

$$\Delta h_w = \frac{\Delta q_s}{\gamma_w} = \frac{8.9}{9.8} = 0.9 \text{ m}$$

Difference in water level from initial yield to failure = $0.9 - 0.72 = 0.28 \text{ m}$.

Step 7: Determine if the soil element will yield under the dead load.

The dead load surface stress = 7 kPa = yield stress

Therefore, the soil element will yield.

Step 8: Determine the short-term and long-term settlements under the dead load.

For surface loads less than the dead load, the soil will behave elastically.

$$e_c = e_o - \kappa \ln R_o = 1.49 - 0.05 \ln 1.59 = 1.47$$

$$E' = \frac{3p'_c(1 + e_o)(1 - 2\nu')}{\kappa} = \frac{3 \times 22.4 \times (1 + 1.47)(1 - 2 \times 0.35)}{0.05} \\ = 996 \text{ kPa}$$

$$G = \frac{E'}{2(1 + \nu')} = \frac{996}{2(1 + 0.35)} = 369 \text{ kPa}$$

$$K' = \frac{E'}{3(1 - 2\nu')} = \frac{996}{3(1 - 2 \times 0.35)} = 1107 \text{ kPa}$$

Under undrained condition (short-term loading), the volumetric strain is equal to zero and $\varepsilon_q = \varepsilon_1 = \varepsilon_z$.

$$\Delta q_{\text{dead load}} = 0.57q_{\text{dead load}} = 0.57 \times 7 = 4 \text{ kPa}$$

$$\varepsilon_z = \varepsilon_p = \frac{\Delta q_{\text{dead load}}}{3G} = \frac{4}{3 \times 369} = 0.0036$$

$$\rho_z = \varepsilon_z H = 0.0036 \times 6000 \approx 22 \text{ mm}$$

Note: Since the element at a depth of 3 m represents the average stress state, the soil thickness to use to calculate settlement is $2 \times 3 = 6 \text{ m}$.

For elastic deformation, $\varepsilon_3 = -\nu' \varepsilon_1$. Therefore, in the case of axisymmetric loading,

$$\varepsilon_p = \varepsilon_1 + 2\varepsilon_3 = \varepsilon_1(1 - 2\nu')$$

and

$$\varepsilon_1 = \varepsilon_z = \frac{\varepsilon_p}{(1 - 2\nu')}$$

$$\Delta p_{\text{dead load}} = 0.4q_{\text{dead load}} = 0.4 \times 7 = 2.8 \text{ kPa}$$

$$\varepsilon_p = \frac{\Delta p_{\text{dead load}}}{K'} = \frac{2.8}{1107} = 0.0025$$

$$\varepsilon_1 = \varepsilon_z = \frac{\varepsilon_p}{(1 - 2\nu')} = \frac{0.0025}{(1 - 2 \times 0.35)} = 0.0084$$

$$p_z = \varepsilon_z H = 0.0084 \times 6000 \approx 50 \text{ mm}$$

$$\text{Total settlement} = 22 + 50 = 72 \text{ mm}$$

Note: $\varepsilon_1 \neq \varepsilon_z$ unless the rotation of principal strains is small.

Step 9: Calculate the height of water to cause failure after consolidation at initial yield.

Let the subscript 1 denote the stresses after consolidation at the initial yield stress:

$$(p'_o)_1 = p'_y + \Delta p_y (= \Delta u_y) = 14.1 + 2.8 = 16.9 \text{ kPa}$$

$$(q_o)_1 = q_y = 13 \text{ kPa}$$

$$(p'_c)_1 = (p'_o)_1 + \frac{(q_o)_1^2}{M^2(p'_o)_1} = 16.9 + \frac{13^2}{1.2^2 \times 16.9} = 23.8 \text{ kPa}$$

$$R_o = \frac{p'_c}{p'_o} = \frac{23.8}{16.9} = 1.41$$

$$(q_f)_1 = M(p'_o)_1 \left(\frac{R_o}{2} \right)^{\lambda} = 1.2 \times 16.9 \times \left(\frac{1.41}{2} \right)^{0.79} = 15.4 \text{ kPa}$$

$$(\Delta q_f)_1 = (q_f)_1 - (q_y)_1 = 15.4 - 13 = 2.4 \text{ kPa}$$

$$\Delta q_s = \frac{\Delta q_f}{0.57} = \frac{2.4}{0.57} = 4.2 \text{ kPa}$$

$$\Delta h_w = \frac{\Delta q_s}{\gamma_w} = \frac{4.2}{9.8} = 0.43 \text{ m}$$

The difference in water heights to failure from initial yield state = $0.43 - 0.28 = 0.15 \text{ m}$. That is, by preloading and consolidating the soil, the surface stress to bring the soil to failure increases.

EXERCISES

Assume $G_s = 2.7$, where necessary.

11.2 Show that the effective stress path in one-dimensional consolidation is

$$\frac{q}{p'} = \frac{3M_c}{6 - M_c}$$

Theory

11.1 Prove that

$$K_o^{nc} = \frac{6 - 2M_c}{6 + M_c}$$

11.3 Show, for an isotropically heavily overconsolidated clay, that $s_u = 0.5Mp'_o(0.5R_o)^{(\lambda-\kappa)/\lambda}$.

11.4 Show that $e_\Gamma = e_c - (\lambda - \kappa) \ln 2$, where e_Γ is the void ratio on the critical state line when $p' = 1$ kPa and e_c is the void ratio on the normal consolidation line corresponding to $p' = 1$ kPa.

11.5 The water content of a soil is 55% and $\lambda = 0.15$. The soil is to be isotropically consolidated. Plot the expected void ratio against mean effective stress if the load increment ratios are (a) $\Delta p'/p' = 1$ and (b) $\Delta p'/p' = 2$.

11.6 Plot the variation of Skempton's porewater pressure coefficient at failure, A_f , with overconsolidation ratio using the CSM for two clays, one with $\phi'_{cs} = 21^\circ$ and the other with $\phi'_{cs} = 32^\circ$. Assume $\kappa = 0.2\lambda$ and the peak shear stress is the failure shear stress.

11.7 A fill of height 5 m with $\gamma_{sat} = 18$ kN/m³ is constructed to preconsolidate a site consisting of a soft, normally consolidated soil. Tests at a depth of 2 m in the soil gave the following results: $w = 45\%$, $\phi'_{cs} = 23.5^\circ$, $\lambda = 0.25$, and $\kappa = 0.05$. Groundwater is at the ground surface.

- (a) Show that the current stress state of the soil prior to loading lies on the yield surface given by

$$F = (p')^2 - p'p'_c + \frac{q^2}{M^2} = 0$$

- (b) The fill is rapidly placed in lifts of 1 m. The excess porewater pressure is allowed to dissipate before the next lift is placed. Show how the soil will behave in (p', q) space and in (p', e) space.

11.8 Plot the theoretical relationship between porosity and undrained shear strength for a 7-m-thick layer of saturated, normally consolidated soil. Assume $\phi'_{cs} = 30^\circ$, $\Lambda = 0.8$, $G_s = 2.7$, and water contents decrease linearly from 80% at the surface to 10% at the bottom of the layer. Groundwater level is below the layer. What conclusion(s) can you draw from this theoretical plot? Search the literature to check whether such a relationship has been observed in practice.

Problem Solving

11.9 The following results were obtained from a one-dimensional consolidation test on a saturated clay of water content $w = 72\%$: $C_c = 0.52$, $C_r = 0.06$, and $OCR = 4.8$. If $K_o^{nc} = 0.5$, calculate λ , κ , e_o , R_o , M_c , and M_e .

11.10 If $\lambda = 0.2$, $\kappa = 0.04$, $e_o = 1.1$, $R_o = 1.4$, and $p'_o = 40$ kPa:

- (a) Calculate e_Γ .
 (b) Plot the loading and unloading/reloading line in (p', e) and $(\ln p', e)$ spaces.

11.11 The following data were obtained from a consolidation phase of a standard triaxial CU test on a clay soil. Determine λ and κ .

p' (kPa)	25	50	200	400	800	1600	800	400	200
e	1.65	1.64	1.62	1.57	1.51	1.44	1.45	1.46	1.47

11.12 The water content of a sample of saturated soil at a mean effective stress of 10 kPa is 85%. The sample was isotropically consolidated with a mean effective stress of 150 kPa. At the end of the consolidation, the water content was 50%. The sample was then isotropically unloaded to a mean effective stress of 100 kPa, and the water content increased by 1%.

- (a) Draw the normal consolidation line and the unloading/reloading lines in (p', e) and $(\ln p', e)$ spaces.
 (b) Calculate λ and κ .
 (c) Draw the initial yield surface and the critical state line in (p', q) , (p', e) , and $(\ln p', e)$ spaces if $\phi'_{cs} = 25^\circ$.

11.13 A saturated sample of soil 38 mm in diameter and 76 mm high was isotropically consolidated to 200 kPa in a triaxial cell. It was decided to stop the consolidation when the excess porewater pressure (Δu) was 20 kPa. The sample was subjected to a standard undrained test ($\sigma_3 = 200$ kPa is kept constant). Failure (critical state) was recorded when $q_f = 64$ kPa. The water content was 40%, $\lambda = 0.16$, and $\kappa = 0.03$. Determine e_Γ , M , and Δu_f .

11.14 Determine the failure stresses under (a) a standard triaxial CU test and (b) a standard triaxial CD test for the conditions described in Exercise 11.12. Calculate s_u for the CU test.

11.15 Estimate the undrained shear strength of a saturated overconsolidated clay under (a) compression and (b) extension, if $\phi'_{cs} = 30^\circ$, $R_o = 5$, $\lambda = 0.2$, $\kappa = 0.04$, and $p'_o = 60$ kPa.

11.16 A CU triaxial test was conducted on a normally consolidated sample of a saturated clay. Its undrained shear strength at a mean effective stress of 100 kPa was 22 kPa. Estimate the undrained shear strength of a sample of this clay if $R_o = 15$ and the initial stresses are the same as the sample that was tested. The consolidation parameters are $\lambda = 0.28$ and $\kappa = 0.06$.

11.17 The natural (is situ) water content of a saturated soil is 64%. Because of undue care, the soil lost 4% water content when it was tested in a standard triaxial CU test. The undrained shear strength of the test was reported as 56 kPa. Estimate the in situ undrained shear strength of the soil if $\lambda = 0.2$.

11.18 The parameters of a soil are $\lambda = 0.2$, $\kappa = 0.04$, $\phi'_{cs} = 28^\circ$, $e_o = 1.08$ at $p'_o = 80$ kPa, and $R_o = 7$. If the soil were to be loaded so that its total stress path $\frac{q}{p} = 2.5$, predict the following.

- (a) Initial yield stresses, p'_y and q_y , under undrained condition.

- (b) Excess porewater pressure at yield for undrained condition.
- (c) The undrained shear strength at initial yield.
- (d) The excess porewater pressure at critical state.
- (e) Would the soil show a peak shear stress? Give reason(s).
- 11.19** The soil parameters from a one-dimensional consolidation test are $C_c = 0.32$, $C_r = 0.06$, and $\phi'_{cs} = 28^\circ$.
- (a) Make a plot of the relationship between $\frac{s_u}{p'_o}$ and R_o for R_o ranging from 2.5 to 7, assuming standard triaxial undrained condition.
- (b) At what value of R_o is the tension cutoff?
- 11.20** For the soil parameters listed in Exercise 11.19, calculate E' , K' , and G if $v' = 0.3$, $R_o = 4$, $p'_o = 50$ kPa, and $e_o = 1$.
- 11.21** Two samples of a soft clay are to be tested in a conventional triaxial apparatus. Both samples were isotropically consolidated under a cell pressure of 250 kPa and then allowed to swell back to a mean effective stress of 175 kPa. Sample A is to be tested under drained condition while sample B is to be tested under undrained condition. Estimate the stress-strain, volumetric strain (sample A), and excess porewater pressure (sample B) responses for the two samples. The soil parameters are $\lambda = 0.15$, $\kappa = 0.04$, $\phi'_{cs} = 26.7^\circ$, $e_o = 1.08$, and $v' = 0.3$.
- 11.22** Determine and plot the stress-strain (q versus ϵ_1) and volume change (ϵ_p versus ϵ_1) responses for an overconsolidated soil under a CD test. The soil parameters are $\lambda = 0.17$, $\kappa = 0.04$, $\phi'_{cs} = 25^\circ$, $v' = 0.3$, $e_o = 0.92$, $p'_c = 280$ kPa, and $OCR = 5$.
- 11.23** Repeat Exercise 11.22 for an undrained triaxial compression (CU) test and compare the results with the undrained triaxial extension test.
- 11.24** A sample of a clay is isotropically consolidated to a mean effective stress of 300 kPa and is isotropically unloaded to a mean effective stress of 250 kPa. An undrained triaxial extension test is to be carried out by keeping the axial stress constant and increasing the radial stress. Predict and plot the stress-strain (q versus ϵ_1) and the excess porewater pressure (Δu versus ϵ_1) responses up to failure. The soil parameters are $\lambda = 0.23$, $\kappa = 0.07$, $\phi'_{cs} = 24$, $v' = 0.3$, and $e_o = 1.32$.
- 11.25** The critical state friction angle of a soil is 30° and $OCR = 20$. Would this soil fail in tension if it were loaded in under plane strain condition? Show calculations to support your answer. Estimate the undrained shear strength under plane strain.
- 11.26** The undrained shear strength of an isotropically consolidated, fine-grained soil in a standard triaxial CU test is 50 kPa. The cell pressure used to consolidate the soil is 225 kPa. Assume $\frac{C_r}{C_c} = 0.25$ and $\phi'_{cs} = 30^\circ$.
- (a) Determine the normalized undrained shear strength.
- (b) Estimate the undrained shear strength of the same soil if $R_o = 6$. Assume the preconsolidation stress is the same.
- (c) Estimate the undrained shear strength if a DSS test was conducted.
- ### Practical
- 11.27** A standard undrained triaxial test was performed on a fine-grained soil. The soil was consolidated to a cell pressure of 120 kPa and then unloaded to a cell pressure of 80 kPa. The axial stress at failure (critical state) was 64 kPa. Assume $\Lambda = 0.8$.
- (a) Determine the normalized undrained shear strength.
- (b) Estimate ϕ'_{cs} .
- (c) Estimate the undrained shear strength of the same soil if it were normally consolidated.
- (d) Estimate the undrained shear strength of the same soil if it were to be subjected to direct simple shear.
- (e) Recommend the undrained shear strength for use in the design of (1) a foundation for an oil tank, and (2) a slope.
- 11.28** A foundation (a slab of concrete) resting on the surface of a saturated overconsolidated clay is to be designed to support a column load including the weight of the foundation of 250 kN. Groundwater level is at the surface. A one-dimensional consolidation test on a sample of the clay at its natural water content of $w = 40\%$ and taken at a depth of 2 m gave the following results: $C_c = 0.54$, $C_r = 0.108$, and $OCR = 12$. Atterberg limit tests gave $LL = 70\%$ and $PL = 30\%$. No other tests were conducted. For a preliminary design, assume a circular footing 2.5 m in diameter and $v' = 0.35$.
- (a) Determine if the increase in stresses from the foundation will cause the clay at a depth of 1 m to yield.
- (b) If the clay does not yield, calculate the factor of safety for undrained condition.
- (c) Calculate the excess porewater pressure due to the foundation load.
- (d) Assuming that the stress state at the depth of 1 m represents the average stress state over a thickness of 2 m of the clay, calculate the settlement of the foundation. Is this settlement elastic or elastoplastic?
- (e) How much long-term settlement would occur from the dissipation of the excess porewater pressure?

11.29 A tank of diameter 5 m is to be located on a deep deposit of lightly overconsolidated homogeneous clay, 25 m thick. The vertical stress imposed by the tank at the surface is 60 kPa. The soil parameters are $\lambda = 0.26$, $\kappa = 0.06$, $OCR = 1.8$, and $\phi'_{cs} = 24^\circ$. The average water content is 42% and groundwater level is at 1 m below the ground surface. Assume the soil above the groundwater is saturated.

- (a) Calculate the excess porewater pressure at depths of 2, 5, 10, and 20 m if the vertical stress were to be applied instantaneously.
- (b) Estimate the undrained shear strength at a depth of 2.5 m.
- (c) Estimate the surface stress to cause the soil at a depth of 2.5 m to yield.

11.30 A sample of soil taken at a depth of 5 m in a homogeneous overconsolidated saturated clay was tested

under standard triaxial CU conditions. Its water content was 48%. The soil was isotropically consolidated to a mean effective stress of 50 kPa and then unloaded to a mean effective stress of 15 kPa. The peak deviatoric stress reported by the soil technician is 20 kPa. The critical state friction angle is 32° . A one-dimensional consolidation test gave the following results: $C_c = 0.32$, $C_r = 0.06$, and $OCR = 6$. In the field, the groundwater level is at the ground surface.

- (a) Is the reported peak deviatoric stress reasonable?
- (b) Is the CU test, as conducted, representative of the in situ conditions? Justify your answer.
- (c) Estimate the undrained shear strength of the in situ soil sample.

BEARING CAPACITY OF SOILS AND SETTLEMENT OF SHALLOW FOUNDATIONS

12.0 INTRODUCTION

In this chapter, we will consider bearing capacity of soils and settlement of shallow foundations. We will also consider the limit equilibrium method of analysis. This is the analysis that Coulomb performed in analyzing the lateral force on fortresses from soil placed behind them (Chapter 1). The limit equilibrium method is used to find solutions for a variety of problems including bearing capacity of foundations, stability of retaining wall, and slopes. We will also consider an alternative to conventional methods of analyses. This alternative method is based on critical state soil mechanics.

When you complete this chapter, you should be able to:

- Calculate the safe bearing capacity of soils.
- Estimate the settlement of shallow foundations.
- Estimate the size of shallow foundations to satisfy bearing capacity and settlement criteria.

You will use the following concepts learned from previous chapters and from your courses in mechanics.

- Statics
- Stresses and strains—Chapter 7
- Consolidation—Chapter 9
- Shear strength—Chapter 10

Importance

Loads from a structure are transferred to the soil through a foundation. A foundation itself is a structure, often constructed from concrete, steel, or wood. So far in our study, we have established the properties of soils and their response to loadings. An important task of a geotechnical engineer is to use the knowledge of the properties of soils and their response to loadings to design foundations. You will have to make decisions on the types of foundations, and their geometries and methods of construction. One type of foundation, often the least expensive, is a shallow foundation. A shallow foundation is one in which the ratio of the embedment depth to the minimum plan dimension (the width) is less than 2.5.

A geotechnical engineer must ensure that a foundation satisfies the following two stability conditions:

1. The foundation must not collapse or become unstable under any conceivable loading. This is called ultimate limit state.
2. Settlement of the structure must be within tolerable limits so as not to impair the design function of the structure. This is called serviceability limit state.

Both requirements must be satisfied. Often, it is settlement that governs the design of shallow foundations.



FIGURE 12.1 Construction of a shallow foundation.

In this chapter, you will learn about some methods to estimate the load-bearing capacity of soils and the geometry of shallow foundations to satisfy ultimate and serviceability limit states. The emphasis is on providing the fundamentals and the assumptions of these methods. The complexities of soils, the high cost of detailed site investigations, the uncertainties in loadings, and our inability to fully understand and model soil behavior accurately lead to methods of estimating foundation geometry that are, at best, classified as semiempirical. Methods in practice are based on simple analyses with simplifying assumptions, simple test methods such as SPT, and experience.

In foundation design, you must consider the method of construction and quality control in making design recommendations. These have significant influence on the soil-bearing resistance. The construction of a shallow foundation is shown in Figure 12.1.

12.1 DEFINITIONS OF KEY TERMS

Foundation is a structure that transmits loads to the underlying soils.

Footing is a foundation consisting of a small slab for transmitting the structural load to the underlying soil. Footings can be individual slabs supporting single columns (Figure 12.2a) or combined to support two or more columns (Figure 12.2b), or be a long strip of concrete slab (Figure 12.2c, d; width B to length L ratio is small, i.e., it approaches zero) supporting a load-bearing wall, or a mat (Figure 12.2e).

Embedment depth (D_f) is the depth below the ground surface where the base of the foundation rests.

Shallow foundation is one in which the ratio of the embedment depth to the minimum plan dimension, which is usually the width (B), is $D_f/B \leq 2.5$.

Ultimate bearing capacity is the maximum pressure that the soil can support.

Ultimate net bearing capacity (q_u) is the maximum pressure that the soil can support above its current overburden pressure.

Ultimate gross bearing capacity (q_{ult}) is the sum of the ultimate net bearing capacity and the overburden pressure above the footing base.

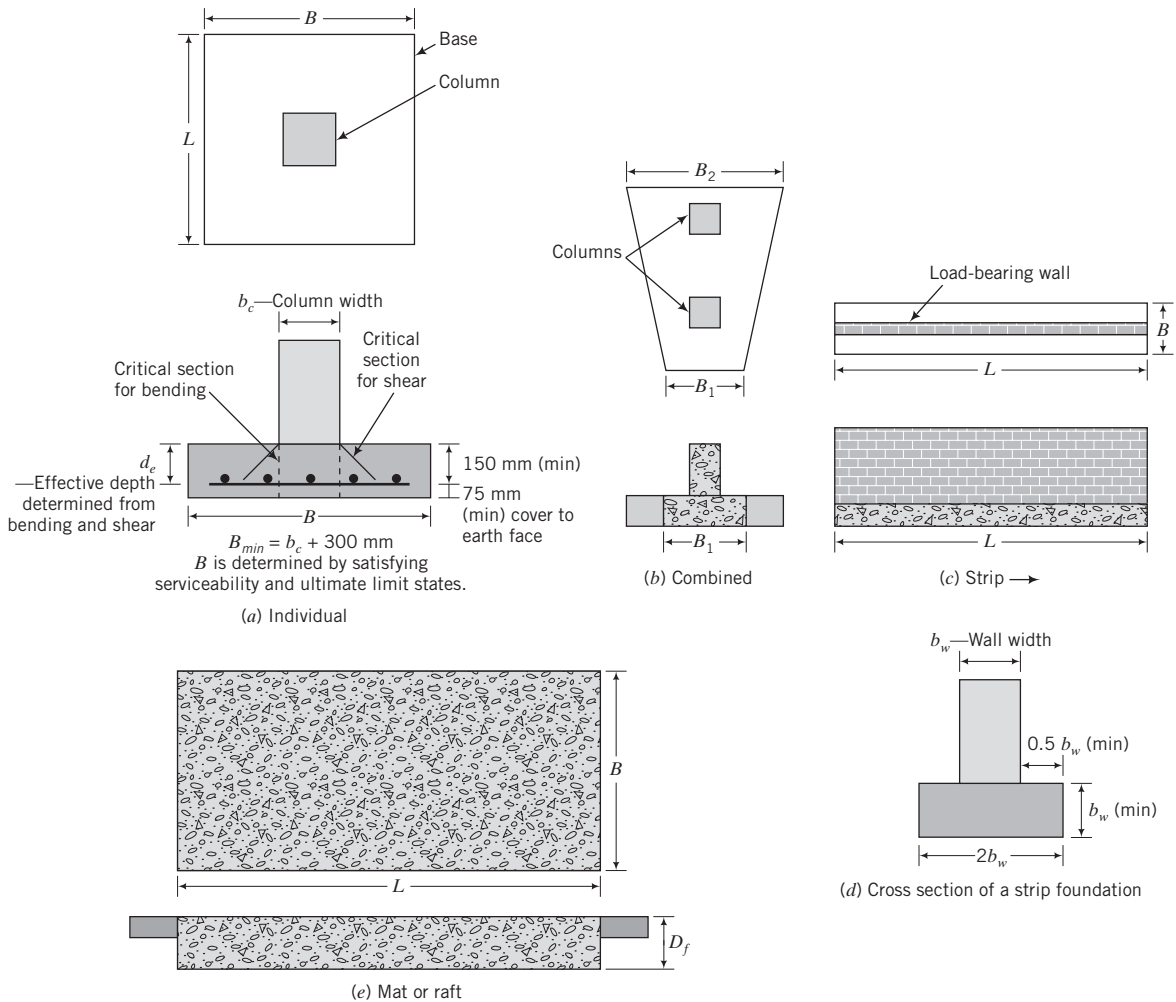


FIGURE 12.2 Type of shallow footing.

Allowable bearing capacity or **safe bearing capacity** (q_a) is the working pressure that would ensure a margin of safety against collapse of the structure from shear failure. The allowable bearing capacity is usually a fraction of the ultimate net bearing capacity.

Factor of safety or **safety factor (FS)** is the ratio of the ultimate net bearing capacity to the allowable net bearing capacity or to the applied maximum net vertical stress. In geotechnical engineering, a factor of safety between 2 and 5 is used to calculate the allowable bearing capacity.

Ultimate limit state defines a limiting stress or force that should not be exceeded by any conceivable or anticipated loading during the design life of a foundation or any geotechnical system.

Serviceability limit state defines a limiting deformation or settlement of a foundation, which, if exceeded, will impair the function of the structure that it supports.

12.2 QUESTIONS TO GUIDE YOUR READING

1. What are the ultimate net bearing capacity and the allowable bearing capacity of shallow footings?
 2. How do I determine the allowable bearing capacity for shallow footings?

3. What are the assumptions made in bearing capacity analyses?
4. What soil parameters are needed to calculate its bearing capacity?
5. What effects do groundwater and eccentric loads have on bearing capacity?
6. How do I determine the size of a footing to satisfy ultimate and serviceability limit states?

12.3 ALLOWABLE STRESS AND LOAD AND RESISTANCE FACTOR DESIGN

There are two design procedures used in practice in North America. One is allowable stress design (ASD); the other is load and resistance factor design (LRFD). In ASD, the ultimate load (stress) resistance is determined, and then this is divided by a factor of safety (FS) to obtain the allowable load (stress).

$$\text{Allowable load (stress or strength)} = \frac{\text{Ultimate load (stress or strength)}}{\text{FS}} \quad (12.1)$$

The factor of safety has no fundamental basis. It is based on experience and judgment of the performance of existing foundations. ASD is the long-standing (conventional) design method.

LRFD is based on reliability methods considering the uncertainties in loads, soil resistance, method of analysis, and construction. The loads are multiplied by load factors, usually greater than one in different combinations, and the ultimate soil resistance is multiplied by a factor, called the performance factor, usually less than one. The governing equation for design based on LRFD is

$$\sum \eta_i \rho_i P_i \leq \varphi_i R_i \quad (12.2)$$

where ρ is load factor; P is load; R is resistance; φ is the performance factor; η is a ductility, redundancy, and operational performance factor; and i is the load type, such as dead load or live load, and the resistance type. Codes (e.g., International Building Code, UBC), engineering organizations (e.g., American Society for Civil Engineers, ASCE), and agencies (e.g., American Association of State Highway and Transportation Officials, AASHTO) have their own recommendations on load and resistance factors and load combinations. In this textbook, we will consider only two types of loads, dead load (DL) and live load (LL), one load combination, and a limited set of performance factors. They are intended only to show how to apply these methods.

The load factors apply only to strength. For settlement calculation, the unfactored load or allowable stress is used.

Load combination

ASD: DL + LL

LRFD: 1.25 DL + 1.75 LL

Performance factor

A set of performance factors is given in Table 12.1. In practice, you should use the appropriate performance factor based on local practice.

A more detailed treatment of ASD and LRFD is presented in the author's textbook *Foundations and Earth Retaining Structures* (Publisher: John Wiley & Sons, NY) and will not be repeated in detail here.

TABLE 12.1 Performance Factors for Bearing Capacity Calculations Using LRFD¹

Bearing capacity	Resistance factor, φ_i
<i>ESA: Coarse-grained and fine-grained soils</i>	
ϕ'_{cs} from lab tests	0.95*
ϕ'_p from lab tests	0.8
ϕ'_p from SPT	0.35
ϕ'_p from CPT	0.45
SPT (N value)	0.45
CPT (cone tip resistance)	0.55
Plate load test	0.55
<i>TSA: Fine-grained soils</i>	
s_u - lab tests (UU triaxial)	0.60
- Vane shear (lab)	0.60
- CPT	0.50
- Field vane shear	0.60
- Plate load test	0.55
Sliding (Concrete slab on 150 mm sand above fine-grained soil)	0.85

¹Collected from different sources. You need to check your local code for recommended values.

*Author's recommendation.

12.4 BASIC CONCEPTS

12.4.1 Soil Response to a Loaded Footing

In developing the basic concepts we will use a generic friction angle, ϕ' , and later discuss whether to use ϕ'_p or ϕ'_{cs} . Failure in the context of bearing capacity means the ultimate gross bearing capacity. For dilating soils, failure corresponds to the peak shear stress, while for nondilating soils, failure corresponds to the critical state shear stress. To distinguish these two states, we will refer to the failure load in dilating soils as the collapse load and reserve the term *failure load* for nondilating soils. Thus, collapse load is the load at peak shear stress, while failure load is the load at critical state. Collapse means a sudden decrease in the bearing capacity of a soil. Recall from Chapter 10 that dilatancy can be suppressed by large confining pressures, and so a peak shear stress may not develop.

The analysis of a footing on a soil is a contact problem of two dissimilar bodies. In making such an analysis, we have to treat soil as an ideal material such as an elastic material or an elastoplastic material or a rigid-perfectly plastic material (Chapter 7). Let us consider soil as a linear elastic-perfectly plastic material (Figure 12.3a) in which the elastic response is small. We assume a strip footing (its length is much longer than its width) traps a wedge of soil, and this wedge, acted on by the footing, pushes its way downward into the soil (Figure 12.3b). If the footing were circular, it would trap a cone of soil.

Centric, vertical loads are now incrementally applied on the footing. Initially, the soil will respond elastically. It will be compressed vertically and laterally (lateral outward movement). The deformation is fully contained within the soil as stored energy. If we were to unload the footing, the deformation would be recoverable. As the load increases, some regions of the soil would yield and behave plastically (plastic flow). The pressure at the apex of the wedge is infinite and leads to infinite differences in principal stresses. Thus, there will be a region around the apex that would yield immediately upon loading. If the soil were a rigid-perfectly plastic material, some regions would flow plastically while other regions would show no deformation. We will call the soil regions that have reached the plastic state the plastic zones. As more loads are added, the plastic zones increase and eventually break free to the surface, and soil "pileup" on the sides of the footing (Figure 12.3b). There is a transition phase

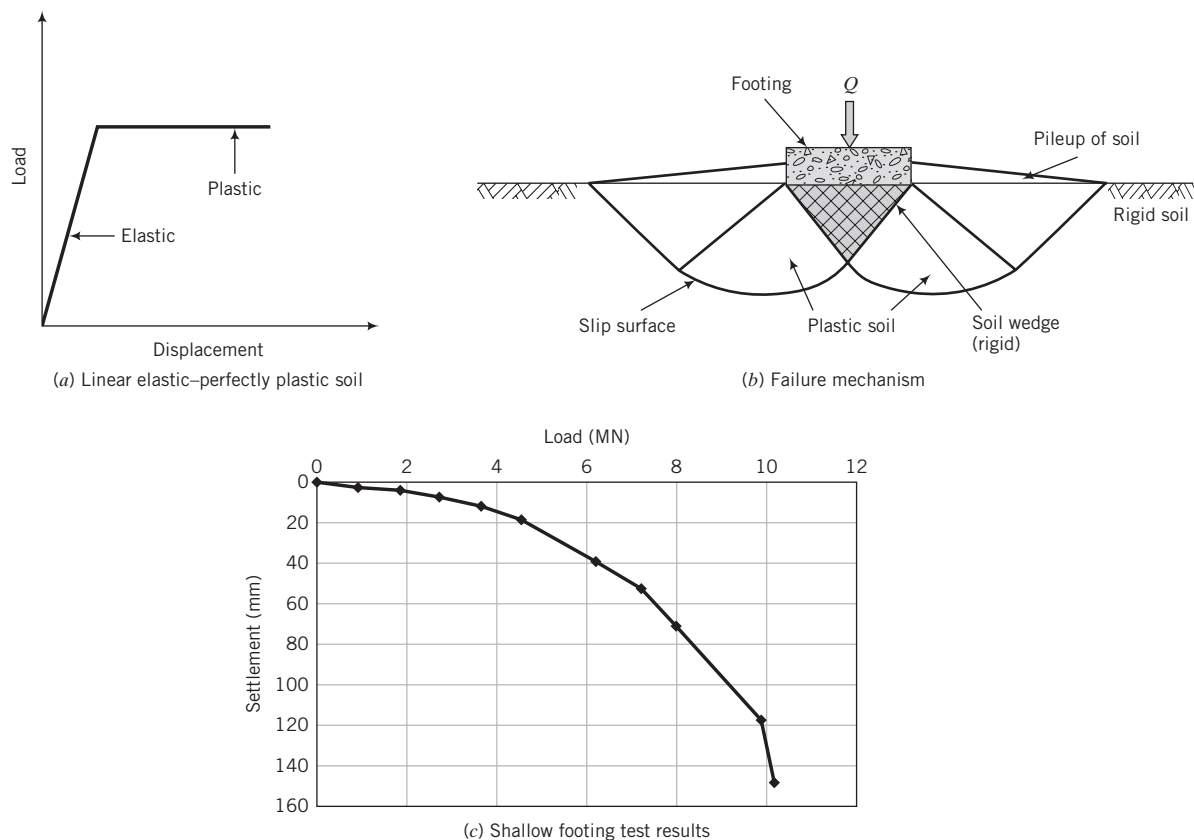


FIGURE 12.3 (a) Load–displacement response of an elastic–perfectly plastic material. (b) Indentation of soil wedge into a soil (no slip at the wedge faces and at the footing–soil interface; slip along the footing thickness). (c) Field test results of a 3-m-square footing on a sand. (Data from Briaud and Gibbens, 1994.)

from elastic to perfectly plastic response whereby the soil behaves as an elastoplastic material and the deformation is essentially in the lateral directions. The surface between the plastic zones and the non-plastic or nondeforming zones (applicable to rigid–perfectly plastic material) is called a slip surface or limiting stress surface.

The “pileup” is influenced by the overburden pressure and the strain-hardening ability of the material. If the footing is embedded in the soil and/or the soil has a large potential to strain-harden, the plastic flow that causes “pileup” of soil around the edges of the footing would be restrained, creating large lateral pressures to force the soil to move laterally. Two consequences are: (1) A soil that would normally show a peak shear stress because of dilatancy and then strain-soften would be forced to behave as a strain-hardening material, pushing the plastic zone farther into the soil mass, and (2) the failure mechanism shown in Figure 12.3b might not develop. Therefore, in this situation, there would not be any distinct collapse load but an increasing load with increasing footing displacement until critical state is achieved. Generally, this would occur at displacements that are intolerable. Tests on shallow footings often show this type of response whereby a peak or collapse load is not discernible (Figure 12.3c).

In the next section, the failure surface assumed in conventional analyses for the collapse load is presented. As you read this section, compare it with the information you just studied.

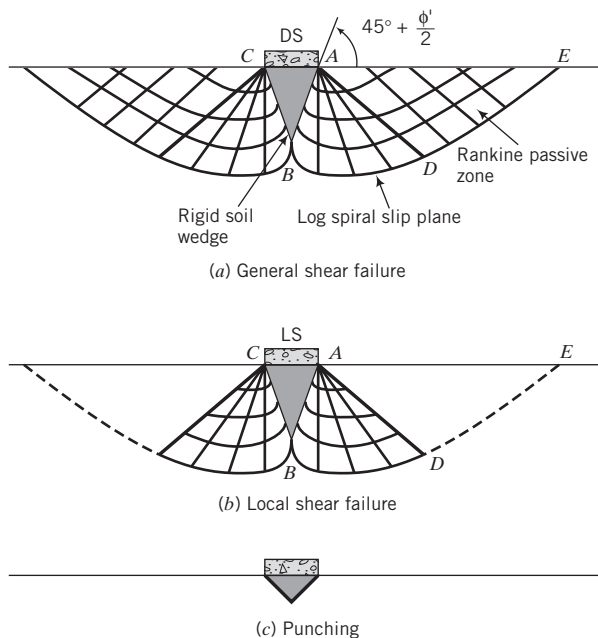


FIGURE 12.4 Conventional failure mechanisms.

12.4.2 Conventional Failure Surface Under a Footing

Prandtl (1920) studied a rigid–perfectly plastic half space loaded by a stiff wedge that is subjected to centric loads. Terzaghi (1943) applied Prandtl's theory to a strip footing with the assumption that the soil is a semi-infinite, homogeneous, isotropic, weightless rigid–plastic material. Recall from the previous section that with these assumptions, plastic flow would occur when the load reached a certain magnitude. The slip surface assumed by Prandtl and adopted by Terzaghi is shown in Figure 12.4a. Two plastic zones form around the rigid wedge—each zone symmetrical about a vertical plane (parallel to the length of the footing) through the center of the footing. One zone, ABD (Figure 12.4a), is a fan with radial slip planes stopping on a logarithmic spiral slip plane. The other zone, ADE , consists of slip planes oriented at angles of $45^\circ + \phi'/2$ and $45^\circ - \phi'/2$ to the horizontal and vertical planes, respectively, as we found in Chapter 7. Zone ADE is called the Rankine passive zone. In Chapter 15, we will discuss Rankine passive zone and also Rankine active zone in connection with retaining walls. Surfaces AB and AD are frictional sliding surfaces, and their actions are similar to rough walls being pushed into the soil. The pressure exerted is called passive lateral earth pressure. If we can find the value of this pressure, we can determine the ultimate gross bearing capacity by considering the equilibrium of wedge ABC . You will recall from Chapter 10 that, according to the Mohr–Coulomb criterion, slip planes form when soils are sheared to failure. No slip plane, however, can pass through the rigid footing, so none can develop in the soil just below the footing. The collapse mechanism shown in Figure 12.4a is called the general shear failure mechanism.

Recall from Section 12.4.1 that the conventional collapse mechanism shown in Figure 12.4a may not develop. Therefore, calculation of a collapse load (Sections 12.5 and 12.6) from this mechanism could be considerably inaccurate.

Other collapse mechanisms have been proposed. For example, it is assumed that for loose soils, the slip planes, if they developed, are expected to lie within the soil layer below the base of the footing and extend laterally. This is called local shear failure (Figure 12.4b). For very loose soil, the slip surfaces may be confined to the surfaces of the rigid wedge. This type of failure is termed punching shear (Figure 12.4c).

THE ESSENTIAL POINTS ARE:

1. The load-displacement response of a footing depends on the stress-strain behavior of the soil and the boundary conditions imposed.
2. When a soil behaves like a rigid-perfectly plastic material, soil piles up near the edges of the footing from plastic flow, and a collapse mechanism develops when there is a free surface. This collapse mechanism may not develop in real soils.
3. The conventional collapse mechanism consists of a rigid wedge of soil trapped beneath the footing bordering radial plastic shear zones under Rankine passive zones.

What's next . . . The bearing capacity equations that we will discuss in this chapter were derived by making alterations to the failure surface proposed by Prandtl. Before we consider these bearing capacity equations, we will find the collapse load for a strip footing resting on a clay soil using a popular analytical technique called the limit equilibrium method.

12.5 COLLAPSE LOAD USING THE LIMIT EQUILIBRIUM METHOD

The bearing capacity equations that are in general use in engineering practice were derived using an analytical method called the limit equilibrium method. We will illustrate how to use this method by finding the collapse load (P_u) for a strip footing. The essential steps in the limit equilibrium method are (1) selection of a plausible failure mechanism or failure surface, (2) determination of the forces acting on the failure surface, and (3) use of the equilibrium equations that you learned in statics to determine the collapse or failure load.

Let us consider a strip footing of width B , resting on the surface of homogeneous, saturated clay whose undrained strength is s_u (Figure 12.5). For simplicity, we will neglect the weight of the soil. Step 1 of the limit equilibrium method requires that we either know or speculate on the failure mechanism. Since we do not know what the failure mechanism is because we have not done any testing, we will speculate that the footing will fail by rotating about the inner edge A (Figure 12.5), so that the failure surface is a semicircle with radius B .

Step 2 is to determine the forces on the failure surface. Along the circumference of the semicircle, there would be shear stresses (τ) and normal stresses (σ_n). We do not know whether these stresses are uniformly distributed over the circumference, but we will assume that this is so; otherwise, we have to perform experiments or guess plausible distributions. Since failure occurred, the maximum shear strength of the soil is mobilized, and therefore the shear stresses are equal to the shear strength of the soil. Now we are ready to move to Step 3. The moment due to the normal force acting on the semicircle about A is zero since its line of action passes through A . The moment equilibrium equation is then

$$P_u \times \frac{B}{2} - s_u \pi B \times B = 0 \quad (12.3)$$

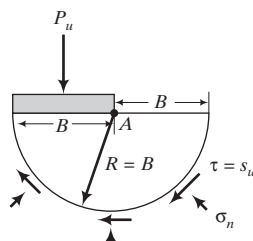


FIGURE 12.5
Circular failure mechanism.

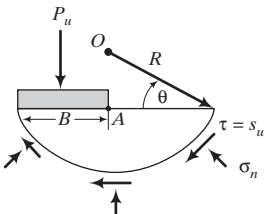


FIGURE 12.6
Circular arc failure mechanism.

and the collapse load is

$$P_u = 6.28Bs_u \quad (12.4)$$

We are unsure that the collapse load we calculated is the correct one, since we guessed a failure mechanism. We can repeat the three steps above by choosing a different failure mechanism. For example, we may suppose that the point of rotation is not A but some point O above the footing such that the radius of the failure surface is R (Figure 12.6).

Taking moments about O , we get

$$P_u(R \cos \theta - B/2) - s_u[(\pi - 2\theta)R]R = 0 \quad (12.5)$$

By rearranging Equation (12.5), we get

$$P_u = \frac{s_u[(\pi - 2\theta)R]R}{(R \cos \theta - B/2)} = \frac{s_u(\pi - 2)R}{(\cos \theta - B/2R)} \quad (12.6)$$

The collapse load now depends on two variables, R and θ , and as such there is a family of failure mechanisms. We must then find the least load that will produce collapse. We do this by searching for extrema (minima and maxima in curves) by taking partial derivatives of Equation (12.6) with respect to R and θ . Thus,

$$\frac{\partial P_u}{\partial R} = \frac{4s_uR(\pi - 2\theta)(R \cos \theta - B)}{(2R \cos \theta - B)^2} = 0 \quad (12.7)$$

and

$$\frac{\partial P_u}{\partial \theta} = \frac{4s_uR^2(B - 2R \cos \theta + \pi R \sin \theta - 2R\theta \sin \theta)}{(2R \cos \theta - B)^2} = 0 \quad (12.8)$$

The solutions of Equations (12.7) and (12.8) are $\theta = 23.2^\circ$ and $R = B \sec \theta$; that is, point O is directly above A . Substituting these values in Equation (12.6), we obtain the collapse load as

$$P_u = 5.52Bs_u \quad (12.9)$$

This is a better solution because the collapse load is smaller than Equation (12.4), but we need to investigate other possible mechanisms, which may yield yet a smaller value of P_u . The exact solution to our problem, using more complex analysis than the limit equilibrium method, gives

$$P_u = 5.14Bs_u \quad (12.10)$$

which is about 9% lower than our second mechanism.

What's next . . . We have just learned the rudiments of the limit equilibrium method. It is an iterative method in which you speculate on possible failure mechanisms and then use statics to find the collapse load. The bearing capacity equations that we will discuss next were derived using the limit equilibrium method. We will not derive the bearing capacity equations because no new concept will be learned. You can refer to the published literature mentioned later if you want to pursue the derivations.

12.6 BEARING CAPACITY EQUATIONS



Computer Program Utility

Access www.wiley.com/college/budhu, click on Chapter 12, and then click on bc.xls for a spreadsheet to calculate bearing capacity of soils.

Terzaghi (1943) derived bearing capacity equations based on Prandtl (1920) failure mechanism and the limit equilibrium method for a footing at a depth D_f below the ground level of a homogeneous soil. For most shallow footings, the depth D_f , called the embedment depth, accounts for frost action, freezing, thawing, and other environmental effects. Building codes provide guidance as to the minimum depth of embedment for footings. Terzaghi assumed the following:

1. The soil is a semi-infinite, homogeneous, isotropic, weightless, rigid-plastic material.
2. The embedment depth is not greater than the width of the footing ($D_f < B$).
3. General shear failure occurs.
4. The angle θ in the wedge (Figure 12.7) is ϕ' . Later, it was found (Vesic, 1973) that $\theta = 45^\circ + \phi'/2$.
5. The shear strength of the soil above the footing base is negligible. Later, Meyerhof (1951) considered the shear resistance above the footing base.
6. The soil above the footing base can be replaced by a surcharge stress ($= \gamma D_f$).
7. The base of the footing is rough.

A plethora of bearing capacity equations, based on limiting equilibrium (e.g., Terzaghi, 1943; Meyerhof, 1963; Hansen, 1970; and Vesic, 1973) has been proposed. We will consider only a set of equations

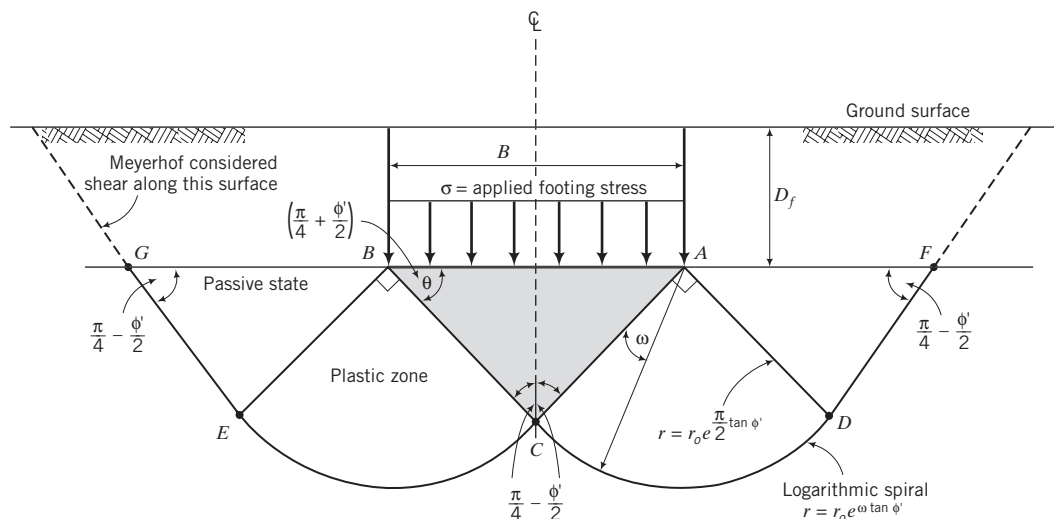


FIGURE 12.7 Conventional failure surface.

for general soil failure that has found general use in geotechnical practice. General shear failure is likely to occur in dense, coarse-grained soils with relative density greater than 70% and in stiff, fine-grained soils. Terzaghi suggested that for local shear failure, ϕ'_p and s_u be reduced to 2/3 their values.

We will consider two limiting conditions. One is short-term condition that requires a total stress analysis (TSA). TSA is applicable to fine-grained soils, and the shear strength parameter is the undrained shear strength, s_u . The other is long-term condition that requires an effective stress analysis (ESA). ESA is applicable to all soils, and the shear strength parameter is the peak friction angle, ϕ'_p , from plane strain tests.

General Loading Conditions

Ultimate Net Bearing Capacity

The ultimate net bearing capacity equations for general failure are

$$\text{TSA: } q_u = 5.14 s_u s_c d_c i_c b_c g_c \quad (12.11)$$

$$\text{ESA: } q_u = \gamma D_f (N_q - 1) s_q d_q i_q b_q g_q + 0.5\gamma B' N_\gamma s_\gamma d_\gamma b_\gamma g_\gamma \quad (12.12)$$

According to Equation (12.11), the bearing capacity of fine-grained soils is not dependent on the size of the footing.

Ultimate Gross Bearing Capacity

The gross bearing capacity is

$$q_{ult} = q_u + \gamma D_f \quad (12.13)$$

Allowable Bearing Capacity

The allowable bearing capacity is

$$q_a = \frac{q_u}{\text{FS}} + \gamma D_f \quad (12.14)$$

where FS is a factor of safety ranging from 2 to 3; FS = 3 is most often used. In practice, some geotechnical engineers use N_q rather than $(N_q - 1)$ in Equation (12.12) and neglect the term γD_f in Equation 12.14 for conservative design.

Vertical Centric Load Only on a Horizontal Footing Resting on a Horizontal Surface

$$\text{TSA: } q_u = 5.14 s_u s_c d_c \quad (12.15)$$

$$\text{ESA: } q_u = \gamma D_f (N_q - 1) s_q d_q + 0.5\gamma B' N_\gamma s_\gamma d_\gamma \quad (12.16)$$

Inclined Load Only on a Horizontal Footing Resting on a Horizontal Surface

$$\text{TSA: } q_u = 5.14 s_u i_c \quad (12.17)$$

$$\text{ESA: } q_u = \gamma D_f (N_q - 1) i_q + 0.5\gamma B' N_\gamma i_\gamma \quad (12.18)$$

where the factors N_q and N_γ are bearing capacity factors that are functions of ϕ'_p ; s_c , s_q , and s_γ are shape factors; d_c , d_q , and d_γ are embedment depth factors; i_c , i_q , and i_γ are load inclination factors; b_c , b_q , and b_γ are base inclination (base tilt) factors; B' is the equivalent footing width (see Figure 12.10); and g_c , g_q , and g_γ are ground inclination factors.

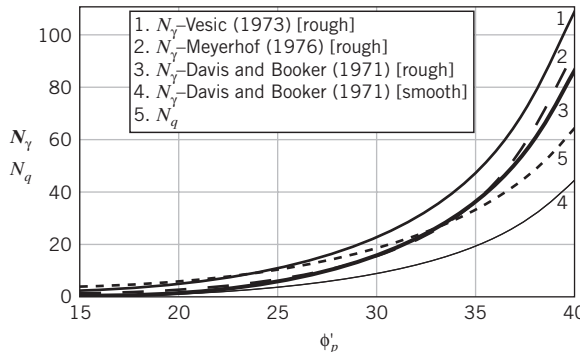


FIGURE 12.8 Comparison of some bearing capacity factors.

Bearing Capacity Factors The bearing capacity factor N_q is

$$N_q = e^{\pi \tan \phi'_p} \tan^2 \left(45^\circ + \frac{\phi'_p}{2} \right); \quad \phi'_p \text{ in degrees} \quad (12.19)$$

Various equations have been proposed for N_γ in the literature. Among the popular equations are:

$$\text{Vesic (1973): } N_\gamma = 2(N_q + 1) \tan \phi'_p; \quad \phi'_p \text{ in degrees} \quad (12.20)$$

$$\text{Meyerhof (1976): } N_\gamma = (N_q - 1) \tan (1.4\phi'_p); \quad \phi'_p \text{ in degrees} \quad (12.21)$$

$$\text{Davis and Booker (1971): } N_\gamma = 0.1054 \exp (9.6\phi'_p) \quad \text{for rough footing; } \phi'_p \text{ in radians} \quad (12.22)$$

$$N_\gamma = 0.0663 \exp (9.3\phi'_p) \quad \text{for smooth footing; } \phi'_p \text{ in radians} \quad (12.23)$$

The differences among these popular bearing capacity factors are shown in Figure 12.8.

The bearing capacity factor, N_γ , proposed by Davis and Booker is based on a refined plasticity method and gives conservative values compared with Vesic. Meyerhof's N_γ values are equal to Davis and Booker's N_γ for ϕ'_p of less than about 35° . In this book, we will adopt the Davis and Booker values for N_γ .

The crucial parameter is ϕ'_p . The attainment of ϕ'_p depends on the ability of the soil to dilate, which can be suppressed by large normal effective stresses. Since neither the loads nor the stresses induced by the loads on the soil mass are certain, the use of ϕ'_p is then uncertain. We can write $\phi'_p = \phi'_{cs} + \alpha_p$, where ϕ'_{cs} is the friction angle at critical state (a fundamental soil property) and α_p is the peak dilation angle (not a fundamental soil property). The uncertainty in ϕ'_p comes mainly from the uncertainty in the value of α_p .

Plane strain conditions have been assumed in developing the theoretical bearing capacity equations. Thus, the values of ϕ'_p should come from plane strain tests such as the direct shear or direct simple shear test. Triaxial tests on the same soil generally give values of ϕ'_p less than plane strain tests. Various conversions have been proposed. For practical purposes, the following conversion can be used:

$$(\phi'_p)_{ps} = \frac{9}{8} (\phi'_p)_{tr} \quad (12.24)$$

where the subscripts ps and tr denote plane strain and triaxial, respectively.

The undrained shear strength, s_u , to be used in Equation (12.11) requires experience and judgment. Recall that s_u is not a fundamental soil property; it is a function of the initial void ratio or initial confining stress. Skempton (1953) used s_u from unconfined triaxial compression tests with success in the postfailure assessment of the failure of the Transcona grain silo foundation mentioned in Chapter 1. However, the limit analysis from which Equation (12.11) was derived requires the use of s_u from plane strain tests. Generally, s_u varies with depth (recall from Chapter 11 that for normally consolidated soils, s_u increases with depth). One practical method for homogeneous soils is to average the s_u values over a depth of $1.5B$ below the bottom of the footing and use that value in Equation (12.11).

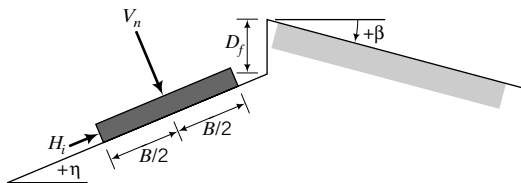


FIGURE 12.9
Footing on a slope.

Rough footing denotes a footing in which full shear is developed at the footing–soil interface. It is common construction practice to compact a layer of coarse-grained soils for the footing to rest on. In this case, N_y for rough footing is appropriate. When a footing rests directly on fine-grained soils, N_y for smooth footing should be used.

Geometric Factors Geometric factors account for the shape and slope of the footing, the load inclination and eccentricity, and the ground slope (Figure 12.9). Several equations have been proposed for these factors. In this book, we will adopt a set of factors proposed in the literature that are used in general practice or have been updated due to more refined analyses or experimental evidence. These factors are listed in Table 12.2 and must be regarded as estimates.

The bearing capacity equations apply for a single resultant load with normal, V_n , and horizontal components, H_B , parallel to the width, B (the short side), and horizontal components, H_L , parallel to the length, L (the long side). When investigating potential failure along the short side, use H_B . For failure along the long side, use H_L .

TABLE 12.2 Geometric Factors for Use in Theoretical Bearing Capacity Equations

Geometric parameters for TSA				
s_c	d_c	i_c	b_c	g_c
$1 + 0.2 \frac{B'}{L'}$	$1 + 0.33 \tan^{-1} \frac{D_f}{B'}$ See note 1	$1 - \frac{nH}{5.14 s_u B' L'}$ See note 2	$1 - \frac{\eta^\circ}{147}$ $\beta < \phi'_p$; $\eta^\circ + \beta^\circ < 90^\circ$ See Figure 12.9	$1 - \frac{\beta^\circ}{147}$ $\beta < \phi'_p$; $\eta^\circ + \beta^\circ < 90^\circ$ See Figure 12.9
Geometric parameters for ESA				
s_q	d_q	i_q	b_q	g_q
$1 + \frac{B'}{L'} \tan \phi'_p$	$1 + 2 \tan \phi'_p (1 - \sin \phi'_p)^2 \tan^{-1} \left(\frac{D_f}{B'} \right)$	$\left(1 - \frac{H}{V_n} \right)^n$ See note 2	$(1 - \eta \tan \phi'_p)^2$ η is in radians	$(1 - \tan \beta)^2$
s_γ	d_γ	i_γ	b_γ	g_γ
$1 - 0.4 \frac{B'}{L'}$	1	$\left(1 - \frac{H}{V_n} \right)^{n+1}$ See note 2	$b_\gamma = b_q$	$g_\gamma = g_q$

Note 1: If the shear strength of the soil above the footing is low compared with that of the soil below the footing, you should set all depth factors to 1. The term $\tan^{-1} \left(\frac{D_f}{B'} \right)$ is in radians.

Note 2: The depth and shape factors for inclined loads should be set to 1. For loading inclined in the direction of the width, B , $\theta = 90^\circ$ in Figure 12.10d, $n = n_B = \left(2 + \frac{B'}{L'} \right) / \left(1 + \frac{B'}{L'} \right)$. For loading inclined in the direction of the length, L , $\theta = 0^\circ$ in Figure 12.10d, $n = n_L = \left(2 + \frac{L'}{B'} \right) / \left(1 + \frac{L'}{B'} \right)$. For other loading conditions, $n = n_L \cos^2 \theta + n_B \sin^2 \theta$.

Eccentric Loads When the location of the resultant load (load center) is not coincident with the centroid (center of area) of the footing, the footing dimensions are theoretically adjusted to align the load center with the centroid. The distances from the center of the area to the location of the vertical component of the resultant load are eccentricities. Applied moments can be converted to a vertical resultant load at eccentricities, e_B and e_L , where

$$e_B = \frac{M_y}{V_n}; \quad e_L = \frac{M_x}{V_n} \quad (12.25)$$

V_n is the resultant vertical load; M_x and M_y are the moments about the X and Y axes, as shown in Figure 12.10c. Some possible cases of eccentric loads are shown in Figure 12.10.

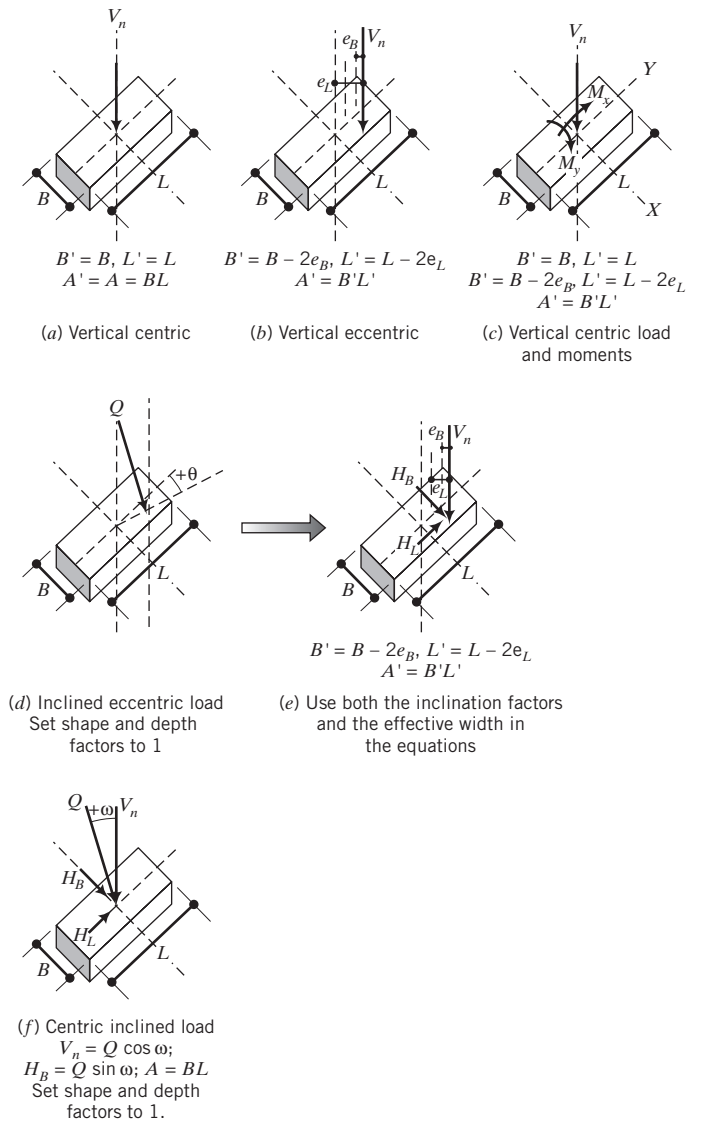


FIGURE 12.10 Some possible load cases.

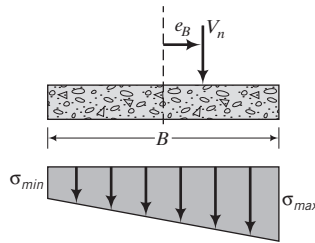


FIGURE 12.11 Vertical stress distribution below an eccentrically loaded footing.

The stresses due to a vertical load at an eccentricity e (moment = $V_n e$) are (from your knowledge of mechanics):

$$\sigma = \frac{V_n}{A} \pm \frac{My}{I} = \frac{V_n}{A} \pm \frac{V_n ey}{I} = \frac{V_n}{A} \pm \frac{V_n e}{Z} \quad (12.26)$$

where I is the second moment of area, y is the distance from the neutral axis to the outer edge, A is the cross-

sectional area, and Z is the section modulus. For a rectangular section, $Z = \frac{I}{y} = \frac{\frac{B^3 L}{12}}{\frac{B}{2}} = \frac{B^2 L}{6}$ or $\frac{BL^2}{6}$,

depending on whether you are considering moment about the Y -axis or the X -axis.

The maximum and minimum vertical stresses along the X -axis are

$$\sigma_{max} = \frac{V_n}{A} + \frac{V_n e}{Z} = \frac{V_n}{BL} \left(1 + \frac{6e_B}{B} \right); \quad \sigma_{min} = \frac{V_n}{A} - \frac{V_n e}{Z} = \frac{V_n}{BL} \left(1 - \frac{6e_B}{B} \right) \quad (12.27)$$

and along the Y -axis are

$$\sigma_{max} = \frac{V_n}{A} + \frac{V_n e}{Z} = \frac{V_n}{BL} \left(1 + \frac{6e_L}{L} \right); \quad \sigma_{min} = \frac{V_n}{A} - \frac{V_n e}{Z} = \frac{V_n}{BL} \left(1 - \frac{6e_L}{L} \right) \quad (12.28)$$

The distribution of vertical stresses below an eccentrically loaded footing on a plane parallel to the direction of its width B and passing through the load point is shown in Figure 12.11.

Let us examine σ_{min} . If $e_B = \frac{B}{6}$ or $e_L = \frac{L}{6}$, then $\sigma_{min} = 0$. If, however, $e_B > \frac{B}{6}$ or $e_L > \frac{L}{6}$, then $\sigma_{min} < 0$, and tension develops. Since the tensile strength of uncemented soil is zero, part of the footing will not transmit loads to the soil. You should try to avoid this situation by designing the footing such that $e_B < \frac{B}{6}$ and $e_L < \frac{L}{6}$.

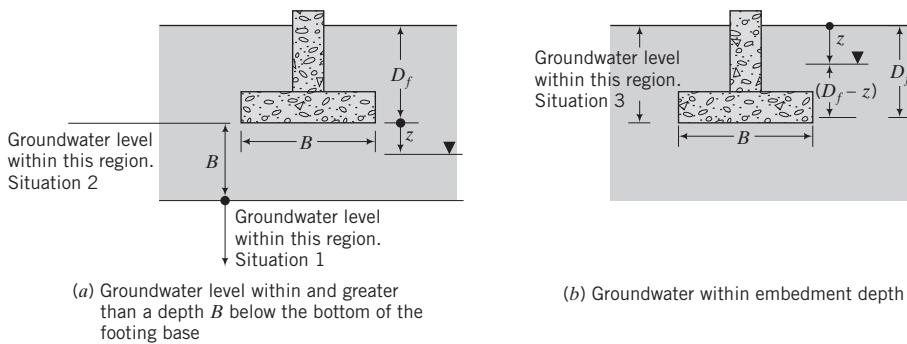
The ultimate net load is:

$$P_u = q_u B' L' \quad (12.29)$$

The effective width, B' , and effective length, L' , giving an effective area $A' = B'L'$ must be used in the theoretical bearing capacity equations. If the load is centric, then $B' = B$ and $L' = L$. For circular footing, $B = L = D$, where D is diameter. The equivalent area for a circular foundation subjected to an eccentric load is

$$A' = \frac{D^2}{2} \left[\cos^{-1} \frac{2e}{D} - \frac{2e}{D} \sqrt{1 - \left(\frac{2e}{D} \right)^2} \right] \quad (12.30)$$

Groundwater Effects You have to adjust the theoretical bearing capacity equations for groundwater condition. The term γD_f in the bearing capacity equations for an ESA refers to the vertical stress of the soil above the base of the foundation. The last term γB refers to the vertical stress of a soil mass of thickness B below the bottom of the footing base. You need to check which one of three groundwater situations given below is applicable to your project.

**FIGURE 12.12** Groundwater effects below base of footing.

Situation 1. If the groundwater level is at a depth greater than or equal to B below the bottom of the footing base (Figure 12.12a), no correction is required.

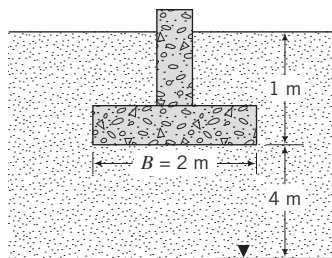
Situation 2. If the groundwater level is within a depth B below the bottom of the footing base such that $0 \leq z < B$ (Figure 12.12a), then the term γB is $\gamma z + (\gamma_{sat} - \gamma_w)(B - z)$ or $\gamma_{sat}z + (\gamma_{sat} - \gamma_w)(B - z)$. The latter equation is used if the soil above the groundwater level is saturated. Note that z is measured from the bottom of the footing base. γD_f remains unchanged.

Situation 3. If the groundwater level is within the embedment depth such that $0 \leq z \leq D_f$ (Figure 12.12b), then the term γD_f is $\gamma z + (\gamma_{sat} - \gamma_w)(D_f - z)$ or $\gamma_{sat}z + (\gamma_{sat} - \gamma_w)(D_f - z)$ if the soil above the groundwater level is saturated. Note that z is measured from the ground surface; $\gamma B = (\gamma_{sat} - \gamma_w)B$.

EXAMPLE 12.1 Allowable Bearing Capacity of a Sand

A footing 2 m square, subjected to a centric vertical load, is located at a depth of 1.0 m below the ground surface in a deep deposit of compacted sand ($\phi'_p = 35^\circ$, $\phi'_{cs} = 30^\circ$, and $\gamma_{sat} = 18 \text{ kN/m}^3$). The groundwater level is 5 m below the ground surface, but you should assume that the soil above the groundwater is saturated. The friction angles were obtained from plain strain tests. Determine the allowable bearing capacity for a factor of safety of 3.

Strategy It is a good policy to sketch a diagram illustrating the conditions given (see Figure E12.1). The groundwater level is located at $(5 \text{ m} - 1 \text{ m}) = 4 \text{ m}$ from the footing base. That is, the groundwater level is more than $B = 2 \text{ m}$ below the base. We can neglect the effects of groundwater.

**FIGURE E12.1**

Solution 12.1

Step 1: Calculate the bearing capacity factors and geometric factors. Assume rough footing. Use $\phi' = \phi'_p = 35^\circ$.

The eccentricity is zero, so $B' = B$ and $L' = L$.

$$N_q = e^{\pi \tan \phi'_p} \tan^2 \left(45^\circ + \frac{\phi'_p}{2} \right) = e^{\pi \tan 35^\circ} \tan^2 \left(45^\circ + \frac{35^\circ}{2} \right) = 33.3$$

$$N_q - 1 = 32.3$$

$$N_\gamma = 0.1054 \exp(9.6 \phi'_p) = 0.1054 \exp \left(9.6 \times \frac{35 \times \pi}{180} \right) = 37.1$$

$$s_q = 1 + \frac{B'}{L'} \tan \phi'_p = 1 + \frac{2}{2} \tan 35^\circ = 1.70$$

$$s_\gamma = 1 - 0.4 \frac{B'}{L'} = 1 - 0.4 \frac{2}{2} = 0.6$$

$$d_\gamma = 1.0$$

$$d_q = 1 + 2 \tan \phi'_p (1 - \sin \phi'_p)^2 \tan^{-1} \left(\frac{D_f}{B'} \right)$$

$$= 1 + (2 \tan 35^\circ) (1 - \sin 35^\circ)^2 \left[\tan^{-1} \left(\frac{1}{2} \right) \times \frac{\pi}{180} \right] = 1.13$$

Step 2: Calculate the ultimate net bearing capacity.

$$q_u = \gamma D_f (N_q - 1) s_q d_q + 0.5 \gamma B N_\gamma s_\gamma d_\gamma$$

$$q_u = (18 \times 1 \times 32.3 \times 1.7 \times 1.13) + (0.5 \times 18 \times 2 \times 37.1 \times 0.6 \times 1.0) \\ = 1515 \text{ kPa}$$

$$q_a = \frac{q_u}{\text{FS}}$$

$$= \frac{1515}{3} + 18 \times 1 = 523 \text{ kPa}$$

EXAMPLE 12.2 The Effects of Groundwater on Bearing Capacity

Compare the ultimate net bearing capacity for Example 12.1 using $\phi'_p = 35^\circ$ when the groundwater is located (a) at 5 m below the ground surface, (b) at the ground surface, (c) at the bottom of the base of the footing, and (d) at 1 m below the base.

Strategy The trick here is to use the appropriate value of the unit weight in the bearing capacity equation.

Solution 12.2

Step 1: Calculate bearing capacity numbers and shape and depth factors. These values are the same as in Example 12.1.

Step 2: Substitute values from Step 1 into Equation (12.14).

(a) *Groundwater level at 5 m below the surface.* The groundwater level is 4 m below the base, which is greater than the width of the footing. Therefore, groundwater has no effect.

$$\text{From Example 12.1: } q_u = 1515 \text{ kPa}$$

(b) *Groundwater level at the ground surface.* In this case, the groundwater level will affect the bearing capacity. You should use

$$\gamma' = \gamma_{sat} - \gamma_w = 18 - 9.8 = 8.2 \text{ kN/m}^3$$

$$q_u = \gamma' D_f (N_q - 1) s_q d_q + 0.5 \gamma' B' N_\gamma s_\gamma d_\gamma \\ = (8.2 \times 1 \times 32.3 \times 1.7 \times 1.13) + (0.5 \times 8.2 \times 2 \times 37.1 \times 0.6 \times 1.0) \\ = 691 \text{ kPa}$$

Alternatively, since the change in the unit weight is the same for both terms of the bearing capacity equation, we can simply find q_u by taking the ratio γ'/γ , that is,

$$q_u = 1515 \times \frac{8.2}{18} = 690 \text{ kPa}$$

- (c) *Groundwater level at the bottom of the base.* In this case, the groundwater level will affect the last term in the bearing capacity.

Thus,

$$\begin{aligned} q_u &= \gamma D_f (N_q - 1) s_q d_q + 0.5 \gamma' B' N_\gamma s_\gamma d_\gamma \\ &= (18 \times 1 \times 32.3 \times 1.7 \times 1.13) + (0.5 \times 8.2 \times 2 \times 37.1 \times 0.6 \times 1.0) \\ &= 1299 \text{ kPa} \end{aligned}$$

- (d) *Groundwater level at 1 m below the bottom of the base.* In this case, the groundwater level is within a depth B below the base and will affect the last term in the bearing capacity, where you should use

$$\gamma' B' = \gamma_{sat} z + \gamma'(B' - z) = 18 \times 1 + 8.2 \times (2 - 1) = 26.2 \text{ kN/m}^2$$

Thus,

$$\begin{aligned} q_u &= \gamma D_f (N_q - 1) s_q d_q + 0.5 (\gamma' B') N_\gamma s_\gamma d_\gamma \\ &= (18 \times 1 \times 32.3 \times 1.7 \times 1.13) + (0.5 \times 26.2 \times 37.1 \times 0.6 \times 1.0) \\ &= 1408 \text{ kPa} \end{aligned}$$

Step 3: Compare results.

We will compare the results by dividing (normalizing) each ultimate net bearing capacity by the ultimate net bearing capacity of case (a).

Groundwater level at	$\frac{q_u}{(q_u)_{(a)}} \times 100$
(b) Ground surface	$\frac{691}{1515} \times 100 \approx 46\%$
(c) Base	$\frac{1299}{1515} \times 100 = 86\%$
(d) 1 m below base	$\frac{1408}{1515} \times 100 = 93\%$

Note: $(q_u)_{(a)}$ is the net ultimate bearing capacity for case (a).

The groundwater level rising to the surface will reduce the bearing capacity by more than one-half.

EXAMPLE 12.3 Allowable Short-term Bearing Capacity of a Clay Soil

A footing $1.8 \text{ m} \times 2.5 \text{ m}$ is located at a depth of 1.5 m below the ground surface in a deep deposit of a saturated overconsolidated clay. The groundwater level is 2 m below the ground surface. The undrained shear strength from a direct simple shear test is 120 kPa and $\gamma_{sat} = 20 \text{ kN/m}^3$. Determine the allowable bearing capacity, assuming a factor of safety of 3, for short-term condition. Neglect the effects of embedment.

Strategy Use the equation for the short-term bearing capacity. You do not need to consider the effect of groundwater when you are evaluating short-term condition.

Solution 12.3

Step 1: Calculate geometric factors.

No eccentricity: $B' = B, L' = L$

$$s_c = 1 + 0.2 \frac{B'}{L'} = 1 + 0.2 \frac{1.8}{2.5} = 1.14, d_c = 1$$

Step 2: Calculate q_u .

$$q_u = 5.14 s_u s_c d_c = 5.14 \times 120 \times 1.14 \times 1 = 703 \text{ kPa}$$

Step 3: Calculate q_a .

$$q_a = \frac{q_u}{\text{FS}} + \gamma D_f = \frac{703}{3} + 1.5 \times 20 = 264 \text{ kPa}$$

EXAMPLE 12.4 Sizing a Rectangular Footing Using ASD and LRFD

Determine the size of a rectangular footing to support vertical centric dead and live loads of 800 kN and 1000 kN, respectively, on a dense, coarse-grained soil. The friction angle obtained from a triaxial test is $\phi'_p = 28.4^\circ$ and $\gamma_{sat} = 18 \text{ kN/m}^3$. The footing is to be located at 1 m below the ground surface. Groundwater level is 6 m below the ground surface. Assume FS = 3, $\eta_i = 1$, and $\phi = 0.8$.

Strategy Neither the footing width nor the length is given. Both of these are required to find q_a . You can fix a length-to-width ratio and then assume a width (B). Solve for q_a , and if it is not satisfactory [$q_a \geq (\sigma)_{max}$], then reiterate using a different B value. You have to convert the triaxial friction angle to an equivalent plane strain value using Equation (12.24).

Solution 12.4

Step 1: Calculate bearing capacity numbers, shape, and depth factors.

Assume $B' = B = 1.5 \text{ m}$ and $\frac{L'}{B'} = 1.5$; that is, $L' = 1.5 \times 1.5 = 2.25 \text{ m}$ and $\frac{B'}{L'} = \frac{1.5}{2.25} = 0.67 \text{ m}$. Footing area $A = B'L' = 1.5 \times 2.25 = 3.375 \text{ m}^2$.

$$(\phi'_p)_{ps} = \frac{9}{8}(\phi'_p)_{tr} = \frac{9}{8} \times 28.4^\circ = 32^\circ$$

$$N_q = e^{\pi \tan 32^\circ} \tan^2(45^\circ + 32^\circ/2) = 23.2$$

$$N_q - 1 = 23.2 - 1 = 22.2$$

Assume rough footing.

$$N_\gamma = 0.1054 \exp(9.6\phi'_p) = 0.1054 \exp\left(9.6 \times \frac{32 \times \pi}{180}\right)$$

$$= 22.5$$

$$s_q = 1 + \frac{B'}{L'} \tan \phi'_p = 1 + 0.67 \tan 32^\circ = 1.42$$

$$s_\gamma = 1 - 0.4 \frac{B'}{L'} = 0.73$$

$$d_q = 1 + 2 \tan \phi'_p (1 - \sin \phi'_p)^2 \tan^{-1} \frac{D_f}{B'}$$

$$= 1 + (2 \tan 32^\circ)(1 - \sin 32^\circ)^2 \left[\tan^{-1} \left(\frac{1}{1.5} \right) \times \frac{\pi}{180} \right]$$

$$= 1.18$$

$$d_\gamma = 1.0$$

Step 2: Calculate the ultimate and allowable bearing capacity.

Substitute the values in Step 1 into the bearing capacity equation, Equation (12.16). The groundwater level is located more than B below the base. Therefore, groundwater will not affect the bearing capacity.

$$\begin{aligned} q_u &= \gamma D_f (N_q - 1) s_q d_q + 0.5 \gamma B' N_\gamma s_\gamma d_\gamma \\ &= (18 \times 1 \times 22.2 \times 1.42 \times 1.18) + (0.5 \times 18 \times 1.5 \times 22.5 \times 0.73 \times 1.0) = 891 \text{ kPa} \end{aligned}$$

$$q_{ult} = q_u + \gamma D_f = 891 + 18 \times 1 = 909 \text{ kPa}$$

$$q_a = \frac{q_u}{\text{FS}} + \gamma D_f = \frac{891}{3} + 18 \times 1 = 315 \text{ kPa}$$

$$R = q_{ult} \times A = 909 \times 3.375 = 3068 \text{ kN}$$

$$P_a = q_a \times A = 315 \times 3.375 = 1063 \text{ kN}$$

Step 3: Calculate the imposed stress based on ASD and LRFD.

$$\text{ASD: } P = \text{DL} + \text{LL} = 800 + 1000 = 1800 \text{ kN}$$

$$\text{LRFD: } P_{uf} = 1.25 \text{ DL} + 1.75 \text{ LL} = 1.25 \times 800 + 1.75 \times 1000 = 2750 \text{ kN}$$

The term P_{uf} is the factored load.

Step 4: Check suitability of assumed foundation size.

$$\text{LRFD: } \varphi R = 0.8 \times 3068 = 2454 \text{ kN} < P_{uf} (= 2750 \text{ kN})$$

Unacceptable; try another footing size.

$$\text{ASD: } P_a (= 1063 \text{ kN}) < P (= 1800 \text{ kN})$$

Unacceptable; try another footing size.

Step 5: Try another width and recalculate.

We need to try a larger B , keeping $\frac{L'}{B'} = 1.5$. Try $B = B' = 2 \text{ m}$. The depth factor for this case changes to 1.14. s_γ and s_q have the same values.

$$\begin{aligned} q_{ult} &= \gamma D_f (N_q - 1) s_q d_q + 0.5 \gamma B' N_\gamma s_\gamma d_\gamma \\ &= (18 \times 1 \times 22.2 \times 1.42 \times 1.14) + (0.5 \times 18 \times 2 \times 22.5 \times 0.73 \times 1.0) + 18 \times 1 \\ &= 942 + 18 = 960 \text{ kPa} \end{aligned}$$

$$q_a = \frac{q_u}{\text{FS}} + \gamma D_f = \frac{942}{3} + 18 \times 1 = 332 \text{ kPa}$$

$$R = q_{ult} \times A = 960 \times (2 \times 3) = 5760 \text{ kN}$$

$$P_a = q_a \times A = 332 \times (2 \times 3) = 1992 \text{ kN}$$

Step 6: Check suitability of assumed foundation size.

$$\text{LRFD: } \varphi R = 0.8 \times 5760 = 4608 \text{ kN} > P_{uf} (= 2750 \text{ kN}); \text{ acceptable.}$$

$$\text{ASD: } P_a (= 1992 \text{ kN}) > P (= 1800 \text{ kN}); \text{ acceptable.}$$

EXAMPLE 12.5 Allowable Bearing Capacity Due to an Inclined Load

Using the footing geometry of Example 12.1, determine q_a for a load inclined at 20° to the vertical along the footing width (see Figure E12.5).

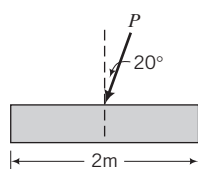


FIGURE E12.5 | 2m |

Strategy You need to use Equation (12.18) for inclined loads. You only need to calculate the inclination factors, since shape and depth factors are not included for load inclination.

Solution 12.5

Step 1: Calculate the inclination factors and depth factors.

$$B' = B; \quad \omega = 20^\circ$$

$$n = n_B = \left(2 + \frac{B'}{L'}\right) / \left(1 + \frac{B'}{L'}\right) = (2 + 1) / (1 + 1) = 1.5$$

$$i_q = \left(1 - \frac{H}{V_n}\right)^n = (1 - \tan \omega)^n = (1 - \tan 20^\circ)^{1.5} = 0.51$$

$$i_y = \left(1 - \frac{H}{V_n}\right)^{n-1} = (1 - \tan \omega)^{n+1} = (1 - \tan 20^\circ)^{1.5+1} = 0.32$$

Step 2: Calculate the ultimate net bearing capacity and allowable bearing capacity.

Use Equation (12.18).

$$q_u = \gamma D_f (N_q - 1) i_q + 0.5 \gamma B N_\gamma i_y = (18 \times 1 \times 32.3 \times 0.51) + (0.5 \times 18 \times 2 \times 37.1 \times 0.32) = 510 \text{ kPa}$$

$$q_a = \frac{q_u}{\text{FS}} + \gamma D_f = \frac{510}{3} + 18 \times 1 = 188 \text{ kPa}$$

The allowable bearing capacity for a vertical centric load is 523 kPa from Example 12.1.

$$\text{Reduction in allowable bearing capacity is } \frac{523 - 188}{523} = 0.64 = 64\%.$$

EXAMPLE 12.6 Factor of Safety of a Footing Subjected to a Vertical Load and a Moment

The footing in Example 12.1 is subjected to a vertical load of 500 kN and a moment about the Y axis of 125 kN.m. Calculate the factor of safety.

Strategy Since we are only given the moment about the Y axis, we only need to find the eccentricity, e_B . The bearing capacity factors are the same as those in Example 12.1.

Solution 12.6

Step 1: Draw a sketch of the problem and calculate e_B .

See Figure E12.6 for a sketch.

$$M_y = 125 \text{ kN.m}, \quad P = 500 \text{ kN}; \quad e_B = \frac{M_y}{P} = \frac{125}{500} = 0.25 \text{ m}$$

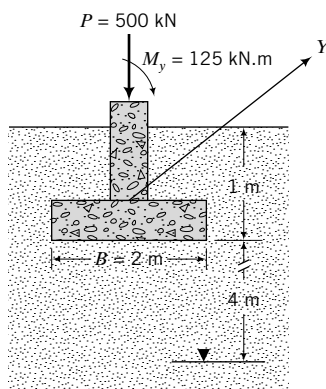


FIGURE E12.6

Step 2: Check if tension develops.

$$\frac{B}{6} = \frac{2}{6} = 0.33 \text{ m} > e_B = 0.25 \text{ m}$$

Therefore, tension will not occur.

Step 3: Calculate the maximum vertical stress.

$$\sigma_{max} = \frac{P}{BL} \left(1 + \frac{6e_B}{B} \right) = \frac{1000}{2 \times 2} \left(1 + \frac{6 \times 0.25}{2} \right) = 438 \text{ kPa}$$

Step 4: Calculate reduced footing size.

$$B' = 2 - 2(0.25) = 1.5 \text{ m}$$

Step 5: Calculate the shape and depth factors.

$$s_q = 1 + \frac{B'}{L} \tan \phi'_p = 1 + \frac{1.5}{2} \tan 35^\circ = 1.53$$

$$s_\gamma = 1 - 0.4 \frac{B'}{L} = 1 - 0.4 \frac{1.5}{2} = 0.7$$

$$d_q = 1 + 2 \tan \phi'_p (1 - \sin \phi'_p)^2 \tan^{-1} \left(\frac{D_f}{B'} \right) = 1 + 2 \tan 35^\circ (1 - \sin 35^\circ)^2 \left[\tan^{-1} \left(\frac{1}{1.5} \times \frac{\pi}{180} \right) \right] = 1.15$$

$$d_\gamma = 1$$

Step 6: Substitute the appropriate values into the bearing capacity equation.

$$\begin{aligned} q_u &= \gamma D_f (N_q - 1) s_q d_q + 0.5 \gamma B' N_\gamma s_\gamma d_\gamma \\ &= (18 \times 1 \times 32.3 \times 1.53 \times 1.15) + (0.5 \times 18 \times 1.5 \times 37.1 \times 0.7 \times 1.0) \\ &= 1373 \text{ kPa} \end{aligned}$$

Step 7: Calculate the factor of safety.

$$FS = \frac{q_u}{(\sigma_a)_{max} - \gamma D_f} = \frac{1373}{438 - 1 \times 18} = 3.3$$

What's next . . . In some projects, spread or individual foundations may overlap each other or differential settlements may be intolerable. One solution is to use a foundation that covers the entire loaded area. These foundations are called mat or raft foundations. Next, we will introduce mat foundations.

12.7 MAT FOUNDATIONS

A mat foundation is conventionally a concrete slab used when:

- Spread or individual footings cover over 50% of the foundation area because of large column loads and/or because the soil is soft with a low bearing capacity.
- Pockets of soft soils are present.
- The structure is sensitive to differential settlement.

A mat foundation can be located at the surface or buried deep in the soil to compensate for all or part of the applied loads. Mat foundations are described frequently as raft foundations because they act like

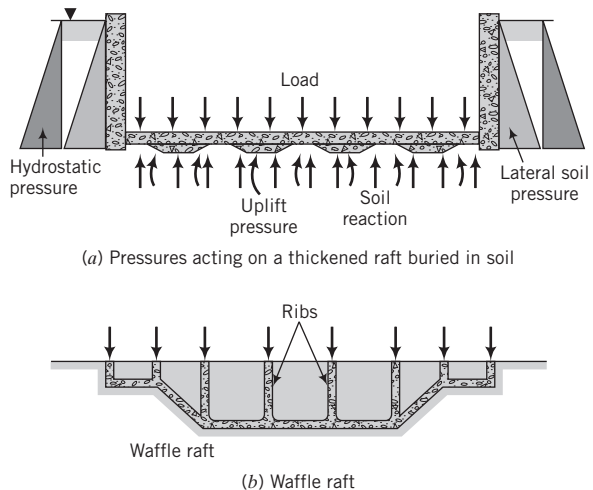


FIGURE 12.13 Two types of mats (rafts).

rafts when part or all of the loads are compensated by embedment. Let us suppose that the average vertical stress at the ground surface from a structure including the self-weight of the raft is 50 kPa and the unit weight of the soil is 20 kN/m³. Then, if the raft is buried at a depth $D_f = 50/20 = 2.5$ m, we get a fully compensated raft. If the raft is buried, say, 2 m, then the compensation is $\frac{2 \times 20}{50} \times 100 = 80\%$.

The raft is then partially compensated. Mat foundations may also be supported on piles to transfer the load to stronger soils. These are called piled rafts. Two types of rafts are shown in Figure 12.13.

Mats are complex soil-structure interaction problems and require advanced analyses that are beyond the scope of this textbook. The bearing capacity of a mat is calculated similar to a spread foundation. However, the settlement of the mat is much more complex. The settlement depends on the rigidity of the mat, type of mat, the type of soil, the homogeneity of the soil, groundwater condition, and construction method. In designing a mat foundation, you should consider:

1. The loads to be supported. Very heavy loads may require a fully or partially compensated raft foundation.
2. The sensitivity of the structure and any machines to settlement.
3. The stability of the mat, particularly if it is embedded in the ground. If groundwater level is below the possible depth of excavation, the theoretical depth of excavation in a fine-grained soil is given by Bjerrum and Eide (1956) as

$$(D_f)_{cr} = N_c \frac{s_u}{\gamma} \quad (12.31)$$

and the factor of safety against bottom heave is

$$FS = N_c \frac{s_u}{\gamma D_f + q_s} \quad (12.32)$$

where $N_c \approx 6 \left(1 + 0.2 \frac{D_f}{B}\right) I_c$ for $\frac{D_f}{B} \leq 2.5$, $N_c = 9 I_c$ for $\frac{D_f}{B} > 2.5$, $I_c = \left(0.84 + 0.16 \frac{B}{L}\right)$, s_u is the undrained shear strength, q_s is the average foundation vertical stress, and B and L are the width and length of the raft, respectively. If the groundwater level is within the possible depth of excavation and the excavation is done under water, replace γ by $(\gamma_{sat} - \gamma_w)$ in Equation (12.32).

4. Heaving. When a fine-grained soil is excavated to embed the raft, it will swell. This will be reversed (reconsolidation) when the foundation is constructed, resulting in settlement.

EXAMPLE 12.7 Allowable Bearing Capacity for a Mat Foundation

A tank foundation 10 m diameter is required to support a vertical centric load of 15,700 kN on the surface of a deep deposit of a stiff clay with $s_u = 80$ kPa and $\gamma_{sat} = 20.8$ kN/m³. Groundwater is at the surface. A 75-mm-thick compacted granular base will be placed on the clay surface prior to the construction of the tank foundation. Calculate the factor of safety.

Strategy The granular base course will impart a rough condition at the soil–foundation interface, but this is not considered in the short-term bearing capacity calculations. Also, the effect of the location of the groundwater is not considered in the short-term bearing capacity calculations.

Solution 12.7

Step 1: Calculate the bearing capacity and geometric factors.

The foundation is at the surface. Set all depth factors to 1.

$$B' = B = D = 10 \text{ m}$$

$$s_c = 1 + 0.2 \frac{B'}{L'} = 1.2$$

Step 2: Calculate the short-term bearing capacity.

$$q_u = 5.14 s_u s_c d_c = 5.14 \times 80 \times 1.2 \times 1 = 493 \text{ kPa}$$

Step 3: Calculate factor of safety.

$$(\sigma_a)_{max} = \frac{\text{load}}{\text{area}} = \frac{15,700}{\pi \frac{10^2}{4}} = 200 \text{ kPa}$$

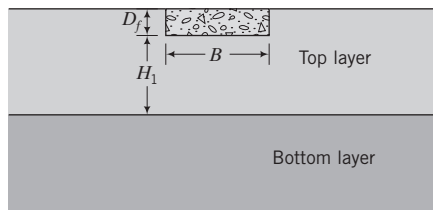
$$\text{FS} = \frac{493}{200} \cong 2.5$$

12.8 BEARING CAPACITY OF LAYERED SOILS

No simple, satisfactory, analytical method is currently available to determine the bearing capacity of layered soils. Analytical methods are available for two layered soils (see the author's textbook *Foundations and Earth Retaining Structures*, John Wiley & Sons, NY). If the thickness, H_1 , of the soil below the footing in the top layer (Figure 12.14) is greater than

$$H_{cr} = \frac{B}{2 \cos \left(45^\circ + \frac{\phi'_p}{2}\right)} \exp [A \tan \phi'_p]; \quad A = \left(45^\circ - \frac{\phi'_p}{2}\right) \text{ in radians} \quad (12.33)$$

the failure surface will be confined in the top layer and it is sufficiently accurate to calculate the bearing capacity based on the properties of the soil in the top layer. Otherwise, the failure surface

**FIGURE 12.14**

Footing on a two-layer soil.

would be influenced by the bottom layer and may extend into it. Alternatively, H_{cr} can be calculated from

$$H_{cr} = \frac{2B \ln \frac{(q_u)_t}{(q_u)_b}}{2\left(1 + \frac{B}{L}\right)} \quad (12.34)$$

where $(q_u)_t$ is the ultimate net bearing capacity of the top layer and $(q_u)_b$ is the ultimate net bearing capacity of the bottom layer with a fictitious footing of the same size and shape but resting on the surface of the bottom layer. A geotechnical engineer can apply a set of practical guidelines or use numerical tools such as the finite element method for analyzing layered soils. The basic problem lies in determining and defining the soil properties for layered soils. We will resort to some practical guidelines for three common cases: a soft clay over a stiff clay, a stiff clay over a soft clay, and thinly stratified soils.

Soft clay over stiff clay: In general, shallow foundations on soft clays should be avoided except for lightly loaded structures such as houses and one-story buildings. You should investigate removing the soft clay and replacing it with compacted fills. An inexperienced geotechnical engineer should calculate the bearing capacity using the methods described previously before making a decision to replace the soft clay.

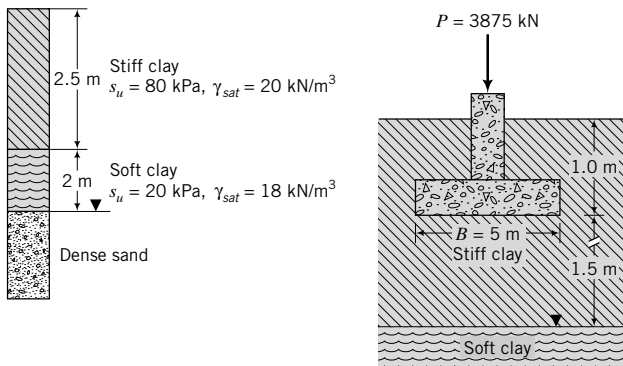
Stiff clay over soft clay: The bearing capacity for this case is the smaller value of (1) treating the stiff clay as if the soft clay layer does not exist and (2) assuming that the footing punches through the stiff clay and is supported on the soft clay. The bearing capacity is the sum of the shear required to punch through a vertical plane in the stiff clay and the bearing capacity of the soft clay layer. Only a fraction, about $\frac{2}{3}$ to $\frac{1}{2}$, of the undrained shear strength should be used in computing the shear resistance on the vertical plane in the stiff clay layer.

Another method is to place an imaginary footing on the soft clay layer with dimensions $(B + t_{sc}) \times (L + t_{sc})$, where B and L are the real width and length of the footing and t_{sc} is the thickness of the stiff clay layer below the base, and then calculate the ultimate net bearing capacity using the bearing capacity equations.

Thinly stratified soils: In this type of deposit, deep foundations should be used. If deep foundations are uneconomical, then the bearing capacity can be calculated by using the shear strength parameters for the weakest layer. Alternatively, harmonic mean values for s_u and ϕ' can be calculated (see Chapter 9), and then these values can be used to calculate the bearing capacity.

EXAMPLE 12.8 Bearing Capacity of a Stiff Clay over a Soft Clay

The soil profile at a site is shown in Figure E12.8. A square footing 5 m wide is located at 1.0 m below ground level in the stiff clay. Determine the safety factor for short-term loading for an applied load of 3875 kN. Neglect effects of embedment.

**FIGURE E12.8**

Strategy Check critical height below footing. If the critical height is less than the soil thickness below the base, check the factor of safety of the stiff clay, assuming that the soft clay layer does not exist. We can then use an artificial footing on top of the soft clay and calculate the factor of safety.

Solution 12.8

Step 1: Check critical height.

$$\phi'_p = 0$$

$$H_{cr} = \frac{B}{2 \cos\left(45^\circ + \frac{\phi'_p}{2}\right)} \exp[A \tan \phi'_p] = \frac{B}{2 \cos 45^\circ} = \frac{5}{2 \cos 45^\circ} = 3.54 \text{ m}$$

The height of soil below the footing to the top of the soft clay is $2.5 - 1 = 1.5 \text{ m} < H_{cr}$. Use stiff clay over soft clay guidelines.

Step 2: Calculate the factor of safety for the stiff clay.

$$s_c = 1 + 0.2 \frac{B'}{L'} = 1.2$$

$$d_c = 1$$

$$q_u = 5.14 s_u s_c d_c = 5.14 \times 80 \times 1.2 \times 1 \\ = 493 \text{ kPa}$$

$$\sigma_{max} = \frac{P}{A} = \frac{3875}{5 \times 5} = 155 \text{ kPa}$$

$$\text{FS} = \frac{q_u}{\sigma_{max} - \gamma D_f} = \frac{493}{155 - 20 \times 1.0} = 3.7$$

Step 3: Check the safety factor for the soft clay.

Artificial footing size: $B + t_{sc} = 5 + 1.5 = 6.5 \text{ m}$; $L + t_{sc} = 5 + 1.5 = 6.5 \text{ m}$

$$q_u = 5.14 s_u s_c d_c = 5.14 \times 20 \times 1.6 \times 1 = 129 \text{ kPa}$$

$$\sigma_{max} = \frac{P}{A} = \frac{3875}{6.5 \times 6.5} = 92 \text{ kPa}$$

$$\text{FS} = \frac{129}{92 - 2.5 \times 20} = 3$$

12.9 BUILDING CODES BEARING CAPACITY VALUES

Building codes usually provide recommended values of bearing capacity for local conditions. You can use these values for preliminary design, but you should check these values using soil test data and the bearing capacity equations. Table 12.3 shows the allowable bearing capacity values for general soil types recommended by the International Building Code (IBC, 2006).

TABLE 12.3 Allowable Bearing Capacity (IBC, 2006)

Soil type	q_a (kPa)
Sandy gravel/gravel (GW, GP)	144
Sand, silty sand, clayey sand, silty gravel (SW, SP, SM, SC, GM, GC)	96
Clay, sandy clay, silty clay, clayey silt (CL, ML, MH, CH)	72

What's next . . . The size of many shallow foundations is governed by settlement rather than bearing capacity considerations. That is, serviceability limit state governs the design rather than ultimate limit state. Next, we will consider how to determine settlement for shallow foundations.

12.10 SETTLEMENT

It is practically impossible to prevent settlement of shallow foundations. At least, elastic settlement will occur. Your task as a geotechnical engineer is to prevent the foundation system from reaching a serviceability limit state. A description of some serviceability limit states is given in Table 12.4.

Foundation settlement can be divided into three basic types: rigid body or uniform settlement (Figure 12.15a), tilt or distortion (Figure 12.15b), and nonuniform settlement (Figure 12.15c). Most damage from uniform settlement is limited to surrounding drainage systems, attached buildings, and utilities. Distortion is caused by differential settlement and may cause serious structural problems, especially in tall buildings. Distortion induces bending in structural elements and is the cause of most cracking in structures. It is quantified by δ/l , where δ is the maximum differential settlement and l is the length over which the settlement occurs. Thus distortion is an angular measurement (radians) and is often referred to as angular distortion. When the foundation rests on an earth fill, the limiting serviceability values are given in Table 12.5. Both Tables 12.4 and 12.5 are only guidelines and can be modified based on local experience.

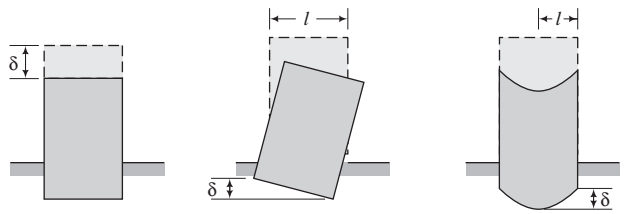
It is desirable to get zero distortion, but this is practically impossible because (1) the properties of building materials and the loading conditions are not known accurately, and (2) the variability of the soils at a site and the effects of construction methods are uncertain. Even if we do know items (1) and (2), the settlement calculations would be very complex.

TABLE 12.4 Serviceability Limit States

Type of structure	Type of damage	Criterion	Limiting value
Framed buildings and reinforced load-bearing walls	Structural damage	Angular distortion	1/150 to 1/250
	Cracking in walls and partitions	Angular distortion	1/500
	Visual appearance	Tilt	1/1000 to 1/1400 for end bays
	Connection to services	Total settlement	1/300
Tall buildings	Operation of elevators	Tilt	50 to 75 mm for sands 50 to 135 mm for clays
	Cracking by relative sag	Deflection ratio*	1/1200 to 1/2000
Unreinforced load-bearing walls	Cracking by relative hog	Deflection ratio*	1/2500 for wall length/height = 1 1/1250 for wall length/height = 5 1/5000 for wall length/height = 1 1/2500 for wall length/height = 5
	Ride quality	Total settlement	100 mm
Bridges	Function	Horizontal movement	38 mm
	Structural damage	Angular distortion	1/250 for multispan 1/200 for single span

*deflection ratio = maximum relative deflection in a panel/panel length

SOURCE: Poulos et al., 2001.



(a) Uniform settlement (b) Tilt or distortion (c) Nonuniform settlement

FIGURE 12.15 Types of settlement.**TABLE 12.5 Serviceability Limit States for Foundations on Earth Fill**

Structure on earth fill	Criterion	Limiting value
Road including bridge approach road	Long-term total settlement after road construction	50 mm
	Differential settlement	20 mm over 5 m
Bridge abutment	Lateral movement after footing installation	25 mm (not applicable if footing is designed for lateral soil movement)
Building on shallow foundations	Angular distortion	1/150 to 1/250 (will depend on the type of building)
Building-service connection through earthfill	Differential settlement	50 mm (will depend on the type of connection)
Buried service pipe	Angular distortion	1/200 (will depend on the type of pipe)
Clay liner	Angular distortion	1/5 to 1/200 (will depend on the type of clay)

SOURCE: Negro et al., 2009.

THE ESSENTIAL POINTS ARE:

1. Distortion caused by differential settlement is crucial in design because it is responsible for cracking and damage to structures.
2. The distortion limits are guidelines that can be modified based on local experience.

EXAMPLE 12.9 Calculation of Angular Distortion

Two shallow footings are located 8 m on center on opposite walls of a framed office building with reinforced load-bearing walls. The vertical, uniform settlements of the two footings are 20 mm and 30 mm, respectively. The footings rest on natural soil.

- (a) Calculate the angular distortion.
- (b) Is the angular distortion satisfactory to reduce wall cracking?

Strategy Determine the difference in settlement and then calculate the angular distortion as the difference in settlement divided by the center line distance of the footings. Compare the result to the limits given in Table 12.4.

Solution 12.9

Step 1: Calculate the differential settlement.

$$\delta = 30 - 20 = 10 \text{ mm}$$

Step 2: Calculate the angular distortion.

$$\frac{\delta}{L} = \frac{10}{8000} = \frac{1}{800}$$

Step 3: Check whether angular distortion is satisfactory.

From Table 12.4, to reduce cracking for end bays, the angular distortion should ideally be between $\frac{1}{1000}$ and $\frac{1}{1400}$. Thus, the calculated angular distortion is not satisfactory. If the client can tolerate the possibility of wall cracking, then the differential settlement is tolerable.

What's next . . . In the next section, we are going to discuss methods to calculate settlement of foundations.

12.11 SETTLEMENT CALCULATIONS

The settlement of shallow foundations is divided into three segments—immediate or elastic settlement, primary consolidation settlement, and secondary consolidation settlement (creep). We have already considered elastic settlement (Chapter 7) and consolidation settlement (Chapter 10). However, we have to make some modifications to the methods described in those chapters for calculating settlement of shallow foundations. These modifications are made to the method of calculating elastic and primary consolidation settlements.

12.11.1 Immediate Settlement

We can use the theory of elasticity to determine the immediate or elastic settlement of shallow foundations. In the case of a uniform rectangular flexible load, we can use Equations (7.45) and (7.46). However, the elastic equations do not account for the shape of the footing (not just L/B ratio) and the depth of embedment, which significantly influence settlement. An embedded foundation has the following effects in comparison with a surface footing:

1. Soil stiffness generally increases with depth, so the footing loads will be transmitted to a stiffer soil than the surface soil. This can result in smaller settlements.
2. Normal stresses from the soil above the footing level have been shown (Eden, 1974; Gazetas and Stokoe, 1991) to reduce the settlement by providing increased confinement on the deforming half-space. This is called the trench effect or embedment effect.
3. Part of the load on the footing may also be transmitted through the side walls depending on the amount of shear resistance mobilized at the soil–wall interface. The accommodation of part of the load by side resistance reduces the vertical settlement. This has been called the side wall–soil contact effect.

Gazetas et al. (1985) considered an arbitrarily shaped rigid footing embedded in a deep homogeneous soil (Figure 12.16) and proposed the following equation for the elastic settlement:

$$\rho_e = \frac{P}{E_u L} (1 - v_u^2) \mu_s \mu_{emb} \mu_{wall}$$

(12.35)

where P is total vertical load, E_u is the undrained elastic modulus of the soil, L is one-half the length of a circumscribed rectangle, v_u is Poisson's ratio for the undrained condition, and μ_s , μ_{emb} , and μ_{wall} are shape, embedment (trench), and side wall factors given as

$$\mu_s = 0.45 \left(\frac{A_b}{4L^2} \right)^{-0.38} \quad (12.36)$$

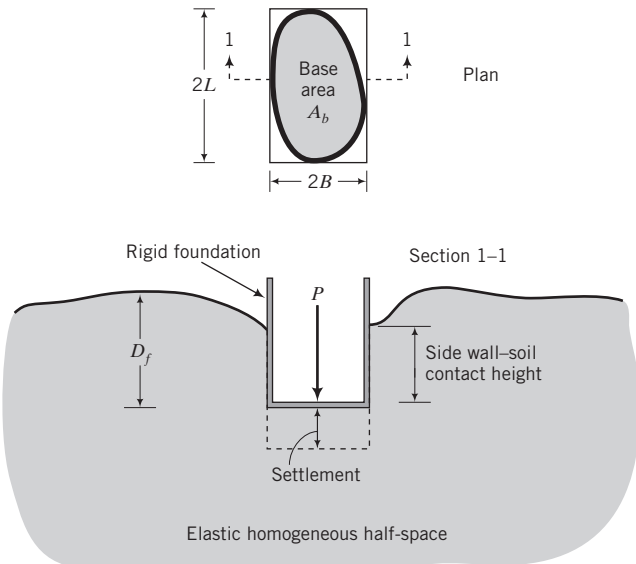


FIGURE 12.16 Geometry to calculate elastic settlement of shallow footings.
(On behalf of the Institution of Civil Engineers.)

$$\mu_{emb} = 1 - 0.04 \frac{D_f}{B} \left[1 + \frac{4}{3} \left(\frac{A_b}{4L^2} \right) \right] \quad (12.37)$$

$$\mu_{wall} = 1 - 0.16 \left(\frac{A_w}{A_b} \right)^{0.54} \quad (12.38)$$

A_b is the actual area of the base of the foundation and A_w is the actual area of the wall in contact with the embedded portion of the footing. The length and width of the circumscribed rectangle are $2L$ and $2B$, respectively. The dimensionless shape parameter, $A_b/4L^2$, has the values for common footing geometry shown in Table 12.6.

The equations proposed by Gazetas et al. (1985) apply to a foundation of arbitrary shape on a deep homogeneous soil. There is no clear definition of what signifies “deep.” The author suggests that the equations of Gazetas et al. can be used when the thickness of the soil layer is such that 90% of the applied stresses are distributed within it. For a rectangular area of actual width B_r , the thickness of the soil layer should be at least $2B_r$.

Equation (7.90) can be modified to account for embedment as

$$\rho_e = \frac{q_s B_r (1 - v_u^2)}{E_u} I_s \mu'_{emb}$$

(12.39)

TABLE 12.6 Values of $A_b/4L^2$ for Common Footing Shapes

Footing shape	$\frac{A_b}{4L^2}$
Square	1
Rectangle	B/L
Circle	0.785
Strip	0

where

$$\mu'_{emb} = 1 - 0.08 \frac{D_f}{B_r} \left(1 + \frac{4B_r}{3L_r} \right) \quad (12.40)$$

where B_r and L_r are the actual width and length, respectively.

The accuracy of any elastic equation for soils depends particularly on the accuracy of the elastic modulus. It is common laboratory practice to determine a secant E_u from undrained triaxial tests or unconfined compression tests at a deviatoric stress equal to one-half the maximum shear strength. However, for immediate settlement it is better to determine E_u over the range of deviatoric stress pertaining to the problem. In addition, the elastic modulus is strongly dependent on depth while Equations (12.35) and (12.39) are cast in terms of a single value of E_u . One possible solution is to divide the soil into sublayers and use a weighted harmonic mean value of E_u (Chapter 10).

The full wall resistance will only be mobilized if sufficient settlement occurs. It is difficult to ascertain the quality of the soil-wall adhesion. Consequently, you should be cautious in relying on the reduction of settlement resulting from the wall factor. If wall friction and embedment are neglected, then $\mu_{wall} = 1$ and $\mu_{emb} = 1$.

Equations (12.35) and (12.39) strictly apply to fine-grained soils under short-term loading. For long-term loading in fine-grained soils and for coarse-grained soils, you should use E' and ν' instead of E_u and ν_u .

EXAMPLE 12.10 Elastic (Immediate) Settlement of a Footing on a Clay Soil

Determine the immediate settlement of a rectangular footing 4 m wide \times 6 m long embedded in a deep deposit of homogeneous clay, as shown in Figure E12.10.

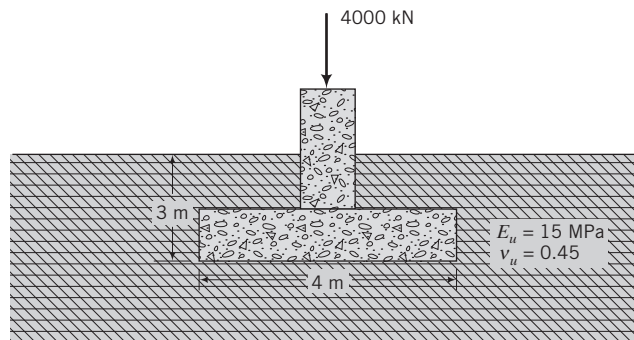


FIGURE E12.10

Strategy You have sufficient information to directly apply Equation (12.35) or Equation (12.39). The side wall effect should not be considered, that is, $\mu_{wall} = 1$, since there really is no wall.

Solution 12.10

Step 1: Determine geometric parameters.

$$A_b = 4 \times 6 = 24 \text{ m}^2, \quad L = \frac{6}{2} = 3 \text{ m}, \quad B = \frac{4}{2} = 2 \text{ m}$$

$$\frac{A_b}{4L^2} = 0.67 \quad \left(\text{Proof: } \frac{A_b}{4L^2} = \frac{2B \times 2L}{4 \times L^2} = \frac{B}{L} = \frac{4}{6} = 0.67 \right)$$

Step 2: Calculate the shape and embedment factors.

$$\mu_s = 0.45 \left(\frac{A_b}{4L^2} \right)^{-0.38} = 0.45(0.67)^{-0.38} = 0.52$$

$$\mu_{emb} = 1 - 0.04 \frac{D_f}{B} \left[1 + \frac{4}{3} \left(\frac{A_b}{4L^2} \right) \right] = 1 - 0.04 \times \frac{3}{2} \left[1 + \frac{4}{3}(0.67) \right] = 0.89$$

Step 3: Calculate the immediate settlement.

$$\begin{aligned} p_e &= \frac{P}{E_u L} (1 - v_u^2) \mu_s \mu_{emb} \mu_{wall} = \frac{4000}{15,000 \times 3} (1 - 0.45^2) \\ &\quad \times 0.52 \times 0.89 \times 1 = 0.033 \text{ m} = 33 \text{ mm} \end{aligned}$$

EXAMPLE 12.11 Immediate Settlement When Elastic Modulus Varies with Depth

Determine the immediate settlement of the foundation shown in Figure E12.11. The undrained elastic modulus varies with depth, as shown in the figure, and $v_u = 0.45$.

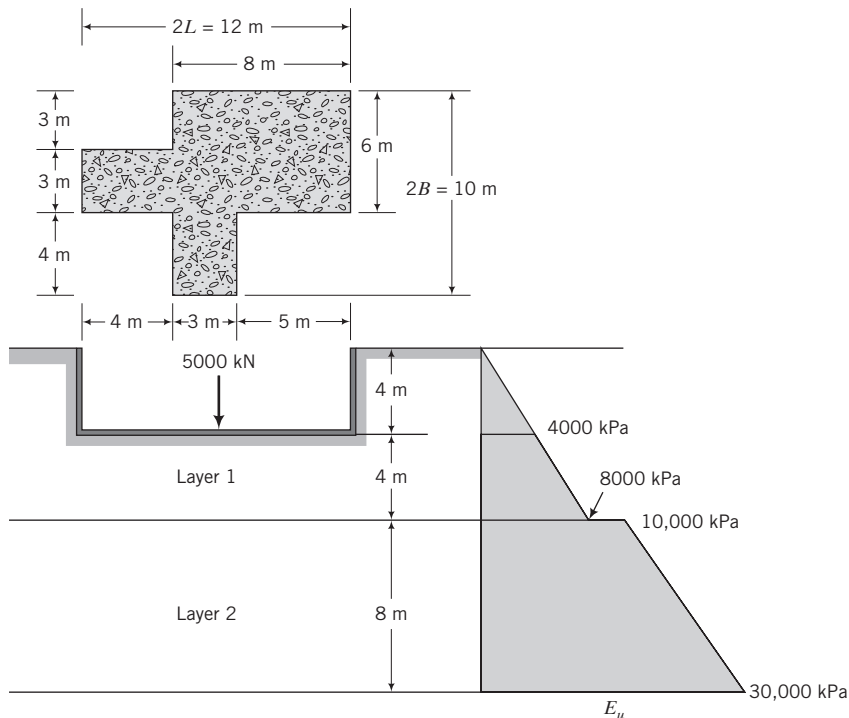


FIGURE E12.11

Strategy You have to determine the length ($2L$) and width ($2B$) of a circumscribed rectangle. The undrained elastic modulus varies with depth, so you need to consider the average value of E_u for each of the layers and then find the harmonic mean. You also need to find the shape parameter $A_b/4L^2$.

Solution 12.11

Step 1: Determine the length and width of the circumscribed rectangle.

$$2L = 8 + 4 = 12 \text{ m}; \quad L = 6 \text{ m}$$

$$2B = 3 + 3 + 4 = 10 \text{ m}; \quad B = 5 \text{ m}$$

Step 2: Determine E_u .

Layer 1

$$E_u \text{ at base level} = \frac{4}{8} \times 8000 = 4000 \text{ kPa}; \quad E_u \text{ at bottom of layer} = 8000 \text{ kPa}$$

$$(E_u)_{avg} = \frac{4000 + 8000}{2} = 6000 \text{ kPa}$$

Layer 2

$$E_u \text{ at top of layer} = 10,000 \text{ kPa}; \quad E_u \text{ at bottom of layer} = 30,000 \text{ kPa}$$

$$(E_u)_{avg} = \frac{10,000 + 30,000}{2} = 20,000 \text{ kPa}$$

Step 3: Find the weighted harmonic mean E_u .

$$E_u = \frac{2(6000) + 1(20,000)}{3} = 10,667 \text{ kPa}$$

Step 4: Find the shape parameter $A_b/4L^2$.

$$A_b = (3 \times 4) + (3 \times 10) + (6 \times 5) = 72 \text{ m}^2; \quad \frac{A_b}{4L^2} = \frac{72}{4 \times 6^2} = 0.5$$

Step 5: Find the shape, embedment, and wall factors.

$$\mu_s = 0.45(0.5)^{-0.38} = 0.59; \quad \mu_{emb} = 1 - 0.04 \frac{4}{5} \left(1 + \frac{4}{3} \times 0.5\right) = 0.94$$

$$A_w = \text{Perimeter} \times \text{depth} = (3 + 4 + 5 + 6 + 8 + 3 + 4 + 3 + 4 + 4) \times 4 \\ = 176 \text{ m}^2$$

$$\frac{A_w}{A_b} = \frac{176}{72} = 2.44; \quad \mu_{wall} = 1 - 0.16(2.44)^{0.54} = 0.74$$

Step 6: Calculate the immediate settlement.

$$\rho_e = \frac{P}{E_u L} (1 - v_u^2) \mu_s \mu_{emb} \mu_{wall} \\ = \frac{5000}{10,667 \times 6} (1 - 0.45^2) \times 0.59 \times 0.94 \times 0.74 = 0.026 \text{ m} = 26 \text{ mm}$$

12.11.2 Primary Consolidation Settlement

The method described in Chapter 10 can be used to calculate the primary consolidation settlement of clays below the footing. However, these equations were obtained for one-dimensional consolidation where the lateral strain is zero. In practice, lateral strains are significant except for very thin layers of clays or for situations when the ratio of the layer thickness to the lateral dimension of the loaded area is small (approaches zero). We also assumed that the initial excess porewater pressure is equal to the change in applied stress at the instant the load is applied. Theoretically, this is possible if the lateral stresses are equal to the vertical stresses. If the lateral strains are zero, then under undrained condition (at the instant the load is applied), the vertical settlement is zero.

Skempton and Bjerrum (1957) proposed a method to modify the one-dimensional consolidation equation to account for lateral stresses but not lateral strains. They proposed the following equation:

$$(\rho_{pc})_{SB} = \int_0^{H_o} m_v \Delta u dz \quad (12.41)$$

where Δu is the excess porewater pressure and H_o is the thickness of the soil layer. Skempton and Bjerrum suggested that the error in neglecting the lateral strains could lead to an error of up to 20% in the estimation of the consolidation settlement. Skempton's equation (Equation 10.50) for the excess porewater pressure in a saturated soil under axisymmetric loading can be algebraically manipulated to yield

$$\Delta u = \Delta \sigma_1 \left(A + \frac{\Delta \sigma_3}{\Delta \sigma_1} (1 - A) \right) \quad (12.42)$$

By substituting Equation (12.42) into Equation (12.41), we get

$$(\rho_{pc})_{SB} = \int_0^{H_o} m_v \Delta \sigma_1 \left(A + \frac{\Delta \sigma_3}{\Delta \sigma_1} (1 - A) \right) dz = \Sigma (m_v \Delta \sigma_z H_o) \mu_{SB} = \Sigma \rho_{pc} \mu_{SB} \quad (12.43)$$

where ρ_{pc} is the one-dimensional primary consolidation settlement (Chapter 10), $\mu_{SB} = A + \alpha_{SB}(1 - A)$ is a settlement coefficient to account for the effects of the lateral stresses, and $\alpha_{SB} = (\int \Delta \sigma_3 dz) / (\int \Delta \sigma_1 dz)$. The values of μ_{SB} typically vary from 0.6 to 1.0 for soft clays and from 0.3 to 0.8 for overconsolidated clays. Values of μ_{SB} for circular and strip footings are shown in Figure 12.17. For square or rectangular footings use an equivalent circular footing of diameter $D = 2\sqrt{A/\pi}$, where A is area of the rectangle or the square. Equation (12.43) must be used appropriately. It is obtained from triaxial conditions and only applies to situations where axial symmetry occurs, such as under the center of a circular footing.

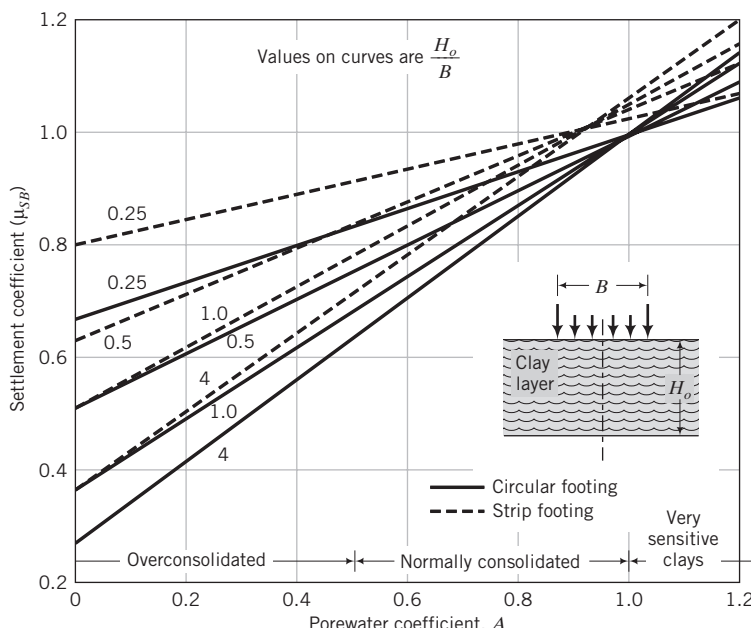


FIGURE 12.17 Values of μ_{SB} for circular and strip footings.
(Redrawn from Scott, 1963.)

EXAMPLE 12.12 Primary Consolidation Settlement of a Footing

Determine the primary consolidation settlement under the square footing shown in Figure E12.12 using the Skempton–Bjerrum method.

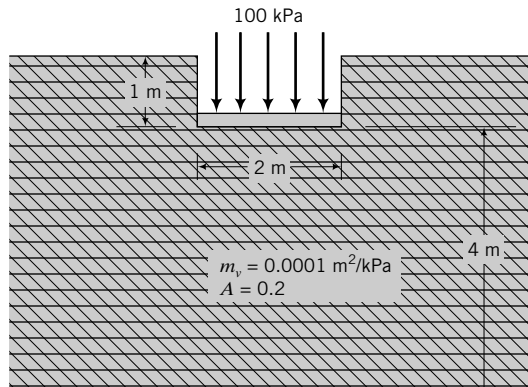


FIGURE E12.12

Strategy First you have to calculate the one-dimensional primary consolidation settlement and then determine μ_{SB} from the chart. Since the clay layer is finite, you should calculate the vertical stress increase using the coefficients in Appendix B.

Solution 12.12

Step 1: Calculate applied stress increase at the center of each layer below the base of the footing.

$$\frac{L}{B} = 1, \quad \frac{H_o}{B} = 2, \quad \frac{z}{B} = 0.5$$

Interpolation from Table C1.2 gives $I_{zp} = 0.72$.

$$\Delta\sigma_z = I_{zp}q_s = 0.72 \times 100 = 72 \text{ kPa}$$

Step 2: Determine μ_{SB} .

Area of base is $2 \times 2 = 4 \text{ m}^2$.

The equivalent diameter of the square footing is

$$D = 2\sqrt{\frac{4}{\pi}} = 2.26 \text{ m}$$

$$\frac{H_o}{B} = \frac{4}{2.26} = 2.21, \quad A = 0.2$$

From Figure 12.17, $\mu_{SB} = 0.43$

Step 3: Calculate the primary consolidation settlement.

$$(\rho_{pc})_{SB} = m_v \Delta\sigma_z H_o \mu_{SB} = 0.0001 \times 72 \times 4 \times 0.43 = 0.0124 \text{ m} = 12.4 \text{ mm}$$

What's next . . . Often, the recovery of soils, especially coarse-grained soils, for laboratory testing is difficult and one has to use results from field tests to determine the bearing capacity and settlement of shallow foundations. Some of the field methods used for coarse-grained soils are presented in the next section.

12.12 DETERMINATION OF BEARING CAPACITY AND SETTLEMENT OF COARSE-GRAINED SOILS FROM FIELD TESTS

We are going to consider the SPT and CPT results in estimating the bearing capacity and settlement of shallow foundations. You need to be extra careful in selecting the N or q_c values to use in the empirical equations given below. You should inspect the results and then eliminate excessively high values of either N or q_c that appear to be spurious. These high values may be due to an obstruction such as from a boulder. A continuous set of low values of N or q_c may indicate a weak soil layer. Depending on the location of this layer, for example, within a depth B below the foundation, it may control the performance of the foundation.

12.12.1 Standard Penetration Test (SPT)



Computer Program Utility

Access www.wiley.com/college/budhu, click on Chapter 12, and then click on bc.xls for a spreadsheet to estimate bearing capacity and settlement from SPT data.

It is difficult to obtain undisturbed samples of coarse-grained soils for testing in the laboratory. Consequently, the allowable bearing capacity and settlement of footings on coarse-grained soils are often based on empirical methods using test data from field tests. One popular method utilizes results from the standard penetration test (SPT). It is customary to correct the N values for overburden pressure. Various correction factors have been suggested by a number of investigators. Energy and other corrections were considered in Chapter 3. Two suggestions for correcting N values for overburden pressure are included in this text. These are

$$c_N = \left(\frac{95.8}{\sigma'_{zo}} \right)^{1/2}; \quad C_N \leq 2 \quad (\text{Liao and Whitman, 1985}) \quad (12.44)$$

$$c_N = 0.77 \log_{10} \left(\frac{1916}{\sigma'_{zo}} \right); \quad C_N \leq 2; \quad \sigma'_{zo} > 24 \text{ kPa} \quad (\text{Peck et al., 1974}) \quad (12.45)$$

where c_N is a correction factor for overburden pressures, and σ'_{zo} is the effective overburden pressure in kPa. A further correction factor is imposed on N values if the groundwater level is within a depth B below the base of the footing. The groundwater correction factor is

$$c_w = \frac{1}{2} + \frac{z}{2(D_f + B)} \quad (12.46)$$

where z is the depth to the groundwater table, D_f is the footing depth, and B is the footing width. If the depth of the groundwater level is beyond B from the bottom of the footing base, $c_w = 1$.

The corrected N value is

$$N_1 = c_N c_w N \quad (12.47)$$

The ultimate bearing capacity for a shallow footing under vertical loads is

$q_{ult} = 32 N_1 B \text{ (kPa)}$

(12.48)

where B is the width in m. In practice, each value of N in a soil layer up to a depth $1.5 B$ below the footing base is corrected, and an average value of N_1 is used in Equation (12.48).

Meyerhof (1965) proposed that no correction should be applied to N values for the effects of groundwater, as these are already incorporated in the measurement. Furthermore, he suggested that q_{ult} calculated from Equation (12.45) using $N_1 = c_N N$ be increased by 50%. In using Equation (12.48), the settlement is assumed to be less than 25 mm.

Burland and Burbidge (1985) did a statistical analysis of settlement records from 200 footings located in quartzitic sand and gravel. They proposed the following equation for the settlement of a footing in a normally consolidated sand at the end of construction:

$$\rho = f_s f_1 \sigma_a B^{0.7} I_c \quad (12.49)$$

where ρ is the settlement (mm),

$$f_s = \text{Shape factor} = \left(\frac{1.25 L/B}{L/B + 0.25} \right)^2 \quad (12.50)$$

$f_1 = (H_o/z_1)(2 - H_o/z_1)$ is a correction factor if the thickness (H_o) of the sand stratum below the footing base is less than an influence depth z_1 , σ_a is the vertical stress applied by the footing or allowable bearing capacity (kPa), B and L are the width and length of the footing (m), respectively,

$$I_c = \text{Compressibility index} = \frac{1.71}{N^{1.4}} \quad (12.51)$$

and N is the uncorrected N value. However, for very fine sand and silty sand, Burland and Burbidge recommended using a corrected $N' = 15 + 0.5(N - 15)$ in Equation (12.51). Further, if the soil is gravel or sandy gravel, use $N' = 1.25N$ in Equation (12.51). The influence depth is the depth below the footing that will influence the settlement and bearing capacity. If N increases with depth or N is approximately constant, the influence depth is taken as $z_1 = B^{0.763}$. If N tends to decrease with depth, the influence depth is $z_1 = 2B$.

If the sand is overconsolidated,

$$\rho = f_1 f_s \left(\sigma_a - \frac{2}{3} \sigma'_{zc} \right) B^{0.7} I_c, \quad \text{if } \sigma_a > \sigma'_{zc} \quad (12.52)$$

$$\rho = f_1 f_s q_a B^{0.7} \frac{I_c}{3}, \quad \text{if } \sigma_a < \sigma'_{zc} \quad (12.53)$$

Burland and Burbidge also recommended a time factor to account for time-dependent settlement. You can check the original reference for this factor.

The procedure for the Burland–Burbidge method is as follows:

1. Determine the influence depth z_1 .
2. Find the average N value within the depth z_1 below the footing.
3. Calculate I_c from Equation (12.51).
4. Determine ρ from the appropriate equation [Equation (12.49) or (12.52) or (12.53)] or, if ρ is specified, you can determine σ_a .

EXAMPLE 12.13 Allowable Bearing Capacity Using SPT Data

The SPT results at various depths in a soil are shown in Table E12.13a.

TABLE E12.13a

Depth (m)	0.6	0.9	1.2	1.5	2.1	2.7	3	3.3	4.2
N (blows/ft)	25	28	33	29	28	29	31	35	41

Determine the allowable bearing capacity for a square footing 2 m wide located at 0.6 m below the surface. The tolerable settlement is 25 mm. The groundwater level is deep and its effects can be neglected.

Strategy The question that arises is what value of N to use. We will estimate the thickness of the soil ($\approx 2B$) below the footing that will be stressed significantly ($>10\%$ of applied stress) and take an average value of N within that layer. The unit weight is not given, so we have to estimate this based on the description and the N values (see Chapter 10, Table 10.4).

Solution 12.13



Computer Program Utility

Access www.wiley.com/college/budhu, click on Chapter 12, and then click on bc.xls for a spreadsheet to estimate bearing capacity and settlement from SPT data.

Step 1: Determine N_1 .

Calculate σ'_{zo} and the correction factor c_N using either Equation (12.44) or (12.45). Use a spreadsheet to do the calculation, as shown in Table E12.13b.

TABLE E12.13b

Bearing capacity from SPT

q_a	1033	kPa				
Width of footing	2	m				
Depth of footing	0.9	m				
Groundwater	5	m				
FS	3					
Vertical effective stress						
Depth (m)	Unit weight (kN/m ³)	(kPa)				
C_n calc.	C_n use	N	N_1			
0	0	0	0	0	0	0
0.6	18.5	11.1	2.9	2.0	25	50
0.9	19	16.8	2.4	2.0	28	56
1.2	20	22.8	2.0	2.0	33	66
1.5	19	28.5	1.8	1.8	29	53
2.1	19	39.9	1.5	1.5	28	43
2.7	19	51.3	1.4	1.4	29	40
3	20	57.3	1.3	1.3	31	40
3.3	20.5	63.45	1.2	1.2	35	43
4.2	20.5	81.9	1.1	1.1	41	44
Avg			Avg	31	48	

Step 2: Calculate q_a .

$$\text{Equation (12.48):} \quad q_{ult} = 32N_1B = 32 \times 48 \times 2 = 3072 \text{ kPa}$$

$$q_a = \frac{q_{ult}}{\text{FS}} = \frac{3072}{3} = 1024 \text{ kPa}$$

The spreadsheet gives $q_a = 1033$ kPa because it uses more significant figures in doing the calculations.

EXAMPLE 12.14 Allowable Bearing Capacity and Settlement Using SPT

Redo using the Burland–Burbidge method for a footing $3 \text{ m} \times 4 \text{ m}$.

Strategy You have to determine whether the sand is normally consolidated or overconsolidated. No direct evidence is provided to allow you to make a decision as to the consolidation state of the sand. One way around this problem is to use Table 10.4 to make an estimate of the consolidation state.

Solution 12.14

Step 1: Determine the consolidation state and find z_1 .

Within a depth equal to B (3 m), the average N value is 29. From Table 10.4, the sand can be classified as medium (N in the range 10–30). A reasonable estimate of the consolidation state is normally consolidated.

$$z_1 = B^{0.763} = 3^{0.763} = 2.3 \text{ m}$$

Step 2: Find an average N for a depth 2.3 m below the base.

Average N value over a depth of 2.3 m below the base is 29. (Note: 2.3 m below the base is equivalent to a depth of 2.9 m, so use the N values up to 3 m.)

Step 3: Calculate I_c .

$$I_c = \frac{1.71}{N^{1.4}} = \frac{1.71}{29^{1.4}} = 0.015$$

Step 4: Calculate q_a .

$$\frac{L}{B} = \frac{4}{3} = 1.33; \quad f_s = \left(\frac{1.25L/B}{L/B + 0.25} \right)^2 = \left(\frac{1.25 \times 1.33}{1.33 + 0.25} \right)^2 = 1.11$$

$f_1 = 1$ (thickness of sand stratum greater than 2.3 m)

$$q_a = \sigma_a = \frac{\rho}{f_s f_1 B^{0.7} I_c} = \frac{25}{1.11 \times 1 \times 3^{0.7} \times 0.015} = 696 \text{ kPa}$$

12.12.2 Cone Penetration Test (CPT)**Computer Program Utility**

Access www.wiley.com/college/budhu, click on Chapter 12, and then click on bc.xls for a spreadsheet to estimate bearing capacity and settlement from CPT data.

Schmertmann (1970) and Schmertmann et al. (1978) proposed a methodology to determine settlement from the quasi-static cone test data for sands. They assumed that the sand is a linearly elastic material, and only stress changes within depths of $2B$ for axisymmetric conditions and $4B$ for plane strain conditions influence the settlement. Settlement is calculated by integrating the vertical strains; that is,

$$\rho = \int \epsilon_z dz \quad (12.54)$$

The equation proposed for settlement (mm) by Schmertmann et al. is

$$\rho = \frac{c_D c_t}{\beta} q_{net} \sum_{i=1}^n \frac{(I_{co})_i}{(q_c)_i} \Delta z_i \quad (12.55)$$

where

$$c_D = \text{Depth factor} = 1 - 0.5 \frac{\sigma'_{zo}}{q_{net}} \geq 0.5 \quad (12.56)$$

$$c_t = \text{Creep factor} = 1.0 + A \log_{10} \left| \frac{t}{0.1} \right| \quad (12.57)$$

β is cone factor [$\beta = 2.5$ for square footing (axisymmetric condition), $\beta = 3.5$ for strip footing (plane strain condition $\frac{L}{B} > 10$)], q_{net} is the net footing pressure in kPa (applied stress minus soil pressure above the base of footing), σ'_{zo} is the original vertical effective stress in kPa at the depth of the footing, t is time in year ($t \geq 0.1$), A is an empirical factor taken as 0.2, Δz_i is the thickness of the i th layer, and $(I_{co})_i$ is the influence factor of the i th layer given as:

Axisymmetric: $L = B$

$$I_{co} = 0.1 + 2(I_{cp} - 0.1) \frac{z}{B} \quad \text{for } \frac{z}{B} \leq \frac{1}{2} \quad (12.58)$$

$$I_{co} = I_{cp} \left[1 - \frac{2}{3} \left(\frac{z}{B} - \frac{1}{2} \right) \right] \quad \text{for } \frac{z}{B} > \frac{1}{2} \quad (12.59)$$

Plane strain: $L > 10B$

$$I_{co} = 0.2 + (I_{cp} - 0.2) \frac{z}{B} \quad \text{for } \frac{z}{B} \leq 1 \quad (12.60)$$

$$I_{co} = I_{cp} \left[1 - \frac{1}{3} \left(\frac{z}{B} - 1 \right) \right] \quad \text{for } \frac{z}{B} > 1 \quad (12.61)$$

where $I_{cp} = 0.5 + 0.1 \sqrt{\frac{q_{net}}{\sigma'_{zp}}}$; $(q_c)_i$ is the cone tip resistance for the i th layer; σ'_{zp} is the original vertical effective stress at the depth where I_{cp} occurs, which is $\frac{B}{2}$ for axisymmetric condition and B for plane strain; and n is the number of sublayers. The unit of B is meters.

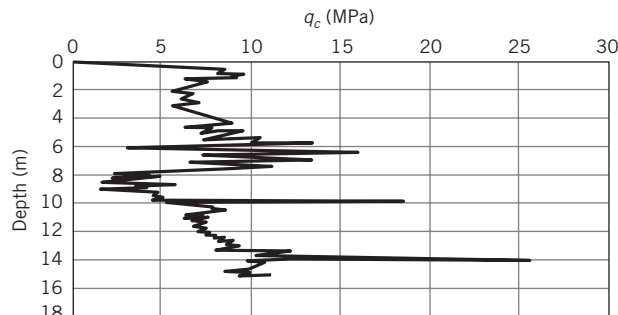
The procedure to determine the settlement from cone data is as follows:

1. Divide the soil below the footing into a number of sublayers. For square footings, the total depth of the sublayers is $2B$ and a reasonable number of sublayers is four. For strip footing, the total depth is $4B$ and a reasonable number of sublayers is eight.
2. Determine the average value of $(q_c)_i$ for each sublayer from the field data of q_c versus depth.
3. Find I_{co} at the center of each sublayer.
4. Estimate ρ using Equation (12.54).

The bearing capacity from the CPT test is estimated by taking a weighted average of the cone resistance over a depth of $2B$ for axisymmetric condition and $4B$ for plane strain condition below the bottom of the footing base.

EXAMPLE 12.15 Allowable Bearing Capacity and Settlement Using CPT Data

A representative set of cone data at a site is shown in Figure E12.15a. A square footing 3 m wide imposing an applied stress of 217 kPa is to be located 1 m below ground level at this site. Determine (1) the bearing capacity and

**FIGURE E12.15a**

(2) the settlement of the footing one year after construction. The bulk unit weight of the sand is 17 kN/m³. Ground-water level is 8 m below the ground surface.

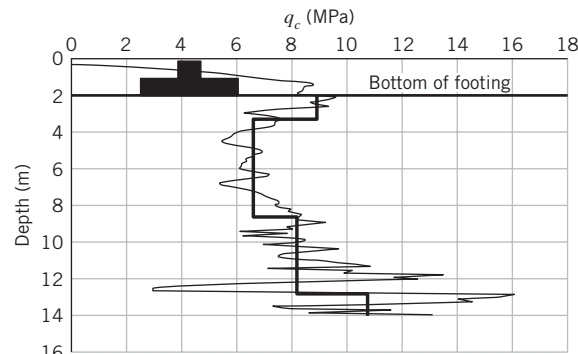
Strategy For a square footing, the influence depth is $2B$. You need to divide this depth into soil layers and then use Equation (12.54).

Solution 12.15

Step 1: Determine the influence depth below base of footing.

$$\text{Influence depth} = 2B = 6 \text{ m}$$

Step 2: Inspect q_c values over the influence depth below the bottom of the base of the footing. Ignore excessively large q_c values and sketch a composite distribution, as shown in Figure E12.15b. Find the average value of q_c , I_{cp} , and ρ over the influence depth.

**FIGURE E12.15b**

Use a spreadsheet program (www.wiley.com/college/budhu_bc.xls; see Table E12.15).

Since this is an axisymmetric case, the depth at which I_{cp} occurs is $B/2$.

q_{ap} = applied pressure, D = depth of footing from original surface, D_f = depth of footing from finished surface.

$$q_{net} = q_{ap} - \gamma D_f = 217 - 1 \times 17 = 200 \text{ kPa}$$

$$\sigma'_{zp} = \gamma \left(\frac{B}{2} + D_f \right) = 17 \times \left(\frac{3}{2} + 1 \right) = 42.5 \text{ kPa}; \quad I_{cp} = 0.5 + 0.1 \sqrt{\frac{200}{42.5}} = 0.72$$

Muni Budhu "Soil Mechanics and Foundations", John Wiley & Sons, NY, 2007
 Bearing capacity and settlement of shallow footings using CPT data

Condition	1 Axisymmetric	HELP	
Settlement	24 mm		
Bearing capacity	6.7 MPa		
q	217 kPa	c_D	0.96
D_f	1 m		1.20
D	1 m		
γ	17 kN/m ³		
B	3 m		
L	3 m		
σ'_{zp}	42.5 kPa		
σ'_{zo}	17 kPa		
σ_{net} or q_{net}	200 kPa		
I_{cp}	0.72		
t	1 yr		
Layer	z	Δz	z/B
m	m	m	
	0		
1	1.00	1.00	0.33
2	2.00	1.00	0.67
3	4.00	2.00	1.33
4	6.00	2.00	2.00
	Sum	6.00	Sum
			0.260 40.3

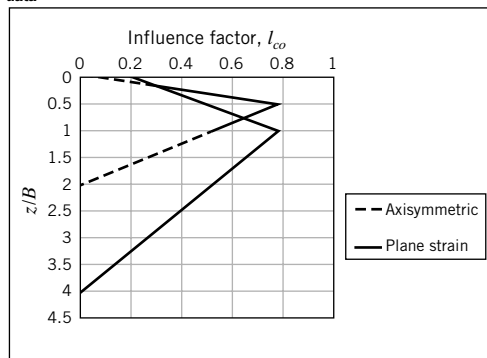


TABLE E12.15

$$\sigma'_{zo} = \gamma D = 1 \times 17 = 17 \text{ kPa}; \quad c_D = 1 - 0.5 \times \frac{17}{200} = 0.96$$

$$c_t = 1 + 0.2 \log_{10} \left| \frac{1}{0.1} \right| = 1.2$$

Step 3: Calculate the bearing capacity.

$$q_{ult} = \frac{\Sigma q_c \Delta z}{\Sigma \Delta z} = \frac{40.3}{6} = 6.7 \text{ MPa}$$

Step 4: Calculate the settlement

$$\rho = \frac{c_D c_t}{\beta} q_{net} \sum_{i=1}^n \frac{(I_{co})_i}{(q_c)_i} \Delta z_i = \frac{0.96 \times 1.2}{2.5} \times 200 \times 0.26 = 24 \text{ mm}$$

12.12.3 Plate Load Test (PLT)

Tests on full-sized footings are desirable but expensive. The alternative is to carry out plate load tests (Figure 12.18) to simulate the load settlement behavior of a real footing. The plates are made from steel, with sizes varying from 150 to 760 mm. Two common plate sizes are used in practice. One is a square plate of width 300 mm and the other is a circular plate of diameter 300 mm. The test is carried out in a pit of depth of at least 1.5 m. Loads are applied in increments of 10% to 20% of the estimated allowable

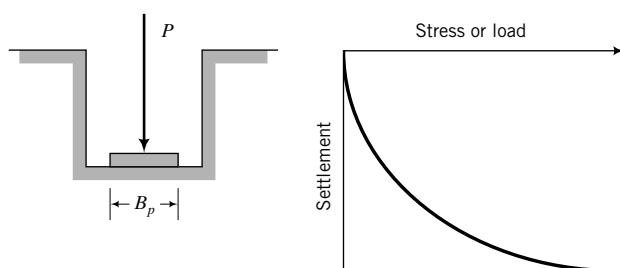


FIGURE 12.18
 Plate load test.

bearing capacity. Each load increment is held until settlement ceases. The final settlement at the end of each loading increment is recorded. Loading is continued until the soil fails or settlements are in excess of 10% of the plate diameter. The maximum load should be at least 1.5 times the estimated allowable bearing capacity.

If the sand were to behave like an elastic material, then the settlement could be calculated from

$$\rho_p = q_{ap} B_p \frac{1 - (v')^2}{E'} I_p \quad (12.62)$$

where ρ_p is the plate settlement, q_{ap} is the applied stress, B_p is the width or diameter of the plate, v' is Poisson's ratio, E' is the elastic modulus, and I_p is an influence factor (0.82 for a rigid plate). The settlement of the real footing (ρ) of width B is related to the plate settlement by

$$\rho = \rho_p \left(\frac{2}{1 + B_p/B} \right)^2 \quad (12.63)$$

In the limit $B_p/B \rightarrow \infty$, $\rho/\rho_p \rightarrow 4$.

Equation (12.63) is only valid if the strains are small (infinitesimal). There are several problems associated with the plate load test.

1. The test is reliable only if the sand layer is thick and homogeneous.
2. The depth of sand that is stressed below the plate is significantly lower than the real footing. A weak soil layer below the plate may not affect the test results because it may be at a depth at which the stresses imposed on the weak layer by the plate loads may be insignificant. However, this weak layer can have a significant effect on the bearing capacity and settlement of the real footing.
3. Local conditions such as a pocket of weak soil near the surface of the plate can affect the test results, but these may have no significant effect on the real footing.
4. The correlation between plate load test results and the real footing is generally problematic. Settlement in a sand depends on the size of the plate. Generally, settlement increases with increases in the plate size. Bjerrum and Eggestad (1963) found that there is significant scatter in the relationship between plate size and settlement for a given applied stress. Bjerrum and Eggestad also reported that field evidence indicates that the limit of ρ/ρ_p ranges between 3 and 5 rather than holding a fixed value of 4.
5. Performance of the test is difficult. On excavation of sand to make a pit, the soil below the plate invariably becomes looser, and this has considerable influence on the test results. Good contact must be achieved between the plate and the sand surface, but this is often difficult. If the plate were above the groundwater, your results would be affected by negative porewater pressure.

What's next . . . In the next section, we examine the use of CSM for the analysis of bearing capacity and settlement of shallow foundations.

12.13 SHALLOW FOUNDATION ANALYSIS USING CSM

An alternative to the conventional analysis for estimating the bearing capacity and settlement of shallow foundation, described in the previous sections in this chapter, is to use CSM. The advantages of using CSM are as follows.

1. It provides for the determination of bearing capacity and settlement in a unified analysis rather than two separate analyses.
2. It represents the soil consistently. In comparison, the conventional method treats the soil mass below the bottom of the footing as a rigid body for the determination of the failure (collapse) load, and then treats that same soil as an elastic material for the calculation of settlement.

3. It is based entirely on effective stresses. Recall that the effective rather than total stresses are responsible for failure and deformation in soils.
4. The foundation is designed for ductility, which is the ability of the soil to deform without rupture or sudden failure.
5. The uncertainty in the elastic modulus to calculate settlement is significantly reduced.
6. Very few soil parameters are needed. These can be obtained from simple soil tests. The minimum soil parameters are $C_r(\kappa)$, OCR (R_o), ϕ'_{cs} (M), and the initial stresses. The latter can be obtained from water content, soil sample depth, and groundwater conditions. If s_u rather than ϕ'_{cs} (M) is known, it is possible to calculate theoretical values of ϕ'_{cs} (M), as will be demonstrated in Example 12.16.
7. It does not require special parameters to account for embedment depth or the shape of the foundation.
8. Ideally, lab tests should duplicate stress conditions in the field. But for certain projects, such tests may be time consuming and uneconomical to conduct. CSM provides a framework to evaluate and modify the appropriate soil parameters from lab tests to be used in the analysis.
9. The theoretical framework provides an understanding of how the soil would behave. For example, you can determine if a soil element under the foundation would be in an elastoplastic (post-yield) state or an elastic state.
10. No failure plane or failure mechanism is presupposed in CSM.
11. It considers the complete stress state of any given soil element.
12. It is an effective tool for evaluating foundation reuse.

CSM, like all the methods we have considered, gives only estimations of the bearing capacity and settlement of soils.

12.13.1 Heavily Overconsolidated Fine-Grained Soil

The basis for the analysis of shallow footings using CSM is that imposed stresses on the footing should be below the stresses to initiate instability. The set of stresses that first bring the soil stress state to the Hvorslev's surface (HV) will be regarded as defining the limiting bearing capacity. This limiting bearing capacity is not the same as the ultimate bearing capacity from limit equilibrium analysis. In fact, a soil may be able to sustain loads higher than the limiting bearing capacity because of the way stresses are redistributed after the HV surface is first reached. However, we cannot predict this redistribution of stresses. Recall, from Chapter 11, that the soil bifurcates on reaching HV surface. So, we need to size the footing so that the applied stresses induce soil stress states that are below the HV surface.

We are going to assume that heavily overconsolidated soils reach a limiting stress state on the HV surface represented by TF in Figure 12.19a. This surface is approximately a linearization of the portion of the initial elliptical yield surface left of the critical state line. Imposed stress states below TF would cause the soil to behave elastically. The line AT in Figure 12.19a is the tension cutoff surface; the surface FC is the Roscoe, Schofield, and Wroth surface (RSW). Heavily overconsolidated soils would have stress states that lie within the area $ATFNA$. Effective stress paths within this area will produce elastic soil response. However, within the area $ATFA$ the soil is likely to initiate discontinuous response. Ideally, our foundation loads should not impose effective stresses within the area $ATFA$. If the imposed effective stresses are within this area, we would be taking a higher level of risk in our design compared with imposed effective stresses within the area AFN . The area, AFC (Figure 12.19a), constitutes the ductile region of soil response (Figure 12.19b).

Let us consider a fine-grained soil in the field that has been one-dimensionally consolidated (ESP, AK in Figure 12.19a, b) to a mean effective stress, p'_k , and deviatoric stress, p_k , and then unloaded (ESP,

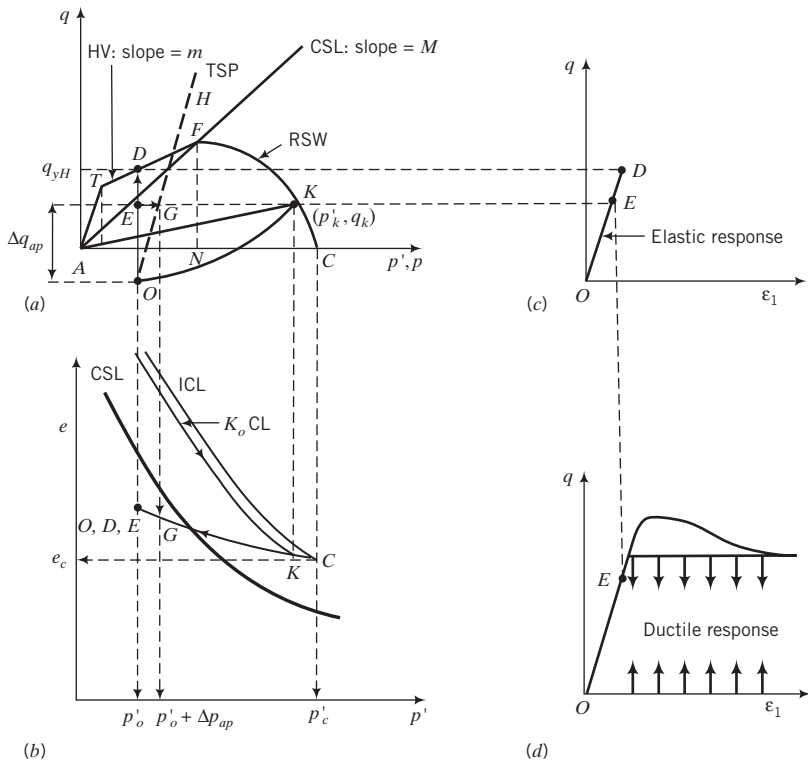


FIGURE 12.19 Response of a heavily overconsolidated fine-grained soil to stresses from a shallow footing.

KO in Figure 12.19a, b) through geological processes such as erosion. We will now construct a shallow, square foundation on this soil. Under the center of a shallow footing, a soil element at a depth z would be loaded axisymmetrically. You may recall that for undrained condition (Chapter 10), the failure of the soil element is independent of the TSP (OH in Figure 12.19a). So the TSP is unimportant for short-term loading except to estimate the excess porewater pressure. Also, you may recall that the ESP for an elastic soil under undrained condition is vertical, as represented by OD in Figure 12.19a. Therefore, if the soil element under the center of the footing is loaded so that the imposed deviatoric stress (recall that deviatoric or shear stress is independent of porewater pressure), Δq_{ap} , is below the limiting deviatoric stress, q_{yH} , on the HV surface (point D in Figure 12.19a), it will respond elastically. The factor of safety with reference to the deviatoric stress on the HV surface, q_{yH} , is

$$FS = \frac{q_{yH}}{q_o + \Delta q_{ap}} = \frac{q_{yH}}{q} \quad (12.64)$$

where q_o is the initial deviatoric stress. A single element that fails ($FS < 1$) does not indicate foundation failure. Failure occurs from a network of connected failure elements. The deviatoric stress on the HV surface is obtained from Equation (11.76), repeated below for easy reference.

$$q_{yH} = p'_o \left[\frac{M - 2n_t t_c}{1 - 2t_c} (1 - t_c R_o) + t_c n_t R_o \right] \quad (12.65)$$

where

$$t_c = \frac{1}{\left(1 + \frac{n_t^2}{M^2} \right)} \quad (12.66)$$

is the tension factor. This factor delineates the mean effective stress, $p'_t = t_c p'_c$ below which the soil will fail in tension; p'_c is the preconsolidation stress. The inverse of t_c is the overconsolidation ratio, R_t , above which the soil will fail in tension. The slope of the tension line, AT , is n_t . For axisymmetric loading, $n_t = 3$ and $M = \frac{6 \sin \phi'_{cs}}{3 - \sin \phi'_{cs}}$, while for plane strain, $n_t = \sqrt{3}$ and $M = \sqrt{3} \sin \phi'_{cs}$.

If tension failure occurs, then

$$q_{tf} = n_t p'_o \quad (12.67)$$

where q_{tf} is the failure deviatoric stress due to tension. Ideally, the imposed deviatoric stress, $q = q_o + \Delta q_{ap}$, should be within the ductile region (Figure 12.19d). That is, from Equation (11.61), $q_o + \Delta q_{ap} < M p_o \left(\frac{R_o}{2} \right)^\Lambda$, where Λ is volumetric strain ratio $= 1 - \frac{\kappa}{\lambda} = 1 - \frac{C_r}{C_c}$, where C_c and C_r are the compression and recompression indices obtained from a plot of void ratio versus the log (base 10) of vertical effective stress and λ and κ are compression and recompression indices from a plot of void ratio versus the natural log of mean effective stress. These compression/recompression indices are related as $\kappa = \frac{C_r}{2.3}$ and $\lambda = \frac{C_c}{2.3}$.

An approximate value for Λ in the absence of information on C_c and C_r is $\Lambda \approx 0.8$, which gives $\frac{C_r}{C_c} = 0.2$.

The elastic deviatoric strain, ε_q , is

$$\varepsilon_q = \varepsilon_z = \frac{\Delta q_{ap}}{3G} \quad (12.68)$$

where ε_z is the vertical strain, $G = \frac{E'}{2(1 + v')}$ is the shear modulus, v' is Poisson's ratio, and E' is the effective elastic modulus (herein called elastic modulus) given by Equation (11.107) as $E' = \frac{3p'_c(1 + e_c)(1 - 2v')}{\kappa} = \frac{6.9p'_c(1 + e_c)(1 - 2v')}{C_r}$, where e_c is the void ratio corresponding to p'_c .

Recall that for undrained condition, the volumetric strain is equal to zero, and from Equations (8.9) and (8.10), $\varepsilon_q = \varepsilon_1 = \varepsilon_z$ for axisymmetric undrained loading. For plane strain undrained condition, $\varepsilon_2 = 0$ and $\varepsilon_q = \frac{2}{\sqrt{3}} \varepsilon_1$. That is, $\varepsilon_1 = \varepsilon_z = \frac{\sqrt{3}}{2} \varepsilon_q$. In general, ε_1 is not equal to ε_z unless the rotation of the principal axis of strain is small.

Now let us see what happens under long-term condition. We will assume that point E in Figure 12.19a represents the imposed deviatoric stress, $q_o + \Delta q_{ap}$, and as such, $FS > 1$. The excess porewater pressure developed during short-term loading, mean stress difference from E to G (Figure 12.19a), would eventually dissipate. The stress path followed during this dissipation (consolidation) is EG (Figure 12.19a, b). The change in void ratio from E to G (Figure 12.19b) is

$$\Delta e = \kappa \ln \left(\frac{p'_o + \Delta p_{ap}}{p'_o} \right) = \kappa \ln \left(1 + \frac{\Delta p_{ap}}{p'_o} \right) \quad (12.69)$$

where Δp_{ap} is the applied mean stress. Note that $\Delta p_{ap} = \Delta p'_{ap}$ when the excess porewater pressure dissipates. The volumetric elastic strain increase during long-term loading is

$$\varepsilon_p = \frac{\Delta e}{1 + e_o} = \frac{1}{1 + e_o} \kappa \ln \left(1 + \frac{\Delta p_{ap}}{p'_o} \right) = \frac{1}{1 + e_o} \frac{C_r}{2.3} \ln \left(1 + \frac{\Delta p_{ap}}{p'_o} \right) \quad (12.70)$$

or

$$\varepsilon_p = \frac{\Delta p_{ap}}{K'} \quad (12.71)$$

where K' is the bulk modulus given by Equation (11.105) as

$$K' = \frac{E'}{3(1 - 2\nu')} = \frac{1 + e_c}{\kappa} p'_c = \frac{2.3(1 + e_c)}{C_r} p'_c \quad (12.72)$$

For elastic deformation, $\varepsilon_3 = -\nu' \varepsilon_1$. Therefore, in the case of axisymmetric loading,

$$\varepsilon_p = \varepsilon_1 + 2\varepsilon_3 = \varepsilon_1(1 - 2\nu') \quad (12.73)$$

From Equations (12.71) and (12.72), we get

$$\varepsilon_1 = \varepsilon_z = \frac{3(1 - 2\nu')\Delta p_{ap}}{E'(1 - 2\nu')} = \frac{3\Delta p_{ap}}{E'} \quad (12.74)$$

For plane strain, $\varepsilon_2 = 0$, and using $\varepsilon_3 = -\nu' \varepsilon_1$, we obtain

$$\varepsilon_p = \varepsilon_1 + \varepsilon_3 = \varepsilon_1(1 - \nu') \quad (12.75)$$

and

$$\varepsilon_1 = \varepsilon_z = \frac{3(1 - 2\nu')\Delta p_{ap}}{E'(1 - \nu')} \quad (12.76)$$

To calculate the settlement, we have to multiply the vertical strain by the effective thickness of the soil stratum. The effective thickness is the soil thickness that is stressed by the imposed load. In most cases, this is about $1.5B$ to $2.0B$, where B is the width of the footing. Recall from Chapter 7 that the increase in stresses below a depth of about $1.5B$ is generally less than 10% of the applied surface stress. Also, the increase in stresses is calculated based on a linearly elastic soil. Since all our calculations for stresses are based on stresses within the area *ATFNA*, then the elastic soil response assumptions made in the calculation of the stress increases from surface loads are valid. Recall from Chapter 7 that the stress increase at a particular depth from surface loads is dependent on the shape of the foundation. Therefore, the effects of shape do not require any additional parameters in calculating the bearing capacity and settlement of a shallow foundation using CSM. Also, the depth of embedment is accounted for in the initial stress state of the soil.

When a uniform vertical surface stress, q_s , is applied on a frictionless strip footing (Figure 7.22a), the maximum (principal) shear stress, $(\Delta\tau)_{max} = \frac{1}{2}(\sigma_1 - \sigma_3) = \frac{q_s}{\pi}$ [see Equation (7.68)], occurs when $\alpha = 90^\circ$ and $\beta = 45^\circ$. The critical depth where the maximum (principal) shear stress occurs is $B/2$ below the bottom of the footing. If you plot the maximum (principal) shear stress under the footing, you will get a circle passing through the edges of the footing and a soil element at a depth of $B/2$. That is, the radius of the maximum (principal) shear stress is $B/2$. Therefore, for a frictionless strip footing with uniform pressure, it is sufficient to consider the stress state of an element at depth $B/2$ below the bottom of the footing.

The increases in mean stresses, $\Delta p_{ap} = I_p q_s$, and the increases in deviatoric stresses, $\Delta q_{ap} = I_q q_s$, where I_p and I_q are stress coefficients, are found from loading of an elastic half-space (Chapter 7). Table 12.7 summarizes these coefficients for strip, square, rectangular, and circular foundations. Combining Equations (12.68) and (12.74), we get for axisymmetric condition

$$\varepsilon_z = \frac{q_s}{E'} \left[\frac{2I_q(1 + \nu')}{3} + 3I_p \right] \quad (12.77)$$

Substituting $E' = \frac{3p'_c(1 + e_c)(1 - 2\nu')}{\kappa}$ into Equation (12.77), we get

$$\varepsilon_z = \frac{q_s \kappa}{3p'_c(1 + e_c)(1 - 2\nu')} \left[\frac{2I_q(1 + \nu')}{3} + 3I_p \right] \quad (12.78)$$

The void ratio at the preconsolidation mean effective stress, e_c , is related to the initial void ratio, e_o , as

$$e_c = e_o - \kappa \ln R_o \quad (12.79)$$

If the stress state at a depth $B/2$ represents the average stress state, then the total settlement is

$$\rho_z = \frac{q_s \kappa B}{3p'_c(1 + e_c)(1 - 2\nu')} \left[\frac{2I_q(1 + \nu')}{3} + 3I_p \right] \quad (12.80)$$

If $\nu' = 0.35$, a reasonable assumption for most soils, Equation (12.80) becomes

$$\boxed{\rho_z \approx \frac{q_s \kappa B}{p'_c(1 + e_c)} \left[I_q + \frac{10}{3} I_p \right] = \frac{q_s C_r B}{2.3p'_c(1 + e_c)} \left[I_q + \frac{10}{3} I_p \right]} \quad (12.81)$$

A conservative estimate of the settlement can be calculated by considering the strains only in vertical direction. This is reasonable at or near the HV surface, where the formation of thin shear bands leads to deformation under approximately zero lateral strains. Putting $R_o = \text{OCR}$, $I_p = I_q = I_z$ where I_z is the influence factor for the vertical stress increase at a depth $B/2$ below the footing and $p'_c = \sigma'_{zc}$ into Equation (12.81) gives

$$\boxed{\rho_z \approx \frac{13}{6.9} \frac{q_s C_r B I_z}{\sigma'_{zc}(1 + e_c)} = 1.88 \frac{q_s C_r B I_z}{\sigma'_{zc}(1 + e_c)}} \quad (12.82)$$

where $e_c = e_o - C_r \log \text{OCR}$. Equations (12.81) and (12.82) serve as the lower and upper limits, respectively, of the range of possible settlement of the footing under axisymmetric loading. By rearranging Equation (12.81), we can obtain the desired width of footing to satisfy a tolerable settlement as

$$\boxed{B = \frac{p'_c(1 + e_c)\rho_z}{q_s \kappa \left[I_q + \frac{10}{3} I_p \right]}} \quad (12.83)$$

In the case of plane strain condition, $\epsilon_3 = -\epsilon_1$ for $\epsilon_p = 0$ and from Equation (8.16), $\epsilon_1 = \frac{\sqrt{3}}{2}\epsilon_q$. Equation (12.80) then becomes

$$\rho_z = \frac{q_s \kappa B}{3p'_c(1 + e_c)} \left[\frac{\sqrt{3}I_q(1 + \nu')}{3(1 - 2\nu')} + \frac{3I_p}{(1 - \nu')} \right] \quad (12.84)$$

If $\nu' = 0.35$, then we can write Equation (12.84) as

$$\boxed{\rho_z \approx \frac{q_s \kappa B}{p'_c(1 + e_c)} \left[\frac{\sqrt{3}}{2} I_q + 1.54 I_p \right]} \quad (12.85)$$

and Equation (12.82) as

$$\boxed{\rho_z \approx \frac{1.05 q_s C_r B I_z}{\sigma'_{zc}(1 + e_c)}} \quad (12.86)$$

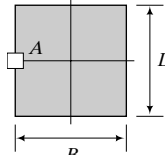
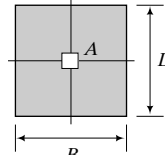
The parameters required for the calculations of the bearing capacity and settlement are all obtained from conventional soil tests. A summary of the soil parameters is ϕ'_{cs} , OCR, e_o , ν' , σ'_{zo} and C_r .

Because we are treating the response of a heavily overconsolidated soil as an elastic material up to the HV surface, any combination of loads, for example, vertical and horizontal loads, can be included by

adding the stresses from each load. The procedure to determine the bearing capacity and settlement of a shallow foundation founded on a heavily overconsolidated, fine-grained soil based on CSM is as follows.

1. Estimate a footing size (see Figure 12.1 for guidance).
2. Calculate the initial stresses at a depth $\frac{B}{2}$ below the bottom of the base of the foundation along its center line for vertical centric load or along an edge where the maximum imposed stress would occur for eccentric load. You can calculate these stresses at different depths below the bottom of the base, if so desired.
3. If s_u is known but not ϕ'_{cs} from lab or field tests, find ϕ'_{cs} from Section 11.7.
4. Assume the soil will behave elastically, and then calculate the increase in stress invariants at depths $\frac{B}{2}$ below the bottom of the foundation base from Chapter 7 (Section 7.4), or use Table 12.7 if only vertical loads are imposed. For vertical centric loads, calculate the increase in mean total stresses and deviatoric stresses along the center line of the footing (Figure 12.20). For eccentric load, calculate the increase in these stresses along the edge of the footing with the highest imposed vertical stress (Figure 12.20). You can calculate these stresses for different depths below the bottom of the base, if so desired. For vertical centric load, the maximum imposed vertical stress is $q_s = \frac{P}{A}$, while for eccentric load it is $q_s = \frac{P}{A} \left(1 + \frac{6e}{B}\right)$, where P is the unfactored load for ASD or the factored load for LRFD, A is the base area, and e is the eccentricity in the direction of the footing width, B . If the eccentricity is along the length, then replace B by L .
5. Check if the soil will fail in tension, i.e., $R_o > R_t$.
6. Check if the imposed deviatoric stress is within the ductile region. That is, $q_o + \Delta q_{ap} \leq Mp'_o \left(\frac{R_o}{2}\right)^\Lambda$, where Λ is volumetric strain ratio $= 1 - \frac{\kappa}{\lambda} = 1 - \frac{C_r}{C_c}$. For LRFD, this check is not required. In fact, the application of CSM to shallow foundation design is best used for ASD rather than LRFD. For an economic design, you can use the limit $1.0 < \frac{Mp'_o \left(\frac{R_o}{2}\right)^\Lambda}{q_o + \Delta q_{ap}} < 1.1$. Increase the footing width or increase the embedment depth if this limit is not satisfied. If ductility limit is satisfied, the factor of

TABLE 12.7 Increases in Stress Invariants for Strip, Square, Rectangular, and Circular Footings Under Vertical Loads

Shape	Edge	Center	
Strip			
	I_p	I_q	
Square	0.35	0.49	0.50
Rectangle ($L/B = 1.5$)	0.22	0.39	0.33
Rectangle ($L/B = 2$)	0.27	0.46	0.40
Circle	0.30	0.49	0.44
	0.25	0.53	0.5
			0.55
			0.55
			0.57
			0.56
			0.62

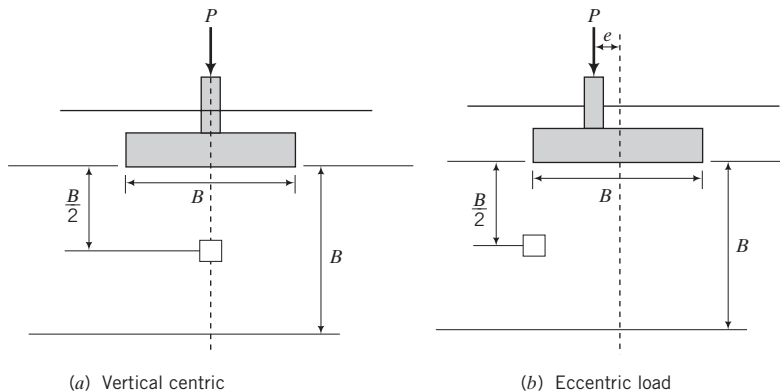


FIGURE 12.20 Locations of soil elements for (a) vertical centric and (b) eccentric loads.

safety is generally greater than 1.25 and steps 7 and 8 can be skipped. However, it is good practice to calculate the factor of safety.

7. Calculate q_{yH} from Equation (12.65).
8. Calculate the factor of safety for ASD [Equation (12.64)] or check that the LRFD condition [Equation (12.2)] is satisfied. If not, change the footing size or embedment and recalculate. $FS > 1.25$ is satisfactory.
9. Calculate the settlement from Equations (12.80) and (12.82). These would give you lower and upper limits of the range of possible settlement for axisymmetric loading. For plane strain, use Equations (12.85) and (12.86).
10. Alternatively, you can calculate the footing width to satisfy the serviceability limit state from Equation (12.83) and then check that the ultimate limit state is satisfied for axisymmetric loading.

12.13.2 Dense, Coarse-Grained Soils

For dense, coarse-grained soils, you can use the same approach as in Section 12.13.1 except that (1) the TSP is equal to the ESP (Figure 12.21) and (2) the HV surface is based on tests on clays. However, observations in simple shear tests (Budhu, 1984) on a dense sand show similar response to heavily overconsolidated clays. Therefore, we will assume that a similar surface is also applicable to coarse-grained soils.

The limiting stresses on the *LS* surface (surface similar to HV) is found from the intersection of the ESP with the *LS* surface (Figure 12.21) as follows.

$$LS \text{ surface: } q_{yLS} = n_t t_c p'_c + m(p'_{yLS} - t_c p'_c) \quad (12.87)$$

where m is the slope of the *LS* surface;

$$ESP: \quad q_{yLS} = n_o(p'_{yLS} - p'_o) + q_o \quad (12.88)$$

where n_o is the slope of the ESP and p'_{yLS} is the mean effective stress at the intersection of the ESP with the *LS* surface.

Solving Equations (12.87) and (12.88) for q_{yLS} , we get

$$q_{yLS} = \frac{t_c p'_c (n_t - m) + m \left(p'_o - \frac{q_o}{n_o} \right)}{1 - \frac{m}{n_o}} \quad (12.89)$$

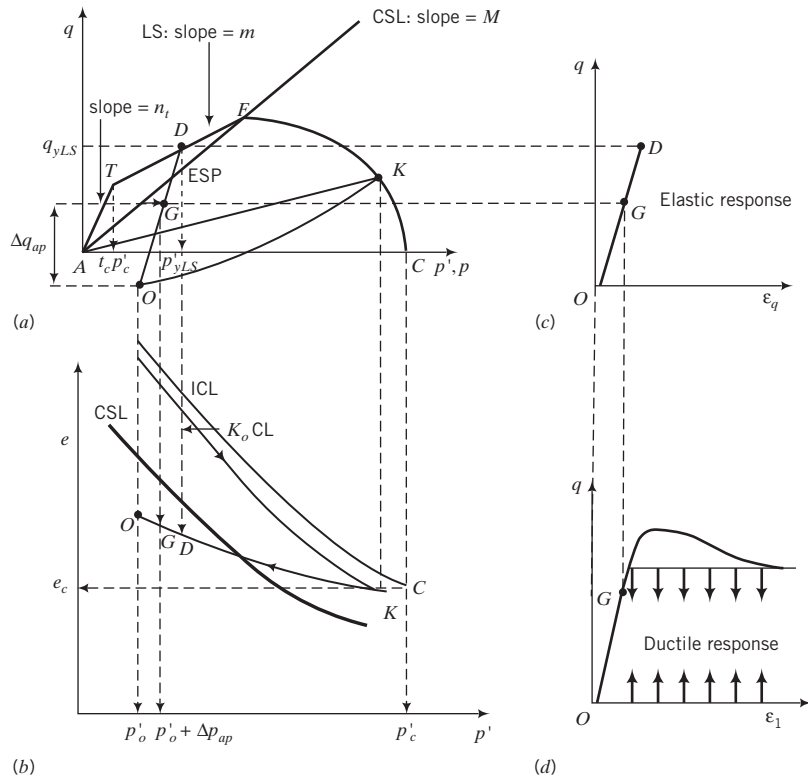


FIGURE 12.21 Response of a dense, coarse-grained soil to stresses from a shallow footing.

Normalizing Equation (12.89) gives

$$\frac{q_{yLS}}{p'_o} = \frac{t_c R_o (n_t - m) + m \left(1 - \frac{q_o}{n_o p'_o} \right)}{1 - \frac{m}{n_o}} \quad (12.90)$$

The vertical strain for Equations (10.41) and (10.42) for axisymmetric condition is

$$\epsilon_z = \epsilon_q + \frac{\epsilon_p}{3} \quad (12.91)$$

The settlement, following a similar approach to that used for heavily overconsolidated clays, is

$$\rho_z = \frac{q_s \kappa B}{3p'_c(1 + e_c)} \left[\frac{2I_q(1 + \nu')}{3(1 - 2\nu')} + \frac{3I_p(1 - 2\nu')}{3(1 - 2\nu')} \right] = \frac{q_s \kappa B}{3p'_c(1 + e_c)} \left[\frac{2I_q(1 + \nu')}{3(1 - 2\nu')} + I_p \right] \quad (12.92)$$

If $\nu' = 0.35$, Equation (12.92) becomes

$$\rho_z = \frac{q_s \kappa B}{3p'_c(1 + e_c)} [3I_q + I_p] = \frac{q_s C_r B}{6.9p'_c(1 + e_c)} [3I_q + I_p] \quad (12.93)$$

A conservative estimate of the settlement is to assume vertical strains only so $R_o = \text{OCR}$ and $I_p = I_q = I_z$, where I_z is the influence factor for the vertical stress increase at a depth $B/2$ below the footing and $p'_c = \sigma'_{zc}$. Equation (12.93) then becomes

$$\rho_z = \frac{4q_s C_r B I_z}{6.9\sigma'_{zc}(1 + e_c)} = \frac{0.58q_s C_r B I_z}{\sigma'_{zc}(1 + e_c)} \quad (12.94)$$

In the case of plane strain (see Chapter 8),

$$\epsilon_q = \frac{2}{3}(\epsilon_1^2 + \epsilon_3^2 - \epsilon_1 \epsilon_3)^{\frac{1}{2}} \quad (12.95)$$

$$\epsilon_p = \epsilon_1 + \epsilon_3 \quad (12.96)$$

Substituting $\epsilon_3 = -v'\epsilon_1$, we get from Equation (12.95) and (12.96)

$$\epsilon_q = \frac{2}{3}\epsilon_1[1 + v' + (v')^2]^{\frac{1}{2}} \quad (12.97)$$

$$\epsilon_p = \epsilon_1(1 - v') \quad (12.98)$$

Solving Equations (12.97) and (12.98) for ϵ_1 , we get

$$\epsilon_1 = \frac{1}{2} \left[\frac{3\epsilon_q}{2[1 + v' + (v')^2]^{\frac{1}{2}}} + \frac{\epsilon_p}{1 - v'} \right] \quad (12.99)$$

Substituting Equations (12.68) and (12.71) into Equation (12.99) and simplifying, we obtain

$$\begin{aligned} \epsilon_1 &= \frac{\kappa}{6p'_c(1 + e_c)} \left[\frac{\Delta q_{ap}(1 + v')}{(1 - 2v')[1 + v' + (v')^2]^{\frac{1}{2}}} + \frac{3\Delta p_{ap}}{1 - v'} \right] \\ &= \frac{\kappa q_s}{6p'_c(1 + e_c)} \left[\frac{I_q(1 + v')}{(1 - 2v')[1 - v' + (v')^2]^{\frac{1}{2}}} + \frac{3I_p}{1 - v'} \right] \end{aligned} \quad (12.100)$$

If $v' = 0.35$ and assuming $\epsilon_1 = \epsilon_v$, then the vertical settlement is

$$\rho_z \approx \frac{0.62\kappa q_s B}{p'_c(1 + e_c)} (I_q + 1.24I_p) \approx \frac{0.27C_r q_s B}{p'_c(1 + e_c)} (I_q + 1.24I_p)$$

(12.101)

Following Equation (12.94), a conservative estimate of vertical settlement is

$$\rho_z \approx \frac{1.39\kappa I_z q_s B}{\sigma'_{zc}(1 + e_c)} \approx \frac{0.6C_r I_z q_s B}{\sigma'_{zc}(1 + e_c)}$$

(12.102)

The procedure for designing a shallow foundation on dense, coarse-grained soil is as follows.

1. Estimate a footing size (see Figure 12.1 for guidance).
2. Calculate the initial stresses at a depth $\frac{B}{2}$ below the bottom of the base of the foundation along its center line for vertical centric load, or along an edge where the maximum imposed stress would

occur for eccentric load. You can calculate these stresses at different depths below the bottom of the base, if so desired.

3. Assume the soil will behave elastically, and then calculate the increase in stress invariants at a depth $\frac{B}{2}$ below the bottom of the foundation base from Chapter 7 (Section 7.4), or use Table 12.7 if only vertical loads are imposed. For vertical centric loads, calculate the increase in mean total stresses and deviatoric stresses along the center line of the footing (Figure 12.20). For eccentric load, calculate the increase in these stresses along the edge of the footing with the highest imposed vertical stress (Figure 12.20). You can calculate these stresses for different depths below the bottom of the base, if so desired. For vertical centric load, the maximum imposed vertical stress is $q_s = \frac{P}{A}$, while for eccentric load it is $q_s = \frac{P}{A} \left(1 + \frac{6e}{B}\right)$, where P is the unfactored load for ASD or the factored load for LRFD, A is the base area, and e is the eccentricity in the direction of the footing width, B . If the eccentricity is along the length, then replace B by L .
4. Check if the soil will fail in tension, i.e., $R_o > R_t$.
5. Check if the imposed deviatoric stress is within the ductile region (Figure 12.21d), that is, $q_o + \Delta q_{ap} < \frac{n_o Mp'_o}{n_o - M}$. For LRFD, this check is not required. For an economic design, you can use the limit $1 < \frac{n_o - M}{q_o + \Delta q_{ap}} < 1.1$. Increase the footing width or increase the embedment depth if this limit is not satisfied.
6. Calculate the deviatoric stresses at the LS surface using Equation (12.89) or Equation (12.90).
7. Calculate the factor of safety for ASD [Equation (12.64)] or check that the LRFD condition [Equation (12.2)] is satisfied. If not, change footing size or embedment and recalculate. $FS > 1.25$ is satisfactory.
8. Calculate the settlement from Equations (12.101) and (12.102).

The difficulty with the above approach is that there is no standard method or even a method to determine the overconsolidation ratio of coarse-grained soils.

An alternative method is as follows.

1. Use the ϕ'_{cs} in Equation (12.12) for long-term condition. If ϕ'_p is available, correct it as described in Section 11.7.
2. Apply a factor of safety of 1.25 for ASD, or a performance factor in the range 0.9 to 0.95 for LRFD.

EXAMPLE 12.16 Design of a Shallow Strip Footing on a Heavily Overconsolidated Clay Using CSM

A shallow strip footing is to support a load of 35 kN/m. The soil is a heavily overconsolidated saturated clay. The average soil parameters over a depth 1 m below the footing are $C_c = 0.28$, $C_r = 0.07$, $OCR = 3$, $\phi'_{cs} = 28^\circ$, and $w = 37\%$. Groundwater is 6 m below the surface. The footing will be located at 1 m below the finished ground surface. Check the suitability of a 1-m-wide footing. The tolerable settlement is less than 25 mm. Assume the effective Poisson's ratio is 0.35.

Strategy The strip footing is best simulated using plane strain condition. Calculate the stresses at a depth $B/2$ below the footing.

Solution 12.16

Step 1: Calculate initial values.

Consider 1 m length of footing.

$$B = 1 \text{ m}$$

$$e_o = wG_s = 0.37 \times 2.7 = 1.0; \quad \gamma_{sat} = \left(\frac{G_s + e_o}{1 + e_o} \right) \gamma_w = \left(\frac{2.7 + 1.0}{1 + 1.0} \right) 9.8 = 18.1 \text{ kN/m}^3$$

$$\sigma'_{zo} = \gamma_{sat} z = \gamma_{sat} \left(\text{embedment depth} + \frac{B}{2} \right) = 18.1 \times \left(1 + \frac{1}{2} \right) = 27.2 \text{ kPa}$$

$$\sigma'_{zc} = \sigma'_{zc} \times 3 = 27.2 \times 3 = 81.6 \text{ kPa}$$

$$\Lambda = \frac{C_c - C_r}{C_c} = \frac{0.28 - 0.07}{0.28} = 0.75; \quad \kappa = \frac{C_r}{2.3} = \frac{0.07}{2.3} = 0.03$$

$$\phi'_{cs} = 28^\circ; \quad M = \sqrt{3} \sin \phi'_{cs} = \sqrt{3} \sin (28^\circ) = 0.81; \quad K_o^{nc} = 1 - \sin \phi'_{cs} = 1 - \sin 28^\circ = 0.53$$

$$K_o^{oc} = K_o^{nc} \text{OCR}^{\frac{1}{2}} = 0.53 \times 3^{\frac{1}{2}} = 0.92$$

Current or initial stresses:

$$p'_o = \frac{1 + 2K_o^{oc}}{3} \sigma'_{zo} = \frac{1 + 2 \times 0.92}{3} \times 27.2 = 25.7 \text{ kPa}$$

$$q_o = \sigma'_{zc}(1 - K_o^{oc}) = 27.2 \times (1 - 0.92) = 2.2 \text{ kPa}$$

$$\frac{p'_c}{\sigma'_{zc}} \approx \frac{1}{3} \left[(3 - 2 \sin \phi'_{cs}) + \frac{(3 - \sin \phi'_{cs})^2}{4(3 - 2 \sin \phi'_{cs})} \right] = \frac{1}{3} \left[(3 - 2 \sin 28^\circ) + \frac{(3 - \sin 28^\circ)^2}{4(3 - 2 \sin 28^\circ)} \right] = 0.946$$

$$p'_c = 0.946 \times 81.6 = 77.2 \text{ kPa}; \quad R_o = \frac{p'_c}{p'_o} = \frac{77.2}{25.7} = 3$$

Alternatively, from Figure 11.29, $R_o = R_o^* = 3$, for OCR = 3.

Step 2: Check if tension failure will govern design.

Plane strain condition, $n_t = \sqrt{3}$

$$t_c = \frac{1}{\left(1 + \frac{n_t^2}{M^2} \right)} = \frac{1}{\left(1 + \frac{(\sqrt{3})^2}{0.81^2} \right)} = 0.18$$

$$R_t = \frac{1}{t_c} = \frac{1}{0.18} = 5.6 > 3. \text{ Therefore, tension will not govern design.}$$

Step 3: Calculate increase in stresses from the surface load.

Assume 1 m length.

$$q_s = \frac{\text{Load}}{\text{area}} = \frac{35}{1 \times 1} = 35 \text{ kPa}$$

Table 12.7: $\Delta p_{ap} = I_p q_s = 0.5 \times 35 = 17.5 \text{ kPa}$

Table 12.7: $\Delta q_{ap} = I_q q_s = 0.55 \times 35 = 19.3 \text{ kPa}$

Step 4: Calculate stresses after the foundation is loaded.

At a depth $\frac{B}{2}$:

$$q = q_o + \Delta q_{ap} = 2.2 + 19.3 = 21.5 \text{ kPa}$$

Step 5: Check if imposed stresses are within the ductile region.

$$\frac{Mp'_o \left(\frac{R_o}{2} \right)^{\lambda}}{q_o + \Delta q_{ap}} = \frac{0.81 \times 25.7 \times \left(\frac{3}{2} \right)^{0.75}}{21.5} = \frac{28.2}{21.5} = 1.31 > 1.10$$

Therefore, the imposed stress state in the soil will be in the ductile region.

Step 6: Calculate the deviatoric stress on the HV surface.

$$\begin{aligned} m &= \frac{M - 2n_t t_c}{1 - 2t_c} = \frac{0.81 - 2 \times \sqrt{3} \times 0.18}{1 - 2 \times 0.18} = 0.3 \\ q_{yH} &= p'_o [m(1 - t_c R_o) + t_c n_t R_o] \\ &= 25.7 \times [0.3(1 - 0.18 \times 3) + 0.18 \times \sqrt{3} \times 3] = 27.6 \text{ kPa} \end{aligned}$$

Step 7: Determine the factor of safety.

$$\text{FS} = \frac{q_{yH}}{q} = \frac{27.6}{21.5} = 1.28 > 1.25; \text{ acceptable.}$$

Step 8: Calculate the settlement.

$$e_c = e_o - \kappa \ln R_o = 1.0 - 0.03 \times \ln 3 = 0.967$$

$$v' = 0.35$$

$$\begin{aligned} \rho_z &= \frac{q_s \kappa B}{p'_c (1 + e_c)} \left[\frac{\sqrt{3}}{2} I_q + 1.54 I_p \right] \\ &= \frac{35 \times 0.03 \times 1 \times 10^3}{77.2 \times 1.967} \left[\frac{\sqrt{3}}{2} \times 0.55 + 1.54 \times 0.5 \right] = 8.6 \text{ mm} \approx 9 \text{ mm} \end{aligned}$$

A conservative estimate of the settlement is

$$\begin{aligned} \rho_z &= \frac{1.05 q_s C_r B I_z}{\sigma'_{zc} (1 + e_c)} \\ e_c &= e_o - C_r \log(\text{OCR}) = 1 - 0.07 \log(3) = 0.966 \end{aligned}$$

$$\text{Equation (7.66): } \Delta \sigma_z = I_z q_s, \text{ where } I_z = \frac{1}{\pi} [\alpha + \sin \alpha \cos (\alpha + 2\beta)]$$

At the center of the footing,

$$I_z = \frac{1}{\pi} \left[\frac{90 \times \pi}{180} + \sin 90 \cos(90 + 2 \times 45) \right] = 0.82$$

$$\rho_z = \frac{1.05q_s C_r B I_z}{\sigma'_{zc}(1 + e_c)}$$

$$= \frac{1.05 \times 35 \times 0.07 \times 1 \times 10^3 \times 0.82}{81.6 \times (1 + 0.966)} = 13.1 \text{ mm} \approx 13 \text{ mm}$$

Step 6: Determine if the footing is satisfactory.

The footing satisfies both serviceability and ultimate limit state requirements. The expected settlement would be in the range 9 mm to 13 mm.

EXAMPLE 12.17 Allowable Bearing Capacity and Settlement of a Shallow Square Foundation on a Heavily Overconsolidated Clay Using CSM

Design a square foundation to support a dead load of 60 kN and a live load of 40 kN on a saturated clay, 12 m thick, overlying bedrock. The overconsolidation ratio of the clay varies with depth. A sample of the clay 50 mm in diameter and 450 mm long was extracted at a depth of 5 m (5 m is the location of the center of the sample). The sample was sealed to prevent moisture content loss. The in situ water content was 40%. Groundwater is located at 3 m below the finished surface but is known to seasonally rise to the surface. A one-dimensional consolidation test on a specimen from the center of the sample at the in situ water content gave the following results: $C_c = 0.32$, $C_r = 0.1$, and $\text{OCR} = 2$. A standard unconfined triaxial compression test was carried out on a specimen 50 mm in diameter and 100 mm long. When the vertical displacement was 1 mm, the vertical (axial) load was 79.1 N, and it remained at this value at further compression. The tolerable total settlement of the footing is 25 mm and less. Determine whether a $2 \text{ m} \times 2 \text{ m}$ square shallow footing located at 1 m below the surface is satisfactory to support the column. Assume the effective Poisson's ratio is 0.3.

Strategy We have only a limited amount of information from two simple soil tests (one-dimensional consolidation and unconfined triaxial compression). We can use the relationships given in Section 11.7 to evaluate the test results and to estimate unmeasured values. The solution of this example is deliberately long to show how CSM can be used to obtain an insight in estimating the appropriate soil parameters and how the soil will respond to the loading from the footing.

Solution 12.17

Step 1: Calculate initial values.

Make a sketch of the problem. See Figure E12.17a.

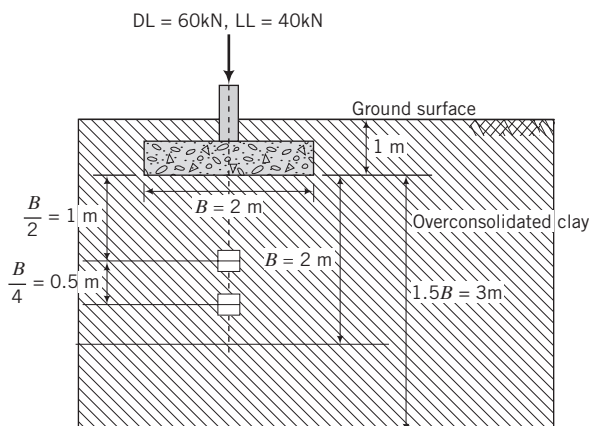


FIGURE E12.17a

$$e_o = wG_s = 0.4 \times 2.7 = 1.08$$

$$\gamma_{sat} = \left(\frac{G_s + e_o}{1 + e_o} \right) \gamma_w = \left(\frac{2.7 + 1.08}{1 + 1.08} \right) 9.8 = 17.8 \text{ kN/m}^3$$

$$\gamma' = \gamma_{sat} - \gamma_w = 17.8 - 9.8 = 8 \text{ kN/m}^3$$

$$\sigma'_{zo} = \gamma'_z = 8 \times 5 = 40 \text{ kPa}; \quad \sigma'_{zc} = \text{OCR} \times \sigma'_{zo} = 2 \times 40 = 80 \text{ kPa}$$

$$P_{max} = 51.4 \text{ N}; \quad \Delta L = 1 \text{ mm}; \quad L = 100 \text{ mm}; \quad \varepsilon_z = \frac{\Delta L}{L} = \frac{1}{100} = 0.01$$

$$D = 50 \text{ mm, initial area, } A_o = \frac{\pi D^2}{4} = \frac{\pi (0.05)^2}{4} = 1.96 \times 10^{-3} \text{ m}^2$$

$$A = \frac{A_o}{(1 - \varepsilon_z)} = \frac{1.96 \times 10^{-3}}{(1 - 0.01)} = 1.98 \times 10^{-3} \text{ m}^2$$

Since the load remained constant, it is likely that the soil has reached critical state.

$$q_f = \frac{P_{max}}{A} = \frac{79.1 \times 10^{-3}}{1.98 \times 10^{-3}} = 40 \text{ kPa}$$

$$(s_u)_f = \frac{q_f}{2} = \frac{40}{2} = 20 \text{ kPa}$$

$$\Lambda = \frac{C_c - C_r}{C_c} = \frac{0.32 - 0.1}{0.32} = 0.686$$

$$\kappa = \frac{C_r}{2.3} = \frac{0.1}{2.3} = 0.043$$

Step 2: Calculate the critical state friction angle.

When the soil was removed from the ground, the total mean stress became zero ($p = 0$) and the porewater pressure became negative (suction). The magnitude of the negative porewater pressures is equal to the initial mean effective stress ($0 = p' + u; u = -p'$). The undrained test was then conducted at the same mean effective stress as in the field. But, we do not know what this value is because we do not know the lateral at-rest coefficient. If we knew ϕ'_{cs} , we could have estimated the lateral at-rest coefficient. We can, however, find ϕ'_{cs} from Equation (11.61) by iterations, i.e., we can substitute various values for $\sin \phi'_{cs}$ until the right-hand side of Equation (11.61) as shown below is about equal to the left-hand side.

$$\left[\frac{(s_u)_f}{\sigma'_{zo}} \right]_{K_o CL} \approx \frac{3 \sin \phi'_{cs}}{3 - \sin \phi'_{cs}} \frac{\left[1 + 2(1 - \sin \phi'_{cs}) \text{OCR}^{\frac{1}{2}} \right]}{3} \left(\frac{R_o^*}{2} \right)^\Lambda$$

$$\text{where } R_o^* \approx \frac{\left[(3 - 2 \sin \phi'_{cs}) - \frac{(\sin \phi'_{cs} - 3)^2}{4(2 \sin \phi'_{cs} - 3)} \right]}{1 + 2(1 - \sin \phi'_{cs}) \text{OCR}^{\frac{1}{2}}} \text{OCR}$$

We know the value of $(s_u)_f$, OCR, and Λ from the lab tests and have calculated σ'_{zo} . We can also rearrange Equation (11.61) to get an expression for $\sin \phi'_{cs}$, but it is simpler to carry out the iterations using a calculator or the Goal Seek function in Excel.

Substituting $(s_u)_f = 20$ kPa, OCR = 2, $\Lambda = 0.686$, and $\sigma'_{zo} = 40$ kPa in the above equation, we get

$$\frac{20}{40} \approx \frac{3 \sin \phi'_{cs}}{3 - \sin \phi'_{cs}} \frac{[1 + 2(1 - \sin \phi'_{cs}) \times 2^{\frac{1}{2}}]}{3} \left\{ \frac{\left[(3 - 2 \sin \phi'_{cs}) - \frac{(\sin \phi'_{cs} - 3)^2}{4(2 \sin \phi'_{cs} - 3)} \right]}{1 + 2(1 - \sin \phi'_{cs}) \times 2^{\frac{1}{2}}} \times 2 \right\}^{0.686}$$

The solution for ϕ'_{cs} is 27.5° .

$$M_c = \frac{6 \sin \phi'_{cs}}{3 - \sin \phi'_{cs}} = \frac{6 \sin 27.5^\circ}{3 - \sin 27.5^\circ} = 1.09$$

$$K_o^{nc} = 1 - \sin \phi'_{cs} = 1 - \sin 27.5^\circ = 0.54$$

$$K_o^{oc} = K_o^{nc} \text{OCR}^{\frac{1}{2}} = 0.54 \times 2^{\frac{1}{2}} = 0.76$$

The current and past consolidation stresses in the field are:

$$\text{Current: } p'_o = \frac{1 + 2K_o^{oc}}{3} \sigma'_{zo} = \frac{1 + 2 \times 0.76}{3} \times 40 = 33.6 \text{ kPa}$$

$$q_o = \sigma'_{zo}(1 - K_o^{oc}) = 40 \times (1 - 0.76) = 9.6 \text{ kPa}$$

In Figure 12.19, point O represents (p'_o, q_o) except q_o is positive.

$$\text{Past: } p'_k = \frac{1 + 2K_o^{nc}}{3} \sigma'_{zc} = \frac{1 + 2 \times 0.54}{3} \times 80 = 55.5 \text{ kPa}$$

$$q_k = \sigma'_{zc}(1 - K_o^{nc}) = 80 \times (1 - 0.54) = 36.9 \text{ kPa}$$

In Figure 12.19, point K represents (p'_k, q_k) .

The preconsolidation stress on the ICL is

$$p'_c = p'_k + \frac{(q_k)^2}{M^2 p'_k} = 55.5 + \frac{36.9^2}{1.09^2 \times 55.5} = 76.2 \text{ kPa}$$

In Figure 12.19, point C represents $(p'_c, 0)$

Step 3: Calculate the variation of OCR with depth.

The sample is taken at a depth of 5 m. So far, all the values we calculated are for this depth. However, the effective depth of the footing (the depth at which the soil will be stressed is approximately $1.5B$) is $1.5 \times 1.0 \approx 1.5$ m. From Chapter 9, we can estimate how the overconsolidation and water content vary with depth. We know e_o , σ'_{zo} , and OCR at 5 m depth. We can then calculate the OCR and s_u at any depth.

The void ratio at the past maximum vertical effective stress is

$$e_k = e_o - C_r \log \frac{\sigma'_{zc}}{\sigma'_{zo}} = e_o - C_r \log (\text{OCR}) = 1.08 - 0.1 \times \log 2 = 1.05$$

The void ratio at any depth, e_z , is then

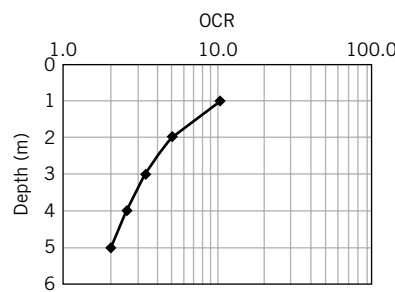
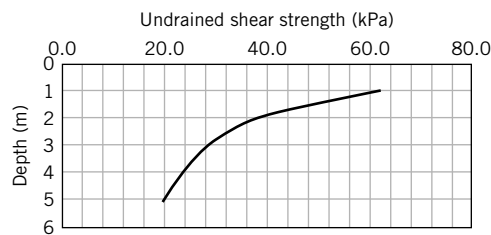
$$e_z = e_k + C_r \log \frac{\sigma'_{zc}}{\sigma'_{zo}} = 1.05 + 0.1 \log \frac{\sigma'_{zc}}{\sigma'_{zo}}$$

where σ'_{zo} is the current vertical effective stress at depth z and σ'_{zc} is past maximum vertical effective stress.

A spreadsheet is useful for this type of calculation. One is shown in Table E12.17a. This table is for illustrative purposes because it is calculated for depths up to 5 m. The depth of 1 m is at the bottom of the base of the footing (Figure E12.17a). See the plot of the variation of OCR and s_u with depth up to 5 m in Figure E12.17b, c. Table E12.17b shows the results for depths at $\frac{B}{2}$ and $\frac{3B}{4}$.

TABLE E12.17a

Depth below surface (m)	e_o	γ_{sat} (kN/m ³)	σ'_{zo} (kPa)	OCR	p'_o (kPa)	R_o	s_u (kPa)
1	1.150	17.5	7.7	10.3	6.5	6.6	41.8
2	1.120	17.7	15.6	5.1	13.1	4.3	30.9
3	1.102	17.7	23.5	3.4	19.8	3.2	25.7
4	1.090	17.8	31.5	2.5	26.5	2.7	22.4
5	1.080	17.8	39.5	2.0	33.2	2.3	20.0

**FIGURE E12.17b****FIGURE E12.17c****TABLE E12.17b**

Depth below surface (m)	e_o	γ_{sat} (kN/m ³)	σ'_{zo} (kPa)	OCR	p'_o (kPa)	R_o (kPa)	q_o (kPa)	s_u (kPa)
2.00	1.120	17.7	15.6	5.1	13.1	4.3	3.7	30.9
2.50	1.110	17.7	19.5	4.1	16.4	3.7	4.6	27.9

Step 4: Calculate increase in stresses from the surface load.

$$q_s = \frac{100}{2 \times 2} = 25 \text{ kPa}$$

Table 12.7: $\Delta p_{ap} = I_p q_s = 0.33 \times 25 = 8.3 \text{ kPa}$

Table 12.7: $\Delta q_{ap} = I_q q_s = 0.55 \times 25 = 13.8 \text{ kPa}$

Slope of TSP is $\frac{\Delta q_{ap}}{\Delta p_{ap}} = n_o = \frac{0.55}{0.33} = 1.67$. (This is not equal to 3 as in the standard triaxial test because $\Delta\sigma_3 \neq 0$.)

The total stress path for the element at depth $\frac{B}{2}$ is $O \rightarrow H$ in Figure 12.19.

Step 5: Calculate stresses after the foundation is loaded.

At a depth $\frac{B}{2}$:

$$p = p_o + \Delta p_{ap} = 13.1 + 8.3 = 21.4 \text{ kPa}$$

$$q = q_o + \Delta q_{ap} = 3.7 + 13.8 = 17.5 \text{ kPa}$$

In Figure 12.19, point G represents (p, q) .

The stresses at $\frac{B}{2}$ and $\frac{3B}{4}$ are given in Table E12.17c and were calculated using Excel.

TABLE E12.17c

Depth below surface (m)	R_o	p'_o (kPa)	q_o (kPa)	Δp (kPa)	Δq (kPa)	q (kPa)	n_o	m	q_{yH} (kPa)	FS
2.0	4.3	13.1	3.7	8.3	13.8	17.5	1.67	0.51	22.9	1.31
2.5	3.7	16.4	4.6	5.0	10.5	15.1	1.67	0.51	25.9	1.71

Step 5: Calculate the deviatoric stress on the HV surface.

For axisymmetric condition, which approximates the stress condition under the center of the footing,

$n_t = 3$. At a depth $\frac{B}{2}$:

$$t_c = \frac{1}{\left(1 + \frac{n_t^2}{M^2}\right)} = \frac{1}{\left(1 + \frac{9}{1.09^2}\right)} = 0.12$$

$$m = \frac{M - 2t_c n_t}{1 - 2t_c} = \frac{1.09 - 2 \times 0.12 \times 3}{1 - 2 \times 0.12} = 0.49$$

$$\begin{aligned} q_{yH} &= p'_o [m(1 - t_c R_o) + t_c n_t R_o] \\ &= 13.1 \times [0.49(1 - 0.12 \times 4.3) + 0.12 \times 3 \times 4.3] = 23.4 \text{ kPa} \end{aligned}$$

The calculations using Excel are shown in Table E12.17c. The difference in results is due to rounding errors.

Step 6: Determine the factor of safety.

$$FS = \frac{q_{yH}}{q_o + \Delta q_{ap}} = \frac{23.4}{17.5} = 1.34 > 1.25; \text{ therefore, acceptable.}$$

Table E12.16c shows calculations using Excel for $\frac{B}{2}$ and $\frac{3B}{4}$ response.

Step 7: Check if the imposed state is within the ductile region.

$$\frac{Mp'_o \left(\frac{R_o}{2} \right)^A}{q_o + \Delta q_{ap}} = \frac{1.09 \times 13.1 \times \left(\frac{4.3}{2} \right)^{0.686}}{17.5} = 1.38 > 1.10$$

Therefore, the imposed stress state in the soil will be in the ductile region.

Step 8: Calculate the settlement.

Assume $\nu' = 0.35$.

$$e_c = e_o - \kappa \ln R = 1.12 - 0.043 \ln(4.3) = 1.06$$

$$\begin{aligned} p_z &\approx \frac{q_s \kappa B}{p'_c(1 + e_c)} \left[I_q + \frac{10}{3} I_p \right] \\ &= \frac{25 \times 0.043 \times 2 \times 10^3}{76.2(1 + 1.06)} \left[0.55 + \frac{10}{3} \times 0.33 \right] = 22.6 \text{ mm} = 23 \text{ mm} \end{aligned}$$

Step 9: Determine if the footing is satisfactory.

The footing satisfies both serviceability and ultimate limit state requirements.

EXAMPLE 12.18 Design of Shallow Foundation on a Coarse-Grained Soil Using CSM for Ductile Soil Response

A square shallow foundation embedded 1 m in a dense quartz sand is required to support a dead load of 150 kN and a live load of 100 kN. The soil parameters from triaxial and one-dimensional consolidation tests are:

$$\phi'_{cs} = 25^\circ, \phi'_p = 29^\circ, \gamma_{sat} = 19.6 \text{ kN/m}^3, C_c = 0.08, C_r = 0.016, \text{OCR} = 9.5, \text{and } \nu' = 0.35$$

Examination of the quartz sand using a light microscope indicated a highly polished surface. This is commonly observed in this type of material and explains the lower-than-average critical state friction angle. The groundwater is at 6 m below the surface. The settlement should not exceed 25 mm. Check whether a shallow footing 1.2 m \times 1.2 m is satisfactory using both ASD and LRFD.

Strategy Follow the procedure given in Section 12.13.2.

Solution 12.18

Step 1: Assume a footing size.

Use the size given. Footing size 1.2 m \times 1.2 m.

Step 2: Calculate initial stresses.

$$\gamma_{sat} = \left(\frac{G_s + e_o}{1 + e_o} \right) \gamma_w$$

$$19.6 = \left(\frac{2.7 + e_o}{1 + e_o} \right) 9.8; \quad e_o = 0.7$$

At a depth $\frac{B}{2}$:

$$\sigma'_{zo} = \gamma_{sat} z = 19.6 \times 1.6 = 31.4 \text{ kPa}$$

$$\sigma'_{zc} = \text{OCR} \times \sigma'_{zo} = 9.5 \times 31.4 = 298 \text{ kPa}$$

$$\Lambda = \frac{C_c - C_r}{C_c} = \frac{0.08 - 0.016}{0.08} = 0.8$$

$$\kappa = \frac{C_r}{2.3} = \frac{0.016}{2.3} = 0.007$$

$$R_o^* \approx \frac{\left[(3 - 2 \sin \phi'_{cs}) - \frac{(\sin \phi'_{cs} - 3)^2}{4(2 \sin \phi'_{cs} - 3)} \right]}{1 + 2(1 - \sin \phi'_{cs}) \text{OCR}^{\frac{1}{2}}} \text{OCR}$$

$$R_o^* \approx \frac{\left[(3 - 2 \sin 25^\circ) - \frac{(\sin 25^\circ - 3)^2}{4(2 \sin 25^\circ - 3)} \right]}{1 + 2(1 - \sin 25^\circ) \times 9.5^{\frac{1}{2}}} \times 9.5 = 6.1$$

$$M_c = \frac{6 \sin \phi'_{cs}}{3 - \sin \phi'_{cs}} = \frac{6 \sin 25^\circ}{3 - \sin 25^\circ} = 0.98$$

$$K_o^{nc} = 1 - \sin \phi'_{cs} = 1 - \sin 25^\circ = 0.58$$

$$K_o^{oc} = K_o^{nc} \text{OCR}^{\frac{1}{2}} = 0.58 \times 9.5^{\frac{1}{2}} = 1.78$$

The current and past consolidation stresses in the field are:

$$\text{Current: } p'_o = \frac{1 + 2K_o^{oc}}{3} \sigma'_{zo} = \frac{1 + 2 \times 1.78}{3} \times 31.4 = 47.7 \text{ kPa}$$

$$q_o = \sigma'_{zo}(1 - K_o^{oc}) = 31.4 \times (1 - 1.78) = -24.4 \text{ kPa}$$

In Figure 12.21a, point O represents (p'_o, q_o)

$$p'_k = \frac{1 + 2K_o^{nc}}{3} \sigma'_{zc} = \frac{1 + 2 \times 0.58}{3} \times 298 = 214.6 \text{ kPa}$$

$$q_k = \sigma'_{zc}(1 - K_o^{nc}) = 298 \times (1 - 0.58) = 125.2 \text{ kPa}$$

In Figure 12.21a, point K represents (p'_k, q_k)

The preconsolidation mean effective stress on the ICL is

$$p'_c = p'_k + \frac{(q_k)^2}{M^2 p'_k} = 214.6 + \frac{125.2^2}{0.98^2 \times 214.6} = 291 \text{ kPa}$$

$$\text{Also, } p'_c = R_o p'_o = 6.1 \times 47.7 = 291 \text{ kPa}$$

In Figure 12.21a, point C represents $(p'_c, 0)$

Step 3: Calculate increase in stresses from the surface load.

$$\text{DL} = 100 \text{ kN}, \text{LL} = 150 \text{ kN}$$

ASD: Design load = DL + LL = 100 + 150 = 250 kN

$$q_s = \frac{250}{1.2 \times 1.2} = 173.6 \text{ kPa}$$

Table 12.7: $\Delta p_{ap} = 0.33 \times 173.6 = 57.3 \text{ kPa}$

Table 12.7: $\Delta q_{ap} = 0.55 \times 173.6 = 95.5 \text{ kPa}$

LRFD: Design load = 1.25 DL + 1.75 LL = $1.25 \times 100 + 1.75 \times 150 = 387.5 \text{ kN}$

$$q_s = \frac{387.5}{1.2 \times 1.2} = 269 \text{ kPa}$$

Table 12.7: $\Delta p_{ap} = 0.33 \times 269 = 88.8 \text{ kPa}$

Table 12.7: $\Delta q_{ap} = 0.55 \times 269 = 148 \text{ kPa}$

The effective stress path, $n_o = \frac{0.55}{0.33} = 1.67$, for the element at depth $\frac{B}{2}$ is $O \rightarrow D$ in Figure 12.21a.

Step 4: Calculate stresses after the foundation is loaded.

At a depth $\frac{B}{2}$:

$$\text{ASD: } p = p_o + \Delta p_{ap} = 47.7 + 57.3 = 105 \text{ kPa}$$

$$q = q_o + \Delta q_{ap} = -24.4 + 95.5 = 71.1 \text{ kPa}$$

In Figure 12.21a, point G represents (p, q) .

$$\text{LRFD: } p = p_o + \Delta p_{ap} = 47.7 + 88.8 = 136.5 \text{ kPa}$$

$$q = q_o + \Delta q_{ap} = -24.4 + 148 = 123.6 \text{ kPa}$$

Step 5: Check if tension will develop.

At the center of the foundation, axisymmetric condition is assumed. Therefore, $n_t = 3$.

At a depth $\frac{B}{2}$:

$$t_c = \frac{1}{\left(1 + \frac{9}{M^2}\right)} = \frac{1}{\left(1 + \frac{9}{0.98^2}\right)} = 0.096$$

Tension cutoff overconsolidation ratio is $R_t = \frac{1}{t_c} = \frac{1}{0.096} = 10.4 > R_o (= 6.1)$. Therefore, the soil will not fail by tension.

Step 6: Check if imposed stresses are within the ductile region.

$$\frac{\frac{n_o M p'_o}{n_o - M}}{q_o + \Delta q_{ap}} = \frac{\frac{1.67 \times 0.98 \times 47.7}{1.67 - 0.98}}{71.1} = 1.59 > 1.10$$

Therefore, the imposed stress state is within the region of ductility.

Step 7: Calculate the deviatoric stress on the LS surface.

$$m = \frac{M - 2n_t t_c}{1 - 2t_c} = \frac{0.98 - 2 \times 3 \times 0.096}{1 - 2 \times 0.096} = 0.5$$

$$q_{yLS} = \frac{t_c p'_c (n_t - m) + m \left(p'_o - \frac{q_o}{n_o} \right)}{1 - \frac{m}{n_o}}$$

$$= \frac{0.096 \times 291(3 - 0.5) + 0.5 \times \left(47.7 - \frac{-24.4}{1.67} \right)}{1 - \frac{0.5}{1.67}} = 144.2 \text{ kPa}$$

Step 8: Determine factor of safety (ASD) and if the applied factored deviatoric stress is below the peak deviatoric stress (LRFD).

$$\text{ASD: } \text{FS} = \frac{q_{yLS}}{q} = \frac{144.2}{71.1} = 2.03 > 1.25; \text{ okay}$$

LRFD: $\phi q_{yLS} = 0.95 \times 144.2 = 137 \text{ kPa} > 123.6 \text{ kPa}$. Therefore, satisfactory.

Step 9: Calculate settlement.

$$e_c = e_o - \kappa \ln R_o = 0.7 - 0.007 \ln (6.1) = 0.687$$

$$\rho_z = \frac{q_s \kappa B}{3p'_c(1 + e_c)} [3I_q + I_p] = \frac{176.3 \times 0.007 \times 1.2 \times 10^3}{3 \times 291 \times (1 + 0.687)} [3 \times 0.55 + 0.33]$$

$$\approx 2 \text{ mm}$$

Conservative estimate of settlement is

$$e_c = e_o - C_r \log \text{OCR} = 0.7 - 0.016 \log (9.5) = 0.684$$

$$\rho_z = \frac{0.6q_s C_r B I_z}{\sigma'_{zc}(1 + e_c)} = \frac{0.6 \times 176.3 \times 0.016 \times 1.2 \times 10^3 \times 0.7}{298 \times (1 + 0.684)} = 2.8 \text{ mm} \approx 3 \text{ mm}$$

Step 10: Decide if footing size is satisfactory.

The footing satisfies both ultimate limit state and serviceability limit state for ASD and LRFD. The footing size can be decreased.

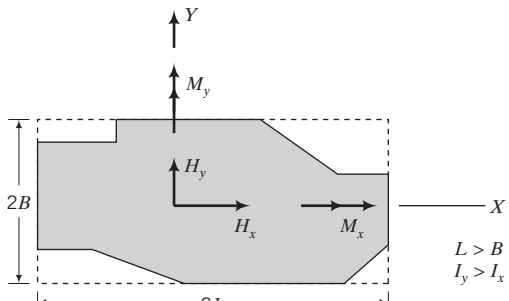
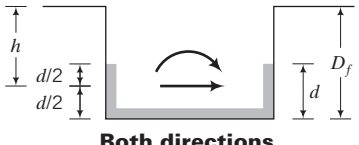
What's next . . . We have considered only vertical settlement under vertical and inclined loads. Horizontal displacements and rotations are important for structures subjected to significant horizontal loads. Using CSM we can calculate the horizontal displacements. For the conventional method, the horizontal displacements and rotations can be estimated by the method presented in the next section

12.14 HORIZONTAL ELASTIC DISPLACEMENT AND ROTATION

Structures such as radar towers and communication transmission towers are subjected to significant horizontal loads from wind, which can lead to intolerable lateral displacement and rotation of their foundations. Gazetas and Hatzikonstantinou (1988) proposed equations based on an isotropic linearly elastic soil to determine the elastic horizontal displacement and rotation of an arbitrarily loaded foundation.

The equations were obtained by curve-fitting theoretical elastic solutions for $\frac{D_f}{B} \leq 2$. A summary of these equations is presented in Table 12.8. You must be cautious (see Section 12.10.1) in using the equations in Table 12.8.

TABLE 12.8 Equations for Estimating the Horizontal Displacement and Rotation of Arbitrarily Shaped Foundations

Loading	Surface foundation  Lateral direction y Longitudinal direction x	Foundation placed in open trench  Both directions
Horizontal	$\rho_e = \frac{H_i}{EL} (2 - \nu)(1 + \nu)\mu_s$ $\mu_{sy} \approx 0.5 - 0.28 \left[\frac{A_b}{4L^2} \right]^{0.45}$ $\mu_{sx} \approx \left[1 + 1.12 \left(\frac{1 - B/L}{1 - \nu} \right) \right] \mu_{sy}$	$(\rho_e)_{emb} \approx \rho_e \mu_{emb}$ $\mu_{emb} \approx 1 - 0.14 \left(\frac{D_f}{B} \right)^{0.35}$
Moment	$\theta_{ry} = \frac{M}{E} \frac{2(1 - \nu^2)}{I_y^{0.75}} (\mu_s)_{ry}$ $(\mu_s)_{ry} \approx 0.43 - 0.10 \frac{B}{L}$	$\theta_{rx} = \frac{M}{E} \frac{2(1 - \nu^2)}{I_x^{0.75}} \left(\frac{B}{L} \right)^{0.25} (\mu_s)_{rx}$ $(\mu_s)_{rx} \approx 0.33 \left(\frac{B}{L} \right)^{0.15}$
Embedded foundation with sidewall-soil contact surface of total areas A_w		
Loading	Lateral direction y 	Longitudinal direction x
Horizontal	$\rho_e = (\rho_e)_{emb} \mu_{wall}$ $(\mu_{wall})_y \approx 1 - 0.35 \left[\frac{h A_w}{B L^2} \right]^{0.2} \approx (\mu_{wall})_x$	
Moment	$\theta = \theta_{emb} (\mu_{wall})_x$ $(\mu_{wall})_{ry} \approx \left\{ 1 + 0.92 \left(\frac{d}{L} \right)^{0.6} \left[1.5 + \left(\frac{d}{L} \right)^{1.9} \left(\frac{D_f}{d} \right)^{0.6} \right] \right\}^{-1} (\mu_{wall})_{rx} \approx \left\{ 1 + 1.26 \frac{d}{B} \left[1 + \frac{d}{B} \left(\frac{D_f}{d} \right)^{0.2} \left(\frac{B}{L} \right)^{0.5} \right] \right\}^{-1}$	

Notes: Substitute the appropriate values for H_i and M in the above equations. For example, if you are considering the X direction, $H_i = H_x$ and $M = M_x$. Also use the appropriate values for μ_s and θ_r . For example, in the X direction, $\mu_s = \mu_{sx}$ and $\theta_r = \theta_{rx}$. For short-term loading, use the undrained values of E and ν ; for long-term loading, use the effective values. The terms I_x and I_y are the second moment of areas about the X and Y axes, respectively, and θ is the rotation caused by the moment.

SOURCE: Gazetas and Hatzikonstantinou, 1988.

12.15 SUMMARY

In this chapter, we described ways in which you can calculate the bearing capacity and settlement of shallow foundations. The critical criterion for design of most shallow foundations is the serviceability limit state. Because of sampling difficulties, the bearing capacity and settlement of coarse-grained soils are often determined from field tests. We showed how to use the results of the SPT, the cone test, and

the plate test to estimate the bearing capacity and settlement of shallow foundations on coarse-grained soils. An alternative method, based on CSM, has been developed to estimate the bearing capacity and settlement of shallow foundations on overconsolidated fine-grained soils and dense coarse-grained soils.

Self-Assessment

Access Chapter 12 at <http://www.wiley.com/college/budhu> to take the end-of-chapter quiz to test your understanding of this chapter.

Practical Examples

EXAMPLE 12.19 Design (Sizing) a Square Footing

Determine the size of a square footing to carry a dead load of 300 kN and a live load of 200 kN using LRFD. The soil at the site is shown in Figure E12.19. The tolerable total settlement is 20 mm. The groundwater level is 3 m below the ground surface and the depth of the footing is 1.5 m. However, the groundwater level is expected to seasonally rise to the surface. You may assume that the clay layer is thin so that one-dimensional consolidation takes place. The performance factor is 0.8.

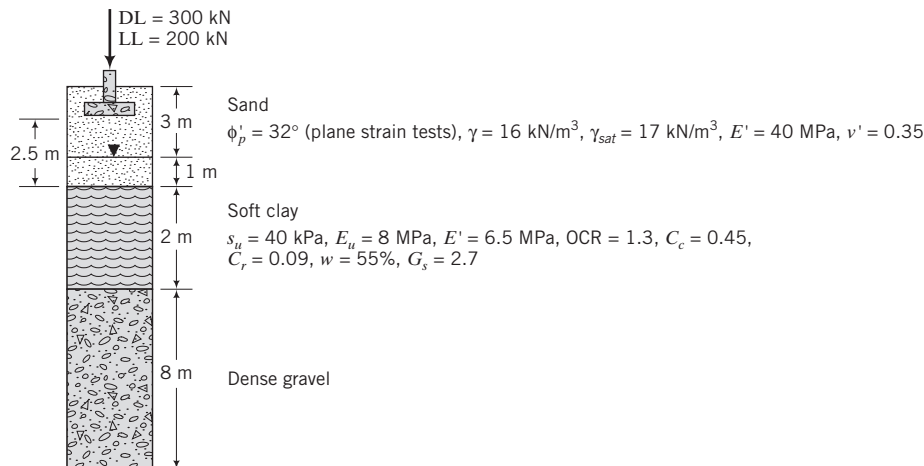


FIGURE E12.19

Strategy The presence of the soft clay layer gives a clue that settlement may govern the design. In this case, we should determine the width required to satisfy settlement and then check the bearing capacity. One can assume a width, calculate the settlement, and reiterate until the settlement criterion is met. Since this is a multilayer soil profile, it is more accurate to calculate the increase in vertical stress for multilayer soils. However, for simplicity, we will use Boussinesq's method for a uniform soil.

Solution 12.19

Step 1: Assume a width and a shape.

Try $B = 3 \text{ m}$, and assume a square footing.

Step 2: Calculate the elastic settlement.

Sand

Neglect side wall and embedment effects; that is, $\mu_{wall} = \mu_{emb} = 1$.

Use Equation (12.39) and Equation (7.93).

$$\text{Equation (7.93): } I_s = 0.62 \ln(L/B) + 1.12 = 0.62 \ln(1) + 1.12 = 1.12$$

$$\rho_e = \frac{q_s B_r [1 - (\nu')^2]}{E'} I_s \mu'_{emb} = \frac{P[1 - (\nu')^2]}{E' L_r} I_s \mu'_{emb}$$

$$\text{Equation (12.39): } = \frac{500(1 - 0.35^2)}{40 \times 10^3 \times 3} \times 1.12 \times 0.81 = 3.3 \times 10^{-3} = 3.3 \text{ mm}$$

Note: In the above equation L_r and B_r are the actual length and width.

Clay

Find the equivalent footing size at the top of the clay layer. Let z_1 be the depth from the base of the footing to the top of the clay layer.

Equivalent width and length of footing at top of clay: $B + z_1 = 3 + 2.5 = 5.5 \text{ m}$.

$$\mu'_{emb} = 1 - 0.04 \frac{4}{(5.5/2)} \left(1 + \frac{4}{3} \times 1 \right) = 0.86$$

$$\mu_s = 0.45$$

For immediate settlement in clays, use undrained conditions with $\nu = \nu_u = 0.5$.

$$\text{Equation (12.35): } \rho_e = \frac{P(1 - \nu_u^2)}{E_u L} \mu_s \mu'_{emb} = \frac{500(1 - 0.5^2)}{8000 \times (5.5/2)} \times 0.45 \times 0.86 = 6.6 \times 10^{-3} = 6.6 \text{ mm}$$

Step 3: Calculate the consolidation settlement of the clay.

$$e_o = wG_s = 0.55 \times 2.7 = 1.49$$

$$\gamma_{sat} = \frac{G_s + e_o}{1 + e_o} \gamma_w = \frac{2.7 + 1.49}{1 + 1.49} 9.8 = 16.5 \text{ kN/m}^3$$

Calculate the current vertical effective stress (overburden pressure) at the center of the clay layer.

$$\sigma'_{zo} = 3 \times 16 + 1(17 - 9.8) + 1(16.5 - 9.8) = 61.9 \text{ kPa}$$

Calculate the stress increase at the center of the clay layer ($z = 3.5 \text{ m}$).

$$\frac{Z}{B} = \frac{3.5}{3} = 1.17$$

From Figure 7.23, $I_z = 0.27$.

$$\sigma_{ap} = \frac{P}{B^2} = \frac{500}{3^2} = 55.6 \text{ kPa}$$

$$\Delta\sigma_z = \sigma_{ap} \times I_z = 55.6 \times 0.27$$

$$\sigma'_{zo} + \Delta\sigma_z = 61.9 + 15 \approx 77 \text{ kPa}$$

$$\sigma'_{zc} = \text{OCR} \times \sigma'_{zo} = 1.3 \times 61.9 = 80.5 \text{ kPa} > \sigma'_{zo} + \Delta\sigma_z (= 77 \text{ kPa})$$

$$\rho_{pc} = \frac{H_o}{1 + e_o} C_r \log \frac{\sigma'_{zo} + \Delta\sigma_z}{\sigma'_{zo}}$$

$$= \frac{2}{1 + 1.49} \times 0.09 \log \frac{77}{61.9} = 6.9 \times 10^{-3} \text{ m} = 6.9 \text{ mm}$$

Step 4: Find the total settlement.

$$\text{Total settlement: } \rho = (\rho_e)_{sand} + (\rho_c)_{clay} + \rho_{pc}$$

$$= 3.3 + 6.6 + 6.9 = 16.8 \text{ mm} < 20 \text{ mm}$$

Step 5: Check bearing capacity.

The groundwater table is less than $B = 3$ m below the footing base, so groundwater effects must be taken into account.

Step 6: Check critical height.

$$H_{cr} = \frac{B}{2 \cos\left(45^\circ + \frac{\phi'_p}{2}\right)} \exp[A \tan \phi'_p]$$

$$A = \left(45^\circ - \frac{\phi'_p}{2}\right) = \left(45^\circ - \frac{32}{2}\right) \frac{\pi}{180} = 0.506 \text{ rad}$$

$$H_{cr} = \frac{3}{2 \cos\left(45^\circ + \frac{32}{2}\right)} \exp[0.506 \tan 32] = 4.24 \text{ m}$$

The height of soil below the footing to the top of the soft clay is 2.5 m < H_{cr} . Therefore, you must consider the bearing capacity of the soft layer.

ESA (sand)

$$d_\gamma = 1, \quad s_q = 1 + \frac{B'}{L'} \tan \phi'_p = 1 + \tan 32^\circ = 1.62$$

$$s_\gamma = 1 - 0.4 \frac{B'}{L'} = 0.6$$

$$d_q = 1 + 2 \tan \phi'_p (1 - \sin \phi'_p)^2 \tan^{-1}\left(\frac{D_f}{B'}\right) = 1 + 2 \tan 32^\circ (1 - \sin 32^\circ)^2 \left[\tan^{-1}\left(\frac{1.5}{3}\right) \times \frac{\pi}{180}\right] = 1.13$$

$$N_q = e^{\pi \tan 32^\circ} \tan^2\left(45 + \frac{32}{2}\right) = 23.2; \quad N_q - 1 = 23.2 - 1 = 22.2$$

$$N_\gamma = 0.1054 \exp\left(9.6 \times 32 \times \frac{\pi}{180}\right) = 22.5$$

Calculate the bearing capacity for the worst-case scenario—groundwater level at surface, i.e., $\gamma = \gamma' = 17 - 9.8 = 7.2 \text{ kN/m}^3$.

$$q_u = \gamma D_f (N_q - 1) s_q d_q + 0.5(\gamma B) N_\gamma s_\gamma d_\gamma$$

$$= (7.2 \times 1.5 \times 22.2 \times 1.62 \times 1.13) + (0.5 \times 7.2 \times 3 \times 22.5 \times 0.6 \times 1.0) = 585 \text{ kPa}$$

$$q_{ult} = q_u + \gamma D_f = 585 + 1.5 \times 7.2 = 596 \text{ kPa}$$

$$Q_{ult} = q_{ult} A = 596 \times 3^2 = 5364 \text{ kN}$$

$$\omega Q_{ult} = 0.8 \times 5364 = 4291 \text{ kN}$$

$$P_{uf} = 1.25 \text{ DL} + 1.75 \text{ LL} = (1.25 \times 300) + (1.75 \times 200) = 725 \text{ kN} < 4291 \text{ kN}; \quad \text{okay}$$

TSA (clay)

Check the bearing capacity of the clay.

Equivalent footing width = $B + z_1 = 3 + 2.5 = 5.5 \text{ m}$.

$$(\Delta\sigma)_{max} = \frac{500}{5.5^2} = 16.5 \text{ kPa}$$

$$q_u = 5.14 s_u s_c d_c$$

$$s_c = 1 + 0.2 \frac{B'}{L'} = 1.2$$

$d_c = 1.0$ because the footing is assumed to be a surface footing on the clay.

$$q_u = 5.14 \times 40 \times 1.2 \times 1.0 = 247 \text{ kPa}$$

$$\omega Q_{ult} = 0.8 \times 247 \times 5.5^2 = 5977 \text{ kN} > 725 \text{ kN}; \text{ okay}$$

Settlement governs the design.

EXAMPLE 12.20 Design (Sizing) of Footings to Limit Differential Settlement

Figure E12.20 shows two isolated footings at the two ends of a building. Your local code requires a maximum distortion of $\delta/\ell = 350$ and a maximum total settlement of 50 mm. Determine the most economical size for each footing to satisfy ultimate and serviceability limit states. Groundwater level is 5 m below the ground surface. Creep effects in the soil are negligible. The embedment depth is 1 m.

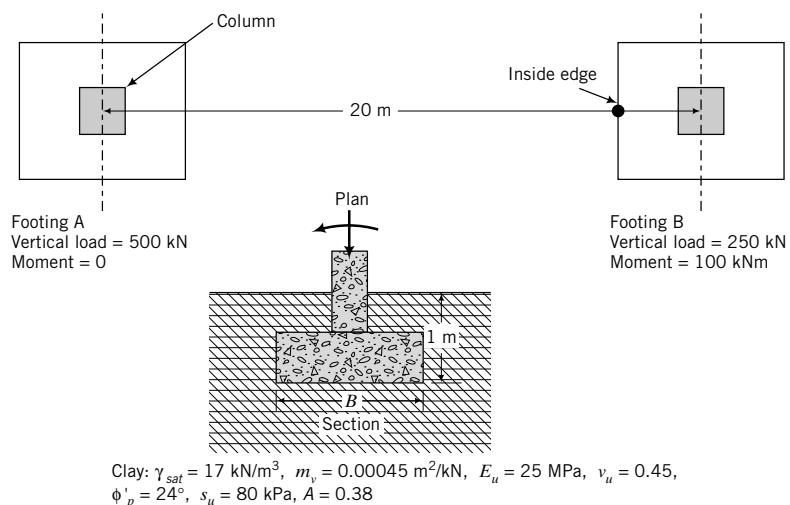


FIGURE E12.20

Strategy The clay layer is very thick, and only a certain thickness below each footing would be stressed. From Chapter 7, you know that the vertical stress increase below a depth of $2B$ for a square footing is less than 10%. So you can use a thickness of $2B$ or $3B$ as the effective thickness of the clay. The Skempton–Bjerrum method for calculating consolidation settlement is suitable for this problem.

Solution 12.20

Footing A

Step 1: Assume a width.

Assume a square footing of width $B = 3 \text{ m}$.

Step 2: Calculate the elastic settlement.

$$\begin{aligned} \text{From Equations (12.35) to (12.38): } \frac{A}{4L^2} &= 1, \quad \mu_{wall} = 1, \quad \mu_s = 0.45 \left(\frac{A_b}{4L^2} \right)^{0.38} \\ &= 0.45 \times 1 = 0.45 \\ \mu_{emb} &= 1 - 0.04 \frac{D_f}{B} \left[1 + \frac{4}{3} \left(\frac{A_b}{4L^2} \right) \right] \\ &= 1 - 0.04 \frac{1}{(3/2)} \left[1 + \frac{4}{3}(1) \right] = 0.94 \\ \rho_e &= \frac{P}{E_u L} (1 - v_u^2) \mu_s \mu_{emb} \mu_{wall} = \frac{500}{25,000 \times (3/2)} (1 - 0.45^2) \\ &\times 0.45 \times 0.94 \times 1 = 4.5 \times 10^{-3} = 4.5 \text{ mm} \end{aligned}$$

Step 3: Compute the consolidation settlement.

Determine the stress increase over a depth $3B = 9$ m (effective depth) below the footing. Divide the effective depth into three layers of 3 m each and find the stress increase at the center of each layer under the center of the footing. Stress overlap is unlikely, as the footings are greater than B apart.

$$\sigma = \frac{P}{B^2} = \frac{500}{3^2} = 55.6 \text{ kPa}$$

Layer	Depth to center of layer, z (m)	$m = n = \frac{(3/2)}{z}$	I_z	$\Delta\sigma_z = 4q_s I_z$ (kPa)
1	1.5	1	0.175	38.9
2	4.5	0.33	0.045	10.0
3	7.5	0.2	0.018	4.0
				$\Sigma 52.9$

Equivalent diameter of footing: $D = 2\sqrt{\frac{A}{\pi}} = 2\sqrt{\frac{9}{\pi}} = 3.38 \text{ m}$

$$\frac{H_o}{B} = \frac{H_o}{D} = \frac{9}{3.38} = 2.7$$

$H_o/B = 5.3$ is outside the plotted limits in Figure 12.17. We will use $H_o/B = 4$, which will result in an overestimation of the primary consolidation settlement. From Figure 12.17, $\mu_{SB} = 0.58$ for $A = 0.38$.

$$\begin{aligned}\rho_{pc} &= \Sigma m_v \Delta\sigma_z H_o \mu_{SB} = 0.00045 \times 52.9 \times 3 \times 0.58 \\ &= 41.4 \times 10^{-3} \text{ m} = 41.4 \text{ mm}\end{aligned}$$

Total settlement = $4.5 + 41.4 = 45.9 \text{ mm} < 50 \text{ mm}$

Total settlement of footing A is okay.

Footing B**Step 4:** Calculate the eccentricity.

$$e = \frac{M}{P} = \frac{100}{250} = 0.4 \text{ m}$$

Step 5: Assume a width.

For no tension, $e/B < 6$; that is, $B > 6e$.

$$B_{min} = 6 \times 0.4 = 2.4 \text{ m}; \text{ try } B = 2.5 \text{ m}$$

Step 6: Calculate the elastic settlement.

$$\mu_{emb} = 1 - 0.04 \times \frac{1}{(2.5/2)} \left(1 + \frac{4}{3}(1) \right) = 0.93$$

$$\rho_e = \frac{500}{25,000 \times 1.25} (1 - 0.45^2) \times 0.45 \times 0.93 \times 1 = 5.3 \times 10^{-3} \text{ m} = 5.3 \text{ mm}$$

Step 7: Calculate the consolidation settlement.

Because of the eccentric loading, the vertical stress distribution under footing B would be nonuniform. The maximum vertical stress, which occurs at the inside edge of magnitude (Equation 12.27), is

$$\sigma_{max} = \frac{250}{2.5^2} \left(1 + \frac{6 \times 0.4}{2.5} \right) = 78.4 \text{ kPa}$$

We need then to find the stress increase under the center of the inside edge of footing B (shown by a circle in Figure E12.20). A table is used for ease of computation and checking.

Layer	Depth to center of layer, z (m)	$m = \frac{B}{z} = \frac{2.5}{z}$	$n = \frac{L}{z} = \frac{1.25}{z}$	I_z	$\Delta\sigma_z = 2q_s I_z$
1	3.0	0.83	0.42	0.10	15.7
2	4.5	0.56	0.28	0.055	8.6
3	7.5	0.33	0.17	0.025	3.9
					$\sum 28.2$

$$\text{Equivalent diameter of footing: } D = 2\sqrt{\frac{A}{\pi}} = 2\sqrt{\frac{2.5^2}{\pi}} = 2.8 \text{ m}$$

$$\frac{H_o}{B} = \frac{H_o}{D} = \frac{9}{2.8} = 3.2$$

From Figure 12.17, $\mu_{SB} = 0.57$.

$$\begin{aligned}\rho_{pc} &= \sum m_v \Delta\sigma_z H_o \mu_{SB} = 0.00045 \times 28.2 \times 3 \times 0.57 \\ &= 22 \times 10^{-3} \text{ m} = 22 \text{ mm}\end{aligned}$$

Step 8: Calculate the total settlement.

$$\rho = \rho_e + \rho_{pc} = 5.3 + 22 = 27.3 \text{ mm} < 50 \text{ mm}$$

Total settlement of footing B is okay.

Step 9: Calculate the distortion.

$$\delta = 45.9 - 27.4 = 18.5 \text{ mm}$$

$$\frac{\delta}{L} = \frac{18.5}{(20 - 1.25) \times 10^3} = \frac{1}{987} < \frac{1}{350}; \text{ therefore, distortion is okay}$$

Note: L is calculated from the center of footing A to the outside edge of footing B because δ is calculated from these points.

Step 10: Check the bearing capacity.

Footing A

Factors

Neglect effects of depth of embedment.

$$B' = B; \quad L' = L; \quad s_c = 1 + 0.2 \frac{B'}{L'} = 1.2; \quad s_\gamma = 1 - 0.4 \frac{B'}{L'} = 0.6$$

$$s_q = 1 + \frac{B'}{L'} \tan \phi'_p = 1 + \tan 24^\circ = 1.45; \quad d_c = d_q = d_\gamma = 1$$

TSA

$$q_u = 5.14 s_u s_c d_c = 5.14 \times 80 \times 1.2 \times 1.0 = 493 \text{ kPa}$$

$$\text{FS} = \frac{493}{55.6 - 17 \times 1} \approx 13 > 3 \quad (\text{okay})$$

ESA

Assume smooth surface.

$$N_q = e^{\pi \tan 24^\circ} \tan^2(45^\circ + 24^\circ/2) = 9.6$$

$$N_\gamma = 0.0663 \exp(9.3\phi'_p) = 0.0663 \exp\left(9.3 \times 24 \times \frac{\pi}{180}\right) = 3.3$$

$$q_u = \gamma D_f (N_q - 1) s_q d_q + 0.5 \gamma B' N_\gamma s_\gamma d_\gamma$$

$$q_u = (17 \times 1 \times 8.6 \times 1.45 \times 1.0)$$

$$+ (0.5 \times 17 \times 3 \times 3.3 \times 0.6 \times 1.0) = 262 \text{ kPa}$$

$$\text{FS} = \frac{262}{55.6 - 17 \times 1} = 6.8 > 1.5 \quad (\text{okay})$$

Footing B

$$B' = B - 2e = 2.5 - 2 \times 0.4 = 1.7 \text{ m}$$

TSA

Same as footing A.

ESA

$$\begin{aligned} q_u &= \gamma D_f (N_q - 1) s_q d_q + 0.5 \gamma B' N_\gamma s_\gamma d_\gamma \\ &= (17 \times 1 \times 8.6 \times 1.45 \times 1.0) \\ &+ (0.5 \times 17 \times 1.7 \times 3.3 \times 0.6 \times 1.0) = 241 \text{ kPa} \end{aligned}$$

$$\text{FS} = \frac{241}{78.4 - 17 \times 1} = 3.9 > 1.5 \quad (\text{okay})$$

Step 11: Recommend footing sizes.

Footing A: 3 m × 3 m; $\rho \approx 46 \text{ mm}$

Footing B: 2.5 m × 2.5 m; $\rho \approx 27 \text{ mm}$

EXAMPLE 12.21 Sizing Footings for a Building Using SPT Data

The column layout for part of a building is shown in Figure E12.21a. Three boreholes are located within this part of the building, and the SPT data are shown in Figure E12.21b, c, d. Determine satisfactory sizes for the foundations under columns B2 and B4 using ASD. The loads on these columns are given in Figure E12.21a. The design criteria based on local codes are maximum settlement = 25 mm and minimum depth of footing = 300 mm, and the finished grade elevation is 780 m. Groundwater was not reached in any borehole.

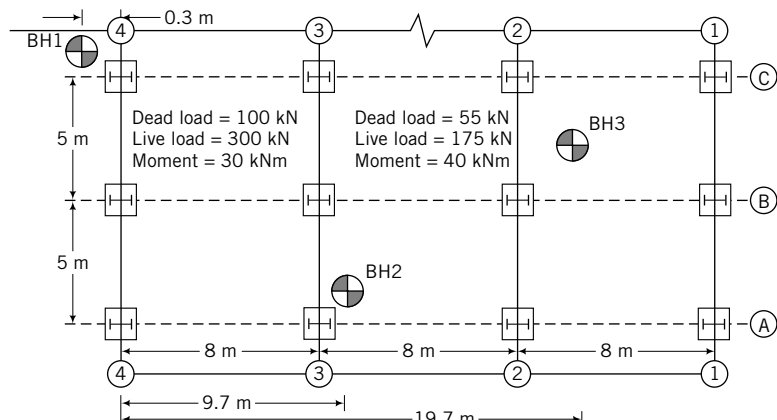


FIGURE E12.21a

								BORING LOG: BH-1							
								SHEET 1 of 1 PROJECT #: _____							
PROJECT: CLIENT: CLIENT PROJECT:								CONTRACTOR: DRILLER: INSPECTOR:							
COORDINATES N: E: LOCATION: Tucson				REF. ALIGNMENT: STATION: OFFSET:				RIG TYPE: DRILLING METHOD: HAMMER TYPE:							
COMMENTS:								SURFACE ELEV.: 781.5 TOTAL DEPTH: 23 START DATE: _____ TIME: _____ FINISH DATE: _____ TIME: _____							
Type/Symbol I.D. O.D. Length Hammer WT. Hammer Fall	Casing	Split Spoon	Ring Sampler	Shelby Tube	Cuttings	Core Barrel	GROUNDWATER DATA								
		S	R	U	CU	C	Date	Time	Water Depth (m)	Casing Depth (m)	Hole Depth (m)				
		34.93mm	63.50mm												
		50.80mm	76.20mm												
		457.20mm	457.20mm												
	622.75 N	Drill Rod Size													
762mm		I.D. (O.D.)													
DEPTH BELOW SURFACE (m) ELEVATION (m) 	SOIL SAMPLE			BLOWS			VISUAL MATERIAL CLASSIFICATION AND REMARKS	RECOVERY (m)	MOISTURE, %	DRY DENSITY	SAMPLES SENT TO LAB				
	TYPE	NUMBER	SYMBOL	DEPTH (m)	0-152.4 mm	152.4-304.8-mm									
				FROM TO	4	5									
	S	S1		0.5 0.957											
	S	S2		6 6.457	20	21									
	S	S3		10 10.457	12	14									
	S	S4		14 14.457	25	30									
					41	71									
780								Silty sand with gravel (SM)							
5								Poorly graded sand with gravel and boulders (SP)							
775								Lean clay, hard, dark brown to gray (CL)							
10								Well graded sand, very dense (SW)							
770								EOB @ 23m. No ground water encountered.							
15															
765															
20															
760															
25															

FIGURE E12.21b

							BORING LOG: BH-2					
							SHEET 1 of 1 PROJECT #:					
PROJECT: CLIENT: CLIENT PROJECT:							CONTRACTOR: DRILLER: INSPECTOR:					
COORDINATES N: E: LOCATION: Tucson							REF. ALIGNMENT: STATION: OFFSET:					
COMMENTS:							RIG TYPE: DRILLING METHOD: HAMMER TYPE:					
Type/Symbol I.D. O.D. Length Hammer WT. Hammer Fall		Casing	Split Spoon	Ring Sampler	Shelby Tube	Cuttings	Core Barrel	GROUNDWATER DATA				
		S	X	R	I	U	I	CU	III	C	X	
		34.93mm		63.50mm								
		50.80mm		76.20mm								
		457.20mm		457.20mm								
		622.75 N		Drill Rod Size								
		762mm		I.D. (O.D.)								
DEPTH BELOW SURFACE (m)		GRAPHIC		SOIL SAMPLE			BLOWS		RECOVERY (m)		VISUAL MATERIAL CLASSIFICATION AND REMARKS	
				TYPE	NUMBER	SYMBOL	DEPTH (m)		N-VALUE		MOISTURE, %	DRY DENSITY
					FROM	TO	0-152.4 mm	152.4-304.8 mm		304.8-457.2 mm		SAMPLES SENT TO LAB
780		S	S1		1	1.457	6	9	10	19	.457	
		S	S2	X	2	2.457	11	12	10	22	.457	Poorly graded sand with trace of gravel (SP)
775		S	S3	X	7	7.457	20	28	20	48	.457	
770		S	S4	X	9	9.457	10	13	15	28	.457	Lean clay, hard, dark brown to gray (CL)
765		S	S5	X	14	14.457	25	35	31	66	.229	Well graded sand, very dense
760												EOB @ 20m. No ground water encountered.
25												

FIGURE E12.21c

							BORING LOG: BH-3				
							SHEET 1 of 1 PROJECT #: _____				
PROJECT: CLIENT: CLIENT PROJECT:							CONTRACTOR: DRILLER: INSPECTOR:				
COORDINATES N: E: LOCATION: Tucson							REF. ALIGNMENT: STATION: OFFSET:				
COMMENTS:							RIG TYPE: DRILLING METHOD: HAMMER TYPE:				
							SURFACE ELEV.: 782 TOTAL DEPTH: 21 START DATE: _____ TIME: _____ FINISH DATE: _____ TIME: _____				
							GROUNDWATER DATA				
Type/Symbol I.D. O.D. Length Hammer WT. Hammer Fall	Casing	Split Spoon	Ring Sampler	Shelby Tube	Cuttings	Core Barrel		Date	Time	Water Depth (m)	Casing Depth (m)
		S	R	U	CU	C				Hole Depth (m)	Symbol
		34.93mm	63.50mm								
		50.80mm	76.20mm								
							622.75 N Drill Rod Size 762mm I.D. (O.D.)				
DEPTH BELOW SURFACE (m) ELEVATION (m)	GRAPHIC			SOIL SAMPLE			BLOWS			VISUAL MATERIAL CLASSIFICATION AND REMARKS	
				TYPE	NUMBER	SYMBOL	DEPTH (m)		N-VALUE	RECOVERY (m)	
					FROM	TO	0-152.4 mm	152.4-304.8-mm		0-152.4 mm	152.4-304.8-mm
				S	S1		2.5	2.957	5	7	9
									16		.457
				S	S2		7.5	7.957	14	15	18
									33		.457
				S	S3		11	11.457	13	14	12
									26		.457
				S	S4		15	15.457	15	23	16
									39		.457
				S	S5		18	18.229	25	36	42
									78		.229
				EOB @ 20m. No ground water encountered.							
							MOISTURE, % DRY DENSITY SAMPLES SENT TO LAB				

FIGURE E12.21d

Strategy It is best to draw an estimated soil profile based on the three borehole data items. It is customary to size the footing under the largest load and then use the maximum vertical stress under this footing to size the other footings. This may not always be satisfactory, as will be shown in this example. Other conditions, such as a footing with a lower load located on a weaker soil layer than the footing with the highest load, may govern the design. This example illustrates the iteration process required in design.

Solution 12.21

Step 1: Draw a composite soil profile based on nearby boreholes.

- Map boreholes in a graph of elevation versus distance using column line (4)–(4) as a reference line (see Figure E12.21e).
- Inspect soil type and N values in each borehole.
- Sketch lines linking similar soil types.
- Divide each soil type, if necessary, into different density groups (dense, medium, loose) based on N values and soil description (see Figure E12.21e). Assign values of unit weight based on Table A.11 in Appendix A.

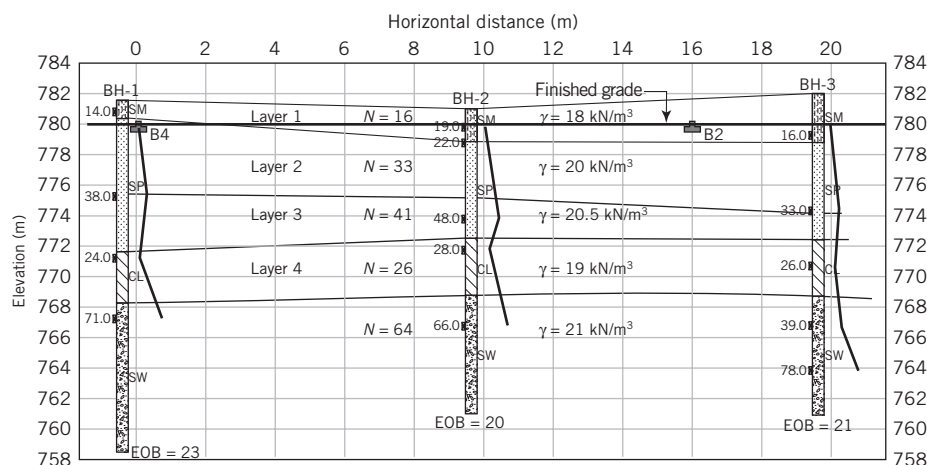


FIGURE E12.21e

Step 2: Decide on the depth for the footing with highest load.

Assume $D_f = 0.5$ m (Elevation: 779.5) for footing B4.
This footing is just below the top of soil layer 2.

Step 3: Assume a footing size for B4.

Assume a square footing 1 m \times 1 m.

Step 4: Correct N values.

Use an average depth of $\frac{1.5B}{2}$ below the footing, i.e., $\frac{1.5 \times 1}{2} = 0.75$ m. (Elevation: 778.75) Original ground level at B4 \approx elevation 781.5 m.

$$\sigma'_{zo} = \gamma z = 18(781.5 - 780.5) + 20(780.5 - 778.75) = 53 \text{ kPa}$$

$$c_N = \left(\frac{95.8}{\sigma'_{zo}} \right)^{\frac{1}{2}} = \left(\frac{95.8}{53} \right)^{\frac{1}{2}} = 1.34 < 2 \quad (\text{okay})$$

$$N_1 = c_N N = 1.34 \times 33 = 44$$

Step 5: Estimate q_{ult} .

$$q_{ult} = 32N_1B = 32 \times 44 \times 1 = 1408 \text{ kPa}$$

Step 6: Calculate maximum imposed vertical stress.

$$V_n = \text{Total vertical load} = 400 \text{ kN}; \quad M = \text{Moment} = 30 \text{ kN.m}$$

$$\text{eccentricity, } e = \frac{M}{V_n} = \frac{30}{400} = 0.075 \text{ m}$$

$$\frac{B}{6} = \frac{1.0}{6} = 0.17 > e; \quad \therefore \text{No tension}$$

$$\sigma_{max} = \frac{V_n}{A} \left(1 + \frac{6e}{B} \right) = \frac{400}{1 \times 1} \left(1 + \frac{6 \times 0.075}{1} \right) = 580 \text{ kPa}$$

Step 7: Check factor of safety.

$$\text{FS} = \frac{q_{ult}}{\sigma_{max}} = \frac{1408}{580} = 2.4$$

Adjust B so that $\text{FS} \approx 3$. Using a spreadsheet makes this easier, as shown in Table E12.21a. With a square footing $1.1 \text{ m} \times 1.1 \text{ m}$, $\text{FS} = 3.3$.

TABLE E12.21a

Finished grade elevation	780 m	Dead load	100 kN				
Width of footing	1.1 m	Live load	300 kN				
Depth of footing	0.5 m	Moment	30 kN.m				
Length of footing	1.1 m	Total load	400 kN				
Groundwater	100 m	e	0.08 m				no tension
FS	3.3	σ_{max}	465.8 kPa				
Elevation (m)	Thickness (m)	Unit weight (kN/m ³)	Vertical effective stress (kPa)	C_N use	N	N_1	q_{ult} (kPa)
781.5	0	0	0.0	0	0	0	0
780.5	1	18	18.0	2.0	16	32	1126
778.7	1.8	20	54.5	1.3	33	44	1540

Step 8: Sizing footing B2.

Assume the depth of footing B2 is at the same elevation as B4. Footing B2 is now located in soil layer 1 with $N = 16$. The key point is that in order for the settlement of footings B2 and B4 to be about equal ($<25 \text{ mm}$), the maximum vertical stress should be the same.

Step 9: Calculate size of footing B2.

$$\text{Total vertical load} = V_n = 55 + 175 = 230 \text{ kN}; \quad \text{Moment} = 40 \text{ kN.m}$$

$$e = \frac{40}{230} = 0.17 \text{ m}$$

$$B_{min} \text{ for no tension} = 6e = 6 \times 0.17 = 1.02 \text{ m}$$

Assume $B = 1.1$ m.

$$\sigma_{max} = \frac{V_n}{A} \left(1 + \frac{6e}{B} \right) = \frac{230}{1.1^2} \left(1 + \frac{6 \times 0.17}{1.1} \right) = 366 \text{ kPa} > 465.8 \text{ kPa} \quad (\text{Table E12.21a})$$

To get $\sigma_{max} = 465.8$ kPa, B must be reduced. But this cannot be done because tension would develop. Therefore, the maximum vertical stress under footing B2 controls the design.

Step 10: Resize footing B2.

It is best to set up a spreadsheet to carry out the calculations, as shown in Table E12.21b. With a footing size of $1.2 \text{ m} \times 1.2 \text{ m}$, the factor of safety is 3.1 and the maximum vertical stress is 298.6 kPa.

TABLE E12.21b

Finished grade elevation	780 m	Dead load	55 kN				
Width of footing	1.2 m	Live load	175 kN				
Depth of footing	0.5 m	Moment	40 kN.m				
Length of footing	1.2 m	Total load	230 kN				
Groundwater	100 m	e	0.17 m				no tension
FS	3.1	σ_{max}	298.6 kPa				
Vertical effective stress							
Elevation (m)	Thickness (m)	Unit weight (kN/m ³)	(kPa)	C_N use	N	N_1	q_{ult} (kPa)
781.0	0	0	0.0	0	0	0	0
778.6	2.4	18	43.2	1.5	16	24	915

Step 11: Resize footing B4.

Use the maximum vertical stress due to footing B2 as allowable stress for B4. The size of footing for B4 is $1.35 \text{ m} \times 1.35 \text{ m}$, with a maximum vertical stress of 292.6 kPa and a factor of safety of 6.2 (see Table E12.21c) from the spreadsheet.

TABLE E12.21c

Finished grade elevation	780 m	Dead load	100 kN				
Width of footing	1.35 m	Live load	300 kN				
Depth of footing	0.5 m	Moment	30 kN.m				
Length of footing	1.35 m	Total load	400 kN				
Groundwater	100 m	e	0.08 m				no tension
FS	6.2	σ_{max}	292.6 kPa				
Vertical effective stress							
Elevation (m)	Thickness (m)	Unit weight (kN/m ³)	(kPa)	C_N use	N	N_1	q_{ult} (kPa)
781.5	0	0	0.0	0	0	0	0
780.5	1	18	18.0	2.0	16	32	1382
778.5	2.0	20	58.3	1.3	33	42	1828

Step 12: Assess design.

The settlement of the two footings will be the same only if the N value and the applied stress distribution are the same. Since footing B2 is located in a weaker soil (lower N value) than footing B4, the settlement is unlikely to be the same.

A better alternative is to locate both footings in layer 2 ($N = 33$) at an elevation of 778.5 m. Additional expenses will occur for excavation to construct the footings, but the settlement of the two footings is now likely to be similar and the footing sizes may be smaller.

Resize footing B2

Try $B = L = 1.1$ m and $D_f = 1.5$ m. From Table E12.21d, $\sigma_{max} = 370.4$ kPa and FS = 3.9.

TABLE E12.21d

Finished grade elevation	780 m	Dead load	55 kN				
Width of footing	1.1 m	Live load	175 kN				
Depth of footing	1.5 m	Moment	40 kN.m				
Length of footing	1.1 m	Total load	230 kN				
Groundwater	100 m	e	0.17 m				no tension
FS	3.9	σ_{max}	370.4 kPa				
Vertical effective stress							
Elevation (m)	Thickness (m)	Unit weight (kN/m ³)	(kPa)	C_N use	N	N_1	q_{ult} (kPa)
781	0	0	0.0	0	0	0	0
779	2	18	36.0	1.6	16	26	919
777.7	1.3	20	62.5	1.2	33	41	1438

Resize footing B4

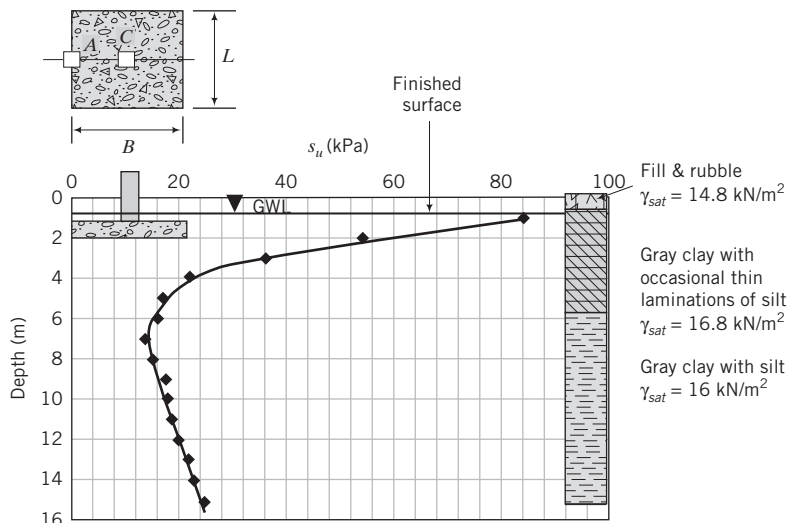
With $B = L = 1.21$ m, $\sigma_{max} = 374.8$ kPa and FS = 3.8 (see Table E12.21e).

TABLE E12.21e

Finished grade elevation	780 m	Dead load	100 kN				
Width of footing	1.21 m	Live load	300 kN				
Depth of footing	1.5 m	Moment	30 kN.m				
Length of footing	1.21 m	Total load	400 kN				
Groundwater	100 m	e	0.08 m				no tension
FS	3.8	σ_{max}	374.8 kPa				
Vertical effective stress							
Elevation (m)	Thickness (m)	Unit weight (kN/m ³)	(kPa)	C_N use	N	N_1	q_{ult} (kPa)
781.5	0	0	0.0	0	0	0	0
780.5	1	18	18.0	2.0	16	32	1239
777.6	2.9	20	76.2	1.1	33	37	1433

EXAMPLE 12.22 Design of a Shallow Foundation Based on Vane Shear Test Data and CSM

The results of a representative field vane shear test at a site are shown in Figure E12.22a. Previous studies reveal $C_r = 0.08$ for the gray clay. A building with different column loads is to be erected on the site. The maximum eccentricity is expected to be 10% of the footing width. The minimum factor of safety is 1.25 for CSM and 2.5 for conventional bearing capacity method. The settlement should not exceed 25 mm. Determine the maximum load that can be supported on square shallow footings up to 3 m × 3 m.

**FIGURE E12.22a**

Strategy We need to inspect and interpret the given data, then follow Section 12.12.1 to design the footing. Assume plane strain condition for the vane shear test. Since the column loads will be eccentric, it is better to assume plane strain (DSS) condition.

Solution 12.22

Step 1: Inspect and interpret vane shear test data.

Inspection of the vane shear test data shows that the soil is overconsolidated above 7 m and normally consolidated below 7 m. Recall that normally consolidated soils tend to show linear increase of shear strength with depth. In other words, the normalized shear strength is constant with depth.

Step 2: Calculate the critical state friction angle.

$$(s_u)_f \text{ at } 7 \text{ m} = 14 \text{ kPa}$$

Vertical effective stress at 7 m is

$$\sigma'_{zo} = 14.8 \times 1 + (16.8 - 9.8) \times 6 = 56.8 \text{ kPa}$$

From Equation (11.73), the normalized undrained shear strength for normally consolidated fine-grained soils is

$$\left[\frac{(s_u)_f}{\sigma'_{zo}} \right]_{DSS} \approx 0.5 \sin \phi'_{cs}$$

$$\therefore \frac{14}{56.8} = 0.5 \sin \phi'_{cs}; \quad \sin \phi'_{cs} = 0.493; \quad \phi'_{cs} = 29.5^\circ$$

$$M_c = \sqrt{3} \sin \phi'_{cs} = \sqrt{3} \times 0.493 = 0.85$$

Step 3: Calculate the initial stresses, overconsolidation ratio, and preconsolidation stress at $B/2$ below the footing.

The calculations will be done for $3 \text{ m} \times 3 \text{ m}$. A spreadsheet will be used for other footing sizes.

The depth from the surface at $B/2$ below the maximum size footing is $2 + (3/2) = 3.5 \text{ m}$.

Vertical effective stress at 3.5 m is

$$\sigma'_{zo} = 14.8 \times 1 + (16.8 - 9.8) \times 2.5 = 32.3 \text{ kPa}$$

$$(s_u)_f \text{ at } 3.5 \text{ m} = 28 \text{ kPa}$$

From Equation (11.72),

$$\left[\frac{(s_u)_f}{\sigma'_{zo}} \right]_{DSS} = \frac{\sqrt{3} \sin \phi'_{cs}}{2} \left(\frac{OCR}{2} \right)^{0.8}$$

$$\left[\frac{28}{32.3} \right]_{DSS} = \frac{0.85}{2} \left(\frac{OCR}{2} \right)^{0.8}$$

$$\therefore OCR = 4.9$$

From Figure 11.29,

$$R_o = 4.2$$

$$K_o^{nc} = 1 - \sin \phi'_{cs} = 1 - \sin 29.5^\circ = 0.51$$

$$K_o^{oc} = K_o^{nc} OCR^{\frac{1}{2}} = 0.51 \times 4.9^{\frac{1}{2}} = 1.13$$

$$\sigma'_{zc} = OCR \times \sigma'_{zo} = 4.9 \times 32.3 = 158.3 \text{ kPa}$$

The current and past consolidation stresses in the field are:

$$\text{Current: } p'_o = \frac{1 + 2K_o^{oc}}{3} \sigma'_{zo} = \frac{1 + 2 \times 1.13}{3} \times 32.3 = 35 \text{ kPa}$$

$$q_o = \sigma'_{zo}(1 - K_o^{oc}) = 32.3 \times (1 - 1.13) = -4.2 \text{ kPa}$$

In Figure 12.19, point *O* represents (p'_o, q_o) .

$$\begin{aligned} \frac{p'_c}{\sigma'_{zc}} &\approx \frac{1}{3} \left[(3 - 2 \sin \phi'_{cs}) + \frac{(3 - \sin \phi'_{cs})^2}{4(3 - 2 \sin \phi'_{cs})} \right] \\ &= \frac{1}{3} \left[(3 - 2 \times 0.493) + \frac{(3 - 0.493)^2}{4(3 - 2 \times 0.493)} \right] \\ &= 0.93 \\ p'_c &= 0.93 \times 158.3 = 147.2 \text{ kPa} \end{aligned}$$

In Figure 12.19, point *C* represents $(p'_c, 0)$

$$\begin{aligned} \gamma_{sat} &= \left(\frac{G_s + e_o}{1 + e_o} \right) \gamma_w \\ 16.8 &= \left(\frac{2.7 + e_o}{1 + e_o} \right) 9.8; \quad e_o = 1.38 \\ \kappa &= \frac{C_r}{2.3} = \frac{0.08}{2.3} = 0.035 \end{aligned}$$

Step 4: Check if the soil element will fail in tension.

$$t_c = \frac{1}{\left(1 + \frac{n_t^2}{M^2} \right)} = \frac{1}{\left(1 + \frac{\sqrt{3}^2}{0.85^2} \right)} = 0.194$$

$$R_t = \frac{1}{t_c} = \frac{1}{0.194} = 5.2 > 4.2$$

Soil will not fail by tension.

Step 5: Calculate the deviatoric stress on the HV surface.

$$m = \frac{M - 2t_c n_t}{1 - 2t_c} = \frac{0.85 - 2 \times 0.194 \times \sqrt{3}}{1 - 2 \times 0.194} = 0.29$$

$$q_{yH} = p'_o [m(1 - t_c R_o) + t_c n_t R_o] = 35 \times [0.29(1 - 0.194 \times 4.2) + 0.194 \times \sqrt{3} \times 4.2] = 51.3 \text{ kPa}$$

Step 6: Estimate the load-to-width ratio to satisfy ultimate limit state.

Since the eccentricity is 10% of the width, then

$$q_s = \frac{P}{B^2} \left(1 + \frac{6e}{B}\right) = \frac{P}{B^2} \left(1 + \frac{6 \times 0.1B}{B}\right) = \frac{1.6P}{B^2}$$

At the edge of footing A (Figure E12.22a), $I_p = 0.22$, $I_q = 0.39$ (Table 12.7).

$$\Delta q_{ap} = I_q q_s = 0.39 \times \frac{1.6P}{B^2} = 0.624 \frac{P}{B^2}$$

$$q_o + \Delta q_{ap} = -4.2 + 0.624 \frac{P}{B^2}$$

$$\text{FS} = \frac{q_{yH}}{q_o + \Delta q_{ap}}$$

$$1.25 = \frac{51.3}{-4.2 + 0.624 \frac{P}{B^2}}$$

$$\frac{P}{B^2} = 72.5; \quad P = 652.5 \text{ kN}$$

Step 7: Estimate the load-to-width ratio to satisfy settlement.

$$e_c = e_o - \kappa \ln R_o = 1.38 - 0.035 \ln(4.2) = 1.33$$

Assume $\nu' = 0.35$; then

$$\begin{aligned} p_z &= \frac{q_s \kappa B}{p'_c(1 + e_c)} \left[\frac{\sqrt{3}}{2} I_q + 1.54 I_p \right] \\ &= \frac{1.6P \times 0.035 \times B}{147.2(1 + 1.33)} \left[\frac{\sqrt{3}}{2} \times 0.39 + 1.54 \times 0.22 \right] \\ &= 1.1 \times 10^{-4} \frac{P}{B} \text{ m} \end{aligned}$$

The settlement from the above equation is dependent only on the P/B ratio because all the other parameters are constant. The maximum allowable settlement is 25 mm. Therefore,

$$0.025 = 1.1 \times 10^{-4} \frac{P}{B}$$

$$\frac{P}{B} = 227; \quad P = 681 \text{ kN}$$

Since the load for bearing capacity consideration is lower than for settlement, bearing capacity governs the design.

Step 8: Determine allowable load using the conventional method.

The maximum footing size is 3 m. Assume an effective depth of B below the footing; then the maximum effective depth is 3 m (5 m below the ground surface). The average undrained shear strength is 28 kPa. The ultimate bearing capacity is

$$q_{ult} = 5.14 s_u s_c d_c = 5.14 \times 28 \times 1.2 \times 1 = 172.7 \text{ kPa}$$

Using FS = 2.5, we get

$$2.5 \times \frac{1.6P}{B^2} = 172.7$$

$$\frac{P}{B^2} = 43; \quad P = 387 \text{ kN}$$

We cannot directly find the elastic modulus. We will assume that all settlement is due to consolidation. The vertical stress increase at the center of the edge of the footing (Figure E12.22a) is found using Figure 7.24 with $B = 3 \text{ m}$, $L = 1.5 \text{ m}$, and $z = 1.5 \text{ m}$. The vertical stress increase coefficient is $I_z = 0.2$.

$$\sigma'_{zo} + \Delta\sigma_z = 32.3 + 2 \times 0.2 \times \frac{1.6P}{B^2}$$

(Note: The multiplier 2 is used because we had to divide the footing into two halves to use Figure 7.24.) We will calculate the settlement assuming that the past maximum vertical effective stress is not exceeded. If it is, we have to know C_c , which is not given. Therefore,

$$\begin{aligned} \rho_{pc} &= \frac{H_o}{1 + e_o} C_r \log \frac{\sigma'_{zo} + \Delta\sigma_z}{\sigma'_{zo}} = \frac{B}{1 + 1.38} \times 0.08 \times \log \frac{\sigma'_{zo} + \frac{0.64P}{B^2}}{\sigma'_{zo}} \\ 0.025 &= \frac{B}{1 + 1.38} \times 0.08 \times \log \left(1 + \frac{\frac{0.64P}{B^2}}{\sigma'_{zo}} \right) \\ \therefore B \log \left(1 + \frac{\frac{0.64P}{B^2}}{\sigma'_{zo}} \right) &= 0.744; \quad \sigma'_{zo} + \Delta\sigma_z < \sigma'_{zc} \\ \frac{P}{B^2} &= \frac{\sigma'_{zo}}{0.64} \left(10^{\frac{0.744}{B}} - 1 \right) = \frac{32.3}{0.64} \left(10^{\frac{0.744}{3}} - 1 \right) = 38.9 \\ P &= 38.9 \times 3^2 = 350 \text{ kN} \end{aligned}$$

Check that $\sigma'_{zo} + \Delta\sigma_z < \sigma'_{zc}$.

$$\sigma'_{zo} + \Delta\sigma_z = 32.3 + 2I_z \frac{1.6P}{B^2} = 32.3 + 2 \times 0.2 \times 1.6 \times \frac{350}{3^2} = 57.2 \text{ kPa} < 158.3 \text{ kPa}$$

∴ okay

Step 9: Compare results.

	CSM load (kN)	Conventional load (kN)
Bearing capacity	652.5	387
Settlement	681	350

For CSM, the maximum load that the footing can support is 652.5 kN, and this is controlled by bearing capacity. For the conventional method, the maximum load that the footing can support is 350 kN, and this is controlled by settlement.

Step 10: Calculate maximum load for other footing sizes.

A spreadsheet can be written to do the calculations for any width. The results from one such spreadsheet are shown in Table E12.22, and the results are also plotted in Figure E12.22b. Differences in results between the preceding calculations and the spreadsheet are due to rounding. The check that $\sigma'_{zo} + \Delta\sigma_z < \sigma'_{zc}$ is to see whether the vertical stress applied is below the past maximum vertical effective stress. If it is not, then the soil will consolidate on the normal consolidation line for the difference between vertical applied stress and the past maximum vertical effective stress (see Chapter 9). For CSM, bearing capacity controls for all footing sizes. For the conventional method, bearing capacity controls the design up to about $B = 2.7$ m, and then settlement controls. The bearing capacity from CSM and from the conventional method is about the same for $B < 1.5$ m. When tension develops, $q_{yH} = q_{tf}$ is adjusted according to Equation (11.61) as $\sqrt{3} p'_o$.

TABLE E12.22

B (m)	σ'_{zo} (kPa)	p'_o (kPa)	q_o (kPa)	R_o p'_o/p'_o	OCR $\sigma'_{zc}/\sigma'_{zo}$	Tension	q_{yH} (kPa)
0	0	0	0	0			
0.5	23.6	25.6	-3.1	5.8	6.7	YES	44.3
0.75	24.4	26.5	-3.2	5.5	6.5	YES	46.0
1	25.3	27.5	-3.3	5.4	6.3	YES	47.6
1.25	26.2	28.4	-3.4	5.2	6.0	YES	49.3
1.5	27.1	29.4	-3.5	5.0	5.9	NO	50.0
2	28.8	31.3	-3.7	4.7	5.5	NO	50.5
2.5	30.6	33.2	-4.0	4.7	5.2	NO	51.1
3	32.3	35.1	-4.2	4.2	4.9	NO	51.6

B (m)	CSM				Conventional			
	BC*		Settlement		BC	Settlement		
B (m)	P/B² (kPa)	P (kN)	P/B (kN/m)	P (kN)	P (kN)	P/B² (kPa)	P (kN)	$\sigma'_{zo} + \Delta\sigma_z$ (kPa)
0	0	0	0	0	0	0	0	0
0.5	61.7	15	227	114	11	1093.8	273	723.6
0.75	64.0	36	227	170	24	336.2	189	239.6
1.0	66.3	66	227	227	43	179.6	180	140.2
1.25	68.6	107	227	284	67	120.1	188	103.0
1.5	69.7	157	227	341	97	90.1	203	84.7
2.0	70.7	283	227	454	172	60.9	244	67.8
2.5	71.8	449	227	568	269	47.0	294	60.6
3.0	72.9	656	227	681	387	38.8	350	57.2

*BC = Bearing capacity

**Check that $\sigma'_{zo} + \Delta\sigma_z > \sigma'_{zc}$

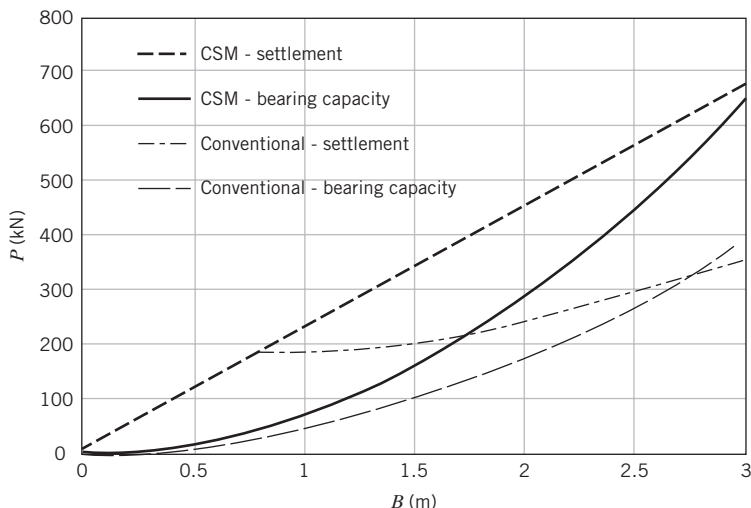


FIGURE E12.22b

EXERCISES

Theory

- 12.1** Show that the ultimate load for a strip footing under long-term conditions using the two triangle failure surfaces shown in Figure P12.1 is $P_u = \frac{1}{2}\gamma B^2 N_y$, where

$$N_y = \frac{2 \tan \phi' (\tan^2 \phi' - 3)}{[(1 + \tan^2 \phi') - 2](1 - \tan \phi')} = \frac{2 \sin 3\phi'}{\cos \phi' - \sin 3\phi'}$$

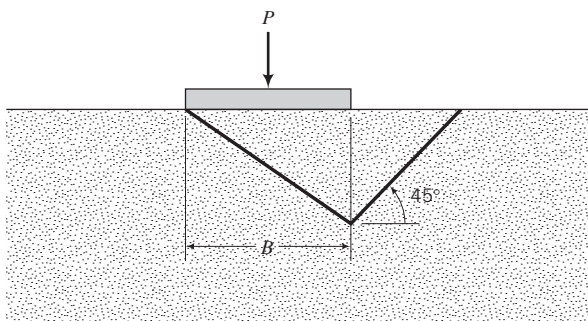


FIGURE P12.1

- 12.2** A strip footing, 5 m wide, is founded on the surface of a deep deposit of clay. The undrained shear strength of the clay increases linearly from 3 kPa at the surface to 10 kPa at a depth of 5 m. Estimate the vertical ultimate load assuming that the load is applied at an eccentricity of 0.5 m right from the center of the footing's width. (*Hint:* Try a circular failure surface, determine the equation for the distribution of shear strength with depth, and integrate the shear strength over the radius to find the shear force.)
- 12.3** The centroid of a square foundation of sides 5 m is located 10 m away from the edge of a vertical cut of depth

4 m. The soil is a stiff clay whose undrained strength is 20 kPa and whose unit weight is 16 kN/m³. Calculate the vertical ultimate load. Assume a circular failure surface for the footing and a planar surface for the cut.

Problem Solving

- 12.4** Calculate the ultimate net bearing capacity of (a) a strip footing 2 m wide, (b) a square footing 3 m × 3 m, and (c) a circular footing 3 m in diameter. All footings are located on the ground surface and the groundwater level is at the ground surface. The soil is medium-dense coarse-grained with $\gamma_{sat} = 17 \text{ kN/m}^3$ and $\phi'_p = 30^\circ$ from direct shear tests.
- 12.5** A strip footing, founded on dense sand ($\phi'_p = 35^\circ$ from direct shear tests and $\gamma_{sat} = 17 \text{ kN/m}^3$), is to be designed to support a vertical load of 400 kN per meter length. Determine a suitable width for this footing for FS = 3. The footing is located 1 m below the ground surface. The groundwater level is 10 m below the ground surface.
- 12.6** A square footing, 3 m wide, is located 1.5 m below the surface of a stiff clay. Determine the allowable bearing capacity for short-term condition if $(s_u)_p = 100 \text{ kPa}$ and $\gamma_{sat} = 20 \text{ kN/m}^3$. If the footing were located on the surface, what would be the allowable bearing capacity? Use FS = 3. Comment on the use of the $(s_u)_p$ value for both the embedded and the surface footing.
- 12.7** A column carrying a load of 750 kN is to be founded on a square footing at a depth of 2 m below the ground surface in a deep clay stratum. What will be the size of the footing for FS = 3 for TSA? The soil parameters are $\gamma_{sat} = 18.5 \text{ kN/m}^3$ and $(s_u)_p = 55 \text{ kPa}$. The groundwater

level is at the base of the footing, but it is expected to rise to the ground surface during rainy seasons.

12.8 Repeat Exercise 12.7 with a moment of 250 kN.m about an axis parallel to the length in addition to the vertical load.

12.9 A square footing located on a dense sand is required to carry a dead load of 200 kN and a live load of 300 kN, both inclined at 15° to the vertical plane along the footing's width. The building code requires an embedment depth of 1.2 m. Groundwater level is at 1 m below the ground surface. Calculate the size of the footing using ASD and LRFD for $\phi'_p = 35^\circ$ from direct shear tests, $\gamma_{sat} = 18.5 \text{ kN/m}^3$, and FS = 3. Assume the soil above the groundwater level to be saturated.

12.10 The footing for a bridge pier is to be founded in sand, as shown in Figure P12.10. The clay layer is normally consolidated, with $C_c = 0.25$, $(s_u)_f = 40 \text{ kPa}$ and $\phi'_{cs} = 30^\circ$. Determine the factor of safety against bearing capacity failure and the total settlement (elastic compression and primary consolidation) of the pier. The friction angle for the dense sand was obtained from direct shear tests.

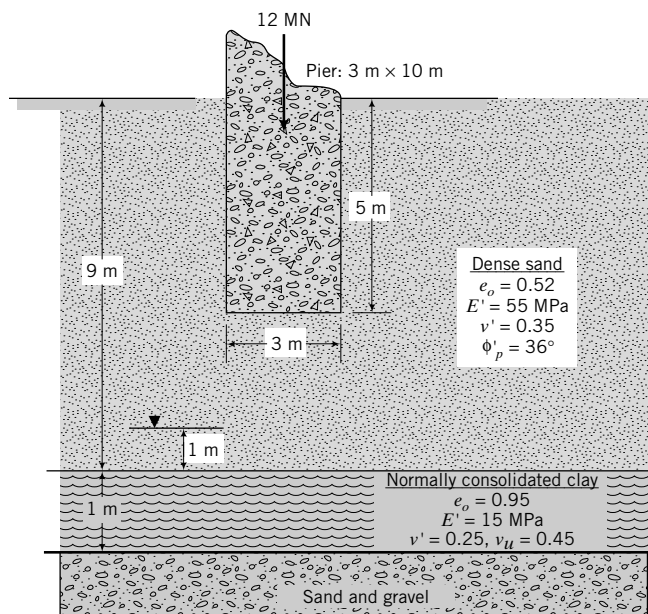


FIGURE P12.10

12.11 A multilevel building is supported on a footing 58 m wide \times 75 m long \times 3 m thick resting on a very stiff deposit of saturated clay. The footing is located at 3 m below ground level. The average stress at the base of the footing is 350 kPa. Groundwater level is at 12 m below the surface. Field and laboratory tests gave the following results:

Depth (m)	0.5	6	25
$(s_u)_p$ (kPa)	58	122	156

$e_o = 0.57$, $C_c = 0.16$, $C_r = 0.035$, $OCR = 10$, $\phi'_p = 28^\circ$, $\phi'_{cs} = 24^\circ$, $E_u = 100 \text{ MPa}$, $v_u = 0.45$, $E' = 90 \text{ MPa}$, and $v' = 0.3$. Determine the total settlement and the safety factor against bearing capacity failure. Assume an effective thickness of $2B$ below the bottom of the footing for settlement calculations. The shear strength parameters were obtained from direct simple shear tests.

12.12 A square footing located on a dense sand is required to carry a dead load of 200 kN and a live load of 300 kN at an eccentricity not to exceed of 10% of the width. The embedment depth is 1 m. Groundwater level is at 1 m below the ground surface. Calculate the size of the footing using CSM for ASD and LRFD. At a depth $B/2$ below the bottom of the footing, the soil parameters are $\phi'_{cs} = 30^\circ$ from direct shear tests, $OCR = 9$, $\Lambda = 0.8$, $C_r = 0.016$, and $\gamma_{sat} = 18.8 \text{ kN/m}^3$. Assume the soil above the groundwater level to be saturated and $v' = 0.35$. Determine the factor of safety of the footing (use the footing size designed according to CSM) using the conventional method.

Practical

12.13 A circular foundation of diameter 8 m supports a tank. The base of the foundation is at 1 m from the ground surface. The vertical load is 20 MN. The tank foundation was designed for short-term loading conditions $((s_u)_p = 80 \text{ kPa}$ and $\gamma_{sat} = 19 \text{ kN/m}^3$). The groundwater level when the tank was initially designed was at 4 m below the ground surface. It was assumed that the groundwater level was stable. Fourteen months after the tank was constructed, during a week of intense rainfall, the tank foundation failed. It was speculated that failure occurred by bearing capacity failure. Establish whether this is so or not. The friction angle is $\phi'_p = 25^\circ$ from direct shear tests.

12.14 The foundation (base) of a long retaining wall is required to support the load (including self-weight of the base and the wall) and moment (this comes from the lateral loads on the wall) shown in Figure P12.14. Determine the factor of safety against bearing capacity failure. Would the settlement of the base be uniform? Discuss your answer.

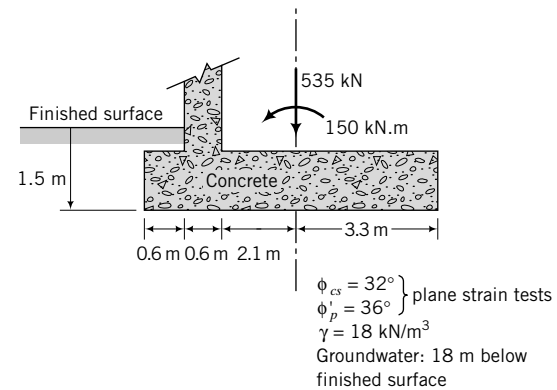


FIGURE P12.14

- 12.15** Calculate the size of a square footing on a soil profile consisting of a medium-dense sand layer with N values, as shown in the table below.

Depth (m)	0	5	10	15
N	0	28	31	37

The dead load is 500 kN and the live load is 200 kN. The footing is embedded 0.5 m into the sand. Groundwater is 4 m below the surface. Consider both ASD with $FS = 3$ and LRFD.

- 12.16** The column load for an office building consists of a dead load of 200 kN and a live load of 250 kN. The soil at the site for the office building is a fairly homogeneous clay. Soil samples at a depth of 2 m gave the following average results. Triaxial tests: isotropic consolidated CU tests on saturated samples, $(s_u)_f = 36$ kPa, confining stress = 144 kPa, and average water content of 40%; one-dimensional consolidation tests: $C_c = 0.16$, $C_r = 0.04$, and $OCR = 9$. The minimum embedment depth of the footing is 1 m. Groundwater level is at the surface. Check the suitability of a 3.0-m-square footing using the conventional ASD method with $FS = 3$. Compare the results of the conventional method with CSM using $FS = 1.25$. Assume $\nu' = 0.35$. The tolerable

settlement is less than 20 mm. Assume the samples represent the soil at a depth $0.5B$ below the bottom of the footing.

- 12.17** The results of a representative field vane shear test at a site are shown in Figure E12.22a. Previous studies reveal that $\Lambda = 0.8$ and $\lambda = 0.12$ for the top gray clay layer. These are average values. A building with different column loads is to be erected on the site. Estimate the maximum centric load that a 2-m-square footing can support using CSM. The minimum factor of safety is 1.25 and the settlement should not exceed 25 mm. Assume $\nu' = 0.35$.

- 12.18** Figure P12.18 shows a proposed canal near a five-story apartment building 30 m wide \times 50 m long. The building is founded on a mat foundation. The existing groundwater level is approximately 1 m below the surface. The proposed normal water level in the canal is 2 m below the surface with 1 m of freeboard. Describe and justify some of the concerns you may have regarding the stability of the building from the construction of a canal. If the owner insists on constructing the canal, research methods that you would consider so that the canal can be designed and constructed safely.

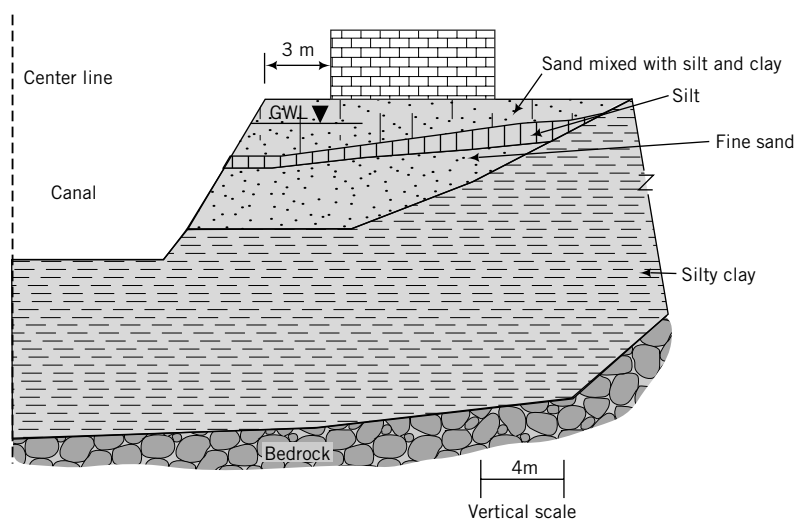


FIGURE P12.18

CHAPTER 13

PILE FOUNDATIONS

13.0 INTRODUCTION

In the previous chapter, we studied the analysis of shallow foundations. In some cases, shallow foundations are inadequate to support the structural loads, and deep foundations (pile foundations) are required.

In this chapter, you will study the bearing capacity (load capacity) and settlement of single and group piles under axial and lateral loads. When you complete this chapter, you should be able to:

- Appreciate and understand the complexity of the stress and strain states imposed by pile installation and structural loads on the soil.
- Estimate the allowable axial load capacity of single piles and pile groups.
- Estimate the allowable lateral load capacity and lateral deflection of single piles.
- Estimate the settlement of single piles and pile groups.

You would need to recall the following:

- Effective stresses—Chapter 7
- Consolidation—Chapter 9
- Statics

Importance

A pile is a slender, structural member installed in the ground to transfer the structural loads to soils at some significant depth below the base of the structure. Structural loads include axial loads, lateral loads, and moments. Another term commonly used in practice for pile foundations is deep foundations. Structures that cannot be supported economically on shallow foundations are normally supported by pile foundations. Pile foundations are used when:

- The soil near the surface does not have sufficient bearing capacity to support the structural loads.
- The estimated settlement of the soil exceeds tolerable limits (i.e., settlement greater than the serviceability limit state).
- Differential settlement due to soil variability or nonuniform structural loads is excessive.
- The structural loads consist of lateral loads, moments, and uplift forces, singly or in combination.
- Excavations to construct a shallow foundation on a firm soil layer are difficult or expensive.

An example of a pile foundation under construction is shown in Figure 13.1 on the next page.

13.1 DEFINITIONS OF KEY TERMS

Pile is a slender, structural member consisting of steel, concrete, timber, plastic, or composites.

Displacement pile is a pile that displaces a large volume of soil. Driven piles with solid sections are displacement piles. Closed-ended pipe piles are displacement piles.



FIGURE 13.1 Concrete piles used for the foundation of a skyscraper.
(© Fritz Henle/Photo Researchers.)

Nondisplacement pile is a pile that displaces only a small volume of soil ($\approx 10\%$) relative to its external volume. Steel H-piles and open-ended pipe piles are nondisplacement piles.

Micropiles are small-diameter piles (50 mm to 340 mm) installed as pipe piles. They are also called mini-piles, pin piles, needle piles, and root piles.

Skin friction stress or shaft friction stress or adhesive stress (f_s) is the frictional or adhesive stress on the shaft of a pile.

End bearing stress or point resistance stress or tip resistance stress (f_b) is the stress at the base or tip of a pile.

Ultimate load capacity (Q_{ult}) is the maximum load that a pile can sustain before soil failure occurs.

Ultimate group load capacity [$(Q_{ult})_g$] is the maximum load that a group of piles can sustain before soil failure occurs.

Skin friction or shaft friction or side shear (Q_f) is the frictional force generated on the shaft of a pile.

End bearing or point resistance or tip resistance (Q_b) is the resistance generated at the base or tip of a pile.

End bearing or point bearing pile is one that transfers almost all the structural load to the soil at the bottom end of the pile.

Friction pile is one that transfers almost all the structural load to the soil by skin friction along a substantial length of the pile.

Floating pile is a friction pile in which the end bearing resistance is neglected.

Drilled shaft or bored pile is a concrete pile cast in a hole created by a spiral auger. These piles are generally cylindrical.

Barrette pile is a drilled shaft created by making an excavation with a grab rather than an auger. Barrette piles have square or rectangular cross sections.

13.2 QUESTIONS TO GUIDE YOUR READING

1. What are the differences among the different types of piles?
2. How do I select a pile for a given application?

3. How is a pile installed in the ground?
4. How do the soil stress states and strain states change by the installation and structural loads?
5. How do I estimate the allowable load capacity of a single pile and pile groups?
6. How do I estimate the settlement of a single pile and pile groups?
7. Is the analysis of the load capacity of a pile exact or is it an approximation?

13.3 TYPES OF PILES AND INSTALLATION

Piles are made from concrete, steel, timber (Figure 13.2), plastic, or composites. The selection of the type of pile required for a project depends on what type is readily available, the magnitude of the loading, the soil type, and the environment in which the pile will be installed, for example, a corrosive environment or a marine environment.

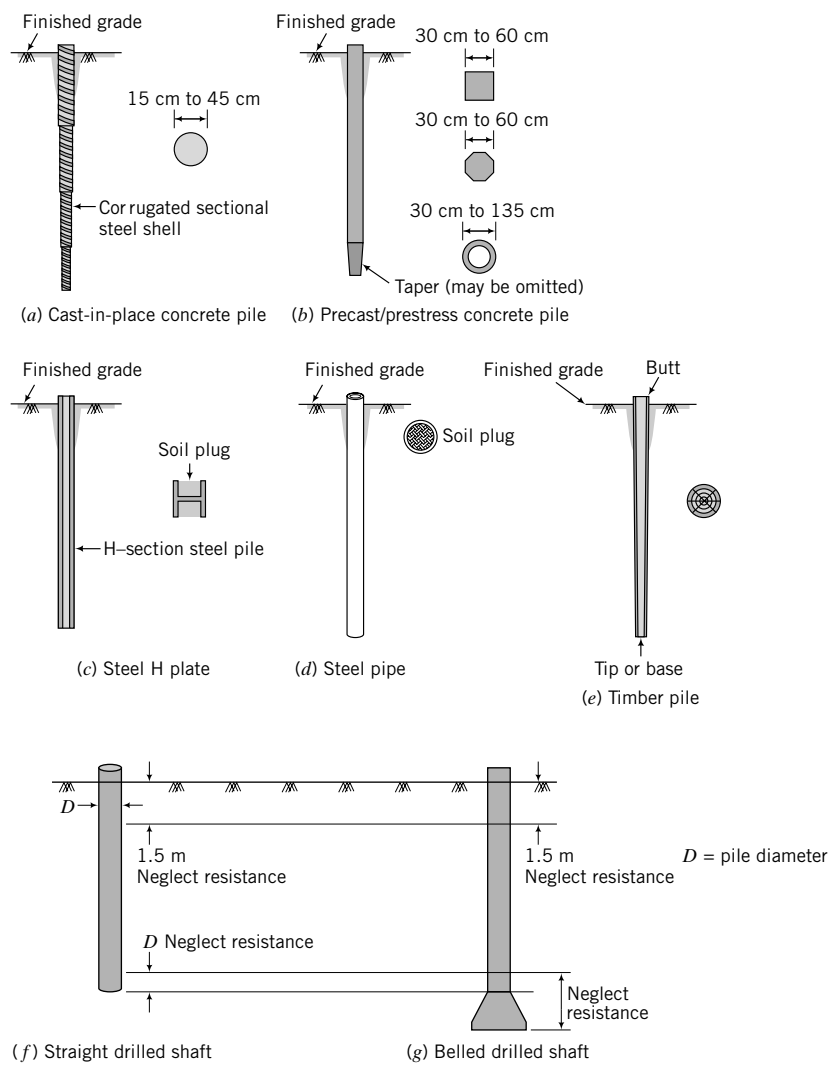


FIGURE 13.2 Pile types.

13.3.1 Concrete Piles

There are several types of concrete piles that are commonly used. These include cast-in-place concrete piles, precast concrete piles, drilled shafts, and barrette piles. Cast-in-place concrete piles are formed by driving a cylindrical steel shell into the ground to the desired depth and then filling the cavity of the shell with fluid concrete. They are called displacement piles. The steel shell is for construction convenience and does not contribute to the load transfer capacity of the pile. Its purpose is to open a hole in the ground and keep it open to facilitate the construction of the concrete pile. Plain concrete is used when the structural load is only compressive. If moments and lateral loads are to be transferred, then a steel reinforcement cage is used in the upper part of the pile. Vigilant quality control and good construction practice are necessary to ensure the integrity of cast-in-place piles.

Precast concrete piles usually have square or circular or octagonal cross sections and are fabricated in a construction yard or a factory from reinforced or prestressed concrete. They are preferred when the pile length is known in advance. The disadvantages of precast piles are problems in transporting long piles, cutting, and lengthening. A very popular type of precast concrete pile is the Raymond cylindrical prestressed pile. This pile comes in sections, and lengths up to 70 m can be obtained by stacking the sections. Typical design loads are greater than 2 MN.

Micropiles (also called minipiles, pin piles, needle piles, or root piles) are small-diameter (50 mm to 340 mm) pipe piles (pushed or driven) or grouted (jet or post or pressure) piles. They are particularly useful for (1) sites with low headroom, (2) congested areas, (3) sites with restricted access, and (4) foundation repair or strengthening.

13.3.2 Steel Piles

Steel piles come in various shapes and sizes and include cylindrical, tapered, and H-piles. Steel H-piles are rolled steel sections. They are nondisplacement piles. Steel pipe piles are seamless pipes that can be welded to yield lengths up to 70 m. They are usually driven with open ends into the soil. A conical tip is used where the piles have to penetrate boulders and rocks. To increase the load capacity of steel pipe piles, the soil plug (Figure 13.2c) is excavated and replaced by concrete. These piles are called concrete-filled steel piles. The soil plug may adhere to the pile surface and moves down with it during driving. This is called plugging.

13.3.3 Timber Piles

Timber piles have been used since ancient times. The lengths of timber piles depend on the types of trees used to harvest the piles, but common lengths are about 12 m. Longer lengths can be obtained by splicing several piles. Timber piles are susceptible to termites, marine organisms, and rot within zones exposed to seasonal changes. Timber piles are displacement piles.

13.3.4 Plastic Piles

Plastic piles comprise a variety of composite materials that include polymer composites, PVC, and recycled materials. These piles are used in special applications such as in marine environments and within soil zones exposed to seasonal changes.

13.3.5 Composites

Concrete, steel, and timber can be combined to form a composite pile. For example, the portion of a timber pile above groundwater level that is likely to suffer from decay due to termites or rot may be replaced by concrete. Similarly, the portion of a steel pile within a corrosive environment can be covered with concrete or other protective materials.

A comparative summary of the different pile types is given in Table 13.1.

TABLE 13.1 Comparison of Different Piles

Pile type	Section* m (in)	Common lengths m (ft)	Average loads kN (kips)	Allowable stress MPa (ksi)	Allowable driving stress – MPa (ksi)	Advantages	Disadvantages
Cast-in-place concrete	0.15 to 1.5** (6 to 60**)	≤35 (115)	600 (135)	4.5 to 8.5 (0.65 to 1.2)	0: 85 f'_c	Can sustain hard driving; resistant to marine organisms; easily inspected; length can be changed easily.	Concrete can arch during placement; can be damaged if adjacent piles are driven before concrete sets.
Precast concrete rebar	0.15 to 0.3 (6 to 12)	≤35 (115)	750 (170)	4.5 to 7 (0.65 to 1)	0.85 f'_c	Economical for specified length; higher capacity than timber.	Cutting and lengthening of piles are expensive; handling is a problem. Shipping long piles is expensive, may crack during driving.
Precast concrete prestressed	0.15 to 0.6 (6 to 24)	≤35 (115)	1000 (225)	$\frac{f'_c}{3} - 0.27 f'_{pe}$ $(f'_{pe})_{min} = 5 \text{ MPa (0.7)}$ $(f'_{pe})_{mix} = 34.5 \text{ MPa (5)}$	0.85 $f'_c - f'_{pe}$	Economical for specified length. Less permeable than reinforced concrete. Very good for marine environment.	Cutting and lengthening cannot be performed. Handling is a problem. Shipping long piles is expensive. Compressive strength decreases with increase in prestressing force. Cost (expensive).
Tapered cylinder	variable	<60 (200)	2,000 (450)	40 to 70 (5.8 to 10)		Can ship in sections; high capacity; long length.	
Steel pipe	0.2 to 1 (8 to 36)	<35 (115)	900 (200)	59 to 83 (8.5 to 12)	186 (27) – ASTM A252, $f_y = 207$ (30) GR 1217 (31.5) ASTM A572, $f_y = 241$ (35) GR 2 310 (40.5) ASTM A572, $f_y = 345$ (50) GR 3	High axial and lateral capacity; can take hard driving, easy inspection and handling; length can be changed easily;	Needs treatment for corrosive environment.
Concrete- filled pipe	0.2 to 1 (8 to 36)	<35 (115)	900 (200)	Concrete: 4.5 to 8.5 (0.65 to 1.2) Steel: 62 to 83 (9 to 12)	186 (27) – ASTM A252, $f_y = 207$ (30) GR 1 217 (31.5) ASTM A572, $f_y =$ 241 (35) GR 2 310 (40.5) ASTM A572, $f_y =$ 345 (50) GR 3	resistant to deterioration. (Similar to steel pipe pile)	(Similar to steel pipe pile)
Steel H-pile	Webs: 1 to 3 (36 to 117) Flange: 0.2 to 0.35 (8 to 14)	<60 (200)	900 (200)	59 to 83 (8.5 to 12)	223 (32.4) – ASTM A36, $f_y = 248$ (36) 310 (40.5) ASTM A572, $f_y = 345$ (50)	Nondisplacement pile, can take hard driving; easy handling; high axial and lateral capacity; length can be changed easily.	(Similar to steel pipe pile)
Timber	0.125 to 0.45 (5 to 18)	12 to 35 (40 to 115)	250 (55)	5.5 to 8.5 (0.8 to 1.2)	5.5 to 8.3 (0.8 to 1.2)	Low cost, easy to handle, renewable resource.	Low capacity. Can deteriorate above groundwater if not protected. Cannot take hard driving.
Micropiles	0.05 to 0.3 (2 to 12)	<25 (80)	1000 (225)	Concrete: 4.5 to 8.5 (0.65 to 1.2) Steel: 59 to 83 (8.5 to 12)	(Similar to concrete and steel pipe pile)	High capacity; low headroom; restricted access; low noise and vibration	

*Diameter or width as appropriate. **The larger sizes (>0.6 m) refer to drilled shafts.

 f'_c = ultimate strength of concrete = 21 MPa, GR = grade, f'_{pe} is prestress.

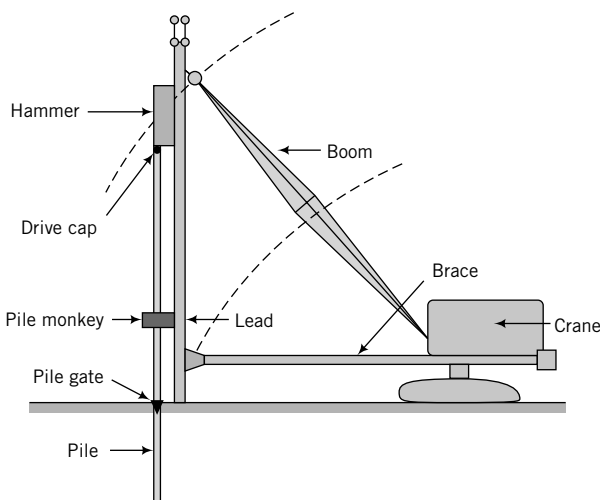


FIGURE 13.3 Key components of pile-driving operation.

13.3.6 Pile Installation

Piles can either be driven into the ground (driven piles) or be installed in a predrilled hole (bored piles or drilled shafts). A variety of driving equipment is used in pile installations. The key components are the leads and the hammer. The leads are used to align the hammer to strike the pile squarely (Figure 13.3). Hammers can be simple drop hammers of weights between 2.5 and 15 kN or modern steam/pneumatic hammers. Two popular types of steam/pneumatic hammers are shown in Figure 13.4. The single-acting hammer utilizes steam or air to lift the ram and its accessories (cushion, drive caps, etc.). The double-acting hammer is used to increase the number of blows/minute and utilizes steam or air to lift the ram and force it down.

The method of installation needs careful consideration because it irreversibly changes the soil stress and strain states and can create intolerable noise and vibration during construction.

The maximum installation stress for piles driven from the top must not exceed the compressive or tensile strength of the pile material (see Table 13.1).

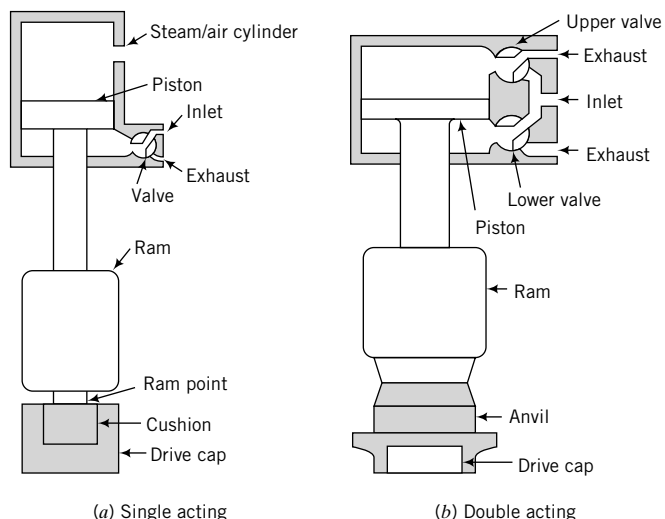


FIGURE 13.4 Two types of pile-driving hammer.

(a) Single acting

(b) Double acting

THE ESSENTIAL POINTS ARE:

1. The selection of a pile type depends on the structural loads, availability, and the environment at the site.
2. Piles can be installed using simple drop hammers but, most often, they are installed using power hammers (e.g., steam or pneumatic).

What's next . . . We have described the various types of piles that are in common use. In the next section, we will develop a basic conceptual understanding of the effects of pile installation and the imposition of structural loads.

13.4 BASIC CONCEPT

Utilizing our knowledge of soil mechanics from previous chapters, especially Chapters 9 through 11, we will construct a simplified framework to understand the effects on the soil from pile installation and structural loads. This would help us to interpret pile test results and understand the limitations of pile load capacity calculations presented later in this chapter. The resistance to vertical loads on a pile is provided by friction along the surfaces of the pile (called skin friction) and by resistance at the base, called end bearing or toe or base resistance (Figure 13.5a).

Pile driving imposes impact load. When the hammer strikes the pile, it sets up a stress wave that propagates through the pile into the surrounding soil. Pushing the pile imposes a continuous (static) load. The installation load is applied quickly so that undrained condition (zero volume change) can be assumed to apply.

The soil fails by imposition of shear stress (interface shear), τ , at the interface of the pile and soil, and radial compression to the soil mass adjacent to the pile (Figure 13.5a, b). The stresses on a soil element, A, at a radius, r , near the shaft are shown in Figure 13.5b. If the soil mass over the length of the pile is layered, then there will be different stresses for each of the layers.

The stresses on the soil element are not simple. Even if we were to solve for these stresses using mechanics, replicating them and the mode of deformation would be difficult for practical applications. The mode of deformation near the shaft is similar to simple shear. An element of soil near the interface is dragged down, as shown for element A in Figure 13.5a.

For displacement or closed-ended pipe piles, a volume of soil that equals the volume of the pile must be displaced during installation. This volume of soil mass is disturbed or remolded. Let us assume a pile of length L and radius r_o . Further, let us assume that a right cylinder of soil is compressed over an annular area of thickness $r - r_o$, where r is the external radius of the disturbed soil (Figure 13.5c). The resulting soil heave is assumed to be ΔL . The minimum disturbed region or disturbed volume of soil around the shaft is as follows.

The volume of the pile is

$$V_p = \pi r_o^2 L \quad (13.1)$$

The disturbed volume of soil must equal the volume of the pile. That is,

$$\pi(r^2 - r_o^2)(L + \Delta L) = \pi r_o^2 L \quad (13.2)$$

Solving for r , we get

$$r = r_o \sqrt{\frac{2L + \Delta L}{L + \Delta L}} \quad (13.3)$$

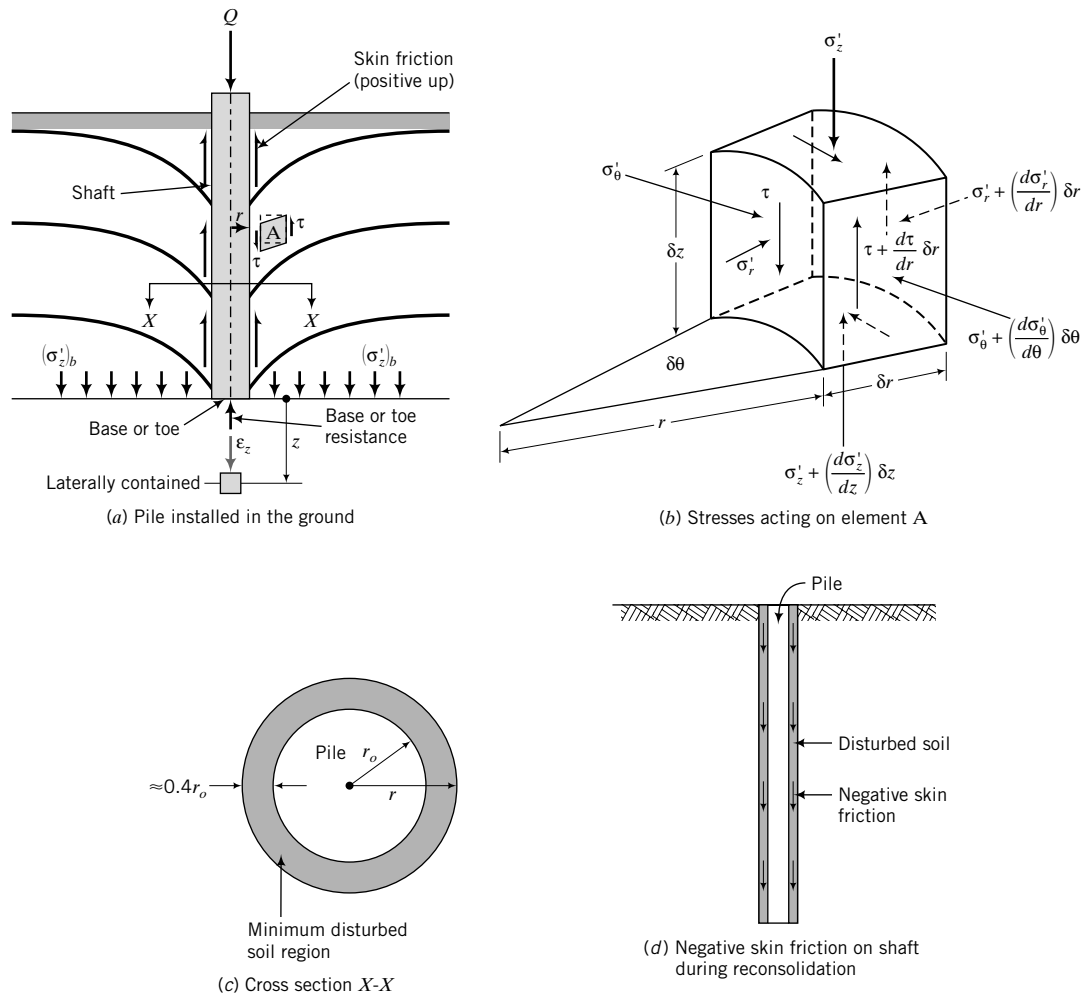


FIGURE 13.5 Stresses and strains near the shaft and base of a pile.

Generally, ΔL is small in comparison to L , and thus

$$r \approx r_o \sqrt{2} \approx 1.4r_o \quad (13.4)$$

Therefore, a cylinder of soil of annular thickness greater than 40% of the pile radius is disturbed. This disturbed zone is a softening zone because the soil stiffness is generally lower than its original (undisturbed) stiffness. The soil mass within the disturbed zone is likely to be at critical state. Interfacial shear stress will further increase the thickness of the disturbed zone.

After pile installation, the cylinder of disturbed soil will reconsolidate because the excess pore-water pressure developed during installation will dissipate. During reconsolidation, negative skin friction (because its direction is the same as the proposed vertical compressive load rather than in opposition to it) would be imposed on the pile shaft, reducing the pile load capacity (Figure 13.5d). However, the soil strength increases because as the excess porewater pressure dissipates, the effective stress increases. Because of the low hydraulic conductivities of fine-grained soils compared to coarse-grained soils, the reconsolidation may occur over a very long time period.

During installation, an element of soil just below the pile base will be under a compressive axial load and will tend to compress as well as shear. Shearing occurs because of the difference between the vertical and lateral stresses. If the soil at the base is dense or is overconsolidated, as is normally the case, we would expect it to dilate at some stage. However, unlike an element of soil around the pile shaft, the soil element just below the base is severely constrained. It is confined laterally, and any heaving or dilatant response is restrained by the pile weight and the friction force at the pile–soil interface. Also, the full overburden pressure [vertical effective stress, $(\sigma'_z)_b$] is acting at the base level to further restrict movement (Figure 13.5a).

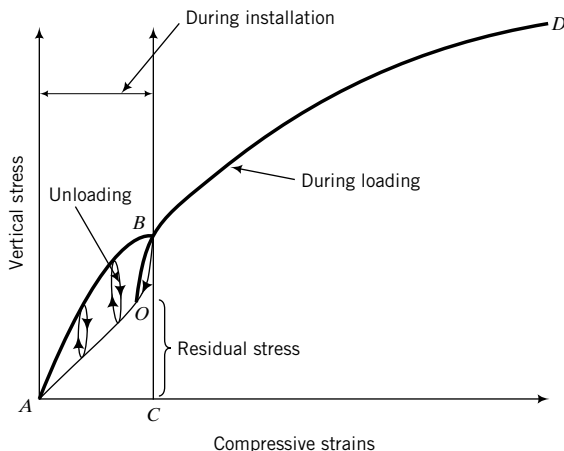
The amount of compression imposed on the element just below the soil base depends on the soil's compressibility, hydraulic conductivity, and crushability, as well as the magnitude and type of load applied. For soils with low hydraulic conductivities such as fine-grained soils, the excess porewater pressures from the tendency of these soils to compress would not dissipate quickly. Because both water and soil solids are practically incompressible, the soil mass just under the base would be practically incompressible. This would provide extraordinary but temporary resistance to pile driving or pushing and can lead to misinterpretation of the long-term pile load capacity. Any vertical compression that takes place at the base during installation is balanced by lateral extension (soil movement is outward), so the soil volume remains constant. The lateral extension of the soil can lead to soil failure by tension at the base.

When installation ceases, the excess porewater pressure dissipates, leading to settlement. For a dense or overconsolidated soil, negative excess porewater pressure develops within the soil below the base, and the effective stress in the soil increases during driving. The net effect is that the soil strength increases temporarily.

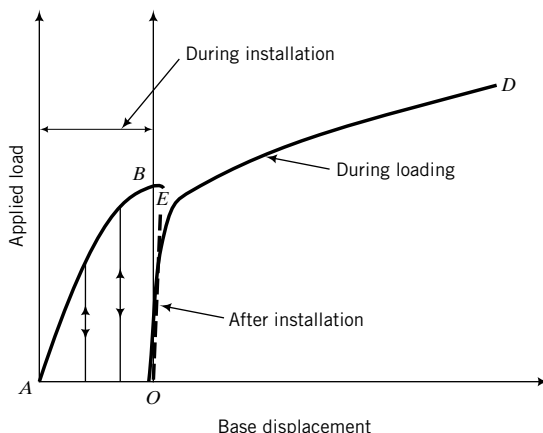
We will now examine the stress–strain response of the soil element just below the base, as illustrated in Figure 13.6. We consider two conceptual illustrations, one that shows the vertical stress–compressive strain relationship (Figure 13.6a) and the other that shows the applied load–pile base displacement (Figure 13.6b), referred to in solid mechanics as a compliance curve. The latter is the de facto standard plot to interpret pile load capacity. Pile driving involves impact loading–unloading–impact reloading. Pushing a pile is a continuous loading process. During impact loading or pushing, the soil element would compress and would follow a vertical stress–compressive strain path shown by *AB* in Figure 13.6a, b. If the soil were a rigid–perfectly plastic material (recall this is the basic assumption of Coulomb, Mohr–Coulomb, and Tresca failure criteria) and no overburden pressure existed at the sides of the pile above the base (free surface), soil would escape around the edges and “pileup” because of plastic flow upon impact. This is called uncontained mode of deformation. The overburden pressure restricts this “pileup” of soil, forcing it to flow radially, but this movement is also constrained by the expanse of the soil in that direction. This is called contained mode of deformation. If the soil were an elastoplastic material, it would tend to compress radially but in a contained mode of deformation.

During unloading in preparation for impact reloading, the soil element would tend to rebound (elastic rebound, as discussed in Chapter 9). This rebound is restrained by the weight of the pile (buoyant weight if the pile is under water) and by negative skin friction at the pile–soil interface mobilized along the shaft (Figure 13.5d). The consequence is that although the installation load is removed (*O* in Figure 13.6b), residual stress (also called locked-in stress) would exist in the soil element (*CO* in Figure 13.6a). The rebound could be fully restrained if the soil swelling force is lower than the sum of the pile weight and the negative skin friction, so that the residual stress is *CB*. The curve *AO* in Figure 13.6a illustrates the buildup of the residual stresses. Over time, the soil may relax and redistribute the residual stresses.

The stress state of the soil is now completely different from its original state. It has changed in ways that are practically indeterminate. The installation confers on the soil an apparent preconsolidation stress. How the soil would behave when the structural loads are applied depends on this preconsolidated stress. Generally, driven piles or displacement piles tend to densify loose, coarse-grained soils near the pile, while they tend to loosen dense, coarse-grained soils. We can expect that the overconsolidation ratio for soft, fine-grained soils or the density for initially loose, coarse-grained soils would be greater than their original overconsolidation ratio or density, but we do not know by how much.



(a) Idealized vertical stress-compressive strain response of soil element under pile base.



(b) Idealized load-base displacement response of soil element under pile.

FIGURE 13.6 Idealized stress-strain and idealized load-base displacement responses for an element of soil under the base.

We have assumed a flat, solid pile base. In reality, the bases of some piles are pointed (conical or wedge-shaped) to facilitate soil penetration. If soil is assumed to be a rigid plastic material, then two plausible mechanisms for soil failure at the base, $ABCDEFGH$ (mechanism I) and $BCDEF$ (mechanism II), are shown in Figure 13.7. A third mechanism is shown in Figure 13.8. Only in rare circumstances, for example, in short piles (length-to-diameter ratio less than 3), would these failure mechanisms possibly develop. The constraints on soil movements at and near the base and the disturbed zone around the shaft discussed earlier would normally prevent these failure mechanisms from developing. In addition, soil is not a rigid-plastic material. While one of these or a similar failure mechanism may be seen in numerical models, the result depends on the soil model used and the skill of the analyst. For example, soil failure based on a Mohr-Coulomb failure criterion is predicated on the soil behaving as a rigid-plastic material or, as used in computer programs, elastic-rigid-plastic material.

When structural loads are applied to the pile after installation, the base soil's initial state would be not at C but at O or B (Figure 13.6a). The initial vertical stress-compressive strain response would be elastic and then elastoplastic, OB (Figure 13.6a). The curve BO is analogous to the unloading line in a one-dimensional consolidation test and OBD , the reloading line. By this analogy, we would expect that ABD would be the complete loading line (normal consolidation line). However, the portion AB is

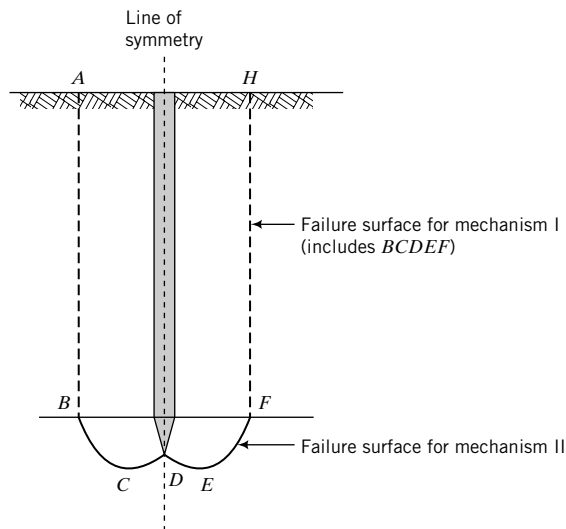


FIGURE 13.7 Two plausible failure mechanisms.

due to impact loading during installation and may not link up smoothly with BD . Because of the large overburden pressure at the pile base, the soil element there would not likely show a peak stress-strain response or to strain-soften when structural loads are applied to the pile. Rather, it would strain-harden (see Chapter 10) until critical state is achieved. The shear or compressive strain necessary to achieve critical state is generally very large ($>10\%$). The corresponding pile displacement (settlement) would be intolerable. Also, fine-grained soils with high overconsolidation ratios or very dense, coarse-grained soils may develop tensile cracking (see Chapter 11).

If we were to plot pile load-displacement data, the failure load might not be discernible unless the pile load were large enough to mobilize the large shear or compressive strains to achieve critical state. This is important in interpreting test pile data, particularly in determining the ultimate end (base) bearing capacity.

Field pile load tests have revealed that to mobilize the full skin friction in a driven pile, a vertical displacement of 2.5 to 10 mm is required. The actual vertical displacement depends on the strength

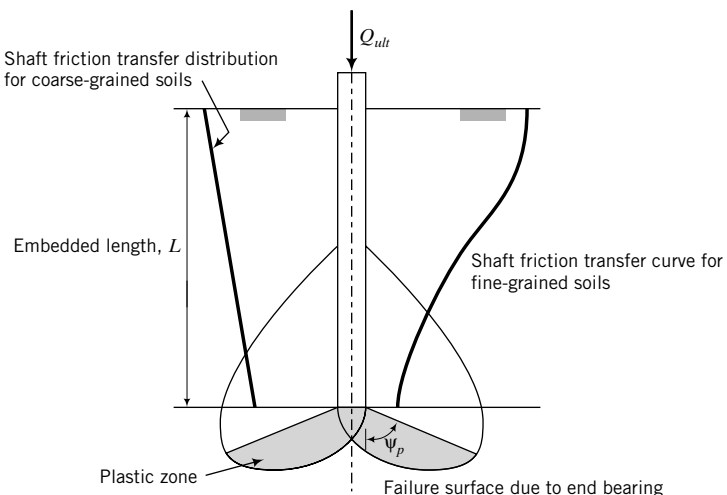


FIGURE 13.8 Load transfer characteristics.

and stiffness of the soil and is independent of the pile length and pile diameter. The full end bearing resistance is mobilized in driven piles when the vertical displacement is about 8–10% of the pile tip diameter. For bored piles or drilled shafts, a vertical displacement of about 30% of the pile tip diameter is required. In many cases, the end bearing resistance is not discernible; the end bearing resistance keeps increasing with increasing settlement. Because the full skin friction and full end bearing are not mobilized at the same displacement, we cannot simply add the ultimate skin friction to the ultimate end bearing resistance unless they are mobilized at the same displacement.

The manner in which skin friction is transferred to the adjacent soil depends on the soil type. In fine-grained soils, the load transfer is nonlinear and decreases with depth, as illustrated in Figure 13.8. As a result, elastic compression of the pile is not uniform; more compression occurs on the top part than on the bottom part of the pile. For coarse-grained soils, the load transfer is approximately linear with depth (higher loads at the top and lower loads at the bottom).

In current practice, the full end bearing resistance is assumed to be mobilized when a failure surface similar to shallow foundations is formed (Figure 13.8). The end bearing resistance can then be calculated by analogy with shallow foundations. The important bearing capacity factor is N_q . Recall from our earlier discussions in this section that such a failure mechanism at the base of the pile may not develop within normal range of loading, and thus the calculation of the end bearing resistance would be unreliable. However, we will use this analogy, as this is common practice. You must be cognizant of the limitation of this analogy.

THE ESSENTIAL POINTS ARE:

- 1. Pile installation has significant effects on pile load capacity.**
- 2. The stresses imposed on the soil mass during pile installation and the application of structural loads are complex.**
- 3. Around the shaft, the soil is compressed by the displacement of the soil to accommodate the pile and sheared by interface friction at the pile–soil interface. A cylindrical volume of soil around the pile is disturbed or remolded, and may reach critical state. The minimum thickness of the disturbed soil is $\approx 40\%$ of the pile radius. In normally and lightly overconsolidated fine-grained soils, and loose coarse-grained soils, positive excess porewater pressures would develop, while in highly overconsolidated fine-grained soils, and dense coarse-grained soils, negative excess porewater pressure would develop, at least in the disturbed soil mass. These excess porewater pressures would dissipate, leading to soil settlement during the design life of the foundation.**
- 4. Below the base of the pile, the soil is mainly subjected to compressive loads, but soil movement is severely constrained laterally and vertically. Highly overconsolidated fine-grained soils, and dense coarse-grained soils, can develop negative excess porewater pressures and cause the soil strength to increase temporarily. This could lead to the overestimation of the pile load capacity.**
- 5. Installation induces residual stresses in the soil mass adjacent to the pile, but particularly under the base because of the constraints on soil movement.**
- 6. The stress state of the soil is very different from the original soil state and is practically indeterminate.**
- 7. You need to consider pile installation effects in using strength and stiffness values for the soil in estimating pile load capacity.**

What's next . . . We now have a basic conceptual understanding of pile installation and loading. In the next section, methods of estimating the load capacity are presented. The load capacity of piles has been studied extensively, but no single satisfactory method of determining the load capacity has evolved. Pile load capacity is mostly based on empirical equations, experience, and judgment. Some of these are at odds with the conceptual understanding that we have developed.

13.5 LOAD CAPACITY OF SINGLE PILES

We know from Section 13.4 that accurate estimation of pile load capacity is a rather difficult task because it is difficult, if not impossible, to account for (a) the changes in stress and strain states from installation effects, (b) the variability of soil types, and (c) the differences in the quality of construction practice. Therefore, calculations of pile load capacity are approximations and rely heavily on empiricism or semiempiricism (part mechanics, part empirical).

The ultimate load capacity, Q_{ult} , of a pile is conventionally taken as consisting of two parts. One part is due to friction (Figure 13.9), called skin friction or shaft friction or side shear, Q_f , and the other is due to end bearing at the base or tip of the pile or pile toe, Q_b . If the skin friction is greater than about 80% of the end bearing load capacity, the pile is deemed a friction pile and, if the reverse, an end bearing pile. If the end bearing is neglected, the pile is called a floating pile.

From statics,

$$Q_{ult} = Q_f + Q_b - W_p \quad (13.5)$$

where W_p is the weight of the pile. In many cases, the weight of the pile is included in the dead load or neglected for piles of small cross-sectional areas ($<0.07 \text{ m}^2$). Equation (13.5), as written, is independent of settlement. Recall from Section 13.4 that Q_f and Q_b are generally mobilized at different values of settlement. Therefore, it is desirable to add mobilized skin friction and mobilized end bearing at the same value of settlement. The conventional methods that will be presented in the next section treat the ultimate pile load capacity and settlement separately. Thus, except for pile load tests (see next section) and numerical methods, it is not possible to add mobilized skin friction and mobilized end bearing at the same value of settlement.

The conventional allowable load capacity for ASD is expressed as

$$Q_a = \frac{Q_{ult}}{\text{FS}} \quad (13.6)$$

where FS is a gross factor of safety usually greater than 2. In practice, the application of a factor of safety greater than 2 is thought of as sufficient to limit settlement to about 25 mm. Nevertheless, you should

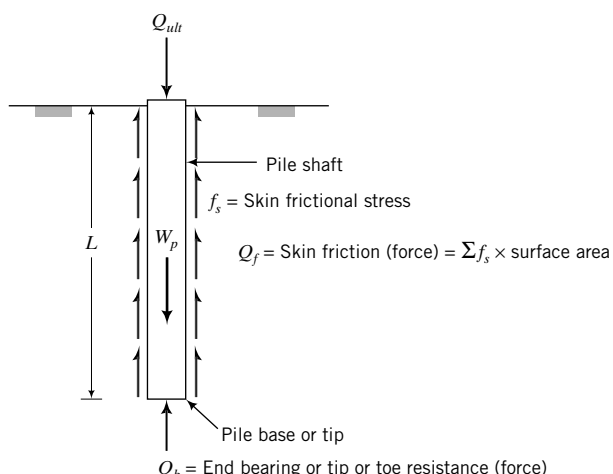


FIGURE 13.9 Pile shaft and end bearing resistance.

estimate the pile settlement as part of good design practice and use it to control the allowable pile load capacity, if necessary. For LRFD,

$$\sum \eta_i \rho_i P_i \leq (\varphi_f Q_f + \varphi_b Q_b) \quad (13.7)$$

where ρ is load factor; P is load; φ_f and φ_b are the performance factors for skin friction and end bearing, respectively; η is a ductility, redundancy, and operational performance factor; and i is the load type.

THE ESSENTIAL POINTS ARE:

1. The ultimate pile load capacity is estimated as the sum of the skin friction and end bearing resistance minus the weight of the pile.
2. The calculation of the ultimate pile load capacity does not take into account the different settlement required to mobilize the ultimate skin friction and the ultimate end bearing resistance.

What's next . . . A variety of methods are available to determine Q_f and Q_b . We will deal with four methods:

- Pile load test
- Statics— α - and β -methods
- Pile-driving formulas
- Wave analysis

We begin with the pile load test.

13.6 PILE LOAD TEST (ASTM D 1143)

The purposes of a pile load test are:

- To determine the load capacity of a single pile or a pile group, especially when the design requires methods that are outside of accepted practice.
- To determine the settlement of a single pile at working loads.
- To verify estimated load capacity.
- To obtain information on load transfer in skin friction and in end bearing.
- To satisfy regulatory agencies.

The ASTM D 1143 provides the standard methods for conducting pile load tests. Only a brief description is presented in this section. In a typical pile load test (conventional load test), the test pile is driven to the desired depth, loads are applied incrementally, and the settlement of the pile is recorded. The axial loads can be applied by stacking sandbags on a loading frame attached to the pile or, more popularly, by jacking against a reaction beam and reaction piles (Figure 13.10). If load transfer information is required, the pile must be instrumented with sensors or strain gages to deduce the strains and stresses along the pile length. The conventional pile load test gives the combined skin friction and end bearing resistance (Figure 13.11a). They cannot be separated easily.

The interpretation of the load capacity depends on the method of loading. Two loading methods are popular. In one method, called the constant rate of penetration (CRP) test, the load is applied at a constant rate of penetration of 1.25 mm/min in fine-grained soils and 0.75 mm/min to 2.5 mm/min in coarse-grained soils. In the other method, called the quick maintained load (QML), increments of load, about 10% to 15% of the expected design load, are applied at intervals of about 2.5 min. At the end of

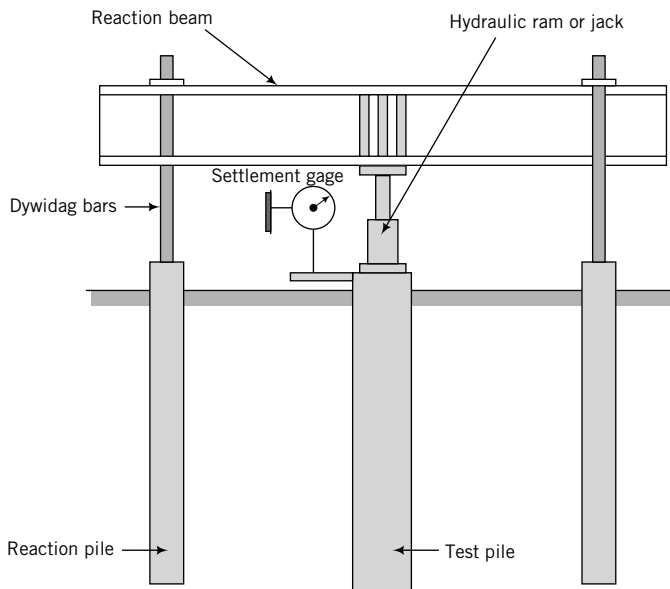
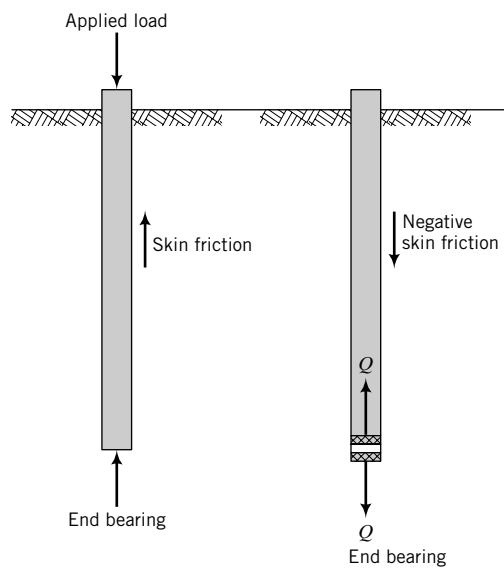


FIGURE 13.10 A pile load test setup.



(a) Conventional load test (b) Load test using O-cell

FIGURE 13.11 Comparison of conventional load test with O-cell load test.

each load increment, the load and settlement are recorded. Usually, the maximum load applied is about twice the expected design load for single piles and about one and a half times the expected design load for group piles. Recall from Section 13.4 that this maximum load may not be enough to bring the soil to critical state. Schematic variations of pile load test plots are shown in Figure 13.12.

The ultimate load is not always well defined. Load-settlement curve (a) in Figure 13.12 shows a well-defined ultimate load, while curve (b) does not. To obtain the ultimate load from curve (b),

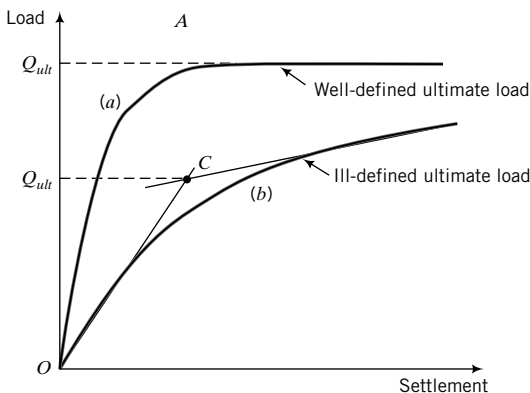


FIGURE 13.12
Load-settlement curves.

various empirical procedures have been suggested. One simple method is to find the intersection of the tangents of the two parts of the curve. The value at the ordinate of the intersection (C in Figure 13.12) is Q_{ult} .

The allowable load capacity is found by dividing the ultimate load by a factor of safety, usually 2. An alternative criterion is to determine the allowable pile load capacity for a desired serviceability limit state, for example, a settlement of 1% of the pile diameter. The settlement at the allowable (working) load capacity is readily determined from the load-settlement plot (Figure 13.12). Relating settlement to the pile diameter is a common practice, but settlement is unrelated to pile geometry. For example, in Section 13.4, we showed that the soil around the pile is displaced in a manner analogous to simple shear. The simple shear strain (see deformation of element A in Figure 13.5a) is not a function of the pile geometry.

You need to be extra-careful in applying the intersection of the tangents method and other similar methods used in practice, especially in interpreting the end bearing capacity, as discussed in Section 13.4 and the following additional discussion.

To separate the skin friction and end bearing resistance, an O-cell called Osterberg cell, after its originator (Osterberg, 1984), is used. This cell is essentially a hydraulic jack installed within the pile unit (Figure 13.13). When the jack is expanded, its upward movement is resisted by the skin friction and its downward movement is resisted by the base resistance. Therefore, the skin friction and the end bearing resistance are measured separately. If the ultimate capacity of either skin friction or end bearing is reached at a value Q using an O-cell, then the equivalent conventional load that has to be applied is $2Q$. The O-cell is not suitable for H-piles, sheet piles, and tapered wooden piles.

Let us consider a load test with an O-cell and the potential load-displacement response. When the O-cell is expanded, it pushes the pile up and negative skin friction is mobilized (Figure 13.11b). The upward movement of the pile is only resisted by skin friction; otherwise, it is free to move vertically. At the same time, the O-cell pushes down on the soil below the base with same force as it pushes the pile up. Recall from Section 13.4 that the soil below the base is severely constrained. It cannot be easily compressed compared with the upward movement of the pile.

The relative displacement to mobilize skin friction and end bearing depends on the shear stiffness and shear strength of the soil adjacent to the pile shaft and the compressive stiffness and strength (mainly compressive) of and constraints on the soil below the base. Because the upward movement of the pile is less constrained than the downward movement of the base soil, the skin friction capacity for a given O-cell load would be mobilized in advance of the end bearing capacity. A possible exception is when the base soil is very weak compared with the soil above the base. As discussed in Section 13.4, if the soil at the base is overconsolidated (fine-grained soil) or is dense (coarse-grained soil), negative excess porewater pressure can develop during loading, creating a portion of the end bearing resistance that would not be there when the excess porewater pressures drain. These (mobilization of ultimate skin friction capacity before ultimate

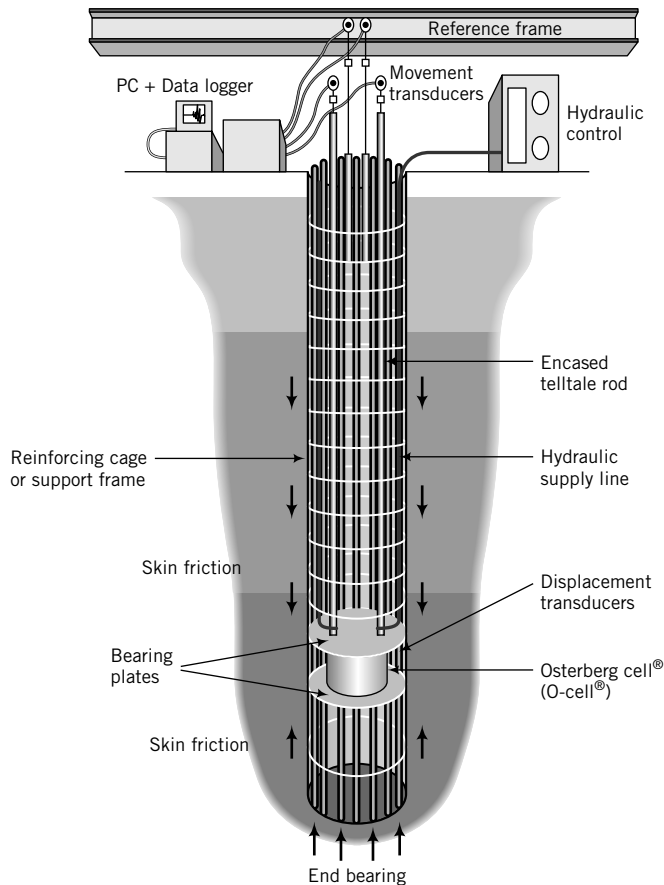


FIGURE 13.13 An O-cell and other instrumentation for a pile test. (Courtesy of Loadtest, Inc.)

end bearing capacity and additional resistance from negative excess porewater pressures) are important considerations in interpreting pile load test results using O-cell and also conventional load tests. The weight of the pile (buoyant weight if the pile is under water) must be subtracted from the maximum upward O-cell load to obtain the actual skin friction capacity. The upward movement also includes the compression of the pile. So the actual relative movement between the shaft and the soil to mobilize the ultimate skin friction is generally small (<10 mm).

In the case of bored piles or drilled shafts, it is practically impossible to remove all the loose material (debris) from the bottom of the predrilled hole. The consequence is that the initial load–displacement response would represent the load–displacement characteristics of this loose material rather than the intact soil at the base. Since each drilled shaft may have different amounts and types of loose material at the base, the load–displacement response of this loose material would be different. A schematic of a drilled shaft load test result using an O-cell is shown in Figure (13.14).

It is best to use the serviceability limit state to decide on a working load capacity, especially when the ultimate end bearing load is ill defined. To combine the skin friction and end bearing, select a given displacement and add the skin friction to the end bearing at that displacement and then subtract the pile weight. This is sometimes called the service load capacity. You need to be careful in doing this for drilled shafts because of the compressibility of the loose material at the base. If the end bearing capacity is less than about 15% of the total load capacity of the drilled shaft, you should consider neglecting the end bearing capacity.

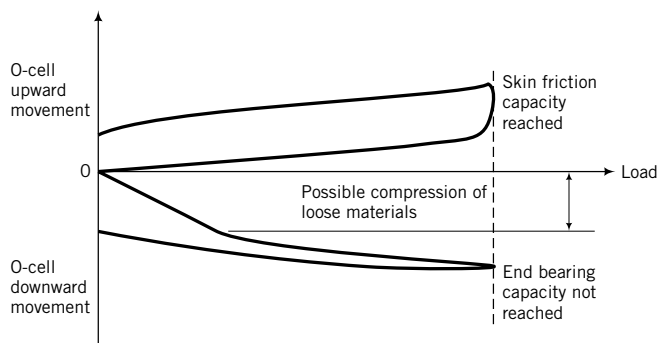


FIGURE 13.14 Schematic of an O-cell pile load test on a drilled shaft.

THE ESSENTIAL POINTS ARE:

1. A pile load test provides the load capacity and settlement of a pile at a particular location in a job site.
2. Various criteria and techniques are used to determine the allowable load capacity from pile load tests.
3. The skin friction and the end bearing capacity are measured separately using an O-cell.
4. Experience coupled with soil mechanics principles are necessary to interpret the pile load capacity.

EXAMPLE 13.1 Interpreting Pile Load Test Data (1)

The results of a load test on a 0.45-m-diameter pile are shown in the table below. The displacements were measured at the pile head. Determine (a) the ultimate pile load capacity, (b) the allowable load for a factor of safety of 2, and (c) the allowable (service) load capacity at 1% pile displacement.

Displacement (mm)	0.0	1.3	2.5	5.1	7.6	10.2	12.7	15.2	17.8	20.3	22.9	25.4	27.9	30.5	33.0
Load (kN)	0	200	350	670	870	1070	1250	1400	1500	1600	1700	1750	1780	1810	1830

Displacement (mm)	35.6	38.1	40.6	43.2	45.7	47.0
Load (kN)	1860	1870	1890	1890	1900	1905

Strategy Plot a graph of displacement versus load and then follow the procedure in Section 13.6.

Solution 13.1

Step 1: Plot a pile head displacement–load graph.

See Figure E13.1.

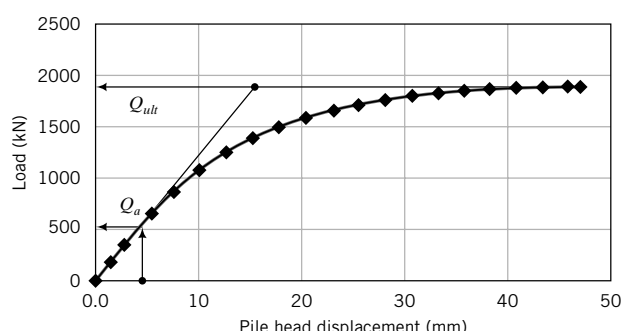


FIGURE E13.1

Step 2: Determine the ultimate pile load capacity.

The failure load appears to be well defined. We will examine the differences between the ultimate load from a horizontal line through the relatively flat part of the load–displacement curve and the ultimate load from the intersection of the tangents at the beginning and the end of the curve. Both give the same ultimate load value of

$$Q_{ult} = 1780 \text{ kN}$$

Step 3: Determine the allowable pile load capacity.

$$\text{FS} = 2$$

$$Q_a = \frac{Q_{ult}}{\text{FS}} = \frac{1780}{2} = 890 \text{ kN}$$

Step 4: Determine the pile load capacity at 1% pile diameter.

$$\text{Pile diameter} = 450 \text{ mm}$$

$$\text{Desired pile head displacement} = 450 \times 0.01 = 4.5 \text{ mm}$$

$$\text{From Figure E13.1: } Q_a = 510 \text{ kN}$$

EXAMPLE 13.2 Interpreting Pile Load Test Data (2)

The results of a load test on a 2-m-diameter pile are shown in Figure E13.2a. Determine (a) the ultimate pile load capacity and (b) the allowable (service) load capacity at a settlement of 1% pile displacement.

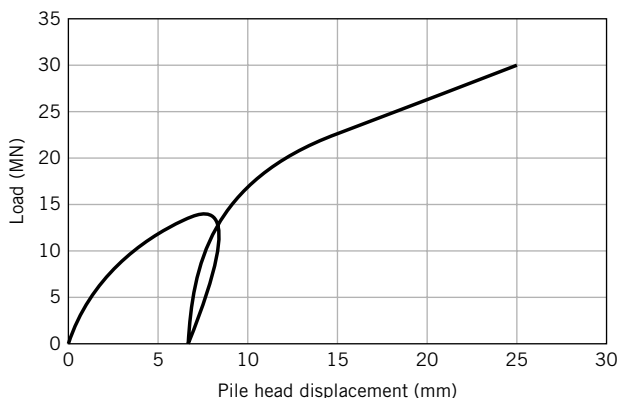
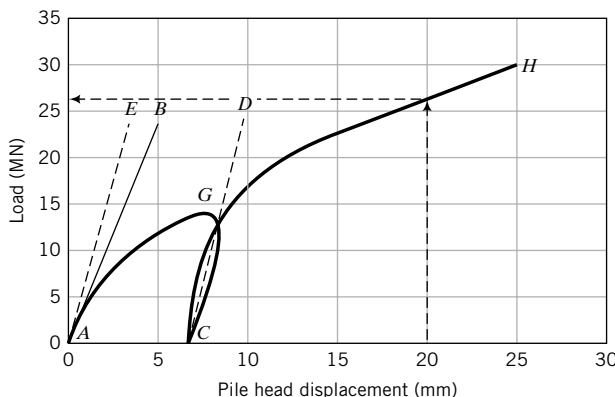


FIGURE E13.2a

Strategy Examine the plot and decide whether the ultimate load is well or ill defined. If it is ill defined, then you have to make a decision as to whether the intersection of tangent method or similar method is appropriate or not.

Solution 13.2**Step 1:** Decide whether the ultimate pile load capacity is well or ill defined.

Inspection of Figure E13.2a shows that the ultimate load is ill defined.

**FIGURE E13.2b**

Step 2: Determine whether the intersection of tangent method is appropriate or not.

The unloading-reloading line can give you a clue to interpret the load-displacement curve. Recall from the one-dimensional consolidation test that the average of the unloading-reloading line of vertical effective stress-void ratio gives C_r , which is related to the elastic response of the soil. We can use this knowledge to evaluate the load-displacement curve. The initial elastic response is shown by line AB (Figure E13.2b; for clarity, the unloading response is not shown). The elastic response from the unloading-reloading line is shown by CD . Normally, the slope of CD is slightly greater than that of AB . If we draw a line parallel to CD through A , line AE , we notice that this line is a bit steeper than AB . The difference in the slopes of AE and AB is very small (<10%) and can be neglected. This indicates that soil is behaving as expected and that the ultimate load has not been achieved at the maximum displacement of 25 mm. Also, the initial loading curve AG merges rather smoothly with the reloading curve CH . Therefore,

$$Q_{ult} > 30 \text{ MN}$$

The intersection of tangent method is not suitable for these test data. If you were to use it on the reloading curve, we would get $Q_{ult} \approx 17.5 \text{ MN}$. But this is not correct.

Step 4: Determine the pile load capacity at 1% pile diameter.

$$\text{Pile diameter} = 2 \text{ m} = 2000 \text{ mm}$$

$$\text{Tolerable pile head displacement} = 2000 \times 0.01 = 20 \text{ mm}$$

From Figure E13.2b: $Q_a = 26 \text{ MN}$

EXAMPLE 13.3 Interpreting O-cell Pile Load Test Data

A load test was conducted on a 1.5-m-diameter drilled shaft of length 14 m fitted with an O-cell (Figure E13.3a). The results are shown in Figure E13.3b. Determine (a) the ultimate and allowable pile load capacity without consideration of settlement for $FS = 2$, (b) the allowable load capacity for a settlement of 6 mm, and (c) the allowable load for a factor of safety of 2 and the settlement. The unit weight of concrete is 24 kN/m^3 .

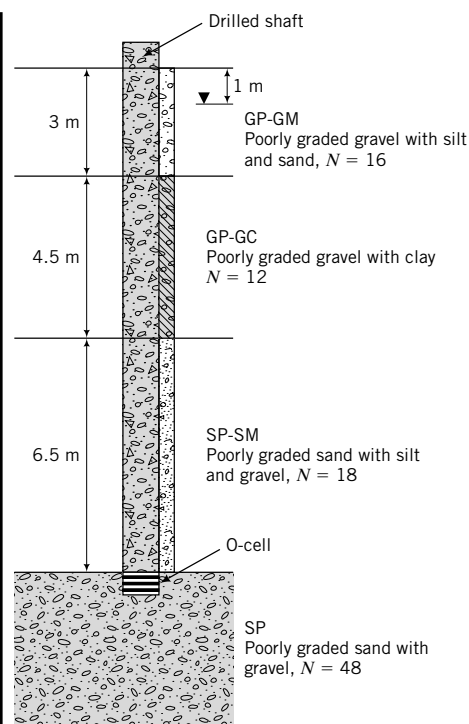


FIGURE E13.3a

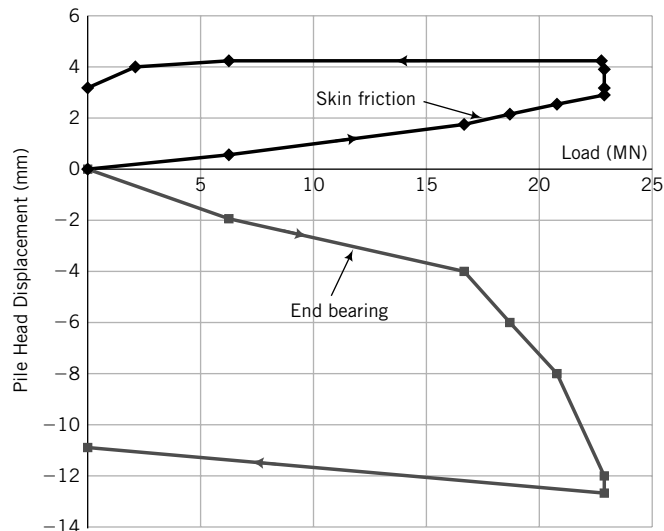


FIGURE E13.3b

Strategy Examine the plot and decide whether the ultimate pile load capacity is well or ill defined.

Solution 13.3

Step 1: Decide whether the ultimate pile load capacity is well or ill defined.

Inspection of Figure E13.3b shows that the skin friction is fully mobilized at about 4.5 mm settlement, but the end bearing capacity has not been fully mobilized. The initial load-displacement response for end bearing appears to be from loose materials at the bottom of the hole (Figure E13.3c).

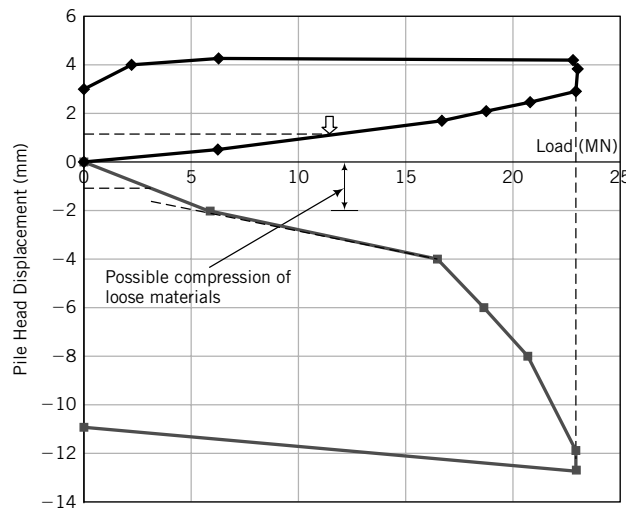


FIGURE E13.3c

Step 2: Determine the ultimate and allowable load capacity without consideration of settlement.

$$Q_f = 23 \text{ MN}$$

The load to compress the loose material is about 6 MN. The actual response from the dense sand at the base is

$$Q_b > (23 \text{ MN} - 6 \text{ MN}) = 17 \text{ MN}$$

$$W_p = \frac{\pi D^2}{4} L \gamma_c = \frac{\pi \times 1.5^2}{4} \times 14 \times (24 - 9.8) = 351 \text{ kN} = 0.35 \text{ MN}$$

The buoyant weight of the pile is used since most of it is below groundwater.

$$Q_{ult} = Q_f + Q_b - W_p = 23 \text{ MN} + (>) 17 \text{ MN} - 0.35 \text{ MN} > 39.7 \text{ MN}$$

$$Q_a = \frac{Q_f + Q_b}{2} - W_p = \frac{23 + 17}{2} - 0.35 = 19.7 \text{ MN}$$

Step 3: Determine the allowable load capacity at 6 mm.

$Q_{f\text{ at }6\text{ mm}} = 23 \text{ MN}$. This is based on the assumption that the ultimate skin friction remains constant. It is not a good practice to extrapolate experimental results because we do not know whether the soil would behave as extrapolated. In this case, there are three test points after the ultimate skin friction with settlement up to 4.4 mm, so it is quite likely that the load will remain relatively constant up to about 6 mm. Also, it is possible that the skin friction can decrease. As engineers, we are often called upon to make decisions based on a limited amount of data. In such cases, we have to use fundamentals and experience in making such decisions.

The end bearing capacity at 6 mm is about $19 \text{ MN} - 6 \text{ MN} = 13 \text{ MN}$. Therefore,

$$Q_{a\text{ at }6\text{ mm}} = 23 + 13 = 36 \text{ MN}$$

At this allowable load capacity, you would mobilize the full skin friction. That is, FS = 1 for skin friction.

Step 4: Determine the allowable load capacity for FS = 2 and the settlement.

Since the skin friction was fully mobilized, the FS will be applied to it.

$$Q_{af} = \frac{23}{2} = 11.5 \text{ MN}$$

The settlement is about 1 mm (Figure E13.3c). The end bearing at the same displacement is 3 MN, but this is the response from the loose material. You can either neglect this load or you can apply an FS to it based on experience. In this case, we will use 1.5 MN. Therefore, the allowable load is $11.5 + 1.5 - 0.35 = 12.7 \text{ MN}$.

You should appreciate the uncertainties in interpreting pile test results and making engineering decisions from them. Since there is no exact answer, it is best to work with a range of possible values. For this situation, the range of allowable load is 12.7 to 19.7 MN, with settlement less than about 3 mm.

What's next . . . Pile load tests are expensive and require careful consideration. To get an estimate of the pile load capacity, at least in the preliminary design stages, recourse is made to statics and to correlations using soil test results. In the next section, we will examine how statics is applied to obtain an estimate of pile load capacity and some correlations between field soil test results and measured pile load capacity.

13.7 METHODS USING STATICS FOR DRIVEN PILES

13.7.1 α -Method

13.7.1.1 Skin Friction The α -method is based on a total stress analysis (TSA) and is normally used to estimate the short-term load capacity of piles embedded in fine-grained soils. In the α -method, a coefficient, α_u , is used to relate the undrained shear strength, s_u , to the adhesive stress (f_s) along the pile shaft. The skin friction, Q_f , over the embedded length of the pile is the product of the adhesive stress ($f_s = \alpha_u s_u$) and the surface area of the shaft (perimeter \times embedded length). Thus,

$$Q_f = \sum_{i=1}^j (f_s)_i \times (\text{surface area})_i = \sum_{i=1}^j (\alpha_u)_i (s_u)_i \times (\text{perimeter} \times \text{length})_i \quad (13.8)$$

where j is the number of soil layers within the embedded length of the pile. For a cylindrical pile of uniform cross section and diameter D penetrating a homogeneous soil, Q_f is given by

$$Q_f = f_s \pi D L = \alpha_u s_u \pi D L \quad (13.9)$$

where L is the embedded length of the pile.

The value of α_u to use in determining the load capacity of piles is a subject of much debate and testing. Most tests to determine α_u are laboratory tests on model piles installed in a uniform deposit of soil. The major problems with these laboratory tests are:

1. It is difficult to scale up the laboratory model test results to real piles.
2. The soils in the field are mostly nonuniform compared with carefully prepared uniform soils in the laboratory.
3. Pile installation in the field strongly influences α_u , which cannot be accurately duplicated in the laboratory.
4. Undefined (peak or critical state and at what initial void ratio) values of s_u have been used in building relationships between s_u and α_u .

Full-scale field tests on real piles are preferred, but such tests are expensive and the results may apply only to the site where the tests are performed. The results from cone penetrometers and the SPT have been linked to α_u , but these are found from statistical correlations with rather low coefficient of correlation.

Recall from Chapters 10 and 11 that s_u is not a fundamental soil property but depends mainly on the initial void ratio or initial confining pressure. Because pile installation changes the initial soil stress state in ways that we can predict, at least easily, the author recommends that s_u should correspond to the critical state value. Converting any known value of s_u to critical state value was presented in Chapter 11.

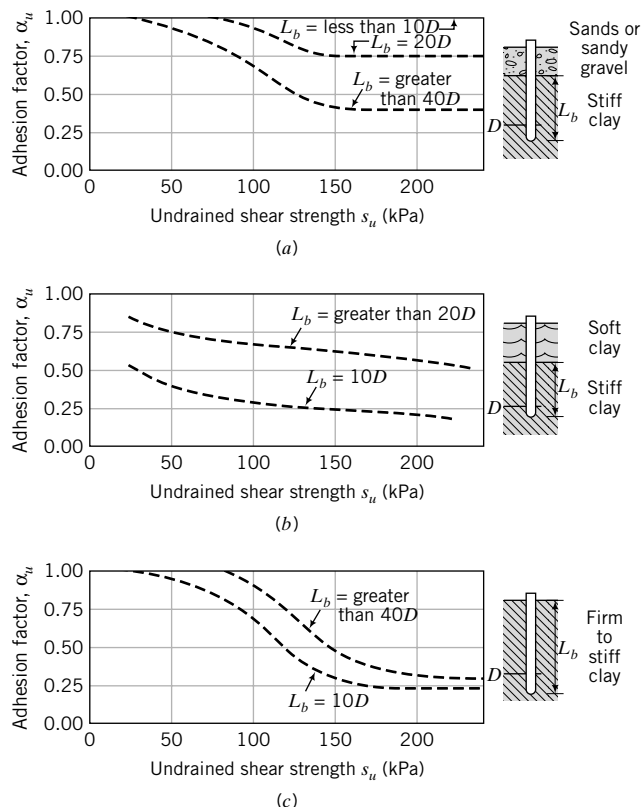
Values for α_u given by Tomlinson (1987) are shown in Figure 13.15. Randolph and Murphy (1985) recommended that f_s be estimated using the lower of the following two expressions:

$$f_s = 0.5 \sqrt{s_u \sigma'_{zo}} \quad (13.10)$$

$$f_s = 0.5 s_u^{0.75} (\sigma'_{zo})^{0.25} \quad (13.11)$$

13.7.1.2 End Bearing The end bearing capacity is found by analogy with the conventional failure mode of shallow foundations and is expressed as

$$Q_b = f_b A_b = N_c(s_u)_b A_b \quad (13.12)$$

FIGURE 13.15 α_u values. (After Tomlinson, 1987.)

where f_b is the base resistance stress, N_c is a bearing capacity coefficient, $(s_u)_b$ is the undrained shear strength of the soil at the base of the pile, and A_b is the cross-sectional area of the base of the pile. Several expressions have been proposed for N_c . In this textbook we will use the following expressions for N_c :

$$N_c = 9 \quad \text{for} \quad \frac{L}{D} \geq 3; \quad (s_u)_b > 25 \text{ kPa} \quad (13.13a)$$

$$N_c = 6 \quad \text{for} \quad (s_u)_b \leq 25 \text{ kPa} \quad (13.13b)$$

13.7.2 β -Method

13.7.2.1 Skin Friction The β -method is based on an effective stress analysis and is used to determine the short-term and long-term pile load capacities of coarse-grained soils and the long-term load capacity of fine-grained soils. The friction along the pile shaft is found using Coulomb's friction law, where the frictional stress is given by $f_s = \mu \sigma'_x = \sigma'_x \tan \phi'_i$, and where μ is the coefficient of friction, σ'_x is the lateral effective stress, and ϕ'_i is the interfacial effective friction angle. The skin friction is expressed as

$$Q_f = \sum_{i=1}^j (f_s)_i (\text{surface area})_i = \sum_{i=1}^j (\sigma'_x)_i \tan \phi'_i \times (\text{perimeter} \times \text{length})_i \quad (13.14)$$

The lateral effective stress is proportional to the vertical effective stress (σ'_z) by a coefficient K (Chapter 7). Therefore, we can write Equation (13.14) as

$$Q_f = \sum_{i=1}^j K_i (\sigma'_z) \tan \phi'_i \times (\text{perimeter} \times \text{length})_i \quad (13.15)$$

We can replace the two coefficients K and $\tan \phi'_i$ by a single factor β to yield

$$Q_f = \sum_{i=1}^j \beta_i (\sigma'_z)_i \times (\text{perimeter} \times \text{length})_i \quad (13.16)$$

Recall from Chapter 7 that for normally consolidated fine-grained soils and coarse-grained soils,

$$K = K_o^{nc} = 1 - \sin \phi'_{cs} \quad (13.17)$$

and for overconsolidated fine-grained soils,

$$K = K_o^{oc} = (1 - \sin \phi'_{cs})(\text{OCR})^{0.5} \quad (13.18)$$

The soil mass adjacent to a pile is expected to reach the critical state or close to it (Section 13.4). You should then use critical state shear strength parameters in determining the long-term load capacity of piles. Loose, coarse-grained soils adjacent to driven piles are densified and $\phi' = \phi'_p$. The actual value of ϕ'_p depends on the magnitude of the normal effective stress. Since the magnitude of the normal effective stress is uncertain, you should be cautious in using ϕ'_p to estimate the long-term load capacity. It would be prudent to use $\phi' = \phi'_{cs}$ in all cases except for some overconsolidated clays with a predominance of parallel aligned particles, where it is advisable to use $\phi' = \phi'_r$.

The value of β is also a subject of many debates, especially for coarse-grained soils. One reason for these debates is the correlation of β with undefined values of ϕ' . In this textbook, we will use ϕ'_{cs} (a fundamental soil property) or ϕ'_r for overconsolidated clays with a predominance of parallel aligned platy particles. The following expressions for β are selected for this textbook.

Fine-grained soils (Burland, 1973)

$$\text{Burland (1973): } \beta = K \tan \phi'_i = K_o^{oc} \tan \phi'_i = (1 - \sin \phi'_{cs})(\text{OCR})^{0.5} \tan \phi_i \quad (13.19)$$

Coarse-grained soils

$$\beta = (1 - \sin \phi'_{cs}) \tan \phi'_i \quad (13.20)$$

$$\text{Calcareous soil (Poulos, 1988): } \beta = 0.05 \text{ to } 0.1 \quad (13.21)$$

Typical ranges of values for ϕ'_i are given in Table 13.2. The vertical effective stress, σ'_z , is calculated at the center of each soil layer.

TABLE 13.2 Typical Range of Interfacial Friction Value

Material	Steel	Concrete	Timber
ϕ'_i	$\frac{2}{3}\phi'_{cs}$ to $0.8\phi'_{cs}$	$0.9\phi'_{cs}$ to $1.0\phi'_{cs}$	$0.8\phi'_{cs}$ to $1.0\phi'_{cs}$

13.7.2.2 End Bearing The end bearing capacity is calculated by analogy with the bearing capacity of shallow footings and is determined from

$$Q_b = f_b A_b = N_q (\sigma'_z)_b A_b \quad (13.22)$$

where $f_b = N_q (\sigma'_z)_b$ is the base resistance stress, N_q is a bearing capacity coefficient that is a function of ϕ' , $(\sigma'_z)_b$ is the vertical effective stress at the base, and A_b is the cross-sectional area of the base.

There is a plethora of expressions for N_q ; some are plotted in Figure 13.16. The differences in ultimate end bearing capacity using these different expressions for N_q can be greater than 900%. Recall from Section (13.4) that the failure mechanism below the base may not develop, so the expressions for N_q may not be representative of the soil response under the base.

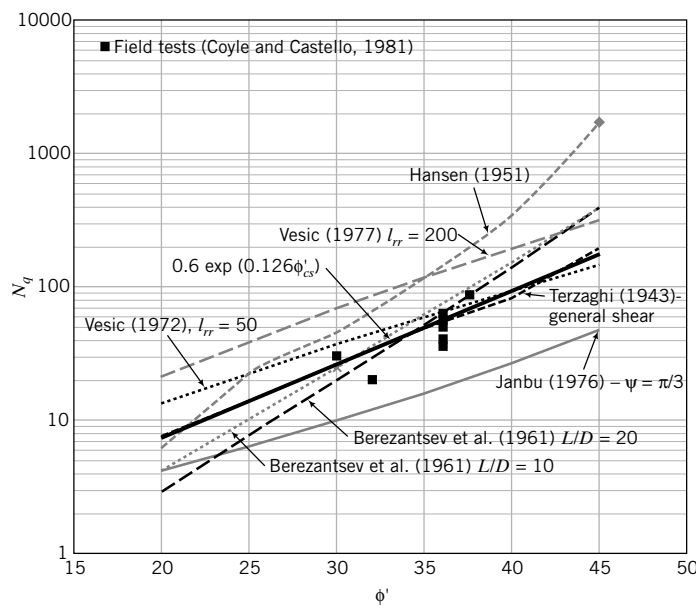


FIGURE 13.16 Comparison of N_q values.

Fine-grained and coarse-grained soils

We will use only two equations for N_q in this textbook. One, proposed by Janbu (1976), is

$$N_q = (\tan \phi' + \sqrt{1 + \tan^2 \phi'})^2 \exp(2\psi_p \tan \phi') \quad (13.23)$$

where the angle ψ_p (called the angle of pastification, as shown in Figure 13.8) varies from $\psi_p \leq \pi/3$ for soft, fine-grained soils to $\psi_p \leq 0.58\pi$ for dense, coarse-grained soils and overconsolidated fine-grained soils. Janbu recommended that for soft, compressible soils, ψ_p should not exceed $\pi/3$, while for dense, coarse-grained soils, ψ_p should not exceed $\pi/2$.

The other equation was developed by the author from field pile test data (Figure 13.16) and is expressed as

$$N_q = 0.6 \exp(0.126 \phi'_{cs}); \quad \phi'_{cs} \text{ is in degrees} \quad (13.24)$$

Janbu's equation would give lower values of N_q compared with Equation (13.24).

THE ESSENTIAL POINTS ARE:

1. The α -method is based on a TSA and is used to estimate the short-term pile load capacity in fine-grained soils.
2. The β -method is based on an ESA and is used to estimate the short-term and long-term pile load capacities in all soil types.
3. The actual values of α_u , β , and N_q are uncertain.

EXAMPLE 13.4 Pile Load Capacity in a Clay Soil

A cylindrical timber pile of diameter 400 mm is driven to a depth of 10 m into a clay with $s_u = 40$ kPa, $\phi'_{cs} = 28^\circ$, OCR = 2, and $\gamma_{sat} = 18$ kN/m³. Groundwater level is at the surface. Estimate the allowable load capacity for a factor of safety of 2. Is the pile a friction pile?

Strategy The solution is a straightforward application of the pile load capacity equations.

Solution 13.4

Step 1: Determine f_s and β .

Calculate the overburden pressure at the center of the embedded length.

$$\sigma'_{zo} = \gamma' \frac{L}{2} = (18 - 9.8) \times \frac{10}{2} = 41 \text{ kPa}$$

f_s is the lesser of

$$f_s = 0.5 \sqrt{s_u \sigma'_{zo}} = 0.5 \sqrt{40 \times 41} = 20 \text{ kPa}$$

and

$$f_s = 0.5 s_u^{0.75} (\sigma'_{zo})^{0.25} = 0.5 \times 40^{0.75} (41)^{0.25} = 20 \text{ kPa}$$

Use $f_s = 20$ kPa.

For OCR = 2, $\phi' = \phi'_{cs}$, and $\phi'_i = \phi'_{cs}$, we get

$$\beta = (1 - \sin \phi'_{cs})(OCR)^{0.5} \tan \phi'_i = (1 - \sin 28^\circ)(2)^{0.5} \tan 28^\circ = 0.4$$

Step 2: Calculate Q_a using a TSA.

$$L = 10 \text{ m}, \quad \text{Perimeter} = \pi D = \pi \times 0.4 = 1.26 \text{ m}$$

$$A_b = \frac{\pi D^2}{4} = \frac{\pi \times 0.4^2}{4} = 0.126 \text{ m}^2; \quad \frac{L}{D} = \frac{10}{0.4} = 25 > 3; \quad N_c = 9$$

$$Q_f = f_s(\pi D)L = 20 \times (1.26) \times 10 = 252 \text{ kN}$$

$$Q_b = N_c(s_u)_b A_b = 9 \times 40 \times 0.126 = 45 \text{ kN}$$

$$Q_{ult} = Q_f + Q_b = 252 + 45 = 297 \text{ kN}$$

$$Q_a = \frac{Q_{ult}}{\text{FS}} = \frac{297}{2} = 149 \text{ kN}$$

Step 3: Calculate Q_a using an ESA.

$$Q_f = \beta \sigma'_z (\pi D L) = 0.4 \times 41 \times (1.26 \times 10) = 207 \text{ kN}$$

Use Janbu's equation for N_q .

$$N_q = \left(\tan \phi'_{cs} + \sqrt{1 + \tan^2 \phi'_{cs}} \right)^2 \exp(2\psi_p \tan \phi'_{cs})$$

For $\phi'_{cs} = 28^\circ$ and assuming $\psi_p = \pi/3$ (soft clay), we find

$$N_q = \left\{ \tan 28^\circ + \sqrt{1 + \tan^2 (28^\circ)} \right\}^2 \exp\left(\frac{2\pi}{3} \tan 28^\circ\right) = 8.4$$

$$Q_b = N_q (\sigma'_z)_b A_b = 8.4 \times (18 - 9.8) \times 10 \times 0.126 = 87 \text{ kN}$$

$$Q_{ult} = Q_f + Q_b = 207 + 87 = 294 \text{ kN}$$

$$Q_a = \frac{Q_{ult}}{2} = \frac{294}{2} = 147 \text{ kN}$$

$$\frac{Q_f}{Q_{ult}} = \frac{207}{294} = 0.7; \text{ pile is not solely a friction pile.}$$

The load capacity from an ESA is slightly less than that from a TSA. Therefore, use the allowable pile load capacity from the ESA, that is, $Q_a = 147$ kN.

Let us compare N_q estimated using Janbu's equation and Equation (13.24).

$$N_q = 0.6 \exp(0.126 \phi'_{cs}) = 0.6 \exp(0.126 \times 28^\circ) = 20.4$$

The ultimate end bearing capacity from Equation (13.24) is then $\frac{20.4}{8.4} = 2.4$ times the ultimate end bearing capacity using Janbu's equation. Using Janbu's equation leads to conservative end bearing capacities (perhaps overly conservative in some cases, and consequently a more costly foundation).

EXAMPLE 13.5 Pile Load Capacity in a Layered Soil Profile

A driven square concrete pile $0.3 \text{ m} \times 0.3 \text{ m}$ is required to support a dead load of 100 kN and a live load of 60 kN. The soil stratification consists of 5 m of medium clay ($s_u = 40 \text{ kPa}$, $\phi'_{cs} = 26^\circ$, $\text{OCR} = 2$, $\gamma_{sat} = 18 \text{ kN/m}^3$) underlain by a deep deposit of stiff clay ($s_u = 80 \text{ kPa}$, $\phi'_{cs} = 24^\circ$, $\text{OCR} = 4$, $\gamma_{sat} = 18.8 \text{ kN/m}^3$). Groundwater level is at 2 m below the ground surface. You may assume that the soil above the groundwater level is saturated. Estimate the length of pile required using ASD with FS = 2 and LRFD with a dead load factor = 1.25 and a live load factor = 1.75, and performance factors $\phi_f = 0.75$ and $\phi_b = 0.7$ for both TSA and ESA.

Strategy You are given Q_a and FS, so you can calculate for ASD, $Q_{ult} = Q_a \times \text{FS}$. Assume an embedment depth and then check that it is satisfactory. You should consider both short-term and long-term conditions.

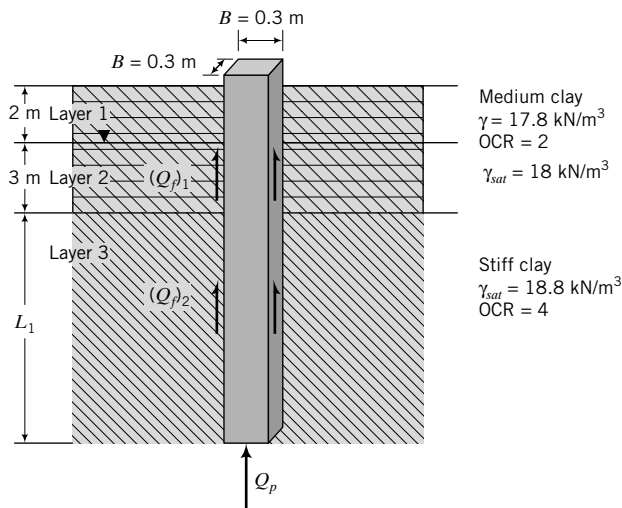
Solution 13.5

Step 1: Determine the ultimate load.

$$\text{ASD: } Q_a = 100 + 60 = 160 \text{ kN}; \quad Q_{ult} = Q_a \times \text{FS} = 160 \times 2.5 = 400 \text{ kN}$$

$$\text{LRFD: } P_u = 1.25 \text{DL} + 1.75 \text{LL} = 1.25 \times 100 + 1.75 \times 60 = 230 \text{ kN}$$

Step 2: Draw a sketch of the soil profile and pile. See Figure E13.5.

**FIGURE E13.5**

Step 3: Determine f_s and Q_f for TSA and ESA.

Assume a pile length of 10 m (5 m penetration in medium clay and 5 m in the stiff clay). Calculate the overburden pressure at the center of the pile length over each layer.

Medium clay:

$$\text{Above groundwater level, } L = 2 \text{ m: Average value of } \sigma'_{zo} = \left(\frac{2}{2} \times 18 \right) = 18 \text{ kPa}$$

$$\text{Below groundwater level, } L = 3 \text{ m: Average value of } \sigma'_{zo} = (2 \times 18) + \frac{3}{2}(18 - 9.8) = 48.3 \text{ kPa.}$$

Stiff clay:

Assume $L = 5 \text{ m}$.

$$\text{Average value of } \sigma'_{zo} = (2 \times 18) + 3(18 - 9.8) + \frac{5}{2}(18.8 - 9.8) = 83.1 \text{ kPa}$$

$$\text{Perimeter} = 2(B + L) = 2(0.3 + 0.3) = 1.2 \text{ m}$$

$$\text{Base area } A_b = BL = 0.3 \times 0.3 = 0.09 \text{ m}^2$$

TSA:

$$f_s \text{ is the lesser of } f_s = 0.5\sqrt{s_u \sigma'_{zo}} \text{ or } f_s = 0.5 s_u^{0.75} (\sigma'_{zo})^{0.25}.$$

$$Q_f = f_s \times \text{perimeter} \times \text{length} = 1.2 f_s L$$

See calculations in the following table.

Soil layer	s_u (kPa)	σ'_{zo} (kPa)	$f_s = 0.5\sqrt{s_u \sigma'_{zo}}$ (kPa)	$f_s = 0.5 s_u^{0.75} (\sigma'_{zo})^{0.25}$ (kPa)	Use $f_s =$ (kPa)	L (m)	Q_f (kN)
1	40	18	13.4	16.4	13.4	2	32
2	40	48.3	22	21	21	3	76
3	80	83.1	40.8	40.4	40.4	5	242
						Total	350

ESA:

For $\phi' = \phi'_i = \phi'_{cs}$, we find the following:

$$\begin{aligned} \text{Medium clay: } \beta &= (1 - \sin \phi'_{cs})(\text{OCR})^{0.5} \tan \phi'_{cs} \\ &= (1 - \sin 26^\circ)(2)^{0.5} \tan 26^\circ = 0.39 \end{aligned}$$

$$\text{Stiff clay: } \beta = (1 - \sin 24^\circ)(4)^{0.5} \tan 24^\circ = 0.53$$

$$f_s = \beta \sigma'_{zo}$$

$$Q_f = f_s \times \text{perimeter} \times \text{length}$$

See calculations in the following table.

Soil layer	β	σ'_{zo} (kPa)	$f_s = \beta \sigma'_{zo}$ (kPa)	L (m)	Q_f (kN)
1	0.39	18	7	2	17
2	0.39	48.3	18.8	3	68
3	0.53	83.1	44	5	264
		Total			349

Step 4: Calculate end bearing.

End bearing resistance in stiff clay

TSA: $\frac{L}{B} = \frac{10}{0.3} = 33.3 > 3$; $(s_u)_b = 80 \text{ kPa} > 25 \text{ kPa}$; $\therefore N_c = 9$
 $Q_b = N_c(s_u)_b A_b = 9 \times 80 \times 0.09 = 65 \text{ kN}$

ESA:

Using Janbu's equation with $\phi' = \phi'_{cs} = 24^\circ$ and $\psi_p = \pi/2$ gives

$$N_q = \left[\tan 24^\circ + \sqrt{1 + \tan^2(24^\circ)} \right]^2 \exp\left(\frac{2\pi}{2} \tan 24^\circ\right) = 9.6$$

$$(\sigma'_z)_b = 2 \times 18 + 3(18 - 9.8) + 5(18.8 - 9.8) = 105.6 \text{ kPa}$$

$$Q_b = N_q(\sigma'_z)_b A_b = 9.6 \times 105.6 \times 0.09 = 91 \text{ kN}$$

Step 5: Check whether assumed length is satisfactory.

$$\text{TSA: } Q_{ult} = Q_f + Q_b = 350 + 65 = 415 \text{ kN}$$

$$\text{ESA: } Q_{ult} = Q_f + Q_b = 349 + 91 = 440 \text{ kN}$$

Since the calculated load capacity from TSA is lower than that of ESA, then TSA governs.

Therefore, $L = 10 \text{ m}$ is satisfactory for ASD.

For LRFD: $P_u \leq \varphi_f Q_f + \varphi_b Q_b$

$$\text{TSA: } \varphi_f Q_f + \varphi_b Q_b = 0.75 \times 350 + 0.7 \times 65 = 308 \text{ kN}$$

$$\text{ESA: } \varphi_f Q_f + \varphi_b Q_b = 0.75 \times 349 + 0.7 \times 91 = 325 \text{ kN}$$

$$P_u = 230 \text{ kN} < 307 \text{ kN}$$

Therefore, $L = 10 \text{ m}$ is satisfactory for LRFD. You can reduce the length by 1 m and it will still satisfy LRFD. Check this for yourself.

EXAMPLE 13.6 Pile Load Capacity in a Clay with s_u Varying Linearly with Depth

A concrete pile 450 mm in diameter and 15 m long is driven into a clay. The undrained strength of the soil varies linearly with depth such that $s_u = 0.22\sigma'_z$. Determine the allowable pile load capacity using a TSA. The factor of safety required is 2 and $\gamma_{sat} = 17 \text{ kN/m}^3$. Groundwater is at the surface.

Strategy Consider the average skin friction. You can also consider an element of thickness dz and perform integration to find the skin friction. But this is rather cumbersome.

Solution 13.6

Step 1: Make a sketch of the problem.

See Figure E13.6.

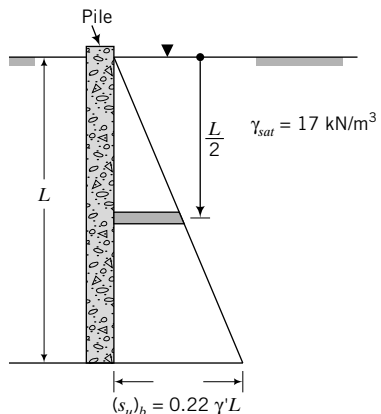


FIGURE E13.6

Step 2: Calculate the skin friction.

$$\text{Perimeter} = \pi D = \pi \times 0.45 = 1.41 \text{ m.}$$

$$\sigma'_{zo} \text{ at } \frac{L}{2} = (\gamma_{sat} - \gamma_w) \frac{L}{2} = (17 - 9.8) \frac{15}{2} = 54 \text{ kPa}$$

f_s is the lesser of $f_s = 0.5\sqrt{s_u\sigma'_{zo}} = 0.5\sqrt{0.22 \times 54^2} = 12.7 \text{ kPa}$ and

$$f_s = 0.5 s_u^{0.75} (\sigma'_{zo})^{0.25} = 0.5 \times (0.22 \times 54)^{0.75} (54)^{0.25} = 8.7 \text{ kPa}$$

Use $f_s = 8.7 \text{ kPa}$.

$$Q_f = f_s \times \text{perimeter} \times \text{length} = 8.7 \times 1.41 \times 15 = 184 \text{ kN}$$

Step 3: Calculate the end bearing capacity.

$$(s_u)_b = 0.22 \times (17 - 9.8) \times 15 = 23.8 \text{ kPa} < 25 \text{ kPa}; \therefore N_c = 6$$

$$A_b = \frac{\pi \times D^2}{4} = \frac{\pi \times 0.45^2}{4} = 0.159 \text{ m}^2$$

$$Q_b = N_c (s_u)_b A_b = 6 \times 23.8 \times 0.159 = 23 \text{ kN}$$

Step 4: Calculate the allowable load capacity.

$$Q_{ult} = Q_f + Q_b = 184 + 23 = 207 \text{ kN}$$

$$Q_a = \frac{Q_{ult}}{\text{FS}} = \frac{207}{2} = 104 \text{ kN}$$

What's next . . . SPT and CPT are popular field tests that are used extensively in estimating pile capacities. We will now consider how to estimate pile load capacities using SPT and CPT results.

13.8 PILE LOAD CAPACITY OF DRIVEN PILES BASED ON SPT AND CPT RESULTS

Various correlations have been proposed among results from SPT and CPT and pile load capacity. We will use only a few of these correlations in this textbook. These correlations and similar ones should be used with caution. Experience is required to successfully apply them to practice.

13.8.1 SPT

Driven piles in coarse-grained soils (Meyerhof, 1956, correlation for sand)

Skin friction: $Q_f = f_s \times \text{perimeter} \times \text{length}$

$$\text{Displacement piles: } f_s = 1.9N_{60}; \quad f_s \leq 100 \text{ kPa} \quad (13.25)$$

$$\text{Non-displacement piles: } f_s = 0.95 N_{60}; \quad f_s \leq 50 \text{ kPa} \quad (13.26)$$

End bearing: $Q_b = f_b A_b$

$$f_b = CN_{60} (\text{kPa}); \quad C = 38 \frac{L_s}{D} \leq 380 \quad (13.27)$$

where L_s is the length of pile driven in sand.

13.8.2 CPT

The cone penetrometer discussed in Chapter 2 was originally developed to estimate the end bearing capacity of piles. The cone resistance, q_c , is a measure of the end bearing capacity and the sleeve resistance, q_{sl} , is a measure of the skin or shaft friction. The ultimate end bearing capacity of a single pile (Xu and Lehane, 2005) is estimated from

$$Q_b = C_b q_{c-av} A_b \quad (13.28)$$

where $C_b = 0.6$ for closed-ended driven pipe piles in sand and $C_b = 0.9$ for jacked piles in sand; q_{c-av} is the average cone tip resistance over a distance 1.5 times the pile diameter above and the same distance below the pile base, and A_b is the area of the pile base. For open-ended pipe piles in siliceous sand (Lehane and Randolph, 2002),

$$C_b = 0.15 \left[1 + 3 \left(\frac{D^*}{D} \right)^2 \right] \quad (13.29)$$

where

$$\frac{D^*}{D} = \left[1 - \min \left\{ 1, \left(\frac{D_i}{1.5} \right)^{0.2} \right\} \left(\frac{D_i^2}{D^2} \right) \right]^{0.5} \quad (13.30)$$

and D is the external diameter, D^* is the effective diameter, D_i is the internal diameter, and min denotes minimum value of the quantity within the braces. Equation (13.29) is based on field tests on piles up to 1.5 m in diameter with lengths greater than 5 times the internal diameter in siliceous sand. The maximum expected settlement from Equation (13.28) is about 10% of the pile diameter.

Several other empirical equations are used in practice. For example, Fleming and Thorburn (1983) suggested that for Equation (13.28), $C_b = 1$ and q_{c-av} is the average cone value over an influence zone of 8 pile diameters above the pile base and 2 pile diameters below the pile base, calculated as follows:

$$q_{c-av} = \frac{q_{c1} + q_{c2} + 2q_{c3}}{4} \quad (13.31)$$

where q_{c1} is the arithmetic average of cone resistance values over 2 pile diameters below the pile base, q_{c2} is the minimum cone resistance value over 2 pile diameters below the pile base, and q_{c3} is the arithmetic average of minimum cone resistance values below q_{c2} over 8 pile diameters above the pile base.

Where the sleeve resistance is measured, either an arithmetic or a geometric mean value of cone resistance over the embedded pile depth is used as the shaft or skin friction. Cone sleeve friction is affected by the relative density of the soil and soil compressibility, while skin friction on a pile is affected by the relative density of the soil, method of installation, soil compressibility, pile geometry, and roughness. In the case of fine-grained soils, the cone sleeve friction value is strongly influenced by soil consolidation around the sleeve. Thus, significant differences between short-term and long-term load capacity can be expected using cone penetrometer results. Pile test results show that the short-term load capacity estimated from cone penetrometer results can be as low as 20% of the long-term load capacity. If the cone sleeve resistance is not measured, an estimate can be made from one of several equations proposed in the literature. Some of these are as follows:

For both open-ended and closed-ended driven pipe piles, the skin frictional stress (Lehane et al., 2005) is given as

$$f_s = C_s q_c A_{rs} \times \left[\max\left(2, \frac{h}{D}\right) \right]^{-0.5} \times \tan \delta_{cv} \quad (13.32)$$

where C_s is a constant (0.03 for compression piles and 0.0225 for tension piles), h is the distance of the pile section under consideration above the pile base, δ_{cv} is the soil–pile interface friction angle correlated to the mean particle size ($\approx 23^\circ$ for $D_{50} = 1$ mm, increasing to 28.8° for $D_{50} = 2$ mm for sand on steel) and A_{rs} is the effective area ratio of the pile shaft given as

$$\text{Closed-ended pipe piles: } A_{rs} = 1 \quad (13.33)$$

$$\text{Open-ended pipe piles: } A_{rs} = 1 - \min\left\{1, \left(\frac{D_i}{1.5}\right)^{0.2}\right\} \left(\frac{D_i}{D}\right)^2 \quad (13.34)$$

$$\text{Eslami and Fellenius (1997): } f_s = C_s q_{cs} \quad (13.35)$$

where q_{cs} is the cone resistance after adjustments for porewater pressure measured at the cone shoulder, and C_s is a coefficient that depends on soil type, as shown in Table 13.3.

$$\text{Vesic (1977)—coarse-grained soils: } f_s = 0.11 \exp(-3 \tan \phi'_{cs}) q_c \quad (13.36)$$

$$\text{Jardine et al. (1998)—coarse-grained soils: } f_s = \sigma'_{rc} \tan \phi_i \quad (13.37)$$

where σ'_{rc} is the radial effective stress on the shaft and is empirically related to the cone resistance as $\sigma'_{rc} = 0.029 q_c \left(\frac{\sigma'_{zo}}{p_a}\right)^{0.13} \left(\frac{h}{R^*}\right)^{-0.38}$, σ'_{zo} = vertical effective stress at a depth z where the shaft friction is considered, p_a = atmospheric pressure, h = depth from pile base to the depth at which the shaft friction is considered, ϕ_i is the interface friction angle ($\phi_i \leq \phi_{cs}$), $R^* = R_o$ for closed-ended pipe piles, R_o is outer radius, $R^* = (R_o^2 - R_i^2)^{0.5}$ for open-ended pipe piles, and R_i is inner radius.

$$\text{Tumay and Fakhroo (1984)—stiff clays: } f_s = 0.5 q_c \quad (13.38)$$

TABLE 13.3 Values of C_s

Soil type	C_s
Soft, sensitive soils	0.08
Clay	0.05
Stiff clay and mixture of clay and silt	0.025
Mixture of silt and sand	0.01
Sand	0.004

The ultimate skin friction is

$$Q_f = f_s \times \text{perimeter} \times \text{length}$$

You have to exercise caution in using these empirical equations, as they were derived from pile load tests and cone penetrometer data in particular soil types and locations. For example, Equations (13.28) and (13.32) were obtained from piles and cone penetrometer data in siliceous sand in an offshore environment in Western Australia.

EXAMPLE 13.7 Pile Load Capacity Using SPT Data

A 450-mm-diameter closed-ended pipe pile is driven into a sand profile to a depth of 10 m. The SPT results are shown in the table below. Estimate the allowable load capacity for a factor of safety of 3.

Depth (m)	1	3	5	6	8	10	11	13
N_{60} (blows/ft)	22	18	25	20	30	36	39	45

Strategy The N values are blows/ft, not blows/m. Use Meyerhof (1956) equations for displacement piles since the pipe pile is closed-ended.

Solution 13.7

Step 1: Determine the skin friction.

$$N_{60} = \text{average } N_{60} = \frac{22 + 18 + 25 + 20 + 30}{5} = 23$$

Displacement pile: $f_s = 1.9N_{60} = 1.9 \times 23 = 44 \text{ kPa} < 100 \text{ kPa}$; use $f_s = 44 \text{ kPa}$

$$q_f = f_s \times \text{perimeter} \times \text{length} = 44 \times \pi \times 0.45 \times 10 = 622 \text{ kN}$$

Step 2: Determine the end bearing and allowable load capacity.

$$f_b = CN_{60}(\text{kPa}); C = 38 \frac{L_s}{D} = 38 \frac{10}{0.45} = 844 > 380; \text{ use } C = 380$$

$N_{60} = 36$ (this is the N value at the base)

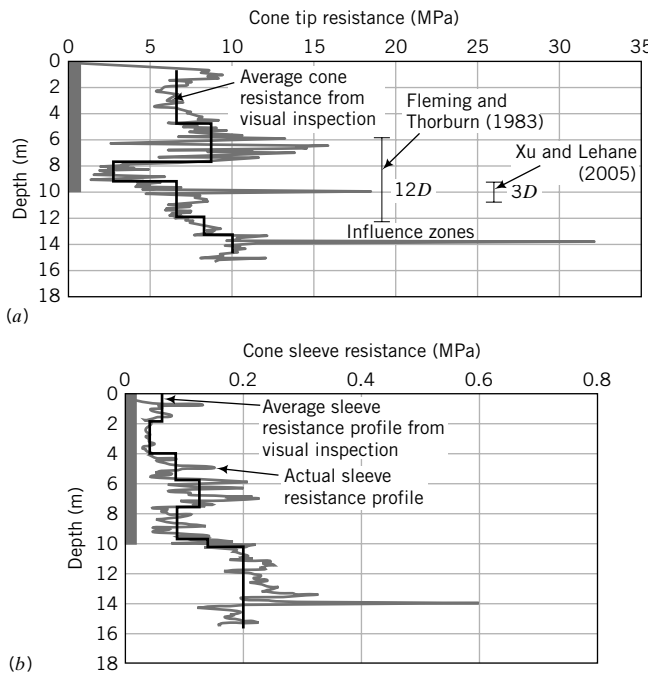
$$Q_b = f_b A_b = 380 \times 36 \times \frac{\pi \times 0.45^2}{4} = 2175 \text{ kN}$$

$$Q_{ult} = Q_f + Q_b = 622 + 2175 = 2797 \text{ kN}$$

$$Q_a = \frac{Q_{ult}}{\text{FS}} = \frac{2797}{3} = 932 \text{ kN}$$

EXAMPLE 13.8 Pile Load Capacity Using CPT Data

The results of cone tip resistance and sleeve resistance from a CPT at a site are shown in Figure E.13.8a. Estimate the ultimate load capacity of a driven closed-ended pipe pile 0.6 m in diameter and 10 m long.

**FIGURE E13.8**

Strategy It is best to select two or more methods to determine the cone resistance and sleeve resistance, and then make a decision on the pile load capacity after conducting the calculations.

Solution 13.8

Step 1: Determine the influence zone.

We will assume the pile is penetrating a weak soil and resting on a strong soil, since the cone tip resistance is increasing just below the pile base.

$$\text{Xu and Lehane (2005): } \text{Above base} = 1.5D = 1.5 \times 0.6 = 0.9 \text{ m}$$

$$\text{Below base} = 1.5D = 1.5 \times 0.6 = 0.9 \text{ m}$$

$$\text{Fleming and Thorburn (1983): } \text{Above base} = 8D = 8 \times 0.6 = 4.8 \text{ m}$$

$$\text{Below base} = 2D = 2 \times 0.6 = 1.2 \text{ m}$$

Step 2: Determine average cone tip resistance.

$$\text{Xu and Lehane: } q_{c-av} = \frac{3 + 6.5}{2} = 4.75 \text{ MPa}$$

$$\text{Fleming and Thorburn: } q_{c-av} = \frac{7.5 + 3 + 2(3.07)}{4} = 4.6 \text{ MPa}$$

Step 3: Determine average sleeve resistance.

You can inspect the sleeve resistance profile and visually draw an average sleeve resistance profile, as shown in Fig. E13.8b.

$$\text{Average sleeve resistance} = 0.075 \text{ MPa over a depth of 10 m}$$

If the sleeve resistance was not measured, you can use one or more of the empirical equations given in Section 13.8.2.

Step 4: Calculate load capacity.

$$\text{Area of base, } A_b = \frac{\pi D^2}{4} = \frac{\pi \times 0.6^2}{4} = 0.28 \text{ m}^2$$

$$\text{Xu and Lehane: } Q_b = 0.6q_{c-av}A_b = 0.6 \times 4.75 \times 0.28 = 0.8 \text{ MN}$$

$$\text{Fleming and Thorburn: } Q_b = q_c A_b = 4.6 \times 0.28 = 1.29 \text{ MN}$$

$$\text{Skin friction, } Q_f = f_s \pi D L = 0.075 \times \pi \times 0.6 \times 10 = 1.41 \text{ MN}$$

$$\text{Xu and Lehane: } Q_{ult} = 0.8 + 1.41 = 2.21 \text{ MN}$$

$$\text{Fleming and Thorburn: } Q_{ult} = 1.29 + 1.41 = 2.7 \text{ MN}$$

There is about 18% difference between the two methods. You can take an average value as an estimate of the ultimate pile load capacity, i.e., $(2.21 + 2.7)/2 \approx 2.5 \text{ MN}$.

13.9 LOAD CAPACITY OF DRILLED SHAFTS

The load capacities of drilled shafts are calculated similarly to driven piles except that the empirical adhesion, friction, and end bearing factors are different.

TSA (fine-grained soils):

- **Adhesion** (O'Neill and Reese, 1999)

$$\alpha_u = 0.55; \frac{s_u}{p_a} \leq 1.5 \quad (13.39a)$$

$$\alpha_u = 0.55 - 0.1 \left(\frac{s_u}{p_a} - 1.5 \right); \quad 1.5 < \frac{s_u}{p_a} \leq 2.5 \quad (13.39b)$$

$$f_s = \alpha_u s_u \leq 380 \text{ kPa} \quad (13.39c)$$

where p_a is atmospheric pressure (101 kPa).

- **End bearing**

$$f_b = N_c (s_u)_b; \quad N_c = 6 \left(1 + 2 \frac{z}{D} \right); \quad N_c \leq 9; \quad f_b \leq 4.0 \text{ MPa} \quad (13.40)$$

where z is the embedded depth of the drilled shaft in the end bearing layer and $(s_u)_b$ is the average undrained shear strength over two diameters below the base. The $(s_u)_b$ value must be obtained from field or laboratory tests within 2 pile diameters below the pile tip. If $(s_u)_b < 25 \text{ kPa}$, the value of N_c should be reduced by one-third.

ESA:

- **Skin friction**

$$\text{Fine-grained soils: } \beta = K \tan \phi'_i = K_o^{oc} \tan \phi'_i = (1 - \sin \phi'_{cs}) (\text{OCR})^{0.5} \tan \phi_i \quad (13.41)$$

Coarse-grained soils (O'Neill and Reese, 1988):

Clean sand

$$\beta = 1.5 - 0.245\sqrt{z}; \quad N_{60} \geq 15, 1.2 \geq \beta \geq 0.25 \quad (13.42a)$$

$$\beta = \frac{N_{60}}{15} (1.5 - 0.245\sqrt{z}); \quad N_{60} < 15, 1.2 \geq \beta \geq 0.25 \quad (13.42b)$$

$$f_s = \beta \sigma'_z \leq 200 \text{ kPa} \quad (13.42c)$$

z = depth (m) measured from the ground surface to the middle of the soil layer.

Gravels and sandy gravels (GW and GP)

$$\beta = 2.0 - 0.15z^{0.75}; \quad 1.8 \geq \beta \geq 0.25; \quad z = \text{depth (m)} \quad (13.43a)$$

$$\beta = 0.25 \quad \text{for } z > 26 \text{ m} \quad (13.43b)$$

$$f_s = \beta\sigma'_z \leq 200 \text{kPa} \quad (13.43c)$$

- **End bearing** (Quiros and Reese, 1977, correlation for cemented sand)

$$f_b = 57.5N_{60}; \quad f_b \leq 2900 \text{ (kPa)}; \quad \frac{L}{D} \geq 10 \quad (13.44a)$$

$$f_b = 5.75LN_{60}; \quad f_b \leq 290L \text{ (kPa)}; \quad \frac{L}{D} < 10 \quad (13.44b)$$

The soil near the top of the drilled shaft is subjected to environmental and construction effects, while the soil just above the base may develop tensile cracking. Consequently, the upper 1.5 m of the shaft and one pile diameter above the base are ignored in calculating skin friction for drilled shafts (see Figure 13.2).

The β for drilled shafts in coarse-grained soils have been obtained from back calculations from load tests on 1-m-diameter drilled shafts in cemented sand at particular locations (Texas Gulf Coast region and Los Angeles, California). They are not related to any soil parameters. They have to be used with careful judgment based on experience.

EXAMPLE 13.9 Load Capacity of a Drilled Shaft in a Layered Soil Profile

A straight drilled shaft of diameter 1 m is installed in a soil profile, as shown in Figure E13.9. SPT were performed at intervals of approximately 1 m below the base. Determine the allowable load capacity for $FS = 2$.

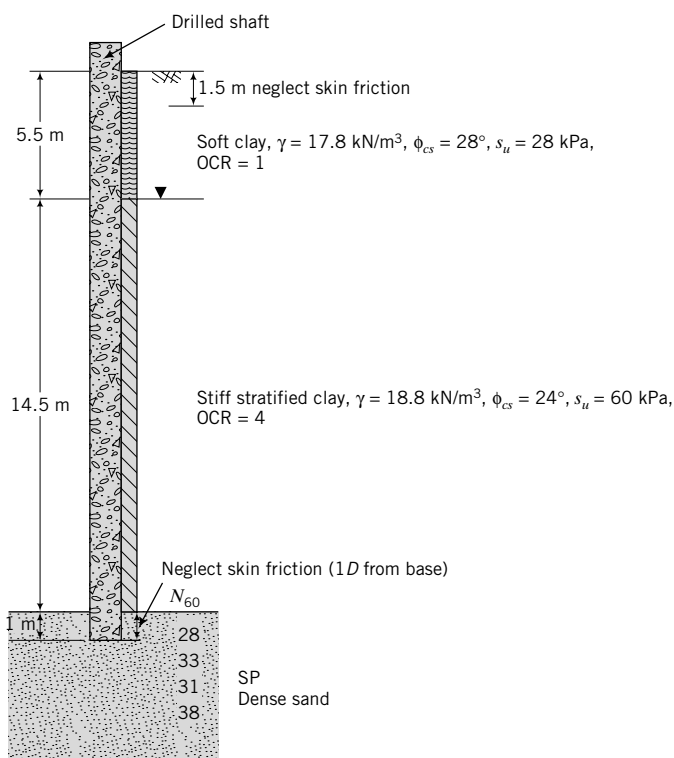


FIGURE E13.9

Strategy The solution is a straightforward application of the empirical equations for drilled shafts.

Solution 13.9

Step 1: Calculate the skin friction.

Neglect the skin friction over top $1.5D = 1.5 \times 1 = 1.5$ m.

Neglect the skin friction one diameter above base = $1D = 1 \times 1 = 1$ m.

TSA:

Diameter	1 m					
Perimeter	3.14 m					
Depth (m)	Soil	L (m)	s _u (kPa)	s _u /p _a	α _u	Q _f (kN)
0–5.5	Soft clay	4	28	0.28	0.55	194
5.5–21.0	Stiff clay	14.5	60	0.59	0.55	1503
				Sum	1697	

ESA: Assume and $\phi' = \phi'_{cs}$, and $\phi'_i = \frac{2}{3} \phi'_{cs}$; $\beta = (1 - \sin \phi'_{cs}) \tan \phi'_i (\text{OCR})^{0.5}$.

Depth (m)	Soil	L (m)	OCR	ϕ'cs	β	σ'zo	Q _f (kN)
0–5.5	Soft clay	4	1	28	0.18	62.3	140
5.5–21.0	Stiff clay	14.5	4	24	0.34	163.2	2529
				Sum	2669		

TSA governs.

Step 2: Calculate end bearing.

Use average N_{60} value over a depth of $2D$ from the base or tip.

$$N_{60} = \frac{28 + 33 + 31}{3} = 31$$

$$\frac{L}{D} = \frac{21}{1} = 21 \geq 10; \text{ use } f_b = 57.5N_{60}; f_b \leq 2900 \text{ (kPa)}$$

$$f_b = 57.5 \times 31 = 1783 \text{ kPa} < 2900 \text{ kPa}; \text{ use } f_b = 1783 \text{ kPa}$$

$$Q_b = f_b A_b = 1783 \times \frac{\pi \times 1^2}{4} = 1400 \text{ kN}$$

Step 3: Calculate Q_a .

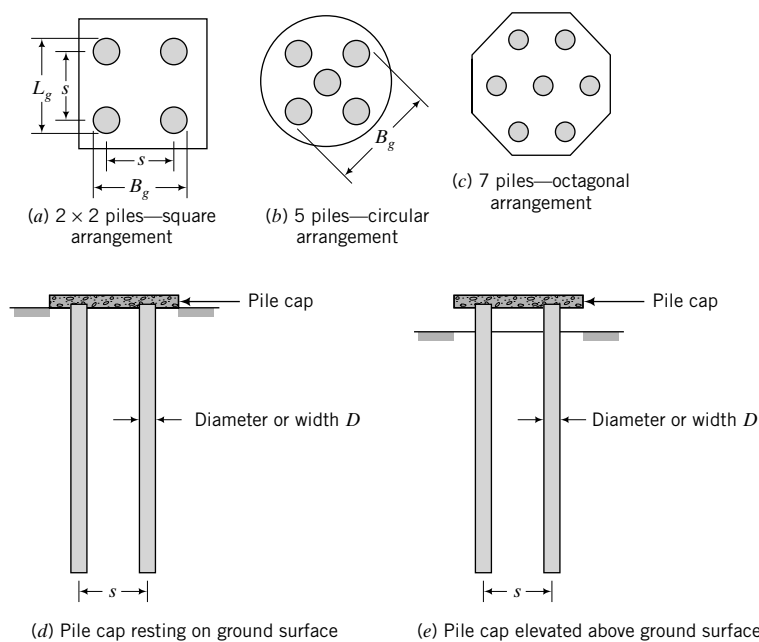
$$Q_{ult} = Q_f + Q_b = 1697 + 1400 = 3097 \text{ kN}$$

$$Q_a = \frac{Q_{ult}}{2} = \frac{3097}{2} = 1549 \text{ kN}$$

What's next . . . Piles are rarely used singly. They are often clustered into groups. Next, we will discuss how to determine the load capacity of pile groups.

13.10 PILE GROUPS

In most practical situations, piles are used in groups. They are arranged in geometric patterns (squares, rectangles, circles, and octagons) at a spacing, s (center to center distance), not less than $2D$ (where D is the diameter or width of the pile). The piles are connected at their heads by a concrete pile cap, which

**FIGURE 13.17**

Pile groups.

(d) Pile cap resting on ground surface

(e) Pile cap elevated above ground surface

may or may not be in contact with the ground (Figure 13.17). If the pile cap is in contact with the ground, part of the load will be transferred directly to the soil.

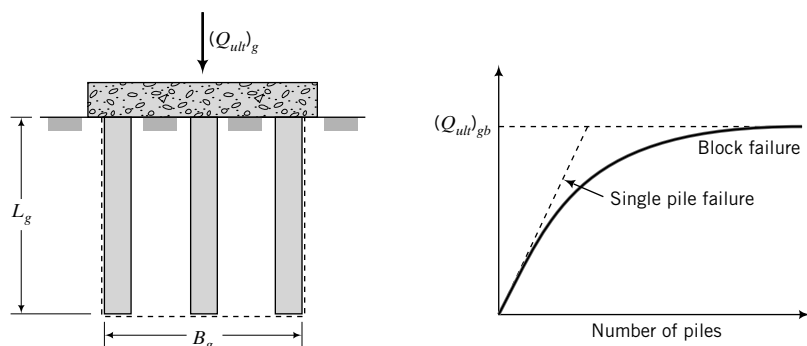
The load capacity for a pile group is not necessarily the load capacity of a single pile multiplied by the number of piles. In fine-grained soils, the outer piles tend to carry more loads than the piles in the center of the group. In coarse-grained soils, the piles in the center take more loads than the outer piles.

The ratio of the load capacity of a pile group, $(Q_{ult})_g$, to the total load capacity of the piles acting as individual piles, (nQ_{ult}) , is called the efficiency factor, η_e ; that is,

$$\eta_e = \frac{(Q_{ult})_g}{nQ_{ult}} \quad (13.45)$$

where n is the number of piles in the group and Q_{ult} is the ultimate load capacity of a single pile. The efficiency factor is usually less than 1. However, piles driven into a loose, coarse-grained soil tend to densify the soil around the piles, and η_e could exceed 1.

Two modes of soil failure are normally investigated to determine the load capacity of a pile group. One mode, called block failure (Figure 13.18), may occur when the spacing of the piles is small enough to cause the pile group to fail as a unit. The group load capacity for block failure mode is

**FIGURE 13.18**

Block failure mode.

ESA:

$$(Q_{ult})_{gb} = \sum_{i=1}^j \left\{ \beta_i (\sigma'_z)_i \times (\text{perimeter})_{ig} \times L_i \right\} + N_q(\sigma'_z)_b (A_b)_g \quad (13.46)$$

TSA:

$$(Q_{ult})_{gb} = \sum_{i=1}^j \left\{ (\alpha_u)_i (s_u)_i \times (\text{perimeter})_{ig} \times L_i \right\} + N_c(s_u)_b (A_b)_g \quad (13.47)$$

where the subscript *gb* denotes block mode of failure for the group.

The other failure mode is single pile failure mode or punching failure mode. The key assumption in single pile failure mode is that each pile mobilizes its full load capacity. Thus, the group load capacity is

$$(Q_{ult})_{gs} = n Q_{ult} \quad (13.48)$$

where the subscript *gs* denotes single pile mode failure.

The values of ψ_p to use in determining N_q in Janbu's equation depend on the s/D ratio and the friction angle. Janbu (1976) showed that

$$\frac{s}{D} = 1 + 2 \sin \psi_p (\tan \phi' + \sqrt{1 + \tan^2 \phi'}) \exp(\psi_p \tan \phi') \quad (13.49)$$

The value of ψ_p is not significantly affected by $s/D \leq 2.5$. As a reminder, Janbu's equation may significantly underestimate the end bearing capacity because the failure mechanism assumed in developing Equation (13.49) may not develop, as discussed in Section 13.4.

THE ESSENTIAL POINTS ARE:

1. The ultimate load capacity of a pile group is not necessarily the ultimate load capacity of a single pile multiplied by the number of piles in the group.
2. A pile group can either fail by the group failing as a single unit, called block failure mode, or as individual piles, called single pile failure mode.

EXAMPLE 13.10 Pile Group Load Capacity in Layered Clays

A pile group consisting of 9 driven piles, each 0.4 m in diameter, is arranged in a 3×3 matrix at a spacing of 1.2 m. The piles penetrate a medium clay soil ($s_u = 40$ kPa, $\phi'_{cs} = 30^\circ$, $\gamma_{sat} = 18$ kN/m 3 , OCR = 2) of thickness 8 m and are embedded 2 m in a stiff clay ($s_u = 90$ kPa, $\phi'_{cs} = 28^\circ$, $\gamma_{sat} = 18.5$ kN/m 3 , OCR = 5). Calculate the group allowable load capacity for a factor of safety of 2. Groundwater level (GWL) is at 2 m below the surface but can rise to the surface due to seasonal changes.

Strategy You need to calculate the ultimate load capacity assuming (a) block failure mode and (b) single pile failure mode. Use a sketch to illustrate the problem.

Solution 13.10

Step 1: Draw a sketch and calculate the geometric properties.

See Figure E13.10.

Single pile: $D = 0.4 \text{ m}$; Perimeter = $\pi D = \pi \times 0.4 = 1.26 \text{ m}$

$$\text{Base area} = A_b = \frac{\pi D^2}{4} = \pi \times \frac{0.4^2}{4} = 0.126 \text{ m}^2$$

Group: Perimeter = $4(2s + D) = 4[2(1.2) + 0.4] = 11.2 \text{ m}$

$$\text{Base area} = (A_b)_g = (2s + D)^2 = 2.8^2 = 7.84 \text{ m}^2$$

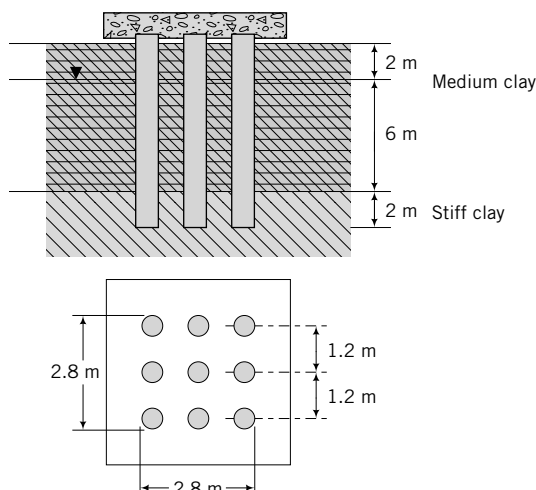


FIGURE E13.10

Step 2: Calculate the ultimate load capacity using TSA.

Calculate the overburden pressure at the center of the pile length. Assume groundwater rises to the surface.

Medium clay:

$$\sigma'_{zo} = \gamma' \frac{L}{2} = (18 - 9.8) \times \frac{8}{2} = 32.8 \text{ kPa}$$

Stiff clay:

$$\sigma'_{zo} = (18 - 9.8) \times 8 + (18.5 - 9.8) \times 1 = 74.3 \text{ kPa}$$

Calculate the skin frictional stress.

f_s is the lesser of $f_s = 0.5\sqrt{s_u \sigma'_{zo}}$ and $f_s = 0.5s_u^{0.75}(\sigma'_{zo})^{0.25}$.

Medium clay:

$$f_s = 0.5\sqrt{s_u \sigma'_{zo}} = 0.5\sqrt{40 \times 32.8} = 18 \text{ kPa}$$

$$f_s = 0.5s_u^{0.75}(\sigma'_{zo})^{0.25} = 0.5 \times 40^{0.75}(32.8)^{0.25} = 19 \text{ kPa}$$

Use $f_s = 18 \text{ kPa}$.

Stiff clay:

$$f_s = 0.5\sqrt{s_u \sigma'_{zo}} = 0.5\sqrt{90 \times 74.3} = 41 \text{ kPa}$$

$$f_s = 0.5s_u^{0.75}(\sigma'_{zo})^{0.25} = 0.5 \times 90^{0.75}(72.3)^{0.25} = 42.6 \text{ kPa}$$

Use $f_s = 41 \text{ kPa}$.

$$Q_f = f_s \times \text{perimeter} \times \text{length}$$

The calculations of Q_f are done using a table, as follows, or a spreadsheet.

Depth (m)	Soil	L (m)	Block		Single
			Perimeter	11.20 m	1.26 m
0–8	Medium clay	8	18	1612.8	181.4
8–10.0	Stiff clay	2	41	918.4	103.3
			Sum	2531.2	284.8

End bearing–stiff clay:

Block mode

$$\frac{L}{D} = \frac{10}{0.4} = 25 > 3; \quad N_c = 9$$

$$(Q_b)_{\text{stiff clay}} = N_c s_u (A_b)_g = 9 \times 90 \times 7.84 = 6350 \text{ kN}$$

Single pile mode

$$(Q_b)_{\text{stiff clay}} = N_c s_u A_b = 9 \times 90 \times 0.126 = 102 \text{ kN}$$

Group load capacity:

Block mode

$$(Q_{ult})_{gb} = (Q_f)_{\text{medium clay}} + (Q_f)_{\text{stiff clay}} + (Q_p)_{\text{stiff clay}}$$

$$(Q_{ult})_{gb} = 2531.2 + 6350 \approx 8881 \text{ kN}$$

Single pile mode

$$(Q_{ult})_{gs} = 9 \times (284.8 + 102) \approx 3481 \text{ kN} < 8881 \text{ kN}$$

Single pile mode governs.

Step 3: Calculate the ultimate load capacity using an ESA.

Assume $\phi'_i = \frac{2}{3}\phi'_{cs}$.

$$\beta = (1 - \sin\phi'_{cs})(OCR)^{0.5} \tan\left(\frac{2}{3}\phi'_{cs}\right)$$

Depth (m)	Soil	L (m)	OCR	ϕ'_{cs}	β	σ'_{zo}	Block	Single
							Perimeter	11.20 m
0–8	Medium clay	8	2	30	0.26	32.8	756.4	85.1
	Stiff clay	2	5	28	0.40	74.3	667.0	75.0
						Sum	1423.4	160.1

End bearing–stiff clay:

Use Janbu's equation with $\phi' = \phi'_{cs}$ and $\psi_p = \pi/2$.

$$N_q = [\tan 28^\circ + \sqrt{1 + \tan^2(28^\circ)}]^2 \exp\left(2 \frac{\pi}{2} \tan 28^\circ\right) = 14.7$$

$$(\sigma'_z)_b = 8 \times (18 - 9.8) + 2 \times (18.5 - 9.8) = 83 \text{ kPa}$$

$$(Q_b)_{gb} = N_q (\sigma'_z)_b (A_b)_g = 14.7 \times 83 \times 7.84 = 9566 \text{ kPa}$$

$$\text{Single pile: } Q_b = 14.7 \times 83 \times 0.126 = 154 \text{ kN}$$

Group load capacity:

Block mode

$$(Q_{ult})_{gb} = 1423.4 + 9566 \approx 10,989 \text{ kN}$$

Single pile mode

$$(Q_{ult})_{gs} = 9 \times (160.1 + 154) \approx 2827 \text{ kN} < 10989 \text{ kN}$$

Single pile mode governs.

Step 4: Decide which failure mode and conditions govern.

Analysis	Load capacity (kN)	
	Block mode	Single pile mode
TSA	8881	3481
ESA	10,989	2827

The lowest ultimate load capacity is 2827 kN for an ESA.

$$\therefore Q_a = \frac{(Q_{ult})_{gs}}{\text{FS}} = \frac{2827}{2} = 1414 \text{ kN}$$

What's next . . . We have discussed methods to determine the ultimate load capacity, that is, the ultimate limit state, which is only one of two limit states required in analysis and design of geotechnical systems. The other limit state is serviceability limit state (settlement). Next, we will examine settlement of piles.

13.11 ELASTIC SETTLEMENT OF PILES

The elastic settlement of a single pile depends on the relative stiffness of the pile and the soil, the length-to-diameter ratio of the pile, the relative stiffness of the soil at the base and of the soil over the pile length, and the distribution of elastic modulus of the soil along the pile length. Laboratory and field soil test results rarely duplicate the installation effects, so you need to be cautious in using soil stiffness from these tests. The relative stiffness of the pile to the soil is $K_{ps} = E_p/E_{so}$, where E_p is the elastic modulus of an equivalent solid cross section of the pile and E_{so} is the elastic modulus of the soil. The elastic modulus of the soil at the base or tip of the pile will be denoted by E_{sb} . Usually, the secant elastic modulus is used in design practice. For short-term loading in fine-grained soils, $(E_{so})_u$ is used, where the subscript u denotes undrained condition.

Various analyses have been proposed to calculate the settlement of single piles and pile groups. Poulos (1989) provided an excellent discussion on the various numerical procedures to calculate settlement of piles. The settlement consists of three components—skin friction, end bearing, and elastic shortening.

Skin friction tends to deform the soil near the shaft, as illustrated in Figure 13.5a. The deformation mode near the shaft is analogous to simple shear strain (Chapter 7), and the shear strain, γ_{zx} , is

$$\gamma_{zx} = \frac{\tau}{G} = \frac{f_s}{G} \quad (13.50)$$

where G is the shear modulus, τ is shear stress, and f_s is the skin frictional stress. The shear strains can be integrated over the pile length to give the elastic settlement (ρ_{es}) resulting from skin friction; that is,

$$\rho_{es} = \frac{1}{G(z)} \int_o^L \tau(z) dz \quad (13.51)$$

where (z) means that the parameter in front of it varies with depth. To solve Equation (13.51), we need to know how G and τ vary with depth, but this we do not know. Therefore, we have to speculate on their variations and then solve Equation (13.51). A further complication arises in that the boundary conditions for a pile problem are complex. Thus, we have to solve Equation (13.51) using numerical procedures. For example, we can assume that

$$\tau(z) = \int F(z, i) \tau(i) di \quad (13.52)$$

where $F(z, i)$ is a stress function and $\tau(i)$ is the shear stress at an ordinate i . We can use finite element or boundary element to solve Equations (13.51) and (13.52). Stress functions for a point load within a half-space were developed by Mindlin (1936).

For a homogeneous soil (E_{so} is constant with depth), a solution of Equation (13.51) using Equation (13.52) for the elastic settlement of a single pile is

$$\rho_{es} = \frac{Q_{af}}{E_{so} L} I \quad (13.53)$$

where I is an influence factor and Q_{af} is the design load transferred as skin friction. An approximate equation for I is

$$I = 0.5 + \log\left(\frac{L}{D}\right) \quad (13.54)$$

Soft soils tend to have elastic moduli that vary linearly with depth; that is,

$$E_{so} = mz \quad (13.55)$$

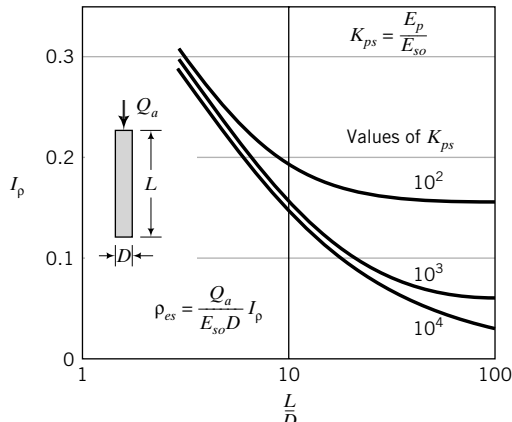


FIGURE 13.19 Influence factor for vertical settlement of a single floating pile.
(After Poulos, 1989.)

where m is the rate of increase of E_{so} with depth (units: kPa/m). For soft soils, the elastic settlement is

$$(\rho_{es})_{so} = \frac{Q_{af}}{mL^2} I_{so} \quad (13.56)$$

where

$$I_{so} = 2.0 \log\left(\frac{L}{D}\right) \quad (13.57)$$

Poulos (1989) developed another solution for the elastic settlement. He showed that ρ_{es} for a floating pile can be determined from

$$\rho_{es} = \frac{Q_{af}}{E_{so}D} I_p \quad (13.58)$$

where I_p is an influence factor that depends on the L/D ratio and K_{ps} , as shown in Figure 13.19.

The soil mass under a pile is subjected to compression from end bearing. We can use elastic analyses (described in Chapter 7) to determine the elastic compression under the pile. For friction piles, the settlement due to end bearing is small in comparison to skin friction and is often neglected.

The elastic shortening of the pile (ρ_p) is found for column theory, which for a soil embedded in a homogeneous soil is

$$\rho_p = C \frac{Q_{af}L}{E_p A_p} \quad (13.59)$$

where C is a reduction factor to account for the fact that the vertical strain reduces with the embedded length of the pile. For most soils, $C \approx 0.5$ except for soft clay soils for which $C \approx 0.7$. Elastic shortening is only significant for slender piles ($E_p/E_{so} < 500$). The total elastic settlement for a floating pile is $\rho_{et} = \rho_{es} + \rho_p$.

Field observations indicate that at design loads, the elastic settlement of a single driven pile is within the range 0.9% to 1.25% of the pile diameter. Hull (1987) found, from numerical analyses, that embedding a pile beyond a certain critical length does not reduce the settlement. The critical length normalized to the diameter (width) is

$$\frac{L_c}{D} = \sqrt{\frac{\pi E_p A_p}{E_{so} D^2}} = \sqrt{\frac{\pi K_{ps} A_p}{D^2}} \quad (13.60)$$

where L_c is the critical length, A_p is the area of the cross section of the pile, and

$$K_{ps} = \frac{E_p}{E_{so}} \quad (13.61)$$

Piles in a group tend to interact with each other depending on the spacing between them. The smaller the spacing, the greater the interaction and the larger the settlement. Pile group settlement is influenced by spacing-to-diameter (or width) ratio (s/D), the number of piles (n) in the group, and the length-to-diameter ratio (L/D). For convenience, pile group settlement is related to a single pile settlement through a group settlement factor R_s , defined as

$$R_s = \frac{\text{Settlement of group}}{\text{Settlement of single pile at same average load}} \quad (13.62)$$

An empirical relationship between R_s and n (Fleming et al., 1985) is

$$R_s = n^\Phi \quad (13.63)$$

where the exponent Φ is between 0.4 and 0.6.

The settlement due to end bearing can be calculated by assuming the pile base is a rigid punch on the surface of the soil relocated at a depth L . The settlement (Timoshenko and Goodier, 1970) is:

$$\rho_b = \frac{Q_b}{r_b G_b} \frac{1 - \nu}{4} \quad (13.64)$$

where r_b and G_b are the radius and shear modulus at the base, respectively, and ν is Poisson's ratio. The settlement for group piles in coarse-grained soils from SPT and CPT can be estimated from:

$$\text{SPT: } \rho_{es} = \frac{0.91 q_s I \sqrt{B_g}}{N_{cor}} \text{ mm} \quad [\text{Units: } q_s \text{ in kPa, } B_g \text{ in m}] \quad (13.65)$$

$$\text{CPT: } \rho_{es} = \frac{41 q_s I B_g}{q_c} \text{ mm} \quad [\text{Units: } q_s \text{ in kPa, } B_g \text{ in m, } q_c \text{ in kPa}] \quad (13.66)$$

where $I = 1 - 0.08 \frac{L}{B_g} \geq 0.5$, L is the embedded length of the pile, N_{cor} is the average N value over $\frac{2L}{3}$ from the finished soil surface and corrected for overburden pressure, q_s is the average allowable vertical stress on the pile group, B_g is the width of the pile group, and q_c is the arithmetic average cone tip resistance over two pile diameters below the cone.

13.12 CONSOLIDATION SETTLEMENT UNDER A PILE GROUP

Sometimes, a pile group may be embedded above a soft clay layer and transfer sufficient load to it (soft clay) to cause consolidation settlement. To estimate the consolidation settlement, the full design load is assumed to act at a depth of $\frac{2}{3}L$ and is then distributed in the ratio of 2:1 (vertical:horizontal). The increase in vertical stress at a depth z in the soft clay layer shown in Figure 13.20 is

$$\Delta\sigma_z = \frac{Q_{ag}}{(B_g + z)(L_g + z)} \quad (13.67)$$

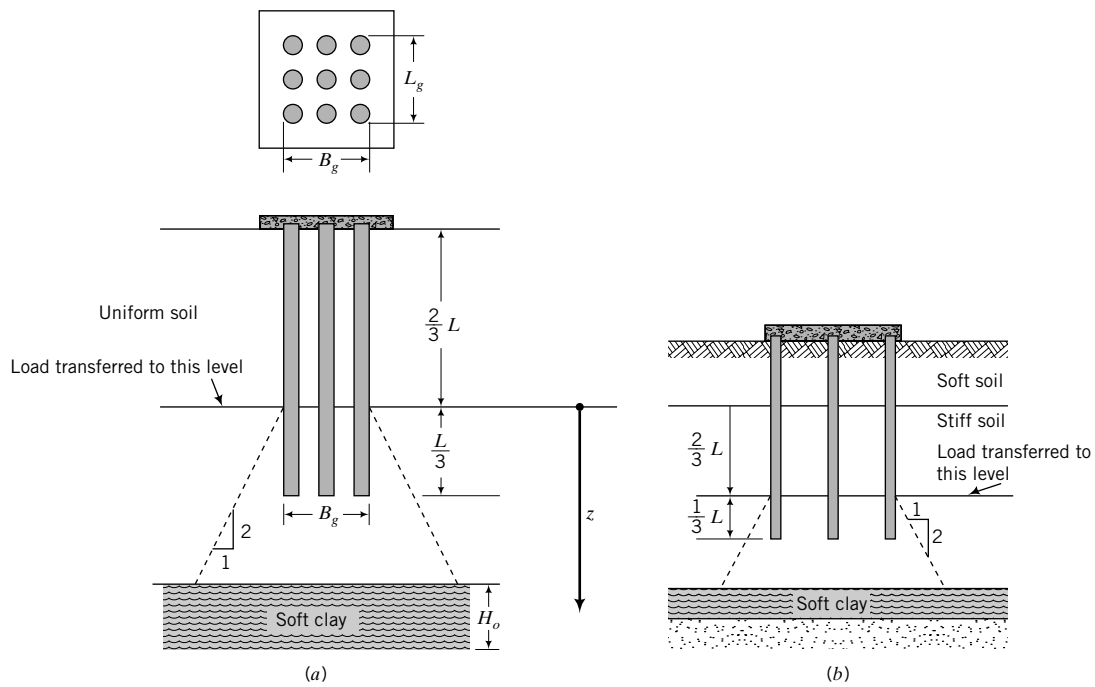


FIGURE 13.20 Assumed distribution of load for calculating settlement of a pile group.

where Q_{ag} is the allowable group load, B_g is the width of the group, L_g is the length of the group, and z is the depth from the load transfer point on the pile group to the location in the clay layer at which the increase in vertical stress is desired. The primary consolidation settlement is then calculated using the procedure described in Section 9.4.

13.13 PROCEDURE TO ESTIMATE SETTLEMENT OF SINGLE PILES AND GROUP PILES

The procedure to estimate the settlement of single piles and group piles is:

1. Obtain the required parameters Q_{af} or Q_{ag} , E_{so} , and E_p .
2. Calculate the elastic settlement, ρ_{es} , for a single pile using Equation (13.53) or (13.56) or (13.58).
3. Calculate the elastic shortening (ρ_p) using Equation (13.59).
4. Calculate the total elastic settlement, $\rho_{et} = \rho_{es} + \rho_p$.

For group piles, skip procedure 4 and continue as follows:

5. Calculate R_s using an estimated value of Φ .
6. Calculate the group settlement from $(\rho_e)_g = R_s \rho_{es} + \rho_p$.
7. Calculate the consolidation settlement, ρ_{pc} , if necessary.
8. Add the elastic and the consolidation settlement to obtain the total group settlement.

THE ESSENTIAL POINTS ARE:

1. Settlement of piles is determined using numerical analyses assuming the soil is an elastic material or empirical correlations.
2. The equations for pile settlement will give only an estimated settlement.

EXAMPLE 13.11 Settlement of a Single Pile

Determine the settlement of the pile in Example 13.4 using $E_p = 20 \times 10^6$ kPa, $E_{so} = 5000$ kPa, and a design shaft friction load $Q_a = 70$ kN.

Strategy This is a straightforward application of the procedure in Section 13.12.

Solution 13.11

Step 1: Determine the influence factor.

$$\frac{L}{D} = \frac{10}{0.4} = 25$$

$$I = 0.5 + \log\left(\frac{L}{D}\right) = 0.5 + \log(25) = 1.9$$

$$K_{ps} = \frac{E_p}{E_{so}} = \frac{20 \times 10^6}{5000} = 4000$$

From Figure 13.19, $I_p = 0.09$ for $K_{ps} = 4000$ and $L/D = 25$.

Step 2: Calculate the elastic settlement.

$$\begin{aligned} \text{Equation (13.53): } \rho_{es} &= \frac{Q_{af}}{E_{so}L} I = \frac{70}{5000 \times 10} \times 1.9 \\ &= 2.7 \times 10^{-3} \text{ m} = 2.7 \text{ mm} \end{aligned}$$

$$\begin{aligned} \text{Equation (13.58): } \rho_{es} &= \frac{Q_{af}}{E_{so}D} I_p = \frac{70}{5000 \times 0.4} \times 0.09 \\ &= 3.2 \times 10^{-3} \text{ m} = 3.2 \text{ mm} \end{aligned}$$

Difference between the two solutions is 0.5 mm. Use an average value of 3 mm.

Step 3: Calculate the elastic shortening of the pile.

$$\begin{aligned} \text{Equation (13.59): } \rho_p &= C \frac{Q_{af}L}{E_p A_p} \\ A_p &= \frac{\pi \times 0.4^2}{4} = 0.126 \text{ m}^2; \quad C = 0.7 \\ \rho_p &= 0.7 \frac{70 \times 10}{20 \times 10^6 \times 0.126} \\ &= 277.8 \times 10^{-6} \text{ m} \cong 278 \times 10^{-3} \text{ mm} \end{aligned}$$

The elastic shortening of the pile is extremely small and can be neglected.

Step 4: Determine the total elastic settlement.

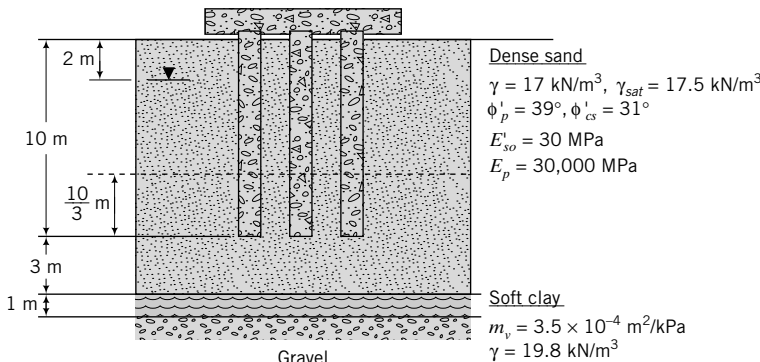
$$\rho_{et} = \rho_{es} + \rho_p = 3.0 + (\approx 0) = 3.0 \text{ mm}$$

The estimated total elastic settlement is approximately 3 mm.

$$\frac{\rho_t}{D} = \frac{3}{400} \times 100 = 0.75\%$$

EXAMPLE 13.12 Settlement of Group Piles

A 3×3 concrete pile group with a pile spacing of 1 m and pile diameter of 0.4 m supports a load of 2.5 MN (Figure E13.12). (a) Determine the factor of safety for the pile group. (b) Calculate the total settlement of the pile group. The piles were driven.

**FIGURE E13.12**

Strategy Follow the procedure in Section 13.13.

Solution 13.12

Step 1: Determine the geometric parameters, β and N_q .

$$D = 0.4 \text{ m}, \frac{L}{D} = \frac{10}{0.4} = 25; n = 9 \text{ piles}, s = 1 \text{ m}$$

$$\text{Single pile: Perimeter} = \pi D = \pi \times 0.4 = 1.26 \text{ m}; A_b = \frac{\pi D^2}{4} = \frac{\pi \times 0.4^2}{4} = 0.126 \text{ m}^2$$

$$\text{Group: } B_g = L_g = 2s + D = 2 \times 1 + 0.4 = 2.4 \text{ m}$$

$$\text{Area of group} = L_g \times B_g = 2.4^2 = 5.76 \text{ m}^2; \text{ Perimeter} = 2(L_g + B_g) = 2(2.4 + 2.4) = 9.6 \text{ m}$$

$$N_q = 0.6 \exp(0.126 \phi'_{cs}) = 0.6 \exp(0.126 \times 31^\circ) = 30$$

$$K_{ps} = \frac{E_p}{E'_{so}} = \frac{30 \times 10^6}{30,000} = 1000$$

$$\text{For } \phi' = \phi'_{l} = \phi'_{cs}, \beta = (1 - \sin \phi'_{cs}) \tan \phi'_{cs} = (1 - \sin 31^\circ) \tan 31^\circ = 0.29.$$

Step 2: Determine the single pile failure mode load capacity.

$$\text{Sand: } \gamma' = 17.5 - 9.8 = 7.7 \text{ k/m}^3$$

Center of sand layer within embedment length of the pile:

$$\sigma'_z = 2 \times 17 + 3 \times 7.7 = 57.1 \text{ kPa}$$

$$\text{At base: } (\sigma'_z)_b = 2 \times 17 + 8 \times 7.7 = 95.6 \text{ kPa}$$

$$\begin{aligned} \text{Skin friction: } Q_f &= \beta \sigma'_z \times \text{perimeter} \times \text{length} \\ &= 0.29 \times 57.1 \times 1.26 \times 10 = 209 \text{ kN} \end{aligned}$$

$$\text{End bearing: } Q_b = N_q (\sigma'_z)_b A_b = 30 \times 95.6 \times 0.126 = 361 \text{ kN}$$

$$\text{Ultimate load capacity: } Q_{ult} = Q_f + Q_b = 209 + 361 = 570 \text{ kN}$$

$$(Q_{ult})_{gs} = n Q_{ult} = 9 \times 570 = 5130 \text{ kN}$$

Step 3: Determine the block failure mode load capacity by proportion.

$$\text{Skin friction: } (Q_f)_{gb} = 209 \times \frac{9.6}{1.26} = 1592 \text{ kN}$$

$$\text{End bearing: } (Q_b)_g = 361 \times \frac{5.76}{0.126} = 16,503 \text{ kN}$$

$$\text{Ultimate load capacity: } (Q_{ult})_{gb} = (Q_f)_g + (Q_b)_g = 1592 + 16,503 = 18,095 \text{ kN}$$

Step 4: Calculate the factor of safety.

The single pile failure mode governs.

$$\therefore \text{FS} = \frac{5130}{2500} \cong 2$$

Step 5: Calculate the elastic settlement of the pile.

$$Q_{af} = \frac{209}{2} \approx 105 \text{ kN}$$

$$\text{For } \frac{L}{D} = 25, \quad I = 0.5 + \log(25) = 1.9$$

$$\rho_{es} = \frac{Q_{af}}{E_{so} L}, \quad I = \frac{105}{30,000 \times 10} \times 1.9 = 0.7 \times 10^{-3} = 0.7 \text{ mm}$$

Neglect elastic shortening of the pile since $K_{ps} > 500$.

Assume $\Phi = 0.5$.

$$R_s = n^\Phi = 9^{0.5} = 3$$

$$(\rho_{es})_g = 0.7 \times 3 \approx 2 \text{ mm}$$

The pile base must support a load of $2500 - 9 \times 105 = 1555 \text{ kN}$.

$$\text{Settlement from end bearing is } \rho_b = \frac{Q_b}{r_b G_b} \frac{1-v}{4}$$

$$\text{Equivalent base radius } r_b = \sqrt{\frac{\text{base area}}{\pi}} = \sqrt{\frac{5.76}{\pi}} = 1.35 \text{ m}$$

$$\text{Shear modulus, assuming } v = 0.3, \text{ is } G_b = \frac{E_{so}}{2(1+v)} = \frac{30,000}{2(1+0.3)} = 11,538 \text{ kPa}$$

$$\therefore \rho_b = \frac{1555}{1.35 \times 11,538} \times \frac{1-0.3}{4} = 0.017 \text{ m} = 17 \text{ mm}$$

$$\therefore (\rho_{es})_g = (\rho_{es})_g + \rho_b = 2 + 17 = 19 \text{ mm}$$

From Section 13.4, we learned that the skin friction is mobilized in advance of the end bearing capacity. Let us consider that the full skin friction is mobilized; then the load to be carried by end bearing is $2500 - 9 \times 209 = 619 \text{ kN}$.

$$\text{Settlement from skin friction is by proportion } \frac{209}{105} \times 0.7 = 1.4 \text{ mm}$$

$$\text{Settlement from end bearing is by proportion } \frac{619}{1555} \times 17 = 6.8 \text{ mm}$$

$$\therefore (\rho_{es})_g = 1.4 \times n^\Phi + 6.8 = 1.4 \times 9^{0.5} + 6.8 \approx 11 \text{ mm}$$

Step 6: Calculate the consolidation settlement.

The design load is transferred to $\frac{2}{3}L$ from the surface. The distance of the load transfer plane to the center

of the clay is $\frac{L}{3} + 3 + \frac{1}{2} = \frac{10}{3} + 3 + \frac{1}{2} = 6.83 \text{ m}$.

$$\Delta\sigma_z = \frac{Q_{ag}}{(B_g + z)^2} = \frac{2500}{(2.4 + 6.83)^2} = 29.3 \text{ kPa}$$

$$\rho_{pc} = m_v H_o \Delta\sigma_z = 3.5 \times 10^{-4} \times 1 \times 29.3$$

$$= 102.7 \times 10^{-4} \text{ m} \approx 10 \text{ mm}$$

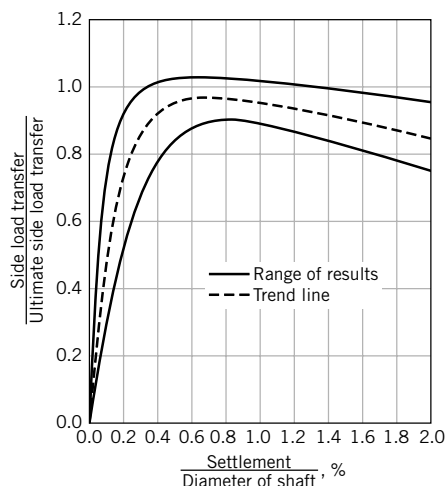
Step 7: Compute the total settlement.

$$\text{Low estimate: } \rho_t = (\rho_{es})_g + \rho_{pc} = 11 + 10 = 21 \text{ mm}$$

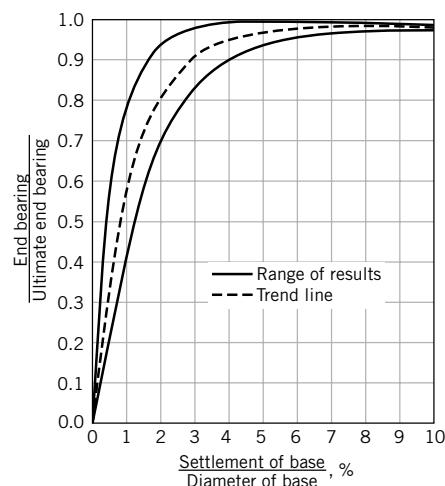
$$\text{High estimate: } \rho_t = (\rho_{es})_g + \rho_{pc} = 19 + 10 = 29 \text{ mm}$$

13.14 SETTLEMENT OF DRILLED SHAFTS

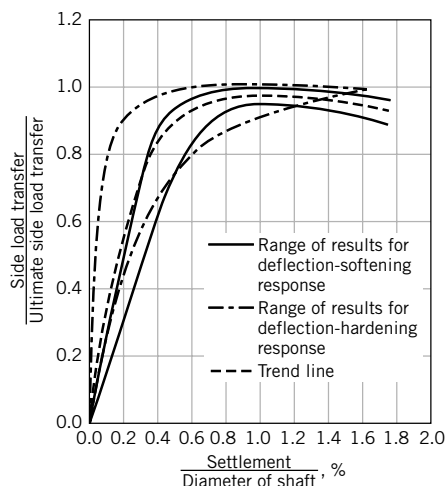
The short-term settlement of drilled shafts, based on field data, is shown in Figure 13.21. The load-settlement curves for fine-grained soils due to skin friction show plateau values between 0.2% and 0.8% of the pile diameter, but for end bearing, the plateau values are between 2% and 5%. For coarse-grained soils, the load-settlement curves show plateau values between 0.1% and 1% for skin friction, but for end bearing, no plateau value was observed. Rather, the load-settlement curve shows increasing settlement. These latter results illustrate the difficulty in predicting the load-settlement response of piles in particularly coarse-grained soils. Consequently, confidence in the prediction depends on experience with similar soil and construction conditions.



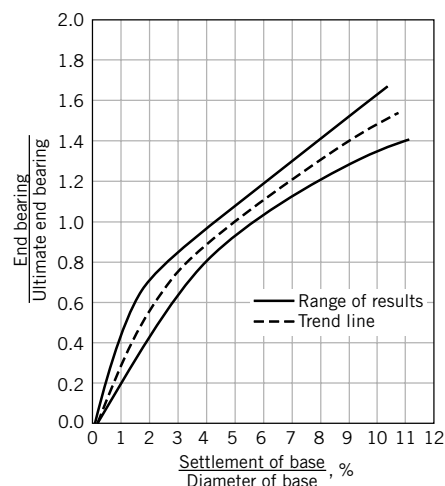
(a) Load transfer in skin friction in fine-grained soils



(b) Load transfer in end bearing in fine-grained soils



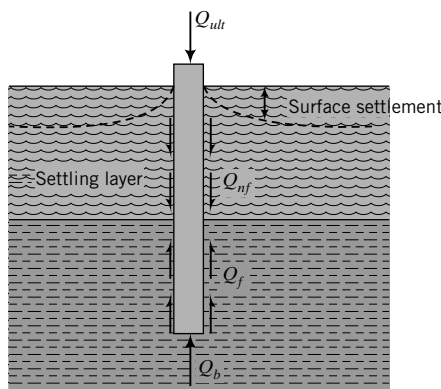
(c) Load transfer in skin friction in coarse-grained soils



(d) Load transfer in end bearing in coarse-grained soils

FIGURE 13.21 Load transfer-settlement curves for drilled shaft.

(Source: Reese and O'Neill, 1988.)

**FIGURE 13.22** Negative skin friction.

13.15 PILES SUBJECTED TO NEGATIVE SKIN FRICTION

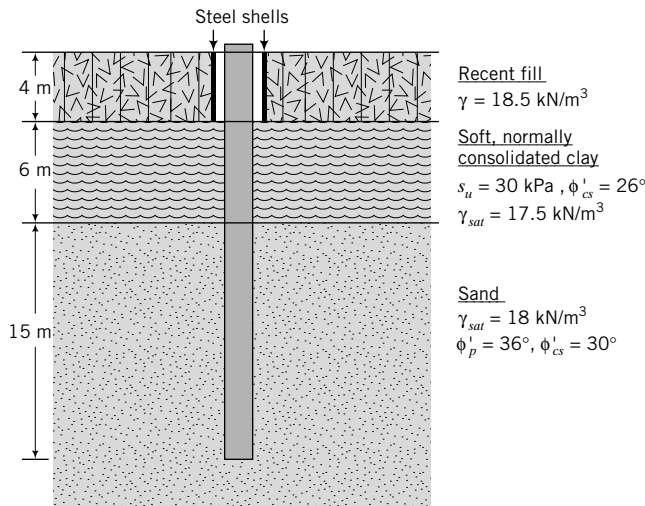
Piles located in setting soil layers (e.g., soft clays or fills) are subjected to negative skin friction called downdrag (Figure 13.22). The settlement of the soil layer causes the friction forces to act in the same direction as the loading on the pile. Rather than providing resistance, the negative friction imposes additional loads on the pile. The net effect is that the pile load capacity is reduced, and pile settlement increases. The allowable load capacity is given, with reference to Figure 13.22, as

$$Q_a = \frac{Q_b + Q_f}{FS} - Q_{nf} \quad (13.68)$$

For a soft, normally consolidated soil, the negative skin friction is usually calculated over one-half its thickness. Negative skin friction should be computed for long-term condition; that is, you should use an ESA.

EXAMPLE 13.13 Negative Skin Friction Due to a Fill

Determine the allowable load capacity of the 0.4-m-diameter pile shown in Figure E13.13. The fill is recent and unconsolidated. To eliminate negative skin friction, a steel shell is proposed around the pile within the fill. The groundwater level is at 1 m below the fill in the soft clay but is expected to rise to the surface. A factor of safety of 2 is required.

**FIGURE E13.13**

Strategy The trick here is to think about what would happen or is happening to the soft clay. Under the load of the fill, the soft clay will settle, dragging the pile down. Therefore, we have to consider negative skin friction imposed by the soft clay. You should use an ESA. Since the pile would likely loosen the dense sand adjacent to it, you should use ϕ'_{cs} rather than ϕ'_p .

Solution 13.13

Step 1: Determine β , N_q , and other relevant parameters.

$$\frac{L}{D} = \frac{25}{0.4} = 62.5; \text{ Perimeter} = \pi D = 0.4\pi = 1.26 \text{ m}$$

$$A_b = \frac{\pi D^2}{4} = \frac{\pi \times 0.4^2}{4} = 0.126 \text{ m}^2$$

Clay

$$\beta = (1 - \sin \phi'_{cs}) \tan \phi'_{cs} (\text{OCR})^{0.5} = (1 - \sin 26^\circ) \tan (26^\circ)(1)^{0.5} = 0.27$$

Sand

$$\beta = (1 - \sin \phi'_{cs}) \tan \phi'_{cs} = (1 - \sin 30^\circ) \tan (30^\circ) = 0.29$$

$$N_q = 0.6 \exp(0.126 \phi'_{cs}) = 0.6 \exp(0.126 \times 30^\circ) = 26.3$$

Step 2: Calculate the negative skin friction for the clay layer.

Assume the groundwater will rise to the surface and the top one-half of the soft clay will be subjected to negative skin friction.

$$\gamma'_{fill} = 18.5 - 9.8 = 8.7 \text{ kN/m}^3$$

$$\gamma'_{clay} = 17.5 - 9.8 = 7.7 \text{ kN/m}^3$$

At center of the upper half of the clay later:

$$\sigma'_z = 8.7 \times 4 + 7.7 \times \frac{3}{2} = 46.4 \text{ kPa}$$

$$Q_{nf} = \beta \sigma'_z \times \text{perimeter} \times \text{length} = 0.27 \times 46.4 \times 1.26 \times 3 = 47 \text{ kN}$$

Step 3: Calculate skin friction of the lower half of soft clay.

At center of the lower half of the clay layer:

$$\sigma'_z = 8.7 \times 4 + 7.7 \times 4.5 = 69.5 \text{ kPa}$$

$$(Q_f)_{clay} = \beta \sigma'_z \times \text{perimeter} \times \text{length} = 0.27 \times 69.5 \times 1.26 \times 3 = 71 \text{ kN}$$

Step 4: Calculate the skin friction and end bearing in sand.

$$\gamma'_{sand} = 18 - 9.8 = 8.2 \text{ kN/m}^3$$

At center of sand layer:

$$\sigma'_z = 8.7 \times 4 + 7.7 \times 6 + 8.2 \times 7.5 = 142.5 \text{ kPa}$$

$$Q_f = 0.29 \times 142.5 \times 1.26 \times 15 = 781 \text{ kN}$$

$$(\sigma'_z)_b = 8.7 \times 4 + 7.7 \times 6 + 8.2 \times 15 = 204 \text{ kPa}$$

$$Q_b = N_q (\sigma'_z)_b A_b = 26.3 \times 204 \times 0.126 = 676 \text{ kN}$$

Step 5: Calculate the allowable load capacity.

$$Q_a = (Q_f)_{clay} + \frac{(Q_f)_{sand} + (Q_b)_{sand}}{2} - Q_{nf} = \frac{71 + 781 + 676}{2} - 47 = 717 \text{ kN}$$

13.16 PILE-DRIVING FORMULAS AND WAVE EQUATION

A number of empirical equations have been proposed to relate the energy delivered by a hammer during pile driving and the pile load capacity. One of the earliest equations is the ENR (*Engineering News Record*) equation, given as

$$Q_{ult} = \frac{\eta_i W_R h}{s_1 + C_1} \quad (13.69)$$

where η_i is an efficiency factor (drop hammer, $\eta_i = 0.75\text{--}1.0$; single-acting hammer, $\eta_i = 0.75\text{--}0.85$; and diesel hammer, $\eta_i = 0.85\text{--}1.0$), W_R is the weight of the ram, h is the height of fall, s_1 is the penetration per blow, and C_1 is a constant. For drop hammers, $C_1 \approx 25$ mm; for steam hammers, $C_1 \approx 2.5$ mm. The units of h and s_1 must be the same. The ENR equation was developed for timber piles using drop hammers for installation, but is used to estimate or check the ultimate load capacity of all types of piles. Equation (13.69) does not account for energy losses due to the elastic compression of the pile. This equation can be modified using an efficiency factor, η_1 ; that is,

$$Q_{ult} = \frac{\eta_1 W_R h}{s_1 + C_1} \quad (13.70)$$

Suggested ranges of values for η_1 are shown in Table 13.4.

When a hammer strikes a pile, the shock sets up a stress wave, which moves down the pile at the speed of sound. From elastic theory, the change in force on the pile over an infinitesimal length Δz , assuming the pile to be a rod, is

$$\frac{\partial F}{\partial z} = E_p A_p \frac{\partial}{\partial z}(\varepsilon_z) = E_p A_p \frac{\partial^2 u}{\partial z^2} \quad (13.71)$$

where $\varepsilon_z = \partial u / \partial z$ is the vertical strain, E_p is Young's modulus of the pile, A_p is the cross-sectional area of the pile, and u is the pile displacement. From Newton's second law,

$$\frac{\partial F}{\partial z} = A_p \frac{\gamma}{g} \frac{\partial^2 u}{\partial t^2} \quad (13.72)$$

where g is the acceleration due to gravity and t is time. Setting Equation (13.72) equal to Equation (13.71), we get

$$E_p A_p \frac{\partial^2 u}{\partial z^2} = \frac{\gamma}{g} A_p \frac{\partial^2 u}{\partial t^2} \quad (13.73)$$

which, by simplification, leads to

$$\frac{\partial^2 u}{\partial t^2} = V_c^2 \frac{\partial^2 u}{\partial z^2} \quad (13.74)$$

TABLE 13.4 Hammer Efficiency

Hammer type	η_1
Drop hammer	0.75–1.0
Single-acting hammer	0.75–0.85
Double-acting hammer	0.85
Diesel hammer	0.85–1.0

where

$$V_c = \sqrt{\frac{E_p g}{\gamma}} \quad (13.75)$$

is the vertical wave propagation velocity in the pile.

The solution of Equation (13.74) is found using appropriate boundary conditions and can be modified to account for soil resistance. Computer programs (e.g., WEAP) have been developed for routine wave analysis of pile-driving operations. These programs are beyond the scope of this book.

Driving records can provide useful information on the consistency of a soil at a site. For example, if the number of blows to drive a pile at a certain depth is A blows at one location and B blows at another location at the same site, then the soil stratification is different. You should reexamine your design and the soil-boring records and make the necessary adjustments—for example, increase or decrease the pile length.

THE ESSENTIAL POINTS ARE:

- 1. A number of empirical equations are available to estimate the pile load capacity from driving records.**
- 2. Driving records can provide some useful information regarding the character of the soil at a site.**
- 3. Careful judgment and significant experience are required to rely on pile load capacity from pile-driving operations.**

What's next . . . Piles are often used to resist lateral loads and moments in addition to vertical loads. The analysis of laterally loaded piles is complex, and only a brief introduction is presented in the next section.

13.17 LATERALLY LOADED PILES



Computer Program Utility

Access www.wiley.com/college/budhu, click on Chapter 13, and download program APILES to predict the response of single, laterally loaded piles.

Structures founded on piles are often subjected to lateral loads and moments in addition to vertical loads. Lateral loads may come from wind, traffic, seismic events, waves, docking ships, and earth pressures. Moments may come from the eccentricity of the vertical force, fixity of the superstructure to the piles, and the location of the lateral forces on the pile with reference to the ground surface.

When a pile is subjected to lateral forces and moments, the pile tends to bend or deflect, as illustrated in Figure 13.23. The deflection of the pile causes strains in the soil mass. To satisfy equilibrium, the soil must provide reactions along the length of the pile to balance the applied loads and moments.

Because soil is a nonlinear material, the soil reaction is not linearly related to the pile deflection. Consequently, at every point along the length of the pile, a nonlinear relationship between soil resistance (p) and pile deflection (y) exists, as illustrated in Figure 13.23.

In designing laterally loaded piles, we need to know the pile deflection, particularly the pile head deflection, to satisfy serviceability requirements and the bending moments for sizing the pile. The pile head deflection depends on soil type, pile installation, pile flexibility (or pile stiffness), loading condition,

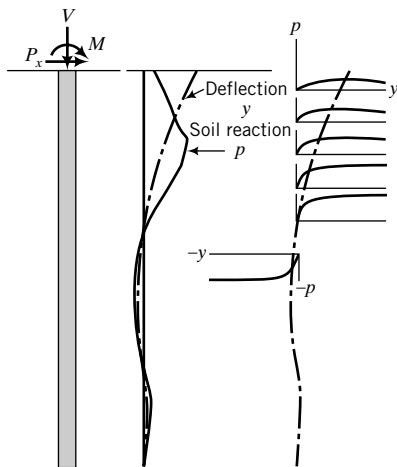


FIGURE 13.23 Pile-soil response to lateral loads and moments.

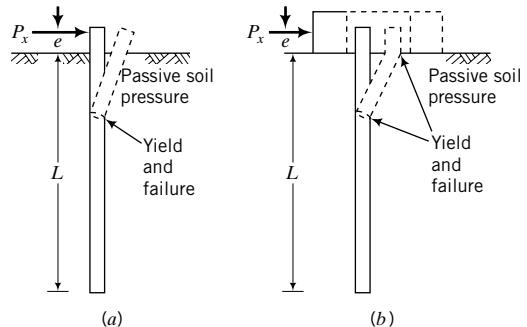


FIGURE 13.24 Possible failure modes for long piles ($L/D > 10$): (a) free head, (b) fixed head.

and how the pile is attached to the superstructure and pile cap. A pile that is attached to the pile cap such that no rotation occurs is called a fixed head pile (Figure 13.24a). A pile that is attached to the pile cap such that rotation is unrestricted is called a free head pile (Figure 13.24b).

The mechanism of failure depends on the length-to-diameter or -width ratio, soil type, and the fixity of the pile head. Free head piles tend to fail by rotation. Lateral loads and moments applied to a free head pile are initially resisted by the soil near ground level. For very small pile deflections, the soil behaves elastically, and as the deflection increases the soil yields, and then permanent soil displacement occurs. The soil resistance is shifted to the lower part of the pile as yielding progressively occurs from the top to the bottom of the pile. Fixed head piles tend to fail by translation. Piles in general are neither fixed head nor free head. They have undermined fixity somewhere between free head and fixed head conditions. You can view fixed head and free head as two limiting conditions in which, in practice, piles will respond somewhere within these limits.

Laterally loaded piles, particularly group piles, are difficult to analyze, mainly because of the complexity of the soil-structure (pile) interaction. The displacements and rotations are in the directions of the resultant lateral load and resultant moment (Figure 13.25). Outer piles in a group are subjected to uplift (pull) and compressive (push) forces, while the piles in the center translate at the level of the superstructure connection. The response of a pile group to lateral loads and moments is influenced by

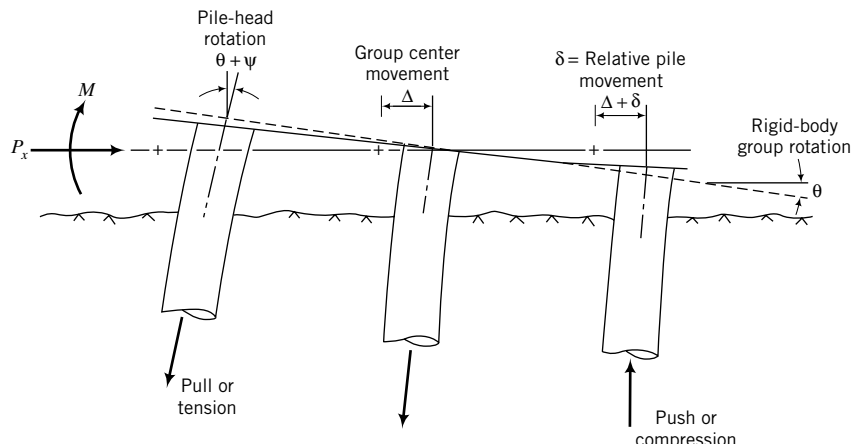


FIGURE 13.25 Group piles subjected to lateral loads.

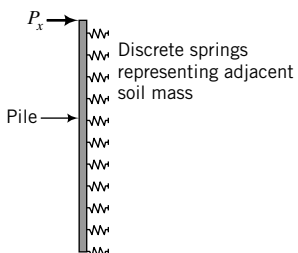


FIGURE 13.26
Simulation of adjacent soil mass as a set of discrete springs.

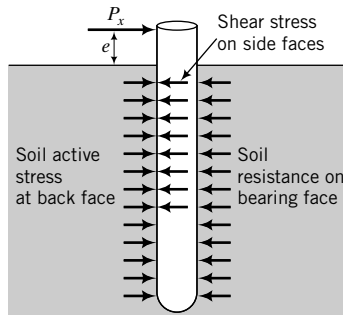


FIGURE 13.27 Soil stresses on a pile segment resulting from lateral loads treating soil as a continuum.

1. Geometry of the group.
2. Pile-soil interaction.
3. Stiffness or flexibility of the piles.
4. Load conditions.
5. Individual pile response.
6. Pile group response resulting from individual pile responses.

Two types of analyses are often used in design practice. One is the p - y (soil resistance-pile deflection) method (Reese, 1984, and others) that represents the soil as discrete springs (Figure 13.26). The p - y relationships are obtained from results of high-quality, instrumented, laterally loaded test piles. General procedures have been developed to construct p - y curves for many soil types, lessening the need to conduct lateral load tests, at least in the preliminary stages of design. However, it is recommended that laterally loaded pile tests be conducted whenever such tests are feasible and economical. Computer programs (e.g., Com624, obtained from <http://isddc.dot.gov/OLPFiles/FHWA/009745.pdf>, and various commercial derivatives of Com624) are available for routine use. The p - y method neglects soil continuity and soil shearing resistance.

The other method is a continuum analysis that represents the soil as a continuous medium, with assumptions made on its stress-strain behavior or constitutive relationships (Figure 13.27). The simplest stress-strain behavior is elastic, described by Hooke's law. The solution gives the load-deformation response of the pile for small strain levels (Poulos, 1971; Randolph, 1981). Soil yielding or pile yielding cannot be obtained from this analysis. To account for soil yielding, the soil can be assumed to be an elastoplastic material (Davies and Budhu, 1986; Budhu and Davies, 1987, 1988). A computer program for the elastoplastic (elastic-rigid plastic) solution is available at www.wiley.com/college/budhu (Chapter 13, APILES) accompanying this textbook. The use of this program and other programs based on the p - y method and the interpretation of the results for practice require significant experience.

THE ESSENTIAL POINTS ARE:

1. Lateral loads and moments cause piles to deflect laterally, and the soil must provide reactions along the length of the pile to balance these applied loads and moments.
2. The analysis of laterally loaded piles is a complex soil-structure interaction problem.
3. Computer programs are available to analyze laterally loaded piles, but the use and interpretation of the results from these programs require significant experience.

EXAMPLE 13.14 Laterally Loaded Single Pile–Continuum Analysis

A 460-mm-diameter timber pile of total length 10 m is embedded to a depth, L , of 9.14 m in a soft, normally consolidated clay deposit of medium plasticity. The strength and elastic modulus of the soil vary linearly with depth. The working stress, σ_w , for timber of this quality is 11 MN/m², and its Young's modulus of elasticity is 10.3 GN/m². A lateral load is to be applied at a height, e , of 690 mm above ground level. Required are: (1) the working load, (2) the lateral deflection at the working load, and (3) the maximum bending moment at the working load. Assume the following: adhesion factor, $\alpha_u = 1$; lateral earth pressure coefficient, $K_o = 1$; effective unit weight, $\gamma' = 9.4 \text{ kN/m}^3$; the slope of the linear variation of undrained shear strength with depth, $c = 2.7 \text{ kN/m}^3$; and the slope of the linear variation of elastic modulus with depth, $m = 2.7 \text{ MN/m}^3$, i.e., $m/c = 1000$.



Strategy Use the program APILES located at <http://www.wiley.com/college/budhu>, Chapter 13.

Solution 13.14

Step 1: Enter input data interactively using the program APILES.

Step 2: Evaluate results.

The echoed input data and the results are given below.

TITLE: Example 13.14

Your input data are as follows.

PILE DATA

Head type: Free head with eccentricity

Eccentricity	=	0.69 m
Length	=	9.14 m
Diameter	=	0.46 m
Young's modulus	=	.10E + 08 kPa
Working stress	=	.11E + 05 kPa

SOIL DATA

Soil type: Soft clay

Effective unit weight of soil	=	9.4000 kN/m ³
Earth pressure coefficient	=	1.00
Adhesion factor	=	1.00
Young's modulus at surface	=	.00E + 00 kPa
Rate of increase of Young's modulus with depth	=	.27E + 04 kN/m ³
Undrained shear strength at surface	=	.00 kPa
Rate of increase of undrained shear strength with depth	=	.27E + 01 kN/m ³

The working load is 42.54 kN; pile head displacement = 31 mm; maximum bending moment is 95 kN.m.

The bending moments and rotations are computed at ground surface.

Load (kN)	Disp. (mm)	Moment (kN.m)	Rotation (radians)	Max. B.M. (kN.m)	Depth to max. B.M. (m)
4.50	1.82	3.10	.04	7.45	1.66
4.91	1.99	3.39	.04	8.14	1.66
6.65	2.74	4.59	.06	11.29	1.66
9.40	4.03	6.48	.08	16.51	1.74
12.96	5.85	8.94	.12	23.45	1.84
13.77	6.27	9.50	.13	25.06	1.85
13.88	6.32	9.57	.13	25.25	1.86

14.48	6.65	9.99	.13	26.42	1.86
18.42	8.88	12.71	.18	34.38	1.92
19.62	9.61	13.54	.19	36.98	1.94
20.79	10.35	14.34	.20	39.64	1.96
23.74	12.31	16.38	.24	46.31	1.99
28.67	15.82	19.78	.30	57.83	2.06
30.96	17.61	21.36	.34	63.71	2.10
31.31	17.90	21.61	.34	64.64	2.10
37.83	23.57	26.10	.44	81.49	2.20
39.94	25.62	27.56	.47	87.52	2.24
45.25	31.14	31.22	.57	102.82	2.34
46.58	32.56	32.14	.59	106.68	2.36
50.68	37.58	34.97	.67	119.38	2.45
55.77	44.17	38.48	.77	135.47	2.54

The load–displacement results are shown in Figure E13.14.

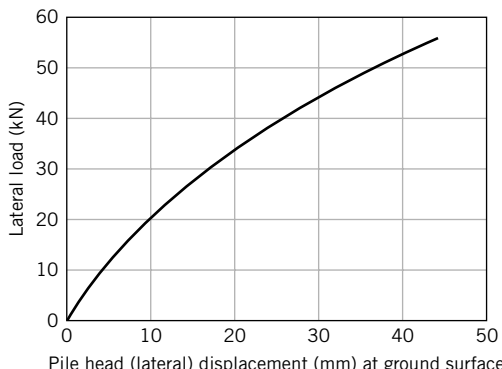


FIGURE E13.14

13.18 MICROPILES

Micropiles, also called minipiles, pin piles, needle piles, or root piles, have been in use in Europe since the 1950s and have grown in popularity globally. They are small-diameter piles, usually less than 300 mm, and are particularly suitable for:

1. Supporting structural loads at sites with restricted access or low headroom.
2. Retrofitting/rehabilitating distressed structures.
3. Underpinning.
4. Excavation and retention systems with restricted access.
5. Seismic retrofit.
6. Expansive soils.

They are also used as alternatives to conventional piles and as anchors in retaining systems and slopes. The method of construction depends on the application (see Table 13.5).

The design of micropiles requires several steps and several years of appropriate experience. It is beyond the scope of this textbook. The reader may refer to “FHWA, Micropile Design and Construction Guidelines, Implementation Manual, Publication No. FHWA-SA-97-070, 2000” for design information.

TABLE 13.5 Summary of Installation and Load Capacity of Micropiles

Type	Soil condition	Installation	Capacity (kN)
Driven or pushed	Loose or soft materials above stiff soils	Driven or pushed through the top soil layer and embedded in the stiff layer.	25–300
Compaction grouted	Loose, sandy soils	Grout is poured into the casing and compacted.	150–750
Jet grouted	Loose soils	Grout applied under pressure.	500–1500
Post grouting	Loose soils	A tube is inserted at the base of the micropile. Grout is applied under high pressure.	400–1000
Permeation grouting	Loose soils	Grout is pressure-injected into the soil to fill void spaces.	250–705
Drilled	Stiff soil or rock	A hole is made by a spiral auger and grouted as the auger is removed, similar to drilled shafts.	500–1000

13.19 SUMMARY

Piles are used to support structural loads that cannot be supported on shallow foundations. The predominant types of pile material are steel, concrete, and timber. The selection of a particular type of pile depends on availability, environmental conditions, pile installation methods, and cost. Pile load capacity cannot be determined accurately because the method of installation invariably changes the soil properties near the pile. We do not know the extent of these changes. The equations for pile load capacities and settlement are, at best, estimates. Load capacities from pile load tests are preferred, but these tests are expensive and may only be cost-effective for large projects.

Self-Assessment

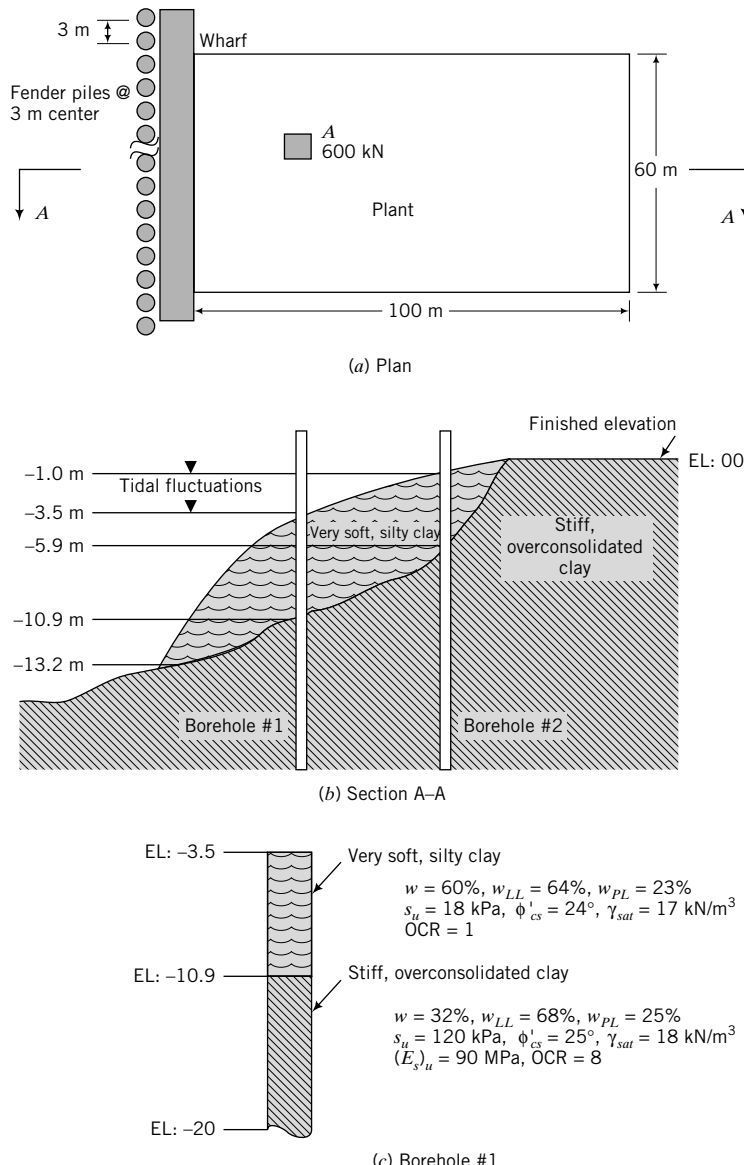
Access Chapter 13 at <http://www.wiley.com/college/budhu> to take the end-of-chapter quiz to test your understanding of this chapter.



Practical Examples

EXAMPLE 13.15 Pile Design for a Fish Port Facility

A fish port facility is to be constructed near a waterfront area, as shown in Figure E13.15a, b. A soil investigation shows two predominant deposits. One is a very soft, normally consolidated clay and the other is a stiff, overconsolidated clay. Soil data on the two deposits are shown in Figure E13.15c. Determine the pile configuration (single or group piles), the pile length, and the expected settlement to support a design column load (working load) of 500 kN at A (Figure E13.15). Timber piles of average diameter 0.38 m and average length 18 m are readily available. The elastic modulus

**FIGURE E13.15**

of the pile is $E_p = 20,000$ MPa. The settlement should not exceed 0.5% of the pile diameter. The pile shafts within the tidal zone will be treated to prevent rot. From experience on this site, it is difficult to drive piles beyond 8 m in the stiff, overconsolidated clay. Driving tends to damage the pile head. You should allow for a 0.25-m cutout from the pile head.

Strategy The very soft, silty clay is likely to cause downdrag on the pile. You should determine the single pile capacity assuming the full available length of the pile will be used. If a single pile is not capable of carrying the load, then you should design a pile group. Use an ESA when you are considering downdrag.

Solution 13.15

Step 1: Determine the geometric parameters, α , β , and N_q .

$$D = 0.38 \text{ m}; \text{ Perimeter} = \pi D = \pi \times 0.38 = 1.19 \text{ m};$$

$$A_b = \frac{\pi D^2}{4} = \frac{\pi \times 0.38^2}{4} = 0.113 \text{ m}^2$$

From borehole #1, the length of pile in soft clay: $L_1 = 7.4$ m

Length of pile in stiff clay: $L_2 = 18 - 7.4 - 3.5 - 0.25 = 6.85$ m

The value 0.25 m is the cutoff length from the pile head and 3.5 m is the distance from the finished elevation to the surface of the soft soil.

$$\text{Soft clay: } \beta = (1 - \sin 24^\circ) \tan 24^\circ (1)^{1/2} = 0.26$$

$$\text{Stiff clay: } \beta = (1 - \sin 25^\circ) \tan 25^\circ (8)^{1/2} = 0.76$$

Assume $\psi_p = \pi/2$. Then,

$$N_q = \left[\tan 25^\circ + \sqrt{1 + \tan^2(25^\circ)} \right]^2 \exp\left(2 \frac{\pi}{2} \tan 25^\circ\right) = 10.7$$

Step 2: Determine the negative skin friction for a single pile.

A conservative estimate is to assume negative skin friction over the whole length of the pile in the very soft clay.

$$\text{Soft clay: } \gamma' = 17 - 9.8 = 7.2 \text{ kN/m}^3$$

$$\text{Center of top half of soft clay: } \sigma'_z = 7.2 \times \frac{3.7}{2} = 13.3 \text{ kPa}$$

$$Q_{nf} = \beta \sigma'_z \times \text{perimeter} \times L_1$$

$$Q_{nf} = 0.27 \times 13.3 \times 1.19 \times 7.4 = 32 \text{ kN}$$

Step 3: Determine the load capacity in the stiff clay for a single pile.

$$\text{Stiff clay: } \gamma' = 18 - 9.8 = 8.2 \text{ kN/m}^3$$

$$\text{Center of stiff clay: } \sigma'_z = 7.2 \times 7.4 + 8.2 \times \frac{6.85}{2} = 81.4 \text{ kPa}$$

$$\text{Base of stiff clay: } (\sigma'_z)_b = 7.2 \times 7.4 + 8.2 \times 6.85 = 109.5 \text{ kPa}$$

$$Q_f = \beta \sigma'_z \times \text{perimeter} \times L_2 = 0.76 \times 81.4 \times 1.19 \times 6.85 = 504 \text{ kN}$$

$$Q_b = N_q (\sigma'_z)_b A_b = 10.7 \times 109.5 \times 0.113 = 132 \text{ kN}$$

Step 4: Determine the allowable load capacity of a single pile.

$$Q_a = \frac{Q_f + Q_b}{3} - Q_{nf} = \frac{504 + 132}{3} - 32 = 180 \text{ kN}$$

A single pile is inadequate for the load.

Step 5: Determine the block failure for the pile group.

$$\text{Number of piles required} = \frac{600}{180} = 3.3.$$

Try 4 piles in a 2×2 matrix at a spacing of 1 m:

$$\frac{s}{D} = \frac{1}{0.38} = 2.6$$

$$B_g = L_g = s + D = 1 + 0.38 = 1.38 \text{ m};$$

$$\text{Perimeter} = (1.38 + 1.38) \times 2 = 5.52 \text{ m}; \quad A_b = 1.38^2 = 1.9 \text{ m}^2$$

$$\text{Soft clay: } Q_{nf} = 0.26 \times 13.3 \times 5.52 \times 7.4 = 147 \text{ kN}$$

$$\text{Stiff clay: } (Q_f)_g = 0.76 \times 81.4 \times 5.52 \times 6.85 = 2339 \text{ kN}$$

$$\text{Stiff clay: } (Q_b)_g = 10.7 \times 109.5 \times 1.9 = 2226 \text{ kN}$$

Step 6: Calculate the allowable load capacity for block failure mode.

$$(Q_a)_g = \frac{(Q_f)_g + (Q_b)_g}{3} - Q_{nf} = \frac{2339 + 2226}{3} - 147 = 1375 \text{ kN}$$

Step 7: Calculate the allowable load capacity for single pile failure mode.

$$\begin{aligned} n &= 4 \text{ piles} \\ (Q_a)_g &= nQ_a = 4 \times 180.6 = 722 \text{ kN} \end{aligned}$$

Therefore, a 2×2 pile group is adequate. Single pile failure mode governs the design.

Step 8: Calculate the settlement.

Assume the full design load of $Q_a = 600$ kN will be carried by skin friction (floating pile) within the stiff clay.

$$\begin{aligned} \text{Load per pile } (Q_{af}) &= \frac{600}{4} = 150 \text{ kN} \\ \frac{L}{D} &= \frac{L_2}{D} = \frac{6.85}{0.38} = 18 \end{aligned}$$

Using Equation (13.53) to calculate the elastic settlement, we get

$$\begin{aligned} I &= 0.5 + \log(18) \approx 1.8 \\ \rho_{es} &= \frac{Q_{af}}{(E_{so})_u L_2} I = \frac{150}{90,000 \times 6.85} \times 1.8 = 0.43 \times 10^{-3} \text{ m} \approx 0.4 \text{ mm} \\ \rho_p &= \frac{0.5Q_{af}L}{E_p A_p} = \frac{0.5 \times 150 \times 6.85}{20 \times 10^6 \times 0.113} = 227 \times 10^{-6} \text{ m} \approx 0.2 \text{ mm} \end{aligned}$$

From Equation (13.63): $R_s = n^\Phi$

Assume $\Phi = 0.5$: $R_s = 4^{0.5} = 2$

$$(\rho_e)_g = R_s \rho_{es} + \rho_p = 2 \times 0.4 + 0.2 = 1.0 \text{ mm}$$

$$\frac{(\rho_{es})_g}{D} = \frac{1.0}{380} = 2.6 \times 10^{-3} \approx 0.2\%$$

EXAMPLE 13.16 Design of Drilled Shafts



Computer Program Utility

Access www.wiley.com/college/budhu, click on Chapter 13, and run piles.xls to calculate the pile load capacity of straight drilled shafts.

A building is to be constructed at a site with a representative soil profile, as shown in Figure E13.16a. Nearby buildings of similar size are constructed on pile foundations. Previous records on driven piles near the site reveal significant heaving of previously installed piles during driving. In addition, pile-driving noise would be a problem with neighborhood groups. Consequently, drilled shafts should be considered. Design straight drilled shafts for the two column loads shown in Figure E13.16b; FS desired = 2.5. The column spacing is 7 m. Groundwater level is 2 m below the finished grade.

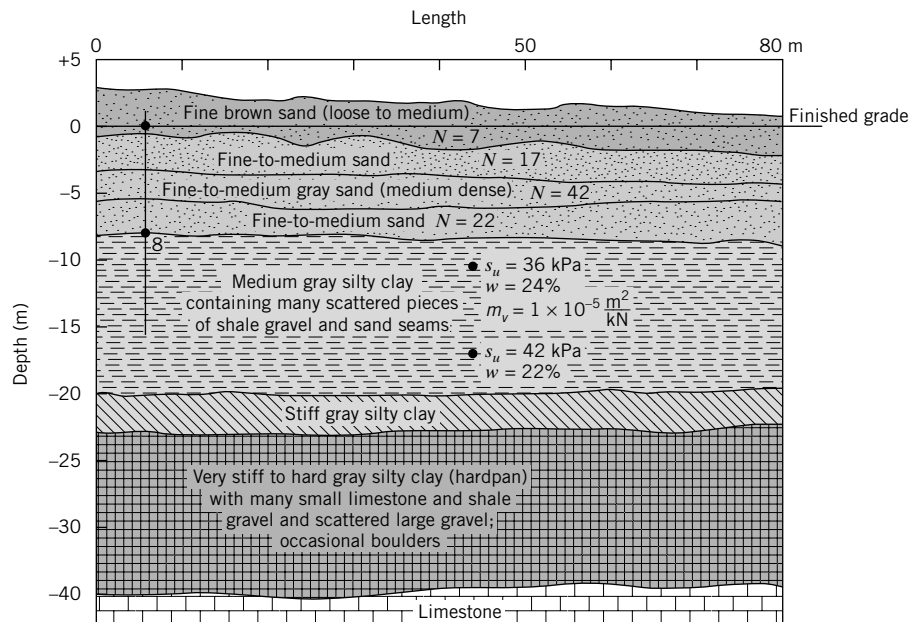


FIGURE E13.16a
Soil profile along
length of building.

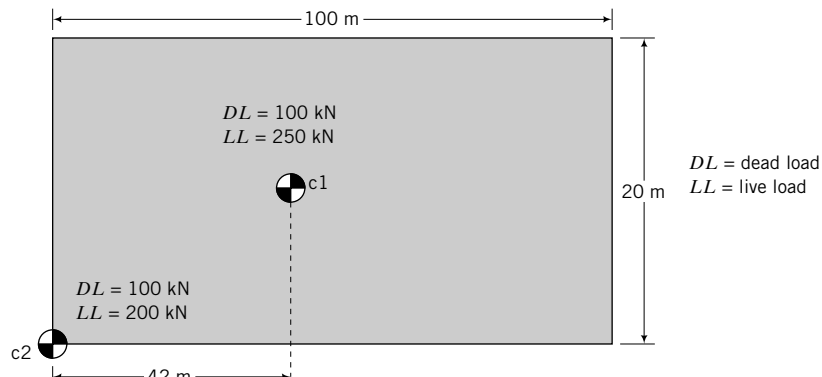


FIGURE E13.16b

Strategy Select drilled shaft diameters by adopting standard sizes used in the area. Study the soil profile and decide which soil layer seems promising as an end bearing layer. Now calculate shaft friction and end bearing resistance for different depths of embedment. For a single shaft layout, you need to check that the maximum diameter (D_{max}) should be such that the column spacing exceeds $3D_{max}$. If not, you will have to consider group action.

Solution 13.16

Step 1: Select drilled shaft diameters.

$$D_{max} < \frac{\text{column spacing}}{3} = \frac{7}{3} = 2.33 \text{ m}$$

Assume $D = 0.6 \text{ m}$.

Step 2: Select end bearing layer.

From inspection of the soil profile, we will try the medium gray silty clay layer as the end bearing layer. We will take an average s_u value of $(36 + 42)/2 = 39 \text{ kPa}$. Although the medium dense sand layer has a high N value, its thickness is too variable. The shaft could punch through this layer. It is best to have a thickness of at least 3 times diameter below the pile tip.

Step 3: Calculate side friction and end bearing capacity for different pile lengths.

For drilled shafts (straight shafts), neglect the skin friction of the top 1.5 m of soil below the finished grade and also the bottom length of one shaft diameter. No information on the unit weight of the sands is provided, so we use the correlations given in Appendix A, Table A.11.

Skin friction

$$\text{Sand: } f_s = \beta \sigma'_z$$

$$\text{Clay: } f_s = \alpha_u s_u$$

See Equations (13.39) and (13.42) for α_u and β .

End bearing

$$\text{Clay: } f_b = N_c(s_u)$$

See Equation (13.40) for N_c .

 Set up a spreadsheet to do the calculation. See spreadsheet piles.xls and worksheet drilledshafts.xls at www.wiley.com/college/budhu.

In the worksheet, the total, effective, and porewater pressures for skin friction are calculated at the middle of each depth segment.

Step 4: Evaluate the calculated skin friction and end bearing capacity and decide on pile length.

In the worksheet drilledshafts.xls, the friction on the top 1.5 m and on a length one diameter above the base is subtracted from the ultimate friction in columns Y and Z. The results show that TSA governs the design.

Pile c1

Applied vertical load = $Q_a = 350 \text{ kN}$

Design load = $Q_{ult} = (\text{FS}) \times Q_a = 2.5 \times 350 = 875 \text{ kN}$

Select pile diameter of 0.6 m.

A copy of a section of the drilled shaft worksheet in pile.xls is shown in Table E13.16a.

TABLE E13.16a

Straight, prismatic drilled shafts

Select units	SI	FS Group	2.5	Ultimate load	875 kN
Design load	350 kN		NO		
Shaft diameter	0.6 m				
Top of base layer	8 m				
Groundwater	2 m				
Use N values	yes				
Perimeter	1.88 m				
Area	0.28 m ²				
Max. end bearing	2900 kPa				

Layer no.	Depth to top of layer (m)	Thickness (m)	Depth to center (m)	Soil type	Unit weight (kN/m ³)	ϕ'	s_u (kPa)	OCR	N_{60}
0	0	0	0		0	0	0	0	0
1	1.5	1.5	0.75	s	15.5				7
2	4	2.5	2.75	s	17				17
3	6	2	5	s	20				42
4	8	2	7	s	17.5		0		22
5	10	2	9	c	20	27	39	4	
6	12	2	11	c	20	27	39	4	

Pile c2

Applied vertical load = $Q_a = 300 \text{ kN}$

Design load = $Q_{ult} = 2.5 \times 300 = 750 \text{ kN}$

Figure E13.16c shows a plot of embedded length (depth) versus the ultimate skin friction and the ultimate load capacity.

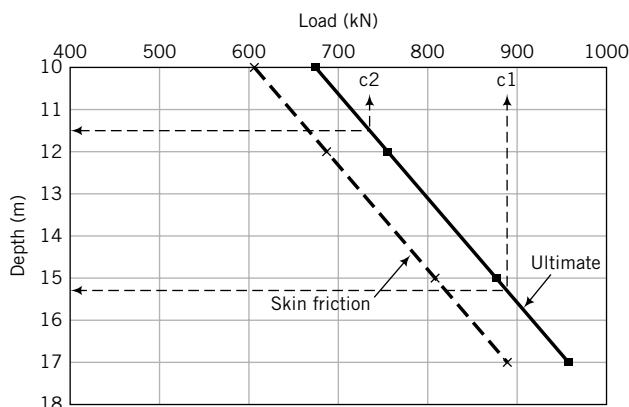


FIGURE E13.16c

A summary of the analysis so far is shown in Table E13.16b

TABLE E13.16b

Drilled shaft	Diameter (m)	Embedded length (m)	$\frac{Q_f}{Q_{ult}}$	$\frac{Q_a}{Q_f}$
c1	0.6	15	$\frac{800}{890} \times 100 = 90\%$	$\frac{350}{800} = 0.44$
c2	0.6	11.5	$\frac{660}{750} \times 100 = 88\%$	$\frac{300}{660} = 0.45$

Most of the load is transferred as side friction. These drilled shafts are friction piles.

Step 5: Evaluate the settlement from skin friction and end bearing.

Assume the working load is transferred as side friction. The settlement using an average $\frac{Q_a}{Q_f} = 0.45$, and the mid-trend line in Figure 13.21c is 0.2% of the pile diameter = $0.002 \times 600 = 1.2 \text{ mm}$.

Step 6: Calculate consolidation settlement.

The working load is transferred to a depth of $2L/3$ from the finished surface (see Figure E13.16d). An effective thickness of soil below the pile base of 3 times the pile diameter is assumed for consolidation settlement calculations. The increase of vertical stress at the center of the effective thickness is calculated using the 2:1 method, as follows.

$$\Delta\sigma_z = \frac{Q_a}{\frac{\pi}{4} \left(D + \frac{L}{3} + \frac{3D}{2} \right)^2}$$

The consolidation settlement is calculated from

$$p_{pc} = m_v H \Delta\sigma_z = m_v (3D) \Delta\sigma_z$$

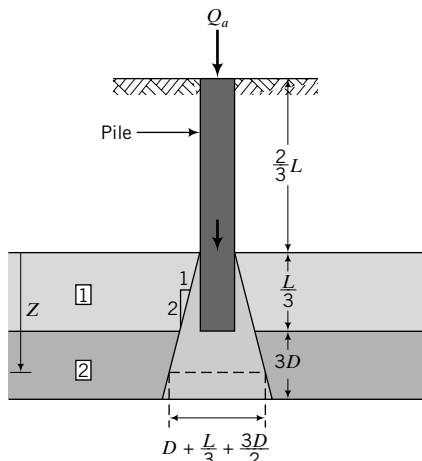


FIGURE E13.16d

See the table below for calculations.

Q_a (kN)	L (m)	$(1/3)L + 3D/2$ (m)	$A = \frac{\pi}{4} \left(D + \frac{L}{3} + \frac{3D}{2} \right)^2$ (m^2)	$\Delta\sigma_z$ (kPa)	ρ_{pc} (mm)
350	15	5.9	33.2	10.5	0.2
300	11	4.6	21.2	14.2	0.3

Step 7: Summarize design.

Pile	Q_a (kN)	Resistance	Total settlement (mm)	Differential settlement (mm)
c1	350	Friction	1.4	≈0
c2	300	Friction	1.5	≈0

You can investigate alternative solutions using different shaft diameters.

EXERCISES

Problem Solving

Use Equation (13.24) for N_q and the pile-soil interface friction angle equal to the critical state friction angle as defaults.

- 13.1** At a site for a factory building, the soil consists of 2.3 m of fill followed by 8 m of soft clay resting on a thick deposit (>10 m) of dense sand. The current groundwater level is at 4 m from the surface but fluctuates seasonally from the surface to about 5 m below it. The average column load consists of 200 kN dead load and 150 kN live

load. For a preliminary design, describe the following: (a) the type of pile you would select, (b) the minimum length you think you would need, and (c) the possible method of installation. Sufficient justification must be given for each answer.

- 13.2** A static pile load test was carried out on a 0.8-m-diameter steel pipe pile installed 21 m into a loose-to-medium sandy soil. The pile was driven into the soil. Selected load-displacement data are shown in the table on the next page. (a) Determine the allowable load if the serviceability limit state is 12 mm. (b) Is the maximum load the ultimate

load? Justify your answer. (c) Discuss some of the issues you would consider in the interpretation of the data.

Load (kN)	0	800	1100	2250	2800	3200	3500	3600	3620	3618
Displacement (mm)	0	2.5	3.8	7.5	10	12.5	15	20	21	26

- 13.3** A static pile load test using an O-cell was carried out on a 1.8-m-diameter, 25-m-long (embedded length) drilled shaft. The soil profile is as given in Table P13.3a (the negative sign means below ground surface). Selected load–displacement data are shown in Table P13.3b. (a) Make a neat sketch of the soil profile and the drilled shaft, as shown in Example 13.3. (b) Determine the ultimate skin friction and ultimate end bearing capacity. (c) If an FS of 2 is required, determine the allowable load and settlement. Justify your answers.

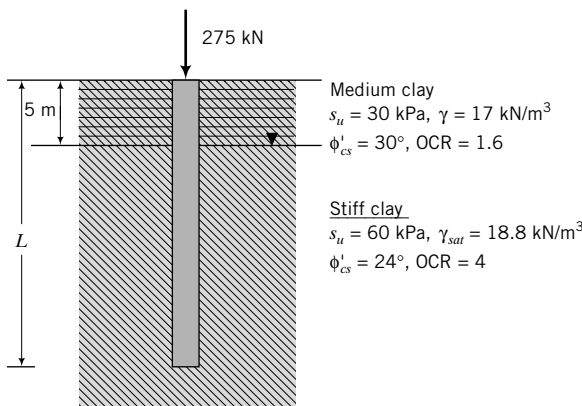
TABLE P13.3a

Elevation (m)	5 to –3.4	–3.4 to –17.6	–17.6 to –38.2
Soil type	Sandy fat clay (CH)	Silty sand with gravel (SM)	Mudstone or weak rock

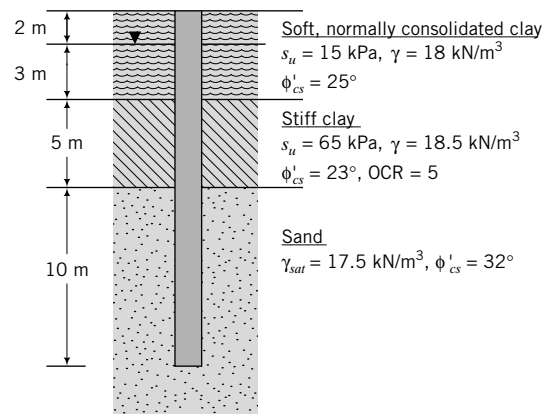
TABLE P13.3b

Load (MN)	0	1	5	8	10	15	20	25	27	27.2	27.1	0
Displacement	0	0.4	0.8	1	1.2	1.5	3.4	6.5	8	9.2	10.8	9.0
up (mm)												
Displacement	0	–0.5	–6	–10	–11	–16	–21	–29	–43	–40	–41	–37
down (mm)												

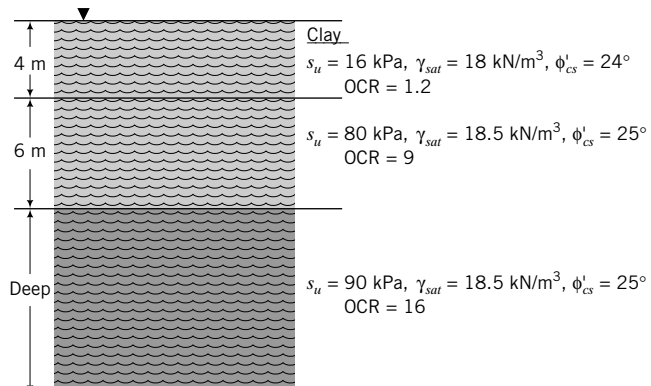
- 13.4** Determine the length, L , of a driven timber pile required to support the load shown in Figure P13.4. The diameter of the pile is 450 mm. A factor of safety of 2 is required. Assume the pile–soil interface friction is equal to the critical state friction angle.

**FIGURE P13.4**

- 13.5** Determine the allowable load for a steel closed-ended pipe pile, 0.4 m in diameter, driven 20 m into the soil profile shown in Figure P13.5. Groundwater is at 2 m below the surface, but you can assume it will rise to the surface. A factor of safety of 2 is required. Neglect negative skin friction.

**FIGURE P13.5**

- 13.6** A square precast concrete pile of sides 0.4 m is to be driven 12 m into the soil strata shown in Figure P13.6. Estimate the allowable load capacity for a factor of safety of 2. Owing to changes in design requirements, the pile must support 20% more load. Determine the additional embedment depth required.

**FIGURE P13.6**

- 13.7** Estimate the allowable load capacity of a 0.5-m-diameter steel closed-ended pipe pile embedded 17 m in the soil profile shown in Figure P13.7. The factor of safety required is 2. The N values are blows/ft. Compare the load capacity for a driven pile and a drilled shaft.

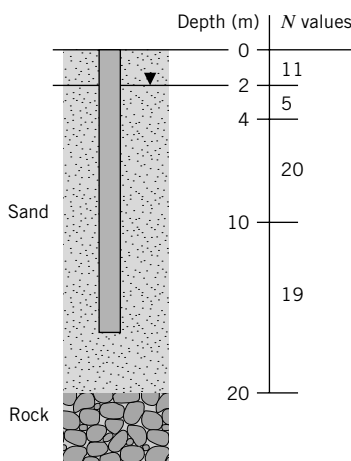


FIGURE P13.7

- 13.8** The soil profile at a site for an offshore structure is shown in Figure P13.8. The height of the pile above the sand surface is 15 m. Determine the allowable load for a driven closed-ended pipe pile with diameter 1.25 m and embedded 10 m into the stiff clay. A factor of safety of 2 is required.

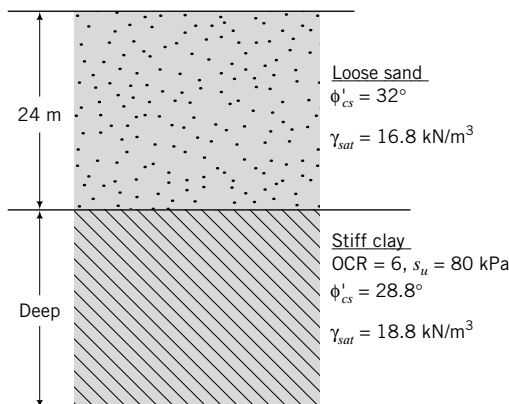


FIGURE P13.8

- 13.9** A soil profile consists of 3 m of a loose, saturated fill ($\phi'_{cs} = 15^\circ$, $\gamma_{sat} = 15 \text{ kN/m}^3$) over a thick layer of clay. The 3-m fill can be assumed to be settling. At a depth of 8 m and greater, $\frac{s_u}{\sigma'_{zo}} = 0.235$, $\text{OCR} = 1$, $\phi'_{cs} = 28^\circ$, and $\gamma_{sat} = 17.8 \text{ kN/m}^3$. Groundwater is at 3 m below the ground surface. Assume that the undrained shear strength of the clay from 3 m to 8 m varies according to $\frac{s_u}{\sigma'_{zo}} = 0.5 \sin \phi'_{cs} (\text{OCR})^{0.8}$ and the average saturated unit weight is 19.8 kN/m^3 . (a) Plot the variation of the shear strength with depth for the clay up to a depth of 20 m. (b) What effect would the fill have on the load capacity of the drilled shaft? Show one method to mitigate any negative effect of the fill on the load capacity. (c) Determine the

ultimate load capacity of a driven precast concrete pile 0.8 m in diameter embedded 18 m from the ground surface.

- 13.10** Estimate the allowable load capacity of a 3×3 timber pile group. Each pile has a diameter of 0.4 m and is driven 15 m into a soft clay ($\text{OCR} = 1.2$) whose undrained shear strength varies linearly with depth according to $s_u = 0.25 \sigma'_z$. The critical state friction angle is 30° and $\gamma_{sat} = 18.8 \text{ kN/m}^3$. The spacing of the piles is 1.5 m. Groundwater level is at ground surface. A factor of safety of 3 is required.

Practical

- 13.11** The soil profile and soil properties at a site are shown in the table below. A group of 12 concrete piles in a 3×4 matrix and of length 12 m is used to support a load. The pile diameter is 0.45 m and pile spacing is 1.5 m. Determine the allowable load capacity for a factor of safety of 2. Calculate the total settlement (elastic and consolidation) under the allowable load. Assume $E_p = 20 \times 10^6 \text{ kPa}$.

Depth (m)	Type of deposit	Soil test results
0 to 3	Sand	$\gamma = 17 \text{ kN/m}^3$, $\phi'_{cs} = 28^\circ$
Groundwater level at 3 m		$E'_{so} = 19 \text{ MPa}$
3 to 6	Sand	$\gamma_{sat} = 17.5 \text{ kN/m}^3$, $\phi'_{cs} = 30^\circ$ $E'_{so} = 18 \text{ MPa}$
6 to 15	Clay	$\gamma_{sat} = 18.5 \text{ kN/m}^3$, $\phi'_{cs} = 27^\circ$ $s_u = 30 \text{ kPa}$ $C_c = 0.4$, $C_r = 0.06$, $\text{OCR} = 1.5$ $E'_{so} = 30 \text{ MPa}$, $\nu' = 0.3$
15 to 17	Soft clay	$\gamma_{sat} = 18 \text{ kN/m}^3$, $\phi'_{cs} = 24^\circ$ $s_u = 20 \text{ kPa}$ $C_c = 0.8$, $\text{OCR} = 1.0$ $E'_{so} = 10 \text{ MPa}$, $\nu' = 0.3$
>17	Rock	

- 13.12** The soil at a site consists of a 30-m-thick deposit of clay. At a depth of 6 m and below, it is normally consolidated. A soil sample from this depth was tested in a direct simple shear (DSS) apparatus. The DSS gave a normalized

undrained shear strength of $\left[\frac{(s_u)_f}{\sigma'_{zo}} \right]_{DSS} = 0.22$, where the subscript *f* denotes failure (critical state). The average saturated unit weight is 19.8 kN/m^3 . Groundwater level is at the surface. From Chapter 11, the normalized undrained shear strength is given by the equation $\left[\frac{(s_u)_f}{\sigma'_{zo}} \right]_{DSS} = \frac{\sqrt{3} \sin \phi'_{cs}}{2} \left(\frac{\text{OCR}}{2} \right)^{0.8}$. (a) Plot the variation of undrained shear strength with depth up to a depth of 30 m. (b) Estimate the allowable load

capacity for a steel closed-ended pipe pile of diameter 1.5 m, length 15 m, and wall thickness 65 mm driven with a driving shoe (displacement pile). Assume FS = 2.

- 13.13** A pile group consisting of ten 500-mm-diameter drilled shafts supports a bridge abutment, as shown in Figure P13.13. The pile spacing in both directions is 2 m. The soil profile consists of a fine sand 2 m thick ($\gamma = 19 \text{ kN/m}^3$) above a medium sand ($\gamma_{sat} = 20 \text{ kN/m}^3$). Groundwater is located at 2 m below ground surface. SPT results are shown in the table. Determine the length of the pile group for FS = 2. Assume the SPT value is constant after 15 m.

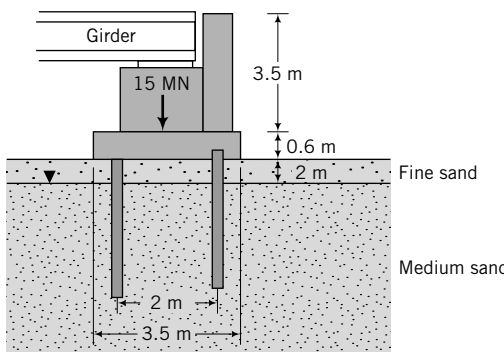


FIGURE P13.13

Depth (m)	1	2	3	5	7	9	10	12	15	>15
N_{60} (below/ft)	5	5	7	12	16	18	19	25	38	42

- 13.14** For the CPT data shown in Figure E13.8, determine the ultimate compressive load for an open-ended pipe pile ($D = 300 \text{ mm}$, $D_i = 270 \text{ mm}$) driven to a depth of 10 m. Assume calcareous material and $\delta_{cv} = 24^\circ$. If the skin friction was not measured, estimate it for $\delta_{cv} = 24^\circ$.

- 13.15** A 500-mm-diameter timber pile of Young's modulus $E_p = 10 \text{ GPa}$ is embedded 8 m into a medium-stiff, homogeneous clay with $s_u = 40 \text{ kPa}$, $\gamma_{sat} = 18.8 \text{ kN/m}^3$, and $E_s = 20 \text{ MPa}$. The working stress of the pile is 10 MPa. Groundwater is at the surface. Using the application software program APILES (www.wiley.com/college/budhu), (a) plot the lateral load–pile head deflection assuming free head pile, an earth pressure coefficient of $K_s = 1$, and an adhesion factor of 0.5; (b) determine the allowable lateral load; (c) determine the maximum bending moment at the allowable load; and (d) determine the pile head deflection at the working load. In APILES, select option 1, stiff clay, and input the effective unit weight of the soil when prompted. APILES creates a text file named apiles.txt in the folder that contains APILES. You can copy the data to Excel and plot the load–deflection curve.

CHAPTER 14

TWO-DIMENSIONAL FLOW OF WATER THROUGH SOILS

14.0 INTRODUCTION

In this chapter, you will study the basic principles of two-dimensional flow of water through soils. The emphasis will be on gaining an understanding of the forces from groundwater flow that provoke failures. You will learn methods to calculate flow, porewater pressure distribution, uplift forces, and seepage stresses for a few simple geotechnical systems.

When you complete this chapter, you should be able to:

- Calculate flow under and within earth structures.
- Calculate seepage stresses, porewater pressure distribution, uplift forces, hydraulic gradients, and the critical hydraulic gradient.
- Determine the stability of simple geotechnical systems subjected to two-dimensional flow of water.

You will use the following principles learned from previous chapters and your courses in mechanics:

- Statics
- Hydraulic gradient, flow of water through soils (Chapter 6)
- Effective stresses and seepage (Chapter 7)

Importance

Many catastrophic failures in geotechnical engineering result from instability of soil masses due to groundwater flow. Lives are lost, infrastructures are damaged or destroyed, and major economic losses occur. The topics covered in this chapter will help you to avoid pitfalls in the analysis and design of geotechnical systems where groundwater flow can lead to instability. Figure 14.1 shows the collapse of a sewer and a supported excavation by seepage forces. You should try to prevent such a collapse.

14.1 DEFINITIONS OF KEY TERMS

Equipotential line is a line representing constant head.

Flow line is the flow path of a particle of water.

Flownet is a graphical representation of a flow field.

Seepage stress is the stress (similar to frictional stress in pipes) imposed on a soil as water flows through it.

Static liquefaction is the behavior of a soil as a viscous fluid when seepage reduces the effective stress to zero.



FIGURE 14.1 Damage to a braced excavation by seepage forces. (Courtesy of George Tamaro, Mueser Rutledge Consulting Engineers.)

14.2 QUESTIONS TO GUIDE YOUR READING

1. What is the governing equation for two-dimensional flow, and what are the methods adopted for its solution for practical problems?
2. What are flow lines and equipotential lines?
3. What is a flownet?
4. How do I draw a flownet?
5. What are the practical uses of a flownet?
6. What is the critical hydraulic gradient?
7. How do I calculate the porewater pressure distribution near a retaining structure and under a dam?
8. What are uplift pressures, and how can I calculate them?
9. What do the terms static liquefaction, heaving, quicksand, boiling, and piping mean?
10. What are the forces that lead to instability due to two-dimensional flow?
11. How does seepage affect the stability of an earth-retaining structure?

14.3 TWO-DIMENSIONAL FLOW OF WATER THROUGH POROUS MEDIA

The flow of water through soils is described by Laplace's equation. Flow of water through soils is analogous to steady-state heat flow and flow of current in homogeneous conductors. The popular form of Laplace's equation for two-dimensional flow of water through soils is

$$k_x \frac{\partial^2 H}{\partial x^2} + k_z \frac{\partial^2 H}{\partial z^2} = 0 \quad (14.1)$$

where H is the total head and k_x and k_z are the hydraulic conductivities in the X and Z directions. Laplace's equation expresses the condition that the changes of hydraulic gradient in one direction are balanced by changes in the other directions.

The assumptions in Laplace's equation are:

- Darcy's law is valid.
- Irrotational flow (vorticity) is negligible. This assumption leads to the following two-dimensional relationship in velocity gradients.

$$\frac{\partial v_z}{\partial z} = \frac{\partial v_x}{\partial x}$$

where v_z and v_x are the velocities in the Z and X directions, respectively. This relationship is satisfied for a uniform flow field and not a general flow field. Therefore, we will assume all flows in this chapter are uniform, i.e., $v_z = v_x = \text{constant}$.

- There is inviscid flow. This assumption means that the shear stresses are neglected.
- The soil is homogeneous and saturated.
- The soil and water are incompressible (no volume change occurs).

Laplace's equation is also called the potential flow equation because the velocity head is neglected. If the soil is an isotropic material, then $k_x = k_z$ and Laplace's equation becomes

$$\frac{\partial^2 H}{\partial x^2} + \frac{\partial^2 H}{\partial z^2} = 0 \quad (14.2)$$

The solution of any differential equation requires knowledge of the boundary conditions. The boundary conditions for most "real" structures are complex, so we cannot obtain an analytical solution or closed-form solution for these structures. We have to resort to approximate solutions, which we can obtain using numerical methods such as finite difference, finite element, and boundary element. We can also use physical models to attempt to replicate the flow through the real structure.

In this chapter, we are going to consider two solution techniques for Laplace's equation. One is an approximate method called flownet sketching; the other is the finite difference technique, which you have encountered in Chapter 9. The flownet sketching technique is simple and flexible and conveys a picture of the flow regime. It is the method of choice among geotechnical engineers. But before we delve into these solution techniques, we will establish some key conditions that are needed to understand two-dimensional flow.

The solution of Equation (14.1) depends only on the values of the total head within the flow field in the XZ plane. Let us introduce a velocity potential (ξ), which describes the variation of total head in a soil mass as

$$\xi = kH \quad (14.3)$$

where k is a generic hydraulic conductivity. The velocities of flow in the X and Z directions are

$$v_x = k_x \frac{\partial H}{\partial x} = \frac{\partial \xi}{\partial x} \quad (14.4)$$

$$v_z = k_z \frac{\partial H}{\partial z} = \frac{\partial \xi}{\partial z} \quad (14.5)$$

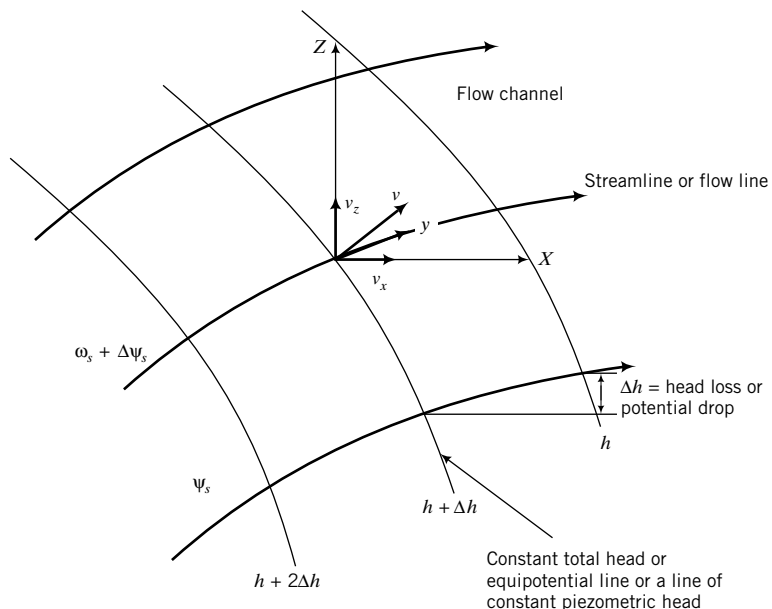


FIGURE 14.2 Illustration of flow terms.

The inference from Equations (14.4) and (14.5) is that the velocity of flow (v) is normal to lines of constant total head, as illustrated in Figure 14.2. The direction of v is in the direction of decreasing total head. The head difference between two equipotential lines is called a potential drop or head loss.

If lines are drawn that are tangent to the velocity of flow at every point in the flow field in the XZ plane, we will get a series of lines that are normal to the equipotential lines. These tangential lines are called streamlines or flow lines (Figure 14.2). A flow line represents the path that a particle of water is expected to take in steady-state flow. A family of streamlines is represented by a stream function, $\psi_s(x, z)$.

The components of velocity in the X and Z directions in terms of the stream function are

$$v_x = \frac{\partial \psi_s}{\partial z} \quad (14.6)$$

$$v_z = -\frac{\partial \psi_s}{\partial x} \quad (14.7)$$

Since flow lines are normal to equipotential lines, there can be no flow across flow lines. The rate of flow between any two flow lines is constant. The area between two flow lines is called a flow channel (Figure 14.2). Therefore, the rate of flow is constant in a flow channel.

THE ESSENTIAL POINTS ARE:

1. Streamlines or flow lines represent flow paths of particles of water.
2. The area between two flow lines is called a flow channel.
3. The rate of flow in a flow channel is constant.
4. Flow cannot occur across flow lines.
5. The velocity of flow is normal to the equipotential line.
6. Flow lines and equipotential lines are orthogonal (perpendicular) to each other.
7. The difference in head between two equipotential lines is called the potential drop or head loss.

What's next . . . The flow conditions we established in the previous section allow us to use a graphical method to find solutions to two-dimensional flow problems. In the next section, we will describe flownet sketching and provide guidance in interpreting a flownet to determine flow through soils, the distribution of porewater pressures, and the hydraulic gradients.

14.4 FLOWNET SKETCHING



Concept Learning, Computer Program Utility, and Self-Assessment

Access <http://www.wiley.com/college/budhu>, Chapter 14 to learn about sketching flownets; calculate porewater pressure and seepage forces through interactive animation.

Click on “2D Flow” to download a finite difference application program that interactively plots flownets for retaining walls and dams. Input different boundary conditions and geometry to explore changes in the flownet. For example, you can drag a sheet pile up or down or position it at different points below a dam and explore how the flownet changes. You can also download a spreadsheet version, 2Dflow.xls.

14.4.1 Criteria for Sketching Flownets

A flownet is a graphical representation of a flow field that satisfies Laplace’s equation and comprises a family of flow lines and equipotential lines.

A flownet must meet the following criteria:

1. The boundary conditions must be satisfied.
2. Flow lines must intersect equipotential lines at right angles.
3. The area between flow lines and equipotential lines must be curvilinear squares. A curvilinear square has the property that an inscribed circle can be drawn to touch each side of the square and continuous bisection results, in the limit, in a point.
4. The quantity of flow through each flow channel is constant.
5. The head loss between each consecutive equipotential line is constant.
6. A flow line cannot intersect another flow line.
7. An equipotential line cannot intersect another equipotential line.

An infinite number of flow lines and equipotential lines can be drawn to satisfy Laplace’s equation. However, only a few are required to obtain an accurate solution. The procedure for constructing a flownet is described next.

14.4.2 Flownet for Isotropic Soils

1. Draw the structure and soil mass to a suitable scale.
2. Identify impermeable and permeable boundaries. The soil–impermeable boundary interfaces are flow lines because water can flow along these interfaces. The soil–permeable boundary interfaces are equipotential lines because the total head is constant along these interfaces.
3. Sketch a series of flow lines (four or five) and then sketch an appropriate number of equipotential lines such that the area between a pair of flow lines and a pair of equipotential lines (cell) is approximately a curvilinear square. You would have to adjust the flow lines and equipotential lines to make curvilinear squares. You should check that the average width and the average length of a cell are approximately equal by drawing an inscribed circle. You should also sketch the entire flownet before making adjustments.

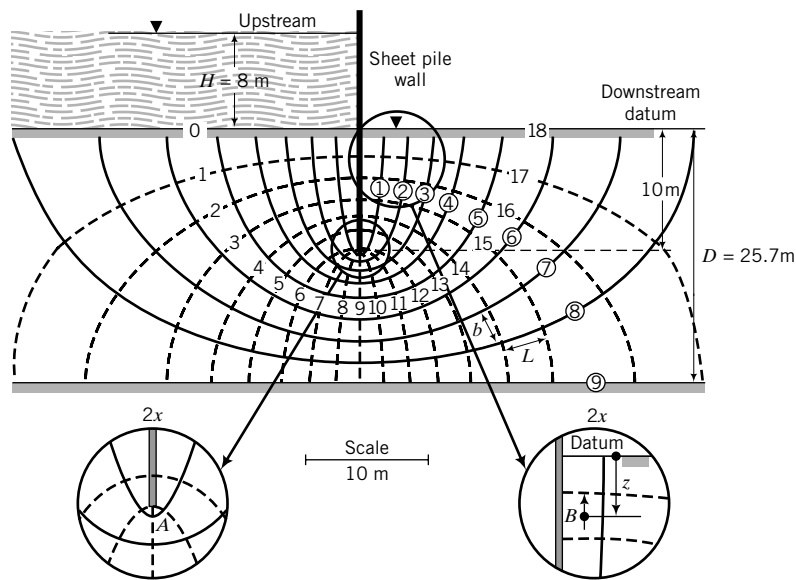


FIGURE 14.3 Flownet for a sheet pile.

The flownet in confined areas between parallel boundaries usually consists of flow lines and equipotential lines that are elliptical in shape and symmetrical (Figure 14.3). Try to avoid making sharp transitions between straight and curved sections of flow and equipotential lines. Transitions should be gradual and smooth. For some problems, portions of the flownet are enlarged and are not curvilinear squares, and they do not satisfy Laplace's equation. For example, the portion of the flownet below the bottom of the sheet pile in Figure 14.3 does not consist of curvilinear squares. For an accurate flownet, you should check these portions to ensure that repeated bisection results in a point.

A few examples of flownets are shown in Figures 14.3 to 14.5. Figure 14.3 shows a flownet for a sheet pile wall, Figure 14.4 shows a flownet beneath a dam, and Figure 14.5 shows a flownet in the backfill of a retaining wall. In the case of the retaining wall, the vertical drainage blanket of coarse-grained soil is used to transport excess porewater pressure from the backfill to prevent the imposition of a hydrostatic force on the wall. The interface boundary, AB (Figure 14.5), is neither an equipotential line nor a flow line. The total head along the boundary AB is equal to the elevation head.

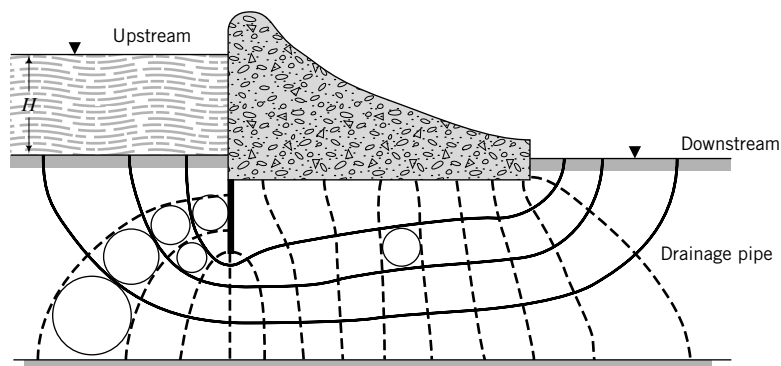


FIGURE 14.4 Flownet under a dam with a cutoff curtain (sheet pile) on the upstream end.

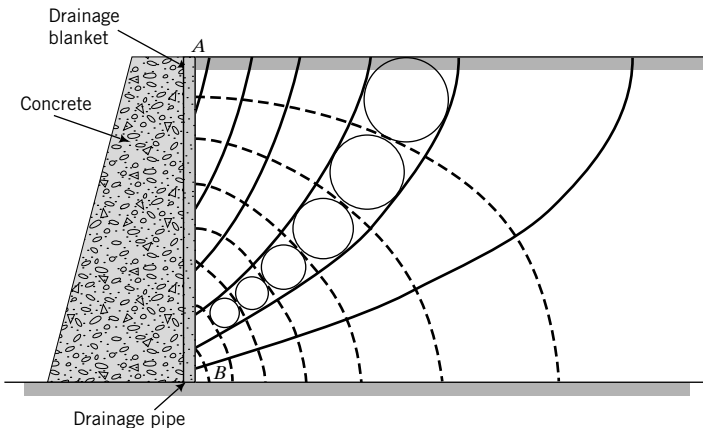


FIGURE 14.5 Flownet in the backfill of a retaining wall with a vertical drainage blanket.

14.4.3 Flownet for Anisotropic Soil

Equation (14.1) is Laplace's two-dimensional equation for anisotropic soils (the hydraulic conductivities in the X and Z direction are different). Let us manipulate this equation to transform it into another form so that we can use the procedure for isotropic soils to draw and interpret flownets. Put $C = \sqrt{k_z/k_x}$ and $x_1 = Cx$. Then,

$$\begin{aligned}\frac{\partial x_1}{\partial x} &= C \\ \frac{\partial H}{\partial x} &= \frac{\partial H}{\partial x_1} \frac{\partial x_1}{\partial x} = C \frac{\partial H}{\partial x_1}\end{aligned}$$

and

$$\frac{\partial^2 H}{\partial x^2} = C^2 \frac{\partial^2 H}{\partial x_1^2}$$

Therefore, we can write Equation (14.1) as

$$C^2 \frac{\partial^2 H}{\partial x_1^2} + C^2 \frac{\partial^2 H}{\partial z^2} = 0$$

which simplifies to

$$\frac{\partial^2 H}{\partial x_1^2} + \frac{\partial^2 H}{\partial z^2} = 0 \quad (14.8)$$

Equation (14.8) indicates that for anisotropic soils we can use the procedure for flownet sketching described for isotropic soils by scaling the x distance by $\sqrt{k_z/k_x}$. That is, you must draw the structure and flow domain by multiplying the horizontal distances by $\sqrt{k_z/k_x}$.

14.5 INTERPRETATION OF FLOWNET

14.5.1 Flow Rate

Let the total head loss across the flow domain be ΔH , that is, the difference between upstream and downstream water level elevation. Then the head loss (Δh) between each consecutive pair of equipotential lines is

$$\Delta h = \frac{\Delta H}{N_d} \quad (14.9)$$

where N_d is the number of equipotential drops, that is, the number of equipotential lines minus one. In Figure 14.3, $\Delta H = H = 8$ m and $N_d = 18$. From Darcy's law, the flow through each flow channel for an isotropic soil is

$$q = AKi = (b \times 1)k \frac{\Delta h}{L} = k \Delta h \frac{b}{L} = k \frac{\Delta H}{N_d} \frac{b}{L} \quad (14.10)$$

where b and L are defined as shown in Figure 14.3. By construction, $b/L \approx 1$, and therefore the total flow is

$$q = k \sum_{i=1}^{N_f} \left(\frac{\Delta H}{N_d} \right)_i = k \Delta H \frac{N_f}{N_d} \quad (14.11)$$

where N_f is the number of flow channels (number of flow lines minus one). In Figure 14.3, $N_f = 9$. The ratio N_f/N_d is called the shape factor. Finer discretization of the flownet by drawing more flow lines and equipotential lines does not significantly change the shape factor. Both N_f and N_d can be fractional. In the case of anisotropic soils, the quantity of flow is

$$q = \Delta H \frac{N_f}{N_d} \sqrt{k_x k_z} \quad (14.12)$$

14.5.2 Hydraulic Gradient

You can find the hydraulic gradient over each square by dividing the head loss by the length, L ; that is,

$$i = \frac{\Delta h}{L} \quad (14.13)$$

You should notice from Figure 14.3 that L is not constant. Therefore, the hydraulic gradient is not constant. The maximum hydraulic gradient occurs where L is a minimum; that is,

$$i_{max} = \frac{\Delta h}{L_{min}} \quad (14.14)$$

where L_{min} is the minimum length of the cells within the flow domain. Usually, L_{min} occurs at exit points or around corners (e.g., point A in Figure 14.3), and it is at these points that we usually get the maximum hydraulic gradient.

14.5.3 Static Liquefaction, Heaving, Boiling, and Piping

Let us consider an element, B , of soil at a depth z near the downstream end of the sheet pile wall structure shown in Figure 14.3. Flow over this element is upward. Therefore, the vertical effective stress is

$$\sigma'_z = \gamma' z - i \gamma_w z \quad (14.15)$$

If the mean effective stress becomes zero, the soil loses its intergranular frictional strength and behaves like a viscous fluid. The soil state at which the mean effective stress is zero is called static liquefaction. Various other names such as boiling, quicksand, piping, and heaving are used to describe specific events connected to the static liquefaction state. Boiling occurs when the upward seepage force exceeds the downward force of the soil. Piping refers to the subsurface “pipe-shaped” erosion that initiates near the toe of dams and similar structures. High localized hydraulic gradient statically liquefies the soil, which progresses to the water surface in the form of a pipe, and water then rushes beneath the structure through the pipe, leading to instability and failure. Quicksand is the existence of a mass of sand in a state of static liquefaction. Heaving occurs when seepage forces push the bottom of an excavation upward. A structure founded on a soil that statically liquefies will collapse. Liquefaction can also be produced by dynamic events such as earthquakes.

14.5.4 Critical Hydraulic Gradient

We can determine the hydraulic gradient that brings a soil mass (essentially, coarse-grained soils) to static liquefaction. Solving for i in Equation (14.15) when $\sigma'_z = 0$, we get

$$i = i_{cr} = \frac{\gamma'}{\gamma_w} = \left(\frac{G_s - 1}{1 + e} \right) \frac{\gamma_w}{\gamma_w} = \frac{G_s - 1}{1 + e} \quad (14.16)$$

where i_{cr} is called the critical hydraulic gradient, G_s is specific gravity, and e is the void ratio. Since G_s is constant, the critical hydraulic gradient is solely a function of the void ratio of the soil. In designing structures that are subjected to steady-state seepage, it is absolutely essential to ensure that the critical hydraulic gradient cannot develop.

14.5.5 Porewater Pressure Distribution

The porewater pressure at any point j within the flow domain (flownet) is calculated as follows:

1. Select a datum. Let us choose the downstream water level as the datum (Figure 14.3).
2. Determine the total head at j : $H_j = \Delta H - (N_d)_j \Delta h$, where $(N_d)_j$ is the number of equipotential drops at point j ; $(N_d)_j$ can be fractional. For example, at B , $H_B = \Delta H - 16.5 \Delta h$.
3. Subtract the elevation head at point j from the total head H_j to get the pressure head. For point B (Figure 14.3), the elevation head h_z is $-z$ (point B is below the datum). The pressure head is then

$$(h_p)_j = \Delta H - (N_d)_j \Delta h - h_z \quad (14.17)$$

For point B , $(h_p)_B = \Delta H - 16.5 \Delta h - (-z) = \Delta H - 16.5 \Delta h + z$.

4. The porewater pressure is

$$u_j = (h_p)_j \gamma_w \quad (14.18)$$

Alternatively, you can find the porewater pressure head as follows. Measure the vertical distance from the upstream water level to the point of interest and then subtract the total head loss up to that point. For example, let us say that the vertical distance from the downstream water level to point B (Figure 14.3) is 4 m. Then, the vertical distance from the upstream water level to point B is 8 m + 4 m = 12 m. The total head loss up to point B is $16.5 \Delta h$. The pressure head is $12 \text{ m} - 16.5 \Delta h$, which is the same as in item 3 above.

14.5.6 Uplift Forces

Lateral and uplift forces due to groundwater flow can adversely affect the stability of structures such as dams and weirs. The uplift force per unit length (length is normal to the XZ plane) is found by calculating

the porewater pressure at discrete points along the base (in the X direction, Figure 14.4) and then finding the area under the porewater pressure distribution diagram, that is,

$$P_w = \sum_{j=1}^n u_j \Delta x_j \quad (14.19)$$

where P_w is the uplift force per unit length, u_j is the average porewater pressure over an interval Δx_j , and n is the number of intervals. It is convenient to use Simpson's rule to calculate P_w :

$$P_w = \frac{\Delta x}{3} \left(u_1 + u_n + 2 \sum_{\substack{i=3 \\ \text{odd}}}^n u_i + 4 \sum_{\substack{i=2 \\ \text{even}}}^n u_i \right) \quad (14.20)$$

EXAMPLE 14.1 Critical Hydraulic Gradient in an Excavation

An excavation is proposed for a site consisting of a homogeneous, isotropic layer of silty clay, 14.24 m thick, above a deep deposit of sand. The groundwater is 2 m below ground level outside the excavation. The groundwater level inside the excavation is at the bottom (see Figure E14.1). The void ratio of the silty clay is 0.62 and its specific gravity is 2.7. What is the limiting depth of the excavation to avoid heaving? Assume artesian condition is not present.

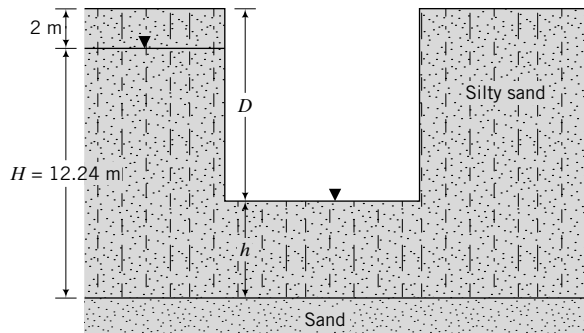


FIGURE E14.1

Strategy Heaving will occur if $i > i_{cr}$. Find the critical hydraulic gradient from the void ratio given and then find the depth at which this hydraulic gradient is reached.

Solution 14.1

Step 1: Calculate i_{cr} .

$$i_{cr} = \frac{G_s - 1}{1 + e} = \frac{2.7 - 1}{1 + 0.62} = 1.05$$

Step 2: Determine D .

Total head difference: $\Delta H = H - h = 12.24 - h$

$$\text{Average hydraulic gradient: } i = \frac{\Delta H}{h}$$

Putting $i = i_{cr}$, we get

$$1.05 = \frac{12.24 - h}{h}$$

Solving for h , we get $h = 5.97$ m.

$$D = (12.24 + 2) - h = 14.24 - 5.97 = 8.27 \text{ m}$$

EXAMPLE 14.2 Flownet Sketching and Interpretation for a Dam

A dam, shown in Figure E14.2a, retains 10 m of water. A sheet pile wall (cutoff curtain) on the upstream side, which is used to reduce seepage under the dam, penetrates 7 m into a 20.3-m-thick silty sand stratum. Below the silty sand is a thick deposit of practically impervious clay. The average hydraulic conductivity of the silty sand is 2.0×10^{-4} cm/s. Assume that the silty sand is homogeneous and isotropic.

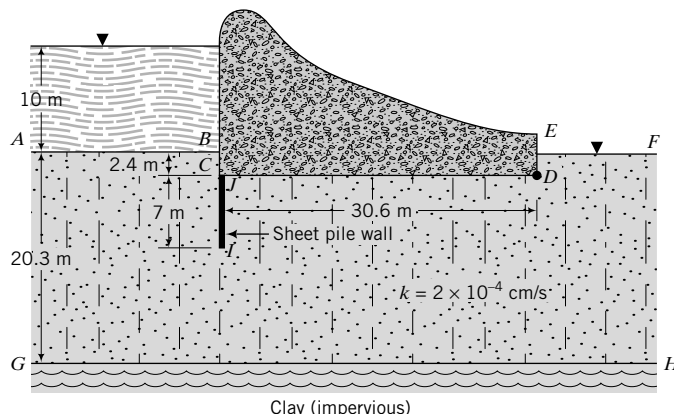


FIGURE E14.2a

Clay (impervious)

- (a) Draw the flownet under the dam.
- (b) Calculate the flow rate, q .
- (c) Calculate and draw the porewater pressure distribution at the base of the dam.
- (d) Determine the uplift force.
- (e) Determine and draw the porewater pressure distribution on the upstream and downstream faces of the sheet pile wall.
- (f) Determine the resultant lateral force on the sheet pile wall due to the porewater.
- (g) Determine the maximum hydraulic gradient.
- (h) Will piping occur if the void ratio of the silty sand is 0.8?
- (i) What is the effect of reducing the depth of penetration of the sheet pile wall?

Strategy Follow the procedures described in Section 14.4 to draw the flownet and calculate the required parameters.

Solution 14.2

Step 1: Draw the dam to scale.

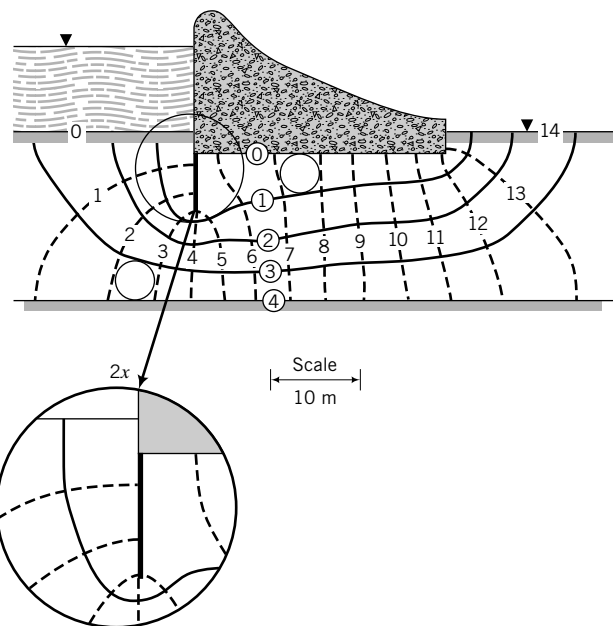
See Figure E14.2b.

Step 2: Identify the impermeable and permeable boundaries.

With reference to Figure E14.2a, AB and EF are permeable boundaries and are therefore equipotential lines. $BCIJDE$ and GH are impermeable boundaries and are therefore flow lines.

Step 3: Sketch the flownet.

Draw about three flow lines and then draw a suitable number of equipotential lines. Remember that flow lines are orthogonal to equipotential lines, and the area between two consecutive flow lines and two consecutive equipotential lines is approximately a square. Use a circle template to assist you in estimating the square. Adjust/add/subtract flow lines and equipotential lines until you are satisfied that the flownet consists essentially of curvilinear squares. See sketch of flownet in Figure E14.2b.

**FIGURE E14.2b**

Step 4: Calculate the flow.

Select the downstream end, *EF*, as the datum. Note: *AB* and *EF* are at the same elevation.

$$\Delta H = 10 \text{ m}$$

$$N_d = 14, \quad N_f = 4$$

$$q = k\Delta H \frac{N_f}{N_d} = 2 \times 10^{-4} \times (10 \times 10^2) \times \frac{4}{14} = 0.057 \text{ cm}^3/\text{s}$$

Note: The flow rate is calculated for 1 cm length of wall, and that is why the unit is cm^3/s .

Step 5: Determine the porewater pressure under the base of the dam.

Divide the base into a convenient number of equal intervals. Let us use 10 intervals; that is,

$$\Delta x = \frac{30.6}{10} = 3.06 \text{ m}$$

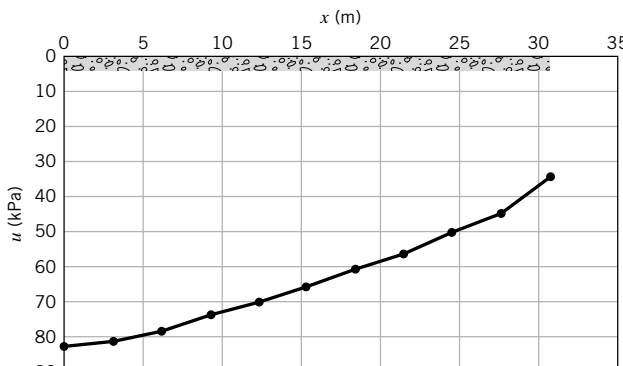
Determine the porewater pressure at each nodal point. Use a table for convenience or, better yet, use a spreadsheet.

$$\Delta h = \frac{\Delta H}{N_d} = \frac{10}{14} = 0.714 \text{ m}$$

The calculation in the table below was done using a spreadsheet program.

Parameters	Under base of dam										
	0	3.06	6.12	9.18	12.24	15.3	18.36	21.42	24.48	27.54	30.6
N_d (m)	5.60	5.80	6.20	6.90	7.40	8.00	8.80	9.40	10.30	11.10	12.50
$N_d\Delta h$ (m)	4.00	4.14	4.43	4.93	5.28	5.71	6.28	6.71	7.35	7.93	8.93
h_z (m)	-2.40	-2.40	-2.40	-2.40	-2.40	-2.40	-2.40	-2.40	-2.40	-2.40	-2.40
h_p (m) = $\Delta H - N_d\Delta h - h_z$	8.40	8.26	7.97	7.47	7.12	6.69	6.12	5.69	5.05	4.47	3.48
u (kPa) = $h_p \gamma_w$	82.3	80.9	78.1	73.2	69.7	65.5	59.9	55.7	49.4	43.9	34.1

Plot the porewater pressure distribution. See Figure E14.2c.

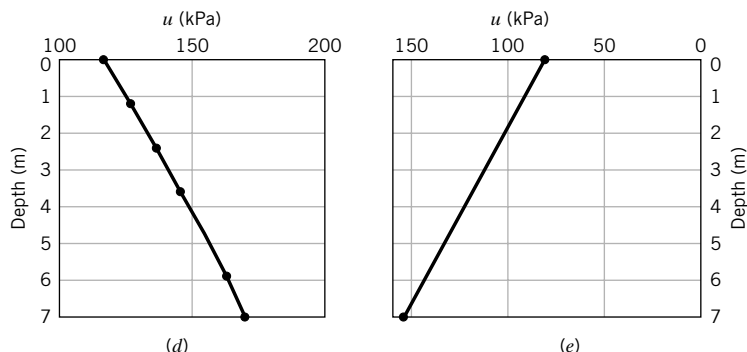
**FIGURE E14.2c**

Step 6: Calculate the uplift force and its location.

Using Simpson's rule [Equation (14.20)], we find

$$P_w = \frac{3.06}{3} [82.3 + 34.1 + 2(78.1 + 69.7 + 59.9 + 49.4) + 4(80.9 + 73.2 + 65.5 + 55.7 + 43.9)] \\ = 1946.4 \text{ kN for one unit length of wall.}$$

Step 7: Determine the porewater pressure distribution on the sheet pile wall. Divide the front face of the wall into six intervals of $7/6 = 1.17 \text{ m}$ and the back face into one interval. Six intervals were chosen because it is convenient for the scaling using the scale that was used to draw the flownet. The greater the number of intervals, the greater the accuracy. Only one interval is used for the back face of the wall, because there are no equipotential lines that meet there. Use a spreadsheet to compute the porewater pressure distribution and the hydrostatic forces. The distributions of porewater pressure at the front and back of the wall are shown in Figure E14.2d, e. Use Simpson's rule to calculate the hydrostatic force on the front face of the wall. The porewater pressure distribution at the back face is a trapezoid, and the area is calculated from one-half the sum of the parallel sides multiplied by the height. For example, the force at the back of the wall is $\left(\frac{155.1 + 82.3}{2}\right) \times 7 = 830.9 \text{ kN}$ for one unit length of wall.

**FIGURE E14.2d, e** Porewater pressure distribution (d) at front of wall and (e) at back of wall

Parameters	Front of wall							Back of wall	
	0	1.17	2.33	3.50	4.67	5.83	7.00	7.00	0.00
$N_d \text{ (m)}$	0.70	1.00	1.30	1.60	1.90	2.40	3.00	5.00	5.60
$N_d \Delta h \text{ (m)}$	0.50	0.71	0.93	1.14	1.36	1.71	2.14	3.57	4.00
$h_z \text{ (m)}$	-2.40	-3.57	-4.73	-5.90	-7.07	-8.23	-9.40	-9.40	-2.40
$h_p \text{ (m)} = \Delta H - N_d \Delta h - h_z$	11.90	12.85	13.81	14.76	15.71	16.52	17.26	15.83	8.40
$u \text{ (kPa)} = h_p \gamma_w$	116.6	126.0	135.3	144.6	154.0	161.9	169.1	155.1	82.3
	Front	Back	Difference						
$P_w \text{ (kN/m)}$	1011.7	830.9	180.8						

Step 8: Determine the maximum hydraulic gradient.

The smallest value of L occurs at the exit. By measurement, $L_{min} = 2$ m.

$$i_{max} = \frac{\Delta h}{L_{min}} = \frac{0.714}{2} = 0.36$$

Step 9: Determine if piping would occur.

$$i_{cr} = \frac{G_s - 1}{1 + e} = \frac{2.7 - 1}{1 + 0.8} = 0.94$$

Since $i_{max} < i_{cr}$, piping will not occur.

$$\text{Factor of safety against piping: } \frac{0.94}{0.36} = 2.6$$

Step 10: State the effect of reducing the depth of penetration of the sheet pile wall.

If the depth is reduced, the value of Δh increases and i_{max} is likely to increase. Therefore, the potential for piping increases.

14.6 FINITE DIFFERENCE SOLUTION FOR TWO-DIMENSIONAL FLOW



Computer Program Utility

Access <http://www.wiley.com/college/budhu>, Chapter 14 and click on “2D Flow” to download a finite difference application program that interactively plots flownets for retaining walls and dams. Input different boundary conditions and geometry to explore changes in the flownet. For example, you can drag a sheet pile up or down or position it at different points below a dam and explore how the flownet changes. You can also download a spreadsheet version, 2Dflow.xls.

In Chapter 9, we used the finite difference technique to solve the governing one-dimensional partial differential equation to determine the spatial variation of excess porewater pressure. We will do the same to solve Laplace’s equation to determine two-dimensional confined flow through soils. Let us consider a grid of a flow domain, as shown in Figure 14.6, where (i, j) is a nodal point.

Using Taylor’s theorem, we have

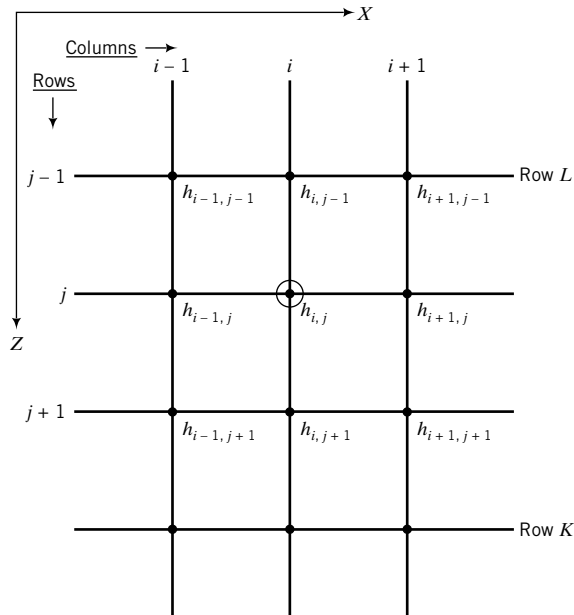
$$k_x \frac{\partial^2 H}{\partial x^2} + k_z \frac{\partial^2 H}{\partial z^2} = \frac{k_x}{\Delta x^2} (h_{i+1,j} + h_{i-1,j} - 2h_{i,j}) + \frac{k_z}{\Delta z^2} (h_{i,j+1} + h_{i,j-1} - 2h_{i,j}) = 0 \quad (14.21)$$

Let $\alpha = k_x/k_z$ and $\Delta x = \Delta z$ (i.e., we subdivide the flow domain into a square grid). Then, solving for $h_{i,j}$ from Equation (14.21) gives

$$h_{i,j} = \frac{1}{2(1 + \alpha)} (\alpha h_{i+1,j} + \alpha h_{i-1,j} + h_{i,j+1} + h_{i,j-1}) \quad (14.22)$$

For isotropic conditions, $\alpha = 1$ ($k_x = k_z$) and Equation (14.22) becomes

$$h_{i,j} = \frac{1}{4} (h_{i+1,j} + h_{i-1,j} + h_{i,j+1} + h_{i,j-1}) \quad (14.23)$$

**FIGURE 14.6** A partial grid of the flow domain.

Since we are considering confined flow, one or more of the boundaries would be impermeable.

Flow cannot cross impermeable boundaries and, therefore, for a horizontal impermeable surface,

$$\frac{\partial h}{\partial x} = 0 \quad (14.24)$$

The finite difference form of Equation (14.24) is

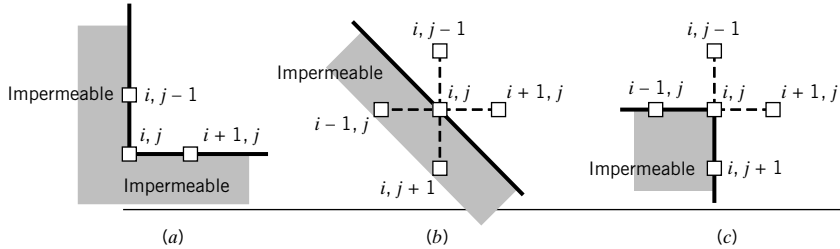
$$\frac{\partial h}{\partial x} = \frac{1}{2\Delta x}(h_{i,j+1} - h_{i,j-1}) = 0 \quad (14.25)$$

Therefore, $h_{i,j+1} = h_{i,j-1}$ and, by substitution in Equation (14.23), we get

$$h_{i,j} = \frac{1}{4}(h_{i+1,j} + h_{i-1,j} + 2h_{i,j-1}) \quad (14.26)$$

Various types of geometry of impermeable boundaries are encountered in practice, three of which are shown in Figure 14.7. For Figure 14.7a, b, the finite difference equation is

$$h_{i,j} = \frac{1}{2}(h_{i+1,j} + h_{i,j-1}) \quad (14.27)$$

**FIGURE 14.7** Three types of boundary encountered in practice.

and, for Figure 14.7c,

$$h_{i,j} = \frac{1}{3} \left(h_{i,j-1} + h_{i+1,j} + h_{i,j+1} + \frac{1}{2}h_{i-1,j} + \frac{1}{2}h_{i+2,j} \right) \quad (14.28)$$

The porewater pressure at any node ($u_{i,j}$) is

$$u_{i,j} = \gamma_w(h_{i,j} - z_{i,j}) \quad (14.29)$$

where $z_{i,j}$ is the elevation head.

Contours of potential heads can be drawn from discrete values of $h_{i,j}$. The finite difference equations for flow lines are analogous to the potential lines; that is, ψ_s replaces h in the above equations and the boundary conditions are specified for ψ_s rather than for h .

The horizontal velocity of flow at any node ($v_{i,j}$) is given by Darcy's law:

$$v_{i,j} = k_x i_{i,j}$$

where $i_{i,j}$ is the hydraulic gradient expressed as

$$i_{i,j} = \frac{(h_{i+1,j} - h_{i-1,j})}{2\Delta x} \quad (14.30)$$

Therefore,

$$v_{i,j} = \frac{k_x}{2\Delta x} (h_{i+1,j} - h_{i-1,j}) \quad (14.31)$$

The flow rate, q , is obtained by considering a vertical plane across the flow domain. Let L be the top row and K be the bottom row of a vertical plane defined by column i (Figure 14.6). Then the expression for q is

$$q = \frac{k_x}{4} \left(h_{i+1,L} - h_{i-1,L} + 2 \sum_{j=L+1}^{K-1} (h_{i+1,j} - h_{i-1,j}) + h_{i+1,K} - h_{i-1,K} \right) \quad (14.32)$$

The procedure to determine the distribution of potential head, flow, and porewater pressure using the finite difference method is as follows:

1. Divide the flow domain into a square grid. Remember from Chapter 9 that finer grids give more accurate solutions than coarser grids, but are more tedious to construct and require more computational time. If the problem is symmetrical, you only need to consider one-half of the flow domain. For example, the sheet pile wall shown in Figure 14.8 is symmetrical about the wall and only the left half may be considered. The total flow domain should have a width of at least four times the thickness of the soil layer. For example, if D is the thickness of the soil layer (Figure 14.8), then the minimum width of the left half of the flow domain is $2D$.
2. Identify boundary conditions, for example, impermeable boundaries (flow lines) and permeable boundaries (equipotential lines).
3. Determine the heads at the permeable or equipotential boundaries. For example, the head along the equipotential boundary AB (Figure 14.8) is ΔH . Therefore, all the nodes along this boundary will have a constant head of ΔH . Because of symmetry, the head along nodes directly under the sheet pile wall (EF) is $\Delta H/2$.
4. Apply the known heads to corresponding nodes and assume reasonable initial values for the interior nodes. You can use linear interpolation for the potential heads of the interior nodes.

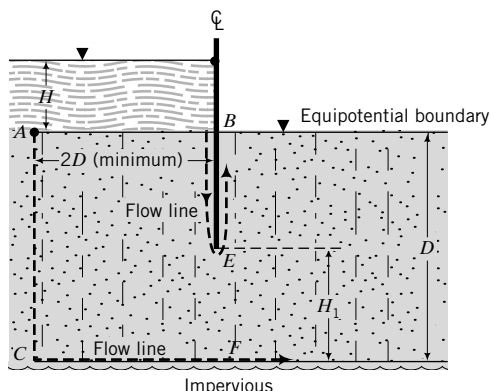


FIGURE 14.8
A sheet pile wall.

5. Apply Equation (14.23), if the soil is isotropic, to each node except (a) at impermeable boundaries, where you should use Equation (14.26), (b) at corners, where you should use Equations (14.27) and (14.28) for the corners shown in Figure 14.7a–c, and (c) at nodes where the heads are known.
6. Repeat item 5 until the new value at a node differs from the old value by a small numerical tolerance, for example, 0.001 m.
7. Arbitrarily select a sequential set of nodes along a column of nodes and calculate the flow, q , using Equation (14.32). It is best to calculate $q' = q$ for a unit permeability value to avoid too many decimal points in the calculations.
8. Repeat items 1 to 6 to find the flow distribution by replacing heads by flow q' . For example, the flow rate calculated in item 7 is applied to all nodes along AC and CF (Figure 14.8). The flow rate at nodes along BE is zero.
9. Calculate the porewater pressure distribution by using Equation (14.29).

A spreadsheet application program (see example at <http://www.wiley.com/college/budhu>, Chapter 14, 2Dflow.xls) can be prepared to automatically carry out the above procedure. However, you should carry out “hand” calculations at selected nodes to verify that the spreadsheet values are correct.

EXAMPLE 14.3 Flownet Using Finite Difference Method

Determine the flow rate under the sheet pile wall (Figure E14.3a) and the porewater pressure distribution using the finite difference method.

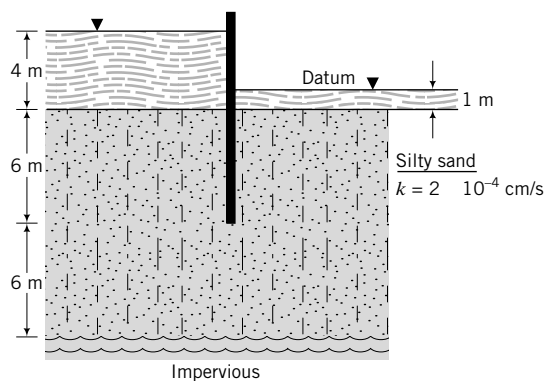


FIGURE E14.3a

Strategy Use a spreadsheet and follow the procedures in Section 14.6.

Solution 14.3

The finite difference solution is shown in Table E14.3 and in Figure 14.3c.

Step 1: Divide the flow domain into a grid.

See Figure E14.3b.

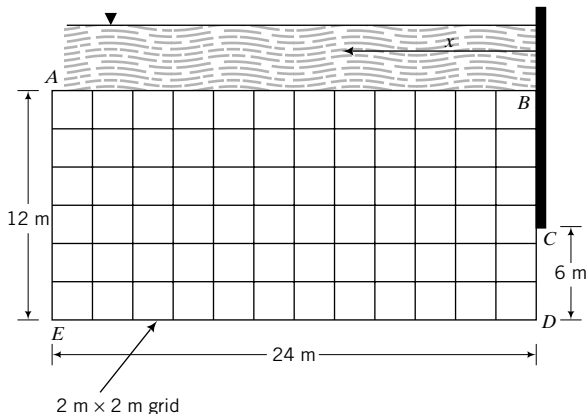


FIGURE E14.3b

Since the problem is symmetrical, perform calculations for only one-half of the domain. Use the left half of the flow domain of width $2D = 2 \times 12 = 24$ m. Use a grid $2\text{ m} \times 2\text{ m}$. The grid is shown as ABCDE in Figure 14.3b.

Step 2: Identify the boundary conditions.

Permeable boundaries: AB and CD are equipotential lines.

Impermeable boundaries: BC , AE , and DE are flow lines.

Step 3: Determine the heads at equipotential boundaries.

Along AB , the head difference is $4 - 1 = 3$ m.

Along CD , the head difference is $3/2 = 1.5$ m.

Step 4: Insert the heads at the nodes.

Set up the initial parameters in column B , rows 3 to 9. Note that cell $B5$ is cell $B3 - B4$. In cells $B12$ to $N12$ (corresponding to the equipotential boundary AB), copy cell $B5$. In cells $N15$ to $N18$, insert cell $B5/2$. Arbitrarily insert values in all other cells from $B13$ to $M18$, $N13$, and $N14$.

Step 5: Apply the appropriate equations.

On the impermeable boundaries— $B13$ to $B18$ (corresponding to AE), $C18$ to $M18$ (corresponding to ED), and $N13$ to $N14$ (corresponding to BC)—apply Equation (14.26). You should note that some nodes (e.g., $B18$) are common. Apply Equation (14.22) to all other cells except cells with known heads.

Step 6: Carry out the iterations.

In Excel (Office 2003), go to Tools → Options → Calculation. Select the following:

- (i) Automatic.
- (ii) Iteration, insert 100 in Maximum iterations and 0.001 in Maximum change.
- (iii) Under Workbook options, select Update remote reference, Save external link values, Accept labels in formulas. You can then click on Calculate now (F9) or Calc.sheet.

In Excel (Office 2007), go to Formulas → Calculation Options → Select Automatic.

TABLE E14.3

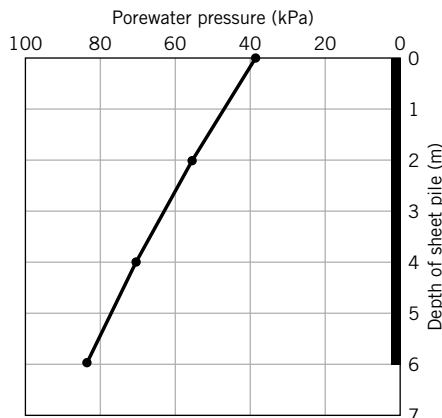


FIGURE E14.3c Porewater pressure distribution.

Step 7: Calculate q .

Use Equation (14.32) to calculate q' for a unit value of permeability. In the spreadsheet for this example, q' is calculated in cell C20 as

$$\{B13-B15+N13-N15+2*(\text{SUM}(C13:M13)-2*\text{SUM}(C15:M15))\}/4$$

The actual value of q is

$$\begin{aligned} q = kq' &= 1.62 \times 2 \times 10^{-4} \times 10^{-2} \\ &= 3.2 \times 10^{-6} \text{ m/s} \quad (10^{-2} \text{ is used to convert cm/s to m/s}) \end{aligned}$$

Step 8: Calculate the flow for each cell (flow lines).

In cells B36 to B42 (corresponding to AE) and C42 to N32 (corresponding to ED), copy q' . The flow at the downstream end (cells N36 to N39) is zero. Apply Equation (14.26) to cells C36 to M41 and N40 to N41. Apply Equation (14.23) to all other cells except the cell with known values of q' . Carry out the reiterations.

Step 9: Calculate the porewater pressures.

From the potential heads, you can calculate the porewater pressure using Equation (14.29). A plot of the porewater pressure distribution is shown in Figure E14.3c.

14.7 FLOW THROUGH EARTH DAMS



Computer Program Utility

Access <http://www.wiley.com/college/budhu>, Chapter 14 and click on Phreatic to download and run an interactive program to calculate and plot the phreatic surface for flow through an earth dam.

Flow through earth dams is an important design consideration. We need to ensure that the porewater pressure at the downstream end of the dam will not lead to instability, and the exit hydraulic gradient does not lead to piping. The major exercise is to find the top flow line called the phreatic surface (Figure 14.9). The pressure head on the phreatic surface is zero.

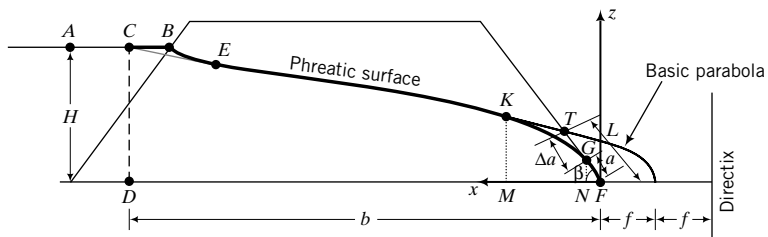


FIGURE 14.9 Phreatic surface within an earth dam.

Casagrande (1937) showed that the phreatic surface can be approximated by a parabola with corrections at the points of entry and exit. The focus of the parabola is at the toe of the dam, point F (Figure 14.9). The assumed parabola representing the uncorrected phreatic surface is called the basic parabola. Recall from your geometry course that the basic property of a parabola is that every point on it is equidistant from its focus and a line called the directrix. To draw the basic parabola, we must know point A , the focus F , and f (one-half the distance from the focus to the directrix). Casagrande recommended that point C be located at a distance $0.3AB$, where AB is the horizontal projection of the upstream slope at the water surface. From the basic property of a parabola, we get

$$2f = \sqrt{b^2 + H^2} - b \quad (14.33)$$

The equation to construct the basic parabola is

$$\sqrt{x^2 + z^2} = x + 2f$$

Solving for z , we obtain

$$z^2 = 4f(f + x) \quad (14.34)$$

or

$$z = 2\sqrt{f(f + x)} \quad (14.35)$$

Since H and b are known from the geometry of the dam, the basic parabola can be constructed. We now have to make some corrections at the upstream entry point and the downstream exit point.

The upstream end is corrected by sketching a transition curve (BE) that blends smoothly with the basic parabola. The correction for the downstream end depends on the angle β and the type of discharge face. Casagrande (1937) determined the length of the discharge face, a , for a homogeneous earth dam with no drainage blanket at the discharge face and $\beta \leq 30^\circ$, as follows. He assumed that Dupuit's assumption, which states that the hydraulic gradient is equal to the slope, dz/dx , of the phreatic surface is valid. If we consider two vertical sections—one is KM of height z , and the other is GN of height $a \sin \beta$ —then the flow rate across KM is

$$q_{KM} = Aki = (z \times 1)k \frac{dz}{dx} \quad (14.36)$$

and across GN is

$$q_{GN} = Aki = (a \sin \beta \times 1)k \frac{dz}{dx} = (a \sin \beta)k \tan \beta \quad (14.37)$$

From the continuity condition at sections KM and GN , $q_{KM} = q_{GN}$; that is,

$$zk \frac{dz}{dx} = (a \sin \beta) k \tan \beta \quad (14.38)$$

which simplifies to

$$z \frac{dz}{dx} = a \sin \beta \tan \beta \quad (14.39)$$

We now integrate Equation (14.39) within the limits $x_1 = a \cos b$ and $x_2 = b$, $z_1 = a \sin \beta$ and $z_2 = H$.

$$\int_{a \sin \beta}^H z dz = a \sin \beta \tan \beta \int_{a \cos \beta}^b dx$$

$$\therefore H^2 - a^2 \sin^2 \beta = 2 a \sin \beta \tan \beta (b - a \cos \beta)$$

Simplification leads to

$$a = \frac{1}{\cos \beta} \left(b - \sqrt{b^2 - H^2 \cot^2 \beta} \right) \quad (14.40)$$

Casagrande (1937) produced a chart relating $\Delta a/L$ (see Figure 14.9 for definition of Δa and L) with values of $\beta > 30^\circ$, as shown in Figure 14.10.

The flow through the dam is obtained by substituting Equation (14.40) into Equation (14.37), giving

$$\begin{aligned} q &= k \sin \beta \tan \beta \left[\frac{1}{\cos \beta} (b - \sqrt{b^2 - H^2 \cot^2 \beta}) \right] \\ &= k \tan^2 \beta (b - \sqrt{b^2 - H^2 \cot^2 \beta}) \end{aligned} \quad (14.41)$$

Because the exit hydraulic gradient is often large, drainage blankets are used at the downstream end of dams to avoid piping. Figure 14.11 shows a horizontal drainage blanket at the toe of an earth dam. Seepage is controlled by the gradation of the coarse-grained soils with or without filter fabric used for the drainage blanket. The phreatic surfaces for dams with drainage blankets are forced to intersect the drainage blankets and do not intersect the downstream faces of the dams. Therefore, no correction to the basic parabola is required on the downstream end of the dam.

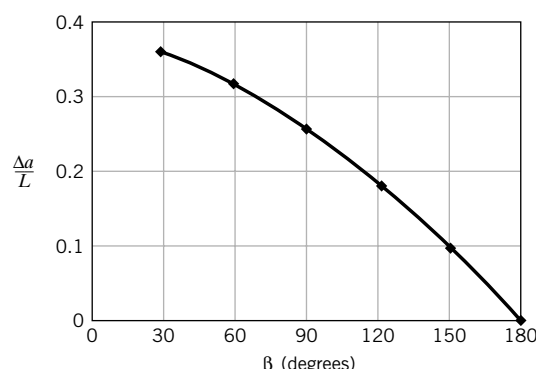


FIGURE 14.10 Correction factor for downstream face.

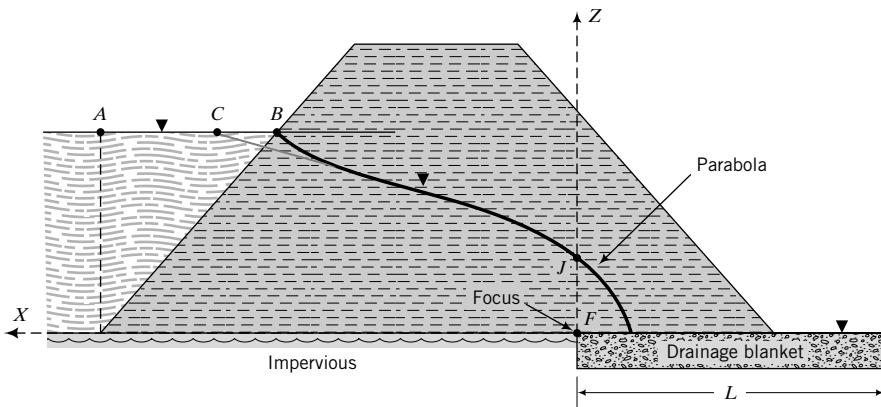


FIGURE 14.11 A horizontal drainage blanket at the toe of an earth dam.

The flow through the dam is

$$q = Aki = Ak \frac{dz}{dx}$$

where dz/dx is the slope of the basic parabola and the area $A = FJ = 1$ (Figure 14.11). From the geometry of the basic parabola, $FJ = 2f$ and the slope of the basic parabola at J is, from Equation (14.34),

$$\frac{dz}{dx} = \frac{2f}{z} = \frac{2f}{2f} = 1$$

Therefore, the flow through a dam with a horizontal drainage blanket is

$$q = 2f \times k \times 1 = 2fk \quad (14.42)$$

The procedure to draw a phreatic surface within an earth dam, with reference to Figure 14.9, is as follows:

1. Draw the structure to scale.
2. Locate a point A at the intersection of a vertical line from the bottom of the upstream face and the water surface, and a point B where the water line intersects the upstream face.
3. Locate point C , such that $BC = 0.3AB$.
4. Project a vertical line from C to intersect the base of the dam at D .
5. Locate the focus of the basic parabola. The focus is located conveniently at the toe of the dam.
6. Calculate the focal distance, $f = (\sqrt{b^2 + H^2} - b)/2$, where b is the distance FD and H is the height of water on the upstream face.
7. Construct the basic parabola from $z = 2\sqrt{f(f+x)}$.
8. Sketch in a transition section BE .
9. Calculate the length of the discharge face, a , using

$$a = \frac{1}{\cos \beta} (b - \sqrt{b^2 - H^2 \cot^2 \beta}); \quad \beta \leq 30^\circ.$$

For $\beta > 30^\circ$, use Figure 14.10 and (a) measure the distance TF , where T is the intersection of the basic parabola with the downstream face; (b) for the known angle β , read the corresponding factor $\Delta a/L$ from the chart; and (c) find the distance $a = TF(1 - \Delta a/L)$.

10. Measure the distance a from the toe of the dam along the downstream face to point G .
11. Sketch in a transition section, GK .
12. Calculate the flow using $q = ak \sin \beta \tan \beta$, where k is the hydraulic conductivity. If the downstream slope has a horizontal drainage blanket, as shown in Figure 14.11, the flow is calculated using $q = 2fk$.

What's next . . . Coarse-grained soils are used with or without filter fabric as filters or drainage blankets to control seepage. Next, we present some simple guidelines for selecting soils for filters and the applications of geotextiles for soil filtration.

14.8 SOIL FILTRATION

The diameter D_{10} (Chapter 2) is called the effective size of the soil and was established by Allen Hazen (1893) in connection with his work on soil filters. The higher the D_{10} value, the coarser the soil and the better the drainage characteristics. The diameter of the finer particle sizes, in particular D_{15} , has been used to develop criteria for soil filters. Terzaghi and Peck (1948), for example, proposed the following set of criteria for an effective soil filter.

$$\frac{D_{15(F)}}{D_{85(BS)}} < 4 \quad (\text{to prevent the filter soil from being washed out}) \quad (14.43)$$

and

$$\frac{D_{15(F)}}{D_{15(BS)}} > 4 \quad (\text{to ensure a high rate of flow of water}) \quad (14.44)$$

where F denotes filter and BS is the base soil.

Most filters are multilayers of sand and gravel. These filters are difficult to construct, and their efficiency is easily compromised by even a small amount of fines. Geotextiles—a permeable, polymeric material—have replaced soil filters in many construction applications. Geotextiles, sometimes called filter fabric, allow the passage of water but not fines. Consequently, the geotextile must be properly sized to prevent clogging. Construction is simple and cost-effective compared with soil filters. Generally, the filter is about 10 to 20 times more permeable than the soil. Two examples of the applications of geotextiles in soil filtration are shown in Figure 14.12. Manufacturers' catalogs and application software programs provide guidance on the selection of the appropriate geotextile.

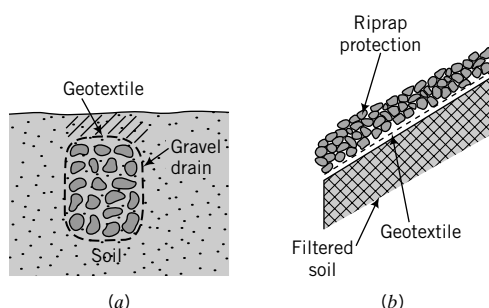


FIGURE 14.12 (a) A geotextile-wrapped gravel drain; (b) geotextile used in filtration of a riprap slope.

14.9 SUMMARY

The flow of water through soils is a very important consideration in the analysis, design, and construction of many civil engineering systems. The governing equation for flow of water through soils is Laplace's equation. In this chapter, we examined two types of solution for Laplace's equation for two-dimensional flow. One is a graphical technique, called flownet sketching, which consists of a network of flow and equipotential lines. The network (flownet) consists of curvilinear squares in which flow lines and equipotential lines are orthogonal to each other. From the flownet, we can calculate the flow rate, the distribution of heads, porewater pressures, seepage forces, and the maximum hydraulic gradient. The other type of solution is based on the finite difference method and requires, in most cases, the use of a spreadsheet or a computer program. Instability of structures embedded in soils can occur if the maximum hydraulic gradient exceeds the critical hydraulic gradient.

Self-Assessment

Access Chapter 14 at <http://www.wiley.com/college/budhu> to take the end-of-chapter quiz to test your understanding of this chapter.

Practical Examples

EXAMPLE 14.4 Determining Flow and Piping for an Excavation

A bridge pier is to be constructed in a riverbed by constructing a cofferdam, as shown in Figure E14.4a. A cofferdam is a temporary enclosure consisting of long, slender elements of steel, concrete, or timber members to support the sides of the enclosure. After construction of the cofferdam, the water within it will be pumped out. Determine (a) the flow rate using $k = 1 \times 10^{-4}$ cm/s and (b) the factor of safety against piping. The void ratio of the sand is 0.59.

There was a long delay before construction began, and a 100-mm layer of silty clay with $k = 1 \times 10^{-6}$ cm was deposited at the site. What effect would this silty clay layer have on the factor of safety against piping?

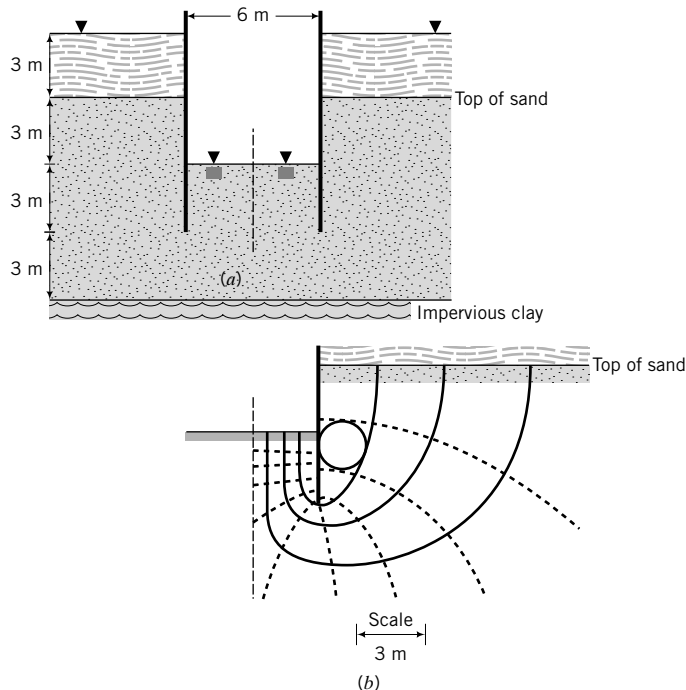


FIGURE E14.4a, b

Strategy The key is to draw a flownet and determine whether the maximum hydraulic gradient is less than the critical hydraulic gradient. The presence of the silty clay would result in significant head loss within it, and consequently the factor of safety against piping would likely increase. Since the cofferdam and the soil are symmetrical about a vertical plane, you only need to draw the flownet for one-half of the cofferdam.

Solution 14.4

Step 1: Draw the cofferdam to scale and sketch the flownet.

See Figure E14.4b.

Step 2: Determine the flow rate per meter length of wall.

$$\Delta H = 6 \text{ m}; \quad N_f = 4, \quad N_d = 10$$

$$q = 2k\Delta H \frac{N_f}{N_d} = 2 \times 1 \times 10^{-4} \times 10^{-2} \times 6 \times \frac{4}{10} = 4.8 \times 10^{-6} \text{ m}^3/\text{s}$$

(Note: The factor 2 is needed because you have to consider both halves of the structure; the factor 10^{-2} is used to convert cm/s to m/s.)

Step 3: Determine the maximum hydraulic gradient.

$$L_{min} \approx 0.3 \text{ m} \quad (\text{this is an average value of the flow length at the exit of the sheet pile})$$

$$i_{max} = \frac{\Delta h}{L_{min}} = \frac{\Delta H}{N_d L_{min}} = \frac{6}{10 \times 0.3} = 2$$

Step 4: Calculate the critical hydraulic gradient.

$$i_{cr} = \frac{G_s - 1}{1 + e} = \frac{2.7 - 1}{1 + 0.59} = 1.07$$

Since $i_{max} > i_{cr}$, piping is likely to occur; the factor of safety is $1.07/2 \approx 0.5$.

Step 5: Determine the effects of the silty clay layer.

Consider the one-dimensional flow in the flow domain, as shown in Figure E14.4c. The head loss through 9 m of sand (6 m outside and 3 m inside of excavation) is 6 m in the absence of the silt layer. Let us find the new head loss in the sand due to the presence of the silt layer.

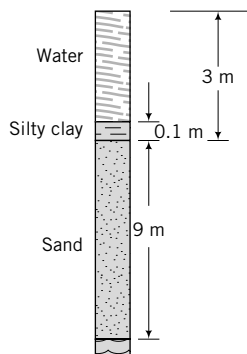


FIGURE E14.4c

From Darcy's law and the continuity condition:

$$k_{sand} i_{sand} = k_{silt} i_{silt}$$

or

$$k_{sand} \frac{\Delta h_{sand}}{L_{sand}} = k_{silt} \frac{\Delta h_{silt}}{L_{silt}}$$

Therefore,

$$\Delta h_{sand} = \frac{1 \times 10^{-6} \times 9\Delta h_{silt}}{1 \times 10^{-4} \times 0.1} = 0.9\Delta h_{silt}$$

But $\Delta h_{sand} + \Delta h_{silt} = 6$ m; that is, $0.9\Delta h_{silt} + \Delta h_{silt} = 6$ m and $\Delta h_{silt} = 3.16$ m. Therefore,

$$\Delta h_{sand} = 6 - 3.16 = 2.84 \text{ m}$$

Thus, the maximum hydraulic gradient would be reduced.

EXAMPLE 14.5 Sizing a Hollow Box Culvert for Uplift

A concrete hollow box culvert is shown in Figure E14.5a.

- (a) Determine the minimum wall thickness to prevent uplift using a factor of safety of 1.2. The groundwater can rise to the surface. The unit weight of concrete is 24 kN/m^3 . Assume the worst-case scenario.
- (b) If the weight of the culvert is restricted so that uplift can occur, show one possible method to prevent uplift.

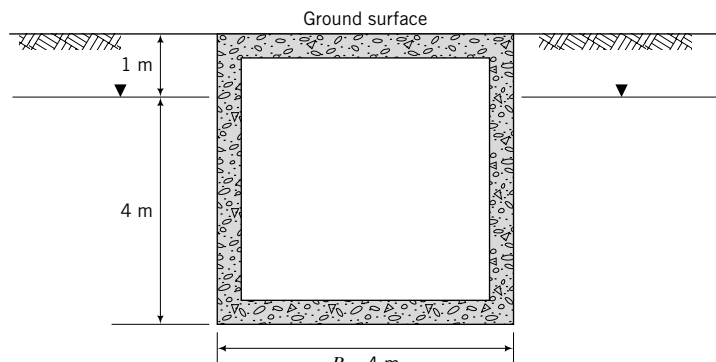


FIGURE E14.5a

Strategy The worst-case scenario is when the groundwater rises to the surface, with no water in the culvert and no side resistance. The solution to this problem requires the use of the force equilibrium equation in the vertical direction.

Solution 14.5

Step 1: Calculate uplift force per unit length of culvert.

The worst-case scenario is when the groundwater rises to the surface.

The uplift pressure is $p_w = h\gamma_w = (4 + 1)9.8 = 49 \text{ kPa}$.

The uplift force, P_{up} , at the base of the culvert is Bp_w .

$$P_{up} = 4 \times 49 = 196 \text{ kN per meter length.}$$

Step 2: Determine the weight of the culvert.

Assume a wall thickness of t .

$$\text{The weight per unit length, } W = [(4 \times 5) - (4 - 2t)(5 - 2t)] \times 24.$$

Step 3: Determine the wall thickness.

$$\text{FS} \times W = P_{up}$$

$$1.2 \times 24 \times [(4 \times 5) - (4 - 2t)(5 - 2t)] = 196$$

$$\therefore t^2 - 4.5t + 1.7 = 0$$

The solution for t is $t = 0.416 \text{ m} = 416 \text{ mm}$.

Step 4: Show one method to prevent uplift.

One potential method to prevent uplift is to use ground anchors, as shown in Figure E14.5b. The anchors must support the difference between the uplift force and the net downward resistance (weight plus side shear resistance) with a sufficient factor of safety (>1.2).

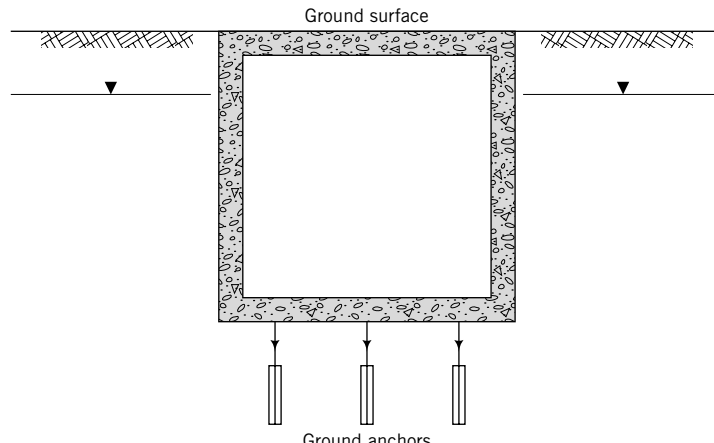


FIGURE E14.5b

EXERCISES

Theory

- 14.1** Derive a relationship between the critical hydraulic gradient, i_{cr} , and porosity, n .

Problem Solving

- 14.2** A sheet pile wall supporting 6 m of water is shown in Figure P14.2.

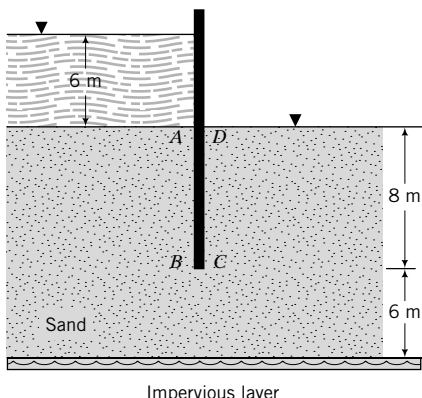


FIGURE P14.2

- (a) Draw the flownet.
- (b) Determine the flow rate if $k = 0.0019 \text{ cm/s}$.
- (c) Determine the porewater pressure distributions on the upstream and downstream faces of the wall.
- (d) Would piping occur if $e = 0.55$?

- 14.3** Assume the height of the wall shown in Figure 14.5 is 3 m high.

- (a) Determine the average flow rate into the drainage blanket if $k = 0.003 \text{ cm/s}$.
- (b) Determine the porewater pressure distribution just before the inflow face of the drainage blanket.
- (c) Calculate the average lateral force from the porewater pressure.

- 14.4** A sheet pile wall supporting 6 m of water has a clay (almost impervious) blanket of 3 m on the downstream side, as shown in Figure P14.4.

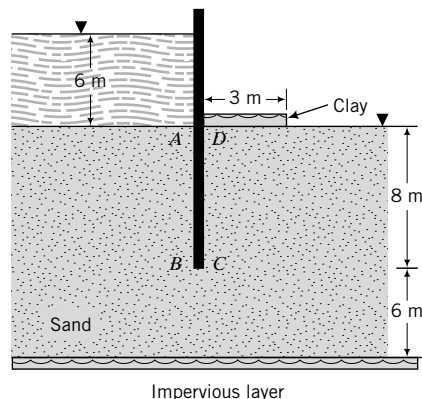
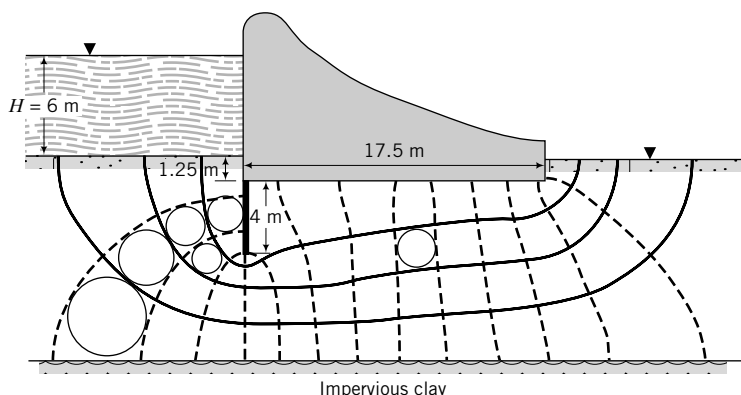


FIGURE P14.4

- (a) Draw the flownet.
- (b) Determine the flow rate if the equivalent hydraulic conductivity is $k = 1.9 \times 10^{-3} \text{ cm/s}$.

**FIGURE P14.6**

- (c) Determine the porewater pressure distributions on the upstream and downstream faces of the wall.

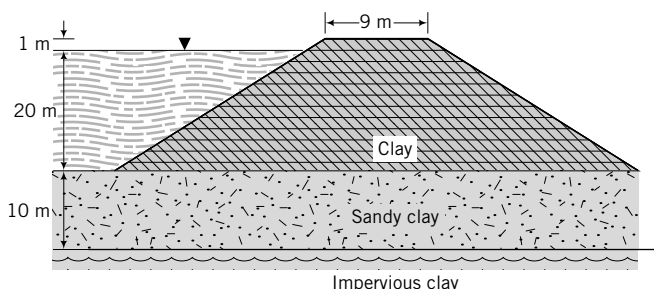
- (d) Would piping occur if $e = 0.55$?

14.5 Repeat Exercise 14.2 using the finite difference method.

14.6 For the dam shown in Figure P14.6,

- (a) Determine the flow rate under the dam if the equivalent hydraulic conductivity is $k = 4 \times 10^{-4}$ cm/s.
- (b) Determine the porewater pressure distribution at the base of the dam.
- (c) Calculate the resultant uplift force and its location from the upstream face of the dam.
- (d) Calculate the weight of the dam to prevent uplift using a factor of safety of 1.2.
- (e) Would piping occur if $e = 0.6$?

14.7 A section of a dam constructed from a clay is shown in Figure P14.7. The dam is supported on 10 m of sandy clay with $k_x = 1.2 \times 10^{-5}$ cm/s and $k_z = 2 \times 10^{-5}$ cm/s and a saturated unit weight of 17.8 kN/m^3 . Below the sandy clay is a thick layer of impervious clay. The upstream and downstream slopes are 1(V):2(H).

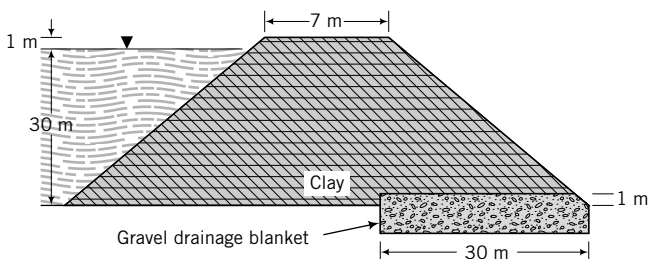
**FIGURE P14.7**

- (a) Draw the flownet under the dam.
- (b) Determine the porewater pressure distribution at the base of the dam.

- (c) Calculate the resultant uplift force and its location from the upstream face of the dam.

14.8 Draw the phreatic surface for the earth dam shown in Figure P14.7. Determine the flow rate within the dam if $k = k_x = 1 \times 10^{-6}$ cm/s.

14.9 Draw the phreatic surfaces and determine the flow rates with and without the drainage blanket for the dam shown in Figure P14.9. Below the dam is a deep deposit of medium clay that is practically impervious. This deposit is not shown in Figure P14.9. The upstream and downstream slopes are 1(V):2(H). The hydraulic conductivity of the clay is $k = k_x = 1.2 \times 10^{-6}$ cm/s.

**FIGURE P14.9**

14.10 Borings at a site for a road pavement show a water-bearing stratum of coarse-grained soil below an 8-m-thick deposit of a mixture of sand, silt, and clay. The water-bearing stratum below the mixture of sand, silt, and clay will create an artesian condition. The excess head is 1 m. One preliminary design proposal is to insert two trenches, as shown in Figure P14.10 on the next page, to reduce the excess head. Draw the flownet and determine the flow rate into each of the trenches if $k = k_z = 1 \times 10^{-5}$ cm/s.

14.11 A retaining wall has a vertical drainage blanket (Figure P14.11 on the next page). After a heavy rainfall, a steady-state seepage condition occurs. Draw the flownet and determine the porewater pressure distribution acting on a potential failure plane AB. The hydraulic conductivity is 1.8×10^{-4} cm/s.

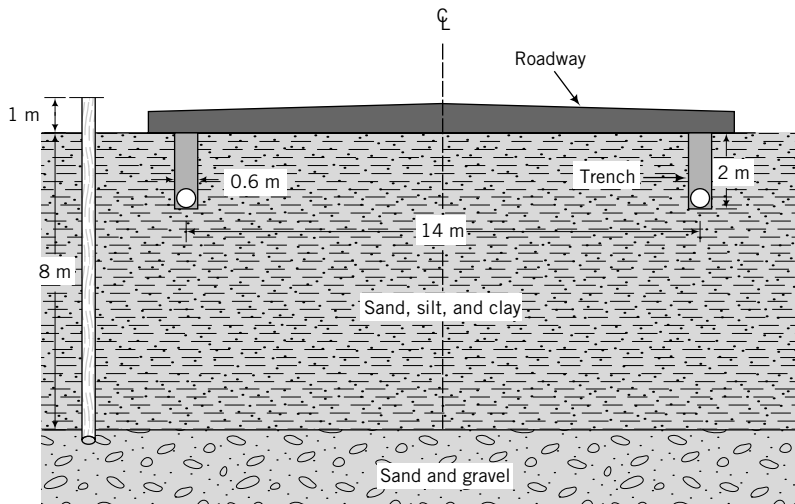


FIGURE P14.10

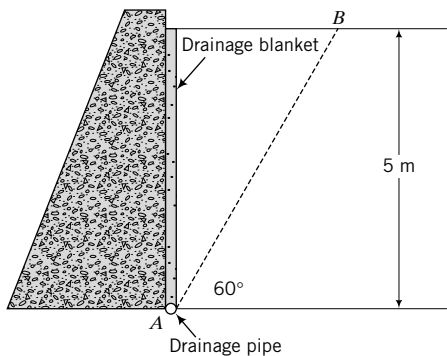


FIGURE P14.11

Practical

14.12 A concrete hollow box culvert is shown in Figure P14.12. A basement for a building is required near the culvert. One proposal is to construct a sheetpile wall to surround the excavation, as shown in Figure P14.12, and pump out the water in the excavation. The lowest groundwater-level profile is as shown in Figure P14.12. The equivalent hydraulic conductivity of the soil is $2 \times 10^{-4} \text{ cm/s}$.

- (a) Draw the flownet.
- (b) Determine the uplift pressure on the box culvert.

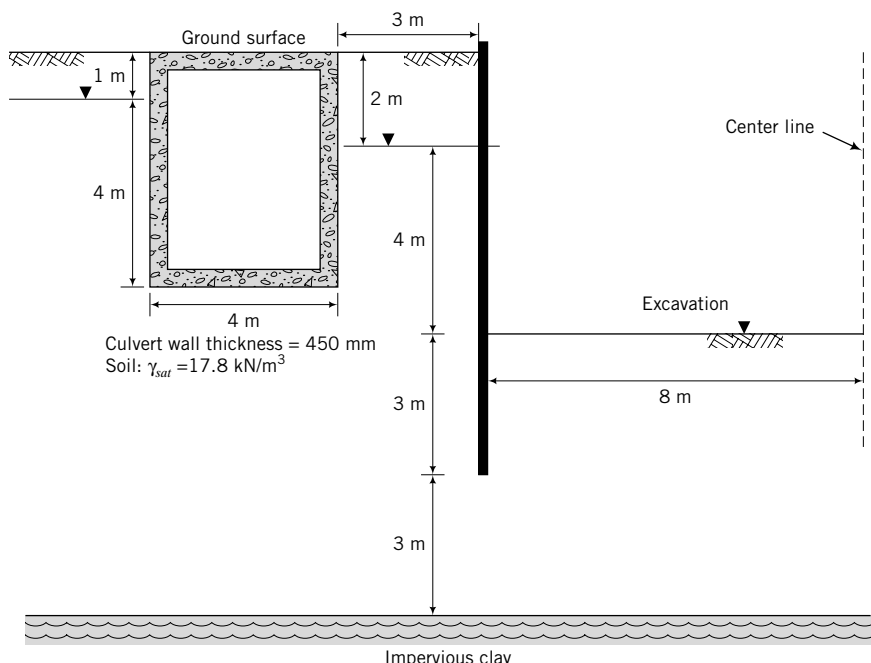


FIGURE P14.12

- (c) Will the culvert be safe against uplift? Assume the frictional resistance per unit length on each side wall is approximately $0.5K_a(\gamma_{sat} - \gamma_w)H^2\tan\left(\frac{2}{3}\phi'_{cs}\right)$, where $K_a = \tan^2\left(45^\circ - \frac{\phi'_{cs}}{2}\right)$ and $\phi'_{cs} = 30^\circ$. The unit weight of concrete is 24 kN/m^3 .
- (d) Determine if piping would occur. (*Hint:* You can calculate the void ratio from the given unit weight.)

- 14.13** A tunnel runs inside an embankment that supports a highway, as shown in Figure P14.13. The equivalent hydraulic conductivity of the embankment soil is $k = 8 \times 10^{-5} \text{ cm/s}$.

- (a) Draw the flownet within the embankment for the worst-case scenario.
- (b) Determine the uplift force per unit length at the base of the tunnel.
- (c) Determine if piping would occur if the unit weight of the soil in the embankment were 18.8 kN/m^3 .

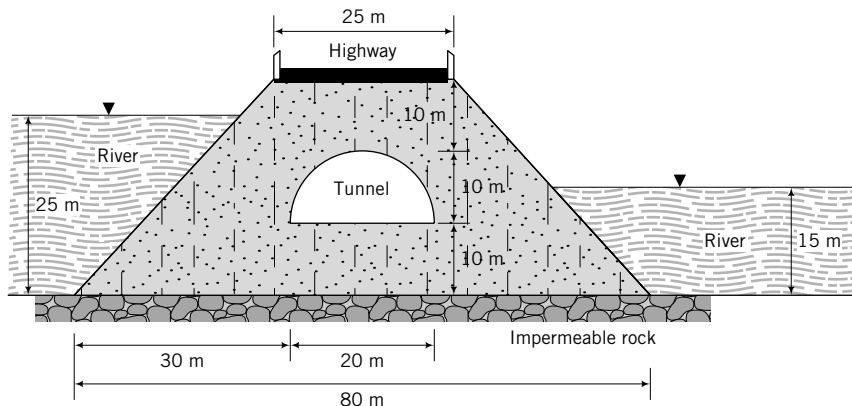


FIGURE P14.13

CHAPTER 15

STABILITY OF EARTH-RETAINING STRUCTURES

15.0 INTRODUCTION

In this chapter, we will analyze some typical earth-retaining structures to determine their stability. The emphases will be on gaining an understanding of the forces that provoke failures and methods of analysis of simple earth-retaining structures.

When you complete this chapter, you should be able to:

- Understand and determine lateral earth pressures.
- Understand the forces that lead to instability of earth-retaining structures.
- Determine the stability of simple earth-retaining structures.

You will use the following principles learned from previous chapters and your courses in mechanics:

- Static equilibrium
- Effective stresses and seepage (Chapter 7)
- Mohr's circle (Chapter 7)
- Shear strength (Chapter 10)
- Two-dimensional flow of water through soils (Chapter 14)

Importance

Earth-retaining structures are ubiquitous in the man-made environment. These structures have the distinction of being the first to be analyzed using mechanics (remember, we mentioned Coulomb's analysis of the lateral earth pressure on the fortresses protected by soil in Chapter 1). There are various types of retaining walls. By convention, these walls are grouped into three categories—mass gravity, flexible, and mechanically stabilized earth walls. Regardless of the category, a geotechnical engineer must ensure that the wall is stable under anticipated loadings. You should recall that stability refers to a condition in which a geotechnical system will not fail or collapse under any conceivable loading (static and dynamic loads, fluid pressure, seepage forces). Stability is synonymous with ultimate limit state, but serviceability limit state is also important. In many circumstances, the serviceability limit state is the deciding design limit state. The methods of analyses that we are going to discuss in this chapter do not consider the serviceability limit state. The analyses involved in determining the serviceability limit state are beyond the scope of this book. An example of a retaining structure in a waterfront area is shown in Figure 15.1.



FIGURE 15.1 A flexible retaining wall under construction.

15.1 DEFINITIONS OF KEY TERMS

Backfill is the soil retained by the wall.

Active earth pressure coefficient (K_a) is the ratio between the lateral and vertical principal effective stresses at the limiting stress state when an earth-retaining structure moves away (by a small amount) from the backfill (retained soil).

Passive earth pressure coefficient (K_p) is the ratio between the lateral and vertical principal effective stresses at the limiting stress state when an earth-retaining structure is forced against a soil mass.

Gravity retaining wall is a massive concrete wall relying on its mass to resist the lateral forces from the retained soil mass.

Flexible retaining wall or **sheet pile wall** is a long, slender wall relying on passive resistance and anchors or props for its stability.

Mechanical stabilized earth is a gravity-type retaining wall in which the soil is reinforced by thin reinforcing elements (steel, fabric, fibers, etc.).

15.2 QUESTIONS TO GUIDE YOUR READING

1. What is meant by the stability of earth-retaining structures?
2. What are the factors that lead to instability?
3. What are the main assumptions in the theory of lateral earth pressures?
4. When shall I use either Rankine's theory or Coulomb's theory?
5. Does Coulomb's theory give an upper bound or a lower bound solution?
6. What is the effect of wall friction on the shape of slip planes?
7. What are the differences among a gravity wall, a cantilever wall, a cantilever sheet pile wall, and an anchored sheet pile wall?

8. How do I analyze a retaining wall to check that it is stable?
9. How deep can I make a vertical cut without wall supports?
10. What are mechanically stabilized earth walls?

15.3 BASIC CONCEPTS OF LATERAL EARTH PRESSURES



Interactive Concept Learning

Access <http://www.wiley.com/college/budhu>, Chapter 15 to learn the basic concepts of lateral earth pressure through interactive visualizations.

We discussed the lateral earth pressure at rest and the lateral increases in stresses on a semi-infinite, isotropic, homogeneous, elastic soil mass from surface loading in Chapter 7. We are now going to consider the lateral earth pressures on a vertical wall that retains a soil mass. We will deal with two theories, one proposed by Coulomb (1776) and the other by Rankine (1857). First, we will develop a basic understanding of lateral earth pressures using a generic ϕ' and make the following assumptions:

1. The earth-retaining wall is vertical.
2. The interface between the wall and soil is frictionless.
3. The soil surface is horizontal and no shear stress acts on horizontal and vertical boundaries.
4. The wall is rigid and extends to an infinite depth in a dry, homogeneous, isotropic soil mass.
5. The soil is loose and initially in an at-rest state.

Consider the wall shown in Figure 15.2. If the wall remains rigid and no movement (not even an infinitesimal movement) occurs, then the vertical and horizontal effective stresses at rest on elements A, at the back wall, and B, at the front wall, are

$$\begin{aligned}\sigma'_z &= \sigma'_1 = \gamma'z \\ \sigma'_x &= \sigma'_3 = K_o\sigma'_1 = K_o\gamma'z\end{aligned}$$

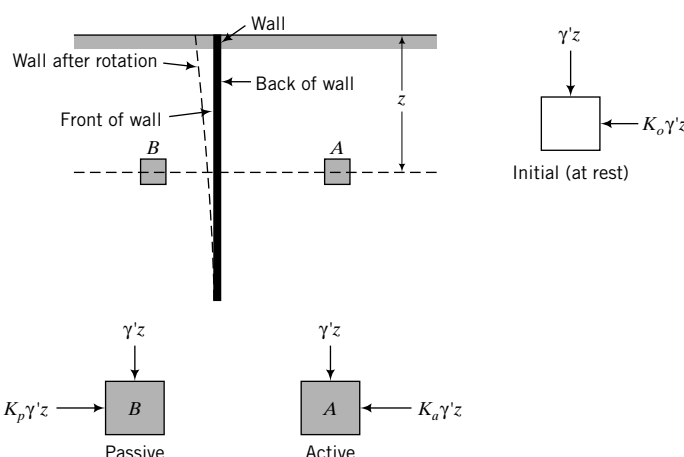


FIGURE 15.2 Stresses on soil elements in front of and behind a retaining wall.

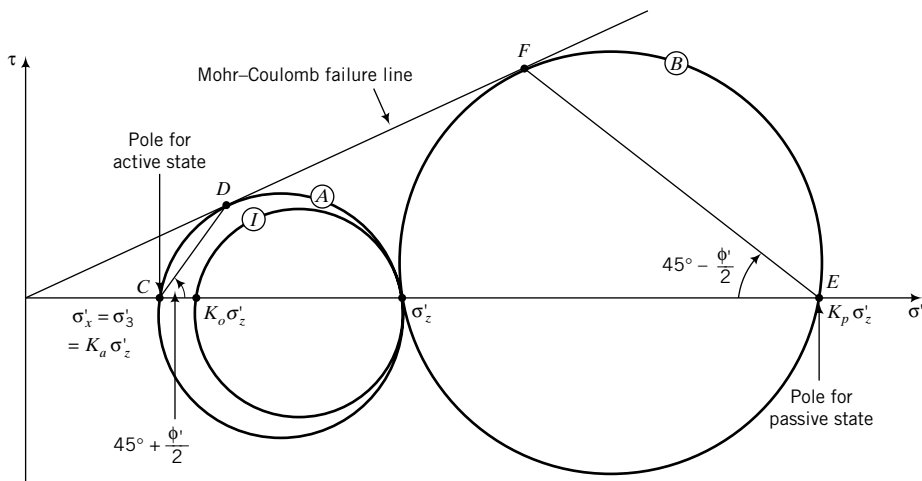


FIGURE 15.3 Mohr's circles at rest, active and passive states.

where γ' is the effective unit weight of the soil and K_o is the lateral earth pressure at rest [Equation (7.50)]. Mohr's circle for the at-rest state is shown by circle (I) in Figure 15.3. Note that if the soil surface were not horizontal, the major and minor principal effective stresses would not be equal to the vertical and lateral effective stresses, respectively.

Let us now assume a rotation about the bottom of the wall sufficient to produce slip planes in the soil mass behind and in front of the wall (Figure 15.4). The rotation, and consequently the lateral strains, required to produce slip planes in front of the wall is much larger than that required for the back of the wall, as shown in Figure 15.5. The soil mass at the back of the wall is causing failure, while the soil mass at the front of the wall is resisting failure. In the latter, you have to rotate the wall against the soil to produce failure.

What happens to the lateral effective stresses on elements A and B (Figure 15.2) when the wall is rotated? The vertical stress will not change on either element, but the lateral effective stress on element A will be reduced, while that for element B will be increased. We can now plot two additional Mohr's circles, one to represent the stress state of element A (circle (A) , Figure 15.3) and the other to represent the stress state of element B (circle (B) , Figure 15.3). Both circles are drawn such that the decrease (element A) or increase (element B) in lateral effective stress is sufficient to bring the soil to the Mohr-Coulomb limiting stress state. For simplicity in this chapter, we will call this limiting stress state the failure state.

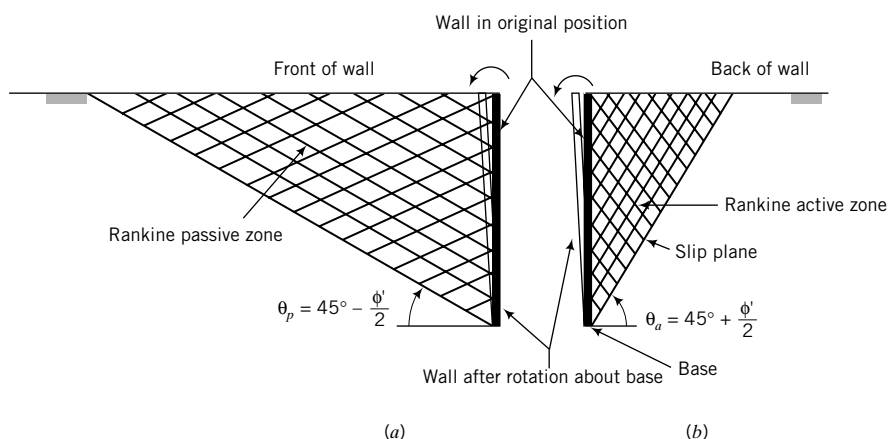


FIGURE 15.4 Slip planes within a soil mass near a retaining wall.

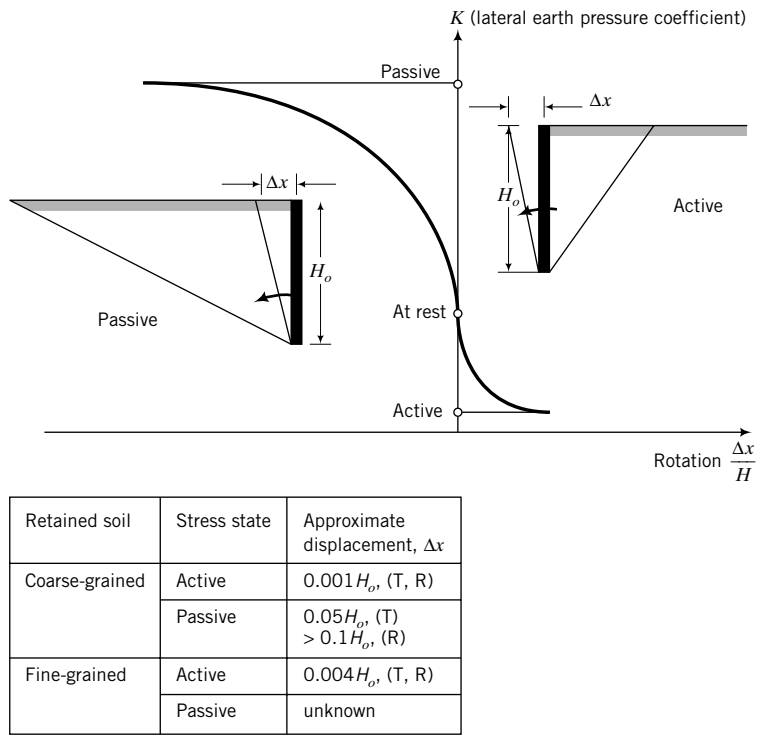


FIGURE 15.5 Rotation required to mobilize active and passive resistance.

This failure state is different from the critical state. For element B to reach the failure state, the lateral effective stress must be greater than the vertical effective stress, as shown in Figure 15.3.

The ratio of lateral principal effective stress to vertical principal effective stress at the limiting stress state is given by Equation (10.26), which, for circle (A) , is

$$\frac{(\sigma'_3)_f}{(\sigma'_1)_f} = \frac{1 - \sin \phi'}{1 + \sin \phi'} = \tan^2\left(45^\circ - \frac{\phi'}{2}\right) = K_a \quad (15.1)$$

where K_a is called the active lateral earth pressure coefficient. Similarly, for circle (B) ,

$$\frac{(\sigma'_1)_f}{(\sigma'_3)_f} = \frac{1 + \sin \phi'}{1 - \sin \phi'} = \tan^2\left(45^\circ + \frac{\phi'}{2}\right) = K_p \quad (15.2)$$

where K_p is the passive earth pressure coefficient. Therefore,

$$K_p = \frac{1}{K_a}$$

If, for example, $\phi' = 30^\circ$, then $K_a = \frac{1}{3}$ and $K_p = 3$.

The stress states of soil elements A and B are called the Rankine active state and the Rankine passive state, respectively [named after the original developer of the theory, Rankine (1857)]. Each of these Rankine states is associated with a family of slip planes. For the Rankine active state, the slip planes are oriented at

$$\theta_a = 45^\circ + \frac{\phi'}{2} \quad (15.3)$$

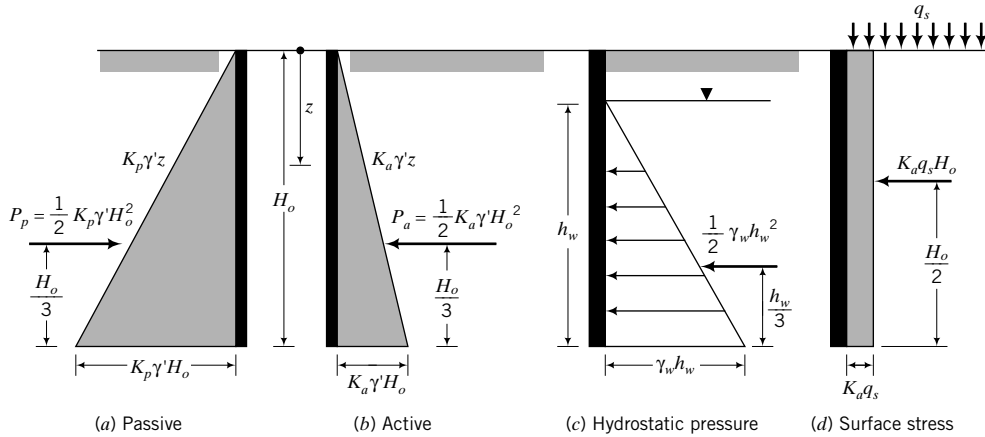


FIGURE 15.6 Variation of active and passive lateral earth pressures, hydrostatic pressure, and a uniform surface stress with depth.

to the horizontal, as illustrated in Figure 15.4b and proved in Chapter 10. For the Rankine passive state, the slip planes are oriented at

$$\theta_p = 45^\circ - \frac{\phi'}{2} \quad (15.4)$$

to the horizontal, as illustrated in Figure 15.4a.

The lateral earth pressure for the Rankine active state is

$$(\sigma'_x)_a = K_a \sigma'_z = K_a \gamma' z \quad (15.5)$$

and for the Rankine passive state it is

$$(\sigma'_x)_p = K_p \sigma'_z = K_p \gamma' z \quad (15.6)$$

Equations (15.5) and (15.6) indicate that, for a homogeneous soil layer, the lateral earth pressure varies linearly with depth, as shown in Figure 15.6a, b. The lateral active and passive coefficients are applied only to effective stresses. For soils above the groundwater level, $\gamma' = \gamma$, while for soils below the groundwater level, $\gamma' = (\gamma_{sat} - \gamma_w)$.

The lateral earth force is the area of the lateral stress diagram, which, for the Rankine active state, is

$$P_a = \int_0^{H_o} K_a \gamma' z = \frac{1}{2} K_a \gamma' H_o^2 \quad (15.7)$$

and, for the Rankine passive state, is

$$P_p = \int_0^{H_o} K_p \gamma' z = \frac{1}{2} K_p \gamma' H_o^2 \quad (15.8)$$

These lateral forces, P_a and P_p , are located at the centroid of the lateral earth pressure distribution diagram. In this case, the centroid is at $H_o/3$ from the base.

If groundwater is present, you need to add the hydrostatic pressure (porewater pressure) to the lateral earth pressure. For example, if the groundwater level is at distance h_w from the base of the wall (Figure 15.6c), the hydrostatic pressure is

$$u = \gamma_w h_w \quad (15.9)$$

and the hydrostatic force is

$$P_w = \frac{1}{2} \gamma_w h_w^2 \quad (15.10)$$

Surface stresses also impose lateral earth pressures on retaining walls. A uniform surface stress, q_s , will transmit a uniform active lateral earth pressure of $K_a q_s$ (Figure 15.6d) and a uniform passive lateral earth pressure of $K_p q_s$. The active and passive lateral earth pressures due to the soil, groundwater, and the uniform surface stresses are then

$$(\sigma_x)_a = K_a \sigma'_z + K_a q_s + (u)_a \quad (15.11)$$

and

$$(\sigma_x)_p = K_p \sigma'_z + K_p q_s + (u)_p \quad (15.12)$$

where u is the hydrostatic pressure and the subscripts a and p denote active and passive states, respectively.

The lateral forces from a line load and a strip load are given in Chapter 7. For other types of surface loads you can consult Poulos and Davis (1974).

THE ESSENTIAL POINTS ARE:

1. The lateral earth pressures on retaining walls are related directly to the vertical effective stress through two coefficients. One is the active earth pressure coefficient,

$$K_a = \frac{1 - \sin \phi'}{1 + \sin \phi'} = \tan^2 \left(45^\circ - \frac{\phi'}{2} \right)$$

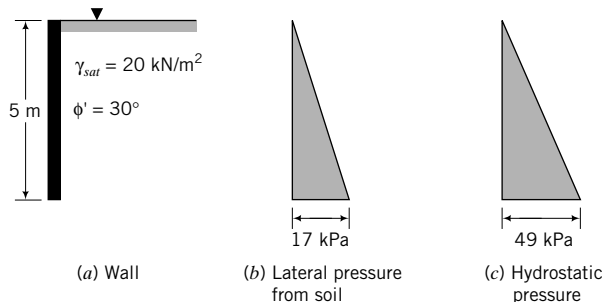
and the other is the passive earth pressure coefficient,

$$K_p = \frac{1 + \sin \phi'}{1 - \sin \phi'} = \tan^2 \left(45^\circ + \frac{\phi'}{2} \right) = \frac{1}{K_a}$$

2. Substantially more movement is required to mobilize the full passive earth pressure than the full active earth pressure.
3. A family of slip planes occurs in the Rankine active and passive states. In the active state, the slip planes are oriented at $45^\circ + \phi'/2$ to the horizontal, while for the passive case they are oriented at $45^\circ - \phi'/2$ to the horizontal.
4. The lateral earth pressure coefficients developed so far are valid only for a smooth, vertical wall supporting a homogeneous soil mass with a horizontal surface.
5. The lateral earth pressure coefficients must be applied only to principal effective stresses.

EXAMPLE 15.1 Lateral Earth Pressure and Force

Determine the active lateral earth pressure on the frictionless wall shown in Figure E15.1a. Calculate the resultant force and its location from the base of the wall. Neglect seepage effects.

**FIGURE E15.1**

Strategy The lateral earth pressure coefficients can only be applied to the effective stresses. You need to calculate the vertical effective stress, apply K_a , and then add the porewater pressure.

Solution 15.1

Step 1: Calculate K_a .

$$K_a = \frac{1 - \sin \phi'}{1 + \sin \phi'} = \frac{1 - \sin (30^\circ)}{1 + \sin (30^\circ)} = \frac{1}{3}$$

$$\text{or } \tan^2\left(45 - \frac{\phi'}{2}\right) = \tan^2\left(45^\circ - \frac{30^\circ}{2}\right) = \frac{1}{3}$$

Step 2: Calculate the vertical effective stress.

$$\text{At the surface: } \sigma'_z = 0, \quad u = 0$$

$$\text{At the base: } \sigma'_z = \gamma' H_o = (20 - 9.8) \times 5 = 51 \text{ kPa}$$

$$u = \gamma_w H_o = 9.8 \times 5 = 49 \text{ kPa}$$

Step 3: Calculate the lateral effective stress.

$$(\sigma'_x)_a = K_a \sigma'_z = \frac{1}{3} \times 51 = 17 \text{ kPa}$$

Step 4: Sketch the lateral earth pressure distributions.

See Figure E15.1b, c.

Step 5: Calculate the lateral force.

$$P_a = P_s + P_w$$

where P_s is the lateral force due to the soil solids and P_w is the lateral force due to the porewater.

$$P_a = \frac{1}{2} (\sigma'_x)_a H_o + \frac{1}{2} u H_o = \left(\frac{1}{2} \times 17 \times 5\right) + \left(\frac{1}{2} \times 49 \times 5\right) = 165 \text{ kN}$$

Step 6: Determine the location of the resultant.

Since both the lateral earth pressure and the porewater pressure distributions are triangular over the whole depth, the resultant is at the centroid of the triangle, that is, $\bar{z} = H_o/3 = 5/3 = 1.67 \text{ m}$ from the base of the wall.

EXAMPLE 15.2 Lateral Earth Pressure in Layered Soils

For the frictionless wall shown in Figure E15.2a, determine the following:

- (a) The active lateral earth pressure distribution with depth.
- (b) The passive lateral earth pressure distribution with depth.

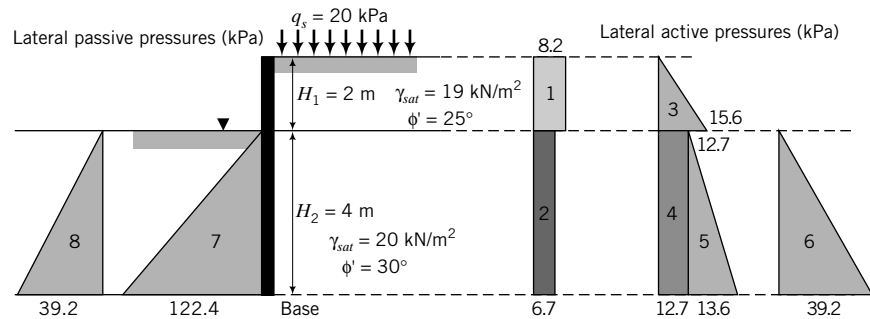


FIGURE E15.2 (f) Porewater (e) Soil (a) Wall (b) Surface stresses (c) Soil (d) Porewater

(c) The magnitudes and locations of the active and passive forces.

(d) The resultant force and its location.

(e) The ratio of passive moment to active moment.

Strategy There are two layers. It is best to treat each layer separately. Neither K_a nor K_p should be applied to the porewater pressure. You do not need to calculate K_p for the top soil layer. Since the water level on both sides of the wall is the same, the resultant hydrostatic force is zero. However, you are asked to determine the forces on each side of the wall; therefore, you have to consider the hydrostatic force. A table is helpful to solve this type of problem.

Solution 15.2

Step 1: Calculate the active lateral earth pressure coefficients.

$$\text{Top layer (0–2 m): } K_a = \tan^2\left(45^\circ - \frac{\phi'}{2}\right) = \tan^2\left(45^\circ - \frac{25^\circ}{2}\right) = 0.41$$

$$\text{Bottom layer (2–6 m): } K_a = \tan^2\left(45^\circ - \frac{\phi'}{2}\right) = \tan^2\left(45^\circ - \frac{30^\circ}{2}\right) = \frac{1}{3}; \quad K_p = \frac{1}{K_a} = 3$$

Step 2: Calculate the active and passive lateral earth pressures.

Use a table as shown below to do the calculations, or use a spreadsheet.

Active	Depth ^a (m)	u (kPa)	σ_z (kPa)	$\sigma'_z = \sigma_z - u$ (kPa)	$(\sigma'_x)_a = K_a \sigma'_z$ (kPa)
Surcharge	0	0	20	20	$0.41 \times 20 = 8.2$
	2–6	0	20	20	$\frac{1}{3} \times 20 = 6.7$
Soil	0	0	0	0	0
	2 [–]	0	$\gamma_1 H_1 = 19 \times 2 = 38$	38	$0.41 \times 38 = 15.6$
	2 ⁺	0	$\gamma_1 H_1 = 19 \times 2 = 38$	38	$\frac{1}{3} \times 38 = 12.7$
	6	$\gamma_w H_2 = 9.8 \times 4 = 39.2$	$\gamma_1 H_1 + \gamma_2 H_2 = 19 \times 2 + 20 \times 4 = 118$	78.8	$\frac{1}{3} \times 78.8 = 26.3$
Passive	Depth (m)	u (kPa)	σ_z (kPa)	$\sigma'_z = \sigma_z - u$ (kPa)	$(\sigma'_x)_p = K_p \sigma'_z$ (kPa)
Soil	0	0	0	0	0
	4	$\gamma_w H_2 = 9.8 \times 4 = 39.2$	$\gamma_2 H_2 = 20 \times 4 = 80$	40.8	$3 \times 40.8 = 122.4$

^aThe – and + superscripts indicate that you are calculating the stress just above (–) and just below (+) 2 m.

See Figure E15.2b–e for the pressure distributions.

Step 3: Calculate the hydrostatic force.

$$P_w = \frac{1}{2} \gamma_w H_2^2 = \frac{1}{2} \times 9.8 \times 4^2 = 78.4 \text{ kN}$$

Step 4: Calculate the resultant lateral forces and their locations.

See the table below for calculations. Active moments are assumed to be negative.

Active Area	Depth (m)	Force (kN)	Moment arm from base (m)	Moment (kN.m)
1	0–2	$8.2 \times 2 = 16.4$	$4 + 1 = 5 = 4.42$	-82.0
2	2–6	$6.7 \times 4 = 26.8$	$\frac{4}{2} = 2$	-53.6
3	0–2	$\frac{1}{2} \times 15.6 \times 2 = 15.6$	$\frac{2}{3} + 4 = 4.67$	-72.9
4	2–6	$12.7 \times 4 = 50.8$	$\frac{4}{2} = 2$	-101.6
5	2–6	$\frac{1}{2} \times 13.6 \times 4 = 27.2$	$\frac{4}{3}$	-36.3
6 (water)	2–6	<u>78.4</u>	$\frac{4}{3}$	<u>-104.5</u>
Σ Active lateral forces = 215.2			Σ Active moments = -450.9	
Passive Area	Depth (m)	Force (kN)	Moment arm from base (m)	Moment (kN.m)
7	2–6	$\frac{1}{2} \times 122.4 \times 4 = 244.8$	$\frac{4}{3}$	326.4
8 (water)	2–6	<u>78.4</u>	$\frac{4}{3}$	<u>104.5</u>
Σ Passive forces = 323.2			Σ passive moments = 430.9	

Location of resultant active lateral earth force:

$$\bar{z}_a = \frac{\Sigma \text{ Moments}}{\Sigma \text{ Active lateral forces}} = \frac{450.9}{215.2} = 2.09 \text{ m}$$

Location of passive lateral force: $\bar{z}_p = \frac{4}{3} = 1.33 \text{ m}$

Step 5: Calculate the resultant lateral force.

$$R_x = P_p - P_a = 323.2 - 215.2 = 108 \text{ kN/m}$$

Step 6: Calculate the ratio of moments.

$$\text{Ratio of moments} = \frac{\Sigma \text{ Passive moments}}{\Sigma \text{ Active moments}} = \frac{430.9}{450.9} = 0.96$$

Since the active moment is greater than the passive moment, the wall will rotate.

What's next . . . The pioneer of earth pressure theory is Coulomb. We are going to introduce his ideas in the next section.

15.4 COULOMB'S EARTH PRESSURE THEORY



Computer Program Utility

Access <http://www.wiley.com/college/budhu>, Chapter 15. Click on K_a and K_p coeff to download and run a computer program that will give the Coulomb and Rankine values of the active and passive coefficients.

Coulomb (1776) proposed that a condition of limit equilibrium exists through which a soil mass behind a vertical retaining wall will slip along a plane inclined an angle θ to the horizontal. He then determined the slip plane by searching for the plane on which the maximum thrust acts. We begin consideration of Coulomb's theory by reminding you of the basic tenets of limit equilibrium. The essential steps in the limit equilibrium method are (1) selection of a plausible failure mechanism, (2) determination of the forces acting on the failure surface, and (3) use of equilibrium equations to determine the maximum thrust.

Let us consider a vertical, frictionless wall of height H_o , supporting a soil mass with a horizontal surface (Figure 15.7a). We are going to assume a dry, homogeneous soil mass and postulate that slip occurs on a plane inclined at an angle θ to the horizontal. Since the soil is dry, $\gamma' = \gamma$. We can draw the free-body diagram as shown in Figure 15.7b and solve for P_a using statics, as follows:

$$\begin{aligned}\Sigma F_x &= P + T \cos \theta - N \sin \theta = 0 \\ \Sigma F_z &= W - T \sin \theta - N \cos \theta = 0\end{aligned}$$

We are using P rather than P_a because P_a is the limiting value.

The weight of the sliding mass of soil is

$$W = \frac{1}{2} \gamma H_o^2 \cot \theta$$

At limit equilibrium,

$$T = N \tan \phi'$$

Solving for P , we get

$$P = \frac{1}{2} \gamma H_o^2 \cot \theta \tan (\theta - \phi') \quad (15.13)$$

To find the maximum thrust and the inclination of the slip plane, we use calculus to differentiate Equation (15.13) with respect to θ :

$$\frac{\partial P}{\partial \theta} = \frac{1}{2} \gamma H_o^2 [\cot \theta \sec^2(\theta - \phi') - \csc^2 \theta \tan(\theta - \phi')] = 0$$

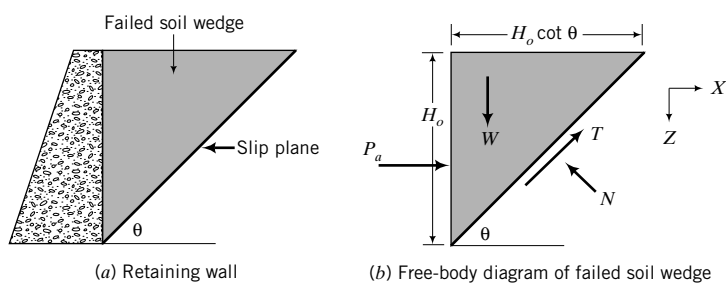


FIGURE 15.7 Coulomb failure wedge.

which leads to

$$\theta = \theta_{cr} = 45^\circ + \frac{\phi'}{2} \quad (15.14)$$

Substituting this value of θ into Equation (15.13), we get

$$P = P_a = \frac{1}{2}\gamma H_o^2 \tan^2\left(45^\circ - \frac{\phi'}{2}\right) = \frac{1}{2}K_a \gamma H_o^2 \quad (15.15)$$

This is the same result obtained earlier from considering Mohr's circle.

The solution from a limit equilibrium method is analogous to an upper bound solution because it gives a solution that is usually greater than the true solution. The reason for this is that a more efficient failure mechanism may be possible than the one we postulated. For example, rather than a planar slip surface we could have postulated a circular slip surface or some other geometric form, and we could have obtained a maximum horizontal force lower than for the planar slip surface.

For the Rankine active and passive states, we considered the stress states and obtained the distribution of lateral stresses on the wall. At no point in the soil mass did the stress state exceed the failure stress state, and static equilibrium is satisfied. The solution for the lateral forces obtained using the Rankine active and passive states is analogous to a lower bound solution—the solution obtained is usually lower than the true solution because a more efficient distribution of stress could exist. If the lower bound solution and the upper bound solution are in agreement, we have a true solution, as is the case here.

Poncelet (1840), using Coulomb's limit equilibrium approach, obtained expressions for K_a and K_p for cases where wall friction (δ) is present, the wall face is inclined at an angle η to the vertical, and the backfill is sloping at an angle β . With reference to Figure 15.8, K_{aC} and K_{pC} are

$$K_{aC} = \frac{\cos^2(\phi' - \eta)}{\cos^2 \eta \cos(\eta + \delta) \left[1 + \left\{ \frac{\sin(\phi' + \delta) \sin(\phi' - \beta)}{\cos(\eta + \delta) \cos(\eta - \beta)} \right\}^{1/2} \right]^2} \quad (15.16)$$

$$K_{pC} = \frac{\cos^2(\phi' + \eta)}{\cos^2 \eta \cos(\eta - \delta) \left[1 - \left\{ \frac{\sin(\phi' + \delta) \sin(\phi' + \beta)}{\cos(\eta - \delta) \cos(\eta - \beta)} \right\}^{1/2} \right]^2} \quad (15.17)$$

The subscript C denotes Coulomb. You should note that $K_{pC} \neq 1/K_{aC}$. Recall that the lateral earth pressure coefficients are applied to the principal effective stress and not the principal total stress.

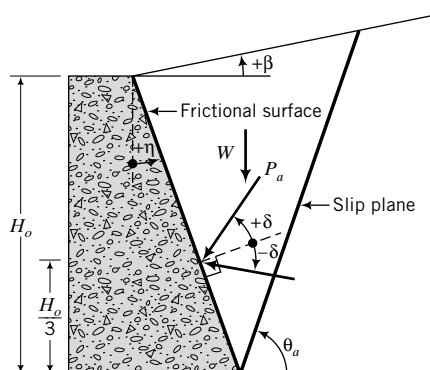


FIGURE 15.8 Retaining wall with sloping back, wall friction, and sloping soil surface for use with Coulomb's method for active condition.

TABLE 15.1 Correction Factors to Be Applied to K_{pC} to Approximate a Logarithm Spiral Slip Surface for a Backfill with a Horizontal Surface and Sloping Wall Face

ϕ'	δ/ϕ'							
	-0.7	-0.6	-0.5	-0.4	-0.3	-0.2	-0.1	0.0
15	0.96	0.93	0.91	0.88	0.85	0.83	0.80	0.78
20	0.94	0.90	0.86	0.82	0.79	0.75	0.72	0.68
25	0.91	0.86	0.81	0.76	0.71	0.67	0.62	0.57
30	0.88	0.81	0.75	0.69	0.63	0.57	0.52	0.47
35	0.84	0.75	0.67	0.60	0.54	0.48	0.42	0.36
40	0.78	0.68	0.59	0.51	0.44	0.38	0.32	0.26

The inclination of the slip plane to the horizontal for a horizontal backfill is

$$\tan \theta = \left[\frac{(\sin \phi' \cos \delta)^{1/2}}{\cos \phi' \{ \sin (\phi' + \delta) \}^{1/2}} \right] \pm \tan \phi' \quad (15.18)$$

where the positive sign refers to the active state ($\theta = \theta_a$) and the negative sign refers to the passive state ($\theta = \theta_p$).

Wall friction causes the slip planes in both the active and passive states to be curved. The curvature in the active case is small in comparison to the passive case. The implication of the curved slip surface is that the values of K_{aC} and K_{pC} from Equations (15.16) and (15.17) are not accurate. In particular, the passive earth pressures are overestimated using Equation (15.17). For the active state, the error is small and can be neglected. The error for the passive state is small if $\delta < \phi'/3$. In practice, δ is generally greater than $\phi'/3$.

Several investigators have attempted to find K_a and K_p using nonplanar slip surfaces. For example, Caquot and Kerisel (1948) used logarithm spiral slip surfaces, while Packshaw (1969) used circular failure surfaces. The Caquot and Kerisel values of K_p are generally used in practice. Table 15.1 lists factors that can be applied to K_{pC} to correct it for a logarithm spiral slip surface.

The lateral forces are inclined at δ to the normal on the sloping wall face. The sign conventions for δ and β are shown in Figure 15.8. You must use the appropriate sign in determining K_{aC} and K_{pC} . The direction of the frictional force on the wall depends on whether the wall moves relative to the soil or the soil moves relative to the wall. In general, the active wedge moves downward relative to the wall and the passive wedge moves upward relative to the wall. The frictional forces developed are shown in Figure 15.9.

The sense of the inclination of active lateral force is then positive, while the sense of the inclination of passive lateral force is negative. Load-bearing walls with large vertical loads tend to move downward relative to the soil. In such a situation the frictional force on both sides of the wall will be downward, and the lateral earth pressures are increased on both sides of the wall. In practice, these increases in pressure are ignored and the sense of the active and lateral forces is taken, as shown in Figure 15.9.

The horizontal components of the lateral forces are $P_{ax} = P_a \cos (\delta + \eta)$ and $P_{px} = P_p \cos (\delta + \eta)$, and the vertical components are $P_{az} = P_a \sin (\delta + \eta)$ and $P_{pz} = P_p \sin (\delta + \eta)$. The point of application of these forces is $H_o/3$ from the base of the wall (Figure 15.8). Typical values of δ for the interfaces of coarse-grained soils and concrete or steel walls range from $\frac{1}{2} \phi'$ to ϕ' , with $\frac{2}{3} \phi'$ most commonly used.

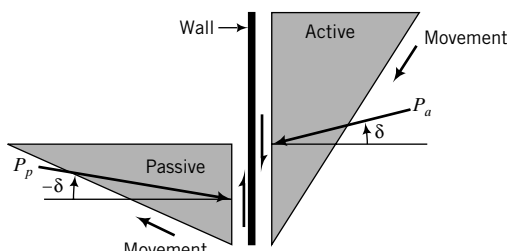


FIGURE 15.9 Directions of active and passive forces when wall friction is present.

THE ESSENTIAL POINTS ARE:

1. Coulomb's analysis of the lateral forces on a retaining structure is based on limit equilibrium.
2. Wall friction causes the slip planes to curve, which leads to an overestimation of the passive earth pressure using Coulomb's analysis.
3. For calculation of the lateral earth pressure coefficients you can use Equations (15.16) and (15.17), and correct K_{pC} using the factors listed in Table 15.1.
4. The active and passive forces are inclined at an angle δ from the normal to the wall face.

What's next . . . Coulomb's analysis is based on a postulated failure mechanism, and the stresses within the soil mass are not considered. Rankine (1857) proposed an analysis based on the stress state of the soil. You have already encountered his approach in Section 15.3. Next, we introduce Rankine's solution for a wall with a sloping backfill and a sloping wall face.

15.5 RANKINE'S LATERAL EARTH PRESSURE FOR A SLOPING BACKFILL AND A SLOPING WALL FACE



Computer Program Utility

Access <http://www.wiley.com/college/budhu>, Chapter 15. Click on K_a and K_p coeff to download and run a computer program that will give the values of the active and passive coefficients for Coulomb and Rankine.

Rankine (1857) established the principle of stress states or stress field in solving stability problems in soil mechanics. We have used Rankine's method in developing the lateral earth pressures for a vertical, frictionless wall supporting a dry, homogeneous soil with a horizontal surface. Rankine (1857) derived expressions for K_a and K_p for a soil mass with a sloping surface that were later extended to include a sloping wall face by Chu (1991). You can refer to Rankine's paper and Chu's paper for the mathematical details.

With reference to Figure 15.10, the lateral earth pressure coefficients according to Rankine's analysis are

$$K_{aR} = \frac{\cos(\beta - \eta)\sqrt{1 + \sin^2\phi' - 2\sin\phi'\cos\omega_a}}{\cos^2\eta(\cos\beta + \sqrt{\sin^2\phi' - \sin^2\beta})} \quad (15.19)$$

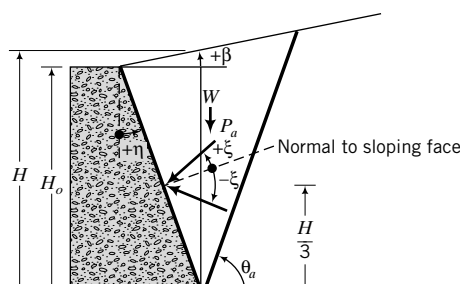


FIGURE 15.10 Retaining wall with sloping soil surface, frictionless soil-wall interface, and sloping back for use with Rankine's method.

and

$$K_{pR} = \frac{\cos(\beta - \eta)\sqrt{1 + \sin^2\phi' + 2\sin\phi'\cos\omega_p}}{\cos^2\eta(\cos\beta - \sqrt{\sin^2\phi' - \sin^2\beta})} \quad (15.20)$$

where the subscript R denotes Rankine, and

$$\omega_a = \sin^{-1}\left(\frac{\sin\beta}{\sin\phi'}\right) - \beta + 2\eta \quad (15.21)$$

$$\omega_p = \sin^{-1}\left(\frac{\sin\beta}{\sin\phi'}\right) + \beta - 2\eta \quad (15.22)$$

The angles of the failure planes to the horizontal for active and passive states are

$$\theta_a = \frac{\pi}{4} + \frac{\phi'}{2} + \frac{\beta}{2} - \frac{1}{2}\sin^{-1}\left(\frac{\sin\beta}{\sin\phi'}\right) \quad (15.23)$$

$$\theta_p = \frac{\pi}{4} - \frac{\phi'}{2} + \frac{\beta}{2} + \frac{1}{2}\sin^{-1}\left(\frac{\sin\beta}{\sin\phi'}\right) \quad (15.24)$$

The sign conventions for η and β are shown in Figure 15.10; counterclockwise rotation is positive.

The active and passive lateral earth forces at the limiting stress state are

$$P_a = \frac{1}{2}K_{aR}\gamma'H_o^2 \quad \text{and} \quad P_p = \frac{1}{2}K_{pR}\gamma'H_o^2$$

These forces are inclined at

$$\xi_a = \tan^{-1}\left(\frac{\sin\phi'\sin\theta_a}{1 - \sin\phi'\cos\theta_a}\right) \quad (15.25)$$

$$\xi_p = \tan^{-1}\left(\frac{\sin\phi'\sin\theta_p}{1 + \sin\phi'\cos\theta_p}\right) \quad (15.26)$$

to the normal of the wall face. The angles ξ_a and ξ_p (reminder: the subscripts a and p denote active and passive) are not interface friction values.

In the case of a wall with a vertical face, $\eta = 0$, Equations (15.19) and (15.20) reduce to

$$K_{aR} = \frac{1}{K_{pR}} = \cos\beta \left(\frac{\cos\beta - \sqrt{\cos^2\beta - \cos^2\phi'}}{\cos\beta + \sqrt{\cos^2\beta - \cos^2\phi'}} \right) \quad (15.27)$$

and the active and passive lateral earth forces act in a direction parallel to the soil surface, that is, they are inclined at an angle β to the horizontal. Thus, $P_{ax} = P_a \cos\beta$ and $P_{az} = P_a \sin\beta$.

THE ESSENTIAL POINTS ARE:

1. Rankine used the stress states of a soil mass to determine the lateral earth pressures on a frictionless wall.
2. The active and passive lateral earth forces are inclined at ξ_a and ξ_p , respectively, from the normal to the wall face. If the wall face is vertical, the active and passive lateral earth forces are parallel to the soil surface.

What's next . . . We considered the lateral earth pressures for a dry soil mass, which is analogous to an effective stress analysis. Next, we will consider total stress analysis.

15.6 LATERAL EARTH PRESSURES FOR A TOTAL STRESS ANALYSIS

Figure 15.11 shows a smooth, vertical wall supporting a homogeneous soil mass under undrained condition. Using the limit equilibrium method, we will assume, for the active state, that a slip plane is formed at an angle θ to the horizontal. The forces on the soil wedge are shown in Figure 15.11.

Using static equilibrium, we obtain the sum of the forces along the slip plane:

$$P \cos \theta + T - W \sin \theta = 0 \quad (15.28)$$

But $T = s_u L = s_u (H_o / \sin \theta)$ and $W = \frac{1}{2} \gamma H_o^2 \cot \theta$. Equation (15.28) then yields

$$P = \frac{1}{2} \gamma H_o^2 - \frac{s_u H_o}{\sin \theta \cos \theta} = \frac{1}{2} \gamma H_o^2 - \frac{2s_u H_o}{\sin 2\theta}$$

We are using P rather than P_a because P_a is the limiting value. To find the maximum active lateral earth force, we differentiate P with respect to θ and set the result equal to zero, giving

$$\frac{dP}{d\theta} = 4s_u H_o \cot 2\theta \csc 2\theta = 0$$

The solution is $\theta = \theta_a = 45^\circ$.

By substituting $\theta = 45^\circ$ into the above equation for P , we get the maximum active lateral earth force as

$$P = P_a = \frac{1}{2} \gamma H_o^2 - 2s_u H_o \quad (15.29)$$

If we assume a uniform distribution of stresses on the slip plane, then the active lateral stress is

$$(\sigma_x)_a = \gamma z - 2s_u \quad (15.30)$$

Let us examine Equation (15.30). If $(\sigma_x)_a = 0$, for example, when you make an excavation, then solving for z from Equation (15.30) gives

$$z = z_{cr} = \frac{2s_u}{\gamma} \quad (15.31)$$

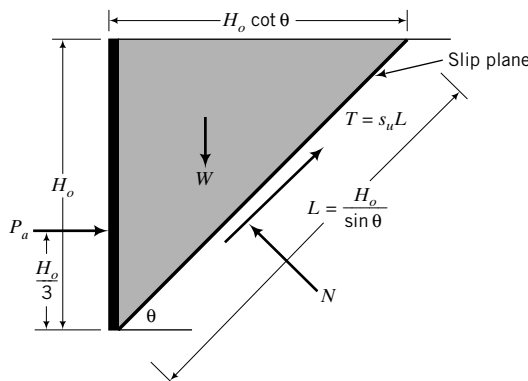


FIGURE 15.11 Forces on a retaining wall for a total stress analysis.

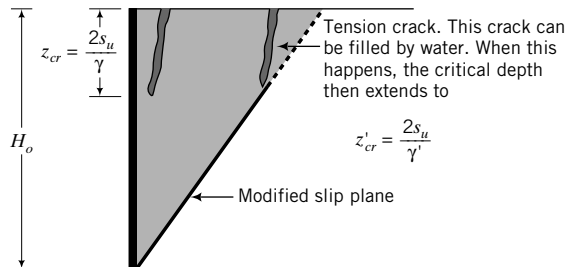


FIGURE 15.12 Tension cracks behind a retaining wall.

Depth z_{cr} is the depth at which tension cracks would extend into the soil (Figure 15.12). If the tension crack is filled with water, the critical depth can extend to

$$z'_{cr} = \frac{2s_u}{\gamma'} \quad (15.32)$$

In addition, the soil in the vicinity of the crack is softened and a hydrostatic pressure, $\gamma_w z'_{cr}$, is imposed on the wall. Often, the critical depth of water-filled tension cracks in overconsolidated clays is greater than the wall height. For example, if $s_u = 80$ kPa, and $\gamma = \gamma_{sat} = 18$ kN/m³, then $z'_{cr} = 19.5$ m. A wall height equivalent to the depth of the tension crack of 19.5 m is substantial. This is substantially more than the average height of the Great Wall of China, which is about 7.6 m. When tension cracks occur, they modify the slip plane, as shown in Figure 15.12; no shearing resistance is available over the length of the slip plane above the depth of the tension cracks.

For an unsupported excavation, the active lateral force is also zero. From Equation (15.29), we get

$$\frac{1}{2}\gamma H_o^2 - 2s_u H_o = 0$$

and, solving for H_o , we obtain

$$H_o = H_{cr} = \frac{4s_u}{\gamma} \quad (15.33)$$

If the excavation is filled with water, then

$$H'_{cr} = \frac{4s_u}{\gamma'} \quad (15.34)$$

We have two possible unsupported depths, as given by Equations (15.31) and (15.33). The correct solution lies somewhere between these critical depths. In design practice, a value of

$$\frac{3.6s_u}{\gamma} \leq H_{cr} \leq \frac{3.8s_u}{\gamma} \quad (15.35)$$

is used for unsupported excavation in fine-grained soils. If the excavation is filled with water,

$$\frac{3.6s_u}{\gamma'} \leq H'_{cr} \leq \frac{3.8s_u}{\gamma'} \quad (15.36)$$

The passive lateral earth force for a total stress analysis, following a procedure similar to that for the active state above, can be written as

$$P_p = \frac{1}{2}\gamma H_o^2 + 2s_u H_o \quad (15.37)$$

and the passive lateral pressure is

$$(\sigma_x)_p = \gamma z + 2s_u \quad (15.38)$$

We can write Equations (15.30) and (15.38) using apparent active and passive lateral earth pressures for the undrained condition as

$$(\sigma_x)_a = \sigma_z - K_{au}s_u \quad (15.39)$$

$$(\sigma_x)_p = \sigma_z + K_{pu}s_u \quad (15.40)$$

where K_{au} and K_{pu} are the undrained active and passive lateral earth pressure coefficients. In our case, for a smooth wall supporting a soil mass with a horizontal surface, $K_{au} = K_{pu} = 2$.

Walls that are embedded in fine-grained soils may be subjected to an adhesive stress (s_w) at the wall face. The adhesive stress is analogous to a wall–soil interface friction for an effective stress analysis. The undrained lateral earth pressure coefficients are modified to account for adhesive stress as

$$K_{au} = K_{pu} = 2\sqrt{1 + \frac{s_w}{s_u}} \quad (15.41)$$

THE ESSENTIAL POINTS ARE:

1. Lateral earth pressures for a total stress analysis are found using apparent lateral earth pressure coefficients K_{au} and K_{pu} . These coefficients are applied to the undrained shear strength. For smooth, vertical walls, $K_{au} = K_{pu} = 2$.
2. Tension cracks of theoretical depth $2s_u/\gamma$, or $2s_u/\gamma'$ if water fills the tension cracks, are usually formed in fine-grained soils and they modify the slip plane. If water fills the cracks, it softens the soil and a hydrostatic stress is imposed on the wall over the depth of the tension crack. You must pay particular attention to the possibility of the formation of tension cracks, and especially so if these cracks can be filled with water, because they can initiate failure of a retaining structure.
3. The theoretical maximum depth of an unsupported vertical cut in fine-grained soils is $H_{cr} = 4s_u/\gamma$ or, if the cut is filled with water, $H'_{cr} = 4s_u/\gamma'$.

What's next . . . You were introduced to Coulomb's and Rankine's analyses of the active and passive lateral earth pressures. Concerns were raised regarding the accuracy of, in particular, K_{pc} because wall friction causes the failure surface to diverge from a plane surface. Several investigators have proposed values of K_p , assuming curved failure surfaces. The question that arises is: What values of K_a , K_p , ϕ' , and s_u should be used in the analyses of earth-retaining structures? Next, we will attempt to address this question. You are forewarned that the answer will not be definite. A geotechnical engineer usually has his/her preferences based on his/her experience with a particular method.

15.7 APPLICATION OF LATERAL EARTH PRESSURES TO RETAINING WALLS

Field and laboratory tests have not confirmed the Coulomb and Rankine theories. In particular, field and laboratory test results showed that both theories overestimate the passive lateral earth pressures. Values of K_p obtained by Caquot and Kerisel (1948) lower the passive lateral earth pressures, but they are still higher than experimental results. Other theories, for example, plasticity theory (Rosenfarb and Chen, 1972), have been proposed, but these theories are beyond the scope of this book and they too do not significantly change the Coulomb and Rankine passive lateral earth pressures for practical ranges of friction angle and wall geometry.

Rankine's theory was developed based on a semi-infinite "loose granular" soil mass for which the soil movement is uniform. Retaining walls do not support a semi-infinite mass but a soil mass of fixed depth. Strains, in general, are not uniform in the soil mass unless the wall rotates about its base to induce a state of plastic equilibrium.

The strains required to achieve the passive state are much larger than those for the active state (Figure 15.5). For sands, a decrease in lateral earth pressure of 40% of the at-rest lateral earth pressure can be sufficient to reach an active state, but an increase of several hundred percent in lateral earth pressure over the at-rest lateral earth pressure is required to bring the soil to a passive state. Because of the large strains that are required to achieve the passive state, it is customary to apply a factor of safety of about 2 to the passive lateral earth pressure.

We have assumed a generic friction angle for the soil mass. Backfills are usually coarse-grained soils compacted to greater than 95% Proctor dry unit weight. If samples of the backfill were to be tested in shear tests in the laboratory at the desired degree of compaction, the samples might show peak shear stresses resulting in ϕ'_p . If you use ϕ'_p to estimate the passive lateral earth pressure using either the Coulomb or Rankine method, you are likely to overestimate it because the shear strains required to develop the passive lateral earth pressure are much greater than those required to mobilize ϕ'_p in the lab. For granular materials, ϕ'_p is mobilized at shear strains $\approx 2\%$ and less. The use of ϕ'_p in the Rankine or Coulomb equations is one reason for the disagreement between the predicted passive lateral earth pressures and experimental results.

Bolton and Powrie (1988) demonstrated that a wall rotation of $0.005H_o$ induces tensile and compressive strains of ± 0.005 corresponding to an average shear strain, $\gamma \approx 1\%$. Tolerable wall rotations are generally less than $0.005H_o$. Consequently, ϕ'_p (which requires $\gamma \approx 2\%$ to be mobilized for clean granular soils) would not be mobilized.

Large shear strains ($\gamma > 10\%$) are required to mobilize ϕ'_{cs} . For a backfill consisting of loose, coarse-grained soils, the displacement of the wall required to mobilize ϕ'_{cs} is intolerable in practice. You should then use conservative values of ϕ' in design. The maximum ϕ'_{design} should be ϕ'_{cs} . In practice, factors of safety are applied to allow for uncertainties of loads and soil properties.

Sometimes it is desirable that the wall remain rigid because of nearby structures that are sensitive to lateral displacements. In this case, you should use K_o as the lateral earth pressure coefficient.

Wall friction causes the active lateral earth pressures to decrease and the passive lateral earth pressures to increase. For active lateral earth pressures, the Coulomb equation is sufficiently accurate for practice, but for passive lateral earth pressures you should use the Caquot and Kerisel (1948) values or similar values (e.g., Packshaw, 1969).

The total stress analysis should only be used in temporary works. But even for these works, you should be cautious in relying on the undrained shear strength. Recall that the undrained shear strength is not a fundamental soil parameter. It depends on the initial void ratio or confining pressure. A total stress analysis should be used in conjunction with an effective stress analysis for retaining structures supporting fine-grained soils.

When a wet, fine-grained soil is excavated, negative excess porewater pressures develop and give the soil an apparent undrained shear strength greater than it was prior to excavation. You should not rely on this gain in strength, because the excess porewater pressures will dissipate with time. On insertion of a wall, the soil at the wall-soil interface is remolded, and you should use conservative values of wall adhesion. The maximum values of wall adhesion (Padfield and Mair, 1984) should be the lesser of

$$\text{Active state: } s_w = 0.5s_u \text{ or } s_w \leq 50 \text{ kPa} \quad (15.42)$$

$$\text{Passive state: } s_w = 0.5s_u \text{ or } s_w \leq 25 \text{ kPa} \quad (15.43)$$

The interface friction between the wall face and the soil depends on the type of backfill used and construction methods. If the surface texture of the wall is rougher than D_{50} of the backfill, the strength characteristics of backfill would control the interface friction. In such a case, the interface friction angle can be taken as equivalent to ϕ'_{cs} . If the wall surface is smooth compared with D_{50} of the backfill, the interface friction value can be assumed, in the absence of field measurements, to be between $\frac{2}{3}\phi'_{cs}$ and $\frac{1}{2}\phi'_{cs}$.

During the life of a retaining wall, a gap may open between the wall and the backfill due to wall movement, deficient construction methods, or unanticipated environmental conditions (drought, rainfall, floods, etc.). You need to be cautious in using adhesion and interface friction because these may become nonexistent during the life of a wall. More importantly, water can seep through the gap and subject the wall to hydrostatic pressures. When a gap could develop, use hydrostatic pressure rather than the lateral soil pressure.

A layer of coarse-grained soil is often used in construction to rest the base of gravity retaining walls (see Section 15.8) founded on clays. The interface friction angle for sliding would then be the lesser of the interface friction between the layer of coarse-grained soil and the wall base, and the interface friction between the layer of coarse-grained soil and the clay.

When cemented soil is either retained as a backfill or is naturally present, the lateral stress would be less than for an uncemented soil. In fact, for temporary works, cemented soils do not require a retaining wall for depths less than that given by Equation (15.36), where s_u is replaced by the cementation strength, c_{cm} , at zero normal effective stress. The cementation strength depends on the degree of cementation, the type of cementing agent, and the uniformity of the bonding of the soil particles with the cementing agent. The shear strains required to mobilize the cementation strength are generally small ($<0.001\%$), so you need to be careful to not exceed the limiting shear strains. Also, cemented soils tend to rupture nonuniformly even before they mobilize their maximum cementation strength. Water can then enter between the rupture surfaces, leading to seepages, stresses, and instability. Under long-term condition, natural cementation bonds tend to diminish and the cementation strength may reduce to zero. Therefore, for long-term condition, you should use ϕ'_{cs} to determine the lateral earth pressure.

Retaining walls are sometimes used to support expansive soils. These soils swell significantly in contact with water. They then impose large lateral pressures on retaining walls. You should take special care to drain water away from these soils. To reduce swell pressures, compressible materials such as geofoam may be used parallel to the wall.

During compaction of the backfill soil, additional lateral stresses are imposed by compaction equipment. For walls with sloping backfill, heavy compaction equipment is generally used. The wall pressures from using heavy compaction equipment can be in excess of the active earth pressures. You should account for the lateral stresses in designing retaining walls. You may refer to Ingold (1979), who used elastic theory to estimate the lateral stresses imposed by construction equipment. Some practicing geotechnical engineers prefer to account for the additional compaction stresses by assuming that the resultant active lateral earth force acts at $0.4H_o$ or $0.5H_o$ rather than $\frac{1}{3}H_o$ from the base of the wall. Alternatively, you can multiply the active earth pressures by a factor (≈ 1.20) to account for compaction stresses.

You should consider active lateral stresses due to surcharges. Surcharges are taken as uniformly distributed pressures, q_s , at the surface. Typical surcharges are:

Buildings on shallow foundations including mat foundation	10 kPa
Highways (live load)	20 kPa
Rural main roads (live loads)	15 kPa
Light traffic roads, footpaths (live loads)	5 kPa

The active lateral pressure is $K_a q_s$ and is assumed to be uniformly distributed over the depth of the wall for backfilled wall. For natural retained soil, the lateral surcharge pressures would be uniform over each layer, and their magnitude would depend on K_a for that layer.

In summary, you should use:

1. $\phi'_{\text{design}} \leq \phi'_{cs}$ because:
 - (a) Uncertainties of loads and soil properties exist.
 - (b) Tolerable rotations of walls ($<0.005 H_o$) would not normally mobilize peak shear strength or critical state shear strength.

- (c) Prior to wall completion, shear bands (thin zones of soil that reached critical state) in the compacted backfill may develop.
 - (d) Quality of construction methods and construction loading, environmental conditions (floods, heavy rainfall, etc.), human and animal interventions (excavation at toe, dumping of materials on top of wall, burrowing of holes, etc.) cannot be estimated (at least, accurately) in advance.
 - (e) You should design the wall so that the backfill soil behaves in a ductile manner. Using ϕ'_{cs} or lower values would allow the soil to respond in a ductile manner.
2. Total stress analysis in conjunction with an effective stress analysis for fine-grained soils.
3. Conservative values for wall friction ($\delta \approx \frac{1}{2}\phi'_{cs}$) and wall adhesion ($s_w = 0.5s_u$, but ≤ 50 kPa for active state and $s_w \leq 25$ kPa for passive case).
 4. A high-quality drainage system to drain water from the backfill and away from the wall.
 5. For a retaining wall with a sloping back, you can use an artificial wall face of height, H , from the heel to the soil surface (Figure 15.10) to calculate the active force. The active horizontal and vertical forces acting on the artificial wall face are $P_{ax} = P_a \cos \delta$ and $P_{az} = P_a \sin \delta$, respectively. In calculating the active lateral earth pressure coefficient use $\eta = 0$ in Equation (15.16).

What's next . . . In the next three sections, we will analyze retaining walls to determine their stability. We will consider an ESA (effective stress analysis) and a TSA (total stress analysis). We begin by considering the possible failure modes.

15.8 TYPES OF RETAINING WALLS AND MODES OF FAILURE

There are two general classes of retaining walls. One class is rigid and consists of concrete walls relying on gravity for stability (Figure 15.13). These are called cast-in-place (CIP) gravity and semi-gravity walls. The other class is flexible and consists of long, slender members of either steel or concrete or wood or plastic and relies on passive soil resistance and anchors for stability (Figure 15.14).

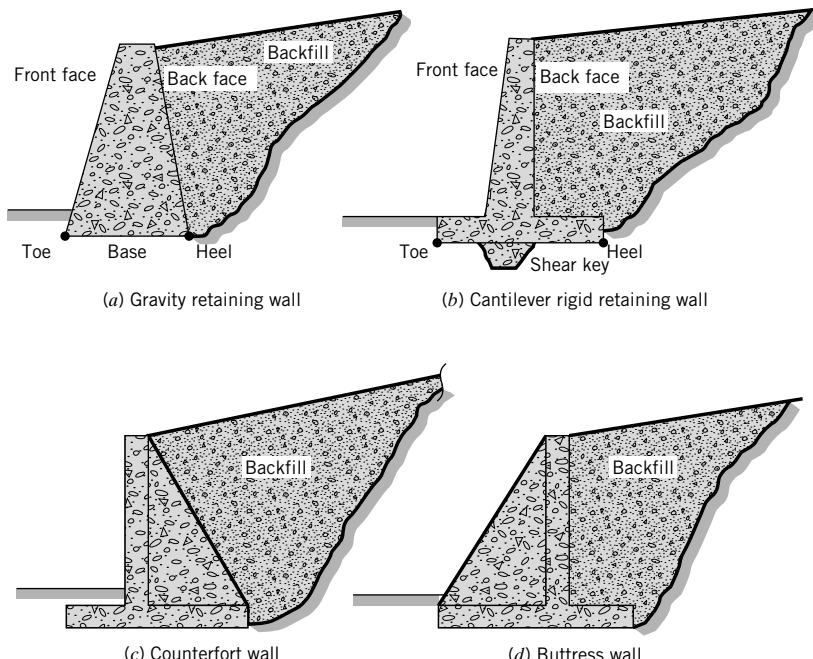


FIGURE 15.13 Types of rigid retaining walls.

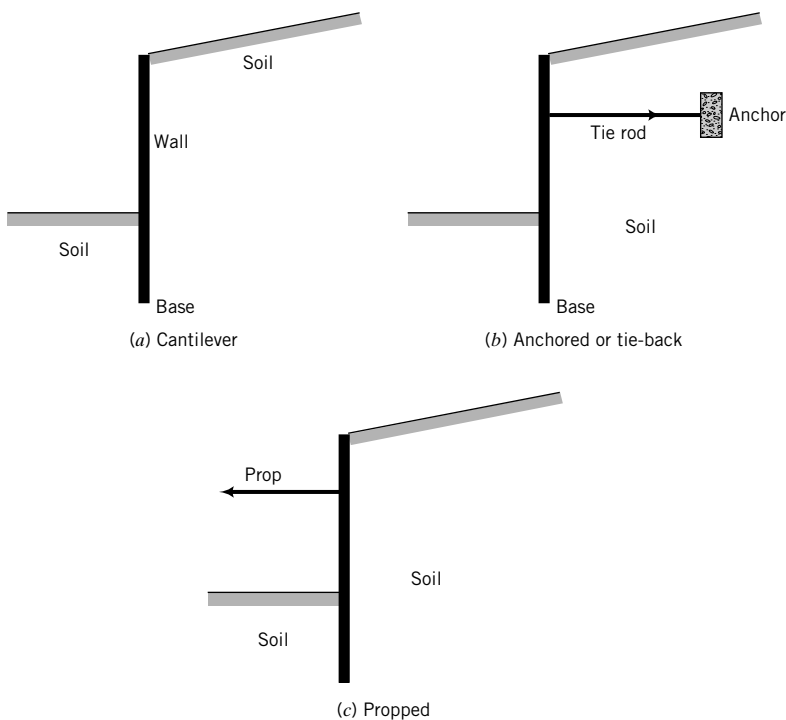


FIGURE 15.14 Types of flexible retaining walls.

There are four modes of failure for rigid retaining walls—translational failure, rotation and bearing capacity failure, deep-seated failure, and structural failure (Figure 15.15). Flexible walls, also called sheet pile walls, fail by either deep-seated failure, rotation at the base, rotation about the anchor or prop, failure of the anchor, bending of the wall, or seepage-induced failure (Figure 15.16).

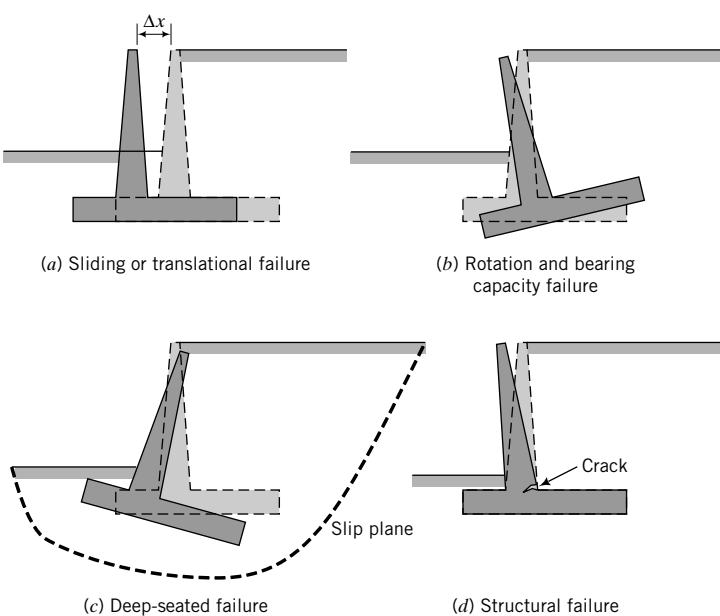
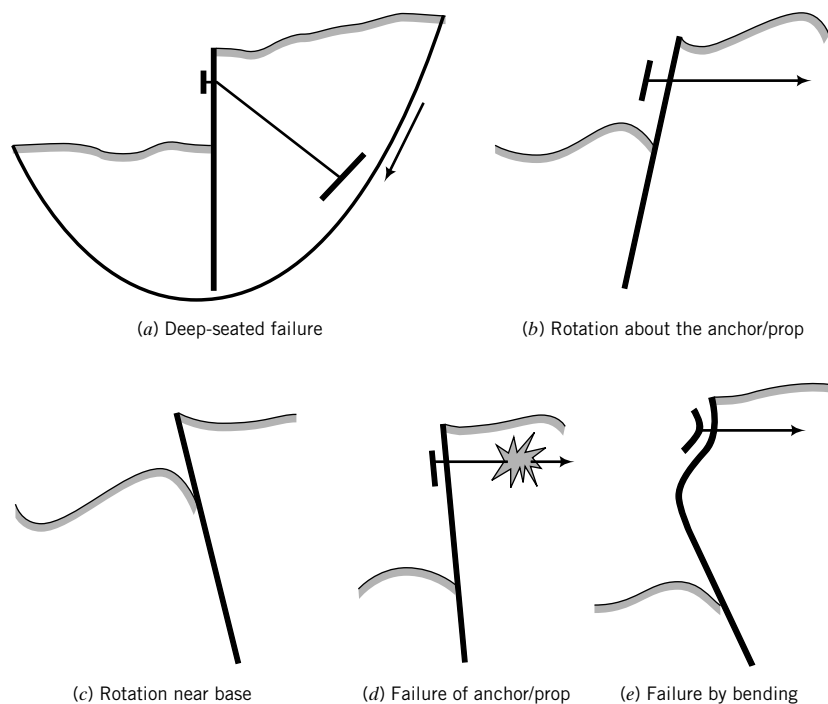
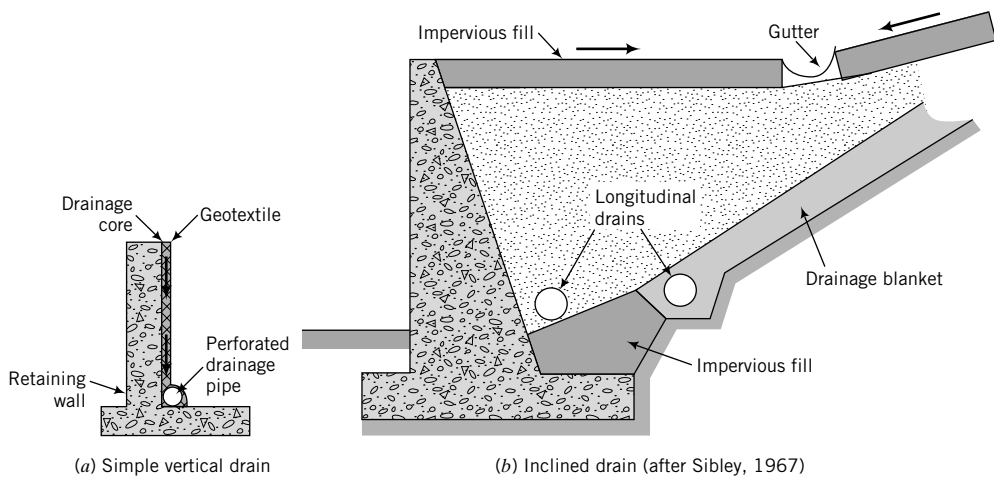


FIGURE 15.15 Failure modes for rigid retaining walls (the dotted lines show the original position of the wall).

**FIGURE 15.16** Failure modes for flexible retaining walls.

Seepage-induced failure is avoided in rigid retaining walls by providing adequate drainage systems, two of which are depicted in Figure 15.17. The design of drainage systems is beyond the scope of this book. Flownets, discussed in Chapter 14, are used in designing drainage systems.

Flexible retaining walls are often used in waterfront structures and as temporary supports for excavations. Seepage forces are generally present and must be considered in evaluating the stability of these walls.

**FIGURE 15.17** Two types of drainage system behind rigid retaining walls.

15.9 STABILITY OF RIGID RETAINING WALLS

CIP gravity retaining walls (Figure 15.13a) are massive concrete walls. Their stability depends mainly on the self-weight of the walls. Cantilever walls (Figure 15.13b)—CIP semigravity walls—utilize the backfill to help mobilize stability and are generally more economical than CIP gravity retaining walls. A rigid retaining wall must have an adequate factor of safety to prevent excessive translation, rotation, bearing capacity failure, deep-seated failure, and seepage-induced instability.

15.9.1 Translation

A rigid retaining wall must have adequate resistance against translation. That is, the sliding resistance of the base of the wall must be greater than the resultant lateral force pushing against the wall. The factor of safety against translation, $(FS)_T$, is

$$(FS)_T = \frac{T}{P_{ax}}; \quad (FS)_T \geq 1.5 \quad (15.44)$$

where T is the sliding resistance at the base and P_{ax} is the lateral force pushing against the wall. The sliding resistance is $T = R_z \tan \phi'_b$ for an ESA, and $T = s_w B$ for a TSA (if the base rests directly on fine-grained soils). R_z is the resultant vertical force, ϕ'_b is the interfacial friction angle between the base of the wall and the soil,

$$\phi'_b \approx \frac{1}{2} \phi'_{cs} \quad \text{to} \quad \frac{2}{3} \phi'_{cs}$$

and B is the projected horizontal width of the base. Typical sets of forces acting on gravity and cantilever rigid retaining walls are shown in Figure 15.18.

Using statics, we obtain, for an ESA,

$$(FS)_T = \frac{[(W_w + W_s + P_{az}) \cos \theta_b - P_{ax} \sin \theta_b] \tan \phi'_b}{P_{ax} \cos \theta_b + (W_w + W_s + P_{az}) \sin \theta_b} \quad (15.45)$$

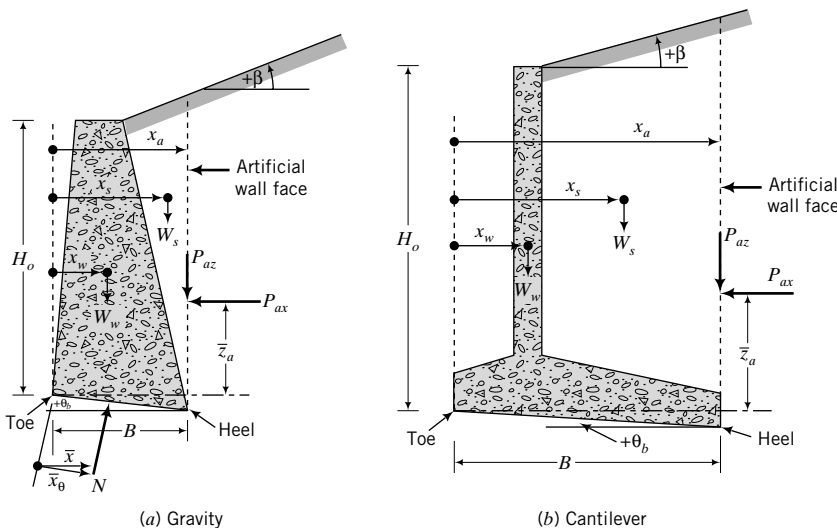


FIGURE 15.18 Forces on rigid retaining walls.

where W_w is the weight of the wall, W_s is the weight of the soil wedge, P_{az} and P_{ax} are the vertical and horizontal components of the active lateral force, and θ_b is the inclination of the base to the horizontal (θ_b is positive if the inclination is counterclockwise, as shown in Figure 15.18). If $\theta_b = 0$ (base is horizontal), then

$$(FS)_T = \frac{(W_w + W_s + P_{az}) \tan \phi'_b}{P_{ax}} \quad (15.46)$$

For a TSA,

$$(FS)_T = \frac{s_w B / \cos \theta_b}{P_{ax} \cos \theta_b + (W_w + W_s + P_{ax}) \sin \theta_b} \quad (15.47)$$

where s_w is the adhesive stress [see Equations (15.42) and (15.43)]. If $\theta_b = 0$, then

$$(FS)_T = \frac{s_w B}{P_{ax}} \quad (15.48)$$

The embedment of rigid retaining walls is generally small and the passive lateral force is not taken into account. If the base resistance is inadequate, the width B of the wall can be increased. For cantilever walls, a shear key (Figure 15.13b) can be constructed to provide additional base resistance against sliding.

15.9.2 Rotation

A rigid retaining wall must have adequate resistance against rotation. The rotation of the wall about its toe is satisfied if the resultant vertical force lies within the middle third of the base. Taking moments about the toe of the base, the resultant vertical force at the base is located at

$$\bar{x}_\theta = \frac{W_w x_w + W_s x_s + P_{az} x_a - P_{ax} \bar{z}_a}{(W_w + W_s + P_{az}) \cos \theta_b - P_{ax} \sin \theta_b} \quad (15.49)$$

where \bar{z}_a is the location of the active lateral earth force from the toe. The wall is safe against rotation if $B/3 \leq \bar{x} \leq 2B/3$; that is, $e = |(B/2 - \bar{x})| \leq B/6$, where e is the eccentricity of the resultant vertical load and $\bar{x} = \bar{x}_\theta \cos \theta_b$.

If $\theta_b = 0$, then

$$\bar{x} = \frac{W_w x_w + W_s x_s + P_{az} x_a - P_{ax} \bar{z}_a}{W_w + W_s + P_{az}} \quad (15.50)$$

15.9.3 Bearing Capacity

A rigid retaining wall must have a sufficient margin of safety against soil bearing capacity failure. The maximum pressure imposed on the soil at the base of the wall must not exceed the allowable soil bearing capacity; that is,

$$(\sigma_z)_{max} \leq q_a \quad (15.51)$$

where $(\sigma_z)_{max}$ is the maximum vertical stress imposed and q_a is the allowable soil bearing capacity.

15.9.4 Deep-Seated Failure

A rigid retaining wall must not fail by deep-seated failure, whereby a slip surface encompasses the wall and the soil adjacent to it. In Chapter 16, we will discuss deep-seated failure.

15.9.5 Seepage

A rigid retaining wall must have adequate protection from groundwater seepage. The porewater pressures and the maximum hydraulic gradient developed under seepage must not cause any of the four stability criteria stated above to be violated and static liquefaction must not occur, that is, $i_{max} < i_{cr}$. Usually,

$$i_{max} \leq \frac{i_{cr}}{(FS)_s}$$

where $(FS)_s$ is a factor of safety for seepage and is conventionally greater than 3. To avoid seepage-related failures, adequate drainage should be installed in the backfill to dissipate excess porewater pressures quickly. Coarse-grained soils are preferable for the backfill because of their superior drainage characteristics compared with fine-grained soils. Blocked drainage not only leads to wall instability but can also cause a dam effect, raising the local groundwater level.

15.9.6 Procedures to Analyze Rigid Retaining Walls

THE ESSENTIAL STEPS IN DETERMINING THE STABILITY OF RIGID RETAINING WALLS ARE AS FOLLOWS:

1. Calculate the active lateral earth force and its components. If the wall is smooth, use Rankine's equations because they are simpler than Coulomb's equations to calculate the active lateral earth pressure coefficient.
2. Determine the weight of the wall and soil above the base.
3. Use Equation (15.45) or Equation (15.46) to find $(FS)_T$.
4. Use Equation (15.49) or Equation (15.50) to determine the location of the resultant vertical force, R_z , from the toe of the wall.
5. Check that the eccentricity is less than $B/6$. If it is, then the wall is unlikely to fail by rotation.
6. Determine the maximum soil pressure from $(\sigma_z)_{max} = (R_z/A)(1 + 6e/B)$.
7. Calculate the ultimate bearing capacity, q_u , described in Chapter 12. In most cases, R_z would be eccentric.
8. For allowable stress design (ASD), calculate the factor of safety against bearing capacity failure: $(FS)_B = q_u/(\sigma_z)_{max}$.
9. For load and resistance factor design (LRFD), the factored lateral and vertical loads must not exceed the performance factor times the resistance in the direction of loading.

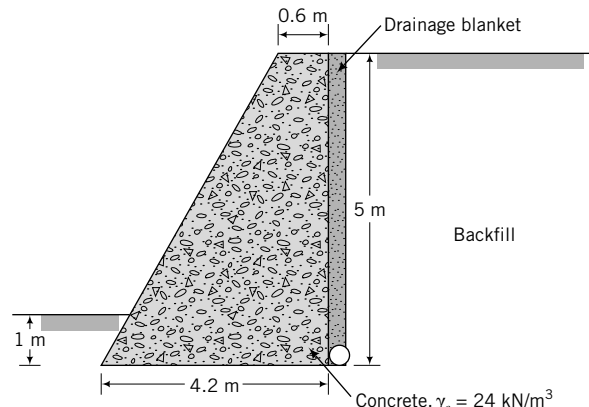
EXAMPLE 15.3 Mass Gravity Wall



Computer Program Utility

Access <http://www.wiley.com/college/budhu>, Chapter 15, and click on retwall.xls to view examples of retaining wall analysis using a spreadsheet. You can change input values and explore how the stability of the walls changes.

A gravity retaining wall, shown in Figure E15.3a, is required to retain 5 m of soil. The backfill is a coarse-grained soil with $\gamma_{sat} = 18 \text{ kN/m}^3$, $\phi'_{cs} = 30^\circ$. The existing soil (below the base) has the following properties: $\gamma_{sat} = 20 \text{ kN/m}^3$, $\phi'_p = 36^\circ$. The wall is embedded 1 m into the existing soil and a drainage system is provided, as shown. The groundwater level is 4.5 m below the base of the wall. Determine the stability of the wall for the following conditions (assume $\delta = 20^\circ$):

**FIGURE E15.3a**

- (a) Wall friction is zero.
- (b) Wall friction is 20° .
- (c) The drainage system becomes clogged during several days of a rainstorm and the groundwater rises to the surface. Neglect seepage forces.

The unit weight of concrete is $\gamma_c = 24 \text{ kN/m}^3$.

Strategy For zero wall friction, you can use Rankine's method. But for wall friction, you should use Coulomb's method. The passive resistance is normally neglected in rigid retaining walls. Since only active lateral forces are considered, K_a from the Rankine and Coulomb methods should be accurate enough. Since groundwater is below the base, $\gamma' = \gamma_{sat}$ over the wall depth.

Solution 15.3

Step 1: Determine K_a .

$$\text{Rankine: } \delta = 0, \quad K_{aR} = \tan^2\left(45^\circ - \frac{\phi_{cs}}{2}\right) = \tan^2\left(45^\circ - \frac{30^\circ}{2}\right) = \frac{1}{3}$$

Coulomb: $\delta = 20^\circ$, $\phi' = \phi'_{cs}$, $\beta = 0$, $\eta = 0$; and from Equation (15.16),

$$K_{aC} = \frac{\cos^2(30^\circ - 0^\circ)}{\cos^2 0^\circ \cos(0^\circ + 20^\circ) \left[1 + \left\{ \frac{\sin(30^\circ + 20^\circ) \sin(30^\circ - 0^\circ)}{\cos(0^\circ + 20^\circ) \cos(0^\circ - 0^\circ)} \right\}^{1/2} \right]^2} = 0.3$$

Step 2: Determine the lateral forces.

All forces are per unit length of wall.

$$\text{Rankine: } P_{aR} = \frac{1}{2} K_{aR} \gamma_{sat} H_o^2 = \frac{1}{2} \times \frac{1}{3} \times 18 \times 5^2 = 75 \text{ kN}$$

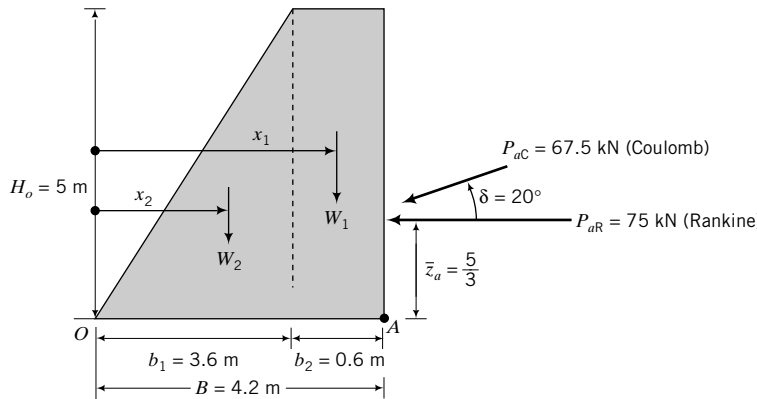
P_{aR} acts horizontally because the ground surface is horizontal.

$$\text{Coulomb: } P_{aC} = \frac{1}{2} K_{aC} \gamma_{sat} H_o^2 = \frac{1}{2} \times 0.3 \times 18 \times 5^2 = 67.5 \text{ kN}$$

P_{aC} acts at an angle $\delta = 20^\circ$ to the horizontal (see Figure E15.3b).

$$\text{Horizontal component of } P_{aC}: (P_{ax})_C = P_{aC} \cos \delta = 67.5 \cos 20^\circ = 63.4 \text{ kN}$$

$$\text{Vertical component of } P_{aC}: (P_{az})_C = P_{aC} \sin \delta = 67.5 \sin 20^\circ = 23.1 \text{ kN}$$

**FIGURE E15.3b**

Step 3: Determine wall stability.

Consider a unit length of wall.

$$W_1 = b_2 H_o \gamma_c = 5 \times 0.6 \times 24 = 72 \text{ kN}$$

$$W_2 = \frac{1}{2} b_1 H_o \gamma_c = \frac{1}{2} \times 3.6 \times 5 \times 24 = 216 \text{ kN}$$

$$W = W_1 + W_2 = 72 + 216 = 288 \text{ kN}$$

or

$$W = \frac{1}{2} (B + b_2) H_o \gamma_c = \frac{1}{2} (4.2 + 0.6) \times 5 \times 24 = 288 \text{ kN}$$

Calculate the location of the resultant from O (Figure E15.3b).

$$\text{Rankine: } M_O = W_1 x_1 + W_2 x_2 - P_{aR} \bar{z}_a = 72(3.6 + 0.3) + 216 \times \left(\frac{2}{3} \times 3.6\right) - 75 \times \frac{5}{3} = 674.2 \text{ kN.m}$$

$$R_z = W = 288 \text{ kN}$$

$$\bar{x} = \frac{M_O}{R_z} = \frac{674.2}{288} = 2.34 \text{ m}$$

$$\text{Coulomb: } M_O = W_1 x_1 + W_2 x_2 + (P_{az})_C \times B - (P_{ax})_C \times \bar{z}_a$$

$$= 72(3.6 + 0.3) + 216 \times \left(\frac{2}{3} \times 3.6\right) + 23.1 \times 4.2 - 63.4 \times \frac{5}{3} = 790.6 \text{ kN}$$

$$R_z = W + (P_{az})_C = 288 + 23.1 = 311.1 \text{ kN}$$

$$\bar{x} = \frac{M_O}{R_z} = \frac{790.6}{311.1} = 2.54 \text{ m}$$

Base resistance: $T = R_z \tan \phi'_b$, where R_z is the resultant vertical force. Assume $\phi'_b = \frac{2}{3} \phi'_p = \frac{2}{3} \times 36^\circ = 24^\circ$.

$$\text{Rankine: } T = 288 \times \tan 24^\circ = 128.2 \text{ kN}$$

$$\text{Coulomb: } T = (288 + 23.1) \times \tan 24^\circ = 138.5 \text{ kN}$$

$$\text{Rankine: } (\text{FS})_T = \frac{T}{P_{aR}} = \frac{128.2}{75} = 1.7 > 1.5; \text{ therefore satisfactory}$$

$$\text{Coulomb: } (\text{FS})_T = \frac{T}{(P_{ax})_C} = \frac{138.5}{63.4} = 2.2 > 1.5; \text{ therefore satisfactory}$$

With wall friction, the factor of safety against translation is greater than without wall friction.

Determine Rotational Stability

$$\text{Rankine: } e = \left| \frac{B}{2} - \bar{x} \right| = \left| \frac{4.2}{2} - 2.34 \right| = 0.24 \text{ m}$$

$$\text{Coulomb: } e = \left| \frac{B}{2} - \bar{x} \right| = \left| \frac{4.2}{2} - 2.54 \right| = 0.44 \text{ m}$$

$$\frac{B}{6} = \frac{4.2}{6} = 0.7 > e$$

The resultant vertical forces for both the Rankine and Coulomb methods lie within the middle one-third of the base and, therefore, overturning is unlikely to occur.

Determining Factor of Safety Against Bearing Capacity Failure Since the resultant vertical force is located within the middle one-third, tension will not develop in the soil.

$$(\sigma_z)_{\max} = \frac{R_z}{A} \left(1 + \frac{6e}{B} \right)$$

$$\text{Rankine: } [(\sigma_z)_{\max}]_R = \frac{288}{4.2 \times 1} \left(1 + \frac{6 \times 0.24}{2.4} \right) = 92.1 \text{ kPa}$$

$$\text{Coulomb: } [(\sigma_z)_{\max}]_C = \frac{311.1}{4.2 \times 1} \left(1 + \frac{6 \times 0.44}{2.4} \right) = 120.6 \text{ kPa}$$

The maximum stress occurs at A (Figure E15.3b) for both the Rankine and Coulomb methods. The base of the wall can be taken as a strip surface foundation, that is, $B/L \rightarrow 0$, and $D_f = 0$. The groundwater level is below $B = 4.2 \text{ m}$ from the base, so groundwater would have no effect on the bearing capacity.

The resultant force, R , is eccentric and inclined to the vertical (Figure E15.3c). Therefore, you should use the bearing capacity equation for inclined load with the width modified for eccentricity.

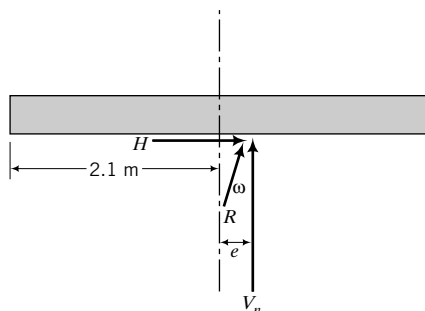


FIGURE E15.3c

$$\text{Rankine: } H = P_{aR} = 75 \text{ kN}; \quad V_n = R_z = 288 \text{ kN}, \quad \frac{H}{V_n} = \frac{75}{288} = 0.26; \quad \omega = \tan^{-1} \frac{H}{V_n} = \tan^{-1} (0.26) = 14.6^\circ$$

$$\frac{B'}{L'} = 0, \quad \text{for a strip footing; } B' = B - 2e = 4.2 - 2 \times 0.24 = 3.72 \text{ m}$$

$$n = \left(2 + \frac{B'}{L'}\right) / \left(1 + \frac{B'}{L'}\right) = 2; \quad i_\gamma = \left(1 - \frac{H}{V_n}\right)^{n+1} = (1 - 0.26)^{2+1} = 0.41$$

$$N_\gamma = 0.1054 \exp(9.6\phi'_p) = 0.1054 \exp\left(9.6 \times 36 \times \frac{\pi}{180}\right) = 43.9$$

$$q_u = 0.5\gamma B' N_\gamma i_\gamma = 0.5 \times 20 \times 3.73 \times 43.9 \times 0.41 = 653 \text{ kPa}$$

$$(\text{FS})_B = \frac{q_u}{[(\sigma_z)_{\max}]_{\text{R}}} = \frac{653}{92.1} = 7.1 > 3; \quad \text{okay}$$

$$\text{Coulomb: } H = (P_{ax})_{\text{C}} = 63.4 \text{ kN}; \quad V_n = R_z = 311.1 \text{ kN}, \quad \frac{H}{V_n} = \frac{63.4}{311.1} = 0.20;$$

$$\omega = \tan^{-1} \frac{H}{V_n} = \tan^{-1}(0.2) = 11.3^\circ$$

$$\frac{B'}{L'} = 0, \quad \text{for a strip footing; } B' = B - 2e = 4.2 - 2 \times 0.44 = 3.32 \text{ m}$$

$$n = \left(2 + \frac{B'}{L'}\right) / \left(1 + \frac{B'}{L'}\right) = 2; \quad i_\gamma = \left(1 - \frac{H}{V_n}\right)^{n+1} = (1 - 0.20)^{2+1} = 0.51$$

$$N_\gamma = 0.1054 \exp(9.6\phi'_p) = 0.1054 \exp\left(9.6 \times 36 \times \frac{\pi}{180}\right) = 43.9$$

$$q_u = 0.5\gamma B' N_\gamma i_\gamma = 0.5 \times 20 \times 3.32 \times 43.9 \times 0.51 = 743 \text{ kPa}$$

$$(\text{FS})_B = \frac{q_u}{[(\sigma_z)_{\max}]_{\text{C}}} = \frac{743}{120.6} = 6.2 > 3; \quad \text{okay}$$

Step 4: Determine the effects of water from the rainstorm.

Using Rankine's method (zero wall friction)

$$P_{aR} = \frac{1}{2} K_a \gamma' H_o^2 + \frac{1}{2} \gamma_w H_o^2 = \frac{1}{2} \times \frac{1}{3} \times (18 - 9.8) \times 5^2 + \frac{1}{2} \times 9.8 \times 5^2 = 34.2 + 122.5 = 156.7 \text{ kN}$$

Location of resultant from *O*

$$M_O = W_1 x_1 + W_2 x_2 - P_{aR} \bar{z}_a = 72(3.6 + 0.3) + 216 \times \left(\frac{2}{3} \times 3.6\right) - 156.7 \times \frac{5}{3} = 538 \text{ kN.m}$$

$$\bar{x} = \frac{M_O}{R_z} = \frac{538}{288} = 1.87 \text{ m}$$

Translation

$$(\text{FS})_T = \frac{97.5}{156.7} = 0.62 < 1$$

The wall will fail by translation.

Rotation

$$e = \left| \frac{B}{2} - \bar{x} \right| = \left| \frac{4.2}{2} - 1.87 \right| = 0.23 < \frac{B}{6} \left(= \frac{4.2}{6} = 0.7 \right)$$

The wall is unlikely to fail by rotation.

Bearing capacity

$$[(\sigma_z)_{\max}]_{\text{R}} = \frac{288}{4.2 \times 1} \left(1 + \frac{6 \times 0.23}{4.2}\right) = 91.1 \text{ kPa}$$

The maximum stress now occurs at *O* rather than at *A*.

The eccentricity of the resultant force, R , is now on the opposite side of the centroid (Figure E15.3d).

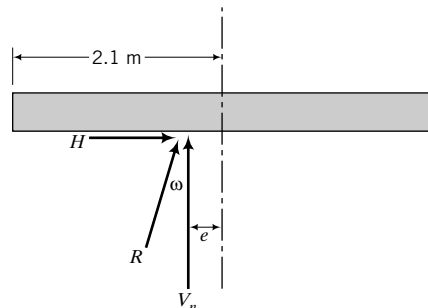


FIGURE E15.3d

$$H = P_{aR} = 156.7 \text{ kN}; \quad V_n = R_z = 288 \text{ kN}, \quad \frac{H}{V_n} = \frac{156.7}{288} = 0.54; \quad \omega = \tan^{-1} \frac{H}{V_n} = \tan^{-1}(0.54) = 28.4^\circ$$

$$B' = B - 2e = 4.2 - 2 \times 0.23 = 3.74 \text{ m}$$

$$n = \left(2 + \frac{B'}{L'}\right) / \left(1 + \frac{B'}{L'}\right) = 2; \quad i_\gamma = \left(1 - \frac{H}{V_n}\right)^{n+1} = (1 - 0.54)^{2+1} = 0.1$$

$$q_u = 0.5 \gamma' B' N_\gamma i_\gamma = 0.5 \times (20 - 9.8) \times 3.74 \times 43.9 \times 0.1 = 83.7 \text{ kPa}$$

$$(\text{FS})_B = \frac{q_u}{[(\sigma_z)_{\max}]_R} = \frac{83.7}{91.1} = 0.9 < 3; \quad \text{not okay}$$

The wall will fail by bearing capacity failure.

EXAMPLE 15.4 Cantilever Gravity Wall

Determine the stability of the cantilever gravity retaining wall shown in Figure E15.4a. The existing soil is a clay and the backfill is a coarse-grained soil. The base of the wall will rest on a 50-mm-thick, compacted layer of the backfill. The interface friction between the base and the compacted layer of backfill is 25° . Groundwater level is 8 m below the base.

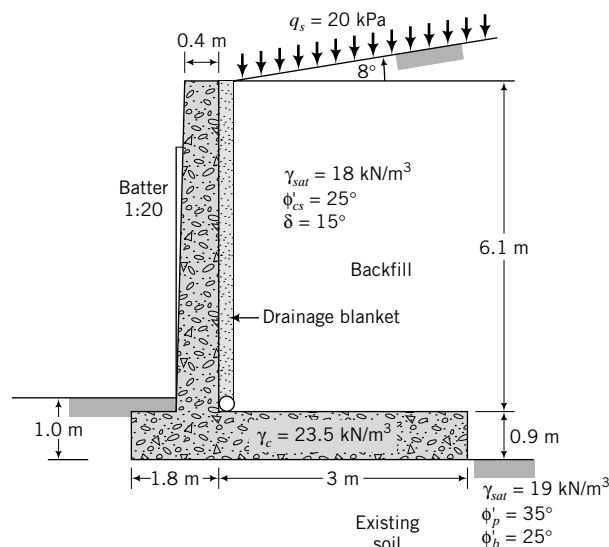


FIGURE E15.4a

Strategy You should use Coulomb's method to determine the lateral earth pressure because of the presence of wall friction. The height of the wall for calculating the lateral earth pressure is the vertical height from the base of the wall to the soil surface. You should neglect the passive resistance of the 1.0 m of soil behind the wall.

Solution 15.4

Step 1: Determine the active lateral force and its location.

See Figure E15.4b. We are given $\eta = 0$, $\beta = 8^\circ$, $\delta = 15^\circ$, and $\phi'_{cs} = 25^\circ$. Therefore, from Equation (15.16),

$$K_{ac} = \frac{\cos^2(25^\circ - 0)}{\cos^2 0^\circ \cos(0^\circ + 15^\circ) \left[1 + \left\{ \frac{\sin(25^\circ + 15^\circ) \sin(25^\circ - 8^\circ)}{\cos(0^\circ + 15^\circ) \cos(0^\circ - 8^\circ)} \right\}^{1/2} \right]^2} = 0.41$$

$$H_o = 0.9 + 6.1 + 3.0 \tan 8^\circ = 7.42 \text{ m}$$

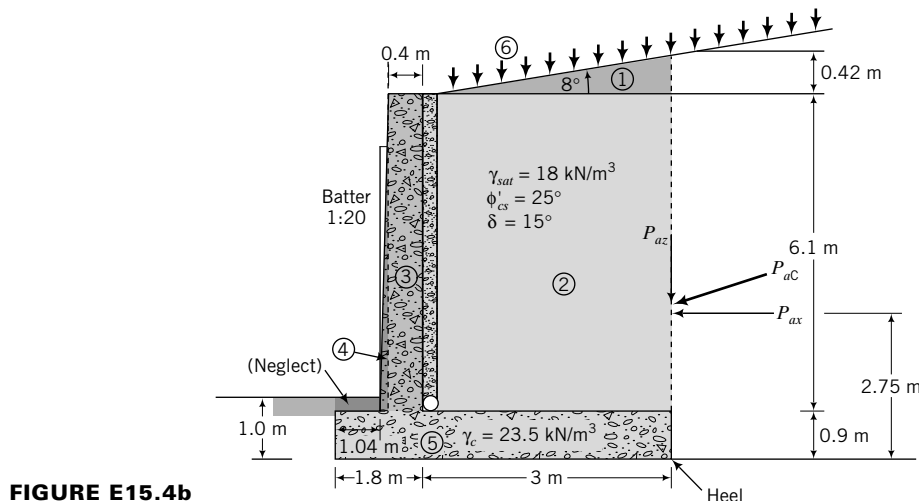


FIGURE E15.4b

Soil mass

All forces are per meter length of wall.

$$\text{Lateral force from soil mass: } P_{ac} = \frac{1}{2} K_{ac} \gamma_{sat} H_o^2 = \frac{1}{2} \times 0.41 \times 18 \times 7.42^2 = 203.2 \text{ kN}$$

$$\text{Horizontal component: } P_{ax} = P_{ac} \cos \delta = 203.2 \cos 15^\circ = 196.3 \text{ kN}$$

$$\text{Vertical component: } P_{az} = P_{ac} \sin \delta = 203.2 \sin 15^\circ = 52.6 \text{ kN}$$

Surcharge

$$F_x = K_{ac} q_s H_o \cos \delta = 0.41 \times 20 \times 7.42 \times \cos 15^\circ = 58.8 \text{ kN}$$

$$F_z = K_{ac} q_s H_o \sin \delta = 0.41 \times 20 \times 7.42 \times \sin 15^\circ = 15.7 \text{ kN}$$

Resultant force components

$$P_{ax} = F_{ax} + F_x = 196.3 + 58.8 = 255.1 \text{ kN}$$

$$P_{az} = F_{az} + F_z = 52.6 + 15.7 = 68.3 \text{ kN}$$

Step 2: Determine the resultant vertical force per unit length and its location.

A table is useful to keep the calculation tidy and easy to check.

Part	Force (kN/m)	Moment arm from toe (m)	Moment (+kN.m)
1	$0.5 \times 0.42 \times 3 \times 18 = 11.3$	3.80	42.9
2	$3 \times 6.1 \times 18 = 329.4$	3.30	1087.0
3	$0.4 \times 6.1 \times 23.5 = 57.3$	1.60	91.7
4	$0.5 \times 0.36 \times 6.1 \times 23.5 = 25.8$	1.28	33.0
5	$0.9 \times 4.8 \times 23.5 = 101.5$	2.40	243.6
6	$3 \times 20 = 60.00$	3.3	198.0
		$\Sigma 585.3$	$\Sigma 1696.2(+)$
P_{az}	68.3	4.8	327.9(+)
R_z	= 653.6		Σ Moments = 2024.1(+)
P_{ax}	255.1	2.75	701.5(-)
			$\Sigma M_o = 1322.6(+)$

The location of the resultant horizontal component of force from the toe is

$$\bar{z} = \frac{F_{ax} \frac{H_o}{3} + F_x \frac{H_o}{2}}{F_{ax} + F_x} = \frac{196.3 \times \frac{7.42}{3} + 58.8 \times \frac{7.42}{2}}{196.3 + 58.8} = 2.75 \text{ m}$$

The location of the resultant vertical component of force from the toe is

$$\bar{x} = \frac{\Sigma M_o}{R_z} = \frac{1322.6}{653.6} = 2.02$$

Step 3: Determine the eccentricity.

$$e = \left| \frac{B}{2} - \bar{x} \right| = \left| \frac{4.8}{2} - 2.02 \right| = 0.38 \text{ m}$$

Step 4: Determine the stability.

Rotation

$$\frac{B}{6} = \frac{4.8}{6} = 0.8 \text{ m} > e (= 0.38 \text{ m}); \text{ therefore, rotation is satisfactory}$$

Translation

$$T = R_z \tan \phi'_b = 653.6 \times \tan 25^\circ = 305 \text{ kN/m}$$

$$(FS)_T = \frac{T}{P_{ax}} = \frac{305}{255.1} = 1.2 < 1.5; \text{ therefore, translation is not satisfactory}$$

In design, you can consider placing a key at the base to increase the factor of safety against translation.

Bearing capacity

$$(\sigma_z)_{max} = \frac{R_z}{B \times 1} \left(1 + \frac{6e}{B} \right) = \frac{653.6}{4.8 \times 1} \left(1 + \frac{6 \times 0.38}{4.8} \right) = 201 \text{ kPa}$$

$$B' = B - 2e = 4.8 - 2 \times 0.38 = 4.06 \text{ m}$$

$$H = P_{ax} = 255.1 \text{ kN}; \quad V_n = R_z = 653.6 \text{ kN}, \quad \frac{H}{V_n} = \frac{255.1}{653.6} = 0.39$$

$$\omega = \tan^{-1} \frac{H}{V_n} = \tan^{-1}(0.39) = 21.3^\circ$$

$$n = \left(2 + \frac{B'}{L'}\right) / \left(1 + \frac{B'}{L'}\right) = 2; \quad i_\gamma = \left(1 - \frac{H}{V_n}\right)^{n+1} = (1 - 0.39)^{2+1} = 0.23$$

$$N_\gamma = 0.1054 \exp(9.6 \phi'_p) = 0.1054 \exp\left(9.6 \times 35 \times \frac{\pi}{180}\right) = 37.2$$

$$q_u = 0.5\gamma B' N_\gamma i_\gamma = 0.5 \times 19 \times 4.06 \times 37.2 \times 0.23 = 330 \text{ kPa}$$

$$(FS)_B = \frac{q_u}{(\sigma_z)_{max}} = \frac{330}{201.5} = 1.6 < 3$$

Therefore, bearing capacity is not satisfactory. Increase width of base.

What's next . . . In the next section, we will study how to determine the stability of flexible retaining walls.

15.10 STABILITY OF FLEXIBLE RETAINING WALLS

Sheet pile walls are flexible and are constructed using steel or thin concrete panels or wood. Two types of sheet pile walls are common. One is a cantilever wall, commonly used to support soils to a height of less than 3 m (Figure 15.14a). The other is an anchored or propped sheet pile wall (Figure 15.14b, c), commonly used to support deep excavations and as waterfront retaining structures. Cantilever sheet pile walls rely on the passive soil resistance for their stability, while anchored sheet pile walls rely on a combination of anchors and passive soil resistance for their stability. The stability of sheet pile walls must satisfy all the criteria for rigid retaining walls described in Section 15.9. Because sheet pile walls are used in situations where seepage may occur, it is necessary to pay particular attention to seepage-related instabilities.

15.10.1 Analysis of Sheet Pile Walls in Uniform Soils

In analyzing sheet pile walls, we are attempting to determine the depth of embedment, d , for stability. The analysis is not exact, and various simplifications are made. The key static equilibrium condition is moment equilibrium. Once we determine d , the next step is to determine the size of the wall. This is done by calculating the maximum bending moment and then determining the section modulus by dividing the maximum bending moment by the allowable bending stress of the material constituting the sheet pile, for example, steel, concrete, or wood.

An effective stress analysis is generally used to analyze sheet pile walls, and as such we must evaluate the porewater pressure distribution and seepage pressures. We can use flownet sketching or numerical methods to determine the porewater pressure distribution and seepage pressures. However, approximate methods are often used in practice. If the groundwater level on both sides of a sheet pile wall is the same, then the resultant porewater pressures and seepage pressures are zero (Figure 15.19a). You can then neglect the effects of groundwater in determining the stability of sheet pile walls. However, you must use effective stresses in your calculations of the lateral earth forces.

The approximate distribution of porewater pressures in front of and behind sheet pile walls for conditions in which the water tables are different is obtained by assuming a steady-state seepage condition and uniform distribution of the total head. Approximate resultant porewater pressure distributions for some common conditions (Padfield and Mair, 1984) are shown in Figure 15.19.

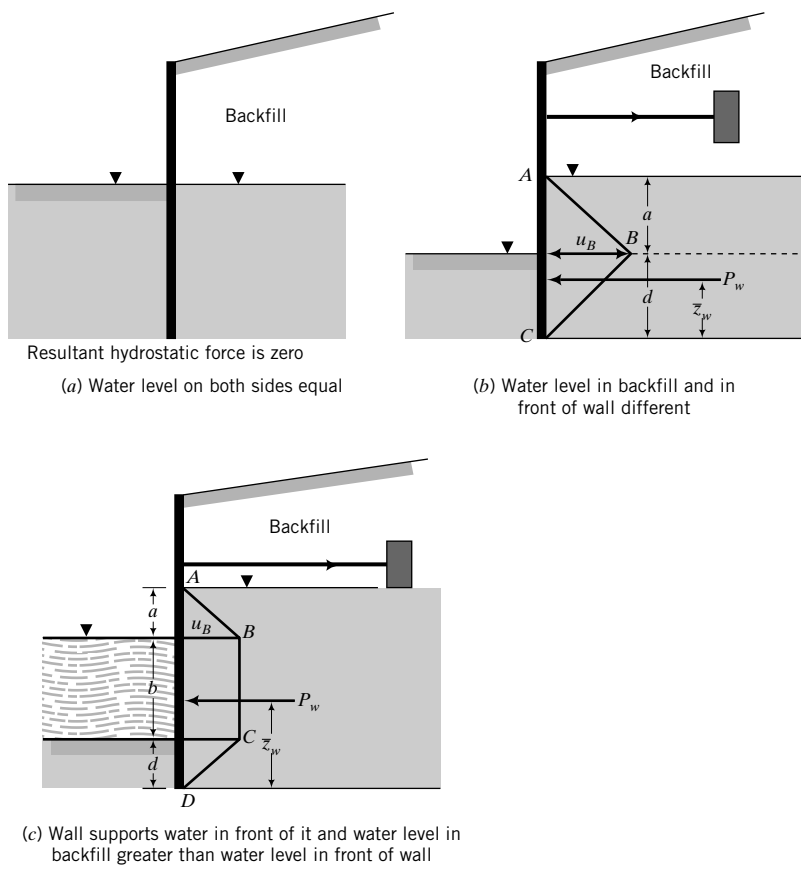


FIGURE 15.19 Approximate resultant porewater pressure distribution behind flexible retaining walls.

The maximum porewater pressures (u_B), maximum porewater forces (P_w) and their locations (\bar{z}_w), and the seepage force per unit volume (j_s) are as follows:

Case (a)—Figure 15.19a

Resultant porewater pressure is zero and the seepage force is zero.

Case (b)—Figure 15.19b

$$u_B = \frac{2ad}{a + 2d} \gamma_w \quad (15.52)$$

$$P_w = \frac{ad(a + d)}{a + 2d} \gamma_w \quad (15.53)$$

$$\bar{z}_w = \frac{a + 2d}{3} \quad (15.54)$$

$$j_s = \frac{a}{a + 2d} \gamma_w \quad (15.55)$$

Case (c)—Figure 15.19c

$$u_B = u_C = \frac{a(b + 2d)}{a + b + 2d} \gamma_w \quad (15.56)$$

$$P_w = \frac{1}{2} \left[\frac{a(b+2d)(a+2b+d)}{a+b+2d} \right] \gamma_w \quad (15.57)$$

$$\bar{z}_w = \frac{a^2 + 3a(b+d) + 3b(b+2d) + 2d^2}{3(a+2b+d)} \quad (15.58)$$

$$j_s = \frac{a}{a+b+2d} \gamma_w \quad (15.59)$$

Recall that j_s is the seepage pressure per unit volume, and the resultant effective stress is increased when seepage is downward (behind the wall) and is decreased when seepage is upward (in front of the wall), as discussed in Chapter 7.

15.10.2 Analysis of Sheet Pile Walls in Mixed Soils

Sheet pile walls may penetrate different soil types. For example, Figure 15.20 shows a sheet pile wall that supports a coarse-grained soil but is embedded in a fine-grained soil. In this case, you should consider a mixed analysis. For short-term condition, an effective stress analysis can be used for the coarse-grained soil but a total stress analysis should be used for the fine-grained soil. For long-term condition, an effective stress analysis should be carried out for both soil types.

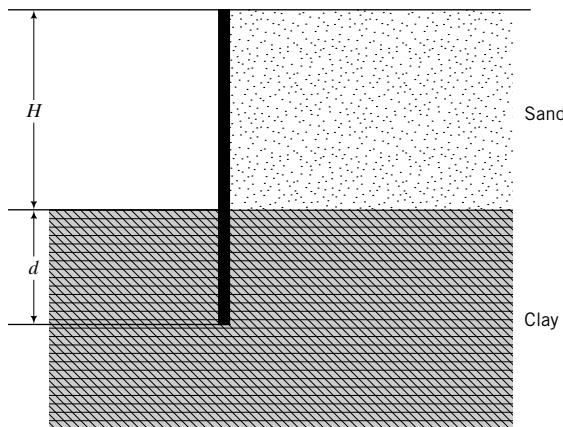


FIGURE 15.20 Sheet pile wall penetrating different soils.

15.10.3 Consideration of Tension Cracks in Fine-Grained Soils

If a sheet pile wall supports fine-grained soils, you should consider the formation of tension cracks. The theoretical depth of a tension crack is

$$z_{cr} = \frac{2s_u}{\gamma} \quad \text{or} \quad \frac{2s_u}{\gamma'} \quad (15.60)$$

The latter is applicable when the tension cracks are filled with water. The depth of a tension crack is sometimes greater than the wall height. In this situation, you can assume a minimum active lateral effective pressure of $5z$ (kPa) as suggested by Padfield and Mair (1984), where z is the depth measured from

the top of the wall. When water fills the tension cracks, you should apply the full hydrostatic pressure to the wall over a depth equivalent to the depth of the tension crack or the wall height, whichever is smaller. In fine-grained soils, loss of moisture at the wall-soil interface can cause the soil to shrink, creating a gap. This gap can be filled with water. In this case, you should apply the full hydrostatic pressure over the height of the wall.

15.10.4 Methods of Analyses

Several methods have been proposed to determine the stability of sheet pile walls. These methods differ in the way the lateral stresses are distributed on the wall and the way the factor of safety is applied in solving for the embedment depth. We will discuss three methods in this book. In the first method, called the factored moment method (FMM), you would determine an embedment depth to satisfy moment equilibrium by applying a factor of safety (FS_p) on the passive resistance, usually between 1.5 and 2.0.

In the second method, called the factored strength method (FSM), reduction factors are applied to the shear strength parameters. These reduction factors are called mobilization factors because they are intended to limit the shear strength parameters to values that are expected to be mobilized by the design loads. A mobilization factor, F_ϕ , is applied to the friction angle, ϕ'_{cs} , and a mobilization factor, F_u , is applied to s_u . The application of these mobilization factors results in a higher active pressure and a lower passive pressure than the unfactored soil strength parameters. The design parameters are

$$\phi'_{design} = \frac{\phi'_{cs}}{F_\phi} \quad (15.61)$$

and

$$(s_u)_{design} = \frac{s_u}{F_u} \quad (15.62)$$

where

$$F_\phi = 1.2 \text{ to } 1.5 \quad \text{and} \quad F_u = 1.5 \text{ to } 2$$

The results from the FSM are sensitive to F_ϕ and F_u .

The third method, called the net passive pressure method (NPPM), utilizes a net available passive resistance (Burland et al., 1981). A vertical line is drawn from the active pressure at the excavation level to the base of the wall (Figure 15.21). The shaded region of pressure on the active side is subtracted from the passive pressure to give the net passive pressure shown by the area hatched by arrows. The factor of safety for the NPPM is

$$(FS)_r = \frac{\Sigma \text{ Moments of net available passive resistance}}{\Sigma \text{ Moments of lateral forces causing rotation}} \quad (15.63)$$

$$(FS)_r = 1.5 \text{ to } 2, \text{ with } 2 \text{ most often used}$$

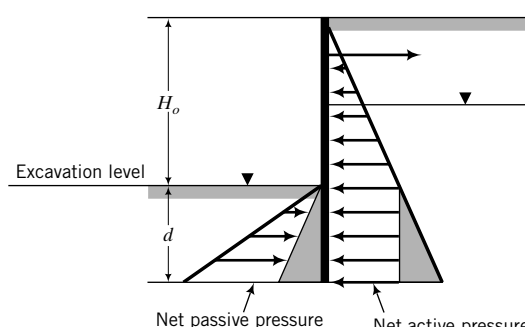


FIGURE 15.21
Net pressures for the NPPM.

The flexibility of sheet pile walls leads to lateral pressure distributions that do not correspond to the Rankine active and passive states. Expected lateral pressure distributions on a “stiff” flexible wall and a less “stiff” flexible wall are shown in Figure 15.22. The deflection (Figure 15.22b) due to yielding of the wall leads to localized constrained soil movements at and near the bulges. The constraint is provided by the intergranular shear stress. Stresses within the soil near the wall are redistributed as the soil tries to establish equilibrium. As a result, different structural arrangements of the particles are created. Sometimes this arrangement and stress redistribution are such that the resistance provided by the soil is analogous to a structural arch. This is called soil arching. The lateral pressures at and near the bulges of the wall are substantially reduced from those calculated using either the Rankine or Coulomb method. This arching action is one reason why some retaining walls have bulged but have remained stable. Recall that a structural arch resists loads through compression and the loads are transferred to the supports. In an anchored retaining wall, arching action may cause large additional loads at the top and bottom of the wall because the arch may find support at these locations. Consequently, the wall has to be designed to support an additional disturbing moment, which could be greater than 30% of the non-arch disturbing moment. So, while arching is beneficial in reducing lateral pressures, it has the negative effect of increasing the disturbing moment. Consideration of soil arching in design is beyond the scope of this book.

Rowe (1957) developed a method, based on laboratory tests, to reduce the calculated maximum bending moment to account for the effects of wall flexibility on the bending moment. Rowe’s moment reduction is applicable when a factor of safety has been applied on the passive resistance, as in the FMM. There is some debate on the applicability of Rowe’s method. Some engineers prefer to calculate the maximum bending moment at limit equilibrium ($(FS)_p = F_\phi = (FS)_r = F_u = 1$) and use it as the design moment. This is the preferred method in this book.

To account for soil–wall interface friction, you need to use K_{aC} and K_{pC} . However, the active and passive coefficients derived by Caquot and Kerisel (1948) are regarded as more accurate than those of Coulomb. For a flexible retaining wall, only the horizontal components of the lateral forces are important. In Appendix D, the horizontal components of the active and passive coefficients of Caquot and Kerisel as tabulated by Kerisel and Absi (1990) are plotted for some typical backfill slopes and soil–wall interface friction angles. We will use the values of the lateral earth pressure coefficients in Appendix D in some of the example problems in this chapter.

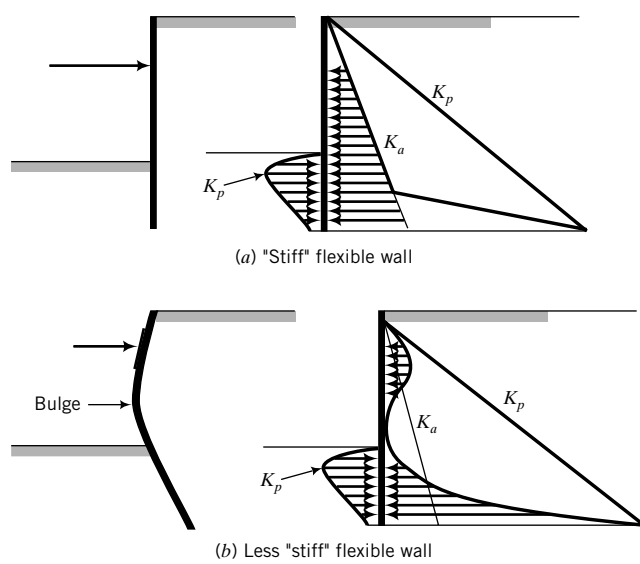


FIGURE 15.22 Lateral pressure distributions expected on a “stiff” flexible wall and less “stiff” flexible wall. (After Padfield and Mair, 1984.)

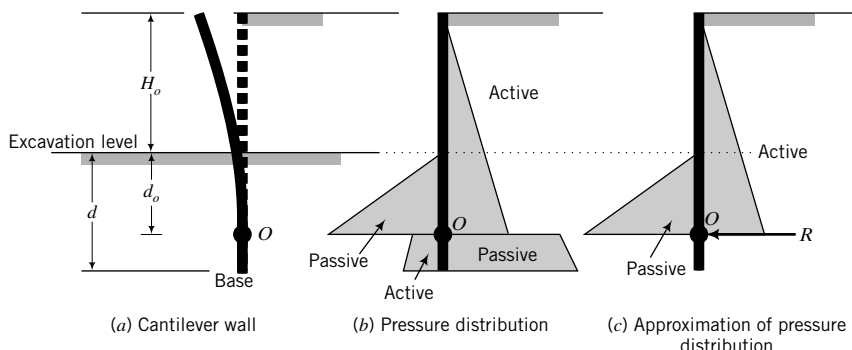


FIGURE 15.23 Approximation of pressure distributions in the analysis of cantilever flexible retaining walls. (Padfield and Mair, 1984.)

15.10.5 Analysis of Cantilever Sheet Pile Walls

Cantilever sheet pile walls are analyzed by assuming that rotation occurs at some point, O , just above the base of the wall (Figure 15.23). The consequence of assuming rotation above the base is that, below the point of rotation, the lateral pressure is passive behind the wall and active in front of the wall (Figure 15.23b). To simplify the analysis, a force R (Figure 15.23c) is used at the point of rotation to approximate the net passive resistance below it (the point of rotation). By taking moments about O , the unknown force R is eliminated and we then obtain one equation with one unknown, that is, the unknown depth, d_o . To account for this simplification, the depth d_o is increased by 20% to 30% to give the design embedment depth, d .

The general procedure for determining d for stability and to determine the wall size is as follows:

1. Arbitrarily select a point O at a distance d_o from the excavation level.
 2. Calculate the active and passive earth pressures using the FMM or FSM or NPPM.
 3. Calculate the net porewater pressure (u) distribution and the seepage force per unit volume (j_s). The effective unit weight is increased by j_s in the active zone and is decreased by j_s in the passive zone. For general design, you should use a minimum difference in groundwater level behind and in front of the wall of not less than one-third the wall height, H_o .
 4. Determine the unknown depth d_o by summing moments about O .
 5. Calculate d by increasing d_o by 20% or 30% to account for simplifications made in the analysis. The depth of penetration d is therefore $1.2d_o$ or $1.3d_o$.
 6. Calculate R by summing forces horizontally over the depth $(H_o + d)$.
 7. Calculate the net passive resistance, $(P_p)_{net}$, over the distance, $d - d_o$, below O .
 8. Check that R is less than $(P_p)_{net}$. If not, extend the depth of embedment and recalculate R .
 9. Calculate the maximum bending moment (M_{max}) over the depth $(H_o + d_o)$ using unfactored passive resistance (FMM), unfactored strength values (FSM), and $(FS)_r = 1$ (NPPM).
 10. Determine the section modulus, $S_x = M_{max}/f_a$, where M_{max} is the maximum bending moment and f_a is the allowable bending stress of the wall material.

15.10.6 Analysis of Anchored Sheet Pile Walls

There are two methods used to analyze anchored sheet pile walls. One is the free earth method, the other is the fixed earth method. We will be discussing the free earth method, because it is frequently used in design practice.

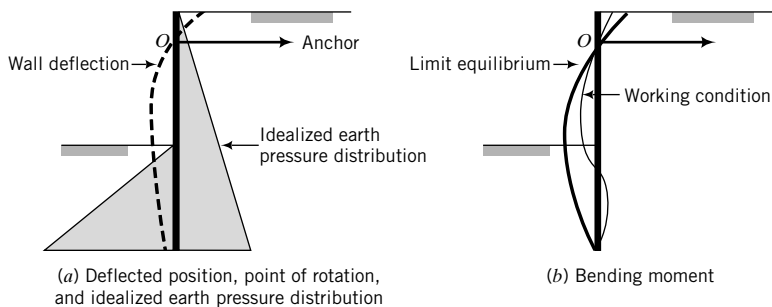


FIGURE 15.24 Free earth conditions for anchored retaining walls.
(Padfield and Mair, 1984.)

In the free earth method, it is assumed that (1) the depth of embedment of the wall is insufficient to provide fixity at the bottom end of the wall, and (2) rotation takes place about the point of attachment of the anchor, O (Figure 15.24a). The expected bending moment diagram, based on the above assumptions, is depicted in Figure 15.24b.

The procedure for analyzing an anchored sheet pile wall is as follows:

1. Assume a depth of embedment, d .
2. Calculate the active and passive pressures using the FMM or FSM or NPPM.
3. Calculate the net porewater pressure (u) distribution and the seepage force per unit volume (j_s). The effective unit weight is increased by j_s in the active zone and is decreased by j_s in the passive zone. For general design, you should use a minimum difference in groundwater level behind and in front of the wall of not less than one-third the wall height, H_o .
4. Determine d by taking moments about the point of attachment of the anchor, O . Usually you will get a cubic equation, which you can solve by iteration or by using a goal seek option in a spreadsheet program or by using a polynomial function solver on a calculator.
5. Recalculate d using unfactored passive resistance (FMM), unfactored strength (FSM), and $(FS)_r = 1$ (NPPM). Use this recalculated depth to determine the anchor force and the maximum bending moment.
6. Determine the anchor force per unit length of wall, T_a , by summing forces in the horizontal direction. The anchor force, T_a , is multiplied by a factor of safety $(FS)_a$, usually 2.
7. Determine the location of the anchor plates or deadmen. Let d_z be the depth of the bottom of the anchor plate from the ground surface (Figure 15.25). The force mobilized by the anchor plate must balance the design anchor force, that is,

$$\frac{1}{2}\gamma'd_z^2(K_p - K_a) = T_a \times (FS)_a$$

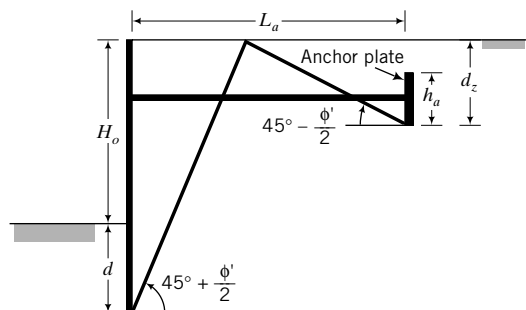


FIGURE 15.25 Location of anchor plates.

Solving for d_z , we get

$$d_z = \sqrt{\frac{2T_a \times (\text{FS})_a}{\gamma'(K_p - K_a)}} \quad (15.64)$$

A passive wedge develops in front of the anchor plate and an active wedge develops behind the retaining wall. The anchor plate must be located outside the active slip plane. The minimum anchor length (L_a) of the anchor rod, with reference to Figure 15.25, is

$$L_a = (H_o + d) \tan(45^\circ - \phi'/2) + d_z \tan(45^\circ + \phi'/2) \quad (15.65)$$

8. Calculate the spacing of the anchors. Let s be the longitudinal spacing of the anchors and h_a be the height of the anchor plate. If $h_a \geq d_z/2$, the passive resistance of the anchor plate is assumed to be developed over the full depth d_z . From static equilibrium of forces in the horizontal direction, we obtain

$$s = \frac{\gamma d_z^2 L_a}{2T_a (\text{FS})_a} (K_p - K_a) \quad (15.66)$$

You need to use the appropriate value of γ . If the anchor is below groundwater level, use γ' . Otherwise use γ_{sat} .

9. Calculate the maximum bending moment (M_{max}) using the embedment depth at limit equilibrium (unfactored passive resistance, unfactored strength values, or $(\text{FS})_r = 1$).
10. Determine the section modulus, $S_x = M_{max}/f_a$, where f_a is the allowable bending stress of the wall material.
11. Select wall size from manufacturer's catalog based on S_x .

EXAMPLE 15.5 Cantilever Flexible Wall



Computer Program Utility

Access <http://www.wiley.com/college/budhu>, Chapter 15, and click *retwall.xls* to view examples of retaining wall analysis using a spreadsheet. You can change input values and explore how the stability of the walls changes.

Determine the depth of embedment required for stability of the cantilever sheet pile wall shown in Figure E15.5a. Compare the results of the three methods—FMM, FSM, and NPPM—using $(\text{FS})_p = 2.0$, $F_\phi = 1.25$, and $(\text{FS})_r = 1.5$. Calculate the maximum bending moment for each of these methods. Groundwater is below the base of the wall. The tolerable rotation is $0.005 H_o$ and less, where H_o is the wall height.

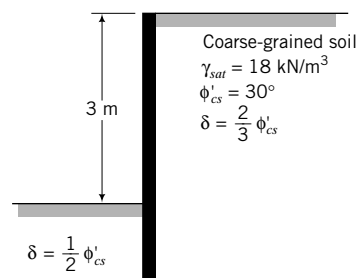


FIGURE E15.5a

Strategy You should use the Kerisel and Absi passive pressures (see Appendix D) and either the Kerisel and Absi or Coulomb active pressures. The key is to determine the lateral forces and then find d_o (an arbitrarily selected embedment depth at which rotation is presumed to occur) using moment equilibrium. Since you have to find the depth for unfactored values to calculate the maximum bending moment, you should determine K_{ax} and K_{px} for factored and unfactored values at the very beginning of your solution.

Solution 15.5

Step 1: Calculate K_{ax} and K_{px} .

$$\text{For FSM: } \phi'_{design} = \frac{\phi'_{cs}}{F_\phi} = \frac{30}{1.25} = 24^\circ$$

$$\text{For FMM and NPPM: } \phi'_{design} = \phi'_{cs}$$

Use the Kerisel and Absi (1990) K_{ax} and K_{px} (Appendix D).

$$\text{FSM: } K_{ax} = 0.36 \quad \left(\phi'_{design} = 24^\circ, \delta = \frac{2}{3} \phi'_{design}, \beta/\phi'_{design} = 0 \right)$$

$$K_{px} = 0.3 \quad \left(\phi'_{design} = 24^\circ, \delta = \frac{1}{2} \phi'_{design}, \beta/\phi'_{design} = 0 \right)$$

$$\text{FMM and NPPM: } K_{ax} = 0.28 \quad \left(\phi'_{cs} = 30^\circ, \delta = \frac{2}{3} \phi'_{cs}, \beta/\phi'_{cs} = 0 \right)$$

$$K_{px} = 4.6 \quad \left(\phi'_{cs} = 30^\circ, \delta = \frac{1}{2} \phi'_{cs}, \beta/\phi'_{cs} = 0 \right)$$

Step 2: Determine the lateral earth pressure distributions.

The lateral pressure distributions for the FMM and FSM have the same shape but different magnitudes because of the different lateral earth pressure coefficients (Figure E15.5b). The lateral pressure distribution for the NPPM is shown in Figure E15.5c. Since groundwater is not within the depth of the retaining wall, $\gamma' = \gamma_{sat} = \gamma$.

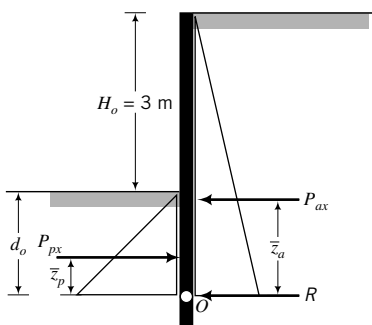


FIGURE E15.5b

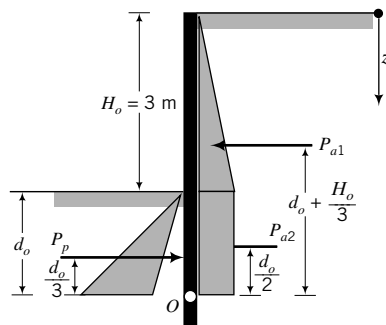


FIGURE E15.5c

With reference to Figure E15.5b:

Active case

$$P_{ax} = \frac{1}{2} K_{ax} \gamma (H_o + d_o)^2 = \frac{1}{2} \times K_{ax} \times 18(3 + d_o)^2 = 9K_{ax}(3 + d_o)^2$$

$$\bar{z}_a = \frac{H_o + d_o}{3} = \frac{3 + d_o}{3}$$

$$(M_O)_a = P_{ax} \bar{z}_a = 9K_{ax}(3 + d_o)^2 \left(\frac{3 + d_o}{3} \right) = 3K_{ax}(3 + d_o)^3$$

Passive case

$$P_{px} = \frac{1}{2} K_{px} \gamma d_o^2 = \frac{1}{2} \times K_{px} \times 18 \times d_o^2 = 9K_{px} d_o^2$$

$$\bar{z}_p = \frac{d_o}{3}$$

$$(M_O)_p = P_{px} \bar{z}_p = 9K_{px} d_o^2 \times \frac{d_o}{3} = 3K_{px} d_o^3$$

Step 3: Find d_o .

All forces are calculated per meter length of wall.

FMM

The passive pressure is factored by $(FS)_p$.

$$K_{ax} = 0.28 \quad \text{and} \quad K_{px} = 4.6$$

$$(M_O)_a = 3 \times 0.28(3 + d_o)^3 = 0.84(3 + d_o)^3$$

$$(M_O)_p = \frac{3 \times 4.6d_o^3}{(FS)_p} = \frac{3 \times 3.3d_o^3}{2} = 6.9d_o^3$$

For equilibrium: $(M_O)_a = (M_O)_p$

$$\therefore 0.84(d_o^3 + 9d_o^2 + 27d_o + 27) = 9.9d_o^3$$

which simplifies to

$$7.21d_o^3 - 9d_o^2 - 27d_o - 27 = 0$$

By trial and error or by using the polynomial function on a calculator, $d_o = 2.95$ m.

FSM

$$K_{ax} = 0.36 \quad \text{and} \quad K_{px} = 3.3$$

$$(M_O)_a = 3 \times 0.36(3 + d_o)^3 = 1.08(3 + d_o)^3$$

$$(M_O)_p = 3 \times 4.6d_o^3 = 9.9d_o^3$$

For equilibrium: $(M_O)_a = (M_O)_p$

$$1.08(d_o^3 + 9d_o^2 + 27d_o + 27) = 6.9d_o^3$$

which simplifies to

$$8.17d_o^3 - 9d_o^2 - 27d_o - 27 = 0$$

By trial and error or by using the polynomial function on a calculator, $d_o = 2.75$ m.

NPPM

$$K_{ax} = 0.28 \quad \text{and} \quad K_{px} = 4.6$$

The pressure diagram for the NPPM is shown in Figure E15.5c.

$$P_{a1} = \frac{1}{2} \times K_{ax} \gamma H_o^2 = \frac{1}{2} \times 0.28 \times 18 \times 3^2 = 22.7 \text{ kN}$$

$$P_{a2} = K_{ax} \gamma H_o d_o = 0.28 \times 18 \times 3 \times d_o = 15.1d_o$$

$$P_p = \frac{1}{2} (K_{px} - K_{ax}) \gamma d_o^2 = \frac{1}{2} (4.5 - 0.28) \times 18d_o^2 = 38.9d_o^2$$

$$(M_O)_a = P_{a1} \left(d_o + \frac{H_o}{3} \right) + P_{a2} \frac{d_o}{2} = 7.6d_o^2 + 22.7d_o + 22.7$$

$$(M_O)_p = P_p \frac{d_o}{3} = 38.9 d_o^2 \times \frac{d_o}{3} = 13 d_o^3$$

$$(\text{FS})_r = \frac{(M_O)_p}{(M_O)_a}$$

For $(\text{FS})_r = 1.5$,

$$1.5(7.6d_o^2 + 22.7d_o + 22.7) = 13d_o^3$$

Rearranging, we get

$$7.67d_o^3 - 7.6d_o^2 - 22.7d_o - 22.7 = 0$$

By trial and error or by using the polynomial function on a calculator, $d_o = 2.41$ m.

Step 4: Calculate the design depth.

$$\text{FMM: } d = 1.2d_o = 1.2 \times 2.95 = 3.54 \text{ m}$$

$$\text{FSM: } d = 1.2d_o = 1.2 \times 2.75 = 3.3 \text{ m}$$

$$\text{NPPM: } d = 1.2d_o = 1.2 \times 2.41 = 2.89 \text{ m}$$

Step 5: Determine R .

$$R = P_{px} - P_{ax}$$

$$\text{FMM: } d_o = 2.95 \text{ m; } R = 9 \times 4.6 \times 2.95^2 - 9 \times 0.28 \times (3 + 2.95)^2 = 271.1 \text{ kN/m}$$

$$\text{FSM: } d_o = 2.75 \text{ m; } R = 9 \times 3.3 \times 2.75^2 - 9 \times 0.36 \times (3 + 2.75)^2 = 109.4 \text{ kN/m}$$

$$\begin{aligned} \text{NPPM: } d_o &= 2.41 \text{ m; } R = 9 \times (4.6 - 0.28) \times 2.41^2 \\ &\quad - (9 \times 0.28 \times 3^2 + 0.28 \times 18 \times 3 \times 2.41) = 166.7 \text{ kN/m} \end{aligned}$$

To calculate the net resistance below the assumed point of rotation, O , calculate the average passive pressure at the back of the wall and the average active pressure in front of the wall. Remember that below the point of rotation, passive pressure acts at the back of the wall and active pressure acts at the front of the wall. The mid-depth between d_o and $1.2d_o$ is $1.1d_o$.

FMM

$$\text{Average passive lateral pressure} = K_{px}\gamma(H_o + 1.1d_o) = 4.6 \times 18 \times (3 + 1.1 \times 2.95) = 517.1 \text{ kPa}$$

$$\text{Average active lateral pressure} = K_{ax}\gamma \times 1.1d_o = 0.28 \times 18 \times 1.1 \times 2.95 = 16.4 \text{ kPa}$$

$$\text{Net lateral pressure} = 517.1 - 16.4 = 500.7 \text{ kPa}$$

$$\text{Net force} = 500.7 \times 0.2d_o = 295.4 \text{ kN} > R (= 271.1 \text{ kN})$$

Therefore, depth of penetration is satisfactory.

FSM

$$\text{Average passive lateral pressure} = K_{px}\gamma(H_o + 1.1d_o) = 3.3 \times 18 \times (3 + 1.1 \times 2.75) = 357.9 \text{ kPa}$$

$$\text{Average active lateral pressure} = K_{ax}\gamma \times 1.1d_o = 0.36 \times 18 \times 1.1 \times 2.75 = 19.6 \text{ kPa}$$

$$\text{Net lateral pressure} = 357.9 - 19.6 = 338.3 \text{ kPa}$$

$$\text{Net force} = 338.3 \times 0.2d_o = 186.1 \text{ kN} > R (= 109.4 \text{ kN})$$

Therefore, depth of penetration is satisfactory.

NPPM

$$\text{Average passive lateral pressure} = K_{px}\gamma(H_o + 1.1d_o) = 4.6 \times 18 \times (3 + 1.1 \times 2.41) = 467.9 \text{ kPa}$$

$$\text{Average active lateral pressure} = K_{ax}\gamma \times 1.1d_o = 0.28 \times 18 \times 1.1 \times 2.41 = 13.4 \text{ kPa}$$

$$\text{Net lateral pressure} = 467.9 - 13.4 = 454.5 \text{ kPa}$$

$$\text{Net force} = 454.5 \times 0.2d_o = 219.1 \text{ kN} > R (= 166.7 \text{ kN})$$

Therefore, depth of penetration is satisfactory.

Step 6: Determine the maximum bending moment.

Maximum bending moment for $(FS)_p = F_\phi = 1$.

Let z be the location of the point of maximum bending moment (point of zero shear) such that $z > H_o$.

$$\begin{aligned} M_z &= \frac{1}{2}K_{ax}\gamma z^2 \times \frac{z}{3} - \frac{1}{2}K_{px}\gamma(z - H_o)^2 \times \frac{(z - H_o)}{3} \\ &= \frac{1}{2} \times 4.6 \times 18 \times \frac{(z - 3)^3}{3} \\ &= 0.84z^3 - 13.8(z - 3)^3 \end{aligned}$$

To find z at which the bending moment is maximum, we need to differentiate the above equation with respect to z and set the result equal to zero.

$$\frac{dM_z}{dz} = 0 = 2.52z^2 - 41.4(z - 3)^2 = 38.9z^2 - 248.4z + 372.6 = 0$$

Solving for z , we get $z = 3.68$ m or 2.53 m. The correct answer is 3.68 m since zero shear cannot occur above the excavation level in this problem (positive shear in the active zone only gets reduced below the excavation level).

$$M_z = 0.84 \times 3.68^3 - 13.8(3.68 - 3)^3 = 36 \text{ kN.m}$$

For this problem, it is easy to use calculus to determine the maximum bending moment. For most problems, you will have to find the shear force distribution with depth, identify or calculate the point of zero shear, and then calculate the maximum bending moment.

EXAMPLE 15.6 Anchored Flexible Wall

Determine the embedment depth and the anchor force of the tied-back wall shown in Figure E15.6a using the FSM.

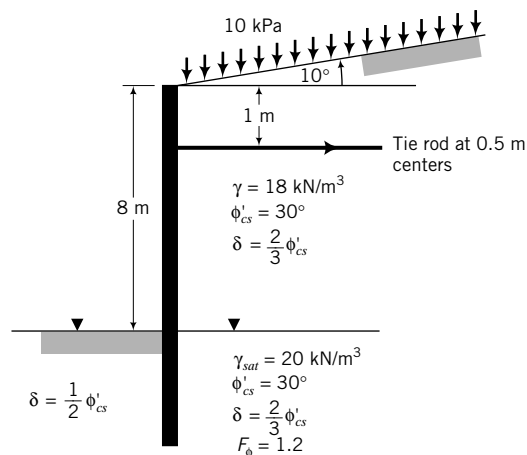


FIGURE E15.6a

Strategy You should use the Kersel and Absi passive pressures (see Appendix D) and either the Kersel and Absi or Coulomb active pressures. Groundwater level on both sides of the wall is the same, so seepage will not occur.

Solution 15.6

Step 1: Determine K_{ax} and K_{px} .

$$\phi'_{design} = \frac{\phi'_{cs}}{F_\phi} = \frac{30}{1.2} = 25^\circ; \quad \frac{\beta}{\phi'_{design}} = \frac{10}{25} = 0.4$$

From Appendix D,

$$K_{ax} = 0.42 \quad \left(\phi'_{design} = 25^\circ, \beta/\phi'_{design} = 0.4, \delta = \frac{2}{3} \phi'_{design} \right)$$

$$K_{px} = 3.4 \quad \left(\phi'_{design} = 25^\circ, \beta/\phi'_{design} = 0, \delta = \frac{1}{2} \phi'_{design} \right)$$

For unfactored strength values,

$$K_{ax} = 0.31 \quad \left(\phi'_{cs} = 30^\circ, \beta/\phi'_{cs} = 10/30 = \frac{1}{3}, \delta = \frac{2}{3} \phi'_{cs} \right)$$

$$K_{px} = 4.6 \quad \left(\phi'_{cs} = 30^\circ, \beta/\phi'_{cs} = 0, \delta = \frac{1}{2} \phi'_{cs} \right)$$

Step 2: Determine the lateral forces and moments.

Use a table to facilitate ease of computation and checking. (See Figure E15.6b.) Below the groundwater level, $\gamma' = 20 - 9.8 = 10.2 \text{ kN/m}^3$.

Part	Horizontal force (kN)	Moment arm from anchor (m)	Moment (kN.m) +
1	$K_{ax}q_s(H_o + d_o) = 0.42 \times 10 \times (8 + d_o) = 4.2d_o + 33.6$	$\left(\frac{H_o + d_o}{2}\right) - h = \left(\frac{8 + d_o}{2}\right) - 1 = 3 + \frac{d_o}{2}$	$-(2.1d_o^2 + 29.4d_o + 100.8)$
2	$\frac{1}{2}K_{ax}\gamma H_o^2 = \frac{1}{2} \times 0.42 \times 18 \times 8^2 = 241.9$	$\frac{2}{3}H_o - h = \frac{2}{3} \times 8 - 1 = 4.33$	-1047.4
3	$K_{ax}\gamma H_o d_o = 0.42 \times 18 \times 8 \times d_o = 60.5d_o$	$H_o - h + \frac{d_o}{2} = 7 + \frac{d_o}{2}$	$-(30.3d_o^2 + 423.5d_o)$
4	$\frac{1}{2}K_{ax}\gamma' d_o^2 = \frac{1}{2} \times 0.42 \times 10.2 \times d_o^2 = 2.1d_o^2$	$H_o - h + \frac{2}{3}d_o = 7 + \frac{2}{3}d_o$	$-(1.4d_o^3 + 14.7d_o^2)$
	$\Sigma 2.1d_o^2 + 64.7d_o + 275.5$		
5	$\frac{1}{2}K_{px}\gamma' d_o^2 = \frac{1}{2} \times 3.4 \times 10.2 \times d_o^2 = 17.3d_o^2$	$H_o - h + \frac{2}{3}d_o = 7 + \frac{2}{3}d_o$	$11.5d_o^3 + 121.1d_o^2$
			$\Sigma M = -(10.1d_o^3 + 74d_o^2 + 452.9d_o + 1148.2)$

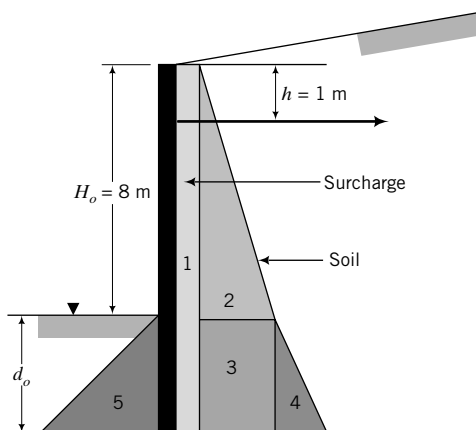


FIGURE E15.6b

Step 3: Determine d_o .

Equate the sum of moments to zero and simplify equation by dividing by the coefficient of d_o^3 .

$$d_o^3 + 7.3d_o^2 - 44.8d_o - 113.7 = 0$$

By trial and error or by using the polynomial function on a calculator, $d_o = 5.38$ m.

Step 4: Determine d_o for the unfactored strength values.

To calculate the new depth of penetration for unfactored strength values, use proportionality, for example,

$$\text{Active moment for unfactored strength} = \text{Active moment for factored strength values} \times \frac{\text{Unfactored } K_{ax}}{\text{Factored } K_{ax}}$$

$$(M_O)_a = -(1.4d_o^3 + 47.1d_o^2 + 452.9d_o + 1148.2) \times \frac{0.31}{0.42} \\ = -(d_o^3 + 34.8d_o^2 + 334.3d_o + 847.5)$$

$$\text{Passive moment: } (M_O)_p = (11.5d_o^3 + 121.1d_o^2) \times \frac{4.6}{3.4} = 15.5d_o^3 + 163.9d_o^2$$

$$\text{Sum of moment: } (M_O)_p + (M_O)_a = 14.5d_o^3 + 129.1d_o^2 - 334.3d_o - 847.5$$

Solving, we get $d_o = 3.38$ m.

Step 5: Determine the anchor force for $d_o = 3.38$ m.

$$\Sigma \text{ Active forces} = (2.1 d_o^2 + 64.7d_o + 275.5) \times \frac{0.31}{0.42} = 381.9 \text{ kN}$$

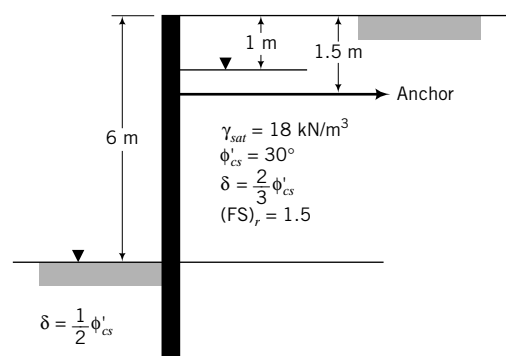
$$\Sigma \text{ Passive forces} = 17.3d_o^2 \times \frac{4.6}{3.4} = 267.4 \text{ kN}$$

$$T_a = 381.9 - 267.4 = 114.5 \text{ kN}$$

$$(T_a)_{\text{design}} = (\text{FS})T_a = 2 \times 114.5 = 229 \text{ kN}$$

EXAMPLE 15.7 Anchored Flexible Wall

Determine the embedment depth and the design anchor force required for stability of the sheet pile wall shown in Figure E15.7a using the NPPM.

**FIGURE E15.7a**

Strategy In the NPPM, you must use the unfactored strength values to calculate K_{ax} and K_{px} and then determine the net active and net passive lateral pressures. To calculate d_o , you have to do iterations. A simple approach to solve for d_o is to set up the forces and moments in terms of the unknown d_o and then assume values of d_o until you find a d_o value that gives the required factor of safety [$(FS)_r \approx 1.5$]. A spreadsheet program or a programmable calculator is

very helpful in solving this type of problem. In Excel, for example, you can use the Goal Seek function to find d_o . It is quite easy to make errors in calculations, so you should recheck your work, and you must conduct a “hand” check when using outputs from computer programs. Since the groundwater levels are different in front of and behind the wall, you need to consider seepage assuming a steady state seepage condition. To calculate the anchor force, you have to find d_o for $(FS)_r = 1$ and then multiply the anchor force by 2 (factor of safety).

Solution 15.7

Step 1: Determine K_{ax} and K_{px} .

From Appendix D,

$$K_{ax} = 0.28 \quad \left(\phi'_{cs} = 30^\circ, \beta/\phi'_{cs} = 0, \delta = \frac{2}{3}\phi'_{cs} \right)$$

$$K_{px} = 4.6 \quad \left(\phi'_{cs} = 30^\circ, \beta/\phi'_{cs} = 0, \delta = \frac{1}{2}\phi'_{cs} \right)$$

Step 2: Determine the net lateral pressures.

Make a table to do the calculations and draw a diagram of the lateral earth pressure distribution.

See Figure E15.7b.

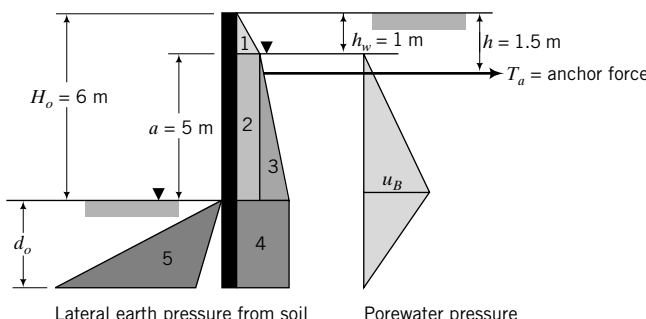


FIGURE E15.7b

Lateral earth pressure from soil Porewater pressure

Below groundwater level

$$\begin{aligned} \text{Average seepage force/unit volume: } j_s &= \left(\frac{a}{a + 2d_o} \right) \gamma_w \\ &= \left(\frac{5}{5 + 2d_o} \right) 9.8 \text{ kN/m}^3 \end{aligned}$$

$$\text{Active zone: } \gamma' = \gamma_{sat} - \gamma_w + j_s = 18 - 9.8 + j_s = 8.2 + j_s \text{ kN/m}^3$$

$$\text{Passive zone: } \gamma' = \gamma_{sat} - \gamma_w - j_s = 18 - 9.8 - j_s = 8.2 - j_s \text{ kN/m}^3$$

Depth (m)	Active pressure (kPa)	Passive pressure (kPa)
0	0	0
1	$K_a \gamma h_w = 0.28 \times 18 \times 1 = 5$	0
6	$K_a \gamma h_w + K_a(\gamma' + j_s)(H_o - h_w)$ $= 0.5 + 0.28 \times (8.2 + j_s) \times 5 = 16.5 + 1.4j_s$	0
$6 + d$	$16.8 + 1.4j_s$	$K_p(8.2 - j_s)d_o - K_a(8.2 + j_s)d_o$ $= 4.6(8.2 - j_s)d_o - 0.28(8.2 + j_s)d_o$ $= (35.4 - 4.88j_s)d_o$
Water	$u_B = \frac{2(ad_o)}{a + 2d_o} \gamma_w = \frac{98.1d_o}{5 + 2d_o}$	

Step 3: Calculate the lateral forces, the moment, and $(FS)_r$.

All forces and moments are per meter length of wall. The moment is the sum of moments about the anchor position and R_x is the resultant active lateral force. In the first column under Moment, a value of d_o is guessed and $(FS)_r$ is calculated. In the second column under Moment, the value of $d_o = 5.75$ m was obtained using a spreadsheet program (the actual value obtained from the spreadsheet program is $d_o = 5.72$ m for $(FS)_r = 1.5$). In Excel, you use Tools → Goal Seek to find d_o to satisfy the desired value of $(FS)_r$.

Part	Forces (kN)	Moment arm (m)	Moment (kN.m)	
			$d = 7 \text{ m}$	$d = 5.75 \text{ m}$
1	$0.5 \times 5.0 \times 1 = 2.5$	$h - h_w + \frac{h_w}{3} = 0.5 + 0.33 = 0.83$	-2.1	-2.1
2	$5.0 \times 5 = 25$	$\frac{a}{2} - (h - h_w) = 2.5 - 0.5 = 2$	-50.0	-50.0
3	$0.5 \times (11.5 + 1.4j_s) \times 5$ $= 28.8 + 3.8j_s$	$\frac{2a}{3} - (h - h_w) = \frac{10}{3} - 0.5$ $= 2.83$	-109.2	-113.4
4	$(16.5 + 1.4j_s) \times d_o$ $= (16.5 + 1.4j_s)d_o$	$H_o - h - \frac{d_o}{2} = 4.5 + \frac{d_o}{2}$	-1126.2	-876.0
	Water: $\frac{ad_o(a + d_o)\gamma_w}{a + 2d_o} = \frac{49d_o(5 + d_o)}{5 + 2d_o}$	$H_o + d_o - h - z_w$ $= 4.5 + d_o - \frac{5 + 2d_o}{3} = \frac{8.5 + d_o}{3}$	-1119.3	-871.9
	$R_x = 56.3 + 3.8j_s$ $+ (16.5 + 1.4j_s)d_o + \frac{49d_o(5 + d_o)}{5 + 2d_o}$		$\Sigma M_d = -2406.8$	-1913.4
5	$0.5 \times (35.4 - 4.88j_s)d_o^2$ $= (17.7 - 2.4j_s)d_o^2$	$H_o - h + \frac{2d_o}{3} = 4.5 + \frac{2d_o}{3}$	$\Sigma M_r = 5179.8$	2912.8
		$(FS)_r = \frac{\sum M_r}{\sum M_d}$	2.15	1.52

Step 4: Calculate the anchor forces for $(FS)_r = 1$.

For $(FS)_r = 1$, $d_o = 4.62$ m. Substituting $d_o = 4.62$ m, we get

Active zone

$$j_s = \left(\frac{5}{5 + 2 \times 4.62} \right) 9.8 = 3.44 \text{ kN/m}^3$$

$$R_x = 56.3 + (3.8 \times 3.44) + (16.5 + 1.4 \times 3.44)4.62 + \frac{49 \times 4.62(5 + 4.62)}{5 + 2 \times 4.62} = 320.8 \text{ kN}$$

Passive zone

$$\text{Passive lateral force} = (17.7 - 2.4 \times 3.44)4.62^2 = 201.6 \text{ kN}$$

$$T_a = \text{Active lateral force} - \text{Passive lateral force} = 320.8 - 201.6 = 119.2 \text{ kN}$$

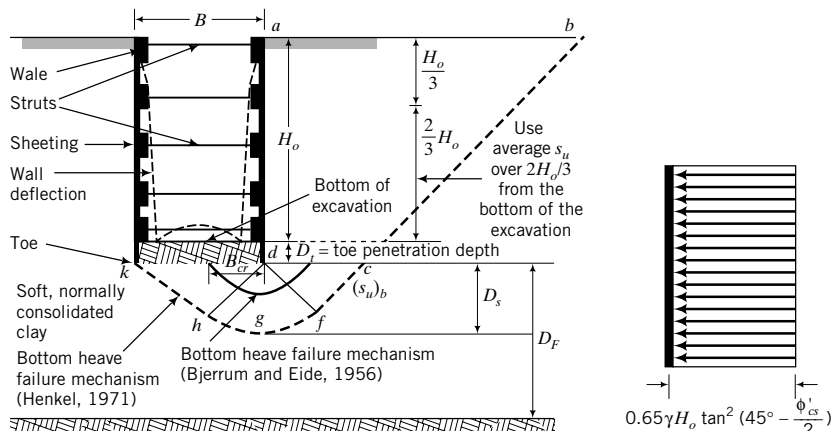
$$\text{Design anchor force} = 2T_a = 248.4 \text{ kN}$$

What's next . . . Sometimes, it is not possible to use an anchored sheet pile wall for an excavation. For example, an existing building near a proposed excavation can preclude the use of anchors. You may have

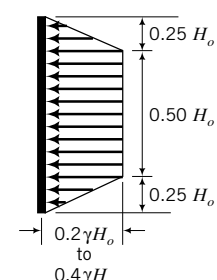
to brace your sheet piles within the excavation using struts. The analysis of braced excavation (also called cofferdam) is presented in the next section.

15.11 BRACED EXCAVATION

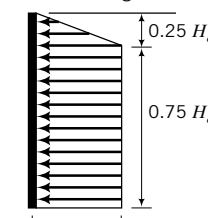
Braced excavations consist of sheet piles driven into the soil to form the sides of an excavation (Figure 15.26a) such as in the construction of bridge piers, abutments, and basements. As excavation proceeds within the area enclosed by the sheet piles, struts are added to keep the sheet piles in place.



(a) Braced excavation

(c) Lateral pressure distribution from fine-grained soils with $\frac{\gamma H_o}{s_u} < 4$

(b) Lateral pressure distribution from coarse-grained soils



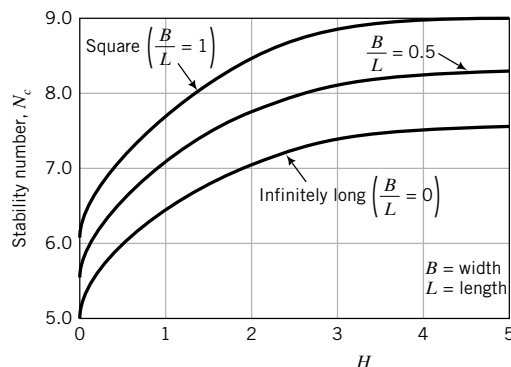
$$K_A = \left(1 - \frac{4 s_u}{\gamma H_o + q_s} \right) + 2\sqrt{2} D_s \frac{1 - \frac{5.14 (s'_u)_b}{\gamma H_o + q_s}}{H_o}$$

$$D_s = \frac{B}{\sqrt{2}} \quad \text{if } D_F > D_s$$

$$D_s = D_F \quad \text{if } D_F < D_s$$

(d) Lateral pressure distribution

$$\text{from fine-grained soils with } \frac{\gamma H_o}{s_u} \geq 4$$



(e) Stability number (Janbu et al., 1956)

FIGURE 15.26 Braced excavations.

The top struts are installed, followed by others at lower depths. The wall displacements before the top struts are installed are usually very small but get larger as the excavation gets deeper. The largest wall displacement occurs at the base (bottom) of the excavation (Figure 15.26a). Wall displacements are inconsistent with all the established earth pressure theories.

The critical design elements in a braced excavation are the loads on the struts, which are usually different because of different lateral loads at different depths, the time between excavations, and the installation procedure. Failure of a single strut can be catastrophic because it can lead to the collapse of the whole system. The analysis for the forces and deflection in braced excavation should ideally consider the construction sequence, and numerical methods such as the finite element method are preferred. Semi-empirical methods are often used for shallow braced excavations and in the preliminary design of deep braced excavations. The finite element method is beyond the scope of this book. We will only discuss a semi-empirical method.

Lateral stress distributions for use in the semi-empirical method are approximations from field measurements of strut loads in different types of soil. The lateral stress distributions used for coarse-grained and fine-grained soils are shown in Figure 15.26b–d. These lateral stress distributions are not real but average approximate stress distributions to estimate the maximum strut load. The real lateral stress distributions are strongly affected by arching action, as discussed in Section 15.10.4. The lateral stress distribution for coarse-grained soils (Figure 15.26b) was extrapolated from strut loads measured for dense sand adjacent to the excavation. The appropriate value of friction angle is ϕ'_p , but because we cannot rely on dilation, the design friction angle should be ϕ'_{cs} . For fine-grained soils, a total stress analysis is used, and the lateral stress distribution depends on the stability number, $\gamma H_o / s_u$ (Peck, 1969). If the stability number is less than 4, the stress state of the soil adjacent to the excavation can be assumed to be elastic, and the recommended lateral stress distribution is depicted in Figure 15.26c. However, if the stability number is greater than or equal to 4, the stress state of the soil adjacent to the bottom of the excavation is expected to be plastic, and the recommended lateral stress distribution is depicted in Figure 15.26d.

If the soil below the base of the excavation is a soft, normally consolidated soil, it is possible that heaving can occur. The soil above the base acts as a surcharge on the soil below it. This surcharge load may exceed the bearing capacity of the soft, normally consolidated soil, resulting in heaving.

Two possible heave mechanisms are shown in Figure 15.26a. One was proposed by Bjerrum and Eide (1956), and the other was proposed by Henkel (1971). Bjerrum and Eide suggested that the excavation could be viewed as a footing of width B and embedment depth H_o . They calibrated their failure mechanism using observations of bottom heave in soft clays and showed that the apparent factor of safety against bottom heave is

$$(FS)_{heave} = N_c \frac{(s_u)_b}{\gamma H_o + q_s} \quad (15.67)$$

where N_c is a bearing capacity coefficient shown in Figure 15.26e, H_o/B is the depth-to-width ratio, q_s is the surcharge on the surface ab (Figure 15.26a), and $(s_u)_b$ is the average undrained shear strength over the depth D_s below the toe of the sheeting. If $(FS)_{heave} < 1.5$, the sheeting should be extended below the base of the excavation for stability. Wall movements, strut loads, and wall moments are sensitive to $(FS)_{heave}$. FEM analyses (Karlsrud and Andresen, 2008) showed that for $(FS)_{heave} > 1.8$, the wall displacement is constant at about 0.2% of H_o , but it is 0.5% of H_o if $(FS)_{heave} = 1.4$.

The apparent lateral pressure for soft, fine-grained soils consists of two terms (Figure 15.26d). The first term $\left(1 - \frac{4s_u}{\gamma H_o + q_s}\right)$ represents the value of K_A that would be calculated from limit equilibrium when $D_s = 0$. That is, failure would occur along a plane parallel to bc and intersect the toe of the sheeting. The value of s_u for the first term should be the average undrained shear strength over a depth starting at $\frac{H_o}{3}$ from the surface and ending at the bottom of the excavation. The second term $\left(1 - \frac{5.14(s_u)_b}{\gamma H_o + q_s}\right)$ represents the component of lateral pressure from heaving. This term must be positive, and as such, $\frac{\gamma H_o + q_s}{(s_u)_b} > 5.14$. When $\frac{\gamma H_o + q_s}{(s_u)_b} < 5.14$, you should neglect the second term. If the levels of

water within the excavation and outside are different, you have to consider hydrostatic pressures and seepage forces.

Using the limit equilibrium method, Henkel (1971) showed that the calculated failure load from his failure mechanism (Figure 15.26a) closely matches observed failure loads from instrumented braced excavations in soft soils in Oslo, Norway, and in Mexico City, Mexico. The soil mass, $abcd$ (Figure 15.26a), behind the excavation slides on a plane, bcf , inclined at 45° to the horizontal and merges with the Prandtl plastic zone, $dfgh$ (Figure 15.26a). The soil wedge, dhk , heaves by sliding on the plane, hk , inclined at 45° to the horizontal. From Equation (12.33), the thickness of the Prandtl plastic zone for soft, normally consolidated clay under undrained condition ($\phi'_p = 0$) is $D_s = \frac{B}{\sqrt{2}}$. If the depth to the firm layer, D_F , is less than D_s , then D_s is equal to D_F .

Bottom heave stability can be improved by:

1. Excavating in steps; this increases N_c .
2. Excavating under pressurized air or under water.
3. Deeply embedding the retaining walls around the excavation.
4. Using cross-wall diaphragm.

The strut loads at each level are found by assuming hinged connections of the struts to the sheet piles. A free-body diagram is drawn for each level, and the forces imposed on the struts are determined using static equilibrium. Displacements of the walls are an important design consideration, as adjacent structures may be affected. The method discussed above does not consider displacements. Analyses using numerical methods (e.g., finite element method) are better suited for the overall analysis of braced excavation. The vertical ground settlement is generally within the range 0.5 to 2 times the lateral wall movement. Tolerable angular distortion (measure of differential settlement) for buildings near excavations is generally less than 2×10^{-3} radians, while tolerable total vertical settlement is less than 50 mm. The actual tolerable value would depend on the type of structure. For example, if the structure is a brick building, the total settlement may be limited to about 25 mm. Lateral wall and vertical ground displacements are dependent on:

1. Soil disturbance from installation, particularly installation of ground anchors and any piling works. The soil strength and stiffness decrease with greater levels of soil disturbance.
2. Soil types. Ground settlements in excavation in soft soils are generally greater than in stiff soils.
3. Soil consolidation from drainage of porewater. Particular attention should be paid to stratified soils with layered coarse-grained and fine-grained soils. Drainage of porewater pressures is enhanced by the presence of the coarse-grained layers. To reduce ground settlements in these types of soils, water leakage to the excavation should be prevented.
4. Stresses from nearby structures.
5. The width of the excavation. Wide excavations with soft soils at and just below the base can heave, resulting in larger ground settlement than in narrow excavations in the same soil.
6. The stress-strain response of the soil. Normally consolidated soils are less stiff than overconsolidated soils, so higher ground displacements can be expected in normally consolidated soils.
7. The geometry of the excavation. Observations of ground movements showed larger differential movements along the ends of excavations than perpendicular to them.

The procedure for analysis of braced excavation is as follows:

1. Check the stability against bottom heave using Equation (15.67). If $(FS)_{heave} < 1.5$, the toe penetration should be extended. This would result in a higher N_c value.
2. Determine the lateral stress on the walls for your soil type (Figure 15.26b-d).
3. Treat the connections of the wall (sheet pile) to the struts as hinges.

4. Draw a free-body diagram at each level of the excavation.

5. Solve for the forces in the struts by applying the static equilibrium equations for each free-body diagram.

The procedure above does not consider ground displacement. Excavations can cause large ground displacements, as discussed before, and should be considered especially for excavations in built-up areas. Numerical methods such as FEM with high-quality soils investigation can make good predictions of wall forces and ground displacements. However, experience is needed in choosing the appropriate soil models, inputting the relevant soil parameters, and considering construction sequencing and environmental conditions.

By restricting $(FS)_{heave}$ to 1.5 and greater, the maximum wall displacement is likely to be less than 0.4% of the excavation depth (H_o). The minimum wall displacement according to the FEM calculations by Karlsrud and Andresen (2008) is 0.2% of H_o . These wall displacements are not universal. They depend also on the structural stiffness of sheeting. The overall factor of safety is

$$FS = \frac{N_c(s_u)_b + 2(s_u)D_t \frac{D_t}{B_{cr}}}{\gamma H_o + q_s} \quad (15.68)$$

where $(s_u)_{D_t}$ is the average undrained shear strength over the depth of the toe penetration, D_t , and B_{cr} is the critical excavation width. The critical width depends on the soil type, wall type, and depth to the firm layer, D_F . If D_F is less than D_s , the firm layer will interfere with the failure mechanism shown in Figure 15.26a. Because B_{cr} has to be found from numerical methods such as FEM, we will assume, for the purposes of this textbook, that $B_{cr} = B$. If the depth to the firm layer, D_F , is less than D_s , we will assume that $B_{cr} = D_F$.

The successful design of excavations requires experience. Many lives have been lost from failure of excavations. An example of a failure in Singapore is briefly described. At about 3:30 p.m. (Singapore time) on April 20, 2004, an open-cut braced tunnel excavation (Figure 15.27) collapsed during the construction of the 33-km-long Circle Line of Singapore's Mass Rapid Transit underground system. Four workers were killed, three were injured, and extensive damage occurred to construction equipment and the main highway (Nicoll Highway) running over the tunnel (http://en.wikipedia.org/wiki/Nicoll_HighwayCollapse). Investigations indicated that there were one or more technical reasons for the collapse. One of these was the incorrect choice of soil model and incorrect soil input parameters in an FEM program (Negro et al., 2009). The Mohr–Coulomb failure criterion was used to model the soft, normally consolidated marine clay present at the site. The Mohr–Coulomb failure criterion (Chapter 10) is a limiting stress criterion and is more appropriate for stiff, overconsolidated clays. The input undrained shear strength used in the model was about 60% higher than expected for the soft, normally consolidated marine clay. The result was an underestimation of the ground displacements and overestimation of the

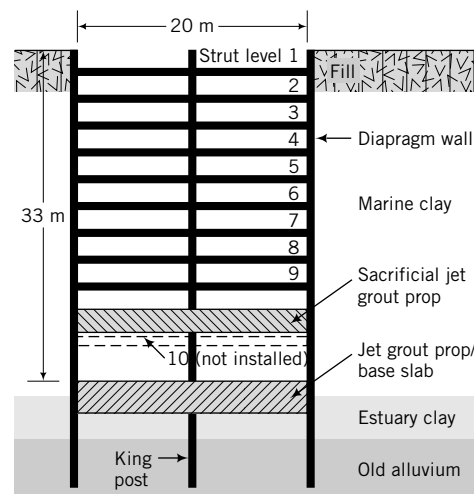


FIGURE 15.27 Typical cross section of the braced excavation as designed. (Negro et al., 2009.)

soil strength. The design loads on the struts were then lower than the actual loads. The contractor allegedly failed to heed warnings from ground displacement monitoring instruments.

Some of the lessons from this failure are:

1. High-quality soil investigations, correct interpretation of the data, high-quality instrumentation, vigilant monitoring, communication, and experience are required to reduce the risk of failures.
2. Numerical analyses are powerful tools, but you must know the basis of these analyses and their limitations, and the fundamentals of the soil models and their limitations. Experience with using these methods, correct choice of soil models, and proper input parameters are essential for the successful use of numerical methods.
3. Ground displacements, soil strength, and loaded structural elements are inclusive. It is not one or the other but all that must be considered in a holistic approach. In the methods we have discussed in this chapter, only soil strength and loaded structural elements are considered. More advanced knowledge is required to consider ground displacements.
4. Temporary works, e.g., excavation, must not be treated lightly. They deserve at least the same weight as, or, in many cases, more weight than the permanent works.

The CSM (Chapter 11) is a good choice for soft, normally consolidated clays. It is good practice to investigate the predictions from various soil models in FEM codes to establish a range of responses and to alert you to any unusual situation.

EXAMPLE 15.8 Braced Excavation

Determine the forces on the struts for the square, braced excavation in a soft, normally consolidated clay, as shown in Figure E15.8a. Assume the water level in the excavation will be maintained at the same elevation as the current groundwater table.

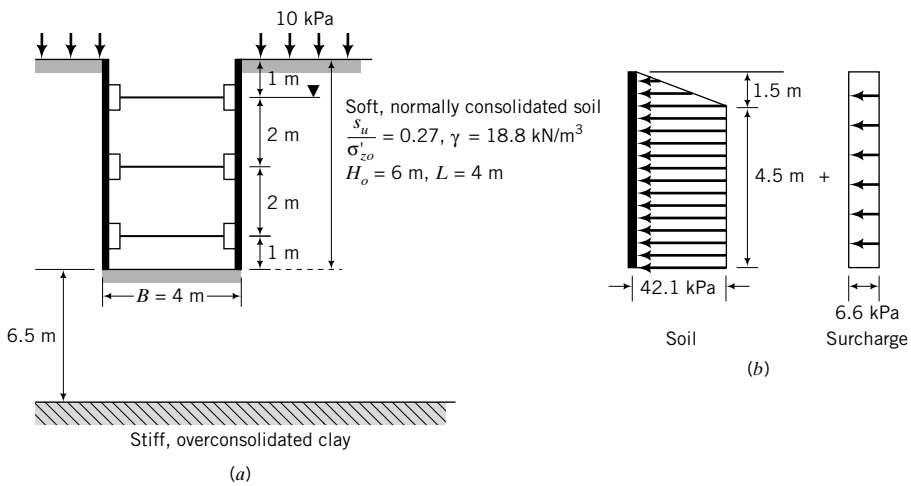


FIGURE E15.8a, b

Strategy You need to determine the approximate lateral stress distribution by calculating $\gamma H_o / s_u$. To find the forces on the struts, draw free-body diagrams—one at each level—and use statics.

Solution 15.8

Step 1: Identify given parameters.

$$B = 4 \text{ m}, H_o = 6 \text{ m}, L = 4 \text{ m}; \frac{H_o}{B} = \frac{6}{4} = 1.5, \frac{B}{L} = \frac{4}{4} = 1$$

Thickness of firm layer, $D_F = 6.5$ m.

Thickness of failure surface, $D_s = \frac{B}{\sqrt{2}} = 2.83$ m.

Therefore, $D_s < D_F$.

$$\frac{s_u}{\sigma'_{zo}} = 0.27, \quad q_s = 10 \text{ kPa}$$

Assume a toe penetration 1.0 m below the bottom of the excavation.

Step 2: Calculate s_u .

Depth	σ_{zo} (kPa)	u (kPa)	σ'_{zo} (kPa)	s_u (kPa)
$\frac{H_o}{3} = \frac{6}{3} = 2$ m	37.6	9.8	27.8	7.5
Bottom of excavation = 6 m	112.8	49	63.8	17.2
Toe of excavation = 7 m	131.6	58.8	72.8	19.7
Center of toe of excavation and base of failure mechanism = $\frac{7 + (7 + 2.83)}{2} = 8.42$ m	158.3	72.7	85.6	23.1

$$s_u = \frac{7.5 + 17.2}{2} = 12 \text{ kPa}; \quad (s_u)_b = 23.1 \text{ kPa}; \quad \text{Use } 23 \text{ kPa.}$$

$$\gamma H_o = 112.8 \text{ kPa}; \quad \frac{\gamma H_o}{s_u} = \frac{112.8}{12} = 9.4 > 4; \quad \text{Use lateral stress distribution given in Figure 15.26d.}$$

$$\gamma H_o + q_s = 112.8 + 10 = 122.8 \text{ kPa}$$

Step 3: Check for stability against bottom heave.

$$\text{For } \frac{H_o}{B} = 1.5 \text{ and } \frac{B}{L} = 1, N_c = 8.2 \quad (\text{Figure 15.26e})$$

$$(\text{FS})_{\text{heave}} = \frac{N_c(s_u)_b}{\gamma H_o + q_s} = \frac{8.2 \times 23}{122.8} = 1.54 > 1.5$$

The toe penetration is satisfactory.

Step 4: Determine the lateral pressure diagram.

$$\frac{\gamma H_o + q_s}{(s_u)_b} = \frac{122.8}{23} = 5.34 > 5.14$$

$$\begin{aligned} K_A &= \left(1 - \frac{4s_u}{\gamma H_o + q_s}\right) + \frac{2\sqrt{2}D_s}{H_o} \left[1 - \frac{5.14(s_u)_b}{\gamma H_o + q_s}\right] \\ &= \left(1 - \frac{4 \times 12}{122.8}\right) + \frac{2\sqrt{2} \times 2.83}{6} \left[1 - \frac{5.14 \times 23}{122.8}\right] \\ &= 0.609 + 0.05 = 0.659. \quad \text{Use } K_A = 0.66. \end{aligned}$$

Since the water levels inside and outside the excavation are equal, we will use the effective stress to calculate the lateral earth pressure.

$$\gamma' = 18.8 - 9.8 = 9 \text{ kN/m}^3$$

$$\text{Soil: } K_A \gamma H_o = K_A [\gamma \times 1 + \gamma'(6 - 1)] = 0.66[18.8 \times 1 + 9 \times 5] = 42.1 \text{ kPa}$$

$$\text{Surcharge: } K_A q_s = 0.66 \times 10 = 6.6 \text{ kPa}$$

Step 5: Calculate the forces on the struts at each level.

All loads are per m length.

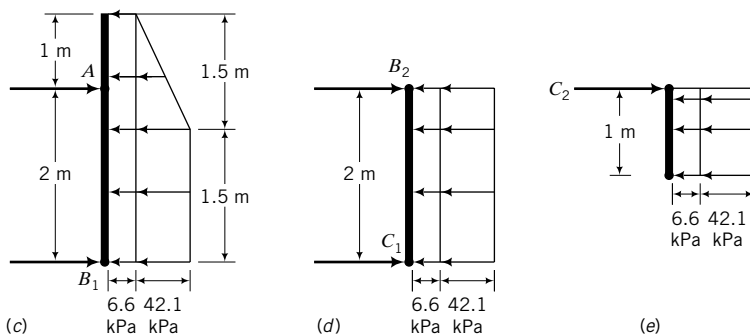


FIGURE E15.8c, d, e

Level 1 (Figure E15.8c)

$$\Sigma M_{B_1} = 2A - \left[\left(6.6 \times 3 \times \frac{3}{2} \right) + 42.1 \times \frac{1.5}{2} \times \left(1.5 + \frac{1.5}{3} \right) + 42.1 \times 1.5 \times \frac{1.5}{2} \right] = 0$$

$$2A = 140 \text{ kN/m}$$

$$A = 70 \text{ kN/m}$$

$$\Sigma F_x = 0$$

$$A + B_1 = (6.6 \times 3) + \left(42.1 \times \frac{1.5}{2} \right) + (42.1 \times 1.5)$$

$$B_1 = 114.5 - 70 = 44.5 \text{ kN/m}$$

Level 2 (Figure E15.8d)

$$B_2 = C_1 = (6.6 + 42.1) \times \frac{2}{2} = 48.7 \text{ kN/m}$$

Level 3 (Figure E15.8e)

Assume cantilever action.

$$C_2 = (6.6 + 42.1) \times 1 = 48.7 \text{ kN/m}$$

Step 6: Calculate resultant forces on struts.

$$A = 70 \text{ kN/m}$$

$$B = B_1 + B_2 = 44.5 + 48.7 = 93.2 \text{ kN/m}$$

$$C = C_1 + C_2 = 48.7 + 48.7 = 97.4 \text{ kN/m}$$

What's next . . . Soils reinforced by metal strips or geotextiles have become popular earth-retaining structures because they are generally more economical than gravity retaining walls. These walls are called mechanical stabilized earth (MSE) walls. A brief introduction to MSE walls is presented next.

15.12 MECHANICAL STABILIZED EARTH WALLS

Mechanical stabilized earth (MSE) walls (Figure 15.28a) are used for a variety of retaining structures. Metal strips (Figure 15.28b), geotextiles (Figure 15.28c), or geogrids (Figure 15.28d) reinforce the soil mass. Other names used are geosynthetics and geocomposites. Geotextile is any permeable textile material used in geotechnical applications. Geosynthetics are polymeric, planar materials (polypropylene, polyethylene, polyester, polyamide, and nylon). Geocomposite is a product made from a combination of geosynthetics. A geogrid is a polymeric product formed by joining intersecting ribs.

Geotextiles are manufactured from filaments and yarns that are combined to form planar products called fabrics. In geotechnical applications, nonwoven and woven facrics are popular. Nonwoven geotextiles are manufactured from continuous filaments formed by extruding polymers through spinnerets or staple fibers (2 cm to 10 cm of filaments). Woven geotextiles are made from yarns knitted using various weave patterns such as plain, twill, satin, or various combinations of these.

The American Society for Testing and Materials (ASTM) has a number of standard tests to determine the physical and mechanical properties of geotextiles. For retaining walls, the key properties are tensile strength, creep, and durability. The ASTM tests for tensile strength and creep are:

1. Grab tensile strength test (ASTM D 4632). This test gives the ultimate tensile load (N) of the geotextile.
2. Wide-width tensile test (ASTM D 4595). This test gives the load per unit width (N/m) of geotextile. You can also obtain the wide-width modulus from this test.
3. Tensile creep test (ASTM D 5262). This test gives the percentage of the ultimate tensile load at which the rate of creep strain approaches zero with time.

Geotextiles suffer strength reduction from ultraviolet light degradation. Consequently, during construction it is essential not to expose the geotextile unduly to sunlight. Specifications normally limit the exposure time to less than 14 days.

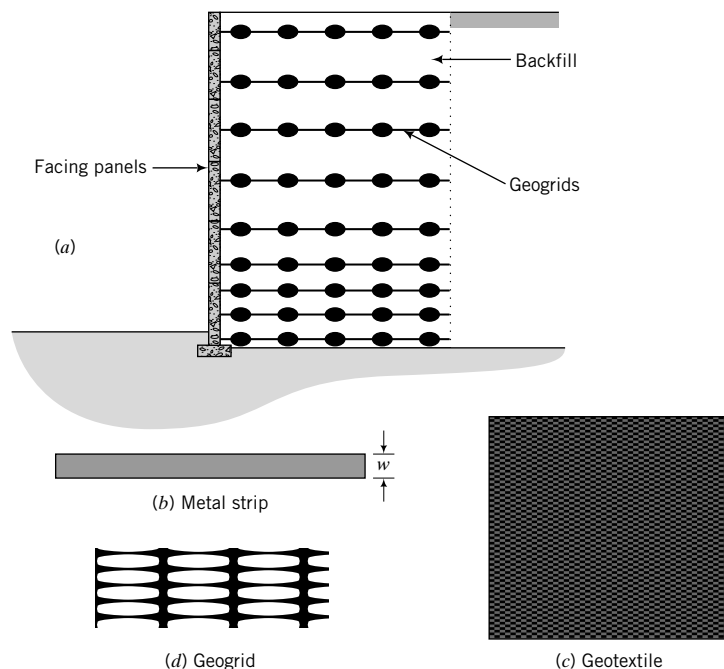


FIGURE 15.28 (a) A geogrid reinforced wall, (b) metal strip, (c) geotextile, and (d) geogrid.

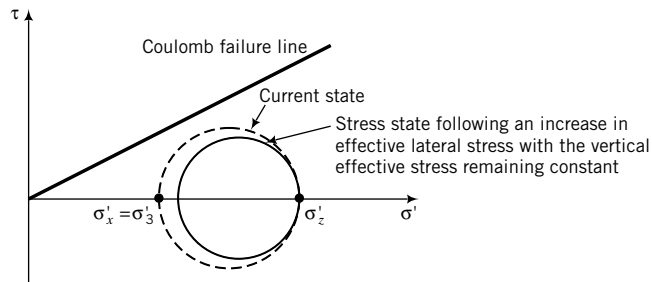


FIGURE 15.29 Effects of increasing the lateral soil resistance by reinforcement.

MSE walls are generally more economical than gravity walls. The basic mechanics of MSE walls is described in the next section.

15.15.1 Basic Concepts

You should recall from Chapter 7 that if a load is applied to a soil mass under axisymmetric undrained condition, the lateral strain (ε_3) is one-half the axial strain (ε_1), as expressed by Equation (10.48). If the undrained restriction is lifted, then you can expect lateral strains greater than one-half the vertical strains. If we were to install strips of metal in the lateral directions of the soil mass, then the friction at the interfaces of the metal strips and the soil would restrain lateral displacements. The net effect is the imposition of a lateral resistance on the soil mass that causes Mohr's circle to move away from the failure line (Figure 15.29). The lateral force imposed on the soil depends on the interface friction value between the reinforcing element and the soil mass and the vertical effective stress. For a constant interface friction value, the lateral frictional force would increase with depth. The reinforcing material will fail if the lateral stress exceeds its tensile strength.

The **essential point** in MSE walls is that the reinforcement serves as an internal lateral confinement that allows the soil to mobilize more shearing resistance than without it.

15.15.2 Stability of Mechanical Stabilized Earth Walls

There are two sets of stability criteria to be satisfied for MSE walls. One is the internal stability; the other is the external stability. The external stability of an MSE wall is determined by analogy to a gravity retaining wall with a vertical face, *FG*, as illustrated in Figure 15.30. The internal stability depends on the tensile strength of the reinforcing material and the slip at the interface of the reinforcing material and the soil. Tensile failure of the reinforcing material at any depth leads to progressive collapse of the wall, while slip at the interface of the reinforcing material and the soil mass leads to redistribution of stresses and progressive deformation of the wall.

Two methods of analysis are used to determine the internal stability. One method is based on an analogy with anchored flexible retaining walls and is generally used for reinforcing material with high extensibility, for example, polymers such as geotextiles and geogrids. The Rankine active earth pressure theory is used with the active slip plane inclined at $\theta_a = 45^\circ + \phi'_{cs}/2$ to the horizontal, as shown in Figure 15.30. The frictional resistance develops over an effective length, L_e , outside the active slip or failure zone. At a depth z , the frictional resistance developed on both surfaces of the reinforcing material (Figure 15.30) is

$$P_r = 2wL_e(\sigma'_z + q_s)\tan\phi_i \quad (15.69)$$

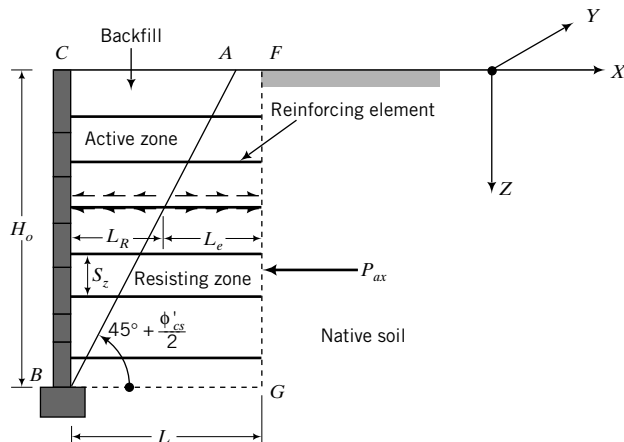


FIGURE 15.30 MSE wall using Rankine's method.

where w is the width of the reinforcing material, σ'_z is the vertical effective stress, q_s is the surcharge, and ϕ_i is the friction angle at the soil–reinforcement interface. Consider a layer of reinforcement at a depth z . The tensile force is

$$T = K_{aR}(\sigma'_z + q_s)S_z S_y \quad (15.70)$$

where S_z and S_y are the spacing in the Z and Y directions and T is the tensile force per unit length of wall. For geotextiles or geogrids, you would normally consider one unit length of wall and one unit width, so $S_y = 1$ and $w = 1$.

By setting $T = P_r$, we can find the effective length of the reinforcement required for limit equilibrium (factor of safety = 1). To find the design effective length, a factor of safety (FS)_t is applied on the tensile force, T , and by solving for L_e from Equations (15.69) and (15.70), we get

$$L_e = \frac{K_{aR}(\sigma'_z + q_s)S_z S_y (FS)_t}{2w(\sigma'_z + q_s)\tan\phi_i} = \frac{K_{aR}S_z S_y (FS)_t}{2w\tan\phi_i} \quad (15.71)$$

where $(FS)_t$ ranges from 1.3 to 1.5.

The total length of reinforcement is

$$L = L_e + L_R \quad (15.72)$$

where L_R is the length of reinforcement within the active failure zone.

Because L_R is zero at the base of the wall, the calculated length of reinforcement at the base is often the shortest. This calculated length, while adequate for internal stability, is often inadequate for translation or bearing capacity (external stability). You should check whether the calculated length of reinforcement at the base is adequate for translation or bearing capacity, as follows:

1. Calculate the maximum lateral active earth force, P_{ax} .

$$P_{ax} = \frac{1}{2}K_{aC}\gamma H_o^2 \cos\delta + K_{aC}q_s H_o \cos\delta = H_o K_{aC} \cos\delta(0.5\gamma H_o + q_s)$$

where K_{aC} is the active lateral pressure coefficient using Coulomb's method with wall friction. The friction angle to use is $\phi' = (\phi'_{cs})_{backfill}$ and the wall friction is $\delta \approx \frac{2}{3}(\phi'_{cs})_{native\ soil}$ to $(\phi'_{cs})_{native\ soil}$. Coulomb's method is used because the interface between the reinforced backfill soil and the native soil (FG , Figure 15.30) is frictional. If the interface friction is neglected, then you can use K_{aR} instead of K_{aC} .

2. Calculate the length of reinforcement required for translation. For short-term loading in clays, the base resistance is $T = L_b s_w$, where L_b is the length of reinforcement at the base and s_w is the adhesion stress. By analogy with sheet pile retaining walls, we will use $s_w = 0.5s_u$ (maximum $s_w = 50$ kPa). For external stability against translation, $T = P_{ax}(\text{FS})_T$, where $(\text{FS})_T$ is a factor of safety against translation; usual range 1.5–3.0. The required length at the base against translation for short-term loading in clays is then

$$L_b = \frac{P_{ax}(\text{FS})_T}{s_w} \quad (15.73)$$

For long-term loading, $T = \sum_{i=1}^n W_i \tan \phi'_b$, where W_i is the weight of soil layer i , n is the number of layers, and ϕ'_b is the effective interfacial friction angle between the reinforcement and the soil at the base. Assuming a uniform soil unit weight throughout the height of the wall, then

$$T = \gamma H_o L_b \tan \phi'_b$$

The length of reinforcement at the base required to prevent translation under long-term loading is

$$L_b = \frac{P_{ax}(\text{FS})_T}{\gamma H_o \tan \phi'_b} = \frac{(K_{aC})_x H_o (0.5\gamma H_o + q_s)}{\gamma H_o \tan \phi'_b} = \frac{(K_{aC})_x (0.5H_o + q_s/\gamma)(\text{FS})_T}{\tan \phi'_b} \quad (15.74)$$

where $(K_{aC})_x$ is the horizontal component of Coulomb's active lateral earth pressure coefficient. You should use the larger value of L_b obtained from Equations (15.73) and (15.74).

The procedure for analysis of a reinforced soil wall using polymeric materials is as follows:

1. Calculate the allowable tensile strength per unit width of the reinforcing polymeric material.

$$T_{all} = T_{ult} \frac{1}{(\text{FS})_{ID} \times (\text{FS})_{CR} \times (\text{FS})_{CD} \times (\text{FS})_{BD}} \quad (15.75)$$

where T_{all} is the allowable tensile strength, T_{ult} is the ultimate tensile strength, FS is a factor of safety, and the subscripts have the following meaning:

- ID—installation damage
- CR—creep
- CD—chemical degradation
- BD—biological degradation

Typical values of the various factors of safety are shown in Table 15.2.

2. Calculate the vertical spacing at different wall heights.

$$S_z = \frac{T_{all}}{K_{aR}(\sigma'_z + q_s)(\text{FS})_{sp}} \quad (15.76)$$

TABLE 15.2 Typical Ranges of Factor of Safety

Factor of safety	Range
$(\text{FS})_{ID}$	1.1 to 2.0
$(\text{FS})_{CR}$	2.0 to 4.0
$(\text{FS})_{CD}$	1.0 to 1.5
$(\text{FS})_{BD}$	1.0 to 1.3

where $(FS)_{sp}$ is a factor of safety between 1.3 and 1.5. It is customary to calculate the minimum vertical spacing using $\sigma'_z = \gamma' H_o$ and then check the vertical spacing required at $H_o/3$ and $2H_o/3$. For practical reasons, the vertical spacing either is kept at a constant value or varies by not more than three different values along the height.

3. Determine the length of reinforcement required at the base for external stability from Equations (15.73) and (15.74).
4. Determine the total length of reinforcement at different levels.

$$L = L_e + L_R$$

where

$$L_R = (H_o - z) \tan\left(45^\circ - \frac{\Phi'_{cs}}{2}\right) \quad (15.77)$$

5. Determine the external stability (translation and bearing capacity). Remember that translation is already satisfied from item 3 above. Overturning is not crucial in MSE walls because these walls are flexible and cannot develop moment. However, you can verify that overturning is satisfied if $e < L_b/6$, where e is the eccentricity of the vertical forces.

The other method is the coherent gravity method (Juran and Schlosser, 1978) and is applicable to low extensible reinforcing materials such as metal strips. Failure is assumed to occur progressively along a path defined by the maximum tensile strains at each level of the reinforcing material. The failure surface is a logarithm spiral that is approximated to a bilinear surface to simplify calculations (Figure 15.31a). The lateral active pressure coefficient is assumed to vary linearly from K_o at the top of the wall to K_{aR} at a depth of 6 m and below (Figure 15.31b).

The variation of lateral stress coefficient with depth (Figure 15.31b) is

$$K = K_{aR} \frac{z}{6} + K_o \left(1 - \frac{z}{6}\right) \quad \text{for } z \leq 6 \quad (15.78)$$

$$K = K_{aR} \quad \text{for } z > 6 \text{ m} \quad (15.79)$$

The length of reinforcement within the failure zone (Figure 15.31a) is

$$L_R = 0.2H_o + \left(0.1H_o - \frac{z}{6}\right) \quad \text{for } z \leq 0.6H_o \quad (15.80)$$

$$L_R = \frac{1}{2}H_o \left(1 - \frac{z}{H_o}\right) \quad \text{for } z > 0.6H_o \quad (15.81)$$

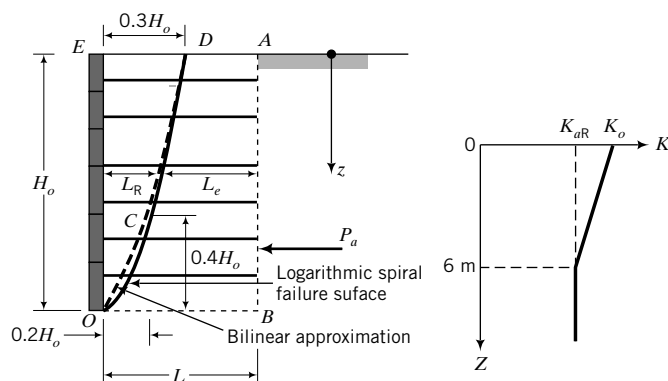


FIGURE 15.31
Coherent gravity method.

(a) Failure surface for the coherent gravity method

(b) Variation of active lateral stress coefficient with depth

The procedure for analyzing an MSE wall using low extensible materials is as follows:

1. Select the spacing of the reinforcement in the Z and Y directions and the width of the reinforcement. Use a manufacturer's catalog to provide information on standard sizes.
2. Calculate the required maximum thickness of the reinforcement.

$$t_r = \frac{K_{aR}(\gamma' H_o + q_s) S_z S_y (\text{FS})_{tr}}{w f_y} \quad (15.82)$$

where K_{aR} is the Rankine active earth pressure coefficient, f_y is the yield stress of the reinforcement, w is the width of the reinforcement, and $(\text{FS})_{tr}$ is a factor of safety, usually 3. The design thickness is the calculated thickness plus a corrosion thickness expected for the design life of the wall.

3. Determine the length of reinforcement required at the base from Equations (15.73) and (15.74).
4. Determine the total length of reinforcement at each level.

$$L = L_e + L_R \quad (15.83)$$

where L_R is given by Equations (15.80) and (15.81) and L_e is determined from Equation (15.71) by using the appropriate value of the active lateral earth pressure coefficient from Equations (15.78) and (15.79).

5. Determine the external stability by assuming the wall is a gravity wall.

EXAMPLE 15.9 Geotextile MSE Wall

Design a 4-m mechanical stabilized earth wall using a geotextile as the reinforcement. The backfill would be a compacted, coarse-grained soil with $\phi'_{cs} = 30^\circ$ and $\gamma_{sat} = 18 \text{ kN/m}^3$. The surcharge is 15 kPa. The geotextile selected has an ultimate wide-width tensile strength of 58.5 kN/m and the soil–geotextile interface friction value is 20° . The native soil is a clay with parameters $\gamma_{sat} = 18.5 \text{ kN/m}^3$, $\phi'_{cs} = 32^\circ$, $\phi'_b = 20^\circ$, and $s_u = 60 \text{ kPa}$.

Strategy Follow the procedure for mechanical stabilized earth walls using a polymeric product.

Solution 15.9

Step 1: Calculate the allowable tensile strength of the geotextile.

From Table 15.2, use $(\text{FS})_{ID} = 1.5$, $(\text{FS})_{CR} = 2$, $(\text{FS})_{CD} = 1.3$, and $(\text{FS})_{BD} = 1.3$.

$$T_{all} = \frac{58.5}{1.5 \times 2 \times 1.3 \times 1.3} = 11.5 \text{ kN/m}$$

Step 2: Calculate the vertical spacing.

$$K_{aR} = \tan^2(45 - \phi'_{cs}/2) = \tan^2(45 - 30/2) = \frac{1}{3}$$

$$\text{Lateral stress due to surcharge: } K_{aR} q_s = \frac{1}{3} \times 15 = 5 \text{ kPa}$$

$$\sigma_x = K_{aR} \sigma'_z + K_{aR} q_s = \frac{1}{3} \gamma' z + 5 = \frac{1}{3} \times 18 \times z + 5 = 6z + 5$$

$$(\sigma_x)_{max} = 6 \times H_o + 5 = 6 \times 4 + 5 = 29 \text{ kPa}$$

From Equation (15.76) with $(FS)_{sp} = 1.3$, we get

$$(S_z)_{min} = \frac{T_{all}}{K_{aR}(\sigma'_z + q_s)(FS)_{sp}} = \frac{11.5}{29 \times 1.3} = 0.305 \text{ m} = 305 \text{ mm}$$

Check spacing requirement at mid-height ($z = 2$):

$$\sigma_x = 6 \times 2 + 5 = 17 \text{ kPa}$$

$$S_z = \frac{11.5}{17 \times 1.3} = 0.520 \text{ m} = 520 \text{ mm}$$

You should try to minimize the number of layers and keep the spacing to easily measurable values. Use $S_z = 250$ mm for the bottom half of the wall and 500 mm for the top half of the wall.

Step 3: Determine the length of reinforcement required at the base for translation.

From Equation (15.16): $K_{aC} = 0.3$, $\delta = 20^\circ$, and $(K_{aC})_x = K_{aC} \cos \delta = 0.3 \times \cos 20 = 0.28$

$$P_{ax} = \frac{1}{2}(K_{aC})_x \gamma H_o^2 + (K_{aC})_x q_s H_o = \left(\frac{1}{2} \times 0.28 \times 18 \times 4^2 \right) + (0.28 \times 15 \times 4) \\ = 57.1 \text{ kN/m}$$

$s_w = 0.5s_u = 0.5 \times 60 = 30 \text{ kPa} < 50 \text{ kPa}$; therefore, use $s_w = 30 \text{ kPa}$

$$\text{Equation (15.73): } L_b = \frac{P_{ax}(FS)_T}{s_w} = \frac{57.1 \times 1.5}{30} = 2.9 \text{ m}$$

$$\text{Equation (15.74): } L_b = \frac{(K_{aC})_x(0.5H_o + q_s/\gamma')(FS)_T}{\tan \phi'_b} \\ = \frac{0.28(0.5 \times 4 + 15/18)1.5}{\tan \left(\frac{2}{3} \times 28 \right)} = 3.5 \text{ m}$$

Use $L_b = 3.5 \text{ m}$.

Step 4: Determine the total length of reinforcement at each level for internal stability.

Use a table to determine the total length, as shown below.

Use $(FS)_t = 1.3$.

z (m)	S_z (m)	$L_R = (H_o - z)$ $\tan(45^\circ - \phi'_{cs}/2)$ (m)	$L_e = \frac{K_{aR}S_z(FS)_t}{2 \tan \phi_i}$ (m)	L (m)
0.50	0.50	2.02	0.3	2.3
1.00	0.50	1.73	0.3	2.0
1.50	0.50	1.44	0.3	1.7
2.00	0.50	1.15	0.3	1.5
2.25	0.25	1.01	0.15	1.2
2.50	0.25	0.87	0.15	1.0
2.75	0.25	0.72	0.15	0.9
3.00	0.25	0.58	0.15	0.7
3.25	0.25	0.43	0.15	0.6
3.50	0.25	0.29	0.15	0.4
3.75	0.25	0.14	0.15	0.3
4.00 (bottom)	0.25	0.00	0.15	0.2

Since L_b is greater than the total length required for internal stability at each level, use $L = L_b = 3.5$ m. The total length can be reduced toward the top of the wall, but for construction purposes it is best to use, in most cases, a single length of polymeric product.

Step 5: Check external stability.

Stability against translation is already satisfied in Step 3.

Check the bearing capacity.

$$(\sigma_z)_{max} = \gamma H_o = 18 \times 4 = 72 \text{ kPa}$$

TSA

$$q_u = 5.14 s_u i_c; \quad i_c = 1 \text{ for strip footing}$$

$$q_u = 5.14 \times 60 \times 1 = 308.4 \text{ kPa}$$

$$(\text{FS})_B = \frac{q_{ult}}{(\sigma_z)_{max}} = \frac{308.4}{72} = 4.3 > 3; \quad \text{okay}$$

ESA

Use rough footing because a layer of geotextile is placed at the interface of the wall and foundation.

$$H = P_{ax} = 57.1 \text{ kN}; \quad V_n = \gamma H_o L_b = 18 \times 4 \times 3.5 = 252 \text{ kN}$$

$$\frac{H}{V_n} = \frac{57.1}{252} = 0.23; \quad \omega = \tan^{-1} \frac{H}{V_n} = \tan^{-1}(0.23) = 13^\circ$$

$$n = \left(2 + \frac{B'}{L'} \right) / \left(1 + \frac{B'}{L'} \right) = 2; \quad i_\gamma = \left(1 - \frac{H}{V_n} \right)^{n+1} = (1 - 0.23)^{2+1} = 0.46$$

$$N_\gamma = 0.1054 \exp(9.6\phi'_p) = 0.1054 \exp\left(9.6 \times 32 \times \frac{\pi}{180}\right) = 22.5$$

$$q_u = 0.5\gamma B N_\gamma i_\gamma = 0.5 \times 18.5 \times 3.5 \times 22.5 \times 0.46 = 335 \text{ kPa}$$

$$(\text{FS})_B = \frac{q_u}{(\sigma_z)_{max}} = \frac{335}{72} = 4.6 > 3; \quad \text{okay}$$

EXAMPLE 15.10 Metal Ties MSE Wall

Design a mechanical stabilized wall 6 m high using metal ties. The backfill is a coarse-grained soil with $\gamma_{sat} = 16.5 \text{ kN/m}^3$ and $\phi'_{cs} = 32^\circ$. Galvanized steel ties are available with a yield strength $f_y = 2.5 \times 10^5 \text{ kPa}$ and a rate of corrosion of 0.025 mm/year. A factor of safety of 3 is desired for a design life of 50 years. The soil-tie interface friction value is 21° . The foundation soil is coarse-grained with parameters $\gamma_{sat} = 18 \text{ kN/m}^3$, $\phi'_p = 35^\circ$, and $\phi'_b = 20^\circ$. The surcharge is 15 kPa.

Strategy You have to guess the spacing of the ties. You can obtain standard widths and properties of ties from manufacturers' catalogs. Follow the procedure for the coherent gravity method.

Solution 15.10

Step 1: Assume spacing and width of ties.

Assume $S_z = 0.5 \text{ m}$, $S_y = 1 \text{ m}$, and $w = 75 \text{ mm}$

Step 2: Calculate required thickness of reinforcement.

$$K_o = 1 - \sin \phi'_{cs} = 1 - \sin 32^\circ = 0.47$$

$$K_{aR} = \tan^2(45 - \phi'_{cs}/2) = \tan^2(45 - 32/2) = 0.31$$

$$t_r = \frac{K_{aR}(\gamma'H_o + q_s)S_zS_y(\text{FS})_{tr}}{w f_y} = \frac{0.31(16.5 \times 6 + 15) \times 0.5 \times 1 \times 3}{0.075 \times 2.5 \times 10^5}$$

$$= 283 \times 10^{-5} \text{ m} = 2.8 \text{ mm}$$

$$t_{\text{corrosion}} = \text{annual corrosion rate} \times \text{design life} = 0.025 \times 50 = 1.25 \text{ mm}$$

$$t_{\text{design}} = \text{calculated thickness} + \text{corrosion thickness} = 2.8 + 1.25 = 4.05 \text{ mm}$$

You will select a tie thickness from standard sizes closest to 4.05 mm. Use $t = 5 \text{ mm}$.

Step 3: Determine the length of reinforcement required at the base.

$$\text{From Equation (15.16): } K_{aC} = 0.28 \quad (\phi'_{cs} = 32, \delta = 20^\circ)$$

$$(K_{aC})_x = K_{aC} \cos \delta = 0.28 \cos 20 = 0.26$$

$$L_b = \frac{(K_{aC})_x(0.5H_o + q_s/\gamma)(\text{FS})_T}{\tan \phi'_b} = \frac{0.26(0.5 \times 6 + 15/16.5)1.5}{\tan 20^\circ} = 4.2 \text{ m}$$

For internal stability, the effective length at the wall base is

$$L_e = \frac{K_{aR}S_zS_y(\text{FS})_t}{2w \tan \phi_i} = \frac{0.31 \times 0.5 \times 1 \times 1.3}{2 \times 0.075 \times \tan 21^\circ} = 3.5 \text{ m} < 4.2 \text{ m}$$

Step 4: Determine the total length of reinforcement.

Use a table, as shown below. $(\text{FS})_t = 1.3$.

z (m)	S_z (m)	K Equation (15.78)	L_e Equation (15.71) (m)	L_r Equation (15.80) (m)	L (m)	Recommended L (m)
0.50	0.50	0.46	5.15	1.72	6.9	7.0
1.00	0.50	0.44	5.00	1.63	6.6	7.0
1.50	0.50	0.43	4.85	1.55	6.4	6.5
2.00	0.50	0.42	4.69	1.47	6.2	6.5
2.50	0.50	0.40	4.54	1.38	5.9	6.5
3.00	0.50	0.39	4.39	1.30	5.7	6.5
3.50	0.50	0.38	4.23	1.22	5.5	6.5
4.00	0.50	0.36	4.08	1.00	5.1	6.5
4.50	0.50	0.35	3.93	0.75	4.7	5.0
5.00	0.50	0.33	3.77	0.50	4.3	5.0
5.50	0.50	0.32	3.62	0.25	3.9	5.0
6.00	0.50	0.31	3.47	0.00	3.5	5.0

Step 5: Check for external stability.

Translation is satisfied because L used at the base is greater than L_b .

Check bearing capacity.

$$(\sigma_z)_{\max} = \gamma H_o = 16.5 \times 6 = 99 \text{ kPa}$$

$$H = 0.5\gamma K_{(aC)x} H_o^2 + K_{(aC)x} H_o q_s = 0.5 \times 16.5 \times 0.26 \times 6^2 + 0.26 \times 6 \times 15 = 100.6 \text{ kN}$$

$$V_n = \gamma H_o L_b = 16.5 \times 6 \times 4.2 = 415.8 \text{ kN}; \quad \frac{H}{V_n} = \frac{100.6}{415.8} = 0.24; \quad \omega = \tan^{-1} \frac{H}{V_n} = \tan^{-1}(0.24) = 13.5^\circ$$

$$n = \left(2 + \frac{B'}{L'}\right) / \left(1 + \frac{B'}{L'}\right) = 2; \quad i_\gamma = \left(1 - \frac{H}{V_n}\right) = (1 - 0.24)^{2+1} = 0.44$$

$$N_\gamma = 0.1054 \exp(9.6 \phi'_p) = 0.1054 \exp\left(9.6 \times 35 \times \frac{\pi}{180}\right) = 37.2$$

$$q_u = 0.5\gamma B N_\gamma i_\gamma = 0.5 \times 18 \times 4.2 \times 37.2 \times 0.44 = 618.7 \text{ kPa}$$

$$(FS)_B = \frac{q_u}{(\sigma_z)_{max}} = \frac{618.7}{99} = 6.2 > 3; \quad \text{okay}$$

15.13 OTHER TYPES OF RETAINING WALLS

There are a variety of retaining walls that are now used in geotechnical and other applications (e.g., landscaping). Some of these are listed below.

15.13.1 Modular Gravity Walls

Modular gravity walls consist of a structural container filled with materials of various types. These walls are used in projects such as highways, dikes, and channels that conventionally utilize cast-in-place concrete gravity walls. The design method is discussed in Section 15.9. Examples of modular gravity walls are:

- *Gabion baskets.* Gabion basket walls consist of prefabricated steel wire or polypropylene or polyethylene or nylon baskets filled with rocks and stacked horizontal and vertically (Figure 15.32). Basket size varies but is normally 2 m in length × 1 m wide × 1 m high. Long baskets exceeding 2 m in length are reinforced with diaphragms to strengthen the baskets for ease of construction. Gabion baskets are suitable for gravity walls where rock fill material is readily available. Common applications are for erosion protection of banks of rivers and streams, and for retaining walls along roads and highways, especially in rugged terrain. Typically the base width is 0.4 to 0.5 m for backfills with $\phi'_{cs} > 30^\circ$, 0.5 to 0.7 m for general types of backfill, and 0.1 to 1 m for backfills with $\phi'_{cs} > 30^\circ$. Gabion baskets are usually inclined at about 6° to 10° from the vertical toward the backfill.
- *Bin walls.* Bin walls are gravity walls in which earth fill is placed in a bin made from metal (steel) or timber or concrete (Figure 15.33). These walls require a small amount of settlement of the vertical corner members. If the foundation is rigid, a compressible cushion of approximately 200 mm of loose fill is placed under the grade plates or concrete base.
- *Precast modular concrete walls.* These walls are constructed by stacking precast blocks made from concrete and other materials. There is a large variety of blocks, the major differences being the material used to make the blocks, size, and interlocking mechanism.



FIGURE 15.32 Gabion basket wall. (Alamy Images.)

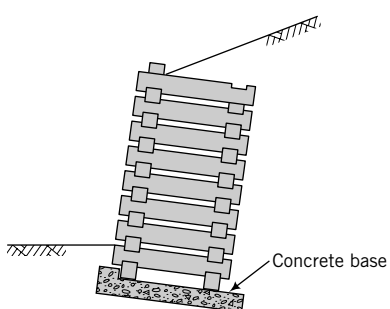


FIGURE 15.33 A crib wall.

15.13.2 In Situ Reinforced Walls

These walls utilize reinforcing elements to form a composite with the soil. The reinforcing elements are nails or small-diameter cast-in-place concrete piles or small-diameter steel pipe piles. One popular in situ reinforced wall is a soil nail wall. Closely spaced nails are installed by drilling inclined holes into the soil and grouting the holes. Shear stresses from the soil are transferred to the nails and are resisted by tensile forces in the nails. The faces of soil nail walls are shotcrete or precast concrete panels or cast-in-place concrete.

15.13.3 Chemically Stabilized Earth Walls (CSE)

CSE walls are in situ soils mixed with chemical grouts such as lime or lime-cement mixtures to form columns of overlapping soils. Sometimes reinforcements are added to the soil-grout mixtures before they harden. CSE walls can retain soils up to great depths. They are also used in seepage control.

15.14 SUMMARY

We have considered lateral earth pressures and their applications to several types of earth-retaining structures in this chapter. Two earth pressure theories are in general use, one developed by Coulomb and the other by Rankine. Coulomb's equations for the lateral earth pressure coefficients are based on limit equilibrium and include the effects of soil–wall friction, wall slope, and backfill slope. Rankine's equations are based on stress states of the backfill and do not account for soil–wall friction. The failure planes in the Coulomb and Rankine methods are planar surfaces. Soil–wall friction causes the failure plane to curve, resulting in higher active lateral earth pressure coefficients and lower passive earth pressure coefficients than those found using Coulomb's equations.

Because of the flexibility of some earth-retaining structures and construction methods used in practice, the “real” lateral earth pressures are different from either the Coulomb or Rankine theories. It is suggested in this book that the appropriate value of friction angle to use in the analysis of earth-retaining structures is ϕ'_{cs} . Three methods of analysis for flexible earth-retaining walls were considered. The differences in the methods result mainly from how the lateral stresses are considered and how the factor of safety is applied.

Self-Assessment

Access Chapter 15 at <http://www.wiley.com/college/budhu> to take the end-of-chapter quiz to test your understanding of this chapter.



Practical Examples

EXAMPLE 15.11 Cantilever Gravity Walls for Material Storage

Ore from a manufacturing plant is to be stored between two cantilever gravity retaining walls, as shown in Figure E15.11a. A gantry crane will run on top of the walls to place the ore. The crane will apply a maximum vertical load of 24 kN and a horizontal load of ± 4.5 kN on each wall. The base of the ore pile is only permitted to come within 0.5 m of the top of the walls. The ore surface should be the maximum admissible slope. The walls will be restrained from spreading outward by steel ties or rods at 1-m centers anchored to the base slab. A 2-m layer of the ore spoils of similar characteristics to the ore to be stored would be compacted to support the base of the wall. Determine (a) the stability of the wall for the geometry shown in Figure E15.11a and (b) the force in the tie rods, assuming they resist all the horizontal loads. If the tie rods were not present, would the walls be safe? Do you expect any alignment problems with the gantry crane?

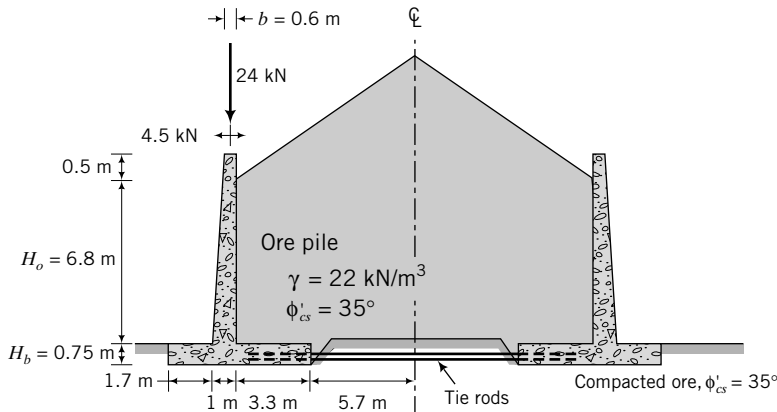


FIGURE E15.11a

Strategy The maximum slope angle would be the friction angle. Since the storage is symmetrical, each wall will carry identical loads. You will have to make an assumption regarding wall friction. You can assume $\delta = \frac{1}{2} \phi'_{cs}$ or $\delta = \frac{2}{3} \phi'_{cs}$ and use Coulomb's method to determine the lateral forces.

Solution 15.11

Step 1: Determine the lateral forces.

The maximum admissible slope is $\beta = \phi'_{cs}$. Therefore, $\beta = 35^\circ$.

$$H_o = 0.75 + 6.8 + 3.3 \tan 35^\circ = 9.86 \text{ m}$$

$$\text{From Equation (15.16): } K_{aC} = 0.7 \quad \text{for } \beta = 35^\circ, \phi' = 35^\circ, \delta = \frac{1}{2} \phi'$$

$$P_a = \frac{1}{2} K_{aC} \gamma H_o^2 = \frac{1}{2} \times 0.7 \times 22 \times 9.86^2 = 748.6 \text{ kN/m}$$

$$P_{ax} = P_a \cos \delta = 748.6 \times \cos 17.5^\circ = 714.0 \text{ kN/m}$$

$$P_{az} = P_a \sin \delta = 748.6 \times \sin 17.5^\circ = 225.1 \text{ kN/m}$$

Step 2: Calculate forces and moments. Draw a diagram (show only one-half because of symmetry; see Figure E15.11b) and use a table to do the calculations.

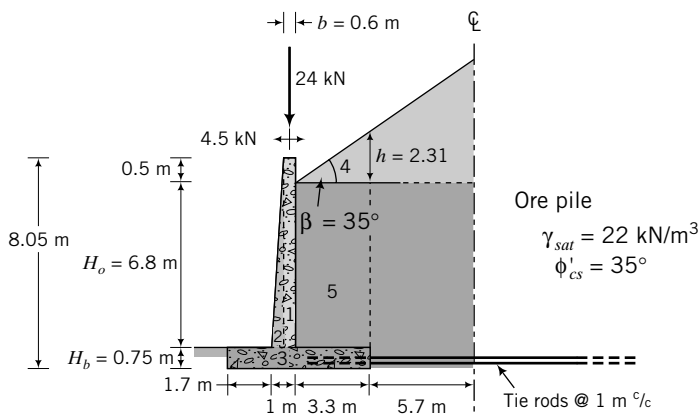


FIGURE E15.11b

Part	Force (kN/m)	Moment arm from 0 (m)	Moment (kN.m)
<i>Wall</i>			
1	<i>Vertical forces</i> $(6.8 + 0.5) \times 0.6 \times 24 = 105.1$	$1.7 + 0.4 + 0.6/2 = 2.4$	+252.2
2	$\frac{1}{2}(6.8 + 0.5) \times 0.4 \times 24 = 35$	$1.7 + \frac{2}{3} \times 0.4 = 1.97$	69.0
3	$0.75 \times 6 \times 24 = 108.0$	$6/2 = 3.00$	+324.0
<i>Soil</i>			
4	$\frac{1}{2} \times 3.3 \times 2.31 \times 22 = 83.9$	$1.7 + 1 + (\frac{2}{3} \times 3.3) = 4.9$	+411.1
5	$3.3 \times 6.8 + 22 = 493.7$	$1.7 + 1 + 3.3/2 = 4.35$	+2147.6
P_{az}	225.1		6
<i>Gantry</i>			
P_z	24	2.4	+57.6
$R_z = \Sigma \text{ Vertical forces} = 1074.8$			
<i>Gantry</i>			
P_x	<i>Lateral forces</i> 4.5	$0.75 + 6.8 + 0.5 = 8.05$	-36.2
<i>Soil</i>			
P_{ax}	714	$9.87/3 = 3.29$	-2349.1
$R_x = \Sigma \text{ Lateral forces} = 718.5$			
$M = \Sigma \text{ Moments} = 2226.8$			

Step 3: Determine stability.

Rotation

$$\bar{x} = \frac{M}{R_z} = \frac{2226.8}{1074.8} = 2.07 \text{ m}$$

$$e = \frac{B}{2} - \bar{x} = \frac{6}{2} - 2.07 = 0.93 \text{ m}$$

$$\frac{B}{6} = \frac{6}{6} = 1 \text{ m}; \quad e < \frac{B}{6}; \quad \text{therefore, wall is safe against rotation}$$

Sliding

$$T = \text{sliding resistance at base} = R_z \tan \phi'_b = 1074.8 \tan 20^\circ = 391.2 \text{ kN}$$

$$(\text{FS})_T = \frac{T}{R_x} = \frac{391.2}{718.5} = 0.54 < 1.5$$

∴ Sliding would occur if tie rods were not present.

Forces on tie rods

$$\text{For } (\text{FS})_T = 1.5: \quad T_a + T = 1.5R_x$$

where T_a is the force on the tie rods/unit length of wall.

$$T_a = 1.5 \times 718.5 - 391.2 = 686.6 \text{ kN/m}$$

Bearing capacity

All horizontal forces are accommodated by tie rods.

$$B' = B - 2e = 6 - 2 \times 0.93 = 4.14 \text{ m}$$

$$V_n = 1074.8 \text{ kN}$$

$$N_y = 0.1054 \exp(9.6\phi'_p) = 0.1054 \exp\left(9.6 \times 35 \times \frac{\pi}{180}\right) = 37.2$$

$$q_u = 0.5\gamma B' N_\gamma = 0.5 \times 18 \times 4.14 \times 37.2 = 1386.1 \text{ kPa}$$

$$(\sigma_z)_{max} = \frac{R_z}{B \times 1} \left(1 + \frac{6e}{B}\right) = \frac{1074.8}{6 \times 1} \left(1 + \frac{6 \times 0.93}{6}\right) = 345.7 \text{ kPa}$$

$$(\text{FS})_B = \frac{1386.1}{345.7} = 4 > 3; \text{ therefore, bearing capacity is satisfactory}$$

Summary of Results

1. The wall is unlikely to rotate significantly.
2. Without the tie rods, the wall will translate.
3. The design tie rod force is $\approx 687 \text{ kN/m}$.
4. The soil bearing capacity is adequate.
5. Assuming that the base slab is rigid and the loading is symmetrical, there should be no alignment problem.

EXAMPLE 15.12 Flexible Wall Near a Lake

A retaining wall is required near a man-made lake in a housing scheme development. The site is a swamp, and the topsoil, consisting mainly of organic material, will be removed up to the elevation of a deep deposit of clay with a silt-and-sand mixture. The wall is expected to retain a sand backfill of height 6 m. It is anticipated that a rapid drawdown condition could occur and the lake could be emptied for a long period. A flexible retaining wall is proposed, as shown in Figure E15.12a. Determine the embedment depth and the force for an anchor spacing of 3 m. A surcharge of 10 kPa should be considered.

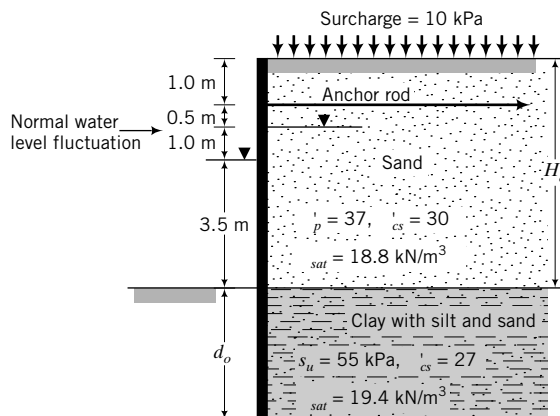


FIGURE E15.12a

Strategy You can use either the FSM or NPPM or both. Because the clay layer has silt and sand, you should consider seepage forces for long-term conditions (assuming that the drawdown level would remain for some time).

Solution 15.12

Step 1: Determine the lateral earth pressure coefficients.

Use NPPM.

Assume a worst-case scenario, that is, $\delta = s_w = 0$.

$$\text{Sand: } K_{ax} = \frac{1}{3} \quad (\phi'_{cs} = 30^\circ, \delta = 0)$$

$$\text{Clay: } K_{ax} = 0.38 \quad (\phi'_{cs} = 27^\circ, \delta = 0)$$

Use Appendix D to find the passive lateral earth pressure coefficient for the clay.

$$K_{px} = 2.9 \quad (\phi'_{cs} = 27^\circ, \delta = 0)$$

Step 2: Determine the seepage forces and porewater pressures.

$$\text{Sand: } \gamma' = 18.8 - 9.8 = 9 \text{ kN/m}^3$$

$$\text{Clay: } \gamma' = 19.4 - 9.8 = 9.6 \text{ kN/m}^3$$

$$j_s = \frac{a}{a + 2d_o} \gamma_w = \left(\frac{3.5}{3.5 + 2d_o} \right) 9.8 = \frac{34.3}{3.5 + 2d_o} \text{ kN/m}^3$$

Active state

$$\text{Sand: } \gamma'_{aj} = \left(9 + \frac{34.3}{3.5 + 2d_o} \right) = \frac{65.8 + 18d_o}{3.5 + 2d_o}$$

$$\text{Clay: } \gamma'_{aj} = \left(9.6 + \frac{34.3}{3.5 + 2d_o} \right) = \frac{67.9 + 19.2d_o}{3.5 + 2d_o}$$

Passive state

$$\text{Clay: } \gamma'_{jp} = \left(9.6 + \frac{34.3}{3.5 + 2d_o} \right) = \frac{19.2d_o - 0.7}{3.5 + 2d_o}$$

$$u_B = \left(\frac{2ad_o}{a + 2d_o} \right) \gamma_w = \left(\frac{2 \times 3.5d_o}{3.5 + 2d_o} \right) 9.8 = \frac{68.6d_o}{3.5 + 2d_o}$$

$$P_w = \frac{1}{2}(a + d_o)u_B = \frac{1}{2}(3.5 + d_o) \frac{68.6d_o}{3.5 + 2d_o} = \left(\frac{120d_o + 34.3d_o^2}{3.5 + 2d_o} \right)$$

$$\bar{z}_w = \frac{a + 2d_o}{3} = \frac{3.5 + 2d_o}{3}$$

Step 3: Carry out the calculations.

Draw a diagram of the pressure distributions. Use a table or a spreadsheet program to carry out the calculations. See Figure E15.12b for the lateral pressure distributions.

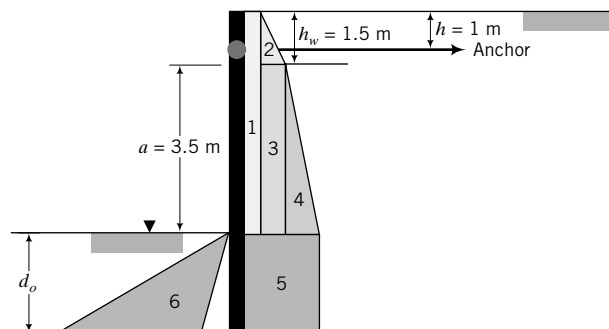


FIGURE E15.12b

See Table E15.12a for the calculations performed using the Excel spreadsheet retwal.xls.

Step 4: Calculate the anchor force.

To calculate the anchor force you must repeat the calculations for the depth of embedment using $(FS)_r = 1$ and then find the anchor force. See Table E15.12b for the calculations.

Design anchor force = 683.7 kN

TABLE E15.12a

Select units		SI					NPPM - Mixed analysis		
q_s	10	kN/m	β	0	deg				
H	6	m	γ'	9	kN/m ³				
ϕ_{cs}	30	deg	j_s	2.0	kN/m ³				
δ_a	0	deg	γ_{aj}	11.0	kN/m ³				
δ_b	0	deg	γ_{pj}	7.0	kN/m ³				
h	1	m	u_c	27.1	kPa				
Depth to water, h_w	1.5	m	P_w	137.7	kN				
γ	18.8	kN/m ³	γ	5.60	m				
a	3.5	m							
Anchor inclination	0	deg							
d_o	6.64	m							
d_{design}	7.97	m							
Clay below excavation									
γ	19.4	kN/m ³	γ'	9.6	kN/m ³				
ϕ_{cs}	27	deg	γ_{aj}	11.6	kN/m ³				
δ'_a	0	deg	γ_{pj}	7.6	kN/m ³				
δ_b	0	deg	s_w	0	kPa				
s_u	55	kPa	s_w	0	kPa				
Drained pressure (kPa)		Force (kN)	Moment arm (m)	Moment (kN.m)					
Part									
1		3.3	20.0	2.00	40.0				
2		9.4	7.0	0.00	0.0				
3		9.4	32.9	2.25	74.0				
4		12.9	22.5	2.83	63.9				
5		25.6	170.2	8.32	1416.3				
Water		27.1	137.7	6.05	832.8				
		Sum	390.4		2427.0				
6		116.2	386.0	9.43	3639.7				
				(FS) _r	1.50				

TABLE E15.12b

Select units		SI					NPPM - Mixed analysis		
q_s	10	kN/m	β	0	deg				
H	6	m	γ'	9	kN/m ³				
ϕ_{cs}	30	deg	j_s	2.5	kN/m ³				
δ_a	0	deg	γ_{aj}	11.5	kN/m ³				
δ_b	0	deg	γ_{pj}	6.5	kN/m ³				
h	1	m	u_c	25.6	kPa				
Depth to water, h_w	1.5	m	P_w	111.4	kN				
γ	18.8	kN/m ³	γ	4.62	m				
a	3.5	m							
Anchor inclination	0	deg							
d_o	5.19	m							
d_{design}	6.22	m							
Drained pressure (kPa)		Force (kN)	Moment arm (m)	Moment (kN.m)					
Part									
1		3.3	20.0	2.00	40.0				
2		9.4	7.0	0.00	0.0				
3		9.4	32.9	2.25	74.0				
4		12.9	22.5	2.83	63.9				
5		25.6	170.2	8.32	1416.3				
Water		27.1	137.7	6.05	832.8				
		Sum	390.4		2427.0				
6		116.2	386.0	9.43	3639.7				
				(FS) _r	1.50				

(continued)

TABLE E15.12b (continued)

Select units	SI	NPPM - Mixed analysis			
Clay below excavation					
γ	19.4	kN/m ³	γ'	9.6	kN/m ³
ϕ'_{cs}	27	deg	γ_{aj}	12.1	kN/m ³
δ_a	0	deg	γ_{pj}	7.1	kN/m ³
δ_b	0	deg	s_w	0	kPa
s_u	55	kPa	s_w	0	kPa
					Active Passive
Part	Drained pressure (kPa)	Force (kN)	Moment arm (m)	Moment (kN.m)	
1	3.3	20.0	2.00	40.0	
2	9.4	7.0	0.00	0.0	
3	9.4	32.9	2.25	74.0	
4	13.4	23.4	2.83	66.4	
5	26.1	135.4	7.59	1028.4	
Water	25.6	111.4	5.56	619.5	
	Sum	330.2		1828.3	
6	83.4	216.2	8.46	1828.7	
				(FS) _r	
				$P_a - P_p$	1.00
					114.0 kN
					683.7 kN
	Horizontal component of anchor force				
	Design anchor force				

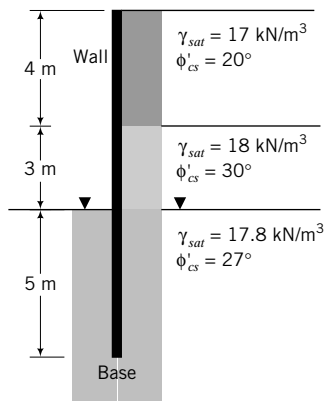
EXERCISES

Theory

- 15.1** Show, using Mohr's circle, that the depth of a tension crack is $z_{cr} = 2s_u/\gamma_{sat}$ for a saturated clay.
- 15.2** Show that a tension crack will not appear in a saturated clay if a surface stress of $q_s \geq 2s_u$ is present.
- 15.3** A trench is to be excavated in a clay soil with $\gamma_{sat} = 20 \text{ kN/m}^3$ and $s_u = 15 \text{ kPa}$.
- Determine the theoretical maximum depth of the trench without lateral support.
 - It was decided to use a bentonite slurry of unit weight γ_f to fill the trench as excavation proceeds. Show that the theoretical maximum depth of the trench is $H_{cr} = \frac{4s_u}{\gamma_{sat} - \gamma_f}$ where γ_{sat} is the saturated unit weight of the soil and s_u is the undrained shear strength.
 - How much deeper can the trench be excavated by using a bentonite slurry of $\gamma_f = 11 \text{ kN/m}^3$?

Problem Solving

- 15.4** Plot the variation of active and passive lateral pressures with depth for the soil profile shown in Figure P15.4.

**FIGURE P15.4**

- 15.5** A retaining wall 8 m high supports a soil of saturated unit weight 18 kN/m^3 , $\phi'_{cs} = 30^\circ$. The backfill is subjected to a surcharge of 15 kPa. Calculate the active force on the wall if (a) the wall is smooth and (b) the wall is rough ($\delta = 20^\circ$). Groundwater is below the base of the wall.
- 15.6** A retaining wall 5 m high was designed to stabilize a slope of 15° . The back of the wall is inclined 10° to the vertical and may be assumed to be rough, with $\delta = 20^\circ$. The soil parameters are $\phi'_{cs} = 30^\circ$ and $\gamma_{sat} = 17.5 \text{ kN/m}^3$.

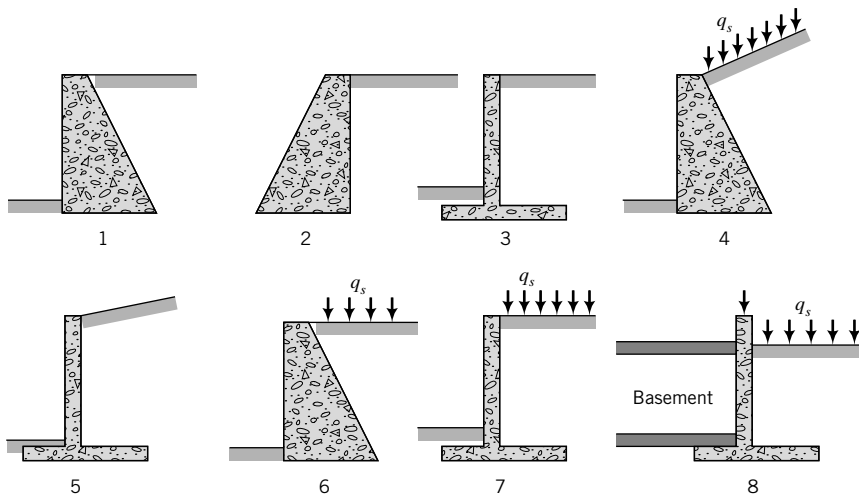


FIGURE P15.7

After a flood, the groundwater level, which is usually below the base of the wall, rose to the surface. Calculate the lateral force on the wall. Neglect seepage effects.

- 15.7** Figure P15.7 above shows rigid walls of height H_o with different geometries. Sketch the distribution of lateral earth pressures on each wall; indicate the location and direction of the resultant lateral force. Show on your diagram what other forces act on the wall, for example, the weight of the wall (W_w) and the weight of the soil (W_s). You should consider two cases of soil–wall friction: (a) $\delta > 0$ and (b) $\delta = 0$.
- 15.8** Which of the two walls in Figure P15.8 gives the larger horizontal force? (Show calculations.)

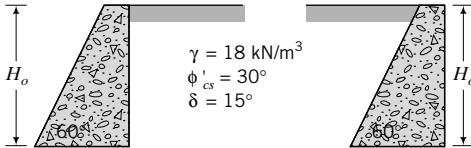


FIGURE P15.8

- 15.9** Determine the stability of the concrete gravity wall shown in Figure P15.9.

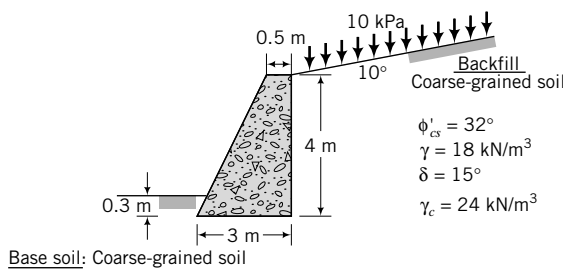


FIGURE P15.9

- 15.10** Determine the stability of the cantilever wall shown in Figure P15.10 and sketch a drainage system to prevent buildup of porewater pressures behind the wall.

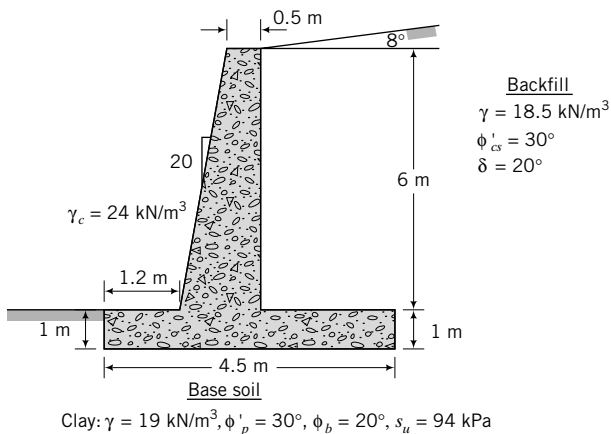


FIGURE P15.10

- 15.11** The drainage system of a cantilever wall shown in Figure P15.11 (on the next page) became blocked after a heavy rainstorm and the groundwater level, which was originally below the base, rose to 1.5 m below the surface. Determine the stability of the wall before and after the rainfall. Neglect seepage effects.

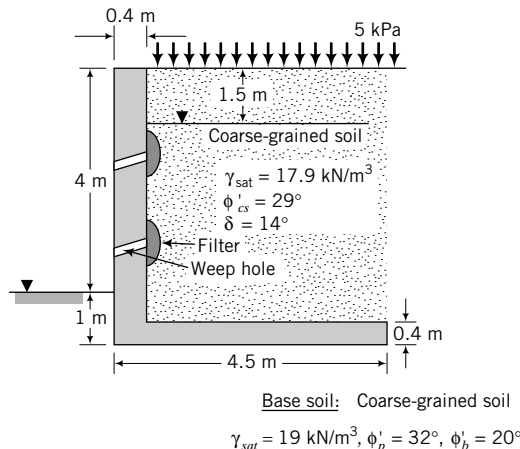


FIGURE P15.11

- 15.12** Determine the embedment depth, d , and maximum bending moment for the cantilever sheet pile wall shown in Figure P15.12. Use the factored strength method (FSM) with $F_\phi = 1.25$.

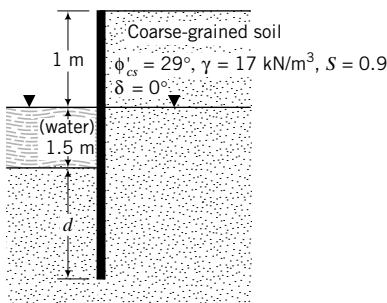


FIGURE P15.12

- 15.13** Determine the embedment depth, d , and maximum bending moment for the cantilever sheet pile wall shown in Figure P15.13 for long-term conditions. Use the FSM with $F_\phi = 1.25$, and the NPPM with $(FS)_r = 1.5$. Compare the results.

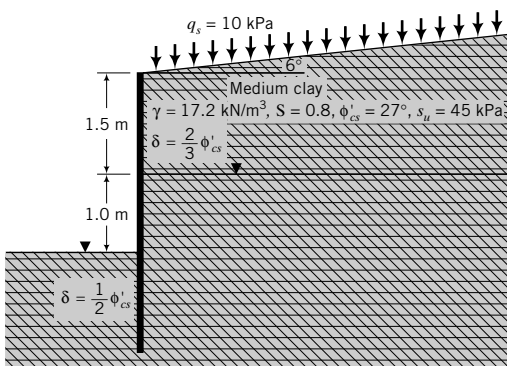


FIGURE P15.13

- 15.14** An anchored sheet pile wall is shown in Figure P15.14. Determine the embedment depth, the maximum bending moment, and the force on the anchor per unit length of wall. Use either FSM ($F_\phi = 1.25$) or the NPPM with $(FS)_r = 1.5$. Assume the soil above the groundwater to be saturated.

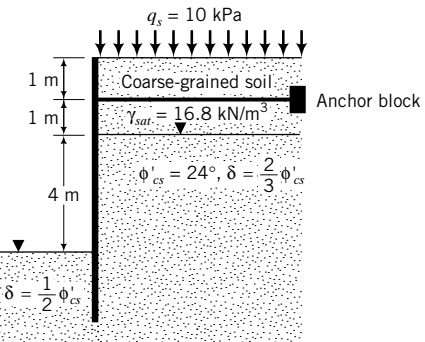


FIGURE P15.14

- 15.15** Determine the embedment depth and the anchor force per unit length of wall for the retaining wall shown in Figure P15.15 using the FMM. Assume the soil above the groundwater to be saturated. Use $FS = 1.5$ to calculate the depth.

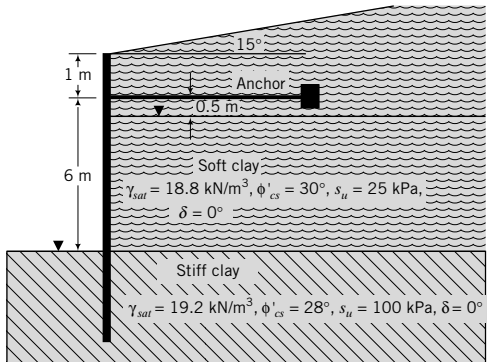


FIGURE P15.15

- 15.16** Calculate the strut loads per meter length for the braced excavation shown in Figure P15.16. The length of the excavation is 10 m.

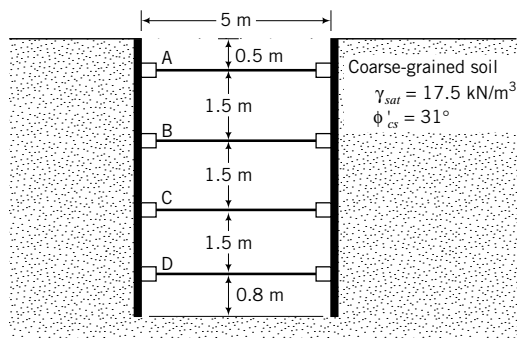


FIGURE P15.16

- 15.17** A braced excavation is required in a soft clay, as shown in Figure P15.17. A stiff clay layer is located 5.9 m from the surface. Determine the load on the struts per meter length and the factor of safety against bottom heave. The length of the excavation is 12 m.

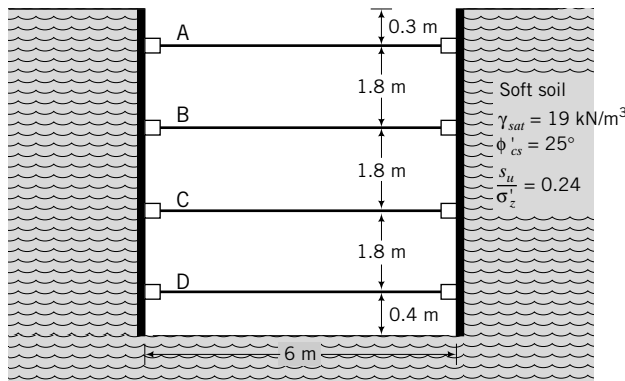


FIGURE P15.17

- 15.18** A 6-m-high geotextile wall is required to support a coarse-grained backfill with $\gamma_{sat} = 17.5 \text{ kN/m}^3$ and $\phi'_{cs} = 29^\circ$. The foundation (base) soil is a clay with $\gamma_{sat} = 18 \text{ kN/m}^3$, $\phi_p = 28^\circ$, $s_u = 72 \text{ kPa}$, and $\phi'_b = 16^\circ$. The ultimate strength of the geotextile is 45 kN/m and the soil-geotextile interface friction angle is 20° . The permanent surcharge is 15 kPa. Determine the spacing and length of geotextile required for stability. Assume $(FS)_{ID} = 1.5$, $(FS)_{CR} = 2$, $(FS)_{CD} = 1.3$, $(FS)_{BD} = 1.3$, $(FS)_{sp} = 1.3$, $(FS)_t = 1.3$, $(FS)_T = 1.5$, and $(FS)_B = 3$.

- 15.19** Redo Exercise using galvanized steel ties 75 mm wide with a yield strength $2.5 \times 10^5 \text{ kPa}$, ties-soil interface friction of 20° , and rate of corrosion of 0.025 mm/yr. The design life is 50 years. Assume $(FS)_{tr} = 3$, $(FS)_T = 1.5$, $(FS)_t = 1.3$, and $(FS)_B = 3$.

Practical

- 15.20** A section of an approach to a bridge is shown in Figure P15.20. The sides of the approach are to be supported

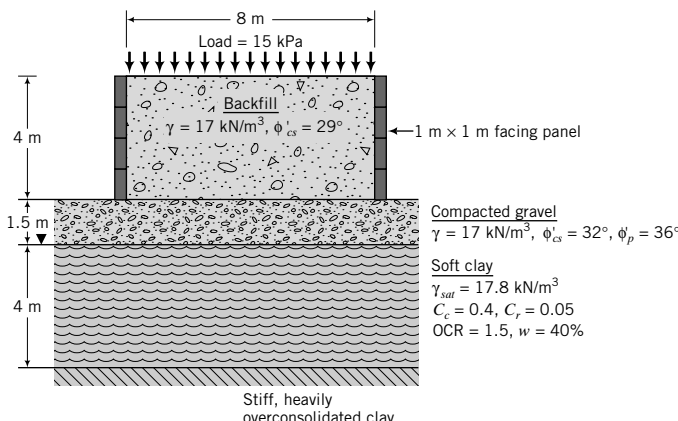


FIGURE P15.20

using MSE walls with $1 \text{ m} \times 1 \text{ m}$ facing panels. Steel ties of width 300 mm are readily available. Determine the length and thickness of the ties required for stability. The design life is 50 years and the rate of corrosion is 0.025 mm/yr . The yield strength is $2.5 \times 10^5 \text{ kPa}$. Assume $(FS)_{tr} = 3$, $(FS)_T = 1.5$, $(FS)_t = 1.3$, and $(FS)_B = 3$.

- 15.21** A cantilever sheet pile wall is required to temporarily support an embankment for an access road, as shown in Figure P15.21. Determine the depth of penetration of the wall into the silty clay soil and the maximum bending moment. Select two methods from FMM, FSM, and NPPM, and compare the results. Groundwater is 10 m below the surface.

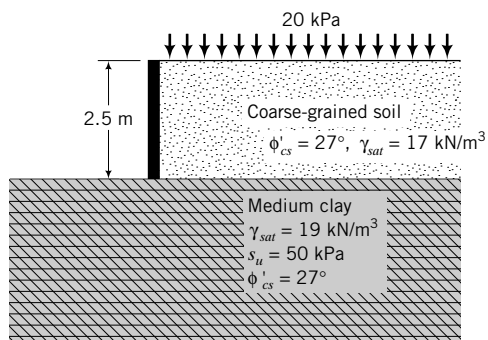


FIGURE P15.21

- 15.22** A cast-in-place (CIP) cantilever wall is required to maintain the grade for a freeway. A preliminary wall dimension is shown in Figure P15.22. Determine the stability of the wall and show how you would provide adequate drainage. Use Rankine's method to calculate the lateral forces. Neglect the passive resistance at the front of the wall.

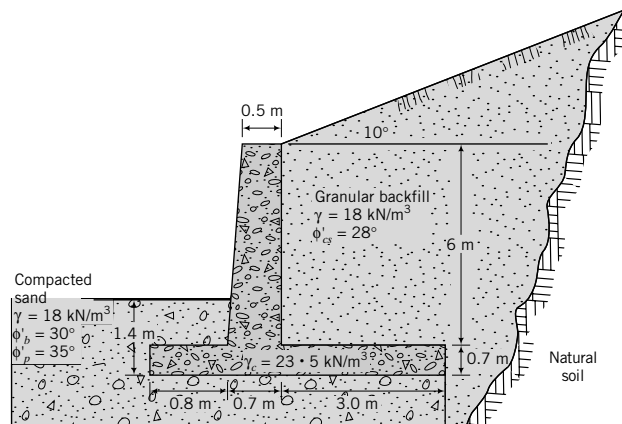
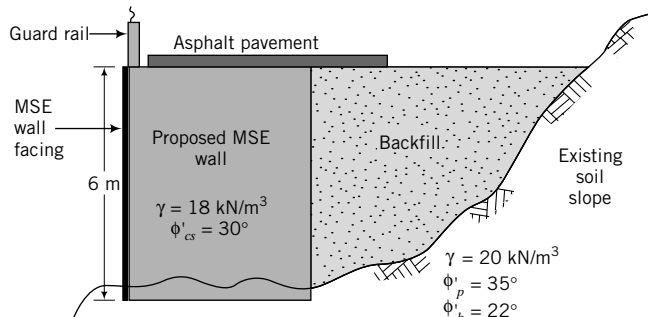


FIGURE P15.22

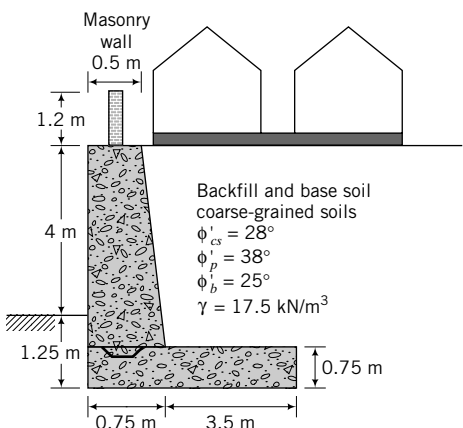
- 15.23** A roadway is to be constructed near an existing slope. The engineer decided to use an MSE wall, as shown in Figure P15.23.

**FIGURE P15.23**

With a surcharge load of 15 kPa (guard rail + pavement + construction), compare designs using:

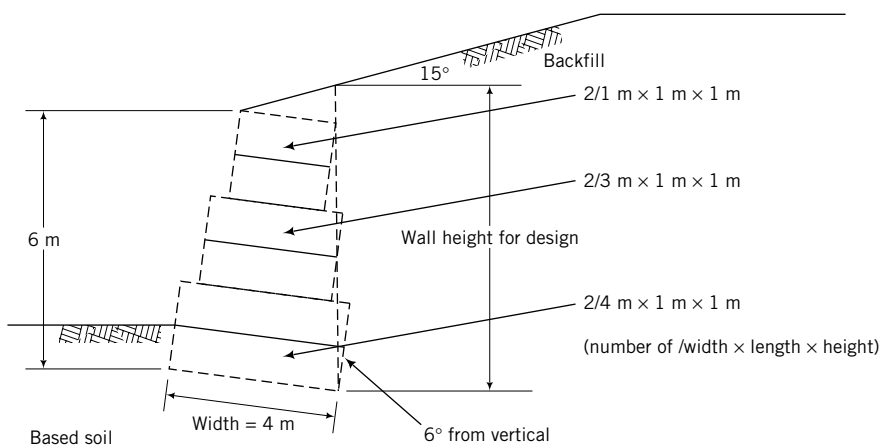
- (a) 4-mm-thick, 50-mm-wide galvanized steel ties; $f_y = 450 \text{ MPa}$, corrosion rate = 0.025 mm/yr, design life = 75 years, soil-tie interface friction = 20° . Assume $(FS)_{tr} = 3$, $(FS)_T = 1.5$, $(FS)_t = 1.3$ and $(FS)_B = 3$.
- (b) Wide-width geotextile of ultimate yield strength 58.5 kN/m and soil-geotextile interface friction = 20° . Assume $(FS)_{ID} = 1.5$, $(FS)_{CR} = 2$, $(FS)_{CD} = 1.3$, $(FS)_{BD} = 1.3$, $(FS)_{sp} = 1.3$, $(FS)_t = 1.3$, $(FS)_T = 1.5$ and $(FS)_B = 3$.

- 15.24** A cantilever retaining wall is required to support a cut near a residential area. A preliminary geometry of the wall is shown in Figure P15.24. A masonry wall 1.2 m high will sit on top of the wall, centered. The masonry wall load (including construction loading) is 9 kN/m and the uniform loading from the homesite is 10 kPa. The wall rotation is limited to $0.0005 H_o$ (H_o is the height of the wall). Check the adequacy of the wall. Determine a suitable wall geometry if the given geometry is unsatisfactory. Sketch a drainage scheme for the wall. Neglect

**FIGURE P15.24**

wall friction. (Hint: The tolerable wall rotation is very small; it is less than the wall rotation to mobilize the active earth pressure.)

- 15.25** A proposed highway embankment runs along a hillside. To construct the embankment, a gabion basket wall (Figure P15.25) is proposed. The unit weight of the granite rocks filling the baskets is 17 kN/m^3 . Determine if the preliminary design shown in Figure P15.25 would be stable. What concern(s) would you have if the site is subjected to annual rainfall that exceeds 0.5 m? How would you modify the design to take care of the concern(s)? Show clear drawings for your answer. (Hint: The design of gabion basket walls is similar to that of gravity walls.) The parameters for the backfill and base soil are: $\phi'_p = 32^\circ$, $\phi'_{cs} = 28^\circ$, $\delta = 20^\circ$, $\phi'_b = 20^\circ$, $\gamma_{sat} = 18 \text{ kN/m}^3$. Groundwater is 5 m below the base. You may assume that the backfill and the base soil are saturated.

**FIGURE P15.25**

CHAPTER 16

SLOPE STABILITY

16.0 INTRODUCTION

In this chapter we will study slope stability, from which you should be able to:

- Understand the forces and activities that provoke slope failures.
- Understand the effects of geology, seepage, and porewater pressures on the stability of slopes.
- Estimate the stability of slopes with simple geometry and geological features.

You will make use of the following:

- Shear strength of soils (Chapter 10)
- Effective stresses and seepage (Chapter 7)
- Flow through dams (Chapter 14)

Importance

Slopes in soils and rocks are ubiquitous in nature and in man-made structures. Highways, dams, levees, canals, and stockpiles are constructed by sloping the lateral faces of the soil because building slopes is generally less expensive than constructing walls. Natural forces (wind, water, snow, etc.) change the topography on Earth and other planets, often creating unstable slopes. Failures of natural slopes (landslides) and man-made slopes have resulted in much death and destruction, economic losses, and environmental damage. Some failures are sudden and catastrophic; others are insidious. Some failures are widespread; others are localized.

Geotechnical engineers have to pay particular attention to geology, surface drainage, groundwater, and the shear strength of soils in assessing slope stability. However, we are handicapped by the geological variability of soils and methods for obtaining reliable values of shear strength. The analyses of slope stability are based on simplifying assumptions, and the design of a stable slope relies heavily on experience and careful site investigation. A slope failure adjacent to a roadway is shown in Figure 16.1. The failed soil mass can move very quickly over large distances. Your job is to prevent such failure.

16.1 DEFINITIONS OF KEY TERMS

Slip or **failure zone** is a thin zone of soil that reaches the critical state or residual state, resulting in movement of the upper soil mass.

Slip plane or **failure plane** or **slip surface** or **failure surface** is the surface of sliding.

Sliding mass is the mass of soil within the slip plane and the ground surface.

Slope angle (α_s) is the angle of inclination of a slope to the horizontal. The slope angle is sometimes referred to as a ratio, for example, 2:1 [horizontal (H):vertical (V)].

Porewater pressure ratio (r_u) is the ratio of porewater force on a slip surface to the total weight of the soil and any external loading.



FIGURE 16.1 Slope failure near a roadway. (Courtesy of Todd Mooney.)

16.2 QUESTIONS TO GUIDE YOUR READING

1. What types of slope failure are common in soils?
2. What factors provoke slope failures?
3. What is an infinite slope failure?
4. What methods of analysis are used to estimate the factor of safety of a slope?
5. What are the assumptions of the various methods of analysis?
6. How does seepage affect the stability of slopes?
7. What is the effect of rapid drawdown on slope stability?

16.3 SOME TYPES OF SLOPE FAILURE

Slope failures depend on the soil type, soil stratification, groundwater, seepage, and the slope geometry. We will introduce a few types of slope failure that are common in soils. Failure of a slope along a weak zone of soil is called a translational slide (Figure 16.2a). The sliding mass can travel long distances before coming to rest. Translational slides are common in coarse-grained soils.

A common type of failure in homogeneous fine-grained soils is a rotational slide that has its point of rotation on an imaginary axis parallel to the slope. Three types of rotational failure often occur. One type, called a base slide, occurs by an arc engulfing the whole slope. A soft soil layer resting on a stiff layer of soil is prone to base failure (Figure 16.2b). The second type of rotational failure is the toe slide, whereby the failure surface passes through the toe of the slope (Figure 16.2c). The third type of rotational failure is the slope slide, whereby the failure surface passes through the slope (Figure 16.2d).

A flow slide occurs when internal and external conditions force a soil to behave like a viscous fluid and flow down even shallow slopes, spreading out in several directions (Figure 16.2e). The failure surface is ill defined in flow slides. Multiple failure surfaces usually occur and change continuously as flow proceeds. Flow slides can occur in dry and wet soils.

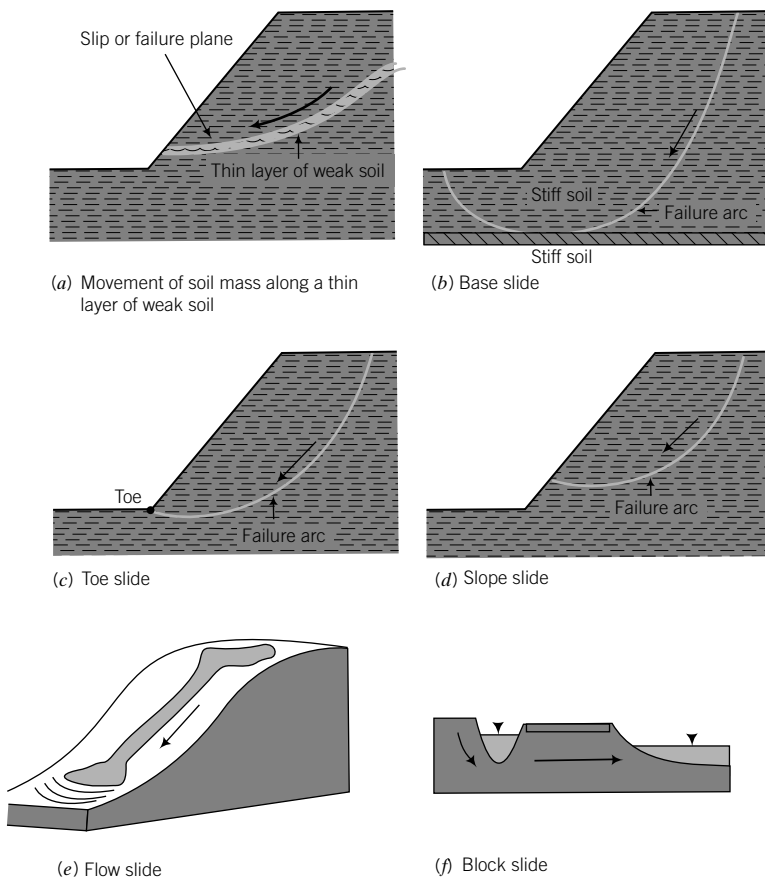


FIGURE 16.2 Some common types of slope failure.

Block or wedge slides occur when a soil mass is shattered along joints, seams, fissures, and weak zones by forces emanating from adjacent soils. The shattered mass moves as blocks and wedges down the slope (Figure 16.2f).

What's next . . . What causes the slope failures that we briefly described above? The causes are many and varied. In the next section, we will describe some common causes of slope failure.

16.4 SOME CAUSES OF SLOPE FAILURE

Slope failures are caused, in general, by natural forces, human misjudgment and activities, and burrowing animals. We will describe below some of the main factors that provoke slope failures.

16.4.1 Erosion

Water and wind continuously erode natural and man-made slopes. Erosion changes the geometry of the slope (Figure 16.3a), ultimately resulting in slope failure or, more aptly, a landslide. Rivers and streams continuously scour their banks, undermining their natural or man-made slopes (Figure 16.3b).

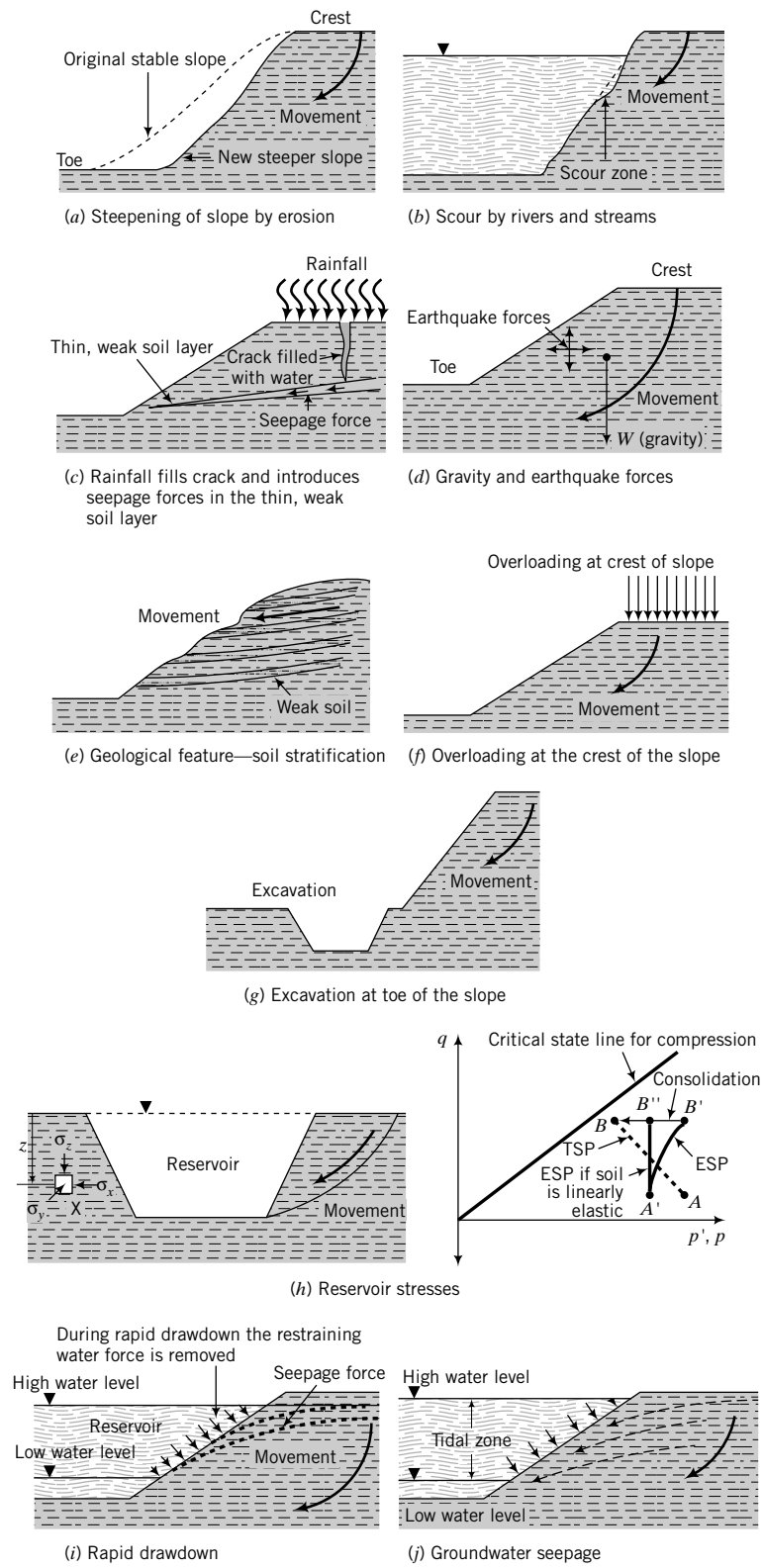


FIGURE 16.3 Some causes of slope failure.

16.4.2 Rainfall

Long periods of rainfall saturate, soften, and erode soils. Water enters into existing cracks and may weaken underlying soil layers, leading to failure, for example, mud slides (Figure 16.3c).

16.4.3 Earthquakes

Earthquakes induce dynamic forces (Figure 16.3d), especially dynamic shear forces that reduce the shear strength and stiffness of the soil. Porewater pressures in saturated coarse-grained soils could rise to a value equal to the total mean stress and cause these soils to behave like viscous fluids—a phenomenon known as dynamic liquefaction. Structures founded on these soils would collapse; structures buried within them would rise. The quickness (a few seconds) with which the dynamic forces are induced prevents even coarse-grained soils from draining the excess porewater pressures. Thus, failure in a seismic event often occurs under undrained condition.

16.4.4 Geological Features

Many failures commonly result from unidentified geological features. A thin seam of silt (a few millimeters thick) under a thick deposit of stiff clay can easily be overlooked in drilling operations, or one may be careless in assessing borehole logs only to find later that the presence of the silt caused a catastrophic failure. Sloping, stratified soils are prone to translational slide along weak layers (Figure 16.3e). You must pay particular attention to geological features in assessing slope stability.

16.4.5 External Loading

Loads placed on the crest of a slope (the top of the slope) add to the gravitational load and may cause slope failure (Figure 16.3f). A load placed at the toe, called a berm, will increase the stability of the slope. Berms are often used to remediate problem slopes.

16.4.6 Construction Activities

Construction activities near the toe of an existing slope can cause failure because lateral resistance is removed (Figure 16.3g). We can conveniently divide slope failures due to construction activities into two cases. The first case is excavated slope and the second case is fill slope.

16.4.6.1 Excavated Slopes When excavation occurs, the total stresses are reduced and negative porewater pressures are generated in the soil. With time the negative porewater pressures dissipate, causing a decrease in effective stresses and consequently lowering the shear strength of the soil. If slope failures were to occur, they would most likely take place after construction is completed.

We can use our knowledge of stress paths (Chapter 8) to provide insight on the possible effects of excavation on slope stability. Let us consider a construction activity involving excavation of a normally consolidated fine-grained soil to construct a reservoir (Figure 16.3h). Let us consider an element of soil, X, at a depth z below the surface. Groundwater is assumed to be at the surface. The soil element, X, is under plane strain condition, but we will use axisymmetric condition for illustrative purposes.

The initial vertical effective stress is $\sigma'_{zo} = \gamma'z$, and the lateral effective stresses are $\sigma'_{xo} = \sigma'_{yo} = K_o\sigma'_{zo}$. The initial porewater pressure is $u_o = \gamma_w z$. The stress invariants are

$$p'_o = \frac{\sigma'_{zo}}{3}(1 + 2K_o), \quad p_o = \frac{\sigma'_{zo}}{3}(1 + 2K_o) + u_o, \quad \text{and} \quad q_o = \sigma'_{zo}(1 - K_o)$$

In stress space $\{p'(p), q\}$, the initial total stresses are represented by point A and the initial effective stresses are represented by point A' . The excavation will cause a reduction in σ_x (i.e., $\Delta\sigma_x < 0$) but very little change in σ_z (i.e., $\Delta\sigma_z \approx 0$) and σ_y (i.e., $\Delta\sigma_y \approx 0$). The change in mean total stress is then $\Delta p = -\Delta\sigma_x/3$, and the change in deviatoric stress is $\Delta q = \Delta\sigma_x$. The total stress path (TSP) is depicted as AB in Figure 16.3h. Although B is near the failure line, the soil is not about to fail because failure is dictated by effective, not total, stresses.

If the soil were a linear, elastic material, the ESP would be $A'B''$ (recall that for elastic material, $\Delta p' = 0$ under undrained condition). Assuming our soil is elastoplastic, then $A'B'$ would represent our ESP. The ESP moves away from the failure line. This is because the excess porewater pressure is negative due to the decrease in lateral stress, and consequently the effective stress increases. Therefore, failure is unlikely to occur during the excavation stage.

After the excavation, the excess porewater pressure would dissipate with time. Since no further change in q occurs, the ESP must move from B' to B , that is, toward the failure line. The implication is that slope instability would most likely occur under drained condition (after the excavation). The illustration of the excavation process using stress paths further demonstrates the power of stress paths to provide an understanding of construction events in geotechnical engineering.

16.4.6.2 Fill Slopes Fill slopes are common in embankment construction. Fill (soil) is placed at the site and compacted to specifications, usually greater than 95% Proctor maximum dry unit weight. The soil is invariably unsaturated, and negative porewater pressures develop. The soil on which the fill is placed, which we will call the foundation soil, may or may not be saturated. If the foundation soil is saturated, then positive porewater pressures will be generated from the weight of the fill and the compaction process. The effective stresses decrease, and consequently the shear strength decreases. With time the positive porewater pressures dissipate, the effective stresses increase, and so does the shear strength of the soil. Thus, slope failures in fill slopes are most likely to occur during or immediately after construction.

16.4.7 Rapid Drawdown

Reservoirs can be subjected to rapid drawdown. In this case the lateral force provided by the water is removed and the excess porewater pressure does not have enough time to dissipate (Figure 16.3i). The net effect is that the slope can fail under undrained condition. If the water level in the reservoir remains at low levels and failure did not occur under undrained condition, seepage of groundwater would occur and the additional seepage forces could provoke failure (Figure 16.3j).

THE ESSENTIAL POINTS ARE:

1. Geological features and environmental conditions (e.g., external loads and natural forces) are responsible for most slope failures.
2. The common modes of slope failure in soils are by translation, rotation, flow, and block movements.

What's next . . . In the next section, we will study how to analyze a slope of infinite extent. We will make use of the limit equilibrium method of analysis and consider long-term and short-term conditions.

16.5 INFINITE SLOPES

Infinite slopes have dimensions that extend over great distances. The assumption of an infinite slope simplifies stability calculations. Let us consider a clean, homogeneous, coarse-grained soil of infinite slope, α_s . To use the limit equilibrium method, we must first speculate on a failure or slip mechanism. We will

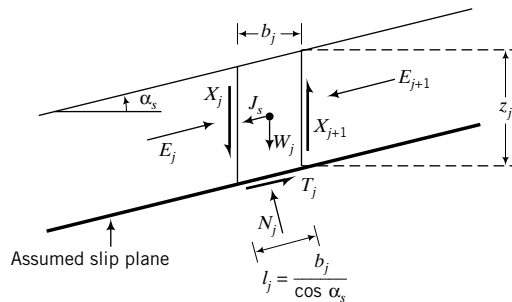


FIGURE 16.4 Forces on a slice of soil in an infinite slope.

assume that slip would occur on a plane parallel to the slope. If we consider a slice of soil between the surface of the slope and the slip plane, we can draw a free-body diagram of the slice, as shown in Figure 16.4.

The forces acting on the slice per unit thickness are the weight $W_j = \gamma b_j z_j$, the shear forces X_j and X_{j+1} on the sides, the normal forces E_j and E_{j+1} on the sides, the normal force N_j on the slip plane, and the mobilized shear resistance of the soil, T_j , on the slip plane. We will assume that forces that provoke failure are positive. If seepage is present, a seepage force $J_s = i \gamma_w b_j z_j$ develops, where i is the hydraulic gradient. The sign of the seepage force depends on the seepage direction. In our case, the seepage force is positive because seepage is in the direction of positive forces. For a uniform slope of infinite extent, $X_j = X_{j+1}$ and $E_j = E_{j+1}$.

To continue with the limit equilibrium method, we must now use the equilibrium equations to solve the problem. But before we do this, we will define the factor of safety of a slope. The factor of safety (FS) of a slope is defined as the ratio of the available shear strength of the soil, τ_f , to the minimum shear strength required to maintain stability, τ_m , that is,

$$\text{FS} = \frac{\tau_f}{\tau_m} \quad (16.1)$$

The shear strength of soils for an effective stress analysis is governed by the Coulomb failure criterion (Chapter 10), that is, $\tau_f = \sigma'_n \tan \phi'$. The shear strength of soils (fine-grained soils) for a total stress analysis is governed by Tresca's failure criterion, that is, $\tau_f = s_u$. The factor of safety is then

$$\text{ESA: } \text{FS} = \frac{\sigma'_n \tan \phi'}{\tau_m} = \frac{N' \tan \phi'}{T_m} \quad (16.2)$$

$$\text{TSA: } \text{FS} = \frac{s_u}{\tau_m} \quad (16.3)$$

where N' is the normal effective force on the slip plane and T_m is the mobilized shear force. Recall that both the Coulomb and Tresca criteria are based on limit stresses where the soil is treated as a rigid-plastic material—no deformation occurs prior to reaching the limiting shear stress.

Let us now use statics to solve for the factor of safety. First, we will consider a slope without seepage and groundwater below the slip plane. Because the groundwater is below the slip plane, the effective stress is equal to the total stress. From statics,

$$N'_j = W'_j \cos \alpha_s \quad \text{and} \quad T_j = W'_j \sin \alpha_s$$

From the definition of factor of safety for the ESA [Equation (16.2)], we get

$$\therefore \text{FS} = \frac{N'_j \tan \phi'}{T_j} = \frac{W'_j \cos \alpha_s \tan \phi'}{W'_j \sin \alpha_s} = \frac{\tan \phi'}{\tan \alpha_s} \quad (16.4)$$

At limit equilibrium, FS = 1. Therefore,

$$\alpha_s = \phi' \quad (16.5)$$

The implication of Equation (16.5) is that the maximum slope angle of a coarse-grained soil cannot exceed ϕ' .

We will now consider groundwater within the sliding mass and assume that seepage is parallel to the slope. The seepage force is

$$J_s = i \gamma_w b_j z_j$$

Since seepage is parallel to the slope, $i = \sin \alpha_s$. From statics,

$$N'_j = W'_j \cos \alpha_s = \gamma' b_j z_j \cos \alpha_s \quad (16.6)$$

and

$$\begin{aligned} T_j &= W'_j \sin \alpha_s + j_s = \gamma' b_j z_j \sin \alpha_s + \gamma_w b_j z_j \sin \alpha_s = (\gamma' + \gamma_w) b_j z_j \sin \alpha_s \\ &= (\gamma_{sat}) b_j z_j \sin \alpha_s \end{aligned}$$

From the definition of factor of safety [Equation (16.2)], we get

$$FS = \frac{N'_j \tan \phi'}{T_j} = \frac{\gamma' b_j z_j \cos \alpha_s \tan \phi'}{\gamma_{sat} b_j z_j \sin \alpha_s} = \frac{\gamma' \tan \phi'}{\gamma_{sat} \tan \alpha_s} \quad (16.7)$$

At limit equilibrium, FS = 1. Therefore,

$$\tan \alpha_s = \frac{\gamma'}{\gamma_{sat}} \tan \phi' \quad (16.8)$$

For most soils, $\gamma'/\gamma_{sat} \approx \frac{1}{2}$. Thus, seepage parallel to the slope reduces the limiting slope of a clean, coarse-grained soil by about one-half.

The shear stress on the slip plane for a TSA, which is applicable to the short-term slope stability in fine-grained soils, is

$$\tau_j = \frac{T_j}{l_j} = \frac{W_j \sin \alpha_s}{l_j} = \frac{W_j \sin \alpha_s \cos \alpha_s}{b_j} = \frac{\gamma b_j z_j}{b_j} \sin \alpha_s \cos \alpha_s = \gamma z_j \sin \alpha_s \cos \alpha_s \quad (16.9)$$

The factor of safety [Equation (16.3)] is

$$FS = \frac{s_u}{\Sigma \tau_j} = \frac{s_u}{\gamma z \sin \alpha_s \cos \alpha_s} = \frac{2s_u}{\gamma z \sin(2\alpha_s)} \quad (16.10)$$

At limit equilibrium, FS = 1. Therefore,

$$\alpha_s = \frac{1}{2} \sin^{-1}(2s_u/\gamma z) \quad (16.11)$$

and

$$z = \frac{2s_u}{\gamma \sin(2\alpha_s)} \quad (16.12)$$

The critical value of z occurs when $\alpha_s = 45^\circ$, that is,

$$z = z_{cr} = 2s_u/\gamma \quad (16.13)$$

which is the depth of tension cracks. Therefore, the maximum slope of fine-grained soils under short-term loading, assuming an infinite slope failure mechanism, is 45° . For slopes greater than 45° and depths greater than $2s_u/\gamma$, the infinite slope failure mechanism is not tenable. The infinite slope failure mechanism is more relevant to coarse-grained soils than fine-grained soils because most slope failures observed in fine-grained soils are finite and rotational.

THE ESSENTIAL POINTS ARE:

1. The maximum stable slope in a coarse-grained soil, in the absence of seepage, is equal to the friction angle.
2. The maximum stable slope in coarse-grained soils, in the presence of seepage parallel to the slope, is approximately one-half the friction angle.
3. The critical slope angle in fine-grained soils is 45° for an infinite slope failure mechanism.
4. The critical depth is the depth of tension cracks, that is, $2s_u/\gamma$.

EXAMPLE 16.1 Infinite Slope Stability Considering Seepage

Dry sand is to be dumped from a truck on the side of a roadway. The properties of the sand are $\phi'_{cs} = 30^\circ$, $\gamma = 17 \text{ kN/m}^3$, and $\gamma_{sat} = 17.5 \text{ kN/m}^3$. Determine the maximum slope angle of the sand in (a) the dry state, (b) the saturated state without seepage, and (c) the saturated state if groundwater is present and seepage were to occur parallel to the slope. What is the safe slope in the dry state for a factor of safety of 1.25?

Strategy The solution to this problem is a straightforward application of Equations (16.5) and (16.8).

Solution 16.1

Step 1: Sketch a diagram.

See Figure E16.1.

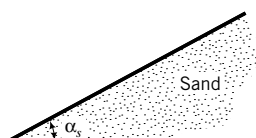


FIGURE E16.1

Step 2: Determine the maximum slope under the dry condition.

$$\text{Equation (16.5): } \alpha_s = \phi'_{cs} = 30^\circ$$

You should note that any small disturbance would cause this slope to fail since it is at limit equilibrium.

The safe slope from Equation (16.4) for $FS = 1.25$ is

$$\alpha_s = \tan^{-1}\left(\frac{\tan\phi'_{cs}}{FS}\right) = \tan^{-1}\left(\frac{\tan 30^\circ}{1.25}\right) = 24.8^\circ$$

Step 3: Determine the maximum slope for the saturated condition.

The value of ϕ'_{cs} is not significantly affected by whether the soil is dry or wet. Therefore, $\alpha_s = 30^\circ$.

Step 4: Determine the maximum slope for seepage parallel to the slope.

$$\begin{aligned} \text{Equation (16.8): } \tan\alpha_s &= \frac{\gamma'}{\gamma_{sat}} \tan\phi'_{cs} \\ \gamma' &= \gamma_{sat} - \gamma_w = 17.5 - 9.8 = 7.7 \text{ kN/m}^3 \\ \tan\alpha_s &= \frac{\gamma'}{\gamma_{sat}} \tan\phi'_{cs} = \frac{7.7}{17.5} \tan 30^\circ = 0.25 \\ \alpha_s &= 14^\circ \end{aligned}$$

EXAMPLE 16.2 Infinite Slope Failure in Clay Soils

A trench was cut in a clay slope (Figure E16.2) to carry TV and telephone cables. When the trench reached a depth of 1.9 m, the excavation was stopped. On resumption, the top portion of the clay suddenly failed when a depth of 2 m was excavated, engulfing the trench and injuring several workers. On investigating the failure, you observed a slip plane approximately parallel to the original slope. Determine the undrained shear strength of the clay.

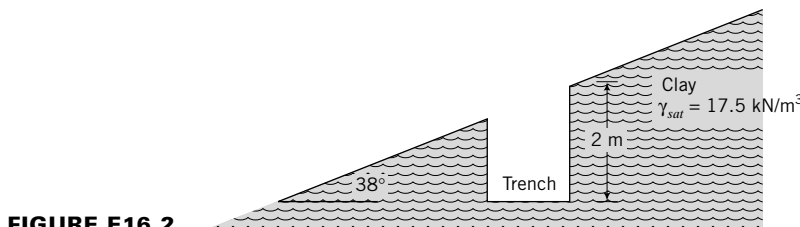


FIGURE E16.2

Strategy The failure observed can be analyzed as an infinite slope failure in a fine-grained soil.

Solution 16.2

Step 1: Determine s_u .

$$\text{From Equation (16.10): } s_u = \frac{\gamma z (\sin 2\alpha_s)}{2} FS$$

Since the slope failed, $FS = 1$.

$$\therefore s_u = \frac{17.5 \times 2 \times \sin(2 \times 38^\circ)}{2} = 17 \text{ kPa}$$

What's next . . . In the next section, we will discuss the methods of analyses used to evaluate the stability of slopes.

16.6 TWO-DIMENSIONAL SLOPE STABILITY ANALYSES

Slope stability can be analyzed using one or more of the following: the limit equilibrium method, limit analysis, the finite difference method, and the finite element method. Limit equilibrium is often the method of choice, but the finite element method (FEM) or the finite difference method (FDM) is more flexible and general. You should recall (Chapters 12 and 15) that in the limit equilibrium method, a failure mechanism must be postulated, and then the equilibrium equations are used to solve for the collapse load. Several failure mechanisms must be investigated, and the minimum load required for collapse is taken as the collapse load. The limit equilibrium method normally gives an upper bound solution (answer higher than the “true” collapse load) because a more efficient mechanism of collapse is possible than those postulated. The limit analysis makes use of the stress–strain characteristics and a failure criterion for the soil. The solution from a limit analysis gives both an upper bound and a lower bound (answer lower than the “true” collapse load). The FEM or FDM requires the discretization of the soil domain, and makes use of the stress–strain characteristics of the soil and a failure criterion to identify soil regions that have reached the failure stress state. The FEM or FDM does not require speculation on a possible failure surface. We will concentrate on the limit equilibrium method in this book because of its simplicity. We will develop the analyses using a generic friction angle, ϕ' . Later, we will discuss the appropriate ϕ' to use. We will use an effective stress analysis (ESA) and a total stress analysis (TSA).

What's next . . . Homogeneous fine-grained soils have been observed to fail through a rotational mechanism. Next, we will consider methods of analyses for two-dimensional slope failure.

16.7 ROTATIONAL SLOPE FAILURES

We will continue to use the limit equilibrium method, but instead of a planar slip surface of infinite extent we will assume circular (Figure 16.5a) and noncircular (Figure 16.5b) slip surfaces of finite extent. We will assume the presence of a phreatic surface within the sliding mass.

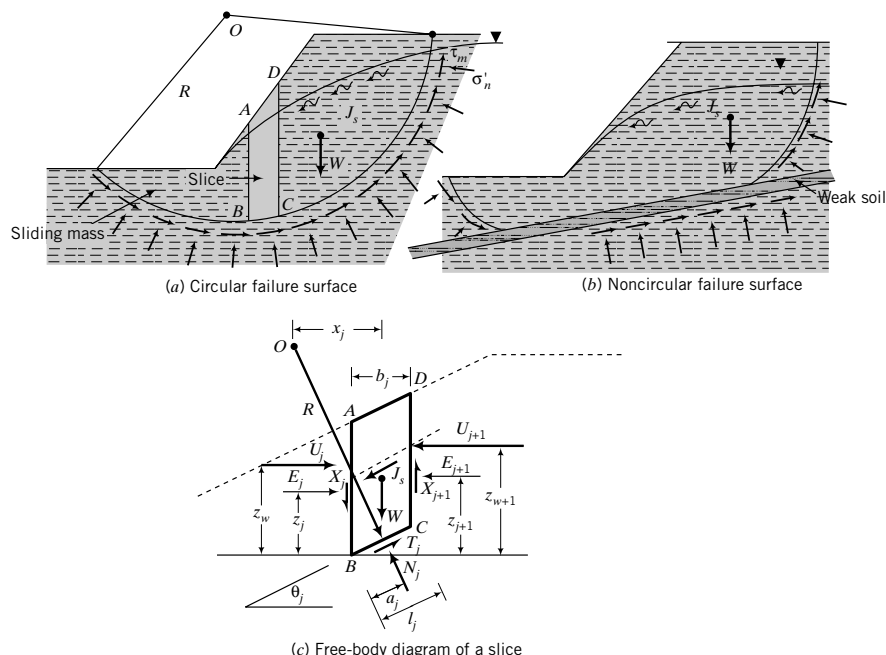


Figure 16.5 Circular and noncircular failure surfaces and the forces on a slice of soil.

A free-body diagram of the postulated circular failure mechanism would show the weight of the soil within the sliding mass acting at the center of mass. If seepage is present, then the seepage forces, J_s , which may vary along the flow path, are present. The forces resisting outward movement of slope are the shearing forces mobilized by the soil along the slip surface.

We must now use statics to determine whether the disturbing forces and moments created by W and J_s exceed the resisting forces and moments due to the shearing forces mobilized by the soil. However, we have several problems in determining the forces and moments. Here is a list.

- It is cumbersome, if not difficult, to determine the location of the center of mass, especially when we have layered soils and groundwater.
- The problem is statically indeterminate.
- We do not know how the mobilized shear strength, τ_m , of the soil varies along the slip surface.
- We do not know how the normal effective stress, σ'_n , varies along the slip surface.
- We do not know how the seepage forces vary within the soil mass and along the failure surface.
- Even the weight of sliding mass is difficult to calculate because of soil layering (different unit weights of the soils) and complex geometry of some slopes.

One approach to solve our problem is to divide the sliding mass into an arbitrary number of slices and then sum the forces and moments of each slice. Of course, the larger the number of slices, the better the accuracy of our answer. Dividing the area inside the sliding mass into slices presents new problems. We now have to account for the internal forces or interfacial forces between the slices.

Let us consider an arbitrary slice, $ABCD$ (Figure 16.5a), and draw a free-body diagram of the forces acting on the slices, as illustrated in Figure 16.5c. The forces have the following meaning:

- W_j is the total weight of a slice including any external load.
- E_j is the interslice lateral effective force.
- $(J_s)_j$ is the seepage force on the slice.
- N_j is the normal force along the slip surface.
- T_j is the mobilized shear force along the slip surface.
- X_j is the interslice shear force.
- U_j is the force from the porewater pressure.
- z_j is the location of the interslice lateral effective force.
- z_w is the location of the porewater force.
- a_j is the location of the normal effective force along the slip surface.
- b_j is the width of the slice.
- l_j is the length of slip surface along the slice.
- θ_j is the inclination of the slip surface within the slice to the horizontal plane.

The side BC is assumed to be a straight line.

We now have to obtain the values of 13 parameters. We can find W_j , U_j , $(J_s)_j$, b_j , l_j , z_w , and θ_j from the geometry of the slice, the unit weights of the soils, and the location of the phreatic surface. We have six unknowns for each slice and only three equilibrium equations; our problem is then statically indeterminate. To solve our problem, we have to make assumptions regarding three of the unknown parameters. Several solution methods have evolved depending on the assumptions made about the unknown

TABLE 16.1 Slope Analysis Methods Based on Limit Equilibrium

Method	Assumption	Failure surface	Equilibrium equation satisfied	Solution by
Swedish method (Fellenius, 1927)	Resultant of interslice force is zero; $J_s = 0$	Circular	Moment	Calculator
Bishop's simplified method (Bishop, 1955)	E_j and E_{j+1} are collinear; $X_j - X_{j+1} = 0, J_s = 0$	Circular	Moment	Calculator
Bishop's method (Bishop, 1955)	E_j and E_{j+1} are collinear; $J_s = 0$	Circular	Moment	Calculator/computer
Morgenstern and Price (1965)	Relationship between E and X of the form $X = \lambda f(x)E$; $f(x)$ is a function ≈ 1 , λ is a scale factor, $J_s = 0$	Any shape	All	Computer
Spencer (1967)	Interslice forces are parallel; $J_s = 0$	Any shape	All	Computer
Bell's method (Bell, 1968)	Assumed normal stress distribution along failure surface; $J_s = 0$	Any shape	All	Computer
Janbu (1973)	$X_j - X_{j+1}$ replaced by a correction factor, f_o ; $J_s = 0$	Noncircular	Horizontal forces	Calculator
Sarma (1975)	Assumed distribution of vertical interslice forces; $J_s = 0$	Any shape	All	Computer

parameters and which equilibrium condition (force, moment, or both) is satisfied. Table 16.1 provides a summary of methods that have been proposed.

We will describe the methods developed by Bishop (1955) and by Janbu (1973) because they are popular methods and require only a calculator or a spreadsheet program. Computer programs are commercially available for all the methods listed in Table 16.1. Before you use these programs, you should understand the principles employed and the assumptions made in their development. The methods of Bishop and Janbu were developed by assuming that soil is a cohesive-frictional material. We will modify the derivation of the governing equations of these methods by considering soil as a dilatant-frictional material. We will also develop separate governing equations for an effective stress analysis and a total stress analysis. However, we will retain the names of original developers. For long-term or drained condition, we have to conduct an effective stress analysis. For short-term or undrained condition in fine-grained soils, we have to conduct a total stress analysis.

16.8 METHOD OF SLICES

16.8.1 Bishop's Method

Bishop (1955) assumed a circular slip surface, as shown in Figure 16.5a. Let us apply the equilibrium equations to the forces on the slice shown in Figure 16.5c, assuming that E_j and E_{j+1} and U_j and U_{j+1} are collinear, N_j acts at the center of the arc length, that is, at $l_j/2$, and $(J_s)_j = 0$.

Summing forces vertically, we get

$$N_j \cos \theta_j + T_j \sin \theta_j - W_j - X_j + X_{j+1} = 0 \quad (16.14)$$

The force due to the porewater pressure (U_j) is $U_j = u_j l_j$. From the principle of effective stress,

$$N'_j = N_j - u_j l_j \quad (16.15)$$

Combining Equations (16.14) and (16.15), we get

$$N'_j \cos \theta_j = W_j + X_j - X_{j+1} - T_j \sin \theta_j - u_j l_j \cos \theta_j \quad (16.16)$$

For convenience, let us define the force due to the porewater as a function of W_j as

$$r_u = \frac{u_j b_j}{W_j} = \frac{\gamma_w (z_w)_j}{(\gamma z)_j} \quad (16.17)$$

where r_u is called the porewater pressure ratio. Substituting Equation (16.17) into (16.16) yields

$$N'_j \cos \theta_j = W_j(1 - r_u) - T_j \sin \theta_j + (X_j - X_{j+1}) \quad (16.18)$$

Bishop considered only moment equilibrium, such that, from Figure 16.5c,

$$\sum W_j x_j = \sum T_j R \quad (16.19)$$

where x_j is the horizontal distance from the center of the slice to the center of the arc of radius R , and T_j is the mobilized shear force. Solving for T_j from Equation (16.19) and noting that $x_j = R \sin \theta_j$, we get

$$\sum T_j = \frac{\sum W_j x_j}{R} = \sum W_j \sin \theta_j \quad (16.20)$$

Recall from Equation (16.1) that the factor of safety is defined as

$$FS = \frac{\tau_f}{\tau_m} = \frac{(T_f)_j}{T_j} \quad (16.21)$$

where T_f is the soil shear force at failure. In developing the governing equation for FS, we will first consider effective stress, and later, total stress. For an ESA,

$$FS = \frac{N'_j \tan(\phi')_j}{T_j} \quad (16.22)$$

By rearranging Equation (16.22), we get

$$T_j = \frac{N'_j \tan(\phi')_j}{FS} \quad (16.23)$$

Substituting Equation (16.23) into (16.18) yields

$$N'_j \cos \theta_j = W_j(1 - r_u) - \frac{N'_j \tan(\phi')_j \sin \theta_j}{FS} + (X_j + X_{j+1}) \quad (16.24)$$

Solving for N'_j , we get

$$N'_j = \frac{W_j(1 - r_u) + (X_j - X_{j+1})}{\cos \theta_j + \frac{\tan(\phi')_j \sin \theta_j}{FS}} \quad (16.25)$$

Putting

$$m_j = \frac{1}{\cos \theta_j + \frac{\tan(\phi')_j \sin \theta_j}{FS}} \quad (16.26)$$

we can write N'_j as

$$N'_j = [W_j(1 - r_u) + (X_j - X_{j+1})]m_j \quad (16.27)$$

Substituting Equation (16.22) into (16.20) gives

$$\frac{\Sigma N'_j \tan(\phi')_j}{FS} = \Sigma W_j \sin \theta_j \quad (16.28)$$

Combining Equations (16.27) and (16.28) yields

$$FS = \frac{\Sigma [W_j(1 - r_u) + (X_j - X_{j+1})] \tan(\phi')_j m_j}{\Sigma W_j \sin \theta_j} \quad (16.29)$$

Equation (16.29) is Bishop's equation for an ESA. Bishop showed that neglecting $(X_j - X_{j+1})$ resulted in about 1% of error. Therefore, neglecting $(X_j - X_{j+1})$, we get

$$FS = \frac{\Sigma [W_j(1 - r_u)] \tan(\phi')_j m_j}{\Sigma W_j \sin \theta_j} \quad (16.30)$$

Equation (16.30) is Bishop's simplified equation for an ESA. If groundwater is below the slip surface, $r_u = 0$ and

$$FS = \frac{\Sigma W_j \tan(\phi')_j m_j}{\Sigma W_j \sin \theta_j} \quad (16.31)$$

Let us now consider a TSA. The mobilized shear force on the slip surface is

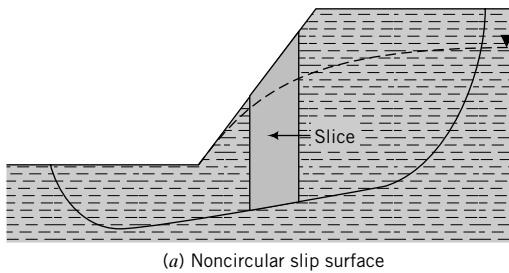
$$T_j = \frac{(s_u)_j l_j}{FS} \quad (16.32)$$

where $(s_u)_j$ is the undrained shear strength of the soil along the slip surface within the slice. Combining Equations (16.20) and (16.22) yields

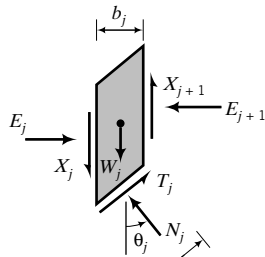
$$FS = \frac{\Sigma (s_u)_j l_j}{\Sigma W_j \sin \theta_j} \quad (16.33)$$

Since $b_j = l_j \cos \theta_j$, Equation (16.33) becomes

$$FS = \frac{\Sigma (s_u)_j \frac{b_j}{\cos \theta_j}}{\Sigma W_j \sin \theta_j} \quad (16.34)$$



(a) Noncircular slip surface



(b) Forces on a slice

FIGURE 16.6 Failure surface proposed by Janbu and forces on a slice of soil.

16.8.2 Janbu's Method

Janbu (1973) assumed a noncircular slip surface (Figure 16.6a). The forces acting on a slice are as shown in Figure 16.6b. Janbu considered equilibrium of horizontal forces and assumed that $E_j - E_{j+1} = 0$.

The factor of safety, defined with respect to equilibrium of horizontal forces, is

$$FS = \frac{\Sigma \text{Resisting forces}}{\Sigma \text{Disturbing forces}} = \frac{\Sigma (T_f)_j \cos \theta_j}{\Sigma [W_j + (X_j - X_{j+1})] \tan \theta_j} \quad (16.35)$$

Noting that $(T_f)_j = T_j (FS) = N_j \tan (\phi')$, FS, we can combine Equations (16.35) and (16.27) to yield, for an ESA,

$$FS = \frac{\Sigma [W_j(1 - r_u) + (X_j - X_{j+1})] m_j \tan \phi' \cos \theta_j}{\Sigma [W_j + (X_j - X_{j+1})] \tan \theta_j} \quad (16.36)$$

Janbu then replaced the interslice shear forces (X_j and X_{j+1}) by a correction factor f_o , as shown in Figure 16.7. The simplified form of Janbu's equation for an ESA is

$$FS = \frac{f_o \Sigma W_j(1 - r_u) m_j \tan \phi' \cos \theta_j}{\Sigma W_j \tan \theta_j} \quad (16.37)$$

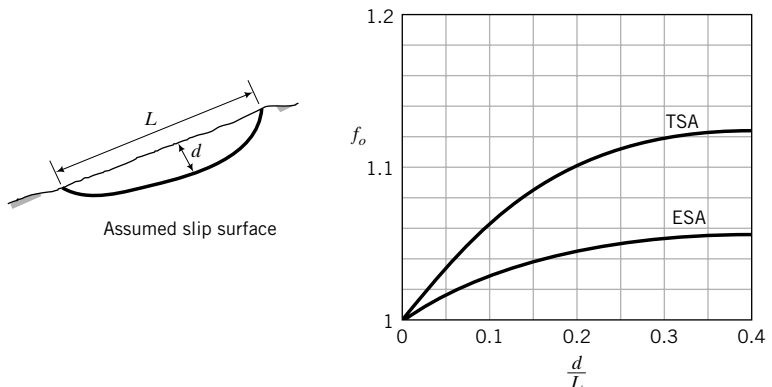


FIGURE 16.7 Correction factor for Janbu's method.

If the groundwater is below the slip surface, $r_u = 0$, and

$$\text{FS} = f_o \frac{\sum W_j m_j \tan \phi'_j \cos \theta_j}{\sum W_j \tan \theta_j} \quad (16.38)$$

For a TSA,

$$\text{FS} = \frac{\sum (s_u)_j b_j}{\sum [W_j + (X_j - X_{j+1})] \tan \theta_j} \quad (16.39)$$

Replacing the effects of $(X_i - X_{i+1})$ by a correction factor f_o (Figure 16.7), we get

$$\text{FS} = f_o \frac{\sum (s_u)_j b_j}{\sum W_j \tan \theta_j} \quad (16.40)$$

16.8.3 Cemented Soils

Equation (16.30) and Equation (16.37) apply to homogeneous uncemented soils. For cemented soils, we can write these equations as

$$\text{FS} = \frac{\sum \{(c_{cm})_j b_j + [W_j(1 - r_u)] \tan (\xi_o)_j m_j\}}{\sum W_j \sin \theta_j} \quad (16.41)$$

$$\text{FS} = \frac{\sum \{(c_{cm})_j b_j + f_o \sum W_j (1 - r_u) m_j \tan (\xi_o)_j \cos \theta_j\}}{\sum W_j \tan \theta_j} \quad (16.42)$$

where c_{cm} is cementation strength (or cohesion) and ξ_o is the apparent friction angle. You need to be very careful in using Equation (16.41) and Equation (16.42). Cemented soils tend to rupture near or at the cementation strength. When rupturing occurs, the flow paths of water through the soil are altered. The rupture planes provide easy flow access, which can lead to destabilization by excess porewater pressure and seepage stresses. The cementation strength and the apparent frictional resistance are not achieved at the same level of shear strains. Consequently, they are not additive. However, the methods considered here are based on limit equilibrium that is independent of soil deformation.

Negative porewater pressures and tree roots confer an apparent shear strength to the soil mass. This apparent shear strength is temporary, as the porewater pressure dissipates and tree roots decay. The apparent shear strength from negative porewater pressure in an unsaturated soil slope can diminish very quickly by infiltration of water from rainfall and leakage from utility pipes. The infiltration of water converts the negative porewater pressure into positive porewater pressure. This causes the effective stresses to decrease and the apparent shear strength to disappear. Equations (16.41) and (16.42) are best used for short term condition under stable environmental conditions and where experience shows that it is safe to do so.

THE ESSENTIAL POINTS ARE:

- 1. Bishop (1955) assumed a circular slip plane and considered only moment equilibrium. He neglected seepage forces and assumed that the lateral normal forces are collinear. In Bishop's simplified method, the resultant interface shear is assumed to be zero.**
- 2. Janbu (1973) assumed a noncircular failure surface and considered equilibrium of horizontal forces. He made similar assumptions to Bishop, except that a correction factor was applied to replace the interface shear.**
- 3. For slopes in fine-grained soils, you should conduct both an ESA and a TSA for long-term loading and short-term loading, respectively. For slopes in coarse-grained soils, only an ESA is necessary for short-term and long-term loading, provided the loading is static.**

16.9 APPLICATION OF THE METHOD OF SLICES

The shear strength parameters are of paramount importance in slope stability calculations. The soils at the slip surface are at or near the critical or the residual state. You should use $\phi' = \phi'_{cs}$ in all slope stability calculations except for fissured overconsolidated clays. Progressive failure usually occurs in fissured overconsolidated clays. The appropriate value of ϕ' to use is ϕ_r —the residual friction angle. The measured undrained shear strength is often unreliable. You should use conservative values of s_u for a TSA. These values should ideally come from direct simple shear tests.

Tension cracks in fine-grained soils tend to develop on the crest and the face of slopes in fine-grained soils. There are three important effects of tension cracks. First, they modify the slip surface. The slip surface does not intersect the ground surface but stops at the base of the tension crack (Figure 16.8). Recall from Equation (16.13) that the depth of a tension crack is $z_{cr} = 2s_u/\gamma$.

Second, the tension crack may be filled with water. In this case, the critical depth is $z'_{cr} = 2s_u/\gamma'$ and a hydrostatic pressure is applied along the depth of the crack. The net effect is a reduction in the factor of safety because the disturbing moment is increased. The additional disturbing moment from the hydrostatic pressure is $\frac{1}{2}\gamma_w z_{cr}^2(z_s + \frac{2}{3}z_{cr})$, where z_s is the vertical distance from the top of the tension crack to the center of rotation (Figure 16.8). The factor of safety using Bishop's simplified method becomes

$$\text{ESA: } \text{FS} = \frac{\sum W_j (1 - r_u) (\tan \theta'_j) m_j}{\sum W_j \sin \theta_j + \frac{\frac{1}{2} \gamma_w z_{cr}^2 \left(z_s + \frac{2}{3} z_{cr} \right)}{R}} \quad (16.43)$$

$$\text{TSA: } \text{FS} = \frac{\sum (s_u)_j \frac{b_j}{\cos \theta_j}}{\sum W_j \sin \theta_j + \frac{\frac{1}{2} \gamma_w z_{cr}^2 \left(z_s + \frac{2}{3} z_{cr} \right)}{R}} \quad (16.44)$$

Third, the tension crack provides a channel for water to reach underlying soil layers. The water can introduce seepage forces and weaken these layers. The locations of the tension cracks and the critical slip plane are not sensitive to the location of the phreatic surface.

Dams and cuts supporting reservoirs can be subjected to rapid drawdown. Consider the earth dam shown in Figure 16.9. When the reservoir is full, the groundwater level within the dam will equilibrate with the reservoir water level. If water is withdrawn rapidly, the water level in the reservoir will drop, but very little change in the groundwater level in the dam will occur. In fine-grained soils, a few weeks of drawdown can be rapid because of the low permeability of these soils. Because the restraining lateral force of the water in the reservoir is no longer present and the porewater pressure in the dam is high,

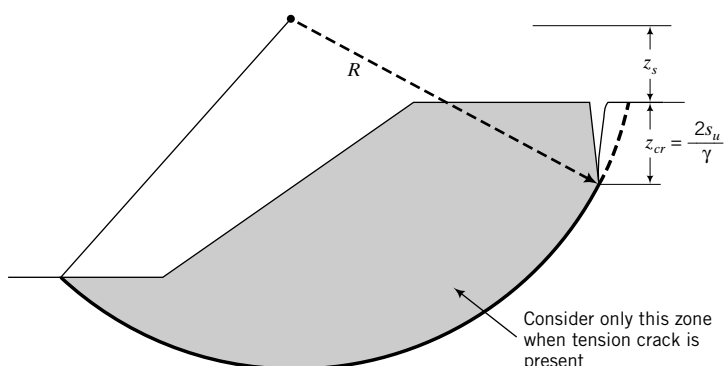


FIGURE 16.8 Effect of tension crack on the slip surface.

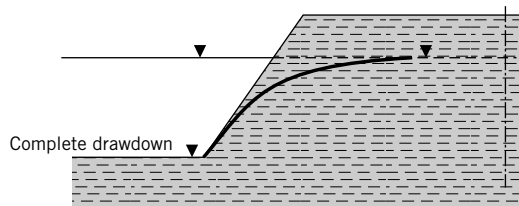


FIGURE 16.9 Drawdown in a reservoir.

the FS will be reduced. The worst-case scenario is rapid, complete drawdown. If a partial drawdown occurs and is maintained, then the phreatic surface will keep changing and seepage forces (resulting from porewater pressure gradients) would be present in addition to the porewater pressures.

16.10 PROCEDURE FOR THE METHOD OF SLICES



Computer Program Utility

Access <http://www.wiley.com/college/budhu>, Chapter 16, for a spreadsheet, slope.xls, on circular and noncircular slope failure analysis. Go to www.grow.arizona.edu and search for “slopes.” Run one of the slope stability programs.

The procedure to determine the factor of safety of slopes using the method of slices, with reference to Figure 16.10, is as follows:

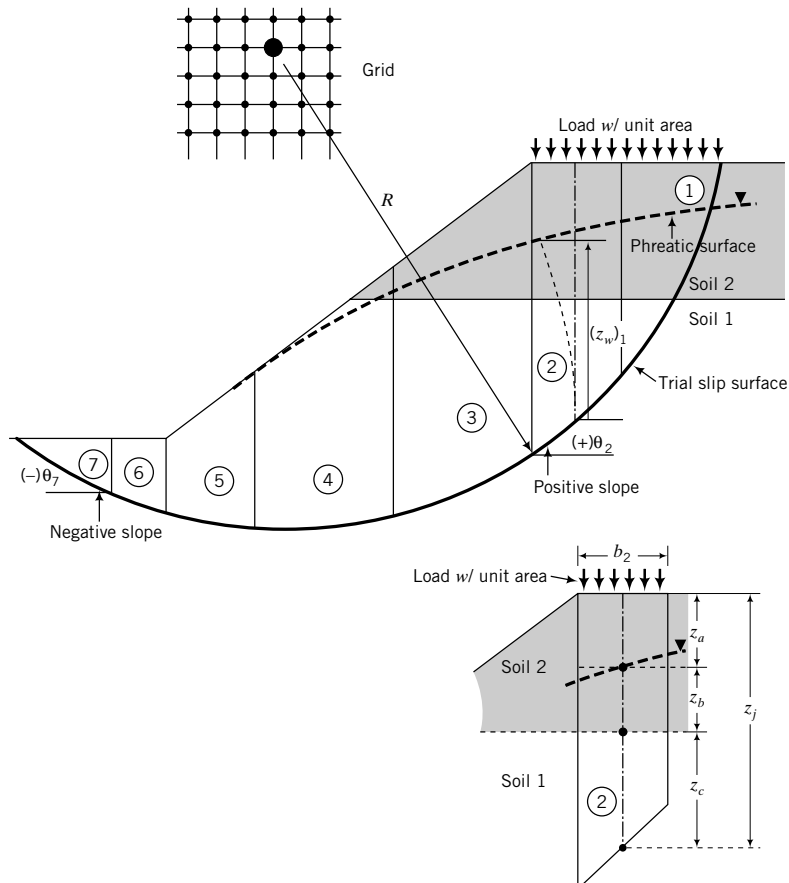


FIGURE 16.10
Method of slices.

1. Draw the slope to scale and note the positions and magnitudes of any external loads.
2. Draw a trial slip surface and identify its point of rotation.
3. Draw the phreatic surface, if necessary (Chapter 14).
4. If the soil is fine-grained, calculate the depth of the tension crack and sketch in a possible location of the tension crack. You can start at the crest and locate a point on your slip surface where the depth matches the depth of the tension crack.
5. Divide the soil mass above the slip surface into a convenient number of slices. More than five slices are needed for most problems.
6. For each slice:
 - (a) Measure the width, b_j .
 - (b) Determine W_j , which is the total weight of a slice including any external load. For example, for the two-layer soil profile shown in Figure 16.10, the weight of slice ② ($j = 2$) is $W_2 = b_2[q_s + z_a(\gamma)_s2 + z_b(\gamma_{sat})_{s2} + z_c(\gamma_{sat})_{s1}]$, where s_1 and s_2 denote soil layers 1 and 2, q_s is the surface load per unit area, and z_a , z_b , and z_c are the mean heights, as shown in Figure 16.10.
 - (c) Measure the angle θ_j for each slice, or you can calculate it if you measure the length, $l_j[\theta_j = \cos^{-1}(b_j/l_j)]$. The angle θ_j can be negative. Angles left of the center of rotation are negative. For example, the value of θ for slice ⑦ is negative, but for slice ②, θ is positive. Alternatively, negative values of the slope of the slip surface in a slice give negative values of θ_j .
 - (d) Sketch an equipotential line starting from the intersection of the vertical center line and the slip surface to intersect the phreatic surface at $\sim 90^\circ$. The vertical projection of the equipotential line is the porewater pressure head, $(z_w)_j$.
 - (e) Calculate $r_u = \gamma_w(z_w)_j / \sum_{j=1}^n \gamma_j z_j$, where n is the number of soil layers within a slice.
7. You now have values for all the required parameters to calculate the factor of safety. Prepare a table or use a spreadsheet program to carry out the calculations. To facilitate calculations using a nonprogrammable calculator, a chart for m_j is shown in Figure 16.11. You have to guess a value of FS and then iterate until the guessed value of FS and the calculated value of FS are the same or within a small tolerance (≈ 0.01). If a tension crack is present, set the term $W_j(1 - r_u)(\tan \phi'_j)m_j$ to zero but keep the term $W_j \sin \theta_j$ for the slices above the tension crack when you are considering an ESA; for a TSA, set $s_u = 0$ for the slices above the tension crack but keep the term $W_j \sin \theta_j$.

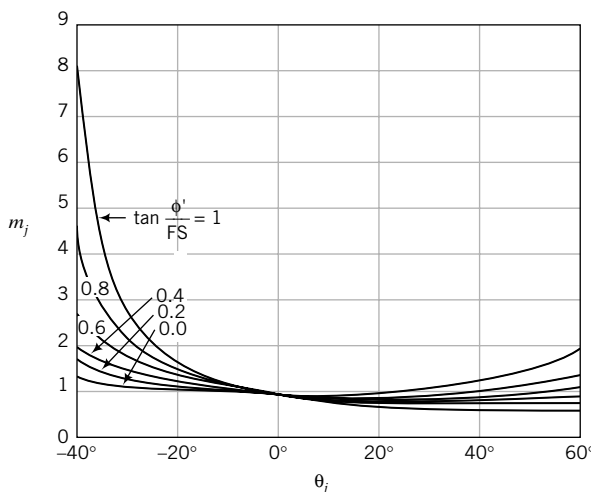


FIGURE 16.11 The m_j to be used in Bishop's method.

8. Repeat the procedure from item 2 to item 7 until the smallest factor of safety is found. There are several techniques that are used to reduce the number of trial slip surfaces. One simple technique is to draw a grid and selectively use the nodal points as centers of rotation. Commercially available programs use different methods to optimize the search for the slip plane with the least factor of safety.

THE ESSENTIAL POINTS ARE:

1. The appropriate value of ϕ' to use is ϕ'_{cs} , except for fissured, overconsolidated fine-grained soils, where you should use $\phi' = \phi'_r$. Use conservative values of s_u . These values should ideally come from direct simple shear tests.
2. Tension cracks in fine-grained soils reduce the factor of safety of a slope. Tension cracks may also provide channels for water to introduce seepage forces and weaken underlying soil layers.
3. For slopes adjacent to bodies of water, you should consider the effects of operating and environmental conditions on their stability.

EXAMPLE 16.3 Slope Stability Using Bishop's Method

Use Bishop's simplified method to estimate the factors of safety of the slope shown in Figure E16.3a. Assume the soil above the phreatic surface to be saturated. Consider three cases: Case 1—no tension crack; Case 2—tension crack; and Case 3—the tension crack in Case 2 is filled with water.

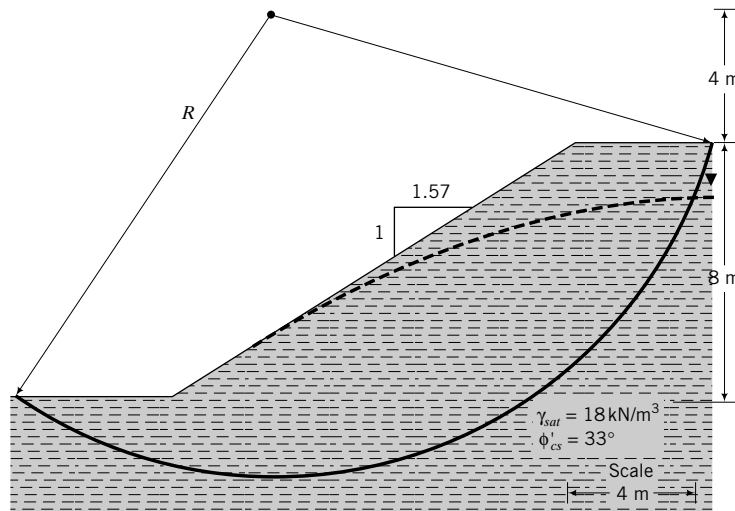


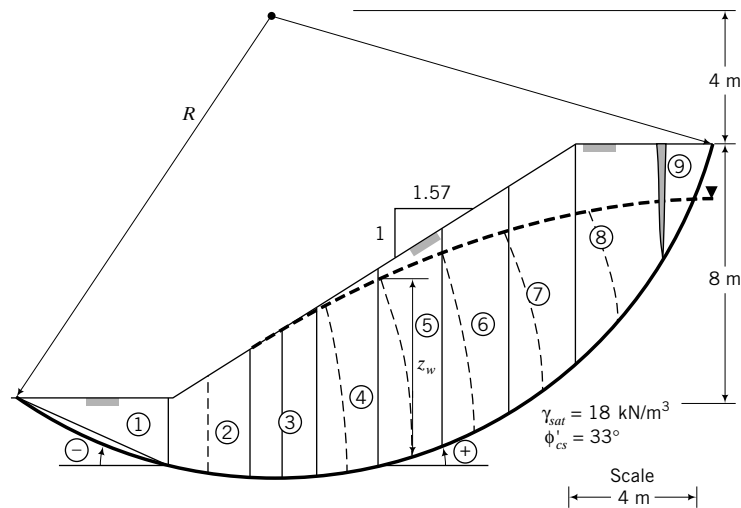
FIGURE E16.3a

Strategy Set up a table to carry out the calculations following the procedure in Section 16.10. If you have access to a spreadsheet program, use it. For the solution of this example, the author used Excel. Before dividing the sliding mass into slices, determine the depth of the tension crack and locate it on the crest of the slope as a side of a slice.

Solution 16.3

Step 1: Redraw the figure to scale.

See Figure E16.3b.

**FIGURE E16.3b**

Step 2: Find the depth of the tension crack.

$$z_{cr} = \frac{2s_u}{\gamma} = \frac{2 \times 30}{18} = 3.33 \text{ m}$$

Step 3: Divide the sliding mass into slices.

Find a height from the crest to the failure surface that equals z_{cr} and sketch in the tension crack. Use this location of the tension crack as a side of a slice. In Figure E16.3b, the sliding mass is divided into nine slices.

Step 4: Set up a spreadsheet.

See Table E16.3.

TABLE E16.3 Bishop's Simplified Method

Homogeneous soil

s_u	30 kPa
ϕ'	33°
γ_w	9.8 kN/m^3
γ_{sat}	18 kN/m^3
z_{cr}	3.33 m
FS	1.05 assumed

No tension crack

Slice	b (m)	z (m)	W = $\gamma b z$ (kN)	z_w (m)	r_u	θ (deg)	m_j	$W \sin \theta$	ESA	TSA
									$W(1 - r_u)(\tan \phi')m_j$	$s_u b / \cos \theta$
1	4.9	1	88.2	1	0.54	-23	1.47	-34.5	38.3	159.7
2	2.5	3.6	162.0	3.6	0.54	-10	1.14	-28.1	54.6	76.2
3	2	4.6	165.6	4.6	0.54	0	1.00	0.0	49.0	60.0
4	2	5.6	201.6	5	0.49	9	0.92	31.5	62.1	60.7
5	2	6.5	234.0	5.5	0.46	17	0.88	68.4	72.2	62.7
6	2	6.9	248.4	5.3	0.42	29	0.85	120.4	80.1	68.6
7	2	6.8	244.8	4.5	0.36	39.5	0.86	155.7	87.6	77.8
8	2.5	5.3	238.5	2.9	0.30	49.5	0.90	181.4	97.5	115.5
9	1.6	1.6	46.1	0.1	0.03	65	1.02	41.8	29.6	113.6
Sum								536.6	570.9	794.8
FS									1.06	1.48

(continued)

Tension crack

FS = 1 assumed										
Slice	<i>b</i> (m)	<i>z</i> (m)	<i>W</i> = $\gamma b z$ (kN)	<i>z_w</i> (m)	<i>r_u</i>	θ (deg)	<i>m_j</i>	<i>W sin θ</i>	ESA	TSA
									<i>W(1 - r_u)(tan φ')m_j</i>	<i>s_ub/cos θ</i>
1	4.9	1	88.2	1	0.54	-23	1.50	-34.5	39.1	159.7
2	2.5	3.6	162.0	3.6	0.54	-10	1.15	-28.1	55.0	76.2
3	2	4.6	165.6	4.6	0.54	0	1.00	0.0	49.0	60.0
4	2	5.6	201.6	5	0.49	9	0.92	31.5	61.8	60.7
5	2	6.5	234.0	5.5	0.46	17	0.87	68.4	71.5	62.7
6	2	6.9	248.4	5.3	0.42	29	0.84	120.4	78.9	68.6
7	2	6.8	244.8	4.5	0.36	39.5	0.84	155.7	85.8	77.8
8	2.5	5.3	238.5	2.9	0.30	49.5	0.87	181.4	95.1	115.5
9	1.6	1.6	46.1	0.1	0.03	65	0.99	41.8	0.0	0.0
									Sum	536.6
									FS	536.2
										681.2
										1.00
										1.27

Tension crack filled with water

R = 14.3 m TCM/R = 23.7 kN FS = 0.95 assumed										
Slice	<i>b</i> (m)	<i>z</i> (m)	<i>W</i> = $\gamma b z$ (kN)	<i>z_w</i> (m)	<i>r_u</i>	θ (deg)	<i>m_j</i>	<i>W sin θ</i>	ESA	TSA
									<i>W(1 - r_u)(tan φ')m_j</i>	<i>s_ub/cos θ</i>
1	4.9	1	88.2	1	0.54	-23	1.53	-34.5	39.9	159.7
2	2.5	3.6	162.0	3.6	0.54	-10	1.15	-28.1	55.3	76.2
3	2	4.6	165.6	4.6	0.54	0	1.00	0.0	49.0	60.0
4	2	5.6	201.6	5	0.49	9	0.91	31.5	61.5	60.7
5	2	6.5	234.0	5.5	0.46	17	0.86	68.4	70.9	62.7
6	2	6.9	248.4	5.3	0.42	29	0.83	120.4	77.8	68.6
7	2	6.8	244.8	4.5	0.36	39.5	0.83	155.7	84.3	77.8
8	2.5	5.3	238.5	2.9	0.30	49.5	0.86	181.4	93.0	115.5
9	1.6	1.6	46.1	0.1	0.03	65	0.96	41.8	0.0	0.0
									Sum	536.6
									FS	531.7
										681.2
										0.95
										1.22

Step 5: Extract the required values.

Follow the procedure in Section 16.10. The weight $W = \gamma_{sat}bz$. When the tension crack is considered, the shear resistance of slice ⑨ is neglected. When water fills the tension crack, the moment of the hydrostatic pressure in the tension crack is

$$TCM = \frac{1}{2}\gamma_w z_{cr}^2 \left(z_s + \frac{2}{3}z_{cr} \right)$$

For an ESA, assume a value of FS and then change this value until it becomes equal to the calculated value.

Step 6: Compare the factors of safety.

Condition	FS	
	ESA	TSA
Without tension crack	1.06	1.48
With tension crack	1.00	1.27
Tension crack filled with water	0.95	1.22

The smallest factor of safety occurs using an ESA with the tension crack filled with water. The slope, of course, fails because $FS < 1$.

EXAMPLE 16.4 Slope Stability Using Bishop's Method for Two-Layered Soils

Determine the factor of safety of the slope shown in Figure E16.4a. Assume no tension crack.

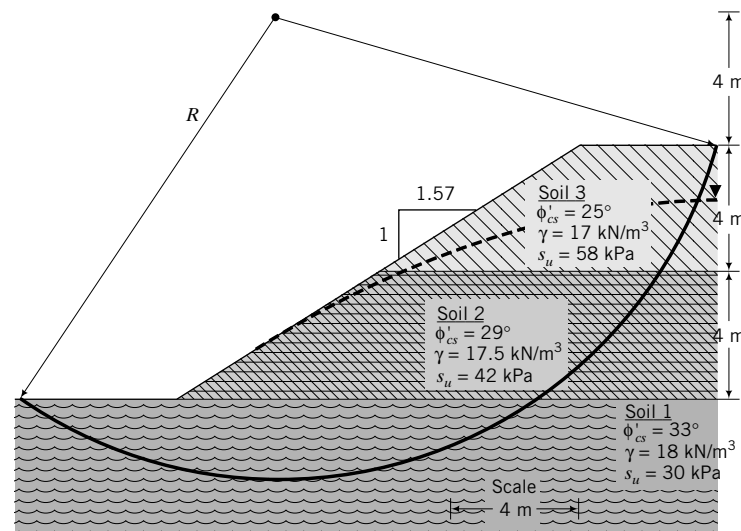


FIGURE E16.4a

Strategy Follow the same strategy as described in Example 16.3.

Solution 16.4

Step 1: Redraw the figure to scale.

See Figure E16.4b.

Step 2: Divide the sliding mass into slices, as shown in Figure E16.4b.

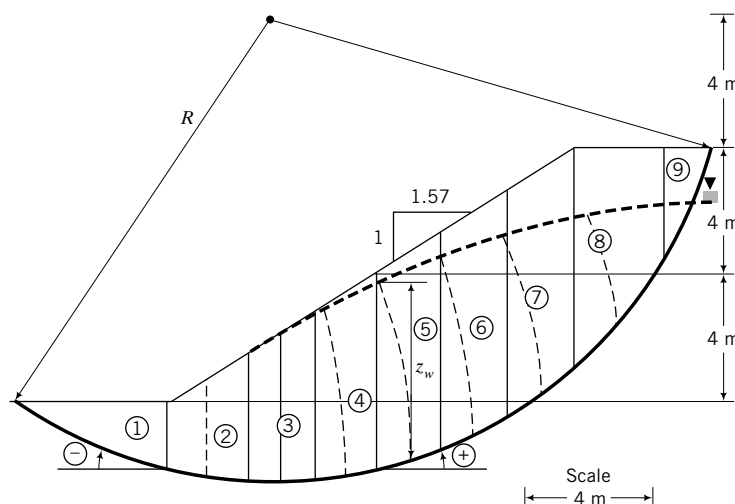


FIGURE E16.4b

Step 3: Set up a spreadsheet.

See Table E16.4.

TABLE E16.4 Three Soil Layers

Slice	b (m)	Soil 1		Soil 2		Soil 3		θ (deg)	m_j	$W \sin \theta$	ESA	TSA
		z_1 (m)	z_2 (m)	z_3 (m)	$W = \gamma b z$ (kN)	z_w (m)	r_u				$s_u b / \cos \theta$	
1	4.9	1	0	0	88.2	1	0.54	-23	1.49	-34.5	39.0	159.7
2	2.5	2.3	1.3	0	160.4	3.6	0.55	-10	1.15	-27.8	53.7	76.2
3	2	2.4	2.2	0	163.4	4.6	0.55	0	1.00	0.0	47.6	60.0
4	2	2	3.6	0	198.0	5	0.49	9	0.92	31.0	59.7	60.7
5	2	0.9	4.1	1.5	226.9	5.5	0.48	17	0.87	66.3	67.6	62.7
6	2	0.8	4.1	2	240.3	5.3	0.43	29	0.84	116.5	74.7	68.6
7	2	0	3.7	3.1	234.9	4.5	0.38	39.5	0.89	149.4	72.6	108.9
8	2.5	0	1.5	3.8	227.1	2.9	0.31	49.5	0.94	172.7	81.1	161.7
9	1.6	0	0	1.6	43.5	0.1	0.04	65	1.19	39.4	23.3	219.6
Sum										513.1	519.1	978.1
FS											1.01	1.91

Step 4: Extract the required values and perform the calculations. Let z_1 , z_2 , and z_3 be the heights of soils 1, 2, and 3, respectively, in each slice. Slice ①, for example, only contains soil 1, while slice ⑥ contains each soil. Use the appropriate value of ϕ'_{cs} and s_u for each of the slices. For example, $\phi'_{cs} = 30^\circ$ and $s_u = 30$ kPa for soil 1 are applicable to slices ① through ⑥, while $\phi'_{cs} = 24^\circ$ and $s_u = 58$ kPa are applicable to slice ⑨.

EXAMPLE 16.5 Slope Stability Using Janbu's Method

A coarse-grained fill was placed on saturated clay. A noncircular slip surface was assumed, as shown in Figure E16.5a. Determine the factor of safety of the slope using an ESA. The groundwater level is below the assumed slip surface.

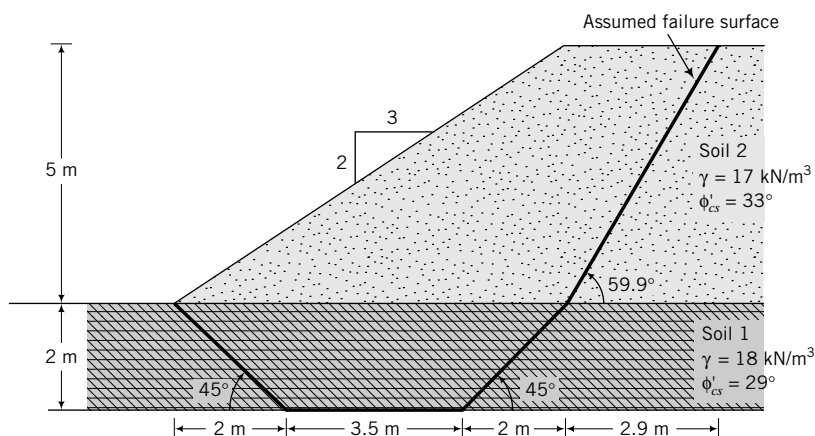


FIGURE E16.5a

Strategy Since a noncircular slip surface is assumed, you should use Janbu's method. Groundwater is below the slip surface; that is, $r_u = 0$.

Solution 16.5

Step 1: Redraw the figure to scale.

See Figure E16.5b.

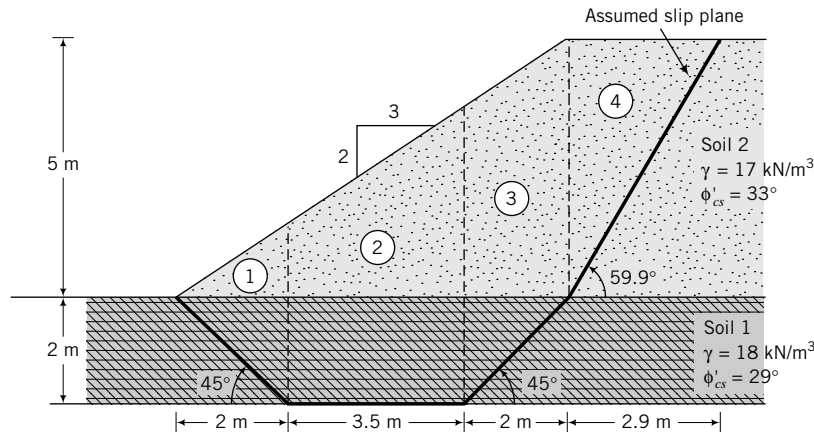


FIGURE E16.5b

Step 2: Divide the sliding mass into a number of slices.

In this case, four slices are sufficient.

Step 3: Extract the required parameters.

Step 4: Carry out the calculations.

Use a spreadsheet, as shown in Table E16.5.

TABLE E16.5 Janbu's Method

	Soil 1	Soil 1
ϕ'	29°	33.5°
γ_w	9.8	kN/m ³
γ_{sat}	18	kN/m ³
d	4.5	m
l	11.5	
d/l	0.39	f_o
FS	1.04	assumed

Slice	b (m)	z₁ (m)	z₂ (m)	W = γbz (kN)	θ (deg)	m_j	ESA	
							W tan θ	W tan φ' (cos θ) m_j
1	2	1	0.7	59.8	-45	3.03	-59.8	71.0
2	3.5	2	2.5	274.8	0	1.00	0.0	152.3
3	2	1	4.3	182.2	45	0.92	182.2	65.9
4	2.9	0	2.5	123.3	59.9	0.95	212.6	38.9
							Sum	335.0
							FS	1.04

What's next . . . Charts can be prepared to allow you to quickly estimate the stability of slopes with simple geometry in homogeneous soils. In the next section, we present some of the popular charts.

16.11 STABILITY OF SLOPES WITH SIMPLE GEOMETRY

16.11.1 Taylor's Method

Let us reconsider the stability of a slope using a TSA, as expressed by Equation (16.34). We can rewrite Equation (16.34) as

$$FS = N_o \frac{\Sigma(s_u)_j}{\Sigma(\gamma z)_j} \quad (16.45)$$

where N_o is called stability number and depends mainly on the geometry of the slope. Taylor (1948) used Equation (16.45) to prepare a chart to determine the stability of slopes in a homogeneous deposit of soil underlain by a much stiffer soil or rock. He assumed no tension crack, failure occurring by rotation, no surcharge or external loading, and no open water outside the slope.

The procedure to use Taylor's chart to determine the safe slope in a homogeneous deposit of soil using a TSA, with reference to Figure 16.12, is as follows:

1. Calculate $n_d = D_o/H_o$, where D_o is the depth from the toe to the top of the stiff layer and H_o is the height of the slope.
2. Calculate $N_o = FS(\gamma H_o/s_u)$.
3. Read the value of α_s at the intersection of n_d and N_o .

If you wish to check the factor of safety of an existing slope or a desired slope, the procedure is as follows:

1. Calculate $n_d = D_o/H_o$.

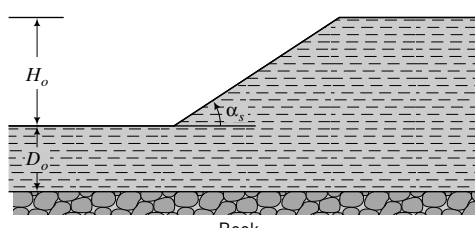
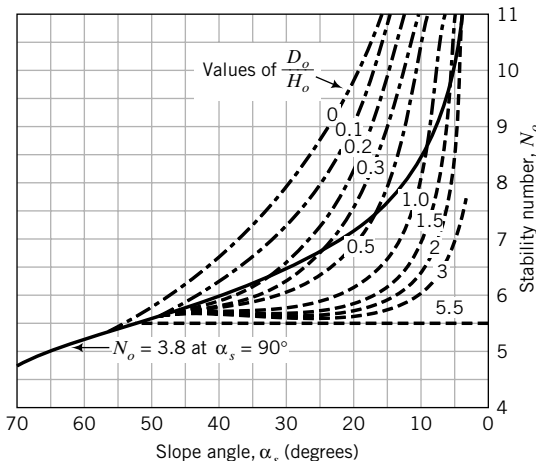


FIGURE 16.12 Taylor's curves for determining the stability of simple slopes.

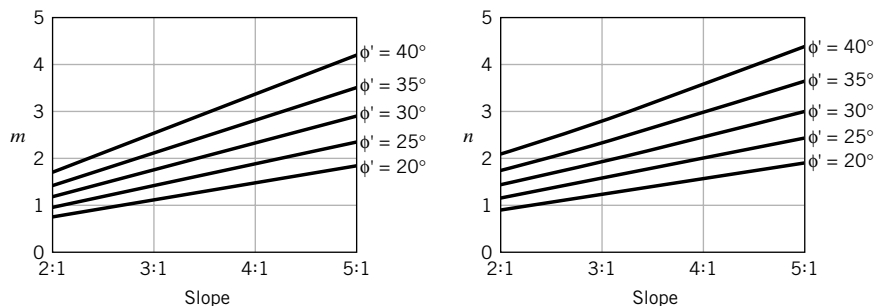


FIGURE 16.13 Values for m and n for the Bishop–Morgenstern method.

2. Read the value of N_o at the intersection of α_s and n_d .

3. Calculate $\text{FS} = \frac{N_o s_u}{\gamma H_o}$.

16.11.2 Bishop–Morgenstern Method

Bishop and Morgenstern (1960) prepared a number of charts for homogeneous soil slopes with simple geometry using Bishop's simplified method. Equation (16.30) was written as

$$\text{FS} = m - nr_u \quad (16.46)$$

where m and n are stability coefficients (Figure 16.13) that depend on the friction angle and the geometry of the slope.

The procedure to use the Bishop–Morgenstern method is as follows:

1. Assume a circular slip surface.
2. Draw the phreatic surface (Chapter 14).
3. Calculate $r_u = \gamma_w(z_w)_j / (\gamma_j z_j)$ (see Figure 16.10). Use a weighted average value of r_u within the sliding mass. A practical range of values of r_u is $\frac{1}{3}$ to $\frac{1}{2}$.
4. With $\phi' = \phi'_{cs}$ and the assumed slope angle, determine the values of m and n from Figure 16.13.
5. Calculate FS using Equation (16.46).

EXAMPLE 16.6 Slope Stability Using Taylor's Method

Determine the factor of safety of the slope shown in Figure E16.6.

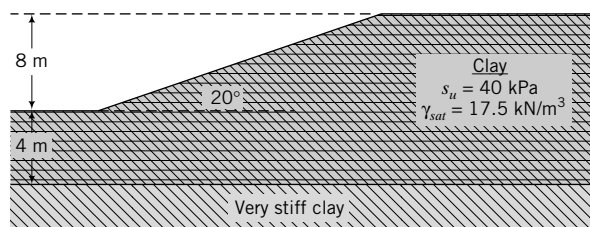


FIGURE E16.6

Strategy Follow the procedures in Section 16.11.

Solution 16.6**Step 1:** Calculate n_d .

$$H_o = 8 \text{ m}, D_o = 4 \text{ m.}$$

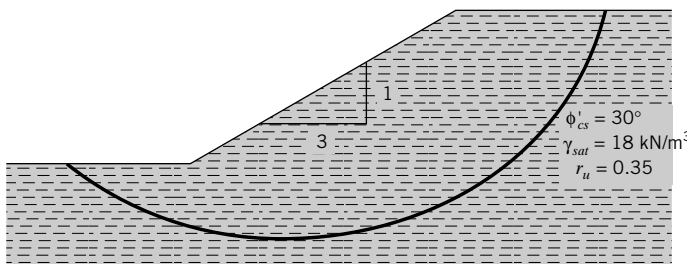
$$n_d = \frac{D_o}{H_o} = \frac{4}{8} = 0.5$$

Step 2: Determine N_o .From Figure 16.12, for $\alpha_s = 20$ and $n_d = 0.5$, we get $N_o = 6.8$.**Step 3:** Calculate FS.

$$\text{FS} = \frac{N_o s_u}{\gamma H_o} = \frac{6.8 \times 40}{17.5 \times 8} = 1.94$$

EXAMPLE 16.7 Slope Stability Using the Bishop–Morgenstern Method

Determine the factor of safety of the slope shown in Figure E16.7.

**FIGURE E16.7**

Strategy Use the Bishop and Morgenstern (1960) charts and equations. Follow the procedures in Section 16.11. Since you are given r_u , you only need to do Steps 4 and 5.

Solution 16.7**Step 1:** Determine m and n .From Figure 16.13, $m = 1.73$ and $n = 1.92$ for a slope of 3:1 and $\phi'_{cs} = 30^\circ$.**Step 2:** Calculate FS.

$$\text{FS} = m - nr_u = 1.73 - 1.92 \times 0.35 = 1.06$$

16.12 FACTOR OF SAFETY (FS)

It is difficult to specify a particular FS for slopes because it is dependent on many factors, including the geological conditions, the population density, types and density of existing and anticipated structures, reliability of soil parameters, groundwater and environmental conditions, and natural hazards. Consequently, the decision on what factor of safety to use is subjective. The usual range of factor of safety is 1.15 to 1.5. In the mining industry, tailing dams are designed with $\text{FS} \approx 1.1$ to 1.2. As a general guide, $\text{FS} \approx 1.3$ is suitable for common slopes such as a cut for a highway. For a dam, $\text{FS} \approx 1.4$ is common.

16.13 SUMMARY

In this chapter, we examined the stability of simple slopes. Slope failures are often catastrophic and may cause extensive destruction and deaths. Slopes usually fail from natural causes (erosion, seepage, and earthquakes) and by construction activities (excavation, change of land surface, etc.). The analyses we considered were based on limit equilibrium, which requires simplifying assumptions. Careful judgment and experience are needed to evaluate slope stability. The geology of a site is of particular importance in determining slope stability. You should consider both an effective stress analysis and a total stress analysis for slopes in fine-grained soils and an effective stress analysis for slopes in coarse-grained soils. The main sources of errors in slope stability analysis are the shear strength parameters, especially s_u , and the determination of the porewater pressures.

Self-Assessment



Access Chapter 16 at <http://www.wiley.com/college/budhu> to take the end-of-chapter quiz to test your understanding of this chapter.

Practical Example

EXAMPLE 16.8 Design of a Slope in a Canal

A lake is required at a housing project for drainage and recreation. The soil profile is shown in Figure E16.8a. Based on historical weather data and nearby drainage conditions, the water level is expected to fluctuate by 2 m. A 1 (V):1.5 (H) slope is selected. Evaluate the stability of this slope.

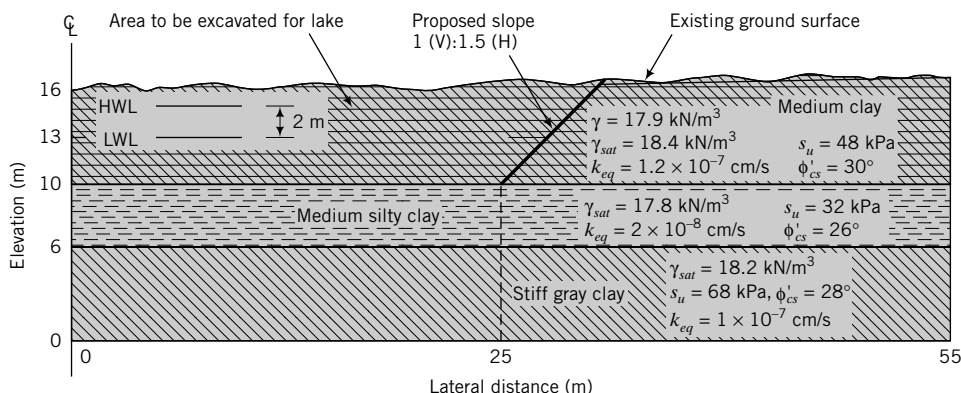


FIGURE E16.8a

Strategy It is best to use a slope stability program. We will use a freely available program, STB2006, which you can obtain from <http://geo.verruijt.net>. This program is based on Bishop's method and treats the soil as a cohesive-frictional material. In this book, soil is treated as a dilatant-frictional material. To use this program for undrained conditions, substitute the undrained shear strength for cohesion and input a friction angle of zero. The worst-case condition is rapid drawdown to the bottom of the proposed lake.

Solution 16.8

Step 1: Input data.

We will investigate two cases. One is a rapid drawdown to the low water level (LWL) and the other is a gradual drawdown, neglecting seepage stresses (the program does not consider seepage stresses). The most serious case is rapid drawdown to the bottom of the proposed lake. We will assume here that the client will maintain the lake level to the LWL. Define nodal points to establish the top of each soil layer and the groundwater level within the slope and in the lake, as shown in Figure E16.8b and c.

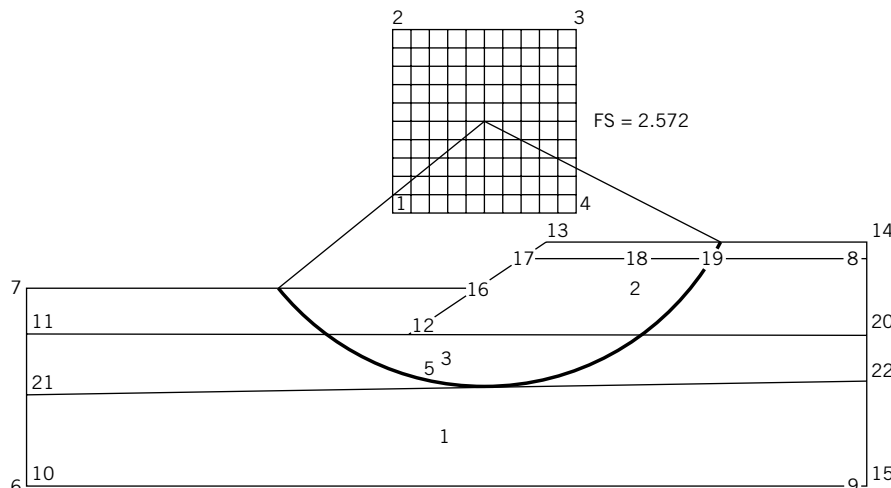


FIGURE E16.8b
Rapid drawdown.

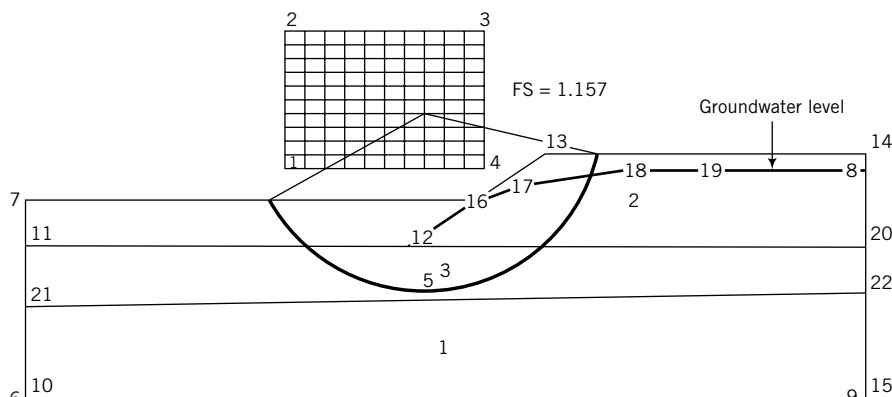


FIGURE E16.8c
Gradual drawdown.

Case 1: During rapid drawdown, the water level within the slope remains constant while the water in the lake drops to the low water level. We can assume that undrained condition prevails. The strength parameter is the undrained shear strength. Partial listing of the input soil parameters is shown in Table E16.8a. Click on "help" when running STB2006 to see the notation used.

TABLE E16.8a Rapid Drawdown

Properties of soils

Soil	Wd kN/m ³	Ws kN/m ³	Ko —	$s_u (c)$ kN/m ²	phi degrees
1	18.200	18.200	1.000	68.000	0.000
2	17.900	18.400	1.000	48.000	0.000
3	17.800	17.800	1.000	32.000	0.000

Coordinates of nodes

Node	x	y
1	20.000	18.000
2	20.000	24.000
3	35.000	24.000
4	35.000	18.000
5		7.000
6	0.000	0.000
7	0.000	13.000

(continued)

TABLE E16.8a (continued)

Node	x	y
8	55.000	15.000
9	55.000	0.000
10	0.000	0.000
11	0.000	10.000
12	25.000	10.000
13	34.000	16.000
14	55.000	16.000
15	55.000	0.000
16	29.554	13.000
17	32.500	15.000
18	40.000	15.000
19	45.000	15.000
20	55.000	10.000
21	0.000	6.000
22	55.000	7.000

Case 2: For gradual drawdown, we have to estimate the groundwater level within the slope for the desired time period (see Chapter 14). The estimated groundwater level for a year is shown in Figure E16.8c. The appropriate shear strength parameter is the friction angle. The input soil parameters for the gradual drawdown are shown in Table E16.8b.

TABLE E16.8b Gradual Drawdown

Properties of soils					
Soil	Wd kN/m³	Ws kN/m³	Ko —	s_u (c) kN/m²	phi degrees
1	18.200	18.200	1.000	0.000	28.000
2	17.900	18.400	1.000	0.000	30.000
3	17.800	17.800	1.000	0.000	26.000

Coordinates of nodes		
Node	x	y
1	17.000	15.000
2	17.000	24.000
3	30.000	24.000
4	30.000	15.000
5	26.100	7.000
6	0.000	0.000
7	0.000	13.000
8	55.000	15.000
9	55.000	0.000
10	0.000	0.000
11	0.000	10.000
12	25.000	10.000
13	34.000	16.000
14	55.000	16.000
15	55.000	0.000
16	29.554	13.000
17	32.500	14.000
18	40.000	14.800
19	45.000	15.000
20	55.000	10.000
21	0.000	6.000
22	55.000	7.000

Step 2: Run the program and evaluate the results.

In STB2006, you have to specify the search area for the centers of rotation of the slip circles. This is done by defining the coordinates of nodes 1 through 4. You have to try different search areas. Also, you have to define the search depth of the slip circles. This is specified by the coordinates of node 5. The minimum FS for Case 1 is 2.572 (Figure E16.8b) while for Case 2 it is 1.157 (Figure E16.8c).

EXERCISES

Theory

- 16.1** A clay slope fails, as shown in Figure P16.1. Derive an equation for the undrained shear strength of the clay.

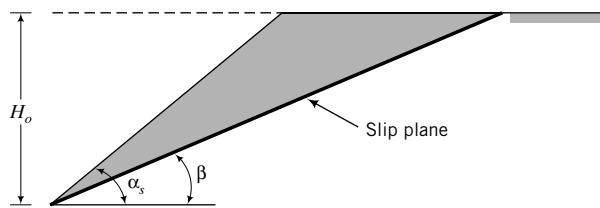


FIGURE P16.1

- 16.2** Derive an equation for the factor of safety of the slope in Figure P16.2 using the mechanism shown.

- 16.3** Figure P16.3 shows the profile of a beach on a lake. It is proposed to draw down the lake by 2 m. Determine the slope angle of the beach below the high water level after the drawdown. You may assume an infinite slope failure mechanism. The critical state friction angle of the sand is 30° .

Problem Solving

- 16.4** A cut for a highway is shown in Figure P16.4. Determine the factor of safety of the slope using an ESA and

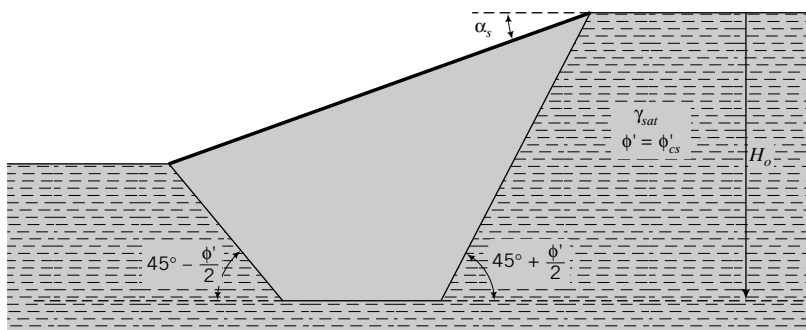


FIGURE P16.2

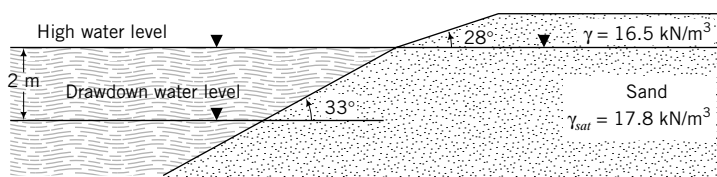


FIGURE P16.3

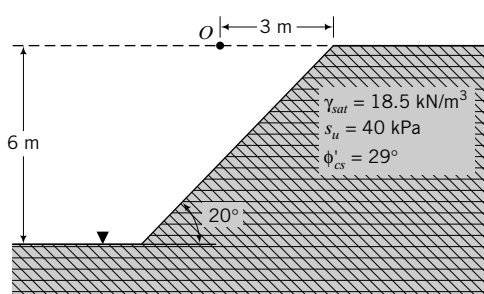


FIGURE P16.4

a TSA. Assume a center of rotation, O , such that the slip surface passes through the toe of the slope.

- 16.5** Determine the factor of safety of the slope shown in Figure P16.5 using an ESA and a TSA. The point of rotation is indicated by O and the line represent-

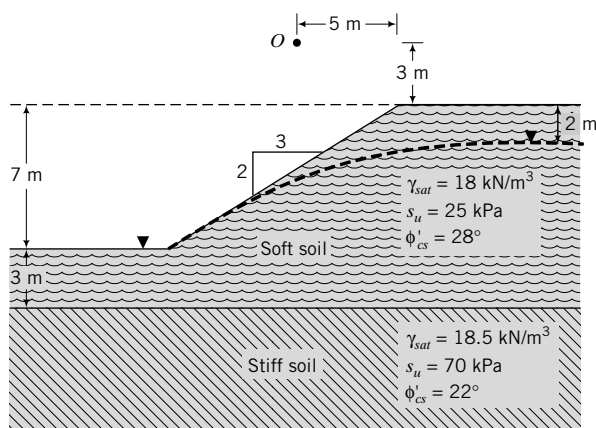


FIGURE P16.5

ing the top of the stiff soil is a tangent to the failure plane.

- 16.6** A compacted earth fill is constructed on a soft, saturated clay (Figure P16.6). The fill was compacted to an average dry unit weight of 19 kN/m^3 and water content of 15%. The shearing strength of the fill was determined by CU tests on samples compacted to representative field conditions. The shear strength parameters are $s_u = 45 \text{ kPa}$, $\phi'_p = 34^\circ$, and $\phi'_{cs} = 28^\circ$. The variation of undrained shear strength of the soft clay with depth as determined by simple shear tests is shown in Figure P16.6, and the friction angle at the critical state is $\phi'_{cs} = 30^\circ$. The average water content of the soft clay is 40%. Compute the factor of safety using Bishop's simplified method. Assume that a tension crack will develop in the fill.

- 16.7** A cross section of a canal is shown in Figure P16.7. Determine the factor of safety for (a) the existing condition and (b) a rapid drawdown of the water level in the canal. Use Bishop's method. The center of rotation of the sliding mass is at coordinates $x = 113 \text{ m}$ and $y = 133 \text{ m}$. The rock surface is tangent

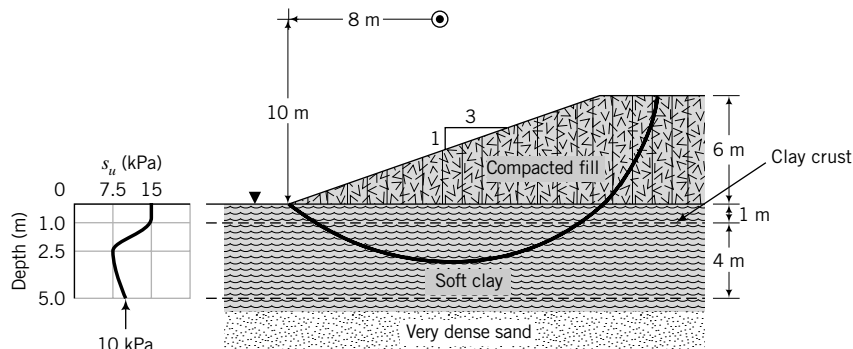


FIGURE P16.6

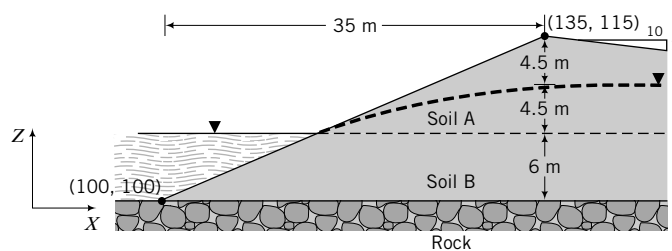


FIGURE P16.7

to the slip plane. Assume the soil above the ground-water level is saturated. The properties of the soil are as follows:

Soil	Description	γ_{sat} (kN/m ³)	s_u (kPa)	ϕ'_{cs} (degrees)
A	Clay	17.8	34	30
B	Clay	18.0	21	28

- 16.8** Use Janbu's method to determine the factor of safety of the slope shown in Figure P16.8. Assume the soil above the groundwater level is saturated.

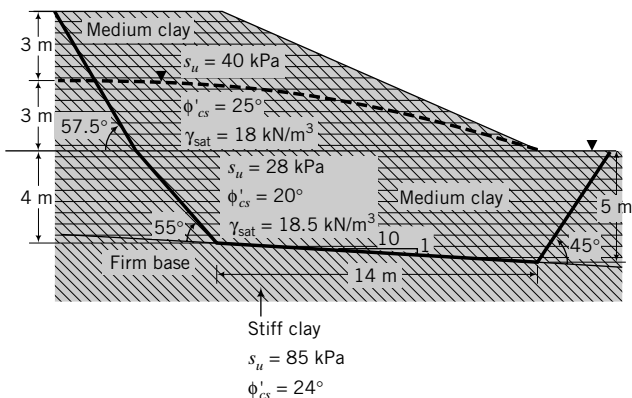


FIGURE P16.8

- 16.9** Use Taylor's method to determine the factor of safety of the slope shown in Figure P16.9.

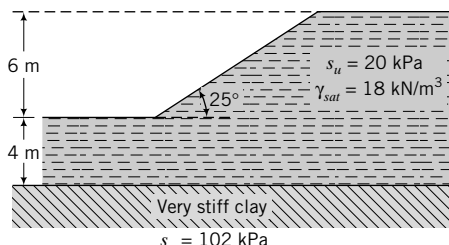


FIGURE P16.9

- 16.10** Use Taylor's method to determine the slope in Figure P16.10 for FS = 1.25.

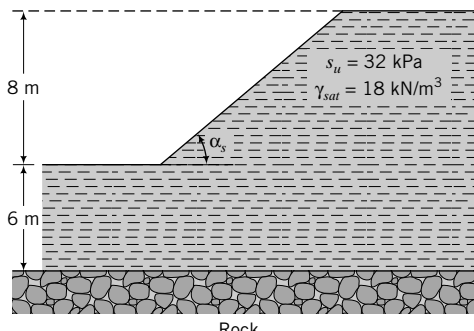
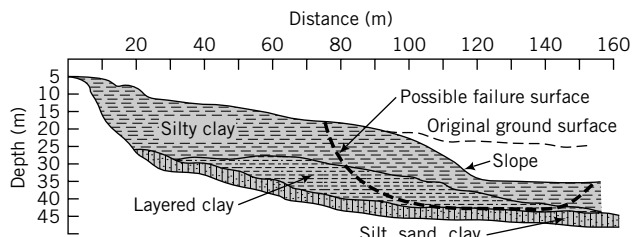


FIGURE P16.10

- 16.11** Determine the factor of safety of a 2:1 slope with $r_u = 0.25$, $\phi'_{cs} = 27^\circ$ using the Bishop–Morgenstern method.

Practical

- 16.12** The soil at a site is shown in Figure P16.12. A slope will be cut to facilitate the construction of a roadway. One possible failure surface is shown in Figure P16.12. Determine the factor of safety. The shear strength parameters were obtained from direct simple shear tests.



Soil	Shear strength parameters		Unit weight γ_{sat} (kN/m ³)
	s_u (kPa)	ϕ'_{cs}	
Silty clay	22	25°	17
Layered clay	48	22°	18
Silt, sand, clay	0	23°	17.5

FIGURE P16.12

- 16.13** A cross section of a levee is shown in Figure P16.13a on the next page. (a) Describe how you would determine the stability of the levee. You must provide sufficient justification for the loading conditions you would consider. (b) Use a slope stability software program such as STB2006 to analyze the stability. Vane shear test data for the medium-to-soft clay is shown in Figure P16.13b. The average water content is 40%. (c) If the upstream slope is subjected to scouring and its gradient can change, research and describe methods you would use to protect it. The subscripts p and cs on the strength parameters in Figure P16.13a denote peak and critical state condition, respectively.

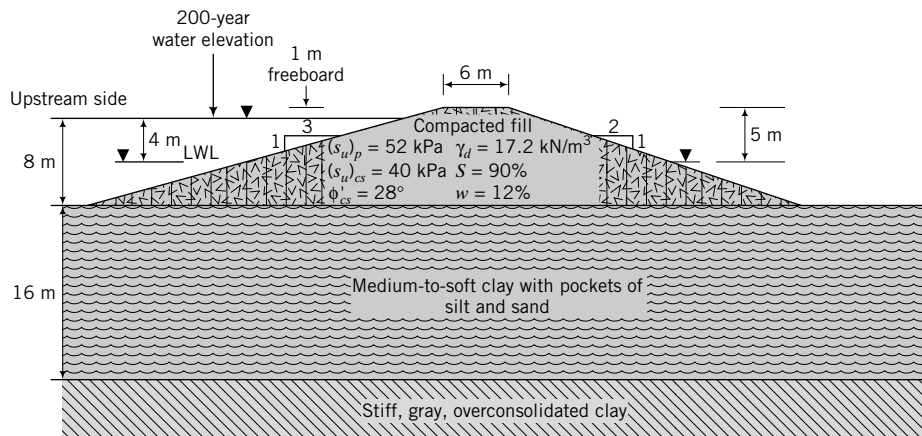


FIGURE P16.13a

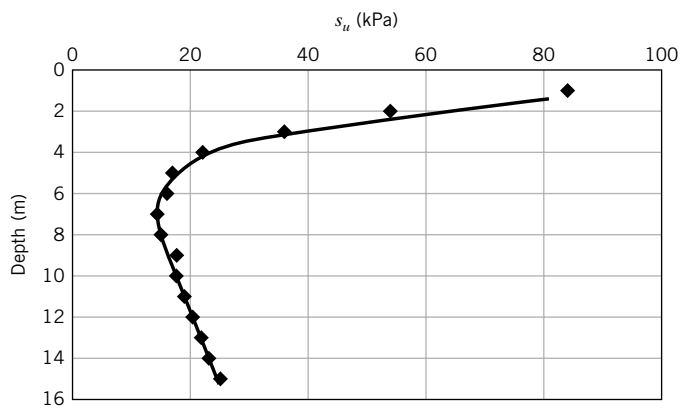


FIGURE P16.13b

A COLLECTION OF FREQUENTLY USED SOIL PARAMETERS AND CORRELATIONS

TABLE A.1 Typical Values of Unit Weight for Soils

Soil type	γ_{sat} (kN/m ³)	γ_d (kN/m ³)
Gravel	20–22	15–17
Sand	18–20	13–16
Silt	18–20	14–18
Clay	16–22	14–21

TABLE A.2 Description of Coarse-Grained Soils Based on Relative Density and Porosity

D_r (%)	Porosity, n (%)	Description
0–20	100–80	Very loose
20–40	80–60	Loose
40–70	60–30	Medium dense or firm
70–85	30–15	Dense
85–100	<15	Very dense

TABLE A.3 Soil Types, Description, and Average Grain Size According to ASTM-CS

Soil type	Description	Average grain size
Gravel	Rounded and/or angular bulky hard rock	Coarse: 75 mm to 19 mm Fine: 19 mm to 4.75 mm
Sand	Rounded and/or angular bulky hard rock	Coarse: 4.75 mm to 2.0 mm Medium: 2.0 mm to 0.425 mm Fine: 0.425 mm to 0.075 mm
Silt	Particles smaller than 0.075 mm exhibit little or no strength when dried	0.075 mm to 0.002 mm
Clay	Particles smaller than 0.002 mm exhibit significant strength when dried; water reduces strength	<0.002 mm

TABLE A.4 Description of Soil Strength Based on Liquidity Index

Values of LI	Description of soil strength
LI < 0	Semisolid state—high strength, brittle (sudden fracture expected)
0 < LI < 1	Plastic state—intermediate strength, soil deforms like a plastic material
LI > 1	Liquid state—low strength, soil deforms like a viscous fluid

TABLE A.5 Typical Atterberg Limits for Soils

Soil type	LL (%)	PL (%)	PI (%)
Sand		Nonplastic	
Silt	30–40	20–25	10–15
Clay	40–150	25–50	15–100
Minerals			
Kaolinite	50–60	30–40	10–25
Illite	95–120	50–60	50–70
Montmorillonite	290–710	50–100	200–660

TABLE A.6 Hydraulic Conductivity for Common Soil Types

Soil type	k_z (cm/s)	Description	Drainage
Clean gravel (GW, GP)	>1.0	High	Very good
Clean sands, clean sand and gravel mixtures (SW, SP)	1.0 to 10^{-3}	Medium	Good
Fine sands, silts, mixtures comprising sands, silts, and clays (SM-SC)	10^{-3} to 10^{-5}	Low	Poor
Weathered and fissured clays			
Silt, silty clay (MH, ML)	10^{-5} to 10^{-7}	Very low	Poor
Homogeneous clays (CL, CH)	< 10^{-7}	Practically impervious	Very poor

TABLE A.7 Typical Values of Poisson's Ratio

Soil type	Description	ν'
Clay	Soft	0.35–0.4
	Medium	0.3–0.35
	Stiff	0.2–0.3
Sand	Loose	0.15–0.25
	Medium	0.25–0.3
	Dense	0.25–0.35

TABLE A.8 Typical Values of *E* and *G*

Soil type	Description	<i>E</i>* (MPa)	<i>G</i>* (MPa)
Clay	Soft	1–15	0.5–5
	Medium	15–30	5–15
	Stiff	30–100	15–40
Sand	Loose	10–20	5–10
	Medium	20–40	10–15
	Dense	40–80	15–35

*These are average secant elastic moduli for drained condition (see Chapter 10).

TABLE A.9 Ranges of Friction Angles (degrees) for Soils

Soil type	ϕ'_{cs}	ϕ'_p	ϕ'_r
Gravel	30–35	30–50	
Mixture of gravel and sand with fine-grained soils	28–33	30–40	
Sand	27–37 ^a	32–50	
Silt or silty sand	24–32	27–35	
Clays	15–30	20–30	5–15

^aHigher values (32° to 37°) in the range are for sands with significant amounts of feldspar (Bolton, 1986). Lower values (27° to 32°) in the range are for quartz sands. The peak delation angle, α_{pr} , ranges from 0 to 15° .

TABLE A.10 A_f Values

Type of Clay	A_f
Highly sensitive	$\frac{3}{4}$ to 1.0
Normally consolidated	$\frac{1}{2}$ to 1
Compacted sandy clay	$\frac{1}{4}$ to $\frac{3}{4}$
Lightly overconsolidated clays	0 to $\frac{1}{2}$
Compacted clay–gravel	$-\frac{1}{4}$ to $\frac{1}{4}$
Heavily overconsolidated clays	$-\frac{1}{2}$ to 0

SOURCE: After Skempton (1954).

TABLE A.11 Correlation of N , N_{60} , γ , D_r , and ϕ' for Coarse-Grained Soils

N	N_{60}	Compactness	γ (kN/m ³)	D_r (%)	ϕ' (degrees)
0–4	0–3	Very loose	11–13	0–20	26–28
4–10	3–9	Loose	14–16	20–40	29–34
10–30	9–25	Medium	17–19	40–70	35–40*
30–50	25–45	Dense	20–21	70–85	38–45*
>50	>45	Very dense	>21	>85	>45*

*These values correspond to ϕ'_p .**TABLE A.12** Correlation of N_{60} and s_u for Saturated Fine-Grained Soils

N_{60}	Description	s_u (kPa)
0–2	Very soft	<10
3–5	Soft	10–25
6–9	Medium	25–50
10–15	Stiff	50–100
15–30	Very stiff	100–200
>30	Extremely stiff	>200

TABLE A.13 Empirical Soil Strength Relationships

Soil type	Equation	Reference
Normally consolidated clays	$\left(\frac{s_u}{\sigma'_z}\right)_{nc} = 0.11 + 0.0037 \text{ PI}$	Skempton (1957)
	$\left(\frac{s_u}{\sigma'_{zo}}\right) = 0.22$	Mesri (1975)
Overconsolidated clays	$\frac{(s_u/\sigma'_z)_{oc}}{(s_u/\sigma'_z)_{nc}} = (\text{OCR})^{0.8}$ See Note 1.	Ladd et al. (1977)
	$\frac{s_u}{\sigma'_z} = (0.23 \pm 0.04)\text{OCR}^{0.8}$ See Note 1.	Jamiolkowski et al. (1985)
Clean quartz sand	$\phi'_p = \phi'_{cs} + 3D_r(10 - \ln p'_f) - 3$, where p'_f is the mean effective stress at failure (in kPa) and D_r is relative density. This equation should only be used if $12 > (\phi'_p - \phi'_{cs}) > 0$.	Bolton (1986)

Note 1: These are applicable to direct simple shear tests. The estimated undrained shear strength from triaxial compression tests would be about 1.4 times greater.

TABLE A.14a Summary of Correlations Among Some Soil Parameters and CSM

Parameter	Relationship	Soil type	Reference
Compressibility	$\lambda \approx 0.59 \text{ PI}$ $C_c = 1.35 \text{ PI}$ PI = plasticity index	Remolded clays	Schofield and Wroth (1968)
Overconsolidation ratio	$\log(\text{OCR}) = \frac{2 - 2\text{LI} - \log\left(15.9 \frac{\sigma'_{zo}}{p_{atm}}\right)}{\Lambda}$ where $\Lambda = 1 - \frac{\kappa}{\lambda} \approx 0.8$	Remolded clays	Wood (1983)
Lateral earth pressure coefficient	$K_o^{nc} = \frac{6 - 2M_c}{6 + M_c}$ nc = normally consolidated, M_c = frictional constant in compression	Normally consolidated clays	N/A
Undrained shear strength	$(s_u)_w = (s_u)_{PL} \exp(-4.6 \text{ LI})$ or $(s_u)_w \approx 200 \exp(-4.6 \text{ LI})$ w = water content, LI = liquidity index	Remolded clays	N/A
	$\left(\frac{s_u}{\sigma'_z}\right) = \frac{\sin \phi'_{cs}[K_o + A_f(1 - K_o)]}{1 + (2A_f - 1)\sin \phi'_{cs}}$	One-dimensionally consolidated remolded clays	Wood (1990)
	A_f = Skempton's porewater pressure coefficient, ϕ'_{cs} = critical state friction angle, K_o = earth pressure coefficient at rest, σ'_z = vertical effective stress		
	$\frac{s_u}{p'_o} = 0.129 + 0.00435 \text{ PI}$ PI = plasticity index (%)	Normally consolidated clays/remolded clays	Wroth & Housby (1985)
	$\left(\frac{s_u}{\sigma'_z}\right) = 0.25$	Normally consolidated clays/remolded clays	Wood (1990)
Friction angle	$\phi'_{cs} = \sin^{-1} \left[0.35 - 0.1 \ln \left(\frac{\text{PI}}{100} \right) \right]$	Remolded clays	Wood (1990)
Stiffness	$E' = \frac{3p'(1 + e_o)(1 - 2\nu')}{\kappa}$ $G = \frac{1.5p'(1 + e_o)(1 - 2\nu')}{\kappa(1 + \nu')}$ $K' = \frac{(1 + e_o)}{\kappa} p'$	Remolded clays	N/A
	$E' = \frac{3p'_c(1 + e_c)(1 - 2\nu')}{\kappa}$ $K'_{max} = \frac{1 + e_c}{\kappa} p'_c$ $G = 0.5K'_{max}$	Overconsolidated clays	Randolph et al. (1979)

N/A = not applicable. These equations have all been derived from the CSM in this textbook.

TABLE A.14b Summary of Relationships Among Soil Strength Parameters from CSM

Relationship	CSM expression	Approximate expression for practical use	Usage
Tension cutoff mean effective stress and overconsolidation ratio	$t_c = \frac{p'_t}{p'_c} = \frac{1}{\left(1 + \frac{n_t^2}{M^2}\right)}$ Axisymmetric compression: $n_t = 3$, $M = M_c = \frac{6 \sin \phi'_{cs}}{3 - \sin \phi'_{cs}}$ Plane strain: $n_t = \sqrt{3}$, $M = M_c = \sqrt{3} \sin \phi'_{cs}$ $R_t = \frac{1}{t_c}$	Axisymmetric compression: $t_c = 0.0002 \phi'_{cs}^{1.92}$; $R_t = 5033 \phi'_{cs}^{-1.92}$ Plane strain: $t_c = 0.0011 \phi'_{cs}^{1.526}$; $R_t = 909 \phi'_{cs}^{-1.526}$ ϕ'_{cs} in degrees	<ul style="list-style-type: none"> To determine the overconsolidation ratio beyond which a soil will rupture from tension
Overconsolidation from stress invariants, R_o , and OCR	$R_o \approx \frac{\left[(3 - 2 \sin \phi'_{cs}) - \frac{(\sin \phi'_{cs} - 3)^2}{4(2 \sin \phi'_{cs} - 3)} \right]}{1 + 2(1 - \sin \phi'_{cs}) \text{OCR}^{\frac{1}{2}}} \text{OCR}$	$R_o \approx 1.45 \text{OCR}^{0.66}$; $\text{OCR} \leq 10$; $25^\circ < \phi'_{cs} < 30^\circ$ $R_o \approx 1.6 \text{OCR}^{0.62}$; $\text{OCR} > 10$; $25^\circ < \phi'_{cs} < 30^\circ$	<ul style="list-style-type: none"> To convert OCR to R_o below tension cutoff
Ratio of normalized yield (peak) shear strength and normalized critical state shear strength under triaxial drained condition	$\alpha_{pcs} = \frac{\frac{\tau_y}{p'_o} = \frac{\left(\frac{p'_y}{p'_o} - 1\right)(3 - M)}{M}}{\frac{\tau_f}{p'_o}}$ $\frac{p'_y}{p'_o} = \frac{(M^2 R_o + 18) + \sqrt{(M^2 R_o + 18)^2 - 36(M^2 + 9)}}{2(M^2 + 9)}$	$\alpha_{pcs} = -1.45 \times 10^{-4} \text{OCR}^{1.32} + 0.31 \text{OCR}^{0.66} + 0.5144$; $\text{OCR} \leq 10$ $\alpha_{pcs} = -1.6 \times 10^{-4} \text{OCR}^{1.14} + 0.34 \text{OCR}^{0.62} + 0.5144$; $\text{OCR} > 10$	<ul style="list-style-type: none"> To estimate critical state shear stress from yield shear stress and vice versa To estimate the range of shear stress for which the soil will behave elastically
Relationship among undrained shear strength, critical state friction angle, and overconsolidation ratio	$\frac{(s_u)_f}{p'_o} = \frac{M \left(\frac{R_o}{2} \right)^\Lambda}{2}$	$\frac{(s_u)_f}{\sigma'_{zo}} \approx \left[1 + 2(1 - \sin \phi'_{cs}) \text{OCR}^{0.5} \right] \frac{\sin \phi'_{cs}}{3 - \sin \phi'_{cs}} \times (0.725)^\Lambda \text{OCR}^{0.66\Lambda}$; $\text{OCR} \leq 10$ $\frac{(s_u)_f}{\sigma'_{zo}} \approx \left[1 + 2(1 - \sin \phi'_{cs}) \text{OCR}^{0.5} \right] \frac{\sin \phi'_{cs}}{3 - \sin \phi'_{cs}} \times (0.8)^\Lambda \text{OCR}^{0.62\Lambda}$; $\text{OCR} > 10$	<ul style="list-style-type: none"> To estimate the normalized undrained shear strength from the critical state friction angle and the overconsolidation ratio and vice versa To estimate the range of shear stress for which the soil will behave elastically

(continued)

TABLE A.14b (continued)

Relationship	CSM expression	Approximate expression for practical use	Usage
Relationship between the normalized undrained shear strength at the critical state for normally consolidated and overconsolidated fine-grained soils	$\alpha_R = \frac{\left[\frac{(s_u)_f}{p'_o} \right]_{oc}}{\left[\frac{(s_u)_f}{p'_o} \right]_{nc}} = (R_o)^\Lambda$	$\alpha_R \approx (1.45 \text{ OCR}^{0.66})^\Lambda; \text{OCR} < 10$ $\alpha_R \approx (1.6 \text{ OCR}^{0.62})^\Lambda; \text{OCR} > 10$	<ul style="list-style-type: none"> To estimate the normalized undrained shear strength for any overconsolidation ratio from normalized undrained shear strength at critical state
Relationship between the normalized undrained shear strength of one-dimensionally consolidated or K_o -consolidated and isotropically consolidated fine-grained soils	$(\alpha_{K_o-ic})_{nc} \approx \frac{1}{3} (3 - 2 \sin \phi'_{cs})$ $\times \left(1 - \frac{(\sin \phi'_{cs} - 3)^2}{4(2 \sin \phi'_{cs} - 3)(3 - 2 \sin \phi'_{cs})} \right)^\Lambda$	$\frac{1}{3} (3 - 2 \sin \phi'_{cs}) \left(1 - \frac{(\sin \phi'_{cs} - 3)^2}{4(2 \sin \phi'_{cs} - 3)(3 - 2 \sin \phi'_{cs})} \right)^\Lambda$	<ul style="list-style-type: none"> To convert the undrained shear strength of an isotropically consolidated soil to that of a K_o-consolidated soil
Relationship between the normalized undrained shear strength at initial yield and at critical state for oveconsolidated fine-grained soils under triaxial condition	$\alpha_{ycs} = \frac{\frac{(s_u)_y}{p'_o}}{\frac{(s_u)_f}{p'_o}} = \frac{\sqrt{R_o - 1}}{\left(\frac{R_o}{2} \right)^\Lambda}$	$\alpha_{ycs} \approx \frac{\sqrt{1.45 \text{ OCR}^{0.66} - 1}}{(0.725 \text{ OCR}^{0.66})^\Lambda}; \text{OCR} \leq 10$ $\alpha_{ycs} \approx \frac{\sqrt{1.6 \text{ OCR}^{0.62} - 1}}{(0.8 \text{ OCR}^{0.62})^\Lambda}; \text{OCR} > 10$	<ul style="list-style-type: none"> To delineate fine-grained soils that would likely exhibit peak undrained shear strengths To estimate the undrained shear strength at initial yield from knowing the undrained shear strength at the critical state and vice versa To estimate the range of shear stress at which a soil would behave elastically

Undrained shear strength under direct simple shear (plane strain) conditions	$\left[\frac{(s_u)_f}{\sigma'_{zo}} \right]_{DSS} = \frac{\sqrt{3}}{4} [1 + (1 - \sin \phi'_{cs}) \text{OCR}^{\frac{1}{2}}] \sin \phi'_{cs} \left(\frac{R_o^*}{2} \right)^{\Lambda}$	$\left[\frac{(s_u)_f}{\sigma'_{zo}} \right]_{DSS} \approx \frac{\sqrt{3} \sin \phi'_{cs}}{2} \left(\frac{\text{OCR}}{2} \right)^{0.8}$ $\left[\frac{(s_u)_f}{\sigma'_{zo}} \right]_{DSS} \approx 0.5 \sin \phi'_{cs}$ for normally consolidated soil	• To estimate the undrained shear strength or critical state friction angle in direct simple shear test
Relationship between direct simple shear test and triaxial test	$\alpha_{DSS-ic} = \frac{\left[\frac{(s_u)_{cs}}{\sigma'_{zo}} \right]_{DSS}}{\left[\frac{(s_u)_{cs}}{\sigma'_{zo}} \right]_{ic}} = \frac{(3 - \sin \phi'_{cs})}{2\sqrt{3}}$	$\alpha_{DSS-ic} = \frac{(3 - \sin \phi'_{cs})}{2\sqrt{3}}$	• To estimate the undrained shear strength for direct simple shear from triaxial test result on an isotropically consolidated soil
Relationship for the application of drained and undrained conditions in the analysis of geosystems	$\alpha_{SL} = \frac{\frac{(s_u)_f}{p'_o}}{\frac{\tau_f}{p'_o}} = \frac{(n_o - M)}{n_o} \left(\frac{R_o}{2} \right)^{\Lambda}; n_o = \text{slope of ESP}$	$\alpha_{SL} \approx \frac{3(1 - \sin \phi'_{cs})}{(3 - \sin \phi'_{cs})} (0.725 \text{OCR}^{0.66})^{\Lambda}; \text{OCR} \leq 10$ $\alpha_{SL} \approx \frac{3(1 - \sin \phi'_{cs})}{(3 - \sin \phi'_{cs})} (0.8 \text{OCR}^{0.62})^{\Lambda}; \text{OCR} > 10$	• To estimate whether short-term or long-term condition is critical; $\alpha_{SL} > 1$, long-term condition is critical or else short-term condition is critical
Relationship among excess porewater pressure, OCR, and critical state friction angle	$A_f = \frac{1}{M} \left[\left(\frac{R_o}{2} \right)^{-\Lambda} - 1 \right] + \frac{1}{3}$	$A_f = \frac{3 - \sin \phi'_{cs}}{6 \sin \phi'_{cs}} [(0.725 \text{OCR}^{0.66})^{-\Lambda} - 1] + \frac{1}{3}; \text{OCR} \leq 10$ $A_f = \frac{3 - \sin \phi'_{cs}}{6 \sin \phi'_{cs}} [(0.8 \text{OCR}^{0.62})^{-\Lambda} - 1] + \frac{1}{3}; \text{OCR} > 10$	• To estimate the porewater pressure coefficient at failure in triaxial test

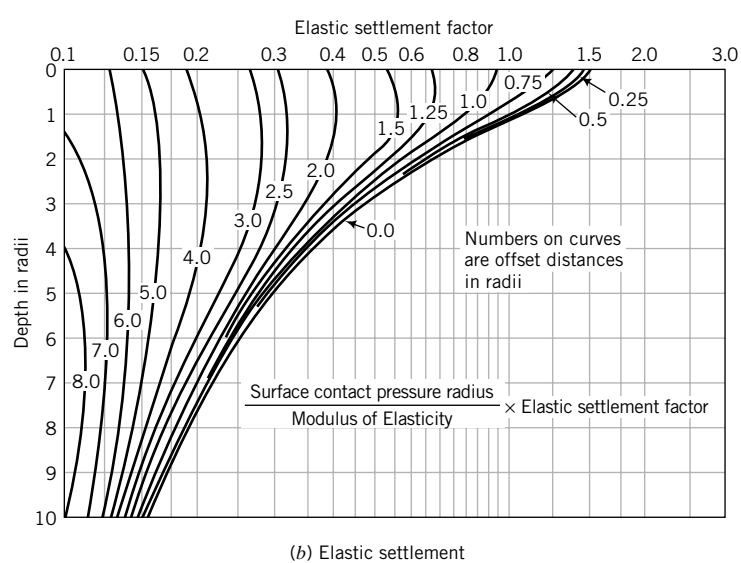
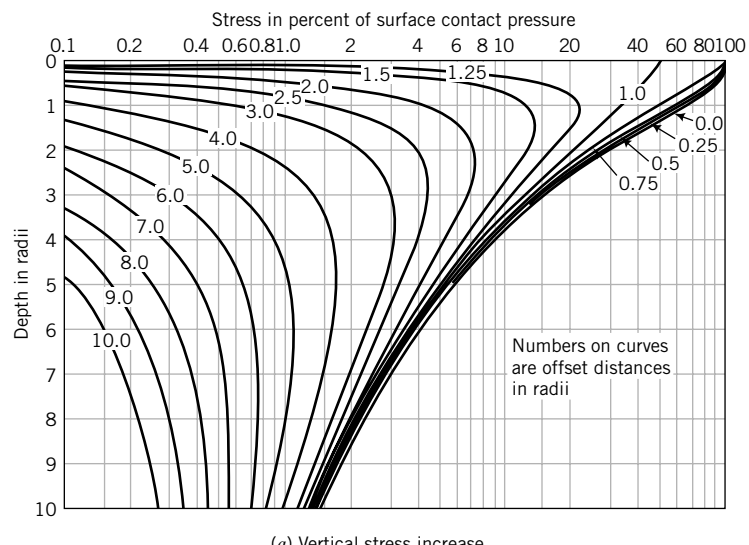
TABLE A.15 Ranges of Free Swell for Some Clay Minerals

Clay minerals	Free swell (%)
Calcium montmorillonite (Ca-smectite)	45–145
Sodium montmorillonite (Na-smectite)	1400–1600
Illite	15–120
Kaolinite	5–60

TABLE A.16 Activity of Clay-Rich Soils

Description	Activity, A
Inactive	<0.75
Normal	0.75–1.25
Active	1.25–2
Very (highly) active (e.g., bentonite)	>6
Minerals	
Kaolinite	0.3–0.5
Illite	0.5–1.3
Na-montmorillonite	4–7
Ca-montmorillonite	0.5–2.0

DISTRIBUTION OF VERTICAL STRESS AND ELASTIC DISPLACEMENT UNDER A UNIFORM CIRCULAR LOAD

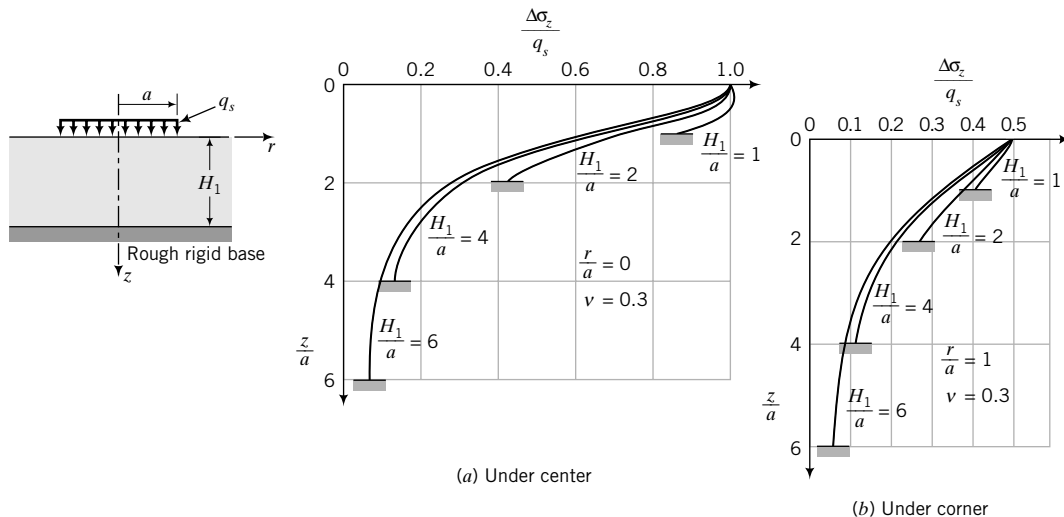


SOURCES: Foster and Alvin (1954); Poulos and Davis (1974).

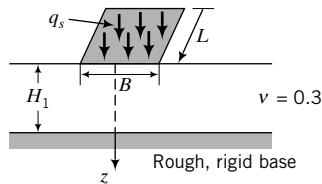
DISTRIBUTION OF SURFACE STRESSES WITHIN FINITE SOIL LAYERS

C1 VERTICAL STRESSES IN A FINITE SOIL LAYER DUE TO A UNIFORM SURFACE LOAD ON A CIRCULAR AREA AND A RECTANGULAR AREA

C1.1 Circular Area (Milovic, 1970)

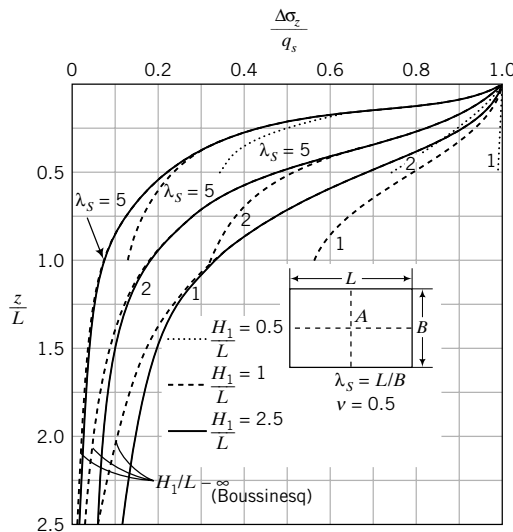


C1.2 Rectangular Area with Rough, Rigid Base (Milovic and Tournier, 1971)

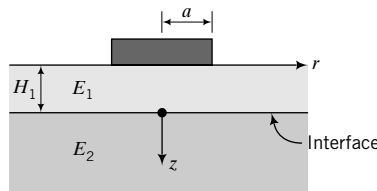


H_1/B	z/B	L/B			L/B		
		Center			Corner		
		1	2	5	1	2	5
1	0.000	1.000	1.000	1.000	0.250	0.250	0.250
	0.100	0.974	0.992	0.996	0.250	0.250	0.250
	0.200	0.943	0.977	0.981	0.250	0.250	0.250
	0.400	0.842	0.924	0.922	0.250	0.250	0.250
	0.600	0.690	0.827	0.832	0.250	0.250	0.250
	0.800	0.570	0.734	0.751	0.238	0.244	0.244
	1.000	0.468	0.638	0.672	0.220	0.232	0.233
	0.000	1.000	1.000	1.000	0.250	0.250	0.250
	0.100	0.970	0.985	0.990	0.250	0.250	0.250
	0.200	0.930	0.963	0.971	0.250	0.250	0.250
2	0.400	0.802	0.878	0.890	0.244	0.249	0.247
	0.800	0.464	0.619	0.670	0.211	0.231	0.230
	1.200	0.286	0.441	0.528	0.172	0.207	0.208
	1.600	0.204	0.340	0.443	0.142	0.183	0.188
	2.000	0.155	0.269	0.377	0.117	0.160	0.168
	0.000	1.000	1.000	1.000	0.250	0.250	0.250
	0.100	0.970	0.982	0.990	0.250	0.250	0.250
	0.200	0.930	0.962	0.969	0.249	0.250	0.249
	0.400	0.799	0.872	0.884	0.241	0.246	0.246
	0.800	0.453	0.599	0.650	0.203	0.222	0.225
3	1.200	0.264	0.405	0.492	0.158	0.191	0.197
	1.600	0.172	0.289	0.395	0.122	0.163	0.174
	2.000	0.124	0.220	0.333	0.098	0.141	0.156
	2.500	0.093	0.171	0.281	0.078	0.120	0.138
	3.000	0.073	0.137	0.238	0.064	0.102	0.123
	0.000	1.000	1.000	1.000	0.250	0.250	0.250
	0.100	0.970	0.981	0.990	0.250	0.250	0.250
	0.200	0.930	0.961	0.969	0.249	0.250	0.249
	0.400	0.798	0.870	0.881	0.241	0.245	0.245
	0.800	0.450	0.594	0.641	0.200	0.219	0.221
5	1.200	0.258	0.394	0.475	0.153	0.184	0.191
	1.600	0.162	0.271	0.368	0.114	0.151	0.164
	2.000	0.111	0.195	0.296	0.087	0.125	0.143
	2.500	0.075	0.139	0.235	0.064	0.100	0.123
	3.000	0.056	0.105	0.193	0.050	0.082	0.108
	3.500	0.044	0.085	0.165	0.040	0.069	0.097
	4.000	0.037	0.071	0.144	0.034	0.060	0.089
	4.500	0.032	0.062	0.128	0.030	0.053	0.082
	5.000	0.027	0.053	0.113	0.026	0.047	0.075

C1.3 Rectangular Area with Smooth, Rigid Base (Sovinc, 1961)



C2 VERTICAL STRESSES IN A TWO-LAYER SOIL UNDER THE CENTER OF A UNIFORMLY LOADED CIRCULAR AREA (Fox, 1948)



a/H_1	z	E_1/E_2				E_1/E_2			
		1	10	100	1000	1	10	100	1000
		Rough interface				Smooth interface			
1/2	0	0.284	0.101	0.0238	0.0051	0.31	0.105	0.0241	0.0051
	H_1	0.087	0.047	0.0158	0.0042	0.141	0.063	0.0183	0.0045
	$2H_1$	0.0403	0.0278	0.0117	0.0035	0.064	0.0367	0.0136	0.0038
	$3H_1$	0.023	0.0184	0.0091	0.0031	0.0346	0.0235	0.0105	0.0033
	$4H_1$	0.0148	0.0129	0.0074	0.0028	0.0212	0.0161	0.0083	0.0029
	0	0.646	0.292	0.081	0.0185	0.722	0.305	0.082	0.019
1	H_1	0.284	0.168	0.06	0.0162	0.437	0.217	0.068	0.0172
	$2H_1$	0.145	0.105	0.046	0.0143	0.225	0.136	0.0525	0.0151
	$3H_1$	0.087	0.07	0.036	0.0124	0.128	0.089	0.0409	0.0133
	$4H_1$	0.057	0.05	0.029	0.011	0.081	0.062	0.0326	0.0117
2	0	0.911	0.644	0.246	0.071	1.025	0.677	0.249	0.067
	H_1	0.646	0.48	0.205	0.0606	0.869	0.576	0.225	0.063
	$2H_1$	0.424	0.34	0.165	0.0542	0.596	0.421	0.186	0.057
	$3H_1$	0.284	0.244	0.133	0.048	0.396	0.302	0.15	0.051
	$4H_1$	0.2	0.181	0.108	0.0428	0.271	0.22	0.122	0.0454

LATERAL EARTH PRESSURE COEFFICIENTS (KERISEL AND ABSI, 1990)

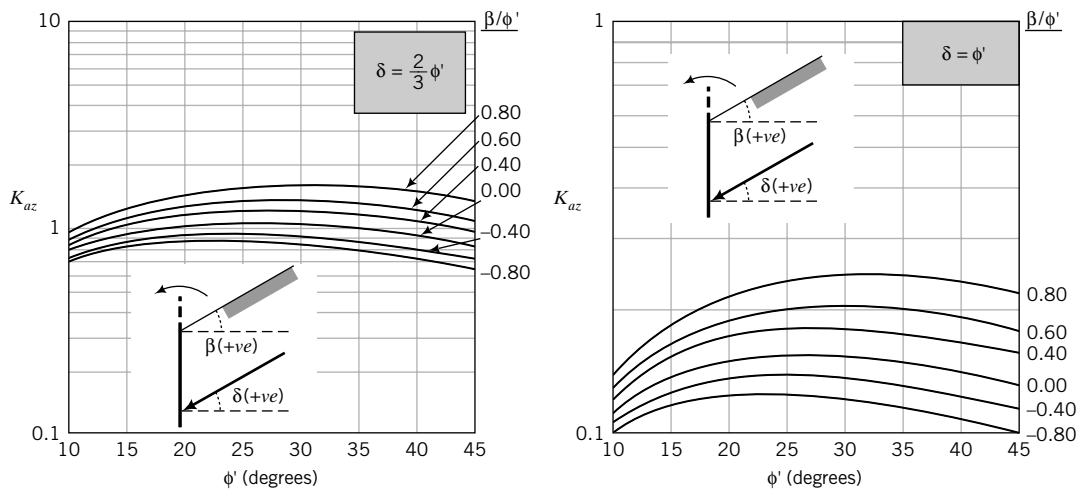


FIGURE D.1 Vertical component of the active lateral pressure coefficient. (Plotted from data published by Kerisel and Absi, 1990.)

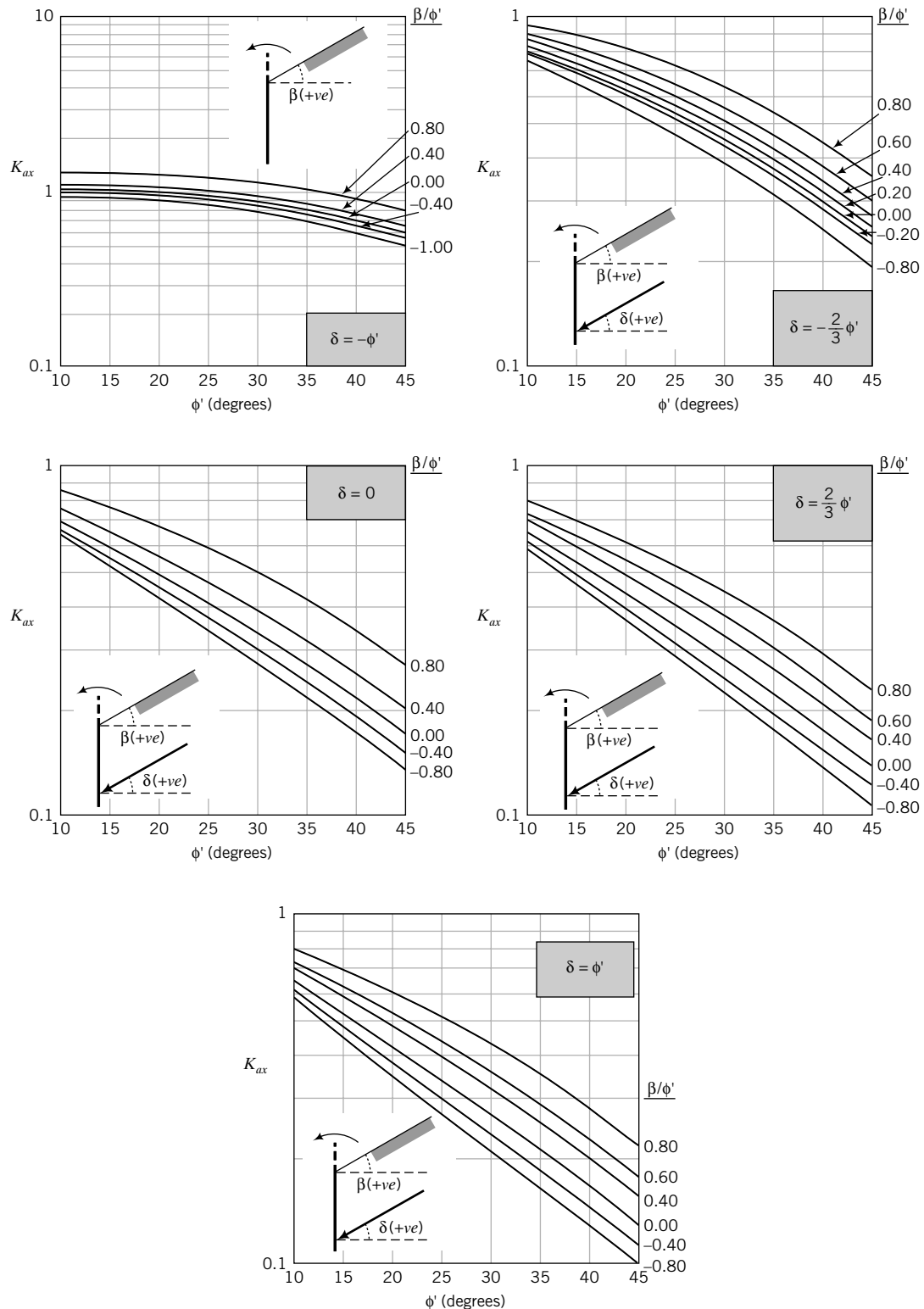


FIGURE D.2 Horizontal component of the active lateral pressure coefficient. (Plotted from data published by Kerisel and Absi, 1990.)

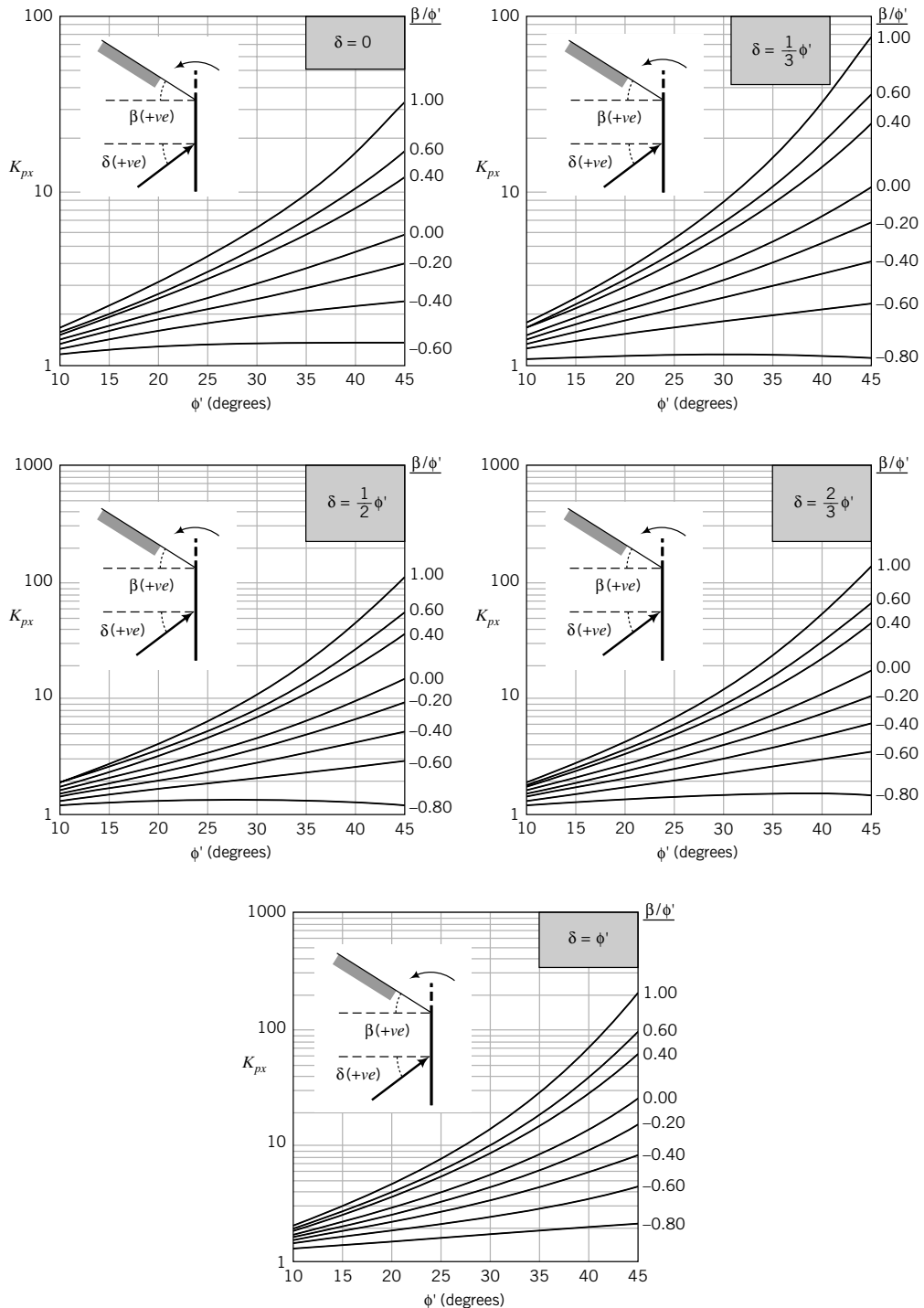


FIGURE D.3 Horizontal component of the passive lateral pressure coefficient. (Plotted from data published by Kerisel and Absi, 1990.)

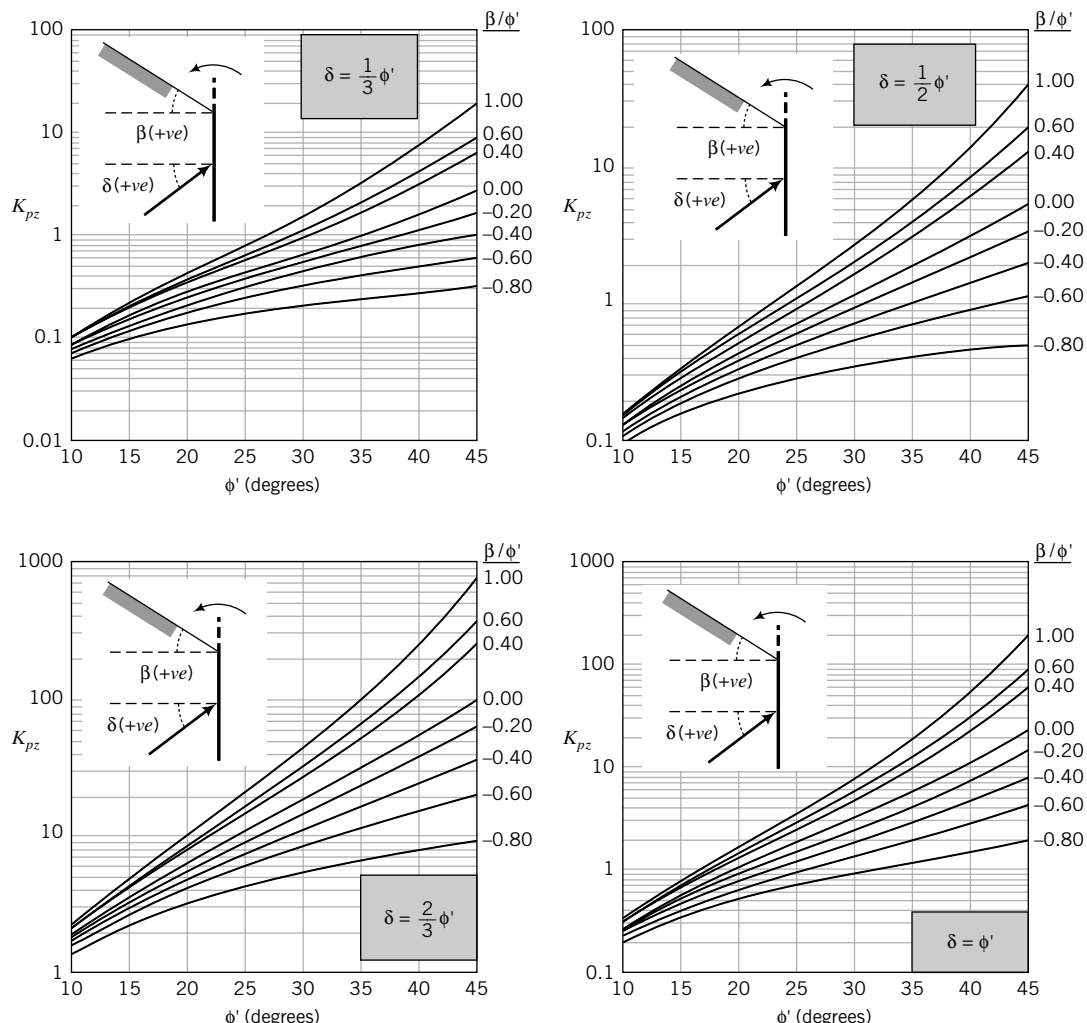


FIGURE D.4 Vertical component of the passive lateral pressure coefficient. (Plotted from data published by Kerisel and Absi, 1990.)

REFERENCES

- Adamson, A. W. (1982). *Physical Chemistry of Surfaces*. Wiley, New York.
- Atterberg, A. (1911). Über die physikalische Bodenuntersuchung und über die Plastizität der Tone. *Int. Mitt. Boden*, **1**, 10–43.
- Azzoz, A. S., Krizek, R. J., and Corotis, R. B. (1976). Regression analysis of soil compressibility. *Soils and Fndns*, **16**(2), 19–29.
- Bell, J. M. (1968). General slope stability analysis. *J. Soil Mech. Found. Eng. Div. ASCE*, **94**(SM6), 1253–1270.
- Berezantzev, V. G., Khristoforov, V. S., and Golubkov, V. N. (eds.) (1961). Load bearing capacity and deformation of piled foundations. *Proceedings of the 5th International Conference on Soil Mechanics and Foundation Engineering*, Paris, Vol. 2, 11–15.
- Bishop, A. W. (1955). The use of the slip circle in the stability analysis of slopes. *Geotechnique*, **5**(1), 7–17.
- Bishop, A. W., and Morgenstern, N. R. (1960). Stability coefficients for earth slopes. *Geotechnique*, **10**(4), 129–150.
- Bjerrum, L. (1954). Geotechnical properties of Norwegian marine clays. *Geotechnique*, **4**(2), 49–69.
- Bjerrum, L., and Eide, O. (1956). Stability of struttied excavations in clays. *Geotechnique*, **1**(1), 32–47.
- Bjerrum, L., and Eggestad, A. (eds.) (1963). Interpretation of loading tests on sand. *Proceedings of the European Conference on Soil Mechanics and Foundation Engineering*, Wiesbaden, Vol. 1, 199–203.
- Blanchet, R., Tavenas, F., and R. Garneau (1980). Behaviour of friction piles in soft sensitive clays. *Canadian Geotechnical Journal*, **17**(2), 203–224.
- Bolton, M. D. (1986). The strength and dilatancy of sands. *Geotechnique*, **36**(1), 65–78.
- Bolton, M. D., and Powrie, W. (1988). The behaviour of diaphragm walls prior to collapse. *Geotechnique*, **38**(2), 167–189.
- Boussinesq, J. (1885). *Application des Potentiels à l'Etude de l'Équilibre et du Mouvement des Solides Élastiques*. Gauthier-Villars, Paris.
- Bozozuk, M. (1976). Tower silo foundation. CBD-177, *Canadian Building Digest*, Ottawa.
- Briaud, J., and Gibbens, R. M. (1994). Predicted and measured behavior of five spread footings on sand. *Geot. Special. Pub. No. 41*, ASCE, 255 pp.
- Budhu, M. (1979). *Simple Shear Deformation of Sands*. Ph.D. Thesis, Cambridge University, Cambridge, England.
- Budhu, M. (1984). Non-uniformities imposed by simple shear apparatus. *Canadian Geotechnical Journal*, **21**(2), 125–137.
- Budhu, M., and Davies, T. G. (1987). Non-linear analysis of laterally loaded piles in cohesionless soils. *Canadian Geotechnical Journal*, **24**, 289–296.
- Budhu, M., and Davies, T. G. (1988). Analysis of laterally loaded piles in soft clays. *Journal of Geotechnical Engineering, ASCE*, **114**(1), 21–39.
- Burland, J. B. (1973). Shaft friction piles in clay—a simple fundamental approach. *Ground Eng.*, **6**(3), 30–42.
- Burland, J. B., and Burbidge, M. C. (1985). Settlement of foundations on sand and gravel. *Proc. Inst. Civ. Eng. Part 1*, **78**, 1325–1381.
- Burland, J. B., Potts, D. M., and Walsh, N. M. (1981). The overall stability of free and propped embedded cantilever walls. *Ground Engineering*, **14**(5), 23–38.
- Caquot, A., and Kerisel, J. (1948). *Tables for the Calculation of Passive Pressure, Active Pressure and Bearing Capacity of Foundations*. Gauthier-Villars, Paris.
- Carter, M., and Bentley, S. P. (1991). *Correlations of Soil Properties*. Pentech, London.
- Casagrande, A. (1932). Research on the Atterberg limits of soils. *Public Roads*, **13**(8), 121–136.
- Casagrande, A. (ed.) (1936). The determination of the preconsolidation load and its practical significance. *1st International Conference on Soil Mechanics and Foundation Engineering*, Cambridge, MA, **3**, 60–64.
- Casagrande, A. (1937). Seepage through dams. *J. N. Engl. Water Works Assoc.*, **L1**(2), 131–172.
- Casagrande, A., and Fadum, R. E. (1940). Notes on soil testing for engineering purposes. *Soil Mechanics Series*, Graduate School of Engineering, Harvard University, Cambridge, MA, **8**(268), 37.
- Chang, M. F. (ed.) (1988). Some experience with the dilatometer test in Singapore. *Penetration Testing*, Orlando, **1**, 489–496.
- Chu, S. (1991). Rankine analysis of active and passive pressures in dry sands. *Soils Founds.*, **31**(4), 115–120.
- COM624 (1993). Laterally loaded pile analysis program for the microcomputer. *FHWASA-91-048*, computer program documentation, by S. T. Wang and L. C. Reese.
- Coulomb, C. A. (1776). Essai sur une application des règles de maximia et minimis à quelques problèmes de statique relatifs à l'architecture. *Mémoires de la Mathématique et de Physique, présentés à l'Académie Royale des Sciences, par divers savants, et lus dans ces Assemblées*. L'Imprimérie Royale, Paris, 3–8.
- Darcy, H. (1856). *Les Fontaines Publiques de la Ville de Dijon*. Dalmont, Paris.
- Davies, T. G., and Budhu, M. (1986). Non-linear analysis of laterally loaded pile in stiff clays. *Geotechnique*, **36**(4), 527–538.
- Davis, E. H., and Booker, J. R. (1971). The bearing capacity of strip footings from the standpoint of plasticity theory. *Proc. First Australia-New Zealand Conference on Geomechanics*, Vol. 1, 276–282.
- Drnevich, V. P. (1967). *Effect of Strain History on the Dynamic Properties of Sand*. Ph.D. Thesis, University of Michigan.
- Dumbleton, M. J., and West, G. (1970). The suction and strength of remoulded soils as affected by composition. LR306, Road Research Laboratory, Crowthorne.

- Eden, S. M. (1974). *Influence of Shape and Embedment on Dynamic Foundation Response*. Ph.D. Thesis, University of Massachusetts.
- Eslami, A., and Fellenius, B. H. (1997). Pile capacity by direct CPT and CPTu method applied to 102 case histories. *Canadian Geotechnical Journal*, **34**, 886–904.
- Fancher, G. H., Lewis, J. A., and Barnes, K. B. (1933). Mineral Industries Experiment Station, Bull. 12, Penn State College.
- Fellenius, W. (1927). *Erdstatische Berechnungen*. W. Ernst und Sohn, Berlin.
- Feng, T. W. (2000). Fall-cone penetration and water content relationship of clays. *Geotechnique*, **50**(2), 181–187.
- Fleming, W., and Thorburn, S. (1983). Recent piling advances. State of the Art Report in *Proc. Conf. on Advances in Piling and Ground Treatment for Foundations*, ICE, London.
- Fleming, W. G. K., Weltman, A. J., Randolph, M. F., and Elson, W. K. (1985). *Piling Engineering*. Halsted Press, New York.
- Foster, C. R., and Ahlvin, R. G. (1954). Stresses and deflections induced by a uniform circular load. *Proc. Highway Research Board*, Vol. 33, 470.
- Fox, L. (1948). Computation of traffic stresses in a simple road structure. *Proc. 2nd Int. Conf. Soil Mech. and Found. Eng.*, Vol. 2, 236–246.
- Gazetas, G., and Hatzikonstantinou, E. (1988). Elastic formulae for lateral displacement and rotation of arbitrarily-shaped embedded foundations. *Geotechnique*, **38**(3), 439–444.
- Gazetas, G., and Stokoe, K. H. (1991). Free vibration of embedded foundations: Theory versus experiment. *J. Geotech. Eng.*, **117**(9), 1362–1381.
- Gazetas, G., Tassoulas, J. L., Dobry, R., and O'Rourke, M. J. (1985). Elastic settlement of arbitrarily shaped foundations embedded in half-space. *Geotechnique*, **35**(2), 339–346.
- Giroud, J. P. (1968). Settlement of a linearly loaded rectangular area. *J. Soil Mech. Found. Div. ASCE*, **94**(SM4), 813–831.
- Graham, J., and Houlsby, G. T. (1983). Elastic anisotropy of a natural clay. *Geotechnique*, **33**(2), 165–180.
- Hansen, B. J. (1951). Simple statical computation of permissible pile loads. *Christiansi and Nielsen Post*, 14–17.
- Hansen, B. J. (1970). *A Revised and Extended Formula for Bearing Capacity*, No. 28. Danish Geotechnical Institute, Copenhagen.
- Hazen, A. (1892). Some physical properties of sand and gravels with special reference to the use in filtration. Massachusetts State Board of Health, 24th annual report.
- Henkel, D. J. (1971). The calculation of earth pressure in open cuts in soft clays. *The Arup Journal*, **6**(4).
- Hull, T. S. (ed.) (1987). *The Static Behaviour of Laterally Loaded Piles*. Ph.D. Thesis, University of Sydney, Sydney, Australia.
- Hvorslev, M. J. (1937). Über die Festigkeitseigenschaften gestörter bindiger Böden. *Ingeniorvidenskabelige skrifter*, A., No. 45, Copenhagen.
- Ingold, T. S. (1979). The effects of compaction on retaining walls. *Geotechnique*, **29**(3), 265–283.
- Jaky, J. (1944). The coefficient of earth pressure at rest. *J. Soc. Hungarian Architects Eng.*, **7**, 355–358.
- Jamiolkowski, M., Ladd, C. C., Germaine, J. T., and Lancellotta, R. (eds.) (1985). New developments in field and laboratory testing of soils. *XIIth International Conference on Soil Mechanics and Foundation Engineering*, San Francisco, Vol. 1, 57–154.
- Janbu, N. (ed.) (1973). Slope stability computations. *Embankment Dam Engineering, Casagrande Memorial Volume*. Wiley, New York, 47–86.
- Janbu, N. (ed.) (1976). Static bearing capacity of friction piles. *Proceedings of the 6th European Conference on Soil Mechanics and Foundation Engineering*, Vol. 1.2, 479–488.
- Janbu, N., Bjerrum, L., and Kjaernsli, B. (1956). Veiledning ved løsning av fundamenteringsoppgaver (Soil mechanics applied to some engineering problems). In Norwegian with English summary. Norwegian Geotechnical Institute Publication 16, 93 pp.
- Jardine, R. J., Overy, R. F., and Chow, F. C. (1998). Axial capacity of offshore piles in dense North Sea sands. *J. Geotech and Geoenvir. Engrg.*, **124**, 171–178.
- Jarquio, R. (1981). Total lateral surcharge pressure due to a strip load. *J. Geotech. Eng. Div. ASCE*, **107**(10), 1424–1428.
- Juran, I., and Schlosser, F. (eds.) (1978). Theoretical analysis of failure in reinforced earth structures. *Symposium on Earth Reinforcement, ASCE Convention, Pittsburgh*. American Society of Civil Engineers, New York, 528–555.
- Karlsrud, K., and Andresen, L. (2008). Design and performance of deep excavations in soft clays. SOA 12. *Proc. 6th Int. Conf. on Case Histories in Geot. Eng.*, Arlington, VA, August, Missouri University of Science and Technology, USA, 1–12.
- Kenny, T. C., Lau, D., and Ofoegbu, G. I. (1984). Permeability of compacted granular materials. *Can. Geotech. J.*, **21**(4), 726–729.
- Kerisel, J., and Absi, E. (1990). *Active and Passive Earth Pressure Tables*. Balkema, Rotterdam.
- Kozeny, J. (1933). Theorie und Berechnung der Brunnen. *Wasserwirtschaft*, **28**, 104.
- Ladd, C. C., Foot, R., Ishihara, K., Schlosser, F., and Poulos, H. G. (1977). Stress-deformation and strength characteristics. *Proceedings of the 9th International Conference on Soil Mechanics and Foundation Engineering*, Tokyo, 421–494.
- Lehane, B. M., and Randolph, M. F. (2002). Evaluation of the minimum base resistance for driven piles in siliceous sand. *Journal of Geotech. and Geoenvir. Eng., ASCE*, **130**(6), 656–658.
- Lehane, B., Schneider, J., and Xu, X. (2005). The UWA-05 method for the prediction of the axial capacity of driven piles in sand. *Int. Symp. on Frontiers in Offshore Geotechnics*, Perth, 683–689.
- Liao, S. S. C., and Whitman, R. V. (1985). Overburden correction factors for SPT in sand. *J. Geotech. Eng. Div. ASCE*, **112**(3), 373–377.
- Love, A. E. H. (1927). *The Mathematical Theory of Elasticity*. Cambridge University Press, Cambridge.
- McCammon, N. R., and Golder, H. Q. (1970). Some loading tests on long pipe piles. *Geotechnique*, **20**(2), 171–184.
- Mayne, P. W., Coop, M. R., Springman, S. M., Huang, An-Bin, and Zornberg, J. G. (2009). Geomaterial behavior and testing. *Proc. 17th Int. Conf. on Soil Mechanics and Geotechnical Engineering*, Alexandria, Egypt, OIS Press, Theme Lecture, Vol. 4, pp. 2777–2872.
- Mesri, G. (1975). Discussion: New design procedure for stability of soft clays. *J. Geotech. Eng. Div. ASCE*, **101**(GT4), 409–412.
- Meyerhof, G. G. (1951). The ultimate bearing capacity of foundations. *Geotechnique*, **2**(4), 301–331.

- Meyerhof, G. G. (1956). Penetration tests and bearing capacity of cohesionless soils. *J. Soil Mech. Found. Eng. Div. ASCE*, **82**(SM1), 1–19.
- Meyerhof, G. G. (1963). Some recent research on the bearing capacity of foundations. *Can. Geotech. J.*, **1**(1), 16–26.
- Meyerhof, G. G. (1965). Shallow foundations. *J. Soil Mech. Found. Div. ASCE*, **91**(SM2), 21–31.
- Meyerhof, G. G. (1976). Bearing capacity and settlement of pile foundations. *J. Geotech. Eng. Div. ASCE*, **102**(GT3), 195–228.
- Milovic, D. M. (1970). Stresses and displacements in an anisotropic medium due to circular loads. *Proc. II Cong. Int. Soc. Rock Mech.*, **3**, 479–482.
- Milovic, D. M., and Tournier, J. P. (1971). Stresses and displacements due to a rectangular load on a layer of finite thickness. *Soils Found.*, **II**(1), 1–27.
- Mindlin, R. D. (1936). Force at a point in the interior of a semi-infinite solid. *J. Appl. Phys.*, **7**(5), 195–202.
- Mitchell, J. K. (1993). *Fundamentals of Soil Behavior*. Wiley, New York.
- Morgenstern, N. R., and Price, V. E. (1965). The analysis of the stability of general slip surfaces. *Geotechnique*, **15**(1), 79–93.
- Negro, A., Karlsrud, K., Srithar, S., Ervin, M., and Vorster, E. (2009). Prediction, monitoring and evaluation of performance of geotechnical structures. *Proc. 17th Int. Conf. on Soil Mechanics and Geotechnical Engineering*, Alexandria, Egypt, OIS Press, Theme Lecture, Vol. 4, pp. 2930–3005.
- Nagaraj, T. S., and Srinivasa Murthy, B. R. (1985). Prediction of the preconsolidation pressure and recompression index of soils. *Geotech. Testing J. ASTM*, **8**(4), 199–202.
- Nagaraj, T. S., and Srinivasa Murthy, B. R. (1986). A critical reappraisal of compression index. *Geotechnique*, **36**(1), 27–32.
- Newmark, N. M. (1942). *Influence Charts for Computation of Stresses in Elastic Foundations*, No. 338. University of Illinois Engineering Experiment Station, Urbana.
- O'Neill, M. W., and Reese, L. C. (1988). Drilled shafts: Construction procedures and design methods. ADSC: The International Association of Foundation Drilling, Publication No. ADSC-TL4, 471 pp.
- O'Neill, M. W., and Reese, L. C. (1999). Drilled shafts: Construction procedures. FHWA-IF-99-025, Federal Highway Administration, Washington, DC.
- Osterberg, J. O. (1984). A new simplified method for load testing drilled shafts. *Foundation Drilling*, Vol. XXIII (6), Association of Drilled Shafts Contractors, August, pp. 9–11.
- Packshaw, S. (1969). Earth pressures and earth resistance. *A Century of Soil Mechanics*. The Institution of Civil Engineers, London, 409–435.
- Padfield, C. J., and Mair, R. J. (1984). *Design of Retaining Walls Embedded in Stiff Clay*. CIRIA, London.
- Peck, R. B. (ed.) (1969). Deep excavation and tunneling in soft ground. *7th International Conference on Soil Mechanics and Foundation Engineering, State-of-the-Art*, Mexico City, Vol. 3, 147–150.
- Peck, R. B., and Bryant, F. G. (1953). The bearing capacity failure of the Transcona Grain Elevator. *Geotechnique*, **11**, 210–208.
- Poncelet, J. V. (1840). Mémoire sur la stabilité des revêtements et de leurs fondations. Note additionnelle sur les relations analytiques qui lient entre elles la poussée et la butée de la terre. *Mémorial de l'officier du génie*, 13.
- Poulos, H. G. (1971). Behavior of laterally loaded piles: Part I—single piles. *ASCE Journal of the Soil Mechanics and Foundations Division*, **97**(SM5), 711–731.
- Poulos, H. G. (ed.) (1988). The mechanics of calcareous sediments. *5th Australia-New Zealand Geomechanics Conference, Australia Geomechanics*, 8–41.
- Poulos, H. G. (1989). Pile behavior—theory and application. *Geotechnique*, **39**(3), 365–415.
- Poulos, H. G., and Davis, E. H. (1974). *Elastic Solutions for Soil and Rock Mechanics*. Wiley, New York.
- Poulos, H. G., Carter, J. P., and Small, J. C. (2001). Foundations and retaining structures—research and practice. *Proc. 15th Int. Conf. on Soil Mechanics and Geotechnical Engineering*, Istanbul, Turkey, A. A. Balkema Publ., Theme Lecture, Vol. 4, pp. 2527–2606.
- Prandtl, L. (1920). *Über die Härte plastischer Körper*, Nachrichten von der Königlichen Gesellschaft der Wissenschaften zu Göttingen (mathematisch-physikalische Klasse aus dem Jahre 1920), Berlin, 74–85.
- Quiros, G. W., and Reese, L. G. (1977). Design procedures for axially loaded drilled shafts. Research Report No. 3-5-72-176, Center for Highway Research, University of Texas at Austin, December.
- Randolph, M. F., Carter, J. P., and Wroth, C. P. (1979). Driven piles in clay—the effects of installations and subsequent consolidation. *Geotechnique*, **29**(4), 361–393.
- Randolph, M. F. (1981). The response of flexible piles to lateral loading. *Geotechnique*, **31**(2), 247–259.
- Randolph, M. F., and Murphy, B. S. (1985). Shaft capacity of driven piles in clay. *Proc. 17th Ann. Offshore Technol. Conf.*, Houston, **1**, 371–378.
- Rankine, W. J. M. (1857). On the stability of loose earth. *Philos. Trans. R. Soc. London*, **1**, 9–27.
- Reese, L. C., and O'Neill, M. W. (1988). *Drilled Shafts: Construction Procedures and Design Methods*. Federal Highway Administration, Washington, DC.
- Reese, L. C. (1984). Handbook on design of piles and drilled shafts under lateral load. FHWA-IP-84/1, FHWA, U.S. Department of Transportation, Washington, DC.
- Reynolds, O. (1885). On the dilatancy of media composed of rigid particles in contact; with experimental illustrations. *Philos. Mag.*, **20**(5th Series), 469–481.
- Richart, F. E. (1959). Review of the theories for sand drains. *Trans. ASCE*, **124**, 709–736.
- Robertson, P. K., and Campanella, R. E. (1983). Interpretation of cone penetration tests. Part I: Sand. *Can. Geotech. J.*, **22**(4), 718–733.
- Roscoe, K. H., and Burland, J. B. (1968). On the generalized stress-strain behavior of “wet” clay. *Engineering Plasticity*, J. Heyman and F. Leckie (eds.). Cambridge University Press, Cambridge, 535–609.
- Roscoe, K. H., Schofield, A. N., and Wroth, C. P. (1958). On the yielding of soils. *Geotechnique*, **8**, 22–53.
- Rosenfarb, J. L., and Chen, W. F. (1972). Limit analysis solutions of earth pressure problems. Fritz Engineering Laboratory Report 35514, Lehigh University, Bethlehem.
- Rowe, P. W. (1957). Anchored sheet pile walls. *Proc. Inst. Civ. Eng., Part 1*, **1**, 27–70.
- Samarasinghe, A. M., Huang, Y. H., and Drnevich, V. P. (1982). Permeability and consolidation of normally consolidated soils. *J. Geotech. Eng. Div. ASCE*, **108**(GT6), 835–850.

- Sarma, S. K. (1975). Stability analysis of embankments and slopes. *Geotechnique*, **25**(4), 743–761.
- Schmertmann, J. H. (1953). The undisturbed consolidation behavior of clay. *Trans. ASCE*, **120**, 1201.
- Schmertmann, J. H. (1970). Static cone to compute static settlement over sand. *J. Soil Mech. Found. Div. ASCE*, **96**(SM3), 1011–1043.
- Schmertmann, J. H., Hartman, J. P., and Brown, P. R. (1978). Improved strain influence factor diagrams. *J. Geot. Eng. Div. ASCE*, **104** (GT8), 1131–1135.
- Schofield, A., and Wroth, C. P. (1968). *Critical State Soil Mechanics*. McGraw-Hill, London.
- Scott, R. E. (1963). *Principles of Soil Mechanics*. Addison-Wesley, Reading, MA.
- Seed, H. B., and Idriss, I. M. (1970). Soil moduli and damping factors for dynamic response analyses. Report EERC 70-10, Earthquake Engineering Research Center, University of California, Berkeley.
- Skempton, A. W. (1944). Notes on the compressibility of clays. *Q. J. Geol. Soc. London*, **100**(C: parts 1 & 2), 119–135.
- Skempton, A. W. (1951). *The Bearing Capacity of Clay*. Building Research Congress, London.
- Skempton, A. W. (ed.) (1953). The colloidal activity of clays. *Proceedings, Third International Conference on Soil Mechanics and Foundation Engineering*, Zurich, Vol. 1, 57–61.
- Skempton, A. W. (1954). The pore water coefficients A and B. *Geotechnique*, **4**, 143–147.
- Skempton, A. W. (1957). Discussion: The planning and design of the new Hong Kong airport. *Proc. Institute of Civil Engineers*, Vol. 7, London, 305–307.
- Skempton, A. W. (1959). Cast-in-situ bored piles in London clay. *Geotechnique*, **9**(4), 153–173.
- Skempton, A. W. (1970). The consolidation of clays by gravitational compaction. *Q. J. Geol. Soc. London*, **125**(3), 373–411.
- Skempton, A. W., and Bjerrum, L. (1957). A contribution to the settlement analysis of foundation on clay. *Geotechnique*, **7**(4), 168–178.
- Slichter, C. (1899). Nineteenth Annual Report, U.S. Geological Survey, Part 2, 360.
- Sovinc, I. (ed.) (1961). Stresses and displacements in a limited layer of uniform thickness, resting on a rigid base, and subjected to a uniformly distributed flexible load of rectangular shape. *5th International Conference on Soil Mechanics and Foundation Engineering*, Paris, Vol. 1, 823–827.
- Spencer, E. (1967). A method of analysis of embankments assuming parallel interslices technique. *Geotechnique*, **17**(1), 11–26.
- Taylor, D. W. (1942). Research on consolidation of clays. Serial No. 82, Massachusetts Institute of Technology, Cambridge.
- Taylor, D. W. (1948). *Fundamentals of Soil Mechanics*. Wiley, New York.
- Terzaghi, K. (1925). *Erdbaumechanik*. Franz Deuticke, Vienna.
- Terzaghi, K. (1943). *Theoretical Soil Mechanics*. Wiley, New York.
- Terzaghi, K., and Peck, R. B. (1948). *Soil Mechanics in Engineering Practice*. Wiley, New York.
- Timoshenko, S. P., and Goodier, J. N. (1970). *Theory of Elasticity*, 3rd ed. McGraw-Hill Book Company, NY.
- Tomlinson, M. J. (1987). *Pile Design and Construction Practice* (3rd ed.). Viewpoint Publications, London, UK.
- Tumay, M. T., and Fakhroo, M. (1984). Pile capacity in soft clays using electric QCPT data. *Proc. Conf. on Cone Penetration Testing and Experience*, St. Louis, MO, Oct. 26–30, 434–455.
- Vesic, A. S. (1973). Analysis of ultimate loads of shallow foundations. *J. Soil Mech. Found. Div. ASCE*, **99**(SM1), 45–73.
- Vesic, A. S. (1975). Bearing capacity of shallow foundations. *Foundation Engineering Handbook*, H. F. Winkerton and H. Y. Fang, eds. Van Nostrand-Reinhold, New York, p. 121.
- Vesic, A. S. (1977). Design of pile foundations, National Cooperative Highway Research Program. *Synthesis of Highway Practice*, No. 42, TRB, National Research Council, Washington, DC.
- Wagner, A. A. (1957). The use of the unified soil classification system by the Bureau of Reclamation. *Proc. 4th Int. Conf. Soil Mech. and Found. Eng.*, London, Vol. 1, 125.
- White, L. S. (1953). Transcona elevator failure: Eye witness account. *Geotechnique*, **11**(5), 209–215.
- Wong, P. K., and Mitchell, R. J. (1975). Yielding and plastic flow of sensitive cemented clay. *Geotechnique*, **25**(4), 763–782.
- Wood, D. M. (1983). Index properties and critical state soil mechanics. *Proc. Symp. on Recent Developments in Laboratory and Field Tests and Analysis of Geotechnical Problems*, Bangkok, Thailand, 301–309.
- Wood, D. M. (1990). *Soil Behavior and Critical State Soil Mechanics*. Cambridge University Press, Cambridge.
- Wood, D. M., and Wroth, C. P. (1978). The correlation of index properties with some basic engineering properties of soils. *Can. Geotech. J.*, **15**(2), 137–145.
- Wroth, C. P. (1984). The interpretation of in situ soil tests. *Geotechnique*, **34**(4), 449–489.
- Wroth, C. P., and Houlsby, G. T. (1985). Soil mechanics: Proper characterization and analysis procedures. *11th International Conference on Soil Mechanics and Foundation Engineering*, San Francisco, **1**, 1–55.
- Wroth, C. P., and Hughes, O. J. M. (eds.) (1973). An instrument for the in-situ measurement of the properties of soft clays. *8th International Conference on Soil Mechanics and Foundational Engineering*, Moscow, Vol. 1, 487–494.
- Xu, X., and Lehane, B. M. (2005). Evaluation of end-bearing capacity for close ended pile in sand from cone penetration data. *Proc. ISFOG 2005*, Perth, Australia.
- Youd, T. L., Idriss, I. M., Andrus, R. D., Arango, I., Castro, G., Christian, J. T., Dobry, R., Liam Finn, W. D., Harder, L. F., Jr., Hynes, M. E., Ishihara, K., Koester, J. P., Liao, S. S. C., Marcuson, W. F. III, Martin, G. R., Mitchell, J. K., Moriwaki, Y., Power, M. S., Robertson, P. K., Seed, R. B. and Stokoe, K. H. II. (2001). Liquefaction resistance of soils: Summary report from the 1996 NCEER and 1998 NCEER/NSF workshops on evaluation of liquefaction resistance of soils." *J. Geot. and Geoenvir. Eng.*, **124**(10), 817–833.
- Youssef, M. S., El Ramli, A. H., and El Demery, M. (eds.) (1965). Relationship between shear strength, consolidation, liquid limit, and plastic limit for remolded clays. *6th International Conference on Soil Mechanics and Foundation Engineering*. Toronto University Press, Montreal, Vol. 1, 126–129.
- Zytnyski, M., Randolph, M. F., Nova, R., and Wroth, C. P. (1978). On modeling the unloading-reloading behavior of soils. *Inf. J. Num. Anal. Methods. Geomech.* **2**(1), 87–93.

INDEX

A

AASHTO. *See* American Association of State Highway and Transportation Officials
absorbed water influences, 13
active earth pressure coefficient
defined, 276, 611
equation, 614
horizontal component, 735
principal effective stress and, 621
vertical component, 734
active lateral earth force, 624, 626
active lateral earth pressures
for undrained condition, 627
wall friction and, 628
activity
calculation, 63–64
defined, 62
adhesion
total stress analysis (TSA), 544
wall, 628
adhesive stress
defined, 510
lateral earth pressure coefficients and, 627
aggregates, requirement determination, 58–59
air
in voids, 50
weight of, 50
allowable bearing capacity. *See also* bearing capacity
building codes values, 448
of clays, 439–440
CPT data example, 462–463
defined, 424
due to inclined load, 441–442
equation, 432
mat foundation example, 445
sand example, 437–438
shallow square foundation example, 477–482
SPT data example, 458–459
allowable stress design (ASD)
allowable load capacity for, 521
defined, 425
factor of safety calculation, 471, 474
rectangular footing sizing example, 440–441
unfactored load, 474
alluvial soils, 10
 α -method. *See also* driven piles
basis, 531

coefficient values, 532
end bearing, 531–532
skin friction, 531
aluminum sheets, 12
American Association of State Highway and Transportation Officials (AASHTO)
soil classification system, 18, 70
classification example, 80
defined, 74
fine-grained soils, 76
group index value, 75
plasticity chart, 76
silt and clay classification, 76
soil groups, 75
soil types, average grain size, description, 74
soil-aggregate mixtures classification, 75
soils classification, 75
American Society for Testing and Materials classification system (ASTM-CS), 71–74
average grain size, 723
classification example, 77–80
coarse-grained soils flowchart, 72
defined, 71
geotextile tests, 666
inorganic fine-grained soils flowchart, 73
organic fine-grained soils flowchart, 74
soil description, 723
soil types, 723
anchor plates, 648, 649, 650
anchored walls
analysis of, 648–650
examples, 654–659
free earth conditions for, 649
illustrated, 631
plate locations, 649
procedure for analyzing, 649–650
angular distortion. *See* distortion
anisotropic soils
defined, 133
flownet for, 585
anisotropy
causes, 145
structural, 145
transverse, 145, 146
apparent cohesion, 262
aquiclude, 36
aquifers
confined, 36
defined, 36
perched, 37
aquitards, 36

ASD. *See* allowable stress design
ASTM-CS. *See* American Society for Testing and Materials classification system
Atterberg limits
defined, 61
typical, 62, 724
average particle diameter, 5, 19
axisymmetric compression, 341
axisymmetric condition. *See also* strains; stresses
application example, 143–144
defined, 142
Hooke's law for, 142
illustrated, 142
matrix form, 142
strain invariant, 188
stress and strain invariants calculation example, 190–191
stress paths due to, 198–200
transverse anisotropic, elastic equations, 145
axisymmetric extension, 341
axisymmetric radial drainage, 246
axisymmetric undrained loading
porewater pressure under, 305–307
Skempton's coefficients and, 306

B

backfill
cemented soil, 629
compaction, 629
defined, 611
flownet in, 585
gap, 629
balloon test. *See also* compaction
apparatus, 100
comparison, 101
procedure, 100
Barrette piles, 510
base slide, 688, 689
bearing capacity
building codes values, 447–448
cone penetration test (CPT), 460–463
dense coarse-grained soils, 471–472
determination from field tests, 457–464
foundation settlement determination, 457–464
groundwater effects example, 438–439
of layered soils, 445–447
mechanical stabilized earth walls, 668–669
overconsolidated fine-grained soil determination, 470–471
parameters for, 469

- plate load test (PLT), 463–464
 rigid retaining walls, 634
 standard penetration test (SPT), 457–459
 two-layer soil example, 446–447
- bearing capacity equations, 429, 431–443
 allowable bearing capacity, 432
 assumptions, 431
 bearing capacity factors, 433
 derivation of, 431
 eccentric loads, 435–436
 geometric factors, 434
 groundwater effects, 436–437
 inclined load only, 432
 plane strain conditions and, 433
 ultimate gross bearing capacity, 433
 ultimate net bearing capacity, 432
 vertical centric load only, 432
- bearing capacity factors
 comparison, 433
 defined, 520
 equation, 433
- β -method. *See also* driven piles
 coarse-grained soils, 533, 534
 end bearing, 534–535
 ESA basis, 532
 fine-grained soils, 533, 534
 interfacial friction value range, 533
 skin friction, 532–533
- bin walls, 675
- Bishop-Morgenstern method. *See also* slope stability
 defined, 714
 example, 715
 procedure, 714
- Bishop's method. *See also* method of slices
 circular slip surface, 699
 equation for ESA, 701
 equation for TSA, 701
 factor of safety, 704
 force due to porewater pressure, 700
 porewater pressure ratio, 700
 slope stability example, 707–710
 slope stability for two-layered soils
 example, 710–711
- block failure mode. *See also* pile groups
 defined, 547
 group load capacity for, 547–548
 illustrated, 547
- block slide, 689
- boiling, 586–587
- bored piles
 debris removal and, 525
 defined, 510
- borehole logs
 defined, 46–47
 elements, 47
 illustrated, 46
- boreholes
 depths of, 34, 35
 number of, 34–35
- braced excavations, 659–665
- analysis procedure, 661–662
 bottom heave stability, 661
 critical design elements, 660
 cross section illustration, 662
 example, 663–665
 failure lessons, 663
 ground displacement and, 662
 heave mechanisms, 660
 illustrated, 659
 lateral earth pressures, 660–661
 lateral stress distributions, 660
 lateral wall and vertical ground displacements, 661
 limit equilibrium method, 661
 Mohr-Coulomb failure criterion and, 662
 sheet piles, 659
 soil below base, 660
 strut loads, 661
 successful design of, 663
 wall displacements, 660
- British Standards (BS), 18
- building systems, 1–2
- bulk unit weight
 defined, 49
 equation, 52
- Burland-Burridge method, 458
- buttress walls, 630
- C**
- calcareous soil, 11
- caliche, 11
- Cambridge Camkometer, 42–43
- cantilever flexible retaining walls. *See also* flexible retaining walls
 analysis of, 648
 example, 650–654
 illustrated, 631
 wall size determination, 648
- cantilever rigid retaining walls. *See also* rigid retaining walls
 example, 640–643
 illustrated, 630
 material storage example, 676–679
- capillarity
 effects of, 153–154
 porewater pressure due to, 154
 simulation in soils, 154
 understanding, 153
- carbonate, in soil identification, 32
- Cartesian coordinate system, 186
- Casagrande cup method
 cup apparatus, 64
 data interpretation example, 68
 defined, 64
 liquid limit results from, 65
- Casagrande's method, 239
- cast-in-place concrete piles. *See also* concrete piles; piles
 characteristics, 513
 defined, 512
 illustrated, 511
- CD. *See* consolidated drained compression test
- cementation
 defined, 262
 effects of, 269, 407
 as nonuniform, 269
 shear strength from, 269
- cemented soils
 backfill, 629
 critical state line, 408
 CSM application to, 407–408
 failure, 408
 method of slices, 703
 retained, 629
 shear strength, 408
 unloading/reloading line, 408
- chemical sedimentary rocks, 7
- chemical weathering, 10
- chemically stabilized earth walls (CSE), 676
- circular arc failure mechanism, 430
- circular area
 uniformly loaded, 167–170
 vertical elastic settlement at surface, 168
 vertical stress increase due to, 168–170
- circular failure mechanism, 429
- circular footings, 455, 470
- circumferential strains, 210
- circumferential stress, 341
- civil engineering, 2–3
- classification schemes
 American Society for Testing and Materials classification system (ASTM-CS), 71–74
 defined, 70
 United Soil Classification System, 71
- clastic sedimentary rocks, 7
- clay fractions
 defined, 63
 plasticity index and, 62
- clay minerals, 11–12, 729
- clay-rich soils, 63
- clays
 AASHTO classification, 76
 allowable short-term bearing capacity of, 439–440
 average grain size, 18
 elastic parameters, 140
 glacial, 11
 homogenous, 111
 hydraulic conductivity, 111
 infinite slope failure example, 696
 Jamiolkowski relationship for, 392
 lightly overconsolidated, 222, 280
 minerals, 11–12
 normally consolidated, 220–221, 280
 overconsolidated, 221, 280
 pile group load capacity example, 548–551
 pile load capacity example, 535–536
 pile load capacity with varying undrained strength example, 538–539
 in Proctor compaction test, 90
 triaxial CU tests on, 302

- coal, 7
 coarse-grained soils. *See also* fine-grained soils
 ASTM flowchart, 72
 behavior prediction using CSM, 337
 β -method, 533, 534
 drainage qualities, 24
 driven piles in, 540
 hydraulic conductivity for, 111, 267
 load-bearing capabilities, 24
 moisture conditions and, 24
 packing, 34
 particle size, 15–16
 porosity, 723
 relative density, 723
 shallow foundation analysis, 471–474
 shallow foundation design example, 482–485
 shear strength, 313
 sieves, 15–16
 specific gravity example, 55–56
 surface areas, 24
 United Soil Classification System
 flowchart for, 71
 coefficient of compression, 214
 coefficient of consolidation
 calculation example, 242–243
 defined, 226
 determination of, 236–238
 log time method, 237–238
 root time method, 236–237
 typical values, 245
 coefficient of curvature, 19
 coefficient of permeability. *See* hydraulic conductivity
 coherent gravity method, 670–671
 cohesion
 apparent, 262
 defined, 262, 267–268
 effects of, 267–268
 collapse loads, 427
 with limit equilibrium method, 429–430
 variable dependence, 430
 colloidal soils, 11
 color, in soil identification, 32
 compaction, 87–104
 balloon test and, 100
 benefits, 95
 data interpretation examples, 92–95
 defined, 88
 degree of, 97
 field, 96–97
 field equipment specification example, 102–103
 field specification illustration, 91
 as inexpensive improvement method, 87
 laboratory tests to determine, 44
 nuclear density meter and, 100–101
 Proctor compaction test, 89–91
 quality control, 97–101
 quality control test comparison, 101
 sand cone and, 97–99
 soil fabric in, 95
 strength and, 92
 zero air voids and, 88
 composite piles, 512
 compressibility
 index, 382–383
 summary, 726
 compression
 elastic, 207, 520
 isotropic, 192, 193
 one-dimensional, 195–196
 secondary, 207, 208, 211, 234
 triaxial, 197
 compression index
 calculation from one-dimensional consolidation test results, 327
 defined, 208, 214, 325
 determining, 240
 empirical relationships, 245
 test data calculation example, 241–242
 typical range of values, 245
 compressive strains, 135, 149
 compressive stresses, 135
 concrete piles. *See also* piles
 cast-in-place, 511, 512, 513
 precast, 511, 512, 513
 types of, 512
 cone penetrometer test (CPT). *See also* in situ testing devices
 allowable bearing capacity example, 462–463
 bearing capacity, 460–463
 characteristics, 42
 cone factor, 461
 defined, 41
 driven piles and, 540–552
 foundation settlement, 460–463
 illustrated, 41
 net footing pressure, 461
 piezocone, 41–42
 pile load capacity example, 542–544
 settlement example, 462–463
 for shear strength, 314
 variants, 41–42
 VisCPT, 42
 confined aquifers, 36
 consistency, in soil identification, 32
 consolidated drained (CD) compression test
 elastic moduli, 296
 ESP/critical state line intersection, 345
 heavily overconsolidated soil, 335, 336
 interpretation example with Mohr-Coulomb failure criterion, 297–300
 isotropic consolidation phase, 295
 normally consolidated soil, 332
 purpose, 295
 results, 297
 shearing phase, 295
 stress paths, 296
 stresses, 296
 consolidated undrained (CU) compression test
 axial displacement measurement, 300
 on clays, 302
 data interpretation example, 302–303
 elastic moduli, 300
 isotropic consolidation phase, 300
 on lightly overconsolidated soil, 333
 on normally consolidated soil, 334
 purpose, 300
 results, 301, 302
 shearing phase, 300
 stress paths, 301
 stresses, 301
 Tresca failure criterion for, 301
 volume of soil, 300
 consolidation
 coefficient of, 226, 236–238
 defined, 208
 degree of, 228, 229
 experimental setup, 210
 governing equation, 225–231
 laboratory versus field, 243–244
 mechanics, 211
 one-dimensional, 207–260
 one-dimensional theory, 225–234
 parameters, mapping of, 327
 preconsolidation, 246–249
 primary, 207, 208, 211
 rate of, 212
 states, 216
 under constant load, 211
 consolidation ratio, 228
 consolidation settlement
 concepts, 209–216
 differential, in nonuniform soil, 254–255
 due to foundation example, 250–253
 due to unexpected field condition example, 254
 of lightly overconsolidated clay, 222
 with modulus of volume compressibility, 222–223
 of normally consolidated clay, 220–221
 one-dimensional, 207–260
 of overconsolidated clay, 221
 primary, calculation of, 216–225
 secondary, 234
 under pile group, 554–555
 constant loads
 consolidation under, 211
 settlement changes, 213
 void ratio, 213
 constant rate of penetration (CRP) test, 522
 constant-head test. *See also* hydraulic conductivity
 data interpretation example, 121
 defined, 118
 process, 118–119
 setup, 119
 viscosity and, 119
 constitutive relationships, 277

- construction
 excavated slopes, 691–692
 fill slopes, 692
 slope failure from, 690, 691–692
 continuum analysis method. *See also*
 laterally loaded piles
 defined, 565
 example, 566–567
 soil stresses illustration, 565
 Coulomb failure line, 326
 Coulomb failure surface, 328
 Coulomb's earth pressure theory, 620–623
 defined, 620
 failure wedge, 620
 limit equilibrium approach, 621
 Coulomb's failure criterion. *See also* shear strength
 application example, 283–284
 for cemented soil, 273
 dilation effects, 272
 equation summary, 282
 failure criteria comparison, 279
 limiting stress basis, 278
 normal effective stress, 272
 shear box test data interpretation
 example, 290–291
 shear box test interpretation example,
 288–289
 shear stress prediction example, 289
 simulation in dense sand, 271
 Coulomb's frictional law, 270
 Coulomb's frictional sliding, 281
 counterfort walls, 630
 creep. *See* secondary compression
 crib walls, 675
 critical hydraulic gradient
 defined, 587
 excavation example, 588
 critical state
 boundary, 337–338
 defined, 262, 264–265
 shear strength, 281
 theoretical ratio for normalized
 undrained shear strength at, 380
 undrained shear strength at, 351,
 374–376
 void ratio, 281
 critical state friction angle
 excess porewater pressure and, 381
 preconsolidation ratio and, 369–370, 381
 preconsolidation stress and, 372
 undrained shear strength and, 369–370
 critical state lines (CSL)
 as boundary, 337–338
 cemented soils, 408
 defined, 325, 328
 ESP intersection, 331
 initial yield surface intersection, 330
 representation, 328
 slope, 325
 TSP intersection, 333
 void ratio of, 342, 343
 yield surface intersection, 329, 340
 critical state model (CSM), 324–421
 cemented soils application, 407–408
 central idea, 325
 critical state parameters, 340–345
 defined, 324
 elements, 339–345
 estimates, 325
 failure lines, 340–343
 failure stresses from, 345–361
 failure surface, 328
 Hvorslev's limiting stress surface
 within, 375
 for lightly overconsolidated fine-grained
 soil simulations, 361
 modifications, 361–364
 practical relationships, 365–389
 prediction of behavior of coarse-grained
 soils, 337
 prediction under drained and undrained
 condition, 335–337
 prediction under drained condition,
 329–332
 prediction under undrained condition,
 332–334
 shallow foundation analysis with, 464–485
 shallow foundation design example, 500–506
 shallow foundation design for ductile soil
 response example, 482–485
 shallow square foundation example,
 477–482
 shallow strip footing design example,
 474–477
 shear bands and, 337
 soil strength parameters relationships,
 727–729
 soil test results evaluation example,
 409–410
 soil yielding, 328–329
 soils as continua treatment, 337
 strains from, 393–399
 summary, 408–409
 volume changes, 338
 yield surface, 339–340
 critical state parameters
 failure line in (p', e) space, 342–343
 failure line in (p', q) space, 340–342
 critical state shear strength
 notation, 281
 sand prediction example, 385–386
 critical state shear stress, 365–367
 critical void ratio, 264, 281
 CRP. *See* constant rate of penetration test
 crystalline materials, 11
 CSE (chemically stabilized earth) walls, 676
 CSL. *See* critical state lines
 CSM. *See* critical state model
 CU. *See* consolidated undrained
 compression test
 cylindrical coordinate system, 186
D
 dams
 earth, flow through, 598–602
 flownet sketching and interpretation
 example, 589–592
 flownet under, 584
 lab test specification example, 318–319
 phreatic surfaces, 600
 Darcy's law
 defined, 106
 equation, 109, 110
 hydraulic conductivity, 109–111
 in pumping test, 123
 validity, 110
 deep-seated failure, rigid retaining
 walls, 634
 degree of compaction, 97
 degree of consolidation
 average, 229
 change in vertical effective stress at,
 231–232
 defined, 228
 time factor, 229
 degree of saturation
 defined, 49
 equation, 52
 dense coarse-grained soils. *See also* coarse-grained soils
 bearing capacity, 471–472
 foundation settlement, 472–474
 shallow foundation design procedure,
 473–474
 shallow foundations, 471–474
 stresses from shallow footing, 472
 dense sands. *See also* sands
 CD test results, 297
 peak shear stresses, 280
 shear box test results, 287
 depression cone, radius of influence, 124
 desk study, 28
 deviatoric stress
 defined, 187
 distortions, 188
 equation, 187
 on HV surface, 466
 illustrated, 187
 dewatering, 124
 differential settlement, 207, 490–493
 diffraction, 30
 diffuse double layer, 13
 dilatancy, in soil identification, 32
 dilating, 281
 dilation
 defined, 262
 occurrence, 273
 dilation angle
 defined, 273
 negative, 280–281
 at peak shear stress, 281
 dip, 5
 direct shear (DS), 45

- direct simple shear (DSS)
 summary, 45
 triaxial tests and, 377–378
 undrained shear strength estimation
 example, 386–389
 undrained shear strength under, 376–377
 dispersed structure, 14
 displacement piles, 509
 distortion. *See also* foundation settlement
 angular, calculation example, 449–450
 causes, 448
 illustrated, 449
 double drainage equations, 229
 drainage path
 defined, 208
 equation, 212
 longer, 212
 shorter, 212
 drained compression tests, 400
 drained conditions
 in analysis of geosystems, 378–380
 existence of, 267
 stress-strain responses example,
 401–406
 drained loading
 effects on volume changes, 267
 undrained loading versus, 268
 drained triaxial test, 345–347
 ESP slope, 346
 extension, 347
 failure, 346
 for overconsolidated soil, 347
 predicting yield stresses example,
 352–353
 yield shear stress, 347
 drawdown, 124, 125
 drilled shafts
 debris removal, 525
 design example, 571–575
 load capacity, 544–546
 load transfer-settlement curves, 559
 piles, 510, 511
 settlement, 559–560
 driven piles
 α -method, 531–532
 β -method, 532–535
 closed-ended, 540, 541
 CPT and, 540–542
 defined, 514
 end bearing resistance, 520
 installation stress, 514
 methods using statics for, 531–539
 open-ended, 541
 pile load capacity, 539–546
 sleeve resistance, 541
 SPT and, 540
 drum-type rollers, 96, 97
 dry density, laboratory tests to determine, 44
 dry soil, 50
 dry unit weight
 defined, 49
 equation, 52
 maximum, 88
 water content relationship, 90–91
 DSS (direct simple shear), 45
 ductility, 280
 due diligence, 27
 dynamic loading, 267
- E**
- Earth
 crust composition, 7
 profile, 6
 section illustration, 6
 earth dams, flow through, 598–602
 correction factor, 600
 drawing phreatic surface procedure,
 601–602
 equation, 600
 flow rate, 599
 horizontal drainage blanket, 601
 phreatic surface, 599, 600, 601–602
 transition curve, 599
 earthquakes, slope failure from, 690, 691
 earth-retaining structures
 braced excavation, 659–665
 chemically stabilized earth walls
 (CSE), 676
 Coulomb's theory, 620–623
 flexible, stability of, 643–659
 importance, 610
 lateral earth pressures, 612–619
 mechanical stabilized, 666–675
 modes of failure, 630–632
 modular gravity walls, 675
 Rankine's principle, 623–624
 rigid, stability of, 633–643
 in situ reinforced walls, 676
 stability, 610–686
 summary, 676
 types of, 630–632
 eccentric loads, 435–436
 economy, as engineering design tenet, 2
 effective bulk modulus, 189
 effective friction angles. *See* friction angles
 effective particle size, 5, 19, 602
 effective stress analyses (ESA)
 β -method based on, 532
 Bishop's equation for, 701
 defined, 280, 432
 end bearing, 545
 group load capacity, 548
 inclined load only, 432
 Janbu's equation for, 702–703
 load capacity of drilled shafts, 544–545
 for sheet pile walls, 643
 skin friction, 544–545
 ultimate net bearing capacity, 432
 vertical centric load only, 432
 effective stress path (ESP)
 CSL intersection, 331
 defined, 194
 effects of, 338
 effects on soil response, 338
 for elastic soil, 195
 equal to TSP, 331
 illustrated, 194
 mean stress difference, 195
 normal, 265–266
 slope, 196
 stress states on, 331
 Young's modulus based on, 215
 effective stresses, 151–160
 changes, 212
 defined, 133, 151
 denotation, 151
 due to geostatic stress fields, 152–153
 effects of capillarity, 153–154
 effects of groundwater condition
 example, 159–160
 effects of seepage, 154–155
 effects of seepage example, 158–159
 horizontal calculation examples, 161, 162
 lateral, 613
 mean, 367–369
 past maximum vertical, 208
 preconsolidation mean, 330
 principle of, 152
 unsaturated soils, 152
 vertical, 212, 231–232
 vertical calculation example, 156
 vertical distribution example, 157–158
 effective unit weight
 defined, 49
 equation, 52
 elastic analysis, 131, 132
 elastic compression
 of piles, 520
 in total settlement, 207
 elastic deviatoric strain, 467
 elastic displacement, 730
 elastic materials
 defined, 133
 linearly, 136
 nonlinearly, 136
 elastic modulus, 137, 140, 242
 elastic parameters
 clay, 140
 determination example, 242
 laboratory tests and, 145
 elastic settlement
 calculation geometry, 451
 defined, 131
 elastic modulus variation example, 453–454
 footing on clay soil example, 452–453
 of piles, 552–554
 with theory of elasticity, 450
 elastic shear strains
 calculation example, 397
 equation, 396
 elastic soil
 ESP for, 195
 triaxial compression test for, 196

- elastic volumetric strains
calculation example, 397
computation of, 395
increment, 390
- elasticity
theory of, 450
Young's modulus of, 215
- elastoplastic materials
defined, 137
idealized stress-strain curves, 137
shear stress-shear strain response, 138
- electrical resistivity, 31
- elevation head, 106
- embankments
height, 179–180
loads, 177
strength test, 315
- embedding depth, 423, 431
- end bearing
 α -method, 531–532
 β -method, 534–535
defined, 510
driven piles, 520
driven piles in coarse-grained soils, 540
effective stress analyses (ESA), 545
skin friction separation, 524
total stress analysis (TSA), 544
- end bearing piles, 510
- end bearing resistance
illustrated, 521
relative displacement to mobilize, 524
in ultimate load capacity, 521
- engineering design, 2
- engineering use chart
defined, 76–77
illustrated, 78–79
- ENR equation, 562
- entrapped gases, 110
- olian soils, 11
- equilibrium equation, 151–152
- equipotential lines
defined, 579
head loss between, 583
intersection and, 583
- equivalent hydraulic conductivity, 117
- erosion, 689, 690
- ESA. *See* effective stress analyses
- excavated slopes, 691–692
- excavation
braced, 659–665
critical hydraulic gradient example, 588
flow and piping determination example, 603–605
strength test, 315
unsupported, active lateral force, 626
unsupported, in fine-grained soils, 626
- excess porewater pressure. *See also*
porewater pressure
calculation, 231
change in, 196
critical state friction angle and, 381
- defined, 208, 209
developed by loading, 267
distribution, 211
distribution with depth, 228
drainage effects, 267
during undrained loading, 349
initial, 210, 212, 230
interpreting from stress path, 197
at level of deviatoric stress, 198
negative, 269
preconsolidation ratio and, 381
shear component, 349
Skempton equation, 455
spatial variation of, 227
total, 334, 349
volume changes and, 338
- expansive soils
defined, 11
retaining wall support, 629
- external loading, slope failure from, 690, 691
- F**
- factor of safety
against translation, 633
for ASD, 471, 474
basis, 425
Bishop's method, 704
defined, 424
footing subjected to vertical load
example, 442–443
Janbu's method, 702
mechanical stabilized earth walls, 669–670
reserved shear strength, 282
of slopes, 705, 715
Taylor's method, 713–714
- factored moment method (FMM), 646
- factored strength method (FSM), 646
- failure criteria
Coulomb's, 270–274
differences among, 279
Mohr-Coulomb, 275–277
practical implications of, 278–280
summary of equations, 282
Taylor's, 274–275
Tresca, 277–278
- failure deviatoric stress, 341
- failure loads, 426
- failure mechanisms
circular, 429
circular arc, 430
- failure stresses
calculation in extension example, 343–344
from CSM, 345–361
drained triaxial test, 345–347
excess porewater pressures and, 356–360
prediction example, 355–356
undrained triaxial test, 347–351
- failure surfaces
conventional, illustrated, 431
Coulomb, 328
- defined, 328
determining forces on, 429
- Janbu, 702
- Mohr-Coulomb, 328
under footing, 428
- failure zone, 687
- failures
cemented soil, 408
geotechnical lessons from, 3–4
local shear, 428
reasons for, 3–4
shear, 432
tension, 467
Transcona Grain Elevator, 4
- fall cone method
apparatus, 66
data interpretation example, 69–70
defined, 65
sample preparation, 65
test results, 66
- falling-head test. *See also* hydraulic conductivity
continuity condition, 120
data interpretation example, 121–122
defined, 119
process, 119–120
setup, 120
- faults, 5
- FDM. *See* finite difference method
- feel, in soil identification, 32
- field compaction. *See also* compaction
with drum-type rollers, 96, 97
lifts, 97
machinery type, 96
with sheepfoot rollers, 96, 97
specification illustration, 91
- field tests
bearing capacity determination, 457–464
- foundation settlement determination, 457–464
- pile load, 519–520
- shear strength determination, 313–314
- soils exploration, 37–43
- fill slopes, 692
- filter fabric, 602
- fine-grained soils. *See also* coarse-grained soils
AASHTO classification, 76
 β -method, 533, 534
- consolidated, primary consolidation
settlement, 217–218
- drainage qualities, 24
- hydraulic conductivity for, 111
- hydrometer test, 16–17
- index properties of, 61–64
- inorganic, ASTM flowchart, 73
- isotropically consolidated, 371–374
- load-bearing qualities, 24
- moisture conditions and, 24
- normally consolidated, 370–371

- fine-grained soils. *See . . . (continued)*
- one-dimensional consolidation
- settlement, 207–260
 - organic, ASTM flowchart, 74
 - overconsolidated, 218, 370–371
 - particle size, 16–17
 - physical states of, 61–64
 - shallow excavations, 268
 - shallow foundation analysis, 465–471
 - shear strength, 313
 - shear strength prediction example, 384–385
 - strength based on liquidity index, 62
 - surface areas, 24
 - tension cracks in, 645–646, 704
 - undrained shear strength, 351
 - United Soil Classification System
 - flowchart for, 72
 - unsupported excavation in, 626
 - walls embedded in, 627
- finite difference method
- flownet example, 595–598
 - for governing consolidation equation, 229–231
 - porewater pressure distribution
 - calculation, 232–234
 - potential head, flow, porewater pressure distribution, 594–595
 - two-dimensional flow, 592–598
 - two-dimensional slope stability analysis, 697
- finite element method (FEM), 697
- finite surface loads, 163
- fissuring, 110
- flat plate dilatometer (DMT). *See also* in situ testing devices
- defined, 43
 - illustrated, 44
 - tests, 43
- flexible retaining walls
- analyses methods, 646–647
 - anchored, 631, 648–650, 654–658
 - cantilever, 631, 648, 650–654
 - defined, 611, 630
 - effective stress analysis, 643
 - factored moment method (FMM), 646
 - factored strength method (FSM), 646
 - lake example, 679–682
 - lateral pressure distributions, 647
 - in mixed soils, 645
 - modes of failure, 632
 - porewater pressures distribution, 643, 644
 - pressure distributions approximation, 648
 - propped, 631
 - soil-wall interface friction, 647
 - stability of, 643–659
 - tension cracks in fine-grained soils, 645–646
 - types of, 631
 - in uniform soils, 643–645
 - uses, 632
- floating piles, 510
- flocculated structure, 14
- flow data, 126–127
- flow lines
- defined, 579
 - intersection, 583
 - sketching, 583
- flow parameters, 112–113
- flow rate, 586
- flow slide, 688, 689
- flownets
- for anisotropic soil, 585
 - in backfill, 585
 - boiling, 586–587
 - criteria, 583
 - critical hydraulic gradient, 587, 588
 - defined, 579, 583
 - examples, 584–585
 - finite difference method example, 595–598
 - flow line intersection, 583
 - flow rate, 586
 - heaving, 586–587
 - hydraulic gradient, 586
 - for isotropic soils, 583–585
 - piping, 586–587
 - porewater pressure distribution, 587
 - for sheet pile, 584
 - sketching, 583–585
 - sketching and interpretation example, 589–592
 - static liquefaction, 586–587
 - under dam, 584
 - uplift forces, 587–588
- fluid pressure, 107
- fluvial soils. *See* alluvial soils
- FMM (factored moment method), 646
- footings
- analysis, 426
 - centroid, 435
 - circular, 455, 470
 - conventional failure surface under, 428–429
 - defined, 423
 - design to limit differential settlement example, 490–493
 - dimensionless shape parameter values, 451
 - eccentric loads, 435–436
 - elastic settlement example, 452–453
 - factor of safety example, 442–443
 - geometric factors, 434
 - groundwater effects below base of, 436–437
 - load transmission, 450
 - loaded, soil response to, 426–428
 - primary consolidation settlement example, 456
 - rectangular, 455, 470
 - rough, 434
 - shallow, 427
 - shape and slope, 434
 - sizing example, 440–441
 - sizing for building example, 493–500
- on slope, 434
- smooth, 434
- square, 470, 477–482, 487–490
- strip, 468, 470, 474–477
- two-layer soil, 446
- force paths, effects, 191
- foundation settlement, 448–450
- calculations, 450–456
 - cone penetration test (CPT), 460–463
 - cone penetration test (CPT) example, 462–463
 - dense coarse-grained soils, 472–474
 - determination from field tests, 457–464
 - differential limit example, 490–493
 - immediate, 450–454
 - nonuniform, 448, 449
 - overconsolidated fine-grained soil determination, 470–471
 - parameters for, 469
 - plate load test (PLT), 463–464
 - prevention and, 448
 - primary consolidation, 454–456
 - serviceability limit states and, 448, 449
 - shallow square foundation example, 477–482
 - standard penetration test (SPT), 457–460
 - standard penetration test (SPT) example, 460
 - tile or distortion, 448, 449
 - time-dependent, 458
 - types, 448
 - uniform, 448, 449
- foundations
- analysis with CSM, 464–485
 - consolidation settlement example, 250–253
 - defined, 422, 423
 - design on overconsolidated clay, 410–414
 - failure calculations example, 316–318
 - horizontal displacement, 485–486
 - mat, 443–445
 - Mohr–Coulomb failure criterion for failure stress example, 285–286
 - pile, 509–578
 - raft, 443–444
 - rotation, 485–486
 - shallow, 423
 - stability conditions, 422
 - stress paths example, 203–205
 - as structures, 422
 - tank, soil response example, 414–418
 - tank, strength test, 315
 - vertical strain increase example, 180–181
 - vertical stress contour example, 171
- Fourier series, governing consolidation equation with, 227–229
- friction angles
- critical state, 369–370
 - defined, 262, 281
 - ranges of, 282, 724
 - simple test to determine, 286
- summary, 726

friction piles, 510
 frictional resistance, 191
 FSM (factored strength method), 646

G
 gabion baskets, 675
 gamma density, 31
 gap-graded soils, 19
 geocomposites, 666
 geographical information system (GIS), 28
 geogrids, 666
 geological dating, 9
 geological features, slope failure from, 690, 691
 geological time, 9
 geology
 discontinuities, 8
 Earth crust composition, 7
 Earth profile and, 6
 plate tectonics, 6–7
 principle of original continuity, 8
 principle of original horizontality, 8
 principle of superposition, 9
 geophones, 30
 georadar, 29
 geostatic stress fields, effective stresses due to, 152–153
 geosynthetics, 666
 geosystems analysis
 drained/undrained conditions and, 378–380
 long-term condition, 379
 short-term condition, 378–379
 geotextiles, 602. *See also* mechanical stabilized earth walls
 ASTM tests, 666
 defined, 666
 illustrated, 666
 manufacture of, 666
 MSE wall example, 671–673
 strength reduction, 666
 glacial clays, 11
 glacial soils, 10, 11
 glacial till, 11
 governing consolidation equation
 derivation of, 225–227
 finite difference solution, 229–231
 solution using Fourier series, 227–229
 GPR (ground-penetrating radar), 29
 grains
 geometry, 272
 size, laboratory tests to determine, 44
 gravel
 average grain size, 18
 hydraulic conductivity, 111
 gravitational flow, 106
 gravity retaining walls
 defined, 611
 example, 635–640
 illustrated, 630
 ground-penetrating radar (GPR), 29

groundwater
 below slip plane, 693
 condition effects on effective stress example, 159–160
 conditions in soils exploration, 36–37
 correction factor, 457
 defined, 105
 depth, 107
 effects below base of footing, 436–437
 effects on bearing capacity example, 438–439
 lowering by wellpoints, 124–126
 pumping tests and, 123
 groundwater level (GWL)
 at depth, 153
 at ground surface, 152–153
 top of, 36
 gypsum, 11

H
 hand augers, 32, 33
 harmonic mean, 219
 head loss, 582
 heads
 defined, 105
 elevation, 106
 hydraulic, 108–109, 113–115
 loss, 117
 loss due to flow, 107
 pressure, 106
 total, 106, 109
 velocity, 106, 581
 heat diffusion equation, 227
 heavily overconsolidated soils
 behavior prediction under drained and undrained conditions, 335–337
 CD test predictive results, 335, 336
 CSM modifications and, 363
 dense-to-medium-dense coarse-grained, 351
 elastic deformation, 337
 fine-grained, 351
 shallow foundation analysis, 465–471
 shallow square foundation example, 477–482
 shallow strip footing design example, 474–477
 stresses from shallow footing, 466
 undrained shear strength determination example, 360–361
 heaving, 586–587
 hollow box culvert, 605–606
 hollow-cylinder apparatus
 illustrated, 312
 purpose, 312
 resonance column tests with, 392
 homogenous clays, 111
 Hooke's law, 139–141
 for axisymmetric condition, 142
 defined, 139
 for displacements from strains and forces, 140

for plane strain condition, 141–142
 for principal stresses, 140
 with stress and strain invariants, 189
 for transverse anisotropic soils, 146

horizontal effective stresses
 calculation examples, 161, 162
 principal, 161

horizontal elastic displacement
 defined, 485
 equations for estimating, 486

horizontal total stresses, 162

HV (Hvorslev's) surface, 465
 with CSM, 375
 defined, 361
 deviatoric stress on, 466
 failure on, 363
 initial deviatoric stress on, 375
 as limiting stress surface, 363
 normalized undrained shear strength and, 375
 soil responses and, 364
 stress states, 362

hydraulic conductivity
 average, 125
 for coarse-grained soils, 111, 267
 for common soil types, 724
 constant-head test, 118–119
 defined, 105, 109
 dependencies, 110
 determination of, 118–124
 empirical relationships, 111–116
 equivalent, 117
 falling-head test, 119–120
 for fine-grained soils, 111
 for homogeneous soil, 111
 in horizontal direction, 248
 pumping test to determine, 122–124
 in radial direction, 248
 for soil types, 111

hydraulic gradient, 123, 586

hydraulic heads. *See also* heads
 calculation and application example, 113–115
 determination example, 108–109

hydrometer test, 16–17

hydrostatic force, 616

hydrostatic pressure
 calculation example, 115–116

variation, 107

I
 ICL. *See* isotropic consolidation line
 igneous rocks, 7
 illite, 11, 12
 immediate settlement
 calculation geometry, 451
 elastic modulus variation example, 453–454
 footing on clay soil example, 452–453
 with theory of elasticity, 450

impervious clays, 111

- in situ reinforced walls, 676
 in situ testing devices
 cone penetrometer test (CPT), 41–42
 flat plate dilatometer (DMT), 43, 44
 pressuremeters, 42–43
 standard penetration test (SPT), 38–41
 types of, 37
 vane shear test (VST), 37–38
 inclined loads, allowable bearing capacity
 due to, 441–442
 incremental loads, in oedometer test, 235
 index test, 44
 infinite loads. *See also* surface loads
 defined, 178
 example, 163
 infinite slopes, 692–696
 clay soils example, 696
 depth of tension cracks, 695
 dimensions, 692
 failure mechanism, 695
 limit equilibrium method, 693
 seepage, 693
 shear stress on slip plane, 694
 stability example, 695–696
 use of, 692–693
 initial excess porewater pressure
 distribution, 231
 estimating, 230
 reduction in, 212
 with vertical load, 210
 initial stresses, strength test, 315
 initial yield
 surface, 329, 340
 theoretical ratio of undrained shear
 strength at, 380
 undrained shear strength at, 374–376
 instantaneous load, 210
 interface friction, 628, 629
 isotropic, 133, 187
 isotropic compression
 defined, 192
 stress path for, 193
 isotropic consolidation line (ICL), 326
 isotropic soils, flownet for, 583–585
 isotropically consolidated fine-grained soils,
 undrained shear strength and, 371–374
- J**
 Janbu's method. *See also* method of slices
 correction factor, 702
 equation for ESA, 702–703
 equation for TSA, 703
 factor of safety, 702
 failure surface, 702
 slope stability example, 711–712
- K**
 kaolinite
 Atterberg limits for, 62
 defined, 11
 structure, 12
- L**
 laboratory tests
 direct shear (DS), 45
 direct simple shear (DSS), 45
 one-dimensional consolidation, 45,
 235–243
 parameters, 37
 phase, 28
 physical properties summary, 44
 results, 37
 samples, 45
 strength, 314, 315
 triaxial (T), 45
 types of, 43–45
 lacustrine soils, 11
 Laplace's equation
 assumptions, 581
 defined, 580–581
 solution, 581
 velocity head and, 581
 lateral earth forces
 active, 624, 626
 in lateral stress diagram, 615
 passive, 624, 626
 lateral earth pressure coefficients
 active, 734–735
 adhesive stress and, 627
 passive, 736–737
 summary, 726
 lateral earth pressures
 active, 627, 628
 active, variation of, 615
 active coefficient, 614
 application to retaining walls, 627–630
 assumptions, 612
 braced excavations, 660–661
 concepts, 612–619
 force example, 616–617
 hydrostatic force, 616
 layered soils example, 617–619
 passive, 627
 passive, variation of, 615
 passive coefficient, 614
 for Rankine active state, 615
 for Rankine passive state, 615
 at rest, 161
 sands and, 628
 stresses, 612
 surface stresses, 616
 for total stress analysis, 625–627
 for vertical frictionless walls, 623
 lateral effective stresses, 613
 lateral strains, 210
 lateral stress
 coefficient variation with depth, 670
 distributions for braced excavations, 660
 soil consolidation example, 250
 laterally loaded piles, 563–567
 analyses, 565
 analysis difficulty, 564
 continuum analysis, 565
 designing, 563–564
 mechanism of failure, 564
 pile groups, 564–565
 pile-soil response, 564
 p-y method, 565
 single pile continuum analysis example,
 566–567
 lateritic soils, 11
 layered soils
 bearing capacity example, 446–447
 bearing capacity of, 445–447
 lateral earth pressure example, 617–619
 load capacity of drilled shaft example,
 545–546
 pile group load capacity example, 548–551
 pile loading capacity example, 536–538
 slope stability with Bishop's method
 example, 710–711
 soft clay over stiff clay, 446
 stiff clay over soft clay, 446
 thinly stratified, 446
 layers
 flow normal to, 117
 flow parallel to, 116
 hydraulic conductivity and, 110
 thick soil, consolidation settlement, 219
 vertical and horizontal flows example,
 117–118
 lifts, 97
 lightly overconsolidated clays
 consolidation settlement, 222
 peak shear stresses, 280
 lightly overconsolidated soils
 behavior prediction under drained
 conditions, 329–332
 behavior prediction under undrained
 conditions, 332–334
 CSM for simulations, 361
 CSM modifications and, 363
 failure in undrained test, 348
 triaxial CU test results, 333
 limit equilibrium method
 braced excavations, 661
 collapse loads, 429–430
 slope analysis based on, 699
 line loads. *See also* surface loads
 defined, 165
 near retaining wall, 165–166
 linear shrinkage ratio, 67
 linearly elastic materials, 136
 liquid limit
 Casagrande cup method for determining,
 64–65
 defined, 49, 61
 fall cone test determination of, 65–66

liquidity index
calculation, 63–64
defined, 62
sensitivity and, 383
soil strength based on, 723
undrained shear strength and, 383
load and resistance factor design (LRFD)
bearing capacity calculations using, 426
defined, 425
factored load, 474
rectangular footing example, 440–441
load capacities of drilled shafts
calculation, 544
ESA, 544–545
layered soils example, 545–546
TSA, 544
load-base displacement response, 517, 518
load-displacement response, elastic-
perfectly plastic material, 427
loaded footings, 426–429
loading history effects, 215
loads
collapse, 427, 429–430
constant, 211, 213
eccentric, 435–436
embankment, 177
failure, 426
finite, 163
inclined, 441–442
incremental, 235
infinite, 163, 178
instantaneous, 210
line, 165–166
point, 163, 164–165
rectangular, 172–175
ring, 167–170
strip, 166–167
surface, 163–178
load-settlement curves, 524
loam, 11
local shear failure, 428
localization, 364
loess, 11
log time method. *See also* coefficient of
consolidation
defined, 237
illustrated, 238
procedure, 238
long-term condition
defined, 267
ESA requirement, 432
in geosystems analysis, 379
volumetric elastic strain during, 467
loose sands. *See also* sands
CD test results, 297
peak shear stresses, 280
shear box test results, 287
Love (LQ) waves, 7
LRFD. *See* load and resistance factor
design
LS surface, 471

M
magma, 7
marine soils, 10, 11
marl, 11
mass gravity retaining wall, 635–640
mat foundations
allowable bearing capacity for, 445
defined, 443
illustrated, 444
location, 443
as raft foundations, 443–444
material storage, cantilever gravity walls
for, 676–679
maximum dry unit weight
defined, 88
knowledge of, 91
in soil compaction, 91–92
theoretical, 88, 89
maximum effective stress obliquity, 277
mean effective stress
preconsolidation, 300, 391, 469
preconsolidation stress and, 367–369
tension cutoff and, 367–369
mean stress
defined, 187
equation, 187
illustrated, 187
TSP and ESP difference, 195
mechanical stabilized earth walls. *See also*
earth-retaining structures
analysis with low extensible materials, 671
bearing capacity, 668–669
coherent gravity method, 670–671
concepts, 667
defined, 611
economy, 667
essential point, 667
external stability, 667
factor of safety, 669–670
geogrids, 666
geotextiles, 666, 671–673
illustrated, 666
internal stability, 667
metal strips, 666
metal ties example, 673–675
Rankine active earth pressure theory,
667–668
stability, 667–671
tensile force, 668
total length of reinforcement, 668
translation, 668–669
types of, 666
Menard pressuremeter, 42
metal ties MSE wall, 673–675
method of slices, 699–703
application of, 704–705
Bishop's method, 699–701
cemented soils, 703
illustrated, 705
Janbu's method, 702–703
procedure for, 705–712
microgravity, 31
micropiles. *See also* piles
characteristics, 513
defined, 510, 512, 567
design of, 567
installation, 568
load capacity, 568
size, 567
uses, 567
minerals
clay, 11–12
defined, 5, 11
free swell, 729
free swell ranges, 54
illite, 11, 12
kaolinite, 11, 12
montmorillonite, 11–12
silicates, 11
minipiles. *See* micropiles
modular gravity walls, 675
modulus of volume compressibility
consolidation settlement using, 222–223
defined, 209, 214
determination of, 240–241
range of vertical effective stress and,
240–241
modulus of volume recompressibility
defined, 215
determination example, 242
Mohr-Coulomb failure criterion. *See also*
shear strength
application example, 284–285
assumptions, 278
braced excavations and, 662
CD triaxial test data interpretation ex-
ample, 297–300
defined, 275
equation summary, 282
failure criteria comparison, 279
failure envelope, 275
failure lines, 276
failure stress due to foundation
example, 285–286
limiting stress basis, 276, 278
Mohr-Coulomb failure surface, 328
Mohr's circle
for at-rest state, 613
geometry, 275
planes in, 148
pole on, 148
for strain states, 148–149
for stress states, 147–148
for UC test, 293–294
for undrained conditions, 278
for UU test, 304
moisture, in soil identification, 32
moment equilibrium equation, 429
montmorillonite
defined, 11–12
structure, 12
as swelling clay, 12

MSE. *See* mechanical stabilized earth walls
mud, 11
multichannel analysis of surface waves (MASW), 30

N

NCL. *See* normal consolidation line
negative skin friction
 calculation, 560
 fill example, 560–561
 piles subjected to, 560–561
neutron porosity, 31
Newmark charts
 defined, 175
 for increase in vertical stress, 162, 175
 normalization, 175
 procedure for using, 175–176
nondilating, 281
nondisplacement piles, 510
nonlinearly elastic materials, 136
nonuniform settlement. *See also* foundation settlement
 defined, 448
 illustrated, 449
normal consolidation line (NCL)
 defined, 213
 slope, 240, 326
 soil settlement following, 218
normal effective stress
 Coulomb's failure criterion, 272
 effects of increasing, 265–266
 peak shear stress plot versus, 269
 Type I soils, 263
 Type II soils, 263–264
normal stresses, 133, 151
normally consolidated clays
 consolidation settlement, 220–221
 peak shear stresses, 280
 soil strength relationships, 316
normally consolidated soils
 behavior prediction under drained conditions, 329–332
 behavior prediction under undrained conditions, 332–334
 CU test results, 334
 defined, 208
 initial elastic response and, 334
 undrained shear strength for, 370–371
nuclear density meter. *See also* compaction
 backscatter measurement, 101
 defined, 100
 direct transmission measurement, 101
 illustrated, 100
 test comparison, 101

O

O-cells (Osterberg cells)
 convention pile load test versus, 523
 defined, 524
 expansion, 524
 illustrated, 525

pile load test schematic, 526
test data interpretation example, 528–530
oedometer test. *See also* one-dimensional consolidation
 apparatus, 235
 data obtained, 236
 defined, 235
 incremental loads, 235
one-dimensional compression, 195–196
one-dimensional consolidation, 45, 207–260
 general equation, 227
 normalized undrained shear strength of, 371–374
 OCR for, 373
 settlement, 207–260
 Terzaghi equation, 227
 theory, 225–234
one-dimensional consolidation test, 235–243
 coefficient of consolidation determination, 236–238
 compression index determination, 240
 data obtained from, 236
 early time response correction, 236
 maximum vertical effective stress determination, 239–240
 modulus of volume change determination, 240–241
 oedometer, 235–236
 recompression index determination, 240
 secondary compression index determination, 241
 void ratio determination, 238–239
one-dimensional consolidation theory, 225–234
 derivation of governing equation, 225–227
 finite difference solution, 229–231
 governing consolidation equation with Fourier series, 227
one-dimensional flows, 105–129
 Darcy's law and, 109–111
 equivalent hydraulic conductivity, 117
 hydraulic conductivity, 109–116
 hydraulic conductivity determination, 118–124
 importance, 105
 normal to soil layers, 117
 parallel to soil layers, 116
 vertical and horizontal example, 117–118
optimum water content
 compaction and, 90–91
 defined, 88, 90
 knowledge of, 91
 Proctor test data calculation example, 92
 in soil compaction, 91–92
organic sedimentary rocks, 7
overconsolidated clays
 consolidation settlement, 221
 foundation design example, 410–414
 peak shear stresses, 280
 soil strength relationships, 316
overconsolidated fine-grained soils
primary consolidation settlement, 218
settlement calculation of, 218
undrained shear strength for, 370–371
overconsolidated soil
 clays, 221, 280, 316, 410–414
 defined, 208
 drained triaxial test, 347
 fine-grained, 218, 370–371
 sand, 458
overconsolidation ratio (OCR)
 defined, 208
 depth and, 216
 effects on peak strength and volume expansion, 266
 equation, 216
 for one-dimensionally consolidated fine-grained soils, 373
 summary, 726
 variation estimation with depth, 223–225

P

packing, coarse-grained soils, 34
parameter mapping, 326–327
particle size
 average diameter, 5, 19
 characterization of soils based on, 17–19
 coarse-grained soils, 15–16
 distribution curves, 16
 effective, 5, 19
 fine-grained soils, 16–17
 hydraulic conductivity and, 110
 laminar flow, 17
 ordinate versus logarithm of, 16
particles
 arrangement in coarse-grained soils, 270–271
 average diameter, 5, 18
 mineral, 11
 rigid assumption, 13
passive earth pressure coefficient
 defined, 276, 611
 equation, 614
 horizontal component, 736
 principal effective stress and, 621
 vertical component, 737
passive lateral earth force, 624, 626
passive lateral earth pressures, for undrained condition, 627
past maximum vertical effective stress
 with Casagrande's method, 239
 defined, 208
 determining, 239–240
 procedure, 239
peak effective friction angle, 281
peak shear strength
 notation, 281
 sand prediction example, 385–386
peak shear stress
 dense sands, 280
 dilation angle at, 281
 envelope, 268

- lightly overconsolidated clays, 280
 loose sands, 280
 mineralogical composition and, 266
 normal effective stress plot versus, 269
 normally consolidated clays, 280
 overconsolidated clays, 280
 Type II soils, 263, 265
 perched aquifers, 37
 perched water tables, 37
 permeability, laboratory test to determine, 44
 phases
 illustrated, 50
 relationships, 50–61
phreatic surfaces. See also earth dams
 approximation, 599
 for dams with drainage blankets, 600
 draw procedure, 601–602
 illustrated, 599
 physical weathering, 10
 piezocene, 41–42
 piezometers, 107, 108
 pile driving
 equations, 562–563
 impact load, 515
 number of blows, 563
 records, 563
 pile foundations, 509–578
 failure mechanisms, 519
 field load tests, 519–520
 load transfer characteristics, 519
 load-base displacement response, 517, 518
 soil stress state, 517
 stress-strain response, 517, 518
 uses, 509
 pile groups, 546–551
 block failure mode, 547–548
 connections, 546–547
 consolidation settlement under, 554–555
 embedded above soft clay layer, 554
 geometric patterns, 546
 illustrated, 547
 lateral loads, 564–565
 load capacity, 547
 load capacity in layered clays example, 548–551
 pile interaction in, 554
 ratio of load capacity, 547
 settlement distribution of load, 555
 settlement estimate procedure, 555–559
 settlement example, 556–559
 single pile failure mode, 548
 spacing, 546
 pile installation
 maximum stress, 514
 methods, 514
 micropiles, 568
 pile load capacity and, 515
 residual stresses, 517
 soil below pile base, 517
 soil stresses, 515
 structural loads applied after, 518–519
 types of, 514
 pile load capacity
 allowable load capacity, 524
 clay soil example, 535–536
 clay with varying undrained strength example, 538–539
 CPT data example, 542–544
 of drilled shafts, 544–546
 on driven piles, 539–546
 estimating, 520
 interpretation of, 522
 layered soil profile example, 536–538
 micropiles, 568
 negative skin friction and, 516
 pile group, 547
 pile installation and, 515
 pile load test and, 522–530
 single piles, 521–522
 SPT data example, 542
 pile load test, 522–530
 conventional versus O-cell, 523
 data interpretation examples, 526–528
 load-settlement curves, 524
 O-cell, 523, 524, 525
 O-cell test data interpretation example, 528–530
 purposes, 522
 schematic variations of plots, 523–524
 setup illustration, 523
 standardized methods for conducting, 522
 pile supporting compressive load, 315
 pile supporting tensile load, 315
 pile-driving hammers
 efficiency, 562
 energy delivered by, 562
 illustrated, 514
 piles
 Barrette, 510
 bored, 510
 composite, 512
 concrete, 511, 512
 defined, 509
 displacement, 509
 distributed volume of soil and, 515
 drilled shaft, 510, 511
 drilled shaft design example, 571–575
 driven, 514
 elastic compression of, 520
 elastic settlement of, 552–554
 elastic shortening of, 553
 end bearing, 510
 fish port facility design example, 568–571
 floating, 510
 friction, 510
 laterally loaded, 563–567
 micropile, 510, 512, 513, 567–568
 negative skin friction, 560–561
 nondisplacement, 510
 plastic, 512
 point bearing, 510
 settlement estimation procedure, 555–559
 settlement examples, 556–559
 steel, 511, 512, 513
 timber, 511, 512, 513
 types of, 511–513
 volume of, 515
 pileup
 defined, 426
 plastic flow causing, 427
 piping, 586–587, 603–605
 plane strain condition. *See also strains; stresses*
 application example, 143
 bearing capacity equations and, 433
 defined, 141
 field conditions and, 196
 Hooke's law for, 141–142
 illustrated, 141
 matrix form, 142
 strain invariant, 188
 undrained shear strength under, 376–377
 plastic limit
 defined, 49, 61
 fall cone test determination of, 65–66
 soil illustration, 65
 test, 65
 plastic materials, 133
 plastic piles, 512
 plastic strains, 394
 plastic volumetric strain ratio, 351
 plastic zones, 428
 plasticity chart
 A-line, 76
 illustrated, 76
 U-line, 76
 plasticity index
 calculation, 63–64
 clay fractions on, 62
 compressibility index and, 382–383
 defined, 61
 plate load test (PLT)
 bearing capacity, 463–464
 foundation settlement, 463–464
 illustrated, 463
 plate sizes, 463
 problems, 464
 plate tectonics, 6–7
 plotting stress paths
 procedure, 197–198
 with stress invariants, 192–196
 with two-dimensional stress parameters, 196–197
 PLT. *See plate load test*
 plugging, 512
 point bearing piles, 510
 point loads. *See also surface loads*
 distribution of stresses for, 163
 vertical stress increase due to, 164–165
 point resistance, 510

- Poisson's ratio
defined, 136
determining, 139
in elastic analysis, 131
generalized, 189
typical values, 136, 724
for undrained condition, 450
poorly graded soils, uniformity
coefficients, 19
pore liquid properties, 110
pore size, 110
porewater
carrying total load, 210
defined, 50
excess, volume of, 210
porewater pressure. *See also* excess
porewater pressure
defined, 105, 133, 151
due to capillarity, 154
maximum change in, 195
measurement, 108
negative, 268
Skempton's coefficients, 306
transducers, 108, 209
under axisymmetric undrained loading,
305–307
variation, 107
vertical and radial dissipation, 248
porewater pressure distribution, 230
calculation example, 232–234
flownet, 587
initial excess porewater pressure and, 230
sheet pile walls, 643, 644
porewater pressure ratio, 687, 700
porosity
calculation example, 56
coarse-grained soils based on, 53, 723
defined, 49
equation, 51
of soils, 51
porous media, two-dimensional flow
through, 580–583
potential drop, 582
potential flow equation. *See* Laplace's
equation
power augers, 32, 33
precast concrete piles. *See also* concrete
piles; piles
characteristics, 513
defined, 512
illustrated, 511
Raymond cylindrical, 512
precast modular concrete walls, 675
preconsolidation, 246–249
preconsolidation mean effective stress, 391
defined, 330
void ratio at, 469
preconsolidation ratio
critical state friction angle and, 369–370, 381
defined, 325
equation, 326–327
excess porewater pressure and, 381
for tension cutoff, 367, 368
undrained shear strength and, 369–370
preconsolidation stress
critical state friction angle and, 372
mean effective stress and, 367–369
tension cutoff and, 367–369
pressure head, 106
pressuremeters. *See also* in situ testing
devices
Cambridge Camkometer, 42–43
characteristics, 43
defined, 42
Menard, 42
primary consolidation
defined, 208
parameters, 214–215
secondary compression versus, 211
in total settlement, 207
under constant load, 211
vertical stresses on, 213–214
primary consolidation settlement
calculation of, 216–225
calculation procedure, 218–219
footing example, 456
foundation, 454–456
of normally consolidated fine-grained
soils, 217–218
for one-dimensional consolidation, 454, 455
of overconsolidated fine-grained soils, 218
thick soil layers, 219
unloading/reloading effects, 216–217
principal stresses
defined, 135
Hooke's law for, 140
horizontal effective, 161
plane, 147
vertical effective, 161
principle of effective stress, 152
principle of original continuity, 8
principle of original horizontality, 8
principle of superposition, 9
Proctor compaction test. *See also* compaction
apparatus, 90
clays, 90
compaction energy, 89
defined, 89
hammer energy, 89
modified, 90–91
results interpretation, 91–95
results interpretation example, 102–103
proped walls, 631
protected fortress, 1
pumping test. *See also* hydraulic
conductivity
Darcy's law in, 123
data interpretation example, 123–124
defined, 122
groundwater and, 123
layout illustration, 122
simple well equation, 122–123
punching shear, 428
p-y analysis method, 565
- Q**
- quick maintained load (QML), 522
quicksand, 587
- R**
- radial displacement, 164
radial stress, in axisymmetric extension, 341
raft foundations, 443–444
rainfall = slope failure, 690, 691
Rankine active state
defined, 614
lateral earth force, 615
lateral earth pressure, 615
slip plane orientation, 614–615
Rankine passive state
defined, 614
lateral earth force, 615
lateral earth pressure, 615
slip plane orientation, 615
rapid drawdown, slope failure from, 690, 692
rate of consolidation, 212
Rayleigh (LR) waves, 7
Raymond cylindrical prestressed pile, 512
recompression index
calculation from one-dimensional
consolidation test results, 327
defined, 209, 215, 325
determining, 240
empirical relationships, 245
typical range of values, 245
reconnaissance, 28
rectangular footings, 455, 470
rectangular loads
approximate method for, 172–173
dispersion of, 173
vertical stress increase due to, 173–175
reflection, 30
refraction, 30
relative density
coarse-grained soils based on, 53, 723
defined, 49, 53
equation, 53
repelling forces, 13
reserved shear strength, 282
residual shear strength, 281
residual shear stress, 263
residual soils, 10
resonance column tests, 392
retaining walls. *See also* earth-retaining
structures
anchored or tie back, 631
braced excavation, 659–665
buttress, 630
cantilever, 630, 631
chemically stabilized earth (CSE), 676
counterfort, 630
embedded in fine-grained soils, 627
expansive soils, 629

- flexible, 611
 forces for total stress analysis, 625
 gravity, 611, 630
 lateral earth pressures, 616
 lateral earth pressures application to, 627–630
 mechanical stabilized earth (MSE), 666–675
 modes of failure, 630–662
 modular gravity, 675
 propped, 631
 in situ reinforced, 676
 slip planes with soil mass, 613
 sloping back, 621
 sloping soil surface, 621
 strength test, 315
 tension cracks behind, 626
 types of, 630–632
 wall friction, 621, 622
 wall/backfill gap, 629
 rigid retaining walls. *See also* retaining walls
 bearing capacity, 634
 cantilever wall example, 640–643
 cantilever wall for material storage example, 676–679
 deep-seated failure, 634
 defined, 630
 drainage systems, 632
 embedment of, 634
 forces, 633
 mass gravity wall example, 635–640
 modes of failure, 631
 procedures for analyzing, 635
 rotation, 634
 seepage, 635
 stability of, 633–643
 translation, 633–634
 types of, 630
 ring loads, 168–170
 rocks
 defined, 5
 igneous, 7
 sedimentary, 7
 weathering of, 10
 root time method. *See also* coefficient of consolidation
 calculation example, 242–243
 defined, 236
 illustrated, 237
 procedure, 237
 rotary drills, 32, 33
 rotation
 defined, 486
 equations for estimating, 486
 rigid retaining walls, 634
 rotational slope failures, 697–699
 circular, 697
 illustrated, 689
 noncircular, 697
 types of, 688
 rough footings, 434
 RSW surface, 362, 465
- S**
 safe bearing capacity, 424
 safety factor. *See* factor of safety
 sand cone test. *See also* compaction
 apparatus, 97–98
 procedure, 98
 results interpretation example, 98–99
 test comparison, 101
 sands
 allowable bearing capacity example, 437–438
 average grain size, 18
 critical state shear strength prediction, 385–386
 dense, 280, 287, 297
 elastic parameters, 140
 hydraulic conductivity, 111
 lateral earth pressure and, 628
 loose, 280, 287, 297
 overconsolidated, 458
 peak shear strength prediction, 385–386
 Seed and Idriss relationship for, 392
 soil strength relationships, 316
 saturated unit weight, 52
 saturation
 degree of, 49
 normal stress and, 151
 Schmertmann's method, 240
 secant elastic modulus, 137
 secondary compression
 defined, 208, 211
 illustrated, 234
 primary consolidation versus, 211
 rate of settlement, 211
 settlement, 234
 in total settlement, 207
 secondary compression index
 defined, 234
 determining, 241
 typical range of values, 245
 sedimentary rocks, 7
 seepage
 defined, 154
 effects of, 154–155
 effects on effective stress example, 158–159
 forces, 154, 155
 infinite slopes, 693
 infinite slopes example, 695–696
 parallel to slope, 694
 rigid retaining walls, 635
 soils illustration, 155
 stresses, 155, 579
 seismic surveys
 reflection, 30
 refraction, 30
 subsurface interfaces, 29–30
 surface wave travel, 29
 sensitivity
 liquidity index and, 383
 soil, 27
 undrained shear strength and, 383
- service load capacity, 525
 serviceability limit states
 as deciding design limit state, 610
 defined, 424
 for foundations on Earth fill, 449
 settlement, 448
 settlement
 calculations, 450–456
 changes under constant load, 213
 of cone data, 461
 consolidation, 207–260
 data plots, 214
 differential, 207
 differential limit example, 490–493
 distortion, 448, 449
 drilled shafts, 559–560
 elastic, of piles, 552–554
 foundation, 448–464
 immediate, 450–454
 levee example, 256–257
 nonuniform, 448, 449
 pile groups example, 556–559
 primary consolidation, 216–219, 454–456
 rate from secondary compression, 211
 secondary compression, 234
 serviceability limit states, 448
 single pile example, 556
 SPT example, 460
 by stress, 132
 time calculations example, 244
 time factor, 243–244
 time rate of, 225
 time-dependent, 458
 total, 207
 uniform, 448, 449
 shaft friction, 510
 shallow excavations, shear strength, 268
 shallow foundations
 allowable bearing capacity example, 477–482
 analysis with CSM, 464–485
 defined, 423
 dense coarse-grained soils, 471–474
 design using CSM for ductile soil response, 482–485
 foundation settlement example, 477–482
 heavily consolidated fine-grained soils, 465–471
 heavily overconsolidated clay example, 474–477
 soil response, 427
 vane shear test data example, 500–506
 shear bands
 CSM and, 337
 development of, 263
 illustrated, 264
 shear box test. *See also* shear strength parameters
 Coulomb failure criterion interpretation, 288–289
 data interpretation example, 290–291
 measurements, 287

- shear box test. *See . . . (continued)*
 results, 287
 shear box illustration, 286
 strength parameters, 287
 vertical forces, 287
 shear deformation
 applying, 262–263
 defined, 263
 illustrated, 263
 shear failure, 432
 shear modulus, 139, 140, 189
 shear strains
 action of intermolecular forces on, 268
 from CSM, 395–396
 defined, 134
 elastic, 396, 397
 illustrated, 134
 intermediate, 391, 392
 maximum, 148
 nonuniform distribution, 392
 soil stiffness and, 391
 soils subjected to, 263
 shear strength, 261–323
 from cementation, 269
 cemented soils, 408
 core penetrometer test (CPT), 314
 Coulomb's failure criterion, 270–274
 critical state, 281
 defined, 262
 field tests, 313–314
 fine-grained soil prediction example, 384–385
 hollow-cylinder apparatus, 312
 interpretation models, 269–278
 interpretation of, 280–286
 measurement devices, 307–313
 Mohr-Coulomb failure criterion, 275–277
 peak, 281
 reserved, 282
 residual, 281
 shallow excavations, 268
 simple shear apparatuses, 307–311
 standard penetration test (SPT), 313
 Taylor's failure criterion, 274–275
 Tresca failure criterion, 277–278
 true triaxial apparatus, 311–312
 undrained, 262, 277, 348
 undrained, from UC test example, 294–295
 undrained, from UU test example, 305
 vane shear test (VST), 313
 shear strength parameters
 consolidated drained (CD) compression test, 295–300
 consolidated undrained (CU) compression test, 300–303
 conventional triaxial apparatus, 291–293
 empirical relationships, 314–316
 friction angle test, 286
 laboratory tests to determine, 286–305
 notation, 281
 shear box test, 286–291
 unconfined compression (UC) test, 293–295
 unconsolidated undrained (UU) test, 304–305
 shear stresses
 critical state, 263, 264, 365–367
 defined, 134
 at failure prediction example, 289
 in hollow-cylinder test, 312
 normalized yield, 365–367
 peak, 263, 265, 266
 pile driving, 515
 residual, 263
 on slip plane, 694
 Type I soils, 263
 Type II soils, 263–264
 yield, 347
 as zero, 135
 shearing
 material response to, 137–138
 resistance, 269
 response illustration, 264
 response of soils to, 262–269
 sheepfoot rollers, 96, 97
 sheet pile walls. *See* flexible retaining walls
 Shelby tube, 35
 short-term condition
 defined, 267
 in geosystems analysis, 378–379
 TSA requirement, 432
 shrinkage index, 67
 shrinkage limit
 defined, 49, 61
 determination, 66–67
 determination example, 70
 equation, 67
 estimating, 67
 side shear, 510
 sieves
 in coarse-grained soil grain size analysis, 15–16
 identification, 16
 stack, 15
 silicate sheets, 11, 12
 silicates, 11
 silt
 AASHTO classification, 76
 average grain size, 18
 hydraulic conductivity, 111
 simple shear apparatuses
 cuboidal sample deformation, 307
 cylindrical sample test, 307
 data interpretation example, 308–310
 failure criteria, 308
 purpose, 307
 shear displacement, 308
 strains interpretation example, 310–311
 stresses and strains, 308
 types of, 307
 simple well equation, 122–123
 single pile failure mode, 548
 Skempton's porewater pressure coefficients, 306
 skin friction
 α-method, 531
 β-method, 532–533
 defined, 510
 driven piles in coarse-grained soils, 540
 effective stress analyses (ESA), 544–545
 end bearing resistance separation, 524
 negative, 560–561
 relative displacement to mobilize, 524
 stress, 510
 ultimate, 542
 ultimate load capacity, 521
 sliding mass, 687
 slip plane
 defined, 687
 determination, 620
 groundwater below, 693
 inclination, 620, 622
 maximum thrust, 620
 Rankine active state, 614–615
 Rankine passive state, 615
 shear stress on, 694
 wall friction and, 622
 slip surfaces
 circular, 697
 defined, 427
 noncircular, 697
 tension crack effect on, 704
 slip zone, 687
 slope angle, 687
 slope failure
 analyses based on limit equilibrium, 699
 base slide, 688, 689
 block slide, 689
 causes, 689–692
 circular mechanism, 698
 from construction activities, 690, 691–692
 from earthquakes, 690, 691
 from erosion, 689, 690
 from excavated slopes, 691–692
 from external loading, 690, 691
 from fill slopes, 692
 flow slide, 688, 689
 from geological features, 690, 691
 from rainfall, 690, 691
 from rapid drawdown, 690, 692
 rotational, 688, 689, 697–699
 slope slide, 688, 689
 toe slide, 688, 689
 types of, 688–689
 slope slide, 688, 689
 slope stability, 687–722
 Bishop-Morgenstern example, 715
 Bishop-Morgenstern method, 714
 Bishop's method example, 707–710
 Bishop's method for two-layered soils example, 710–711
 canal example, 716–719
 importance of, 687

- Janbu's method example, 711–712
 with simple geometry, 713–715
 summary, 716
 Taylor's method, 713–714
 Taylor's method example, 714–715
 slopes
 excavated, 691–692
 factor of safety of, 705, 715
 fill, 692
 infinite, 692–696
 seepage as parallel to, 694
 smell, in soil identification, 32
 smooth footings, 434
 soil behavior
 Coulomb's law in modeling, 270
 critical state model for interpretation, 324–421
 loading history and, 215
 prediction of Coarse-grained soils, 337
 prediction under drained and undrained condition, 335–337
 prediction under drained condition, 329–332
 prediction under undrained condition, 332–334
 Region I, 362
 Region II, 362
 Region III, 362–363
 soil classification
 AASHTO, 74–76, 80
 ASTM-CS, 71–74, 77–80
 schemes, 70–76
 soil profile estimation example, 82–83
 USCS, 71, 72, 77–80
 uses, 70
 soil constituents
 calculation example, 57–58
 deriving relationships example, 54–55
 relationships application examples, 59–61
 soil fabric, 13–15
 in compaction, 95
 defined, 13
 dispersed, 14
 flocculated, 14
 illustrated, 14
 loading history, 215
 response, stability, failure of, 192
 as space frame, 191–192
 soil filtration, 602
 soil formation, 10
 soil identification
 carbonate, 32
 color, 32
 consistency, 32
 dilatancy, 32
 feel, 32
 moisture, 32
 packing, 34
 shape, 32
 smell, 32
 structure, 32
 weathering, 32
 soil mechanics, 2
 soil models
 Coulomb's failure criterion, 270–274
 defined, 269–270
 Mohr-Coulomb failure criterion, 275–277
 Taylor's failure criterion, 274–275
 Tresca failure criterion, 277–278
 soil profiles
 construction site, 27
 estimation example, 82–83
 soil quantities
 dam example, 81–82
 highway embankment example, 81
 soil resistance, 1
 soil ruptures, 368
 soil sampling
 objective, 35
 with Shelby tube, 35–36
 soil sensitivity, 27
 soil states
 consolidation, 216
 fine-grained soil, 61
 impending instability, 279–280
 impossible, 279
 interpretation of, 279
 stable, 280
 water content and, 62
 soil stiffness, 389–393
 calculation example, 393
 depth and, 450
 relationships, 392
 shear strains and, 391
 soil strength
 defined, 261
 empirical relationship, 725
 parameter relationships, 727–729
 shear, 261–323
 water content and, 61
 soil tension
 defined, 262, 268
 effects of, 268–269
 large, 268
 soil yielding, 328–329
 soils
 alluvial, 10
 calcareous, 11
 caliche, 11
 cemented, 407–408
 colloidal, 11
 composition of, 10–15
 defined, 5
 drying of, 13
 as engineering material, 1
 elolian, 11
 expansive, 11, 629
 glacial, 10, 11
 glacial clays, 11
 glacial till, 11
 gypsum, 11
 lacustrine, 11
 lateritic, 11
 loam, 11
 loess, 11
 marine, 10, 11
 marl, 11
 mud, 11
 particle size determination, 15–19
 performance uncertainties, 2
 residual, 10
 types of, 10–11
 soils exploration
 with electrical resistivity, 31
 field tests, 37–43
 geophysical methods, 31–32
 with ground-penetrating radar (GPR), 29
 groundwater conditions, 36–37
 identification, 32–34
 laboratory tests, 37, 43–46
 methods, 29–32
 number/depth of boreholes, 34–35
 phase, 28
 program, 29–46
 sampling, 35–36
 with seismic surveys, 29–30
 soils investigation
 desk study phase, 28
 importance of, 26
 laboratory testing phase, 28
 phases, 27–29
 preliminary reconnaissance phase, 28
 purposes of, 27
 soils exploration phase, 28, 29–46
 soils report phase, 29, 46–47
 soils reports
 defined, 46
 example illustration, 46
 minimum requirements, 46–47
 phase, 29
 solid state, 61
 sonic-VDL, 31
 specific gravity
 coarse-grained soil example, 55–56
 defined, 51
 determination, 52
 equation, 51–52
 laboratory tests to determine, 44
 soil solids, 88
 specific volume, 51
 spheres
 dense packing of, 14, 15
 loose packing, 14, 15
 spread footings, strength test, 315
 SPT. *See* standard penetration test
 square footings, 470, 487–490
 square foundations
 allowable bearing capacity example, 477–482
 foundation settlement example, 477–482
 vertical stress contour below, 171

- stability
 bottom heave, 661
 earth-retaining structure, 610–688
 as engineering design tenet, 2
 flexible retaining walls, 643–649
 foundation, 422
 infinite slope example, 695–696
 mechanical stabilized earth walls, 667–671
 rigid retaining walls, 633–643
 slope, 687–722
 structure, 3
 two-dimensional slope analyses, 697
 ultimate limit state and, 610
- stability number, 713
 standard axial test condition, 379
 standard penetration test (SPT). *See also* in situ testing devices
 allowable bearing capacity examples, 458–460
 bearing capacity, 457–459
 characteristics, 39
 corrected N value, 39, 457
 correction factors, 38–39, 40
 defined, 38
 drive sequence illustration, 39
 driven piles in coarse-grained soils, 540
 foundation settlement, 457–460
 foundation settlement example, 460
 groundwater correction factor, 457
 pile load capacity example, 542
 results of, 36
 shear strength from, 313
 sizing footings example, 493–500
 value correction example, 40–41
- static equilibrium, 625
 static liquefaction
 defined, 579
 quicksand, 587
 steady-state condition, 106
 steel piles. *See also* piles
 characteristics, 513
 displacement, 515
 illustrated, 511
 plugging, 512
 types of, 512
 stiffness
 matrix, 140
 summary, 726
 Stokes's law, 17
 strain invariants, 187–191
 axisymmetric condition, 188
 axisymmetric loading calculation example, 190–191
 deviatoric strain, 188
 Hooke's law using, 189
 plane strain, 188
 volumetric strain, 188
 strain states, 148–149
 strains
 axisymmetric condition, 142–143, 188
 calculation example, 396–398
- circumferential, 210
 compressive, 135, 149
 from CSM, 393–399
 defined, 133
 deviatoric, 188
 importance, 277
 lateral, 210
 pile, 516
 plane strain condition, 141–142, 188
 plastic, 394
 shear, 134–135, 148, 395–396
 simple shear test interpretation example, 310–311
 tensile, 135, 149
 vertical strain, 210
 volumetric, 134, 188, 210, 393–395
- strength tests, laboratory
 defined, 314
 illustrated, 315
 stress invariants, 187–191
 axisymmetric loading calculation example, 190–191
 calculation, 197
 deviatoric stress, 187–188
 Hooke's law using, 189
 incremental form, 192
 mean stress, 187
 plotting, 197
 plotting stress paths with, 192–196
- stress parameters, 196–197
 stress paths, 191–202
 consolidated drained (CD) compression test, 296
 consolidated undrained (CU) compression test, 301
 defined, 187
 determining, 192
 determining for loading conditions, 195
 due to axisymmetric loading, 198–200
 effective (ESP), 194, 195, 196, 330–331
 for isotropic compression, 193
 one-dimensional compression, 196
 plot representation, 192
 plotting procedure, 197–198
 plotting with stress invariants, 192–196
 plotting with two-dimensional stress parameters, 196–197
 in spaces for soil elements, 200–202
 summary, 203
 total (TSP), 194, 195, 196, 315, 331
 for UC test, 293
 unconsolidated undrained (UU) test, 304
 under foundation example, 203–205
- stress states
 critical, 281
 defined, 133, 147
 on ESP, 331
 HV surface, 362
 Mohr's circle, 147–148
 Mohr's circle example, 149–151
 peak, 281
- pile installation and, 517, 518
 stresses
 adhesive, 510
 axisymmetric condition, 142–143
 beyond yield curve, 138
 circumferential, 341
 compressive, 135
 consolidated drained (CD) compression test, 296
 consolidated undrained (CU) compression test, 301
 defined, 133
 deviatoric, 187–188, 466
 distribution of, 163
 due to applied loads, 134
 effective, 133, 151–160
 failure, 343–344
 general state of, 139–140
 increments of, 192
 initial, 315
 lateral, 250
 lateral earth pressure, 612
 locus, 138
 mean, 187
 normal, 133
 pile, 516
 plane strain condition, 141–142
 preconsolidation, 367–369
 principal, 135, 140
 radial, 341
 seepage, 155, 579
 shear, 134–135
 skin friction, 510
 surface, 132
 from surface loads, 162–178
 total, 133, 151
 triangular, 167
 types applied to soils, 132
 unconfined compression (UC) test, 293
 unconsolidated undrained (UU) test, 304
 at unloading and reloading, 161
 yield, 352–355
- stress-strain response, 399–406
 drained compression tests, 400
 prediction example, 401–406
 undrained compression tests, 400, 401
- strike, 5
 strip footings. *See also* footings
 design example, 474–477
 stress invariants, 470
 strip loads. *See also* surface loads
 area transmitting triangular stress, 167
 defined, 166
 uniform stress near retaining wall, 167
 uniform surface stress, 166–167
 vertical displacement due to, 167
- structural anisotropy, 145
 structure, in soil identification, 32
 surcharges, 629
 surface forces, 12–13
 surface loads

- classes, 163
 embankment loads, 177
 finite, 163
 infinite, 163, 178
 line load, 165–166
 point load, 163–165
 rectangular, approximate method for, 172–175
 ring, 167–170
 stresses, 162–178
 strip load, 166–167
 uniformly loaded circular area, 167–170
 uniformly loaded rectangular area, 170–172
 vertical stress below arbitrarily shaped areas, 175–177
 surface stresses
 distribution within finite soil layers, 731–734
 lateral earth pressures, 616
 swell factor
 defined, 49
 equation, 53
- T**
- tangent elastic modulus, 137
 tank foundation
 soil response prediction example, 414–418
 strength test, 315
 Taylor's failure criterion. *See also* shear strength
 application example, 283–284
 equation summary, 282
 extension, 275
 external energy, 274
 failure criteria comparison, 279
 internal energy, 274
 peak dilation angle, 275
 physical mechanism of failure, 274
 Taylor's method. *See also* slope stability
 defined, 713
 example, 714–715
 factor of safety, 713–714
 procedure, 73
 Taylor's theorem, 230, 592
 tensile strains, 135, 149
 tensile stresses, 135
 tension cracks
 behind retaining walls, 626
 channel for water, 704
 depth of, 695
 effect on slip surface, 704
 in fine-grained soils, 645–646, 704
 water filling, 646
 tension cutoff
 mean effective stress and, 367–369
 preconsolidation ratio for, 367, 368
 preconsolidation stress and, 367–369
 tension factor, 467
 tension failure, 467
 Terzaghi one-dimensional consolidation equation, 227
 test pits, 32, 33
 thinly stratified soils, 446
 timber piles
 characteristics, 513
 defined, 512
 illustrated, 511
 time factor, 243–244
 defined, 243
 equation, 243
 in vertical direction, 248
 time-dependent settlement, 458
 time-settlement calculations, 244
 tip resistance, 510
 toe slide, 688, 689
 total excess porewater pressure, 349
 total settlement, 207
 total stress
 defined, 133, 151
 horizontal, 162
 vertical, 152–153
 total stress analysis (TSA)
 adhesion, 544
 a-method basis, 531
 Bishop's equation for, 701
 defined, 277, 432
 end bearing, 544
 group load capacity, 548
 inclined load only, 432
 Janbu's equation for, 703
 lateral earth pressures for, 625–627
 load capacity of drilled shafts, 544
 ultimate net bearing capacity, 432
 vertical centric load only, 432
 total stress path (TSP)
 CSL intersection, 333
 defined, 194
 effects of, 338
 ESP equal to, 331
 illustrated, 194
 mean stress difference, 195
 slope, 196, 197
 strength tests, 315
 in total excess porewater pressure, 334
 for triaxial compression, 197
 Transcona Grain Elevator failure, 4
 translation
 factor of safety against, 633
 mechanical stabilized earth walls, 668–669
 rigid retaining walls, 633–634
 transverse anisotropy
 application example, 146
 defined, 145
 Tresca failure criterion. *See also* shear strength
 for CU test, 301
 defined, 277
 equation summary, 282
 failure criteria comparison, 279
 total stress analyses (TSA), 277
 for UC test, 294
 for UU test, 304–305
 triangular stress, 167
 triaxial (T), 45
 triaxial apparatus
 average stresses and strains, 292–293
 defined, 291
 sample area, 293
 schematic, 292
 versatility, 293
 triaxial compression, 367, 368
 test, 196
 TSP for, 197
 triaxial tests
 direct simple shear tests and, 377–378
 drained, 345–347
 from isotropically consolidated samples, 378
 undrained, 347–351
 true axial apparatus
 cuboidal sample, 311
 purpose, 311
 schematic, 311
 stress/strains measured in, 311, 312
 TSA. *See* total stress analysis
 2:1 method, 172
 two-dimensional flows, 579–609
 boiling, 586–587
 boundary types, 593
 critical hydraulic gradient, 587, 588
 earth dams, 598–602
 effective size of soil, 602
 excavation determination example, 603–605
 finite difference solution for, 592–598
 flow domain grid, 593
 flow rate, 582, 594
 flownet interpretation, 586–592
 flownet sketching, 583–585
 heaving, 586–587
 horizontal velocity, 594
 hydraulic conductivity, 581
 hydraulic gradient, 586
 importance, 579
 Laplace's equation, 580–581
 piping, 586–587
 porewater pressure distribution, 587
 soil filtration, 602
 static liquefaction, 586–587
 through earth dams, 598–602
 through porous media, 580–583
 uplift forces, 587–588
 velocity, 582
 two-dimensional slope stability analyses, 697
 two-layer soils
 bearing capacity example, 446–447
 common cases, 446
 footing, 446
 slope stability with Bishop's method example, 710–711
 vertical stresses in, 733
 Type I soils, 263, 265

- Type II soils, 263–265
 compression, 264
 critical state shear stress values, 265
 defined, 263
 peak shear stress, 263
- U**
- UC. *See* unconfined compression test
 ultimate bearing capacity
 defined, 423
 for shallow footing, 457
 ultimate gross bearing capacity
 defined, 423
 equation, 432
 ultimate group load capacity, 510
 ultimate limit state
 defined, 424
 stability and, 610
 ultimate load capacity
 defined, 510
 parts, 521
 ultimate net bearing capacity
 defined, 423
 for general failures, 432
 of two-layer soil, 446
 ultimate skin friction, 542
 unconfined compression (UC) test
 Mohr's circle, 293–294
 in preliminary analyses, 305
 purpose, 293
 results, 294
 stress paths, 293
 stresses, 293
 Tresca failure criterion for, 294
 undrained shear strength example, 294–295
 unconsolidated undrained (UU) test
 advantage, 305
 isotropic compression phase, 304
 Mohr's circles for, 304
 in preliminary analyses, 305
 purpose, 304
 shearing phase, 304
 stress paths, 304
 stresses, 304
 Tresca failure criterion for, 304–305
 undrained shear strength example, 305
 undrained, 194
 undrained compression tests, 400–401
 undrained conditions
 active/passive lateral earth pressures for, 627
 in analysis of geosystems, 378–380
 existence of, 267
 Poisson's ratio for, 450
 stress-strain responses example, 401–406
 undrained elastic modulus, 450
 undrained loading
 drained loading versus, 268
 effects on volume changes, 267
 excess porewater pressures during, 349
- undrained shear strength
 comparison, 349
 at critical state, 351, 374–376
 critical state friction angle and, 369–370
 defined, 262, 348
 direct simple shear example, 386–389
 fine-grained soils, 351
 HV surface and, 375
 at initial yield, 374–376
 at liquid limit, 382
 liquidity index and, 383
 for normally consolidated soils, 370–371
 of one-dimensionally consolidated
 soils, 371–374
 for overconsolidated soils, 370–371
 at plastic limit, 382
 preconsolidation ratio and, 369–370
 prediction in compression and extension
 tests example, 360–361
 rupture normalized, 368
 sensitivity and, 383
 summary, 726
 theoretical ratio at critical state, 380
 UC test example, 294–295
 under direct simple shear, 376–377
 UU test example, 305
 water content change effects example, 361
 undrained triaxial test, 347–351
 failure, 348
 predicting yield stresses example, 353–354
 shear component, 349
 total volume change, 347
 undrained shear strength at critical state,
 351
 undrained shear strength comparison, 349
- Unified Soil Classification System
 (USCS), 71
- uniform settlement. *See also* foundation
 settlement
 defined, 448
 illustrated, 449
- uniformitarianism, 6
- uniformity coefficient, 18–19
- uniformly loaded circular area, 167–170
- unit weight
 bulk, 49, 52
 defined, 52
 dry, 49, 52, 88
 effective, 49, 52
 saturated, 52
 typical values, 53, 723
- United Soil Classification System (USCS)
 classification example, 77–80
 coarse-grained soils flowchart, 71
 defined, 71
 fine-grained soils flowchart, 72
- unloading/reloading
 index. *See* recompression index
 void ratio at, 389–390
- unloading-reloading line (URL)
 cemented soils, 408
- defined, 214
 notation, 326
 slope, 326
 void ratio, 390
- unprotected fortress, 1
- uplift forces, 587–588
 per unit length, 587–588
 sizing a hollow box culvert example, 605–606
 structure stability and, 587
- URL. *See* unloading-reloading line
- USCS. *See* United Soil Classification System
- UU. *See* unconsolidated undrained test
- V**
- vane shear test (VST). *See also* in situ
 testing devices
 characteristics, 37
 defined, 37
 illustrated, 38
 shallow foundation design example,
 500–506
 undrained shear strength from, 313
- velocity
 average, 110
 Darcy's law, 110
 horizontal, 594
 two-dimensional flow, 582
- velocity head, 106, 581
- vertical displacement, 164, 167
- vertical effective stress
 calculation example, 156
 change at degree of consolidation, 231–232
 distribution calculation example, 157–158
 at liquid limit, 382
 modulus of volume compression and,
 240–241
 past maximum, determination of, 239–240
 at plastic limit, 382
- vertical elastic settlement, 171
- vertical strains
 calculation example, 242
 increase due to foundation example,
 180–181
 volumetric strain and, 210
- vertical stresses. *See also* stresses
 applied, 212
 below arbitrarily shaped areas, 175–177
 circular area, 731
 contour below square foundation, 171
 distribution, 163, 170
 distribution below eccentrically loaded
 footing, 436
 distribution under uniform circular
 load, 730
 effects on primary consolidation, 213–214
 embankment height for increase
 example, 179–180
 in finite soil layer, 731–733
 increase due to electric power transmission
 pole example, 178–179

- increase due to embankment, 177
 increase due to irregular loaded area, 176–177
 increase due to point load, 164–165
 increase due to rectangular load, 173–175
 increase due to ring load, 168–170
 Newmark charts for, 162, 175
 rectangular area, 732–733
 total, 152–153
 in two-layer soil, 733
 X-axis, 436
 Y-axis, 436
 virgin consolidation line, 213
 viscosity
 in constant-head test, 119
 dynamic, 119
 hydraulic conductivity and, 110
 VisCPT, 42
 void ratio
 calculation example, 56
 constant load, 213
 critical, 264, 281
 of critical state line, 342, 343
 defined, 49
 at end of loading step, 238–239
 equation, 51
 hydraulic conductivity and, 110
 initial, back-calculating, 239
 maximum/minimum, 53
 preconsolidation mean effective stress, 469
 at unloading/reloading, 389–390
 voids
 air, 50
 defined, 14, 50
 volume of, 50
 water, 50
 zero air, 88
 volume changes
 drained/undrained conditions on, 267
 OCR effects on, 266
 volumetric strains
 from CSM, 393–395
 elastic, 390, 395, 467
 equation, 134
 total change in, 393
 vertical strain and, 210
 VST. *See* vane shear test
- W**
- wall adhesion, 628
 wall displacements, 660
 wall friction
 active force and, 622
 active lateral earth pressures and, 628
 passive force and, 622
 retaining wall with, 621
 wash boring, 32, 33
 water
 expulsion from micropores, 234
 one-dimensional flows, 105–129
 two-dimensional flows, 579–609
 in voids, 50
 weight of, 50
 water content
 calculation example, 58
 change effects on undrained shear strength, 361
 defined, 49
 dry unit weight relationship, 90–91
 equation, 51
 finding, 51
 laboratory test to determine, 44
 optimum, 88, 90–91
 soil strength and, 61
 weathering
 chemical, 10
 physical, 10
 in soil identification, 32
 well-graded soils, 19
 wellpoints
 data interpretation example, 126
 defined, 124
 groundwater lowering by, 124–126
 illustrated, 125
 Wheatstone bridge, 108
 wick drains
 defined, 246
 effects on time, 247
 flow into, 248
 illustrated, 246
 preconsolidation with, 246–249
 purpose, 246
 spacing, 248
 spacing example, 248–249
 square grid plan, 247
 surcharge height, 248
 triangular grid plan, 247
 vertical section illustration, 247
- Y**
- yield shear stress
 critical state shear stress relationship, 365–367
 drained triaxial test, 347
 yield stresses
 drained condition prediction example, 352–353
 excess porewater pressures and, 356–360
 initial estimation example, 354–355
 undrained condition example, 353–354
 yield surface
 critical state line intersection, 329, 340
 as CSM element, 339–340
 defined, 138, 328
 as ellipse, 329
 equation, 339
 expanded, unloading from, 331
 expansion, 329
 expansion example, 398–399
 initial, 329, 340
 initial size estimation example, 354–355
 shear strains and, 395
 theoretical basis, 340
 Young's modulus
 based on effective stresses, 215
 in elastic analysis, 131
 of elasticity, 215
 in radial displacement, 164
 in vertical displacement, 164

NOTATIONS

Note: A prime (') after notation for stress denotes effective stress.

A	Area	K_p	Passive lateral earth pressure coefficient
B	Width	K_o	Lateral earth pressure coefficient at rest
c_o	Cohesion or shear strength from intermolecular forces	L	Length
c_{cm}	Cementation strength	LI	Liquidity index
c_t	Soil tension	LL	Liquid limit
C	Apparent undrained shear strength	LS	Linear shrinkage
C_c	Coefficient of curvature	m_v	Modulus of volume compressibility
C_c	Compression index	N	Standard penetration number
C_r	Recompression index	N_c, N_q, N_γ	Bearing capacity factors
C_h	Horizontal coefficient of consolidation	n	Porosity
C_v	Vertical coefficient of consolidation	NCL	Normal consolidation line
C_a	Secondary compression index	OCR	Overconsolidation ratio with respect to vertical effective stress
C_u	Uniformity coefficient	PI	Plasticity index
CSL	Critical state line	PL	Plastic limit
CSM	Critical state model	p	Mean total stress
D	Diameter	p'	Mean effective stress
D_f	Embedment depth	q	Deviatoric stress or shear stress
D_r	Relative density	q_a	Allowable bearing capacity
D_{10}	Effective particle size	q_{ap}	Applied deviatoric stress
D_{50}	Average particle diameter	q_s	Surface stress
e	Void ratio	q_u	Ultimate net bearing capacity
e_T	Void ratio on CSL for $p' = 1$ kPa	q_{ult}	Ultimate gross bearing capacity
E	Modulus of elasticity	q_y	Deviatoric stress at initial yield
E_i	Initial tangent modulus	q_{yH}	Deviatoric stress on reaching the Hvorslev's surface
E_p	Modulus of elasticity of pile	q_{yLS}	Deviatoric stress on reaching the limiting stress surface
E_s	Secant modulus	q_w	Flow rate of wick material
E_{so}	Modulus of elasticity of soil	q_z	Flow rate in vertical direction
E_t	Tangent modulus	Q	Flow, quantity of flow, and also vertical load
f_b	Ending bearing stress	Q_b	End bearing or point resistance
f_s	Skin friction	Q_f	Skin or shaft friction
FS	Factor of safety	Q_{af}	Allowable skin friction
F_ϕ	Mobilization factor for ϕ	Q_{ult}	Ultimate load capacity
F_u	Mobilization factor for s_u	$(Q_{ult})_g$	Ultimate group load capacity
G	Shear modulus	R_T	Temperature correction factor
G_s	Specific gravity	R_x	Resultant lateral force
h_p	Pressure head	R_z	Resultant vertical force
h_z	Elevation head	R_o	Preconsolidation ratio with respect to mean effective stress invariants
H	Head, also horizontal force	s_u	Undrained shear strength
H_o	Height	S	Degree of saturation
H_{dr}	Drainage path	SI	Shrinkage index
i	Hydraulic gradient	SL	Shrinkage limit
I	Influence factor	SR	Shrinkage ratio
I_s	Settlement influence factor		
k	Hydraulic conductivity		
K_a	Active lateral earth pressure coefficient		

S_t	Sensitivity	ϕ'_p	Peak friction angle
SPT	Standard penetration test	ϕ'_r	Residual friction angle
t_c	Tension factor	γ	Bulk unit weight
T	Sliding force or resistance	γ'	Effective unit weight
u	Porewater pressure	γ_{sat}	Saturated unit weight
U	Average degree of consolidation	γ_d	Dry unit weight
URL	Unloading/reloading line	$\gamma_{d(max)}$	Maximum dry unit weight
v	Velocity	γ_w	Unit weight of water
v_s	Seepage velocity	γ_{zx}	Shear strain
V	Volume	κ	Recompression index
V'	Specific volume	λ	Compression index
V_a	Volume of air	μ	Viscosity
V_n	Vertical resultant force	μ_s	Shape coefficient
V_s	Volume of solid	μ_{emb}	Embedment coefficient
V_w	Volume of water	μ_{wall}	Wall friction coefficient
V_{sh}	Shear wave velocity	ν	Poisson's ratio
w	Water content	ρ_e	Elastic settlement
w_{opt}	Optimum water content	ρ_{pc}	Primary consolidation
W	Weight	ρ_{sc}	Secondary consolidation settlement
W_a	Weight of air	ρ_t	Total settlement
W_s	Weight of solid	σ	Normal stress
W_w	Weight of water	τ	Shear stress
z	Depth	τ_{cs}	Critical state shear strength
α	Dilation angle	τ_f	Shear strength at failure
α_p	Peak dilation angle	τ_p	Peak shear strength
α_s	Slope angle	τ_r	Residual shear strength
α_u	Adhesion factor	ξ	Velocity potential
β	Skin friction coefficient for drained condition	ξ_o	Apparent friction angle
δ	Deflection or settlement; also wall friction angle	ψ	Inclination of principal plane to the horizontal plane
ϵ	Normal strain	ψ_p	Plastification angle for piles
ϵ_p	Volumetric strain	ψ_s	Stream potential
ϵ_q	Deviatoric strain	,	Prime used throughout to indicate effective stress condition
ϕ'	Generic friction angle		
ϕ'_{cs}	Critical state friction angle		

HELPFUL CONVERSION FACTORS

U.S. Customary SI Units

Units

Length

1.00 in.	=	2.54 cm
1.00 ft	=	30.5 cm

Mass and Weight

1.00 lb	=	454 g
1.00 lb	=	4.46 N
1 kip	=	1000 lb

Area

1.00 in. ²	=	6.45 cm ²
1.00 ft ²	=	0.0929 m ²

Volume

1.00 ml	=	6.00 cm ³
1.00 l	=	1000 cm ³

$$1.00 \text{ ft}^3 = 0.0283 \text{ m}^3$$

$$1.00 \text{ in.}^3 = 16.4 \text{ cm}^3$$

Temperature

°F	=	1.8(°C) + 32
°C	=	(°F - 32)/1.8

Pressure

1.00 psi	=	6.895 kPa
1.00 psi	=	144 psf
1.00 ksi	=	1000 psi

Unit Weight and Mass Density

1.00 pcf	=	16.0 kg/m ³
1.00 pcf	=	0.157 kN/m ³

Universal Constants

g	=	9.81 m/s ²
g	=	32.2 ft/s ²